PRICM 10

CONTENTS

Greetings from the Conference Chair

Dear Colleagues,

On behalf of The Chinese Society for Metals, I am pleased to welcome you all to The 10th Pacific Rim International Conference on Advanced Materials and Processing (PRICM10) being held on August 18-22, 2019 in Xi'an.

Over the last 27 years, the conference has been jointly organized and in-rotation hosted by The Chinese Society for Metals (CSM), The Japan Institute of Metals and Materials (JIM), The Korean Institute of Metals and Materials (KIM), Materials Australia (MA), and The Minerals, Metals & Materials Society (TMS). It is the third time that PRICM is hosted by China since its start in 1992 in Hangzhou and we will continue the tradition of bringing together researchers and experts involved in advanced materials and processing from all over the world, to discuss the latest advance in materials science and share their knowledge and experiences.

After reviewed by the symposium organizers, 1213 papers from 41 countries and regions have been included in the technical program of PRICM10, together with 5 plenary lectures, 116 keynote presentations, 268 invited presentations, 542 contributed presentations and 282 poster presentations, which cover the field of advanced materials and processing.

The Chinese Society for Metals would like to take this opportunity to express its gratitude to all the authors, keynote and invited speakers, and chairpersons of conference sessions. We believe that their contributions will help to make the conference as outstanding as it has been. Special acknowledgement is given to all the sponsoring organizations, local co-organizations, symposium organizers, In-Country Technical Representatives, members of International Organizing Committee and International Advisory Board for their great assistance and support.

Finally, I hope you enjoy the conference and your stay in Xi'an.

Prof. Huibin Xu
Member of Chinese Academy of Engineering
President of Beihang University
Chairman of PRICM10

ZEISS 3D Correlative Microscopic Imaging Solution for Material Research

From cm to nm, pure imaging to micro analysis

XRM

- High resolution (Sub-um) 3D imaging of large samples
- High Contrast
- Non-destructive

FIB-SEM

- High resolution (nm scale) 3D Imaging
- High contrast, High accuracy sample preparation
- High resolution 3D micro analysis

3D Correlative analysis of Al-Cu Alloy

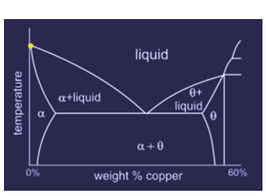

Phase diagram of Al-Cu Alloy

3D XRM → **3D FIB-SEM** → **EDS**

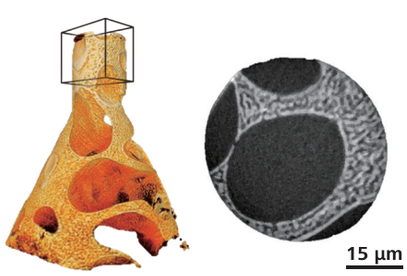

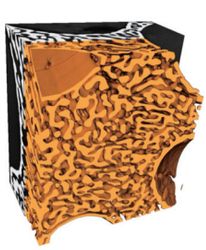

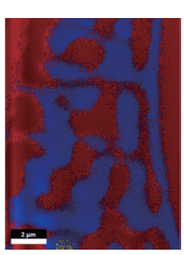

XRM

- Time evolution 3D data (4D)
- Non-destructive 3D analysis
- Positioning of ROI

FIB-SEM

- High resolution data aquisition of selected ROI
- Analysis of Chemical compositions and structures (EDS, EBSD)

Carl Zeiss (Shanghai) Co., Ltd.

ZEISS China Service Hotline: 400-6800-720
www.zeiss.com.cn/microscopy
Scan the QR code to follow us on Wechat

ZEISS
Seeing beyond

Organizers / Committees

Organized by

The Chinese Society for Metals (CSM)

Sponsored by

The Chinese Society for Metals (CSM)
The Japan Institute of Metals and Materials (JIM)
The Korean Institute of Metals and Materials (KIM)
Materials Australia (MA)
The Minerals, Metals & Materials Society (TMS)

Local Co-organized by

Beihang University
China Powder Metallurgy Alliance
Northwest Institute for Nonferrous Metal Research
Northwestern Polytechnical University
Xi'an Jiaotong University
Xi'an University of Architecture and Technology

Supported by

Chinese Materials Research Society

Sponsors

Carl Zeiss (Shanghai) Co., Ltd.

Park Systems

Honorary Chairman

Yuqing Weng Chinese Academy of Engineering

Conference Chairman

Huibin Xu Beihang University

In-Country Technical Representatives

CSM

Prof. Chengjia Shang, University of Science & Technology Beijing
Email: cjshang@ustb.edu.cn

JIM

Prof. Haruyuki Inui, Kyoto University
Email: inui.haruyuki.3z@kyoto-u.ac.jp

KIM

Prof. Sung-Joon Kim, POSTECH
Email: sjkim1@postech.ac.kr

MA

Prof. Jian-Feng Nie, Monash University
Email: jianfeng.nie@monash.edu

TMS

Dr. George T. Gray III, Los Alamos National Lab
Email: rusty@lanl.gov

International Organizing Committee Members

CSM	Fusheng Pan	Chongqing University
	Chengjia Shang	University of Science & Technology Beijing
	Zhiling Tian	Center Iron & Steel Research Institute
	Weihua Wang	The Institute of Physics, Chinese Academy of Sciences
	Guoqing Zhang	Beijing Institute of Aeronautical Materials
	Tongyi Zhang	Shanghai University
	Pei Zhao	The Chinese Society for Metals
	Shaoming Zhang	China Iron & Steel Research Institute Group
JIM	Yoshitsugu Kojima	Hiroshima University
	Nobuhiro Tsuji	Kyoto University
	Satoshi Sugimoto	Tohoku University
	Hideharu Nakashima	Kyushu University
KIM	Young-Chang Joo	Seoul National University
	Hyuck-Mo Lee	KAIST
	Woo-Young Lee	Yonsei University
MA	Allan Morton	Monash University
	Ming-Xing Zhang	University of Queensland
	Daniel East	CSIRO
TMS	Saryu Fensin	Los Alamos National Lab
	Brajendra Mishra	Worcester Polytechnic Institute
	Dan Thoma	University of Wisconsin - Madison

International Advisory Board Members

CSM	Yafang Han	Chinese Materials Research Society
	Xishan Xie	University of Science & Technology Beijing
	Zengyong Zhong	The Chinese Society for Metals
JIM	Hiroshi Fukutomi	The Open University of Japan
	Tomoyuki Kakeshita	Fukui University of Technology
	Mitsuo Niinomi	Tohoku University
KIM	Kyung Tae Hong	KIST
	Chang Hee Lee	Hanyang University
	Chong Soo Lee	POSTECH
MA	Matthew Barnett	Deakin University
	Simon Ringer	University of Sydney
	David StJohn	University of Queensland
TMS	Diran Apelian	Metal Processing Institute (MPI)
	Marc Meyers	University of California San Diego
	Robert Shull	National Institute of Standards & Technology

Secretary General

Xinjiang Wang The Chinese Society for Metals

F1 QUJIANG INTERNATIONAL CONVENTION CENTER

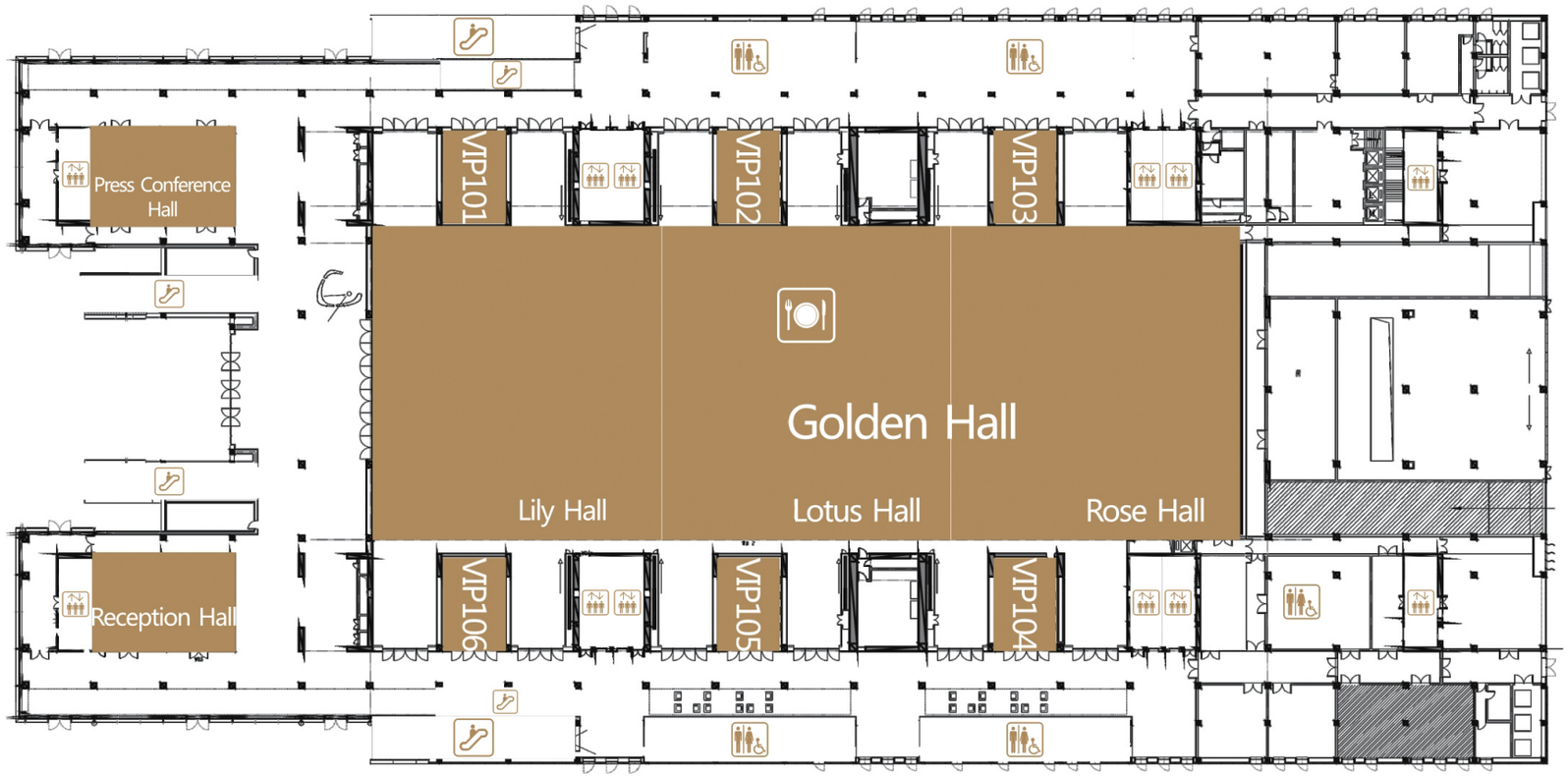

F2

QUJIANG
INTERNATIONAL
CONVENTION
CENTER

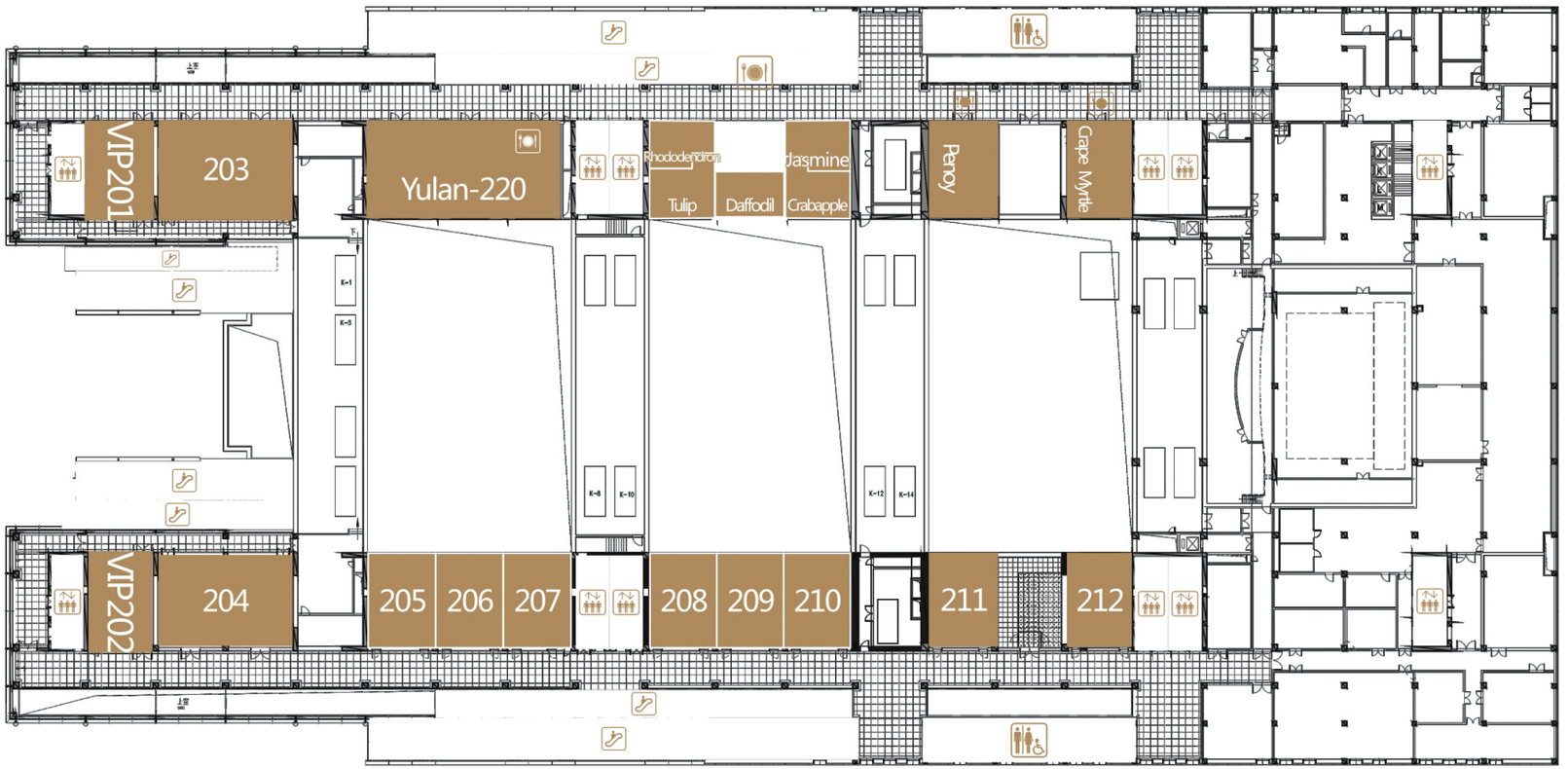

Floor Maps

F3 QUJIANG INTERNATIONAL CONVENTION CENTER

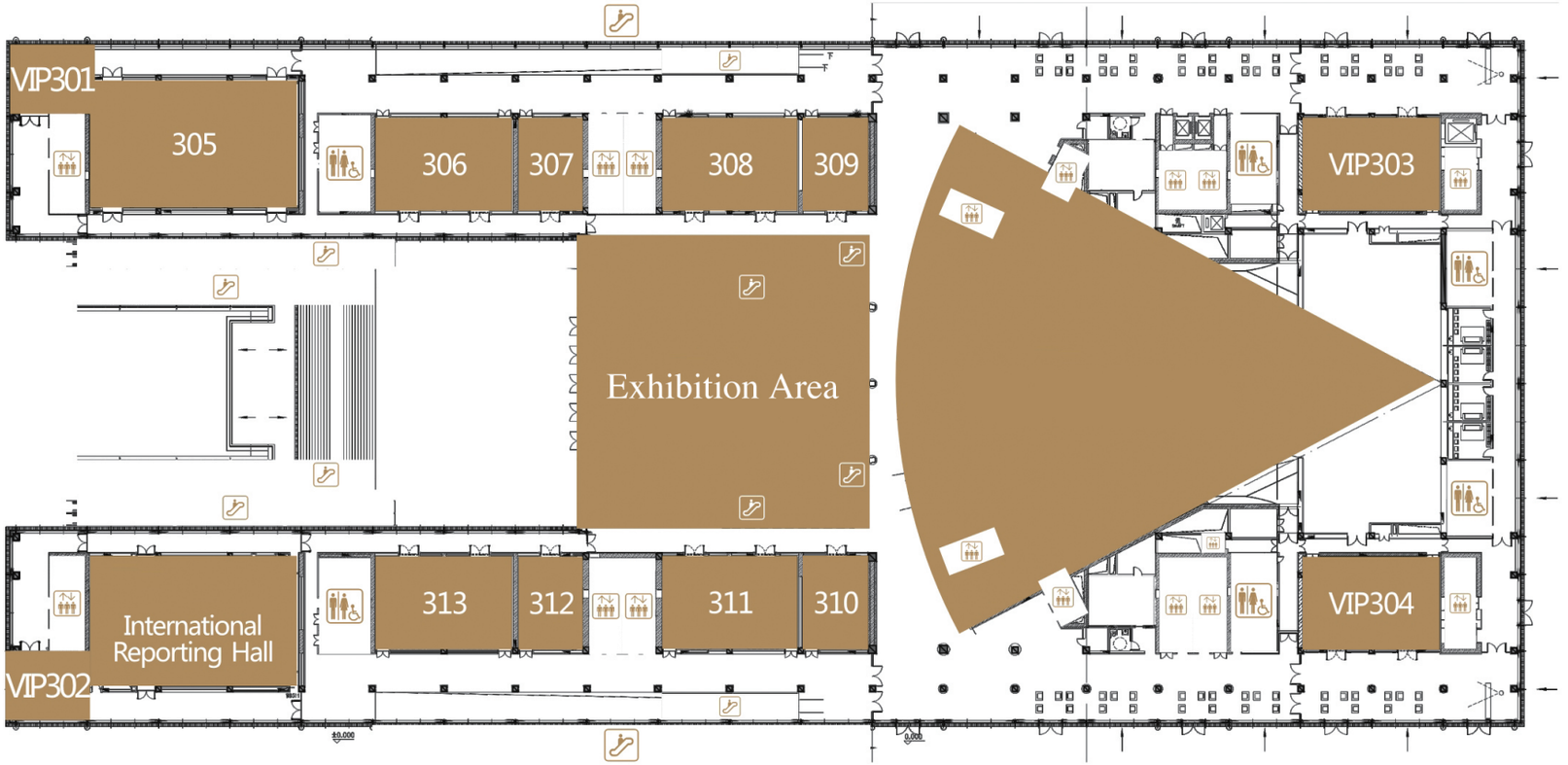

F4
QUJIANG
INTERNATIONAL
CONVENTION
CENTER
VIP401
International
Conference Hall
Presidium
Conference Room
402
405
406

Schedule At-A-Glance

August 18, 2019		
13:00-21:00	Registration	1st Floor of QICEC
14:30-18:00	ZEISS Workshop	Room 305 (3rd Floor) of QICEC
18:00-19:30	Welcome Reception	Golden Hall (1st Floor) of QICEC
August 19, 2019		
07:30-16:00	Registration	1st Floor of QICEC
08:30-12:30	Plenary Session	Golden Hall (1st Floor) of QICEC
12:00-13:30	Lunch	1st Floor of QICEC
13:30-18:00	Parallel Sessions	1st , 2nd, 3rd and 4th Floor of QICEC
08:30-18:30	Exhibition and Poster Sessions	3rd Floor of QICEC
August 20, 2019		
08:00-16:00	Registration	1st Floor of QICEC
08:30-12:30	Parallel Sessions	1st , 2nd, 3rd and 4th Floor of QICEC
08:30-12:00	Big Data Intelligence and Knowledge Services Forum 2019 (I)	International Reporting Hall (3rd Floor) of QICEC
12:00-13:30	Lunch	1st Floor of QICEC
13:30-18:00	Parallel Sessions	1st , 2nd, 3rd and 4th Floor of QICEC
13:30-17:30	Big Data Intelligence and Knowledge Services Forum 2019 (II)	International Reporting Hall (3rd Floor) of QICEC
19:00-21:00	Conference Dinner	Golden Hall (1st Floor) of QICEC
08:30-18:30	Exhibition and Poster Sessions	3rd Floor of QICEC
August 21, 2019		
08:00-16:00	Registration	1st Floor of QICEC
08:30-12:30	Parallel Sessions	1st , 2nd, 3rd and 4th Floor of QICEC
09:00-12:00	2nd China-Korea Symposium on Light Metals (I)	Room 304 (3rd Floor) of QICEC
12:00-13:30	Lunch	1st Floor of QICEC
13:30-18:00	Parallel Sessions	2nd, 3rd and 4th Floor of QICEC
13:30-17:00	2nd China-Korea Symposium on Light Metals (II)	Room 304 (3rd Floor) of QICEC
08:30-14:00	Exhibition and Poster Sessions	3rd Floor of QICEC
August 22, 2019		
08:00-16:00	Registration	1st Floor of QICEC
08:30-12:30	Parallel Sessions	2nd, 3rd and 4th Floor of QICEC
12:00-13:30	Lunch	1st Floor of QICEC
13:30-18:00	Parallel Sessions	2nd and 4th Floor of QICEC

Session Schedule

Symposium Name / Session Name	Date	Time	Room	Page
Programming Highlights				
Plenary Session	MON, Aug. 19	AM	Lily Hall of Golden Hall (1st Floor)	18
A. Advanced Steels and Processing				
Advanced Steels and Processing I	MON, Aug. 19	PM	Room 205+206+207 (2nd Floor)	20
Advanced Steels and Processing II	TUE, Aug. 20	AM	Room 205+206+207 (2nd Floor)	82
Advanced Steels and Processing III	TUE, Aug. 20	PM	Room 205+206+207 (2nd Floor)	150
Advanced Steels and Processing IV	WED, Aug. 21	AM	Room 205+206+207 (2nd Floor)	223
Advanced Steels and Processing V	WED, Aug. 21	AM	Room 208+209+210 (2nd Floor)	227
Advanced Steels and Processing VI	WED, Aug. 21	PM	Room 205+206+207 (2nd Floor)	290
Advanced Steels and Processing VII	WED, Aug. 21	PM	Room 208+209+210 (2nd Floor)	294
Advanced Steels and Processing VIII	THU, Aug. 22	AM	Room 205+206+207 (2nd Floor)	355
Advanced Steels and Processing VIIII	THU, Aug. 22	PM	Room 205+206+207 (2nd Floor)	393
B. High Temperature Structural Materials				
Power Generation	MON, Aug. 19	PM	Room 305 (3rd Floor)	24
Intermetallics	MON, Aug. 19	PM	Room VIP (1st Floor)	26
Fundamentals of Superalloys	TUE, Aug. 20	AM	Room 305 (3rd Floor)	85
Creep, Fatigue and Deformation Behavior	TUE, Aug. 20	PM	Room 305 (3rd Floor)	154
Processing and Alloy Design	WED, Aug. 21	AM	Room 305 (3rd Floor)	232
Novel Concepts	WED, Aug. 21	PM	Room 305 (3rd Floor)	298
Casting and Manufacturing	THU, Aug. 22	AM	Room 305 (3rd Floor)	359
C. Light Metals and Alloys				
Plenary Session of Light Metals and Alloys	MON, Aug. 19	PM	Room 406 (4th Floor)	30

C1. Light Metals and Alloys-Aluminum

Light Metals and Alloys-Aluminum I	TUE, Aug. 20	AM	Presidium Conference Room (4th Floor)	88
Light Metals and Alloys-Aluminum II	TUE, Aug. 20	PM	Presidium Conference Room (4th Floor)	156
Light Metals and Alloys-Aluminum III	WED, Aug. 21	AM	Presidium Conference Room (4th Floor)	235
Light Metals and Alloys-Aluminum IV	WED, Aug. 21	PM	Presidium Conference Room (4th Floor)	302
Light Metals and Alloys-Aluminum V	THU, Aug. 22	AM	Presidium Conference Room (4th Floor)	363
Light Metals and Alloys-Aluminum VI	THU, Aug. 22	PM	Presidium Conference Room (4th Floor)	397

C2. Light Metals and Alloys-Magnesium

Light Metals and Alloys-Magnesium I	TUE, Aug. 20	AM	Room 406 (4th Floor)	92
Light Metals and Alloys-Magnesium II	TUE, Aug. 20	PM	Room 406 (4th Floor)	160
Light Metals and Alloys-Magnesium III	WED, Aug. 21	AM	Room 406 (4th Floor)	239
Light Metals and Alloys-Magnesium IV	WED, Aug. 21	PM	Room 406 (4th Floor)	306
Light Metals and Alloys-Magnesium V	THU, Aug. 22	AM	Room 406 (4th Floor)	366

C3. Light Metals and Alloys-Titanium

Light Metals and Alloys-Titanium and Others I	TUE, Aug. 20	AM	Room 304 (3rd Floor)	96
Light Metals and Alloys-Titanium and Others II	TUE, Aug. 20	PM	Room 304 (3rd Floor)	165
Light Metals and Alloys-Titanium and Others III	THU, Aug. 22	AM	Room 304 (3rd Floor)	371

D. Advanced Processing of Materials

Advanced Processing of Materials I	MON, Aug. 19	PM	Room 208+209+210 (2nd Floor)	33
Advanced Processing of Materials II	TUE, Aug. 20	AM	Room 208+209+210 (2nd Floor)	99
Advanced Processing of Materials III	TUE, Aug. 20	PM	Room 208+209+210 (2nd Floor)	168
Advanced Processing of Materials IV	WED, Aug. 21	AM	International Reporting Hall (3rd Floor)	243
Advanced Processing of Materials V	WED, Aug. 21	PM	International Reporting Hall (3rd Floor)	312

E. Thin Films and Surface Engineering

Thin Films and Surface Engineering I	MON, Aug. 19	PM	Room 313 (3rd Floor)	36
Thin Films and Surface Engineering II	TUE, Aug. 20	AM	Room 313 (3rd Floor)	102
Thin Films and Surface Engineering III	TUE, Aug. 20	PM	Room 313 (3rd Floor)	173
Thin Films and Surface Engineering IV	WED, Aug. 21	AM	Room 312 (3rd Floor)	247

F. Biomaterials

Functional Biomaterials	MON, Aug. 19	PM	Room 306 (3rd Floor)	41
Biodegradable Magnesium Alloys	TUE, Aug. 20	AM	Room 306 (3rd Floor)	105
Surface Modification	TUE, Aug. 20	PM	Room 306 (3rd Floor)	177
Biomedical Titanium and Zirconium Alloys	WED, Aug. 21	AM	Room 306 (3rd Floor)	249
Interface	WED, Aug. 21	PM	Room 306 (3rd Floor)	317
Bioactive Materials	THU, Aug. 22	AM	Room 306 (3rd Floor)	374

G. Smart and Magnetic Materials

Permanent Magnetic Materials	MON, Aug. 19	PM	Room Yulan-220 (2nd Floor)	44
Permanent Magnetic Materials and Smart Materials	TUE, Aug. 20	AM	Room Yulan-220 (2nd Floor)	109
Permanent and Soft Magnetic Materials	TUE, Aug. 20	PM	Room Yulan-220 (2nd Floor)	181
Magnetocaloric and Elastocaloric Materials	WED, Aug. 21	AM	Room Yulan-220 (2nd Floor)	253
Shape Memory Materials	WED, Aug. 21	PM	Room Yulan-220 (2nd Floor)	320
Magnetostrictive Materials and Soft Magnetic Materials	THU, Aug. 22	AM	Room Yulan-220 (2nd Floor)	377

H. Materials Characterisation and Evaluation

Materials Characterisation and Evaluation I	MON, Aug. 19	PM	Room 308 (3rd Floor)	49
Materials Characterisation and Evaluation II	TUE, Aug. 20	AM	Room 308 (3rd Floor)	112
Materials Characterisation and Evaluation III	TUE, Aug. 20	PM	Room 308 (3rd Floor)	184

Materials Characterisation and Evaluation IV	WED, Aug. 21	AM	Room 308 (3rd Floor)	256
Materials Characterisation and Evaluation V	WED, Aug. 21	PM	Room 308 (3rd Floor)	323

I. Composite Materials

Composite Materials I	TUE, Aug. 20	AM	Room 307 (3rd Floor)	116
Composite Materials II	TUE, Aug. 20	PM	Room 307 (3rd Floor)	189
Composite Materials III	WED, Aug. 21	AM	Room 307 (3rd Floor)	260
Composite Materials IV	WED, Aug. 21	PM	Room 307 (3rd Floor)	328

J. Amorphous and High Entropy Alloys

Amorphous Alloys I	MON, Aug. 19	PM	Room 405 (4th Floor)	55
Amorphous Alloys II	TUE, Aug. 20	AM	Room 405 (4th Floor)	120
Amorphous Alloys III	TUE, Aug. 20	PM	Room 405 (4th Floor)	192
Amorphous Alloys IV	WED, Aug. 21	AM	Room 405 (4th Floor)	264
Amorphous Alloys V	WED, Aug. 21	PM	Room 405 (4th Floor)	331
High Entropy Alloys I	MON, Aug. 19	PM	Room 303 (3rd Floor)	59
High Entropy Alloys II	TUE, Aug. 20	AM	Room 303 (3rd Floor)	124
High Entropy Alloys III	TUE, Aug. 20	PM	Room 303 (3rd Floor)	197
High Entropy Alloys IV	WED, Aug. 21	AM	Room 303 (3rd Floor)	268

K. Nanocrystalline Materials, and Ultra-Fine Grained Materials

Nanocrystalline Materials, and Ultra-Fine Grained Materials I	MON, Aug. 19	PM	Room 309 (3rd Floor)	63
Nanocrystalline Materials, and Ultra-Fine Grained Materials II	TUE, Aug. 20	AM	Room 309 (3rd Floor)	128
Nanocrystalline Materials, and Ultra-Fine Grained Materials III	TUE, Aug. 20	PM	Room 309 (3rd Floor)	201
Nanocrystalline Materials, and Ultra-Fine Grained Materials IV	WED, Aug. 21	AM	Room 309 (3rd Floor)	271
Nanocrystalline Materials, and Ultra-Fine Grained Materials V	WED, Aug. 21	PM	Room 309 (3rd Floor)	336

Nanocrystalline Materials, and Ultra-Fine Grained Materials VI	THU, Aug. 22	AM	Room 309 (3rd Floor)	381

L. Computational Design and Simulation of Materials

Computational Design and Simulation of Materials I	MON, Aug. 19	PM	Room 204 (2nd Floor)	67
Computational Design and Simulation of Materials II	TUE, Aug. 20	AM	Room 204 (2nd Floor)	132
Computational Design and Simulation of Materials III	TUE, Aug. 20	PM	Room 204 (2nd Floor)	205
Computational Design and Simulation of Materials IV	WED, Aug. 21	AM	Room 204 (2nd Floor)	274
Computational Design and Simulation of Materials V	WED, Aug. 21	PM	Room 204 (2nd Floor)	339
Computational Design and Simulation of Materials VI	THU, Aug. 22	AM	Room 204 (2nd Floor)	385
Computational Design and Simulation of Materials VII	THU, Aug. 22	PM	Room 204 (2nd Floor)	401

M. Renewable Energy and Nuclear Materials

Renewable Energy and Nuclear Materials I	MON, Aug. 19	PM	Room 311 (3rd Floor)	70
Renewable Energy and Nuclear Materials II	TUE, Aug. 20	AM	Room 311 (3rd Floor)	135
Renewable Energy and Nuclear Materials III	TUE, Aug. 20	PM	Room 311 (3rd Floor)	209
Renewable Energy and Nuclear Materials IV	WED, Aug. 21	AM	Room 311 (3rd Floor)	277
Renewable Energy and Nuclear Materials V	WED, Aug. 21	PM	Room 311 (3rd Floor)	343

N. Additive Manufacturing and Powder Metallurgy

Powder Preparation & Simulation	MON, Aug. 19	PM	Room 402 (4th Floor)	74
Titanium & Titanium Alloy I	TUE, Aug. 20	AM	Room 402 (4th Floor)	139
Titanium & Titanium Alloy II	TUE, Aug. 20	PM	Room 402 (4th Floor)	212
Medium/High Entropy Alloy	WED, Aug. 21	AM	Room 402 (4th Floor)	280
Other Preparation Methods	WED, Aug. 21	AM	Room 313 (3rd Floor)	284
Materials Characterization & Properties	WED, Aug. 21	PM	Room 402 (4th Floor)	345
Composites	WED, Aug. 21	PM	Room 313 (3rd Floor)	351

Refractory Metal & Superalloy	THU, Aug. 22	AM	Room 402 (4th Floor)	388
Steel & Other Alloys	THU, Aug. 22	PM	Room 402 (4th Floor)	404

O. Electronic and Spin-Electronic Materials

Electronic and Spin-Electronic Materials I	MON, Aug. 19	PM	Room 312 (3rd Floor)	79
Electronic and Spin-Electronic Materials II	TUE, Aug. 20	AM	Room 312 (3rd Floor)	143
Electronic and Spin-Electronic Materials III	TUE, Aug. 20	PM	Room 312 (3rd Floor)	216
Electronic and Spin-Electronic Materials IV	WED, Aug. 21	AM	Room VIP (1st Floor)	288

P. Dynamic Behaviour of Materials

Dynamic Behaviour of Materials I	TUE, Aug. 20	AM	Room VIP (1st Floor)	146
Dynamic Behaviour of Materials II	TUE, Aug. 20	PM	Room VIP (1st Floor)	219

Posters

Poster Sessions	Aug. 19-21	PM	Exhibition Area (3rd Floor)	407

Events

ZEISS Workshop: Study Structure-Property Relations in Materials Using Analytical and In-Situ Microscopy Characterization Techniques	SUN, Aug. 18	PM	Room 305 (3rd Floor)
Big Data Intelligence and Knowledge Services Forum 2019 (I)	TUE, Aug. 20	AM	International Reporting Hall (3rd Floor)
Big Data Intelligence and Knowledge Services Forum 2019 (II)	TUE, Aug. 20	PM	International Reporting Hall (3rd Floor)
2nd China-Korea Symposium on Light Metals (I)	WED, Aug. 21	AM	Room 304 (3rd Floor)
2nd China-Korea Symposium on Light Metals (II)	WED, Aug. 21	PM	Room 304 (3rd Floor)

PRICM 10

Technical Program

Plenary Session

Monday AM | August 19, 2019
Room: Lily Hall of Golden Hall (1st Floor)

Chair:
Yafang Han, President, International Union of Materials Research Societies, China
Zhiling Tian, Central Iron & Steel Research Institute, China

8:30-8:50

Opening Remarks

Huibin Xu (Conference Chairman), Beihang University, China

8:50-9:30

Recent Progress in Space Materials Science and Technology

Bingbo Wei, Northwestern Polytechnical University, China

The extraordinary physical and chemical states of outer space provide a special environment to design, investigate and apply advanced materials. Owing to the continuous achievements of manned space flight programs, world-wide researchers have got rid of the narrow-minded and dubious privilege of microgravity. Instead, space materials science and technology is evolving into a vigorous cross-disciplinary research field. Almost all categories of typical materials, from aluminum through superalloys to semiconductors and even artificial bones, were taken into account for space experiments. This presentation tries to make a brief survey about the essential progress in the recent decade. Since China is greeting our era of space station in the years to come, both ground simulation study and space experiment design are conducted extensively. Although the keynote of such a field is still mainly for fundamental research, some promising application approaches from novel materials to creative techniques are proposed for discussion. With respect to the speaker's own work, both the space experiments of ternary eutectic growth on board China's Spacelab TG-II and the most up-to-date investigations on containerless rapid solidification of W-based refractory alloys are presented in detail.

9:30-10:10

High Entropy Alloy and Microstructure Design, Mechanical Properties, and Processing

Hyoung Seop Kim, POSTECH, Korea

Multi-principal element alloys also referred to as high-entropy alloys (HEAs), have attracted considerable attention due to their great potential with an endless playground for alloy design. Most of the HEA researchers have focused on the alloying effect, phase evolution, mechanical properties, and deformation behavior of HEAs developed based on intuition and incomplete thermodynamic database with microstructural and deformation theories. Also, few studies on processing, up-scaling, and applications have been tried so far. The successful development of HEAs and their industrial applications critically depend on processing and formability for industrial products as well as fundamental understanding. In this presentation, systematic approaches for new HEA design and microstructural optimization using sequential alloy selection and computer simulation approaches, such as molecular dynamics, finite element method, machine learning, and their integrations are introduced. For an excellent combination of tensile strength and ductility, multiple-stage deformation-induced phase transformation, as well as strong solid solution strengthening, was employed. The in-situ neutron diffraction studies make it clear that the martensite formation and the concurrent load partitioning between the fcc and the bcc phases play an important role in the increase in strength. This multiple mechanism strengthening results in heterogeneous microstructures, which can be optimized using machine learning. This result and optimization scheme underlines insights to provide expanded opportunities for the future development of HEAs for cryogenic applications. Lastly, the processability of the HEAs and its sheet formability are investigated using Erichsen testing, deep drawing testing, and hole expansion testing. Mechanical properties and microstructure characterization are investigated to obtain a basic understanding of the sheet formability and deformation behavior.

10:10-10:30 Tea Break

10:30-11:10

Understanding and Developing Nanostructured Materials with Requisite Properties and Stability

Kevin Hemker, Johns Hopkins University, United States

The focus on nanoscience has greatly advanced our ability to synthesize, characterize, and model nanomaterials with unprecedented physical and chemical properties that are derived from dimensional constraints. In applications where engineered comp-onents must withstand load, structural nanomaterials show clear promise owing to "smaller is stronger" trends. Dislocation activity in nanocrystalline metals is mitigated by the greatly reduced volume in which they can exist. Comparisons of experiments and molecular dynamics simulations have elucidated unique plasticity mechanism and highlighted the inherent mechanical and thermal instability of nanocrystalline metals. Challenges in bridging nano-to-mesoscale fabrication and microstructural instabilities present serious obstacles to the wide spread commercialization of structural nano materials.

Nanotwinned metals have received considerable attention in recent years to do their unique balance of properties. Nanotwinning has historically been observed in low stacking fault metals and alloys, and to date most studies have focused on nanotwinned Cu. Our recent observation of nanotwins in sputter deposited NiMoWfilms was unexpected, but subsequent characterization of this material indicates that the nanotwins underpin ultrahigh mechanical strength, extreme anisotropic plasticity, low electrical resistivity, low thermal expansion, and superior thermal and mechanical microstructural stability.

We have produced a compositional spread of solid solution NiMoW films, revealing ultrahigh strengths exceeding 3.5GPa and an exceptional balance of thermal, mechanical and physical properties due to the presence of nanotwins. We have further demonstrated the ability to shape and micromachine NiMoW metal MEMS cantilevers with the requisite dimensional precision and stability. To date, the vast majority of MEMS devices have been made of silicon, but NiMoW has the potential to supplant silicon in extreme MEMS applications. Thus, use of high temperature MEMS materials like nanotwinned NiMoW, that possess a balance of properties (e.g. high strength, electrical conductivity, dimensional stability and microscale manufacturability) well beyond what is possible with silicon, may pave the way for widespread digital monitoring and control and enable what is widely referred to as the Internet of Things (IoT).

11:10-11:50

Research and Development of Metallic Biomaterials for Inhibiting Stress-Shielding Between Implant and Bone

Mitsuo Niinomi, Tohoku University / Osaka University/ Meijo University/Nagoya University, Japan

In the very early stage of titanium usage for biomedical applications, only pure titanium and (alpha + beta)-type Ti-6Al-4V ELI were used. These materials are still widely used. However, V-free titanium alloys were developed in the 1980s when it was discovered that V is a harmful element for human beings. Then, when Al was also determined to be a harmful element, V- and Al- free titanium alloys were developed in the 1990s. V-free, and V- and Al-free titanium alloys for biomedical applications are all (alpha + beta)-type alloys. In the middle of the 1990s, researchers were focusing on the stress shielding problem between metallic implants and bone, which is the inhomogeneous stress transfer between implant and bone; bone resorption occurs because the stress is preferentially transferred through implants because they have higher Young's moduli than that of the bone. The research and development of beta-type titanium alloys compose of non-toxic and allergy-free elements with low Young's modulus were started in the 1980s, and are currently being continued; they are mostly Ti-Nb, Ti-Ta, Ti-Mo, Ti-Zr-beta stabilizing element based alloys. It was found in the case of the surgical operation of scoliosis diseases using spinal fixation devices that high Young's modulus of the rod, which is one of the parts of spinal fixation devices, is advantageous for surgeons because they need to bend it to fix spin with keeping bent shape, but the low Young's modulus of the rod is advantageous for patients. To satisfy these conflicting demands simultaneously, it should be possible to increase the Young's modulus of the bent parts of the rod via deformation at room temperature to introduce a deformation-induced secondary phase with high Young's modulus, while allowing the Young's modulus of the remainder of the rod to remain unchanged at a low Young's modulus. Then, the Young's modus changeable beta-type titanium alloys for biomedical applications, especially for spinal fixation rods were developed.

During research and development of the aforementioned beta-type titanium alloys, peculiar deformation behaviors were found in some low Young's modulus beta-type titanium alloys used for biomedical applications. In this case, mainly the effects of the non-toxic and allergy-free light weight interstitial element, oxygen (O) on the biological mechanical properties is highly interesting.

The research and development of beta-type titanium alloys composed of non-toxic and allergy-free elements with low Young's moduli for biomedical applications will be discussed. Then, the peculiar deformation behaviors found in some beta-type titanium alloys with low Young's moduli used for biomedical applications will be also discussed.

11:50-12:30

Finding the Atoms that Matter in Functional Materials

Joanne Etheridge, Monash University, Australia

In many materials, it can be a small subset of atoms that control the important properties of the whole. These are the atoms that matter! Finding them and identifying their role can be challenging. In modern transmission electron microscopes, electron wavefields can be focussed to a point less than an Ångström in diameter, providing a powerful tool with which to probe small volumes of matter. By tuning the incident probe and harvesting selected parts of the scattered signal, specific structural, chemical and/or electronic information can be obtained. This talk will give an overview of these methods. It will illustrate them with a range of applications to functional materials, such as crystal growth and shape control in metal nanoparticles; structure-property relationships in photoactive perovskites and III-V semiconducting quantum wells; Li-driven superlattices in Li-ion conductors; surface plasmon polaritons in metallic nanostructures; and 'imaging' the distribution of electrons as they scatter within an atomic lattice.

A. Advanced Steels and Processing: I

Symposium Organizers:

Han Dong, Shanghai University, China; Zhigang Yang,Tsinghua University, China; Yoshitaka Adachi, Nagoya University, Japan; Dong-Woo Suh, Pohang University of Science and Technology (POSTCEH), Korea; Christopher Hutchinson, Monash University, Australia; Amy Clarke, Colorado School of Mines, USA

Monday PM Room: 205+206+207(2nd Floor)
August 19, 2019 Symposium: A

Chairs:
Chengjia Shang, University of Science and Technology Beijing, China
Mattihias Militzer, The University of British Columbia, Canada

13:30-14:00 Keynote

Modelling of Heat Affected Zone Microstructures in Advanced Line Pipe Steels

Matthias Militzer, Nicolas Romualdi, Madhumanti Mandal, Warren Poole, The University of British Columbia, Canada

State-of-the-art line pipe steels are microalloyed low-carbon steels that combine high strength and fracture toughness with good weldability. The weld heat affected zone (HAZ) is a critical aspect for the integrity of pipelines as the HAZ experiences rapid thermal cycles resulting in a graded microstructure that can be significantly different from that of the as-hot rolled microstructure. In particular, intercritically annealed portions of the coarse grained HAZ (CGHAZ) are of concern as they may be particularly susceptible to crack propagation. Based on systematic experimental studies microstructure evolution models have been developed for selected line pipe grades to describe austenite formation, austenite grain growth, dissolution of NbC precipitates and the austenite decomposition kinetics into complex ferrite-bainite microstructures for HAZ thermal cycles. The models have been formulated using the state variable approach and have also been implemented into phase field simulations. The status of incorporating the role of steel chemistry into the models will be reviewed. Further, mechanical properties have been determined by tensile and Charpy testing. The ductile-brittle transition temperature increases significantly when an intercritical austenite film forms at prior austenite grain boundaries thereby confirming the higher risk of crack propagation in the intercritically reheated CGHAZ. An outlook is provided for integrating microstructure and property models.

14:00-14:20

Improving Strength of Cold-Drawing Steel Wire by Martensitic Transformation in 65Mn Steel

Junjie Sun, Yongning Liu, Xi'an Jiaotong University, China

Usually ultra-high strength steel wire can be produced by severe cold-drawing of high-carbon steel with pearlitic structure, but the strength improvement is heavily relying on the large plastic deformation. Therefore, it is difficult to make large-section steel wire with strength exceeding 2GPa by this method. For a 2mm diameter 65Mn steel wire with a cold-drawing strain of 1.7, the strength and elongation are about 1.8GPa and 6%, respectively. Here we report a new method to improve strength of steel wire by combination of cold-drawing and austenitizing followed by oil quenching and low temperature tempering. The above cold-drawing steel wire was heated at 780˚C for 9s and oil quenched to room temperature and subsequently tempered at 250˚C for 2h. The austenite grain size of the new process treated steel wire was refined to about 5.4μm, and the martensite substructure preferred to change from twin to dislocation by grain refinement, which renders the high-carbon steel wire both strong and tough, and the strength was improved from 1.8GPa to 2.4GPa while still maintaining 5% ductility. For the traditional oil quenched high-carbon steel wire, it has larger grains of 12～15μm and the martensite substructure contained many twins, and it is very brittle in low temperature tempered state, the plasticity can be improved by increasing tempering temperature but with much lose of strength. It’s worth mentioning that the tensile strength and ductility of the new method processed steel wire are comparable with that of existing maraging steels, such as C350, the highest strength in commercialized level, in which more than 20% precious alloy elements such as Co, Mo, Ni and Ti are contained, and the cost of our material is only about 1/50 of the C350. This may provide a new method to produce ultra-high strength steel wire in a simple and economic way.

14:20-14:40

The Investigation of Reheat-Cracking Susceptibility in Modified T23 Steel

Renyuan Zhou, Shixian Li, Lihui Zhu, School of Materials Science and Engineering Shanghai University, China; Guoli Zhai, Baoshan Iron & Steel Co., Ltd., China

T23 steel (2.25Cr-1Mo-1.6W-0.24V-0.05Nb) has been

widely used as water walls, superheater and reheater tubes in ultra-super critical (USC) power plants. However, the reheat-cracking susceptibility in T23 steel resulted in the bursting of the tubes and leaking of water walls, which hazarded the safety of USC power plants. Therefore, it is necessary to modify T23 steel in order to reduce reheat-cracking susceptibility. The hardness, tensile strength, impact toughness of modified T23 steel (2.64Cr-0.63Mo-0.44W-0.24V-0.02Nb) were measured, and the microstructure was systematically investigated by OM, SEM and TEM. Considering that reheat-cracking susceptibility is inter-granular cracking in coarse grain heat-affected zone (CGHAZ), Gleeble 3800 thermal simulator was used to simulate the CGHAZ in modified T23 steel via thermal simulation of welding, and its reheat-cracking susceptibility at high temperature was evaluated using isothermal slow strain rate tensile test at Gleeble 3800. The results showed that the mechanical properties of modified T23 steel meet the ASME standard. Moreover, the modified T23 steel exhibits an enhanced reheat-cracking susceptibility compared with T23 steel. Under tensile load at high temperature, it is not easy for the micro-voids and micro-cracks to form at the grain boundaries, which is related to the carbides and M/A constituents in the modified T23 steel.

14:40:15:00

Mechanical Properties and HIC Susceptibility of X80 Pipeline Steels with Low Manganese Addition

Qingyun Sha, Ansteel Group Corporation Limited, China; Dahang Li, Ansteel Iron and Steel Research Institute, China

In recent years, there are many studies about the pipeline steel with low manganese addition due to their superior resistance of hydrogen induced cracking (HIC). However, most steel grades in these studies are up to X70 grade and very few studies are about X80 pipeline steel with low manganese addition. In this investigation, an API X80 pipeline steel with low manganese addition has been developed for sour service application based on conventional high Mn X80 pipeline steel. The content of manganese in this investigation is less than 1.20% which is quite lower than that in conventional X80 pipeline steel. The mechanical properties, HIC susceptibility and microstructure of the steel were studied. Yield strength levels up to 595MPa, tensile strength levels up to 721MPa and toughness levels up to 100% of shear area at -15℃ for drop wear tear test (DWTT) were achieved while no HIC cracks were observed. The above mechanical properties and HIC susceptibility meet the minimum requirements of X80 pipeline steel. The microstructure predominantly consisted of acicular ferrite (AF) together with small amount of granular bainite (GB) and martensite/austenite (M/A) constituent. The microstructure also contained high dislocation density and dislocation substructure. Precipitates in different morphologies and size range were observed. Cuboidal precipitates are in the range of 70~100nm while 80~120nm for irregular precipitates, 30~70nm for spherical precipitates and 5~10nm for fine precipitates. The precipitates were characterized as (Nb,Ti) (C, N) and NbC. The lower HIC susceptibility for the X80 pipeline steel in this study is associated with the addition of copper, fine and uniform microstructure which results from alloy system design and strictly controlled processing condition in this study. The results indicate that the X80 pipeline steel with low manganese addition in this investigation is suitable for sour service application. Some suggestions are also given to improve the current study in the future.

15:00-15:20

Effecet of Shot Peening on the High-Temperature Steam Oxidation Behavior of Ferritic Heat-Resistant Steel

Kang Shen, *Wenhe Cai,* Xuexing Zhang, Shuangming Du, Shuqing Dong, Dawei Gao, Institute of Thermal Power Technology, China Datang Corparation Science and Technology Institute, China; Yin Bai, Institute for Special Steels, Central Iron and Steel Research Institute, China

In this paper, shot peening treatment was carried out at the inner wall of G115 which was a ferritic heat-resistant steel pipe, and the 650℃ high temperature steam oxidation behavior of P92 and G115 steel with and without shot peening was studied by using a high temperature steam oxidation test device. The peening layer and oxide layer were characterized by SEM, EBSD and other methods. The results show that the inner wall of G115 pipe treated by shot peening represented the characteristics of slip zone and cross slip, which was the strain layer caused by shot peening. Oxide stratification occurred in both P92 and G115 steel. The outermost layer was enriched in Fe, while the middle layer was enriched in Fe and Cr, and the innermost layer was inner oxide layer. The weight gain of G115 steel was far less than that of P92 steel at the same time of steam oxidation. The steam oxidation resistance of G115 steel was better than that of P92 steel while the content of Cr was roughly equivalent. The Cu rich phase precipitated at the interface of two layers of oxides which was an important reason for the difference of their oxidation properties. At the same oxidation time, the weight gain of G115 steel treated by shot peening was smaller than that of G115 steel without shot peening. Shot peening process could improve the steam oxidation resistance of G115 ferrite heat-resistant steel to some extent. For such a 9%Cr content G115 steel, the increased slip band, dislocation and martensite lath boundary caused

by shot peening provide a channel for the diffusion of Cr elements to the surface, and accelerate the diffusion rate of Cr elements to the surface in the matrix. The oxide of G115 steel formed rich Cr layer, and the steam oxidation resistance of G115 steel was improved.

15:20-15:40

Microstructure Characterization and Microhardness of ODS Eurofer Subject to Designed Heat Treatments

J. Fu, J. C. Brouwer, I. M. Richardson, M. J. M. Hermans, Delft University of Technology, Netherlands

Oxide dispersion strengthened (ODS) ferritic-martensitic steels are promising candidates for structural materials in advanced fusion and fission power plant due to good creep strength and radiation tolerance. ODS steels are usually produced by a powder metallurgy route involving mechanical alloying, consolidation and subsequent heat treatment. Hot isostatic pressing and hot extrusion are the most commonly used consolidation techniques. However, the processing times and costs are issues to be considered. The present work deals with ODS Eurofer steel fabricated by mechanical alloying and spark plasma sintering. A heat treatment route including normalizing and tempering was applied to the as-produced steel, based on differential scanning calorimetry (DSC) measurement. The microstructure was characterized by scanning electron microscopy (SEM). The results show that the condition of normalizing at 1150℃ for 1h and tempering at 700℃ for 1h is a suitable heat treatment route for the as-produced steel. The Vickers microhardness of the sample after the designed heat treatment is more uniform compared to the as-produced condition. The grain size distribution in the material is bimodal, with ultrafine grains and coarse grains formed in the microstructure, which is beneficial for the mechanical properties.

15:30-16:10 Tea Break

16:10-16:40 Keynote

A New Advanced Austenitic Heat-Resisting Steel with Nano-Size Phase (MX, Cu-Rich Phase , Nb CrN) Precipitation Strengthening for 630~650℃ USC Boiler Superheater / Reheater Application

Xishan Xie, University of Science and Technology Beijing, China

For raising thermal efficiency and decreasing CO_2 emission, China had constructed and put in service more than one hundred 600~620℃, 1000MW ultra supercritical (USC) electric power units in service. Recently China is also planning to develop 630~650℃ high efficiency USC power units. Up to now the routinely used austenitic heat resisting steels, such as TP347H, Super304H, and HR3C for 600~620℃ USC units can not meet the severe requirements of 630~650℃ high efficiency USC units. To fulfill this severe requirement China has developed and patented a new austenite heat resisting steel SP2215 (07Cr23Ni15Cu4NbN) which is based on 22Cr-15Ni with certain amount of Cu and also Nb and N for multiple nanosized phase (MX, Cu-rich phase and NbCrN) precipitation strengthening in Fe-Cr-Ni austenite matrix and M23C6 carbide precipitated at grain boundaries. This new austenitic steel characterizes with high stress rupture strengths (650, 105h >126MPa, 700℃, 105h>78MPa) and good oxidation /corrosion resistance . 650~700℃ long time aging till to 10,000hrs shows good structure stability without harmful phase formed. SP2215 austenitic heat resistant steel has been commercially produced for tube product form and recommended for superheater / reheater components of 630~650℃ high efficiency USC boiler application.

16:40-17:00

Influence of Alloying Elements in Low Transformation Temperature Filler Metals on Microstructure and Mechanical Properties

Doohyeon Kim, Youngchai Lee, Jae Hee Lee, Changhee Lee, Hanyang University, Korea

Welding process has been widely used in many industries such as shipbuilding, automobiles and railroads. However, due to the rapid thermal cycles during welding, the residual stress is generated in the weld region, which results in deformation of products and reduction of fatigue strength. To relieve the residual stress, various processes such as shot peening or post weld heat treatment are used, all these increase product cost and reduce price competitiveness. Recently, studies are underway of low transformation temperature (LTT) filler metals that control residual stresses of welds using volume expansion during transformation from austenite to martensite. Applying LTT filler metals has advantage in that it can control residual stress without changing welding techniques or replacing production facilities. In many previous studies on LTT filler metals, the residual stress is reduced by controlling the chemical composition to delay martensite transformation. In this study, the effect of alloying elements into martensite start (Ms) temperature and mechanical properties were analyzed. The compositions of LTT were designed to have various Ms temperature groups, and different

alloying element contents in each Ms temperature group. LTT filler metals were produced with a vacuum induction furnace and the Ms temperature and thermal expansion of phases were measured by dilatometry. Depending on the content of alloying elements, the volume expansion due to martensitic transformation including Ms temperature was changed, which affected the residual stress reduction. Butt-welding was performed using gas tungsten arc welding (GTAW) process to simulate weld joints. Actual residual stress measurement after welding was conducted by hole-drilling method, and a comparison was made between dilatometric behavior and actual residual stress. Microstructure analyses were carried out by SEM, XRD and TEM to determine the optimum Ms temperature and retained austenite fraction that effectively reduce the residual stress in welds. Mechanical properties of as-weld specimens were evaluated using hardness, tensile and charpy impact tests.

17:00-17:20

An Improved Methodology of Enhancing the Toughness of Coarse Grained Heat Affected Zone: the Significance of Stabilizing Austenite Grain

Xuelin Wang, Zhiquan Wang, Zhenjia Xie, Jingliang Wang, Shang Chengjia, University of Science and Technology Beijing, China

Coarse grained heat affected zone (CGHAZ) always exhibit the worst impact toughness because of the formation of undesirable microstructure during welding. Altering the heat input is by far the best way to obtain the optimum microstructure and good impact toughness in CGHAZ. However, the optimal heat input is often low, which is not conducive to improving the welding efficiency. Therefore, another feasible method is put forward in this paper, i.e., stabilizing prior austenite grain of CGHAZ by slightly extending the time of austenite homogenizing. The results indicated that extending the time of the sample holding at peak temperature from 1 to 3s can significantly improve the low temperature (-40˚C) impact toughness of CGHAZ, and its value can be increased from ~85 to 165J. The impact toughness was maintained at the level of ~150J by further prolonging the austenitizing time to 60s. The characterization of microstructure showed that the austenite grain size can be increased and homogenized by prolonging the holding time. The large austenite grain with high content of solid solution alloys and high hardenability could promote more crystallographic variants from different Bain groups, and thereby increasing the density of high angle grain boundaries, which is associated with block boundary with misorientation higher than 45° . Meanwhile, the combination with controlled inter-spacing of block boundaries by self-accommodation below the critical Griffith crack length, micro-crack can be arrested by these high angle grain boundaries thereby suppressed brittle fracture initiation and increased fracture properties.

17:20-17:40

Effect of Ni and Mn on the Mechanical Property and Corrosion Resistance of Duplex Stainless Steel Weldments

Youngchai Lee, Chang Min Lee, Doohyeon Kim, Changhee Lee, Hanyang University, Korea; Tae-Ho Lee, Korea Institute of Materials Science, Korea

The offshore industries require materials with combination of high mechanical strength and corrosion resistance since the environment in which it is used harsh and maintenance is limited. Duplex stainless steel (DSS), which has about half the Ni content than austenitic stainless steel, is in high demand due to its excellent mechanical strength and corrosion resistance. These good properties are attributed to the duplex structure, which consists of about same ratio of austenite and ferrite without undesirable precipitates or secondary phase such as sigma phase. However, during the welding process, the ferrite/austenite balance of the weldment is broken and nitrides and secondary phase are produced due to welding thermal cycle, which results in deterioration in mechanical property and corrosion resistance. In general, filler metal with about 2%~4%Ni added is used to maintain the ferrite/austenite ratio of the DSS weldment. In this study, filler metal for leanized DSS was investigated in which expensive elements such as Ni were reduced based on the commercial DSS2205. Leanized filler metal was fabricated using vacuum induction melting furnace and bead on plate welding was performed using GTAW in order to simulate welds. The phase ratio between ferrite and austenite as a changing of the alloying elements was measured using ferrite scope. In addition, microstructure analysis was performed using SEM and TEM. The elemental distribution of each phase were quantified using EPMA. Tensile strength tests and potentiodynamic polarization tests were carried out to clarifying the effect of alloying elements and microstructure change for mechanical properties and corrosion resistance. As the Ni and Mn increased, the ferrite content in weldment decreased, and the austenite stabilization effect of Ni was more than twice that of Mn. As the Mn increased, the difference in Mn content in ferrite and austenite was almost constant, but the difference in Ni content was increased as Ni increased.

B. High Temperature Structural Materials: Power Generation

Symposium Organizers:

Qiang Feng, University of Science and Technology Beijing, China; Shengkai Gong, Beihang University, China; Hyun Uk Hong, Changwon National University, Korea; Damon Kent, University of Sunshine Coast, Australia; Sammy Tin, Illinois Institute of Technology, USA; Hiroyuki Yasuda, Osaka University, Japan; Jun Zhang, Northwestern Polytechnical University, China

Monday PM
August 19, 2019

Room: 305 (3rd floor)
Symposium: B

Chair:
Qiang Feng, University of Science and Technology Beijing, China

13:30-13:35 Open Remarks

13:35-14:05 Keynote

A New Ni-base Superalloy GH750 for 700℃ Advanced Ultra-Supercritical Power Plant application

Xishan Xie[1]
1.University of Science and Technology Beijing,China

The world tendency of coal fired electrical power plant development is intended to reach high temperature up to 700˚C for raising thermal efficiency and decreasing CO_2 emission. A new Ni-based superalloy Ni-Cr-Co-Mo-W-V-Nb-Ti-Al-C-B-Zr-La named GH750 has been designed and produced as tube product to fulfill the 700˚C A-USC boiler application. GH750 is based on Ni-Cr-Co austenitic matrix for solid solution strengthening by addition of W and Mo and mainly strengthening γ'- Ni_3(Nb, Ti,Al) precipitation and combined with grain boundary carbide formation. The basic structure of GH750 after standard heat treatment is mainly about 15% γ' precipitated in γ-matrix and a certain amount of $M_{23}C_6$ carbide formed at grain boundaries. No any kind of harmful phases (such as Ni_3Ti type η phase, σ phase and other TCP phase) formed after 10,000 hrs long time aging in the temperature range of 700~800˚C. It shows excellent structure stability at high temperature application. Long time stress rupture strengths for 105h extrapolated by Larson Miller method at 700, 750 and 760˚C can reach 207MPa, 122MPa and 108MPa respectively. It clearly meet the requirement of 760˚C/105h stress rupture strength higher than 100MPa. GH750 not only characterizes with high stress rupture strength but also good long time stress rupture ductility, as example after 750˚C, 180MPa, stress rupture tests (longer than 15,000hrs), the elongation can keep in a high range of 15%~18%. The manufacturing performance of GH750 is excellent. It can be melted by VIM+ESR or VIM+VAR. Ingots are easy to forge, hot extrusion and cold rolling for required tube sizes. GH750 has been evaluated as a candidate A-USC superheater / reheater materials for 700˚C A-USC test loop in China.

14:05-14:25

Research on the Long-Term Microstructural Stability and Mechanical Properties Changes of Nickel-Base superalloys for 700℃ Advanced Ultra-Supercritical Power Plants

Shuangqun Zhao[1], Rui Fu[1], Yanfeng Wang[1]
1.Shanghai Power Equipment Research Institute, China

Ultra-supercritical coal-fired power generation technologies are developing worldwide for raising thermal efficiency and reduction of CO_2, SO_x and NO_x emission. The research and development of high strength nickel-base superalloys for key and high temperature components of advanced ultra-supercritical power units have been gaining remarkable progress during the past years. Several nickel-base superalloys, such as Haynes 282, Inconel alloy 740H, Nimonic 263 and alloy 617B, have been selected as the main candidate materials in the developing project of advanced ultra-supercritical power plants in the world and were expected to be applied as the boiler tube or pipe, steam turbine rotor or casing, etc. In order to get the results of microstructure evolution and mechanical properties changes of Haynes 282, Inconel alloy 740H, Nimonic 263 and alloy 617B in the proposed long-term service temperature range, these four nickel-base superalloys, and a Chinese new superalloy GH750 developed for boiler tube, were heat-treated at 700˚C ,760˚C and 800˚C for times up to 10000h, and its mcirostructural stability were examined by SEM, EDX and TEM. The experimental results show that the m phase forms in the alloy of Haynes 282 after aged at 760˚C and 800˚C for 3000h. In addition to the growth of γ' phase, no other phases form in samples of Inconel alloy 740H. The h phase forms in the alloy of Nimonic 263 after aged at 760˚C for 5000h and after aged at 800˚C for 3000h. The dense and uniform γ' particles precipitate in the sample of alloy 617B during aging at 700˚C. However, the quantity of γ' particles decreases obviously during aging at 760˚C and especially in 800˚C. Microstructure observation indicates that no harmful and brittle TCP phases were found in the specimens of GH750 after long term exposure at 700~850˚C except the coarsening of γ' particles. The test results of mechanical property show that the tensile strength keeps the high values and the impact ductility decreases firstly

and then keeps stable during long thermal exposure. Furthermore, the influence of the main elements of chemical composition on the phase stability for these five nickel-base superalloys was discussed according to the thermodynamic calculation results.

14:25-14:45

Influence of Lamellar Structure on Creep Property of Cellular Precipitating Ni-38Cr-3.8Al Alloy

Yoshihiko Koyanagi[1], Hiroyuki Takabayashi[1], Hiroyuki Yasudai[1]
1.Osaka University, Japan

Ni-Cr binary alloys containing high amount of Cr precipitate gamma/alpha-Cr lamellar structure by cellular precipitation(CP) reaction from grain boundary. The mechanism of CP reaction is caused by supersaturated Cr in gamma phase. Supersaturated Cr content influences on driving force for CP reaction and lamellar spacing. Moreover, the Ni based alloys with high Cr containing added Al significantly increase the hardness and strength due to very narrow lamellar structure. Al addition brings on Ni consumption in the matrix by precipitation of gamma prime. Therefore, Cr supersaturates dramatically in the matrix. The wrought Ni-38Cr-3.8Al (mass%), reaches extremely high tensile strength, which is over 2GPa, after aging treatment. Even though chemical composition of Ni-38Cr-3.8Al is simple, the microstructure is complex because it consists of gamma / alpha Cr lamellar structure with the gamma prime. In order to clarify the possibility for further applications at high temperature, it is necessary to understand the creep behavior. However, there is not enough the investigation of thermal stability of microstructure in Ni-Cr and Ni-Cr-Al system alloys. Therefore, stability of lamellar structure at high temperature creep properties and were investigated in Ni-38Cr-3.8Al. Thermal exposure test and creep test were performed at 600, 700 and 800℃. The lamellar structure is significantly influenced by the temperature during exposure. The lamellar structure began to collapse mainly at the grain boundary of prior gamma phase and lamellar colony boundary up to 700℃exposure. However, the lamellar structure rapidly collapsed at 800℃ exposure. The hardness was still high compared with conventional Ni-based alloys after exposure. Activation energy of creep was similar to pure-Ni or Ni-Cr binary alloys, even though most of lamellar structure was stable up to 700℃. Creep deformation predominantly generated in gamma phase which collapsed the lamellar structure during creep test. Therefore, it was verified that the creep property of Ni-38Cr-3.8Al is strongly influenced by the thermal stability of lamellar structures.

14:45-15:05

Tensile Deformation Mechanisms in a New Ni-Fe-Base Superalloy at 750℃

Peng Zhang[1], Yong Yuan[1], Yuefeng Gu[1], Jingbo Yan[1], Yingying Dang[1], Jintao Lu[1], Hongfei Yin[1], Jincheng Wang[1]
1.Xi'an Thermal Power Research Institute Co., Ltd., China

A new precipitation-hardened Ni-Fe-base superalloy HT700 containing around 20 vol.% of γ' precipitates has been developed, which is evaluated as a candidate material for 700℃ A-USC boiler tube application. After a standard heat treatment and subsequently thermal aging for 8220h at 750℃, the tensile behavior of HT700 is studied, and the evolution of dislocation structures with strain has been analyzed using transmission electron microscopy during tensile deformation at 750℃. It is found that contrary to previous findings widely reported in Ni-base superalloy used for multiple critical components in aero-engines and land-based gas turbine, the initial plastic deformation of the experimental alloy is achieved mainly by the climb and cross-slip of dislocations together with Orowan looping process when the average size of γ' precipitates is around 140nm. Additionally, the experimental observations reveal that as the tensile deformation proceeds, more and more a/2<110> matrix dislocations surround the same γ' precipitate, and stacking fault shearing also operates actively, which is rarely reported in the literature. Based on the experimental observations, it is deemed that the transition in the deformation mechanism with strain accounts for the variation of the flow stress with the strain. This study provides new insights into understanding the relationship between the operating deformation mechanisms and the deformation behavior of Ni-base/Ni-Fe-base superalloys.

15:05-15:25

New Generation of Cast & Wrought Superalloy for A-USC Boiler Application Beyond 700℃

Fei Sun[1], Furuhara Tadashi[1]
1.Tohoku University, Japan

The 700℃-class advanced ultra-supercritical (A-USC) boiler is a promising technology for new generation of high-efficiency coal-fired thermal power plants. A-USC technoloy will realize both higher thermal efficiency of coal-fired power plants and lower CO_2 emission to prevent global warming.
A new type cast & wrought Ni-Fe-based alloys with high strength and low cost has been developed recently. Considering the materials cost and workability for large component during application, high content Fe and

no Co element were added into Ni-based alloys. The strength of the Ni-Fe-based alloy is much higher than some other existing Ni-Fe-based alloys and even some Ni-based superalloys. The cost of the Ni-Fe-based alloy is almost one half of that of In740 alloy. This Ni-Fe-based alloys have been evaluated as candidate materials for 700˚C class A-USC boiler applications.

Creep property acts as one of the most important materials properties for boiler materials. After creep deformation at intermediate temperatures, microstructure analysis of the Ni-Fe-based alloys were performed by SEM, TEM and HRTEM-EDS. Alloying elements distribution behaviors were detected at nanoscale. Innovative deformation behaviors and strengthening mechanisms are presented that (i) double Orowan looping processes occurred in grain interiors, which could improve the creep strength more effectively, (ii) α-Cr precipitates formed and could act as effective obstacles to impede the dislocation gliding and thus increase the creep strength, and (iii) the coarsening γ' precipitates along grain boundaries contribute to strengthening the grain boundaries, resulting in the crack initiation and propagation in the relative soft region at the opposite side of the grain boundaries along the {111} slip planes. The results presented are helpful in providing a new approach to design and develop novel high-performance alloys for A-USC boiler applications.

15:25-16:10 Tea Break

16:10-16:30

Effects of Ti Addition on Mechanical Properties of RAFM steel

Soyoung Im[1], J O Moon[2], C H Lee[2], Hyun Uk Hong[1]
1.Changwon National University,Korea
2.Korea Institute of Materials Science, Korea

Reduced activation ferritic-martensitic (RAFM) steels are considered as structural materials for blanket module of nuclear fusion reactors because of their good thermo-physical properties with low activation capability, good high-temperature mechanical properties and long-life for nuclear applications. In this study, the effects of Ti addition on microstructure stability and mechanical properties of RAFM steel have been investigated. Ti addition of 0.01wt% to conventional Eurofer 97 steel was intended to promote fine MX precipitation in order to enhance microstructure stability and mechanical properties. As a result, the Ti-added RAFM (Ti-RAFM) steel showed excellent high temperature tensile and creep properties. Eurofer 97 steel and the Ti-RAFM steel showed 592h and 1823h of creep life, respectively, after creep test at 550˚C, 200MPa. From these results, excellent fatigue properties were also expected for the Ti-RAFM steel. Low cycle fatigue tests were therefore conducted under 550˚C, 0.0024s^{-1} with total strain amplitudes of 0.4%, 0.8% and 1.2%, respectively. Ti-RAFM steel surprisingly showed poor fatigue life of 2888, 720, 374 cycles in correspondence to each strain amplitude respectively, compared to Eurofer 97 steel with 3504, 1375, 502 cycles. This is thought to be related to the softening rate. Yield strength was higher in Ti-RAFM steel than in Eurofer 97 steel and stress reduction was also higher. In other words, it implies that resistance for recovery is very low. On the other hand, Creep-Fatigue Interaction (CFI) resembling the actual plasma on/off & operation conditions of the fusion reactor was conducted under 550˚C, 0.0024s^{-1}, $\Delta\varepsilon_t$=0.8%, tensile hold time = 600 sec. As a result, Eurofer 97 steel and Ti-RAFM steel showed 397 cycles and 578 cycles of life, respectively. Ti-RAFM steel therefore showed excellent properties in CFI compared to Eurofer 97 steel, indicating that creep is more effective in CFI. In conclusion, Ti addition effectively increases microstructure stability and mechanical properties of RAFM steels.

B. High Temperature Structural Materials: Intermetallics

Symposium Organizers:

Qiang Feng, University of Science and Technology Beijing, China; Shengkai Gong, Beihang University, China; Hyun Uk Hong, Changwon National University, Korea; Damon Kent, University of Sunshine Coast, Australia; Sammy Tin, Illinois Institute of Technology, USA; Hiroyuki Yasuda, Osaka University, Japan; Jun Zhang, Northwestern Polytechnical University, China

Monday PM
August 19, 2019

Room: Room VIP (1st Floor)
Symposium: B

Chairs:
Hiroyuki Yasuda, Osaka University, Japan
Yongwang Kang, AECC Beijing Institute of Aeronautical Materials, China

13:30-14:00 Keynote

Design Approaches and Properties of Novel Wrought TiAl Alloys for Jet Engine Applications

Masao Takeyama[1]
1.Tokyo Institute of Technology, Japan

A five-year National project of "Structural Materials for Innovation (SM4I)" in Cross-ministerial Strategic Innovation Promotion Program (SIP) in Japan starting from 2014 is coming to an end. In this project of SM4I, a focus is placed on innovative structural materials applicable to LPT and HPC blades for jet engines, where the author at Tokyo Tech has played a key role as a technical leader to develop novel TiAl alloys, in collaboration with Hokkaido University and industries (Kobe Steel, Ltd and IHI Co.). Tokyo Tech

has taken responsibility for alloy design based on phase diagram study and microstructure/mechanical property relationships. Hokkaido University has worked on oxidation behavior and mechanisms of the alloys proposed by Tokyo Tech. Kobe Steel is in charge of casting and recycling process technologies, and IHI is in charge of the blade fabrication and forming process technologies. Eventually, we have successfully developed novel TiAl alloys applicable at 1073K, with superior performance to the existing alloys.

It is needless to say that the reliable phase diagrams are extremely important for the alloy design but commercially available existing database (DB) for the phase diagram calculations are not reliable, so that we firstly built up our own thermodynamic DB in Ti-Al-M1-M2 multi-component systems, to reproduce experimentally determined phase diagrams, by optimizing the interaction parameters among the elements in the following each phase of β-Ti, α_2-Ti_3Al, α-Ti and γ-TiAl existing in the systems, with careful considerations of temperature, aluminum and M1/M2 concentration dependencies. The proposed alloys exhibit excellent hot workability even under faster strain rate of 10/s and with room temperature ductility of more than 1%. An introduction of bcc β phase and microstructure design using a unique phase transformation pathway of β+α→α→β+γ in the multi-component systems makes it possible to develop the alloys with excellent properties in both process and service temperatures. The detailed microstructure control method to obtain the excellent mechanical/chemical properties will be presented.

Part of this study was carried under the research of SIP in JST (Japan Science and Technology Agency).

14:00-14:20

Mechanical Properties of TiAl Alloys with Unique Layered Microstructure Fabricated by Electron Beam Melting

Ken Cho[1], Masahiro Sakata[1], Jong Yeong Oh[1], Hiroyuki Y Yasuda[1], Mitsuharu Todai[2], Ayako Ikeda[3], Minoru Ueda[4], Masao Takeyama[5], Takayoshi Nakano[1]

1. Osaka University, Japan
2.Institute of Niihama National College of Technology, Japan
3. Institute of Metal Research, Chinese Academy of Sciences, China
4. Technology Co., Ltd.,
5. Tokyo Institute of Technology, Japan

The specific strength of TiAl alloys is much higher than that of other high temperature materials such as Ni-based superalloys. Moreover, the alloys exhibit excellent high-temperature strength and good oxidation resistance. Therefore, the alloys have been used for low-pressure turbines for aircraft jet engine. Electron beam melting (EBM) is a new technology for additive manufacturing, which is able to fabricate 3D products with high degree of complexity by adding layer-on-layer of materials. This process has attracted much attention as a fabrication process for TiAl alloys because of its high energy density and low residual stress as compared to other additive manufacturing processes.

In this study, microstructure and mechanical properties such as tensile and fatigue properties of the TiAl cylindrical rods fabricated by EBM were investigated focusing on an angle (theta) between the building and cylinder directions. As a result, we found that it is possible to obtain unique layered microstructure consisting of duplex-like regions and equiaxed gamma grains regions (gamma bands) under optimum process parameters. This layered microstructure is formed by repeated thermal effect from the melting pool. Therefore, the layered microstructure is always aligned perpendicular to the building direction. In other words, it is possible to control orientation of the layered microstructure by changing angle theta. We also found that mechanical properties of the alloy rods with the layered microstructure is strongly dependent on the angle theta. The rods fabricated at theta = 45 deg shows approximately 4 times higher elongation at room temperature than those fabricated at theta = 0 deg. Moreover, the theta = 45 deg rods exhibit better fatigue strength at room and high (750˚C) temperature compared to casting alloys even without hot isostatic pressing process. These excellent mechanical properties of theta = 45 deg rods are attributed preferential deformation at gamma bands. These results indicate that the alloys with the unique layered microstructure have a great potential for aerospace applications.

14:20-14:40

Effect of Zr on Microstructure and Mechanical Properties of Nb-Si Based Multi-Element Alloys

Yongwang Kang[1], Fengwei Guo[1], Ming Li[1]

1. AECC Beijing Institute of Aeronautical Materials, China

Nb-Si based alloys have the attractive characters such as higher melting points(＞1750˚C), relatively lower densities(6.6~7.2g/cm^2) and excellent high-temperature strength in comparison with Ni based superalloys, which are greatly potential to serve in the condition with the temperature range of 1200~1400˚C as a family of ultrahigh temperature structural materials to replace Ni base superalloy for jet engines. Based on the previous development, the mechanical properties and oxidation resistance of Nb-Si based alloys have been improved greatly. However, its comprehensive properties still did not fit the demand of engines. In order to improve the comprehensive properties, the influences of Zr on the microstructures and mechanical properties of Nb-Ti-Si-Cr-Al-Hf-Mo and Nb-Ti-Si-Cr-Al-V based multi-element

materials were investigated.
We found that Zr segregated in silicide and was able to induce the formation of γ-Nb_5Si_3 phase, which would accelerate the phase transformation of γ-Nb_5Si_3 to α-Nb_5Si_3 and refine the microstructure with the increase of Zr content during the high temperature heat treatment. In addition, the room temperature (H.T.) fracture toughness and hardness of the heat-treated alloys are higher than those of as-cast alloys. For heat-treated alloys, the room temperature fracture toughness and the hardness were improved with the higher addition proportion of Zr.

14:40-15:00

Microstructural Evolution and Hardness of Rapidly Solidified Nb-Si Based Alloys

Yueling Guo[1], Lina Jia[1], Hui Peng[1], Zhang Hu[2]
1. Northwestern Polytechnical University, China
2. Beihang University, China

Nb-Si based alloys have shown great potential for future gas turbine and jet engine applications, because of their high melting temperatures (>1750℃) and attractive creep resistance. The overall performance of cast Nb-Si based alloys has been significantly improved in the past three decades, but the low fracture toughness and insufficient oxidation resistance still impose restrictions on their practical application, owing to the coarse and complex microstructures. Microstructural refinement achieved by rapid solidification is an effective method to improve the mechanical property and the oxidation resistance of materials, which had been scarcely reported for Nb-Si based alloys.
In this context, we employed electron beam surface melting (EBSM), a typical rapid solidification method, to refine the microstructures of Nb-18Si-24Ti-2Cr-2Al (at.%) alloys. Prior to scanning, in order to prevent the cracking of brittle Nb-Si based alloys, each original substrate was preheated to 1200℃ by the high-energy electron beam. To determine their microstructure stability at high temperatures, the present work also investigated the microstructural evolution of Nb-Si based alloys processed by EBSM and subsequent heat treatment.
Results showed that a crack-free remelted layer on the original alloy produced by vacuum induction melting (VIM), with a significantly refined microstructure, was created by EBSM treatment. The grain size of silicides ranged from 15 to 113μm for the VIM alloy, while it reduced to below 13μm in the remelted layer. The Nbss and α-Nb_5Si_3 phases in the VIM alloys were transformed into Nbss and Nb_3Si after EBSM upon rapid solidification. The eutectoid reaction of Nb_3Si→Nbss+α-Nb_5Si_3 was triggered by HT at 1200℃ for 5h. A higher HT temperature at 1450℃ for 5h not only enabled the completion of the eutectoid decomposition of Nb_3Si, but also promoted the growth and the coarsening of α-Nb_5Si_3 grains. The average hardness of the EBSM alloy was 829HV0.2 in the as-processed state, but reduced to 662HV0.2 and 578HV0.2, after the heat treatment at 1200℃ and 1450℃ for 5h, respectively.

15:00-16:10 Tea Break

16:10-16:35 Invited

Good Compatibility of Ultrahigh-Temperature Strength and Room-Temperature Fracture Toughness for MoSiBTiC Alloy

Kyosuke Yoshimi [1]
1. Tohoku University, Japan

Mo-Si-B-based alloys are promising candidates as ultrahigh temperature materials beyond Ni-based superalloys. Unfortunately, in general for structural materials, room-temperature fracture toughness comes at the expense of high-temperature strength, and the same is equally true of the Mo-Si-B based alloys. However, quite recently, the room-temperature fracture toughness of cast Mo-Si-B alloys has been well improved by TiC addition without impairing high-temperature strength. The TiC-added Mo-Si-B alloy, so-called MoSiBTiC alloy, shows a room-temperature fracture toughness value better than 17MPa$(m)^{1/2}$ after heat treatment and a heatproof temperature better than 1350℃ which is defined as the temperature given by the creep lifetime of 1000h under 137MPa. The good compatibility between ultrahigh-temperature strength and room-temperature fracture toughness is a big question for the MoSiBTiC alloy.
One possible mechanism responsible for the improved room-temperature fracture toughness is the ductile phase toughening with Mo solid solution (Moss). The volume fraction of Moss in the MoSiBTiC alloy is less than 50%, but Moss percolation in the microstructure is considerably improved compared with that in the ternary Mo-Si-B system. The microstructural improvement would come from the Mo/TiC eutectic reaction. The Mo/TiC eutectic reaction occurs at about 2175℃ as a second solidification step, which is much higher than those of other solidification reactions involving constituent phases such as Mo_5SiB_2 (T2) and Mo_2B as well as Moss and TiC. As a result, the Mo/TiC eutectic reaction appears to form the frame of the microstructure during solidification. This would be the reason why the Moss percolation is improved by the TiC addition.
The cast microstructure also largely affects tensile-creep behavior in the ultrahigh temperature region of 1400 ~1600℃. T2 formed during solidification has a plate-like shape on a several-tens micron scale. The plate surface is parallel to the (001) basal plane and the <100] directions of T2 preferentially grow along the cooling direction, and thus in a cast ingot, T2 has

a strong texture though Mo and TiC show randomly-oriented distribution. During creep, T2 plates largely rotate and Moss works as sticky ligament in the small-plate-reinforced metal-matrix composites. This would be the reason why the MoSiBTiC alloy shows excellent creep resistance. Therefore, the unique microstructure formed during solidification is considered as the key of the good compatibility between ultrahigh-temperature strength and room-temperature fracture toughness for the MoSiBTiC alloy.

16:35-16:55

Effect of Ti Content on Microstructure and Oxidation Resistance of MoSiBTi$_2$C alloys

Tomotaka Hatakeyama [1], Kyosuke Yoshimi[1]
1. Tohoku University, Japan

TiC added MoSiB alloy (MoSiBTiC alloy) has a great attention as a promising candidate for next generation ultra-high temperature materials. This alloy mainly consists with Mo solid solution (Moss), Mo_5SiB_2 (T2), as well as TiC phase and exhibits outstanding high-temperature strength, creep strength, and room-temperature fracture toughness, yet it has poor oxidation resistance at elevated temperature. Recently, we developed a MoSiB-Ti-TiC (MoSiBTi$_2$C) alloy consists with Moss, T2, TiC, and Ti_5Si_3 phase by the addition of 28% Ti and successfully reduced the density with improved oxidation resistance by keeping the mechanical properties. However, the oxidation resistance of the MoSiBTi$_2$C alloy is still insufficient especially at intermediate temperature for the practical applications. The poor oxidation resistance of MoSiBTiC alloys mainly result from the continuous sublimation of volatile Mo oxide (MoO_3), which disturbs the formation of continuous scales. In other words, the decline of activity of Mo in the alloy expected to improve the oxidation resistance. In this study, the increase in Ti concentration in MoSiBTi$_2$C alloy was investigated for further improvement of oxidation resistance.

(74-x)Mo-xTi-14Si-6C-6B (x=28 to 50, mol%) were prepared by conventional arc-melting and homogenized at 1600˚C for 24 hours in argon atmosphere. Microstructure were analyzed by means of X-ray diffraction (XRD), Scanning electron microscope (SEM), and Energy dispersive X-ray spectroscopy (SEM-EDX). Isothermal oxidation tests were carried out at 800, 1100, and 1200˚C for up to 100 hours. Oxidized samples were also analyzed by XRD, SEM, and SEM-EDX.

Microstructure of the alloys kept their original Moss-T2-Ti_5Si_3-TiC four phases even if Ti content reached 50mol%. According to the EDX analysis, Ti was distributed in all phases by substituting Mo-site. The weight loss by oxidation became smaller as Ti content increased and 50Ti alloy exhibited the best oxidation resistance at 800 to 1200˚C due to the formation of dense TiO_2 scale.

16:55-17:15

Microstructural Evolution During Ultrahigh-Temperature Tensile Creep of MoSiBTiC Alloy

Sojiro Uemura[1], Takateru Yamamuro[1], Kyosuke Yoshimi[2], Shiho Yamamoto Kamata[2], Shunichi Nakayama[2], Gunther Eggeler[3], Kouichi Maruyama[2], Sadahiro Tsurekawa[1]
1. Kumamoto University, Japan
2. Tohoku University, Japan
3. Ruhr-Universität Bochum, Japan

A MoSiBTiC alloy (65Mo-5Si-10Ti-10C(at.%)) has high potential for ultrahigh-temperature materials to replace Ni-base superalloys, because the alloy has a low density, a high creep resistance showing the rupture time of over 1000h under 137MPa at 1360˚C and a high fracture toughness over 15MPa(m)$^{1/2}$. The microstructure of the alloy is dominantly composed of the molybdenum solid solution (Moss), Mo_5SiB_2 (T2) and (Ti, Mo)C_x phases, in which the Moss phase would contribute to the good ductility and Mo_5SiB_2 and (Ti, Mo)C_x phases to high strength. In this study, we focused on the evolution of microstructure in the MoSiBTiC alloy during creep deformation at high temperatures.

Tensile creep test was conducted under 137MPa at 1500˚C in vacuum. Microstructure at creep strain of 0, 3, 12, 32, 53, 72% was observed by SEM, SEM-EBSD, TEM.

SEM observations revealed that the void formed at interface between Moss phase and other phases and the number of voids drastically increased just before the specimen was ruptured. SEM-EBSD and TEM observations revealed that the orientation dispersion and the KAM value of the Moss phase increased with increasing creep strain. In addition, fine (sub-) grains of dislocation free were formed due to the large Moss grains formed in cast ingots are divided, which suggested that dynamic recovery and recrystallization was occurred. The T2 phase, which has a plate shape of orientation (001) for the plate surface and <100] for side ones, rotated with increasing creep strain. The <100] strongly oriented the direction of the tensile axis and the plate surface of tensile specimen, and (001) oriented in the direction of the side of tensile specimen. Therefore, it is considered that the suppression for formation and concatenation of voids by the rotation of T2 phase and function of Moss phase like ligament is one of the reasons of MoSiBTiC alloy shows excellent high-temperature tensile creep resistance.

C. Plenary Session of Light Metals and Alloys

Symposium Organizers:

Baiqing Xiong, GRINM Group Co. Ltd., China; Xianhua Chen, Chongqing University, China; Yongqing Zhao, Northwest Institute for Nonferrous Metal Research, China; Yoshihito Kawamura, Kumamoto University, Japan; Young Min Kim,Korea Institute of Materials Science (KIMS), Korea; Jian-Feng Nie, Monash University, Australia; Diran Apelian, Worceste Polytechnic Institute, USA

Monday PM
August 19, 2019

Room: 406 (4th Floor)
Symposium: C

Chairs:
Yongqing Zhao, Northwest Institute for Nonferrous Metal Research, China
Alan Luo, The Ohio State University, USA

13:30-13:40

Opening Remark

Fusheng Pan, Chongqing University, China

13:40-14:10 Keynote

Advanced Light Metals and Processing: Alloy Development and Process Innovations

Alan Luo, The Ohio State University, United States

Advanced light metals (aluminum, magnesium and titanium alloys) are increasingly being used in the automotive, aerospace and consumer industries for weight reduction and structural efficiency. This talk will provide examples of designing and developing new lightweight metallic materials, including i) Al and Mg alloys for high-pressure die casting; ii) Mg alloys for extrusion and sheet applications; iii) Ti alloy for permanent mold casting; and iv) high-entropy alloys for solidification and powder-based processing. The talk will also summarize some of the latest process innovations in developing/optimizing casting, extrusion, sheet forming and multi-material manufacturing processes. Vacuum assisted high pressure die casting (HPDC) and super vacuum die casting (SVDC) processes are used to produce integrity and thin-wall Al and Mg die castings. A new setup including an induction skull melting (ISM) system, a gravity tilt-pour system, and a ceramic-coated steel mold has been developed to produce near-net-shape titanium castings, using low-cost permanent mold casting process. Improved extrusion, sheet and tube forming processes have been developed for Al and Mg alloys. While a single material cannot always meet all requirements of specific applications, multi-material systems often provide better solutions. Overcasting is a key enabling technology developed for multi-material structures where Al- and Mg-based light alloys can be cast around dissimilar material substrates. Integrated Computational Materials Engineering (ICME) is defined as the integration of materials information, captured in computational tools, with engineering product performance analysis and manufacturing-process simulation. This talk presents some examples of alloy development and advanced processing of light alloys using ICME tools. Advanced solidification and precipitation models for light alloys has been developed using computational thermodynamics and kinetics, combined with microstructure and process modeling techniques. These solidification and precipitation models are being integrated to predict location-specific mechanical properties, based on location-specific microstructure, of light alloy castings for structural applications. The future trends in lightweight multi-material structures and the research needs will also be discussed.

14:10-14:40 Keynote

Forming and Formability of Aluminium Sheet Alloys

Peidong Wu, Mechanical Engineering, McMaster University, Canada

There is considerable societal and government legislative pressure on the automotive producers to reduce the fuel consumption and exhaust gas emissions from vehicles. One of the most effective ways to achieve this is by the weight reduction that can be obtained by replacing steel with aluminum, magnesium or advanced high strength steel in the vehicle structure and body panels. However, these materials have a number of perceived and real technological limitations, the most significant of which is their reduced formability as compared with conventional steel. It is believed that this could be eliminated by the development of improved materials, or must be circumvented by the development of new application methods, so that they can be used effectively in the volume manufacturing of reduced weight automobiles. In the present lecture, we start with listing limits to sheet metal forming. We then very briefly summarize the past and current research projects aiming for understanding these limits. We proceed by demonstrating how crystal plasticity theory can be applied to study sheet metal formability. Finally, the effect of the cube texture on sheet metal formability is investigated as an example. It is found that, while the ideal cube texture decreases formability, a spread about cube significantly delays the initiation of localized necking when a sheet undergoes biaxial tension. The effect of the cube texture on the predicted Forming Limit Diagrams (FLDs) is discussed in terms of the sharpness of the yield locus near equi-biaxial tension.

14:40-15:10 Keynote

The Effect of Texture Anisotropy on the Dwell Fatigue Properties of Ti-6Al-4V Forged Bar

Kenichi Mori, Shotaro Hashimo, Mitsuo Miyahara, Nippon Steel Corporation, Japan

It is known that the fatigue life is significantly suppressed in α+β and near-α titanium alloys if the load is held at maximum value instead of continuously cycled. This failure mode occurring at room temperature to about 200˚C is known as cold dwell fatigue. Previous studies have pointed out the influence of microstructure, texture or MTR (Micro Texture Region) on crack initiation, propagation and characteristic facet formation in dwell fatigue. It is desired to clarify these damage mechanisms and establish a method to appropriately evaluate the dwell fatigue life. For that purpose, it is necessary to examine the damage accelerating mechanism including fatigue and creep interaction, with clarifying the influence of macro-texture and micro-texture.

The dwell fatigue behavior of Ti-6Al-4V forged round bar with highly textured, fine equiaxed microstructure was compared with that of cyclic fatigue and room-temperature creep. The influence of macro-texture was examined by setting the load direction as the axial direction (L-direction) or radial direction (T-direction) of the bar. Furthermore, the influence of micro-texture was examined by analyzing the fracture surface and cross section of the sample using SEM and EBSD.

The results of fatigue tests were summarized using the ratio of maximum stress to 0.2% proof stress (0.2%PS). The influence of the loading direction on the fatigue life was appeared only in the dwell fatigue. The fatigue life in T-direction was shorter than that in L-direction. In the range of 93%~95% of 0.2%PS, characteristic large facets and little striations were observed in the T-direction in dwell fatigue. As a result of detailed analysis, the coarse facets consisted of multiple initiation facets and propagation facets. Facet face and crack propagation direction of propagation facet corresponded almost to (0001) <10-10> of α phase.

15:10-15:40 Keynote

Review of Recent Research on Mg Alloys with Low Corrosion Rates

Andrej Atrens, Zhiming Shi, Matt Dargusch, Akif Soltan, The University of Queensland, Australia

Twenty years ago stainless Mg was a research goal, and this goal remains relevant today. Most research has studied Mg corrosion in aqueous solutions, particularly in concentrated chloride solutions, because these are expected to provide information relevant for the corrosion of Mg in auto applications and for aerospace usage. It should also however be noted that Mg alloy corrosion in the atmosphere can be much less, for example the atmospheric corrosion rate can be lower than the common aluminium alloys or steel. The main metallurgical factors controlling corrosion of Mg alloys in aggressive chloride environments were clear: (i) corrosion acceleration by micro-galvanic corrosion by second phases, including Fe-rich phases, (ii) improved protectiveness of the surface film on the alpha-Mg matrix by alloying, and (iii) decreased corrosion rate by microstructural refinement. These factors remain the metallurgical factors of importance for Mg corrosion. Over the last twenty years, there has been much research carried out with the aim of producing Mg alloys with low corrosion rates. The bench mark is the intrinsic corrosion rate of Mg of ~0.3mm/y in a concentrated chloride solution and in a synthetic body fluid like Hanks' solution. It should be mentioned that the corrosion mechanistic insights from the studies in concentrated chloride solutions are also relevant to the biocorrosion of Mg. This paper reviews the recent research on Mg alloy development and focusses on Mg alloys with low corrosion rates that are comparable to, or lower than, the benchmark of the intrinsic corrosion rate of high-purity Mg.

15:40-16:00 Tea Break

16:00-16:30 Keynote

Prediction of Bendability and Deep Drawability Based on Orientation Distribution Function for Polycrystalline Aluminum Alloy Sheets

Hirofumi Inoue, Osaka Prefectural University, Japan

Bendability and deep drawability of aluminum alloys are closely related to recrystallization textures of rolled and annealed sheets. It is necessary to quantitatively predict their in-plane anisotropies for improvement in sheet metal formability. A method for predicting the in-plane anisotrories of bendability and deep drawability on the basis of the average Taylor factor as a polycrystalline metal which can be calculated by using the orientation distribution function. The normalized Taylor factor, which means the average Taylor factor of a textured material devided by that of a non-oriented material, and the r-value were used as indicators of bendability and deep drawability, respectively. The predicted results from ideal orientations demonstrated that {001}<uv0> texture components such as a {001}<100> cube orientation showed excellent bendability and poor deep drawability, whereas {111}<uvw> texture components such as a {111}<110> orientation showed poor bendability and excellent deep drawability. It is estimated that {123}<634> orientation has poor bendability and the effect of the

r-value improvement is not so much as expected due to remarkable in-plane anisotropy. The predicted results for some commercial aluminum alloy sheets suggested that conventionally cold-rolled and annealed sheets consisting mainly of a {001}<100> cube orientation would be favorable to bendability, and that the addition of asymmetric warm rolling at a low reduction to cold rolled sheets would improve deep drawability in the annealed sheets with a {111}<110> orientation, which was formed by additional shear deformation of asymmetric warm rolling and then developed through recrystallization during solution treatment. In other words, it is important to control recrystallization textures according to sheet forming methods. The application of the {111}<110> component to inner panels of automobile bodies using T4-treated 6xxx series aluminum alloys can be expected in the future. In contrast, the conventionally cold-rolled and T4-treated 6xxx series aluminum alloys with the {001}<100> cube component seem to be suitable for outer panels which requires hemming in automobile bodies.

16:30-17:00 Keynote

Uncovering Deformation Mechanisms in Metastable Beta Titanium Alloys

Elena Pereloma, Ryan Naseri, Frank Niessen, Gilberto Casillas, David Mitchell, Azdiar Gazder, Ahmed Saleh, University of Wollongong, Australia; Dmytro Savvakin, Institute for Metal Physics, Australia

From aerospace to biomedical industries, metastable β-Ti (body centred cubic, bcc) alloys find wide applications due to their unique combination of strength and ductility. In these alloys, deformation is accommodated via stress-induced phase transformation and twinning along with slip. The relative activities of the operative deformation mechanisms depend on several factors including the stability of the β phase, loading path and deformation conditions (temperature and strain rate).

In the present ongoing research project, various in-situ and ex-situ experimental techniques are used to evaluate the effects of the β matrix stability, strain and loading path (tension, compression, cyclic tension-compression and bending) on the microstructure evolution and the associated deformation mechanisms in metastable β Ti-V-Fe-Al alloys. The matrix stability was manipulated by the formation of different volume fractions of α phase (hexagonal close packed, hcp) and the associated rejection of β-stabilisers back into the β matrix. The evolution of microstructures during in-situ mini-tensile tests in transmission electron microscope and during in-situ bending test in scanning electron microscope were followed. In-situ neutron diffraction during monotonic tension and cyclic tension-compression loading (±2% strain) of fully β microstructure was also carried out. The latter revealed a significant tension-compression asymmetry (with the maximum stress in compression always higher than tension) along with a pronounced strain recovery during unloading. The former is associated with easier α" martensite (orthorhombic) formation under tension than compression, whereas the latter suggests that either reverse transformation of α" martensite back to the β matrix or de-twinning could be occurring during load reversal. The neutron diffraction results were supported by ex-situ microstructure characterisation. The effects of β phase stability, strain and strain path were analysed and discussed.

17:00-17:30 Keynote

Plastic Deformation Behavior of Magnesium Single Crystals

Kwang Seon Shin, Seoul National University, Korea

Plastic deformation behavior of magnesium single crystals was examined in this study. Single crystals of pure magnesium and magnesium alloys were prepared by the Bridgeman method. Single crystal specimens with different orientations were deformed at various temperatures in order to determine the critical resolved shear stress (CRSS) values for various slip and twin modes. The deformed samples were examined with optical and scanning electron microscopy. The visco-plastic self-consistent (VPSC) simulation was carried out in order to obtain the CRSS and hardening parameters for various deformation modes, when multiple deformation modes were involved in plastic deformation due to the loading direction of a single crystal specimen. The change in crystal orientation due to plastic deformation and/or recrystallization was also examined.

Plastic deformation behavior of magnesium single crystals was examined in this study. Single crystals of pure magnesium and magnesium alloys were prepared by the Bridgeman method. Single crystal specimens with different orientations were deformed at various temperatures in order to determine the critical resolved shear stress (CRSS) values for various slip and twin modes. The deformed samples were examined with optical and scanning electron microscopy. The visco-plastic self-consistent (VPSC) simulation was carried out in order to obtain the CRSS and hardening parameters for various deformation modes, when multiple deformation modes were involved in plastic deformation due to the loading direction of a single crystal specimen. The change in crystal orientation due to plastic deformation and/or recrystallization was also examined.

D. Advanced Processing of Materials: I

Symposium Organizers:

Wanqi Jie, Northwestern Polytechnical University, China; Jianguo Li, Shanghai Jiaotong University, China; Hideyuki Yasuda, Kyoto University, Japan; Myoung-Gyu Lee, Seoul National University, Korea; Huijun Li, University of Wollongong, Australia; Dan Thoma, University of Wisconsin- Madison, USA

Monday PM
August 19, 2019

Room: 208+209+210 (2nd Floor)
Symposium: D

Chairs:
Glenn Daehn, The Ohio State University, USA
Young Suk Kim, Kyungpook National University, Korea

13:30-14:00 Keynote

Neutron Scattering - Novel Non-Destructive Tool for Characterization of Advanced Processing and Manufacturing

Anna Paradowska, Ulf Garbe, Mark Reid, ANSTO, Australia

Two neutron instruments: KOWARI and DINGO at The Australian Nuclear Science and Technology Organisation (ANSTO) at Lucas Heights, are vital non-destructive characterisation tools for modern advance manufacturing, engineering and life extension. The primary function of the KOWARI instrument is the determination of residual stresses and texture within the interior of bulk engineering components. Residual stresses induced in the fabrication of components may lead to distortion and significant loss of strength in a steel structure. Therefore, research on the residual stress distribution in complex components is becoming very important for manufacturing industry. Experimental measurements are essential to establish a quantitative understanding of the sign, magnitude and distribution of the residual stresses around the critical regions, within acceptable limit. DINGO is a neutron radiography/ tomography and imaging beamline often used to assessing defects and dimensional tolerance of internal features engineering components well suited for thick and complex's metallic and composite components. The instruments provide valuable information that could have direct impact on optimization of modern manufacturing processes in particular welding and additive manufacturing. They can also improve product reliability, enhanced design performance, reduced production cost, and extended life prediction on significant engineering assets (e.g. power-station utilities, gas pipelines, aircrafts, trains, etc.). This paper will focus on how the ANSTO team can assist welding and advanced processing/ manufacturing industry. Examples of resent industry driven collaboration projects will be highlighted.

14:00-14:25 Invited

Fracture of Austenitic Steel in Hot Forming Condition by Considering Grains Effect

Zhenshan Cui, Xiaoqing Shang, Haiming Zhang, Shanghai Jiao Tong University

Very large grains are often encountered in heavy forgings and lead to crack with different fracture behavior in the hot forming process. Austenite steel 316LN is a material that often used to manufacture the huge main pipe for nuclear power plant. Experiments and crystal plasticity finite element simulation were applied to this material to study the effect of grain size on the fracture behavior. The investigation demonstrated that the growth of inside voids depends on the microscopic non-uniform deformation induced by the mis-orientation of grains. Coarse grains result in severe strain concentration, leading to a wide variation of void growth. Based on the Rice-Tracey model, a modified void growth model was established by involving the grain size effect. For the hot deformation condition, the grain size evolution was characterized by dynamic recrystallization fraction. Experiments demonstrated that the fracture strain of 316LN depends linearly on the Zener-Hollomon parameter and dynamic recrystallization fraction. Assuming that the effect of stress triaxiality and Lode factor on the fracture is the same as in cold deformation, a damage model for hot working was established. The model was applied to a study of forging parameters of a head-shaped forging, and the tendency of crack initiation was predicted.

14:25-14:50 Invited

Principle and Application of Infrared Local Heating in Sheet Metal Forming Process

Eun-Ho Lee, Handong University, Korea

Since infrared (IR) heating technology has advantages of fast response, being clean, high power capability, easy to control, and high energy efficiency, some of industry fields have employed IR heating for heat treatment process. While home heating, soldering, and food industries actively have used IR heating technology, sheet metal forming industry has relatively few examples of infrared heating applications. This paper introduces IR heating and discusses the potential of IR heating application for sheet metal forming process in order to improve the formability and reduce springback. The first section of this work explains the principle of IR heating which is the cause of the advantages of IR heating. Application examples in other industries (food, home heating, and soldering) then are introduced to evaluate

the possibility of industrial application in the second section. In the third section, lab scale tests of IR heating for sheet metal forming are presented. Finally, industrial applications of IR heating for sheet metal forming are presented. The study on IR heating for sheet metal forming includes the thermal-mechanical simulation results as well as experiment results. Based on the experimental and simulation results, this work shows that IR heating technology has enough potential to be applied to sheet metal forming process.

14:50-15:10

Competition between Hydrogen Induced Hardening and Softening Effect for Hot Workability of Titanium Matrix Composites

Xuan Wang, Baifeng Luan, Chongqing University, China; Wang Liang, Su Yanqing, Harbin Insititute of Technology, China

The hot workability of titanium matrix composites was decided by microstructure of matrix alloy and distribution of reinforcements. In this paper, (TiB+TiC)/Ti-6Al-4V composites were in situ synthesized and hydrogenated by melt hydrogenation (melting alloys in gas mixture of hydrogen and argon). The distribution of ceramic particles in the composites with different hydrogen content showed that the distribution changed from homogeneous dispersion distribution to approximate network distribution as the hydrogen content increased. The main reason was that hydrogen caused overheat on the melt surface and activated the diffusion of atoms, which in turn increased the the growth rate of the primary β phase and leaded to the coarsening of grains. Results of high temperature compression showed that there was a competition between hydrogen induced hardening and softening effect. When the deformation was below 850℃, the hydrogen induced softening on the matrix was weak, and the network-like distribution of the ceramic particles increased the flow stress due to the grain boundary strengthening effect, and the hardening was the dominant effect. When the temperature was 850℃, hydrogen induced improvement on β-phase content, DRX and dislocation mobility, the stronger softening effect of hydrogen on the matrix reduced the flow stress of the composites, and the softening was the dominant effect. The dynamic material model was used to establish the constitutive equation for the high temperature deformation of composites. The calculated results showed that the thermal activation energy of the composites before and after hydrogenation was 339.65kJ/mol and 286.5kJ/mol, respectively. Hydrogen narrowed the destabilization zone during hot processing of composite, and expanded hot processing window and ideal deformation zone. The microstructure of deformed composites under same hydrogen content and deforming conditions were observed. After hydrogenation, the crushed ceramic particles distributed more homogeneoulty, which was mainly due to hydrogen increasing the high temperature flowing ability of matrix alloy. TEM and EBSD results on DRX, dislocations and phase content after hot deformation of composites showed that hydrogen slightly increased the β-phase content, significantly increased the DRX volume fraction, and increased the proportion of low-density dislocation regions.

15:10-15:30

Thixoextrusion of Mg-Al-Mn Magnesium Alloy

Qiang Chen, Zude Zhao, Hong Zhan, Southwest Technology and Engineering Research Institute, China; Baoguo Yuan, Hefei University of Technology, China

Thixoextrusion, which belongs to semisolid metal processing, is a relatively new method for extruding alloys in the semisolid condition to near net shaped products. As-cast AM60 magnesium alloy billet was subjected to hot extrusion. Experimental procedures are as follows: Direct chill semi-continuously cast AM60 magnesium alloy with an initial diameter of 360mm was subjected to hot extrusion at 380℃. The extrusion ratio was about 13. The liquid fraction-temperature relationship was obtained by a DSC analysis. Based on the DSC results, the solidus and liquidus temperatures for the extruded AM60 alloy were 545℃ and 621℃, respectively. Before partial remelting experiments, samples with dimensions 7mm×7mm×14mm were cut from the extruded bars. Samples were reheated at different temperatures for various holding times. When target holding time was arrived, samples were quickly quenched into ice water. The partial remelting process carried out in the condition of Ar atmosphere in order to prevent oxidation. For thixoextrusion, billets with size of ϕ100mm×60mm were machined from extruded bars. The billets were rapidly reheated to the target temperatures. The die applied to thixoextrusion was heated at 400℃ for holding 3h for avoiding shock chilling. When target parameters were reached, the billet was immediately subjected to thixoextrusion. Exerted pressure was about 40MPa. The evolution of the microstructures was analyzed by optical observation. Results show that during hot extrusion, fine and equiaxed grains were obtained due to dynamic recrystallisation. After reheating above the solidus, liquid firstly appeared at local grain boundaries. During partial remelting, with prolonged holding time and raising temperature, solid particles became more spheroidal and grew to some extent. Thixoextrusion for extruded AM60 alloy resulted in successfully filling the die. Under optimized parameters, the tensile strength, yield strength and elongation for AM60 alloy thixoextruded from starting material produced by the SIMA process are 307MPa, 226MPa and 12%, respectively.

15:30-16:10 Tea Break

16:10-16:35 Invited

Superior Mechanical Properties of Microalloyed Bainitic Steels Subjected to Warm Deformation

Kostryzhev Andrii, Carpenter Kristin, Chen Liang, Li Huijun, University of Wollongong, Australia

Global economy requires steel with further increasing mechanical properties and simultaneously decreasing price. In mass production three major ways can be taken to increase strength: increase microalloy additions (increases cost), decrease finish deformation temperature and/or increase cooling rate after high temperature processing (both can be challenging for equipment). Minimisation of deformation of casting semi-product is an effective way to reduce cost. However, mechanical properties can be missed due to insufficient microstructure development (in particular, too large grain size and sluggish precipitation of hard phases). In this work we investigate a recently proposed technology based on Austenite Conditioning followed by Accelerated Cooling and Warm Deformation (AC2WD). Two low carbon steels containing 0.095C-0.012Ti or 0.081C-0.1Mo-0.064Nb-0.021Ti (wt.%) were subjected to three processing routes with two (route A), one (route B) or no deformation (route C) of cast semi-product in the austenite temperature region, followed by quick cooling and finishing deformation in the bainite temperature region. The processing was carried out in Gleeble and included for route A: austenitising at 1250˚C, first deformation at 1100˚C to 0.35 strain, second deformation at 975˚C to 0.50 strain, cooling to 675˚C (temperature below *A*1 = 750˚C for the studied steels) at a cooling rate of 40˚C s^{-1}, third deformation at 675˚C to 0.25 strain, holding at 600˚C for 300s and slow cooling to room temperature. From route A the route B differed in the absence of deformation at 1100˚C, and the route C differed in the absence of both deformations at 1100˚C and 975˚C. Such processing schedules were designed to provide dynamic recrystallization (DRX) of austenite and retention of substructure in austenite (route A), absence of DRX but retention of austenite substructure (route B), and retention of cast microstructure due to absence of any austenite deformation (route C). For various austenite conditions the 0.095~0.012Ti and 0.081C-0.1Mo-0.064Nb-0.021Ti steels exhibited 680~770MPa and 800~950MPa of the yield stress, respectively, with simultaneously high elongation to failure in the range of 20%~30%. It is worth to highlight, that optimum parameters of austenite conditioning varied with steel composition. A detailed microstructural analysis of the studied steels was carried out using optical, scanning and transmission electron microscopy. The nature of strengthening mechanisms associated with the AC2WD technology is discussed.

16:35-17:00 Invited

Advanced Thermo-Mechanical Processing of HSLA Steels with Hierarchical Microstructures

Primig Sophie, Chakraborty Arnab, Pratiwi Hafsah I., Ledermueller, Carina, UNSW Sydney, Australia

Steels exert a profound impact on society, enabling innovations in transport, construction, mining, and beyond. Stronger steels enable mechanical designs with thinner sections achieving weight savings that confer environmental benefits in terms of emissions and fuel efficiency. Therefore, the overall aim of this research is to design a new steel processing technology that will simultaneously increase strength and ductility via multi-scale hierarchical microstructures of ultrafine grained ferrite decorated with nanoscale precipitates. Here, the approach is to overcome common challenges around low work hardening rates and delamination of ultrafine-grained mild steels via advanced thermo-mechanical processing (aTMP) of modern HSLA steels.
In our recent research on aTMP optimisation, we have studied the microstructural evolution during plane strain compression of modern Mo-Nb, Cr-Nb and Mo-Nb-Ti HSLA steels with Carbon contents of around 0.05wt.% in a Gleeble 3500 simulator followed by direct aging, supported by thermo-kinetic modelling using the software 'MatCalc'. A combination of electron channelling contrast imaging, electron backscatter and transmission Kikuchi diffraction, and transmission electron microscopy revealed a hierarchy of ultrafine grain sizes (mean diameter ~500nm), cementite (~150nm) decorating grain boundaries, and smaller Mo/Cr-Nb/Ti-rich precipitates (~15nm) on dislocation networks. The predominant mechanism behind grain refinement is continuous dynamic recrystallization, with initial grains subdividing into smaller crystallites confined by a mix of subgrain and high-angle grain boundaries with a characteristic ferrite rolling texture. However, in areas of Carbon segregation, particle stimulated nucleation seems to occur as a second mechanism, and the resulting grains are not only finer, but more randomly oriented and confined by high-angle grain boundaries mostly. The higher strengthening achieved by the latter mechanism suggests that future alloy optimisation should explore modern HSLA steels with increased Carbon contents.

17:00-17:25 Invited

A Combined Extrusion for a Drive Shaft with Spur Gear and Internal Spline: Process Design and Application

KuTae-Wan, Kang Beom-Soo, Pusan National University, Korea

A combined cold extrusion process for fabricating a

drive shaft with forward extruded spur gear geometry and backward forged internal spline structure is proposed in this study. The drive shaft is required to be about 92.0mm for the face width of the top land on the spur gear part and roughly 22.7mm for the groove depth of the internal spline section. Because it seems to experience excessive plastic deformation during the combined cold extrusion, a preform is adopted as an intermediate workpiece. AISI 1035 medium carbon steel bar with a diameter of 50.0mm and a length of 121.0mm is spheroidized and annealed in order to improve its mechanical properties and forgeability, thereafter, a series of uni-axial tensile and compression tests are performed so as to assess the mechanical properties of the raw and the heat-treated specimens. In the process design, the preform is designed using a volume apportioning scheme from the required target shape, thereafter, the initial round billet is outlined. Two shoulder angles of the preform and the drive shaft are considered to be the main geometric process parameters influencing the dimensional quality of the drive shaft. Three-dimensional finite element simulations are carried out in order to investigate the effects of each shoulder angle on the dimensional accuracy. Moreover, the cold forging loads are predicted so as to determine the proper forging press capacity required to actualize the preform and the drive shaft. With consideration of the results obtained from the numerical simulations, the tool components are prepared and applied to the preform forging and the combined extrusion experiments.

17:25-17:45

Effect of Deformation Conditions of Cyclic Rotating Bending Process on Microstructure and Mechanical Properties of Medium-Carbon Steel Tube

Zicheng Zhang, Northeastern University, China / The University of Tokyo, Japan; Tsuyoshi Furushima, The University of Tokyo, Japan; Ken-ichi Manabe, Tokyo Metropolitan University, Japan; Bin Li, Northeastern University, China

In the last several decades, with the development of the lightweight technology in the transportation machinery field, the solid parts of the transportation machine were gradually replaced by the hollow structures. To meet the strength and ductility requirements of the hollow structures used in the transportation machine, the tube for producing the hollow structures should have good strength as well as ductility. However, the steel tubes produced with conventional methods such as piercing, hot rolling, cold drawing etc. are often accompanied with coarse grains, uneven microstructure and poor mechanical properties. In this study, to investigate the effect of the deformation conditions of the CRB process on the microstructure and mechanical properties of the steel tube, the cyclic rotating bending process (CRB) of the seamless medium-carbon steel tube of STKM17C (JIS) were carried out with different deformation temperatures and bending angles. The microstructure of the processed tube by the CRB processes with different deformation conditions were investigated by the Optical Microscope (OM) and the Scanning Electronic Microscope (SEM) equipped with Electron Back-Scattered Diffraction (EBSD). The mechanical properties of processed tubes were studied by the conventional tensile test at room temperature. The results revealed that the microstructure refinement of steel tube was successfully realized with the CRB process. Recrystallization occurs when the deformation temperature was 600˚C. The grain refinement results in the improvement of the combination of strength and ductility. As a result, the tube with an average grain size of 5.86μm which also exhibited highly excellent ductility was successfully obtained with the CRB process with the deformation temperature of 700˚C, the bending angle of 172° , deformation time of 5min and the rotation speed of 20r/min. And the elongation and the strength-ductility balance of the processed tube is increased by 35% and 35.6%, respectively, compared to those of the tubes heat-treated with temperature of 700˚C for 5min. And the elongation and the strength-ductility balance of the processed tube increased by 77.4% and 23.7%, respectively, compared to those of the as-received tube.

E: Thin Films and Surface Engineering: I

Symposium Organizers :

Chuang Dong, Dalian University of Technology, China; Hongbo Guo, Beihang University, China; Hiroshi Masumoto, Tohoku University, Japan; Ho Won Jang, Seoul National University, Korea; Mingxing Zhang, University of Queensland, Australia

Monday PM
August 19, 2019

Room: 313 (3rd Floor)
Symposium: E

Chairs:
Robert Vassen, Forschungszentrum Jülich GmbH, Germany
Christopher Berndt, Swinburne University, Australia

13:30-14:00 Keynote

Engineered Surface Properties of Quasicrystalline Materials

Jean-Marie Dubois, Institut Jean Lamour / Institut Jean Lamour, France

Quasicrystals are crystals like others from a thermodynamics point of view. They grow through a peritectic reaction upon cooling a liquid alloy of the appropriate composition. They may also form surface coatings and thin films when processed with adequate

technologies. They order on the long distance, giving rise to sharp spots in diffraction experiments. Yet, the ordering scheme is different from the one in normal crystals because translational symmetry does not operate in conventional 3-dim space, but in higher dimensions. As a result, electron transport and more generally transport properties are by essence very different from what they are in classical metals, alloys and intermetallic compounds.

This characteristic leads to very different surface properties compared to normal crystals. The first and most important property is the surface energy, which is found significantly below the values inherent to the metallic constituents. From this on, other properties that are related to the surface energy like solid-solid adhesion and friction are also found much different from what they are in normal crystals.

The author studied those properties in close collaboration with Pr Esther Belin-Ferré (1939-2018) who measured partial densities of states in a wealth of sintered specimens and surface treated samples and the group of Pr Jackson Guedes de Lima (1948-2018) who dealt with HVOF coatings. The purpose of the conference will be to give a rapid account of the most salient results obtained in this frame and which appeared in the articles listed below. These topics are: friction and surface energy, wetting and surface energy, self-lubricating coatings made of quasicrystals, other applications if time allows.

14:00-14:25 Invited

Surface Severe Plastic Deformation for Improved Mechanical Properties and Optimum Reactivity

Thierry Grosdidier, Université de Lorraine, France

As failure is often initiated from the surface, surface treatments involving severe plastic deformation of the outer part of a work piece are being developed. Mechanical surface treatment techniques, deriving from the traditional pre-strain shot peening but involving much longer treatment durations, have been developed for which the shots are set in motion within a confined chamber and have a wide variety of incidence angles when colliding onto the surface. They are found in the literature under different names such as Surface Mechanical Attrition Treatment (SMAT) or Ultrasonic Shot Peening (USP).

While the effect of using cryonenic temperature (CT) has been used to reduce further the grain sizes on Cu or carbon steels, this presentation focusses on the effect of CT in metals susceptible to form martensite: the austenitic stainless steels. It will be shown that the use of cryogenic temperature did not increase the surface hardness significantly but greatly increased the subsurface hardness and, in some cases, changed the martensitic phase transformation sequences. Another new interesting aspect of surface modifications by applying SMAT will be demonstrated by the analysis of Ti-V-Cr alloys used for H-storage applications. While bulk SPD such as high pressure torsion did not allow H-storage reversion, the alloys that were mechanically activated by SMAT and processed a gradient microstructure could activate and store reversibly hydrogen.

14:25-14:50 Invited

Morphology, Structure and Mechanical Properties of Titanium Alloy Processed via Surface Severe Plastic Deformation

Yingang Liu, The University of Queensland, Australia

Titanium and titanium alloys are the advanced structural materials and widely used in aerospace engineering. The usage amount of titanium and titanium alloys in aeroengine is up to thirty percent of the components, such as the fans, compressor discs and blades. Therefore, service environment for titanium and titanium alloys is extremely harsh, including high temperature, high pressure, high rotational speed, friction, scour and so on. Fatigue failure of blades and fans in aeroengine has become the biggest difficulty which affects reliability of the aeroengine in practical application. Solving fatigue fracture of blades and fans in aeroengine has been determined to be the key technology of aeroengine. Surface strengthening and surface modification are the most economical and effective approaches to solve this key problem. Based on severe plastic deformation, manufacturing of gradient nanostructure with the grain size gradually changing from nanometer scale at the topmost surface to micrometre scale in the substrate materials is an effective approach to improve the mechanical performance of the components. Shot peening is a well-developed and widely-used surface mechanical treatment method to introduce compressive residual stress on the surface of metallic component in order to improve the fatigue life. In this research, high energy shot peening (HESP) driven by the computerized numerical control was adopted to fabricate gradient nanostructure in the surface layer of titanium alloy. The surface morphology, microstructure, fine structure, hardness and tensile properties of titanium alloy after HESP were examined in depth by means of 3D confocal microscopy, scanning electron microscope, electron back scattering diffraction, high-resolution transmission electron microscope, hardness tester and electronic universal testing machine. On this basis, the formation and evolution of nanostructure in titanium alloy were analysed. The results showed that gradient nanostructure was created in titanium alloy via HESP and the thickness of nanocrystalline layer was up to 40μm. Correspondingly, the increased hardness, enhanced strength and plasticity were achieved.

14:50-15:10

VO_2-Based Thermochromic Smart Glazing Coatings

Xun Cao, Hongjie Luo, Ping Jin, State Key Laboratory of High Performance Ceramics and Superfine Microstructure, Shanghai Institute of Ceramics, Chinese Academy of Sciences, China

Energy consumption has become an urgent issue not only for the global environment, but also for people's lives. Among total energy consumptions, buildings take nearly 30%. For buildings, energy exchange through windows accounts for over 50% by means of conduction, convection and radiation. To reduce energy consumption, we must develop new structures for glass surfaces to enhance their thermal insulation properties. Vanadium dioxide (VO_2) is the most well-known thermochromic material, which exhibits a notable optical change from transparent to reflecting in the infrared upon a semiconductor-to-metal phase transition. Thermochromic window coatings offer some possibilities to achieve energy efficiency in window. In this presentation, I will sort out the urgent problems and critical obstacles which we are facing on the present VO_2 research for smart window applications. First, the VO_2 films without impurity can be fabricated by different methods including sputtering deposition, sol-gel synthesis, and pulsed laser deposition. Second, it is a big challenge to get a high-quality VO_2 films with good performance of proper phase-change transition temperature, high visible luminance transmittance, high solar modulation ratio, as well as good durability at a relative low growth temperature. Third, the mechanism of the phase-transition behavior in VO_2 materials is also very interesting. Realizing control of properties of VO_2 by defects modulation is an efficient route for understanding the nature of phase-transition and developing novel functional devices for practical applications.

15:10-15:30

Contributed Surface Functionalization of 2D Materials for Flexible Low-Power Electronics

Qiong Peng, Jian Zhou, Zhimei Sun, Beihang University, China

Surface engineering plays an essential role in modulating the performance of 2D monolayer and heterostructure materials for electronic devices. Meanwhile, the mechanistic investigation on surface engineering from the atomic level is of great significance for the predictive design of advanced materials. Yet the understanding of the fundamental relationship between structure and performance is falling far behind the synthesis and empirical researches. Here, on the basis of first-principles calculations, we report that surface functionalization can not only effectively modulate nontrivial topological transitions in group-III monochalcogenides, but also controllably regulate Schottky barriers in metal-semiconductor heterostructures. For the fully O-functionalized GaSe monolayer, GaSeO, a novel quantum spin Hall state is revealed with a large bandgap of 178meV, in which the nontrivial band topology originates from the s-p band inversion in the crystal field. In addition, for 2D metal-semiconductor heterostructures composed of Nb_2CT_2 (T = OH, F, and O) MXenes and MoS_2, the Schottky barriers (SB) at the contact interfaces can be effectively modulated via appropriate functionalization of MXenes. Particularly, a n-type SB-free contact is available in $MoS_2/Nb_2C(OH)_2$ heterostructure and a different p-type Schottky contact is found in MoS_2/Nb_2CO_2 heterostructure, in which the controllable Schottky barriers are derived from the tunable metal work function induced by functionalized termination. Our work provides significantly mechanistic insights into the surface engineering on 2D materials for flexible low-power electronics.

15:30-16:10 Tea Break

16:10-16:40 Keynote

Atomic Layer Deposition Techniques: Electrocatalysts and Charge Transporting Layers

Hyunjung Shin, Sungkyunkwan University, Korea

Atomic layer deposition (ALD) is now being recognized as a powerful, general tool for modifying the surfaces of nanomaterials in applications for many renewable energy conversion devices. However, ALD involves slow processes particularly when it is subjected to nanoporous media with high-aspect ratios. A comparative study of the ALD coating onto two distinctive templates having nanopores, i.e., two- and three-dimensionally ordered media (DOM), of similar porosity and pore dimension. Comparison of the ALD coating profiles across the thickness of both templates reveals fundamentally distinct coating mechanism; while a uniform growth zone develops along the pores of the 2-DOM, a gradual decrease in the deposition is observed in those of the 3-DOM as ALD pulse time increases. The present model study helps universally predict the ALD behaviors into nanoporous media even with different types of pore connectivity.

ALD techniques are now utilizing in forming electrocatalytic as well as charge transporting layers for photo electrochemical and solar cells. Exposing edges of few layers of MoS_2 as efficient electrocatalysts can be formed by ALD in this study. CH3NH3PbI3 with perovskite crystal structure has attracted considerable interest for high power conversion efficiency (PCE, now certified 23.7%). ALD chemistry for TiO_2 and ZnO are well known and the process requires relatively low deposition temperature as low as ~ 100°C, which is applicable to deposit onto the halide perovskite layer.

In this presentation, highly efficient perovskite solar cells having a long-term stability that adapts uniform and dense inorganic charge transport layers grown by ALD are reported. The devices shows excellent water-resistant properties and long-term stability at 85˚C under illumination compared to devices without ETL grown by ALD.

16:40-17:05 Invited

ALD Enabled Synthesis of Nanostructured Materials and Its Applications

Se Hun Kwon, Pusan University, Korea

One-dimensional nanostructured materials such as nanodots, nanowires, nanotubes, nanorods, and nanobelts have attracted special attention because they possess unique structural one dimensionality and possible quantum confinement effects in two dimensions. As a result, they are expected to play an important role as building blocks in future nanoscale functional devices. Potential applications for these nanostructured materials have been expanded through the efforts of several researchers. To date, various approaches have been developed for the fabrication of various nanostructured materials such as hydrothermal synthesis, anodization of metal sheets, template-assisted growth, and seeded growth. Of these methods, the template-assisted approach combined with atomic layer deposition (ALD) has been distinguished from the others as a simple and well-controlled method. Because ALD is a vapor-phase non-line-of-sight deposition process, it can provide excellent control over the wall thickness of nanostructures at the sub-angstrom scale and can be used to create highly conformal coatings of dense inorganic film even on nano-sized templates with high aspect ratios.
Herein, highly ordered freestanding nanostructure arrays with atomic layer control of wall thickness were fabricated by a hybrid process of versatile nanoporous template and ALD. The ultrafine thickness tunability of the ALD process made it possible to develop functional nanostructures with various wall thicknesses. In addition, various ALD processed metal and oxides enalbed us to creat various functionality, which is useful for various advanced applications. In this presentation, we will discuss some recent examples and emerging application areas.

17:05-17:30 Invited

Wafer-Scale Growth and Assembly of 2D Semiconductors

Kibum Kang, KAIST, Korea

High-performance semiconducting films with precisely engineered thicknesses and compositions are essential for developing next generation electronic devices, which are becoming more integrated, complex, and multifunctional. My talk will introduce the novel processes that enable atomic-scale control of the thickness and spatial composition of semiconducting films on the wafer-scale. These processes include: (i) the wafer-scale generation of monolayer van der Waals semiconductors such as transition metal dichalcogenides (TMDCs) via metal-organic chemical vapor deposition (MOCVD), (ii) the atomic-level engineering of vertical thickness and composition through the layer-by-layer assembly of TMDC monolayers, and (iii) the transfer of atomically engineered films, using their van der Waals nature, onto arbitrary substrates. These capabilities provide a new material platform for both fundamental research and practical applications, including incorporation into existing integrated circuit technology to form hybrid materials (i.e. TMDC/CMOS) and boost electrical and optical functionality.

17:30-17:50

The New Application of Traditional DC Pulsed Magnetron Sputtering Technique on Deposition of Film with Preferred Orientation

Wanyu Ding, Zhixuan Lv, Weichao Chen, Dalian Jiaotong University, China; Jindong Liu, Dalian Jiaotong University, China / Jilin Institute of Chemical Technology, China

The traditional DC pulsed magnetron sputtering technique has been widely used in the field of film deposition. In general, the film deposited by traditional DC pulsed magnetron sputtering technique displays amorphous structure or crystal structure without preferred orientation. Actually, for some special film, such as TiO_2 film, ITO film, and so on, the different lattice plane could display the different property. So, it is interesting to prepare film with some special preferred orientation, such as anatase TiO_2 film with (001) preferred orientation, bcc bixbyite ITO film with (100) preferred orientation. This presentation introduces the new application of traditional DC pulsed magnetron sputtering technique on deposition of TiO_2 and ITO film film with preferred orientation, as well as the special application of TiO_2 and ITO film with preferred orientation.
Firstly, the traditional DC pulsed magnetron sputtering technique was used to prepare anatase TiO_2 film with (001) preferred orientation. With lower sputtering power density, the deposited TiO_2 film was amorphous structure with nano-size anatase crystal nucleus. After annealing treatment, anatase TiO_2 film displays (001) preferred orientation. In case of anatase TiO_2 films with (001) preferred orientation, during N ion beam bombardment process, the stable structure for implanted N was to bond with two 2-fold O at outer layer of (001) surface and one 5-fold Ti at sublayers of (001) surface, for both

substitutional and interstitial doping N. On the contrary, the stable structure for implanted N was to bond with one 2-fold O and two 5-fold Ti at (101) surface for both substitutional and interstitial doping N. With same N ion beam bombardment process, anatase TiO_2 films with (001) preferred orientation could effectively improve the formation of N-Ti bond.

Secondly, the traditional direct current pulsed magnetron sputtering technology was used to prepare ITO film. In case of the sputtering power density higher than critical point, parts kinetic energy of incident particles was transformed as the crystal energy in ITO crystal lattices, which worked for the growth of ITO grains along the certain direction. Besides, the incident In-O and Sn-O group should be considered, which resulted in the growth ratio along normal direction of film surface was much higher than those of parallel to film surface. For this reason, ITO columnar crystalline gains were formed and ITO film displayed (100) preferred orientation. ITO film with (100) preferred orientation displays the satisfactory optical and electrical properties, respectively. In case low energy methyl cation beam bombardment process, ITO film with (100) preferred orientation could effectively restrain the diffusion of methyl cation.

17:50-18:10

Novel Methods for Thin Film Thickness Measurements and Chemical State Analysis

Wenbing Yun, Sylvia Lewis, Benjamin Stripe, Xiaolin Yang, SH Lau, Srivatsan Seshdri, Ruimin Qiao, Sigray Inc., USA

Driven by device scaling and new materials, the non-destructive precise metrology of ultrathin films and elemental dose measurement with high spatial resolution and high throughput is desired capability for semiconductor IC manufacturing and nanotechnology research. Current challenges for such metrology include: non-destructive capabilities for buried layers, thickness measurements on 3D structures, and sufficiently high sensitivities to detect sub-Angstrom equivalent thicknesses.

Here we present three major x-ray characterization systems enabled by patented new innovations in the x-ray source and x-ray optic technology. The first system, the AttoMap micro X-ray fluorescence (microXRF) system, provides down to 0.1A equivalent film thickness measurements for dopants and can achieve accuracy better than 1% within seconds. The second system, the QuantumLeap X-ray absorption spectroscopy (XAS) system, enables chemical information on microns-thick films such as oxidation states and chemical bond lengths.

We will first review the AttoMap's intrinsic advantages for thin film measurements, including nondestructive, non-contact, ultrahigh trace level sensitivity, and high precision, and high spatial resolution for thin films and 3D IC structures. The system achieves spatial resolution at 10~40 micrometers. Examples, including demonstrations of sensitivity for 0.1A equivalent film thickness will be shown, in addition to the system's linearity and accuracy characterization. Because it can be used in ambient pressure, this non-destructive technique can be used as a complementary upstream technique to SIMS or FIB-SEM to identify regions of interest.

Recent results from the QuantumLeap XAS will furthermore be reviewed. The QuantumLeap is the first laboratory, non-synchrotron X-ray absorption spectroscopy system with sub-eV resolution and 100 μm spatial resolution. The system achieves fingerprinting measurements of samples down to seconds and has demonstrated advantages for catalyst characterization.

The final is a new design for X-ray photoelectron spectroscopy (XPS) enabled by an ultrahigh brightness, multi-energy X-ray source for depth-dependent characterization of interfaces and of hydrated interfaces.

18:10-18:30

(B,Al)-(C,Si)-Mg Amorphous Thin-Film Materials Designed Using the Cluster-Plus-Glue-Atom Model

Yanping Ma, Dalian University of Technology/Hainan University, China; Xuyang Zhou, Aimin Wu, Chuang Dong, Dalian University of Technology, China

According to the cluster-plus-glue-atom model developed for amorphous metals, an ideal metallic glass with a high glass forming ability always satisfies the [cluster](glue atom)1 or 3 composition formulas, where the cluster is a coordination polyhedron from a devitrification phase, and each unit cluster formula contains nearly 24 valence electrons (Han et al. Acta Mat. 2012). The hardness at this specific composition also reaches the maximum. In the present work, we applied this new composition design method in developing superhard amorphous boride (B,Al)-(C,Si)-Mg thin film materials. Relevant ideal amorphous composition formulas were reached using clusters from superhard phases AlB14Mg and B12C2Mg. Then magnetron sputtering was employed to synthesize the thin films. It was shown that the thin films satisfying the ideal cluster formulas and the 24-electron criterion did present hardness extremes, thus pointing to a new route towards designing superhard ceramic film materials with superior comprehensive properties.

F. Biomaterials: Functional Biomaterials

Symposium Organizers:

Yufeng Zheng, Peking University, China; Luning Wang, University of Science and Technology Beijing, China; Takayoshi Nakano, Osaka University, Japan; Seung-Kyun Kang, Korea Advanced Institute of Science and Technology (KAIST), Korea; Cuie Wen, RMIT University, Australia; Marc Meyers, University of California, San Diego, USA

Monday PM
August 19, 2019

Room: 306 (3rd Floor)
Symposium: F

Chairs:
Luning Wang, University of Science and Technology Beijing, China
Takayoshi Nakano, Osaka University, Japan

13:30-14:00 Keynote

Targeting Early Inflammatory Response for the Design of Functional Bone Biomaterials

Xiao, Yin, Queensland University of Technology, Australia / Australia-China Centre for Tissue Engineering and Regenerative Medicine, Australia

Native tissue repair and regeneration are initiated by the infiltration of inflammatory cells, which not only scavenge the damaged tissues, but also regulate cytokines for stem cell recruitment and differentiation. Functional biomaterials are designed to enhance tissue regeneration by activation of stem cell differentiation, regulation of local tissue inflammatory reaction and angiogenesis. The early inflammation and immune cells influxes into the injury sites after the application of biomaterials are critical in the subsequent cascade of tissue healing processes. The unique biomaterials-inflammation microenvironment determines the outcome of tissue regeneration. Our current strategies on the development of functional biomaterials for skeleton tissue regeneration point out that manipulation of inflammatory cells, such as macrophages, polymorphonuclear neutrophils (PMNs), dendritic cells can significantly control the osteo-immune responses, leading to stem cell differentiation and bone regeneration.

14:00-14:25 Invited

Biologically Inspired Multi-Functional Composites

Kisailus, David, University of California at Riverside, America

There is an increasing need for the development of multifunctional lightweight materials with high strength and toughness. Natural systems have evolved efficient strategies, exemplified in the biological tissues of numerous animal and plant species, to synthesize and construct composites from a limited selection of available starting materials that often exhibit exceptional mechanical properties that are similar, and frequently superior to, mechanical properties exhibited by many engineering materials. These biological systems have accomplished this feat by establishing controlled synthesis and hierarchical assembly of nano-to micro-scaled building blocks. This controlled synthesis and assembly require organic that is used to transport mineral precursors to organic scaffolds, which not only precisely guide the formation and phase development of minerals, but also significantly improve the mechanical performance of otherwise brittle materials. However, Nature goes one step further, often producing materials with that display multi-functionality in order to provide organisms with a unique ecological advantage to ensure survival.

In this work, we investigate a variety of organisms that have taken advantage of hundreds of millions of years of evolutionary changes to derive structures, which are not only strong and tough, but also demonstrate multifunctional features dependent on the underlying organic-inorganic components. Specifically, we discuss (i) the hyper-mineralized combative dactyl club of the stomatopods, a group of highly aggressive marine crustaceans, (ii) the heavily crystallized radular teeth the chitons, a group of elongated mollusks that graze on hard substrates for algae. From the investigation of synthesis-structure-property relationships in these unique organisms, we are now developing and fabricating cost-effective and environmentally friendly multifunctional engineering composites with impact resistance and biologically inspired nanomaterials for energy conversion and storage.

14:25-14:50 Invited

Preferential Orientation of Collagen/Apatite as a Bone Quality Parameter and Biomedical Implant Design Based on the Bone Tissue Anisotropy

Takayoshi Nakano , Osaka University, Japan

It is known in the field of biomaterials science that crystallographic texture and orientation—long-range ordered arrangements of atoms, ions, and molecules—strongly dominate the mechanical and/or functional properties of materials like metals, ceramics, polymers, and their composites. The biological apatite crystal, for example, is a major inorganic component of bone that belongs to a hexagonal system, which normally has greater anisotropy than the cubic crystal.

In this study, the implants design such as artificial hip joint, dental implant and vertebral fusion cage which are suitable for the preferential orientation of apatite and the related collagen fiber in bone tissues was proposed. The apatite orientation based on collagen fiber is introduced

as a bone quality parameter to understand the anisotropy of the intrinsic and extrinsic properties of various bones. The degree of apatite c-axis orientation significantly changes and positively correlates with the mechanical parameter of bone in the regenerated bone and in other bones such as intact and pathological bones.

To arbitrarily control or enhance the mechanical properties during bone regeneration, artificial induction of the oriented apatite structure is effective. Artificial control of the apatite orientation has been tried on the basis of mainly two strategies: i) control of the principle stress and subsequent continuous stress transfer between host bone and metal implants by facilitating an adaptive response to change the degree of apatite orientation and ii) usage of anisotropically-patterned substrates to align bone forming osteoblasts for secreting an oriented extracellular matrix.

Future artificial implants are finally concluded be develop based on the control of the apatite/collagen arrangement for clinical use in the biomedical fields.

14:50-15:10

Bioinspired Functional Coatings Based on Marine Plants

Bin Wang, Shenzhen Institutes of Advanced Technology, Chinese Academy of Sciences, China; Miaomiao Cui, Shenzhen Institutes of Advanced Technology, Chinese Academy of Sciences, China / City University of Hong Kong, China

Polymeric coating has become a widely used protective means because of its low cost, simple construction technology and excellent protection performance. However, during its application, the corrosive ions will gradually reach the coating/metal interface as the water travels into the coating, causing corrosion reaction of the metal substrate. Effectively inhibiting the transmission of erosive ions is a key factor to improve the protective performance of coatings. Mangrove is one type of marine plants growing in tropical and subtropical intertidal zone, and its harsh growing environment is very similar to that of organic coatings serving in the marine environment. This paper studies the salt-secreting tissue-salt gland of mangrove in terms of developing bioinspired anticorrosion coatings, and uses ion exchange resin to modify the epoxy organic coating to fabricate bionic anti-corrosion coating with selective ion permeability. With the salt selective ability, bionic anti-corrosion coating can inhibit the transmission of corrosive ions to film/metal interface, and improve the protection ability of the metal. The results show that the salt gland of Ceriops tagal (perr.) C. B. Rob. (one species of mangrove) is distributed on the upper and lower surfaces of the leaves, and regulates the salt ions. The cationic coating and anionic coating prepared mimicking the salt gland function have selective permeability for Cl^- and Na^+, respectively. Using fourier transform infrared spectroscopy, it is found that the resin/coating interface in both coatings has good stability, ion selectivity of ion-coating and the stability of the resin/coating interfaces in coatings are the key factors to restrain the corrosive ion intrusion and delay the metal corrosion.

15:10-15:30

Novel Defense Mechanisms in the Armor of the Scales of the "Living Fossil" Coelacanth Fish

Haocheng Quan, Marc Meyers, University of California, San Diego, America; Wen Yang, University of California, San Diego, America / Lawrence Berkeley National Lab, America; Robert Ritchie, University of California, Berkeley, America / Lawrence Berkeley National Lab, America

The elasmoid scales are the prevailing type of fish scales which provide effective protection for most of living fish species today. Typically, the elasmoid scales have two layers macroscopically: the mineralized outer layer providing hardness to prevent penetration by predators' teeth and the collagenous inner providing deformability to improve damage-tolerance. All the well studied collagen layer of elasmoid scales exhibit an arrangement of the collagen fibrils that follows an orthogonal or twisted plywood structure (also called the "Bouligand-type" structure), which can accommodate the imparted deformation through fibrous lamellae rotation, fibril straining, and interfibrillar sliding. Here, we present a primitive type of elasmoid scale with a unique structure and deformation mechanisms. Such a primitive type of scale is from the "living fossil" coelacanth fish. Coelacanth is one of two living groups of lobe-finned fish which is regarded as the envolutionary missing link between aquatic creatures and terrestrial tetropods. We characterized the intricate and ingenious structure of their scales, that of bundled collagen fibrils which follow a unique form of a double twisted Bouligand-type pattern comprised of orthogonal bilayers embedded in a through-the-thickness collagenous matrix. Our tensile tests of intact and notched samples indicate that this fibrous hierarchical structure can not only accommodate the excessive deformation by delocalizing an imposed load and dissipating any excessive energy, but also can effectively arrest any local fractures, thereby enhancing the toughness of the scale both intrinsically and extrinsically. Various toughening mechanisms including crack deflection, fiber reorientation, twisting, stretching, delamination, and the deformation of fibrous matrix are identified by post-mortem scanning electron microscopy (SEM) observation under both in situ and ex situ loading. We also applied in situ synchrotron small-angle X-ray scattering (SAXS) techniques for real-time analysis of mechanical tensile tests on bulk scale samples to reveal the novel deformation and toughening mechanisms within the collagenous inner core in the scale of this ancient creature.

15:30-16:10 Tea Break

16:10-16:35 Invited

3D Tissue Processing Using Stimuli-Responsive Biomaterials

Masaya Yamamoto, Tohoku University, Japan

Stimuli-responsive biomaterials have been widely investigated not only as a drug carrier to enhance the efficacy of drugs in the body, but also as a material to be utilized for stem cell culture as a tunable substrate. The physicochemical properties of the stimuli-responsive biomaterials could be altered in response to an external stimulus without cytotoxicity, such as heat, light, magnetic field, chemical compounds. We designed stimuli-responsive biomaterials as a scaffold to be used for three dimensional (3D) tissue processing. In this presentation, I will introduce two types of hydrogel scaffolds with a stimulus-responsiveness to fabricate 3D tissue-like constructs in vitro.

One is a sugar-responsive hydrogel scaffold that has been developed as a sacrificial template to introduce a defined vascular channel structure into a collagen hydrogel. As a sugar-responsive hydrogel scaffold, m-aminophenylboronic acid (APBA) with the ability to bind a sugar molecule was introduced into gelatin, followed by being fabricated with a defined structure using a computer-controlled dispensing apparatus. The viscoelastic property of an aqueous solution of the APBA-introduced gelatin was investigated to optimize the fabrication of the sugar-responsive hydrogel scaffold. The sugar-responsive hydrogel scaffold with a vascular endothelial cell was placed into a collagen gel and removed from the collagen gel by adding sorbitol as a sugar molecule to transfer the attached vacular endothelial cells to the collagen gel. The resulting collagen hydrogel with a vascular channel structure could be utilized as a soft microfluidic device for disease researches. Sulfobetain-based polymeric nanoparticles with a thermo-responsiveness will be introduced as an intracellular carrier being capable of cell membrane translocation for anti-tumor drugs, and the permeability of the nanoparticles through vascular endothelial cells was investigated using the soft microfluidic device.

The other is an iron oxide nanoparticles-containing hydrogel as a magnetic responsive hydrogel scaffolds to be used for inducing spontaneous tubule formation of an epithelial cell in vitro. The epithelial tubule-like construct could function as a means to transplant cells with high bioactivities.

16:35-17:00 Invited

Photo-Inspired Antibacterial Biomaterials

Shuilin Wu, Tianjin University, China

Bacterial infections and the ensuing complications often result in the failure of implants used for repair or replacement of hard tissue; such infections are traditionally treated by systemic antibiotic therapy. However, the abuse of antibiotics has been reported to induce bacterial resistance and even multidrugresistant superbugs. Bacteria tend to colonize and adhere to medical devices such as medical implant by forming sessile multicellular communities known as biofilms, which can be the source of persistent chronic device-related infections. For example, Staphylococcus aureus (S. aureus) comprises up to two-thirds of all pathogens in orthopedic implant-related infections, and S. aureus biofilm can attach and persist on host tissues to cause local purulent infection or even other systemic inflammatory problems. Because of increased antibiotic resistance of bacteria and their efficient mutations to evade the host immune system, implant-related biofilms infections are difficult to be eliminated completely, and typically show recurring symptoms even after cycles of traditional antibiotic therapy, and associated with high mortality rates. In addition, once protective bacterial biofilms form on the surface of implants, antibiotic therapy have been reported to have poor outcome. The coating strategy is proposed to prevent implant-related bacterial infections because functionalized coatings can endow the implant materials with highly effective self-antibacterial efficacy. Our recent studies developed a series of photo-sensitive surface systems such as Graphene Oxide/Ag/Collagen, Tannic Acid/Fe^{3+}/Ag, black phosphorus nanosheets (BPSs)/poly (4-pyridonemethylstyrene) endoperoxide (PPMS-EPO), Chitosan/MoS_2, Ag@AgCl and so on, in which lights with different wavelengths can inspire the photocatalytic or/and photothermal properties of coatings to produce large amount of radical oxygen species (ROS) or hyperthermia through electron transition or oscillations during light irradiation. ROS and/or hyperthermia can kill the bacteria directly by damaging the bacterial membrane and the inside masses such as proteins and DNA, thus endowing the coatings with highly photodynamic and photothermal antibacterial ability. Sometimes, photothermal and photodynamic therapy for bacterial infection can be combined with each other or other techniques, thus exhibiting desirable synergistic effects for antibacterial therapy and tissue repair or reconstructions.

17:00-17:25 Invited

Transient Electronics

Sukwon Hwang, Korea University, Korea

An ultimate goal of a conventional silicon-based integrated system is its capability to last forever without any malfunction and physical deformation, in almost any practical uses. Recent works demonstrate a new class of silicon electronics that has the opposite

behavior -- it physically dissolves or disappears in water, environment or biofluids, in a controlled fashion, at predefined times or on demand and with programmed rates. For example, (i) a complete collection of transient electronic building blocks, including n- and p-channel silicon nanomembrane (NM) metal oxide field effect transistors (MOSFETs), and their integration into circuits that disappear or functionally transform, (ii) sensors of light, temperature and strain, each of which uses functional materials and formats common to those for the electronics, (iii) photovoltaic and inductive devices for power supply, (iv) experimentally validated, analytical models of transience, suitable as design tools for engineered behaviours and (v) integrated examples in wirelessly controlled, bio-resorbable devices that provide thermal therapy in an implantable form. This 'transient' technology opens up completely new application opportunities for electronic devices in areas, such as implantable medical devices that exist for medically useful timeframes but then dissolve and disappear completely by resorption into the body. Use scenarios range from integration with living hosts (human/animal/insect/plant; on-dwelling or in-dwelling) to indoor/outdoor environments such as buildings, roadways or materiel. Enabled devices include medical monitors that fully resorb when implanted into the human body ("bio-resorbable") to avoid adverse long-term effects, or environmental monitors that dissolve when exposed to water ("eco-resorbable") to eliminate the need for collection and recovery. Other concepts involve circuits that incorporate strategic regions with timed transience, to affect controlled transformation in function. This talk summarizes recent work on 'transient' technology, ranging from fundamental chemistry of the key materials, to development of various components and systems for biosensors, to in vivo toxicity tests for biocompatibility.

17:25-17:45

A Novel Antibacterial High-Strength Maraging Stainless Steel

Muhammad Babar Shahzad, Wei Wang, Yiyin Shan, Ke Yang, Institute of Metal Research, Chinese Academy of Sciences, China

The novel concept of antibacterial metals has been in spotlight in recent years, owing to unimpeded efforts to overcome certain barriers to pave its way from laboratory scope to diverse commercial applications. Bio-functioning of stainless steel concept relies on its alloying with copper element and appropriate heat treatment to endow it superb antibacterial property.
We devised a systemic experimental approach to develop a novel Cu-bearing high-strength maraging stainless steel by optimizing Cu-content, aging temperature and aging time to achieve superior mechanical properties, good corrosion resistance and novel antibacterial function. A range of techniques were employed for experimental characterization to find the role and effects of Cu-content, aging temperature and time on Cu-precipitation behavior, Cu ion-release, corrosion properties and antibacterial mechanism to refine the integrated performance of this new stainless steel for conventional and new applications.
An appropriate amount of copper addition into to maraging stainless provided a threefold advantage as Cu-rich phase improved its UTS (ultimate tensile strength), through precipitation strengthening, enhanced the corrosion resistance and endowed it with a novel antibacterial function. The novel antibacterial function of high strength maraging steel would enable it to use for certain medical applications, as well as provide it an excellent protection against MIC (microbiologically influenced corrosion) in the conventional structural applications.

G. Smart and Magnetic Materials: Permanent Magnetic Materials I

Symposium Organizers:

Shaoxiong Zhou, Center Iron & Steel Research Institute, China; Chengbao Jiang, Beihang University, China; Satoshi Sugimoto, Tohoku University, Japan; Haein Yim, Sookmyung Women's University, Korea; Sean Li, New South Wales, Australia; Bob Shull, National Institute of Standards and Technology, USA

Monday PM Room: Yulan Hall-220 (2nd Floor)
August 19, 2019 Symposium: G

Chairs:
Shiratsuchi Yu, Osaka University, Japan
Xiangyi Zhang, Yanshan University, China

13:30-14:00 Keynote

Designing Hybrid Nanostructures Towards High Energy Density

Xiangyi Zhang, Yanshan University, China

Hybrid nanostructures consisting of two or more functional components have recently attracted extensive attention and are emerging as hot research topic in energy-related fields, owing to their potential to yield enhanced or novel functional properties. However, bulk hybrid nanostructures that make strong permanent magnets are difficult to devise, because it has been proven very challenging to precisely control bulk complex nanostructures, especially aligning nanocrystals. This challenge has been considered as an engineering nightmare.
Through developing new fabrication principle and technologies, we have recently made breakthrough progress in engineering bulk hybrid nanomaterials with desired structures. The engineered layered,

multicomponent nanostructures comprising hard and soft-magnetic nanocrystals exhibit a record-high energy density for this class of nanocomposite magnets, with soft-magnetic fraction exceeding 20wt%. Such hybrid nanostructure outperforms its corresponding pure rare-earth magnet with ~75% enhancement in energy product. These findings open up new opportunities for creating high-performance permanent-magnet materials with reduced rare earths and for engineering next-generation permanent magnets.

14:00-14:30 Keynote

Current Status and Prospect of Ceramic Permanent Magnets

Sang-Im Yoo, Kang-Hyuk Lee, and Sung-Jun Choli, Seoul National University, Korea

M-type hexaferrties with the chemical formula of $MeFe_{12}O_{19}$ (Me=Ba, Sr) have been well known as ceramic permanent magnets. Their magnetic properties, including coercivity (BHc,), remanence (Br) and the maximum energy product (BH)max, have been improved in the order of BaM, SrM, (La, Sr)(Fe,Co)12-xO19, and (La, Ca)(Fe,Co)12-xO19, representing that the enhancement of the uniaxial magnetocrystalline anisotropy without degrading their saturation magnetization (Ms), leading to improved BHc, has been obtainable via a cation substitution for both Me^{2+} and Fe^{3+} sites. On the other hand, to achieve the c-axis alignment of each grain, the forming process under the applied magnetic field is essential, and to achieve high sintered density together with the suppression of grain growth, a small amount of additive should be used. In this talk, first, I will explain the progress in the improvement of intrinsic magnetic properties, including Ms and anisotropy field (Ha) through the cation substitution. Next, I will describe the important factors affecting the extrinsic properties, including BHc, Br, and (BH)max, for the system of La0.15Sr0.85Fe10.75Co0.15O19. Finally, I will discuss the prospect of higher-performance ceramic permanent magnets.

14:30-14:55 Invited

Local Demagnetization Processes in the Fractured Surface of a Nd-Fe-B Sintered Magnet: A Soft X-Ray Magnetic Circular Dichroism Spectromicroscopy Study

Kentaro Toyoki, David Billington, Hiroyuki Okazaki, Tetsuya Nakamura, Japan Synchrotron Radiation Research Institute, Japan / National Institute for Materials Science, Japan; Yoshinori Kotani, Japan Synchrotron Radiation Research Institute, Japan; Satoshi Hirosawa, National Institute for Materials Science, Japan

Understanding the demagnetization processes is the key to controlling the coercivity, which is crucial for permanent magnet. From this perspective, magnetic imaging plays an important role. However, conventional magnetic microscopes have limitations when applied to real systems, e.g. low applied fields, and fabrication to optically flat surfaces or transmittable thin films, in which magnetic domain structures are seriously affected. To bridge the gap to the realistic magnetization behavior, a scanning soft X-ray magnetic circular dichroism spectromicroscope with 100nm spatial resolution and high applied magnetic fields up to 8T was developed at BL25SU, SPring-8, and its usefulness was demonstrated in magnetic domain observations on fractured surfaces of a Nd-Fe-B magnet by showing that the grains maintained 90% of bulk coercivity.

Using this magnetic microscope, the fractured surface in Nd-Fe-B magnet were observed with stepwise fields. Some of local magnetization curves were displaced along the field-axis by as much as 0.2~0.3T. These large shifts were mostly observed in pairs of grains with shifts of opposite sign and likely originate from the following two processes: First, because of a thermal fluctuation, the order of magnetization reversal in pairs are stochastic and different in the descending and ascending branches. Second, once a grain has reversed, the antiparallelly-magnetized state is stabilized by the magneto-static coupling between the grains. These considerations suggest that the demagnetization process of sintered magnets is influenced not only by micromagnetic domain wall pinning and nucleation, but also by stochastic nature combined with long-range magneto-static interactions.

The authors thank Dr. T. Nishiuchi from Hitachi Metals, Ltd. for supplying the sample. Part of this work is supported by ESICMM under the outsourcing project of MEXT.

14:55-15:15

Microstructure and Magnetic Properties of Multi-Main-Phase Ce-Fe-B Spark Plasma Sintered Magnets by Dual Alloy Method

Qingzheng Jiang, Lunke He, Weikai Lei, Qingwen Zeng, Sajjad Ur Rehman, Lili Zhang, Renhui Liu, Jiajie Li, Shengcan Ma, Zhenchen Zhong, Jiangxi University of Science and Technology, China

Much demanded and overused are the critical rare earth elements such as Pr, Nd, Dy and Tb with increasing need of Nd-Fe-B-type rare earth permanent magnets in the world. The soaring price of these four critical rare earth elements and the roller-coaster-type price fluctuation in rare earth raw materials in general have caused a considerable pressure on the Nd-Fe-B manufacturing industry and instability in their downstream applications. However, the most abundant rare earth element Cerium (Ce) is overstock and the utilization efficiency is very low

for a long time. So, it is quite important and necessary to do research and develop Ce-containing permanent magnetic materials with higher ratio of performance over cost for national strategic security and the reduction of the costs of raw materials.

Ce-Fe-B spark plasma sintered (SPSed) magnets prepared with different ratio of alloys of Ce-Fe-B and Pr-Nd-Fe-B by dual alloy method are investigated in this paper. As expected, the remanent magnetization Jr, coercivity Hci and maximum energy product (BH) max of SPSed magnets increase obviously with increasing weight percentage of Pr-Nd-Fe-B alloy. The magnetic properties of Jr = 0.71T, Hci = 915kA/m, (BH) max = 72kJ/m^3 are obtained for the SPSed magnets with 80wt% Pr-Nd-Fe-B alloy. There are three Curie temperatures in this type magnet, which implies the coexistence of three hard magnetic phases. The second Curie temperature depends on the Pr-Nd-Fe-B content. With increasing Pr-Nd-Fe-B alloy content, the volume fraction and width of coarse grain zone decrease. It is shown by the microstructure analysis that the rare earth elements diffuse during sintering process resulting in the formation of Pr-Nd-Ce-Fe-B hard magnetic phase. The intergranular exchange coupling strength is enhanced with increasing Pr-Nd-Fe-B content. The present research may be a potential reference for further research and development of this type Ce-containing nanocrystalline permanent magnetic materials.

15:15-15:35

The Effect of Additional Element (Re) on the Magnetic Properties of (Sm1-x-yRexZry)(Fe0.8Co0.2)11Ti with ThMn12 Structure

Jihoon Park, Hui-Dong Qian, Jung Tae Lim, Jong-Woo Kim, Chul-Jin Choi, Korea Institute of Materials Science, Korea

Iron-rich rare-earth (RE) alloys with tetragonal ThMn12 structure have been extensively studied as a potential high performance permanent magnetic material due to its high saturation magnetization of 1.78T, anisotropy field of 12T and Curie temperature of 859K. However, its low intrinsic coercivity prohibits its use as a permanent magnetic material. Therefore, in this work, we have synthesized light RE elements doped Sm-Fe-Ti alloys, and modified grain boundaries with Sm-based diffusion materials to investigate microstructure and magnetic properties.

(Sm1-x-yRexZry)(Fe0.8Co0.2)11Ti ribbons were prepared by arc-melting raw materials and melt-spinning. The melt-spun ribbons were ground, and sintered at various temperatures range from 800 to 1000˚C for various sintering time. The synthesized (Sm1-x-yRexZry)(Fe0.8Co0.2)11Ti powders were mixed with a grain boundary diffusion material using ultra-sonication in ethanol. The mixture was then dried in a glove box and hot-pressed under 500MPa at different temperatures to produce grain boundary modified (Sm1-x-yRexZry)(Fe0.8Co0.2)11Ti bulk.

The hysteresis loops of all samples were measured under 20kOe at 295K, showing that the intrinsic coercivity increases with doping rare-earth such as La and Ce. In order to investigate the Curie temperature, we have observed the temperature dependence of magnetization. The obtained grain boundary modified (Sm1-x-yRexZry)(Fe0.8Co0.2)11Ti bulk tend to have significantly increased intrinsic coercivity and reduced magnetization. The details of the microstructure and magnetic properties of the synthesized (Sm1-x-yRexZry)(Fe0.8Co0.2)11Ti bulk will be discussed.

15:35-16:10 Tea Break

16:10-16:35 Invited

2D Layered Semiconducting Materials and Terahertz Non-Destructive Inspection

Tadao Tanabe, Yutaka Oyama, Tohoku University, Japan

For optical applications using two-dimensional (2D) layered semiconductors in our group, GaSe and InSe were grown by a low temperature liquids phase solution method under a controlled Se vapor pressure. The stoichiometry-controlled crystals realize highly device performance. On the other hand, 2D layered material is easily broken because layered crystals combine thin sheets by out-of-plane van der Waals interaction. For practical use of 2D layered materials, the mechanical strengthen needs to be high. Therefore, quantitative and direct measurements of the bonding energy have to be evaluated. In our group, a tensile testing machine was constructed for the direct quantitative determination of the interlayer van der Waals bonding force. Furthermore, a novel friction induced crystal growth method has been implemented for synthesizing atomic layers of MoS_2.

The low-temperature solution growth method is suitable for very high quality compound semiconductors fabrication, which results to reduce numbers of defects. GaSe crystal has birefringent properties, which allows collinear phase-matching for a terahertz (THz) wave generation. Thus, higher-power and simply-structured THz emitter is realized using the GaSe crystal.

The energy of THz wave corresponds to molecular interactions such as hydrogen bonding, van der Waals interactions and lattice interactions. Thus, THz wave has high permeability for non-polar materials, which is expected to be used as non-destructive evaluation. Besides, THz wave has low quantum photon energy, so that it is safe for human tissues. Our group has created a database of THz permeability characteristics for

industrial materials, and successfully constructed non-destructive THz diagnosis of building blocks, insulated copper cable and hot-dip galvanized steel sheet. As tunable-frequency THz source in wide range, our group developed differential frequency generation (DFG) of GaSe crystals. The layered GaSe semiconductor combines thin sheets by out-of-plane van der Waals interactions. For practical applications that use 2D layered GaSe semiconductors, the mechanical strength needs to be high. For example, device fabrication processes, such as dicing and wire bonding, require the crystal to be mechanically strong. However, no direct experimental determination has been carried out up to now for van der Waals bonding energy. Therefore, quantitative and direct measurements of the bonding energy are urgently required in order to obtain crucial understandings of 2D semiconductor materials. By our group, a tensile testing machine was constructed for the first quantitative detemination of the interlayer van der Waals bonding force, where two stainless steel L-shaped sliders were combined, with a strain gauge between them. Then, the interplanar binding strength of layered GaSe crystals was directly determined using the tensile testing machine.

Molybdenum disulfide (MoS_2) is one type of 2D transition metal dichalcogenides (TMDC). MoS_2 having an ultrathin atomic layered structure is an interesting semiconductor material for high speed, low power transistors, superconductors and as highly active catalysts. For these studies, the MoS_2 crystals were prepared by two methods. One was mechanical exfoliation, the other was chemical vapor deposition (CVD). On the other hand, layered MoS_2 has also been used as a lubricant. This reduces friction at the interface between mechanical parts, where each layer slides easily under a small shear stress as a result of the weak van der Waals bonding force of the layered structure. At the interface, MoS_2 is mechanochemically synthesized from molybdenum dialkyldithiocarbamate (MoDTC) in a synthetic oil. A low friction interface is realized in well-stacked layered MoS_2. This reduction reaction is used to reduce piston ring friction in car engines. We have proposed a novel method in which the friction is used to induce the growth of 2D layered MoS_2 crystals. The structure of MoS_2 crystals grown by this friction induced method was layered with the c-axis perpendicular to the surface. The thickness was N-layers (N>6). The photoluminescence (PL) peak of the neutral exciton emission was observed at room temperature, which suggests that the crystalline quality was good with low impurities and defects. Such MoS_2 crystals can be used for fabricating semiconductor devices. In addition, selective growth of MoS_2 films at specified positions using this friction-induced method enables savings to be fabricated, since a dry vacuum pump is not necessary and a photolithography process can be omitted from the fabrication process, making it similar to a rubbing process. In our study, friction induced crystal growth has been realized for the first time.

16:35-17:00 Invited

Magnetic Properties and Nicrostructure of High Coercivity Zn-Bonded Sm-Fe-N Magnets

Masashi Matsuura, Ryo Matsunami, Nobuki Tezuka, *Satoshi Sugimoto,* Tohoku University, Japan; Tetsuya Shoji, Noritsugu Sakuma, Toyota Motor Corporation, Japan / MagHEM, Japan

Sm2Fe17N3 has a high saturation magnetization, a large anisotropy field, and a high Curie temperature, however, this compound cannot be sintered because of decomposition above about 600˚C. To obtain high performance Sm-Fe-N bulk magnet, Zn-bonded Sm-Fe-N magnets is expected. Our group prepared Zn-bonded Sm-Fe-N magnets using Zn fine powder with low oxygen content (d50= 0.23mm, oxygen content= 680ppm), and the low oxygen Zn-bonded Sm-Fe-N magnets showed high coercivity of 2.66MA/m (15wt% Zn).

In this study, we investigated relationship between microstructure and coercivity. In magnets without Zn, coercivity decreased and there were a-Fe grains at the surface of Sm-Fe-N powder after annealing. However, in high coercive Zn-bonded magnets, Zn-diffused layer existed between the Fe-rich and Sm2Fe17N3 phases after annealing. This indicates that the Zn-diffused layer isolates Sm2Fe17N3 phase from soft magnetic phase (Fe-rich phase), therefore the magnetic isolation can induce high coercivity.

17:00-17:25 Invited

Compression-Based Elastocaloric Cooling: Recent Advances in Materials and Systems

Ichiro Takeuchi, University of Maryland, USA

We have been pursuing different materials and devices for compression-based elastocaloric cooling. From heat-exchanging point of view, it is desirable to be able to fabricate elastocaloric materials of different shapes at will. To this end, we are fabricating superelastic NiTi using additive manufacturing. We have been able to consistently obtain adiabatic DT of 4K in as-printed NiTi. Because of its unusual microstructure, 3D-printed NiTi displays stress-strain curves with narrow hysteresis, which can help to increase its materials COP. We have studied fatigue behavior of as-printed NiTi, and found that their elastocaloric properties do not decay for at least up to 1 million cycles. Following our previous work on hydraulically-driven compressive elastocaloric cooling

systems, we have constructed a single-stage active regenerator using a bundle of 10" long commercially-available NiTi tubes. Starting with materials DT of 8K at compression strain of 5%, we have been able to achieve DT of 22.5K in the regenerator to date operating at 100W. We are also pursuing devices based on Cu-based shape memory alloys. Recently, we have demonstrated a compact low-field magneto-elastocaloric cooling device by combining a magneto strictive terfenol and a piece of Cu-Mn-Al elastocaloric material. By applying a relatively small field (170mT), magnetostriction in terfenol is used to apply stress to Cu-Mn-Al, resulting in DT as large as 4K. Such a multiferroic composite device can be used to circumvent shortcomings of existing technologies such as the high magnetic-field requirement of the magnetocaloric materials and the need for high-stress actuation mechanism for elastocaloric materials, while enabling new applications such as compact remote cooling devices. This work is carried out in collaboration with Huilong Hou, David Catalini, Nehemiah Emaikwu, Jan Muehlbauer, Naila Hassan, Suxin Qian, Jun Cui, Yunho Hwang, and Reinhard Radermacher. The projects are funded by the U.S. Department of Energy.

17:25-17:50 Invited

Special Microstructure Evolution and Enhanced Magnetic Properties of Ce-Fe-B-Based Spark Plasma Sintered Magnets with Core-Shell Structure by NdCu Addition

Zhenchen Zhong, Qingzheng Jiang, Sajjad Ur Rehman, Weikai Lei, Lunke He, Qingwen Zeng, Jiangxi University of Science and Technology, China

Much demanded and overused are the critical rare-earth elements such as Pr, Nd, Dy, and Tb with increasing need of NdFeB-type rare-earth permanent magnets in the enlarging application areas, developing new high-tech industries, and emerging cutting-age frontiers. The balance and efficient use of rare-earth resources comes into being the national strategy, national defense, and border safety for many major countries and regions in the world. (Nd, Ce)FeB-based permanent magnetic materials, which can not only reduce cost but also offer a feasible way for integrated and effective utilization of rare earth resources, have received much attention in recent years.

Ce-Fe-B-based rare earth permanent magnets are prepared by spark plasma sintering (SPS) technique, and low melting NdCu alloy is added to improve its magnetic properties and thermal stabilities. The X-ray diffraction (XRD) result indicates that the lattice constants of the unit cell of 2:14:1 phase increase with NdCu addition. The remanent magnetization, coercivity and maximum energy product are enhanced remarkably from 0.37T, 227kA/m, 16kJ/m^3 for the sintered magnets without NdCu addition to 0.47T, 476kA/m, 30kJ/m^3 for those with 20wt.% NdCu addition. There are two Curie temperatures in the Ce-based magnets with NdCu addition, which implies the coexistence of two hard magnetic phases. It is shown by the microstructure analysis that a typical core-shell structure is formed with Ce-rich core and Ce-lean shell by NdCu addition. Furthermore, it is displayed that Nd atoms prefer to diffuse into the Ce-lean flakes. The Nd-Ce exchange mechanism and immigration behavior of elements are finally investigated. The intergranular exchange coupling strength is enhanced in NdCu-added magnet. It is found out that the core-shell structure plays an important role in the special microstructure evolution and the enhancement of the magnetic properties for the typical Ce-Fe-B-based SPSed magnets by NdCu addition.

17:50-18:10

Microstructure, Magnetic Properties and Thermal Stabilities of Alnico Ribbons

Sajjad Ur Rehman, Qingzheng Jiang, Lunke He, Jie Song, Han Ouyang, Zhenchen Zhong, Jiangxi University of Science and Technology, China

Reducing the spatial dimension of ferromagnetic (α_1) phase is the promising route for improving the coercivity of alnico alloys. It is an experimental fact that the spatial dimension of α_1 phase cannot be reduced below a certain limit (~25nm) by using conventional processing methods. To obtain fine and narrow α_1 phase, alnico ribbons with nominal composition of 32.2Fe-36Co-13.5Ni-7.6Al-6.2Ti-3.8Cu-0.5Zr-0.2B have been fabricated by melt spinning and subsequent simplified heat treatments. By subjecting to various heat treatments, it is confirmed that the alnico ribbons have much wider treatment range as compared to alnico bulk alloys. Fine Fe-Co rich (α_1) rods of the order of 5nm diameter and 100nm length (aspect ratio ~20) embedded in Al-Ni rich matrix are obtained. Magnetic properties of Hcj = 815Oe, Br = 6.70kG and (BH)max = 1.88MGOe are obtained after simplified heat treatment. These are promising properties which would be helpful to develop high performance alnico permanent magnets. Furthermore, it is shown that alnico ribbons have unprecedented thermal stability described in terms of temperature coefficient of remanence (α) and temperature coefficient of coercivity (β) by measuring magnetic properties at temperature range 300~800K. The microstructures of the alloys have been analyzed by Scanning Electron Microscope and Transmission Electron Microscope. The magnetic properties are measured by using PPMS, and the phase transition temperatures have been observed by DTA.

18:10-18:30

Enhancement of Magnetic Property in RE-Fe-Co-B (RE=Nd, Ce, Pr) Ribbons by Modifying the Intergranular Phase

Xiaohua Tan, Qin Deng, Yang Liang, Yang Yang, Hui Xu, Shanghai University, China

RE-Fe-B (RE=rare earth) permanent magnets have found applications in a wide range of fields including electronic, data processing and medical devices due to their outstanding hard magnetic properties. Developing economically more attractive RE-Fe-B permanent alloys is extremely important because of the limited natural resources and high cost of critical rare earth metals in recent years. The rapid solidification technique of melt-spinning is one of the most important techniques for producing RE-Fe-B ribbons which are currently used as raw materials for the production of bonded magnets and hot-pressed magnets. Hence, optimizing the microstructure of melt-spun ribbons is critical to improving the magnetic properties of RE-Fe-B permanent magnets. The intergranular phase including non-ferromagnetic or ferromagnetic one has a strong influence on the magnetic properties. In this work, we used the annealing in an applied magnetic field of 1T and additive Co to adjust the distribution and chemistry of the intergranular phase. The atom probe tomography (APT) results showed that ferromagnetic intergranular phase was both found in (Nd0.8Ce0.2)2.4Fe12Co2B melt-spun and annealed ribbons. Moreover, the magnetic field annealing-treatment increased the remanence by enhancing the exchange coupling interaction, leading to a maximum product energy ((BH)max) which is 16% higher than that of melt-spun ribbons. It is found that the substitution Co for Fe in (Nd0.8Pr0.2)2.2Fe14-xCoxB (x=0, 2, 2.25) alloys improved the magnetic properties by modifying the intergranular phase. That is, ferromagnetic intergranular phase was found in (Nd0.8Pr0.2)2.2Fe14B (x=0) alloy, whereas non-ferromagnetic and ferromagnetic intergranular phase were both observed for Co-containing with x=2.25 alloy. In comparison to x=0 alloy, both increase of coercivity and remanence (enhanced by 7% and 4%) of (Nd0.8Pr0.2)2.2Fe11.75Co2.25B (x=2.25) alloy was due to the combined contributions of two types of intergranular phase. Our findings provide a new idea to design prospective permanent alloys by tuning the distribution and chemical composition of the intergranular phase.

H. Materials Characterisation and Evaluation: I

Symposium Organizers:

Zhiwei Shan, Xi'an Jiaotong University, China; Xiaodong Han, Beijing University of Technology, China; Satoshi Hata, Kyushu University, Japan; Ju-Young Kim, Ulsan Institute of Science and Technology (UNIST), Korea; Jin Zou, University of Queensland, Australia; Jennifer Carter, Case Western Reserve University, USA

Monday PM
August 19, 2019

Room: 308 (3rd Floor)
Symposium:H

Chairs:
Ian Gentle, The University of Queensland, Australia
Jianghua Chen, Hunan University, China

13:30-14:00 Keynote

Atomic-Resolution Electron Microscopy for Aluminum Alloys as High-Performance Industry Materials

Jianghua Chen, Hunan University,China

Developments of high-strength aluminum alloys have always faced a difficult problem: owing to their small size, the early-stage strengthening precipitates are difficult to characterize in terms of composition, structure and evolution. Here we employ atomic-resolution transmission electron microscopy (TEM) imaging and first-principles energy calculations to address these problems. Recent years, we have investigated tens of typical high strength aluminum alloys, such as 2xxx (AlCu, AlCuMg and AlCuLiMg), 6xxx (AlMgSi and AlMgSiCu) and 7xxx (AlZnMg and AlZnMgCu) alloys, with different compositions and with varying thermal processes for understanding their property-structure-process correlations. Using aberration-corrected high-resolution TEM (HRTEM) and aberration-corrected scanning TEM (STEM), much of our attention has been paid to revisit the strengthening precipitates in these important alloys and to clarify the controversies left in the past about their precipitation behaviors. Our study demonstrates the followings: (1) Atomic-resolution imaging in STEM can provide straightforward structure models at the atomic-scale, whereas atomic-resolution imaging in HRTEM with rapid quantitative image simulation analysis can provide the refined structures with high precision beyond the resolution limitation of the microscope. The combination of the two techniques can be more powerful in solving difficult structure problems in materials science. (2) Most of the early-stage precipitates in aluminum alloys are highly dynamic in both composition and structure. Typically, having their characteristic genetic

skeletons to guide their evolution, these dynamic precipitates initiate, mature and grow with thermal aging following characteristic evolution paths. The fine precipitation scenarios revealed in our studies are rather different from previous understandings in the textbooks and literatures published thus far.

14:00-14:25 Invited

3D TEM Characterization of Heterogeneous Precipitation at Dislocations in an Age-Hardened Al-Cu-Mg Alloy

Xiaoxu Huang, Zongqiang Feng, Chengwei Lin, Rui Fu, Guilin Wu, Chongqing University, China

It is well-known that a dislocation structure characterized by straight and curved dislocation lines, dislocation loops, and dislocation helixes is generated after solid solution treatment and quenching of Al-Cu-Mg alloys. Several previous studies have shown that heterogeneous nucleation of strengthening precipitates at dislocations occurs during subsequent aging, which influences the morphology and distribution of the precipitates in the Al matrix and the mechanical properties of the aged material. It has also been shown that the heterogeneous nucleation of precipitates at the dislocations of various geometrical features exhibits two kinds of preferred selections: selection of crystallographic variants fulfilling the orientation relationship between the precipitate and the matrix Al, and selection of nucleation sites along a given dislocation feature. However, the underlying mechanisms responsible for these preferred selections are not well understood due to the lack of detailed crystallographic information such as the dislocation types (namely, edge, crew or mixed, which is determined by the Burgers vector and line direction of a given dislocation), the normal to a dislocation loop, the axis of a dislocation helix. In this study, we selected an Al-Cu-Mg alloy to investigate the correlation between the dislocation structure and the precipitation with an aim to understand how the characteristics of dislocations affect the preferred selections associated with the nucleation of precipitates. We first carried out detailed characterization of 3D arrangements of dislocations in the solution-treated and quenched state by means of correlative electron tomography and crystallography of dislocations, which provided detailed and precise characterization of the geometrical and crystallographic features of the dislocation structure. And then in situ TEM heating of the same specimen was carried out to follow the precipitation process during aging. The correlative 3D characterization of dislocations and in situ TEM observations of precipitation of the same area revealed that both the preferred selections of the precipitation process are strongly related to the crystallographic features of the dislocation structure, which will be discussed in detail in the presentation.

14:25-14:50Invited

Picometer Scale Fine Structure of Materials and Emergent Properties in Noether's Vision

Lin Gu, The Insitute of Physics, Chinese Academy of Sciences, China

The origin of functional materials is divided into two parts, multi-electronic system and single electronic system. Multi-electronic system is determined by various fields, while single electronic system is determined by local symmetry. From Noether’ s vision, to every differentiable symmetry generated by local actions there corresponds a conserved flux. Materials with broken symmetry destroy the conserved quantities and therefore have functionality. Even the change under picometer scale in functional materials could break the symmetry. As a powerful characterization method, Spherical aberration corrected electron microscopy could acquire information about atomic-scale structure and electronic structure, which could get rid of the structure-activity relationship under the constraint condition of periodic potential field, single electron approximation, and adiabatic approximation theories in solid material. In our recent work, we realized broken symmetry in functional material by electrochemical operation（Gong, Gu* et al. J Am Chem Soc, 2017, 139(12), 4274-4277）(Gong, Gu* et al. Nature Communications, 2018, 9, 1-8). For example, the interface regions, including surfaces and internal boundaries, may have a substantial impact on battery performance. Both the spatial inversion symmetry and translational symmetry are broken by the interfacial structure itself. This report will focus on electrochemical operation of functional oxide materials, physical mechanism of electrochemical energy storage materials, and electron structure of catalyst materials, to discuss the correlation between microstructure and electronic structure in the broken symmetric system.

14:50-15:10

Structural Analysis of Au-Ru Alloy Nanoparticles by Atomic-Resolution Electron Tomography

Tomokazu Yamamoto, Koji Shigematsu, Syo Matsumura, Kyushu University, Japan; Quan Zhang, Kohei Kusada, Hiroshi Kitagawa, Kyoto University, Japan

Bimetallic nanoparticles has attracted a great deal of interests in many field due to their novel properties in the recent years. Structural characterization of nanoparticles is essential to consider their properties because the nanoparticle properties depend on their sizes, shapes, compositions, surface structures, elemental distributions. The electron tomography is a powerful characterization tool to investigate three-dimensional (3D) structure of nanoparticles. In recent years, Yang et al.developed the new tomographic

reconstruction algorism termed as a generalized Fourier iterative reconstruction (GENFIRE) and achieved atomic resolution tomographic reconstruction of the FePt nanoparticle with elemental distinction. In this study, we investigated structures of Au-Ru nanoparticles synthesized by a liquid-phase chemical reduction method using atomic resolution tomography with the GENFIRE algorism. Au-Ru system is immiscible system. However it is possible to synthesized non-equilibrium super-saturated nanoparticles controlling the reduction speeds. The purpose of this study is analysis of local elemental configrations in the AuRu alloy nanoparticles. $AuRu_3$ solid-solution NPs with fcc structure were synthesized using a polyol reduction method. Hydrogen tetrabromoaurate (III) hydrate ($HAuBr_4 \cdot nH_2O$) and potassium pentachloronitrosylruthenate (II) ($K_2Ru(NO)Cl_5)_{12}$ were dissolved in diethylene glycol (DEG) with a 1:3 molar ratio. The metal precursor solution was slowly dropped into an ethylene glycol (EG) solution containing polyvinylpyrrolidone (PVP) at 190℃. The synthesized $AuRu_3$ nanoparticles were observed using an Aberration-corrected STEM (JEOL JEM-ARM200F) at acceleration voltage of 120kV. A tilt series of HAADF-STEM images was acquired between angle ranges from -65° to 65° . Tomographic reconstruction were performed using the GENFIRE-Python software developed by Pryor Jr. et al. HAADF-STEM observation revels that AuRu3 nanoparticles synthesized in this study were around 10nm in size and polycrystalline. The nanoparticles contained many twins. The compositional fluctuations were observed by STEM-EDX elemental mapping. Atomic-resolution tomographic reconstruction was achieved successfully by GENFIRE algorism. The resolution of the reconstructed object depends on directions against tilting axis. In the reconstructed object, {100}, {110} and {111} planes were clearly observed from some directions. Three dimensional compositional fluctuation patterns were evaluated with nanometer scale using the reconstructed object. This segregation tendency were derived from the originally immiscible nature of the Au–Ru system.

15:10-15:30

Revealing the Three-Dimensional Dislocation Structure in an Al-Cu-Mg Alloy

Zongqiang Feng, Chengwei Lin,Guilin Wu, Xiaoxu Huang, Chongqing University, China

Dislocations play essential roles in plastic deformation and phase transformation of crystalline materials such as metals and alloys. The dislocation characteristics can be described by their geometrical and crystallographic parameters. For the former, examples are straight and curved dislocation lines, dislocation loops, dislocation helixes, and dislocation networks and dislocation boundaries formed as a result of dislocation interactions. For the latter, examples are Burgers vector and line direction that determine the character of a dislocation (edge, screw or mixed), normal to the dislocation loop plane and axis of the dislocation helix. Statistical determination of these features is crucial to understand the mechanisms responsible for the phenomena occurring during plastic deformation and phase transformation. However by means of conventional two dimensional (2D) electron microscopy techniques it is often impossible to quantify the morphological and crystallographic characteristics of a complex dislocation structure. However this can be done by three-dimensional characterization based on correlative electron tomography and crystallography of dislocation structures. Recently we have established such a technique based on transmission electron microscopy which enables a precise and high-throughput characterization of the geometrical and crystallographic parameters of individual dislocations and dislocation structures with significantly enhanced efficiency. This technique has been applied to quantify the 3D dislocation structure in a water-quenched Al-Cu-Mg alloy to compare with the 2D observations reported in the literature. The geometrical and crystallographic characteristics have been analyzed not only for the individual dislocation lines, loops and helixes but also for the low angle dislocation boundaries observed in the quenched sample. The current 3D characterization results reveal much more details than what already known from the conventional 2D observation with respect to both the geometrical and crystallographic features. The new results form a basis for an in-depth discussion about the evolution mechanisms of the intrinsic dislocation structure in the as-quenched state and their potential effects on the nucleation of strengthening precipitates during subsequent aging.

15:30-16:10 Tea Break

15:30-16:00 Keynote

Diffusion and Stability in Organic Optoelectronic Devices

Ian Gentle, The University of Queensland, Australia

Organic optoelectronic devices such as organic light emitting diodes (OLEDs), solar cells and sensors that use luminescent polymers are critically dependent on the diffusion of organic materials for their properties. In each type of device diffusion plays a different role. In the case of OLEDs, diffusion can lead to intermixing of the various layers of which a device is composed, such

as the active layer and charge transport layers. Such intermixing causes degradation in performance and so materials need to be chosen to minimize diffusion, particularly at elevated temperatures. For organic solar cells, on the other hand, diffusion of one organic material into another to form a bulk heterojunction is essential for good performance. Devices are typically annealed to ensure that the appropriate structures are formed and again materials choice is critical. Finally, fluorescent sensors rely on the diffusion of an organic analyte, such as an explosive material, through the film of sensing material to quench fluorescence and lead to a sensitive signal. For a reusable sensor it is desirable to have controlled diffusion so that the analyte can be removed when desired to enable subsequent sensing events. Over several years our group in the Centre for Organic Photonics and Electronics (COPE) has studied the effect of diffusion on the structures and performance of each of the above types of devices using mainly neutron reflectometry and we are now in a position to begin to understand the relationships between molecular structures, diffusion and device performance.

16:00-16:25 Invited

Atomic Scale Magnetic and Structural Imaging by Achromatic Electron Microscopy

Xiaoyan Zhong, Tsinghua University, China

The atomic-level knowledge of local spin configuration of the magnetic materials is of great importance to predict and control their physical properties, in order to meet the challenges of ever-increasing demands on performance of functional materials. However, it is highly challenging to experimentally characterize magnetic properties of such materials with atomic scale spatial resolution. The leading techniques in spatially resolved magnetic imaging are magnetic exchange force microscopy and spin polarized scanning tunneling microscopy. However, as they are surface sensitive, very little information can be obtained regarding bulk or buried materials. The X-ray magnetic circular dichroism (XMCD) combined with photoelectron emission microscopy (PEEM) technique is a very attractive alternative because it has the spatial resolution as high as the polarized x-ray beam size besides element specific feature, as it is less surface sensitive and can be used to look at the interior of the thin films. However, the length scale of magnetic contrast using highly brilliant left and right circularly polarized X-ray beams is around 15nm. The best option to push the spatial resolution of the spectromicroscopies lies in the electron beam equivalent technique electron energy-loss magnetic chiral dichroism (EMCD), which is also called electron magnetic circular dichroism. Physically, XMCD and EMCD shares the same underlying physics in which the angular momentum transferred during X-ray absorption or inelastic electron scattering can selectively excite magnetic sublevels in atoms. The structured electron beams generated through interference of suitably phased plane waves can produce beams with orbital angular momentum. Electron beams can be easily focused compared with X-rays, allowing for atomic scale magnetism to be probed. Previously, we have found a strong EMCD signal in transition metal oxides allowing them to use standing wave methods to identify the different spin states of Fe atoms with site specificity. In principle EMCD can offer higher spatial resolution and greater depth sensitivity due to the short de Broglie wavelength and penetration of high-energy electrons compared to XMCD. Recently by using EMCD and achromatic electron microscopy, we are able to access the magnetic circular dichroism with unit-cell resolution and even with atomic resolution. Combining with advanced capobility of structural and chemical imaging by using aberration-corrected transmission electron microscopy, all the information including magnetic polarization, atomic configurations, chemical states can be simultaneously accessed from the very same sample region. In the examples of complex oxides including Sr_2FeMoO_6, $NiFe_2O_4$ and La0.7Sr0.3MnO3, we would like to show how to achieve local atomic-scale magnetic, chemical and structural information and understand the structure-property relationship of these magnetic materials at the atomic level. This work was financially supported by National Key Research and Development Program (2016YFB0700402), National Natural Science Foundation of China (11834009, 51761135131, 51822105, 51671112, 51788104), National Basic Research Program of China (2015CB921700) and Fund of Key Laboratory of Advanced Materials of Ministry of Education (2018AML12). This work made use of the resources of the National Center for Electron Microscopy in Beijing. The author thanks to the colleagues and students at Tsinghua University, Forschungszentrum Jülich, Uppsala University and University of Tsukuba for their strong supports.

16:25-16:50 Invited

Mechanical Properties Characterization of Materials at Multiple Scale

Qian Yu, Zhejiang University, China

Solid materials are very important market consumes in real industry and are holding the leading roles as structural materials and functional materials. Regardless of the application, the development of solid materials is associated with solid mechanics and microstructure

characterization. Traditional mechanical/electrical/thermal testing experiments and material characterization techniques are frequently separate, so they lack the in-situ information resolution required to directly relate the measured properties with individual microstructure evolution events. The broad field of electron microscopy instrumentation development holds great promise for addressing these problems due to its inherently high spatial resolution and the strong interactions between electrons and solids. It is believed to be the ideal tool to exploit materials properties, especially at small scale. Here, I will present recent results investigating materials properties at multiple scales by coupling the in situ TEM/SEM techniques with other characterization techniques such as HRTEM and EBSD. For instance, by using transmission electron microscopy and nanomechanical characterization, we report that the intense hardening effect of dilute oxygen solutes in pure a-Ti is due to the interaction between oxygen and the core of screw dislocations that mainly glide on prismatic planes, which was thought unlikely based on traditional understanding of solid solution strengthening mechanisms. Also we studied the deformation mechanisms that are responsible for the ultra-high toughness of high entropy alloys. We report on the salient atomistic to micro-scale mechanisms underlying the origin of these properties. We identify a synergy of multiple deformation mechanisms, rarely achieved in metallic alloys, which generates high strength, work hardening and ductility, including the easy motion of Shockley partials, their interactions to form stacking-fault parallelepipeds, and arrest at planar slip bands of undissociated dislocations, in FeCoNiCrMn. We further show that crack propagation is impeded by twinned, nanoscale bridges that form between the near-tip crack faces and delay fracture by shielding the crack tip.

16:50-17:10

Direct Observation and Characterization of H/D in Ti Alloys Using Atom Probe Tomography Combined with Cryogenic Focused Ion Beam Technique

Yanhong Chang, Wenjun Lu, Leigh Stephenson, Isabelle Mouton, Dirk Ponge, Dierk Raabe, Baptiste Gault, Max-Planck-Institut für Eisenforschung GmbH, Germany; Abigail Ackerman, David Dye, Department of Materials,Royal School of Mines,Imperial College, UK

It is well documented that hydrogen has detrimental effects on a variety of metallic materials, including steels and nonferrous Ni-, Al-, Ti-, Zr-, or Mg - based alloys. Many mechanisms for hydrogen embrittlement such as hydrogen - enhanced local plasticity (HELP), hydrogen - enhanced decohesion (HEDE), or hydride - induced cracking, etc., have been proposed. However, precisely how H behaves within materials at the nanoscale remains mostly unresolved due to the experimental challenge in characterizing the H distribution within metals, in particular at specific microstructural features. Atom probe tomography (APT), as a mass spectroscopy technique with near-atomic spatial resolution, enables us to characterize and visualize the 3D distribution of H within engineering materials. However, specimen fabrication for APT measurements, by electropolishing or conventional focused ion beam (FIB) milling, has a high tendency to trigger undesired H ingress and possibly hydrides formation in Ti or Zr alloys. Cryogenic FIB technique was deployed to avoid undesired introduction of H from the environment during specimen preparation, and in the same time, to prevent out-diffusion of H/D purposely charged into the material, by significantly lowering H/D diffusion rate. Using APT combined with cryogenic FIB milling for sample fabrication, we imaged H/D as solute, hydride/deuteride and segregation at interfaces in a set of Ti-alloys. We visualized H/D partitioning between α and β phases, and local H/D segregation at α' martensite lath boundaries. H solubility in different matrix phases, β phase > α phase with Al alloying or Mo oversaturation > pure α Ti, was clearly revealed. Combining with transmission electron microscopy and atom probe crystallography, we identified nano-sized hydrides/deuterides, with approx. 50at.% H/D, forming in the vicinity of α grain boundaries and α/β interfaces. Moreover, we evaluated the quantitativeness of H/D measurement by APT by systematically analyzing the composition of titanium deuteride (TiD~2, stoichiometry of 65.0~66.6at.% D) with various experimental conditions. Direct observation and characterization of H/D opens an access for more closely understanding the H behaviors and furthermore hydrogen embrittlement mechanism within materials.

17:10-17:30

Atomic Imaging and Modelling of Defects in Hexagonal GST

Jiangjing Wang, Wei Zhang, Xi'an Jiaotong University, China; Chunlin Jia, Peter Grünberg Institute and Ernst Ruska-Centre for Microscopy and Spectroscopy with Electrons,Forschungszentrum Jülich GmbH, Germany / Xi'an Jiaotong University, China

Disorder plays an essential role in shaping the transport properties of GeSbTe phase-change materials (PCMs) to enable non-volatile memory applications. Recently, increasing efforts have been undertaken to investigate disorder in the layer-structured GST compounds, especially a special type of swapping bilayer defects. In

this work, we focus on hexagonal GST. The samples were prepared by magnetron sputtering and were annealed at 300˚C for half an hour. We thoroughly characterized the structural and chemical features of the major defects in hexagonal GST at atomic scale through chemi-scanning transmission electron microscopy (STEM) experiments. By combining nanoscale density functional theory (DFT) modelling and simulations, we identify that the intermixing of Sb and Te in the bilayers is crucial to stable the defects, and attribute their abundance to the small energy cost. Another special triple layer defects were also observed in Te-rich thin film prepared with the same method as above. The composition was confirmed to be $GeTe_2$ by energy dispersive X-ray spectroscopy (EDX) at atomic resolution, and the central Ge atom is octahedrally coordinated. Both of the bilayer and trilayer defects are demonstrated to be ineffective in altering the electron localization nature but may affecting the quantitative value of electrical resistance in hex-GST.

17:30-17:50

Probe the Ultrafine Cerium Oxide Nanocrystals by Aberration Corrected Scanning Transmission Electron Microscopy

Xiaodong Hao, Shufang Ma, Gaohui Du, Shaanxi University of Science & Technology, China; Mitsuhiro Saito, The University of Tokyo, Japan; Chunlin Chen, Tohoku University, Japan / Institute of Metal Research, Chinese Academy of Science, China; Bingshe Xu, Shaanxi University of Science & Technology, China / Taiyuan University of Technology, China; Tadafumi Adschiri, Tohoku University, Japan; Yuichi Ikuhara, Tohoku University Japan / The University of Tokyo, Japan

Cerium oxide (CeO_2) has been recognized as one of the best candidates in applications as diverse as solid oxide fuel cells, catalytic antioxidants for treating oxidative stress-related diseases, and catalytic converters for cleaning vehicle exhaust gas. Most of its interesting properties, including its extraordinarily high capacity to store oxygen, stem from the flexible valence switching between cerium cations (Ce^{4+} and Ce^{3+}). To gain insights into the atomic surface structure, valence states distribution behaviors and their relationship to chemical properties of CeO_2, we have focused on the ultrafine CeO_2 nanocrystals (NCs) using the state-of-the-art aberration corrected scanning transmission electron microscopy (STEM) imaging and electron energy loss spectra (EELS). Based on these technologies, we have provided the robust solutions for the direct imaging of organic surfactant molecules on CeO_2 NCs. The EELS elemental mapping spectra offer the explicit evidences for the existence and distribution of organic surfactant on CeO_2 NCs surface; and the optimized STEM imaging condition provides enhanced contrast for the direct imaging of surfactant molecules, which will advance our understanding of the surface chemistry of surfactant-modified nanocrystals. In addition, the quantitative analysis of Ce valence state layer by layer across a single CeO_2 NC perpendicular to its (100) exposed facet is also achieved. Combining the structure analysis and theoretical simulation, the relationship between the lattice parameters and the formation of oxygen vacancies with respect to the NCs size are the systematic discussed. The quantitative analysis of the valence state distribution, combined with local structural transformation and nano-size effect, provides a basis for understanding the intrinsic features of cerium oxide nanocrystals, and it will further provide critical guidance for designing and fabricating novel oxygen-storage materials that can be used as catalysts and solid electrolytes.

17:50-18:10

Atomic-Scale Understanding of Stress-Induced Phase Transformation in Cold-Rolled HCP Metals

Song Ni, Henglv Zhao, Min Song, Central South University, China

Identifying the character and the source of partial dislocations associated phase transformation from a hexagonal close-packed (HCP) structure to a face-centered cubic (FCC) structure is essential for understanding phase transformation mechanisms, but was rarely done using microscopy. Here, we report a stress-induced HCP to FCC phase transformation in pure hafnium and zirconium during cold rolling. Two distinctive orientation relations between HCP phase and FCC phase were observed, which were denoted as B-type and P-type orientation relations according to whether the phase interface is parallel to the basal plane or prism plane of the HCP matrix. The mechanisms for the phase transformation generating the two different HCP-FCC orientation relations were thoroughly analyzed. B-type orientation relation was achieved when HCP to FCC phase transformation occurred via collective gliding of Shockley partial dislocations on basal planes, while P-type orientation relation was attained through pure-shuffle and shear-shuffle mechanisms. Detailed transmission electron microscopy investigations revealed that transformation-related partials stemmed from the dissociation of <a>-type dislocations. Successive gliding of partials on every other basal plane resulted in the orientation relationship between the two phases. Besides, a new way to form a twin relationship in the FCC structure was discovered. The growth of FCC lamella can also be realized by merging small lamella with the same orientation or with a twin relationship.

J. Amorphous and High Entropy Alloys: Amorphous Alloys I

Symposium organizers:

Weihua Wang, The Institute of Physics, Chinese Academy of Sciences, China; Zhaoping Lv, University of Science and Technology Beijing, China; Hidemi Kato, Tohoku University, Japan; Hojin Ryu, Korea Advanced Institute of Science and Technology (KAIST), Korea; Michael Ferry, New South Wales, Australia; Evan Ma, Johns Hopkins University, USA

Monday PM
August 19, 2019

Room: 405 (4th Floor)
Symposium: J

Chairs:
Zhaoping Lu, University of Science and Technology Beijing, China
Lina Hu, Shandong University, China

13:30-14:00 Keynote

Liquid-Like Behaviours of Low-Dimensional Metallic Glassy Nanoparticles at Room Temperature

Weihua Wang, C. R. Cao, H. Y. Bai, Institute of Physics, Chinese Academy of Sciences, China

Direct atomic-scale observations and measurements on dynamics of amorphous metallic nanoparticles (a-NPs) are challenging owing to the insufficient consciousness to their striking characterizations and the difficulties in technological approaches. In this work, we report the observation of coalescence process of low-dimensional a-NPs at atomic scale. We measure the viscosity of the a-NPs through the particles coalescence by in situ method. We find that the a-NPs have fast dynamics, and the viscosity of the a-NPs exhibits a power law relationship with size of the NPs. The NPs with sizes smaller than 3nm are in supercooled liquid state and exhibit liquid-like behaviours with a decreased viscosity by four orders of magnitude lower than that of bulk glasses. These results reveal the intrinsic flow characteristics of glasses in low demention, and pave a way to understand the liquid-like behaviours of low dimension glass, and are also of key interest to develop size-controlled nanodevices.

14:00-14:25 Invited

Making Glassy Solids Ductile at Room Temperature by Imparting Flexibility into Their Amorphous Structure

Evan Ma, Johns Hopkins University

Glasses lack ductility at RT. A long-sought goal is therefore to impart ductility without conceding strength. Here we advocate purposely enhanced flexibility, in an otherwise compositionally uniform and single-phase amorphous structure, for stress-driven profuse bond-switching events to carry shear transformations throughout the sample volume and therefore distributed flow without severe shear banding. We highlight how to retain flexibility from the parent liquid, or rejuvenate the glass structure to restore flexibility, for making MGs, a-silica and a-Si all plastically deformable at RT. To devise a universal structure parameter, we introduce "flexibility volume" as a single indicator of the glassy state. It quantitatively predicts the shear modulus on both atomic and macroscopic levels, reflecting the barrier to overcome in deformation, and advantageous over the widely cited "free volume", which is ambiguous and inapplicable to open-structure glasses such as a-silicon and a-silica. Z. Fan et al., review in Materials Research Letters 6 (2018) 570-583; J. Ding et al., Nature Communications 7 (2016) 13733.
The speaker did his graduate work at Tsinghua University and Caltech, followed by postdoc sojourns at MIT and Univ. of Michigan. He is currently a professor in the Department of Materials Science and Engineering at Johns Hopkins University (with an adjunct professorship at Xi'an Jiaotong Univ.). He has published ~320 papers (with ~26,000 citations and h index=84, according to SCI; and ~34,000 citations and h index=97, according to Google Scholar) and presented ~220 invited talks at international conferences and seminars. He has been named a Fellow of American Society for Metals, American Physical Society, and Materials Research Society. Dr. Ma's current research interests include amorphous metals (metallic glasses), chalcogenide phase-change alloys for memory applications, ductility and plasticity mechanisms of nanostructured metals and high-entropy alloys, and in situ transmission electron microscopy of small-volume materials exposed to mechanical, thermal and environmental stimuli.

14:25-14:50 Invited

Order and Structural Variability in Metallic Glasses Studied by Electron Nanodiffraction

Amelia Liu, Amelia Liu, Espen Bojesen, Laure Bourgeois, Joanne Etheridge, Timothy Petersen, Monash University, Australia; Ryan Ott, Mikhail Mendelev, Ames Laboratory, USA; Matthew Kramer, Ames Laboratory, USA/ Iowa State University, USA; Peter Harrowell, University of Sydney, Australia; Alessio Zaccone, University of Milan, Italy

The role of local structures in the formation and properties of glasses has been notoriously hard to

determine due to the difficulty of characterizing the type and degree of order in systems that lack translational symmetry. For crystals, translational invariance imposes tight restrictions on the solution-space, and even biological molecules with hundreds of thousands of atoms can be solved using diffraction. In contrast, in glasses, every atom occupies a statistically unique position; conventional diffraction cannot be used to find a unique structural solution.

In developing a "generalized crystallography" that will include glasses and other disordered materials, electrons have a unique role to play. They interact strongly with atomic potentials and can be focussed to a quasi-parallel probe with dimensions tuned to the correlation length of interest in the material. In an electron nanodiffraction (END) pattern, the characteristic diffuse amorphous rings from large-volume diffraction, break up into discrete areas of diffracted intensity that reflect the local atomic structure illuminated by the probe.

In this presentation, I will describe some key advances in the physics of diffraction from disordered materials that have enabled us to interpret the features in END patterns from glasses. In particular, weak angular correlations can be extracted from ensembles of END patterns and statistically analysed to yield new information about the number and symmetry of distinct local structures. This information may provide the key to understanding why some systems are good glass-formers and what local structures determine the mechanical properties of glasses.

The authors acknowledge use of the facilities at the Monash Centre for Electron Microscopy (FEI Titan3 80-300 FEGTEM funded by ARC LE0454166). Espen Bojesen would like to thank VILLUM FONDEN for the funding via the research grant (VKR023371). Amelia Liu gratefully acknowledges support from the ARC (FT180100594).

14:50-15:10 Invited

Understanding Atomic-Scale Features of High-Temperature Non-Arrhenius Crossover Phenomenon in Metallic Glass-Gorming Liquids

Lina Hu, Nannan Ren, Shandong University, China; Pengfei Guan, Beijing Computational Science Research Center, China

The structural relaxation of metallic glass-forming liquids (MGFLs) slows down upon cooling and, accompanied with it, many interesting dynamic phenomena have been discovered such as liquid-liquid transition, the breakdown of S-E relation and the fragile-to-strong transition phenomenon. Most of these dynamic anomalies occur in the supercooled liquid region or approaching the liquidus temperature Tl. At higher temperatures, the MGFLs are generally regarded as homogeneity which results in a constant dynamic mechanism described by Arrhenius equation. However, recent studies show that there is a crossover from this Arrhenius to non-Arrhenius behavior even at high temperature well above Tl (defined as TA in some literatures) during cooling. The high temperature non-Arrhenius crossover of structural relaxation behavior is an interesting phenomenon in MGFLs, but what happens near TA remains mystery from the atomic scale. Through molecular dynamics (MD) simulations in Fe80P20 marginal system, straight evidence is found that TA (≈1600K) is the onset of the notable increase of dynamic heterogeneity deviating from Arrhenius during cooling. Accompanied with it, the structural correlation of characteristic atoms with high five-fold local symmetry (FFLS) becomes stronger. These findings indicate that the information involved in glass transition is already in embryo in liquids from TA, which in turn helps to clarify the key roles of FFLS during the inheritance from the liquid to glassy solids in MGFLs. Further studies show that by using TA as a scaling parameter, a scaling collapse between dynamic heterogeneity and structural relaxation exists in different MGFLs. The extent of dynamic heterogeity in different MGFLs is almost the same at the crossover temperature TA. This quantitative analysis shows us a direct link between dynamic heterogeneity and structural relaxation behavior in liquids.

15:10-15:30

In-Situ Scattering Study of an Unusual Phase Transformation Pathway in Zr-Ti-Cu-Ni-Al Bulk Metallic Glasses

Si Lan, Weixia Dong, Jiacheng Ge, Sinan Liu, Nanjing University of Science and Technology, China; Yang Ren, Argonne National Laboratory, USA; Li Zhu, Nanjing University of Aeronautics and Astronautics, China; Haiyan He, Xunli Wang, City University of Hong Kong, China

The multicomponent Zr-Ti-Cu-Ni-Al alloy has excellent glass-forming ability. The pathway during amorphous-to-crystalline transformation in Zr-Ti-Cu-Ni-Al bulk metallic glasses (BAM 11) still remains controversial so far. A great deal of studies revealed evidence of amorphous phase separation or the formation of metastable phases in the supercooled liquid before crystallization. However, the others denied above scenarios because of the negative heat of mixing nature among the main constituent elements for Zr-Ti-Cu-Ni-Al alloys. Most recently, evidence of the liquid-liquid phase transition has been found in a series of bulk metallic glasses, which

opens a new window to study this long-standing issue. Here, a suite of state-of-the-art techniques, including differential scanning calorimetry (DSC), time-resolved simultaneous wide- and small-angle X-ray scattering (WAXS/SAXS), in-situ pair distribution function (PDF) and in-situ transmission electron microscopy (TEM), were employed to have a deep insight into the phase transformation pathway in BAM 11 supercooled liquid. Multiscale structure evidence reveals an unusual phase transformation pathway in the following sequence upon isothermal annealing the BAM 11 supercooled liquid: incubation, liquid-liquid phase transition, chemical phase separation, crystallization stage I and crystallization stage II. An incubation period before phase transitions and a latent heat release at different annealing temperatures together suggest a first-order nature of the phase transitions. In addition, the structure evolution in real space illustrates that the enhancement of cluster connectivity plays essential roles in the early stage of the phase transformation. In addtion, we also use a specific model to fit the SAXS data, the results of model fitting are in good agreement with the experimental results. To sum up, our results suggest that the occurrence of the phase transformation in such an unusual pathway enables different value of free energy in this system. It is not a process of free energy decreasing step by step, which would be a universal behavior for alloys of excellent glass-forming ability.

15:30-16:10 Tea Break

16:10-16:35 Invited

Middle Range Ordering of Zr-Based Amorphous Alloys

Kazumasa Sugiyama, Toru Kawamata, Tohoku University, Japan

The atomic ordering in both the short-range region and the middle-range region in amorphous alloys is known to be correlated with unique material properties. As an example, the icosahedral and icosahedral-like local atomic arrangement is suggested to be one of the unique topological short range orderings (TSROs) in the case of Zr-based bulk amorphous alloys and such icosahedral-like TSRO is also discussed with the crystallization behavior of the quasi-crystalline phase. In addition, some researchers have developed an idea that TSRO is associated with the solute-centered chemical short range ordering (CSRO) together with the formation of the middle range ordering (MRO). However, the picture of the atomic ordering reaching to next shell of the first nearest neighbor region, has not been fully revealed yet.

In order to analyze the detailed structure of amorphous alloys, anomalous X-ray scattering (AXS) method is a powerful diffraction technique, which allows us to obtain the environmental structural information of constituents. Further application of the reverse Monte-Carlo (RMC) simulation serves a reasonable three dimensional structural image with respect to TSRO and CSRO. Recently, we have developed a new approach for describing structural features of amorphous alloys on the bases of classical Bernal polyhedral units and the combinatorial analysis of AXS-RMC and this approach is useful to elucidate MRO which could not be reproduced in the dense packing sphere model. For example, the present analytical approach revealed that the non-Bernal typed TSRO is associated with the medium range ordering of Pt-Pt pair in Zr80Pt20 amorphous alloy. And these geometrical features appears to be similar to those in Mackay clusters found in the crystalline approximants for the icosahedral phase, in particular.

The present paper introduces AXS-RMC analysis for the amorphous alloys together with corresponding evaluation methods. Some selected examples of the structural analysis for Zr-based amorphous alloys are also demonstrated together with their features in SRO and MRO.

16:35-16:55

Does Structure Determine Property in Amorphous Solids: A General Atomistic View

Yunjiang Wang, Institute of Mechanics, Chinese Academy of Sciences, China

What determines the glass properties remains an unsolved major problem in both condensed matter physics and materials science. Despite extensive works have been done trying to identify possible structural motifs in glasses which govern properties, obeying the conventional philosophy of "structure determines property" in matters, the hidden rule about why some proposed structures predict properties effectively but others do not is still not thoroughly revealed. Here we revisit some earlier proposed successful 'structural motifs', such as vibrational mean-square displacement, flexibility volume, phonon low-frequency participation fraction, and two-body excess entropy, correlating them with the system's long-time property probed via the local activation energy for athermal and thermally activated atom rearrangement from the potential energy landscape. We find that all the four structures correlate strongly with activation energy, presenting large Pearson's correlation coefficients. By examining the spatial feature

and auto-correlation function of the activation energy and structure motifs, a common nature comes up that there exists a critically characteristic correlation length up to nanometer, which is far beyond the short-range order of glassy structure. We further demonstrate the concept of long-range order, or complex structure determining property by manipulating the cutoff distance used to define the two-body excess entropy. Only if this structure feature is defined beyond the short-range order, it reproduces the long-range spatial correlation feature. Our findings question the prevailing approach of materials science aimed at identifying simple structural motifs responsible for glass properties. The presence of a common correlation length strongly indicates that it is a necessity to take into account the spatial correlation of a complex super-structure in medium-, or long-range order for the dynamic property of general glassy materials.

16:55-17:15

Local-Structure Change Rendered by Electronic Localization–Delocalization Transition in Ce-Based Metallic Glasses

Qiang Luo, Southeast University, China

The metallic bonding nature endows metallic glasses (MGs) with densely-packed structure and unique local atomic configuration, which leads to many superior mechanical, magnetic and chemical properties. The solute-centered atomic clusters are considered as the basic building blocks of MGs, but their packing schemes to form medium-range order (MRO) structures remain elusive. The local structure change of MG with composition has been intensively investigated, focusing on glass formation and material design with required properties. Besides, temperature and pressure have been used to tune the short-range order (SRO), MRO and properties of MGs. The investigation of structure change with temperature is mainly focused on glass transition and crystallization events in MGs. Recently, pressure induced amorphous-to-amorphous transition has been reported in some rare earth-based MGs, which originates from the change of 4f electronic configuration, which attracts intensive interest. These works indicate a significant impact of electronic configuration on the structure of MGs and offer a new perspective of the amorphous configuration of MGs. Actually, since the work of Nagel and Tauc, it has been realized that the electronic configuration near the Fermi level correlates with the glass forming ability of MGs. Moreover it was found that the strength and ductility of MGs depended on the detailed features of s-character/pd-hybrid bonds. The correlation between atomic structure and electronic configuration underpins our understanding of the nature of MGs, which is still a longstanding challenge. Here we report, at ambient pressure and below room temperature, a novel local-structure change of topological and chemical short-range orders, along with an unusual large volume shrinkage in two Ce-based MGs. The Ce L3-edge X-ray absorption spectroscopy (XAS) measurements, along with results of the Ce2p3d resonant inelastic X-ray scattering (RIXS) spectra showing well-resolved features of the unoccupied (f0) and singly (f1) and doubly (f2) occupied 4f states, uncover a 4f-electron localization-to-delocalization transition as the main mechanism of the abnormal local-structure change and unusual large volume contraction.

17:15-17:35

Enhanced Kinetic Stability of a Bulk Metallic Glass by High Pressure

Rongjie Xue, Jiangsu University of Technology, China / Institute of Physics, Chinese Academy of Sciences, China; Linzhi Zhao, Chenglong Shi, Xuekui Xi, Meng Gao, Ping Wen, Xiaohui Yu, Changqin Jin, Mingxiang Pan, Haiyang Bai, Weihua Wang, Institute of Physics, Chinese Academy of Sciences, China; Teng Ma, Institute of Physics, Chinese Academy of Sciences, China / Jilin University, China; Pingwen Zhu, Jilin University, China

Owing to the metastable nature of metallic glasses (MGs), the lack of stability of MGs has hindered their applications. We report the formation of an ultrastable Pd-based MG with bulk size of 3mm in diameter and 3mm in length under high pressure at room temperature. The ultrastable MG shows remarkably enhanced thermal and kinetic stability with substantially increased glass transition temperature Tg (11K increased under 17GPa), crystallization temperature Tx (11K increased under 17GPa), density (1% increased under 17GPa) and hardness (8% increased under 17GPa). The unique thermal and kinetic stability can be further reinforced by higher pressure and maintained even at high temperature conditions. High pressure squeezes atoms, changes local electronic states, local electronic band structure, and heightens the potential energy landscape barriers that restrict atomic mobility. The 63Cu nuclear magnetic resonance isotropic shift reveals that the local electronic states and the local electronic band structure have changed during high pressure processing, and this could be the physical mechanisms underlying the enhanced thermal and kinetic stability. This result provides a unique and effective method to produce bulk ultrastabl emetallic glasses with excellent properties, which could advance the glass design and the understanding of fundamental issues in glasses.

J. Amorphous and High Entropy Alloys: High Entropy Alloys I

Symposium organizers:

Weihua Wang, The Institute of Physics, Chinese Academy of Sciences, China; Zhaoping Lv, University of Science and Technology Beijing, China; Hidemi Kato, Tohoku University, Japan; Hojin Ryu, Korea Advanced Institute of Science and Technology (KAIST), Korea; Michael Ferry, New South Wales, Australia; Evan Ma, Johns Hopkins University, USA

Monday PM
August 19, 2019

Room: 303 (3rd Floor)
Symposium: J

Chairs:
Yong Yang, City University of Hong Kong, China
Rajarshi Banerjee, University of North Texas, America

13:30-14:00 Keynote

Self and Interdiffusion in High Entropy Alloys: What We Now Know

Irina Belova, Mohhamad Afikuzzaman, Graeme Murch, The University of Newcastle, Australia

High entropy alloys (HEAs) are a novel class of materials with many atomic components (between 5 and 13) at about equal compositions. One of the important properties of HEAs is slow mass diffusion. This should be vital for enhancing the apparent stability of HEAs as well as their high-temperature technological applications. In this overview, recent experimental and theoretical findings of diffusion in HEAs are presented and discussed. The discussion concentrates on the tracer (or self-) diffusion and inter- diffusion (quasi-binary diffusion couple technique in chemical gradients). The newly developed combination of the standard interdiffusion and radiotracer diffusion technique is also discussed. This technique allows for measurement of tracer diffusion as a function of composition in the interdiffusion sample.
From a theoretical point of view, the diffusion kinetics behaviour of the Onsager phenomenological transport coefficients, interdiffusion coefficients and tracer diffusion coefficients of atomic components in multicomponent alloys is discussed. These are investigated by extending and applying three classical diffusion kinetics approaches in the model case of fcc CoCrFeMnNi HEA. In the case of this alloy, the combined analysis of tracer diffusion coefficients with interdiffusion coefficients is also presented. Furthermore, extensive Kinetic Monte Carlo (KMC) simulation results are used for the testing of the possible interdiffusion composition profiles in a model HEA.

14:00-14:25 Invited

Large-Area Synthesis of Freestanding Ultra-Thin Films of Complex Alloys: from Amorphous to High Entropy Alloys

Yong Yang, Tianyu Wang, City University of Hong Kong, China

In this talk, we would like to present a novel and facile method to synthesize freestanding ultra-thin films of complex alloys. This is done through a series of well controlled preparation of hydrogels which have a nanometer scale surface roughness and are bonded to silicon wafers within a carefully selected temperature-time window. Afterwards, metal films are deposited onto the hydrogels through inert gas condensation to form a metal-polymer multilayer. such that a cleave fracture can be triggered along the metal-hydrogel interface once the hydrogels are soaked in water for a limited period of time. The film thickness so obtained can be varied from nanometers to micrometers while the film width can span from a few hundred micrometers to a few centimeters. With the aid of finite element simulations, theoretical modeling and experiments, we also discuss the limitations of this method, focusing on the underlying mechanistic understanding of the interfacial fracture process, which is related to the combined effect of elastic mismatch and toughness of films, hydrogel and their interface. As a demonstration, we will present a few freestanding films of amorphous and high entropy alloys and briefly discuss their structures and basic mechanical properties. In principle, our methods can be extended to diverse materials systems, including molecular glasses, polymers and ceramics. On one hand, the freestanding thin films so obtained provide the model systems to understand the physical/chemical behavior of amorphous and high entropy alloys in a nearly two dimensional space, which is very useful to deepen our understanding of the longstanding issues, such as glass transition, mechanical size effect, surface effect, oxidation and corrosion, which has never been done before with freestanding films; on the other hand, the freestanding thin films could have extensive potential use in a variety of applications, ranging from optical devices, micro-electro-mechanical systems, lubrication and catalysts.

14:25-14:50 Invited

Study on Thermodynamic Properties of High Entropy Alloys

Hiroshi Ohtani, Masanori Enoki, Tohoku University, Japan

The objective of the present study is to clarify the thermodynamic properties inherent to the high entropy alloys (HEA) by means of free energy calculations based on the first principles technique. For the

computational method, we employed the cluster variation method (CVM) in which the ordered structures of the base solid solution were divided into various clusters, and the interatomic energies for those clusters were evaluated using the cluster expansion method. The free energy at finite temperatures were calculated from the configurational entropy and internal energies. Understanding of the formation tendency for ordered structures is also significant in HEA, hence the stable structures in the ground state were calculated using the genetic algorithm. In this method, many random structures were generated from the component elements at the beginning. Then structural relaxation was performed on each structure using the first principles technique, and variation operators such as heredity, mutation, permutation, and so on were used to generate offspring from the stable structures. These calculations were repeated until the simulation reached the convergence criteria for the most stable structures. The calculated enthalpies of formation in the ternary and the quaternary systems constituting the Cr-Mn-Fe-Co-Ni alloy indicates that the interactions between neighboring atoms could be almost negligible. On the other hand, the mixing entropy was approximately equal to that of the complete disordered state. These results indicate that this alloy behaves as an ideal solution. Furthermore, the calculation by the genetic algorithm clarified that the formation of compound phases was restricted in each component ternary system. Some other evaluated alloys in which a solid solution appears at the equiatomic compositions showed the similar behavior to that of the Cr-Mn-Fe-Co-Ni alloy.

14:50-15:10

FCC to L12 Ordering Transformation in Equimolar FeCoNiV High-Entropy Alloy

Shubin Wang, Shihao Chen, Da Shu, Yongbing Dai, Baode Sun, Shanghai Jiao Tong University, China; Fuyang Tian, University of Science and Technology Beijing, China

The ordered L12 phase generally appears as dispersed precipitates in FCC high-entropy alloys. In this work, a single L12 ordered intermetallic is obtained in the annealed equimolar FeCoNiV solid solution alloy. Experiments show that the FCC to L12 ordering transformation occurs below 778˚C, accompanied by lattice contraction, anti-phase boundaries formation and low-temperature magnetic moment decrease. The L12 ordered alloy exhibits strong linear strain hardening rate up to 5.0GPa during the tensile deformation at room temperature, meanwhile, keeps 20% tensile elongation, although the yield strength is not significantly changed. The ab initio calculations based on the exact muffin-tin orbitals in combination with coherent potential approximation (EMTO-CPA) predict that V atoms prefer to occupy the cubic corner sites of L12 sublattice, and the FCC phase becomes more stable with respect to L12 phase above 849˚C considering the competition between enthalpy and entropy. The ab initio molecular dynamic simulations (AIMD) indicate that V atoms prefer to bond with the unlike atoms (Fe, Co and Ni) in liquid FeCoNiV, which is consistent with the cubic corner site occupation of V in L12 ordered structure. The present work demonstrates a new design strategy of high-entropy alloys which focus on single phase ductile intermetallic compounds.

15:10-15:30

Development of High Performance Co-Rich High Entropy Alloys

Daixiu Wei, Weicheng Heng, Yuichiro Koizumi, Hidemi Kato, Akihiko Chiba, Tohoku University, Japan; Xiaoqing Li, KTH-Royal Institute of Technology, Sweden; Won-Mi Choi, Byeong-Joo Lee, Hyoung Seop Kim, Pohan University of Science and Technology, Korea

Equiatomic FeCoCrNi high entropy alloys (HEAs) have attracted extensive academic interests. Recently, twinning-induced plasticity (TWIP) and transformation-induced plasticity assisted dual phase (TRIP-DP) non-equiatomic Fe-rich HEAs were developed, inspired by the plasticity and strengthening mechanisms in low stacking fault energy (SFE) metals and alloys. The two types of HEAs exhibit high tensile strengths and large elongations that overcome the strength-ductility trade-off. The low SFE of the alloys are gained from tuning the chemical compositions and concentrations. On the other hand, Co-based superalloys have been widely used in manufacturing vanes and metallic orthopedic implants, owing to the superior mechanical properties and corrosion resistance. Generally, the SFE of these alloys is extremely low, reaching negative values at room temperature for some compositions.

In the present study, we designed novel Co-rich HEAs with manipulated mechanical properties and deformation behaviors by lowering the SFE and the fcc phase stability, achieved by adjusting the elemental concentrations of the equiatomic CoCrFeNi alloy. We adopted quaternary HEAs described as CoxCr25(FeNi)75-x (x= 25, 35, 45, 55, 65). The Gibbs free energy difference between hcp phase and fcc phase of the various alloys, were calculated using Thermo-Calc software with the TCFE2000 thermodynamic database and its upgraded version. The generalized stacking fault energy of the alloys were calculated by ab initio calculations based on density functional theory (DFT) method, and the Kohn-Sham equations were solved using the exact muffin-tin orbitals method (EMTO).

The results indicated that an increase in Co content leads to a decrease in fcc phase (γ phase) stability in the CoxCr25(FeNi)75-x alloys. Moreover, γ phase is more stable at elevated temperatures whereas the hcp phase

(ε phase) tends to be more stable at lower temperatures. On the other hand, It was found that the Fe and Ni stabilize the γ phase in the alloys, and In independent reduction of Ni concentration or an increase in the Co concentration does significantly lower the SFE. Among the alloys, the Co35Cr25Fe20Ni20 and Co45Cr25Fe15Ni15 alloys with metastable single fcc phase possess superior combination of strength and ductility compared to other single fcc phase counterparts, contributing to the TWIP and TRIP effect, respectively. The findings here provide a feasible guideline for developing high performance HEAs.

15:30-16:10 Tea Break

16:10-16:35 Invited

Effect of Co Content on the Mechanical Properties of A2 and B2 Phases in AlCoxCrFeNi High-Entropy Alloys

Young-Sang Na, Ka-Ram Lim, Jong-Woo Won, Heoun-Jun Kwon, Korea Institute of Materials Science, Korea; MinJu Kang, Johns Hopkins University, USA

High entropy alloys are now offering new explorable topics and strategies to physical metallurgist since the first announcement of its concept by B. Cantor and J.W.Yeh, separately. High entropy alloys are no longer limited to a single phase system even if it was first suggested that single solid solution like FCC-structured CoCrFeMnNi would be stabilized due to the high entropy effect. Actually, second phases like precipitate is regarded to be essential in metallic systems for strengthening. We dealt with dual-phase high entropy alloys with BCC structure, in this study.
AlCoCrFeNi-based high entropy alloys such as AlxCoCrFeNi, and AlCoCrFeNiTix have been studied as representative BCC HEAs. Despite their high strength and wear resistance, there are practical problems due to the high cost of the alloying elements. In particular, Co is more than six times as expensive as the other elements, and is becoming even more expensive with the growth of the secondary cell industry.
In this study, the effect of Co content on the strengths of the A2 and B2 phases in AlCoxCrFeNi high entropy alloys was investigated. The strength of AlCoxCrFeNi (x=0, 0.25, 0.5, 0.75, and i) was considerably reduced when the Co content was zero. This was attributed to the low hardness of the A2 phase due to reduced configurational entropy. On the other hand, the ordered B2 phase showed the opposite tendency. In summary, AlCoxCrFeNi (x=0.25, 0.5, 0.75, and ii) high entropy alloys showed improved compressive properties as the Co content decreased; however, Co0 exhibited a large drop in yield strength. The subtraction of Co decreased the entropy of the A2 and B2 phases. Lower entropy resulted in the decreased and increased hardness of the disordered and ordered phases, respectively. This result shows that the configurational entropy causes opposing effects on disordered and ordered phases, and the importance of considering the effects of elements and entropy on each phase when an alloy is composed of two or more phases.

16:35-17:00 Invited

Competition Between L12 and B2/L21 Precipitation in FCC Based High Entropy Alloys: Multi-scale Microstructures and Tuning Mechanical Properties

Rajarshi Banerjee, Sriswaroop Dasari, Bharat Gwalani, Talukder Alam, University of north texas, America; Yao-Jen Chang, An-Chou Yeh, National Tsinghua University, Taiwan, China; Stephane Gorsse, CNRS, ICMCB, UPR 9048, 33600 Pessac, France

Often the experimentally observed single phase high entropy alloy (HEA) is the result of second phase precipitation constrained by thermodynamic and kinetic factors. This raises some fundamental questions regarding the impact of thermo-mechanical processing on the phase transformation pathways in these HEAs. These pathways lead to different combinations of phases, at multiple length scales, within these alloys. This presentation will focus on investigating and rationalizing how such transformation pathways can dramatically alter the microstructure and mechanical properties in face-centered cubic (FCC) based HEAs. Example systems to be considered include FCC-based 3d transition series alloys, such as Al0.3CoCrFeNi, Al0.5Co1.5CrFeNi1.5, and Al0.2Ti0.3Co1.5CrFeNi1.5. All these alloys inherently exhibit a competition between the precipitation of different ordered intermetallic phases, such as the L12, B2, and L21, within the FCC solid solution matrix. The thermodynamic rationale underlying such competition is the complex interplay between the driving force and the nucleation barrier associated with each of these phases. This interplay will be investigated in detail as a function of different thermo-mechanical treatments, resulting in differences in the homogeneous versus heterogeneous nucleation of the intermetallic phases. The resultant microstructural diversity within the same HEA can lead to dramatically different mechanical properties, as aspect which can be used for tuning their properties for various applications.

17:00-17:20

Design of D022 Superlattice with Superior Strengthening Effect in High Entropy Alloys

Feng He, Da Chen, Bin Han, C.T. Liu, Ji-jung Kai, City University of Hong Kong, Hong Kong, China; Feng He, Qingfeng Wu, Zhijun Wang, Northwestern Polytechnical University, China; Shaolou Wei, Massachusetts Institute of Technology, USA; Daixiu Wei, Tohoku University, Japan

High entropy alloys (HEAs) with face centered cubic (FCC) crystal structure have attracted broad scientific

interests by showing excellent toughness at both room and cryogenic temperatures. Their yield strength, however, is too low for structural applications, and thus the precipitation-strengthening of FCC HEAs has been widely investigated. The L12 phase-strengthened HEAs keep good ductility but possess modest yield strength. The intermetallic particles lead to high yield strength but relatively bad ductility. Therefore, designing a better reinforcing phase is of great importance for precipitation-strengthened HEAs. In the present work, we demonstrated an overall valence electron concentration (OVEC) strategy to design reinforcing precipitates with excellent strengthening effect. A D022 phase-strengthened HEA has been developed by using the OVEC strategy. Nano-size lenticular precipitates with D022 structure were obtained in a novel Ni2CoCrFeNb0.15 HEA. Different from traditional Ni3Nb-type D022 phase, the current high-entropy D022 phase possesses an stoichiometry of (Ni,Co,Cr,Fe)3(Nb,Fe). TEM inspection indicated there are three different variants with crystallographic orientation relationships of [001]γ"//<001>γ and (001) γ″ //{100}γ. The high-entropy D022 phase showed excellent strengthening effect. A small volume fraction of D022 phase (~7%) caused an increase of 670MPa in yield strength, resulting superior yield strength-ductility combination among precipitation-strengthened HEAs. The superb strengthening effect of D022 phase was attributed to the combination of ordering strengthening and coherency strengthening. Our results provided a convenient strategy to design reinforcing phase for HEAs and developed a promising D022-strengthened HEA for structural applications. These findings will not only benefit the development of precipitation-hardened HEAs but deepen the fundamentals of the precipitates design for other complex concentrated alloys as well.

17:20-17:40

Effect of Stacking Fault Energy on Deformation Behavior of AlCoCrFeNi-Based High-Entropy Alloy Thin Film

Seungjin Nam, Hyunjoo Choi, Kookmin University, Koera; Se Hoon Kim, Korea Automotive Technology Institute, Korea

High-entropy alloy (HEA) has been widely investigated as novel alloy materials composed of at least five principal elements with equiatomic or near-equiatomic ratio. Induced from atomic size difference of the alloying elements, severe lattice distortion can result in enhancement of strength and suppression of atomic diffusion at high temperatures. Interestingly, HEAs have revealed outstanding fracture toughness even at cryogenic temperatures due to their low stacking fault energy (SFE). The SFE plays an important role for deformation behavior of HEAs, wherein deformation twinning can be activated in the alloys with a decrease of the SFE. Since the SFE of HEAs is varied depending on their composition, the compositional effect on deformation behavior have been widely investigated in the bulk or powder metallurgy HEA materials. However, there have been limited systematic studies on relation between the SFE and deformation behavior because of the non-homogeneous microstructures and elemental distributions induced during fabrication processes. In this study, we investigated the deformation behavior in a series of AlCoCrFeNi-based HEAs with various composition produced via multilayer deposition. After deposition of multilayer films on wafers using E-beam evaporation, heat treatment was conducted to form equilibrium phases under a high vacuum (~ 10^{-6} torr) at high temperatures. The phase formed in the heat-treated films was determined using grazing incidence X-ray diffraction (GIXRD). While a solid solution phase with a face-centered cubic (FCC) structure was identified regardless of the composition, sigma phase was formed in films with high concentration of Cr. Furthermore, nano-indentation was utilized to evaluate the mechanical properties of the film. In order to determine the deformation behavior of films, the microstructure was observed using transmission electron microscopy (TEM) from the specimen prepared on the deformed area using focused ion beam (FIB) technique. Hence, the evolution of microstructures and deformation behavior of HEAs will be discussed with consideration of the SFE.

17:40-18:00

Effects of Al Addition on Hot Deformation Behavior and Processing Maps of CoCrFeMnNi High Entropy Alloy

Hee-Tae Jeong, Woo-Jin Kim, Hongik University, Korea; Hyung-Ki Park, Kwangsuk Park, Tae-Wook Na, Korea Institute of Industrial Technology, Korea

The high-temperature deformation mechanism and processing maps of cast Al0.5CoCrFeMnNi that comprises FCC and BCC phases (where BCC phase is a minor phase) were studied at temperatures in the range of 1023 to 1323K and at strain rates in the range of $10s^{-3}$ to $101s^{-1}$. During hot compression, the hard BCC phase provided nucleation sites for dynamically recrystallized (DRXed) grains in the soft FCC matrix through particle stimulated nucleation (PSN). Continuous dynamic recrystallization (CDRX) simultaneously occurred with the PSN-induced DRX. As a result, the fraction of DRXed grains was notably higher and the size of the DRXed grain size was considerably smaller in Al0.5CoCrFeMnNi than those in CoCrFeMnNi with a single FCC phase. The effect of the BCC phase on the fraction of DRXed grains was especially pronounced at high strain rates ($10s^{-1}$), which is important for the practical use of cast Al0.5CoCrFeMnNi

in the hot-working industry. Solute drag creep appeared at low strain rates and at high temperatures as the rate-controlling deformation mechanism due to the presence of Al solutes in the FCC matrix. The activation energy for plastic flow associated with solute drag creep was measured to be 251kJ/mole. This value most likely represents the activation energy for the interdiffusivity of aluminum solutes in Al0.5CoCrFeMnNi. The solute drag creep behavior could be predicted by the Weertman model, indicating that AlCoCrFeMnNi behaves similar to a typical class I solid solution metal alloy.
By adding aluminum to CoCrFeMnNi, the hot workability was greatly improved, according to the processing maps and microstructure analysis. The power dissipation efficiency was increased, and the flow instability regime decreased in size. The instability disappeared at $10s^{-1}$ and at 1323K in Al0.5CoCrFeMnNi, agreeing with the microstructural evidence for the occurrence of a considerable extent of DRX at the corresponding condition.

K. Nanocrystalline Materials, and Ultra-Fine Grained Materials: I

Symposium Organizers:

Yue Zhang, University of Science and Technology Beijing, China; Zhiyong Tang, National Center for Nanoscience and Technology, China; Nobuhiro Tsuji, Kyoto University, Japan; Jae-il Jang, Hanyang University, Korea; Kenong Xia, University of Melbourne, Australia; Nathan Mara, University of Minnesota, USA

Monday PM
August 19, 2019

Room: 309(3rd Floor)
Symposium: K

Chairs:
Jin-Yoo Suh, Korea Institute of Science and Technology, Korea
Kenji Higashida, Kyushu University, now at National Institute of Technology, Japan

13:30-14:00 Keynote

Effect of Grain Refinement Due to Severe Plastic Deformation on the Brittle-to-Ductile Transition in a Low Carbon Steel

Kenji Higashida, Kyushu University, now at National Institute of Technology, Sasebo College, Japan, Masaki Tanaka, Kyushu University, Japan; Tomotsugu Shimokawa, Kanazawa University, Japan

Brittle fracture of materials is a major concern for the safety in their structural application.Since dislocations in bcc crystals have rather high Peierls potential, plastic behaviors in those crystals highly depend on deformation temperatures. They fail in a brittle manner at low temperatures, but they tend to be ductile with increasing temperature. This is termed brittle-to-ductile transition (BDT). The mechanism behind this phenomenon has been investigated from the view point of the crack-dislocation interaction. An explanation for the transition is made by the crack-tip shielding due to dislocations, where the internal stress field of the dislocations emitted around the crack-tip shields the crack-tip stress intensity. This means that the stress intensity due to the dislocations generated around the crack-tip relieves the external applied stress concentration around the crack-tip. The stress relieving process due to crack-tip shielding depends on dislocation mobility as well as dislocation source densities,Grain refinement due to severe plastic deformation (SPD) has attracted much attention because materials with ultra-fine grained structures demonstrate remarkable increase not only in yield strength but also in fracture toughness at low temperatures. However, the fundamental mechanism behind the both enhancements of strength and ductility in fine-grained structures has been still ambiguous. In the present study, it was attempted to reveal the mechanism of the enhancement of toughness at low temperatures after the SPD process. The dependence of the BDT on the grain size will be discussed, basing on the crack-tip shielding theory.

14:00-14:25 Invited

Accumulated Roll Bonding of High Cr Steel at Elevated Temperatures

Jin-Yoo Suh, ae-Hyeok Shim, Korea Institute of Science and Technology, Korea; Min Seong Kim, Shi-Hoon Choi, Sunchon National University, Korea

Martensitic stainless steels with high carbon and chromium contents are characterized by the combination of superior strength and corrosion resistance. The inherent brittleness of the steel could be alleviated by tempering process but the unavoidably accompanying loss in strength might be unacceptable for some applications. In such a context, there have been some efforts to create a multilayered structure of a martensitic steel and a ductile metal to secure the maximum strength and reasonable ductility simultaneously. However, in this study, we studied the multilayered structure composed of only one martensitic steel roll-bonded at elevated temperature to check the feasibility of the microstructural and mechanical optimization of the multilayered steel plate.
Multilayered 0.8C-15Cr martensitic steel plate was produced by utilizing the concept of accumulated roll bonding at elevated temperature up to 3 times to result in 8 layers. Because of the rolling temperature as high as the austenite region, highly accumulated strain together with the repeated phase transformation produced a fine-grained structure. Also, the decarburization of surfaces

taking place right before the roll-bonding process resulted in carbon-depleted layers with lower hardness in between the layers of the initial steel composition. To further tailor the microstructure and mechanical behavior, heat treatment at different temperatures, 1073, 1123, 1173, and 1223K was carried out. Microstructure and mechanical behavior characterized by SEM-EBSD and microhardenss-tensile test, respectively, will be discussed in the presenation to further present the properties of the high-strength multilayered steel.

14:25-14:50 Invited

Strength–Ductility Balance in an Ultrafine-Grained Non-Equiatomic Fe50(CoCrMnNi)50 Medium-Entropy Alloy with a Fully Recrystallized Microstructure

Nokeun Park, Minku Choi, Ibrahim Ondicho, Yeungnam University, Korea; Nobuhiro Tsuji, Kyoto University, Japan

High-entropy alloys (HEAs) contain five or more principal elements in a concentration range of 5~35at.%. Recent studies have revealed CoCrFeMnNi has a single FCC phase when annealed at temperatures above 800˚c, but second-phase precipitates are formed when it is annealed below this temperature. In this study, we explored the phase stability and mechanical properties of an ultrafine-grained non-equiatomic Fe50(CoCrMnNi)50 medium-entropy alloy (MEA). The alloy was processed by conventional cold rolling and then annealed at temperatures between 500˚c and 800˚c. X-ray diffraction revealed that this alloy has a single face-centered cubic structure even below 800˚c, where the equiatomic CoCrFeMnNi mostly forms second phases. The kinetics of recrystallization of this alloy demonstrated that a fully recrystallized microstructure with an ultrafine grain size of 0.97μm is achieved after annealing at 600˚c for 1h. The experimental data show excellent agreement with the JMAK theoretical model, with the recrystallized exponent m = 1.6 indicating that the kinetics of recrystallization in this alloy are slow. This might be due to the sluggish effect of multicomponent alloys and low annealing temperature. Tensile results further revealed that this alloy displays an excellent combination of strength and ductility with YS, UTS, and TE of 550MPa, 700 MPa, 51%, respectively, although it contains a UFG microstructure. It is imperative to note that the alloy was processed using conventional cold rolling and annealing which are practically applicable in the industry unlike severe plastic deformation techniques.A discontinuous yielding phenomenon was observed in both partially recrystallized and fully recrystallized UFG specimens. In the partially recrystallized specimens, discontinuous yielding resulted from pre-existing dislocations and the partially recrystallized UFG specimen, although this combined effect is still weaker than that observed in a fully recrystallized UFG specimen. In the fully recrystallized specimen, the discontinuous yielding was caused by the fully UFG microstructure, which requires a higher stress to nucleate new dislocations.

14:50-15:10

Application of Harmonic Structure Design to a Medium Carbon Steel

Ryohei Iritani, Kenta Hori, Mie Kawabata, Ristumeikan University, France; Guy Dirras, David Tingaud, Université Paris 13, France

Harmonic structure (HS) design is one of the heterogeneous microstructure design, and it is heterogeneous on micro- but homogeneous on macro-scales. In the present work, the HS design has been applied to an Fe-0.3mass%C steel, via a powder metallurgy route consisting of controlled severe plastic deformation of the corresponding powder and subsequent consolidation. By mechanical milling (MM) process, i.e., a severe plastic deformation - powder metallurgy (SPD-PM) process, nano ferritic grains formed in the surface region of the powder while a coarse grain structure was maintained in the middle of the powder. Increase of austenite phase was observed especially in the Shell-network structure after sintering. It is noteworthy that acceleration of the austenite phase nucleation took place in the nano grain region, and it resulted in the Shell structure. Subsequent heat treatments of the compacts resulted in a microstructure with tempered martensite Shell-network and ferrite/tempered martensite Core. Those sintered compacts with appropriate heat treatments showed superior mechanical properties such as high strength with ductility compared to the homogeneous microstructure counterparts. This behavior was essentially related to the ability of the HS to promote the uniform distribution of strain during plastic deformation, leading to improved mechanical properties by avoiding or delaying localized plastic instability. In other words, the characteristic "micro-scale stress concentration" and "macro-scale stress dispersion" by the Shell-network structure are assumed to lead a large work hardening and a constraint of the deformation localization.

This work was supported by JSPS KAKENHI Grant Number JP18H05256 and the JFE 21st Century Foundation. These supports are gratefully acknowledged.

15:10-15:30

Effect of Grain Size on Hydrogen Embrittlement of Ultrafine-Grained Iron Processed by High-Pressure Torsion

Hideaki Iwaoka, Shuhei Morimoto, Shoichi Hirosawa, Yokohama National University, Japan

Hydrogen embrittlement is a phenomenon in which

hydrogen atoms intrude into a metal, thereby the mechanical properties of the metal is decreased and the metal becomes brittle. It is considered that the mechanism of hydrogen embrittlement is closely related to lattice defects. In the case of dislocations, it is reported that hydrogen atoms promote movement of dislocations and enhance plastic deformation at vicinity of a crack tip by localization of shear strain. On the other hand, as for grain boundaries which also control deformation and fracture of metals, detailed research of effect on hydrogen embrittlement has not been carried out sufficiently. Therefore, we conducted tensile tests while hydrogen charging for an ultrafine-grained iron processed by high-pressure torsion (HPT) and investigated the effect of grain boundaries on hydrogen embrittlement.Pure iron (99.99% purity) discs were annealed at 1173K for 3h and processed by HPT under a pressure of 1.5GPa for 5 turns. The HPT samples were heat-treated at various temperatures from 225 to 350℃ to change the grain size. Tensile tests were conducted for these samples while cathodic hydrogen charging in NaOH electrolytic solution. The fracture surface and fracture part of tensile specimen were observed by scanning electron microscope (SEM) and laser microscopy, respectively.

The tensile strength of HPT sample without hydrogen charging is significantly improved by grain refinement and the elongation is decreased. The grain coarsening is occurred by heat treatment after HPT processing, thereby the tensile strength degrades and the elongation recovers. The elongation of these samples is decreased by hydrogen charging, which indicates that hydrogen embrittlement was occurred. The reduction of area obtained from observation of fracture surface also shows degradation of ductility by hydrogen charging. Especially in the HPT samples heat-treated over 275℃, the fracture type changes and the reduction of area is rapidly decreased. It is revealed that hydrogen embrittlement of ultrafine-grained iron is affected by grain size.

15:30-16:10 Tea Break

16:10-16:30

Fabrication of Ultrafine Grained Fe-24Ni-0.3C without Severe Plastic Deformation

Wenqi Mao, Si Gao, Kyoto University, Japan; Gao, Myeong-Hoem Park,Yu BAI, Akinobu Shibata, Nobuhiro Tsuji, Kyoto University, Elements Strategy Initiative for Structural Materials, Japan

It has been reported that metastable austenitic steels having ultrafine grained (UFG) microstructures can be fabricated simply by cold rolling (CR) and subsequent annealing without very high strains, using deformation induced martensitic transformation and its reverse transformation to austenite. However, the efficiency of grain refinement in this method greatly depends on the amount of martensite formed during CR. In a previous study by the present authors, the minimum grain size obtained by CR and subsequent annealing was 1.3μm in an Fe-24Ni-0.3C alloy, due to limited amount of martensite formed by CR. In order to fabricate UFG Fe-24Ni-0.3C having sub-micrometer grain sizes, an attempt has been made in the present study to accelerate the formation of deformation induced martensite during CR by increasing dislocation density in starting material via ,repetitive martensitic transformation cycles. Repetitive rolling and annealing processes were performed on the Fe-24Ni-0.3C alloy. The starting plate having a thickness of 20mm was firstly subjected to sub-zero quenching in liquid nitrogen to get thermally induced martensite, and then heated up to 600℃ for 30s in a salt bath followed by water quenching to get reversed austenite. Such transformation cycling was repeated for 5 times. Then the plate was cold rolled from 20mm to 10mm in thickness. In order to further reduce the grain size, the plate was subjected to another 5 times of the transformation cycling treatment and then cold rolled to 1mm in thickness. The cold rolled sheet was finally annealed at 650℃for 30s using a salt bath followed by water quenching. UFG Fe-24Ni-0.3C with a mean austenite grain size of 0.5μm was successfully fabricated by the simple repetition of cold rolling and annealing. According to microstructure observations at different stages of the process, the dislocation density of the material was significantly increased by the repetition of thermal martensitic transformation and reverse transformation. As a result, the deformation induced martensitic transformation during CR was greatly accelerated, which made an important attribution to the formation of UFG austenite. The UFG specimen exhibited an excellent combination of high strength along with good ductility (ultimate tensile strength of 1.1GPa and uniform elongation of 70%).

16:30-16:50

Ihomogeneous Deformation of Ultra-Fine Grained 304 Stainless Steel during Tensile Test

Si Gao, Yu Bai, Wenqi Mao, Akinobu Shibata, Nobuhiro Tsuji, Kyoto University, Japan; Ruixiao Zheng, Beihang University, China; Yanzhong Tian, Northeast University, China; Akinobu Shibata, Nobuhiro Tsuji , Kyoto University, Japan

Austenitic stainless steels (ASSs) exhibit excellent corrosion resistivity and deformability, but usually low yield strength around 300~400MPa due to their FCC structure. Previous studies have found that the ultra-fine grained (UFG) ASSs exhibit good combinations of strength and tensile ductility, as well as good fatigue properties, which make them prospective materials for future industrial applications. On the other hand,

unusual tensile behaviors have been sometimes observed in such UFG ASSs. Long stress plateaus after the yield-drop are often observed on tensile stress-strain curves of some UFG ASSs, which seems classical Lüders deformation that typically occurs in carbon steels. However, detailed mechanisms of such an unusual tensile behavior have not yet been made clear. The present study aims to clarify the mechanism of the prominant Lüders-like deformation for the first time, using an austenitic stainless steel having UFG microstructures fabricated by cold rolling and annealing processes.

A commercial 304 stainless steel having ultra-fine grained (UFG) microstructures with the minimum average grain size of 0.3 micro-meter was successfully fabricated by simple cold rolling and subsequent annealing processes. Tensile test at room temperature revealed excellent combinations of tensile strength and uniform elongation in the UFG specimens in comparison with the coarse grained counterpart, which was attributed to the grain refinement strengthening in austenite and the occurrence of deformation induced martensitic transformation during the tensile test. On the other hand, it was noteworthy that the UFG specimens exhibited yield point phenomena with Lüders-band-type inhomogeneous deformation while their coarse-grained counterparts showed continuous yielding with homogeneous deformation. The yield point phenomena became more prominent as the grain size decreased, accompanying with the dramatically increased Lüders strain which was precisely measured by the digital image correlation (DIC) technique. SEM-EBSD was employed to characterize the microstructures within the Lüders band. The prominent Lüders deformation was explained in terms of the grain size effect on early plastic instability (necking) of austenite and the enhanced strain hardening by the deformation induced martensitic transformation, which could be revealed by comparing the tensile behavior of the UFG specimen at room temperature and at elevated temperatures.

16:50-17:10

Mechanical Properties of Cu-Zn Binary Alloys with Various Grain Sizes

Zhangfan Deng, Yu Bai, Akinobu Shibata, Nobuhiro Tsuji, Kyoto University, Japan; Yu Bai, Myeong-heom Park, Akinobu Shibata, Nobuhiro Tsuji, Kyoto University, Japan

Grain refinement is an effective approach to enhance strength of metallic materials. However, tensile ductility usually decreases with increasing strength, which is known as a trade-off relationship between strength and ductility. On the other hand, some studies reported that face-centered cubic (FCC) alloys with low stacking fault energy (SFE) showed good balance of strength and ductility. Since the SFE could be controlled by addition of alloying elements, Cu alloys are appropriate to understand the fundamental deformation mechanisms of low-SFE FCC alloys showing good balance of mechanical properties. The deformation mechanism in Cu alloys has been conventionally focused on coarse-grained structures or nano-structures with deformed state. However, the mechanical properties of Cu alloys with fully recrystallized ultrafine-grained (UFG) microstructure have been rarely reported.

In the present study, Cu-10wt%Zn and Cu-30wt%Zn alloys with various average grain sizes ranging from 0.23μm to 12.2μm were fabricated by high pressure torsion (HPT) and subsequent annealing. Mechanical properties were evaluated by a uniaxial tensile test at room temperature. It was found that yield strength and tensile strength increased with decreasing the grain size in both alloys. The Cu-30Zn alloy exhibited higher yield strength and tensile strength than those in the Cu-10Zn alloy with similar grain sizes. In addition, the discontinuous yielding with a yield drop phenomenon, which is a unique behavior of UFG materials, occurred when the grain size was smaller than 0.69μm in the Cu-10Zn alloy, and the yield drop became sharper with decreasing the grain size. However, discontinuous yielding with a small yield drop was only observed in the Cu-30Zn alloy with the grain size of 0.23μm. In this presentation, the reason for the interesting mechanical behaviors in the Cu-Zn alloys, including difference in the yield drop in the UFG specimens will be discussed.

17:10-17:30

Microstructure Evolution in 99.9% Pure Copper and Cu-0.1Fe-0.03P Deformed by High-Strain Torsion at Various Temperatures

Reza Gholizadeh, Yu Bai, Akinobu Shibata, Nobuhiro Tsuji, Kyoto University, Japan

A pure copper with 99.9wt.% purity and a precipitate-containing copper alloy (Cu-0.1Fe-0.03P) were continuously deformed to high strains (> 6) by torsion. The deformation was carrid out at different temperatures ranging from room temperature to 650˚C, and the flow stress-strain data were measured simultaneously. Torsion specimens were water-quenched immediately after the deformation, and microstructures under various deformation conditions were investigated by electron back-scattering diffraction (EBSD) method and transmission electron microscopy (TEM). The EBSD measurements were carried out in a field emission scanning electron microscope (JEOL JSM 7100F), and the TEM observation was conducted in a TEM microscope (JEOL JEM 2010F) operated at 200kV. The observation section on the gage part of the round-bar specimen was normal to the radial direction at a radial distance of 0.9R from the center. The results showed that increase in the deformation temperature resulted in a gradual transition in microstructures. Firstly, the

deformation at low temperatures led to the formation of the ultrafine lamellar structures (< 1μm) which were caused by so-called grain subdivision mechanism. As the deformation temperature increased, however, the grain morphology changed to relatively equiaxed ones, and simultaneously the grain size increased and reached to several micrometers in the Cu-0.1Fe-0.03P alloy and several ten micrometers in the 99.9% pure copper. The increase in the grain size with increasing the deformation temperature was accompanied with a decrease in the flow stress, indicating that softening mechanisms such as boundary migration and dynamic recrystallization (DRX) became dominant during the deformation at elevated temperatures. Additionally, it was found that fine precipitates in the Cu-0.1Fe-0.03P alloy remarkably hindered grain growth and therefore the flow-stress softening, compared to those in the pure copper. Different mechanisms of the microstructure evolution, e.g., the grain subdivision at low temperatures and the grain growth and DRX at elevated temperatures, in the heavily deformed coppers with and without precipitates will be discussed in details: G.H. Xiao, N.R. Tao, K. Lu, Scripta Materialia, 65 (2011) 119-122.

L. Computational Design and Simulation of Materials: I

Symposium Organizers:

Tongyi Zhang, Shanghai University, China; Zhimei Sun, Beihang University, China; Shigenobu Ogata, Osaka University, Japan; Byeong-Joo Lee, Pohang University of Science and Technology (POSTCEH), Korea; Salvy Russo, RMIT, Australia; Saryu Fensin, Los Alamos National Lab, USA; Michele Manuel, University of Florida, USA

Monday PM
August 19, 2019

Room: 204 (2nd Floor)
Symposium: L

Chairs:
Zhimei Sun, Beihang University, China
Jeffrey Reimers, Shanghai University, China

13:30-14:00 Keynote

Surface Induced Size-Dependent Thermodynamic Properties of Nanomaterials

Tongyi Zhang, Shanghai University, China

Multi-scale and trans-scale simulations and calculations are considerably challenging in the academic research and engineering practices. Theoretical modeling has the power to solve the multi-scale and trans-scale issues. As an example, the present presentation introduces the surface induced size-dependent ultimate tensile strength, size- and temperature-dependent Young's modulus, and size-dependent thermal expansion coefficient of thin films and nanowires. Theoretically, the surface eigenstress model and surface eigendisplacement model are developed within the continuum frame based on mechanics and thermodynamics and thereby lead to analytic formulas of the size-dependent material properties. These formulas present the coupling behaviors of multiply physics fields and are multi-scale and trans-scale in nature. First-principle calculations and molecular dynamics simulations are conducted to study the size-dependent properties, and the results verify perfectly the derived equations and determine the values of the parameters involved in the models. The eigenstress model has been further developed to study the size-dependent solubility in nanomaterials for open and closed systems, e.g., the grain size-dependent solubility in nanograined polycrystals for open systems and the thickness size-dependent surface segregation in nanofilms for closed systems. These derived formulas are also verified by experimental results or/and atomistic simulations. The developed surface models might, in general, establish the foundation for the further development of size-dependent thermodynamics.

14:00-14:30 Keynote

Materials Design by Computation

Kwang-Ryeol Lee, Xiaowei Li, Korea Institute of Science and Technology, Korea

Computational research at the atomistic scale could provide significant insight into the structure-property relationships in materials. Atomic scale understanding of the phenomena involving surface and interface became viable in atomic (subatomic) scale computations. However, the interfacial properties are not sufficiently characterized by only the experimental analysis approach. Thin film structures are frequently governed by the initial period of deposition when the intermixing or epitaxial misfit occurs. Tribological behavior of carbon surface could be more systematically investigated by massive computation of atomic scale tribology simulation. The physical and chemical properties of hybrid (composite) materials are also governed with the interfacial properties. Owing to the rapid increase in computing power and successful development of the computation methodology, molecular level simulation has driven new paradigm of materials research. Increased predicting power of the ab initio calculation combined with molecular dynamics approach can now guide the experimental research. In this talk, I will present the major results of computational research at KIST to understand the surface or interfacial phenomena in various materials systems. Finally, I will

introduce the recent effort of KIST to build a web-based materials design platform. This platform would become an essential infrastructure for future computational and data-driven research where researchers or developers can perform the required elaborate simulation with relatively low entrance barrier to computational research. The platform is further important for accumulating and managing the computation data, which accelerated the data-driven materials design.

14:30-15:00 Keynote

The Materials Science of Josephson Junctions: Modelling Their Formation and Electrical Response from an Atomistic Point of View

Jared Cole, RMIT University, Australia

The basis for superconducting electronics is the Josephson junction: a thin insulating barrier that separates two superconducting leads and thereby behaves as a tunneling barrier. These junctions are the nonlinear circuit element inside superconducting quantum interference devices, microwave electronics, and superconducting quantum computers. The width of this barrier can be as thin as two nanometers and the electronic properties of such junctions are therefore strongly dependent on the morphology of the barrier, both at the interfaces of the superconducting leads and within the metal oxide itself.

We perform molecular dynamics simulations of the oxidation and deposition process, in order to develop atomistic models of aluminium-oxide tunnel junctions. Junction models constructed with this methodology are compared to models based on simulated annealing in which the characterisitics of the junction can be controlled systematically. We then perform a quantitative analysis of structural differences as a function of oxide density and the stoichiometric O/Al ratio in the barrier layer. By simulating the fabrication process, we aim to determine what characteristics naturally emerge from the fabrication process, and how they can be controlled by modifying the fabrication conditions.

To understand the electrical response of these model junctions, we have developed a new approach that captures the physics of the junction morphology using a three-dimensional electrostatic potential computed from molecular dynamics simulations. We calculate the normal resistance of a Josephson junction using the non-equilibrium Green's functions formalism and investigate the effect of changing the stoichiometry and oxide density of the insulating barrier.

Our results provide new insights into the influence of fabrication conditions on the electrical response of metal-oxide barriers and the resulting performance of quantum technologies constructed from them.

15:00-15:30 Keynote

Van Der Waals Forces Control both the Internal Chemical Structure within ABP2X6 Monolayers and Ferroelectric/Antiferroelectric Interlayer Stacking

Jeffrey Reimers, Sherif Tawfik, Shanghai University, China; Michael Ford, University of Technoology Sydney, Australia

Van der Waals forces between atom pairs can be very strong, especially if soft atoms like Cu, S, and Se are involved. We show that in CuBiP2Se6 and CuInP2S6 monolayers, these forces outcompete traditional covalent-bonding forces to determine the copper coordination (tetrahedral, trigonal planar, octahedral, etc.). Further, their strong 1/r^6 dependence is shown to lead to quite different energies for ferroelectric and antiferroelectric layer stackings. This effect is used to explain different stacking patterns found in nanocrystals and in 3D materials. The energy difference between two large van der Waals contributions cancel somewhat, but still overpower the Coulomb forces associated with dipole alignment to control stacking. These are just examples of many examples demonstrated in the last few years of net interatomic van der Waals forces outcompeting traditional covalent and ionic bonding, eg, controlling gold-sulfur bonds on surfaces and nanoparticles and hence nanoparticle formation. Whilst the van der Waals force is normally taken to be additive, like gravity, means of switching it off are also demonstrated. Different modern computational methods are shown to describe these effects in very different ways, and different methods appropriate for different situations are described. Basic requirements for new and improved computational approaches are discussed, focusing on the need for consistent treatments of many-body effects at the short-range and long-range limits.

15:30-16:10 Tea Break

16:10-16:35 Invited

High Throughput Screening of Alloy Catalysts for PEMFC and Machine Learning Prediction of Chemisorption

Hyuck Mo Lee, Jung Woo Choi, KAIST, Korea; Soonho Kwon, California Institute of Technology, USA

Much progress has been made in hydrogen production and its utilization through fuel cell application to exploit this renewable energy source without any limitation from

diurnal variation in local insolation. For rational design of new cathode catalysts for sluggish oxygen reduction reaction (ORR), theoretical approaches using density functional theory (DFT) have provided comprehensive explanations for enhanced performance of new catalysts. Based on solid concepts in heterogeneous catalysis, we conducted high-throughput screening of L12-type alloys for proton-exchange membrane fuel cell (PEMFC) application to find a new ORR electrocatalyst. In this study, we introduce a highly durable & active catalyst candidate and describe its chemistry on the corresponding surface by higher-level of calculations for verification.

In general, many computational screening studies have been done by fixing the surface structure without changing symmetry because of its simple construction of model surfaces and a limitation from the computing capacity. Here, however, we carried out symmetry-unconstrained screening to find a new Ag-based ORR catalyst for the anion-exchange membrane fuel cell (AEMFC). We considered not only the catalytic activity but also the phase stability from each phase diagram and heat of formation to secure the durability of catalysts. A further systematic approach to move closer towards optimal alloying design escaping from a known database, such as the Materials Project, is also discussed.

Given that one has a proper size of the database for a specific property, prediction through machine learning can be a good choice. Here, using a large database from the screening we had performed above, we trained an artificial neural network (ANN) to predict surface – adsorbate interaction to estimate the catalytic performance within an error range of < 0.2eV. In this way, one can reduce computational cost significantly and broaden the screening window for materials exploration. Also, we will show how the accuracy of the machine learning model and types of input features depend on the size of a training set.

16:35-17:00

Integrated Computational Materials Engineering for Advanced Materials: A Brief Review

Yi Wang, Jinshan Li, Weimin Liu, Northwestern Polytechnical University, China; Zikui Liu, Pennsylvania State University, USA

After developing the simulation-based design approach of materials for decades, computational materials science/engineering present the power in accelerating the discoveries and the applications of novel advanced materials through a digital-twin design paradigm of integrated computational materials engineering (ICME). While the short goals of ICME are almost accomplished, those long goals are on the right way, highlighting the concept/strategy of materials by design. In this brief review, the recent frameworks of data-driven ICME in the last two years are discussed, presenting key aspects of principles, benchmarks, standards, databases, platforms and toolkits via various case studies. The author and his collaborators display a routine of data-driven ICME utilized in the investigations of Mg alloys through integrating the high-throughput first-principles calculations and the CALPHAD approach. It is highlighted that the bonding charge density could not only provide an atomic and electronic insight into the physical nature of chemical bond of pure elements, alloys, metal melts, oxides and semiconductors, surface and interfaces, but also reveal the fundamental solid-solution strengthening/embrittlement mechanism and the grain refinement mechanism, paving a path in accelerating the development of advanced materials. It is believed that the combinations of high-throughput multi-scale computations and fast experiments/manufacturing will build the advanced algorithms in the development of a promising digital fabricating approach to overcome the present and future challenges, illuminating the way toward the digital-twin intelligent manufacturing era.

17:00-17:25 Invited

Continuum Dislocation-Density based Models for the Dynamic Shock Response of Single-Crystal and Polycrystalline Materials

Darby Luscher, Los Alamos National Laboratory, USA

The dynamic thermomechanical responses of polycrystalline materials under shock loading are often dominated by the interaction of defects and interfaces. For example, polymer-bonded explosives (PBX) can initiate under weak shock impacts whose energy, if distributed homogeneously throughout the material, translates to temperature increases that are insufficient to drive the rapid chemistry observed. In such cases, heterogeneous thermomechanical interactions at the mesoscale (i.e. between single-crystal and macroscale) lead to the formation of localized hot spots. Within metals, a prescribed deformation associated with a shock wave may be accommodated by crystallographic slip, provided a sufficient population of mobile dislocations is available. However, if the deformation rate is large enough, there may be an insufficient number of freely mobile dislocations. In these cases, additional dislocations may be nucleated, or alternate mechanisms (e.g. twinning, damage) activated in order to accommodate the deformation. Direct numerical simulation at the mesoscale offers insight into these physical processes that can be invaluable to the development of macroscale constitutive theories, if the mesoscale models adequately represent the anisotropic nonlinear thermomechanical response of individual crystals and their interfaces.

This talk will briefly outline a continuum mesoscale modeling framework founded upon local and nonlocal variations of dislocation-density based crystal plasticity

theory. The nonlocal theory couples continuum dislocation transport with the local theory. In the latter, dislocation transport is modeled by enforcing dislocation conservation at a slip-system level through the solution of advection-diffusion equations. The configuration of geometrically necessary dislocation density gives rise to a back-stress that inhibits or accentuates the flow of dislocations. Development of the local theory and application to modeling the explosive molecular crystal RDX and polycrystalline PBX will be discussed. The talk will also emphasize recent implementation of the coupled nonlocal model into a 3D shock hydrocode and simulation results for the dynamic response of polycrystalline copper in two and three dimensions.

M. Renewable Energy Materials and Nuclear Materials: I

Symposium Organizers :

Min Zhu, South China University of Technology, China; Yuan Deng, Beihang University, China; Guanghong Lu, Beihang University, China; Tetsuya Uda, Kyoto University, Japan; Taek-Soo Kim, Korea Institute of Industrial Technology (KITECH), Korea; Dmitri Golberg, Queensland University of Technology, Australia; Assel Aitkaliyeva, University of Florida, USA

Monday PM
August 19, 2019

Room: 311(3rd Floor)
Symposium: M

Chairs:
Min Zhu, South China University of Technology, China
James Stubbins, University of Illinois at Urbana-Champaign, United States

13:30-14:00 Keynote

Construction of Superlattice-Like Sandwich Structures from 2D Oxide and Hydroxide Nanosheets towards Superior Energy Storage and Conversion

Takayoshi Sasaki, National Institute for Materials Science, Japan

We have developed a variety of transition metal oxide and hydroxide nanosheets via delamination of precursor layered compounds into single layers. The resulting colloidal nanosheets are molecularly thin 2D nanocrystals, extending laterally up to several tens micrometers. Because of their highly redox activity and large surface area, they are promising as a building block for electrode materials and catalysts. One drawback to be overcome is their poorly conducting nature. We combined these oxide and hydroxide nanosheets with graphene oxide (GO) or its reduced form (rGO) into heteroassembled superlattice-like materials through solution-based processes based on electrostatic self assembly.

The oxide nanosheets as well as GO and rGO are negatively charged while hydroxide sheets are positively charged. We can turn their charge by modifying their surface with an appropriate polyelectrolyte, keeping the monodisperse nature. Then such oppositely charged nanosheets were mixed, spontaneously producing bulk-scale flocculates of unique superlattice-like sandwich structures where oxide or hydroxide nanosheets and GO or rGO are alternately stacked at molecular level. We showed that such heteroassembled lamellar composites exhibited superior performance in electrochemical charging/discharging and water electrolysis, showing promise for applications in supercapacitors, Li or Na ion batteries and electrocatalysts.

14:00-14:25 Invited

Role of Irradiation and Weld-Induced Post-Irradiation Annealing on Deformation Mechanisms in 304L Stainless Steel

Wharry Janelle, Purdue University, USA; Keyou Mao, Purdue University & Idaho National Laboratory, United States; Cheng Sun, Idaho National Laboratory; Freyer Paula, Westinghouse Electric Company, LLC; Garner Frank, Texas A&M University, USA

This presentation will describe recent advancements in micro-mechanical testing that inform how deformation mechanisms in 304L stainless steels (SS) are affected by the presence of irradiation-induced defects. Austenitic 304L SS is one of the most widely utilized structural alloys in nuclear energy systems, but the role of irradiation on its underlying mechanisms of mechanical deformation remains relatively poorly understood. Now, recent advancement of micro-scale mechanical testing in a scanning electron microscope (SEM), coupled with site-specific transmission electron microscopy (TEM), enables us to precisely determine deformation mechanisms as a function of plastic strain and grain orientation.

We focus on AISI 304L stainless steel irradiated in EBR-II to 20 displacements per atom (dpa) at 415℃, and contain ~3 atomic parts per million (appm) He amounting to 1.5% swelling. A portion of the specimen is laser welded in-hot cell; the laser weld heat affected zone is studied and considered to have undergone post-irradiation annealing (PIA). An archival, virgin specimen is also studied as a control. We conduct nanoindentation testing, then subsequently prepare TEM lamellae from the plastic zone of the nanoindents using site-specific focused ion beam (FIB) milling. TEM investigation reveals nucleation of deformation-induced α' martensite in the irradiated specimen, and metastable ε martensite in the PIA specimen.

Meanwhile, the unirradiated control specimen exhibits evidence only of dislocation slip; this is unsurprising given that alternative deformation mechanisms such as twinning and martensitic transformation are typically observed only near cryogenic temperatures in austenitic SS. Surface area of irradiation-produced voids contribute sufficient free energy to accommodate the martensitic transformation. The lower population of voids in the PIA material enables ε martensite formation, while the higher void number density in the irradiated material causes α' martensite formation. SEM-based micropillar compression tests confirm nanoindentation results. Irradiation damage could enable fundamental, mechanistic studies of deformation mechanisms that are typically only accessible at extremely low temperatures.

14:25-14:50 Invited

High-Density Uranium Silicide Fuels – Radiation Response and Oxidation Resistance

Jie Lian, Rensselaer Polytechnic Institute, USA

U_3Si_2 is being considered as a leading form of the accident tolerant fuels for light water reactors due to its excellent thermal conductivity and higher fissile element density. In this talk, the microstructure evolution and radiation response of U_3Si_2 under extensive ion beam irradiation are summarized with the focus on radiation-induced amorphization, grain subdivision, and grain growth. U_3Si_2 is sensitive to ion beam radiation-induced amorphization at room temperature. Above a critical temperature, U_3Si_2 is highly resistant against amorphization, and radiation-induced polygonization and grain subdivision occur. Isothermal annealing was performed on pre-amorphized U_3Si_2, leading to the formation of high-density nano-sized silicide. The critical doses for radiation-induced amorphization and grain subdivision and the kinetics of the grain coarsening are determined, providing experimental data for the development and validation of the MARMOT fuel performance models.

In addition, U_3Si_2 is prone to oxidation at low temperatures under synthetic air and steam conditions. Innovative fuel design and fabrication are required for the development of the high-density silicide fuels with enhanced oxidation and water corrosion resistance. Monolithic and composite U_3Si_2 fuels with sintering additives are fabricated by spark plasma sintering (SPS), and the microstructure and phase behavior of the SPS-densified silicide fuels are characterized and correlated with the sintering process. Dynamic oxidation and mechanical tests of the densified fuels are also performed and compared with the silicide fuels fabricated by conventional sintering. The concepts of using chemical doping and sintering additives for developing U_3Si_2 fuels with enhanced oxidation and corrosion resistance are also highlighted.

14:50-15:10

Dehydration-Hydration Behaviors of Lanthanum Compounds as Potential Thermochemical Heat Storage Materials

Naoyuki Hatada, Kunihiko Shizume, Kazuaki Toyoura, Tetsuya Uda, Kyoto University, Japan

Thermal energy storage based on chemical reactions (thermochemical heat storage) is a prospective technology for the reduction of fossil-fuel consumption by storing and using waste heat. For widespread application, a critical challenge is to find appropriate reversible reactions that occur below 250˚C, where abundant low-grade waste heat and solar energy might be available. Previously proposed reactions include dehydration-hydration reactions of alkaline-earth compounds such as $Mg(OH)_2$, $CaCl_2{\cdot}nH_2O$, and $CaSO_4{\cdot}1/2H_2O$. However, there is still need to find materials satisfying all of the following criteria: high energy density, adequate storage temperature for low-grade waste heat, sufficient reversibility of reactions, non-corrosiveness, low cost, etc. It should be noted that most of rare-earth compounds except for $La(OH)_3$ have been left uninvestigated as thermochemical heat storage materials to date while the prices of yttrium, lanthanum and cerium have dropped due to oversupply. Therefore, we have investigated dehydration-hydration behaviors of several lanthanum compounds, namely, $La(OH)_3$, $La_2(SO_4)_3{\cdot}H_2O$, $La_2(SO_4)(OH)_4$, and $A La(SO_4)_2{\cdot}xH_2O$ (A=Na, K, Rb), as potential thermochemical heat storage materials.

Thermogravimetry revealed that $La(OH)_3$ and $La_2(SO_4)_3{\cdot}H_2O$ reversibly dehydrate/hydrate on heating / cooling at 50~400˚C under humidified argon atmospheres (water vapor pressure: 0.12~0.23 atm). Especially, the reactions of $La_2(SO_4)_3{\cdot}H_2O$ proceeded in the temperature range from 50 to 250˚C with remarkably small thermal hysteresis of less than 50˚C at the heating/cooling rate of 20˚C/min, and thus it emerges as a new candidate system for thermal energy storage. By contrast, the other compounds dehydrated on heating but hardly rehydrated on cooling.

Detailed study on $La_2(SO_4)_3$ was then conducted. High-temperature X-ray diffraction analysis and first-principles molecular dynamics simulation revealed that the dehydration/hydration reactions proceed through an unusual mechanism for sulfates: water molecules are removed from, or inserted in $La_2(SO_4)_3{\cdot}xH_2O$ with progressive change in hydration number x without phase change. In addition, a characteristic microstructure of $La_2(SO_4)_3$ polycrystalline particles consisting of 200nm-thick fine platy grains was found to facilitate the fast hydration reaction, by thermogravimetry, transmission electron microscope and gas adsorption studies. The standard enthalpy change of the dehydration reaction of $La_2(SO_4)_3{\cdot}H_2O$ was assessed to be 91kJ/mol, or 154kJ/

kg-monohydrate. This value is comparable to those of typical phase change materials (PCM) and renders the need for further enhancement of energy density.

15:10-15:30

$NiCo_2S_4/Ni_3S_2$ Heterostructure on Nickel Foam as Self Supporting Electrodes for Water Splitting

Weiji Dai, Ye Pan, Southeast University, China

Nowadays, the increasing consumption of nonrenewable fossil fuels, such as coal, petroleum and natural gas has caused a series of severe environmental problems, ranging from air and water pollution to global warming. Therefore, the development of new type energy with environmental friendly, high efficiency and sustainable development, such as solar energy and wind energy, as well as hydrogen energy, is an significant and urgent task for the scientific community. Among this, with the zero carbon emission and high energy density output, hydrogen has been regarded as an ideal renewable resource to replace the increasingly depleted fossil fuels. Furthermore, water splitting technology has widely recognized as a promising and appealing strategy to convert electrical energy into renewable hydrogen energy. Therefore, the development of high efficiency and earth abundant electrocatalysts materials for the two half reactions of water splitting: the hydrogen evolution reaction (HER) at the cathode and the oxygen evolution reaction (OER) at the anode is the uppermost challenge. To date, the most efficient HER catalysts are platinum (Pt)-based noble metal materials and the state-of-the-art OER catalysts are iridium (Ir) and ruthenium (Ru)-based oxides, however, the scarce abundance and high cost severely limited their large-scale applications. Great efforts have been devoted to developing transition metal-based electrocatalysts for HER and OER. Herein, we report the controllable synthesis of $NiCo_2S_4/Ni_3S_2$ Heterostructure on Nickel foam and their application as an efficient bifunctional electrocatalyst for overall water splitting. The $NiCo_2S_4/Ni_3S_2$ heterostructure is achieved by the facile one-step hydrothermal approach without preparation of any precursor. The resultant $NiCo_2S_4/Ni_3S_2$ electrode exhibits as an effective bifunctional electrocatalyst, to achieve an current density of 10 $mA{\cdot}cm^{-2}$ for HER and OER it need overpotentials of only 167 and 280mV respectively in 1M KOH solution. Such enhanced electrocatalytic performance can be credited to (i) the interface effect of $NiCo_2S_4/Ni_3S_2$ Heterostructure, (ii) the flower like morphology of $NiCo_2S_4/Ni_3S_2$ could expose massive active sites. This work not only provides a new efficient and stable catalyst for overall water splitting, but also proposes an interface design principle for Nickel Foam based high-performance water splitting electrocatalysts materials.

15:30-16:10 Tea Break

16:10-16:35 Invited

Neutron Irradiation Behavior of Fe-Cr Alloys, from Model to Engineering Alloy Compositions

Weiying Chen, Argonne National Lab, Lemont, USA; Xiang Liu, Idaho National Lab, Idaho Falls, USA; Huan Yan, Hoon Lee, *James Stubbins,* Department of Nuclear, Plasma and Radiological Engineering, University of Illinois at Urbana-Champaign, Urbana, USA

A number of alloys ranging from simple binary and ternary Fe-Cr alloys to commercial ferritic/martensitic alloys were irradiated in the Advanced Test Reactor at Idaho National Lab over a range of displacement doses from 0.01dpa to 10dpa at nominal irradiation temperatures of 300˚C, 450˚C and 550˚C. The intent of this large irradiation matrix was to develop an understanding of the behavior of these alloy systems by building on the response of simple alloy systems up to very complex systems. The irradiations included specimens for microstructural examination as well as tensile testing.

This talk will discuss the findings of microstructural behavior and its relationship to mechanical properties performance for a range of alloys and irradiation conditions. This includes a presentation of the understanding of the development of the α' phase (a Cr-rich Fe-Cr phase) which is not found in heavy ion irradiations of the same materials, and is difficult to identify in experimental techniques that rely on diffraction scattering analysis. The relationship between materials composition and irradiation conditions for the formation of this phase are still in dispute, as is the equilibrium phase boundary.

The talk will also cover some in situ tensile tests of certain of these alloy conditions to show the advantages of dynamic straining to elucidate which microstructural features are playing a role in the deformation process and to what extent. Plans for future testing will also be discussed.

16:35-16:55

Effect of Phase Composition and Local Crystal Structure on Transport Properties of Solid Solutions ZrO_2-Gd_2O_3

Filipp Milovich, Tabachkova, National University of Science and Technology "MISIS", Russian Federation; Mihail Borik, Elena Lomonova, Valentina Myzina, Alexey Kulebyakin, Prokhorov General Physics Institute, Russian Academy of Sciences, Rusia; Polina Ryabochkina, Tatyana Volkova, Ogarev Mordovia State University, Republic of Mordovia, Russia; Ekaterina Agarkova, Institute of Solid State Physics, Russian Academy of Sciences, Russia

Currently, the use of materials based on zirconia as

a solid electrolyte for solid oxide fuel cells (SOFC) is associated with the need to solve a number of scientific and technological problems. The production of materials with high conductivity in the range of average temperatures (500~700˚C) and the increase in the stability of the electrophysical characteristics of solid electrolyte at operating temperatures for a long time are some of these issues. In accordance with this, the identifying of various factors, such as phase composition and local crystal structure, affecting the magnitude of oxygen-ionic conductivity of zirconia-based solid solutions, is a relevant research topic.

Comprehensive studies of the phase composition and local structure of zirconium dioxide crystals stabilized by gadolinium oxide in a wide range of compositions from 2.7 to 38mol.% were performed and the effect of Gd_2O_3 on the transport characteristics of crystals of these solid solutions was established. The presence of transformable t and untransformable t' tetragonal phases was established in crystals of zirconia partially stabilized by gadolinium oxide, with a concentration of 2.7 and 3.6mol.%, and their crystal structure parameters were determined. The presence of a twin structure formed during the transition of the high-temperature cubic phase to the tetragonal phase is shown in ZrO_2 crystals with a content of 8mol.% Gd_2O_3 by transmission electron microscopy and Raman spectroscopy. It was established that the twin structure is absent with the same content of yttrium oxide in ZrO_2-8mol.% Y_2O_3 crystals, and the structure of the crystals corresponds to the structure of the t''-phase. Studies of the features of local crystal structure ZrO_2-Gd_2O_3 were carried out using optical spectroscopy methods. Eu_2O_3 was used as a spectroscopic probe. It has been established that the local structure of the ZrO_2-Gd_2O_3 solid solutions is determined mainly by the concentration of stabilizing oxides Gd_2O_3. It was shown that the decrease in ionic conductivity in the concentration range of stabilizing oxides above 12mol.% Gd_2O_3 is due to the increase in the relative fraction of Gd^{3+} cations with oxygen vacancy in the nearest crystalline surroundings, and in the concentration range above 20mol.% Gd_2O_3 the formation of two anionic ions vacancies in the nearest crystalline surroundings of Gd^{3+} ions.

The work was carried out with financial support in part from the RSF (№ 18-79-00323).

16:55-17:15

Reversible Hydration-Dehydration Reaction of Yttrium Sulfate as a New Candidate of Thermal Energy Storage Material for Low-Temperature Waste Heat.

Kunihiko Shizume, Naoyuki Hatada, Shoko Yasui, Tetsuya Uda, Kyoto University, Japan

Thermal energy storage based on chemical reactions (thermochemical heat storage) is a prospective technology for the reduction of fossil fuel consumption by storing and reusing industrial waste heat. For widespread application, a critical challenge is to find appropriate reversible reactions which occur below 250˚C where abundant low-grade waste heat might be available. Hydration (endothermic)-dehydration (exothermic) reaction cycle of inorganic solids with water vapor is one of the practical reaction systems due to its safety and easy storage of water. However, many hydration reactions of inorganic solids are slower compared with their dehydration reactions when their reaction temperatures are about 300˚C or less. Exceptionally, hydration reactions of calcium sulfate $CaSO_4$ and lanthanum sulfate $La_2(SO_4)_3$ can proceed promptly even by exposure to air by water insertion into the pore in their crystal structure. However, they form hydrates with only small hydration numbers such as hemihydrate $CaSO_4 \cdot 1/2H_2O$ and monohydrate $La_2(SO_4)_3 \cdot H_2O$. Therefore, the enthalpy changes of the reactions are not large enough for practical application. In this work, we have focused on yttrium sulfate $Y_2(SO_4)_3$ as a new candidate material. Dehydration reaction of yttrium sulfate octahydrate $Y_2(SO_4)_3 \cdot 8H_2O$ has been reported to complete below 200˚C, but rehydration behavior of the anhydrate is unknown. If the anhydrate reacts with water vapor rapidly to form the hydrates $Y_2(SO_4)_3 \cdot nH_2O$ with large hydration number n, it will be a prospective candidate for thermochemical heat storage material.

We conducted thermogravimetry (TG) on $Y_2(SO_4)_3 \cdot 8H_2O$ during heating-cooling cycles under a humidified argon atmosphere (Ar–1%~2% H_2O). It revealed that $Y_2(SO_4)_3 \cdot 8H_2O$ dehydrated to $Y_2(SO_4)_3$ at between 150 to 270˚C during heating at a rate of 20˚C·min^{-1}, and then during cooling to 27˚C, $Y_2(SO_4)_3$ rehydrated to form $Y_2(SO_4)_3 \cdot nH_2O$ where n increased step by step with the range from 0 to 6. At least two hydration/dehydration reaction processes were observed at different reaction temperature ranges when heating/cooling rate was 1˚C·min^{-1}. At between 80 to 130˚C, hydration number varied from 0 to approximately 1 with small thermal hysteresis of less than 50 ˚C as follows:

$Y_2(SO_4)_3$ (s) + H_2O (g) ⇄ $Y_2(SO_4)_3$ H_2O (s) (80~ 130˚C)

This hydration/dehydration reaction temperature range is narrower than that of $La_2(SO_4)_3$ (80~250˚C) and nearly equal to that of $CaSO_4$ (70~120˚C). At lower temperature range, further hydration of $Y_2(SO_4)_3 \cdot H_2O$ proceeded. The hydration number reached about 6 at below 30˚C on cooling process, and the partial formation of $Y_2(SO_4)_3 \cdot 8H_2O$ was confirmed by X-ray diffraction (XRD). The reaction is written as follows:

$Y_2(SO_4)_3 \cdot H_2O$ (s) + $7H_2O$ (g) ⇄ $Y_2(SO_4)_3 \cdot 8H_2O$ (s) (27~90˚C)

It is interesting that hydration number reached as large as 8 without any high water vapor partial pressure treatments. In fact, $La_2(SO_4)_3 \cdot 9H_2O$ and $CaSO_4 \cdot 2H_2O$ are stable hydrates, but can not be formed from their

anhydrate under the same atmosphere (Ar–1%~2% H_2O). Therefore, if the hydration/dehydration reaction between $Y_2(SO_4)_3$ and $Y_2(SO_4)_3{\cdot}8H_2O$ is applied to thermochemical heat storage, higher heat storage density is expected than those of other candidates. The mechanisms of the reaction will be discussed on the basis of the change of crystal structure and microstructure of $Y_2(SO_4)_3{\cdot}nH_2O$ during hydration/dehydration reaction revealed by high temperature XRD and gas adsorption measurements.

17:15-17:35

Ordered Mesoporous Carbon Supporting Well-Dispersed Active Co Nanoclusters for Low Temperature CO_2 Methanation

Feng Li, Chunxia Zhao, Hang Li, Wen Chen, Wuhan University of Technology, China; Yunxia Yang, The Commonwealth Scientific and Industrial Research Organization, Australia

An energy efficient process must be developed for utilizing CO_2 as a carbon source to produce commodity chemicals aligned to industrial needs because of the serious environmental problems and resources limitation. The Sabatier reaction (also known as CO_2 methanation) reduces CO_2 with H_2, over a catalyst, to produce methane at elevated temperatures and pressures. A high-efficiency CO_2 methanation catalyst is the key of this reaction. At present, Ni-based metal oxide supported catalysts such as Ni/Al_2O_3, Ni/TiO_2, Ni/SiO_2 and Ni/CeO_2, are easily deactivated at high temperature and humidity. So, it is necessary to study new types of low-temperature catalysts and expand the diversity of catalyst support materials. In comparison, cobalt based catalyst exhibits almost the same methanation activity as Ni catalyst, but it has lower activation energy. Thus it is possible that cobalt is applied to low temperature CO_2 methanation. With respect to catalytic supports, carbon materials, including CNTs, graphene, AC, mesoporous carbon etc, have different chemistry and structures from metal oxides. However, there are relatively few studies on CO_2 methanation catalysts based on carbon materials.

Ordered mesoporous carbon, CMK-3, has a two-dimensional hexagonal mesoporous structure and a large specific surface area which could provide a good environment to highly disperse catalysts. In our work, Co@CMK-3 catalyst with well-dispersed Co nanoclusters on the channels of ordered mesoporous carbon was synthesized by impregnation method with $Co(NO_3)_2$ as Co source and CMK-3 as support and then were activated in situ under methanation reaction conditions at 350˚C . The prepared Co@CMK-3 catalysts have high specific surface area of 957m^2/g and uniform pore size of 3.61nm. As a result, a CO_2 conversion rate of 16.22% is obtained by this catalyst at 300˚C and 30bar. Then, the influences of CMK-3 surface modification and Ru, Co co-loading on the catalytic activity of CO_2 methanation are investigated. It is found that The acid-pretreated CMK-3 can promote the low-temperature catalytic performance of the composite catalyst, and the CO_2 conversion rate is 37.17% at 300˚C and 30bar. Ru and Co co-loading can also significantly improve the low temperature catalytic performance, and the CO_2 conversion rate is increased to 45.01% at the same reaction condition.

N. Additive Manufacturing and Powder Metallurgy: Powder Preparation & Simulation

Symsposium Organizers:

Huiping Tang, Northwest Institute for Nonferrous Metal Research, China; Yong Liu, Central South University, China; Yuichiro Koizumi, Osaka University, Japan; Kee-Ahn Lee, Inha University, Korea; Qian Ma, RMIT, Australia; Ed Herderick, Ohio State University, USA

Monday PM
August 19, 2019

Room: 402 (4th Floor)
Symposium: N

Chairs:
Yunping Li, Central South University, China
Yoon Suk Choi, Pusan National University, Korea

13:30-14:00 Keynote

Development and Applications of Gas Atomisation and Spray Forming for High Performance Alloys

Guoqing Zhang, Zhou Li, Wenyong Xu, Hua Yuan, Na Liu, Liang Liu, Yang Zheng, Yufeng Liu, Beijing Institute of Aeronautical Materials, China

Gas atomised powders and deposited preforms have been developed for high performance alloys. Advances in the gas atomisation technologies of three types of highly alloyed structural materials, nickel based superalloys, titanium aluminides and high speed steels are evaluated in this paper. The equipment, process and research results of gas atomisation technologies at BIAM will be presented. BIAM initiated the research and development of gas atomisation and deposition for superalloys, intermetallics and special steels in early 1990s. A serial gas atomisation and deposition plants with melt capacity of 50 to 350 kilograms have been designed, established and modified. Typical alloys were vacuum induction melt, gas atomised, consolidated, and hot processed. Simulation and modification of the atomisation and deposition process were investigated to optimise the melting, atomising and forming parameters to make designed and clean powders and preforms for manufacturing sound components. The results exhibit that the high quality powders and preforms, with high

yield and low oxygen contents, can be achieved after the optimisation of melting and atomising parameters. Argon atomised powders of Ni and TiAl based alloys with a range of particle size, oxygen contents, chemistry are utilised to produce components by both additive manufacturing and normal powder metallurgy techniques. The metallurgical quality and mechanical properties of components are shown to be closely related to melt droplets or powders quality charactered with purity, morphology, particle size, and sphericity.

14:00-14:25 Invited

Ultrahigh Oxidation Resistance and High Electrical Conductivity in Copper Silver Powder

Yunping Li, Central South University, China

The electrical conductivity of pure Cu powder is typically deteriorated at elevated temperatures due to the oxidation by forming non-conducting oxides on surface, while enhancing oxidation resistance via alloying is often accompanied by a drastic decline of electrical conductivity. Obtaining Cu powder with both a high electrical conductivity and a high oxidation resistance represents one of the key challenges in developing next-generation electrical transferring powder. Here, we fabricate a Cu-Ag powder with a continuous Ag network along grain boundaries of Cu particles and demonstrate that this new structure can inhibit the preferential oxidation in grain boundaries at elevated temperatures. As a result, the Cu-Ag powder displays considerably high electrical conductivity and high oxidation resistance up to approximately 300℃, which are markedly higher than that of pure Cu powder. The successful use of inert and conducting Ag rich in GBs of a Cu-Ag powder represents a remarkable step forward in realizing high electrical conductivity and high oxidation resistance for a broad range of electrical transfer applications. It is interesting to find that the aging-treated Cu-Ag at 200~350℃ demonstrates a Q value as high as that of pure Cu at high temperature, implying that the oxidation of aged Cu-Ag powder is possibly linked to the lattice diffusion of Cu, since the diffusion of Cu at GBs is blocked due to the continuous distribution of Ag phase. The Q of as-atomized Cu-Ag powder at 200~350℃ is close to that of 6N copper at intermediate temperatures of 600~850℃, where the oxidation relies on both GB diffusion and lattice diffusion. Our results demonstrate, for the first time, that the unique resultant microstructure leads to the effective inhibition of oxidation of the Cu powder while not sacrificing the electrical conductivity. Such an outstanding combination of oxidation resistance and electrical conductivity in Cu-Ag powders holds substantial promise as a new material platform for further development of electrical transfer powder. This study paves a new pathway for developing novel Cu powders with much enhanced electrical conductivity and oxidation resistance in service.

14:25-14:50 Invited

Research and Development Progress in Production of Refractory Metal Powders by Plasma Rotating Electrode Process

Changshu Xiang, Xi'an Sailong Metal Materials Co. Ltd, China

Compared with gas atomization, the powder produced by plasma rotating electrode process(PREP) boasts high sphericity, less or even none hollow powder, none satellite powder and non-agglomerated powder, etc. Moreover, by using our proprietary high-power and high-energy-density transferred arc plasma torch technology, the limitation of the melting point of the materials can be broken, then refractory metal powders with higher melting point can be manufactured. Since 2016, Sailong Metal has adopted the technology to produce high-quality metal powders including Ti-Nb alloy, Ti-Ta alloy, Nb-W alloy, pure Mo, pure Ta, pure W, etc. This report: (i) shows Sailong Metal's research and development in the production of the above-mentioned powders; (ii) analyzes the comprehensive properties of above mentioned powders; (iii) presents the exploration we conducted in the refractory metal materials by electron beam powder bed additive manufacturing.

14:50-15:10

Spray Processing of Particulate Reinforced Metal Matrix Composite Particles

Xinggang Li, Qiang Zhu, Southern University of Science and Technology, China

The idea is brought up that particulate reinforced metal matrix composite (MMC) particles could be produced through mixing melt droplets and particulate reinforcements in a spray atomization and co-injection process. The in-flight formation of composite droplets occurs due to collisions of metal droplets with particulate reinforcements in the spray cone. As a result of collisions, particles may adhere to the surface of the droplets or penetrate into the droplets, forming composite droplets, which are subsequently solidified as particulate reinforce MMC particles. By this way, the problems associated with the deposition stage in a spray forming process can be avoided but the advantages relative to rapid solidification can be retained. A composite particle is composed of a metallic matrix incorporated with particulate reinforcements. Such composite particles will not demix during a subsequent process like hot processing (HP), sintering or additive manufacturing to produce parts of various shapes or thermal spraying to generate coatings. Especially in MMC particles, the inhomogeneous distributions of particulate reinforcements are limited within a scale of metal powder size in several 10~102 micrometers. Several atomization methods for the production of the

MMC particles are introduced, such as conventional gas atomization, centrifugal atomization and pressure swirl gas atomization (PSGA). Multi-scale descriptions of particle-droplet interactions in spray processing of MMC particles are realized based on Multiphase Computational Fluid Dynamics (M-CFD) models, which deal with the macro-scale mixing process of metallic droplet sprays and ceramic particulate jets during melt atomization and spray, the meso-scale collision process of ceramic particulates with an arbitrary metallic droplet along the droplet trajectory, and the micro-scale penetration process of a ceramic particle into a metallic droplet. The multi-scale simulation results indicate that a large quantity of particulate reinforcements could be incorporated into the matrix or captured by the surface of the MMC particles by optimizing the process operation conditions, which proves that atomization of a melt with co-injection of particulates is a viable approach to generate particulate reinforced MMC particles.

15:10-15:30

Metal-Metal Core-Shell Fine Powders Fabricated by Coating of Low-Oxygen Metal Powders with Different Metals

Wataru Yamaguchi, Rikio Soda, Kenta Takagi, National Institute of Advanced Industrial Science and Technology, Japan

Metal-metal core-shell fine powders were prepared by a simple and versatile process. In the process, preparation of a fine metal powder by a dry pulverizing process is followed by formation of a different metal layer on the powder surface by using a dry coating technique. In order to ensure oxide-free, direct metal-metal interfaces, all the processes are carried out in an environment where oxygen is thoroughly excluded. Since the process does not involve any chemical treatments, there is no need to use special reagents like organometallic compounds, and the very materials with the target compositions for the core and the shell are available as raw materials. The process is also applicable to solids other than metals and can therefore be of wide application.
Metal powders with sizes of 1 to 2 micrometers are prepared by pulverizing coarse powders by a jet mill mounted in a glove box filled with highly purified nitrogen gas. The coarse powders are commercially available products and initially have surface oxides, but newly formed surfaces through the pulverization are not exposed to oxygen. Drastic increase of the surface area results in reduction of the ratio of oxidized part to the whole surface. The low-oxygen powder thus prepared is transferred to a coating apparatus connected to the glove box. The coating layer is formed on the powder surface by a dry coating technique.
Oxides in the metal-metal interface of the core-shell powders were analyzed by X-ray photoelectron spectroscopy. A core-shell powder prepared from a commercially available fine powder and that from a low-oxygen powder were compared. Changes in chemical states along the depth direction were investigated by alternately performing spectroscopy and etching by Ar sputtering. Only for the core-shell powder from the commercial source, signals corresponding to some oxides appeared in the spectra as the etching progresses.

15:30-16:10 Tea Break

16:10-16:35 Invited

Numerical and Experimental Studies on Melt-Pool Scale Behaviors of Metal Layers Processed by Direct Energy Deposition (DED) and Powder Bed Fusion (PBF) Techniques

Yoon Suk Choi, Seul-Bi Lee, Jae-Woong Kim, Pusan National University, Korea; Jae-Keun Hong, Institute of Materials Science, Korea

Melt-pool scale micro-cracks were experimentally and numerically examined for a medium carbon steel layer (AISI H13) additively deposited on cast iron using a direct energy deposition (DED) technique and for Ti4822 (Ti-48Al-2Cr-2Nb) tracks additively deposited on a Ti4822 plate using a powder bed fusion (PBF) technique. The formation of micro-cracks was thoroughly investigated using the optical microscopy, electron microscopy, chemistry mapping and the topology analysis. A finite element method (FEM) with fully coupled thermal and mechanical responses was also utilized in order to predict local thermal profiles and residual stresses, and to understand the mechanisms for the micro-crack formation. For the H13 layer deposited on cast iron, micro-cracks were observed along the graphite accompanied by plate martensite. No micro-cracks were observed for the single track. However, single, double and triple layers showed micro-cracks formed near the interface. This result indicated that repeated heating and cooling cycles during the DED process are responsible for micro-cracking of the H13 layer deposited on cast iron. For Ti4822 tracks deposited by the PBF process, distinctive micro-crack patterns were identified depending on process conditions (the laser power and speed). Those micro-crack patterns are L-type (cracks parallel to the laser scan direction), T-type (cracks perpendicular to the laser scan direction) and D-type (cracks diagonal between the L- and T-types). The through-thickness melt-pool geometry varied with the PBF process condition, changing from the conduction mode toward the key-hole mode, which was classified by the depth-to-width ratio. The results indicated that the micro-crack pattern changes toward the L-type and the melt-pool dimension changes toward the key-hole mode as the energy density increases. The FEM simulation also showed a strong tensile residual stress distribution

along the laser scan direction under the condition of the low energy density. The detailed micro-crack patterns, track surface topologies and surface/through-thickness microstructures were analysed in conjunction with FEM simulations of the single track PBF process in order to clarify the micro-crack formation. The mechanism responsible for micro-cracking will be discussed based upon experimental observations combined with numerical simulations.

16:35-16:55

Setup and Validation of Additive Manufacturing Directed Energy Deposition Simulations via In-Situ and Post-Process Measurements

Max Biegler, Benjamin Graf, Fraunhofer Insitute of Production Systems and Design Technology (IPK), Germany; Michael Rethmeier, Fraunhofer Insitute of Production Systems and Design Technology (IPK) / Federal Institute of Materials Research and Testing (BAM)y / Institute of Machine Tools and Factory Management, Technical University Berlin, Germany

Due to rapid and repeated, localized heating, melting and cooling, distortions develop in additive manufacturing (AM) directed energy deposition (DED) components, leading to reduced dimensional accuracy, excessive localized stresses and even cracking. Currently, a new build-job has to be set up experimentally with many iterations in order to optimize the path-planning strategies, the process parameters (such as laser power, forward speed and layer-height) and the filler-material flow. The experimental optimization can not be readily transferred from one part to the next because of non-linear interactions, occupying valuable machine- and personnel-time for each new build. Structural numerical welding simulations can predict these deviations and optimize new parts before any experimental effort but the approaches are still in development for AM DED and largely untested. To establish the simulation tool for use in an industrial context, user-firendly pre- and post-processing needs to be developed and comprehensive validations with experimental results need to be conducted in order to generate trust in the new methods. In this contribution, a thermo-mechanical simulation of a thin-walled, arbitrarily curved DED geometry from 1.4404 stainless steel is shown. Special consideration is given to efficient finite-element modelling and to the thermal calibration process. For the validation of transient, in-process displacements, the distortions are measured experimentally via the GOM Aramis in-situ digital image correlation system on the newly-built geometry. After build-up, 3D-scans are conducted for the final shape-deviations before and after "electric-discharge machining" (EDM) removal from the substrate plate. Subsequently, a comparison is made between the experimental in-situ and post-process distortion measurements and the simulated predictions. According to the results, the performance of structural welding simulation approaches in additive manufacturing DED is discussed in terms of result accuracy, calculation time and usability. Finally, recommendations are given for future use of numerical simulations in AM and areas requiring further research are identified.

16:55-17:15

Selective Laser Melting of Spherical Tantalum Powder Prepared by Induction Plasma

Xin Liu, Xinhua Mao, Chao Ding, Qi Shi, Guangdong Institute of Materials and Processing, Guangdong Academy of Sciences, National Engineering Research Center of Powder Metallurgy of Titanium & Rare Metals, China

Recently tantalum is gaining more attention with development of additive manufacturing. In this study, spherical tantalum powder was prepared by induction plasma, and microstructure and mechanical properties of selective laser melted (SLMed) tantalum was investigated. Spherical tantalum powder was obtained by induction plasma through controlling carrier gas flow rate, feed rate, chamber pressure, injection probe position, and sheath gas flow rate. Compared with raw tantalum powder produced by Na reduction, the tantalum powder after induction plasma shows better sphericity, finer particle size distribution, broader X-ray diffraction peaks, and lower oxygen content. For the spherical tantalum powder with the size from 15 to 53μm, the oxygen content can be lower than 500ppm, apparent density is higher than 9.0g/cm^3, tap density is higher than 10.0g/cm^3, and Hall flow rate is lower than 6s/50g. With the increase of laser power from 160 to 240W, the surface of the SLMed tantalum becomes denser. With the increase of scanning speed from 650 to 750mm/s under low laser power, the surface of SLMed tantalum appears more pores. The surface roughness decreases with the increase of energy density from 133.33 to 230.77J/mm^3 and the values are from 4.3 to 6.4μm. The relative density of the SLMed tantalum increases with the increase of energy density and can reach full density nearly. Compared with spherical tantalum powder, the X-ray diffraction peaks of the SLMed tantalum become broader, and shifts to higher angles when the energy density increases. The <111> crystal direction is the preferred direction along the building direction and a few grains with a <100> direction along the building direction are also present. With the increase of energy density, the ultimate tensile strength and yield strength of the SLMed tantalum show no obvious change, but the elongation to failure increases obviously. The tensile fracture surface displays a mixture of cleavage facets, microvoids and dimples under relative low energy density, and more dimples under relative high energy density. The optimal σ_b, $\sigma_{0.2}$, and δ of the SLMed tantalum is 693MPa, 616MPa, and 28.5%, respectively. Compared with the

SLMed tantalum using tantalum powder of hydrogenation / dehydrogenation as raw material, the $\sigma_{0.2}$, and δ of the SLMed tantalum using spherical tantalum powder prepared by induction plasma increases by about 36%, and 14 times, respectively, although the σ_b decreases by about 6%.

17:15-17:35

Preparation and Characterization of Biomedical TiNbZrTaSi Alloy Powder for Additive Manufacturing Technology

Kun Yang, Jilin University / Northwest Institute for Nonferrous Metal Research, China; Huiping Tang, Jian Wang, Northwest Institute for Nonferrous Metal Research, China; Yuanyuan Li, Jilin University, China

Biomedical Ti65.0Nb23.33Zr5.0Ta1.67Si5.0 (TNZTS, at %) alloy powders were produced by rapid solidification via plasma rotating electrode process (PREP). The obtained TNZTS powders exhibited good sphericity and smooth surfaces, which is mainly in the size distributions of 45~200μm. The as-obtained TNZTS powder was sieved into 6 size fraction given by the sieve sizes: <46μm, 46~75μm, 75~105μm, 105~150μm, 150~200μm, and >200μm. It is found that the phase constituents of TNZTS powders are particle size independent, which is mainly composed by single β phase. In additional, the PREPed powder demonstrates a dendrite structure, which is related to solidification path and cooling rate of molten droplets in PREP process. An increased Vickers micro-hardness is obtained and is associated with decreasing particle size, which is mainly because of the effects of grain refinement. Finally, selective electron beam melting (SEBM) technology is applied to access the additive manufacturing processability of the PREPed TNZTS powder. The results indicated that the as-built bulk TNZTS parts reached a relative density of 99.95%, which are dominated by the mixture of the bcc β-Ti matrix and hexagonal S2 reinforced phase. In addition, the TNZTS lattice samples with the porosity from 63%~92% were also obtained.

17:35-17:55

Macroscopic Morphology and Microstructure of Spherical Ti-1Al-8V-5Fe Alloy Powders

Liqing Wang, Ye Li, Shaoyang Zhao, Jingou Yin, Zengfeng Li, Ping Tan, Huiping Tang, Northwest Institute for Non-ferrous Metal Research, China

Spherical Ti alloy powders play a paramount role in the additive manufacturing (or 3D printing) process, and it was typically prepared by gas atomization process (GA), plasma rotating electrode process (PREP) and plasma atomization process (PA). Ti-1Al-8V-5Fe (Ti185) alloy is a kind of low cost β-Ti alloy, containing lower cost alloying element Fe. Ti185 alloys exhibited high tensile and shear strengths, toughness and corrosion resistance, which would be a candidate for transportation application with the purpose of light-weighting. Besides, the microstructure and mechanical properties can be regulated through heat treatment process, which provides a method to improve the mechanical properties of 3D-printed parts. Therefore, the 3D-printed Ti185 alloys have attracted a lot of attention to reduce the segregation and porosity, and regulate the mechanical properties. In this work, we focused on the preparation, microstructure and properties of the spherical Ti185 powders to provide high-quality raw materials for 3D printing. The spherical Ti185 powders were prepared by the PREP process, and its macroscopic morphology, microstructure and hardness were characterized. The average size of the spherical Ti185 powders was about 100μm. The powder exhibited excellent surface smoothness and sphericity. Evolution of the microstructure and the hardness of the Ti185 powder with different sizes was also discussed.

17:55-18:15

Fabrication of TaC Powder by SHS Process from Recycled Ta Scrap

JaeJin Sim, SangHoon Choi, JaeHong Lim, Kyoung Tae Park, Korea Institute of Industrial Technology, Korea

Tantalum (Ta), with a melting point of 3017°C and density of 16.69g/cm^3, is a critical material for applications in industries such as electronics, medical, material processing and numerous more. However, Ta is among the material found in regions afflicted with conflicts. Therefore it is necessary to refine the currently available Ta scraps in order to adjust with fluctuation of its market supply. In this study, the Ta scrap is recycled into Ta powder and the recycled Ta powder was subsequently treated to manufacture TaC powder with excellent properties for their use in carbide tool, carbide mold and nozzle coating. Ta metal scraps such as Ta targets, sheets and metal turning were used. The scrap pretreated using pulverization and acid leaching. The resultant product was further processed using hydrogenation/dehydrogenation technique followed by powder milling to achieve high purity recycled Ta powder. The recycled powder was then used to fabricate TaC powder by Self-propagating High-temperature Synthesis (shortly SHS). SHS offers high process efficiency and faster production rate. Furthermore, SHS process could design that feed stock does not contact with other structural components like a crucible and requires no additional heat after ignition. Nitric acid of 63% concentration was utilized for removal of impurities from Ta scrap. During the next step the hydrogenation temperature was varied between 300 ~ 700°C followed by dehydrogenation to study the particle size control for

the preparation of Ta powder. The powder thus prepared had a mean size of 14.75μm. The TaC powder prepared by using the SHS method had a particle size of 8.91μm. Wet ball milling of the as synthesized powder resulted in a final particle size of 1.24μm. It was confirmed that Ta can be recycled through leaching, hydrogenation / dehydrogenation, and powder manufacturing process from Ta scrap for production of TaC powder which is used for applications such as semiconductors, carbide tools, and biomaterials.

O. Electronic and Spin Electronic Materials: I

Symposium Organizers :

Hongda Chen, Institute of Semiconductors, Chinese Academy of Sciences, China; Feng Pan, Tsinghua University, China; Rie Y. Umetsu(Ms.), Tohoku University, Japan; Joonyeon Chang, Korea Institute of Science and Technology (KIST), Korea; Lianzhou Wang, University of Queensland, Australia

Monday PM
August 19, 2019

Room: 312 (3rd Floor)
Symposium: O

Chairs:
Hongda Chen, Institute of Semiconductors, Chinese Academy of Sciences, China
Feng Pan, Tsinghua University, China
Rie Y. Umetsu, Tohoku University, Japan
Joonyeon Chang, Korea Institute of Science and Technology, Korea
Lianzhou Wang, The University of Queensland, Austraila

13:30-14:00 Keynote

Imaging Topological Electron-Spin Textures by Using Atomic-Resolution Lorentz TEM

Xiuzhen Yu, RIKEN, Japan

The nanometer-scale vortex-like spin textures, such as vortex-anrivortex pairs in ferromagnetic (FM) domain walls, votices in superconductors, skyrmion (lattice) and antiskyrmions in magnets with inversion symmetry, have recently attracted enormous attention owing to their emergent phenomena. To confirm such minute complex spin textures and their dynamics with external stimuli, ultrafast real-space high-resolution imaging technique, such as time-resoved X-ray microscopy or Lorentz transmission electron microscopy (TEM) is useful.
In this talk, I will present several vortex-like spin textures realized by Lorentz TEM with atomic resolution in several systems, such as chiral magnets, ferromagnets with uniaxial anisotropy and the fluctrated magnets with Ruderman–Kittel–Kasuya–Yosida (RKKY) interaction. In addition to the hexagonal skyrmion lattice (hex-SkL), a square lattice of merons and antimerons (sq-ML)—topologically distinguish with skyrmions—have been observed. By finely varying the external magnetic fields, the transformation between the sq-ML and a hex-SkL have been induced. We found that the skyrmions were very robust, lasting even as we lowered the temperature of the thin plate, but the merons and antimerons were much more sensitive, and relaxed into spin helices as the temperature fell.
Futhermore, the transition between skyrmions (topological "particals") and antiskyrmions ("antiparticles") via non-topological magnetic bubbles have been also demonstrated by means of the in-situ Lorentz TEM observations in a chiral system with D2d-symmetry. The control of topological nature among various magnetic vortices with external stimuli will be shown.
These works have been done in collaboration with Profs. Yoshinori Tokura, Naoto Nagaosa, Taka-hisa Arima, Yusuke Tokunaga, Shinichiro Seki and Fumitaka Kagawa, and with Drs. Wataru Koshibae, Yasujiro Taguchi, Khanh Nguyen, Daisuke Morikawa, Naoya Kanazawa, Tomoyuki Yokouchi, Kiyou Shibata, Licong Peng and Yoshio Kaneko.

14:00-14:30 Keynote

Spin-Orbit Technologies: From Magnetic Memory to Terahertz Generation

Hyunsoo Yang, National University of Singapore, Singapore

Spintronic devices utilize an electric current to alter the state of a magnetic material and thus find great applications in magnetic memory. Over the last decade, spintronic research has focused largely on techniques based on spin-orbit coupling, such as spin-orbit torques (SOTs), to alter the magnetic state. The phenomenon of spin-orbit coupling in magnetic heterostructures was also recently used to generate terahertz emission and thus bridge the gap between spintronics and optoelectronics research.
I will introduce the basic concepts of SOTs, such as their physical origin, the effect of SOTs on a magnetic material, and how to quantitatively measure this effect. Next, I will discuss the latest trends in SOT research, such as the exploration of novel material systems like topological insulators and two-dimensional materials to improve the operation efficiency. Following this, some of the technical challenges in SOT-based magnetic memory will be highlighted. Moving forward, I will introduce the process of terahertz generation in magnetic heterostructures, where the spin-orbit coupling phenomenon plays a dominant role. I will discuss the details of how this terahertz emission process can be extended to novel material systems such as ferrimagnets and topological materials. The final section will focus on how the

terahertz generation process can be used to measure SOTs in magnetic heterostructures, thus highlighting the interrelation between terahertz generation and the SOTs, which are linked by the underlying spin-orbit coupling.

14:30-14:55 Invited

Magnetic Skyrmions-and-Bobbers-Based Racetrack Memory

Haifeng Du, High Magnetic Field Laboratory of the Chinese Academy of Sciences, China; Jing Tang, High Magnetic Field Laboratory of the Chinese Academy of Sciences, China

Magnetic skyrmions and bobbers are two kinds of different nanoscale vortex-like spin configurations that can coexist in chiral magnets. They both possess high stability and particle-like properties and are then proposed to be utilized as binary bits to build the racetrack memory device, where the data bits are encoded by a chain of magnetic domains moving electrically along a given racetrack. The ability to controllably manipulate the two magnetic objects in confined geometries is the prerequisite to realize the device. In this talk, we show by numerical simulations that an isolated skyrmion and bobber can be interconverted by using spin-polarized current in a stepped magnetic nanostructure. They both can be driven collectively by current-induced spin torques. But, they show different dynamical behavior. In addition, we further demonstrate the feasibility of encoding data bits by a series of skyrmions and bobbers. Our results not only propose an accessible and controllable method to create the magnetic bobber by electric, but also provide a guide for future magnetic racetrack memory design based on binary magnetic topological structures.

14:55-15:20 Invited

Spintronics in Quantum Materials

Wei Han, Peking University, China

Quantum materials have recently exhibited many unique spin-dependent properties, which could be promising material candidates for spintronics. On the other hand, pure spin current, flow of spin angular momentum without the company of any charge current, can be a useful probe for interesting quantum materials/states.
In this talk, I will present our recent experimental results on spintronics in quantum materials. I will first talk about the using topological insulators for spintronics, such as spin and charge conversion, and modificatoin of the magnetic properties in the YIG/(BixSb1-x)2Te3 heterostructures, which are due to the spin-momentum locked properties of the topological surface states. Then I will discuss the pure spin current transport in canted antiferromagnet Cr_2O_3, suggesting the existence of spin superfluid ground state at low temperatures. A large enhancement of the nonlocal spin signal is observed below ~ 20K, and it saturates from ~ 5K down to 2K. We show that the spins can propagate over very long distances (~ 20μm) in such spin superfluid ground state and the nonlocal spin signal decreases very slowly as the spacing increases with an inverse relationship, which is consistent with theoretical prediction. The experimental demonstration of the spin superfluid ground state in canted antiferromagnet will be extremely important for the fundamental physics on the BEC of spin-1 bosons and paves the way for future spin supercurrent devices, such as spin-Josephson junctions.

15:30-16:10 Tea Break

16:10-16:40 Keynote

Magnon Valve and Magnon Junction Effects

Xiufeng Han, Institute of Physics, Chinese Academy of Sciences, China

Compared with the electron based spintronic devices, the magnon based spintronic devices have many attractive features, including minimization of Joule heating, much longer magnon coherence length and additional phase degree of freedom. It has been expected that a device, used a core structure of Magnetic insulator [MI1]/Space [S]/Magnetic insulator [MI2], can also operate by method of magnon current similar to a classical spin valve (SV) and a magnetic tunnel junction (MTJ). Here, we first demonstrated a magnon valve (MI1/S/MI2, YIG/Au/YIG) which consists of two magnetic insulators (MI=YIG) and a nonmagnetic spacer (S=Au). Instead of regulating transport of spin-polarized electrons, the magnon valve regulates flow of magnons. We used the temperature gradient to excite the magnon current in YIG, and inverse spin Hall effect (ISHE) to detect the magnon current across the magnon valve by the electrical method. Our results show that the magnon current transmission between two magnetic insulating layers (YIG) mediated by a nonmagnetic metal (Au) has high efficiency, and the transmission of the magnon current in a magnon valve becomes high (low) as magnetizations of the two magnetic insulators are parallelly (anti-parallelly) configured. We interpret the Magnon Valve Effect (MVE) by the angular momentum conversion and propagation between magnons in two YIG layers and conduction electrons in the Au layer. The temperature dependence of Magnon Valve Ratio (MVR=11% at room temperature) shows approximately a power law, supporting the above magnon-electron spin conversion mechanism. This work conceptually proves the possibility of using magnon

valve structures to manipulate the magnon current in magnetic insulators, which has potential applications in magnon based devices.

Then, we designed and manufactured an all-insulating magnon junction with sandwich structure MI1/S/MI2 (S=AFI, antiferromagnetic insulator, such as YIG/NiO/YIG), in order to achieve pure magnon transport. The devices were made on magnetron sputtering system which is a technique used for industrial large-scale production. Necessarily, the transport and manipulating properties of magnon were investigated. When the temperature gradient was applied, the magnon current would flow from one MI to the other MI through the AFI. So the magnon current in any MI are easily influence by the other MI layer. Then setting a heavy metal Pt on the top MI layer for detecting magnon, one could find an effect that the signal of ISHE is related to the magnetization structure of both MI layers, similar to the TMR effect in an MTJ. Furthermore, the magnon valve ratio in such magnon junctions can be increase to 100%. Hence, the electric-insulating magnon junctions can be used for developing magnon-based circuits, including non-Boolean logic, memory, diode, transistors, magnon waveguide and switches with sizable on-off ratio.

16:40-17:05 Invited

A Novel Electric-Field-Assisted-Switching STT-MRAM Design for Sub-Nanosecond Low Energy Writing

Tai Min, Xi'an Jiaotong University, China

Magnetic Random Access Memory (STT-MRAM) is one of the next generation of new nonvolatile memory, which has the most industrial prospects and followed lots of new ideas. Recently, we found that under a small electric bias voltage induced by Ionic liquid gating, the synthetic anti-ferromagnetic multilayer system (FeCoB/Ru/FeCoB and $(Pt/Co)_2/Ru/(Co/Pt)_2$) can be changed from an antiferromagnetic coupling state to a ferromagnetic coupling state. Based on this phenomenon, we propose a new type of STT-MRAM with SAF free layer in which the critical write current can be reduced significantly. Micro magnetic simulation has been used to investigate the switching behavior and the magnetic dynamics of this SAF free layer design under the impact of the electric field, and found that the switching current density at sub-ns region can be reduced by three – six times of this design, making it a potential candidate to replace L1/2-SRAM at sub-10nm technology node. And to understand the physical origin of the abnormal phenomenon, a toy model has been proposed, in which, the external E-field controlled sign change of the RKKY interaction in SAF gives an extra contribution to rise up the total energy to help the spins climb over the barrier and breaking the processional switching mechanism.

17:05-17:30 Invited

Microscopic Studies of Spin Dynamics with Combined Effect of Multidimensional Magnetic Field and Electric Current

Weisheng Zhao, Xueying Zhang, Beihang University, China; Anni Cao, Huaiwen Yang, Xiaoxuan Zhao, Vernier Nicolas, University Paris-Saclay, France

Spintronics devices play an important role in the era of information and intelligence by providing various solutions for data storage and computing. Studies on spin dynamics are interesting for the development of novel spintronic devices, for the characterization of properties of spintronic materials and for the understanding of underlying physics. In this talk, we present several recent research results on the spin dynamics under the combined effect of various stimulation conditions via a multifunctional Kerr microscope. First, using the coordinated work of fast magnetic field pulses and a permeant magnetic field, we have nucleated micron-size domain bubbles and directly observed the their spontaneous deflation induced by the effect of domain wall (DW) surface tension; Second, using the combined effect of in-plane and the perpendicular magnetic field, we are able to quantify the strength of Dzyaloshinskii-Moriya interactions in Pt/Co/MgO film by observing the asymmetrical expansion of magnetic bubble and find an effective method to tune the strength of DMI; Third, using the combined effect of perpendicular magnetic field and electrical current, we have observed the linear dependence of DW motion velocity on the current density in the Ta/CoFeB/MgO stripes; the effective spin-polarization of CoFeB is found to be as low as 0.26, which can explain the difficulty of DW motion induced by pure spin-transfer torque in this materials; Last, using the combined effect of in-planed magnetic field and electric current, we are able to observe the ultra-efficient spin-orbit toque induced magnetic switching in a W/CoFeB/MgO Hall bar structure, which is very beneficial for the development of novel SOT-based spintronic device.

We believe the above several research shows the importance of spin dynamics study with multiple test conditions. The research results are interesting for the development of novel spintronics devices based on the combined effect of various stimulations.

A. Advanced Steels and Processing: II

Symposium Organizers:

Han Dong, Shanghai University, China; Zhigang Yang,Tsinghua University, China; Yoshitaka Adachi, Nagoya University, Japan; Dong-Woo Suh, Pohang University of Science and Technology (POSTCEH), Korea; Christopher Hutchinson, Monash University, Australia; Amy Clarke, Colorado School of Mines, USA

Tuesday AM Room: Room 205+206+207(2nd Floor)
August 20, 2019 Symposium: A

Chairs:
Zhaoping Lv, University of Science and Technology Beijing, China
Mei Zhang, Shanghai University, China

8:30-9:00 Keynote

Formability Evaluation and Fracture Mechanism of 10Mn5 Sheet Steel

Zhang Mei, Shanghai University, China

Medium manganese steel with multiphase microstructure, consisting of amount of ferrite, retained austenite and martensite, shows good strength-plasticity balance and attracts more and more attention from both steel and auto-making. Previous studies have focused on their formability of the structural components of body in white (BIW). To date, the nature of medium manganese's fracture mechanism remains unclear. Against this background, formability evolution and fracture mechanism of 10Mn5 medium manganese sheet steel were extensively investigated based on mechanical test and microstructure observation in this study. Firstly, the mechanical properties of 10Mn5 medium-manganese steel have been tested at different strain rates within the range of 0.00006~0.06667s^{-1} uniaxial tension tests. The steel has superior elongation (EL 40%), TRIP effect and fine ferrite phase are main contributor to such high EL. The strain rates have little influence on mechanical performance. And isotropic mechanical tests of this material have also been measured and show good performance. Other tests including erichsen test, hole expansion test, and parts forming (A-pillar reinforcement beam, Y-tube and endcone) are examined. The dome height can steady reach 10~12mm. Its hole expansion ratio differs largely for different sample preparation conditions (excess 80% for the wire cutting and down to below 30% for punching). And the formability of 10Mn5 sheet steel was tested systematically by conventional cold stamping of a complex A-pillar reinforcement beam. All results show that 10Mn5 sheet steel has a well-behaved mechanical property and fairly good formability. It is indicated that 10Mn5 medium manganese steel is a potential lightweight material for extra-deep drawing quality (EDDQ) automotive parts.

9:00-9:25 Invited

Effect of Intermediate Temperature Annealing on the Stability of Retained Austenite and Mechanical Properties of Medium Mn-TRIP Steel

Xuejun Jin, Lianbo Luo, Wei Li, Shanghai Jiao Tong University, China; Li Wang, Baosteel Research Institute, China

It is well known that the stability of austenite plays a key role in the process of martensitic transformation; hence, the mechanical properties of the TRIP steel. The stability of austenite in medium Mn-TRIP steel is influenced by many factors, including the chemical compositions (in particular C and Mn), grainsize, constraints such as the morphology and residual stress, and deforming temperature. The ultrafine ferrite grains have limited strain hardening capability and the generation of dislocations from the grain boundary sources is the main plasticity mechanism. An enhanced work hardening capacity requires the collaborative effect of dislocation accumulation in ferrite and austenite transformation, and the latter provides the sources for dislocation nucleation and also accumulation in the surrounding ferrite grains. When the deforming temperatures increase (e.g. warm formation), the TRIP effect and working hardening capacity are compromised due to the increasing stability of austenite. However, the early plastic instability occurred when the deforming temperature increased to 100℃ due to the lack of work hardening in ultrafine grains and deformation induced martensitic transformation.
In this study, the effects of austenite and precipitate on deformation behaviors were investigated on the medium Mn-TRIP steels. Our conclusions are as follows:
(1) Based on intermediate temperature annealing heat treatment, approximately 6vol% austenite in the sample transforms into ferrite and precipitates in the matrix. At the same time, some clusters are formed in the austenite grain boundaries with C-Mn segregation, reducing the stability of austenite.
(2) 7Mn-annealed sample showed higher strength and larger ductility than the as-received one at 100℃ The strengthening mechanism is from the precipitation pinning and the boosted TRIP effect, both increased the dislocations density inferrite and inhibited the plastic instability.

9:25-9:50 Invited

Dynamic Strengthening and Phase Transformation Mechanisms of Metastable Austenite in ART-Annealed 0.2C5Mn Steel

Wenquan Cao, Chang Wang, Haifeng Xu, Han Dong, Yuqing Weng, Central Iron and Steel Research Institute (CISRI), China

In this study, a hot rolled 0.2C5Mn steel was annealed

at 650˚C with holding time varied from 5 minutes to 12 hours. Tensile deformation was carried out at different temperatures ranged from +400˚C to -196˚C to examine the annealing time and deformation temperature effects on mechanical property and austenite stability. The microstructure evolution during deformation at different temperature was examined by electron back scattered diffraction pattern (EBSD), transmitted electron microscopy (TEM) and x-rays diffraction (XRD). Microstructure evolution characterization revealed that the metastable austenite gradually transformed into a-martensite controlled by deformation strain and deformation temperature. Mechanical property examination indicated that the tensile deformation behavior was mainly determined by the austenite volume fraction and the deformation temperature. At last, the austenite to martensite phase transformation mechanism during deformation process and the ductility dependence on the austenite volume fraction and mechanical stability were derived and analyzed, which provided a thorough understanding on the TRIP behavior of the ductility enhanced steel aided by the austenite transformation.

9:50-10:10

Chemical Patterning of Austenite as an Additional Degree of Freedom in Microstructural Design of Steels

Christopher Hutchinson, Ruomo Zhang, Xiaohen Weng, Yuxiang Wu, Lingyu Wang, Monash University, Australia; Wenwen Sun, Nanjing University of Science and Technology, China

Third generation advanced high strength steels (AHSS) are multiphase composite materials that exploit the stress or strain induced transformation of austenite to achieve impressive combinations of ductility and *UTS*. The critical aspect of their design is the control of austenite stability so that its transformation into martensite is tuned as a function of temperature, strain and strain-rate to maximise the *UTS*-ductility combination obtained. The austenite stability depends on its chemistry, size and shape, as well as the mechanical constraints imposed by the surrounding phases.

In this contribution, we present a new processing route for controlling both the stability and spatial distribution of metastable austenite in a ferritic matrix in medium Mn steels. It exploits a fine scale (~100nm) chemical patterning of Mn in austenite that may be obtained by the austenitisation of a pearlite structure formed under conditions with strong Mn partitioning between ferrite and cementite. The resulting 'ghost pearlite' ferrite/austenite can be subsequently treated to exhibit an interesting combination of ultimate tensile strength (UTS) (> 2000MPa) and ductility (10% elongation). The simple steel composition and short processing provides a UTS-ductility combination similar to maraging steels and super bainitic steels.

The new concept is one of exploiting a chemically patterned austenite as a template for subsequent phase transformations to design new microstructures that were previously not possible. It represents a new degree of freedom for the microstructural designer and opens new possibilities for the combinations of mechanical properties obtained.

10:10-10:35 Invited

Design of Microstructure for Achieving High Strength in an Fe-10Mn-3Al-0.2C Based Alloy

Yoon-Uk Heo, Sung-Joon Kim, Pohang University of Science and Technology, Korea

Yielding and work hardening behaviors were studied using $\alpha+\gamma$ and $\alpha'+\gamma$ fine lamellar structures in an Fe-10Mn-3Al-0.2C based alloy. An alloy of Fe-10.62Mn-2.84Al-0.17C-0.5Mo (wt.%) steel was prepared by vacuum induction melting. The ingot was homogenized at 1150˚C for 2h, then hot-rolled to 4-mm-thick plates. The plates were solution-treated at 900˚C for 20min then quenched with water. To obtain the $\alpha + \gamma$ lamellar structure, intercritical annealing was performed at 550˚C for 16h (Fig. 1). A plate was then annealed at 800˚C for 1min and cooled in air. Another plate was annealed at 850˚C for 3min and water-quenched. Yielding in $\alpha'+\gamma$ lamellar structure occurred much faster than that in $\alpha+\gamma$ lamellar structure. After yielding, $\alpha'+\gamma$ lamellar structure showed abrupt increase of strength compared to gradual work hardening of $\alpha + \gamma$ lamellar structure. The origin of two different yielding and work hardening behavior was investigated using a transmission electron microscopy (TEM). TEM results demonstrate the importance of neighboring phase contacting with soft γ and mechanical stability of γ for yielding. Abrupt work hardening in $\alpha' +\gamma$ lamellar structure was related with deformation induced martensitic transformation of γ lamella. When g lamella is mechanically stable, yielding occurs by the propagation of pile-up dislocations in α to γ or α' to γ. To understand this yielding mechanism, the stress for the propagation of pile-up dislocations in one phase into another phase is calculated using Hall-Petch behaviors of corresponding phases. Effective grain size of a lamella is determined to calculate the contribution of each boundary of a lamella to dislocation pile-up. Comparison of stresses required to drive α-to-γ and γ-to-α, and α'-to-γ and γ-to-α' propagations of pile-up dislocations suggests that $\alpha+\gamma$ and $\alpha'+\gamma$ lamellar structures yield by propagation of pile-up dislocations in a lamella to γ lamella or α' lamella to γ lamella. Based on the experimental results, the concept for achieving high strength was developed.

10:35-11:10 Tea Break

11:10-11:30

Influence of the Pre-Annealing Treatment on the Retained Austenite and Mechanical Properties of Medium-Mn Steels

Baojia Hu, CAS, China / University of Science and Technology of China, China; Chengwu Zheng, Dianzhong Li, CAS, China

The advanced high strength steel (AHSS) is desirable for developing lightweight structural components in the automotive industry, with a purpose to reduce fuel consumptions and improve the passenger's safety. Among various candidates of the new generation AHSS, the medium Mn transformation induced plasticity (TRIP) steel is considered to the most appropriate due to its lean alloying design with high strength and good ductility. Austenite reversion transformation (ART) in the medium Mn steel has been received wide attentions in view of its close correlation with not only the stability of the metastable austenite but also its potential practice relevance with final microstructures and properties of the final product. However, the medium manganese steel with high strength and ductility is mainly produced by long-time processing of the ART, which limits its industrial production.

In this study, a novel intercritical annealing processing, which involved a pre-annealing before the normal ART treatment (A-ART), was adopted to produce multi-phase microstructural constituents of ferrite, martensite and retained austenite in order to develop a method of potentially short-processing to produce medium Mn steels with high strength and ductility. Here, a 0.2C-5Mn medium Mn steel was used. The specimens were firstly pre-annealed at 680℃ to form a mixture structure, and then reheated to 650℃ for the conventional ART. The underlying microstructures were examined by transmission electron microscopy (TEM), electron back-scattered diffraction (EBSD), and X-ray diffraction (XRD).

The results show that the reversed austenite during the first pre-annealing stage was partly transformed into fresh martensite. The precipitation of carbides was inhibited, which was noticeably different from their precipitation behavior during the low temperature ART annealing at 650℃. After the A-ART process, the final multiphase microstructure was consisted of fresh martensite, lathy ferrite and a large amount of retained austenite. The A-ART process was found dramatically increase the amount of the reversed austenite. This is because the fresh martensite transformed from the unstable reversed austenite at first pre-annealing stage has provided abundant dispersive sites for nucleation of the reversed austenite in the ART at 650℃. The steel after the A-ART exhibited a high tensile strength of 995 MPa together with a total elongation of 32.7%. And an excellent combination of strength and ductility of 32.5 GPa% could be obtained. It is thus proposed that the A-ART is a promising way to simplify the traditional processes of the medium Mn steel and further improve its mechanical properties as well.

11:30-11:50

A Novel 900MPa Grade High Yield Strength Duplex Medium-Mn Lightweight Steel with Distinguished Cold Formability

Degang Liu, Xiao Hu, Hua Ding, Minghui Cai, Northeastern University, China

High strength-ductility synergy and the vehicles' weight reduction as well as low-cost production and environmental friendliness have become critical issues for automotive steel applications. In addition, as passenger compartments enclosed in a strict safety cage, structural reinforcement components require high yield strength to prevent or minimize the deformation for serving spaces around passengers. Thus, the cold stamping formability of advanced high strength steels with high yield strength has become a hot area of research due to some unique advantages. However, as the yield strength of steels increases, their cold stamping properties would decrease significantly. Therefore, it is necessary to develop automotive steels with good formability. In order to meet the requirements of light weighting effect and safety, a novel high yield strength (ferrite + austenite) duplex lightweight steel has been developed, which is characterized by both high yield strength of ~ 900MPa and large elongation of ~ 33%. The enhanced overall tensile properties are found to result from typical planar dislocation glide in the austenite sustained by the uniform arrangement of nano-sized intra-granular κ-carbides, together with the wave slip configuring dislocation tangles in ferrite. Specifically, the high yield strength steel sheets exhibit no obvious cracking or heavy springer back after cold stamping using the U-shaped dies at room temperature, implying a distinguished cold formability. In view of a combination of high strengths and good formability, the present medium-Mn lightweight steel sheets show excellent potentials for applications in the automotive industry at low costs.

11:50-12:10

Enhancement of Both Strength and Ductility by Grain Refinement in Dual Phase Steels

Myeong-heom Park, Akinobu Shibata, Nobuhiro Tsuji, Kyoto University, Japan

Low-carbon dual phase (DP) steels composed of ferrite (soft phase) and martensite (hard phase) are widely used for industrial applications due to their high strength, adequate ductility and excellent formability. It is considered that this well-balanced mechanical property of DP steels results from an interaction between ferrite and martensite under deformation. Since the microstructures of DP steels are micro-scale mixtures of ferrite and martensite, the mechanical interaction should be clarified to fully understand its mechanical

properties. In this study, we thoroughly investigated the mechanical interaction between ferrite and martensite in DP steels having different grain sizes. We fabricated DP structures with different ferrite grain sizes ranging from 58.3μm to 4.1μm, having the same martensite distribution (network-shaped martensite morphology) and the same martensite volume fraction (f_M = 43%) by various heat treatments. The hardness of ferrite and martensite was measured by a nano indentation test to confirm the hardness ratio between two phases of the DP structures. We found that the hardness ratio of the DP structures having different grain sizes was almost identical. In order to evaluate mechanical properties of the DP structures with different grains sizes, an uniaxial tensile test was carried out at a quasi-static strain rate at room temperature. It was found from the tensile tests that the fine-grained DP structure showed higher strength and larger elongation than the coarse-grained DP structure. To clarify details of their microscopic deformation behaviors, strain-partitioning between ferrite and martensite was quantitatively investigated by Digital Image Correlation (DIC) method. It was clearly found that the coarse-grained DP structure showed large strain localization in the ferrite phase, meanwhile the fine-grained DP structure was homogeneously deformed without large strain concentration. This reveals that the effective suppression of strain localization, demonstrated in the fine-grained DP structure, results in enhancing its ductility, as well as strength.

B. High Temperature Structural Materials: Fundamentals of Superalloys

Symposium Organizers:

Qiang Feng, University of Science and Technology Beijing, China; Shengkai Gong, Beihang University, China; Hyun Uk Hong, Changwon National University, Korea; Damon Kent, University of Sunshine Coast, Australia; Sammy Tin, Illinois Institute of Technology, USA; Hiroyuki Yasuda, Osaka University, Japan; Jun Zhang, Northwestern Polytechnical University, China

Tuesday AM | Room: 305 (3rd floor)
August 20, 2019 | Symposium: B

Chairs:
Hongbiao Dong, University of Leicester, UK
Michael Mills, The Ohio State University, USA

8:30-9:00 Keynote

New Insights into Rate Limiting Deformation Processes in Ni-Base Superalloys

Michael Mills[1]
1. The Ohio State University, USA

Polycrystalline Ni-based superalloys are vital materials for disks in the hot section of aerospace and land-based turbine engines due to their exceptional microstructural stability and strength at high temperatures. In the drive to increase operating temperatures and hold times, hence increasing engine efficiency and reduction of carbon emissions, the creep properties of these alloys is becoming increasingly important. At higher temperatures, new and unexpected deformation modes become active. For instance, twinning and stacking fault shearing are important operative mechanisms in the 600~800˚c temperature range. Advanced characterization techniques-based on scanning transmission electron microscopy using diffraction contrast imaging, high resolution imaging, and energy dispersive spectroscopy-have been used to gain new insights into these mechanisms and the rate-limiting processes during high temperature deformation. It is becoming increasing clear that localized phase transformations at stacking faults which shear the precipitates can alter the active deformation mechanisms and provide either strengthening or softening effects at higher temperature, and that these effects are also very sensitive to the alloy composition. This presentation will summarize some of these recent findings and will also highlight the modeling efforts of our NSF-funded DMREF program that seek to predict the active deformation mechanisms, incorporate them into enhanced creep behavior models, and provide insights that can lead to alloys with higher temperature capability.

9:00-9:25 Invited

The Effect of Segregation of Solutes at Crystal Defects on the Mechanical Performance of Superalloys

Paraskevas Kontis[1], Lola Lilensten[1], Phillip Kürnsteiner[1], Alice Cervellon[1], Jonathan Cormier[2], Dierk Raabe[1], Baptiste Gault[1]
1. Max-Planck-Institut für Eisenforschung GmbH, Germany
2. Institut Pprime, Germany

Development of new enhanced superalloys will allow operational temperatures of aero-engines and land-based gas turbines to increase, resulting in lower carbon emissions and improved performance. However, a better understanding of the deformation mechanisms at elevated temperatures is required for the development of smart material-design strategies. For instance, the mechanism controlling the complete or partial dissolution of γ' precipitates at elevated temperatures by the presence of high dislocation density is not well understood. We also have limited information on the deformation of secondary grain boundary phases, such as borides, which can control the mechanical performance of polycrystalline superalloys. Finally, it is still unclear how the undesirable topologically-closed packed phases forming in highly deformed regions

during deformation at elevated temperatures. For all the above open questions we provide new fundamental insights into the role of crystalline imperfections, such as dislocations and stacking faults, on the lifetime of single and polycrystalline nickel-based superalloys. We have performed systematic high resolution characterization studies at the near-atomic scale by using atom probe tomography (APT) in nickel-based superalloys deformed under creep and fatigue conditions at various temperatures. We will present quantitative, near-atomic scale segregation of solutes at crystal defects in γ' precipitates and grain boundary borides. Direct observation of the segregation of particular solutes at crystal defects, allow us to elucidate the physical mechanisms controlling the mechanical performance of superalloys.

9:25-9:45

Interface Structures in Nickel-Based Single Crystal Superalloys during Rafting at High Temperatures

Dongqing Qi[1,2], Peng Zhao[1], Li Wang[1], Jian Zhang[1], Hengqiang Ye[1], *Kui Du* [1]
1 Institute of Metal Research, Chinese Academy of Sciences, China
2 University of Science and Technology of China, China

Single crystal nickel-based superalloys show excellent mechanical properties, especially high creep strength, and are widely used for turbine blades of aircraft engines and gas turbines. In recent years, with the increasing service temperature of turbine blades, the creep deformation behaviors above 1000˚C have been attracted strong attention. At such high temperatures, interfacial grooves from γ phase intruding into γ' phase were observed at γ/γ' interfaces during both creep and aging in nickel-based single crystal superalloys. It is worthy to note that there is often one dislocation at the tip of each groove. The types of dislocations at the tip of grooves have been comprehensively investigated. These grooves are determined being induced by the stress field of interfacial dislocations. In addition, some γ-forming elements, mainly Re, Co and Cr, are enriched around the dislocation at the tip of each groove. The enrichment of these elements with slow diffusion coefficients could impede the movement of dislocations along the interfaces. During cooling, the cooling rate has significant effects on the evolution of interfacial grooves, due to the swelling of primary γ' phases contending with the precipitation of secondary γ' phases in γ matrix. With a slow cooling rate, such as cooling in furnace, the swelling of primary γ' phases is more dominant. Therefore, the swelling of primary γ' phases during cooling could further increase the depth of grooves, especially with a slow cooling rate. While attentions were focused on the formation mechanisms of grooves before, there are many effects induced by grooves on the deformation mechanism, such as the evolution of γ/γ' interfaces and the evolution of γ' phases. In this work, the γ/γ' interface structures and their evolution during both creep and aging at 1120˚C are investigated in a third-generation single crystal superalloy with aberration-corrected scanning transmission electron microscopy in addition to energy dispersive spectroscopy.

9:45-10:05

The Tetrahedral-Octahedral Site Trajectories of Boron in $L1_2$ Ni_3Al and Its (010) Antiphase Boundary

Yi Wang[1, 2], Kristopher A Darling[3], Hongyeun Kim[2], Shunli Shang[2], Laszlo J Kecskes[4], Qiang Feng[5], Xidong Hui[5], Jinshan Li[1], Zikui Liu[2]
1 Northwestern Polytechnical University, China
2 Pennsylvania State University, USA
3 U.S. Army Research Laboratory, USA
4 Johns Hopkins University, USA
5 University of Science and Technology Beijing, China

The development of superalloys has been driven by the more aggressive operating conditions of gas turbines in power plants (gasified coal, low-grade oil and gas with high sulfur content) and aircraft engines (high temperature and stress). To reveal the high-temperature strength, strengthening mechanism and the anomalous flow stress of superalloys, it is necessary to discuss their structural defects, such as stacking faults, anti-phase boundaries (APB) and dislocations. Being an important minor alloying element, boron (B) is commonly added to strengthen γ/γ' Ni-based superalloys while dramatically improving the room temperature ductility of γ', enhancing the tolerance for minor solidification defects and suppressing the intergranular fractures. Knowledge of site occupations of B in the γ' Ni_3Al phase is essential in revealing its interactions with key alloying elements. Furthermore, investigating site occupation of B in antiphase boundaries (APBs) of Ni_3Al is necessary to study the role that APBs play in the anomalous yield behavior of Ni-based superalloys. In this work, we demonstrate the preferred octahedral site occupations of boron in $L1_2$ Ni_3Al and its (010) type APB. Based on the electronic structures of (010) type APB, 12 initial tetrahedral sites for B are identified and reduced to 6 distinct configurations, which finally transform into 4 independent octahedral sites presented by the atomic trajectories. Far away from the fault layers of APB, the most energetically favorable octahedral site for B was dominated by energy differences associated to the tetrahedral-octahedral transition, which is attributed to a lower electron density of octahedral site than that of tetrahedral ones. This work provides an insight into the atomic and electronic basis for solid-solution strengthening mechanism of $L1_2$ Ni_3Al and its (010) type APB.

10:05-10:20 Tea Break

Chairs:
Lei Wang, Northeastern University, China
Sophie Primig, UNSW Sydney, Australia

10:20-10:45 Invited

Designing the Microstructure of Alloy 718

Sophie Primig[1], Felix Theska[1], Vitor Rielli[1], Simon P Ringer[2]
1. UNSW Sydney, Australia
2. The University of Sydney, Australia

Nickel-based superalloys require critical properties such as high strength, low creep rates, wear, and corrosion resistance for operation under extreme environments. Alloy 718 is one of the most commonly used high temperature superalloys for contemporary aircraft engine disc applications. Conventional thermo-mechanical processing of alloy 718 turbine discs is carried out via multi-stage forging followed by solution annealing and double-ageing for controlled precipitation of secondary phases as precipitates and nanometer-sized clusters. In order to achieve higher yield strength, a 'direct age process' developed in the late 1970s can be utilized instead. Even if this process is used for processing the majority of modern aircraft engine discs, the underlying microstructural mechanisms are not fully understood.
Therefore, we developed a correlative microscopy approach that allows imaging over multiple length scales covering the grain structure down to the atomic order to understand the corresponding processing-structure-property relationship during direct ageing. The chemical and structural similarities of precipitates and nanometer-sized clusters to the surrounding matrix material require high-resolution characterisation techniques including scanning electron and atom probe microscopy. We recently presented a model for the microstructural evolution during direct versus conventional ageing which where we report a remarkable structuring within and between the nanoscale gamma' and gamma" precipitation. Not only did we find an increase in both the volume fraction and size of the gamma" precipitates, we found a prevalence of gamma'/gamma" co-precipitation stacked in a variety of sequences depending on the nucleation condition. This finding opens up new degrees of freedom in the design of superalloy microstructure, raising fundamental questions as to which precipitate dispersions are the most effective, and how novel direct ageing-type processes might be devised that generate properly tailored microstructures.

10:45-11:05

Deformation Behavior and Strengthening-Toughening of GH4169 Alloy with Multi-Field Coupling

Lei Wang [1], Jinlan An[1, 2], Yang Liu[1], Xiu Song[1]
1. Northeastern University, China
2. Shenyang Aerospace University, China

Nickel-base GH4169 superalloy shows excellent combination properties including good fatigue property, good oxidation resistance and corrosion property. For satisfying high performance of aero-engine, both strength and ductility of GH4169 alloy at high temperature are required to be simultaneously improved for safety servicing. It is an effective method to strengthen alloys by adding alloying elements, which unavoidably leads to hard deforming and plasticity declining. Therefore, it is key to find method realizing strengthening-toughening and without any losing of hot-deforming ability. In present research, the multi-field (electric-pulse current (EPC)/ temperature/stress) coupling was applied to GH4169 superalloy. The strengthening-toughening mechanisms and plastic deformation behavior of GH4169 alloy with multi-field coupling were investigated. The results show that deformation resistance decreases and plastic deformation ability increases of GH4169 alloy with multi-field coupling. It is found that the thermal vibration of atoms enhances leading to decreasing of Peierls force with multi-field coupling, which is the essential factor on deformation resistance decrease and plastic deformation coordinate ability increase. When the alloy aged with electric-pulse treatment (EPT)/temperature coupling, the ultimate strength, yield strength and fracture elongation increase simultaneously. The vacancy concentration increases of the alloy aged with EPT/temperature coupling. Vacancy induces ultrafine nm-sized γ" phase to precipitate during tensile deformation at high temperature, which is the key factor on strength and ductility improvement.

11:05-11:25

Influence of Heat Treatment on Microstructures and High-Temperature Mechanical Properties of Selective Laser Melted Inconel 625

Jiwon Lee[1], Jinhyeok Kim[1], Sunyoung Jun[1], T Mathieu[1], C Etienne[1], L Philippe[1], H Hyunuk[1]
1. Changwon National University, Korea

Inconel 625 has been widely used for submarine, aerospace, power generation applications where superior mechanical resistance is required. Today, feasibility of manufacturing Inconel 625 by additive manufacturing (AM) is considered in the frame of near net shape fabrication. Although studies on AM are actively in progress world wide, microstructure as well as appropriate post heat treatment are not well understood yet. In this study, Inconel 625 is fabricated by

selective laser melting (SLM) with proper manufacturing conditions (Power: 275W, Scanning speed: 760mm/s) ensuring 0.33% of relative porosity fraction. On as-built sample, X-Ray diffraction residual stress measurement along the building direction resulted in normal and shear stress respectively of Min. 245MPa average deviation 34MPa and Min. 7MPa average deviation 5MPa. Heat treatment is then applied to some of as-built samples with two different objectives. The first one is designed for recrystallization and homogenization; standard heat treatment. The second one is conducted to induce the grain boundary serration (GBS) as for strengthening the material and enhancing its creep properties; GBS heat treatment. The microstructure and the mechanical properties of as-built and heattreated samples are compared to that of standard wrought Inconel 625. The microstructure of as-built sample shows epitaxial grown columnar structures with interdendrite segregation dominantly composed with Nb and C due to rapid cooling and heating during fabrication. After standard heat treatment, recrystallization occurs on the whole sample, however NbC carbides still remain in inter and intra granular regions. Grain boundary serration is successfully obtained with over 70% in volume fraction on wholly recrystallized grains by specially designed heat treatment. NbC carbides are precipitated on some parts of the grain boundaries and $M_{23}C_6$ carbides are also observed simultaneously in grain boundary serration heat treated samples. Based on these microstructural analysis, high temperature mechanical properties are evaluated and discussed.

11:25-11:45

Morphological Characterization of Multimodal Microstructure for Ni-Based Superalloy Udimet 720Li

Yoshiya Yamaguchi[1], Hiromu Hisazawa[2], Terada Yoshihiro[1]
1. Tokyo Institute of Technology, Japan
2. Tokushima University, Japan

Ni-based superalloys are used for aerospace jet-engine components due to superior mechanical properties. It is important to control γ' morphology for improving high-temperature strength in the superalloys. It is known that various γ' morphology and γ' sizes are exhibited during an isothermal aging for the alloys. Multimodal γ' microstructure usually appears for the superalloys with higher γ' volume fraction for disc applications. In recent years, researches have been attempted to the construct models predicting the high-temperature strength for Ni-based superalloys with multimodal γ' microstructures. The aim of the present study is to evaluate the γ' morphology quantitively by using the absolute moment invariants for Udimet 720Li.
Wrought Ni-based superalloy Udimet 720 is used in this study. The alloy was solution treated at the super-solvus temperature followed by various cooling methods; such as water quenching (WQ), oil quenching (OQ), air cooling (AC) and furnace cooling (FC). Isothermal aging was carried out at 1073–1173K for up to 3000h. Microstructure observation was conducted by using field emission scanning electron microscopy (FE-SEM) and transmission electron microscopy (TEM). The morphology of γ' precipitates is quantitively evaluated by using the absolute moment invariants. Micro-Vickers hardness tester was used for hardness measurement.
The secondary γ' precipitates are observed in this study for every cooling condition, while tertiary γ' precipitates are observed only for the FC alloy. That is, the slow cooling from the super-solvus temperature results in the multimodal distribution of γ' precipitates. The size of secondary γ' precipitates, d, increases continuously with the decrease of cooling rate, v, along with the following equation; $d \propto v^{-0.4}$. It is clarified that the morphology of secondary γ' precipitates evolves from a spherical to a cubic and/or octo-dendrite shape with the decrease of cooling rate, while the aspect ratio remains unchanged. The effect of isothermal aging on the size and morphology of secondary γ' precipitates are examined for the OQ and FC alloys. In the case of the OQ alloy, the value of d continuously increases with aging time at 1173K, while the spherical shape remains unchanged during aging. The Ostwald ripening of secondary γ' precipitates occurs for the OQ alloy. On the contrary, for the FC alloy, the morphology of secondary γ' precipitates evolves from an octo-dendrite to a spherical shape with aging time under the almost constant value of d.

C1. Light Metals and Alloys-Aluminum: I

Symposium Organizers:

Baiqing Xiong, GRINM Group Co. Ltd., China; Yoshihito Kawamura, Kumamoto University, Japan; Young Min Kim, Korea Institute of Materials Science (KIMS), Korea; Jian-Feng Nie, Monash University, Australia; Diran Apelian, Worceste Polytechnic Institute, USA

Tuesday AM — Room: Presidium Conference Room (4th Floor)
August 20, 2019 — Symposium: C1

Chairs:
Brajendra Mishr, Worcester Polytechnic Institute, United States
Jianghua Chen, Hunan University, China

8:30-9:00 Keynote

Electron Microscopy for Aluminum Alloys as Light-Weight Industry Materials

Jianghua Chen, Hunan University, China

Developments of high-strength aluminum alloys have always faced a difficult problem: owing to their small size, the early-stage strengthening precipitates are

difficult to characterize in terms of composition, structure and evolution. Here we employ atomic-resolution transmission electron microscopy (TEM) imaging and first-principles energy calculations to address these problems. Recent years, we have investigated tens of typical high strength aluminum alloys, such as 2xxx (AlCu, AlCuMg and AlCuLiMg), 6xxx (AlMgSi and AlMgSiCu) and 7xxx (AlZnMg and AlZnMgCu) alloys, with different compositions and with varying thermal processes for understanding their property-structure-process correlations. Using aberration-corrected high-resolution TEM (HRTEM) and aberration-corrected scanning TEM (STEM), much of our attention has been paid to revisit the strengthening precipitates in these important alloys and to clarify the controversies left in the past about their precipitation behaviors. Our study demonstrates the followings:

(1) Atomic-resolution imaging in STEM can provide straightforward structure models at the atomic-scale, whereas atomic-resolution imaging in HRTEM with rapid quantitative image simulation analysis can provide the refined structures with high precision beyond the resolution limitation of the microscope. The combination of the two techniques can be more powerful in solving difficult structure problems in materials science.

(2) Most of the early-stage precipitates in aluminum alloys are highly dynamic in both composition and structure. Typically, having their characteristic genetic skeletons to guide their evolution, these dynamic precipitates initiate, mature and grow with thermal aging following characteristic evolution paths. The fine precipitation scenarios revealed in our studies are rather different from previous understandings in the textbooks and literatures published thus far.

9:00-9:20

Anisotropic Behavior and Related Deformation Mechanism of Al/Mg/Al Clad Sheet

Toko Tokunaga, Kumamoto University, Japan

In terms of energy and resource savings, Al and Mg alloys are ideal materials for vehicles because of their low density and high recyclability. These attractive characteristics lead to wide attention of using these alloys together in one component. The authors have developed a fabrication process of Al/Mg/Al clad sheet by hot extrusion and subsequent hot rolling. The sheet exhibited a significant tensile elongation of more than 700% at 300˚C and at $1.0\times10^{-3}s^{-1}$. No cracks were observed at the Al/Mg interface after the elongation. The large elongation of the sheet is classified into the superplasticity in terms of the elongation and the strain rate sensitivity. Considering the poor formability of Mg alloys, deep drawing process is known to be one of the best processes to manufacture thin-walled Mg alloy parts. Thus, the Al/Mg/Al sheet can be deformed by deep drawing process by taking advantage of its superplastic characteristic. Formability by the deep drawing process is significantly influenced by the anisotropy of materials. Therefore, in the present study, anisotropic behavior of the Al/Mg/Al sheet is investigated. To understand the behavior, the anisotropy was discussed in the light of the crystallographic orientation of the Al and the Mg alloy.

Pure Al (99.99%) and AZ80 Mg alloy (Mg-8.2Al-0.56Zn-0.44Mn (mass%)) were used for the cladding and substrate layers, respectively. The Al/Mg/Al sheet was fabricated by hot extrusion followed by hot rolling. The processing temperature and the reduction ratio of the materials were 290˚C and 90% for the extrusion, and 350˚C and 81% for the rolling, respectively. To investigate the anisotropic behavior of the sheet, tensile tests were conducted. The tensile specimens were wire-cut from the sheet to have 0, 45, and 90° between the tensile and the rolling directions. Tensile tests were conducted at 25, 200, 250, and 300˚C, and at 1.0×10^{-2}, 5.0×10^{-3}, and $1.0\times10^{-3}s^{-1}$. Crystallographic orientations of the Al and the Mg alloy were investigated by Electron BackScatter Diffraction (EBSD) before and after the tensile tests.

At room temperature, the highest elongation and strength were obtained with the Al/Mg/Al sheet tensile-tested in 90° direction at any strain rates. There was no big difference in elongation and strength in the samples tensile-tested in 0 and 45° directions. At elevated temperatures, neither anisotropy in elongation nor strength was not observed in any specimens, and the reasons for this result is considered as follows. In the Al/Mg/Al sheet, the Mg alloy is much thicker than the Al layers and therefore the Mg alloy dominated the deformation of the sheet. It is known that the Mg alloy deformed with the grain boundary sliding during the superplastic deformation. Thus, the Al/Mg/Al sheet deformed mainly with grain boundary sliding at elevated temperatures. Since the anisotropy is mainly arisen by dislocation slip, the Al/Mg/Al sheet did not show anisotropy in the present study. Consequently, there was no anisotropy in the superplastic behavior of the Al/Mg/Al sheet.

9:20-9:40

Precipitation in Aluminium Alloys: Shake or Bake?

Christopher Hutchinson, Wenwen Sun, Yuman Zhu, Qi Zhang, Lingyu Wang, Xiang Gao, Monash University, Australia; Ross Marceau, Deakin University, Australia

High strength Al alloys exploit solid state precipitation to tailor their mechanical response. This precipitation requires two ingredients: a thermodynamic driving force and atomic mobility. For a given alloy chemistry, the heat treatment (precipitation) temperature is chosen as a compromise between having sufficient driving force

for precipitation and sufficient atomic mobility so that the precipitation reaction occurs in a reasonable time and results in a 'not too coarse' precipitate distribution. It is this compromise that frames the competition between nucleation, growth and coarsening that constrains the possible precipitate distributions and hence mechanical responses.

In this presentation, we demonstrate a new approach to precipitation hardening that does not use thermal treatments and therefore allows independent control over the thermodynamic driving force and atomic mobility. This provides a means to fully alter the competition between precipitate nucleation, growth and coarsening and new microstructures, with new combinations of properties are obtained.

The approach uses small amplitude cyclic plasticity at room temperature as a means of continually pumping vacancies into the system to achieve atomic mobility under conditions of high thermodynamic driving force. The approach is self-regulating (in both space and particle size) and results in extremely uniform and fine-scale microstructures. The approach can be used either as a new processing route for high strength Al alloys, or as a 'training' routine to improve the high cycle fatigue properties of precipitate strengthened Al alloys. Both examples will be shown in this presentation.

9:40-10:00

Effect of Alloy Elements on Non-Basal Slips in Magnesium Single Crystals

Shinji Ando, Kumamoto University, Japan / Magnesium Research Center, Japan; Tomohiro Hanada, Kosuke Hayashi, Kumamoto University, Japan / Graduate School of Science and Technology, Japan; Hiromoto Kitahara, Kumamoto University, Japan / Institute of Pulsed Power Science, Japan

Magnesiumand magnesium alloys are candidate materials for energy saving of transportation vehicles and devices due to their high specific strength and low density. However, the plasticity of magnesium at room temperature is poor since basal slip system, which is their main slip system, has limited number of independent slip systems available to accommodate applied plastic deformation. Therefore, activation of non-basal slip systems is necessary to show good ductility. Recently, effect of yttrium on ductility of magnesium and discussion for activity of (c+a) pyramidal slips has been reported. In this study, to investigate effects of yttrium and other alloying elements, such as aluminium, zinc and cerium, on non-basal slips, [11-20] tensile and [0001] compression tests of magnesium alloy single crystals were carried out at 77K, 293K and 473K. Specimen sizes of tensile test and compression tests were 20 x 3 x 0.3mm^3 and 6 x 3 x 3mm^3, respectively. Cross head speed of both tests was 0.05mm/min. Complex alloying effects on the deformation behaviour of magnesium in tension and compression were observed. In compression tests of Mg-0.5Al, Mg-0.5Zn, Mg-0.5Y, Mg-1.45Al-0.15Zn and Mg-2.7Al-0.4Zn, second order pyramidal slips (SPCS) were observed, and the critical resolved shear stresses (CRSS) of SPCS sere increased by alloying. In tensile tests of Mg - 0.052Ce, SPCS was observed and the CRSS was decreased. In Mg-0.5Al, Mg-1.0Al and Mg-2.6Al-0.3Zn, the alloys were yield due to {10-11} twin instead of SPCS. Mg-(0.6-0.9)Y single crystals were yielded due to first order pyramidal slip instead of SPCS, and showed high ductility than in pure magnesium. (c+a) edge dislocation immobilization by thermal activation process following double cross slip of (c+a) screw dislocation, have been proposed as deformation mechanism for SPCS in pure magnesium. Based on the mechanism, effect of alloying elements on ductility of magnesium was discussed.

10:00-10:20

Effect of Various Texture Components on the Formability of Al Alloy AA5182 at the Plane Strain Condition

Zhenshan Liu, Jingwei Zhao, Kangcai Yu, Lei Fu, Pizhi Zhao, Chinalco Materials Application Research Institute Co. Ltd., China

During the stamping of automotive parts, the cracking usually happens in the plane strain zone. This paper studied the influence of grain orientation on the plane strain at the forming limit curve (FLC) in Al alloy AA5182, utilized as automotive inner panel. To achieve different grain orientation distribution with the same grain size, cold rolled sheets are annealed at various approaches, Continuous Annealing air furnace (CA), Salt Bath (SB), and Box type Air furnace (BA). FLCs of these annealed samples, which only difference in texture distribution, are tested along various directions with digital image correlation technique. It is found that the plane strain at FLC, exactly speaking minimum major strain (FLCmin) varies in the range from 0.191 to 0.208 for these annealed AA5182 sheets. The texture components in annealed AA5182 sheet scatter far away to their ideal orientation. In the sample annealed with CA and SB (500˚C × 1min), Q and random texture take the dominance; in the sample annealed with BA (450˚C × 2 hours), Cube, Brass, R and Q are the main texture components. This difference of texture components has limited effect on FLCmin, only 1% of it. FLCmin shows good linear relationship with elongation, uniform elongation, work hardening index, but has no clear correlation with r value. Hence, r value is not a suitable parameter to characterize the formability during the stamping of automotive aluminum sheet.

10:20-10:45 Tea Break

10:45-11:10 Invited

In-Situ Processes for Production of Aluminum-Matrix Nanocomposites

Brajendra Mishra, Jeremy Fedors, Worcester Polytechnic Institute, United States

Increasing the mechanical properties of cast aluminum components at temperatures in the vicinity of 300˚C will allow for lightweighting opportunities, especially in automotive and aerospace applications. Metal-matrix nanocomposites show great promise in this regard, in the form of aluminum as a matrix containing well-dispersed ceramic nanoparticles. These have been shown to retain most of the ductility of the matrix alloy, while adding strength and stiffness at far lower reinforcement fractions than are required in microcomposites. Unfortunately, metal-matrix nanocomposites are plagued by issues which limit commercialization, such as high costs of production, issues with particle wetting and dispersion, low potential for scalability and poor castability. In this work, two existing metal-matrix nanocomposite manufacturing processes showing promise to overcome some of these obstacles were developed further: the in-situ gas-liquid reaction, and self-propagating high-temperature synthesis. Composites reinforced with aluminum nitride and titanium carbide were produced, alloyed with several matrix compositions and squeeze cast. The in-situ gas-liquid reaction simply introduces nitrogen gas into liquid aluminum at a set temperature and a controlled flow rate, which allows the reaction to form aluminum nitride nanoparticles. The SHS process uses fine titanium, carbon, copper oxide and aluminum particles to cause the formation reaction for titanium carbide. Insights into the effects of process design on microstructure and properties were gained, and potential process improvements and areas to focus future research have been identified.

11:10-11:30

Influence of Retrogression Regimes on Microstructure and Properties in a High Zinc Al-9.5Zn-2.1Mg-1.7Cu Alloy

Xiwu Li, Kai Wen, Hongwei Yan, Lizhen Yan, Zhihui Li, Yongan Zhang, GRIMAT Engineering Institute Co., Ltd., China; Baiqing Xiong, GRIMAT Engineering Institute Co., Ltd./GRINM Group Co., Ltd., Beijing, China

In the present work, the influence of various retrogression regimes on hardness, electrical conductivity and mechanical properties of a high Zn-containing Al-9.5Zn-2.1Mg-1.7Cu alloy is investigated and several retrogression regimes subjected to a fixed temperature (170˚C /45, 90, 135min) and time (170, 180, 190˚C/90min) are proposed. The precipitates are investigated by means of transmission electron microscopy (TEM) techniques. The results show that the main precipitates vary from GP zones and η' phase to η' phase and η phase with the prolonging of retrogression time under a fixed temperature of 170˚C. Similarly, the increase of retrogression temperature under a fixed time of 90min also leads to a variation from η' phase to η' phase and η phase. Besides, the matrix precipitates and grain boundary precipitates enlarge with the increase of temperature or the prolonging of time. The influence of precipitates on mechanical properties is discussed through the interaction relationship between precipitates and dislocations.

11:30-11:50

Indentation Microstructure and Stress Analysis of Age-Hardenable 7050 Aluminum Alloy

Ryo Muramatsu, Shinji Muraishi, Shinji Kumai, Tokyo Institute of Technology, Japan

The nano-indentation test is a simple method of measuring the micro hardness and Young's modulus from the load-displacement response of the material surface by a micro-indenter. It is known that characteristic surface displacements such as pile-up and sink-in occur around the impression, but the shape of the plastic region and the residual stress influence on the surface displacement is not clear yet. Therefore, in this study, in order to investigate the relationship between plastic deformation behavior around the indentation by a nano-indentation and aging precipitation, we measured the surface displacement around the indentation of the 7050 precipitation strengthened type aluminum alloy and observed the dislocation structure and the expansion of the plastic zone just under the indentation.

Iindentations were made by nano-indentation test on loading 100 to 50000mgf on the an as-quench (A.Q.) material subjected to solution treatment to 7050 aluminum alloy, a quasi-aging and a peak aging material subjected to aging treatment for 1 hour and 10days at 120˚C after solution treatment. In the load-displacement curve in nano-indentation, the elastic recovery rate increased with increasing aging time. It is considered that fine precipitates due to age hardening act as obstacles of dislocation lines, and the elastic field of these dislocations increased the elastic recovery rate of the impression surface.

Surface displacement around the impression was measured with a laser scanning microscope (LSM) and a scanning probe microscope (SPM). Since the peak of pile-up tends to be located in the outer direction of the indentation under the low load condition where the indentation depth is small, in addition to the plastic displacement of the vertical component of the indenter, the plastic displacement of the tangential component due to the dislocation motion contributes to the formation of pile-up.

The cross-sectional structure just under the indentation

was observed with a transmission electron microscope (TEM). Regardless of the aging condition, the plastic region showed a shape close to an ellipse, and as the aging time increased, the size of the plastic region for the indentation decreased. The characteristic shape of this plastic region is attributable to the dislocation motion occurring on the slip plane diagonal to the loading axis and the size of the plastic region decreased due to the inhibition of dislocation movement by precipitation strengthening.
The average stress and average strain in the plastic zone predicted by TEM observation results and the plastic work of nano-indentation showed good agreement with the yield stress of the present alloy.

11:50-12:10

Impurity Effects on Mechanical Properties of 1xxx Series Aluminum Thin Foils

Toshihiro Hara, Daisuke Egusa, The University of Tokyo, Japan; Mami Mihara, Hiroki Tanaka, UACJ Corporation, Japan; Eiji Abe, The University of Tokyo, Japan / National Institute for Materials Science, Japan

Commercial pure aluminium (Al) thin foils are used for various ways, e.g. packaging foods, electrodes of lithium-ion battery, and electrolytic capacitor. Commercial pure Al alloys inevitably contain impurities which mainly consist of Fe/Si. Mechanical properties of those Al alloys usually understood as in the view of work hardening, however it is also accepted that distributions of Fe/Si elements also affect mechanical properties of the alloys. There are reports on the distributions of these impurities, e.g., precipitation on dislocations or segregations around grain boundaries. Since the behaviour seems to be depend on history of process, details are still unclear. We investigated microstructures of 1050 Al foils with/without inter annealing (denoted IA/NIA, hereafter), especially focusing on distributions of Fe/Si elements. Based on tensile testing of the foils, it is found that elongations are remarkably different, 2.8% for IA and 5.6% for NIA, although the work hardening behaviours are almost same while the testing. This result contradicts usual point of view, suggesting effect of Fe/Si elements on the properties. The states of Fe/Si elements within the foils were identified as $Al_{13}Fe_4$, Al-Fe-Si ternary compounds and pure Si by XRD, SEM and TEM observations. Volume fractions of each state were estimated by XRD profiles, showing that volume fraction of pure Si only was different between IA and NIA. We investigated distributions of pure Si by SEM-EDS/EBSD, resulting that almost pure Si exists along high-angle grain boundaries. Pure Si were few micrometers in radius and their sizes were larger in IA foil. Based on the observations, we designed a mechanism of coarsening of pure Si on grain boundaries by Ostwald ripening during inter annealing process. Such coarsened pure Si on grain boundaries can be a candidate for initiation of fracture, which lead decrease in elongation. The validity of the above mechanism was investigated with SEM and TEM observations of samples before foil rolling.

C2. Light Metals and Alloys-Magnesium: I

Symposium Organizers:

Xianhua Chen, Chongqing University, China; Yoshihito Kawamura, Kumamoto University, Japan; Young Min Kim, Korea Institute of Materials Science (KIMS), Korea; Jian-Feng Nie, Monash University, Australia; Diran Apelian, Worceste Polytechnic Institute, USA

Tuesday AM
August 20, 2019

Room: 406 (4th Floor)
Symposium: C2

Chairs:
Nack J Kim, Postech, Korea
Liming Peng, Shanghai Jiao Tong University, China

8:30-8:55 Keynote

Kink Strengthening of LPSO and Mille-Feuille Structures in Mg Alloys

Eiji Abe, The University of Tokyo, Japan,

Dilute Mg alloys containing a few atomic percent of transition-metal and rare-earth element have attracted increasing attentions because of their excellent mechanical properties. The remarkable microstructural feature common for all of these Mg alloys is formation of a novel type of long-period stacking/order (LPSO) structures; though, it is found that the LPSO structures themselves are not directly responsible for the excellent properties, but the properties can be realizedonly when the kink-deformation regions are densely introduced through the warm-extrusion process. From the extensive studies of the LPSO-structured Mg alloys for more than a decade, it has become apparent that the kink regionsindeed play a critical role for effective strain storage of the alloys, but its detailed mechanism is not fully understood yet.
In order to deepen our understanding of the veiled work-hardening mechanism related to kink, we have just launched the new project aiming the establishment of the "Kink strengthening phenomenon" as a universal strengthen principle. In the meantime, the LPSO structure can be generally viewed as "Mille-feuille structure (MFS)", in the sense that they are constructed by alternate stacking of microscopic hard- and soft-layer. Our preliminary studies have confirmed that the MFS Mg alloys indeed reveal the kink strengthening, whose effect seems to be more prominent than LPSO

Mg alloys. Therefore, solving the critical condition and universality on the kink-strengthening phenomenon will certainly lead to a further development of lightweight structural materials, including novel Al and Ti alloys, and even polymer materials in the future.

8:55-9:20 Keynote

Casting and Solidification of Magnesium Alloys

Yuanding Huang, Kainer Karl, Norbert Hort, Helmholtz-Zentrum Geesthacht, Germany

Magnesium alloys have a high specific strength with their good castability and machinability which are interesting for lightweight construction applications. However, they have a poor room temperature formability and low high-temperature strength. Microstructural modifications such as refining and precipitation were popularly used to improve their ductility and strength. Regarding the subsequent microstructural optimizations, the first step casting and solidification plays a key important role because the quality of initial microstructure directly influences the subsequent one. The present paper introduces some recent investigations on the casting and solidifications in MagIC. First, the influence of alloying elements on the hot tearing of magnesium alloys is simply summarized, including the elements Al, Zn, Y, Gd and Ca. With the increment of alloying element content, the hot tearing susceptibility increases till to a maximum, and then reduce with further increasing the content of alloying element. Second, the applications of synchrotron radiations in the in-situ observations of solidification is introduced for magnesium alloys. It was found that synchrotron radiations could identify the solidification process and also the solidified phases. Finally, the grain refinement of magnesium alloys inoculated by the external particles SiC is reported. When adding the SiC particles to Mg-Al alloys, the casting microstructure was largely refined. The responsible refinement mechanism is due to the formation of Al_2MgC_2 by the reactions of SiC particles with Mg-Al melt. This ternary compound has a very close crystal structure to that of magnesium. As observed in Mg-Al alloys, the additions of SiC particles could also refine the grains of as-cast Mg-Zn alloys. But the refinement mechanism is different from that for Mg-Al alloys. It is attributed to the formation of (Mn, Si)-enriched intermetallics by the interactions between SiC and impurity Mn in Mg-Zn alloys.

9:20-9:40 Invited

Achieving High Strength and High Ductility of Ultrahigh Pressure Mg Alloys

Qiuming Peng, State Key Laboratory of Metastable Materials Science and Technology, China

The compelling need for lightweight, energy-efficient, environmentally benign engineering systems is driving the development of a wide range of structural and functional materials for energy generation, energy storage, propulsion, and transportation. As the lightest metallic structural materials, Mg-Li alloys have been used for various industrial products such as automobile, aerospace, defence, biomedical, sporting and electronic goods sectors owing to their high stiffness, good castability, good electro-magnetic shielding and high damping properties. However, the strength of Mg-Li alloys is reduced with the increasing of Li content. A lot of work has demonstrated that it is possible to improve both strength and ductility simultaneously, but this has mostly been limited to systems with ultrafine microstructures, such as nanotwin Cu or twinning-induced plasticity steels. A high strength duplex-phase Mg-Li alloy without sacrificing the ductility was prepared by ultrahigh pressure technique. The strengthening mechanism is attributed to densely hierarchical {101(—)1}-{101(—)1} double contraction nanotwins (DCTWs) and full-coherent hexagonal close-packed (HCP) particles in twin boundaries. These hierarchical nanoscaled DCTWs with stable interface characteristics not only bestow a large fraction of twin interface but also form interlaced continuous grids, hindering possible dislocation motions. Meanwhile, orderly aggregated particles offer supplemental pinning effect. In addition, the phase transformation of the coherent phase was investigated. Those cutting-edge results provide underlying insights toward designing alternative and more innovative hcp-type structural materials with superior mechanical properties.

9:40-10:00 Invited

Effects of Microstructure on Fracture Toughness of Wrought Mg-8Gd-3Y-0.5Zr Magnesium Alloy

Li Jin, Jing Li, Jie Dong, Fenghua Wang, Shuai Dong, Shanghai Jiao Tong University, China

Fracture toughness is a critical property for Mg alloys applied as structural parts. However, its improvement mechanism has rarely been investigated on newly developed Mg-Gd-Y-Zr alloys. Here, The toughness and uniaxial tensile tests were conducted on a Mg-8Gd-3Y-0.5Zr (wt.%) alloy (GW83) prepared by three different processing methods: rolling, extrusion and forging. The effects of microstructure on the fracture toughness were investigated. The results showed that the fracture toughness was highest in the forged sample but lowest in the rolled sample, which due to the secondary phase strips and high-density dislocations in the forged samples. Careful microstructural characterization revealed that the secondary phase strips which could cause dimples and secondary cracks, and then deflect the main cracks to enhance the fracture resistance for the extruded and forged sample. In addition to the reactivation of the mobile dislocations, initial substructures and dislocations by increasing strain hardening in the plastic zone led to

high fracture toughness for the forged sample further. Moreover, it was proposed that fracture toughness and ductility did not always show the same trend, which was due to the difference in the magnitude of plastic zone and stress field in two test samples and thus resulted in different deformation mechanisms.

10:00-10:20 Invited

Improved Understanding of the Microstructure and Mechanical Behaviour of Mg-Al-RE Alloys

Mark Easton, Suming Zhu, Charlotte Wong, Hua Qian Ang, Dong Qiu, RMIT University, Australia; Trevor Abbott, Magontec Ltd, Australia; Kazuhiro Nogita, Stuart McDonald, David StJohn, University of Queensland, Australia; Jian Feng Nie, Monash University, Australia; Mark Styles, Mark Gibson, CSIRO, Australia

Magnesium – Aluminium – Rare Earth alloys are the most commonly used specialty alloy system with alloys such as AE42 and especially AE44 being commonly used in powertrain applications. Over the past few years, we have been investigating the microstructure and mechanical behaviour of these alloys. The microstructure of the alloys include intermetallics found at grain boundaries (and sometimes within grains). The morphology and identity of these intermetallics and the ternary phase diagrams are not fully consistent with what has been reported previously including the identification of a previously unknown phase. Whilst the particular rare earth additions affect the identity of intermetallic phases, it is actually the Mn content that is critical to the mechanical properties and creep response of these alloys due to precipitation hardening. This means that using low cost REs such as La and Ce to produce alloys without Nd and Pr additions does not significantly degrade the properties. With strength matching AZ91 and ductility matching AM60, the Mg-Al-RE alloys, particularly AE44, are excellent candidates for structural applications. However, since the Mg-Al-RE alloys are primarily strengthened through grain refinement, dispersion strengthening by grain boundary intermetallics and precipitation hardening, they do behave differently to AZ91 and AM60 which have a significant contribution from solid solution strengthening. In particular, AE44 is more strain rate sensitive and has less anelasticity at low strain rates compared with AZ91 and AM60, especially in the aged condition.

10:20-10:35

Experimental Investigation on the Anisotropy of Extruded AZ31 Magnesium Alloys by Combined Tension-Torsion Test

Baodong Shi, Chong Yang, Yan Peng, Yanshan University, China

The urgent need for reducing CO_2 emissions due to the accelerated deterioration of environment is driving increased applications of lightweight engineering materials in automobiles. The properties of magnesium alloys (e.g. low density, high specific strength, good castability and recyclability) make them attractive replacement for the more mass-intensive materials, and the promising energy efficiency improvements with Mg alloys as vehicle components are significant. However, as one of the Hexagonal Closed Packed (HCP) metals, rolled magnesium alloy sheets typically exhibit strong anisotropy (including tension-compression yield strength asymmetry, known as Strength Differential effect, SD effect) due to the presence of a strong basal texture, with the c-axis of the crystals parallel to the norm direction of the sheet. This strong anisotropy contributes to poor cold formability and hinders wider applications of this material. Although the microscale modelling work is straightforward to characterize the mechanical behaviour of metals, there are still difficulties with the deformation of macro-scale parts due to computational efficiency. From this point of view, macroscale modelling of the anisotropic behaviour based on phenomenological descriptions are more promising.
Focusing on the strong anisotropy during forming process of HCP metals, the distortional evolution of yield surfaces of AZ31 Mg alloy are investigated experimentally and numerically under combined tension-torsion/tension-tension test. Strong anisotropy including initial strength differential effect and subsequent distortional hardening are observed. The underlying deformation mechanisms are discussed based on microstructure observation. In particular, isotropic, kinematic and distortional hardening are employed to capture the anisotropic deformation of AZ31 Mg alloy. The expansion, movement and distortional shape evolution of yield surfaces are governed by specifically designed evolution equations. It is found that the number of twinning decrease with pre-axial tension stress increasing, resulting from the restricted activity of twinning with c/a ratio decreasing. Furthermore, the subdivision of twin boundaries leads to large strain hardening rate. Therefore, the strain hardening rate and flow stress under pure torsion are much higher than other loading paths. Consequently, the strong anisotropy is obtained during large plastic deformation.

10:35-10:50 Tea Break

10:50-11:10 Invited

Significantly Enhanced Mechanical Properties of Mg-9Al Alloy by Using Multi-Walled Carbon Nanotubes

Wenbo Du, Beijing University of Technology, China,

In the present study, Mg-9Al/MWCNTs composites were synthesized by using powder metallurgy followed hot

extrusion techniques. MWCNTs were dispersed in Mg-9Al matrix with an ionic gemini dispersant. The results of the present study established that MWCNTs could be effectively and uniformly dispersed by the ionic gemini dispersant C12-DSDM without structural damage. Matrix-MWCNT was found to be absence of voids and debonding. The addition of MWCNTs could significantly affect the size of Mg17Al12 phase, which decreased from micron to nano length scale.

Compared to Mg-9Al alloy, the mechanical properties of Mg-9Al/MWCNTs composites, especially the ductility, were significantly enhanced. In the case of Mg-9Al/0.4MWCNTs composite, the elongation and UTS were 15% and 355MPa, showing 150% and 18% increase, respectively. The remarkable enhancement of the mechanical properties achieved was mainly attributed to two factors: (i) The nanoscale distributed Mg17Al12 s phase in composite, which was in situ formed by using MWCNTs as heterogeneous nucleus substrates and (ii) the strong and effective interface bonding between MWCNTs and matrix due to the partially inserted interface relationship with Mg matrix. This work may provide an alternative method to fabricate MWCNTs reinforced metal matrix composite, which could efficiently enhance ductility and strength of Mg-9Al matrix simultaneously.

11:10-11:25

Dislocation-Templated Gd Nano-Fiber Patterns: a New Strategy of Tailoring Mechanical Properties in Mg Alloys

Yangxin Li, Xiaoqin Zeng, Shanghai Jiao Tong University, China,

Microstructure engineering is a persistently vigorous technique in altering material's properties through tailoring geometrical features of structural units at multiple length scales and modifying three-dimensional arrangements of structural units. Structural units can be classified into three, two, one, or zero dimensions, such a s three-dimensional volumes (phases, grains, particles/precipitates), two-dimensional surfaces (boundaries, interphases), one-dimensional lines (triple lines, edges, dislocations) or zero-dimensional points (quadruple points, vertices on polyhedral particles). In advancing the material's performance resulted from these structural units, arranging their distribution provides different strategies in addition to regulating the dimensions and shapes of these structural units. To realize specific microstructure, heat treatment, mechanical deformation, and/or their combinations can be applied while adjusting chemical compositions of a material.

Rare-earth (RE) elements has a demonstrated significance in tuning the microstructure of Mg alloys, such as weakening basal texture of Mg alloys, refining grain sizes, forming long-period stacking-ordered structure, etc. RE solutes can also be trapped in twin boundaries, and in turn, impeding migration of twin boundaries. In addition, the elastic interactions between solutes and dislocations lead to solute segregation and depletion around dislocation cores. Such a solute atmosphere, which can maintain their confined structural and chemical states over a range of evaluated temperatures, produces a drag force on the moving dislocations, pins the dislocation motion, and thus modifies the mechanical performance of materials.

Here, we reported self-assembled hexagonal patterns of Gd-segregated dislocations that have a <c>-rod shape. These pinned dislocations act as the predictable inhibitor for basal slips because the glide of basal dislocations must cut them, but less affect the glide of non-basal prismatic dislocations because they are on the parallel planes. Additionally, the crystal domains, strengthened by such pinned dislocation patterns, can effectively impede twin propagation. As a result, such dislocation patterns can change the relative mobility of plastic deformation carriers (dislocations and twins).

11:25-11:40

Microstructure and Properties of Ultrasonic Assisted Magnesium Alloy MAO Coating

Guanqun Chen, Sheng Lu, Jinwei Zhang, Zexin Wang, Lei Xu, JiangSu University of Science and Technology, China

Magnesium alloys are the best candidates for implant materials and can avoid reoperation and stress shielding because of excellent biodegradability, bio-safety and similar density and elastic modulus with human bone. However, inferior corrosion resistance of magnesium alloys could cause fast degradation during clinic application therefore cannot meet the requirements of implants. Ultrasonic-assisted micro-arc oxidation(UMAO) is a promising surface modification technology to improve the density and biological activity of coatings prepared by micro-arc oxidation(MAO). In the present work, the ultrasonic power is adjusted in the optimized composite bio-electrolyte system and the ZK60 magnesium alloy is subjected to MAO treatment. The processing current-time curve was recorded to analyze the growth characteristics of MAO coating. Scanning electron microscopy (SEM) coupled with energy disperse spectroscopy (EDS) and X-ray diffraction (XRD) were used to analyze the micro-morphologies, chemical components and phase. And Nanoscratch tester was used to characterize the adhesion of the coating. Electrochemical workstation was used to evaluate the degradation behavior. The results show that the peak current of MAO decreases after applying ultrasonic waves, it is possible that

the explosion of the ultrasonic cavitation bubble provides energy, reducing the voltage drop required for breakdown; the thickness decreases first and then increases; the phases of the film layer was Mg, MgO, Mg_2SiO_4, $Mg_3(PO_4)_2$ and $CaCO_3$; the wetting angle of the film layer was 13.47° and the coating exhibited good hydrophobicity; the corrosion current density decreased by one order of magnitude compared to bare ZK60 alloy which demonstrates excellent corrosion resistance; the highest critical load is 9.91N, This is mainly due to the compact, uniform coating with high bonding strength.

11:40-11:55

Grain Refinement of Magnesium Alloy for Road Wheel Application

Jun Ho Bae, Ha Sik Kim,Young Hoon Moon,Young Min Kim, Bong Sun You, Korea Institute of Materials Science, Korea

In recent years, demands of light weight in transportation systems dramatically increase because of more stringent environment regulations and changing in consumer perceptions of fuel efficiency improvement. For this reason, magnesium alloy, the lightest structure material, has been used increasingly in transportation systems. Although magnesium alloys have been used for many decades, in order to expand the application area more aggressively, it is necessary to develop new technology and alloys capable of satisfying various requirements of the field such as high strength, toughness, corrosion resistance. Grain refinement is an effective way to improve the mechanical properties of both cast and wrought magnesium alloys. It can also lead to more uniform microstructural features and enhancement of strength, ductility and workability, leading to considerable cost reduction, and it enables further increase the industrial applications of magnesium alloys. However, the grain refinement technology rarely used for casting industries, which make up a significant portion of magnesium alloy parts, except high-pressure die casting due to the absence of high-efficiency grain refinement techniques for various casting processes. Recently, several grain refinement methods focused on a suitable technology, i.e. effective, reliable and easy to apply for industry, have been developed, such as carbon inoculation, melt conditioning, master alloy addition, etc. In this presentation, it is investigated that how to use the grain refinement technology in industrial casting process effectively. The SiC containing grain refiner was applied to 1 ton scale low pressure die casting for the fabrication of magnesium road wheel. And its grain size and mechanical properties compared to commercial AZ91 alloy was investigated.

C3. Light Metals and Alloys: Ti and Others I

Symposium Organizers :

Yongqing Zhao, Northwest Institute for Nonferrous Metal Research, China; Yoshihito Kawamura, Kumamoto University, Japan; Young Min Kim,Korea Institute of Materials Science (KIMS), Korea; Jian-Feng Nie, Monash University, Australia; Diran Apelian, Worceste Polytechnic Institute, USA

Tuesday AM
August 20, 2019

Room: 304 (3rd Floor)
Symposium:C3

Chairs:
Kenichi Mori, Nippon Steel & Sumitomo Metal Corporation, Japan
Robert Wilson, Commonwealth Scientific and Industrial Research Organization, Australia

8:30-9:00 Keynote

Titanium Particulates to Titanium Products

Robert Wilson, CSIRO, Australia

CSIRO is involved in working across the titanium metal value chain, ranging from licensed technologies to synthesize novel titanium metal powders, technologies and strategies to recycle titanium machining swarf to powder for further qualification, developing technologies to make titanium wire and sheet from powder and particulate feeds, and metallic 3D printing/additive manufacturing of titanium components from powder feeds via additive manufacturing methods. An overview will be given defining this value chain and then a specific focus will be given to the recycling of titanium metal machining chips to generate powders for further consolidation. The two powder to product consolidation methods employed by CSIRO are the continuous extrusion particulate to wire (TiWi) and powder to sheet (direct powder rolling/hot roll densification, DPR/HRD) technologies. The output stream for the wires is targeted at wire fed additive manufacturing and wire fed powder atomisation. A description and the current status of the wire and sheet technologies from virgin and recycled powder materials will also be provided. As part of the fabrication of titanium samples by 3D printing, the progress in understanding the processing / microstructure / properties relationship of Laser Engineered Net Shaping (LENS) fabricated Ti-6Al-4V will also be discussed in terms of thermal exposure and microstructures to induce high ductility response.

9:00-9:25 Invited

Hot Forging Design for TiAl Alloys based on Dynamic and Metadynamic Recrystallization Investigations

Bin Tang, Lin Xiang, Xiaofei Chen, Hongchao Kou, JInshan Li, Northwestern Polytechnical University, China

The γ-TiAl alloys are considered to be the most important candidate to replace Ni-based superalloys for jet engine. However, the intrinsic brittleness and hard processability of TiAl alloys limit the application. Hot forging is one of the most important approaches to obtain an ingot with fine and uniform microstructure and excellent mechanical performances. In the present work, a multi-direction hot forging route was designed to obtain a fine-grained and uniform microstructure for TiAl alloys based on dynamic recrystallization (DRX) and metadynamic recrystallization (MDRX) studies. Two typical TiAl alloys were taken as examples, Ti-43Al-4Nb-1Mo-0.1B (TNM) and Ti-48Al-2Cr-2Nb (Ti-4822). Results show that both of DRX and MDRX play an important role in the forging process of TNM alloy, while DRX is the single controlling factor for the forging process of Ti-4822 alloy. By using the hot forging techniques designed by present work, a microstructure with uniform and fine grain size of 8~30μm was obtained. Besides, the constitutive model and recrystallization grain size model were established to predict the hot deformation behaviour and grain size after forging. The proposed hot forging method in the present work yields important information for the development of hot deformation techniques and microstructure controlling strategies of TiAl alloys.

9:25-9:50 Invited

Understanding Local Deformation Behaviour of Titanium and Its Alloys Using Experimental Micromechanics

Tea-Sung (Terry) Jun, Incheon National University, South Korea

The deformation mechanisms of titanium and its alloys are still unclear due to their highly localised deformation and elastic/plastic anisotropy inherent to hcp crystal structure. Further complexities arise from microstructural heterogeneity, macro- and micro-texture and/or phase interactions. Small-scale experiments on a localised, confined area are therefore required to improve the understanding of fundamental mechanism on the level of the individual constituents. In recent years, much attention has been paid to developing in-situ micromechanical testing techniques to examine mechanical deformation process at small-scale. Micropillar compression particularly shows an effective way to characterise real time deformation and failure modes of a wide range of materials including complex multi-phase alloys. Further development shows that this technique can be combined with EBSD, allowing quantitative analysis of local elastic strain (hence stress) and the distributions of GND contents during compression. In the present study, combined nanoindentation, micropillar compression and/or (HR)EBSD techniques are used to investigate the evolution of heterogeneous deformation in Ti and its alloys. The in-situ compression tests are performed using a displacement-controlled Alemnis nanoindentation platform set inside a SEM and EBSD patterns were captured using a TSL-EDAX EBSD system. Analysis of each map was performed offline using CrossCourt from BLG productions (Bristol, UK). These experimental approaches present new exciting mechanistic insight into important deformation mechanisms, as well as opening up further studies of new alloy design.

9:50-10:10

Effect of the Initial Microstructure on Aging Behavior in Si-Bearing Near Alpha Titanium Alloy

Tatsuaki Sakamoto, Ehime University, Japan; Hiroaki Akiyama, Shinwa Kogyo Co., Ltd., Japan; Seiya Tange, Primetals Technologies Japan, Ltd., Japan

Aging behavior of a Si-bearing near alpha titanium alloy Ti-1100 has been investigated using specimens having two different initial microstructures: alpha phase and alpha-prime martensite (hereafter denoted as alpha specimen and alpha-prime specimen, respectively). The alpha specimen and the alpha-prime specimen were made by the following heat treatment. Firstly, solid solution treatment was conducted at 1060˚C for 25min, followed by air cooling for the alpha specimen and by iced brine quenching for the alpha-prime specimen. The alpha and alpha-prime specimens consist of almost all alpha phase and alpha-prime martensite, respectively. Silicides are hardly observed in both specimens after the solid solution treatment. Aging was carried out at 600˚C from 5min to 42 day for both specimens. In the case of the alpha specimen, Vickers microhardness decreases during aging from 5 to 625min, and then increases until 42 day. TEM observation revealed that the first decrease in hardness is due to the decrease in dislocation density and the second increase is due to precipitation of silicide and Ti_3Al. On the other hand, in the case of alpha-prime specimen, Vickers microhardness decreases during aging from 5 to 25min, increases from 25min to 625min, decreases from 625min to 4 day, and then increases until 42 day. TEM observation revealed that the first decrease in hardness is due to the decrease in dislocation density, the second increase is due to the precipitation of silicides, the third decrease due to coalescence of the silicides and the last increase due to precipitation of Ti_3Al. The alpha prime specimen initially has considerable dislocations within itself, resulting in promotion of precipitation of silicide showing the peak

of hardness during the aging. It is likely that the initial microstructure affects high temperature deformation behavior because precipitation of silicides is related to high temperature deformation in this alloy.

10:10-10:30

Tensile Properties at 700℃ of Ti-Al-Sn-Zr-Mo-Nb-W-Si High-Temperature Titanium Alloys with Different Mo Addition

Xiaoyun Song, Yuwei Diao, Wenjing Zhang, Wenjun Ye, Songxiao Hui, GRIMAT Engineering Institute Co., China

High-temperature titanium alloys have been widely used in the aerospace industry, due to their exceptional properties of strength-to-weight ratio, corrosion resistance, workability and weldability. With increasing the flight speed of short-term high-speed aircraft, the short-time service temperature has reached 700℃, and traditional long-term high temperature titanium alloys have been unable to meet the requirements. In our previous work, novel Ti-Al-Sn-Zr-Mo-Nb-W-Si short-term high-temperature titanium alloys were designed and the tensile behaviors of the alloys at temperatures to 650℃ have been studied. However, the properties of alloys higher than 650℃ or even 700℃ have not been systematically investigated. In this paper, three Ti-6.5Al-2Sn-4Zr-xMo-2Nb-1W-0.2Si (x =1, 2, 4) alloys (hereinafter termed as 1M2N1W, 2M2N1W and 4M2N1W, respectively) were prepared by vacuum consumable electrode method. The ingots were hot-rolled into 12-mm-diameter bars in two-phase region. The effects of Mo content on the microstructure and tensile properties at 700℃ were investigated through optical microscopy (OM), scanning electron microscopy (SEM) and tensile tests. The results show that after single annealing, the alloys are composed of bimodal structure with equiaxed primary α-phase (α_p) and lamellar transformed β structure (β_t). Fine secondary-α (α_s) that precipitated in the β_t structure. As the content of Mo increases, the average size of the α_p phase is gradually reduced, with the size of β_t is gradually increased, and the thickness of the lamellar α_s phase is also getting finer and finer. Tensile tests at 700℃ show that with the increase of Mo content, the yield strength (YS) decreases while the elongation increases. But the alloy with 2at% Mo addition shows higher ultimate tensile strength (UTS) than the other two alloys. It is considered that the interface strength is weakened dramatically at high temperature especially 700℃. As the Mo content increases, the α_p phase and α_s phase in the alloy become smaller with the β_t phase increases. The grain is remarkably refined, so the YS shows a decreasing trend, and the plasticity of the alloy has been improved. Moreover, compared to 650℃, the strengthening effect of Mo element is weakened at 700℃.

10:30-10:45 Tea Break

10:45-11:10 Invited

Heterogeneous Microstructure in Beta Type Ti-Mo Alloy Through Thermomechanical Treatment

Satoshi Emura, Xin Ji, Koichi Tsuchiya, National Institute for Materials Science, Japan

Beta type Ti-Mo alloy exhibits excellent properties such as good balance of mechanical properties and high corrosion resistance. Mechanical properties of titanium alloys are known to be strongly affected by their microstructure. In this talk, I would like to introduce some of our efforts to apply heterogeneous microstructure in Ti-Mo alloys. (i) Mo is an important element for stabilizing beta phase in titanium alloys, but is prone to segregate, i.e. unevenly distributed in Ti-Mo alloys. We use this segregated structure for enhancing mechanical properties of Ti-Mo alloys. Swirly or layered structure caused by elemental segregation was successfully applied through simple thermomechanical treatment, namely hot forging and hot rolling. Using this segregated structure, we can locally control the precipitation behavior of omega phase (hard second phase) and successfully enhance the strength-ductility balance of Ti-Mo alloy. (ii) Recently, long period stacking structure (LPSO) was found in magnesium alloys and this type of layered structure (so called Mille-feuille structure) seems to have some effects on mechanical properties of other materials than magnesium. We have obtained Mille-feuille like layered precipitation of alpha phase in beta matrix by the combination of slight cold rolling and following aging treatment.

11:10-11:35 Invited

Deformation Compatibility in Dual Phase Ti Alloys Under Compression

Renlong Xin, Ke Wang, Qing Liu, Chongqing University, China

Dual phase titanium (Ti) alloys are widely used as airplane structural parts due to their high specific strength and very attractive combinations of strength, toughness and fatigue resistance. Such superior mechanical properties are intimately related to the deformation compatibility between the alpha and beta phases. Fracture usually initiates at phase interface during fabrication and service of Ti alloys. Therefore, it is important to investigate the behaviors of deformation and crack initiation in dual Ti alloys and hence figure out the correlations with microstructural and crystallographic features. Based on the observations on slip trace and crystallographic orientation, the activated slip systems in TC21 and TA19 Ti alloys are determined after compression deformation, and their corresponding Schmid factor (SF) and

geometric compatability parameter (m') were calculated and analyzed. The m' for most active slip systems of alpha and beta phases in TC21 has a high value, indicating a good strain compabitility at phase interface. Difficult slip transfer occurs at a low m' or low SF in TA19, which induces stress concentration at grain boundaries, and then causes a corresponding crack nucleation. Moreover, the displacement gradient induced by dislocation glides in one phase is transferred to another phase by tensor analysis, which is then used to explain the observed strain compatibility phenomena at phase interface. These deformation and fracture behaviors in dual phase Ti were discussed and considered as crystallographic orientation dependent.

11:35-11:55

The Influence of Chemical Composition on the Grain Boundary Network Characteristics in Ti Alloys

Hossein Beladi, Ehsan Farabi, Peter Hodgson, Deakin University, Australia

The effect of chemical composition on the intervariant boundary network characteristics during martensitic phase transformation was studied using the crystallographic theories of displacive transformation and the 5 parameter boundary analysis. The martensitic microstructure of two titanium grades, namely commercially pure Ti (CP-Ti) and Ti-6Al-4V alloy; was examined using TEM and EBSD techniques. The CP-Ti had a coarse martensitic microstructure consisting of dislocated laths while the Ti-6Al-4V alloy showed fine twinned laths. There was a distinct difference in misorientation angle distribution of two martensitic microstructures, although the peaks were consistent with the Burgers orientation relationship. The martensitic CP-Ti had a distinct peak at the 60° misorientation angle corresponding to the 60° / [1 1 -2 0] intervariant boundary while the Ti-6Al-4V had a peak around the 63.26° misorientation angle related to the 63.26° / [-10 5 5 -3] intervariant boundary. This discrepancy was rationalized using phenomenology theory of martensite transformation. It was predicted that the difference in the chemical composition leads to different strain levels during the martensitic transformation. This resulted in the occurrence of a local variant selection mechanism to self-accommodate the transformation strain. In this regard, different variant clustering in martensitic CP-Ti (i.e., 3-variant, triangular morphology) and Ti-6Al-4V (i.e., 4-variant, quadrilateral morphology) was predicted and observed. It was concluded that the local variant selection during martensitic transformation influenced by the chemical composition stimulated specific intervariant boundaries in the Ti-alloy microstructure. Finally, the change in the self-accommodation morphology resulted into the promotion of pyramidal (1 0 -1 1) interfaces in the CP-Ti martensite, while the prismatic interfaces was favoured in the Ti-6Al-4V martensite.

D. Advanced Processing of Materials: II

Symposium Organizers:

Wanqi Jie, Northwestern Polytechnical University, China; Jianguo Li, Shanghai Jiaotong University, China; Hideyuki Yasuda, Kyoto University, Japan; Myoung-Gyu Lee, Seoul National University, Korea; Huijun Li, University of Wollongong, Australia; Dan Thoma, University of Wisconsin- Madison, USA

Tuesday AM
August 20, 2019

Room: 208+209+210 (2nd Floor)
Symposium: D

Chairs:
Anna Paradowska, ANSTO, Australia
Sophie Primig, UNSW Sydney, Australia

8:30-9:00 Keynote

Study of Single Point Incremental Forming and Its Formability

Kim Young Suk, Do Van Cuong, Xiao Xiao, Oh Seok Hwan, Kyungpook National University, Korea

Single point incremental forming (SPIF) technology - a flexible manufacturing method is used widely in small batch production and rapid prototyping. In this forming process, the product is formed incrementally by using a computer numerical controlled machine or a robot that can control the path of the semi-spherical tool moving along the trajectory of the outer shape of the product. Nowadays, the application of this flexible manufacturing technology has expanded into a variety of asymmetric and symmetric stockpile products such as the front end of a high-speed train, aircraft shell components, and dental parts. In the incremental sheet forming, the formability in very high in compared with conventional stamping method but the springback phenomena is more critical. To minimize the springback, many optimization schemes were studied to improve the profile accuracy of final parts. In addition, finite element method based on numerical simulation is a strong tool for studying formability of SPIF in which the flow curve, yield behavior of sheet materials are strongly affected on the simulation results. This paper reviews the current advances in SPIF and investigates main plasticity topics of SPIF: formability, forming limit, springback optimization and numerical simulation.
In this paper, we shortly summarized the basic concept of ISF and its application to engineering and in industries. Asymmetric incremental single-point sheet forming is viable for making complicated shapes from sheet metal. It makes the forming of sheet metal a flexible operation, and it is an easy operation for facilities with access to a three-axis CNC machine. The process has tremendous potential, and it can possibly be used in many applications in the future.

The formability is strongly depended on forming parameters such as tool diameter, vertical step, toolpath. The hole bridge implements the stretching and bending effect in order to get the maximum forming angle up to 90 degree.

In addition, a new method and the associated apparatus are introduced to define FLCF experimentally. With the four-wing star toolpath, a homogeneous minimum thickness area at the center of forming part will lead to fracture occurrence with equi-biaxial strain state. The FLCF is the material property, not depended on the forming parameter.

Optimization method such as Taguchi method, RSM and ANN are the great tools to predict and minimize the springback value. Taguchi method with grey relational grade can give multi objectives optimization with simple calculation. Meanwhile RSM offers the visible dependence of springback amount on forming parameter. ANN with PSO quickly determines the weights of the neural network with global minimum.

In the explicit code simulation, the NAFR yield behavior using Hill 1948 and Kim-Tuan flow curve that is best fitted for large strain flow curve is applied to predict well the fracture occurrence as well as thickness distribution. This method using mass scale and time scale leads to short computational time in order to be applied for large part simulation of real industrial part.

9:00-9:30 Keynote

Metamorphic Manufacturing – Forming High Quality Components on Demand

Daehn Glenn, The Ohio State University, USA

Digital manufacturing has seen two impactful waves of innovation. The first was CNC machining. The second, now underway, is in additive manufacturing. The third natural wave is likely to come in reshaping. Think of robotic blacksmithing where an automata senses the shape of an object and uses tools like hammers, rollers an presses to squeeze it into a target shape. Like a blacksmith, a wide variety of shapes can be made with very simple and lightweight tools. However, much greater levels of control, power and reproducibility can be developed with such a system. This has been dubb ed metamorphic manufacturing because both the shape and properties are changed, or morphed and like a blacksmith, thermomechanical processing can be used to alter local chemistry or properties. Many underlying technologies such as open-die forging and manual blacksmith operations demonstrate the fundamentals, and advances in sensing, artificial intelligence and robotics bode well for rapid advancement. TMS led an in-depth expert study on the status, potential and pathways to market for this potentially revolutionary technology. This presentation will provide a review of the study and recent advances. Acknoweldgements are due to many collaborators including those at LIFT, Ohio State and TMS and the National Study Committee.

9:30-9:50

Precipitation Hardening Behavior of Al-Based Alloys Processes by Additive Manufacturing

Konda Gokuldoss Prashanth, Tallinn University of Technology, Estonia / Austrian Academy of Science, Austria

Selective Laser Melting (SLM) is one of the additive manufacturing processes (AM) that has gained increasing attention because of its ability to process a wide spectrum of materials including Al-based, Ti-based, Fe-based, Cu-based, Co-based, Ni-based and Si-based alloys. In addition, different classes of materials including polycrystalline, amorphous, nano-crystalline, quasi-crystalline alloys and high entropy alloys were attempted using SLM process. SLM also has the capability of producing parts with added functionality and complex shapes theoretically without any restriction. The parameter optimization process for any materials for SLM is difficult and a tedious process involving several hundreds of parameters including, laser power, laser scan-speed, layer thickness, hatch distance, hatch style, spot-size of the laser, etc. However, it is relatively easier than the other powder bed fusion process like the electron beam melting process and hence offers the possibility of processing a wide spectrum of materials. Al-based, Fe-based and Ti-based alloys have been widely produced using SLM, because of their direct applications as structural materials. Both Al-Si10-Mg and Al-12Si have been fabricated and studied extensively using SLM because of their fluidity (where it is widely used as casting alloys because of its fluidity), which makes them easy to process via SLM. However, researchers have slowly shifted the focus towards the precipitation hardenable Al-based alloys. Several precipitation hardenable Al-alloys have been processed using SLM with the traditional idea of improving the mechanical property of these parts with natural aging or with artificial thermal treatment (involving solutionizing and/or aging), where fine precipitates evolve out in the Al-matrix. However, the results do not show a drastic increase in the properties compared to the original base alloy. The present talk will discuss the processing of age/precipitation hardenable Al-based alloys by SLM where their merits and demerits will be discussed in detailed. The scientific reasons behind the possible improvement/degradation of properties will be explored.

9:50-10:10

High Efficiency Sintering of ZrB_2 Ceramics at Medium-Temperature Using Polymer-Derived SiBCN as a Sintering Aid

Bingyang Li, Pengfei Wang, Yingze Cao, China Academy of Space Technology, China

The rapid development of polymer-derived ceramics(PDCs) makes it possible to be the sintering

aids for ultra-high temperature ceramics (UHTCs). However, the present method of introducing additives by PDCs route follows the traditional ways of using crystalline powder as the sintering aid. The pyrolysis product of polymer precursor keep amorphous structure for a period of time and the then begins to separate out crystals at about 1200℃ while the sintering temperature of UHTCs are almost above 1800℃. The effects of the ceramization process of PDCs including polymer decomposition, amorphous structure construction and crystallization are nearly ignored, and those effects may contribute to the densification of the UHTCs at medium-temperature. Here we choose polymer-derived SiBCN as the sintering aid to hot-pressing ZrB_2 ceramics. Without heat pretreatment, the liquid polymer precursor is directly introduced into ZrB_2 powders and the ceramic densification proceeds along with polymer transformation. This work is focused on the assisting sintering efficiency at medium temperatures from 1000℃ to 1600℃, accordant with the conversion stage of amorphous SiBCN to crystal ceramic. The results show that ZrB_2 ceramics using polymer-derived SiBCN as sintering aid displayed high sintering efficiency at medium temperature, which was different from the general sintering of non-oxide ceramics with additives such as metals, oxides, and carbides. The microstructure and densification behavior of ZrB_2-SiBCN samples were mainly studied. The densification performance was attributed to the structural evolution of polymer-derived SiBCN and the interactions between pyrolysis products and ZrB_2 matrix. Especially, the relative density of ZrB_2-SiBCN samples increased by 22% in the temperature range of 1300~1400℃, when the rearrangement of amorphous SiBCN network was in an active stage and the migration of chemical bonds like Si-C and Si-N drove the movement of ZrB_2 particles. The uncombined carbon from pyrolysis products could remove oxide purities by carbothermal reduction reactions and promote the formation of ZrC. The diffusions and reactions at the interface were also beneficial to the relatively dense microstructure of ZrB_2-SiBCN ceramics sintered at 1600℃.

10:10-10:30

Role of Shoulder Diameter on Aluminum 6061-T6 and Pure Copper Joint During Friction Stir Flat Welding (FSFW)

Soni Neetesh, Singh Ambrish, Southwest Petroleum University, China

The work focuses on the shoulder diameters and tool pin profile design during friction stir flat welding of dissimilar metals joints. The dissimilar materials joining by friction stir welding is typical because both materials are in different in nature such as melting temperature, density, and microstructural features. It is an advancement to used simulation and proper parameters of the joining of dissimilar metals without any defect's formations. The scenarios are more demanding of these types of joint because of the economic, reliable and perfects matching with as per required industries. The diameters of shoulder influencing the quality of weldment during friction stir flat welding. Tools pin profile evaluated across the weld interface. In this research work, the effect of tool shoulder geometry, tool rotational speed and traverse speed on the microstructure, material flow and microhardness of the fabricated aluminum 6061-T6 and pure copper joint were studied. The result shows that with increase of tool shoulder diameter like 18mm, 20mm, 22mm, and 24mm ductility decreases thereby hardness is found to increases after certain critical limit and with changed the tools pin profile such as cylindrical, tapered cylindrical, tapered threaded, the strength increases upto the critical limit and beyond that it decreases. The average Microhardness of the surface on the weldment is achieved as ~150-172HV with 24mm shoulder diameter of the tool. The results were concluded with the analysis of data using SEM, microstructure analysis, Microhardness, and tools geometry of dissimilar joints.

10:30-10:45 Tea Break

10:45-11:10 Invited

Dynamic Failure of Spot Welds under Combined Axial and Shear Loading Conditions

Jung-Han Song, Gi-hyun Bae, Namsoo Park, Jongsup Lee, Wooram Noh, Korea Institute of Industrial Technology, Korea

This paper is concerned with the evaluation of the dynamic failure strength and empirical failure criterion of the spot weld under combined axial and shear loading at various loading speeds. The testing fixture is designed to impose the combined axial and shear load on the spot weld. Using the proposed testing fixtures and specimens, quasi-static and dynamic failure tests of the spot weld are conducted with seven different combined loading conditions. The failure load and failure behavior of the spot weld are investigated with different loading conditions. Effect of loading speeds on the failure load of the spot weld, which a critical for structural crashworthiness, is also examined based on the experimental data. Dynamic sensitivities of failure loads with various combined loading conditions were also analyzed. Experimental results indicate that the failure contour is expanded with increasing strain rates and failure loads shows similar dynamic

sensitivity with respect to the loading angles. Based on the experimental data, a novel dynamic failure criterion was constructed. The dynamic sensitivity of the failure load was interpolated with an exponential function of the logarithm of the strain rates. It was confirmed that the proposed failure criterion provides a fairly accurate interpolation of the failure contours of a spot weld at various loading speeds.

11:10-11:35 Invited

ALE Based Finite Element Simulation of Friction Stir Welding and Its Application to the Prediction of Joint Strength

Myoung-Gyu Lee, Dongjoon Myung, Seoul National University, Korea; Sung-Tae Hong, University of Ulsan, Korea

As a solid state welding technology, the friction stir welding (FSW) has been introduced to join hard-to-weld materials such as aluminum alloys as potential lightweight sheet metals for automotive parts. The FSW involves complex mechanical-metallurgical process that determines final welding quality and joint strength. Therefore, optimal welding parameters should be sought before welding in order to enhance the mechanical properties of welded parts. Due to this complex deformation process during the FSW, experimental analyses on the detailed material flow around the FSW tool are not readily available, which required numerical approach for understanding the coupled effect of frictional heat generation and material flow around the rotating tool. In the present study, the FSW process was numerically simulated by the finite element (FE) method, from which detailed temperature histories and severe deformation patterns in the welding region were analysed. As for a model material, aluminum alloy sheet was selected due to its frequent application to the real FSW parts. As for the finite element simulation, the fully coupled thermal-mechanical analysis based on the arbitrary Lagrangian-Eulerian (ALE) scheme, which is particularly beneficial for solving the numerical challenge with severe mesh distortion during the FSW process, was utilized. The plastic strain, plastic strain rate and temperature distribution could be successfully predicted using the ALE based finite element simulation. Then, the mechanical properties of the welded joint were estimated from the well-known dislocation density based strengthening mechanism and the calculated temperature histories in the FE simulation. Finally, a numerical simulation based deterministic method for evaluating the quality of the welded joint is additionally discussed in this study.

E: Thin Films and Surface Engineering: II

Symposium Organizers :

Chuang Dong, Dalian University of Technology, China; Hongbo Guo, Beihang University, China; Hiroshi Masumoto, Tohoku University, Japan; Ho Won Jang, Seoul National University, Korea; Mingxing Zhang, University of Queensland, Australia

Tuesday AM
August 20, 2019

Room: 313 (3rd Floor)
Symposium: E

Chairs:
Jean-Marie Dubois, Institute Jean Lamour / Institute Jean Lamour, France
Hyunjung Shin, Sungkyunkwan University, Korea

8:30-9:00 Keynote

Advanced Ceramic Coatings for High Temperature Use Made by Thermal Spray Techniques

Robert Vassen, Forschungszentrum Jülich GmbH, Germany

Thermal spray technologies offer the possibility to manufacture coatings with a wide range of different microstructures. Such coatings especially for the use at high temperatures are applied on structural components in gas turbines. Several examples will be given in the presentation.
First, thermal barrier coatings (TBCs) which are used to protect metallic parts are addressed. Different microstructures are used for this application. The standard are micro-cracked coatings produced by atmospheric plasma spraying (APS). More advanced coatings show a columnar microstructure with high strain tolerance. The manufacture of these coatings by suspension plasma spraying (SPS) and by plasma spray - physical vapor deposition (PS-PVD) will be described, furthermore also characteristics of theses coatings will be given.
More recently, ceramic matrix composites are introduced into gas turbines. Although their temperature capability is higher than these of metallic substrates, they need protective coatings against water vapor recession. These coatings have to be rather dense to avoid the water vapor attack. Also such coatings can be produced by thermal spray techniques. Examples of $Yb_2Si_2O_7$ coatings prepared by APS, PS-PVD, SPS and high velocity oxygen fuel (HVOF) will be described. In addition to the high density also a high crystallinity is of importance for a good performance of the coatings.

9:00-9:25 Invited

New TBC Materials and Structures

Xueqiang Cao, Wuhan University of Technology, China

Thermal barrier coatings (TBCs) have very important applications in gas turbines for higher thermal efficiency and protection of components at high temperature. TBCs of rare earth materials such as lanthanum zirconate ($La_2Zr_2O_7$, LZ), lanthanum cerate ($La_2Ce_2O_7$, LC), lanthanum cerium zirconate ($La_2(Zr0.7Ce0.3)_2O_7$, LZ_7C_3) were prepared by electron beam-physical vapor deposition (EB-PVD) and atmospheric plasma spraying (APS). The composition, crystal structure, surface and cross-sectional morphology, cyclic oxidation behavior of these coatings were studied. These coatings have partially deviated from their original compositions due to the different evaporation rates of oxides, and the deviation could be reduced by properly controlling the deposition condition. A double ceramic layer-thermal barrier coatings (DCL-TBCs) of LZ_7C_3 and LC could also be deposited with a single LZ_7C_3 ingot by properly controlling the deposition energy. The failure of DCL-TBCs is a result of the sintering of LZ_7C_3 coating and the chemical incompatibility of LC and TGO. Since no single material that has been studied so far satisfies all the requirements for high temperature applications, DCL-TBCs is an important development direction of TBCs.

9:25-9:50

Highly Stretchable Ag-PTFE Hybrid Electrodes for Highly Stretchable Strains Sensor and Touch Screen Panels

Sungyoung Yoon, Shuai Lan, Ju-Ri Lim, Han-Ki Kim, Sungkyunkwan University, Korea

High-performance wearable electronics require highly stretchable and conductive materials that are prepared by simple, scalable processes to be implemented in the essential roles of electrodes and interconnects. Here, we demonstrate room temperature fabrication of highly stretchable electrodes consisting of self-connected Ag nano-porous sponges embedded in polytetrafluoroethylene (PTFE) matrices on stretchable polyurethane substrates using a metal-polymer co-sputtering process. The metallic Ag nano-porous sponge networks embedded in PTFE matrices showed minimal changes to resistance even after stretching by 50% and after 10,000 cycles under 20% strain due to the well-connected Ag nano-porous sponge network and the stretchable PTFE matrix. We demonstrated the feasibility of this hybrid material as stretchable interconnects and electrodes for stretchable thin film heaters and strain sensors. Because the Ag nano-porous sponges embedded in PTFE matrices were simply fabricated by a typical sputtering process, which is compatible with current electronics fabrication processes, we strongly expect that the Ag-PTFE hybrid electrodes can be easily applied as universal stretchable electrodes for wearable thin film heaters, stretchable interconnectors, and stretchable strain sensors. Furthermore, as promising applications of Ag-PTFE nano-composite electrodes, we suggested stretchable and wearable and stretchable touch sensors. Succesful operation of stretchable strains sensors, interconnectors and touch sensors verified the outstanding stretchability of Ag-PTFE nano-composite electrodes.

9:50-10:10

Toughened $Gd_2Zr_2O_7$ for Thermal Barrier Coating Applications

Lei Guo, Zheng Yan, Fuxing Ye, Tianjin University, China

Thermal barrier coatings (TBCs) are commonly used to protect metallic components of turbine engines from oxidation and erosion, leading to increased operating temperature and improved engine efficiency. The widely used TBCs are made of yttria stabilized zirconia (YSZ), however, its sustainable temperature is not higher than 1200℃. With an ever-growing demand for increasing the engine operating temperature, there is thus on-going research to develop alternative TBC materials. $Gd_2Zr_2O_7$ has excellent high-temperature capability and low thermal conductivity, which has been considered as a promising TBC candidate. However, $Gd_2Zr_2O_7$ TBCs have not been used in industry mainly due to the poor toughness.

To improve the toughness of $Gd_2Zr_2O_7$, our group has done much work and obtained some interesting results. Sc_2O_3 doped $Gd_2Zr_2O_7$ was produced, and its ordering degree decreased and the lattice parameter increased with increasing the Sc_2O_3 content, which caused an increase in the toughness. Non-stoichiometry Gd_2-$_x$$Zr_2$+$_x$$O_7$+ $_x$/2 (x = 0, 0.1, 0.3, 0.5, 0.7) ceramics was designed, and excess ZrO_2 in the compound benefited the fracture toughness, probably attributed to the increased fracture energy, ferroelastic toughening and compressive stress. RE_2O_3 (RE=Yb, Dy, Er, Y) stabilized ZrO_2 with a ferroelastic phase structure was doped into $Gd_2Zr_2O_7$, which caused an obvious increase in the toughness. Composition - microstructure - mechanical property relationships and toughening mechanisms of $GdPO_4$-doped $Gd_2Zr_2O_7$composites were investigated. $GdPO_4$ existed as a second phase in the matrix, which refined $Gd_2Zr_2O_7$ grains, strengthened grain interfaces, and introduced residual stress in the composites. At low dopant contents < 30mol%, the toughness of composites increased without sacrificing hardness and Young's modulus. The strengthened interfaces, and cracks deflection, bridging and bifurcation in $GdPO_4$ grains resulting from the layer structure and the generated tensile stress contributed to the initial increase in the

toughness.

10:10-10:30

The Design of Novel Gradient Y_2O_3 Doped ZrO_2 Coatings and the CMAS Corrosion Resistance

Jian He, Pin Cao, Hui Peng, Hongbo Guo, Beihang University, China

As the turbine inlet temperature increases continually, the calcium-magnesium-alumina-silicate (CMAS) from volcanic ash, air dust, runway debris, etc. ingested by engines can be melted and deposited on thermal barrier coatings (TBCs), which leads to severe degradation of TBCs. Especially for the EB-PVD YSZ TBCs, the columnar structures will accelerate the CMAS attack because the columnar intergranular gaps can act as fast infiltration paths for the molten CMAS. In viewing of this, novel gradient Y_2O_3 doped ZrO_2 coatings were designed and prepared by EB-PVD in this paper. The CMAS corrosion behavior at 1250˚c was investigated and the protection mechanism of the novel coatings against CMAS was clarified. Meanwhile, the thermal shock resistance was evaluated at 1100˚c.
The results showed that the Y_2O_3 contents at the top of coatings reached 50wt.% and decreased gradually along the thickness. The resistance to CMAS corrosion of the gradient coatings got much improved, compared with the traditional YSZ coatings, since they could react with CMAS to form dense continuous apatite and melilite phases. The phases can prevent the further infiltration of the molten CMAS by occupying the infiltration paths. In addition, the thermal cycle lifetime of the coatings was not reduced because the columnar structures were remained.

10:30-10:50 Tea Break

10:50-11:20 Keynote

Thermal Spray Coatings: Relating Processing Conditions to Microstructural Evolution

Christopher Berndt, Andrew Ang, Swinburne University, Australia

Thermal spray coatings (TSCs) and the associated technology represent a USD$14 billion global industry. Pre-1950 TSCs were based on flame spray, wire sprayings and low energy plasma techniques in relatively low risk applications. Advancements over the last 70 years have focused on matching temperature and velocity distributions of the thermal spray process zone to the particle size chemistry, morphology and size distribution. The applications of these coatings has now extended to the harsh and extreme conditions that are experienced under mechanical wear, corrosion and thermal environments.
The overall outcome is that the microstructural building blocks of TSCs have evolved from being ad hoc and unpredictable to heterogeneous structures that can be classified into ordered taxometric classifications. Moreover, the 3-dimensional structure of TSCs arises under dynamic conditions because the ground state of the coatings changes as multiple layers a created. The thermal spray process is constrained by the rules of physics. The rapid solidification processes are founded on the pioneering work of J. Madejski, i.e., where is the flattening ratio of the particle diameter to splat thickness and may be related to the Reynold's number of the thermal spray process. There have been many technical and theoretical advancements to the Madejski proposition over the past 4 decades. Thus, the traditional Madejski approach must be modified to account for real-time conditions.
The scientific outcome is that the flattening ratio (the diameter-to-thickness ratio of a splat) can be found. A thorough understanding this scientific question will enable the manufacture of improved products on the basis of fundamental science that is related to the wetting behaviour and viscosity of the impacting particles. There is a compelling and urgent need to provide a rigorous scientific understanding behind TSCs. The basis for this fundamental framework will be presented by describing how processing conditions influence microstructures for the growing family of thermal spray technologies.

11:20-11:40

Development of A Novel Long Laminar Plasma Jet on Atmospheric Plasma Spray Process

Senhui Liu, Guanjun Yang, Chengxin Li, Changjiu Li, Xi'an Jiaotong University, China; Juan Pablo Trelles , University of Massachusetts Lowell, USA; Anthony B. Murphy, CSIRO Materials Scienece and Engineering, Australia; Hong-Bo Guo, Beihang University, China

We propose a novel atmospheric plasma spray method, which by using a newly development plasma torch that can generate a long, stable and silent plasma jet in atmospheric environment without any other auxiliary equipment. The lengths of these plasma jets vary from 100 mm to 1000 mm in an atmospheric environment. The fluid characteristics of plasma jets present a laminar or quasi-laminar with a low-level noise (< 80 dB) through numerical simulation and experimental analysises. Moreover, the lengths of the plasma jets are increased by the increasing of the output power at every constant gas flow rate in the ranging of 8 ~ 15 SLPM and decreased as the increasing of total gas flow rate at every constant output power in the ranging of 8 ~ 100 kW. It can provide a super-long particle flight time in the atmospheric plasma spray process. The research history and current researches of this laminar plasma technologies are listed in the paper. The microstructure evolution, particle heating and motion in this work are all present in the followings. The effects of particle

flowing characteristics to the formation of coatings are discussed. This method may provide a new selection for the atmospheric plasma spray technology.

11:40-12:05 Invited

Neutron Residual Stress Analysis of Single- and Two-Phase Cold-Sprayed Coatings

Vladimir Luzin, Australian Nuclear Science and Technology Organisation / School of Engineering, The University of Newcastle, Australia; Mingxing Zhang, School of Mechanical and Mining Engineering, The University of Queensland, Australia

Neutron diffraction for residual stress analysis is a powerful technique in application to coatings of different kinds, provided that they are metallic or ceramic. This non-destructive stress measurement technique combines advantages of high spatial resolution up to 0.1mm and high accuracy of just few MPa. Also, in contrast to any mechanical methods, the neutron diffraction is exceptionally beneficial when two-phase are to be investigated because different phases can be studied through different diffraction reflection in the overall diffraction pattern. In case of multiple phases, not only mechanical stress (macro-stress) can be determined, but also phase incompatibility stress (micro-stresses) can be studied, both providing experimental basis for understanding of the macro- and micro-mechanics.
The results of through-thickness residual stress profiling achieved by the neutron diffraction experiments at the Australian OPAL research reactor are reported in the case of selected one-phase and two-phase (metal-ceramic composite) coatings. Although with focus on the cold spray technique, the approach is easily generalized to other spraying techniques, e.g. HVOF or plasma sprays. The link of the experimental results to the mechanisms of macro- and micro-stress formation, which usually combine the thermal and plastic deformation mechanisms, as well as connection of these mechanisms to spraying parameters, will be discussed.

12:05-12:25

Microstructures of $La_2Ce_2O_7$ Coatings Produced by Plasma Spray-Physical Vapor Deposition

Cong Zhao, Wenting He, Liangliang Wei, Hongbo Guo, Beihang University, China

$La_2Ce_2O_7$ (LC) coatings were produced by plasma spray-physical vapor deposition (PS-PVD). To achieve the quasi-columnar microstructure, the process-structure relationships response for net power, spray distance and carrier gas flow were investigated. It was found that the net power and carrier gas flow played more significant roles than the spray distance to acquire high-ratio vapors. The corresponding phase and chemical compositions of coatings were studied by X-ray diffraction (XRD) and energy dispersive spectrometer (EDS), respectively. The results indicate that the lattice parameters of LC phases have positive correlations with average La/Ce ratios of the coatings. This may be related to different ionic radii between La^{3+} and Ce^{4+}. As the ionic radius of La^{3+} is larger, if the lattice parameter of LC phase is high, the La/Ce ratio is supposed to increase. The regional characteristics of the optimized coating were investigated by transmission electron microscope (TEM). The selected area electron diffraction (SAED) patterns confirmed Face Centered Cubic (FCC) structure, which is in accordance with defect fluorite structure. It is widely accepted as the structure of traditional LC phase. However, super-lattice patterns revealed it is not defect fluorite but pyrochlore structure. The "particle-interruption" mechanisms in the quasi-columnar coating were also discussed, mainly divided into two aspects: surface temperature and sub-column growth route.

F. Biomaterials: Biodegradable Magnesium Alloys

Symposium Organizers:

Yufeng Zheng, Peking University, China; Luning Wang, University of Science and Technology Beijing, China; Takayoshi Nakano, Osaka University, Japan; Seung-Kyun Kang, Korea Advanced Institute of Science and Technology (KAIST), Korea; Cuie Wen, RMIT University, Australia; Marc Meyers, University of California, San Diego, USA

Tuesday AM
August 20, 2019

Room: 306 (3rd Floor)
Symposium: F

Chairs:
Hyun Kwang Seok, Korea Institute of Science and Technology (KIST), Korea
Andrej Atrens, The University of Queensland, Australia

8:30-9:00 Keynote

Outlook on the Clinical Translation and Commercialization of Biodegradable Metals

Hyun Kwang Seok, Y-C Kim, H-S Han, KIST, Korea; H-C Jung, U&i Inc, Korea; K-J Han, Ajou Hospital, Korea

The concept of bone replacement has been dominant in the development of metallic implants and the biodegradable metals with the potential to stimulate bone formation have recently captured the attention of scientists. Among these metals, magnesium alloy is an attractive biodegradable material with unique set of properties. The corrosion of magnesium is accompanied by hydrogen evolution and a local increase in pH,

which impose constraints on many potential biomedical applications. We have overcome these limitations and created a road map to the next generation of metallic biodegradable implant materials with the addition of completely biocompatible elements.

Along with the addition of Ca, which is a biocompatible element that plays major in bone formation and remodeling, excellent material properties were achieved through the special mechanical extrusion machine. The state of the art method to synchronize the corrosion potentials of two constituent phases (Mg + Mg_2Ca) with the selective doping of Zn into Mg_2Ca was developed to control the corrosion rate. Furthermore, mechanical extrusion broke the connectivity of the Mg_2Ca phases, which prevented continuous corrosion and the formation of a galvanic circuit that caused severe corrosion of the Mg-Ca alloy. Animal studies confirmed the large reduction in hydrogen evolution and revealed good tissue compatibility with increased bone deposition around the newly developed Mg alloy implants. Newly developed set of K-RESOMET implants have the mechanical strength, ability to stimulate bone growth and controlled slow degradation rate to be considered as an ideal candidate for biodegradable implant applications.

With all the extensive in vivo experience using developed magnesium alloy material over the past 5 years, we were able to receive an approval from Korea Food and Drug Administration (KFDA) for the first human clinical trial of orthopedic biodegradable metallic implant devices in Korea. Working closely with hospitals, we have performed several hundreds of cases of small bone fixation screws in the past two years and have received approval for sale in Korea.

9:00-9:25 Invited

In Vivo Degradation Behavior of Hydroxyapatite-Coated Magnesium Alloys for Bone Implant Application

Sachiko Hiromoto, National Institute for Materials Science, Japan; Etsuro Nozoe, Kagoshima University, Japan; Kotaro Hanada, National Institute of Advanced Industrial Science and Technology, Japan

To moderate the corrosion speed and to improve the bone conductivity of biodegradable magnesium alloys, we developed hydroxyapatite (HAp) and octacalcium phosphate (OCP) coatings using Mg-3mass% Al-1mass% Zn (AZ31) and Mg-4mass% Y-3mass% RE (WE43) alloys. The HAp and OCP coatings reduced the corrosion speed of AZ31 and the inflammation reaction under the skin of mice.

In this study, HAp-coated WE43 and Mg-Ca alloys were implanted into the femoral bone of rats. The HAp coating accelerated the bone formation around the implanted alloys. The corrosion retardation of substrate depended on the alloy. The corrosion of WE43 was moderated for 6 weeks of implantation period although the corrosion proceeded under the coating. The corrosion of Mg-Ca was retarded initially; however, the corrosion under the coating formed a gap between HAp coating and substrate, and then the HAp coating was not able to retard the corrosion of Mg-Ca. In the case of WE43, a gap was not formed between HAp coating and substrate. The HAp coating remained almost original shape for 6 weeks regardless of the substrate alloy. Macrophage and osteoclast-like cells were cultured on HAp-coated WE43 or AZ31, and the degradation of HAp coating was not observed. The HAp coating is thus suitable for the devices which should support load for relatively long period.

Accordingly, carbonated apatite (CAp) coatings were developed as a biodegradable coating recently, because CAp is generally degraded by osteoclast cells in vivo. The in vitro degradation behavior of CAp-coated WE43 will be presented in the conference.

9:25-9:50 Invited

Computational Design of Mg Alloys with Minimal Galvanic Corrosion

Pil-Ryung Cha, Kookmin University, Korea; Yu-Cha Kim, Hyun-Kwang Seok, T Krishnamohan, Kookmin University, Korea; Seung-Cheo Lee, Kookmin University, Korea / Korean Institute of Science and Techonology, Korea

Replacement metals have been found in the skulls and teeth of ancient humans, which implies that metallic implants have been used for several millennia. The concept of bone replacement has been dominant in the development of metallic implants. However, biodegradable metals with the potential to stimulate bone formation have recently captured the attention of scientists. Among these metals, magnesium alloy is an attractive biodegradable material. However, its corrosion is accompanied by hydrogen evolution and a local increase in pH, which impose constraints on many potential biomedical applications. In this study, we propose a new computational alloy design methodology to minimize the galvanic corrosion that is the main corrosion mechanism in biodegradabe Mg alloys. The standard redox potentials for more than 40 metals with one-electron to four-electron are calculated using the Born-Haber cycle, and it was confirmed that the calculated potentials are in good agreement with experimental values available in literature. The concept is extended for use with multicomponent alloys by calculating redox potentials that are in accordance with standard redox potential; this is achieved through calculation of the formation free energy for alloys using density functional theory with reasonable assumptions. Then we propose a method to calculate the equilibrium concentrations of various phases existing in arbitary multi-component and multi-phase alloy systems based

on cluster expansion method. We apply our proposed methodology to Mg-Sr-Zn and Mg-Ca-Zn ternary alloy systems and estimate the ideal concentration of Zn which minimizes the galvanic corrosion in the systems. The results show very good agreement with experimental data, which confirms the validity of the alloy design methodology proposed in this study.

9:50-10:10

The Effect of High-Pressure Torsion on Biodegradable Pure Magnesium, Mg-1Ca and Mg-2Sr Alloys

Wenting Li, Xiao Liu, Danni Shen, Yufeng Zheng, Peking University, China; Kelvin Yeung, The University of Hong Kong , Hong Kong, China; Ruslan Valiev, Ufa State Aviation Technical University, Russia

In recent years, magnesium and its alloys have attracted great attentions as biodegradable materials without the need of implant-removal surgery in orthopedic field due to their biodegradability, similar mechanical properties to cortical bone, invading ‘stress shielding’ effect, and the biocompatibility of the magnesium ion, which is an essential element for bone growth. However, how to improve their mechanical properties and corrosion resistance simultaneously is a key issue for the material scientists. In this study, we used a severe plastic deformation method, high-pressure torsion(HPT), to treat as-cast P-Mg, Mg-1Ca and Mg-2Sr alloys in order to achieve improvement of their biodegradable properties and mechanical performance simultaneously by reducing their crystal size to nanoscale. The comparative analyses of microstructure, mechanical properties, degradable performance and in vitro biocompatibilities of as-cast, extruded and HPT materials were conducted by optical microscope, SEM, TEM, tensile tests, immersion tests and cell toxicity tests. After that, we evaluated the biocompatibilities of HPT P-Mg, Mg-1Ca and Mg-2Sr alloys in vivo by implanting the materials into the lateral epicondyle of the rat femur. The results showed that after high-pressure torsion with proper parameters, P-Mg, Mg-1Ca and Mg-2Sr alloys with nanoscale crystals have higher tensile strength and lower corrosion rate than those of the as-cast or extruded materials. In vitro cytotoxicity tests using MC3T3-E1 cell showed that P-Mg, Mg-1Ca and Mg-2Sr alloys after high-pressure torsion had Grade I cytotoxicity. In vivo implantation experiments showed that after the severe plastic deformation the degradation rates of the alloys were relatively low. The appropriate release rate of Mg, Ca and Sr ions contributed to the promotion of osteoblastic differentiation. Although there are some gas cavities around the implant during the first 4 weeks after the implantation, the new bone gradually formed in the bone marrow cavity in the vicinity of the implant after that. The project successfully improved the mechanical properties, corrosion resistance and biological properties of the material itself by severe plastic deformation and provided a new idea for the development of biomedical magnesium alloys.

10:10-10:30

Comparative Study of the Biodegradable Behaviors of Extruded, Rolled and Stamped Mg-2Zn-Nd (ZN20) Alloy

Iniobong Etim, Institute of Metal Research, Chinese Academy of Sciences, China / University of Science and Technology of China, China; Wen Zhang, Institute of Metal Research, Chinese Academy of Sciences, China / Central South University, China; Lili Tan, Ke Yang, Institute of Metal Research, Chinese Academy of Sciences, China;

Mg-2Zn-Nd alloy (ZN20) was processed by extrusion, rolling and stamping. The microstructure, crystallographic orientation and corrosion performance of the different processing methods was investigated to reveal the influence of the different processing route on the degradation rate of Mg-2Zn-Nd (ZN20). The degradation rate was measured by immersion of the Mg-2Zn-Nd alloy in simulated body fluid using Electrochemical Impedance Spectroscopy, Potentiodynamic polarization and mass loss. The in vitro degradation result reveals that the extruded Mg-2Zn-Nd has a lower degradation rate of 0.1mm/year compared to the stamped and rolled alloy. The material behavior was correlated to the changes in texture during extrusion, rolling and stamping. The metallurgical features were monitored by Optical Microscopy (OM), Scanning Electron Microscope (SEM) and Electron Back Scattered Diffraction (EBSD). The result reveals that crystallographic orientation significantly influenced the corrosion performance of Mg-2Zn-Nd alloy. The degradation rates largely increased with decreased 0001 crystallographic plane intensity while the 10-10 and 11-20 crystallographic plane intensities increased. This result reveals that degradation rate can be modified to some extent by controlling the texture during processing.

10:30-10:45 Tea Break

10:45-11:10 Invited

Understanding Mg Corrosion in Vivo

Andrej Atrens, Sean Johnston, Zhiming Shi, Matt Dargusch, The University of Queensland , Australia

Mg alloys are attractive for biodegradable medical implants. For this application, corrosion which is normally an unwanted feature of Mg alloys, becomes critical for the

success of the Mg alloy in this application. Nevertheless, it is vital to understand and control the corrosion rate. Over the last decade, Mg alloys have progressed from a laboratory concept to significant clinical successes. Parallel research has been carried out to understand the environmental factors controlling Mg corrosion in the body (in vivo). In vitro research has identified the following factors as the most important in vivo: (a) the inorganic ions like calcium, chlorides, bicarbonates, phosphates; and (b) the organic compounds including proteins, amino acids and vitamins. The best estimates for Mg corrosion rates (based on in vitro measurements) are larger than the corrosion rates measured in vivo. This suggests that the Mg corrosion mechanism in vivo is not adequately characterized, or the in vivo environment is not equivalent to immersion in a solution as used in the in vitro experiments. In fact, recent examination of specimens implanted subcutaneously into Sprague-Dawley rats indicated that the in vivo environment was not at all equivalent to immersion in a solution, but rather the environment could be better described as damp. The implications are discussed.

11:10-11:35 Invited

Electrochemical Functionalization of Biometals: Realization of Tissue-Regenerative and Cell-Selective Fully Metallic Devices

Myoung-Ryul Ok, Korea Institute of Science & Technology, Korea

Historically, biomedical applications of metallic devices have depended upon their mechanical and chemical stabilities in-vivo: metals have good combination of excellent strength and fracture toughness compared to other biomaterials in competition. However, chemical stability of biometals with their dense and stable native oxides is the result of suppressed chemical interactions between biometals and human bodies, including positive interactions like tissue regeneration or cell control. So, to endow bioactive functions to biometals, researchers have used ceramic or organic coatings, but this strategy caused other problems such as safety and/or reliability issues of the coating materials or at the biometal/coating interfaces. Thus, it has been a dream of biometal field to invent fully metallic implants with bioactive functions. Reactive oxygen species (ROS), naturally produced by metabolism, have ambivalent effects in the biological systems: the well-known oxidative stress to DNA and cells, but various types of cell signaling and promotion of angiogenesis. Recently, Park et al. reported an fully-metallic implant prototype spontaneously generating reactive oxygen species (ROS) via electrochemical processes and accelerating blood vessel regeneration. The 'tissue-regenerative fully-metallic implant system' is a galvanic couple consisting of inert bio-metal (Ti alloys, SUS, etc. widely in use) and biodegradable metal (Mg, Zn, Fe, etc.) and spontaneously generates hydrogen peroxide (H_2O_2) to promote angiogenesis. Indeed, ROS have different effects depending on the cell types: activating the functions of endotherial cells while preventing proliferation and migration of other cell types like smooth muscle cells(SMCs). This cell-selective nature can be used in stents, accelerating re-endothelialization of the stent surface while minimizing the migration of SMCs, for example. The system can also be applied to the sterilization of biomedical devices or environmental applications.

11:35-11:55

Optimization of Microstructure, Mechanical Properties and Degradation Behavior of a Degradable Orthopaedic Mg-Zn-Y-Nd Alloy

Beining Du, Liyuan Sheng, Zhiping Xiao, Yufeng Zheng, Tingfei Xi, Shenzhen Institute, Peking University, China

A new type of Mg-Zn-Y-Nd alloy for degradable orthopedic implants was developed. In the present study, the Zn and Y, Nd contents were adjusted and different extrusion processes were adopted, and then the influences alloying elements and processing techniques on the microstructures, mechanical properties and degradation behaviors were discussed. The results showed that the change of Zn content does not change the grain structure of the extruded Mg-Zn-Y-Nd alloy, while the increase of Y, Nd content would reduce the size and volume fraction of the equiaxed DRXed grains. The tensile properties are very little affected by Zn content because of the similar grain structure. As Y and Nd content increase, the tensile yield strength (TYS) and ultimate strength (TUS) increases while the elongation decreases, which is caused by the combining effects of grain refinement, texture strengthening, precipitation strengthening and twin strengthening. The increase of alloying elements would decrease the corrosion resistance of the Mg-Zn-Y-Nd alloy. In addition, different extrusion passes were applied to Mg-Zn-Y-Nd alloy, and the results showed that after one-pass extrusion, the incomplete dynamic recrystallization has led to a mixed grain structure with fine equiaxed grains and coarse elongated grains. After two-pass hot extrusion, dynamic recrystallization continues and both equiaxed grains and elongated grains are further refined. The increase of extrusion passes would not only enhance the mechanical properties, but also improve the corrosion resistance of the alloy remarkably.

G. Smart and Magnetic Materials: Permanent Magnetic Materials II

Symposium Organizers:

Shaoxiong Zhou, Center Iron & Steel Research Institute, China; Chengbao Jiang, Beihang University, China; Satoshi Sugimoto, Tohoku University, Japan; Haein Yim, Sookmyung Women's University, Korea; Sean Li, New South Wales, Australia; Bob Shull, National Institute of Standards and Technology, USA

Tuesday AM Room: Yulan Hall-220 (2nd Floor)
August 20, 2019 Symposium: G

Chairs:
Yang Sun, Institute of Physics, Chinese Academy of Sciences, China
Hiroaki Sukegawa, National Institute for Materials Science (NIMS), Japan

8:30-9:00 Keynote

Antiferromagnetic Domain Control by Magnetoelectric Effect

Yu Shiratsuchi, Osaka University, Japan

Antiferromagnet used to be regarded as useless materials because of the absence of spontaneous magnetization. This limitation restricts the application of the antiferromagnet to the static use, e.g. the induction of the exchange bias in the spin-valve film. Recent progress of the spin manipulation technique enabled us to manipulate the antiferromagnetic (AFM) spin based on spin torque effect, electric field (voltage) etc. Owing to these developments, the antiferromagnets are now expected to yield novel spintronic applications such as THz device and high-density magnetic storage.
Cr_2O_3 is an oxide antiferromagnet and exhibits the unique properties because of the combination of crystal structure and spin alignment, i.e. the magnetoelectric (ME) effect. The ME effect refers as the magnetization induction by an electric field or the electric polarization by a magnetic field. The ME effect of Cr_2O_3, has a long history since the discovery in 1950's, coupled with the above-mentioned recent development of the spin manipulation technique, and now, it was utilized as the principle of the AFM spin control. In the ferromagnetic (FM)/Cr_2O_3 stacked system, the FM spin (magnetization) can couple with the AFM domain state of Cr_2O_3 via the exchange bias. Then, the ME-controlled AFM order parameter can be detected through the FM domain. In this keynote, we overview the history of the ME control of Cr_2O_3 domain state and the detection via the FM domain. In addition, we present the recent development of this technique including the switching dynamics, i.e, the AFM domain wall velocity driven by the ME effect.

9:00-9:30 Keynote

Suppression of Eddy Current Generation in Nd-Fe-B-Type Magnet under Alternating Magnetic Field by Enhancing Electrical Resistivity

Hae-Woong Kwon, K. M. Kim, M. S. Kang, Pukyong National University, Korea; J. G. Lee, J. H. Yu, Korea Institute of Materials Science, Korea; K. H. Shin, Kyungsung University, Korea

Rotor magnet in traction motor of hybrid electric vehicle (HEV) and electric vehicle (EV) operates under alternating magnetic field from stator ripples and windings. Unless the rotor magnet possesses high enough electrical resistivity, generation of eddy current in the magnet is inevitable. Magnet exclusively used for rotor in the traction motor is Nd-Fe-B-type magnet thanks to its superior magnetic performance. Despite having excellent performance, the Nd-Fe-B-type magnet has drawback due particularly to its low Curie temperature (~310˚C), and it leads to poor thermal stability. In particular, high temperature coefficient of coercivity (b) of the Nd-Fe-B-type magnet has been a worrisome for the motor designers. Operating temperature of the rotor magnet in actual operation rises up to as high as 150 ~200˚C, coercivity of the magnet is radically decreased and in worst case the magnet is demagnetized, thus malfunction of motor can occur. Current approach for solving this problem is sufficiently enhancing room temperature coercivity of the magnet so as to still have enough coercivity at the operating temperature. Overly high operating temperature of the rotor magnet in traction motor is due largely to eddy current in the magnet generated during operation. As the Nd-Fe-B-type magnet is essentially metallic and hence has high electrical conductivity, eddy current is readily generated in the magnet by alternationg magnetic field from stator slot ripples and windings. Enhancing electrical resistivity in the magnet can, therefore, have immense benefit for suppressing over-rise of operating temperature of the rotor magnet. In this presentation, suppression of eddy current generation, hence temperature-rise, in the Nd-Fe-B-type magnet under alternating magnetic field by enhancing electrical resistivity is to be discussed. Temperature-rise in the Nd-Fe-B-type magnet was evaluated using a closed-type alternating magnetic field circuit for anisotropic Nd-Fe-B-type magnets with high electrical resistivity. Highly resistive magnets were fabricated by hot-pressing or die-upsetting the mixture of Nd-Fe-B-type magnetic particles (melt-spun flakes, HDDR-treated powder) and dielectrics (Dy salt, oxide) with low melting point.

9:30-9:55 Invited

Halide Ion-Mediated Synthesis of L10-FePt Nanoparticles with Tunable Magnetic Properties

Yongsheng Yu, Harbin Institute of Technology, China

L10-ordered FePt nanoparticles (NPs) with face-

centered-tetragonal (fct) phase structure have aroused extensive attention for potential applications in ultra-high-density magnetic recording media, magnetic energy storage and electrocatalysis because of their large magneto-crystalline anisotropy constant (Ku > 107erg/cm^3), high coercivity, outstanding corrosion resistance and eminent catalytic activity. Solution phase chemical synthesis of monodispersed FePt NPs with controllable size, composition and regular shapes have been reported over the last few decades. In general, the as-synthesized FePt NPs from solution phase reactions have a face-centered cubic structure (fcc), which is superparamagnetic at room temperature and cannot be applied in areas of data storage and permanent magnetic materials. For obtaining hard magnetic L10-phase, high temperature (>550˚C) annealing of the as-made NPs under a reducing or inert atmosphere is required. However, the protective organic layer surrounding the NPs will decompose at high temperature condition, and resulting in particle agglomeration that will lead to the growth up of particles with irregular shapes and sizes. Among various preparation processes, a direct synthetic process that can produce fct phase FePt NPs without post-synthesis annealing has attracted special interest. However, it is still desirable, albeit challenging to directly prepare L10-FePt NPs by a liquid phase synthesis process that does not require further annealing or the addition of noble metal atoms additives.

Here, a halide-ions (Cl^-, Br^- or I^-) mediated strategy for synthesis of fct-FePt NPs was developed. The FePt NPs structure can be controlled to be either fcc (without halide ions) or poly-crystalline fct (with different amounts of halide ions) through co-reduction of Fe(acac)3 and Pt(acac)2 in OAm. The systematic investigation on the synthetic mechanism confirm that the key control factor to form fct-FePt NPs is the strong binding force between halide ions and Fe or Pt ions, which are crucial for favoring FePt NPs growing in a more thermodynamic stable way and forming more stable fct phase structure. L10-FePt NPs with a room-temperature coercivity as high as 8.64 kOe and saturation magnetization of 64.21emu/g can be directly obtained by controlling the amount of the halide ions. This halide ion-assisted strategy may demonstrate a general route to tune the phase structure, magnetic properties and morphology of the FePt NPs by addition of different kinds of halide ions or in various amounts. The strategy also provides opportunities to prepare other magnetically hard Pt-based bimetallic NPs in a more controllable manner.

9:55-10:20 Invited

Fabrication of Rare Earth Free New Mn Based Permanent Magnetic Materials

Chul-Jin Choi, Jihoon Park, Ping-Zhan Si, Hui-Dong Quin, Jong-Woo Kim, Korea Institute of Materials Science, Korea

With the advent of high performance permanent magnets based on the rare earth elements such as Sm-Co, Nd-Fe-B alloys in the 1980s, the application areas have been extended from the electronics to hybrid electric vehicles and wind turbines etc. Since the high costs and environmental issues of the rare earth metals boosts up the price of the high performance rare earth permanent magnets, there is much interest on development of the various kind of new rare earth free permanent magnets Therefore, many researchers have paid much attention on the non-rare earth element, i.e. the metallic based permanent magnetic materials. In recent years, the researches on several materials systems have been focused on the nanocomposite made from transition-metallic alloys, tetragonal L1o FeCo alloys, anisotropic Mn-based alloys and body centered tetragonal $Fe_{16}N_2$ iron nitride alloys, etc. A variety of methods are available to manufacture rare earth free, high Clarke element based permanent magnetic materials in bulk, nanostructure, nanocomposite and thin films. Recently, among them, the magnetic Mn based system has attracted much interest due to low cost and strong uniaxial magnetocrystalline anisotropy., etc.

To develop the rare earth free permanent magnetic materials with large energy product, the new alloy design and microstructure modification should be solved. In this paper, we outline the challenges, prospects and research status for several potential Mn based alloys which could replace Nd based permanent magnetic materials.

10:20-10:35 Tea Break

10:35-11:05 Keynote

Smart "Binary Materials" for Photodetection from Mid-Infrared, Visible, to X-Ray

Tom Wu, UNSW, Australia

Light-matter interaction is a long-lasting theme in condensed matter physics and optoelectronics. Light detection in different wavelength regimes is the foundation of a wide range of sensing, imaging, medical and surveillance technologies. In this talk I will discuss the use of transition-metal oxides, hybrid organo-metal perovskites and other nanomaterials in "binary" mixed-dimensional heterostructures with proper bandgaps and architectures to detect photons with different wavelengths. First, for visible light detection, we demonstrate that combining 3D hybrid perovskites (CH3NH3PbI3) with high-mobility 1D carbon nanotubes or 2D two-dimensional metal dichalcogenides significantly enhances charge transport and device performance. Second, we report a mid-infrared (up to 10μm) mixed-dimensional photodetector enabled via coupling graphene with a narrow bandgap (0.1eV) oxide semiconductor Ti_2O_3. Finally, I will first discuss a nonvolatile memory made of ferroelectric Sm0.1Bi0.9FeO3 and semiconductor Nb-doped $SrTiO_3$, where a tunnelling electroresistance

as large as 10^5 is achieved, which is accompanied by a tunable photovoltaic effect.Furthermore, a colossal persistent photoconductivity was observed at room temperature in such thin-film junctions, where the junction conduction is enhanced by six orders in magnitude under X-ray illumination.

11:05-11:30 Invited

Smart Windows: State-of-Art and Outlook

Ping Jin, Xun Cao, Shanghai Institute of Ceramics, Chinese Academy of Sciences, China; Hongjie Luo, Shanghai University, China

Smart windows are such that enable a control of solar/light irradiation in response to environmental change or human needs. They can be made either by coating thin films on rigid glass or coating/blending with polymers to form soft foils. Smart windows are expected to be the next generation of window to replace partially the low-E and solar control films for buildings and vehicles. There are a variety of smart windows according to their chromogenic responses and color-change mechanisms. The most popular ones are known as electrochromic, thermochromic, photochromic, and gasochromic, with chromogenic responses to electric field, temperature, light, and gas species (i.e., diluted hydrogen), respectively. Among the categories, the most interest has been focused on the electrochromic window, worldwide and particularly in China, for its conveniency, high energy efficiency and comfort, and matured manufacture technology. Although products have been produced in USA and sold worldwide, innovations are still required for new materials, new structures, simplified machines and manufacturing process to scale-up the market under a substantial reduction in the cost.

An increasing attention has been paid to the thermochromic window that enables an automatic solar/heat irradiation control in response to environmental temperature using the metal-insulator phase transition of vanadium dioxide thin films. The first generation of thermochromic foil product has been launched in China and tested on buildings and cars.

A photochromic window can be made by chemical methods (WOx nano-particles and foils) and physical deposition (YOxHy films). They are characterized by high regulation rate in energy with pleasant color, but still with obstacles in the response time and durability towards a product.

The alloy-film-based gasochromic window is almost the only one capable of the reverse change from transmitting to high reflecting (mirror). The materials and film stack has been optimized for scale-up, and the switching system has been simplified towards large-scale production. Such type is expected to find applications in the future.

Based on the long-term research experience over a wide range of smart windows of the author, the state-of-art and outlook of the above windows will be presented with our most recent advances.

11:30-11:50

Catalytic Synthesis and Magnetic Properties of Iron Nitrides Nanostructures Synthesized in a Tetraethylenepentamine Solution

Da Li, Yong Li, Zhidong Zhang, Institute of Metal Research, CAS, China; Chuljin Choi, Korea Institute of Materials Science, Korea

Hard magnetic materials with large coercive fields are widely used in many application fields, such as high-density data storage media and permanent magnets. High coercivity property originates from large magnetocrystalline anisotropy and shape anisotropy. Magnetocrystalline anisotropy is usually obtained by high-temperature annealing for the chemically ordered phase of a hard magnetic material, while the shape anisotropy arises entirely from the demagnetizing field Hd. By combining shape anisotropy and size effect, the lower dimensionality may enable to enhance magnetic properties of magnetic nanostructures. In comparison of the top-down physical method, chemical synthetic route can simply synthesize uniform magnetic nanostructures with controlled size and shape. Our recent research has focused on low-temperature synthesis and enhanced magnetic properties of iron nitride nanostructures. In this presentation, tetraethylenepentamine (TEPA) is considered as both the reductant and the precursor of N and C elements. By means of a new, facile and one-pot reaction of iron(II) acetylacetonate in TEPA, carbon coated iron nitride magnetic nanostructures have been synthesized and low temperature nitrogenation mechanism has been demonstrated by kinetically controllable syntheses in various reaction conditions. For example, ε-Fe_3N@C nanoparticles show an excellent saturation magnetization of 135.5emu/g at 300K and an enhanced Curie temperature (TC) of 614K, much higher than the TC values in the previously reported maximum TC (=575K) for ε-Fe_3N obtain by A. Leineweber and his cooperator. Moreover, carbon coated Fe nitrides nanorods have been synthesized by our chemical route. Such nanorod-like Fe nitride nanostructures show a ratio of length to diameter (~20:1). The reaction time dependent on the ratio of Fe and N has been studied to expect for the synthesis of $Fe_{16}N_2$ with excellent hard magnetic properties.

11:50-12:10

Enhanced Thermal Stability of Piezoelectricity in Lead-Free (Ba,Ca)(Ti,Zr)O_3 Systems Through Tailoring the Phase Transition Behaviors

Mengye Yin, Chao Zhou, Shuai Ren, Yanshuang Hao, Minxia Fang, Jinghui Gao, Tianyu Ma, Lixue Zhang, Sen Yang, Xiaobing Ren, Xi'an Jiaotong University, China

Good thermal stability of lead-free $BaTiO_3$-based ceramics is one important concern for their applications above room temperature. Two pseudo-binary Pb-free

BaTiO3-based ferroelectric systems, (1-x)Ba(Ti0.8Zr0.2)O3-x(Ba0.65Ca0.35)TiO3) ((1-x)BZ0.2T-xBC0.35T) and (1-y)Ba(Ti0.8Zr0.2)O3-y(Ba0.95Ca0.05)TiO3 ((1-y)BZ0.2T-yBC0.05T), were fabricated via the traditional solid-state method. Phase transition behaviors for these two systems has been tailored due to different contents of Zr and Ca. Temperature dependences of piezoelectric coefficient d33 for the compositions on the tetragonal to orthorhombic phase boundary for these two systems, 0.55BZ0.2T-0.45BC0.35T and 0.20BZ0.2T-0.80BC0.05T, have been compared from 20℃ to the paraelectric to ferroelectric phase transition temperature (Tm). And enhanced temperature stable piezoelectricity has been achieved for the latter. The variation of d33 together with the value normalized by the room temperature piezoelectricity d33/d33|RT for this composition with less Zr are 183pC/N and 58.2%, while those for the former are 463pC/N and 91.3%. And the different phase transition behaviors can be revealed from the different responses of the temperature dependent dielectric permittivity, hysteresis loops and in-situ domain structure for these two samples. We found that the composition with improved thermal stability shows higher Tm (115.7℃) and less degree of diffusion (degree of diffusion constant = 1.35), compared with the phase transition behaviors for the other composition Tm = 81.3℃ and = 1.65. Thus, our work provides a considerable aspect for designing piezoelectric materials with good thermal stability through tailoring the phase transition behaviors.

H. Materials Characterisation and Evaluation: II

Symposium Organizers:

Zhiwei Shan, Xi'an Jiaotong University, China; Xiaodong Han, Beijing University of Technology, China; Satoshi Hata, Kyushu University, Japan; Ju-Young Kim, Ulsan Institute of Science and Technology (UNIST), Korea; Jin Zou, University of Queensland, Australia; Jennifer Carter, Case Western Reserve University, USA

Tuesday AM
August 20, 2019

Room: 308 (3rd Floor)
Symposium: H

Chairs:
Heung Nam Han, Seoul National University, Korea
Dmitri Golberg, Queensland University of Technology, Australia

8:30-9:00 Keynote

In situ Nanomaterial Property Studies in a High-Resolution Transmission Electron Microscope

Dmitri Golberg, Queensland University of Technology (QUT), Australia

Understanding mechanical, electrical, thermal, thermoelectric, optical, optoelectronic and photovoltaic properties of a material, in particular on the individual nanostructure level, is of key importance as far as its effective integration into any modern technology is concerned.

However, in the vast majority of cases, these property measurements are performed by means of instruments with no direct access to the materials' atomic structure, its crystallography, spatially-resolved chemistry and existing point and/or linear structural defects. This fact largely limits the relevance of the collected data because all particular structural features of an object prior, during and after its testing are typically hidden. Therefore, the acquired results can hardly be linked to a particular material morphology, atomic structure, and defect network. Thus, a wide scatter in the reported data has been commonly observed between various samples and research groups. Till now this drawback has greatly confused practical engineers and technologists and led to many uncertainties in regards to materials' practical applications and industrial potentials.

In this contribution I demonstrate the full usefulness of newly designed in situ high resolution transmission electron microscopy (HRTEM) probing techniques for diverse property analyses of many advanced materials, e.g. individual inorganic nanotubes, graphene-like nanosheets, nanowires and nanoparticles.

Elasticity, plasticity, fracture strength and toughness, electrical conductance, thermal gradients, photocurrents, photovoltages and spatially-resolved cathodoluminescence are now may accurately be measured inside HRTEM, while employing piezo-driven nanomanipulators and/or optical fibers inserted into the microscope column.

9:00-9:25 Invited

New Functions on Electron Tomography: Magnetic-Field-Free Diffraction Contrast Imaging and In-Situ Specimen Straining

Satoshi Hata, Hikaru Saito, Kyushu University, Japan; Mitsuhiro Murayama, Kyushu University, Japan / Virginia Tech, USA

Electron tomography (ET) is a three-dimensional (3D) nanostructural imaging method using transmission electron microscopy (TEM) or scanning transmission electron microscopy (STEM). Here, we present our recent activities on developing new functional ET imaging methods: magnetic-field-free diffraction contrast ET and in-situ ET with straining a specimen in TEM. The former, magnetic-field-free diffraction contrast ET, is useful for observing 3D crystalline microstructure in ferromagnetic materials, for example, dislocations in Fe with a body-centered cubic structure. In order to realize the magnetic-field-free ET method, an aberration-corrected objective lens-less STEM mode, demagnetization of the objective lens system and a tri-axial high-tilt specimen holder are essential techniques. The latter, the in-situ straining and

ET system, consists of (i) an in-situ specimen-straining and tomography holder, (ii) the in-situ straining and subsequent tilt-series data set acquisition software to control the holder, imaging devices and the specimen stage in an integrated manner and (iii) ex-situ 3D reconstruction and visualization software. We applied the in-situ straining and ET system to dynamic 3D imaging of plastic deformation in a Pb–Sn solder alloy specimen.

9:25-9:50 Invited

Nanostructure Analyses of Hafnia-Based Ferroelectric Thin Films by Aberration-Corrected Electron Microscopy

Takanori Kiguchi, Takahisa Shiraishi, Toyohiko J. Konno, Tohoku University, Japan; Takanori Mimura, Takao Shimizu, Hiroshi Funakubo, Tokyo Institute of Technology, Japan

Recently, the novel polar orthorhombic phase (Pbc21) of SiO_2–HfO_2 with ferroelectricity has been found. The important point of the polar orthorhombic phase is metastable phase, which is stabilized just under the chemical (dopant) and the strain effect. After that, many researches found that various dopants were also effective for stabilization of the polar orthorhombic phase in polycrystalline HfO_2-based thin films.
On the other hand, the growth and characterization of the HfO_2-based epitaxial thin films has been limited. Shimizu prepared the 7~8mol% $YO1.5$–HfO_2 (YHO) epitaxial thin films on the $YO1.5$–ZrO_2 (YSZ)(100) substrate by a pulsed laser deposition (PLD), showing the ferroelectric P-E hysteresis curve, and found that the phase was the polar orthorhombic phase with Pbc21 symmetry using an aberration-corrected scanning transmission electron microscopy (STEM). Katayama has controlled and analyzed the domain orientation by X-ray diffraction. Kiguchi has conducted the epitaxial growth of ZrO_2–HfO_2 (HZO) thin films on YSZ(100) substrate by solid state epitaxy using ion-beam sputtering and the atomic structure observation of the 90° domain structure using the STEM. The domain structure is rather different from the conventional perovskite-type ferroelectric thin films such as $PbTiO_3$ and the detail of the domain structure has not been understood well.
In the present study, we have focused on the YHO epitaxial thin films in order to exclude the complexity for the detail analysis of the domain and the domain wall structures by pushing out the extra factors such as grain size, grain boundary, and random orientation. The observed domain walls were composed of {100} and {110} types. The longest axis is b-axis under the symmetry Pbc21, while the length of the polar c-axis is quite close to that of the shortest a-axis. This fact infers that the orientation relationship between neighbor domains is decided by the relationship between the longest b-axis in each domain and the rotation axis between domains. We have elucidated that the orientation relationship between neighbor domains is decided by two factors: (i) tilt or twist relationship between the longest b-axis in the domains, and (ii) parallel or perpendicular relationship between the rotation axis and the longest b-axis.
This research was supported by Japan Society for the Promotion of Science (JSPS) KAKENHI 16K14378, 17H05327, SUZUKI Foundation, Yashima Environment Technology Foundation, Shorai Foundation For Science And Technology, Hosokawa Powder Technology Foundation.

9:50-10:10

Amorphization and Dislocation Emission Accompanied by Detwinning at Crack Tip of Aluminium Observed in Situ by HRTEM

Yanqing Yang, Zongde Kou, Zongqiang Feng, Northwestern Polytechnical University, China

The microstructure ahead of crack tip is very important for studying the fracture mechanism of materials. We conducted tensile tests on 2024 Al alloy and pure Al and observed in situ by HRTEM. Two phenomena are special in front of the crack tip. First, it was found that amorphous structure appears around some nanovoids ahead of the crack tip of 2024 alloy. As the strain increases, the nanovoid becomes larger, leading to the forward propagation of the main crack. The amorphous structure was also identified in the fractured part. Second, during tensile deformation, twinning was observed at the crack tip because of high stress concentration. Then the twin tip becomes thinner, and detwinning of the thinned twin tip happens due to the high stacking fault energy of Al, and at the same time, a dislocation is emitted from the twin tip to pure Al matrix, which is a new way for dislocation multiplication at the crack tip of aluminium with high stacking fault energy. It was also found that lattice dislocation can be absorbed to the twin boundary and forms a sessile step. As twinning and detwinning, the sessile step moves to the twin tip gradually and the dislocation emits into lattice.

10:10-10:30

4D In-Situ XRM and LabDCT Applications on Material Science

Chunjie Cao, Carl Zeiss (Shanghai) Co. Ltd, China

In recent years, Zeiss X-ray microscopy technology has become more and more popular in the fields of scientific research and industrial inspection. Its unique performance has opened up a new research method for high resolution nondestructive analysis. ZEISS Xradia X-ray Microscopes bring synchrotron capabilities to the lab.The following are the main technical features of the product:
(1)ZEISS Xradia Versa architecture uses a two-stage

magnification technique that produces sub-micron resolution imaging at large working distances (RaaD) for a diverse set of sample sizes and types. Sample imaged independent of distance to source, enabling interiors of larger samples to be imaged non-destructively at higher resolution.
(2)ZEISS Xradia Versa delivers flexible, high contrast imaging for even your most challenging materials – low atomic number (low Z) materials, alloy composite, soft tissue, polymers, fossilized organisms encased in amber, and other materials of low contrast.
(3)ZEISS X-ray microscopes uniquely enable the most advanced in situ experiments. These studies require samples to be further away from the X-ray source to accommodate various types of in situ rigs. On traditional microCT systems, this significantly limits the resolution achievable for your samples. ZEISS XRM are uniquely equipped with dual-stage magnification architecture with Resolution at a Distance (RaaD) technology that enables the highest resolution for in situ imaging.
(4)With LabDCT option exclusively available on Xradia 620 Versa, ZEISS brings you the first ever laboratory-based diffraction contrast tomography imaging module. This unique grain imaging analytical technology enables non-destructive mapping of orientation and microstructure in 3D. No longer confined to conventional 2D metallographic investigations, direct visualization of 3D crystallographic grain orientation opens up a new dimension in the characterization of metal alloys and polycrystalline materials.
The presentation will introduce the advantages of ZEISS X-ray microscopy and its applications in metal research. The first section of the presentation is focused mainly on the working principle and instrumentation in X-ray microscopy. The following sections will list the application cases of XRM on metal research, including alloy, AM, TBC , 4D in-situ experiment etc. The last sections will introduce diffraction contrast tomography technology on ZEISS x-ray microscopy. The application of DCT in metal crystal orientation analysis will also be introduced.

10:30-10:45 Tea Break

10:45-11:15 Keynote

Analysis on Mechanical Softening of Nano-Ceramics induced by Electron-Beam Irradiation

Heung Nam Han, Sung-gyu Kang, Woojin Cho, In-suk Choi, Seoul National University, Korea

Plasticity of material has a direct correlation to formability. Ceramics, which are the most widely known low-plasticity material, only exhibit the brittle fracture when subjected to stress, unless placed at a high temperature condition. In order to fabricate a ceramic-based structural material, complex processes must be involved: High temperature heating or sintering for a bulk scale, deposition methods for micro/nano scales. Especially for nano-ceramics, simple geometries, such as wires, films, and spheres, are only valid to fabrication. Despite the exceptional mechanical properties of the 3D nanoceramic with complex geometries and their novel applications from a damage tolerance material to advanced electronics reported recently, low plasticity limits their potential for wider application.
Recent researches have made a breakthrough in the plasticity of ceramics by utilizing an electron-beam (henceforth, referred to as "E-beam") irradiation. Amorphous silica spheres of submicron size exhibit mechanical softening and substantial permanent deformation when uniaxially compressed under the E-beam irradiation in a transmission electron microscopy (TEM). However, since most researches have focused on the E-beam effects on deformation behaviors of amorphous silica, only a few results for other amorphous ceramics have been reported. In addition, the majority of studies have investigated the E-beam effects on the deformation behaviors of amorphous silica within the TEM. TEM not only generates a fixed high energy electron beam of several hundred keV, but also only allows very simple mechanical tests, such as tensile test of a nanowire and compression test of a particle, owing to its limited chamber size. Despite, the in-situ TEM system simultaneously provides information on microstructural changes of the material during the E-beam irradiation, but not sufficient to rigorously investigate the E-beam induced deformation behaviors and to confirm the improved formability of the material in various ways.
In this talk, we utilize an in-situ scanning electron microscopy (SEM) compression system to explore the E-beam induced mechanical softening of the ceramic materials. The beauty of SEM is that we can easily utilize the low energy E-beam with various conditions by regulating the acceleration voltage and the beam current in each pixel. With the E-beam of the SEM, we rigorously investigated the low energy E-beam induced mechanical softening of the amorphous silica and its relationship with the E-beam parameters, such as the acceleration voltage, the beam current, etc. Experiments and simulations have shown that the interacting volume between the material and the incident electrons is an important factor for the mechanical softening. Moreover, we expand the concept of the E-beam induced mechanical softening to various ceramics, including amorphous and crystalline ceramics, by confirming similar mechanical softening behavior under the E-beam of SEM.

11:15-11:40 Invited

Recent Progress in High Resolution X-Ray Tomography at High X-Ray Energies

Hiroyuki Toda, Kyosuke Hirayama, Han Su, Kazuyuki Shimizu, Osamu Takakuwa, Akihisa Takeuchi, Kentaro Uesugi, Kyushu University, Japan

Recently, high resolution X-ray tomography techniques

at high X-ray energies, such as 20~30keV, have been developed in the Japanese synchrotron radiation facility, SPring-8. The X-ray energy range available for high resolution X-ray microscopes has been limited to ~ 10keV or so in X-ray energy due mainly to the difficulty in the preparation of the magnifying optics with nanoscopic structures for high X-ray energies. Recently, SPring-8 has successfully developed so-called an apodization Fresnel zone plate, by which the difficulty in the fabrication of high X-ray energy devices can be remarkably mitigated together with improved diffraction efficiency. In May, 2017, a large-scale 20keV X-ray microscope, which has a camera length of 165m, was realized and thereby spatial resolution of X-ray microtomography technique has been improved by one order of magnitude for light metals such as aluminum alloys. In May, 2018, the X-ray energy available for the X-ray microscope was successfully raised to 30keV by which titanium alloys and steels can be visualized in 3D. The Zernike phase contrast imaging technique has been used together with an appropriate illumination system. This enables to visualize dual phase structures in steels and titanium alloys, which have sometimes very small density difference, without time-consuming phase retrieval techniques.

In-situ observation techniques are employed with the high resolution imaging facilities. Since then the high resolution imaging techniques have been applied to various materials science related issues such as fatigue cracking in titaniumu alloys, hydrogen nano void formation in aluminum alloys, stress corrosion cracking in high Mg Al-Mg alloys, the in-situ observations of the deformation-induced transformation of an austenite phase in TRIP steels, etc. In this presentation, technological features of the high resolution imaging techniques will be introduced at the beginning, and then the various applications will be demonstrated together with the introduction of ongoing challenging development such as an amalgamation of X-ray CT and XRD for advanced crystallographic analyses in polycrystalline materials.

11:40-12:00

Rapid Solidification and Microstructure Evolution of Ternary Al-Si-Fe Alloy Droplets

Xiaoyu Lu, Weili Wang, Ying Ruan, Northwestern Polytechnical University, China

Ternary Al51.8Si35.4Fe12.8 peritectic alloy was undercooled and rapidly solidified under free fall condition in a 3m drop tube, the droplets sized 180~1000mm were obtained, and the rapid solidification mechanism of them was researched. The near equilibrium solidification processing was accomplished by DSC experiment, and the liquidus temperature of the alloy was measured as 1162K. Based on the Newton cooling model, the cooling rate and the undercooling of the droplets are calculated, and both of them increase sharply with the decrease of the droplets' diameter, in this study the maximum cooling rate and undercooling are 2.09´104K/s and 226K respectively. It is deduced that during the solidification, the growth of the primary phase, the ternary peritectic reaction and ternary eutectic reaction happened in succession, the final microstructure contains (Si) phase, t_4 phase and ternary eutectic phase which is composed of (Si)、(Al) and Al2Si phase. The t4 phase has a shape of lath, other phases are distributed in the gap of the t_4 lath, and with the decrease of the droplets' diameter, the t_4 lathes become finer, the spacing of them reduce. Also the solute trapping effect happens distinctly, with the decrease of the droplets' diameter, the solubility of Al and Fe in (Si) phase increase sharply, and the microhardness of the droplets increases obviously.

12:00-12:20

Quantifying the Microstrain Evolution and Micromechanism for the Structural and Functional Materials by In-Situ Neutron Diffraction under Multi-Field Coupled Loading

Changsheng Zhang, Hongjia Li, Fangjie Mo, Beibei Pang, Hong Wang, Jian Li, Zhaolong Yang, Yi Tian, Yaling Huang, Guangai Sun, Key Laboratory for Neutron Physics of Chinese Academy of Engineering Physics, Institute of Nuclear Physics and Chemistry

The multiscale internal strains may be deemed as the fingerprints of the deformation for materials. Residual Stress Neutron Diffractometer (RSND) at the China Mianyang Research Reactor (CMRR) has been expected to show fundamental significance in both the applications of engineering and materials science due to its multifunction RSND provides the unique tool for accessing the internal stress distribution inside components and guiding the reliability assessment. Besides, RSND also provides the powerful method for revealing the mechanism underlying the macroscopic mechanical/physical responses in the structural and functional materials. We shall show those results and progresses on the microresponses for the structural and functional materials, which are addressed by the in-situ neutron diffraction. Recently, the intergranular and intragranular stresses in the polycrystalline hexagonal have been quantified through neutron diffraction, which show a composite behavior and tuned significantly by the temperature and strain rate effects. The intergranular stress and stored energy are large for the soft-oriented grains (SOGs), while the intragranular stress and stored energy are large for the hard-oriented ones (HOGs). Both of those stresses are significantly high for the dynamic strain rate while they are relatively low for the elevated temperature. The large internal stresses in the dynamically compressed specimen should be attributed to the large number of twins and high density of dislocations. Elastic-tension-induced

lattice distortions have been revealed in DD10 single crystal nickel-based superalloy by a newly-developed in situ neutron diffraction method, which might provide the directly experimental evidence to the origin of rafting. Meanwhile, we have developed a two-phase elastic-plastic self-consistent model to account for lattice coherency for nickel-based superalloys. In-situ neutron diffraction has been also used to investigate simultaneously the macroscopic and microscopic stress-strain behaviors as well as the microstructure evolution in α″ -martensitic U-Nb shape memory alloys (SMAs). The aging-effect-modulated mechanical properties are achieved through the modified twinning-detwinning process. The initial yielding strength is significantly increased. The in-situ observations show that the strength enhancement arises from the aging-induced resistance during the twinning-detwinning process. The in-situ neutron diffraction has been also employed to demonstrate the structural stability for the novel-designed stress tolerant soft magnets. RSND at CMRR is therefore ready for more experiments from the multidisciplinary users, which could be helpful for the design and development of materials.

12:20-12:40

Solidification and Microstructure of A Hypereutectic Zn-Al Alloy

Hongfa Hu, University of Windsor, Canada

Zinc-aluminium alloys, in particular the eutectic Zn-Al alloy, are often employed to coat steel for corrosion protection. With additional Al contents, hypereutectic Zn-Al alloys provide improved corrosion resistance. Since Zn-Al coating on steel involves solidification, it is essential to develop scientific understanding of its solidification behavior and relation to microstructure evolution. In this work, Zn-6wt.% Al hypereutectic alloy was solidified under different cooling rates of 0.04, and 10˚C/s. The effect of cooling rates on the solidification of the alloy was investigated according to thermal histories recorded by temperature measurements on cooling curves. The slow cooling of 0.04˚C/s reveals the detailed solidification sequences, at which different phases form, due to its near-equilibrium condition. The observation of no apparent undercooling on the cooling curve of the alloy under the high cooling condition implies a significant refinement of the matrix microstructure structure. The metallographic analyses by scanning electron microscopy (SEM) and energy dispersive X-ray spectroscopy (EDS) indicate that four different phases, the primary γ-ZnAl phase, the eutectic β-Zn phase, and the eutectoid α-Al and eutectoid β-Zn phases decomposed from the eutectic γ-ZnAl phase appear in the samples solidified under the difference cooling rates. However, as the cooling rate increases to 10.00˚C/s, which suppresses the eutectic and eutectoid reactions, the average size of the eutectic phase is significantly reduced by more than an order of magnitude from the micron size (7.58μm) for the cooling rate of 0.04˚C/s to the nano size (0.58μm = 580nm) for the cooling rate of 0.04˚C/s. The results of the measured eutectic spacing indicate that an increase in the undercooling decreases the spacing between eutectics, and the eutectic spacing is inversely proportional to the undercooling. Evidently, the high cooling rate of 10˚C/s suppresses the growth of the eutectoid phases, and results in the formation of the nano-sized eutectoid α-Al and eutectoid β-Zn phases, and the considerably refined microstructure.

I. Composite Materials: I

Symposium Organizers:

Lin Geng, Harbin Institute of Technology, China; Boming Zhang, Beihang University, China; Junya Inoue, Tokyo University, Japan; Sang Bok Lee, Korea Institute of Materials Science (KIMS), Korea; Hao Wang, University of Southern Queensland, Australia; Rusty Gray III, Los Alamos National Lab, USA

Tuesday AM
August 20, 2019

Room: 307(3rd Floor)
Symposium: I

Chairs:
Lin Geng, Harbin Institute of Technology, China
Tapas Laha, Indian Institute of Technology (IIT) Kharagpur, India

8:30-9:00 Keynote

Carbon Nanotubes Reinforced Superprofile

Hansang Kwon, Dasom Kim, Kwangjae Park, Pukyong National University, Korea; Kyungju Kim, Next Generation Materials Co. Ltd., Korea; Yuske Hirayama, Kenta Takagi, National Institute of Advanced Industrial Science and Technology (AIST), Japan

Carbon nanotubes (CNT) or graphene nanotubes were used as a reinforcing materials enhending for aluminum (Al) alloys matrix composite profile by mechanical ball milling and the directl hot extrusion processes with special billet preparation. Multi layered CNT-Al alloys superprofile was successfully fabricated as a world first in mass production line.
The superprofiles could be used for composed of various frame elements and brackets needed for assembling with T-slot structure which has advantage of no welding, simple designed, short manufacturing time and easy to recycling and so on. The mechanical properties were increased and especially elastic modulus of the superprofile showed around four times higher than that of Al alloys. Moreover, thermal conductivity of the superprofile was enhenced almost 30% of that of Al alloy.The grains of Al alloy texture are aligned with (001) orientation. The high-alignment properties are

attributed to the effect of extrusion direction. However, orientation of the CNT in Al alloy matrix is difficult to observe because CNT is nano scale and encapsulated into the soft Al matrix during direct extrusion process.
Some of strengthening mechanisms such as load transfer effect, grain refinement and other factors was introduced in this study to explain the higher mechanical properties than theoretical values. The theoretical strength of superprofile was predict respectively based on the Kelly-Tyson equation and Hall-Petch equation to compare with experimental values. In the results, it was shown theoretical and experimental values significantly were matched.
It is possible to apply for general automation system frames, electric vehicle parts and customized solar battery frames and so on.

9:00-9:25 Invited

Graphene Reinforced Aluminum Composite Prepared by Cold Drawing

Xuexi Zhang, Jianchao Li, Lin Geng, Harbin Insitute of Technology, China

Dispersion of graphene in aluminum matrix has been a key factor that affects the strengthening efficiency of graphene reinforced aluminum matrix composites. Here, GNP/Al composites reinforced with graphene nano-platelets (GNP) were fabricated by powder metallurgy (PM) followed by a multi-pass cold drawing at ambient temperature in order to eliminate the GNP aggregates. The microstructure evolution and the mechanical properties of the GNP/Al composites were investigated. Results showed that GNP cracked into pieces along the drawing direction, leading to improved GNP distribution. GNP aggregates were eliminated in 0.4wt% GNP/Al at an equivalent drawing strain of 6.00 compared with that in the as-extruded composite, while some still exist in the 2.0wt% GNP/Al composite. The ultimate tensile strength (UTS) of as-drawn 0.4 wt% GNP/Al composites was ~52% higher than that of the Al alloy. While, the mechanical properties of 2.0 wt% GNP/Al composites deteriorated because of the existence of GNP aggregates. The dispersed GNP with strong interfacial bonding in 0.4wt% GNP/Al composites exhibited significant load transfer strengthening effect, which contributed to the improvement in UTS. The strengthening efficiency (R) of graphene in the cold-drawn composite wires reached ~80%, which is comparable to that of the composites fabricated by wet chemistry method.

9:25-9:45

Fabrication and Microstructure of Porous Material Using CNTs Block for Fabrication of Matrix Composites Materials

Fei Gao, Yongbum Choi, Kazuhiro Matsugi, Kenjiro Sugio, Gen Sasaki, Xingxing Zhao, Hiroshima University, Japan

With the rapid development of electronic industry, the heat sink material of semiconductor and optoelectronic is required of as high as TC (200 or more $W \cdot m^{-1} \cdot K^{-1}$), compatible CTE with those of electronic components (6~7ppm/K) and low density. But as heat sink material, aluminum and copper are unable to simultaneously meet the requirements. Carbon nanotubes (CNTs) reinforced metal matrix composite are focused for the advantages of low density and high thermal conductivity, etc. However, when CNTs were applied to composite materials, the difficulty of dispersion of CNTs leads to the deterioration of thermal property. Thus, this study developed porous material consisting of undispersed and self-aligned CNTs block as preform for fabrication of Al matrix composite.
Electroless Cu plating were conducted on CNTs block with 15, 30, 60 and 180s, respectively. 10vol.% of electroless Cu plated CNTs block were mechanically mixed with 90vol.% NaCl at tilting 45 degree for 600s using a glass rod. Mixtures were put into a graphite mold, then was compacted by a pressure of 60MPa. Compacted mixtures were sintered in Ar. The sintering conditions of electroless Cu plated CNTs block were 973K and 1.8ks. Sintered samples were immersed into distilled water for 48h to dissolve NaCl then were dried. The size of the preform is 3mm in height and 10mm in diameter.
Cu was uniformly plated on surface of CNTs blocks. The thickness of Cu electroless coated CNTs block with 15s, 30s, 60s and 180s was 2.60, 3.55, 5.21 and 9.25μm respectively. And the porous materials with porosity of 90% were fabricated. In the cell wall of porous materials, CNTs block were covered by Cu layer. Thus, the porous material can be utilized as preform for fabrication of Al matrix composite.

9:45-10:05

Effects of Alloying Additives X (X=Si, Al, Cr, Mn, Ni, Mo) on the Properties of TiB_2/Fe Interface: A First-Principles Study

Yefei Li, Bing Xiao, Yangzhen Liu, Yiran Wang, Shengqiang Ma, Zhiwei Liu, Qiaoling Zheng, Xi'an Jiaotong University, China

Accompanying with the rapid development of the modern industry, ceramic particles reinforced iron composites or also known as ceramics/iron composites have been becoming an intensively investigated novel type of wear resistant materials. Among many ceramics/iron composites, TiB_2/Fe composite combines the desirable properties of TiB2 and iron, and which also offers several advantages in terms of large elastic modulus, high mechanical strength, superior hardness and wear resistance.
In this work, we investigate the atomic structures, chemical bonding, stability and fracture mechanism of B- and Ti-terminated TiB_2 (0001)/Fe (111) interfaces using first-principles calculations. It is found that all Ti-

terminated interfaces (Ti-HCP, Ti-MT and Ti-OT) as well as B-HCP interface are non-diffusive type. Meanwhile, B-MT and B-OT configurations are diffusive interfaces due to the formation of additional FexB intermetallic compound at the original Fe/TiB_2 interface. The calculated works of adhesion and interfacial energies of all six configurations indicate that Ti-HCP and B-HCP are the most stable structures. Based on HCP configurations, the segregation behavior of alloying additives X (X=Si, Al, Cr, Mn, Ni, Mo) on the interface of TiB_2 ceramic reinforced iron matrix composite as well as the effects of these additives on the interfacial adhesion, electronic and magnetic properties were studied. The results indicated that Cr, Mn and Mo may segregate at the TiB_2 (0001)/Fe (111) interface because of their low heat of segregation barrier. Moreover, compared with the work of adhesion of different alloying doping interfaces, the introduction of Cr, Mn improves the adhesive strength of TiB_2(0001)/Fe (111) interface through strong covalent interactions between Cr/Mn and B atoms. The best strengthening effect on TiB_2 (0001)/Fe (111) interface can be attributed to Mn because of the highest interfacial work of adhesion and critical stress of Mn-doped interface; we also have the following order of this interface system: indicating the mechanical strength of the interface is more remarkable than both TiB_2 and Fe slabs, and the mechanical failure will initiate at the Fe interior. Besides, the effects of the alloying additives on interfacial electronic and magnetic properties are also discussed in this paper.

10:05-10:25

In Situ Synthesis of High Content Graphene Nanoplatelets Reinforced Cu Matrix Composites

Siyuan Guo, Chunsheng Shi, Naiqin Zhao, Tianjin University, China

Metal matrix composites (MMCs) are made by dispersing reinforcements into a metal or alloy matrix, aiming at improving comprehensive properties of the metal matrix. The MMCs have been widely used in aerospace, automotive and electronics industries. In recent years, graphene and its derivatives with the excellent mechanical, electrical and thermal properties have been considered as ideal reinforcements for the composites. MMCs reinforced with graphene have been expected to improve the mechanical properties while remain or even further improve the functional properties of the whole materials. Low content graphene and its derivatives are adopted to improve the mechanical properties of the composites, but only high content reinforcement phase can improve the thermal properties of the composites. However, it is inevitable to encounter the problems of agglomeration of reinforcements and weak interface bonding between the reinforcement and the matrix, which will affect the mechanical properties of the composites. So far, most of the existing research mainly focuses on the improvement of mechanical properties or thermal properties, further exploration is needed to enhance the comprehensive performance of the composites. In this work, high content graphene nanoplatelets (GNPs) were synthesized on the surface of Cu by using chemical vapor deposition with solid carbon source and impregnation reduction, which made GNPs uniformly dispersed and improved the interface bonding between GNPs and Cu matrix. Then, the bulk composites were densified by vacuum hot pressing sintering followed by multi-step hot rolling process, during which the orientation distribution of GNPs was achieved. After a rolling reduction of 70%, composite materials containg 12vol% GNPs provide increase by 44%(256MPa) in yield strength compared with pure Cu (178MPa). Furthermore, the in-plane thermal conductivity is increased by 17% (441W/mK) when GNPs content reaches 15vol%. The microstructure analysis shows that Cu matrix composites with uniform and orientation distribution of high content GNPs were prepared by our strategy. Both the mechanical properties and the thermal conductivity of the composites were improved, which lays a foundation for the application of the composite in electronic packaging.

10:25-10:45 Tea Break

10:45-11:05

A Facile Method to Prepare Multifunctional Materials for Oil Removal and in Situ Contaminants Reduction and Adsorption from Wastewater

Yingze Cao, Pengfei Wang, Bingyang Li, Qian Xuesen Laboratory of Space Technology, China Academy of Space Technology, China

In recent decades, rapid development of science and technology has been significantly promoting the global industry innovation, which further improved the quality of the human life greatly. However, it also led to serious environmental problems. Massive discharge of oily wastewater from industry and agriculture has become a serious problem of environment, threatening our living conditions and ecosystems. In most cases, oily wastewater contains various contaminiants, for instance, metal ions and organic molecules. Therefore, it is of great significance to develop materials can deal with complex wastewater consists of both water insoluble oil and water soluble contaminiants.

In our study, the multifunctional materials have been developed through two-step immersion to deal with water insoluble oily compounds and water-miscible inorganic and organic molecules. Firstly, PVA sponge as substrates were coated with polydopamine and polyethylenepolyamine codeposition films through mussel inspired chemistry, and then Ag nanoparticles was reduced and anchored on sponge by immersion in a $AgNO_3$ solution. The as-prepared sponge exhibits

superhydrophilic and underwater superoleophobic property so that it can selectively separate oil droplets from oily wastewater. The sponge possess abundant amino groups which can adsorb copper ions though coordination. The anchored Ag nanoparticles endow the sponge with the catalytic ability, which is able to decompose water soluble 4-nitrophenol instantly with adding $NaBH_4$. The adsorption of copper ions and reduction of 4-nitrophenol can be realized as the oily wastewater flow though sponge. The oil removal efficiencies of various oil/water mixtures are above 99.9% in a single unit operation with high fluxes, and copper ions and 4-nitrophenol can be effectively removed during the filtration. The as-prepared materials have good property in recycle as the separation efficiency was above 99.9% after 50 cycles and the reduction has rarely obvious change. This method is simple, facile, and low-cost and can be used to prepare large-scale materials. The multifunctional composite sponge allows continuous treatment of polluted oily wastewater and has broad potential in purification engineering.

11:05-11:25

First-Principles Calculation on the Adhesion Strength and Electronic Structure of the NiTi (111)// α -Al_2O_3 (0001) Interface

Lu Chen, Yefei Li, Qiaoling Zheng, Xi'an Jiaotong University, China; Qingkun Liu, Changmeng Zhou, Shandong Huifeng Casting Technology Co., Ltd., China

The work of adhesion (Wad), and electronic structure of NiTi(111)// α -Al_2O_3(0001) interfaces are investigated using first-principles calculations. Considering different stacking sequences (MT-, and HCP-site) and different terminations (Al-, O-, Ni- and Ti-terminated), totally four different interfaces are studied. The local positions of Ni (Ti)-Al-HCP and O-Ti-MT interfacial atoms remain after relaxation, but for the Ni-O-MT site, the Ni atoms are in the middle of the edge and the chemical attraction of the surrounding O atoms is large, making the Ni atoms shift. The calculation of adhesion strength shows that O-terminated interfaces have larger Wad and smaller d0 than Al-terminated interfaces, implying the chemical reaction between O-terminated Al_2O_3 (0001) surface and Ni, Ti atoms at outmost of NiTi (111) surface is stronger than that of Al-terminated Al_2O_3 (0001) surface. In addition, the Ti-O-MT interface has the largest Wad, while the Wad of Ti-Al-HCP interface is the smallest, showing lowest stability. The further PDOS and charge density distribution analysis indicate that the interfacial electron redistribution is rather localized and restricted to the first or second layer nearby the interface. And the dominant interfacial bonding for the Ni-Al and Ti-Al interface is the mixed metallic/ionic bond, while the O-Ti interface exhibits mixed covalent/ionic character with higher interfacial bonding strength.

11:25-11:45

Fabrication and Hybrid-Strengthening Effects of CNTs-SiCp or CNTs-Al_2O_3w Dual-Nano Reinforcements in Aluminum Matrix Composites

Xin Zhang, Shufeng Li, Deng Pan, Xi'an University of Technology, China

Carbon nanotubes (CNTs) reinforced aluminum matrix composites (AMCs) are widely concerned due to the excellent performance of integrated CNTs and Al. However, uniform dispersion of CNTs and the control of the interfacial reaction between CNTs and Al are the bottlenecks for its development. Aiming to solve the key scientific problems which restrict the exertion of the compound effect of CNTs reinforced AMCs, the second reinforcing phase (nano SiCp or in situ formed nano Al_2O_3w) was induced in CNTs reinforced AMCs preparing by flake powder metallurgy. The results show that a significant hybrid strengthening effect of CNTs-SiCp or CNTs-Al_2O_3w in AMCs can be exerted effectively, which benefit from the uniform dispersion of reinforcements and good interfacial bonding with Al matrix. The tensile strength of 0.5CNTs-0.5SiCp/Al reaches 247MPa, which is increase by 94% compare with pure Al, 14% compare with 1.0CNTs/Al and 56% compare with 1.0SiCp/Al. The strengthening mechanisms of CNTs-Al_2O_3w reinforced AMCs are summed as load transfer, grain refinement, thermal mismatch and Orowan looping theory. The predicted values indicate that load transfer mechanism from both CNTs and Al_2O_3w is dominant, improving UTS of 0.5CNTs reinforced AMCs (228MPa) by more than 79.5% in comparison with pure Al. The experimental strengths of AMCs containing 0.25 and 0.5vol.% CNTs are well matched with the theoretical values calculated by mixture rule. And the differences between them are less than 2.9%, which is highly effective for predicting the mechanical properties of CNTs-Al_2O_3w reinforced AMCs. In addition, the elongation and conductivity of the dual-nano reinforcements AMCs are also maintained about 20% and 50%IACS at the same level of pure Al. This study provides a practical research method for giving full play to the excellent properties of CNTs in AMCs.

11:45-12:05

Homogeneous Distribution of Coarse Grain in a Tri-Modal Al-Based Composites via Local Grain Growth Induced by Difference of Thermal Stability

Chuandong Wu, Wuhan University of Science and Technology / Wuhan University of Technology, China; Zhanghua Gan, Jing Liu, Wuhan University of Science and Technology, China; Guoqiang Luo, Qiang Shen, Lianmeng Zhang, Wuhan University of Technology, China

The bimodal/multi-modal structure has been manipulated

to influence the trade-off between strength and ductility/plasticity. Typically, the bimodal/multi-modal structure can be induced by traditional thermomechanical methods in bulk sample or consolidation of mixture with pre-selected various grain size. The key point to enhance the ductility/plasticity is to achieve the homogeneous distribution of the CG in the bimodal/multi-modal material. We reported an investigation of homogeneous distribution of coarse grain in a tri-modal Al-based composites via local grain growth induced by difference of thermal stability. The incorporation of Nano-B4C, combined with the in-situ dispersion particles, could contribute to the enhancement of the stabilization in Nano-B4C rich zone, which could inhibit the grain growth during consolidation. Representative high-angle annular dark/bright field STEM images displayed the distribution of UFG/CG in the Nano-B4C free zone. The GP zone and η' precipitates distributed in grain interior, while several η precipitates located at GB. Noted that yield strength of the tri-modal composite is 817±32MPa with acceptable strain of 9.3%, which could be ascribe to the homogenization of CG in the tri-modal composites. Multiple "vein-like" structure caused by deformation during the compressive testing was detected in the fracture surface. In addition to the "vein-like" structure, the backscattered electron diffraction image shows the CG could inhibit the propagation of the micro-cracks.

J. Amorphous and High Entropy Alloys: Amorphous Alloys II

Symposium Organizers:

Weihua Wang, The Institute of Physics, Chinese Academy of Sciences, China; Zhaoping Lv, University of Science and Technology Beijing, China; Hidemi Kato, Tohoku University, Japan; Hojin Ryu, Korea Advanced Institute of Science and Technology (KAIST), Korea; Michael Ferry, New South Wales, Australia; Evan Ma, Johns Hopkins University, USA

Tuesday AM
August 20, 2019

Room: 405 (4th Floor)
Symposium : J

Chairs:
Baolong Shen, Southeast University, China
Xidong Hui, University of Science and Technology Beijing, China

8:30-9:00 Keynote

Correlating Structural Heterogeneity to Deformation in Metallic Glasses

Jinwoo Hwang, Soohyun Im, Pengyang Zhao, Yunzhi Wang, Ohio State University, USA; Geun Hee Yoo, Eun Soo Park, Seoul National University, Korea

We investigate the potential connection between the nanoscale structural heterogeneity and the deformation behavior of metallic glasses (MGs) using a combination of novel 4-dimensional scanning transmission electron microscopy (4D-STEM) and mesoscale deformation simulation. While lacking long-range atomic ordering, MGs are known to contain medium-range ordering (MRO) within its nanometer scale structure. Intuitively, the type and degree of MRO and the resulting structural heterogeneity can change as we change the composition and thermal history of the MGs. Such change in heterogeneity has recently been documented using several experimental methods. Computational simulations have also provided useful insights on how the heterogeneity may affect deformation behavior of MGs. However, establishing direct connection between the heterogeneity and deformation still remains challenging, due to the difficulty in (i) measuring the details of heterogeneity, including their type, size, distribution, and volume fraction of MRO, and (ii) incorporating the experimentally-determined information into simulation to fully calculate the deformation comparable to the spatial and temporal scales of the real deformation. Our current approach aims to overcome these challenges. We use 4D-STEM based on electron nanodiffraction using a new-generation pixel array STEM detector that captures the heterogeneity information spatially resolved at the atomic scale. Using this method, we determine the type, size, distribution and volume fraction of MRO, the parameters that have been difficult to obtain using any other experimental or simulation methods. We incorporate the experimentally-determined parameters into the mesoscale simulation that assumes heterogeneously distributed shear transformation zones (STZs). By postulating certain relationships between the measured structure and STZs, the simulation investigates the potential connection between the structural heterogeneity and overall deformation behavior at realistic spatial and temporal scales, which we compare to the mechanical properties of real MGs to gain insights on the missing structure-property relationship.

9:00-9:25 Invited

Study on the Correlation of the Plasticity/Toughness with the Physical Properties and Structural Heterogeneity for Zr-Based Bulk Metallic Glasses

Xidong Hui, University of Sciecne and Technology Beijing, China

Metallic glasses (MGs) have shown great potential applications due to their high strength and elastic limit, excellent corrosion resistance and soft magnetic properties etc. Since the atomic packing in MGs is disordering in long-range but ordering in short-range, many MGs have been found to exhibit poor, or even zero macroscopic plasticity before fracture at room temperature, which restricts their application for

structural engineering materials. Therefore, it is of great significance to develop MGs with macroscopic plasticity and to study the intrinsic mechanism of plasticity and toughness. In the present presentation, Zr-based bulk metallic glasses (BMGs) were chosen for the object of study. In order to explore the origin of the plasticity of BMGs, the physical parameter which can character the properties of glass formation liquid has been employed to study the relationship among the molten liquid, fragile-to-strong transition, relaxation, structure and plasticity. By adding the elements which have the positive mixing enthalpy with those in BMGs, the effects of phase separation and β-relaxation on the compressive plasticity at room temperature has been investigated. The correlation of phase separation and deformation induced nanocrystallization (DINC) to compressive plasticity/toughness of Zr-based BMGs have been further studied. It has been found that DINC takes place, and the nanocrystallines with the size smaller than 5 nm have been formed in the whole region, especially in shear bands (SBs). The tendency of the instability of SBs can be greatly decreased by DINC, and multiple SBs are formed, resulting in the improvement of plasticity or toughness. Two step work-hardening phenomenon has been discovered for the first time in Zr-Cu-Fe-Al-Nb-Co-Mo BMG by the combined addition of Mo, Nb, Fe and Co elements and the adjustment of the proportion of Zr to Cu in the BMG. Under the effect of two step work-hardening, the compressive strain of this BMG reaches above 20% at room temperature.

9:25-9:45

Structural Heterogeneity in U-Based Metallic Glasses

Haibo Ke, Huogen Huang, China Academy of Engineering Physics, China

Nano-scale structure inhomogeneity has been identified to be an inherent characteristic of metallic glasses (MGs). Structural heterogeneities are also found to play a key role in designing and tuning the mechanical and relaxation behavior of MGs. U-based MGs show novel unique properties desirable for nuclear industries, such as excellent anti-corrosion ability. What's more, the 5f electron of U-based glassy systems may provide a good candidate for further understanding the electronic structure behavior of MGs. However, owing to the absence of stable glass forming alloys in this class in the past decades, their atomic structures still lack understanding. In the present work, two newly developed stable U-based MGs with compositions of U65Fe30Al5 and U60Fe27.5Al12.5 were chosen for study. The two U-Fe-Al MGs, whose amorphous structures were confirmed by X-ray diffraction and thermal analysis, were systematically investigated with nanoindentation technique of high sensitivity. It is found that they exhibit significantly different mechanical response for the primary and secondary creeps and U60Fe27.5Al12.5 shows better creep resistance than U65Fe30Al5at varying loading rates and peak loads. With the combination of the viscoelastic creep model and the relaxation spectra of the two MGs, a series of parameters associated with structural heterogeneity were obtained, which indicated that U60Fe27.5Al12.5 MG is in a more rigid state and possesses a more compact atomic structure. Furthermore, the schematic maps of atomic structure for the two U-Fe-Al MGs were constructed, which exhibits that U65Fe30Al5 possesses a more relaxed state with a larger number of liquid-like regions or flow units. In other words, dissimilar structure heterogeneity can be derived for these two MGs to account for their difference in creeping behavior. These results would be beneficial for deeply understanding the structure features of U-based MGs and for designing U-based glassy materials with desirable mechanical properties by tuning alloy composition. What's more, they also provide crucial insight into the structure-property relationship of amorphous materials.

9:45-10:05

Revealing β-Relaxation Mechanism Based on Energy Distribution of Flow Units in Metallic Glass

Zhen Lu, Mathematics for Advanced Materials-OIL, AIST, China

Glasses can be formed through quenching from highly viscous liquid and lost their ability to flow. In the cooling process, the structure relaxation of a glass forming liquid, which is known as α-relaxation, dramatically slows down and freezes at the glass transition temperature Tg. It is also well established that, in addition to the α-relaxation, there also exists another slow relaxation mode, which is universally observed in glass state and known as the slow β-relaxation (or Johari-Goldstein relaxation). The β-relaxation, which is the source of the dynamics in glass state and has practical signifcance to relaxation and mechanical properties of glasses, has been an open question for decades.
In this work, we performed stress relaxation experiments under isothermal and linear heating modes and molecular dynamics simulations to investigate the different β-relaxation behaviors of various metallic glasses and the correlation between β-relaxation and flow units based on the activation energy distribution of flow units. In order to purposefully study the microstructural origin of β-relaxation, three representative MGs of Cu46Zr46Al8, Pd40Ni10Cu30P20 and La55Ni20Al25 with obviously different β-relaxation behaviors were investigated. We show that the β-relaxation originates from the flow units in metallic glasses, and the activation energy distribution of flow units modulates the β-relaxation modes such as

excess wing, shoulder and peak in their dynamic spectra. The La55Ni20Al25 with the most obvious β -relaxation presents the sharpest activation energy spectrum, while Cu46Zr46Al8 is the opposite one. In other words, the MGs with relatively narrow activation energy distribution of flow units show obvious β-relaxation. Through the molecular dynamics simulations, we creatively design various artificial metallic glass systems and build a direct relation between β-relaxation behavior and features of flow units. The results provide a better understanding of the structural origin of β-relaxation and also afford a method for designing metallic glasses with obvious β-relaxation and better mechanical properties.

10:05-10:25

Relaxation and Rejuvenation of a Heterogeneous Zr-Cu-Al Bulk Metallic Glass

Wei Guo, Huazhong University of Science and Technology, China / Tohoku University, Japan; Junji Saida, Tohoku University, Japan; Yuman Shao, Mi Zhao, Shulin Lv, Shusen Wu, Huazhong University of Science and Technology, China

The rapid quenching during the fabrication of most bulk metallic glasses (BMGs) makes them possess higher configurational energy than their crystallized counterparts. Thus, during annealing process, their microstructure tends to change towards a lower energy state, which is so-called relaxation. In contrast, the energy state can be also tailored to an even higher state or a more metastable state via thermal or mechanical method, which is so-called rejuvenation. Generally, relaxation embrittles the BMGs and rejuvenation plasticizes them. However, in this study, abnormal plasticization during relaxation and embrittlement during rejuvenation have been firstly observed in a heterogeneous Zr-Cu-Al BMG. The relaxation was achieved by annealing the as-cast sample at ~1.05Tg for 2min followed with a 20K/min cooling. The rejuvenation was achieved by quenching the relaxed sample with 100, 300 and 700K/min after annealing at 1.05Tg for 2min. Although a broad peak was observed for all samples, the relaxation state and heterogeneity of the samples varies due to different thermal treatment history. Besides the microstructure change due to relaxation/rejuvenation, nano-sized clusters are found to evolve during the thermal treatment in this structurally unstable BMG. More thermal treating time induces more nano-clusters. The less initiation of shear bands in relaxed BMGs causes a higher shear band temperature during deformation, which contributes to the stress-induced crystallization behavior and subsequently the plasticization of the sample. In contrast, more shear bands are initiated in rejuvenated sample and the temperature of shear bands is not high enough to induce the crystallization during deformation, although some nano-clusters do grow to a larger size. Once the crystallization occurs, the propagation of shear bands can be hindered by these secondary phase, causing them stopped, branched or multiplied. For each shear band accommodate a certain amount of plastic deformation, the multiple shear bands correspond to the improved plasticity of relaxed sample. This study provides a new vision on the mechanical property of BMGs upon relaxation or rejuvenation, which needs overall consideration including both relaxation state and heterogeneity evolution.

10:30-10:45 Tea Break

10:45-11:10 Invited

Preparation and Mechanical Properties of FeNiMoPCBSi Ferromagnetic Bulk Metallic Glasses

Baolong Shen, Southeast University, China

Fe-based bulk metallic glasses (BMGs) have attracted great attention due to their excellent soft magnetic properties, high strength, good corrosion resistance and relatively low material cost. However, the catastrophic fracturing at room temperature hinders their widespread applications as structural and functional materials.
In this work, a novel ductile Fe56Ni20Mo4P11C4B4Si1 BMG with saturation magnetization of 0.93T, coercivity of 1.9A/m and plastic strain of 7% was successfully synthesized. Effects of Ni and Si additions on mechanical properties and serrated flow behavior of Fe-Mo-P-C-B BMGs were systematically investigated. It was found that the simultaneous additions of Ni and Si are effective to improve the plasticity of Fe76Mo4P12C4B4 BMG as indicated by the increase in the plastic strain from 1.7% to 7%. Serrated flow behavior is not observed in Fe76Mo4P12C4B4 BMG. However, the chaos state occurs in Fe56Ni20Mo4P12C4B4 BMG, and eventually the self-organized critical (SOC) behavior appears in Fe56Ni20Mo4P11C4B4Si1 BMG. In addition, morphologies of deformed Fe76-xNixMo4P12-yC4B4Siy (x = 0, 10, 20; y = 0, 1, 2at.%) BMGs were observed to investigate the relationship between shear-band dynamics and plasticity. The Fe76Mo4P12C4B4 BMG deforms through a single shear band movement, exhibiting poor plasticity. For the Fe56Ni20Mo4P12C4B4 BMG, a few secondary shear bands occur around the primary shear band, which propagating randomly in chaotic dynamics. But for the Fe56Ni20Mo4P11C4B4Si1 BMG, multiple shear bands form and interact with each other following the SOC dynamics, leading to large plastic strain. Thus, the improvement of plasticity might result from an increased number of potential shear transition zone sites and a

stronger tendency of forming shear band interactions. This work provides a perspective from serrated flow behavior to understand plastic deformation mechanism in Fe-based BMGs with different plasticity, which has important scientific significance and practical value for promoting the theoretical development of the Fe-based BMGs, as well as guiding the exploration of novel Fe-based BMGs with large plasticity.

11:10-11:30

Structure Origin of Good Plasticity of a Zr-Cu-Fe-Al Nanostructured Bulk Metallic Glass

Sinan Liu, Min Chen, Yangxin Gu, Hao Lu, Xiangyi Zhang, Jiacheng Ge, Weixia Dong, Nanjing University of Science and Technology, China; Chenyu Lu, Zhengqiao Li, City University of Hong Kong, China; Dong Ma, Chemical and Engineering Materials Division, Oak Ridge National Laboratory, USA; Xunli Wang, City University of Hong Kong, China / City University of Hong Kong Shenzhen Research Institute, China; Si Lan, Nanjing University of Science and Technology, China / City University of Hong Kong, China

It was proposed that the plasticity of Zr-Cu-Al bulk metallic glasses (BMGs) can be significantly improved by the addition of Fe to introduce nanoscale heterogeneous structure. However, the microstructure origin of the superplastic deformation of Zr-Cu-Fe-Al BMG is still unclear. We have prepared two Zr-based BMGs, Zr59Cu33Al8 (Z0) and Zr59(Cu0.55Fe0.45)33Al8 (Z2). The thermophysical behavior, atomic and nanometer scale structure, mechanical properties and their internal relations of Z0 and Z2 bulk metallic glasses were studied by differential scanning calorimetry (DSC), small/wide angle synchronous X-ray scattering (SAXS/WAXS), synchrotron radiation high energy X-ray diffraction (HE-XRD), neutron diffraction, and X-ray photoelectron spectroscopy (XPS). Our results show that the Z0 alloy has no abnormal structural changes during solidification at different casting temperature. In contrast, the Z2 alloys prepared at lower suction casting temperatures undergo liquid-state phase separation (LSPS) during the cooling process. The small-angle X-ray scattering results illustrate that the heterogeneity of Z2 BMGs increases with the decrease of the casting temperature. Further mechanical tests showed that Z2 BMGs with LSPS have better mechanical properties, including higher yield strength, and better significant compressive ductility as well as more complex serrated flows behavior in compressive stress-strain curve. The neutron and synchrotron pair distribution function (PDF) analysis illustrate that the change of bonding length between solute atoms caused by LSPS may be the internal reason for the improvement of plasticity. The XPS tests found that the peak position of the profile of the Zr 3d binding energy in the Z2 alloy has a downward shift comparing with that of Z0 alloy, whereas no distinct changes of Cu 2p and Al 2p binding energy can be found in two BMGs. Therefore, the XPS results confirmed that the softening of the bonds related to the solvent atom Zr, which may play a more critical role in plastic deformation than the solute atoms Cu and Al. This study may shed lights on the research and development of nano-structured BMGs with flexible structure and performance.

11:30-11:50

Shear Banding and Fracture Behavior in Bulk Metallic Glasses under Quasi-static and Dynamic Shearing

Ding Zhou, Bingjin Li, Naidan Hou, Zihao Ma, Xianhang Zhao, Bing Hou, Yulong Li, Northwestern Polytechnical University, China

Bulk Metallic Glasses (BMGs) have shown increasing promise as engineering materials because of their excellent mechanical, physical and biomedical properties. Different from crystal materials, the plastic deformation of BMGs is localized in narrow shear bands, in which local strain is accommodated by 'shear transformation'. Such an event essentially refers to atomic clusters undergo a shear displacement. While originated from inelastic shear distortion, shear banding behavior in BMGs is strongly affected by normal stress. Besides, loading rate also affects shear banding behavior. In previous studies, strain-rate effect is often studied by compressive testing. Thus, it is of great importance to decouple the normal stress effect and strain rate effect by shear-dominated loading. This study focuses on shear banding and fracture behavior in BMGs under quasi-static and dynamic shearing. With specially designed double-shear sample, shear-dominated stress state is achieved in the shear zones of the sample. The shear responses of BMGs under quasi-static and dynamic loading rates are measured by test machine and modified split Hopkinson pressure bar. Meanwhile, in-situ high-speed photographing is used to capture the real-time deformation process from shear-band initiation and propagation to fracture. Digital image correlation (DIC) is introduced to measure the real-time strain evolution. Combined with shear responses, real-time deformation images and SEM observations, we conclude the strain-rate effect on the mechanical properties of BMGs under shear loading. The plastic deformation is dominated by multiple shear banding under quasi-static shearing, while dominated by single shear banding under dynamic shearing. In addition, rate effect on the transition from shear band to crack is studied owing to the absence of normal stress

effect during shear banding process. The transition is originated from cavity formation along a shear band under quasi-static loading, while from direct crack-opening at shear band tip under dynamic loading. The rate effect on shear-band-to-crack transition might be due to growing temperature rise within shear bands with increasing strain rate.

11:50-12:10

Real-Time Measuring of Temperature Rise during Shear Banding in Bulk Metallic Glasses (BMGs) under Quasi-Static and Dynamic Loading

Ruoyun Song, Ding Zhou, Bing Hou, Yulong Li, Northwestern Polytechnical University, China

Bulk metallic glasses (BMGs) have a great potential in various applications, due to their excellent mechanical properties, such as high strength and hardness, large elastic strain, good corrosion and fatigue resistances. However, BMGs exhibit non-uniform plastic deformation at room temperature and high strain rate, which is related to highly-localized shear bands. Shear banding in BMGs significantly affects their macroscopic plastic flow and fracture. These shear bands initiate and propagate rapidly with softening inside, thereby leading to catastrophic brittle fracture, severely limiting their processing and application. Most studies have confirmed that BMGs turn into a pre-failure state through a shear softening mechanism, such shear transformation zone (STZ). But some researches show the local softening is closely related to temperature rise in shear bands. It is noted the heat evolution during shear banding and cracking is a high-disputed issue. Present experiment evidences do not directly confirm whether a mature shear band propagates with a cold front or a hot/melted tail. Great advance in the estimation of temperature rise during shear banding has been achieved by Lewandowski and Greer, i.e., temperature rise is estimated to be greater than 1000K by coupled thermal and mechanical measurements. However, such estimation did not rule out the temperature rise during fracture stage. In addition, rate-dependent shear band operations have been widely observed. How strain rate controls shear banding by rate-dependent structural softening or thermal effect remains unresolved. In this study, a real-time heat evolution during shear banding in BMGs is measured under quasi-static and dynamic loading, trying to find the relationship between strain rate and temperature rise. Based on the temperature rises at different loading rates, we could investigate whether the initiation of shear band is cold or hot. Besides, how thermal effect affects shear banding process is further studied by comparing with our previous real-time photographing observations.

J. Amorphous and High Entropy Alloys: High Entropy Alloys II

Symposium Organizers:

Weihua Wang, The Institute of Physics, Chinese Academy of Sciences, China; Zhaoping Lv, University of Science and Technology Beijing, China; Hidemi Kato, Tohoku University, Japan; Hojin Ryu, Korea Advanced Institute of Science and Technology (KAIST), Korea; Michael Ferry, New South Wales, Australia; Evan Ma, Johns Hopkins University, USA

Tuesday AM
August 20, 2019

Room: 303 (3rd Floor)
Symposium : J

Chairs:
Zhaoping Lu, University of Science and Technology Beijing, China
Young-Sang Na, Korea Institute of Materials Science, Korea

8:30-9:00 Keynote

Ten Surprises Confronting Dislocations in High Entropy Alloys

Evan Ma, Qingjie Li, Johns Hopkins University, USA

We present the first atomistic simulations, employing a realistic interatomic potential for the NiCoCr model system, to reveal unusual dislocation behavior in multi-principal-element solid solutions. We have found that these high entropy alloys are indeed different from the familiar (such as FCC) metals and solid solutions, in terms of the ruggedness of the energy landscape that govern dislocation activities. These lead to 10 new features, including low and variable stacking fault energy, local anti-phase boundary energy in the absence of a sublattice, difficulty in twin widening, slip localization resulting in "planar slip", wavy dislocation line, intermittent nanoscale segment detrapping, small activation volume, elevated activation barrier, elevated lattice friction (mechanical strength), and increased temperature and strain rate sensitivity. We show how these new and puzzling options facing dislocations affect the selection of dislocation pathways in slip, faulting, twinning, and martensitic transformation, resulting in behaviors unexpected for conventional FCC metals. We also illustrate how the variation in local environments due to concentrated compositions necessitates a new mechanism for dislocation motion, strengthening the high entropy alloy. All these open a vast playground not accessible to traditional metals and ground-state intermetallics, making HEAs a wonderland for dislocations (and other defects), with rich opportunities to tune mechanical (and possibly transport) properties.

9:00-9:25 Invited

Research Status and Prospects of High Entropy Bulk Metallic Glasses

Z. P. Lu, University of Science and Technology Beijing, China

High-entropy bulk metallic glasses (HEBMGs) is a new kind of amorphous alloy which has both the composition characteristics of multi-elements high entropy alloy and the stacking characteristics of long-range disordered atomic structure of amorphous alloy. Due to its unique composition and structure, high entropy alloys exhibit a series of unique physical, chemical and mechanical properties. Therefore, HEBMGs have attracted much attention since they were discovered. The first part of this report will briefly review the current research progress of HEBMGs, mainly introducing the characteristics and related research progress in terms of composition, structure and performance. The second part of the report will combine our research group in recent years in the aspect of a series of work about HEBMGs and put forward several scientific problems needed to be solved in the field of HEBMGs.

How to understand the effect of high entropy on the formation of HEBMGs? HEBMGs have the characteristics of high-mixing entropy due to their composition characteristics of multiple principal components (at least 5 components) and equal atomic ratio (or near-atomic equal ratio). According to the law of chaos, high-entropy is beneficial to the formation of amorphous structure. However, it is found that HEBMGs have worse GFA than traditional BMGs. At the same time, it is also found that there is an abnormal relationship between the GFA and their thermal stability of HEBMGs.

Structure and thermodynamic properties of HEBMGs: High entropy effect and slow diffusion effect have important effects on microstructure and properties of HEBMGs. How do these effects affect the structure and thermodynamic properties of HEBMGs? Our preliminary study shows that HEBMGs have more uniform stacking structure than traditional BMGs. It is also found that the supercooled liquid of HEBMGs has an abnormally small excess specific heat capacity. The physical nature of these phenomena warrants further investigation.

Abnormal thermal stability of HEBMGs: Many physical phenomena in metallic glasses (such as structural relaxation and crystallization, etc.) are closely related to their thermal stability. Due to the high entropy effect and slow diffusion effect, HEBMGs show unique crystallization behavior during the heating process. It is found that, unlike conventional BMGs, the first exothermic peak of the HEBMGs on differential thermal analysis (DSC) curve is not caused by crystallization, but by the ordering of atomic structure in the supercooled liquid phase. Moreover, the crystallization kinetic of HEBMGs is very slow. Therefore, it is expected to produce new high-entropy bulk nanostructured materials with uniform nanocrystal distribution through the crystallization of HEBMGs

9:25-9:50 Invited

First-Principles Predictions of Dislocation Motion in High-Entropy Alloys

Tomohito Tsuru, Mitsuhiro Itakura, Japan Atomic Energy Agency, Japan; Koretaka Yuge, Kyoto University, Japan; Yoshiteru Aoyagi, Momoji Kubo, Tohoku University, Japan; Tomotsugu Shimokawa, Kanazawa University, Japan; Shigenobu Ogata, Osaka University, Japan

High entropy alloys (HEAs) are chemically complex single- or multi-phase alloys with crystal structures. There are no major components but five or more elements are included with near equiatomic fraction. In such a situation, deformation behavior can no longer be described by conventional solid solution strengthening model. Some HEAs, indeed, show higher strengthening behavior and anomalous slip. However, the mechanisms of these features have yet to be understood. Dislocation structure and motion should be the key to identify the unique feature of mechanical properties of HEAs. In the present study, we investigate the core structure of dislocations in BCC-HEAs using density functional theory (DFT) calculations. Special quasirandom structures (SQS) scheme was employed to construct randomly-distributed five-component MoNbTaVW HEAs with equiatomic fraction. Here, MoNbTaVW alloy is one of the most stable BCC-phase HEAs, and has been actually confirmed by experiments. Dislocation quadrupolar was inserted into the perfect SQS models. DFT calculations were then carried out to obtain stable configuration after fully relaxation. We found that core structure of a screw dislocation is identified as is the case with common BCC metals. On the other hand, dislocation motion should be different from pure BCC metals because of chemical and configurational disorder around dislocation core. We confirmed the specific feature of dislocation motion in HEAs by two-dimensional Peierls potential surface.

9:50-10:10

Reactive Molecular Dynamics Simulation of Crack Propagation Process of High Entropy Alloy under Pressurized High Temperature Water

Narumasa Miyazaki, Chang Liu, Qian Chen, Honami Yanagisawa, Yusuke Ootani, Nobuki Ozawa, Momoji Kubo, Tohoku University, Japan

Equimolar composition alloys called as high entropy alloys (HEA) or medium entropy alloys (MEA) have more excellent properties such as hot wear resistance and high temperature strength than typical dilute alloys. Therefore HEAs are promised as the heat resistant alloy such as airplane structural materials. Moreover

their working temperature is increasing year by year due to the demand of airplanes and improvement of fuel efficiency, hence the necessities of high-temperature oxidation resistance and corrosion resistance are also increasing. Especially, at the corrosion environment under tensile stress state, the creep life time and the yield strength decrease drastically. Therefore it is necessary to understand the stress corrosion cracking mechanism to obtain guidelines of alloy designing for airplane materials. Then we elucidate crack propagation process by tensile deformation tests under high temperature corrosive environment using reactive molecular dynamics simulation.

First, we simulate pure iron model for the comparison with the HEA model. We constructed symmetrical tilt grain boundary of sigma 5(310), and modeled pre-clack along with grain boundary. For the interatomic potential, we applied the reactive force field (reaxff) potential to describe the chemical reaction. To simulate the stress corrosion cracking process based on this reaxff potential, we used "LASKYO" reactive molecular dynamics simulator which is developed by our group.

We simulated tensile deformation tests with constant strain rate of $109s^{-1}$ for the pure iron with the pre-crack model under both pressurized high temperature water and vacuum environments at 600K. Under water environment, H_2O molecules dissociated to H^+ and OH^-, and OH^- bound with iron atom at the surface. According to the tensile deformation, small cracks were formed around the pre-crack under water environment, and dislocations propagated from the head of pre-crack. From above results we elucidate that the complex process of dislocation propagation and the chemical reaction of the Fe-OH bonding at the surface promotes the elementally process of the cracking propagation. At the meeting, we will talk about the comparison of iron metal model and FeNi-based HEA model and discuss about the effect of solution elements on the stress corrosion cracking mechanism.

10:10-10:30

Compositional Design of Novel High-Entropy Alloys with Enhanced Strength and Plasticity

Rong Guo, Lin Liu, Huazhong University of Science and Technology, China

The improvement in plasticity is usually compensated by the reduction of strength in structural materials, which is a long-standing conflict referred as the strength- plasticity trade-off. In recent years, a new type of structural materials of high-entropy alloys (HEAs) with equiatomic or near-equiatomic concentrations have attracted increasing attention due to their unique mechanical and physical properties. However, HEAs with BCC structure exhibit high strength but low plasticity, while the HEAs with FCC structure show inversely high plasticity and low strength. The formation of the complex structures (i.e, FCC+BCC) is a good approach to solve the problem. In this work, a BCC-based AlCoCrFeTi0.5 high-entropy alloy (HEA) was modified by the addition of a certain amount of Ni, the FCC stabilizer, to improve the plasticity. The new HEAs have the composition of AlCoCrFeTi0.5Nix (x=0~3mol%), which were prepared by arc melting following by copper mold casting. The effect of Ni concentration on the microstructures and mechanical properties of AlCoCrFeTi0.5Nix alloys were systematically studied. The result shows that Ni element has the capacity to induce phase transformation from BCC phase containing brittle ordered B2 to FCC phase containing ductile ordered L12 nano-precipitates as the Ni concentration increased from 0mol% to 3mol%. A good combination of strength and plasticity was achieved for the HEA with an optimizing Ni content of 2.5mol%, which has the yield strength of 1.4GPa and compressive plastic strain of 42.7%. The mechanism for the improvement of plasticity of the HEAs is discussed.

10:30-10:45 Tea Break

10:45-11:05

Novel Metastable Engineering in Single-Phase High-Entropy Alloy

Ruixin Wang, Yu Tang, Shun Li, Hong Zhang, Yuanlin Ai, Shuxin Bai, National University of Defense Technology, China

High-entropy alloy (HEA) has attracted increasing attention since it was first proposed due to its unique characteristics and great application potential. Unlike the traditional phase rule, HEA composed of four or more metallic elements forms a single-phase solid solution (SSS) with unordered atom occupation. The unique structure of HEA results in some special performances, such as a low diffusion coefficient, high irradiation resistance, and excellent mechanical properties at extreme environment including low temperature, high temperature and high strain rate.

However, the application of HEA is still restricted by the trade-off between strength and ductility, which is the most common dilemma for structural materials. To meet the demand for high strength and ductility, the metastability engineering strategy, which has been widely used in high-Mn steels and titanium alloys, has been used for HEAs. According to metastability engineering strategy, the high-temperature structure of HEAs is destabilized to promote strain-induced transformation. The process of strain-induced transformation results in the uniform plastic deformation by delaying the onset of necking and releasing internal stress and the occurrence of the transformation-induced plasticity (TRIP) effect. Furthermore, the strength of HEA will be significantly enhanced by co-contribution from the interface hardening

from the dual phases and the transformation hardening from the metastability (named as transformation-induced strength, TRIS). This combined increase in strength and ductility provides a useful guide for designing HEA and other structural materials.

However, all of the reported TRIP-HEAs are dual-phase alloys to date, which limits the popularization of the metastability engineering strategy. It is possible for strain-induced transformation and then the TRIP effect to occur in single-phase HEA via strain-induced element diffusion. When element diffusion occurs during loading, element segregation and dual-phase microstructures will form in the original metastable single-phase HEA. Thus, the strain-induced transformation and TRIP effect can be facilitated as continuous load is applied. Alternatively, it is possible that a fracture has generated along a brittle region before the TRIP effect works in the HEA composited of ductile and brittle phases. This risk can be avoided in TRIP single-phase HEA. Moreover, the elemental fluctuation caused by element diffusion may result in coherent nano-precipitation, which increases strength without ductility loss. Therefore, it is significant to explore the novel HEA with the SSS structure and TRIP effect.

In this work, this novel strategy was applied to a brittle body-centered cubic (BCC) refractory high-entropy alloy (RHEA) because of applicability as a high-temperature and energetic structural materials and the pressing demand for both high strength and ductility. Considering the formation of BCC SSS and the strain-induced transformation based on component elements, the equiatomic NbZrTiTa RHEA was selected and prepared by vacuum arc melting. As known, while all of the constituents had the same BCC structure at high temperature (HT), the room temperature (RT) structures of IV B elements (Ti and Zr) and V B elements (Ta and Nb) were different, which would result in severe drive force for separation. The low compatibility between constituents results in element rearrangement and the in-situ formation of TiZr-rich and TaNb-rich regions when the NbZrTiTa alloy is energized, including annealing and loading. Element diffusion results in changed structure stability and solid solubility in different regions, and then it leads to a transformation from the BCC to BCT structure and coherent nano-precipitation during loading. The strength of the NbZrTiTa alloy is increased by TRIS effect and precipitation strengthening induced by coherent nano-precipitation. The ductility of NbZrTiTa is improved to an unreported value as a result of the TRIP effect based on element diffusion, although the fracture mechanism is the typical intergranular fracture. While the in-situ formation of the two-phase regions ensures contribution of the TRIP effect, the participation and presence of the metastable intermediate structure reveals promising potential for single-phase metastable HEA with the in-situ induced TRIP effect.

11:05-11:25

Microstructure and Tensile Mechanical Properties of a CoCrFeNiMn High Entropy Alloy with Secondary Phase Nano-Particles Produced by Powder Metallurgy

Jiamiao Liang, Yuehuang Xie, Jun Wang, Shanghai Jiao Tong University, China; Deliang Zhang, Northeastern University, China

A CoCrFeNiMn high entropy alloy with secondary nano-particles was successfully synthesized by high energy mechanical milling (HEMM) followed by spark plasma sintering (SPS) and hot extrusion (HE). HEMM led to the mechanical alloying of the powders and the formation of a dual phase microstructure including BCC phase and FCC phase in the as-milled powders, and it transformed into a single FCC phase after SPS. Meanwhile, Cr-rich M23C6 carbide particles and spinel $(Cr, Mn)_3O_4$ oxide particles were formed during sintering due to the C and O element introduced during milling. The carbide particles with sizes of 350~550nm were much larger than the oxide particles with sizes of 30~60nm. The as-synthesized alloy exhibited a bimodal microstructure consisting of larger equiaxed grains with sizes of 900~1200nm distributed at the prior powder boundaries and finer equiaxed grains with sizes of 300~600nm inside the prior powder particles. This alloy had an average yield strength and ultimate tensile strength of 1272 and 1288MPa respectively which are clearly higher than those of most of the CoCrFeNiMn high entropy alloys reported in the literatures. The further improvement of tensile strength was achieved by reducing the grain size. It can be found that the significant refinement of grains lead to a yield drop phenomenon and the critical size to maintain uniform elongation is about 500nm. Intragranular particles may pin dislocations and improve ductility while intergranular particles may have an opposite effect. The analysis of the strengthening mechanisms demonstrated that grain boundary strengthening and Orowan strengthening play a major role in strengthening.

11:25-11:45

Modeling of Twinning-Induced Plasticity of High Entropy Alloy Based on Crystal Plasticity

Takuya Tsukuda, Yoshiteru Aoyagi, Tohoku university, Japan

In recent years, high entropy alloys (HEAs) consisted of various kinds of elements in equiatomic or near equiatomic concentrations have been attracting attention as new materials because of its encouraging mechanical properties such as high strength, wear resistance, and corrosion resistance. Defining features of HEAs comparing with common alloys are that HEAs

consist entirely or primarily of a single phase solid solution structure and have high entropy of mixing. It is considered that HEAs such as the equiatomic FeMnNiCoCr alloy have a high strength due to twinning-induced plasticity. The mechanical twinning caused by applied shear stress introduces microstructures separated by twin boundaries into materials, and high strength and high ductility appear. Formations of additional twins remarkably reduce migration path of dislocations, and high strain hardening rate results. Plastic deformation of HEAs is mainly caused by slip due to the movement of dislocations and twinning. A reduction of stacking fault energy of materials promotes the formation of twins. In order to improve the mechanical properties of HEAs, it is necessary to understand the information on macroscopic deformation, mesoscopic structural change, and microscopic dislocation behavior, simultaneously. However, although the number of research on twinning-induced plasticity for HEAs is increasing, there are few studies on multiscale modeling of deformation of HEAs.

In this study, we construct a twinning-induced plasticity model describing plastic deformation for mechanical twinning based on the crystal plasticity considering information of dislocation. Mechanical twinning at a material point of a continuum body is expressed as a superimpose of plastic strain originated in slip and twinning. The volume fraction of induced twins determines deformation in the mixture phase of the matrix and the induced twins. We conduct finite element analysis using the presented multiscale crystal plasticity model and investigate mechanical properties and deformation of HEAs from the viewpoint of twin-induced plasticity according to obtained results.

11:45-12:05

Design of Dual-Phase Refractory High Entropy Alloy

Hosun Jun, Pyuck-Pa Choi, Korea Advanced Institute of Science and Engineering, Korea

Refractory high entropy alloys (HEAs) have received great attention due to their high-temperature mechanical properties (e.g., strength and creep resistance) and hence the potential to be the next generation high-temperature alloys for key engineering applications. It was recently found that Al additions to refractory HEAs with BCC structure could result in a dual-phase B2/BCC microstructure. While most reported B2/BCC refractory HEAs have a brittle B2 matrix with discontinuous BCC precipitates, fabricating refractory HEAs with a ductile BCC matrix and coherent hard B2 precipitates is expected to increase creep resistance at elevated temperatures due to a precipitation hardening effect.

In the present study, refractory HEAs with a microstructure consisting of BCC matrix and B2 precipitates were designed by a novel approach of mixing two alloys, namely Ti-25at.% Nb and HfAl. Their mixing ratio was controlled to form a supersaturated solution after homogenization and induce phase separation during the ageing treatments. Ageing temperature and time were altered for systematical studies of elemental partitioning behavior.

The microstructure of the newly designed alloys after heat treatment were studied by multiple characterization techniques including X-ray diffraction, transmission electron microscopy (TEM), and atom probe tomography (APT). TEM and APT characterization showed that refractory HEAs with a BCC matrix and coherent B2 nanoprecipitates of 2~3nm in size could indeed be successfully fabricated.

K. Nanocrystalline Materials, and Ultra-Fine Grained Materials: II

Symposium Organizers:

Yue Zhang, University of Science and Technology Beijing, China; Zhiyong Tang, National Center for Nanoscience and Technology, China; Nobuhiro Tsuji, Kyoto University, Japan; Jae-il Jang, Hanyang University, Korea; Kenong Xia, University of Melbourne, Australia; Nathan Mara, University of Minnesota, USA

Tuesday AM
August 20, 2019

Room: 309(3rd Floor)
Symposium: K

Chairs:
Kei Ameyama, Ritsumeikan University, Japan
Ruslan Valiev, Saint Petersburg State University, Ufa State Aviation Technical University, Russia

8:30-9:00 Keynote

Nanostructural Design of Metallic Materials for Superior Properties

Ruslan Valiev, Saint Petersburg State University, Ufa State Aviation Technical University, Russia

Multiple studies in recent years have proved severe plastic deformation (SPD) techniques as a very efficient way to produce nanostructured metals and alloys with significantly improved mechanical and functional properties. At the same time advanced properties affected by several nanostructured parameters, including ultrafine grains and also the defect structure of boundaries in SPD-processed nanomaterials. This report presents the recent results of complex studies of the formation of different grain boundaries (low angle and high angle ones, special and random, equilibrium and non-equilibrium with strain-distorted structure as well as with the presence of grain boundary segregations and precipitations) in nanostructured materials processed

using SPD with various regimes and routes. This entails the materials with superior multifunctional properties, i.e. the combination of high mechanical and functional properties (superplasticity corrosion and radiation resistance, electrical conductivity, etc.) that are induced by grain boundaries. Particular emphasis is laid on the physical nature and the use of multifunctional nanomaterials for their innovative applications in medicine and engineering.

9:00-9:30 Keynote

Harmonic Structure Design: Creation of Innovative High Performance Metallic Materials

Kei Ameyama, Ritsumeikan University, Japan

Over many years, fabrication of materials with superior combinations of high strength and high elongation remains a hot issue in material engineering. Ultra-fine grained (UFG) metals have been proved to be attractive structural materials because of superior strength, especially when compared to their coarse-grained (CG) counterparts. However, the downside of homogeneous UFG materials is typically in a low elongation because of the plastic instability in the early stage of deformation. The Harmonic Structure (HS) design can be a candidate materials design, which combines high strength with high ductility at the same time. As opposed to a "Homogeneous-UFG" material, "HS" material has a unique heterogeneous "Three-dimensionally (3D) Gradient Microstructure" wherein the UFG areas form an interconnected three-dimensional network surrounding CG regions, and CG and UFG areas are periodically arranged in all the directions. In the present research, the harmonic structure design has been applied to many kinds of pure metals and alloys via a severe plastic deformation powder metallurgy (SPD-PM) route and subsequent sintering. At a macro-scale, the harmonic structure materials exhibited significantly better combination of strength and ductility, as compared to their homogeneous microstructure counterparts. Since the area under the stress-strain curve is considered as a representation of the tensile toughness of a material, the HS materials also exhibited improved tensile toughness. This behavior was essentially related to the ability of the harmonic structure to promote the uniform distribution of strain during plastic deformation, leading to improved mechanical properties by avoiding or delaying localized plastic instability. In other words, the characteristic "micro-scale stress concentration" and "macro-scale stress dispersion" by the Shell-network structure are assumed to lead a large work hardening and a constraint of the deformation localization. In addition, such a stress concentration in the Shell region leads to high density of dislocation generation and hence it results in a preferential recrystallization in the Shell. And the well-developed Shell structure by the preferential recrystallization provides further improvement of the mechanical properties.

9:30-9:55 Invited

Interplay between Thermal Stability and Environmental Tolerance in Nanocrystalline Alloys

Jessica Krogstad, Pralav Shetty, Caelin Muir, Megan Emigh, University of Illinois, Urbana-Champaign, America

Enhanced thermal stability of nanocrystalline metallic alloys is necessary for improving processing routes, preserving desirable mechanical properties that arise from the ultra-fine microstructure, and expanding available applications spaces. Segregation of solute atoms to the grain boundaries in nanocrystalline metals has been explored as a potential route for microstructural stabilization. Decoration of grain boundaries either with distinct precipitates or more subtle concentration enhancements not only changes the mobility of the grain boundaries, but also of diffusing species along the grain boundary. As a result, we will show that microstructural thermal stability is also central to promoting the environmental tolerance of these materials. A series of DC magnetron sputtered thin film Ni-based alloys have been subjected to both in situ and ex situ heating and oxidation. Characterization via transmission electron microscopy and atom probe tomography has confirmed that those alloys, wherein the onset of recrystallization and rapid grain growth is shifted moderately (~100℃), exhibit improved passivating oxide quality (density, adherence and continuity). These observations are related to clustering of minor alloying additions in the vicinity of the original grain boundaries, which both reduce grain boundary mobility and also modify the grain boundary diffusion kinetics of desirable oxide forming alloying elements (e.g. Cr and Al).

9:55-10:15

Zn Single Crystals Deformed by a Single Pass of ECAP

Hiromoto Kitahara, Yuta Matsuo,Yuki Oda, Masayuki Tsushida, Shinji AndoKumamoto University, Japan

A single pass of equal channel angular pressing (ECAP) at 223K was applied to six kinds of Zn bulk single crystals with different crystal orientations, and the deformation behavior was investigated, such as grain refinement and texture development. Six types of Zn single crystals are prepared in this study. Here, in the early stage of ECAP process, compression in the normal direction (ND) is simply loaded to a sample, as well uniaxial compression. Therefore, the deformation behavior in the early stage was expected, and the six types of Zn single crystals were employed and categorized into three groups. Twinning and basal slips were expected to occur in ND compression in Sample 1 and 2, with basal planes parallel and perpendicular

to the theoretical shear plane. Twinning was expected to occur in ND compression in Sample 3 and 4, with c-axes are parallel to ND. In Sample 5 and 6 whose c-axes are parallel to the transverse direction (TD) and extrusion direction (ED), twinning and basal slips never occur in ND comp. However, the results depended on the group. The initial orientation of Sample 3 rotated due to {10-12} twinning above the shear plane in the early stage, and it corresponded to the initial orientation of Sample 6. Sample 3 and 6 fractured in the early stage of ECAP. In samples 1 and 2, twinning and double twinning occurs above the shear plane in the early stage. Also, recrystallization occurred and equiaxed grains were observed above the shear plane. Beneath the shear plane in the final stage, many grain were observed. That is, a large grain with several millimeters can be divided into a number of grains with several tens micron meters by a single pass of ECAP in Samples 1 and 2. On the other hand, in Samples 4 and 5, many {10-12} twins were observed above the shear plane, but recrystallization did not occur. Recrystallization above the shear plane is a key for the grain refinement in Zn. Increase in twin boundaries, due to twinning and activation of basal slips within the twins, are required for occurrences of the recrystallization.

10:15-10:35

Nanograin Formation of Second Phase-Strengthened High-Entropy Alloy: Grain Refinement Versus Particle Strengthening

Jeong-Min Park, Dong-Hyun Lee, Jae-il Jang, Hanyang University, Korea; Zhaoping Lu, University of Science and Technology Beijing, China; Jin-Yoo Suh, Korea Institute of Science and Technology, Korea; Megumi Kawasaki, Oregon State University, America; Upadrasta Ramamurty, Nanyang Technological Unoversity, Singapore

A face-centered cubic (fcc) (CoCrFeNi)94Ti2Al4 high-entropy alloy (HEA) with and without Ni3(Ti,Al) second phase particles was subjected to high-pressure torsion (HPT) to examine the possibility of deriving the benefits of particle and grain boundary (GB) strengthening simultaneously. A marked reduction in the average grain size, from ~57μm before HPT to nm-scale, upon HPT was noted. This, in turn, increases the hardness substantially. Transmission electron microscopy analysis with elemental mapping of the alloy subjected to HPT reveal that dissolution of a large amount of the second phase particles and structural transformation (from L12 to disordered fcc) of the remnant ones occur concomitantly with the grain refinement. This precludes the accrual of benefits of simultaneous strengthening of the examined HEA through grain refinement and particle strengthening. Strain rate sensitivity measurements indicate that the former mechanism not only enhances the strength, but may also increase the HEA's ability for accommodating plastic deformation. This appears to occur, as indicated by the estimates of the activation volume for deformation, due to a transition from lattice distortion controlled processes in the coarse grained HEA to grain boundary controlled ones in the nanocrystalline HEA. These observations provide key directions for the design of strong and ductile HEAs.
This work was supported by the National Research Foundation of Korea (NRF) grants funded by the Ministry of Science and ICT (No. 2015R1A5A1037627 and No. 2017R1A2B4012255).

10:30-10:45 Tea Break

11:45-11:10 Invited

Utilizing Solute Solution Drag of Nb in Ni for Fabricating Multilayered Structures in a Sheet Metal

Zakaria Quadir, Curtin University, Australia

Solute solution strengthening has been a subject in many metallurgical phenomena. The required level of concentration for creating an effective drag has been a key question for many years. In this investigation, it was found that the solute drag effect of Nb atoms in Ni slows down the thermal restoration process. This was a reflected from the changes in deformation structures during annealing. This phenomenon was observed in a Ni sheet containing 0.5 atomic percentage of Nb in the form of a homogeneous solid solution. The sheet was roll bonded with commercial purity of Ni to a high strain by a severe plastic deformation (SPD) process known as accumulative roll bonding (ARB). ARB involves successive bonding of sheets for many iterations while the thickness of the sheet remains constant. This investigation shows the change in crystallographic textures and microstructures with ARB processing and subsequent annealing heat treatments. This investigation incorporates a range of advanced characterization techniques that include scanning electron microscopy (SEM), electron backscattered diffraction (EBSD), transmission Kikuchi diffraction (TKD), transmission electron microscopy (TEM) and atom probe tomography (ATP). Discoveries are made on the maximum level of refinements by rolling, and concentration of solute for preventing coarsening in ARB formed microstructures.

11:10-11:35 Invited

Analysis on Temperature- and Rate-Dependent Nanomechnical behavior of Nanocrystalline High-Entropy Alloys Through High-Temperature Nanoindentation

In-Chul Choi, Kumoh National Institute of Technology, Korea; Dong-Hyun Lee, Max Planck Institute for Iron Research, Korea; Jae-il Jang, Hanyang University, Korea; Ruth Schwaiger, Karlsruhe Institute of Technology, Germany

High-entropy alloys (HEAs) which are multicomponent

alloys containing five or more elements in (near-)equal atomic percent, have attracted significant research interest over the past decade due to their simple microstructures with interesting mechanical properties. Recently, it has been reported that the mechanical performance of HEAs can be further enhanced by reducing the grain size to the nanocrystalline (nc) regime. One of the ways to obtain a nc HEA is through the high-pressure torsion (HPT) process. The mechanical behavior of such nc HEAs is also reasonably well understood; this was mostly accomplished by employing small-volume mechanical testing techniques such as a nanoindentation and a micro-pillar compression due to the due to limited volume of material available. However, most of these studies are confined to room temperature (RT). In this study, high-temperature nanoindentation experiments in the temperature (T) range of 298 and 573K were performed to determine the hardness, strain-rate sensitivity (m), activation volume (V*) and activation energy (Q) for the plastic flow in a nc CoCrFeMnNi HEA, which was synthesized using HPT process. The operating deformation mechanisms are interpreted on the basis the data obtained. First of all, the value of m remains almost constant (~0.015) until 423K and increases from 473K onwards with T. In contrast, V* a peak at 423K. Although these results do indicate a possible change in the deformation mechanism, they are insufficient to confirm a mechanistic transition whereas, Q, being a thermodynamic parameter for the thermally-activated plastic flow can provide such confirmation. Especially, the activation energy of the nc CoCrFeMnNi HEA suddenly increases from ~0.5 to ~1.8eV at a T of 473K. It was revealed that this increase is not by the microstructural instability but by the change in deformation mechanism, i.e., enhanced plasticity due to GB diffusion at high T.

11:35-12:00 Invited

Multiscale Simulation Based on Macroscopic Deformation Model Predicted by Microstructure Information of Ultrafine-Grained Metals

Yoshiteru Aoyagi, Atsushi Sagara, Tohoku University, Japan; Chihiro Watanabe, Kanazawa University, Japan; Masakazu Kobayashi, Yoshikazu Todaka, Hiromi Miuragnes, Toyohashi University of Technology, Japan

A uniaxial tensile test generally determines mechanical properties of materials by neglecting a directional dependency of the materials. Advanced materials such as ultrafine-grained metals (UFGMs) having peculiar mechanical properties that are not found in conventional materials have attracted a great deal of attention due to an increase in industrial demand for materials. It is reported that UFGMs improve the tensile strength that is about four times stronger than the usual materials. UFGMs produced by severe plastic deformation such as accumulative roll-bonding (ARB) processing show mechanical anisotropy depending on strong rolling texture. Therefore, it is difficult to determine the mechanical properties of UFGMs by an only uniaxial tensile test. It is necessary to take the information of microstructure into account for accurate comprehension of the mechanical properties of advanced materials.
In this study, yield functions for severely rolled pure aluminum, A1050, was constructed in order to investigate the effects of microstructures on mechanical properties. The yield function is estimated from the contours of plastic work obtained by uniaxial and biaxial tensile tests with yield function of Yld-2000-2D. Moreover, the yield function is predicted by crystal plasticity analyses based on the microstructure observed using EBSD method and the curve fitting with a stress-strain curve obtained by a uniaxial tensile test. Comparison of both results verifies the validity of the numerical prediction of the yield function. The practical CAE system based on microstructures of materials is constructed by introducing the yield function predicted by the crystal plasticity simulation into a general-purpose CAE software.

12:00-12:20

In Situ Atomistic Observation of Disconnection-Mediated Grain Boundary Migration

Qi Zhu, Guang Cao, Jiangwei Wang, Zhejiang University, China

Shear-coupled grain boundary (GB) migration is of general significance in the deformation of nanocrystalline and polycrystalline materials, but comprehensive understanding of the migration mechanism at the atomic scale remains largely lacking. Here, we systematically investigate the atomistic migration of $\Sigma 11(113)$ coherent GBs in gold bicrystals using a state-of-art in situ nanofabrication and shear testing technique inside aberration-corrected transmission electron microscope, combined with molecular dynamic simulations. We show that shear-coupled GB migration can be realized by the consecutive nucleation and lateral motion of GB disconnections, where both single-layer (b=1/22<471>) and double-layer (b=1/22<332>) disconnections have important contributions to the GB migration through their frequent (energy driven) composition and (GB kinetics induced) decomposition. Such disconnection-mediated GB migration is also confirmed in other high angle GB structures in our experiments, which should represent a general deformation phenomenon in the GB dominated plasticity; in the meantime, the disconnection-mediated GB migration mechanism is weakly influenced by the interaction between GBs and lattice defects, including dislocations and stacking faults. We further reveal the consecutive nucleation of GB disconnections from the triple junction, which is a prevalent structure in engineering polycrystalline and nanocrystalline materials. Moreover, we demonstrate

that the disconnection-mediated GB migration is fully reversible in shear loading cycles without the emission of lattice defects, which enhances the deformability of nanostructured materials, inspiring the tuning of mechanical properties through proper design of GB structures. This talk is based on our recent publication in Nature communications (Nature Communications, 2019, 10, 156)

L. Computational Design and Simulation of Materials: II

Symposium Organizers:

Tongyi Zhang, Shanghai University, China; Zhimei Sun, Beihang University, China; Shigenobu Ogata, Osaka University, Japan; Byeong-Joo Lee, Pohang University of Science and Technology (POSTCEH), Korea; Salvy Russo, RMIT, Australia; Saryu Fensin, Los Alamos National Lab, USA; Michele Manuel, University of Florida, USA

Tuesday AM
August 20, 2019

Room: 204 (2nd Floor)
Symposium: L

Chairs:
Alan Luo, The Ohio State University, USA
Zhe Liu, The University of Melbourne, Australia

08:30-08:55 Invited

Accelerating Phase-Change Materials Design by Integrating High-Throughput Ab Initio Calculations with Experiments

Zhimei Sun, Shuwei Hu, Zhen Li, Bin Liu, Jian Zhou, Beihang University, China

Phase-change (PC) materials, especially chalcogenide PC materials, are the foundation for phase-change random access memory (PCRAM) techonolgy. As one pristine PC material hardly meet all the criteria of PCRAM, doping is commonly used to optimize or enhance the performance of PC materials. Nevertheless, the identification of optimal dopants for various PC material is laborious and is usually carried out in a fashion by intuition and time-consuming trial and error. In this talk, using Sb_2Te_3 as an example, we show that rapid identifying optimal-dopants for Sb_2Te_3 to meet the criteria of PCRAM can be achieved by integrating high-throughput ab initio calculations with "artificial intelligence". On the basis of high-throughput ab initio calculations Scandium (Sc), Yttrium (Y) and Mercury (Hg) are identified as the optimal dopants for Sb_2Te_3. Then using Sc and Y as examples we have extensively investigated the doping effect on the structure and property of Sb_2Te_3. Based on ab initio calculations, Sc will randomly substitute for Sb, while Y prefers an ordered subsitition of Sb, nevertheless, both dopants linearly increases the band gap of Sb_2Te_3 with increasing doped concentrations. Our experimental results confirm the above theoretical findings. The underline mechanism has been analyzed by density of states, electron localization function and charge transfers. Furthermore, by the semi-classical Boltzmann transport theory, the calculated results show that Sc and Y can significantly decrease the electrical conductivity and thermal conductivity of Sb_2Te_3, and thus reduced power consumption of Sb_2Te_3-based PCRAM is expected. Finally, the ab initio molecular dynamics simulations demonstrated that Sc and Y can significantly improve the thermal stability of amorphous Sc-doped Sb_2Te_3, and hence the enhanced data retention of Sb_2Te_3-based PCRAM. Our experiments confirms the conclusions. The present work provides fundamentals for fast screening optimal dopants to improve the overall performance of chalcogenide phase-change materials for PCRAM, and the present method can be extended to other similar semiconductor materials.

08:55-09:20 Invited

Computational Design of Two-Dimensional Smart Energy Conversion and Energy Storage Materials

Zhe Liu, The University of Melbourne, Australia

This presentation will cover our recent research works on computational materials physics for, two-dimensional smart actuation materials (energy conversion); and ion storage/transport in nanoslits enclosed by two-dimensional materials (energy storage).

Fast growing miniaturization technology has been facilitating the development of nanoelectromechanical devices (NEMS) in a myriad of fields ranging from biomimetic robotics to aerospace industry. One of the key objectives is to make the futuristic electromechanical systems more intelligent and autonomous. It is mandatory to design high performance miniaturized actuators and sensors (core components in NEMS) at nanoscopic or ultimately atomistic scales. Our recent works show that the electromechanical properties of two-dimensional materials are unique and exciting. They have exceptional strain output (up to 28%), volumetric work capacities (as much as 29 times greater than common high modulus ferroelectrics), and fast response rate (up to GHz). I will provide an overview of our density functional theory simulation studies of the piezoelectric and shape memory effects of some two-dimensional materials.

Ion transport in severe nanoconfinement (< 2nm in one characteristic dimension) can be very different from that in bulk and has been a subject of extensive research

across both scientific and engineering disciplines, for many different applications such as batteries, electrochemical capacitors, salinity gradient energy harvesting, and capacitive deionisation systems. I will present some recently discovered novel ion transport properties/phenomena under nanoconfinement, taking advantage of our graphene membrane experimental platform that has continuously tunable nanoslit size from 10nm down to 0.5nm. This includes a quantitative and statistical representative microstructure model to describe the cascading nanoslit system embedded in graphene membranes; a scaling law correlating ion conductance with nanoslit size in the whole sub-10nm range, and recently discovered low-voltage modulation of ion diffusion through layered graphene-based membranes. These new properties/phenomena cannot be explained by the conventional theory, which opens up the prospect of scientific research in future.

09:20-09:40

Thermotransport in Liquid Alloys and Extension to the Solid State

Graeme Murch, Irina Belova, Tanvir Ahmed, The University of Newcastle, UK; Zikui Liu, Pennsylvania State University, USA; Rafal Kozubski, Jagiellonian University, Poland; Andreas Meyer, German Aero Space Center (DLR), Germany

In this contribution, we present a newly developed theoretical formalism for describing interdiffusion and thermotransport in a liquid binary metallic alloy with several examples of molecular dynamics calculation of the thermotransport and interdiffusion and tracer diffusion parameters for a range of compositions in Ni-Al and Cu-Ag liquid alloys. The coupling of mass and heat flows (Thermotransport) is generally understood from its resulting segregation of the liquid components in a temperature gradient (the Soret effect). Until recently, thermotransport in binary and multicomponent liquid alloys did not have a general theory that can both piece the experimental facts together and provide an understanding that has predictive power. In this paper, we also present the pathway to building this theory is presented. Further examples of molecular dynamics calculation of thermotransport and interdiffusion and tracer diffusion parameters for a range of temperatures and compositions in Co-Ni-Al liquid alloys are discussed in this presentation.
The extension of the formalism to describing thermotransport in the solid state A-B-vacancy 'ternary' system will also be discussed and analysed. It is known that in the solid state the heat of transport must include (in some form) the vacancy formation enthalpy. It was recently shown that, using the binary-ternary liquid alloy analogy, this term should be simply added to the standard heat of transport that appears in the analysis of thermotransport in the binary liquid alloys.

09:40-10:00

Investigation of Atomic Order and Molar Volume of the Sigma Phase

Wei Liu, Xiaogang Lu, Yi Liu, Shanghai University, China

Sigma phase is a non-stoichiometric intermetallic compound designated as tetragonal structure with 30 atoms distributed on five inequivalent sites (2a, 4f, 8i1, 8i2, 8j). The formation of the sigma phase in technologically important materials, such as Ni-based supperalloys, influences greatly their mechanical properties. Fundamental knowledge on the sigma phase is demanded to understand the phase stability and reasonably control its precipitation. In the present work, the atomic order (i.e. atomic constituent distribution or site occupancy preference on inequivalent sites of a crystal) and molar volume of the binary sigma phase are systematically investigated by using first principles calculations combining with the experimental data from the literature. Firstly, we observe that the atomic order of the sigma phase is affected by both the size factor and electron configuration of the constituent elements. Furthermore, we dissociate the effect of the individual influencing factor on atomic order. Secondly, the molar volume of the sigma is found affected by both atomic mixing and atomic order. Our calculation results show the influence of atomic mixing on molar volume is related to the tendency of electron loss or gain of the two constituent elements; the influence of atomic order on molar volume is related to the atomic bonding. Thirdly, we develop a new integrated thermodynamic and molar volume model of the sigma phase to consider physically both atomic mixing and order factors. The integrated thermodynamic and molar volume databases can predict successfully the molar volume of the binary and ternary sigma compounds.

10:00-10:20

Photoexcitation Dynamics at Nanoscale Interfaces

Run Long, Beijing Normal University, China

Advancing organohalide perovskite solar cells requires understanding of carrier dynamics. Electron–hole recombination is a particularly important process because it constitutes a major pathway of energy and current losses. Non-adiabatic molecular dynamics combined with ab initio real-time time-dependent density functional theory enable us to model time-resolved laser experiments in real time and at the atomistic level, emphasizing realistic aspects of the materials, such as defects, dopants, boundaries, humidity, chemical bonding, etc. In this talk, we will discuss the factors influencing electron-hole recombination in perovskite $CH_3NH_3PbI_3$ and $CH_3NH_3PbI_3/TiO_2$ interface, including how dopants control electron-hole recombination,

how grain boundaries accelerate recombination while Cl doping decreases the recombination rate, how the interplay between localized and free charge carries rationalizes the hog Fluorescence in $CH_3NH_3PbBr_3$, how humidity and Lewis basis passivation affect electron-hole recombination, how quantum decoherence determines electron-hole recombination in multiple two-dimensional perovskites, how photoinduced localized hole delays charge reconbination in $CsbPBr_3$, and how chemical bonds determine electron injection from $CH_3NH_3PbI_3$ into TiO_2.

It was found that strong interactions between perovskite and TiO_2 facilitate ultrafast photoinduced charge transfer, that Cl and Br doping reduces losses of the photogenerated charges, that grain boundaries provide a major pathway for the charge recombination, that perovskite interaction with water depends strongly on the amount of water on the perovskite surface, and that Lewis base localizes the electron wave functions in different way for suppressing electron-hole recombination, that the localized and free charge carriers are responsible for normal and delayed hot fluorescence respectively, and that quantum decoherence affects significantly electron-hole recombination in multiple two-dimensional perovskites. The predicted changes in the charge and energy transfer and relaxation processes arise due to a complex interplay of charge localization, trapping, elastic and inelastic electron-phonon interactions, and thermal disorder. The reported dynamics studies formulate detailed conclusions which may further guide technological efforts towards design of optimal perovskite materials for photovoltaic purposes.

10:20-10:40 Tea Break

10:40-11:05 Invited

Integrated Computational Materials Engineering (ICME) for Lightweight Metallic Materials and Manufacturing

Alan Luo, The Ohio State University, USA

Lightweight alloys (aluminum, magnesium and titanium alloys) and metal matrix nanocomposites (aluminum and magnesium-based MMNCs) are increasingly being used in the automotive, aerospace and consumer industries for weight reduction and structural efficiency. Integrated Computational Materials Engineering (ICME) is defined as the integration of materials information, captured in computational tools, with engineering product performance analysis and manufacturing-process simulation. This talk presents examples of alloy development and advanced processing of lightweight metallic materials using ICME tools. The talk will first demonstrate how CALPHAD (CALculation of PHAse Diagrams) modeling, when combined with critical experimental validation, can be used to guide the design of new Al, Mg and Ti alloys and Al-based composites. The talk will then summarize some of the latest process innovations in cast and wrought products and the use of ICME in developing/optimizing these processes. The microstructural evolution and microsegregation of a series of Mg alloys during solidification with respect to cooling rate have been investigated using a CALPHAD-based model incorporating the back-diffusion effect in the solidified solid. The solidification microstructure of aluminum alloys is simulated using a three-dimensional (3-D) multi-component model based on cellular automaton (CA) and process simulation, to predict grain size of high pressure die castings (HPDC). Precipitation strengthening plays a critical role in controlling the yield strength of multi-component light alloys. As an example, concurrent precipitation of Mg17A112 and Mg_2Sn phases in Mg-Al-Sn alloys has been simulated using a Kampmann–Wagner numerical (KWN) model coupled with a newly developed Mg mobility database and thermodynamic database. The evolution of key microstructure features including volume fraction, number density, and precipitate sizes at different aging temperatures and aging times were predicted. These solidification and precipitation models are being integrated to predict location-specific mechanical properties, based on location-specific microstructure, of light alloy castings for structural applications. The future trends and research needs in light metal castings are also discussed.

11:05-11:25

Discovery of Ternary Electrides by High-Throughput Calculations

Junjie Wang, Northwestern Polytechnical Unviersity, China

Electrides are said to be a class of unconventional ionic materials which contain excess valence electrons confined in the void space and playing the role of anions. Due to its room temperature stability, electrides enable many technological applications such as the splitting of carbon dioxide at room temperature, synthesis of ammonia from atmospheric nitrogen under mild conditions and using as a low electron-injection barrier for organic light-emitting diodes (OLEDs).

A high-throughput screening based on first-principles calculations was performed to search for new ternary inorganic electrides. From the available materials database, we identified a series of new thermodynamically stable materials as potential electrides made by main group elements, in addition to the well known Mayenite based electride ($Ca_6Al_7O_{12}$). Different from those conventional inorganic electrides in which the excess electrons play only the role of anions, the new materials, resembling the electrides found in simple metals under high pressure, possess

mixed ionic and metallic bonding. The interplay between two competing mechanisms, together with the different crystal packing motifs, gives rise to a variety of topologies in anionic electrons, and rich physical phenomena such as ferromagnetism, superconductivity and metal-insulator transition. Our finding here bridges the gap between electrides found at ambient and high pressure conditions.

Among those newly identified ternary electrides, we found that LaCoSi is an efficient and stable catalyst for N_2 activation to produce NH_3. The ammonia synthesis is significantly promoted by shifting the reaction bottleneck from the sluggish N_2 dissociation to NHx formation, which few catalysts have achieved. Theoretical calculations reveal that the negatively charged cobalt mediates electron transfer from lanthanum to the adsorbed N_2, which further reduces the activation barrier of N_2 dissociation. Most importantly, the specific LaCoSi geometric configuration stabilizes the N_2 adsorption with a strong exothermic effect, which dramatically decreases the apparent energy barrier of N_2 activation. Consequently, LaCoSi shows a superior activity ($1250 \mu mol \cdot g^{-1} \cdot h^{-1}$), with a 60-fold increase over the activity of supported cobalt catalysts under mild reaction conditions (400˚c , 0.1MPa).

11:25-11:45

Multiphase-Field Study of Eutectic Formation in Superalloy Solidification

Cong Yang, Qingyan Xu, Baicheng Liu, Tsinghua University, China

In superalloy solidification, coarse γ/γ' eutectic structure with highly segregated refractory alloy elements can be found in the interdendritic region, and a heat treatment process afterwards is necessary to dissolve the coarse γ' phase. Therefore, predicting the eutectic structure in superalloy castings is vital for determining the heat treatment process. However, the complex eutectic microstructure evolution in multicomponent superalloy solidification was not fully understood.

In this work, a quantitative multiphase-field method was developed to study the eutectic growth at the final stages of DD6 superalloy solidification. In the model, three phases (liquid, γ, γ') and are nine alloy components (Al, Co, Cr, Hf, Mo, Nb, Re, Ta, W) including the matrix Ni are considered. Realistic superalloy thermodynamic and kinetic data from CALPHAD database were used in the multiphase-field and diffusion simulations. To achieve large scale phase-field simulations, a previously developed GPU-based parallel computing scheme was used to accelerate the computation.

Previous work has indicated that the γ' phase nucleates at the γ/liquid interface at eutectic point. Hence, two types of initial conditions for γ/γ' eutectic structure were considered. One is the laminar γ/γ' phases settled at the bottom of simulation domain, and the other is nuclei of γ' phase placed on the γ/liquid interface. The eutectic morphology evolution and microsegregation behavior of each alloy component under different cooling rates were analyzed. The simulated microsegregation behavior was in good agreement with the EPMA analysis results of DD6 superalloy at the eutectic region, which demonstrates the capability of the developed model. Moreover, the typical eutectic morphology changes from fine γ/γ' network to coarse γ/γ' phase was reproduced by current model. The coarse γ' phase at the end of eutectic solidification can be ascribed to the fast growth of γ phase at early eutectic solidification stage.

M: Renewable Energy Materials and Nuclear Materials: II

Symposium Organizers :

Min Zhu, South China University of Technology, China; Yuan Deng, Beihang University, China; Guanghong Lu, Beihang University, China; Tetsuya Uda, Kyoto University, Japan; Taek-Soo Kim, Korea Institute of Industrial Technology (KITECH), Korea; Dmitri Golberg, Queensland University of Technology, Australia; Assel Aitkaliyeva, University of Florida, USA

Tuesday AM
August 20, 2019

Room: 311(3rd Floor)
Symposium: M

Chairs:
Chenyang Lu, Xi'an Jiaotong University, China
Yuan Deng, Beihang University, China
Ying Chen, Deakin University, Australia
Shaojun Guo, Peking University, China

8:30-9:00 Keynote

Solving Major Challenges in Lithium-Sulfur Batteries

Ying Chen, Deakin University, Australia

Lithium–sulphur (Li-S) batteries have a much higher energy density than Li ion batteries and thus are considered as next generation batteries. However, the problem of rapid capacity fading due to the shuttling of soluble polysulfides between electrodes remains main obstacle for practical applications. We use different approaches to decrease the charge transfer resistance and mitigate the shuttling problem. (i)The Li-S cells use a porous-CNT/S cathode coupled with a sulfur–nitrogen dual-doped graphene (SNGE) interlayer to benefit from excellent electric conductivity of SNGE and efficiently trapping LiPS ions. These cathodes exhibit ultrahigh cyclability when cycling at 8C for 1000 cycles, and a low capacity degradation rate of 0.01% per cycle. (ii) A composite interlayer is built simply by coating the cathode surface with a functionalized boron nitride nanosheets (FBN). Using this thin and ultralight composite interlayer, the specific capacity and cycling

stability of Li-S batteries are improved significantly with a life of over 1000 cycles, an initial specific capacity of 1100mAh·g^{-1} at 3C and a cycle decay as low as 0.0037% per cycle. (iii) New separators are constructed by incorporation of FBN nanosheets with negative charged groups onto a commercial Celgard separator. The FBN separator is capable to prevent PSs migration through the separator effectively due to strong ion-repelling of negatively charged PSs by the negatively-charged FBN nanosheets. The Li-S cell with a FBN separator exhibits an excellent long-term cycling stability up to 2000 cycles and a high capacity of 585mAh·g^{-1} at a very high current of 10C (1.68A·g^{-1}). (iv) For Li metal anodes, composite anodes are fabricated via melt infusion of lithium into graphene foams decorated by metal oxide nanoflake arrays, which successfully controls the formation and growth of Li dendrites, and alleviate volume change during cycling. A resulting Li-Mn/Graphene composite anode demonstrates a super long and stable lifetime for repeated Li plating/stripping of 800 cycles at 1mA cm^{-2} without voltage fluctuation, which is 8-fold longer the normal lifespan of a bare Li foil under the same conditions. (v) These huge improvements in the life time of the Li-S cells enable Li-S batteries to be used in electric vehicles and other large-scale electrochemical energy storage systems in near future.

9:00-9:25 Invited

Stain-Controlled Energy Electrocatalysis on Multimetallic Nanomaterials

Shaojun Guo, Peking University, China

Proton exchange membrane fuel cells (PEMFCs) are generally expected to be the ideal alternative to traditional internal combustion engine as energy-supplying devices for transportation, which consumes nearly 25% of the global energy. However, to guarantee the wide-adoption of PEMFCs, it still requires an efficient electrocatalyst, with higher activity/stability and lower Pt usage than the state-of-the-art carbon supported platinum nanoparticles (Pt/C), towards the cathodic oxygen reduction reaction. But, the absence of low-platinum, high-activity and satisfied-durability electrocatalysts for oxygen reduction reaction has bottlenecked the wide-adoption of PEMFCs for decades. To address this challenge, an efficient strategy is to modify the electronic structure of Pt by alloying with other cheap transition metals (M), normally called ligand or electronic effect. Tuning or controlling the surface strain in multimetallic nanomaterials is a robust method to boost electrocatalytic performance, and tremendous progress has been made in this area in the past decade. In this talk, I will show recent important advances in how to tune the compressive and tensile strain in multimetallic nanocrystals to achieve more efficient energy conversion by electrocatalysis. I will start with the introduction of stain and the basic information on how to tune the strain for the electronic structure tuning. Then, I will give several examples on designing metal-based materials with interesting strain effects for boosting oxygen reduction and hydrogen evolution reaction catalysis. In particular, I will highlight our recent important results on making PtPb/Pt core/shell nanoplates with biaxial strain for boosting oxygen reduction catalysis, which exhibit much higher activity and stability for oxygen reduction catalysis. Furthermore, I will show that our strain tuning concept will be extended to other Pd-based and transition metal-based materials system for greatly enhancing oxygen reduction and hydrogen evolution catalysis. Finally, I will give the conclusion and perspective on the strain-tuned energy catalysis of different metal-based material system.

9:25-9:50 Invited

High-Performance Thermoelectric Materials: Progress and Applications

Zhigang Chen, University of Southern Queensland, Australia

Thermoelectrics, enabling the interconversion between heat and electricity, become a typical component in the drive for eco-friendly energy technology. The mass-market application demands a high energy conversion efficiency, evaluated by the figure-of-merit (zT), which is proportional to power factor and reciprocal of lattice thermal conductivity. Besides, thermoelectric materials are supposed to be environmentally benign. GeTe is the competent choice to replace the highly toxic Pb-based alloys that are commonly used as mid-temperature thermoelectric materials. Recently, super-high zT over 2.0 for GeTe-based materials has been reported by several research groups. Particularly, our innovative contributions have significantly promoted the advance of high-performance GeTe (Adv. Mater. 2018, 30, 1705942 and Adv. Energy Mater. 2018, 8, 1702333).
Herein, we review the most recent research outcomes in GeTe-based thermoelectric materials. First, we summarize the features of GeTe (i.e., crystal structures, phase transition, multiple sub valence bands, and phonon dispersions), which endow diverse degrees of freedom to manipulate the thermoelectric properties for GeTe. Accordingly, the strategies for enhancing power factor are settled, including alignment of multiple valence bands, resonant distortion of density-of-states, and an increase of band degeneracy induced by slight symmetry reduction. To decrease thermal conductivity, we highlight the methods of strengthening intrinsic phonon-phonon interactions and introducing various lattice imperfections as scattering centers. Then, we overview the current GeTe-based thermoelectric devices, including the technical challenges and the solutions. In the end, we propose possible future directions for developing GeTe. The significance of this review can be summarized as: (i)The delivered information will bridge the communications among physicists, chemists, and

engineers to further enhance the performance of GeTe and to facilitate the establishment of large-scale thermoelectric devices with high conversion efficiency. (ii)The achieved high thermoelectric performance in GeTe-based thermoelectric materials with the rationally developed strategies could serve as references for broader materials to pursue high performance.

9:50-10:10 (1222207)

Effect of Yttrium Contents on the Microstructure and Texture of a Hot Rolled Ferrite/Martensite12Cr-ODS Steel

Changhao Wang, Institute of Material, China Academy of Engineering Physics / Chongqing University of Technology, China; Qingzhi Yan, University of Sciences and Technology Beijing, China; Jinru Luo, Guomin Le, Institute of Material, China Academy of Engineering Physics, China; Jian Tu, Hong Ye, Zhonglin Yan, Chongqing University of Technology, China

Oxide dispersion strengthened (ODS) steel is one of the most important candidate structural material for the fuel cladding and fusion reactor cladding of the fourth generation nuclear reactor fission fast reactor for its excellent high temperature creep performance and radiation resistance, thus attract the attentions of many researchers and become a hot research topic nowadays. As a cladding tube material, hot deformation is the necessary manufactural process for the ODS steel. And the mechanical performance can be improved through hot deformation such as rolling or extrusion by means of microstructural optimization. Therefore, the understanding on the deformation and recrystallization mechanisms and the subsequent microstructural evolution of the material during hot deformation become very important for mechanical performance design and optimization. In the present study, a 12Cr-ODS ferrous alloy containing 0.3wt.% Y_2O_3 has been hot rolling to various strain levels at different temperature. The microstructure and texture of rolled samples has been characterized by optical microscope (OM), X-ray diffractometer (XRD) and a scanning electron microscope (SEM) equipped with electron back-scattered diffraction (EBSD) detector. The shape, size and distribution of the second phase particles were mainly examined by electron microscopes. The microstructural and textural evolutions of the ODS steel rolled to various strain at different temperature have been discussed with considering the effect of thermal activation and deformation energy on the dynamic recrystallization and phase transition of the matrix and the coarsening of the second phase particles. Microhardness has also been applied to estimate the mechanical performance of the deformed samples. The relationships between the microstructure the mechanical properties of the rolled samples have also been discussed in the present study by telling the effects of work hardening and grain refinement of the matrix grains and the density and particle size of the ODS phase.

10:30-10:45 Tea Break

10:45-11:10 Invited

Enhancing Irradiation Tolerance in Single-Phase Concentrated Solid Solution Alloys by Tuning Chemical Complexity

Chenyang Lu, Xi'an Jiaotong University / University of Michigan, China; Fei Gao, Lumin Wang, University of Michigan, China

Single-phase concentrated solid solution alloys (SP-CSAs), including high entropy alloys (HEAs) are a novel family of materials for studying defect dynamics without preexisting defect sinks. In contrast to conventional alloys, SP-CSAs are composed of two to five principal elements in equal or near-equal molar ratios that form random solid solutions in either a simple face-centered cubic (fcc) or simple body-centered cubic (bcc) crystal lattice structure. Significant suppression of void formation at elevated temperatures has been achieved with increasing compositional complexity in Ni-containing SP-CSAs. In our research, we demonstrated the modification of alloy complexity by increasing the number, the type and the concentration of alloying elements in SP-CSAs.

A group of SP-CSAs (Ni, NiCo, NiFe, NiCoFe, NiCoFeCr, NiCoFeCrMn) irradiated by Ni ions at 773K has been studied by cross-sectional transmission electron microscope (TEM). This study demonstrates the enhancement of radiation tolerance by showing two orders of magnitude of decrease on void swelling with increasing number of alloying elements. The controlling mechanism of defect movements was determined through detailed TEM characterization of defect clusters distributions and Molecular dynamics (MD) simulations. The enhanced swelling resistance is attributed to the tailored interstitial defect cluster motion in the alloys, from a long-range one-dimensional (1-D) mode to a short-range three-dimensional (3-D) mode, which leads to enhanced point defect recombination.

The effect of alloying elements on radiation-induced microstructural evolution has been studied in Ni and Ni-20*X* (*X*=Fe, Cr, Mn and Pd) binary alloys. The 3-D migration mode is identified to be the dominating migration mechanism for interstitial clusters in these binary alloys, contrary to the 1-D mode dominated in dilute alloys. It is found that the solute atomic volume size factor plays a key role in the migration and interaction of defect clusters. The total void swelling generally decreases as the atomic volume factor increases, accompanying with a significantly sluggish interstitial migration and smaller dislocation loop size.

The effects of elemental concentration on radiation

tolerance in Ni-Fe alloys have been studied. Void swelling and dislocation loop evolution are both suppressed or delayed with increasing iron concentration. Furthermore, the dominating migration behavior of interstitial clusters shifted from 1-D to 3-D mode with increasing iron concentration. It has been demonstrated that the transition between 1-D and 3-D is a continuous process, and can be quantitatively characterized by the mean free path of the interstitial defect clusters.

This talk demonstrates the enhancement of radiation tolerance in SP-CSAs, and more importantly, reveals its controlling mechanism through a detailed analysis of microstructure characterizations and atomistic computer simulations.

11:10-11:30

Hydrogen Storage Properties of Nano-Crystalline Mg_2Ni Prepared from Compressed $2MgH_2$-Ni Powder

Khan Darvaish, Shanghai Jiao Tong University, China

Limited fossil fuel, climate change and increasingly severe environmental pollution problems, clean energy have been given increasingly widespread attention. The use of clean renewable energy has become an inevitable trend. Hydrogen is a predominant candidate as a future energy carrier for sustainable development. For the wide application of hydrogen-powered fuel cell vehicles, it is of considerable importance to develop a feasible on-board hydrogen storage system. Nevertheless, safe and compact storage of hydrogen in a solid medium is the most demanding and challenging requirement for realizing a hydrogen economy as far as mobile and stationary applications are concerned. Generally, hydrogen can be stored in the form of high-pressure gas, cryogenic liquid, or chemically or physically bonded to a suitable solid-state material. For the safe solid state hydrogen storage, various studies have been carried out, however, Mg-based hydrides stand out due to their high gravimetric storage capacity (7.6wt% for MgH_2), low cost, environmental friendliness, and high natural abundance. Practical applications of Mg-hydrides for stationary or on-board energy sectors are limited due to slow hydrogen absorption kinetics, high thermal stability and very high reaction activity towards oxygen. The sluggish hydrogenation kinetics are due to slow dissociation rate of H_2 molecules on the Mg surface, the low hydrogen diffusion rate on the Mg because it extremely difficult after a MgH_2 layer forms on the surface of Mg because the H_2 diffusion coefficient in MgH_2 ($1.5 \times 10^{-16} m^2/s$) is considerably smaller than Mg ($4 \times 10^{-13} m^2/s$), and formation of Mg/MgH_2 oxides on the surface of Mg/MgH_2. The slow dehydrogenation kinetics is due to the strong bond between Mg and H, the low diffusion rate of H in MgH_2, the high energy required for the nucleation of Mg on the surface of MgH_2, and the combination of hydrogen atoms to form the H_2 molecule on the Mg surface. However, its high decomposition temperature (T>300˚C) is due to the strong ionic characteristics of the Mg-H bond.

We prepared nanocrystalline Mg_2Ni with an average size of 20~50nm was prepared via ball milling of a $2MgH_2$-Ni powder followed by compression under a pressure of 280MPa. The phase component, microstructure, and hydrogen sorption properties were characterized by using X-ray diffraction (XRD), scanning electron microscope (SEM), transmission electron microscope (TEM), pressure-composition-temperature (PCT) and synchronous thermal analyses (DSC/TG). Compared to the non-compressed $2MgH_2$-Ni powder, the compressed $2MgH_2$-Ni pellet shows lower dehydrogenation temperature (290˚C) and a single-phase Mg_2Ni is obtained after hydrogen desorption. PCT measurements show that the nanocrystalline Mg_2Ni obtained from dehydrogenated $2MgH_2$-Ni pellet has a single step hydrogen absorption and desorption with fairly low absorption (-57.47kJ/mol H_2) and desorption (61.26kJ/mol H_2) enthalpies. It has very fast hydrogen absorption kinetics at 375˚C with about 3.44wt.% hydrogen absorbed in less than 5min. The results gathered in this study show that ball milling followed by compression is an efficient method to produce Mg-based ternary hydrides.

11:30-11:50

Nanoconfinement of Mg by Ultrathin Carbon Layer with Enhanced Hydrogen Storage Properties

Tong Liu, Xiubo Xie, Ming Chen, Miaomiao Hu, Beihang University, China

A facile way has been developed to fabricate ultrathin carbon layer encapsulated air-stable Mg nanoparticles (Mg@C NPs) by methane plasma metal reaction method. Compared with pure Mg NPs, the nanoconfinement of Mg by carbon layer can not only reduce particle size but also prevent Mg from oxidation. By adjust methane from 10 to 300ml, average size of Mg@C NPs reduces from 140 to 60nm and thickness of carbon layer increases from 1 to 4nm. After exposure in air for 3 months, little MgO can be detected in Mg@C NPs. In these Mg@C samples, Mg@C (CH4:50ml) with size of 80nm and ultrathin amorphous carbon shell of 3nm shows the highest hydrogen capacity of 6.3wt% H_2. In comparison, the hydrogen capacities of Mg@C (CH4:10ml) and Mg@C (CH4:300ml) are only 5.4wt% H_2 and 4.3wt% H_2, respectively. Mg@C (CH4:50ml) also displays the highest hydrogenation and dehydrogenation rates which can absorb 4.8wt% H_2 within 10min at 573K and desorb 5.0wt% H_2 within 20min at 623K. The apparent energies for hydrogenation and dehydrogenation of Mg@C (CH4:50ml) are 64.1 and 107.2kJ·mol^{-1}, both smaller than Mg@C (CH4:10ml) of 66.7 and 118.9kJ·mol^{-1} and Mg@C (CH4:300ml) of 67.7 and 137.8kJ·mol^{-1}. The enhanced hydrogen storage properties of Mg@C (CH4 : 50ml) are attributed to smaller particles size and excellent antioxidant properties provided by the ultrathin carbon layer.

N. Additive Manufacturing and Powder Metallurgy: Titanium & Titanium Alloy I

Symposium Organizers:

Huiping Tang, Northwest Institute for Nonferrous Metal Research, China; Yong Liu, Central South University, China; Yuichiro Koizumi, Osaka University, Japan; Kee-Ahn Lee, Inha University, Korea; Qian Ma, RMIT, Australia; Ed Herderick, Ohio State University, USA

Tuesday AM
August 20, 2019

Room: 402 (4th Floor)
Symposium: N

Chairs:
Ming Yan, Southern University of Science and Technology, China
Yoshimi Watanabe, Nagoya Institute of Technology, Japan

8:30-9:00 Keynote

Effects of Powder Quality on Fatigue Strength of Ti-6Al-4V Alloy Fabricated by Electron Beam Additive Manufacturing

Akihiko Chiba, Tohoku University, Japan

To establish the benefits of electron beam melting (EBM) for the fabrication of Ti–6Al–4V alloy components, it is necessary to properly understand the fatigue performance of the alloy. In the present study, we investigated the high-cycle fatigue behaviors of EBM-fabricated Ti–6Al–4V alloy component samples and systematically assessed their correlation with the microstructure, porosity, and (quasistatic) tensile properties of the material. The associated defects formed in the samples fabricated from the plasma atomization and plasm rotating electrode process were also examined. The employed samples were post-processed by hot isostatic pressing (HIP) and heat treatment (HT) at 920˚C for 2h with and without the application of 100MPa gas pressure, respectively. The as-built samples consisted of fine acicular α (hcp) microstructures, attributable to the β (bcc) → α' (hcp) martensitic transformation during the EBM process, and these microstructures were coarsened by the HIP and HT processes. However, the fatigue properties of the HIP samples were found to be superior to those of the other samples despite the coarsened microstructure and reduced tensile strength. Notably, a small amount of porosity was observed in the as-built and HT samples, although all the samples were almost fully dense, having relative densities of ~100%. The pores were found to act as crack initiation sites, with the defects having a greater effect on the fatigue properties of the samples than the microstructures. Optimization of the parameters of both the EBM process and the raw powder production process is required to enhance the performance of EBM-fabricated Ti–6Al–4V alloy components.
It has been revealed for the first time that without HIP process after build, the samples fabricated from the PREPed powder show the excellent fatigue strength compared with the ones fabricated from plasma atomized powder.

9:00-9:25 Invited

Selective Laser Melting of Ti-6Al-4V and Al with Heterogeneous Nucleation Site Particles

Yoshimi Watanabe, Nagoya Institute of Technology, Japan

Australia has researched multiple pathways to providing near net shapes for high value added materials such as Titanium for several decades. Building of Australia's mineral wealth of Titanium bearing ore, CSIRO has assisted in building a new Titanium Additive Manufacturing industry in Australia, developing technologies for the entire value chain from powder to product. The TIRO™ process is a continuous direct production of titanium powder consisting of two stages. The first stage is a bed reactor (FBR) in which TiCl4 is reacted with magnesium powder to form solid magnesium chloride particles about 350 µm in diameter in which micron sized titanium particles are dispersed. The second stage is a continuous vacuum distillation operation where the titanium is separated from the magnesium chloride and sintered to form a friable sponge precursor material. The sponge precursor can be directly feed into a novel Powder Manipulation Technology (PMT) that achieves significant improvements in powder morphology, particle size distribution, flowability and the tap density in solid state without the need for atomization or hydride de-hydride (HDH). The end-process produces a low-cost titanium powder that can be used for Additive Manufacturing of parts to affordable conversion of shaped intermediates such as pipe, sheet, preforms and wire mill products. CSIRO titanium innovations extend the entire titanium value chain to patented melt-less consolidation technologies namely Cold Spray for the manufacture of billet, preform and pipe, to Direct Powder Rolling and Hot Rolling process for the continuous fabrication of thin Titanium sheet and strip and a continuous extrusion process for the fabrication of rod and wire, all directly from binder-less powder feedstock. Our Additive Manufacturing modelling capabilities extend from the powder bed raking through to modeling the melting (EBM or Laser) and part distortion. We actively seek, partner and licence our technologies to Australian and international companies assisting in the development of a new titanium industry in Australia. The strengths and opportunities of each novel Titanium technology and its potential impact to the emerging Additive Manufacturing in the Aerospace, Defense and Medical industries in

Australia will be presented and examined.

9:25-9:50 Invited

Development of a Titanium Manufacturing Industry in Australia

Stefan Gulizia, Leon Prentice, Peter King, Christian Doblin, Robert Wilson, Nazmul Alam, Darren Fraser, Alejandro Vargas Uscategui, Vu Nguyen, CSIRO, Australia

To explore the electron beam melting (EBM) , new alloys development is High Entropy Alloys (HEAs) have attracted significant research interest in recent years due to the novelty of the underlying alloy design principle as well as their promising mechanical properties, such as good corrosion resistance, excellent wear resistance, high strength, and exceptional ductility, of the massive solid solution microstructure. Here, we detailed characterize the equiatomic CoCrFeNiMn HEA powder produced by gas atomization. It is revealed that gas atomized HEA powder is suitable for additive manufacturing (AM). The printability of the pre-alloyed CoCrFeNiMn and mixed CoCrFeNiMn-x ($0 < x < 2$) is investigated by electron beam melting (EBM), which is one of powder-bed-fusion AM. For the pre-alloyed CoCrFeNiMn powder, the processing window narrow and the EBM-built parts exhibit comparable mechanical properties to their conventional cast counterparts. For the mixed CoCrFeNiMn-xTi powder, the chemical composition parts are obtained by EBM and the in situ formed precipitates enhance the strength. The microstructure and deformation mechanism of the EBM-built HEAs are presented and the formation of caused by the in situ reaction during the process is also discussed. These findings are expected to be usefully for understanding the relations between the AM part quality and the feedstock powder, the AM part deformation mechanism, and the role of cellular sub-structure on the AM part mechanical properties.

9:50-10:10

Designed and Manufactured Open-Cell Titanium Foams with Different Unit Cell Geometries

Xuezheng Yue, University of Shanghai for Science and Technology, China; Yuxuan Lin, An-Yang Normal University, China; Xuejie Yue, Xinxiang University, China

Titanium foams are a class of lightweight materials with novel physical, mechanical, thermal, electrical and acoustic properties. They offer potential for lightweight structures, energy absorption, and thermal management. Titanium foams are used for structural applications or for aerospace engineering because of their low density, high strength and excellent corrosion resistance.
Additive Manufacture process enables to manufacture open-cell geometry consisting of periodic space-filling polyhedrons. Though there are several space-filling polyhedrons, the present study focusses on two polyhedrons, truncated octahedron and rhombic dodecahedron. Truncated octahedron, which is one of Archimedean solids, has 14 faces (8 hexagons and 6 squares), 36 edges and 24 vertices. Rhombic dodecahedron, which is one of Catalan solids, has 12 rhombic faces, 24 edges and 14 vertices. Of course, titanium foams with these polyhedron cell morphologies have been reported in the previous study. However, the relationship between the porosity, cell edge length, cell diameter and cell orientation has not been discussed systematically.
In the present study, mechanical properties of titanium foams with truncated octahedron and rhombic dodecahedron cells are investigated systematically. Different compression direction was in order to estimate mechanical properties of open cell Titanium. Unit cell geometries of open cell titanium foam was studied. Optimal cell geometry for mechanical properties such as plateau stress and energy absorption are clarified through the compressive tests.

10:10-10:30

Study of Structure and Mechanical Properties in Biocompatible Ti-6Al-4V Alloys Manufactured by Selective Laser Melting with Different Built Orientation

Nataliya Kazantseva, Institute of Metal physics Ural branch of Russian Academy of Sciences / Ural Federal University, Russia

The method of selective laser melting (SLM) is very promising, especially for medicine, because it allows to obtain parts of complex structures and take into account the personal characteristics of the human body. Laser power, quality and size of powder, distance between layers are important in a selective laser melting because all of these affect the porosity and the level of residual stresses in the material and, accordingly, its mechanical properties. It is known that metallic samples obtained by additive manufacturing show a layered structure. The appearance of such a structure in conventional materials leads to anisotropy of physical and mechanical properties. In this paper, we conducted a study of the effect of SLM sample orientation on its structure and mechanical properties.
Study of the Ti-6Al-4V samples manufactured by selective laser melting was done with TEM, SEM and X-ray analysis. Different built orientation of the samples such as vertical, flat, 30, 45 degree is used. Samples were produced with the EOSINT M280 machine (EOS GmbH) equipped with an Ytterbium fiber laser operating at 1075nm wavelength (IPG Photonics Corp.). The chemical composition of powders complies with the ASTM B348 (grade 23) standard for surgical implant applications. It was found that the micro hardness,

Young's modulus and microstructure depend on the build orientation of the samples. The horizontally built sample, had the highest hardness, and the sample which was grown at an angle of 30 degrees, had the lowest hardness and elastic modulus. The presence of tensile residual stresses was found in as-built samples. Level of residual stresses in the samples depends on the build orientation also. Dependence of mechanical properties on the direction of construction of the SLM sample is explained by cyclic heating during its manufacture. During the selective laser melting process, the heating and rapid cooling of each molten layer occurs cyclically as the laser is scanned and the next layer of powder is added. A change in the width of the construction zone changes the boundaries of the temperature zone (its length) into which each layer gets into during the operation of the laser. The narrower the scanning area, the narrower the temperature range during thermal cycling. The maximum temperature for narrow and wide samples is the same, but the narrow zone warms up and cools faster.

This work was supported by Russian Found of Basic Research N 17-03-00084, State programs: "Diagnostics" AAA-A18-118020690196-3 and "Pressure" AAA-A18-118020190104-3.

10:30-10:45 Tea Break

10:45-11:10 Invited

Ultra Low Cost Powders for Additive Manufacturing of Ti and Ti Alloys

Ming Yan, Southern University of Science and Technology, China

In recent years, people have made significant progress in terms of hardware development, i.e. the various 3D printers, for additive manufacturing & 3D printing. The raw materials end, however, is only slowly moving forward. People in both research sector and in business world have to face the pressure from high cost on raw materials, i.e. the expensive AM powders, particularly Ti powders, which is one of the main contributing factors to a still very limited industry size for the AM technology. We report in this presentation our latest efforts in developing ultra low cost but high performance AM Ti and Ti alloys that is based on modifying the hydrogenation-dehydrogenation (HDH) Ti powder. We will show that not only cost-effective CP-Ti can be produced into excellent mechnical properties using our approach, but also those typical important Ti alloys such as Ti1023 and Ti-6Al-4V, as well as Ti-based composite such as Ti+TiB_2.
Implications of the results will be discussed; pros and cons of the current approach will be analysed. Future direction will be addressed in the report as well. It is believed that the findings will make decent impacts to the rapid development of the AM Ti business as well as its R&D.

11:10-11:30

Ultrahigh-Properties TiNi Shape Memory Alloys by 4D Printing

Chao Yang, China University of Technology, China

With the significant advancements in additive manufacturing or 3D printing, the terminology of 4D printing is introduced to witness technological evolution. In essence, 4D printing is 3D printing of intelligent materials. Until now, 4D printing is applicable usually to polymers, rarely to TiNi shape memory alloys (SMAs). Additionally, 3D printing provides great flexibility in obtaining controlled microstructures by nonequilibrium rapid solidification resulted from complicated combination of manufacturing parameters. Undoubtedly, the two aspects improve the difficulty level in achieving desired properties by tailoring microstructures and manufacturing parameters.
Recently, a limited number of attempts have been made by selective laser melting (SLM). These works mainly focus on Ni-rich TiNi SMAs, and confirm exactly that energy inputs applied to SLM of TiNi SMAs is low enough, generally in the range of 50~100J/mm^3. Also, related contents investigated cover various properties of damping property and Elinvar effect, superelasticity under compression, actuation response, and mechanical properties, in addition to microstructure evolution. As the most preferential properties needed to be considered, unfortunately, mechanical properties of SLMed TiNi SMAs have been paid much attention but little progress has been made in previous works. This is embodied by that these mechanical properties were tested mostly under compressive conditions, probably owing to the coexistence of micro-pores and micro-cracks in SLMed TiNi SMAs. Until now, only reported tensile properties by SLM is 606MPa ultimate tensile strength and 6.8% elongation aiming to the alloy Ni-rich NiTi. This scenario raises an interesting question. For TiNi SMAs, can they be manufactured by 4D printing (or SLM) to achieve high properties specifically under high enough energy inputs?
In this work, ultrahigh-properties Ti-rich TiNi shape memory alloys (SMAs) were fabricated by 4D printing of selective laser melting under high enough energy inputs. Interestingly, the printed SMAs have ultrahigh ultimate tensile strength and elongation, about 200MPa and 2% higher than published values of equivalent materials, respectively. Meanwhile, their shape memory effect is far greater than that of equivalent materials. Accordingly, this work substantiates, for the first time, high enough energy inputs in SLM can be applied to print ultrahigh-properties TiNi SMAs.

11:30-11:50

Optimizing HIP Parameters for EBM Ti-6Al-4V

Chuanlong Hao, Anders Eklund, James Shipley, Quintus Technologies AB,China

Hot isostatic pressing (HIP) is widely used today to

eliminate internal defects in metallic materials produced by powder bed fusion. The internal defects are mostly lack-of-fusion defects generated during the printing process and entrapped gas porosity coming from the powder particles. These defects acts like stress concentrations and crack initiation points in the material which decreases the material properties. By eliminating these defects within the material, the ductility and especially the fatigue properties are improved.

But after HIP, normally the yield strength of the AM part will decrease, an investigation of HIP parameters for EBM Ti-6Al-4V has been performed by Arcam AB and Quintus Technologies AB with the aim to maximize the strength of the HIP:ed material. A lower HIP temperature of 800˚C and a higher pressure of 200MPa gives the highest strength and is also enough to eliminate all internal defects. By printing material with intentionally induced porosity combined with an optimized HIP cycle the highest strength can be obtained.

In another project, the influence of hot isostatic pressing (HIP) and thermal cycling as standalone post processing techniques on the microstructure of electron beam powder bed deposited Ti-6Al-4V has been investigated. Electron beam powder bed deposition is an effective technology for fabricating complex net shape components that cannot be manufactured with conventional processes. However, material deposited by this technology results in columnar grain growth which is detrimental for many applications. For Ti-6Al-4V, it has been found that thermal cycling alone is not sufficient to breakdown the columnar microstructure that is typical of electron beam powder bed technology. HIP, on the other hand, has the potential to be an effective technique to break down the columnar microstructure of Ti-6Al-4V into a more equiaxed and refined grain structure, and provide a more homogeneous microstructure compared to the thermally cycled samples. Based on the unique thermal cycle and the application of pressure in the HIP vessel, Ti-6Al-4V e-beam deposited microstructures were modified from columnar grain growth to equiaxed microstructures; a significant outcome to this collaboration.

11:50-12:10

Selective Electron Beam Melting (SEBM) Fabricated Ti-6Al-4V Cantilever Struts for Lattice Design

Xuezhe Zhang, Northwest Institute for Nonferrous Metal Research, China / RMIT University, China; Huiping Tang, Northwest Institute for Nonferrous Metal Research, China; Qian Ma, RMIT University, China

Ti-6Al-4V lattices can relegate the modulus of solid Ti-6Al-4V to match with the modulus properties of various human bones and offer an innovative biological form for fixation by promoting bone tissue ingrowth into its open-celled structures. In addition, lattice-like open cellular structures are more conducive to inserting antibiotics to eliminate or help control infection. Fine metal lattice structures are finding increasing applications enabled by the powder-bed-fusion based additive manufacturing (AM) processes including selective electron beam manufacturing (SEBM). We report a systematic study of the SEBM manufacturability of Ti-6Al-4V cantilever struts with design diameters ranging from 0.05mm to 3.0mm and inclination angles from 0° to 90°, totaling 165 samples. Detailed characterization was made of these samples in terms of the discrepancy between design and manufactured diameters, surface roughness, and three-dimensional (3D) internal defect features. Manufactured struts with design diameters in the range of 0.1~1.5mm turned out to be oversized (i.e., > design diameter) while those with design diameters of 2.0~2.5mm were undersized. Strut surface roughness depends on both the design diameter and the inclination angle, but the latter is more influential. Struts manufactured at small inclination angles contain more lack-of-fusion defects per unit volume than do those manufactured at large inclination angles due to the much increased hatch line length in the former case. The comprehensive experimental data provide an essential manufacturability database for design of SEBM Ti-6Al-4V lattices.

12:10-12:30

Microstructure and Mechanical Properties of In-Situ Laser Additive Manufactured Ti-Mo Alloys

Nan Kang, Kai Wu, Qiuge Li, Xin Lin, Weidong Huang, Northwestern Ploytechnical University, China

Laser additive manufacturing (LAM) process is used to produce the self-standing 3D parts in complex morphology without any material waste. In general, the powder mixture, which used as feedstock materials in LAM, always bring the undesirable problems in microstructure and then mechanical properties, given to the inhomogeneous chemical composition and stability. The Ti-7.5Mo alloy possesses a metastable α" phase after rapid solidification process and the α" phase shows low Young's modulus with low content of Mo, which could reduce the density of implant replacement. In this work, the almost dense Ti-Mo alloy (over 99.5%) was manufactured by LAM from powder mixture of pure Ti and pure Mo (7.5wt.%). Then, microstructure was determined by using XRD, SEM, EBSD and TEM with focus on grain size, phase, residual stress and dislocation. As the laser scanning speed decreases from 1700mm/s to 1000mm/s, the sample's relative density increases from 85.5% to 99.5%. The microstructural analysis indicates that Mo particle was mostly fully melted during laser melting. But, some large sized Mo particles

were partial melted, which possesses gradient interface structure. Then, the tensile properties of as-fabricated samples under several laser scanning speeds were determined. The results shows that the as-fabricated dense sample presents Young's modulus, ultimate tensile strength and strain at failure about of 70GPa, 740MPa and 9.2% respectively. During the SLM process, the Mo, which possesses high melting temperature, was partial melted and then driven by Marangoni flow in molten pool. Thus, the micro-segregation appears with the result of this special conchoid structure. The reason behind it can be attributed to the formation of sandwich structure, which consists by hcp α-Ti and bcc β-Ti. Given to it, the Young's modulus reduced from 110GPa to about 70GPa with stable phase. Given to this low Young's modulus, which is approximate to bone of 30GPa, the LAM processed Ti-7.5Mo shows great application potential in implant component.

12:30-12:50

Simulation of Ti-6-4 β Phase Grain Evolution during Additive Manufacturing

Weizhao Sun, Tao Jing, Tsinghua University, China; Feihu Shan, AVIC Manufacturing Technology Institute, China; Hongbiao Dong, University of Leicester, UK

To predict and further control β phase grain evolution of Ti-6-4 during additive manufacturing (AM), modelling and simulation will play a critical role. The key is to fill the gap between processing modelling (~mm) and microstructure/grain evolution modelling (~μm) and make a compromise between computational precision and efficiency. In this study, combined with thermal field calculated previously and independently, kinetic Monte Carlo (MC) and a novel probabilistic cell captured method are applied to simulate the β phase grain evolution during recrystallizing, coarsening, melting and solidifying. Specially, the probabilistic cell captured method is to deal with grain front-tracking during solidification. The accuracy of simulation is validated by experiments in both qualitative and quantitative ways. The texture featured substrate, recrystallized and coarsened grains featured heat affected zone (HAZ) and epitaxial growing and coarse grain featured fusion zone (FZ) are demonstrated in order. Two characters distinguished in AM, i.e. curved growth and epitaxial growth, are well computed. The distribution of grain size agrees with that from experiments to some degree. Besides, formation mechanisms of artificial equiaxed dominated region are also revealed, which originate from the competition between grains normal to the plane and those in the plane. We believe that the multi-scale framework helps predicting grains evolution efficiently and accurately.

O. Electronic and Spin Electronic Materials: II

Symposium Organizers :

Hongda Chen, Institute of Semiconductors, Chinese Academy of Sciences, China; Feng Pan, Tsinghua University, China; Rie Y. Umetsu(Ms.), Tohoku University, Japan; Joonyeon Chang, Korea Institute of Science and Technology (KIST), Korea; Lianzhou Wang, University of Queensland, Australia

Tuesday AM
August 20, 2019

Room: 312 (3rd Floor)
Symposium: O

Chairs:
Hongda Chen, Institute of Semiconductors, Chinese Academy of Sciences, China
Feng Pan, Tsinghua University, China
Rie Y. Umetsu, Tohoku University, Japan
Joonyeon Chang, Korea Institute of Science and Technology, Korea
Lianzhou Wang, The University of Queensland, Austraila

8:30-9:00 Keynote

Spin-Orbit Interaction at Epitaxial Fe/GaAs Interfaces & Spin Injection and Detection in 2DES

Dieter Weiss, University of Regensburg, German

All-electrical spin injection, detection and manipulation by using spin-orbit interaction (SOI) are at the heart of semiconductor spintronics with the Datta-Das spin transistor as an example, which uses all three ingredients. SOI provides also a promising avenue for switching magnetization electrically.
In my presentation, I am going to discuss two topics, SOI at epitaxial Fe/GaAs interfaces and electrical spin injection and detection in a two-dimensional electron system (2DES). An epitaxially grown Fe layer on top of doped or undoped GaAs is a particularly clean system to study SOI and features both Rashba- and Dresselhaus SOI at its interface. Experimental manifestations of the latter is an anisotropic tunneling magnetoresistance (TAMR) and crystalline anisotropic magnetoresistance (CAMR). Driving an electrical current through the iron layer generates, due to the interfacial spin-orbit fields (SOFs), a spin-orbit torque acting on the iron's magnetization. The strength and the direction of the interfacial spin orbit fields can be influenced via an applied gate voltage at a Schottky diode, thus tuning the interfacial electric field.
Despite significant experimental efforts during the last decades, spin-injection into 2DES showed discouragingly low spin signals DR with DR/R<1%. Here, I discuss our recent experiments on all electrical spin injection and detection in 2DES using (Ga,Mn)As/GaAs Esaki diode junctions as spin sensitive contacts, which show large spin signals with DR/R up to 80%, in standard spin valve geometry. In contrast to non-local measurements,

the two ferromagnetic contacts serve as both injector and detector of spins. For low bias currents, the size of the spin signal can be tuned by means of gates placed outside the current path employing the difference in spin accumulation in open and closed systems.
Work carried out in collaboration with Mariusz Ciorga, Franz Eberle, Jürgen Moser, Martin Oltscher, Thomas Hupfauer, Lin Chen, Werner Wegscheider, Dieter Schuh, Martin Utz, Dominique Bougeard, Martin Gmitra, Alex-Matos Abiague, Jaroslav Fabian, Christian Back

9:00-9:30 Keynote

Spin-Orbit Torque in Epitaxial Pt/Co Bilayer Systems

Junsaku Nitta, Tohoku University, Japan

The Rashba spin orbit coupling (SOC) induced by structural inversion asymmetry is now at the heart of condensed matter physics and its applications for spin-orbitronics. The spin-orbit torque (SOT) is expected to be an innovative way towards fast domain wall motion and magnetization switching. There are two possible origins for the SOT in heavy metal/ferromagnet (HM/FM) bilayer systems, namely, the Rashba-Edelstein effect (REE) at the interface and the bulk spin Hall effect. Although a large spin splitting due to the Rashba SOC is observed at the surfaces of HMs, the contribution of the Rashba SOC in the HM/FM systems is still controversial. It is required to enhance the SOT efficiency by clarifying the origins.We have found that the D' yakonov-Perel' spin relaxation mechanism due to the Rashba SOC in epitaxial Pt thin films is dominant over the Elliot-Yafet mechanism. Here in this work, we compared the SOT efficiencies between epitaxial and polycrystalline Pt/Co bilayers from spin Hall magnetoresistance (SMR) and spin torque ferromagnetic resonance (ST-FMR) measurements. The average roughness of the Pt/Co interface for epi-samples is determined to be below 0.1nm from the X-ray reflectivity measurement, demonstrating interfacial flatness at the atomic scale. In contrast, the roughness for poly-Pt/Co interface is above 0.3nm. The SMR and ST-FMR measurements demonstrate enhancement of SOT efficiency in epi-samples with Pt films having lower resistivity than poly- samples. This result is different from the previous reports and suggests that the REE at the Pt/Co interface plays a role for the enhancement. Our study provides experimental evidence that SOT can be significantly modulated with hetero-interface control.

9:30-10:00 Keynote

Manipulating Exchange Bias by Spin-Orbit Torque

Chih-Huang Lai, Pohung Lin, Boyuan Yang, Hsiu-Hau Lin, National Tsing Hua University, China

Exchange bias (EB) effect, arising from the interfacial coupling between a ferromagnetic (FM) layer and an adjacent antiferromagnetic (AFM) layer, may lead to a unidirectional pinning of the FM, manifesting a shift in the hysteresis loop. Ever since its discovery about 60 years ago, it has wide implications in fundamental science explorations and numerous device applications such as spin valves and magnetic random access memory (MRAM). It is generally believed that the exchange coupling at the FM/AFM interface and the AFM configurations are of crucial importance. However, these two properties are hard to probe experimentally because the volume fraction of the interface is small and the net moment of AFM layer virtually vanishes. On the other hand, by applying electrical current pulses, it has been demonstrated that the generated spin-orbit torque (SOT) serves as an effective means to manipulate the magnetization of the FM layer. To explore the possibility of electrical manipulation for EB, we investigate the SOT switching in the NM/FM/AFM tri-layer system, where NM is a non-magnetic layer (Pt) with strong spin-orbit interaction, and FM and AFM layers consist of Co and IrMn respectively. The SOT generated by current pulse causes concurrent switching of FM magnetization and EB together. This is strikingly different from the SOT switching with uniaxial anisotropy in all previous studies. The current-pulse method to manipulate EB we found here is fundamentally different from the conventional field-annealing approach. This implies that the ferromagnetic magnetization and exchange bias can be manipulated independently. Our work demonstrates that spin-orbit torque in ferromagnet/antiferromagnet heterostructures facilitates independent manipulations of distinct magnetic properties, motivating innovative designs for future spintronics devices.

10:00-10:25 Invited

Complementary Logic Operation Based on Spin-Orbit Torque

Byong-Guk Park, Korea Advanced Institute of Science and Technology, Korea

Nowadays, a rapid increase in power consumption of semiconductor-based memory and logic devices in computers and mobile phones is one of the most challenging technical issues to overcome. To this regard, spintronic devices as alternatives to traditional semiconductor-based electronic devices attract considerable interest as they offer zero quiescent power, built-in memory, scalability, and reconfigurability. To realize spintronic logic gates for practical use, a complementary logic operation is essential but still missing despite recent progress in spin-based logic devices. Here, we report the development of a complementary spin logic device using electric-field controlled spin-orbit torque (SOT) switching. In heavy metal/ferromagnet/oxide structures, the critical current for SOT-induced switching of perpendicular magnetization is efficiently modulated by an electric field via voltage-controlled magnetic anisotropy (VCMA) effect in a non-volatile manner. This facilitates the

basic working principle of the spin logic performing a programmable logic operation based on the gate voltage and input clock current. Moreover, the polarity of the VCMA is tuned by the modification of oxidation state at the ferromagnet/oxide interface. This allows us to fabricate both "n-type" and "p-type" spin logic devices and to enable a complementary logic operation, paving the way for the development of non-volatile and reconfigurable logic devices.

10:30-10:45 Tea Break

10:45-11:15 Keynote

Spin-Orbit Torque Switching in Heavy Metal-Ferromagnet Junctions for Memory Devices

Young Keun Kim, Korea University, Korea

Switching magnetization direction of a ferromagnetic layer with high speed as well as low energy consumption has drawn emerging technological interest, for example, in the area of next-generation magnetic random access memory (MRAM) applications. Lately, a new switching principle so called spin-orbit torque (SOT) switching has been discovered in various sets of junctions consisting of nonmagnet (NM)/ferromagnet (FM)/oxide/capping layers such as (Ta, W)/CoFeB/MgO. In these junctions, an in-plane current injection induces magnetization reversal in perpendicularly magnetized layers. This switching is resulted from the spin-orbit interaction of either spin Hall effect or Rashba origin or mixed of the two. Therefore, many research efforts are being pursued worldwide to understand underlying physics, to search new sets of HM/FM material systems and device structures, and to manipulate interfacial structures to get high SOT efficiencies beneficial for reducing critical current densities for switching. Being the 5d heavy metals, Ta and W have large spin-orbit coupling and are compatible with semiconductor processing. We investigate variations of SOT in Ta/W/CoFeB/MgO Hall bars as a function of the W insertion layer thickness. The SOT efficiency increases as the W thickness increases and reaches its maximum at 1.5~2.0nm, and then reduces as W thickness increases further. Microstructural analyses by x-ray microdiffraction suggest that the crystal phase of W changes from beta- to alpha-phase as the W thickness increases.

11:15-11:40 Invited

Heat Controlled Magnetic Anisotropy Effect

Minori Goto, Yosuke Wakatake, Ugwumsinachi Oji, Natsumi Furuichi, Shinji Miwa, Osaka University, Japan; Nikita Strelkov, Bernard Dieny, Grenoble Alpes University, Japan; Hitoshi Kubota, Kay Yakushiji, Akio Fukushima, Shinji Yuasa, National Institute of Advanced Industrial Science and Technology, Japan; Yoshishige Suzuki, Osaka University, Japan

Fast and efficient spin-torque is significant for realizing communication, memory, and neuromorphic devices in spintronics. The electrical control of magnetic anisotropy is one of the promising techniques for generating spin-torque. In this study, we report that the Joule heating can generate fast and efficient spin-torque in nano-scale system.Fast and efficient spin-torque is significant for realizing communication, memory, and neuromorphic devices in spintronics. The electrical control of magnetic anisotropy is one of the promising techniques for generating spin-torque. In this study, we report that the Joule heating can generate fast and efficient spin-torque in nano-scale system.

In general, the heat engine in macro-scale is slow and efficient, on the other hand, that in nano-scale is fast and inefficient because of rapid heat dissipation in nano-scale. To control the heat efficiency and speed, the interfacial thermal conductivity is important. The film stack, buffer layer | CoFeB(2) reference layer | MgO(1.1) | FeB(1.7) free layer | MgO(1.0) | cap layer, was deposited on Si | SiO_2 substrate (nm in thickness). The Fe|MgO interface has low thermal conductivity which enhances the temperature increase in free layer. The magnetic anisotropy as a function of voltage is measured by spin-torque diode technique. We characterized the magnitude of heat controlled magnetic anisotropy (HCMA) as −5.3 μJ/Wm.

The advantage of HCMA compared to the voltage controlled magnetic anisotropy (VCMA) is that the Joule heating can control not only the interfacial anisotropy but bulk anisotropy. One of the promising applications to control the bulk anisotropy is magnetic dot reservoir system. Because its interaction is dipole coupling, thicker film is preferable, and in this case, HCMA is feasible.The advantage of HCMA compared to the voltage controlled magnetic anisotropy (VCMA) is that the Joule heating can control not only the interfacial anisotropy but bulk anisotropy. One of the promising applications to control the bulk anisotropy is magnetic dot reservoir system. Because its interaction is dipole coupling, thicker film is preferable, and in this case, HCMA is feasible.

11:40-12:00

Spin Valve Effect Induced by Spin-Orbit Torque Switching

Ruiqi Zhang, Cheng Song, Feng Pan, Tsinghua University, China; Jian Su, Jianwang Cai, Institute of Physics, Chinese Academy of Sciences, China

The spin valve effect in sandwich structures stands out as a seminal phenomenon in the emerging field of spintronics, read head, magnetic memories, magnetic sensors, and isolators, etc. In general, the spin valve effect is obtained via scanning the magnetic field. There is a great demand on the low power consumption for spintronics, thus electrical (current and electric field) switching of magnetization becomes the mainstream. High and low resistance states can be achieved by

these electrical means, giving rise to hysteresis loop-like switching curves, but no spin valve-like switching behavior has been realized.
Here we investigate a spin valve effect via spin-orbit torque switching in perpendicularly magnetized CoFeB/Mo/CoFeB sandwiches where the two CoFeB layers are ferromagnetically coupled. Spin current generated in the Mo space layer flows upward and downward, causing the seperate switching of the two CoFeB layers. When scanning the current, the two CoFeB layers can be switched from one antiparallel state to a parallel state, and then to the other antiparallel state, producing an unprecedentedly current-dependent spin valve effect. Such a spin valve-like switching is sensitive to the additional magnetic field direction. We successfully replicate the experimental observations by the Landau-Lifshitz-Gilbert equation simulation. Besides the fundamental interest, our finding would add a different dimension to energy efficient memories and sensors.

P. Dynamic Behaviour of Materials:I

Symposium Organizers :

Marc Andre Meyers, University of California, USA; Na Yan, Northwestern Polytechnical University, China

Tuesday AM
August 20, 2019

Room: VIP (1st Floor)
Symposium: P

Chairs:
Lanhong Dai, Institute of Mechanics, China
Na Yan, Northwestern Polytechnical University, China

8:30-9:00 Keynote

Superior Dynamic Response of CrCoNi-Based High-Entropy Alloys

Marc Andre Meyers, University of California, San Diego, United States

High impact resistance of the CrCoNi-based high-entropy alloys (HEAs) is expected from their excellent high-strain-rate plasticity. The high strain-hardening ability of the Al0.3CoFeCrNi and CrMnFeCoNi high-entropy alloys, enabled by solid-solution hardening, forest dislocation hardening, and mechanical twinning, marked strain-rate sensitivity and modest thermal softening, result in an excellent resistance to shear localization. The resistance to shear localization was studied by dynamically-loading hat-shaped specimens to induce forced shear localization. However, no adiabatic shear band could be observed for Al0.3CoCrFeNi high-entropy alloy. For the CrMnFeCoNi high-entropy alloy, a shear strain of ~7 has been found to be required for shear-band propagation (using a hat-shaped specimen that enables one single shear band to initiate and grow). This compares very favorably to a shear strain of ~1 for a Ti-6Al-4V alloy, ~3 for 1006 steel and ~5.5 for copper. The superior resistance to shear localization is originated from twinning due to its low stacking-fault energy. We build the slip-twinning relationship for CrMnFeCoNi high-entropy alloy. Dislocation prefers to slip at low strain-rates and high temperature. In comparison, twinning happens at high strain-rates and low temperatures. In addition, twinning often happens at a larger strain when dislocation slip gets difficult. Recrystallized ultrafine-grained grains (diameters of 100~300nm) are revealed inside the shear band. Their formation is explained by the classical rotational dynamic recrystallization mechanism. A high density of recrystallization twins was formed in the CrMnFeCoNi high-entropy alloy during the dynamic recrystallization process inside the shear band. The “pop-out” mechanism does not require concurrent grain-boundary movement for the formation of recrystallization (or annealing) twins and is therefore a possible mechanism, enabled by the lower stacking-fault energy. Results on shock hardening (front surface) and spalling (rear surface) of the CrMnFeCoNi high-entropy alloy employing laser ablation shock compression have also been revealed. The remarkable high-strain-rate plasticity is significant for ballistic applications.

9:00-9:25 Invited

Bioinspired Ceramic/Polymer Segmented Armour

Pedro Miranda, University of Extremadura, Spain

Here we report on the development of multi-segmented ceramic/polymer armour elements inspired in the armadillo and boxfish carapaces, which consist of rigid hexagonal segments connected by collagen fibres. This ingenious armour design, created by nature through billions of years of evolution, ensures protection as well as flexibility. First, finite element modelling (FEM) is used to analyse the effect of scale geometry and other impact parameters on the ballistic protection provided by a segmented ceramic armour. The impact of cylindrical fragment simulating projectiles (FSPs) onto alumina-epoxy scaled plates is simulated, while scale geometrical parameters (size, thickness and shape) and impact conditions (FSP diameter, speed, location) are varied. The amount of damage produced in the ceramic tiles and the final residual velocity of the FSP after the impact are evaluated. Segmentation drastically reduces the size of the damaged area without significantly reducing the ballistic protection in centred impact, provided the tile size is kept over a critical value. Such critical tile size (~20mm for impacts at 650m/s) is independent of the scale thickness, but decreases with projectile speed, although never below the diameter of the projectile. Off-centred impacts reduce the ballistic protection and increase the damaged area, but an appropriate tile shape can minimize this effect. Hexagonal scales, like those found in the natural dermal armours of the

boxfish and armadillo, are found to be optimal, with ballistic protection varying by less than 12% with impact location. Preliminary results on the fabrication and characterization of the proposed ceramic/polymer segmented armours are also presented; and design guidelines for the fabrication of segmented protection systems are discussed.

9:25-9:50 Invited

The Effect of Texture on the Evolution of Adiabatic Shear Band: Experiment and Simulation

Tao Suo, Northwestern Polytechnical University, China

The dynamic (or high strain rate) responses of nanostructured face-centered-cubic alloys with different stacking fault energies after severe plastic deformation (ECAP, equal channel angular pressing) were investigated under uniaxial compression. It is found that adiabatic shear bands were easier to appear in those alloys with lower stacking fault energy, even though under quasi-static loading more obvious hardening behavior was observed with decreasing stacking fault energy. To understand the formation mechanism of adiabatic shear bands, firstly thermal softening during dynamic loading was considered. Dynamic tests within a wide range of temperature and interrupted loading revealed that adiabatic temperature rise prior to plastic instability has only minor effect on the onset of shear localization. Unlike medium/high stacking fault energy materials, strong textures have always been reported after severe plastic deformation in the metals with low stacking fault energy. Hence, influence of texture on the propensity to adiabatic shear bands was taken into account. The dynamic anisotropic behaviors show that the pre-existing texture formed during severe plastic deformation is responsible for the initiation of localized deformation, and the adiabatic temperature rise in the localized region promotes the formation of adiabatic shear bands. For understanding the mechanism for adibatic shear l; ocalization int this unuausal naostructured face centered cubic (FCC) metal, the crystal plasticity mehod was emplyed. To verify the effect of texture on the formation of adiabatic shear bands we have incorporated preferred orientation of grains into finite element modeling based on crystal plasticity. An elastic-viscoplastic continuum slip constitutive relation was adopted to describe the mechanical response of materials, in which the dependence of slip systems' resistance on the temperature evolution was also considered. The simulation results are in good accordance with the experimental results. As such a more comprehensive picture of the formation of adiabatic shear bands in such materials has been uncovered along with the underlying mechanism.

9:50-10:10

Effect of Microstructural Aspects in the Heat-Affected Zone (HAZ) of High Strength Pipeline Steels on the Stress Corrosion Cracking (SCC) Mechanism : in Simulated Acidic Soil Solution

Xueda Li, China University of Petroleum (East), China

Three types of microstructure, which consist of bainite/ferrite matrix and varied distribution of martensite-austenite (M-A) constituent, in the heat-affected zone (HAZ) of high strength pipeline steel were simulated using Gleeble simulation. Effect of microstructural aspects on the stress corrosion cracking (SCC) behavior was studied through slow strain rate tensile (SSRT) test in simulated acid soil solution at open circuit potential. The results showed that three types of microstructure exhibited significant difference in the SCC sensitivity. Analysis on the SCC mechanism showed that the distribution of martensite-austenite (M-A) constituent had large effect on the initiation of SCC microcracks. Galvanic effect and stress concentration between M-A and matrix, as well as hydrogen involvement are attributed to assist the formation of microholes at M-A/matrix interface, and SCC microcracks could readily nucleate through coalescence of these microvoids, especially when the M-A constituent are in continuously distributed along the prior austenite grain boundaries. Consequently, distribution of M-A constituent had large effect on the SCC sensitivity. When the M-A constituent was in dispersive state, the SCC sensitivity was low. As to the propagation, SCC microcracks preferred to propagate along the interface between elongated M-A constituent and upper bainite laths, whereas acicular ferrite and quasi-polygonal ferrite could inhibit the crack propagation. The present work revealed the SCC mechanism from the perspective of initiation and propagation process of SCC cracks, which can give contribution to the welding design and microstructure control in the HAZ.

10:10-10:30

Microstructure and Mechanical Properties of Ti-6Al-4V Titanium Alloy under Laser Processing

Chen Zhen, Central South University, China

Ti-6Al-4V titanium alloy is a typical α-β two-phase titanium alloy containing 6% α stable element Al and 4% β stable element V and widely used in aerospace medical fields. Laser welding is a solid-state connection process that can melt a material in a very short time and cooling rapidly. Microstructure and mechanical properties of the Ti-6Al-4V titanium alloy under laser welding was investigated by optical microscope (OM), electron probe microanalysis (EPMA), transmission electron microscope(TEM) and

nanoindentation, respectively. Results show that the structure of the hardened phase in melting is very tiny, and the microstructure of the titanium alloy consist of crossed β-phase lath crystals and nanosized equiaxial grains. On the one hand, the martensite nucleates at the edge of β-phase lath crystals, and the other lattice remodeling through shear phase transformation forms a more staggered martensite structure. On the other hand, nanograins appear at the intersection of the crossed β-phase laths. The heat-affected zone near the welding core is composed of residual α phase and the lath acicular structure. In terms of mechanical properties, the tensile strength of the welded joint is higher than the matrix and the microhardness values of the titanium alloy increases from the matrix to the welding zone. The nanoindentation tests show that during the loading stage, the applied load in the ultrafine grains in the weld zone is larger than that for the heat-affected zone grain and matrix grains under the same displacement. The displacement of the weld zone is approximately 200nm, which is consistent with the width of the martensite observed in the TEM. During the holding time, the creep displacement value of the melt zone is the smallest, indicating that the creep resistance of the melt zone is better than matrix. Formation of the microstructure of titanium alloy under the laser processing is discussed at the final section.

10:30-10:45 Tea Break

10:45-11:15 Keynote

Dynamic Fracture of Metallic Glasses under Shock Loadings

Lanhong Dai, Chinese Academy of Sciences, China

Bulk metallic glass (BMGs), due to lack of long-range order and the absence of tranditional defects such as dislocations and grain boundaries, have a series of intrinsic mechanical properties. Although considerable works on fracture behavior of BMGs have been made during past decades, how BMGs fail at impact loadings is relatively unclear. In this talk, we will demonstrate the physical picture of dynamic microdamage nucleation and evolution of BMGs under shock loadings and reveal the underlying mechanism via couple of examples, including spallation, cavitation instability, dynamic fracture surface pattern evolution etc. For study of spallation behavior of BMGs, we develop a multi-stress pulse technique via the specially designed double flyers based upon single-stage light gas gun. This technique leads the samples to be subjected to dynamic tensile loadings of identical amplitude but with different durations. By using this technique, spallation fracture is revealed clearly to be originated from microvoid. Furthermore, theoretical model was estabilished and the explicit expressions for the void nucleation rate as well as the critical pressure for cavitation instabilities were obtained. It is found that a dimensionless inertial number controls dynamic void growth, where the inertial effects can suppress the void growth while the viscous effects will suppress vibrating growth. d growth, where the inertial effects can suppress the void growth while the viscous effects will suppress vibrating growth.

11:15-11:40 Invited

Rate-Dependent Plastic Instability Mechanisms of Aluminum Alloy with the Effect of Interface Behaviors

Pengfei Wang, Hebin Jiang, Songlin Xu, University of Science and Technology of China, China

In this work, the rate-dependent behaviors of 2A12 aluminum alloy with hollowed cylinder geometry were designed for analyzing the dynamic adiabatic shear instability mechanisms. The stress drop was observed in the stress strain curves as the strain rate increases to $3600s^{-1}$. Metallographic images of recovery specimens showed obvious localized deformation band under dynamic loading. The plastic deformation behavior with the lubricated interface state shows a prominent shear instability property, the numerical results reveal the shear band runs through the two surfaces with different interface friction coefficients. The high speed camera and digital image correlation (DIC) methods were used to analysis the instability deformation process. The initial surface state of ring-shaped specimen not only influences the onset strain and the yield strength, but also controls the duration of plastic instability stage. The formation mechanism of localized deformation bands and the constitutive equation of the stress drop stage were then theoretically analyzed.

11:40-12:05 Invited

Microstructure and Mechanical Properties of a FeCoNiCrMn High Entropy Alloy at High Velocity Loading

Bingfeng Wang, Central South University, China

The equiatomic CoCrFeMnNi high-entropy alloy owning a single-phase solid solution with the face-centered-cubic structure is one of the extensively investigated high entropy alloys. Powder metallurgy is an promising way to prepare the high-strength CoCrFeMnNi high-entropy alloy with homogeneous compositions and microstructures. The deformation behavior of the high-entropy alloy deformed under quasi-static conditions has been widely studied. However, the study of high-entropy

alloys under high strain rates (beyond $1\times10^{3}s^{-1}$) was rarely reported. As we know, the application of the high-entropy alloy often requires the study of its mechanical performance and microstructural evolution in dynamic deformation processes, such as penetration, impact cyclic loading, and shock loading. The CoCrFeMnNi high-entropy alloy prepared by powder metallurgy has homogenous microstructure and little segregations. The deformation behavior of the CoCrFeMnNi high-entropy alloy at strain rates ($1\times10^{3}s^{-1}$ to $4\times10^{5}s^{-1}$) was investigated, including the serration behavior and the shear localization of the alloy under dynamic conditions. Results indicate that the CoCrFeMnNi high-entropy alloy has only small serrations on the stress-strain curves even deformed at high strain rates (>$1000s^{-1}$), and the value of the yield strength of the powder-metallurgy high-entropy alloy CoCrFeMnNi is larger than that of the as-casting high-entropy alloy CoCrFeMnNi and the other steels. Shear band is an important deformation mechanism for the CoCrFeMnNi high entropy alloy at dynamic loading. Microstructure and mechanical properties in a shear band are investigated by the transmission electron microscope (TEM) and the nanoindentation technique. Core of the shear band is composed of ultrafine grains. It can be revealed that the ultrafine grained materials in the shear band have much higher hardness and a small strain rate sensitivity. Combined the mechanical properties obtained via the nanoindentation and the microstructure, the formation of a shear band in a CoCrFeMnNi high entropy alloy is caused by a rotational dynamic recrystallization mechanism.

12:05-12:25

Quasi-Static and Dynamic Compression Properties of Modified TC4 Titanium Alloys

Rui Liu, GRIMAT Engineering Institute Co., China

This paper aimed to study the quasi-static and dynamic properties of modifed TC4 titanium alloys. The ingots in weight of 20kg, with nominal compositions of commercial Ti-6Al-4V, Ti-6Al-3V-0.3O, and Ti-6Al-4V-0.3O-0.1B were melted, and then multi-forged into bars with 50mm in diameter. The bars were heat treated at temperatures of 30~60˚C above their β-transus temperature in purpose of obtaining homogeneous Widmannstatten microstructure. The quasi-static tensile properties were tested by MTSTM testing system at strain rate of $10^{-3}s^{-1}$. The dynamic compression properties were tested by Split Hopkinson Pressure Bar system at strain rate of 2000~$4000s^{-1}$. The results show that the quasi-static properties of Ti-6Al-3V-0.3O alloy are comparable to commercial Ti-6Al-4V alloy, while Ti-6Al-4V-0.3O-0.1B alloy shows a better strength. Among the three alloys, Ti-6Al-4V-0.3O-0.1B alloy exhibits the best bearing capacity under dynamic compression loading. Visible damages can be observed in commercial Ti-6Al-4V and Ti-6Al-3V-0.3O specimens at strain rate of 2200~$2500s^{-1}$, while in Ti-6Al-4V-0.3O-0.1B alloy at strain rate of 3200~$3500s^{-1}$. The average dynamic flow stress of Ti-6Al-3V-0.3O alloy is comparable to commercial Ti-6Al-4V, over 200MPa lower than that of Ti-6Al-4V-0.3O-0.1B alloy. The value of maximum strain during homogeneous dynamic plastic deformation of Ti-6Al-4V-0.3O-0.1B alloy is approximately 0.24, 50% ~ 60% higher than that of Ti-6Al-3V-0.3O and commercial Ti-6Al-4V alloy.

12:25-12:45

Experimental Study on 2D-C/SiC Subjected to the Unpenetrated Impact and Post-Impact Mechanical Behavior

Wei Hu, Northwestern Polytechnical University, China

In this paper, the impact behavior of 2D-C/SiC at different velocities was investigated by experimental method. The specimens were impacted at the speed of 50m/s, 70m/s, 90m/s and 110m/s respectively by a steel sphere with the diameter of 4mm. It can be seen from the picture of high-speed camera, the debris cloud size from the back of the specimen increases with the impact velocity before 90m/s. The debris cloud size was larger at 110m/s than the one at 90m/s, which indicates that the damage mode was different than before. There was double-zone damage mode on the surface of the impact area, including compression-based damage in the internal part and the tension-based damage in the annular part. At the lower velocities of 50m/s, there was no visible damage on the surface of the back side. When it comes to the speed of 70m/s, the corner fracture could be found on the edge of the specimen. The reason is that the compressive wave propagates to two related free surfaces, then the two unloading tensile waves interacted with each other. The spallation occurred at the velocity of 90m/s and 110m/s, coupled by one-fracture mode and three-fracture mode respectively. When the specimen was impacted at 110m/s, the back surface initially fractured at the center of the impact zone, followed by the two fractures near the center. The difference between the two modes can be attributed to the different interfacial strength and fiber strength. If the compressive wave is not strong enough, the unloading wave is more dissipated in the delamination instead of in the breakage of higher-strength fibers. Moreover, the DIC method was adopted to measure the strain of the impact area to understand the post-impact tensile behavior of 2D-C/SiC. As the impact velocity increases, the residual strength of the material decreases slowly initially, and then it drops sharply.

A. Advanced Steels and Processing: III

Symposium Organizers:

Han Dong, Shanghai University, China; Zhigang Yang,Tsinghua University, China; Yoshitaka Adachi, Nagoya University, Japan; Dong-Woo Suh, Pohang University of Science and Technology (POSTCEH), Korea; Christopher Hutchinson, Monash University, Australia; Amy Clarke, Colorado School of Mines, USA

Tuesday PM
August 20, 2019

Room: 205+206+207(2nd Floor)
Symposium: A

Chairs:
Xuejun Jin, Shanghai Jiaotong University, China
Wenquan Cao, Central Iron & Steel Research Institute, China

13:30-14:00 Keynote

Serrations in the Tensile Curve of C-Bearing TWIP Steel

Young-Kook Lee, Seon-Keun Oh, Yonsei University, Korea

Type A serrations in the tensile stress-strain curves of C-bearing twinning-induced plasticity (TWIP) steels without Al, Si, and Cr have been frequently observed even at room temperature when tensile testing was performed at quasi-static strain rates. It is well-known that serrations are associated with the Portevin-Le Châtelier (PLC) band, which is induced by dynamic strain aging (DSA). Because C-free TWIP steels reveal no serrations in their tensile curves, the DSA phenomenon has been primarily explained by the following two models based on C diffusion; dislocation-arrested model and reorientation model of C-Mn complexes. The dislocation-arrested model explains that DSA occurs due to the additional pinning of dislocations arrested at obstacles in advance by long-range pipe-diffused C atoms. Meanwhile, the reorientation model of C-Mn complexes explains that DSA occurs due to the obstruction of the movement of partial dislocations by the short-range reorientation of C-Mn complexes because TWIP steels have low stacking fault energy (SFE). Therefore, the DSA mechanism for type A serrations occurring in C-bearing TWIP steels is still controversial. Accordingly, in this presentation various DSA mechanisms for serrations would be introduced, and the comparatively analyzed with the assistance of new experimental results to make the room-temperature DSA mechanism occurring in C-bearing TWIP steels clear.

14:00-14:25 Invited

Revisit the Work Hardening Mechanism of TWIP Steels

Mingxin Huang, The University of Hong Kong, China

Deformation twins are frequently cited as the major mechanism responsible for the excellent mechanical properties of twinning-induced plasticity (TWIP) steels. Nevertheless, our recent experiments show that the high strain hardening rate of TWIP steel is not mainly related to the deformation twins, but is mainly caused by its high dislocation density. In addition, the deformation twins do not contribute much to the reduced average dislocation glide distance. The high dislocation density in TWIP steels is caused by the high carbon content. The TWIP steel without carbon addition has low dislocation density and low strain hardening rate, although there are intensive deformation twins generated during deformation. TWIP steels with high carbon content processes high dislocation density, even when they are deformed at 300˚C at which no deformation twins are generated. The results presented in the present work provides new understanding on the work hardening behaviour of TWIP steels. For the design of new TWIP steels which require high work hardening rate, high ultimate tensile strength, interstitial alloying elements such as C or N are required. Without the addition of interstitial alloying elements, the TWIP steels will behave as normal austenitic steel such as 316L stainless steel, which provides design guideline for future development of TWIP steels.

14:25-14:50 Invited

Development of High Strength Automotive Suspension Spring Steels with Superior Corrosion Fatigue Characteristics

Kwanho Kim, Youngsoo Chun, Byounggab Lee, Technical Research Laboratories, POSCO, Korea

The corrosion fatigue resistance of suspension spring steels has attracted more attention than ever before as the tensile strength of the steel increases for the light weighting of vehicles. This is because the automotive suspension springs are naturally exposed to corrosion environments including deicing salts and have the latent possibilities of the breakage of paintings by impacting gravels and grains of sands during driving. Furthermore, the higher strength steels are more susceptible to hydrogen embrittlement. Since the breakage of suspension springs can be attributed to the pitting corrosion and the hydrogen delayed fracture, this research was focused on both points. With regard to the pitting corrosion resistance, the Cr content plays an important role in controlling the aspect ratio of corrosion pits. The higher Cr content can make corrosion pits

deeper by reducing pH value inside of pits. The addition of Cu and Ni has a positive effect on this viewpoint. The smaller the aspect ratio of the corrosion pits on the steel surface, the longer the corrosion fatigue life. On the other hand, the resistance to hydrogen delayed fracture is enhanced by microalloying such as V, Nb, and Mo, resulting in the precipitation of nano-sized fine carbides to trap diffusible hydrogen atoms. Of many trap sites such as interfaces, precipitates, dislocations, etc, only precipitates can play as the favorable and irreversible trap site which can be manipulated metallurgically. It should be noticed that the nano-sized fine carbides used for trapping diffusible hydrogen atoms in this research is the ones not precipitated during conventional tempering process but precipitated during and after hot rolling. The developed steel shows higher tensile strength than 1950MPa after quenching and tempering, and its resistance to hydrogen delayed fracture is 2.3 times as 54SiCr6 or SAE9254 in the same strength level. By using the developed steel, the highly corrosion fatigue resistant automotive suspension springs can be available with design stress over 1300MPa.

14:50-15:10

Comparative Analysis of the Twinning Behavior and Tensile Properties in Fe-13/22Mn-1.0C TWIP Steels

Dongdong Li, Yanshan University, China

High manganese austenite twinning-induced plasticity (TWIP) steels exhibit high tensile strength and excellent plasticity, having attracted much attention. The role of Mn content in varying the tensile properties of Fe-Mn-Al-C TWIP steels has been analyzed; however, the results available in literature are different. In addition, several studies have been devoted to investigating the effect of Mn content on the tensile properties of Fe-Mn-C TWIP steels, but the results obtained are also not consistent. Obviously, it is ambiguous how Mn content affects the tensile properties and microstructure evolution in twinning-dominated high manganese austenitic steels. Here, we focus on the understanding of the tensile deformation and twinning behavior in Fe-13Mn-1.0C and Fe-22Mn-1.0C steels, at two kinds of grain size (a fine-grained and a coarse-grained).
Monotonic tensile tests were performed at room temperature, and deformation twinning versus tensile strain was examined by optical, scanning electron and transmission electron microscopes. Results show that the yield and tensile strengths of the steels exhibit a downward trend with the increase of Mn content; however, the elongation to fracture is greatly improved. Moreover, the steel with a higher Mn content shows differences in dynamic strain aging behavior, as compared with the steel with a lower Mn content. Based on the statistical analysis of the parallel lamellae twins arising from TEM images, the steel with a higher Mn content promotes the formation of thinner and denser deformation twins than the steel with a lower Mn content. Furthermore, according to SEM image results, the increasing Mn content suppresses the formation of deformation twins at low strains, but allows deformation twins to form continuously and steadily up to higher strains, which provides more persistent strain-hardening and delays the instability of plastic deformation.

15:10-15:30

Effect of Grain Boundary Characters on Low Cycle Fatigue Behavior of Hydrogen Charged High-Mn TWIP Steels

Gyeong hyeon Jang, Chong Soo Lee, GIFT, POSTECH, Korea

High-manganese twinning-induced plasticity (TWIP) steels receive great attention nowadays due to their excellent combination of tensile strength and elongation. However, TWIP steels often reveal hydrogen embrittlement (HE), i.e., hydrogen delayed fracture, leading to the catastrophic failure of the structural components. In order to prevent or suppress HE, high stacking fault alloying element such as Al is added in the TWIP steels. Recently, an alternative approach is used by the application of grain boundary engineering (GBE), a method to increase the fraction of coincidence site lattice (CSL) by imposing a small amount of strain and annealing. CSL boundary, which have lower energy state, prevents hydrogen from migrating through grain boundaries. That can prevent degradation of mechanical properties of steel without adding other alloying elements. The aim of this study is to investigate the effect of grain boundary engineering on low cycle fatigue (LCF) properties of hydrogen charged TWIP steels. High-Mn austenitic TWIP steels with compositions of Fe-17Mn-0.6 was produced by vacuum induction melting. The cast ingot was solution-treated at 1473K for 2 hours and hot-rolled to a thickness of 17mm. Using as-received TWIP steel, GBE processed TWIP steel was prepared by heat treatment at 1173K 13min after imposing 10% strain. Although the CSL fraction of GBE processed TWIP steel was increased by about 35% compared to AR, grain size and tensile properties of AR and GBE processes TWIP steels are nearly identical. Fatigue life curve results showed that LCF properties of GBE processed TWIP steels were similar to those of as-received TWIP steels in the hydrogen uncharged condition, while the degradation of low cycle fatigue life of the former was not significant in the hydrogen charged condition. Stress concentration on grain boundary under cyclic loading, however, higher fraction of CSL could relief those stress effectively than the other random boundaries.

15:30-16:10 Tea Break

16:10-16:30

Effect of Decarburization Layer on Corrosion Resistance of Low-Density Steel

Dan Liu, Xuemin Wang, Xiangyu Xu, Wei Zhang, University of Science and Technology Beijing, China

Low-density steels have a wide application prospect in marine and offshore engineering. To achieve low-density, the aluminum content in low-density steel is higher than that of traditional low-carbon steels, in addition high strength and corrosion resistance are achieved at the same time. As the aluminum content increased, the austenite phase zone was shrunk and the experimental steel cannot be completely austenitized (the volume fraction of austenite is maximized at 1160˚C), so the experimental steel was a laminated multi-phase structure. Compared with ferritic single-phase steel, there is galvanic corrosion behavior in multi-phase structure during corrosion, therefore multi-phase low-density steel has a problem of insufficient corrosion resistance. Before the hot plate rolling, the decarburization layer will inevitably form on the surface of the slab in the insulation process, which may be beneficial to improve the corrosion resistance of the experimental steel. The composition of experimental steel was Fe-0.18C-3.93Al-2.4Mn-2.0Ni-0.048 Nb-0.3Si-0.011Ti(wt.%). The decarburization rate of high-aluminum multi-phase steel is faster than that of ordinary low-carbon steel. The EPMA experiment results showed that the decarburization phenomenon of the experimental steel was accompanied by dealumination. Because the diffusion of carbon is faster than the diffusion of aluminum, dealumination phenomenon always occurs after decarburization. As the carbon content in the decarburization layer decreased, the multi-phase microstructure in the decarburization layer of the experimental steel transformed into ferrite phase, and the corrosion resistance of the ferrite is superior to that of multi-phase, so the decarburization layer contributes to improve the corrosion resistance of the experimental steel. However, dealumination is not conducive to the corrosion resistance of steel. Therefore, the thickness of the decarburized layer and the degree of dealumination should be controlled by controlling the insulation process before hot plate rolling, and the best reheating process had been achieved while the best corrosion resistance was also achieved.

16:30-16:50

Characterization of Serration Behaviors in 22Mn-0.6C Steel

Sukyoung Hwang, Yu Bai, Akinobu Shibata ,Nobuhiro Tsuji, Myeong-Heom Park, Kyoto University, Japan

High-Mn austenitic steels are well known to show the outstanding mechanical properties combining high strength and large ductility, which result from the formation of mechanical twin during deformation. On the other hand, serration behaviors are frequently observed in carbon containing high-Mn austenitic steels. Serration behaviors are often characterized by strain localization such as Portevin-Le Chatelier (PLC) bands. The PLC band is known to arise from pinning and de-pinning of mobile dislocations by interstitial carbon atoms, which is also known as dynamic strain aging (DSA). However, the role of serration behaviors on mechanical behaviors in high-Mn austenitic steels still remains unclear. The present study aims to explore nature of serration behaviors in high-Mn austenitic steel. A 22Mn-0.6C austenitic steel having fully recrystallized microstructures with a mean grain size of 5.1μm was produced through 4 cycles of the repeated cold-rolling and annealing treatment. Between every cold rolling step, the specimen was annealed at 600˚C for 0.6ks followed by water quenching to restore deformability in the next cold rolling step. Mechanical properties were evaluated by an uniaxial tensile test at room temperature at a strain rate of $8.3 \times 10^{-4}s^{-1}$. The specimen showed a good combination of strength and ductility with yield strength of 350MPa (0.2% proof stress), tensile strength of 1090MPa and total elongation of 77%. Serration behaviors during tensile tests were quantified by the aid of digital image correlation (DIC) method. It was revealed that observed serrated flows corresponded with inhomogeneous deformation in the tensile specimen, which was described as PLC bands. Serration behaviors were also evaluated by in-situ synchrotron diffraction. There was a significant change in microstructures with respect to the PLC band migration. Detailed results will be shown and discussed in the presentation.

16:50-17:10

Effect of Aging Temperature on Microstructure and Tensile Properties in a Fe-Mn-Al-C Lightweight Steel Microalloyed by Nb and Mo

Zhuang Li, Jiaxin Liang, Jinke Du, Beijing Institute of Technology, China; Yingchun Wang, Xingwang Cheng, Shukui Li, Beijing Institute of Technology, China / National Key Laboratory of Science and Technology on Materials under Shock and Impact, China

An investigation was conducted to study the effect of aging temperature over a range of 400~700˚C after solid solution treatment on the microstructure and tensile properties of Fe–27Mn-8Al–1.6C lightweight steel with addition micro-alloying elements Nb and Mo. The results show that the microstructures of the steel after solution treatment is composed of equaxied austenite grains within annealing twins and two types of nanoscale precipitates, the (Nb, Mo)C and κ-carbide,

distributed uniformly in the matrix. After aged at different temperatures, the grains are coarsened slightly with increasing aging temperature and the average grain sizes remained ~13μm without considering the annealing twins. After aging up to 600℃, the (Nb, Mo)C particles keep unchanged in size, morphology and distribution. This is considered that the Nb and Mo are both heavy so that it is difficult for them to migrate up to 600℃. Meanwhile, an increase of the nano-sized intragranular k precipitates in volume fraction and size are observed as aging temperature increases to 600℃. However, after aging at 700℃, the number of the (Nb, Mo)C particles decreases significantly with the presence of a great number of boundary k-carbides with size less than 1μm and intragranular k-carbides coarsening. By comparison with solution treatment, aging increases the strength but decreases the ductility. With aging temperature rise from 400 to 600℃, the strength increases and the ductility decreases continuously and the strain hardening capacity gradually weakens. After aging at 700℃, the strength and ductility decrease simultaneously and the strain hardening rate improves. The difference in strain hardening rate is related to the interaction between dislocations and the k-carbides and the fraction decrease of (Nb, Mo)C particles. To further study the deformation mechanism, the stacking fault energy of the lightweight steel was calculated to be ~77mJ/m^2, which is considered high enough to suppress the transformation induced plasticity(TRIP) and twinning induced plasticity(TWIP).

17:10-17:30

Origin of Resistance to Temper Softening in Low-Carbon Martensitic Steels by Microalloying of V, Nb and Ti

Yongjie Zhang, Goro Miyamoto, Tadashi Furuhara, Tohoku University, Japan

Substitutional alloying elements are generally added to martensitic steels to suppress the softening during high-temperature tempering. Strong carbide-forming alloying elements like V, Nb and Ti are particularly effective to provide resistance to temper softening. In this study, a series of Fe-0.1C-1.5Mn-0.05Si(mass%) alloys, with microalloying (up to 0.4mass%) of V, Nb and Ti, were used to investigate their alloying effects and underlying origin of resistance to tempering softening.

The as-quenched alloys were isothermally tempered at various temperatures (623~923K) for various times (60s~43.2ks). Vickers hardness of these tempered specimens was measured under the load of 9.8N, while their microstructure was characterized by optical microscopy and scanning electron microscopy. Afterward, three-dimensional atom probe and X-ray diffraction analyses were performed to reveal the nano-scale microstructural evolutions.

With similar hardness in as-quenched condition in all the alloys used, hardness of tempered martensite is increased by microalloying, particularly after treatment at higher temperature with longer time. In V-added alloys, hardness increment from the base alloy becomes larger by increasing V content. When compared with the same amount of addition, the resistance to temper softening of Nb and Ti are similar, but much stronger than the case of V. The results of atom probe measurements reveal that at higher temperature of 923K, high density of nano-sized alloy carbides are formed in those microalloyed steels. At lower temperature of 723K, however, almost no inhomogeneous distribution of V, Nb and Ti atoms can be detected. With negligible difference in the distribution of cementite by microalloying, the reduction in dislocation density during tempering is found to be strongly retarded by V, Nb and Ti additions through analyzing X-ray line profiles of the tempered specimens. This should be the major reason for their resistance to temper softening at relatively lower temperature, even without nano-precipitation of alloy carbides.

17:30-17:50

Stabilizing Austenite via a Core-Shell Structure in the Medium Mn Steels

Xinhao Wan, Yang Zhigang, Chi Zhang, Hao Chen, Tsinghua University, China

The metastable retained austenite has been found to play a significant role in the strength-ductility balance of medium Mn steels due to transformation induced plasticity (TRIP) effect during deformation, and thus its optimization is of great importance. In this contribution, a new processing route (Flash-Austenite Reversion Treatment, Flash-ART) was proposed to design retained austenite with a compositional core-shell structure in a 0.20C-7.76Mn-1.99Al (wt%) steel. This kind of core-shell structured retained austenite was experimentally verified by Nano-Auger Electron Spectroscopy-Electron Backscatter Diffraction (Nano-AES-EBSD) and Scanning Transmission Electron Microscopy (STEM). It was interestingly found that the austenite core, which should transform into martensite based on its composition and size, was stabilized by the Mn enriched shell. Flash-ART allows us to obtain more retained austenite compared with the conventional ART. The formation mechanism of core-shell structured retained austenite and its mechanical response will be discussed in details.

B. High Temperature Structural Materials: Creep, Fatigue and Deformation Behavior

Symposium Organizers:

Qiang Feng, University of Science and Technology Beijing, China; Shengkai Gong, Beihang University, China; Hyun Uk Hong, Changwon National University, Korea; Damon Kent, University of Sunshine Coast, Australia; Sammy Tin, Illinois Institute of Technology, USA; Hiroyuki Yasuda, Osaka University, Japan; Jun Zhang, Northwestern Polytechnical University, China

Tuesday PM
August 20, 2019

Room: 305 (3rd floor)
Symposium: B

Chairs:
Lin Liu, Northwestern Polytechnical University, China
Jonathan Cormier, Institut Pprime, France

13:30-14:00 Keynote

Crack Initiation Mechanisms during VHCF of Ni-Based Single Crystal Superalloys

Jonathan Cormier[1], Cervellon Alice[1], Mauget Florent[1], Hemery Samuel[1]
1. Institut Pprime, France

Ni-based single crystal superalloys (SX) are widely used in gas turbine engines for the manufacturing of high pressure turbine blades due to their exceptional mechanical properties at high temperature. Service operations of blades may lead to fatigue controlled failure mechanisms due to the vibration introduced by the gas flow in addition to the centrifugal forces. These failures are difficult to forecast, as up to 90% of the fatigue life is spent in the crack initiation phase. To study crack initiation in these materials, an uniaxial ultrasonic fatigue testing system has been developed to operate at 1000°C, 20kHz and under different stress ratios. A wide range of SX superalloys having a <001> orientation have been tested to investigate the crack initiation mechanisms. CMSX-4 SX alloy cast using a Bridgman process is taken as reference. Bridgman cast MAR-M200, AM1 and CMSX-4 Plus alloys in addition to AM1 cast using a high rate solidification process have been used to expand the database. Crack initiation sites have been carefully characterized by SEM and EBSD to identify the role of their size and localization, how plasticity develops in their vicinity as well as the most detrimental casting defects. In this presentation, a critical analysis of the VHCF life sensitivity to the casting pore size and gamma/gamma-prime microstructure degradation (i.e. gamma-prime rafting) will be performed, by using a specifically tailored crack initiation model. Moreover, for VHCF life in excess of 10^9 cycles, crack initiation occurs either through an internal Fine Granular Area (FGA) process or at the surface due to oxidation. By varying the casting process or the oxidation resistance among the different alloys studied, a map of crack initiation mechanisms in VHCF will finally be proposed for alloys. Moreover, the different stages leading to the formation of the FGA (including microstructure evolutions) and subsequent crack initiation will be detailed.

14:00-14:20

Vibration Characteristics of High Speed Rotating Blades

Hua Wei[1]
1. Zhejiang University, China

Turbine blades are one of the key high speed rotary compnents in aerocraft engines. It is very crucial to ensure the safe and reliable operation of engines. Many studies have showen that the vibration-induced blade failure is one of the important reasons resulting in blade failure. The study foucused on the investigation of the natural vibration characteristics of blades coupled with the finite element analysis and experimens performed using the atomized liquid jet excitation technology for high speed rotary blades.

The atomized liquid jet excitation platform for high speed rotary blades was designed and constructed. The in-situ stress-strain testing system under the high rotation speed was set up. The high speed electric slip rings were used to transmit strain signals which were obtained through strain gauges attached to the root of blades. The vibration characteristics of blades, such as the modal frequency and resonance amplitude, was obtained by means of the in-situ stress-strain testing system under the specific rotation speed. Using the constructed platform, the vibration characteristics of blades was studied coupled with ANSYS software. The modal analysis of blades was carried out under static condition and high rotation speed, respectively. The influence of the centrifugal force caused by the high rotation speed on the inherent vibration characteristics of blades was investigated. The harmonic response analysis of blades were also made. The vibration characteristics of blades with or without damping blocks were finally compared under high rotation speed.

The obtained results showed that with the increase in injection excitation force, the peak strain of blades increased gradually but the change of injection excitation force could not affect the resonance frequency of blades. Because of the influence of centrifugal acceleration, the measured strain values of blades were greater in the deceleration stage than in the acceleration stage. In order to obtain the strain values of high speed rotary blades as accurately as possible, it was necessary to

reduce the ratary acceleration of blades. The amplitudes of vibration strain of the damped blades were 50% lower than that of the undamped blades, and the inherent frequency of blades was reduced by 0.25%. It meaned that the damping blocks had good vibration reduction effect.

14:20-14:40

Effect of Secondary Dendrite Orientation on the Low Cycle Fatigue Behaviors of a Third Generation Ni-Base Single Crystal Superalloy

Li Wang[1], Guodong Sun[1], Yifei Li[1], Chen Li[1], Wei Zheng[1], Dong Wang[1], Langhong Lou[1], Jian Zhang[1]
1. Institute of Metal Research, Chinese Academy of Sciences, China

Effect of secondary dendrite orientation on the low cycle fatigue (LCF) behaviors of a third generation nickel-base single crystal (SX) superalloy was investigated in the present paper. SX bars were directionally solidified with high rate solidification technique. Then, those bars within 3° deviated from <001> were selected and full heat treated. LCF samples were machined with secondary dendrites about 0°, 26° and 45°, respectively, relative to the sample surfaces. To determine the role of holes on the LCF behaviors another group of samples were prepared with a hole in the center of the gauge section. LCF tests were carried out at 950°C, with a strain ratio of R=0.1. It was found that for samples without holes LCF life decreases in the sequences of secondary dendrite around 45°, 0°, and 26°. When a hole presented in the center of the gauge section, samples with secondary dendrite around 0° relative to the sample surface exhibit the longest life, and the samples with secondary dendrite around 26° experience the shortest life. It was discussed from micro to macro structures based on the oxidation, secondary dendrite orientation and the effect of the holes. Some of the LCF tests were interrupted to reveal the initiation and propagation of cracks during the process.

14:40-15:00

Re Segregation at Dislocations in the γ' Phase of Ni-Based Single Crystal Superalloys

Xiaoxiang Wu[1], Surendra Makineni[1], Baptiste Gault[1], Gunther Eggeler[1]
1. Ruhr-Universität Bochum, Germany

Ni-based single crystal superalloys have long been used as essential materials in gas turbines and power plants, due to their superior mechanical performance with respect to creep, fatigue and resistance to oxidation at elevated temperatures. The addition of a small amount of Re into Ni-based single crystal superalloys improves the creep properties significantly. However, the understanding of the role of Re is still limited and somehow unclear. Other researchers confirm that there is no observation of Re clusters at the γ matrix phase. To better understand the role of Re in superalloys and its role in creep, in the present work, we investigate the creep behavior of a second-generation Ni-based single crystal superalloy (ERBO1, equivalent to CMSX-4) at low temperature and high stress condition, using state-of-art transmission electron microscopy (TEM) and atom probe tomography (APT). We analyse the microstructure evolution in great detail for the interpretation of a peculiar double minimum creep behaviour at the primary creep stage. We report evidence of Re and Mo segregation (up to 2.6 at.% and 1 at.% resp.) along with Cr and Co to the dislocations inside of γ' precipitates after 5% creep deformation at 750°C under an applied stress of 800 MPa in the [001] orientation. The observation of Re segregating to dislocations inside of γ' precipitates is new and can be utilised for a better unserstanding of Re effect in superalloys. The observed segregation effects can be rationalized through bridging the solute partitioning behaviour across the γ/γ' interface and pipe diffusion mechanism along the core of the dislocation line. In combination with TEM investigations, the peculiar creep behaviour is further rationalised with the observed Re and Mo segregating to dislocations inside of γ' phases. The current results can improve our understanding with regard to the role of Re in Ni-based single crystal superalloys and provide new input for advanced alloy design.

15:00-15:20

Microstructure Characteristics and Tensile Behavior of Ni-Co Base Superalloy Manufactured by Additive Manufacturing

Ling Tang[1,2], Chuanyong Cui[1], Jingjing Liang[1]
1. Institute of Metal Research, Chinese Academy of Sciences, China
2. University of Science and Technology of China, China

A newly developed Ni-Co base superalloy with different contents of Co manufactured by additive manufacturing (AM) has been investigated. The microstructures were studied using OM, SEM, TEM, ICP-AES and EPMA. The results showed that the Ni-Co base superalloy made by AM showed a columnar microstructure. After heat treatments, primary γ', secondary γ' and tertiary γ' precipitated. The heat treatments also promoted the precipitation of η phase. The ICP-AES and EPMA investigation showed that loses and segregation of elements could account for the formation of η phase. Increasing of Co could promote the precipitation of γ' and decreased the segregation of Ti in the heat-treated state and was beneficial for decreasing the precipitation of η phase. The tensile tests were performed at temperatures ranging from room temperature to 800°C with a strain rate of 3×10^{-4}. The yield strength, ultimate

tensile strength, elongation, work hardening index of Ni-Co base superalloy were achieved. It has been found that yield and tensile strengths decreased and elongation showed an increasing trend with the rising of temperature. The tensile properties could be influenced by the strengthening elements and the volume of strengthening phases. In addition, columnar grain could also influence the tensile properties. Columnar grain had no transverse grain boundaries which could play an important role in strengthening at lower temperatures. What's more, the adverse effect of transverse grain boundaries at higher temperatures could also be eliminated correspondingly in columnar microstructure. The fracture observations of Ni-Co base superalloys showed that the fractures were predominately cleavage.

15:30-18:00 Tea Break

C1. Light Metals and Alloys-Aluminum: II

Symposium Organizers:

Baiqing Xiong, GRINM Group Co. Ltd., China; Yoshihito Kawamura, Kumamoto University, Japan; Young Min Kim, Korea Institute of Materials Science (KIMS), Korea; Jian-Feng Nie, Monash University, Australia; Diran Apelian, Worceste Polytechnic Institute, USA

Tuesday PM Room: Presidium Conference Room Room（4th Floor）
August 20, 2019 Symposium: C1

Chairs:
Zhihui Li, GRIMAT Engineering Institute Co., Ltd., China
Malcolm Couper, Chongqing University, China

13:30-13:55 Invited

The Relationship of Solid Solubility to the Precipitation Sequence in Aluminium Alloys

Malcolm Couper, Chongqing University, China

The room temperature equilibrium solid solubility of many elements, or combinations of elements, in aluminium is very low. For binary aluminium alloys, the highest room temperature equilibrium solubilities occur for Ga (8at%) and Mg (2.3at%), followed by Zn (approx 0.5at%), Li, and Ge, though for the latter, extrapolation from higher temperature is required (e.g. Li, 3.3at%, 500K; Ge, 0.2at%, 450K). Most other common additions to aluminium have extrapolated room temperature equilibrium solubilities of <0.01x at% with the highest being probably Ag (0.04at%) and Cu (0.02at%). In other cases the data is typically extrapolated from 500~800K. For ternary aluminium alloys, the solubility is sometimes reported to increase, for example Cu with addition of Zn (at 730K), or decrease, for example Mn with addition of Si or Zn. For Al-Mg-Si/Ge ternary alloys, the solubility is reduced by the formation of the equilibrium phase (Mg_2Si / Mg_2Ge) and further reduced by an excess of Mg. The solubility of Ge at 650K is 2at% in Al-Ge but in Al-Mg_2Ge it reduces to 0.03at%Ge. For Al-Si at 650K it is 0.24at% but in Al-Mg_2Si it reduces to 0.12at%Si. Solubilities at room temperature or normal ageing temperatures have not been reported.

Super-saturation of solute can be realised by rapid solidification or more commonly, by quenching a solid solution from a high temperature, typically within the alpha phase region, with the solution temperature as high as possible, but also recognising the need to minimise the risk of incipient melting. The subsequent precipitation has been studied extensively, with the focus on the precipitation sequence, including compositions and structures that results in age-hardening or other combinations of properties. This paper attempts to describe and interpret the somewhat limited data available on the variation of solute levels in the matrix throughout the precipitation sequence and the degree to which equilibrium solubility is approached or reached during ageing. The potential opportunities for alloy design will also be considered.

13:55-14:15

Effect of GP(I) and GP(II) Zones on Precipitation Microstructure and Hardness in A7050 Aluminum Alloy by Means of Two Step Aging

Yuta Sano, Shinji Muraishi, Yohei Harada, Shinji Kumai, Tokyo Institute of Technology, Japan

Steel fastener, bolts, nuts and screws, has been widely used for mechanical joint of various different metal parts, where the contact points of dissimilar metals by aluminum and steel acting as the site of internal stress and corrosion due to the difference of material properties, elastic modulus, thermal expansion coefficient, corrosion resistance, etc. Furthermore, during remelting process, impurity elements from steel parts are inevitably incorporated into aluminum alloy, which reduces potential recyclability of aluminum alloy. In present study, we have chosen A7050 aluminum alloy (Al-Mg-Zn based alloy) as the candidate of aluminum screw to achieve good mechanical fastening ability by age-hardening. The precipitation sequence of Al-Zn-Mg based alloy is as follows,

SSSS → GP zone → η' → η ($MgZn_2$)

Recently, existence of two types of GP zones are reported in Al-Zn-Mg alloy, which are spherical GP(I) zone and plate-shaped GP(II) zone on {111} plane. However, contribution of different types of GP zones on age-hardening behavior is still unclear. Therefore, the ageing treatment for the formation of different types of

GP zones and their roles in evolution microstructure and resultant hardness by η' phase was investigated by means of two step aging treatment at different temperatures. TEM observation revealed that the amount of {111} type GP (II) can be increased at the aging temperature ranging from 333 to 393K, where conventional spherical GP(I) are simultaneously formed with GP(II).

By conducting several different two step aging, where preferential formation of GP (I) or GP (II) is expected at the first step of aging with different temperatures (room temperature, 333, 393, 423K) and subsequent second step aging at 423K, it is found that there exists no significant difference in the peak hardness by the second step aging at 423K regardless of the preliminary formed GP zones. This implies that the effect of two different types of GP zones on the precipitation and hardening behavior of η' phase is similar by several different two step aging conditions in present study.

14:15-14:35

Study of Deformation Mechanisms in Ma-Ca Alloy by In-Situ EBSD and 3DXRD

Gaoming Zhu, Leyun Wang, Xiaoqin Zeng, Shanghai Jiaotong University, China

The addition of a small amount of Ca improves the ductility of Mg alloys. However, the mechanism underlying this effect is not well understood. In this work, in-situ tensile tests of an extruded Mg-0.47 wt.%Ca alloy were conducted both in a scanning electron microscope equipped with electron backscattered diffraction (EBSD) detector and at a synchrotron X-ray beamline with three dimensional X-ray diffraction (3DXRD) capability. EBSD-based slip trace analysis indicates strong activity of prismatic slip and pyramidal <a> slip in addition to basal slip, and the fraction of non-basal slip increased with strain. Some transmission electron microscopy (TEM) experiments were performed at the strain of 8%, <c+a> dislocations were identified under this strain. However, only <a> type dislocations were identified at the strain of 4% and below. In order to clarify the dislocation type on pyramidal I plane, a TEM sample was cut by focused ion beam (FIB) on the surface of a grain with pyramidal I slip lines at the strain of 4%. By combining slip trace analysis and TEM, the type of dislocations in this grain was identified as (1-101)[-1-120]. According to TEM experiment, we think that <a> dislocation was the dominate type on pyramidal I plane at the initial deformation stage. With the strain increasing, <c+a> dislocation plays an important role gradually. Our first-principles calculations found that solute Ca atoms would reduce the generalized stacking fault energies for slip systems in Mg. 3DXRD experiment provide orientations and stresses for grains inside the materials. We could calculate the grain rotation and stress evolution for each grain in the tensile test. Then the deformation mode was identified by calculating the grain rotation axis and grain rotation angle. In addition, the diffraction spots for each grain were tracked at every loading steps, then the deformation of specified slip system can be quantified.

14:35-14:55

Computational Process Optimization for Wrought Aluminum Alloys

Hailin Chen, Qing Chen, Thermo-Calc Software, Sweden

This work is to demonstrate the application of CALPHAD calculations and simulations to process optimization for typical wrought aluminum alloys from casting to various heat treatments. Such applications usually follow three steps:

First of all, Scheil and equilibrium calculations are performed to predict the sequence of formation of solid phases during solidification, as well as their amounts and compositions. Intermetallic compounds that form after the start of the precipitation of (Al) accounts for the particles at grain boundaries in as-cast alloys. Primary phases formed earlier than the (Al) phase are either embedded within (Al) grains or pushed to grain boundaries. Calculated compositions of the (Al) phase can be used for predicting the composition profile of the (Al) matrix and account for its compositional micro-segregation.

Secondly, thermodynamic calculations and DICTRA diffusion simulations are utilized to optimize the processing temperature and holding time for subsequent homogenization and solution treatments. With equilibrium stepping calculations, the temperature range for heat treating a specific alloy can be preliminarily determined so that the particles at grain boundaries can be dissolved completely or to a large extent. DICTRA simulations help to evaluate the holding time, which is needed for eliminating the composition segregation in the matrix and for dissolving the particles, at a selected isothermal holding temperature or to determine an optimal (more energetically and costly efficient) non-isothermal heating time-temperature profile.

Finally, TC-PRISMA is employed to simulate the precipitation kinetics during aging treatment. From the output results, typically, particle size distribution, volume fraction and particle number density, one can easily determine the peak-aging state.

14:55-15:15

Effect of Cu and Mg on the Intergranular Corrosion Properties of 2024 Aluminum Alloy

Xiang Xiao, Cheng Liu, Xiaodong Mao, Zhongyu Yang, Zeyu Zhou, Chinalco Materials Application Research Institute Co., Ltd., China

Al-Cu-Mg aluminum alloys with high specific strength, good fracture toughness, excellent fatigue damage tolerance have been found important applications in

the aerospace industry. The rapid development of aerospace industry has put forward higher and higher requirements for the comprehensive properties of Al-Cu-Mg aluminum alloy, which requires not only high strength and toughness, but also the corrosion resistance. Intergranular corrosion is the main corrosion form of Al-Cu-Mg aluminum alloy, which seriously reduce the lifetime of aircraft structural parts. In this paper, the microstructure and the intergranular corrosion behavior of 2024 alloy with varying Cu and Mg content has been studied in details by scanning electron microscope (SEM), transmission electron microscope (TEM) and three dimensional atom probe (3DAP). The results show that the there are nano-scale θ (Al_2Cu) and S (Al_2CuMg) particles precipitate along grain boundary after quenching. The nano-cluster is the main strengthening phase in the 2024 alloy after natural aging for 96 hours. The intergranular corrosion susceptibility is greatly affected by the presence of θ (Al_2Cu) and S (Al_2CuMg) phase along grain boundary. Specifically, Cu-rich precipitates and intermetallics are known to act as local cathodes, which facilitate oxygen reduction reactions and ultimately drive anodic dissolution of the surrounding matrix material. The intergranular corrosion resistance of the alloy decreases with the increase of the content of Cu and Mg elements. The results also show that the corrosion resistance of 2024 alloy with lower Mg content is significantly improved compare with the 2024 alloy with a more common composition (Cu to Mg mass ratio of 2.9). Attempts are made to explain the observed corrosion behavior of the alloy of various contents of Cu and Mg elements. The research results can provide theoretical guidance for the composition design of 2xxx aluminum alloy with high corrosion resistance.

15:15-16:10 Tea Break

16:10-16:35 Invited

As-Cast Microstructure and Its Evolution during Homogenization of a Novel High Alloying Al-Zn-Mg-Cu Alloy

Zhihui Li, Kai Wen, Xiwu Li, Hongwei Yan, Da Xu, Yongan Zhang, GRIMAT Engineering Institute Co., LTD., China; Baiqing Xiong, GRIMAT Engineering Institute Co., LTD., China / GRINM Group Co., LTD., China

The second phases in as-cast Al-Zn-Mg-Cu alloy could dissolve into the matrix or undergo transformation during homogenization treatment. The microstructure of as-cast and as-homogenized alloy was investigated by means of scanning electron microscope (SEM), transmission electron microscope (TEM), differential scanning calorimetry (DSC), hardness and electrical conductivity tests. AlZnMgCu phase in as-cast alloy possessed a similar structure of $MgZn_2$. A transformation from AlZnMgCu phase to Al_2CuMg phase occurred via a homogenization treatment at 380˚C while AlZnMgCu phase directly dissolved into the matrix with no phase transformation at 470˚C. Homogenization temperature influenced diffusion rates of Zn, Mg and Cu atoms determined an obvious diffusion rate gap between Zn and Cu atoms for homogenizing at 380˚C, leading to a transformation to Al_2CuMg phase. On the contrast, homogenizing at 470˚C gave rise to a small gap so as to the AlZnMgCu phase dissolution. Abundant Al_3Zr particles with small size and dispersive distribution generated in the alloy after two stage homogenization treatment. Al_3Zr particle showed a round shape with a first stage homogenization temperature of 400˚C. When the first stage homogenization temperature varied from 400˚C to 450˚C, Al_3Zr particles with blocky morphology appeared and its proportion enlarged. The formation of blocky Al_3Zr particle was speculated.

16:35-16:55

Prediction of Mechanical Properties for Al-Mn Alloys Subjected to Prolonged Heating at High Temperatures

Nobuhiro Makii, Shoichi Hirosawa, Yokohama National University, Japan

The mechanical strength of alloys decreases when exposed to high temperatures, but the rate of the decrease is generally very small under the conventional service condition of products. Therefore, it is required to predict in advance the definitive strength after a service for, for example, several decades. Temperature-accelerated test and full-annealing treatment test are examples of such prediction methods, and highly expected to provide good estimates instead of the experimentally unmeasurable definitive strength. Al-Mn alloys are one of the aluminum alloys used for high-temperature components, but further improvement of the strength and thermal stability is in great demand. In this study, powder metallurgy (PM) extrudes of Al-2.5mass%Mn (25M), Al-3.0mass%Mn (30M) and Al-4.0mass%Mn (40M) with larger amounts of Mn than its solubility limit were newly developed by gas atomization and cold isostatic press (CIP). And then the mechanical strength after prolonged exposure at 373~673K (i.e., temperature-accelerated test above a service temperature) or after controlled cooling at 1K/h from a solution treatment at 793K for 10h (i.e., full-annealing treatment test) were compared to those of the conventional A3004-H112 Al-Mn alloy by means of tensile test and Vickers hardness measurement. The obtained time–temperature–hardness curves by temperature-accelerated test showed that the hardness of A3004-H112 monotonously decreases with increasing exposure time above 523K, but 25M, 30M and 40M hardly decrease in hardness even when exposed at 573K for 10000h. The hardness decreases of 25M, 30M and 40M after full-annealing treatment

test were also very small compared to A3004-H112, thus disallowing numerical analyses by, for example, Larson-Miller parameter (LMP) and Arrhenius models to be worked. Such endurance of mechanical strength of newly developed PM extrudes was attributed to thermally stable Al6Mn dispersed phase, and thus the definitive microstructures after a prolonged service was attempted to elucidate by a phase field simulation. The calculated little microstructural change in 40M even after a prolonged exposure at 573K was in good agreement with the results of the two prediction methods concerning the excellent thermal stability of the extrude.

16:55-17:15

Grain Refinement and Macrosegregation Behavior of Direct Chill Cast 2024 Aluminum Alloy under Intensive Melt Shearing

Xudong Liu, Qingfeng Zhu, Rui Wang, Yubo Zuo, Northeastern University, China

Grain refinement and improvement of macrosegregation are very important for direct chill (DC) casting of high quality wrought aluminum alloy ingots. In this paper, intensive melt shearing was introduced to refine the as-cast structure and improved macrosegregation during DC casting 2024 aluminum alloy. Intensive melt shearing was achieved by the application of a stator-rotor high shearing device and was applied directly to the melt in the sump during DC casting process to control the as-cast structure and macrosegregation of 2024 aluminum alloy ingot with a diameter of 300mm. Temperature measurement was carried out to study the temperature field during casting process and to understand the mechanism of the grain refinement effect of intensive melt shearing on the DC casting process. The experiment results show that intensive melt shearing can reduce the cold folds, which make the surface of ingot smooth. The thickness of the solid shell increases with the application of intensive melt shearing. After the application of intensive melt shearing, the grain structure is transformed from the mixture of columnar grains, feathery grains and coarse equiaxed grains to fine equiaxed grains. The uniformity of as-cast structure is also greatly improved. The intensive melt shearing shows a significant effect on the distribution of elements. The negative macrosegregation in the center region of the ingot is obvious reduced. At the same time, it has no obvious effect on the strong positive surface segregation and negative subsurface segregation. In conventional DC casting process, the temperature of the melt in the sump is high and the temperature field in the sump is non-uniform. During the DC casting process with intensive melt shearing, the liquid melt from the launder is cooled with a high cooing rate directly to 2~4℃ below the liquidus and the temperature field in the sump is quite uniform. This is believed results in the enhanced heterogeneous nucleation and improved the survival of the nuclei.

17:15-17:35

Compressive Properties and Energy Absorption of CNTs/Al Composite Foam Filled Aluminum Alloy Tubes

Jiali Xu, Chunnian He, Naiqin Zhao, Tianjin University, China; Xudong Yang, Civil Aviation University of China, China

The composite structures prepared by aluminum foam combined with other dense materials became more and more valuable in engineering application. Recently, there has been some literatures on the foam fill tubes (FFTs) structures, concluding that using aluminum foams as cores inside the metal tubes can improve the energy absorption of simple tubes. However, the strength of the aluminum foam core was generally low. It was difficult to achieve synergetic deformation with the metal tube, and the interaction between foam and tube can't be maximized. In this study, CNTs/Al composite foam filled 6061 aluminum alloy thin-walled tube was prepared. The combination of CNTs/Al composite foam with tube was achieved by simple mechanical contact. CNTs had high reinforcement efficiency owing to low density, high modulus. The composite aluminum foam fabricated by space-holder method had the consistent pore size and precise porosity. The addition of CNTs and the controllable foam structure improved the deformation strength and stability of the composite foam, respectively. Benefit from the properties of the CNTs/Al composite foam, the CNTs/Al composite FFTs structure showed high strength, certain toughness and excellent energy absorption properties.

The experiment studied the compressive deformation and energy absorption capability of the FFTs structure. Due to the synergetic deformation between the CNTs/Al composite foam and alloy tube, CNTs/Al composite FFTs structure exhibited more excellent properties than that of the superposition of alloy tube and CNTs/Al composite foam. The plateau stress and energy absorption of composite structure were 57.4MPa and 28.4MJ/m^3, which were ~0.23 and ~0.87 times higher than that of the superposition of alloy tube and CNTs/Al composite foam, respectively. More importantly, the energy absorption efficiency of composite structure was 1.23 times that of the superposition of tube and composite foam. Compared to pure aluminum FFTs structure, CNTs/Al composite foam with high strength can significantly increase the plateau stress, energy absorption capacity of the FFTs structure. CNTs/Al composite FFTs structure's plateau stress and energy absorption were ~0.51 and ~0.67 times higher than that of pure aluminum FFTs structure, respectively.

Generally, CNTs could improve foam's strength while reducing its density. The CNTs/Al composite foam and tube deformed cooperatively, further preventing the foam and tube from collapsing instantaneously, stabilizing the FFTs structure. The specific energy absorption and specific strength of the FFTs structure were obviously improved.

C2. Light Metals and Alloys-Magnesium: II

Symposium Organizers:

Xianhua Chen, Chongqing University, China; Yoshihito Kawamura, Kumamoto University, Japan; Young Min Kim, Korea Institute of Materials Science (KIMS), Korea; Jian-Feng Nie, Monash University, Australia; Diran Apelian, Worceste Polytechnic Institute, USA

Tuesday PM Room: 406 (4th Floor)
August 20, 2019 Symposium: C2

Chairs:
Eiji Abe, The University of Tokyo, Japan
Wenbo Du, Beijing University of Technology, China

13:30-13:55 Keynote

Development of Corrosion Resistant Magnesium Alloys

Bong Sun You, Young Min Kim, Korea Institute of Materials Science, Korea; Jong Il Kim, Chungnam National University, Korea; Hui Yu, Hebei University of Technology, China

The main reason for abandoning magnesium alloy after the beginning of the active use in the automobile and aircraft industries in the 1940s, which is still the key issue not to use very large amounts of magnesium alloys in the automobile industry, is its high corrosion rate compared with other metals. Studies have been done to develop corrosion resistant magnesium alloys vie the addition of active metallic elements in commercial alloys, but there have not been any meaningful results except when using certain rare earth elements. As in the case of Cr addition to stainless steel to make a dense oxide film that can act as passive film to resist continuous corrosion, we need new additional elements for magnesium alloys to make stable passive films. However, almost all the elements that have been studied have shown negative results for corrosion resistance. The only interesting result is that it has been found if we make high purity alloys by minimizing some harmful elements such as Fe, Cu and Ni, the corrosion resistance improves significantly.
KIMS have been studied on new corrosion resistant magnesium alloys by the addition Ca and Y together which was originally designed to improve non-flammability of AZ series magnesium alloy. A controlled amount Ca and Y containing phases and the formation of multi-layered protective oxides consisting of CaO, Y_2O_3, $MgAl_2O_4$, and MgO effectively improve the corrosion resistance. This paper introduces the mechanism of corrosion resistance of Ca and Y containing alloys, and compares the corrosion behaviour with that of commercial alloys. Also, it introduces field test results on several items which are made by die casting, billet making and extrusion processes for the application in electronic, railway, automotive and aerospace industries.

13:55-14:20 Keynote

Study of the Alloying Effect on Mg's Ductility by in Situ Synchrotron X-Ray and Electron Microscopy Experiments

Xiaoqin Zeng, Shanghai Jiao Tong University, China,

14:20-14:40 Invited

Advanced Protective Coating Strategy for Mg Alloys

Xiaobo Chen, RMIT University, Australia

Utilisation of light-weight magnesium (Mg) alloys as engineering materials is limited due to their high affinity for oxygen and water, and hence vulnerability to corrosion. Many efforts have been attempted to address the corrosion issue of Mg alloys to pave a path for wider implementation of Mg in various applications, such as automotive, airplane, electronic devices and biomaterials.
There are two straightforward methodologies to suppress corrosion progress of Mg alloys. Addition of alloying elements, such as Al, Zn and even As, into the bulk Mg matrix which may lead to favorable microstructure, grain size or kinetic restriction to corrosion kinetics (with attendant changes in properties and cost). The other intensively exploited approach is applying stable and inert coatings onto the surface of Mg alloys as a barrier to provide protection functionality. Compared to alloying, surface properties will be altered rather than the fundamental properties of the bulk materials and desirable protection can be obtained by means of simply and efficient processing procedures.
The most successful commercial coatings are chromate based, however, the extreme carcinogenicity to organisms and environments has led to a strict ban on the utilisation of chromate coatings globally. Therefore, there is an urgent need to develop alternative coatings to tackle the corrosion issue of Mg alloys as chromate did. Herein, we introduce some advanced techniques to develop coatings onto Mg alloys to perform either as a barrier or functional coating in order to address the corrosion of Mg. The coating characteristics, formation mechanism and their specific roles in corrosion protection will be presented and discussed. In addition, a novel pretreatment method will be introduced to demonstrate its vital role in generating a homogenous surface condition that is favorable for subsequent growth of desirable coatings. The results indicate that superior corrosion resistance of Mg alloys could be yielded through high-performance coatings.

14:40-15:00 Invited

Quantitative Prediction of Texture Effect on Hall–Petch Slope for Magnesium Alloys

Yunchang Xin, Bo Guan, Qing Liu, Xiaoxu Huang, Chongqing University, China

The high texture dependence of a Hall–Petch slope (k) for Mg alloys has been frequently reported. Several important equations used to calculate k have been previously developed, and although they seem to work well for fcc and bcc materials, they often fail to predict the highly texture-dependent k in Mg alloys. A new equation based on the dislocation pile-up model was developed in this study. The validity of this new equation was tested through a comparison of the predicted k values with the experimental values as well as the calculations from older equations. The results indicate that the new equation can achieve an accurate prediction for several previously reported texture effects on k, whereas the k values predicted by the older equations often exhibit a clear deviation. The reasons for this were analyzed and discussed. The strong deformation anisotropy for Mg alloys leads to a complex texture effect on k, including the effects from both external and internal stresses. Both effects are well expressed in the new equation. In contrast, the old equations consider the external stress effect, but do not express well the internal stress effect. In addition, the old equations consider only the predominant deformation mode. However, our results indicate that the activation of a portion of another deformation mode other than the predominant one plays an important role in the k value. Using the important parameters of the new equation, the mechanisms for several texture effects on k as previously reported were discussed and new understandings were obtained.

15:00-15:20 Invited

Age Hardening Effect and Superelasticity of Martensitic Transformable Mg-Sc Based Alloys

Daisuke Ando, Keisuke Yamagishi, Yuji Suto, Junichi Koike, Tohoku University, Japan; Yukiko Ogawa, National Institute for Materials Science, Japan

Mg alloys have been expected as a next generation structural material for many decades. Especially, Mg-Al based and Mg-Zn based alloys have been developed and used for various industrial products due to weight reduction. However, these conventional Mg alloys show poor plastic deformability at room temperature because of their hexagonal closed packed (hcp) structure, which exhibits high plastic anisotropy. And also, the strength of Mg alloys is insufficient compared with Al based alloy. These poor workability and insufficient strength of most Mg alloys limit their practical application. Therefore, many attempts have been made to improve those properties.

Among them, Li addition is very effective method to enhance the ductility of Mg alloys. Small addition of Li can reduce the c/a ratio of hcp lattice and enhance the activation of <c+a> slip, which leads to the enhancement of ductility. The alloys with Li content between 5.5 and 8.5wt.% have a bcc/hcp dual phase structure. The dual phase alloys have an excellent ductility and show super-plasticity at 423K. Furthermore, it was reported that the alloys with Li contents up to 12.5wt.% have a bcc single phase structure. Recently, the low corrosion resistance has improved by the alloy composition and thermo-mechanical processing routes. These Mg-Li alloys were accepted as main flame material in mobile notebook PC. However, according to the phase diagram of Mg-Li alloy, the dual-phase boundary is almost vertical up to high temperature, which indicates that the volume fraction ratio of the bcc/hcp dual phase can be controlled only by Li content, but not by temperature. It means phase transformation could not happen during thermo-mechanical processing.

In this study, we propose Mg-Sc alloys with phase transformability. This alloy shows ultra-high strength after aging due to fine hcp precipitation from metastable bcc matrix. The maximum Vickers hardness is over 230HV aging at 200 degree C for 25 hours. The sample exhibits brittle fracture in tensile deformation at room temperature because of severe strain hardening during phase transformation. However, after straightening anneal at 300 degree C for a few minutes, the samples shows excellent mechanical properties at room temperature and elevated temperature.

Furthermore, the alloys show super-elasticity of 4.4% at -150 degree C and shape recovery upon heating. The shape memory properties are caused by reversible martensitic transformation from bcc to orthorhombic phase. This behavior resembles that of Ti alloys. The martensitic transformation temperature strongly depends on the Sc contents. After optimizing the Sc contents, Mg-Sc alloy shows super-elasticity even at room temperature. The density of Mg-Sc alloy is around 2g/cm^3, which is one-third less than that of practical TiNi Shape memory alloy.

The study shows a possibility to use metastable bcc phase for novel microstructural control and adding functionality into Mg alloys.

15:20-15:35

Enhanced Mechanical Properties of a Mg-Gd-Y Alloy Processed by Multi-Directional Impact Forging

Songhe Lu, Institute of Metal Research, Chinese Academy of Sciences, China / University of Science and Technology of China, China; Di Wu,Rongshi Chen,Enhou Han, Institute of Metal Research, Chinese Academy of Sciences, China

The solution-treated Mg-6.58Gd-5.7Y-0.55Zr alloy was

subjected to multi-directional impact forging (MDIF) with 520℃. The microstructure and mechanical properties of the two MDIFed samples were investigated. Their deformed microstructure was typical bimodal grain structure consisting of deformed coarse grains and dynamic recrystalliziation grains. A MDIFed sample exhibits an average 0.2% proof stress (YS) of 306MPa, an average ultimate tensile strength (UTS) of 354MPa and an average elongation to failure of 3.3% at room temperature. Nevertheless, the other MDIFed sample exhibits lower YS (212MPa) and UTS (297MPa), which is attributed to its weaken random texture. On the other hand, static recrystalliziation (SRX) behavior of as-MDIFed Mg-6.58Gd-5.7Y-0.55Zr alloy were investigated by annealing treatment at 520℃ with different time using in-situ-optical microscopy (OM). During this process the deformed coarse grains were gradually replaced by recrystalliziation grains and they almost have been consumed by SRX grains at annealing time of 5min. Finally, a completely recrystalliziation microstructure with average grain size of ~50μm was obtained at annealing time of 10min. After annealing treatment, UTS decrease but elongation-to-failure significantly increases. This should be ascribed to further texture randomization and vanishing work hardening caused by SRX during annealing treatment.

15:35-16:05 Tea Break

16:05-16:25 Invited

Improvement in Room-Temperature Yield Asymmetry of Extruded AZXW9100 Alloy by Precipitation Hardening

Joung Sik Suh, Korea Institute of Materials Science, Korea; David Klaumuenzer, Volkswagen AG, Korea; Young Min Kim,Bong Sun You, Korea Institute of Materials Science, Korea / Korea Institute of Geoscience and Mineral Resources, Korea

Tension-compression yield asymmetry at room temperature of extruded AZ91 based Mg alloy is investigated regarding precipitation hardening. Non-flammability is a key prerequisite for application of Mg extrusion products to advanced transport such as aircraft and high-speed train. It has been known that conventional Mg alloys are reactive in molten state and thus rapidly ignited as contacting with oxygen in air. In order to solve this problem, a non-flammable high-strength Mg alloy was developed by a trace addition of Ca and Y to AZ91 (Mg-9Al-0.8Zn-0.1Mn-0.3Ca-0.2Y bal. wt. denoted as AZXW9100). As engineering materials, one of the main challenges is how tension-compression yield asymmetry of Mg alloys can be reduced so as to suit industrial applications. It is well known that Mg alloys are low-symmetry materials with hexagonal-close packed structures having axial ratios of around 1.633. In this case, yield asymmetry can be attributed to the prevalence of {10-12} twinning. Based on this, the analysis of mechanical behavior of extruded AZXW9100 plates presents that aging treatment increases yield strength in uniaxial tension and compression. Especially, this distinct increase in compressive yield strength makes close to yield symmetry compared with as-extruded condition. This reduction in yield asymmetry is attributed to the presence of Ca containing Mg17Al12 precipitates, which suppress tensile twinning in compression. EBSD measurements confirms a reduction in the scale and area fraction of {10-12} tension twins in aging-treated samples at equivalent levels of strain.

16:25-16:40

Effect of Ca, Sm and La Additions on Microstructures and Tensile Properties of As-Cast and As-Extruded AZ31 Alloys

Li Fu, Zheng Jia, Shenyang University, China; Qichi Le, Yanxia Niu, Yonghui Jia, Northeastern University, China

Magnesium alloys are more and more attractive for structural materials of metal in automotive due to their low density and easy recycling, while their applications are still limited due to their lower absolute strength and plasticity at room temperature, especially they can not work for a long time when the temperature is over 120℃. Alloying of rare earths is recognized to be an effective method improving properties of magnesium alloys. In this study, 1.3%Ca is first added to AZ31 alloy and 1.0% Sm+0.3% La is further added, then microstructures and tensile properties of AZ31 alloys with Ca, Sm and La additions are investigated. Detailed analysis and characterization results on structures and morphologies of second phases by XRD and SEM-EDS indicate that Al2Ca is formed after Ca additions, while Al2Sm irregular strips and Al2Sm polygons are formed with further additions of Sm and La. Formations of these new phases could decrease Mg17Al12 phases and refine grains of both as-cast and as-extruded AZ31 alloys obviously. Texture analysis results of as-extruded AZ31 alloy by XRD show that (0002) basal texture changes little with Ca additions, while it is significant strengthened with further additions of Sm and La. Tensile tests results at room temperature reveal that Rp0.2 (Yield strength) of as-extruded AZ31 alloy is enhanced by about 20MPa and A (elongation) is approximate to 25% with Ca additions, while with further adding Sm and La, Rp0.2 is enhanced by over 50MPa and A is decreased to less than 20%. Tensile tests results at 150℃ reveal that both Rp0.2 and Rm (ultimate tensile strength) is significantly enhanced with Ca additions, which change little with further additions of Sm and La.

16:40-16:55

Study of the Dislocation Activity in a Mg-Y Alloy by Differential Aperture X-Ray Microscopy

Leyun Wang, Bijin Zhou, Xiaoqin Zeng, Wenjiang Ding, Shanghai Jiao Tong University, China; Wenjun Liu, Argonne National Laboratory, USA; Jian Wang, University of Nebraska-Lincoln, USA

As the lightest metallic structural material, Mg and its alloys have strong potential for weight reduction applications in the automotive and aerospace industries. Yet, the ductility of Mg still needs to be improved to ensure good formability at room temperature. Recent studies have shown that the addition of yttrium (Y) can substantially improve the ductility of Mg alloys. This phenomenon was attributed to the enhanced activity of non-basal <a> and <c+a> slips according to previous TEM studies. However, relative activity among different non-basal slip modes and how non-basal slips improve the material's ductility is still unclear due to the small observation area associated with TEM and the post-mortem sample status. In this paper, a novel technique of differential aperture X-ray microscopy (DAXM) with submicron resolution is employed to map the distribution of geometrically necessary dislocations (GNDs) among five grains in a Mg-5wt%Y alloy (grain size ~ 100mm) after an in situ bending test. The DAXM experiment was conducted at Beamline 34-ID-E of the Advanced Photon Source. The GND contents are determined voxel by voxel based on the diffraction peak streaking in the corresponding Laue diffraction patterns. Among those voxels with peak streaking, 56% contain GNDs associated with basal slip, while the other 44% contain GNDs associated with prismatic slip (8%), pyramidal <a> slip (13%), and pyramidal <c + a> slip (23%). The deviatoric part of the elastic strain tensor was further calculated for each voxel from the Laue diffraction patterns. It is found that non-basal GNDs were often related to local stress concentrations. Long-range lattice rotation that was measured from the position movement of diffraction peaks across multiple voxels is not always consistent with the distribution and characters of GNDs in the grain. We attribute the high ductility of Mg-Y alloys to the extensive activation of non-basal <a> and <c+a> slip to prevent premature crack initiation at grain boundaries.

16:55-17:10

Atomistic Microstructure of Kinks Formed in Dilute Mg Alloys

Daisuke Egusa, The University of Tokyo, Japan; Eiji Abe, The University of Tokyo, Japan / National Institute of Materials Science, Japan

Magnesium (Mg) alloys are promising for structural materials due to their high strength-to-weight ratio. Recently, Mg alloys with a small addition of TM (Transition Metals) and RE (Y and Rare Earth elements) have attracted much attention, owing to their high strength by simply applying a conventional hot extrusion. Microstructural features, which are believed to essential for the excellent properties of the alloys, are formation of long period stacking/order (LPSO) phase and activations of kink deformations.

The LPSO structures are consist of 2H (ABAB) structure and I2-type stacking faults (ABCA), which are interpreted as periodical stacking of close-packed planes. In addition, TM/RE elements located at the layers relevant to stacking faults. Owing to these structural and chemical order along the stacking direction, LPSO phases have anisotropic structural features which is accepted to cause limitations of several deformation modes, such as non-basal slip and twinning.

Due to these limitations, kink deformation is one of the important deformation modes for homogeneous deformations of the alloys. Hess et al proposed a microscopic mechanism of kink deformation, which comprehend "kinks" as cooperative motion of basal dislocations; however, details have not clarified yet. Based on the proposed model, kink deformation introduces high dense of dislocation which cause dynamic recovery/recrystallization during hot workings, so that kink as itself cannot contribute the strength of alloys without suppressing the recovery/ recrystallization behavior. This fact suggests a presence specific microstructural feature within kinks of the Mg-TM-RE alloys which make kinks stable once they were formed.

In the present study, we investigated microstructural features of kink formed in dilute Mg-TM-RE alloys with transmission electron microscopy (TEM) and scanning transmission electron microscopy (STEM). Based on TEM observations and image analysis, atomic structure of faults embedded in kinks are identified as Shockley-type and Frank-type partial dislocations that form I2-type and I1-type stacking faults within hcp structure, respectively. In addition, STEM images show that there are characteristic distributions of trace elements that are combined with faults around kinks. The selective enrichments of trace elements on these faults, considered as Suzuki segregation and Cottrell atmosphere, suggest occurrences of structural accommodation within kink formation which may be origin of thermodynamic stability of kink. We will discuss about formation mechanism of kink in Mg-TM-RE alloys based on microscopic features of kinks.

17:10-17:25

High Stretch Formability of As-Rolled Magneiusm Alloys with Additions of Er/Zn at Ambient Temperature

Ke Liu, Wenbo Du, Zhaohui Wang, Shubo Li, Jinxue Liu, Beijing University of Technology, China

As a lightweight structural material, the wrought

magnesium alloy has a unique advantage in 3C fields owing to its high specific strength and excellent electromagnetic shielding characteristic. However, as the hexagonal close packed structure (HCP), it is difficult to make the magnesium alloy undergo a homogeneous deformation. In generally, the wrought magnesium alloy has a strong basal texture and a notable anisotropy, which is harmful to the formability. Modifying texture is one of key factors to improve formability at room temperature. In the present investigation, the microstructure, mechanical properties and stretch formability at room temperature of magnesium/magnesium alloy sheets were investigated. The magnesium alloys were alloyed with different alloying elements (Zn/Er). The result suggested that a trace addition of Zn and Er played a key role in texture modification, shear bands formation and nano-scale secondary phase precipitation, which resulted in obvious increase in stretch formability and mechanical properties at the same time. It was indicated the Mg-0.5Zn-0.5Er alloy sheet exhibited better tensile strength along the rolling direction. The values of yield strength (YS) and ultimate tensile strength (UTS) were 180MPa and 201MPa, respectively, companying with superior Erichsen value (IE) of 7.0mm at room temperature. The good performances of the alloy sheet were ascribed to the weak basal texture intensity, formation of shear bands and precipitation of nano-slcae W-phase ($Mg_3Zn_3Er_2$).

17:25-17:40

The Effect of Frequency on Solidification of AZ80 Magnesium Alloy during Electromagnetic DC Casting

Yonghui Jia, Qichi Le, Qiyu Liao, Lei Bao, Northeastern University, China

The effect of frequency on solidification of AZ80 magnesium alloy billet during electromagnetic DC casting was investigated experimentally. The billet with diameter 320mm was solidified in an oscillation electromagnetic field with the imposition of a pulse current at the frequency of 20, 30, and 40Hz when the time-averaged current intensity is 80A and duty cycle is 20%, from which a pulse electromagnetic force is yielded. The macrostructure evolution was quantitatively examined in terms of the grain size and its distribution, and the electrical conductivity was measured to evaluate the characteristics of solidified microstructure. The effects of electromagnetic frequency on macro- and microstructure evolution, phase distribution, element segregation, and conductivity distribution were discussed in detail. It was observed that the solidified structure under pulse oscillation electromagnetic field is sensitive to the electromagnetic frequency, which has an effective frequency range. The grain size can be effectively controlled with different electromagnetic parameters. The grain size decreases from 815 ~ 951μm (without MF) to 402 ~ 486μm at the frequency of 30Hz. The segregation ratio is reduced evidently at the frequency of 30Hz. As the frequency decreases or increases, the grain size and segregation ratio increase. As the frequency further increases to 40Hz, the grain size and the difference of electrical conductivity on the cross section of billet increases. In addition, the conductivity distribution of the cross section of the billet is more uniform, which is closely related to the solidification structure of the billet in the presence of oscillation electromagnetic field.

17:40-17:55

Superelastic Property of Mg-Sc Binary Alloys at Room Temperature

Keisuke Yamagishi, Daisuke Ando,Yuji Sutou,Junichi Koike, Tohoku University, Japan

Mg alloys have been expected as a next generation structural material for many decades due to its light weight and high specific strength. However, conventional Mg alloys show a poor formability at room temperature because of their hcp structure, which exhibits a high plastic anisotropy. Therefore, many researchers have attempted to change hcp crystal structure to bcc crystal structure in Mg-Li alloy system. These Mg-Li alloy with bcc structure show excellent ductility and superplasticity with fine grain even at room temperature. But the volume fraction of the bcc phase is uniquely determined upon the Li composition. Mg-Sc alloy system is only other Mg alloy which transforms from hcp structure to bcc structure depending on temperature even at the same composition. It means that microstructure can be controlled by thermomechanical treatment like Ti alloys and the metastable bcc phase might transform to other phase during deformation like stress-induced martensitic transformation. Actually, we found and reported for the first time in Mg based alloy that Mg-20.5 at.%Sc alloy shows stress-induced martensitic transformation from bcc phase to orthorhombic phase, therefore exhibits superelasticity at a low temperature of -150˚C. The density of this alloy is about 2.0, which is one-third of that of NiTi based shape memory alloys. However, the working temperature of the superelasticity is too low to use this Mg-20.5 at.%Sc alloy for various industrial applications.

Now, we have challenged to develop a room temperature superelastic Mg-Sc alloy. In previous study, we have noticed that its martensitic transformation temperature shows a strong dependence on the alloy composition and increases with decreasing Sc content. Therefore, in this study, we investigated the martensitic transformation temperature of Mg-(18-19) at.%Sc alloys and confirmed that the transformation temperature certainly increases with decreasing Sc composition. Furthermore, we have successfully realized superelasticity at room temperature in this composition range. In this presentation, I would like to show our results in detail.

C3. Light Metals and Alloys: Ti and Others II

Symposium Organizers :

Yongqing Zhao, Northwest Institute for Nonferrous Metal Research, China; Yoshihito Kawamura, Kumamoto University, Japan; Young Min Kim, Korea Institute of Materials Science (KIMS), Korea; Jian-Feng Nie, Monash University, Australia; Diran Apelian, Worceste Polytechnic Institute, USA

Tuesday PM
August 20, 2019

Room: 304 (3rd Floor)
Symposium: C3

Chairs:
Elena Pereloma, University of Wollongong, Australia
Yongqing Zhao, Northwest Institute for Nonferrous Metal Research, China

13:30-14:00 Keynote

R & D of New Titanium Alloys in China

Yongqing Zhao, Northwest Institute for Nonferrous Metal Research, China

Because of their excellent comprehensive properties, Ti and its alloys have been wide used in many industry fields. This paper review the R & D of new titanium alloys developed in China in recent 10 years, such as TC21 alloy with high strength and high toughness, TC4-DT alloy with middle strength and high toughness, Ti-1300, Ti26 and Ti-B19 alloys with super high strength, Ti75 and Ti31 alloys used for shipbuilding and so on. And also this paper will show the applications of these new alloys.

14:00-14:25 Invited

Modelling of Materials Flow at Elevated Temperatures

Zhanli Guo, Sente Software Ltd., UK

Materials flow is governed fundamentally by deformation mechanisms, which should remain unchanged regardless of the means of experimental investigations. However, for historical reasons, deformation mechanisms have been presented in various laws depending on the means of testing. For example, the deformation mechanism maps proposed by M. F. Ashby are based on creep mechanisms, whereas many of the laws describing strain or work hardening are derived from tensile or compression testing. There are many constitutive equations available describing the stress-strain behaviour at elevated temperatures. Strictly speaking, these equations are not based on deformation mechanisms, but rather empirical in nature. All these laws can be unified, at least in principle, if the common assumption that stress-strain relation is path-independent prevails. This paper looks at materials flow of various alloy systems such as Ti^{-}, Al^{-} and Mg-alloys. The constitutive equations, such as the Johnson-Cook type or the Norton-Hoff type which are used to describe flow stress curves at elevated temperatures, can now be replaced by appropriate creep laws.

14:25-14:50 Invited

Creep Deformation of Near-Alpha Ti Alloys

Yoko Yamabe-Mitarai, Tetsuya Matsunaga,Yoshiaki Toda, National Institute for Materials Science, Japan; Kei SHIMAGAMI, Haruki Masuyama, Shibaura Institute of Technology, Japan; Tsutomu Ito, Toyama Prefectural University, Japan

Near alpha Ti alloys are used as compressor blades or disks in jet engine. However, Ti alloys can not be used above 600˚C because oxidation and creep resistances become low above 600˚C. Operation temperature of jet engine is raising to reduce green gas and fuel consumption. Then, Ni-based superalloys with density twice as high as that of Ti alloys are used even in the high-temperature latter parts in compressors. However, using Ni-based superalloys increase the weight of jet engine. Then, it is very important to develop new high-temperature Ti alloys. Generally, microstructure related with mechanical properties is drastically changed by plastic deformation such as forging and rolling. Then, in this paper, the way to control microstructure of Ti alloys by changing forging and rolling condition was investigated. Then, using samples with different microstructure formed by different plastic deformation, the effect of microstructure factor on creep deformation was systematically investigated to understand creep deformation and decide the direction of alloy design. At first, the role of alloying elements was investigated to improve oxidation resistance. It is found that Sn degrades oxidation resistance and Nb improves oxidation resistance. Although Sn is a mandatory element for a-Ti alloys to stabilize a phase and strengthen a phase by solid solution hardening, we have attempted to design new Ti alloys without Sn. Nb is chosen as alloying element to improve oxidation resistance. To expect solid-solution hardening, Zr is also added to the alloys. The alloy ingots were melted using the cold-crucible levitation melting method, forged and groove-rolled to produce a bar with 14mm in diameter at 900 and 1000˚C with different deformation ratio. Samples were cut from a bar and heat treated in different conditions. The model microstructures such as equiaxed single alpha phase, equiaxed alpha phase with Ti_3Al precipitates, equiaxed alpha phase with silicide precipitates, alpha + alpha' -martensite phase and equiaxed alpha phase surrounded by beta phase were prepared by changing heat treatment. The creep behavior of the model microstructure was investigated at temperature range between 550 and 650˚C under stress range between 69

and 242MPa. The effect of each microstructure factor, such as Ti_3Al precipitates, silicide, alpha' and beta phases on creep deformation was clarified.

14:50-15:10

The Mechanism of {332}<113> Twinning Combining Metastable Phases in Metastable β-Type Ti-Mo Alloys Based on Cluster Structure

Mingjia Li, Xiaohua Min, Dalian University of Technology, China

Metastable β-type Ti alloys have attracted considerable attention as promising materials for biomedical and marine engineering applications due to their excellent properties such as low Young's modulus, good biocompatibility, high resistance to corrosion, shape memory effect and superelasticity. Twinning is an important deformation mechanism and plays a very important role in twinning-induced plasticity (TWIP) effect as it results in an extra strain hardening. An unusual twinning mode, {332}<113> twinning, is one unique deformation mechanism metastable β-type Ti alloys and is described by several models such as, shear and shuffle mode, α″ martensite transformation mode, dislocation mode and lattice instability mode. However, the modes as described above did not considered the influence of metastable phases, and the origin of {332}<113> twinning remains unclear. In this paper, the mechanism of {332}<113> twinning was investigated by considering the existence of the metastable phases (ω-phase and O'-phase) in body-centered-cubic (bcc) β-matrix. The magnitudes of twinning shear and shuffle were evaluated in different modes to find out the most possible mode to describe the formation of {332}<113> twinning. Besides, comparing the magnitudes of shear and shuffle between {112}<111> and {332}<113> twinning to clarify the competing relationship between them. The results showed that the shear magnitude of {332} plane along <113> direction was $5\sqrt{11}/22a\beta$ ($0.7538a\beta$) when {332}<113> twinning proceeded via the single shear mode. However, in the shear and shuffle mode, the magnitude of atomic displace were $\sqrt{11}/44a\beta$ ($0.0754a\beta$) and $\sqrt{22}/11a\beta$ ($0.4264a\beta$), respectively, which were less than the former mode. Moreover, under the softening effect of shear modulus along <111> direction (G111), the {112} plane moved along <111> to form ω-phase, which made the shuffle magnitude reduced to $0.2843a\beta$ at most concerning the influence of Mo content and cluster structure. The low tetragonal shear elastic constant (C') of β-phase made the {110} plane shuffled along <110> direction to form O'-phase. In this process, the atoms were shuffled to their correct twin positions. Therefore, the formations of metastable phases were conductive to {332}<113> twinning. In addition, the magnitudes of shear and shuffle in {332}<113> twinning were smaller than those in {112}<111> twinning via the formations of metastable phases. Therefore, the new mechanism of the {332}<113> twinning presented in this study can explain how the metastable phases preferentially activates the {332}<113> twinning in metastable β-Ti alloys instead of the {112}<111> twinning which is a major twinning mode observed in alloys with stable bcc structure.

15:10-15:30

Investigation of Strain Rate Strengthening and Work Hardening Behaviors in a Twinning-Induced Plasticity Ti-15Mo Alloy

Kai Yao, Xiaohua Min, Dalian University of Technology, China; Satoshi Emura, Koichi Tsuchiya, National Institute for Materials Science, Japan

The metastable β titanium alloys with twinning-induced plasticity (TWIP) effect show a wide application prospect in the aerospace, biomedicine, and energy industries due to their excellent mechanical properties with high strength, high ductility, and excellent work-hardening behavior. Some studies demonstrated that the mechanical properties of metastable β titanium alloys with TWIP effect remarkably depended on the strain rate, which exhibited the negative strain rate sensitivity (SRS). The SRS should be divided into instantaneously strain rate sensitivity (ISRS) and strain rate sensitivity of work-hardening (SRSW). The former part represented the effect of strain rate on flow stress, and the latter part represented the strain rate effect on microstructural evolution, i.e. the change of work-hardening rate. In the present study, the continuous tensile experiments at various strain rates and strain rate jump experiments were designed to investigate ISRS and SRSW in a twinning-type Ti-15Mo alloy, and a slip-type Ti-6Al-4V as a comparison material. The Ti-15Mo and Ti-6Al-4V alloys were prepared by cold crucible levitation and vacuum consumable arc melting. After solidification, the ingots were subjected to homogeneous treatment, hot forging, hot rolling and solution treatment. The tensile specimens with a gauge length of 25mm(l)×4mm (w)×1mm(t) were cut from the solution treated plates. The monotonic tensile tests up to fracture were performed on an UTM4204X testing machine at different strain rates ranging from 1.11×10^{-5} to $1.11\times10^{-1}s^{-1}$. The tensile specimens were stretched to various true strains (0.00, 0.05, 0.10, 0.15, 0.20 and 0.25) at constant strain rates of $1.11\times10^{-4}s^{-1}$ and $1.11\times10^{-1}s^{-1}$. The tensile specimens were first loaded with a stain rate of $1.11\times10^{-4}s^{-1}$ to the true strains of 0.00, 0.05, 0.10, 0.15 and 0.20, and then instantaneously jumped to higher strain rate up to fracture. In the Ti-15Mo alloy, the yield stress monotonously increased, while the ultimate tensile strength and elongation gradually decreased as increasing strain rate. The Ti-15Mo alloy exhibited negative SRS, and the coefficient of SRS was positive at a smaller strain level (<0.08), further decreased to the negative value as increasing strain. It demonstrated a positive ISRS in this alloy, which gradually increased as increasing jumping strain. The negative SRS was attributed to the much negative SRSW, i.e. lower work-hardening rate at higher strain rate. In the $Ti^{-6}Al^{-4}V$ alloy,

as increasing strain rate, the yield stress and ultimate tensile stress gradually increased, while the elongation decreased. The SRS and SRSW of this alloy were also negative, and a positive ISRS was found, which was stable regardless of jumping strain.

15:30-16:10 Tea Break

16:10-16:30

In-Situ EBSD Investigation of As-Built Laser Direct Melting Deposited (LDMD) Ti-6Al-4V Component at Moderate Temperature 200℃

Rafi Ullah, Beijing University of Technology, China

Laser direct metal deposition (LDMD) is quite new developed additive manufacture (AM) process. LDMD based Ti-6Al-4V component promisingly offers cost-effective alternate route to meet the severe demands of the modern aircraft industry. The OM and SEM results show that the structure of the as-built sample is more complex with beta columnar grains solidified in the building direction with interior covered of fine randomly oriented alpha laths which can lead to different unbalance deformation behavior during tensile test that needs to be better understood. Analysis of EBSD reveals that the as-built sample structure contains 89% volume fraction of alpha phase with small amount 11% of beta phase, rogue alpha grain combinations and different crystal orientations. Microstructural features relation with deformation behavior, and interesting effect of grain orientation, recrystallized fraction, schmid factor at moderate temperature 200℃ were investigated by direct In-situ EBSD observation technique during tensile testing. With the increase of tensile stress, maximum intensity of the texture of alpha phase first slightly increases from 33.01 to 35.63 and then dropped to 28.59. It has been observed that alpha plates having axes roughly parallel to the tensile axis easily deformed and present high discontinuity. Moreover, crystal in which the c-axis of the unit cell roughly inclined to the tensile axis exhibited easily slip lines after tensile.

16:30-16:50

True Stress - True Strain Curve up to Large Strain Obtained by Image Analysis Tensile Test Method at Elevated Temperature in Ti-17 Alloy

Atsushi Ito, Kiminori Taga, Shiro Torizuka, University of Hyogo, Japan

For aerospace applications, Ti-17 alloy has been applied for engine parts due to its excellent strength and toughness. They are mainly formed parts by hot forging. To evaluate hot forgeability, uniaxial compression test is common test method. However, in uniaxial compression tests, strain distribution is not introduced uniformly inside of the specimen due to the friction between a specimen and an anvil, resulting in large strain concentration in the center of the specimen. On the other hand, in tensile test strain is introduced uniformly inside a specimen up to the start of necking. However, the strain of necking start is generally small, it's difficult to obtain stress-strain curve up to large strain. To solve this problem, we have developed the image analysis tensile test method enabled us to evaluate accurate stress-strain curves after necking up to fracture at room temperature. The image analysis devices equipped with thermomechanical treatment simulator enables us to measure the change in the necking geometry during a tensile test at elevated temperature. From the necking geometry data, true stress after necking can be calculated by Bridgeman equation. In the present work, the image analysis tensile test method at elevated temperature is carried out and the accuracy of obtained true stress- true strain curves are evaluated in Ti-17 alloy. True stress decreased slightly after yielding at 1000℃ and at the strain rate of $0.01s^{-1}$ tensile test. In conventional compression test, at the strain rate of 0.1 and $1s^{-1}$, true stress decreased largely. On the other hand, true stress in tensile test increased after yielding. The microstructure in the specimen compressed at the strain rate of $1s^{-1}$ was deformed microstructure including little recrystallized grains. Therefore, in compression test, geometrical change and non-uniform strain distribution in a specimen rather than metallurgical structural change inside largely affect true stress – strain curve, resulting in the inaccuracy in the curve. This image analysis tensile test method can obtain accurate true stress – strain curve which is directly attributed to metallurgical structural change.

16:50-17:10

Direct Imaging of Short-Range Displacive Order in a Pre-Martensitic State of Ti-Ni-Fe Shape Memory Alloys

Ryouhei Kinoshita, Daisuke Egusa, University of Tokyo, Japan; Yasukazu Murakami, Graduate School of Engineering, Kyusyu University, Japna; Eiji Abe, National Institute for Materials Science, Japan

Pre-martensitic phenomena are critical issues for understanding B2-phase to R-phase martensitic transformations of Ti-Ni-Fe alloys, which are well known as shape memory materials. The phenomena are characterized by such as diffuse scattering in electron diffraction which suggest structural modulations formed by small atomic displacements correlated to the martensite shear. Based on the electron diffractions, the modulations are interpreted as a transvers-type displacement wave, whose propagation and displacement vectors are <110> and <1-10>, respectively. However, details of this precursor phenomena are still unclear, because magnitude of expected displacements is quite small, which is considered on order of picometers. To clarify the phenomena, we investigated atomistic details of pre-martensitic states in Ti50Ni48Fe2 alloys with HAADF-STEM observations. [1-11] projected STEM image shows fluctuation of column intensities that form intensity

modulation along <110> directions, although there is no difference in [1-11] projected potentials between atomic columns. We found out that such intensity fluctuations derived from small atomic displacements with transvers-type modulation that affect the scattering behavior of electrons contributing for HAADF imaging, based on multi-slice STEM simulations. The modulations of image intensity are also confirmed by diffuse scattering appear in a power spectrum of filtered HAADF-STEM image, which correspond with the one shown in conventional electron diffraction. We constructed a structural model of the transverse-type atomic displacements based on the image analysis and STEM simulations. In addition, based on diffuse scattering within the power spectrum, it is suggested that sizes of each modulation modes were estimated as about 1~2nm in diameter, and they form domains with each of 6 variants of modulation waves. Distributions of those domains uniformly spread in the specimen, implying that the pre-martensitic phenomena are second-order-like transition process. Entropy difference accompanying with the transition was estimated by configurational entropy of domains based on the model, showing close value to the one accompanied with B2 to R transformation.

17:10-17:30

Synergistic Effect of Pre-Deformation Microstructures and Isothermal ω-Phase on Mechanical Properties of Ti-10Mo Alloy

Shichao Ma, Xiaohua Min, Dalian University of Technology, China; Satoshi Emura, Koichi Tsuchiya, National Institute for Materials Science, Japan

β titanium alloys have been widely used in aerospace, biomedical and other industrial fields owing to its high specific strength, corrosion resistance, excellent aging strengthening (ω and α phase) and many other excellent properties. A simultaneous improvement in both strength and ductility by means of a single deformation mode or second-phase precipitated appears to be difficult for β titanium alloys to achieve large uniform elongation while keeping high yield strength. An improved strength-ductility in twinning-type Ti-15Mo alloy was found by means of pre-deformation induced {332}<113> twinning and subsequently isothermal ω phase precipitation. However, relatively little attention has been given to the complex deformation modes consisting of α" martensite, {332}<113> twining and dislocation in β titanium alloys. The purpose of this study is to confine the suitable degree of pre-deformation and appropriate aging temperature on the tensile properties in Ti-10Mo alloy. An approximately 1kg ingot of Ti-10Mo alloy was prepared by cold crucible levitation. After solidification, the ingot was homogenized at 1273K for 3.6ks and then hot-forged at 1273K, hot-rolling at 1173K, subsequent aging at 473~673k for 3.6ks. Four types of samples were used in this study: ST (solution-treated) and STA (solution-treated and aged) samples, which were tensile specimens (gauge dimensions: 20(*l*)mm × 4(*w*)mm × 1(*t*) mm), STD (solution-treated and deformed) and STDA (solution-treated, deformed, and aged) samples, which were pre-deformation specimens made by deforming ST specimens to 2%, 5%, 10%, 20% and 30% tensile strain prior to aging. Tensile tests were performed at room temperature in a tensile test machine Instron-5581 at an initial strain rate of $2.78 \times 10^{-4} s^{-1}$. Vickers hardness was measured with a load of 1kgf at ten positions on the transverse plane of each sample, with their average taken as the value for that sample. The microstructure was observed by optical microscopy (OM). Phase identification was made by X-ray diffraction (XRD) with an EMPYREN diffractometer using CuKα radiation. More stress induced α" martensite and {332}<113> mechanical twins were refined with the increasing degree of pre-deformation. The Vickers hardness gradually increased with an increase of precipitating temperature, which was resulted from the precipitation of brittle ω phases. The favourable strength-ductility tradeoff in Ti-10Mo alloy was achieved through the 20% pre-deformation and aging at 523K for 3.6ks. The high yield strength was mainly dominated by the precipitation strengthening of isothermal ω phase, and the enhanced uniform elongation was attributable to pre-existing twins and α" martensite as well as the subsequently dynamic microstructural refinement due to the {332}<113> twin and α" martensite during tensile deformation.

D. Advanced Processing of Materials: III

Symposium Organizers:

Wanqi Jie, Northwestern Polytechnical University, China; Jianguo Li, Shanghai Jiaotong University, China; Hideyuki Yasuda, Kyoto University, Japan; Myoung-Gyu Lee, Seoul National University, Korea; Huijun Li, University of Wollongong, Australia; Dan Thoma, University of Wisconsin- Madison, USA

Tuesday PM
August 20, 2019

Room: 208+209+210 (2nd Floor)
Symposium: D

Chairs:
Zhenshan Cui, Shanghai Jiao Tong University, China
Myoung-Gyu Lee, Seoul National University, Korea

13:30-13:55 Invited

Value and Challenges in Industry/University Collaboration on Advanced Materials and Processing Technologies

Abu-Zahra Nidal, University of Wisconsin-Milwaukee, USA

Advanced materials discovery continues to drive various forms of innovations and technologies, and impacts all aspects of our daily life such as financial,

health, energy, and food securities. However, it is worth noting that new materials are unlikely to have high intrinsic value on their own. Instead it is the way that they are integrated into components and systems to enable new designs, deliver improved performance, and reduce manufacturing costs. In addition, most important future materials developments will involve integration of "new" and "old" materials with increasing precision and sophistication, down to the nanoscale. Consequently, much of the value in future materials, will lie in the ability to operate competitively at the intersection of design, materials science and manufacture. Concurrently, it has been a challenge to separate materials developments from manufacturing innovations, as each drives the other in a remarkable spiral of improvement towards optimum performance. Similarly, advances in basic and applied science are needed if the availability and performance of advanced materials is to be accelerated, given that performance advancements often rely on improved fundamental understanding of materials properties, chemistry, and physics. Advanced materials breakthroughs at the laboratory scale can face major barriers related to manufacturing process scale-up and eventual market acceptance, which can significantly limit a material’s potential for large-scale impact on our economic system. Materials research involves leading edge equipment for imaging, synthesis, manipulation, and measurements, all of which require substantial capital investments. On-going support is also needed for staffing research teams and lengthy experimental and computational processes that can lead to materials breakthroughs. Market readiness programs, pilot and demonstration projects, and extension efforts are some of the mechanisms which can be used to help usher such technologies through the so-called "valley of death" between proof of concept and market adoption.

Although there are several government interventions to stimulate scalability in materials development, there also need to be incentives and mechanisms for investments in the scale-up of state-grown materials and manufacturing ideas and capabilities. Without this, there is a danger that regional and local materials manufacturing research will become overly dependent on using standardized, pre-production technologies, thus reducing our ability to secure valuable early-stage intellectual property in materials and manufacture. It is no secret that the most valuable knowledge and intellectual property associated with a "new" material often only comes to light once scale-up manufacturing is pursued. Therefore, it is vital that local and regional economic development offices and industry leaders work closely with the research and academic institutions in the region to develop effective mechanisms for enabling sustainable collaborations between academy and industry all the way from materials design or discovery through commercialization.

Among the challenges undermining the development efforts of new materials and processing technologies, one of the greatest is the effective integration of these new materials with existing technologies and workforce in a well-established industry. Creative solutions to this challenge can only be revealed through direct communication and strong collaboration between the various stakeholders and leadership influencing the state's economy and higher education systems. Academic institutions and research labs provide fertile ground for developing talent and shaping the skills of future workforce and entrepreneurs. Industry partners provide a market-driven perspective, helping balance scientific curiosity, engineering imagination, with their needs and constraints. This relationship can take different forms, ranging from frequent communication and active collaboration through strategic partnerships built on mutual recognition of each other's needs and valued contribution to the partnership. Academic centers of excellence, which are designed on these principles, can offer strong platforms with effective mechanisms to harness the power of collaboration between various constituents and stakeholders in the targeted technology.

13:55-14:15

Influence of Mandrel Parameters on Wall Thickness Variation of H96 Rectangular Tube in Small-Radius Bending

Hong Zhan, Southwest Technology and Engineering Research Institute, China / Northwestern Polytechnical University, China; Dayu Shu, Jun Lin, Qiang Chen, Yang Wu, Southwest Technology and Engineering Research Institute, China; Yuli Liu, Northwestern Polytechnical University, China

H96 thin-walled small-radius bent tubes are widely used in the fields of aviation, radar and automobile manufacturing because of their merits of compact structure, lightweight and large medium circulation. However, wall over-thinning and thickening easily occur in small-radius rotary draw bending process of tube due to its structural characteristics of hollowness and thin wall, which seriously affect the microwave transmission characteristics as well as mechanical properties. Rotary draw bending of tubes is a complicated forming process of multi-dies precision collaboration and strict coordination, and different dies, such as bending die, clamp die, pressure die and mandrel, play distinct roles in bending. Mandrel parameters have a vital effect on wall thickness variation of H96 rectangular tube, especially in the condition of small-radius bending. Thus, taking H96 brass rectangular tubes as research objects, the influence of mandrel parameters on wall thickness variation of tube in small-radius bending was investigated using the reliable 3-D finite element models. The results show that: (i) On the basis of ABAQUS/Explicit platform, the 3D-FE model of small-radius rotary draw bending of H96 rectangular tube is established, and its reliability

is successfully verified by experiment; (ii)With the increase of mandrel extrusion em, the wall thinning ratio and wall thickening ratio of H96 rectangular tube both aggravate in totally. The increase of friction coefficient between core and tube μc results in the decrease of wall thinning ratio and the growth of wall thickening ratio, but their variation just changes a little as a whole; (iii) As the increase of clearance between core and core Δ, wall thinning ratio as well as wall thickening ratio of rectangular tube increase simultaneous, which are due to its enlarged core supporting zone to tube.

14:15-14:35

Compressive Response and Energy Absorption Characteristic of Aluminum Composites Foams Reinforced by Graphene Nanosheets

Weiting Li, Chunnian He, Jiajun Li, Naiqin Zhao, Tianjin University, China; Xudong Yang, Civil Aviation University of China, China

Aluminum (Al) foams have been widely utilized due to their combination of structural and functional characteristics such as energy absorption, vibration reduction as well as noise elimination. The global properties of Al foams are strongly connected to the strut properties and the pore morphology. The performance of the strut material can be achieved through adding alloying elements, electro-deposition and incorporating reinforcements. Graphene nanosheets (GNSs) is considered to be a promising reinforcement for Al foam because of their extraordinarily high strength to weight ratio and high interface area to volume ratio. We successfully designed and fabricated the GNSs reinforced Al (GNSs/Al) composite foam via the method combined with the shift-speed ball-milling and the space-holder, during which the GNSs was prepared through in-situ NaCl template-assisted with the decoration of Cu nanoparticles. The influence of the GNSs content and the relative density on compressive responses and corresponding energy absorption characteristics of GNSs/Al composite foams was investigated. Moreover, the compressive responses of composite foams were characterized by quasi-static compression test. The scanning electron microscopy (SEM) and transmission electron microscopy (TEM) are employed to deeply comprehend deformation and fracture behavior and strengthening mechanism of the composite foam compared with pure Al foam. The results show that the mechanical compressive property of composite foam generally increased first and then decreased with the increase of GNSs content. The energy absorption capacity is well consistence with the variation law of the mechanical compressive property. Besides, with the introduction of GNSs, the composite foam with lower relative density can process the supreme energy absorption capacity in a wider range of stress, which is beneficial for lightweight of composite foam. What's more, the fracture behavior of Al foam changes from single ductile failure mode to ductile&brittle failure mode with the addition of the GNSs. The strengthening mechanisms of GNSs/Al composite foams are the combination of grain refinement strengthening, load transfer strengthening and dispersion strengthening.

14:35-14:55

Experimental and Constitutive Characterization on the Anisotropic Evolution of Yield Surfaces of Mg Alloy Rolled Sheet by Means of Biaxial Tensile test

Baodong Shi, Chong Yang, Yan Peng, Yanshan University, China; Fusheng Pan, Chongqing University, China

Magnesium alloys are promising materials to aid in the "lightweight" of many structural parts in automotive, aircraft, aerospace, and 3C industries due to their low density, high specific strength, good castability and damping capacity. Compared with die-cast products, wrought Mg alloy products, such as extruded profiles, rolled sheets with higher strength and ductility are developed for high-performance structural applications. However, the limited formability and strong anisotropy at temperatures below 200 degree limit the wider application of existing wrought Mg alloys.
The forming process of Mg alloy is strongly affected by the anisotropic mechanical behaviour due to crystallographic texture. Traditionally, the anisotropic behaviour is captured by uni-directional loadings along different directions (e.g. RD, TD and 45 from RD directions). Two questions rise under traditional uni-directional loadings. Firstly, the whole evolution of mechanical behaviour along all dimensions (i.e. Sigma xx, Sigma yy, Sigma zz, Sigma xy, Sigma yz and Sigma zx) instead of uni-directional mechanical property, determines the subsequent deformation behaviour and plastic flow of metals. Secondly, since the metal forming process is under multi-axial instead of uni-directional loading, the anisotropic plastic flow behaviour of metals under multi-axial loading are crucial to the forming technology. Clearly both questions cannot be answered by traditional uni-directional loading test. In line with the state of the art progress in Elasticity and Plasticity theory at finite strain, the aforementioned questions can be clarified by the anisotropic evolution of yield surfaces, i.e., distortional hardening. Therefore, in this work, evolution of yield surface of AZ31 rolled sheet under uniaxial tension was probed experimentally by means of compression and biaxial tensile test with specifically designed non-proportional strain paths. Anisotropic evolution of yield surface is observed under uniaxial tension, and underlying deformation mechanism is discussed based on microstructure and texture analysis. A thermodynamically consistent constitutive model at finite strain is employed to capture the anisotropic behaviour. The anisotropic evolution of yield surfaces of

AZ31 rolled sheet under uniaxial loading along RD and TD directions are predicted and validated after model parameters identification.

14:55-15:15

Effect of Cooling Rate on Mechanical Properties of Solution Heat Treated 7075 Aluminum Alloy for Cold Forming Application

Chanmi Moon, Yumi Choi, Myoung-Gyu Lee, Seoul National University, Korea

Lightweight vehicles in the automotive industry requirematerials with high specific strength as a future material solution. The high strength aluminum alloys such as 6000 and 7000 series are strong candidates to replace high strength steels. As an alternative to the forming of high strength aluminum alloys at elevated temperature (namely, hot forming of aluminum) developed for increasing formability, a cold forming technology using solution heat treated sheets has been developed. This forming technology utilizes the solution heat treatment (SHT) before stamping and quenching, resulting in the dissolution of alloying elements which precipitates into the matrix. The sheet with a microstructure of supersaturated solid solution (SSS) has enhanced formability and the strength can be recovered by the artificial ageing process after forming. Due to the nature of room temperature forming, it has lower manufacturing cost, better surface finish, and can use conventional stamping facilities. However, the strength of the heat treated sheet is higher than that of the sheet which is result of hot stamping process. This higher strength leads to larger springback which should be carefully controlled by an appropriate tool design. Moreover, the sheet during the quenching after SHT can be distorted by the non-uniform temperature distribution, which may require additional sheet leveling process before forming. As an alternative to the water quenching, die quenching can be a potential cooling method. In this study, the effect of cooling rate on the mechanical properties of solution heat treated (SHTed) 7075 aluminum alloy sheet is investigated. To control the cooling rate, three different cooling methods are applied: water quenching, die quenching and air cooling. The formability and springback of the SHTed sheet are evaluated, and the mechanical properties after the post artificial aging are comparatively investigated among different cooling methods.

15:15-15:35

Creep Behavior of Polycrystalline Zirconia Ceramics under DC Current

Koji Morita, Yoshida Hidehiro, Byung-Nam Kim, National Institute for Materials Science (NIMS), Korea

Flash sintering phenomena, which occurs by applying DC current directly to ceramic powder compacts, can succeed to lower the sintering temperature of several ceramic powders. On the other hand, Conrad and his colleagues examined the effect of electric fields on the high temperature tensile properties of 3Y-TZP and confirmed that the fields can lower the tensile flow stresses of 3Y-TZP enough to attain superplasticity. The enhanced deformation was explained by suppressed grain growth due to the electric bias effect. However, the effect of electric field on the high temperature deformation is still unclear. In order to clarify the effect of electric current on high temperature deformation, therefore, the present study was carried out to examine the tensile behavior of polycrystalline zirconia ceramics under the several temperature and electric field/current conditions.

By applying the electric power higher than a critical value Ec, the flash event similar to that of powder sintering occurs even in dense zirconia ceramics. At around 1000˚C, for example, the Ec value is about 100~200mW/mm^3, which is slightly larger than those reported in the powder compacts. For lower than Ec, the applied electric current increases sample temperature depending on the applied value, but does not enhance the rate of deformation. For higher than Ec, on the other hand, the electric current enhances the rate of the deformation to about several times as compared with that of without current conditions. The enhanced deformation cannot be interpreted only by the increment of sample temperatures and is likely to occur by the flash event. After the deformation under the electric current conditions, the tested sample shows slight gray color even in air, suggesting that the enhanced deformation would be related to oxygen vacancy formation. In the presentation, we will discuss the detailed current effect obtained at wide range testing conditions.

15:35-16:15 Tea Break

16:15-16:40 Invited

Advanced Surface Coatings Solutions for Marine Hydraulic Components

Ang Andrew, Wade Scott, Swinburne University of Technology, Australia / ARC Training Centre - Surface Engineering for Advanced Materials (SEAM), Australia / DMTC Ltd, Australia; Piola Richard, DST Group, China; Howse Hugo, United Surface Technologies Ltd, Australia; Leigh Matthew, MacTaggart Scott Australia, Australia; Berndt Christopher, Swinburne University of Technology, Australia / ARC Training Centre - Surface Engineering for Advanced Materials (SEAM), Australia

This work focuses on advanced surface coatings developed for protection of critical hydraulic machine components that are subjected to aggressive marine

operating conditions. Specifically, it relates to providing a superior solution to address the issues of corrosion and biofouling for shafts, piston rods or spline components that are often partially or fully immersed in stagnant seawater that often accelerates failures. The project started at a very early technology development stage that included laboratory testing to select the suitable candidate material and optimise the coating process using high velocity oxygen fuelled (HVOF) thermal spraying. This was followed by a series of longer term field trials at several locations around the Australian coast with different environmental conditions to assess the corrosion, biofouling, surface roughness and hydraulic sealing performance of these novel single layer HVOF coatings. Twelve months of static field immersion exposures, as well as subsequent scaled prototype actuators tested in under water environments, showed no coating delamination failures for both WC-NiCr or WC-Hastelloy®-based HVOF coatings. The biofouling rate of these HVOF coatings was 2~3 times less than those of a standard control coating. The surface metrology results also showed that the surface roughness of these HVOF coatings did not vary significantly over the field testing trials and is within the specification requirements of a functional hydraulic shaft. These two candidate coatings (WC–NiCr and WC–Hastelloy® C) are currently being tested in on-board trials.

16:40-17:00

Effect of Different Shot Peening Treatments on Fatigue Strength of Stainless Steel

Yasunori Harada, University of Hyogo, Japan; Takahashi Katsuhiko, Natioanl Institute of Technology, Toyama College, Japan

The effects of peening conditions on the surface characteristics and fatigue life of stainless steel was investigated using microshot peening and ultrasonic shot peening. Shot peening is a surface treatment technology widely used in the automobile industry, and has the effect of improving the fatigue characteristics of mechanical parts. The technique improves the fatigue strength by creating a work-hardened layer, leaving a compressive residual stress in the surface. In recent years, the microshot peening (MSP) and ultrasonic shot peening (USP) technologies have attracted attention. The use of microshot peening technology with minute media has become more widespread in consideration of the reduction of the notch effect in the material surface. The ultrasonic shot peening that uses media of several millimeters in size with ultrasonic vibration has attracted attention as a means to reduce the surface roughness. However, the influence of these technologies on stainless steel has not been much studied. In particular, it is the current situation that little research on USP has been done. In the present study, an air-type and an ultrasonic type machine were used. In the microshot peening process, the media used was high-carbon cast steel and the hard powder, with an average diameter of 0.1mm. The workpieces were three types of stainless steel, SUS304, SUS316, SUS316L. In the MSP, work hardening was evident to the depth of approximately 0.1mm from the surface. This depth was approximately equal to the steel ball diameter. However, the influence of the peening time on the hardness distribution was not great. In the USP, work hardening was deeper in the material. This is because the diameter of the media used for ultrasonic machining was large. The compressive residual stress was added in the surface vicinity on MSP workpieces. In the case of USP, the region with added residual stress extended toward the inside of the material. This is because the diameter of the media used for ultrasonic machining was large and the collisions caused by ultrasonic vibration were more frequent. The fatigue limit was thought to be greater in the USP because the work-hardened layer was formed near the workpiece surface.

17:00-17:20

Characteristics of Oxide Scale Formed on an Equiatomic CrMnFeCoNi Alloy during Early Stages of High Temperature Oxidation

Paeng Jeong In, Swaminathan Srinivasan, Kang Yoon Gu, Jun In-Ho, Myoung-Gyu Lee, Han Heung Nam, In-Suk Choi, Seoul National University, Korea; Min-Gu Jo, Jin-Yoo Suh, Dong-Ik Kim, Korea Institute of Science and Technology, Korea

The equiatomic multi-element metallic alloys are relatively new class of materials that gained considerable interest over recent years. Though these alloys contain high concentrations (nearly 20at.%) of multiple elements with different crystal structures but can crystallize as a single phase. We examined a five-element equiatomic alloy CrMnFeCoNi, which forms a single phase face-centered cubic solid solution. In the present work, oxide scale evolution on a five-element equiatomic alloy CrMnFeCoNi at 700˚c, in ambient air has been investigated, in continuous and discontinuous manner. Ex-situ mass change oxidation kinetics (up to 500h) is determined by using an electronic balance, whereas for in-situ oxidation kinetics, the thermogravimetric (TG) experiment has been conducted for 25h. The microstructural, morphological and chemical analyzes (including the in-depth distribution of chemical element within the oxide layer) have been carried out using XRD, SEM/EDX/EBSD, and Dynamic SIMS techniques. It will be shown that the oxidation rate is initially linear but became parabolic at longer times. In this talk, it will be discussed that how the diffusion of reactants (Mn and Cr) influence the progress of oxidation, and further, the high temperature oxidation resistance of this alloy will be compared with the alloy 740H.

E: Thin Films and Surface Engineering: III

Symposium Organizers :

Chuang Dong, Dalian University of Technology, China; Hongbo Guo, Beihang University, China; Hiroshi Masumoto, Tohoku University, Japan; Ho Won Jang, Seoul National University, Korea; Mingxing Zhang, University of Queensland, Australia

Tuesday PM
August 20, 2019

Room: 313 (3rd Floor)
Symposium: E

Chairs:
Soo Young Kim, Chung Ang University, Korea
Xueqiang Cao, Wuhan University of Technology, China

13:30-14:00 Keynote

Corrosion, Wettability, and Cytocompatibility of Ta and Ta-N Films Deposited on Ti6Al4V by Cathodic Arc Deposition

Yue Zhao, Sina Jamali, University of Wollongong, Australia; Aychingh Hee, University of Adelaide, Australia; Huiliang Cao, SICCAS, China; Avi Bendavid, Phil Martin, CSIRO, Australia

Tantalum and tantalum nitride thin films were produced by filtered cathodic vacuum arc deposition method as a bio-stable surface treatment on Ti_6Al_4V titanium alloy for knee/hip joint implant applications. Effect of nitrogen to argon gas ratio on microstructure of the deposited film was observed by TEM. Corrosion behavior of the films in simulated biological fluid solution was examined by electrochemical impedance spectroscopy. It was found that both the Ta and Ta-N films enhanced corrosion resistance of the Ti_6Al_4V substrate with the best protective characteristics achieved by the Ta-N film deposited at 0.25 N_2/Ar gas ratio. The protective characteristic was attributed to the formation of tantalum oxide and oxynitride compound at the surface, as verified by X-ray photoelectron spectroscopy. Increasing N_2/Ar gas ratio increased susceptibility to localized corrosion. The effect of bias voltage on the substrate was investigated and it was found The Ta/−100V showed a significant improvement in corrosion resistance because of good cohesion to the substrate and a stable passivation layer on the film surface. The in-vitro cytocompatibility of the materials was investigated using rat bone mesenchymal stem cells, and the results show that the Ta films have no adverse effect on mammalian cell adhesion and spreading proliferation.

14:00-14:25 Invited

Metallic Glass Coatings with Beneficial Properties for a Wide Range of Applications

Jinn Chu, National Taiwan University of Science and Technology, Taiwan, China

Glass-forming metallic coating have received increasing attention in recent years because these materials could be obtained readily using PVD processes such as magnetron sputter deposition. Metallic glass coatings are thus now available not only in monolayer and multilayer forms but also in nanotube arrays with sizes up to tens of mm. With the advent of these materials exhibiting unique physical and mechanical properties, the thin-film metallic-glass (TFMG) materials are also of great importance for scientific research and engineering application. In this presentation, some important properties are reviewed, with focuses on the high strength, excellent room-temperature ductility and extremely low coefficient of friction. Then, the TFMG-based applications are introduced, including enhancing electrospun polyacrylonitrile (PAN) membrane for oil/water separation. In this work, which has been published in Surface and Coatings Technology, Vol. 344, p. 33-41 (2019), we used magnetron sputtering to coat PAN membrane with Zr-based TFMG ($Zr_{53}Cu_{26}Al_{16}Ni_5$) to enable the separation of oil and water. The proposed coating also provides protection from chemical and thermal degradation as well as irreversible internal fouling. The smooth TFMG coating also provides a strongly hydrophobic surface (water contact angle of 136°). We also investigated the effects of sodium dodecyl sulfate (SDS) surfactant on oil/water separation performance. The resulting combination of the hydrophobic TFMG-coated membrane with the surfactant enabled oil rejection performance ranging from 95% to 100%, depending on the concentration of SDS. This work confirms that membrane-related problems such as fouling, chemical, and thermal stability can be resolved through the application of metallic glass coatings.

14:25-14:50 Invited

The Oxide Reinforcement Effect of Be on the Oxidation Resistant Be-Containing Mg Alloys

Qiyang Tan, The University of Queensland, Australia

The present experimental work investigated the effect of trace addition of Be on the high temperature oxidation resistance of various Mg alloys, including AZ91, Mg-2Zn, Mg-2Sn, Mg-2Y, AS21, AM60, ZK20 and ZC63. It was found that microalloying with Be significantly improved the oxidation resistance of AZ91, Mg-2Zn, Mg-2Sn, AS21 and ZC63 alloys. But, Be microalloying marginally influenced the oxidation behaviours of the ZK20, AM60 and Mg-2Y alloys. The effectively improved oxidation resistance of the AZ91, Mg-2Zn, Mg-2Sn, AS21 and ZC63 alloys was attributed to the reinforcement effect

on the initially formed oxide layer on the alloy surface. It was indirectly confirmed that Be can segregate in the initially formed MgO layer, (i) forming (Mg, Be)O solid solution; and (ii) refining the oxide grains during the oxidation process. The (Mg, Be)O layer with refined grains exhibited higher mechanical properties, including (i) the interfacial adhesion strength between the substrate and the oxide layer; (ii) the hardness; and (iii) the internal bonding strength of the layer. During high-temperature oxidation, the fine-grained (Mg, Be)O layer provided sufficient strength to withstand the internal stress generated by the internal tension stress and the vigorous Mg vaporisation, and therefore prevented oxide layer from cracking and debonding from the substrate. Hence, the oxidation incubation period was effectively increased. For the ZK20 and AM60, experiment exploited that the Zr and Mn solutes in these alloys chemically reacted with Be added, forming thermally stable Be-containing intermetallic compounds and therefore arrested the role of Be in improving their oxidation resistance. For the Y-containing Mg-2Y alloy, as Y can effectively improve the oxidation resistance, the effect of trace addition of Be was covered.

14:50-15:10

Microstructure and Oxidation Resistance of a Pt Modified α+γ+γ' Coating

Liangliang Wei, Beihang University, China

Platinum modified NiAl coatings, especially single-phase β-NiPtAl coating are widely used as oxidation-resistant coatings or as the bond coats in the thermal barrier coatings (TBCs) system . According to recent research, the single-phase β-NiPtAl coating are not compatible with the new-generation Ni-based single crystal (SC) superalloys contain high amount of refractory elements such as Re, Ru, W and Ta, because numerous topologically closed-packed phases (TCP) and second reaction zone (SRZ) are formed in the SC alloys due to the interdiffusion between the β-NiPtAl coating and SC alloy.

Pt modified γ+γ' coatings were produced by electroplating of Pt films on a second generation Ni-based single crystal (SC) superalloy, followed by diffusion treatment at high temperature. The effects of processing parameters such as Pt film thickness, diffusion temperature and time on the microstructures of the coatings were investigated. Initial Pt thickness, vacuum diffusion temperature and time have important effects on the microstructures and chemical compositions of the Pt modified γ+γ' coatings. A new type of Pt modified α+γ+γ' coating with high contents of Pt and Al was produced by 1h diffusion treatment at 1000℃, which exhibited good oxidation-resistance at 1100℃ but also good compatibility with the SC superalloy.

15:10-15:30

Effect of High Energy Shot Peening on Wear Resistance of TiN Films on TA2 Surface

Conghui Zhang, Xi'an University of Architecture and Technology, China

As a kind of high quality hard film, TiN film can significantly improve the surface hardness and wear resistance of materials, and has been widely used in the fields of dies, cutting tools and so on. In present work,the TiN films were deposited on the surface of pure titanium TA2 without and with high energy shot peening (HESP) by the pulsed magnetron sputtering. The morphology and crystal structure of TiN thin films were analyzed by scanning electron microscopy (SEM) and X-ray diffraction (XRD). The film-substrate adhesion, hardness and modulus of elasticity of TiN films were measured by scratch tester and nanoindentation tester. The wear resistance of TiN films was measured by micro-tribotester. The results showed that: compared with original pure titanium, TA2 surface treated by HESP could produce a large number of defects and have high chemical activity, which can quickly capture and fix Ti and N plasma during the sputtering process to refine the grain size of TiN film and make the film thicker and denser. With the prolongation of HESP time, the film-substrate adhesion increased from 19.6N of original TA2 to 44.2N of 40min HESP-treated TA2, and the nanohardness of TiN films increased from 14.0GPa of original TA2 to 28.4GPa of 40min HESP-treated TA2. HESP treatment could improve wear resistance and stable friction coefficient of TiN thin films. The specific wear rate of TiN films decreased from 0.061mm^3/N.m of original TA2 to 0.019mm^3/N·m of 40min HESP-treated TA2.

15:30-15:50 Tea Break

15.50-16:15 Invited

Understanding Mechanical Failure of Metal/Ceramic Interfacial Regions Through Microscale Mechanical Testing and Multiscale Simulations

Wenjin Meng, Louisiana State University, USA

We summarize our recent efforts in microscale measurements of the mechanical response of metal/ceramic interfacial regions under shear, compression, and tension loading. Utilizing the nanoscale machining capabilities of focused ion beam (FIB) instruments, microscale pillar specimens containing ceramic-coating/adhesion-interlayer/substrate interfacial regions were fabricated, with the interfacial region at different inclinations with respect to the pillar axis. Quantitative ex-situ and in-situ micro mechanical testing was carried out through axial compression and tension loading on the micro-pillar specimens, and was coupled

with morphological/structural characterizations and multiscale simulations, including density functional theory (DFT), molecular dynamics (MD), and crystal plasticity finite element analysis (CPFEA). This combination offers new data and new insights into how metal/ceramic interfacial regions fail under mechanical loading, and suggests approaches for engineering the mechanical performance of metal/ceramic interfaces. Relevance to engineering mechanical integrity of coating/substrate interfaces will be discussed.

16:15-16:40 Invited

Quantitative Measurement of Adhesion Strength for Anti-Corrosive Coating Layers on Steel Sheet

Young-Rae Cho, Pusan National University, Korea

Quantitative measurement of adhesion strength for anti-corrosive coating layers such as paint or zinc layer on steel sheet is very important. Also, corrosion is one of the major concerns for the metals degradation in shipbuilding industry. To protect ship steels from these corrosion problems, anti-corrosive paint has been developed. To obtain the intended results, the anti-corrosive paint should be strongly bonded to the steel-sheet substrate. The bonding (adhesion) strength between the paint and the substrate is governed by the degree of contamination on the substrate surface. When the bonding strength is insufficient, the corrosion resistance of the substrate is greatly degraded. The purpose of this study is to investigate the effect of surface contamination or different coating layers on the bonding strength of epoxy-based paint on the carbon steel for ships application. In particular, the effect of the contaminated area on the bonding strength was investigated. In order to understand these phenomena, we used structural steel (SPCC) and anti-corrosive epoxy paint which is mainly used in the shipbuilding or automotive industry. The adhesion strength between SPCC and anti-corrosive paint was measured by using Elcometer 510 made by Elcometer Corp. Dolly is made of aluminum (Al) with a diameter of 20mm. Especially, the theory of adhesion strength for paint or zinc (Zn) layer on the metallic substrate and effect of surface contamination on the adhesion strength will be discussed in details.

16:40-17:00

Research on A New Rust Stabilization Treatment of Weathering Steel and Its Corrosion Resistance Behavior

Lijun Gao, Jianwei Yang, Jianping Cao, Shengrong Wang, Shougang Group, China

The using of weathering steel without coating had become a new trend. But this using of weathering steel would cause rust scattering and environmental pollution. The formation of stable rust layer would be very long and some areas with high salt content, the dense rust layer would be difficult to form. To solve the problem that rust liquid appeared sagging and flying apart during the initial stage of the using of bare weathering steel. A new rust stabilization surface treatment agent was prepared. The effect of rust stabilization treatment on the rust structure and anticorrosion of weathering steel in the stimulated marine atmosphere were investigated through periodic immersed corrosion test, rust microscopic analysis and electrochemical measurement. The new rust stabilization surface treatment agent was mainly composed of a water-soluble acrylic resin and water is used as a solvent. Additional components added included a promoter, a pigment and a dispersant. Among them, the aqueous solution replaces the organic solvent component added to most of the conventional treatment agents, thereby achieving the purpose of greatly reducing the air pollution and achieving environmental protection effects. The results showed that rust layer of weathering steel after treatment was divided into continuous inner layers and outer layers. After 168h of accelerated corrosion, compared to bare steel, the corrosion rate of treatment weathering steel was reduced to 3.31g·m^2·h^{-1} from 5.71g·m^2·h^{-1}. The corrosion rate was reduced by 42%. The rust layer resistance of treatment steel increased up to 167.7Ω·cm^2 from 96Ω·cm^2. The rust layer resistance increased by 75%. As the corrosion processing, Cr element aggregated on the junction of inner rust layer and substrate as α-（Fe1-xCrx）OOH. The new stabilization agent could obviously improve rust structure, refine the crystal grain and hinder the permeation of Cl^-, which was helpful for the generation of compact, continuous, stable layers on surface of weathering steel.

17:00-17:20

Grain Shape Effects on the Fracture Toughness of Yttria Partially Stabilized Hafnia Ceramics

Chun Li, Yue Ma, Hongbo Guo, Beihang University

The fracture toughness of ceramics served as top coat in thermal barrier coating system is of great importance. Numerous studies have attempted to improve the fracture toughness of some potential TBC materials which have excellent thermal properties by introducing second phase. In this work, 8mol.% Y_2O_3 partially stabilized HfO_2 ceramics (Hf0.92Y0.08O1.96, YSH8) with C phase/ M phase/ C phase sandwich structure was utilized to enhance the fracture toughness. YSH8 specimens with different grain shape were obtained by sintering for 2~16h at 1500℃. X ray diffraction (XRD) and scanning electron microscope (SEM) were used to study the microstructure of YSH8, and indentation

method was utilized to measure the fracture toughness. Results shows that YSH8 samples sintered for different time have identical phase composition, and all the specimens had a C phase/ M phase/ C phase sandwich structure except for the different length to width ratio of M phase. YSH8 sintered for 4h maintained the highest fracture toughness of ~2.4MPa·$m^{0.5}$, mainly because of the relatively high length to width ratio of the M phase inside the sandwich structure. Finite element simulation of the stress state in the sandwich structure was further investigated to study the effect of grain shape on the fracture toughness. The statistics of the sandwich structures in YSH8 samples were counted and two crack propagation resistance factors further explained the relationship of grain shape of YSH8 ceramics and the fracture toughness. This study put forward a simple way to improve the fracture toughness by conventional sintering method, and an effective approach to roughly predict the crack propagation resistance by FEM method.

17:20-17:40

Effect of Interfaces Discontinuity on Effective Thermal Conductivity of APS Lamellar Thermal Barrier Coating

Shiyi Qiu, Yue Ma, Beihang University, China; Chenwu Wu, Institute of Mechanics, Chinese Academy of Sciences, China

The thermal barrier coating obtained by atmospheric plasma spraying has a distinct lamellar microstructure and good thermal insulation properties. The 'splat' boundaries in APS TBCs run parallel to the metal/ ceramic interface, which are highly effective in reducing the thermal conductivity of APS TBCs. In this paper, the concept of discontinuity in 'splat' boundaries is introduced. Using the finite element simulation method, the microstructure model with random distribution of discontinuous boundaries is established, to investigate the effect of interlayer discontinuity on thermal conductivity. The results show that with the increase of interface discontinuity, the thermal conductivity of the coating decreases, and with the increase of the longitudinal distribution density of interlayer discontinuous boundaries, the thermal conductivity of the coating decreases. The discontinuous boundaries overlap distribution model is an optimization model, which has the lowest effective thermal conductivity because the heat transfer path is the longest. In the discontinuous boundaries overlap distribution model, the discontinuous boundaries distribution is more dispersed, and the thermal conductivity of the coating is larger, but the increasing trend tends to be gentle. These results provide a theoretical reference for the microstructure design of thermal barrier coatings.

17:40-18:00

Theoretical Investigation of the Catalytic Activity of Goethite (α-FeOOH) for the Electrochemical Water Oxidation

Tae Hyung Lee, Howon Jang, Seoul National University, Korea; Donghwa Lee, Postech, Korea

Recently, to replace the expansive noble metals in electrocatalyst, transition metals with low cost and comparable performances are chosen as substitutes. Among transition metals, iron, which is one of the most abundant metal in the earth crust, is relatively out of the attention as an electrocatalyst. Due to its earth abundance and well-organized production system, iron has the one-tenth price of nickel, and even one-fiftieth price for cobalt. Considering that the ultimate goal of the water electrocatalysis system is an integrated system with a photovoltaic cell which demands the scale-up processing, the cost competitiveness can be maximized for the commercialization.

To enjoy the strong cost competitiveness of the iron, the poor catalytic property of the iron based electrocatalysts, particularly its low current density should be enhanced. According to several studies, it is known that certain phase, iron oxyhydroxide, can have much higher current density than existing iron-based electrocatalysts. Especially, iron oxihydroxide (FeOOH) belongs to thermodynamically stable form among iron oxides and presented to have enhanced catalytic property by experiments. Though, there are not enough theoretical investigations on its catalytic activity.

Herein, we investigate the water oxidation mechanism on the Iron oxyhydroxide(FeOOH) electrocatalysts using first-principles calculations based on Density Functional Theory. With calculations of relative surface stabilities and adsorbate coverages, the most stable low-index surfaces of FeOOH will be determined. Next, with the determined FeOOH surfaces, we will compare the theoretical overpotentials achieved by calculating each oxygen evolution reaction steps. For each step, the magnetic state will be checked for the explanation of oxygen evolution reaction process. Furthermore, impacts of the various dopants such as Mn, Ni, Co will be also investigated. With the calculation using hybrid functional, the electronic structure of the iron oxyhydroxide, with and without dopants, will be obtained and it will give the explanation of different OER catalytic activity shown by iron oxyhydroxide with different dopants.

For the strict verification of the calculation data, experiment results of the bare and doped FeOOH will be also presented. All the alpha FeOOH samples are synthesized with electrodeposition method and their electrocatalytic properties will be evaluated. With the comparison of calculation and experiment data, it is expected to figure out how the dopants affect bulk properties, reaction at the surface of the FeOOH and eventually influence the electrocatalytic properties.

F. Biomaterials: Surface Modification

Symposium Organizers:

Yufeng Zheng, Peking University, China; Luning Wang, University of Science and Technology Beijing, China; Takayoshi Nakano, Osaka University, Japan; Seung-Kyun Kang, Korea Advanced Institute of Science and Technology (KAIST), Korea; Cuie Wen, RMIT University, Australia; Marc Meyers, University of California, San Diego, USA

Tuesday PM
August 20, 2019

Room: 306 (3rd Floor)
Symposium: F

Chairs:
Takao Hanawa, Tokyo Medical and Dental University, Japan
Donghui Zhu, University of North Texas, USA

13:30-14:00 Keynote

Biofunctionalization of Metals with Development of New Alloy, Manufacturing Process and Surface Modification

Takao Hanawa, Tokyo Medical and Dental University, Japan

Over 70% of implant devices are made of metals, because of their high strength, toughness, and durability. Metals are generally superior to ceramics and polymers on the above properties for medical devices. Therefore, it is difficult to replace metals in medical devices with ceramics or polymers. In this regard, research and development of metals continue on the purpose of improving mechanical and surface properties, which govern their mechanical and interfacial compatibility. Research and development of metals continue with the purpose of improving mechanical and surface properties, which govern their mechanical and tissue compatibility.
After micro arc oxidation (MAO), bone formation on titanium is accelerated. Silver is easily contained in the surface oxide layer by the addition of silver in the electrolyte for MAO. In this case, live bacteria were killed and simultaneously calcification occurred in a certain silver amount. This result reveals that bone formation and antibacterial property are simultaneously performed by addition of calcium, phosphate, and silver to surface oxide layer by MAO. It is possible to obtain and control dual-functional property by this technique.
To clarify the effects of micron/nano hybrid topography on cell behavior and morphology, we investigated the adhesion of human mesenchymal stem cell (hMSC) to titanium surfaces with three different topographies; namely, Micron, Nano, and Hybrid grooves which created using a femtosecond laser. In addition, immune-fluorescent detection of the differentiation of hMSC cultured on specimens after differentiation was conducted. Four cell types, neurocytes, adipocytes, osteocytes, and chondrocytes, were differentiated from hMSC. The different surface features had different effects on the differentiation of hMSC. In particular, the Hybrid surface topography promoted the osteogenic differentiation and chondrogenic differentiation.
On the other hand, we have developed Zr-based alloys, showing low magnetic susceptibility, high strength and corrosion resistance, to decrease MRI artifact. A large-amount melting of Zr-1mass%Mo alloy and investigated mechanical properties, crystal phase, and magnetic susceptibility, for the commercialization of the alloy was performed. Finally, MRI artifact of spinal instruments consisting of the alloy and implanted in sheep spine was observed. 3T MRI artifact of spinal instruments consisting of the alloy and implanted into sheep spine occupied in 2mm and the vertebral canal appeared. Therefore, this alloy is a candidate of MRI compatible alloy.

14:00-14:25 Invited

Engineering a Bioactive Coating on Zinc Metallics for Enhanced Biocompatibility and Antibacterial Property

Donghui Zhu, Yingchao Su, University of North Texas, America; Yufeng Zheng, Peking University, China

Statement of Purpose: Zinc (Zn) has been cited as the "calcium of the twenty-first century", and recently emerged as a novel biodegradable metal thanks to its important physiological roles and promising degradation behavior. However, cytocompatibility and antibacterial property of pure Zn is still suboptimal, in part, due to the excessive Zn ions released during degradation. To enhance the biocompatibility of Zn metallics, bioactive coatings including zinc phosphate (ZnP), zinc oxide (ZnO), and zinc hydroxide ($Zn(OH)_2$) were prepared on pure Zn to enhance its biocompatibility and antibacterial property. These ZnP coated materials can be further developed as bone implants for orthopaedic and other applications.
Methods: ZnP, ZnO and $Zn(OH)_2$ coatings were prepared on pure Zn using chemical conversion methods and characterized by XPS, XRD and SEM-EDS. The coatings were then optimized in regard to the surface morphology and degradation rate through controlling the composition and pH of coating solution. Degradation was carried out using weight loss of immersion in simulated body fluid as well as electrochemical testing. Osteoblast and vascular cell attachment, viability and growth are analyzed using both indirect and direct culture methods. Then the pre-osteoblast differentiation toward bone tissue was examined using ALP and Alizarin Red staining. Moreover, the antibacterial property of the materials were investigated using standard testing in vitro. Last, the in vivo biocompatibility of the new materials was analyzed using μCT and histological staining.

Results: Data shows that ZnP, not ZnO or $Zn(OH)_2$, significantly enhances its biocompatibility. The surface morphology and controlled Zn ion release were shown to be pivotal for the cytocompatibility and antibacterial performance of ZnP coated materials. The decreased Zn ion release and surface morphology significantly enhanced the pre-osteoblast and vascular cell adhesion, viability, and proliferation. Moreover, the micro- and nano-structures of ZnP formed on Zn surface significantly reduced the bacterial adhesion and growth. In vivo data also showed that the Zn materials had good radiopacity without gas shadow and the mechanical integrity maintained for at least 8 weeks. In addition, Zn with ZnP coating showed better osteointegration and osteogenesis property than uncoated control.
Conclusions: Taken together, ZnP coating on Zn-based biomaterials appears to be a viable approach to enhance the biocompatibility and antibacterial property of Zn-based bone implant as well as to control its degradation rate, and could be applied as a novel surface coating to improve biocompatibility of different implants.

14:25-14:50 Invited

Biofunctionalization of Metallic Implants by Synergistic Effects of Micro/Nano-Patterning and Surface Coating

Fuzeng Ren, Mingyu Zhu, Haixia Ye, Ju Fang, Southern University of Science and Technology, China

Implant-associated infection and lack of osteointegration are two key factors to cause failure of metallic implants. Thus, engineering the metallic implant surface with enhanced osteogenic differentiation and antibacterial activity is in great demand for clinical practice. Considering topographical cues play an important role in directing cell behavior, herein, we first demonstrate a fast, cost-effective, and feasible approach to the precise fabrication of shape- and size- controlled micropatterns on titanium substrates using a combination of photolithography and inductively coupled plasma–based dry etching. Then, using this approach, we have designed a series of micropatterned Ti Topochips with varying groove and ridge widths to explore the relationship between topographical parameters, osteoblast proliferation, cell morphology and orientation, and alkaline phosphatase (ALP) activity and osteogenic genes expressions in a high-throughput manner. After identifying the optimal microgroove pattern that can effectively align the cells and promote osteogenic differentiation, we deposited a sandwich-structured Ta-TaCu coating on the micro-patterned Ti. Using the synergistic effects of micro/nano-patterning and chemical coating, the developed titanium implants had dual-functions of enhanced osteogenic differentiatioon and antimicrobial activity. This study not only offers a microfabrication method that can be extended to fabricate various shape- and size-controlled micropatterns on titanium and its alloys, but also provides insight into the surface biofunctionalization of orthopedic and dental implants.

14:50-15:10

Nanorod-Shaped Si Substituted Hydroxyapatite Coating on Ti for Percutaneous Implants

Kai Li, Ting Yan, Lan Zhang, Yong Han, Xi'an Jiaotong University, China

A ideal intraosseous transcutaneous implant should form firm biointegration with natural bone and soft tissue at the bone-fixed and percutaneous positions, simultaneously. Notably, a tight seal between the underlying dermis and implant surface, which prevents soft tissue recession and bacterial infection, plays a key role in the service life of a percutaneous implant. Natural soft tissue mainly consists of collagen fibrils, and such a fibrous framework is an ideal extracellular matrix that can host cells capable of dynamically remodeling the tissue. In this paper, Si substituted hydroxyapatite (Si-HA) nanorods were designed on Ti to simulate the microstructure of natural tissue and improve the biointegration of Ti with soft tissue. The nanorods were fabricated by alkali-heat treatment followed with hydrothermal treatment (HT). The microstructure, phase composition, chemical state, surface roughness, and wettability of the Si-HA as well as pure HA nanorods were characterized. The hydrothermal formation mechanism of the Si-HA nanorods was explored. The skin-forming cell (fibroblast) behaviors in vitro and skin integration in vivo of the Si-HA nanorods were evaluated, and pure HA nanorods coated Ti were used as controls. The obtained results show that the incorporation of Si did not significantly alter the phase component, morphology, roughness and wettability of HA. Comparing to HA nanrods and Ti substrate, Si-HA nanrods enchanced cell behaviors including proliferation and fibrotic phenotype in vitro and skin integration, such as reducing epithelial down growth and stimulating collagen deposition in vivo. It should be due to the releasing of Si and nantopography of Si-HA nanorods. Coating Ti with Si-HA nanorods could be an option to improve and accelerate skin integration for percutaneous implants in clinic.

15:10-15:30

Promotion of Osteoconductivity of Titanium with Multi-Scaled Hierarchical Patterned Topography Fabricated by Femtosecond Laser Irradiation

Peng Chen, Maki Ashida, Yusuke Tsutsumi, Takao Hanawa, Tokyo Medical and Dental University, Japan; Keisuke Takenaka, Masahiro Tsukamoto, Osaka University, Japan

The next generation surface modification on medical and dental implants is coatings of tissue or stem cells on them.

To promote cellular attachment and formation of tissues on artificial substrate, the control of patterned surface topography is an alternative method. As in previous reports, the surface topography of a material governs its biocompatibility; for example, in the case of titanium (Ti), nanometer scale topographical features influence cell spreading and micrometer scale topography promotes stem cell differentiation in vitro. To clarify the role of patterned multiscale hierarchical topographies on the biocompatibility and osteoconductivity of metallic biomaterials, we investigated the adhesion and calcification of mouse preosteoblast (MC3T3-E1) to Ti surfaces with three surface patterned micro/nano grooves topography fabricated by single-shot femtosecond laser irradiation.

Ti (grade 2) was mirror-polished (m_{Ti}) and the surface was scanned with a femtosecond laser. As a result, Ti surfaces with three patterned micro/nano grooves topography were fabricated: full surface pattern (f_{Ti}), half surface pattern (h_{Ti}), and chessboard pattern (c_{Ti}). The surface morphology and chemical state of the Ti surfaces before and after laser irradiation were characterized using scanning electron microscope (SEM) and X-ray photoelectron spectroscope (XPS), respectively. The cell extension morphology after 6h incubation was visualized by fluorescent staining. The cell proliferation on Ti with surface patterns was evaluated with cell counting kit-8 over five continuous days. The osteogenic differentiation was induced with induction medium. Calcification of MC3T3-E1 cultured on Ti substrates was evaluated with alizarin red S staining.

The SEM images showed a successful fabrication of clear micro-grooves with nano-ripples periodic interval on Ti. For this surface processing with femtosecond laser irradiation, XPS results showed that there was no significant difference of surface compositions and chemical states among Ti specimens with and without laser scanning. Cells cultured on surface with micro/nano grooves topography were highly aligned. However, a lower growth rate was showed by cells culture on the full patterned surface (f_{Ti}) comparing with smooth surface (m_{Ti}). In addition, larger extracellular calcified deposition areas were observed by f_{Ti} and c_{Ti} compared with that observed by m_{Ti} and h_{Ti}, indicating that the multi-scaled hierarchical topography promoted calcification in vitro. Interestingly, similar calcified deposition areas were obtained by m_{Ti} and h_{Ti}, and also f_{Ti} and c_{Ti}, respectively. In our current work, Ti with three surface patterned micro/nano grooves topography was fabricated by femtosecond laser scanning. A high orientated cellular morphology showed by cells on Ti surface with micro/nano grooves topography. Notably, compared with mirror surface, cells cultured on the micro/nano grooves topography showed a larger calcified area, which indicated superior osteoconductivity. Moreover, the chessboard-patterned Ti surface with a better balance between proliferation and calcification is expected to provide a basis for designing novel biomaterial–cell interfaces to promote the osteoconductivity of metallic biomaterials.

15:30-16:10 Tea Break

16:10-16:35 Invited

Surface Modification and Biomechanical Compatibility of Biomedical Titanium Alloy

Zhentao Yu, Northwest Institute for Nonferrous Metal Research, China

Biomedical titanium alloy is widely used in the production of surgical implants for hard tissue repair or replacement. The biomechanical compatibility between titanium alloys implant and bone is a key factor in its long-time service period. The surface morphology of Titanium alloys also limits the service life of implant. It is necessary to investigate new high strength and low modulus medical titanium alloys and related surface modification technology to get more compatible implant with bone tissue. We have developed a novel Beta-type Ti alloy Ti3Zr2Sn3Mo25Nb (TLM) with E = 60~80GPa and R_m = 700~1020MPa, shows an excellent comprehensive performance and wide application. A unique dealloying idea has also been used to modify the TLM surface and got (i) porous surface by micro-arc oxidation method, can induce osteoblast adhesion, differentiation and proliferation; (ii) antibacterial surface by Ag atom addition, show a long duration of action; (iii) colourful coating by TiO_2, can improve the efficiency of surgery. It has also been found that the biological friction interface and bioactive interface between titanium alloys implant and bone are where the failure of implants originated. To develop a long-life titanium alloys implant, we try to investigate the relationship between implant interfaces and biomechanical compatibility.

16:35-17:00 Invited

Oxygen Tolerant RAFT Polymerisation: Application in the Design of Anti-Microbial Polymers

Cyrille Boyer, Jonathan Yeow, Peter Judzewitsch, Thuy-Khanh Nguyen, Sihao Xu, Gervase Ng, Nathanial Corrigan, Rashin Namivandi-Zangeneh, Zahra Sadrearhami, Sivaprakash Shanmugam, Chenyu Wu, UNSW, Australia;

The presence of oxygen during controlled/living radical polymerisation (CLRP) can be detrimental owing to its rapid quenching of carbon-centred radicals. As a result, CLRPs are typically performed after the removal of dissolved and atmospheric oxygen by nitrogen sparging or freeze-pump-thaw cycling. This requires specialist equipment and sealed reaction vessels, which can limit the scalability of CLRP particularly when considering high throughput polymer synthesis at low reaction

volumes. Furthermore, improving the tolerance to oxygen in CLRP can significantly improve or expand the scope of polymer applications in surface modification, biomolecule functionalisation and (micro)flow chemistry by removing the need for deoxygenation processes. Furthermore, the development of such process can fast track the synthesis of polymer libraries.

As a result, in recent years, there has been renewed interest in performing CLRP without the need to first apply physical deoxygenation techniques. Our team has focused on the development of photopolymerisation technique named photoinduced electron/energy transfer – reversible addition fragmentation chain transfer (PET-RAFT) polymerisation, which can convert oxygen into inactive species. The PET-RAFT process uses photoredox catalysts, including organo-dyes and metal based photoredox catalysts, and in the presence of a suitable reducing agent, polymerisations can be conducted in the presence of oxygen (or air) at microlitre volumes (> 10μL) and at low concentration. These polymerisations proceed under mild conditions at room temperature in water or organic solvents, with excellent polymerisation control achievable even at molecular weights approaching 100 000g/mol. These RAFT polymerisations are compatible with a range of monomer families and can be performed in microtiter well plates and even in discrete droplets. Using this platform, we demonstrate that the ability to perform multiple parallel polymerisations can greatly aid in the synthetic optimisation of polymeric architectures such as star polymers and self-assembled nanoparticles (spherical-, worm-micelles and vesicles). We have demonstrated the effectiveness of this fast throughput strategy via the rapid preparation of a library of anti-microbial polymers and test their antimicrobial activities against different gram-negative bacteria. Using this process, we have been able to rapidly prepare library of anti-microbial polymers and test their antimicrobial activities against different gram-negative bacteria. Interestingly, the anti-microbial activities can be affected by the monomer placement in the polymer chain as well as by the monomer structure and polymer composition. To improve anti-microbial activity, Nitric oxide donor molecules were conjugated to the polymer structure. Nitric oxide donors can release NO gas under specific conditions, which promotes the dispersion of bacterial biofilm. By combining NO and anti-microbial polymers, we can see synergetic anti-microbial activities against a range of different bacteria.

17:00-17:25 Invited

Osteoanabolic Implant Materials for Orthopedic Treatment

Xiaobo Chen, RMIT University, Australia; Rachel Li, Paul Smith, Nick Birbilis, Australian National University, Australia; Mitsuo Niinomi, Tohoku University, Japan

Osteoporosis is becoming more prevalent due to the aging demographics of many populations. Osteoporotic bone is more prone to fracture than normal bone, and current orthopedic implant materials are not ideal for the osteo-porotic cases. A newly developed strontium phosphate ($SrPO_4$) coating is reported herein, and applied to Ti-29Nb-13Ta-4.6Zr (wt%), TNTZ, an implant material with a comparative Young's modulus to that of natural bone. The $SrPO_4$ coating is anticipated to modulate the activity of osteoblast (OB) and osteoclast (OC) cells, in order to promote bone formation. TNTZ, a material with excellent biocompatibility and high bioinertness is pretreated in a concen-trated alkaline solution under hydrothermal conditions, followed by a hydro-thermal coating growth process to achieve complete $SrPO_4$ surface coverage with high bonding strength. Owing to the release of Sr ions from the $SrPO_4$ coating and its unique surface topography, OB cells demonstrate increased proliferation and differentiation, while the cellular responses of OC are suppressed, compared to the control case, i.e., bare TNTZ. This TNTZ implant with a near physiologic Young's modulus and a functional $SrPO_4$ coating provides a new direction in the design and manufacture of implantable devices used in the management of orthopedic conditions in osteoporotic individuals.

17:25-17:45

Fabrication of Biodegradable MgxCu(x=0, 0.1, 0.4, 0.7) Coating on Ti6Al4V Alloy as Orthopedic Implants Materials with Enhanced Antibacterial Property

Muhammad Ibrahima, Junxiu Chena, University of Science and Technology of China, China; Xiaoming Yu, Lili Tan, Ke Yang, Institute of Metal Research, Chinese Academy of Science, China; Huazhe Yang, China Medical University, China

Titanium and its alloys are widely used as implant materials, because of their reliable and favorable mechanical properties, such as high strength and rigidity etc. However, surface modification is necessary to increase their bioactivity. In this study, a bioactive MgCu coating was successfully fabricated on Ti6Al4V substrates by arc ion plating (AIP). The surface composition of the sample was characterized by X-ray diffraction and the surface morphology was characterized by scanning electron microscope (SEM) equipped with energy dispersive spectroscopy (EDS), while the Cu contents were analyzed by inductively coupled plasma-atomic emission spectrometry (ICP). The fabricated MgCu coating was proved with fine particle size. The electrochemical experiment showed the corrosion rate of pure Mg coating was lower than the MgCu coating. Antibacterial assays proved that the MgCu coating could successfully reduce the viability of Staphylococcus aureus (S.aureus). So it is expected that MgCu coated Ti6Al4V with improved antibacterial properties can be used for the orthopedic application.

G. Smart and Magnetic Materials: Permanent and Soft Magnetic Materials

Symposium Organizers:

Shaoxiong Zhou, Center Iron & Steel Research Institute, China; Chengbao Jiang, Beihang University, China; Satoshi Sugimoto, Tohoku University, Japan; Haein Yim, Sookmyung Women's University, Korea; Sean Li, New South Wales, Australia; Bob Shull, National Institute of Standards and Technology, USA

Tuesday PM Room: Yulan Hall-220 (2nd Floor)
August 20, 2019 Symposium: G

Chairs:
Hae-Woong Kwon, Pukyong National University, Korea
Yongsheng Yu, Harbin Institute of Technology, China

13:30-14:00 Keynote

Fabrication and Potential Applications of Magnetic Nanomaterials

Yanglong Hou, Kai Zhu, Junjie Xu, Peking University, China

Magnetic nanomaterials (MNMs) have attracted significant interest in the past few decades due to their unique properties such as superparamagnetism, which results from the influence of thermal energy on a ferromagnetic nanoparticle. To understand the fundamental behavior of nanomagnetism and develop relevant potential applications, various preparation routes have been explored to produce MNMs with desired properties and structures, among which chemical synthesis, especially high-temperature organic-phase method, play an indispensable role in which the microstructures and physical/chemical properties of MNMs can be tuned by controlling the reaction conditions such as precursor, surfactant, or solvent amounts, reaction temperature or time, reaction atmosphere, etc. In this talk, we first introduce the fundamental of high-temperature organic-phase method, and present the progress on the synthesis of plenty of MNMs, including monocomponent nanostructures (like metals, metal alloys, metal oxides/carbides) and multicomponent nanostructures (heterostructures and exchange-coupled nanomagnets). Considering the latter type not only retain the functionalities from each single component, but also possess synergic properties that emerge from interfacial coupling, with improved magnetic, optical or catalytic features, and therefore, we will discuss the potential applications of MNMs in many areas, including biomedicine, catalysis, environmental purification and etc. For an instance, Fe_5C_2, one kind of representative iron carbide, have shown infinite possibilities. It showed intrinsic catalytic properties during Fischer–Tropsch synthesis, no matter in efficiency and selectivity. On the other hand, through modification of affinity proteins (ZHER2:342), Fe_5C_2 NPs can selectively bind to HER_2 overexpressing cancer cells. T2-weighted MRI and PAT signals are readily observed, and tumors are effectively ablated by PTT under NIR irradiation. To enhance cancer therapeutic efficiency, anticancer drug doxorubicin is loaded into bovine serum albumin coated Fe_5C_2 NPs, combining PTT with chemotherapy. Such nanoplatform can respond to NIR and acidic environments, and exhibit burst drug release. In summary, we overview the rational design, fabrications of magnetic nanomaterials, this kind of materials give great application potential in biomedicine and nanocatalysis.

14:00-14:25 Invited

Topological Electronic Transport of Magnetic Weyl Semimetal in $Co_3Sn_2S_2$ Nanodevices

Enke Liu, Institute of Physics, Chinese Academy of Sciences, China

As a topological physical state, magnetic Weyl semimetals (WSMs) motivate increasing interests in the condense matter physics for low-consumption electronic devices and topological quantum computation. Originating from topologically non-trivial band characters in time-reversal symmetry broken systems, magnetic WSMs host two-fold degenerate Weyl fermions acting as magnetic monopoles of Berry curvature. Thus magnetic WSMs are expected to generate a strong intrinsic anomalous Hall effect (AHE) and Nernst effect (ANE). Recently, the quasi-two-dimensional, kagome-lattice magnetic WSM candidate $Co_3Sn_2S_2$ was realized experimentally, with chiral-anomaly-induced negative magnetoresistance, giant AHE, and large ANE, showing a promising potential for topological spintronic. The topological transport behaviors in nanoscale are highly desired for the device applications.
In this talk, I will present a transport study on nanodevices of $Co_3Sn_2S_2$. The devices with a thickness of 180nm have been prepared by micro-fabrications. The thin films show stable out-of-plane ferromagnetism and enhanced AHE, with a Curie temperature of 171K. The anomalous Hall conductivity, Hall angle, and coercive force were measured as 1500S/cm, 23%, and 5T, respectively, which are much larger than the bulks. The comparisons of anomalous Hall angle and factor with other materials will be presented. The results indicate the topological transport behaviors can be enhanced in nanoscale, which are important for potential applications. Magnetic Weyl semimetal $Co_3Sn_2S_2$ can provide an ideal system for device physics and applications under the connection of topological physics and spintronic.

14:25-14:50 Invited

Lattice-Matched Magnetic Tunnel Junctions Using a Spinel Barrier for Advanced Spintronic Devices

Hiroaki Sukegawa, National Institute for Materials Science (NIMS), Japan

A magnetic tunnel junction (MTJ) having a ferromagnet (FM)/tunnel barrier/FM trilayer structure has been widely used for spintronic practical applications such as read sensors in hard disk drives and memory cells of magnetoresistive random access memories. Typically, an MTJ has a thin oxide tunnel barrier, which controls its magnetoresistive performance. Especially, tunnel magnetoresistance (TMR) ratio, the resistance change ratio for parallel and antiparallel magnetization configurations, determines the electrical output of a device. Recent MTJ applications dominantly use MgO as a barrier since large TMR ratios more than 100% can be easily obtained by the coherent tunneling mechanism. However, MgO has a non-negligible lattice-mismatch with various FM layers, which limits MTJ performance. Recently, the lattice mismatch was effectively reduced by the use of a new barrier, $MgAl_2O_4$ (spinel). Therefore, $MgAl_2O_4$ is expected to be a promising barrier material for achieving a defect-free MTJ suitable for various spintronic applications.
In this talk, I will introduce recent progress of our spinel barrier technology. Thanks to the perfect lattice-matching with CoFe based alloys, large TMR ratios of 200%~300% were demonstrated at room temperature in epitaxial $MgAl_2O_4$ based MTJs prepared by various methods: post-oxidation, a direct sputtering, and electron-beam evaporation. In addition, a CoFeB/ $MgAl_2O_4$ /CoFeB-type polycrystalline MTJ with a large TMR ratio ~ 260% was achieved by controlling the $MgAl_2O_4$ interface, demonstrating the industrial viability of spinel-based MTJs. I will also introduce a new spinel barrier with a low barrier height, $MgGa_2O_4$, which significantly reduces a junction resistance (~1/50 of $MgAl_2O_4$ at a given barrier thickness). The remarkable features including the tunability of a lattice-constant and a barrier-height are likely to pave the way for constructing advanced spintronic devices.
This work was partly supported by the ImPACT Program, and JSPS KAKENHI Nos. 16H06332 and 16H03852.

14:50-15:15 Invited

Spin-Orbit-Torque Engineering in Multiferroic Heterostructure

Kangkang Meng, Yong Jiang, University of Science and Technology Beijing, China

The ability to manipulate magnetic states in an ultrathin ferromagnetic (FM) layer has been widely studied for device applications such as nonvolatile magnetic memory. It was found that the combination of STT with spin-orbit coupling led to a new type of torque: Spin-orbit torque (SOT). SOT is that an in-plane electric current applied in a heterostructure with large spin-orbit interaction or its structural inversion asymmetry gives rise to a torque, and the advantages of SOT are generally fast reaction, reliable operation, operation and feasible integration, and the origin of SOT arises from the bulk spin Hall effect (SHE) in the heavy metal (HM) and/or the interfacial Rashba effect at interfaces.
In the last few years, the idea of electric manipulations in ferromagnetic heterostructures has been proposed for the next generation spintronic devices. Among them, the magnetization switching via spin-orbit torque (SOT) has been intensely pursued due to its high stability and scalability. In this talk, a novel way was introduced to manipulate the switching current of SOT, and the $BiFeO_3$ (BFO) based heterostructures with opposite spontaneous polarization largely changes the perpendicular magnetic anisotropy and SOT switching. The harmonic Hall voltage measurements were taken to measure damping-like torque, and then a change up to 272% in effective spin Hall angle can be calculated with different polarizationx. Our findings may pave the way towards multiferroic spin current control and reconfigurable logic devices.

15:15-15:35

Overcoming Synthetic Metastability and Achieve Widely Tunable Metal to Insulator Transitions Achieved in D-Band Correlated Rare-Earth Nickelates

Jikun Chen, University of Science and Technology Beijing, China

Effective synthesis of meta-stable materials challenging the thermodynamic limits will largely broaden the horizon in material designs and further device applications. As one typical example, the d-orbital bands correlated perovskite structured rare-earth nickelates ($ReNiO_3$) exhibits high thermodynamic instability and cannot be synthesized via conventional chemical reactions. Such metastable nickelates provskite system has extremely complex electronic orbital configurations and phase diagrams, enabling unconventional functionalities such as the metal-insulator transition (MIT) and multiple magnetic ground states. This has greatly enriched the respective applications in fields such as artificial intelligence (Nat. Commun. 2017, 8, 240), high-performance energy conversion (Nature, 2016, 534, 231), biological sensing (Nature, 2018, 553, 68) and multifunctional logic/memory devices (Nature, 2017,

546, 124). Nevertheless, these applications are vitally bottlenecked by the ineffective growth of $ReNiO_3$ thin films in electronic level, which heavily relies on complicated and vacuum-based procedures at the current stage.

The discovery of a more convenient synthetic approach that is free of utilizing any vacuum process to grow metastable $ReNiO_3$ thin films in high quality and electronic level will lead profound impacts, promoting both their more-in-depth fundamental exploration and device applications. Herein, this vital issue is addressed as we developed a wet-chemical based and vacuum free approach to effectively row single crystalline $ReNiO_3$ thin films with widely regulatable rare-earth compositions, i.e. Nd, Sm, Eu, Gd, Sm1-xNdx, Sm1-xEux, Sm1-x-yNdxEuy and Sm1-x-yNdxGdy. As compared to the previous synthesis of $ReNiO_3$, our approach largely simplifies the fabrication procedure, reduces the cost, and achieves high flexibility in regulating the electronic structures via compositions and interfacial strains as indicated by synchrotron spectroscopy. As-grown $ReNiO_3$ exhibit a sharper metal-to-insulator transition with a broadly tunable transition temperature across 400K, compared with the best performance reported previously. The largely enhanced effectiveness in synthesizing $ReNiO_3$ is expected to further pave the way to explore their new applications in emerging electronic devices.

15:35-16:10 Tea Break

16:10-16:40 Keynote

Nonvolatile Memory and Synaptic Devices Based on the Magnetoelectric Effects

Yang Sun, Jianxin Shen, Peipei Lu, Dashan Shang, Yisheng Chai, Institute of Physics, Chinese Academy of Sciences, China

From a symmetry concern, there should be a fourth fundamental circuit element defined from the relationship between charge q and magnetic flux j, in addition to the well-known resistor, capacitor, and inductor. We demonstrate that a two-terminal passive device employing the magnetoelectric (ME) effects exhibits a direct relationship between q and ϕ, and thus acts as the fourth fundamental circuit element. Both the linear element and nonlinear memelement, termed transtor and memtranstor, respectively, have been experimentally realized using multiferroic materials showing the ME effects. A full map of fundamental circuit elements consisting of four linear (resistor, capacitor, inductor, and transtor) and four nonlinear-memory (memristor, memcapcitor, meminductor, and memtranstor) elements is constructed. Especially, the memtranstor has a great potential in creating next-generation nonvolatile memory devices. The principle is to utilize the states of the magnetoelectric coefficient, instead of magnetization, electric polarization, or resistance, to store binary information. We have demonstrate in a series of experiments nonvolatile multilevel memory as well as artificial synaptic devices based on the memtranstors made of multiferroic heterostructures and hexaferrites. This kind of nonvolatile memory based on the memtranstors has practical merits such as the simple structure, low power consumption, parallel reading, fast speed, and so on.

16:40-17:05 Invited

Spin Colossal Magnetoresistance

Zhiyong Qiu, Dalian University of Technology, China; Dazhi Hou, Eiji Saitoh, Tohoku University, Japan

Spin - the key element of spintronic - has been regarded as a powerful substitution for the charge in the next generation of information technology, in which spin will be the carrier of information and/or energy just as the charge has done in the framework of electronics. The great feature of spin, transport of which is free from the electron motion, makes spin transport in insulator becoming one of the hot topics, and magnetic ordering insulators are the most compelling material systems.

Here, we report a new effect in an antiferromagnetic insulator, named spin colossal magnetoresistance (SCMR). In an electric system, CMR refers to a large change in conductivity induced by a magnetic field in the vicinity of a metal-insulator transition and has inspired extensive studies for decades. We demonstrate an analogous spin effect near the Neel temperature TN=296K of the antiferromagnetic insulator Cr_2O_3. Using a yttrium iron garnet YIG/Cr_2O_3/Pt trilayer, we injected a spin current from the YIG into the Cr_2O_3 layer and collected via the inverse spin Hall effect the signal transmitted in the heavy metal Pt. We observed a change by two orders of magnitude in the transmitted spin current within 14K of the Neel temperature. This transition between spin conducting and nonconducting states could be also modulated by a magnetic field in isothermal conditions. This effect, that we term spin colossal magnetoresistance (SCMR), has the potential to simplify the design of fundamental spintronic components, for instance enabling the realization of

spin current switches or spin-current based memories.

17:05-17:30 Invited

Electric-Field Control of Magnetic Materials

Zhiqi Liu, Beihang University, China

Using an electric feld instead of an electric current (or a magnetic feld) to tailor the electronic properties of magnetic materials is promising for realizing ultralow-energy-consuming memory devices. In this talk, I would like to present our experimental results on giant magnetization and resistivity modulation in a metamagnetic intermetallic alloy, FeRh, which is achieved by electric-feld-controlled magnetic phase transitions in multiferroic heterostructures. Furthermore, this approach is extended to colossal electroresistance memory devices, topological antiferromagnetic spintronic, and new antiferromagnetic memory devices.

17:30-17:50

Spin Glass Properties Mapped by Coercivity in Ferromagnet/Spin Glass Bilayers

Xiaodan Chi, Yong Hu, Northeastern University, China

We report a study on the spin glass (SG) anisotropy (KSG) and interfacial exchange coupling (JIF) dependent coercivity (HC) at ferromagnet (FM)/SG interface, based on modified Monte Carlo Metropolis algorithm. It is shown that KSG and JIF are interdependent while take effect on different magnetic degrees of freedom and different time scales, resulting in complicated HC behaviors. On the one hand, the KSG dependence of HC is nonmonotonic (initially increases and then decreases to level off) at small JIF, while monotonically increases at large JIF. On the other hand, HC vs. JIF decreases monotonically at small KSG while exhibits a minimum value at intermediate JIF for large KSG. The complicated HC behaviors, not shown in the conventional ordered magnets, image the complex SG nature. By means of a micromagnetic approximation approach, we analytically explained the HC behaviors with respect to KSG and JIF. The dynamic SG surplus magnetization and the SG spin rotatability at the interface, hard to be detected experimentally, have proven to play crucial roles. This paper elucidates the weak anisotropy dependence of SG magnetic properties, and predicts that the SG features can be tunable at will by precisely controlling the magnetic parameters. Therefore, the SG physics picture in nanostructures is clear.

H. Materials Characterisation and Evaluation: III

Symposium Organizers:

Zhiwei Shan, Xi'an Jiaotong University, China; Xiaodong Han, Beijing University of Technology, China; Satoshi Hata, Kyushu University, Japan; Ju-Young Kim, Ulsan Institute of Science and Technology (UNIST), Korea; Jin Zou, University of Queensland, Australia; Jennifer Carter, Case Western Reserve University, USA

Tuesday PM
August 20, 2019

Room: 308 (3rd Floor)
Symposium: H

Chairs:
Ryo Ishikawa, The University of Tokyo, Japan
ShiHoon Choi, Sunchon National University, Korea

13:30-14:00 Keynote

Heterogeneous Deformation Behaviors and Microstructure Evolution of Mg Alloys during Mini-V-Bending, Erichsen and In-Situ Tension Tests

ShiHoon Choi, Jaiveer Singh, Min-Seong Kim, Sunchon National University, Korea

Improvement in the stretch or bend formability of Mg alloys sheets at room temperature (RT) is needed to expand their range of applications. Texture modifications of Mg alloys via the micro-alloying of rare earth (RE) metals or pre-twinning/stretching is now commonly used to improve the formability of Mg alloys at RT. In this study, heterogeneous deformation behaviors and microstructure evolution of magnesium (Mg) alloy sheets were investigated via mini-V-bending and conventional Erichsen testing at room temperature (RT). Formability of Mg alloys was discussed in terms of punch stroke (PS) and Erichsen index (IE) during mini-V-bending and Erichsen tests, respectively. Microstructure evolution in E-form and AZ31 Mg alloys was studied via ex-situ mini-V-bending tests. The microtexture heterogeneity through the thickness direction of the E-form Mg alloy sheets deformed by different PSs was discussed in terms of deformation twinning and detwinning during Erichsen tests. The evolution of the microtexture, twin, and KAM (kernel average misorientation) was analyzed via electron back-scattered diffraction (EBSD) technique. The EBSD results revealed how twin bands (TBs) developed at different PSs in the deformed grains made a significant contribution to the localized deformation zones in both Mg alloys under the mini-V-bending process. High-resolution cross-sectional t-EBSD analysis showed that surface relief allowed the grains residing on the free surface to be less affected

by stress concentration while the sub-surface grains were more affected by stress concentration, which promoted the development of twinning during the mini-V-bending process. Furthermore, we investigated the detwinning behaviors of in-plane compressed E-form Mg alloy systematically using in-situ tensile test with EBSD technique. Microtexture evolution was analyzed at different tensile strains. The detwinning in E-form Mg alloy was found to be linked to both twin boundary mobility and the interaction of their boundaries with dislocations. The effect of detwinning on mechanical behavior and formability of the E-form Mg alloy was also examined. In-situ tensile test EBSD results indicate that most of the deformation twins formed during in-plane compression were removed when the load is reversed during a tensile test.

14:00-14:25 Invited

Holistic Characterisation of Biomedical Materials Produced by CSIRO's Additive Manufacturing Centre

Natasha Wright, CSIRO, Australia

Characterisation of additive manufactured products, in particular those developed for Biomedical applications, can be a significant challenge due to the complex systems and interface interactions of the constituents, which can be at levels ranging from subnano - to micro-scale. The ability to holistically characterise these distributions and interactions has continued to grow in importance within CSIRO compared with conventional, bulk analyses.

In this paper the application of ultra- high resolution imaging (including 3D tomography), thin film X-ray diffraction, spectroscopic and various surface analysis techniques (XPS, AFM) have been employed to holistically characterise several examples of custom engineered products for Biomedical applications produced by CSIRO's Additive Manufacturing Centre.

Characterisation of additive manufactured products, in particular those developed for Biomedical applications, can be a significant challenge due to the complex systems and interface interactions of the constituents, which can be at levels ranging from subnano - to micro-scale. The ability to holistically characterise these distributions and interactions has continued to grow in importance within CSIRO compared with conventional, bulk analyses.

In this paper the application of ultra- high resolution imaging (including 3D tomography), thin film X-ray diffraction, spectroscopic and various surface analysis techniques (XPS, AFM) have been employed to holistically characterise several examples of custom engineered products for Biomedical applications produced by CSIRO's Additive Manufacturing Centre.

14:25-14:50 Invited

Environmental Attack in Metals Revealed by in Situ ETEM

Degang Xie, Yuecun Wang, Zhiwei Shan, Xi'an Jiaotong University, China

Environmental TEM is a powerful technique for corrosion science, not only in uncovering the micro-nano-mechanism behind environmental attack, but also in chemically modifying materials for higher corrosion resistance. In this talk, examples of both aspects from our group will be delivered to demonstrate how fundamental research at micro- and nano-scale can help understand materials behavior and improve materials property. This talk will include two workflow, the first one is hydrogen induced blistering and hydrogen-dislocation interaction in Al, while the other one is using exited CO_2 to improve the corrosion resistance of Mg and its alloys. In the Al-H part, despite that that hydrogen has long been known to cause blisters in Al/Al alloys and result in the spallation of protective film, but all current models fail to explain how a nanoscale gas bubble manages to reach its critical size at the metal/oxide interface before the oxide layer can deform. Our work revealed how tiny blisters came into being at this very early stage as well as the subsequent developing process at room temperature and at elevated temperature, to eventually cause the failure of protective oxide film. Once dissolved into the metal substrate, hydrogen will also impact dislocation behavior. In this aspect, we performed carefully-designed experiments to provide direct evidence that hydrogen can lead to strong pinning effect on dislocation motion, mediated by forming hydrogenated vacancies, at odds with previous understanding. In the Mg-CO_2 part, knowing that the origin to inadequate corrosion resistance of Mg and its alloys is the porous and unprotective surface layer mainly consisting of MgO and $Mg(OH)_2$, we exploit the electron-beam-excited CO_2 inside ETEM to purposely transform the pre-existing surface layer into a compact $MgCO_3$ layer, which render much better corrosion resistance to the metal. The $MgCO_3$ layer shows strong adherence to the metal substrate and can simultaneously strengthen the near-surface layer. The above findings have broad implications for coating performance in nuclear, petroleum, and transportation industries, and can help optimize the material design strategies to alleviate a broad range of environmental induced materials failures (Xie et al, Nature Materials, 2015 ; Xie et al, Nature Communications, 2016; Li, Xie al, Nature Communications, 2017; Zhang et al, Nature Communications 2018; Wang et al, Nature Communications, 2018).

The authors acknowledge supports from the National Key Research and Development Program of China (No. 2017YFB0702001), the Natural Science Foundation of China (51701151), and the Natural Science Foundation of Shaanxi Province (2017JQ5110)

14:50-15:10

Crack Tip, Dislocation Structure and Hydrogen

Shuai Wang, Southern University of Science and Technology, China / University of Wisconsin-Madison, USA; Akihide Nagao, Kyushu University, Japan / JFE Steel Corporation, Japan; Petros Sofronis, Kyushu University, Japan / University of Illinois at Urbana-Champaign, USA; Ian M. Robertson, University of Wisconsin-Madison, USA

The presence of hydrogen accelerated the fatigue crack growth in a BCC low carbon steel and an FCC 316L stainless steel. To reveal the underlying relationship between the failure process in macroscale and the dislocation behavior in nanoscale, cracks generated in both materials were halted at similar stress intensity in the presence and absence of hydrogen, and the surface slip traces and the microstructure as a function of distance from the halted crack tip were investigated. At the region of interest, electron transparency samples were extracted by using focused ion beam machining, and the microstructures were observed by using scanning transmission electron microscopy. The distribution of flow stress ahead of the crack tip was accessed by using the characteristic length of dislocation structure, and the difference between the evolved dislocation structure and the free surface feature was discussed. In both BCC and FCC materials, the presence of hydrogen resulted in the formation of a smaller and more equiaxed dislocation cell structure that extended further from the crack tip than the one generated in air. Qualitative assessment of the dislocation structure ahead of the crack tip found the stress ahead of the crack tip to vary linearly as ln(1/x), where x is the distance from the crack tip irrespective of the test environment. These results indicated hydrogen shielding effect of dislocation motion enlarged the range of intensive plastic stress around the crack tip and the accumulation of plastic damage was much faster in the presence of hydrogen.

15:10-15:30

Effect of Carbon and Nitrogen on Hydrogen Embrittlement of Metastable Austenitic Stainless Steels

Kyung-Shik Kim, Sung-Joon Kim, Graduate Institute of Ferrous Technology(GIFT), POSTECH, Korea

Austenitic stainless steels are gathering attention as structural materials for hydrogen environment due to high resistance to hydrogen embrittlement. In commercial metastable austenitic stainless steels, adding interstitial elements (C and/or N) is reported to decrease the detrimental effect of hydrogen. To study the effects of interstitial elements in detail, hydrogen embrittlement in metastable austenitic steels having Fe-15Cr-15Mn-4Ni as base composition was investigated with varying C or N content up to 0.2wt.%. The steels deformed mainly via ε-martensite transformation and mechanical twinning, and ductile fracture was observed. With increasing C or N concentration, austenite stability increased, which suppressed ε-martensite transformation during deformation. The susceptibility to hydrogen embrittlement was studied by electrochemical charging of hydrogen and subsequent slow-strain-rate tensile testing. In general, from hydrogen pre-charging, ductility loss was observed. The ductility loss decreased with higher content of interstitial elements. Hydrogen pre-charging also increased the amount of ε -martensite and decreased α'-martensite after deformation in the hydrogen affected zone. In this zone, the fracture mode was brittle, and the depth decreased with more C and N. Cracks initiated from the grain boundaries with adjacent ε-martensite, in the surface area where hydrogen was diffused into. From the results, austenite stability and the depth of hydrogen affected zone which differed from C and N content were found to be responsible for the hydrogen embrittlement in these metastable austenitic stainless steels. Carbon and nitrogen however, had different aspects. Carbon was more effective than nitrogen in enhancing the resistance to hydrogen embrittlement at low contents until 0.1wt.%, whereas it reversed at 0.2wt.%. Moreover, in carbon containing steels, the strain hardening rate decreased after some strain while in nitrogen containing steels, it dropped with early strain. Interaction between hydrogen and interstitial elements is responsible for these results. Detailed explanation on the effect of carbon and nitrogen on hydrogen embrittlement will be discussed.

15:30-16:10 Tea Break

16:10-16:35 Invited

Complex Point Defect Analysis by Atomic-Resolution STEM

Ryo Ishikawa, The University of Tokyo, Japan / JST-PRESTO, Japan; Naoya Shibata, Yuichi Ikuhara, The University of Tokyo, Japan / Japan Fine Ceramics Center, Japan

Following the establishment of high purity technology for germanium, silicon and the other semi-conductors, it has been shown that dilute doping of functional single atoms in semiconductors can dramatically enhance their physical or chemical properties such as electrical transport, catalysis, magnetism, and optoelectronics. These properties are sensitive to the location of impurity atoms and it is therefore important to identify the occupation site and their valence state of single dopants. Atomic-resolution scanning transmission electron microscopy (STEM) has a significant capability to directly observe even single atoms embedded bulk materials. Here, we show the direct determination of complex defect structure of single dopants in nitrides by

combining Z-contrast STEM with electron energy-loss spectroscopy. We also show the recent progress on three-dimensional imaging by optical depth sectioning with larger-angle illumination STEM. In addition to the long historical Z-contrast STEM imaging, we also discuss with the recent progress on the electric field imaging of atomistic defects in monolayer graphene by using segmented-type detectors in the bright-field region. A part of work was supported by NEDO-RISING2 project.

16:35-16:55

Phase Field Crystal Modeling for Mechanism of Crack Extension and Brittle-Ductile Transition Behavior on Nano-Scale

Yingjun Gao, Physical School of Guangxi University, China

The phase field crystal method was used to simulate the nano-crack propagation for samples with different pre-deformations, under uniaxial tensile strain. By observing the crack evolution, the free energy change of system during crack propagation and the stress-strain curve was analyzed, and also the curve of the crack area fraction and the perimeter curve of the crack. The results show that for the pre-deformation sample under the tensile strain, when the strain reaches the critical value, the dislocations initiate at the notch to make the strain energy of the concentration release. The extension of the crack tip was accompanied by dislocation slip. No dislocation was emitted from the crack tip, and cleavage propagation of the crack appears at the later stage. For the sample with pre-shear deformation of 1% and 2%, there is a pair of dislocation on the left and right crack in the stages of the crack propagation. The two dislocations slip alternately along their cross glide planes, which make the crack tip propagate alternately along the two glide directions. The edge of the crack is serrated. At the later stage of the extension of the crack, only one dislocation is at the crack tip, which is of only one gliding direction. The crack propagation is in cleavage. For the sample with pre-deformation of 3%, a dislocation at the crack tip is emitted, and a string of the isolated hole is induced in the slip zone, and then, the holes develop into cavities and connect to become cracks. In addition to the main crack, secondary cracks also generate from the cavities. The whole crack propagation is in a mode of ductile propagation. With the increase of pre-deformation, the crack propagation can be changed from brittle to ductile.The copper metal is taken as an example of the calculation, and the obtained result is a good agreement with that of the experiment.

16:55-17:15

An Integrated In-Situ Solution for Mechanical Testing in SEM

Fang Zhou, Carl Zeiss Microscopy GmbH, Germany

In-situ material testing in SEM is an emerging trend among SEM applications, since it is the powerful method to link mechanical properties to the microstructures of materials. To understand the connection between microstructures and mechanical properties helps to design new advanced materials in a most effective way. A well-integrated solution, combining SEM imaging with mechanical testing stage and EDS/EBSD analytical methods is currently developed.

In this work the solution which enables tailored in-situ workflows based on Python scripting is introduced. The automated workflow can generate meaningful data with highest reproducibility and precision. On the other hand, such automated workflows make high throughput data acquisition at high resolution and precisely controlled mechanical load or tempering process in SEM possible. The high quality of the acquired datasets facilitates post processing and data analysis, for e.g. strain mapping by means of digital imaging correlation (DIC). Further advancements such as automated feature tracking help to realize true one-button-start workflows and experiments.

Preliminary results such as grain boundary transition or grain deformation imaged using backscattered electron detector (BSD) will be shown. Examples of measuring grain misorientation during mechanical load by means of high resolution EBSD as well as high resolution strain mapping by means of digital imaging correlation will be discussed.

17:15-17:35

Effect of Surface Area of Grain Boundaries on Internal Stress during Stress Relaxation in Pure Copper

Yurina Suzuki, Yoshinori Kusuda, Kodai Murasawa, Shinsuke Suzuki, Waseda University, Japan; Masato Takamura, RIKEN Center for Advanced Photonics, Japan; Tomoyuki Hakoyama, Gifu University, Japan; Takayuki Hama, Kyoto University, Japan

Internal stress is an important term for understanding plastic deformation behavior. The internal stress value σ_i is expected to be affected by piled-up dislocations at grain boundaries. Therefore, it is suggested that σ_i is affected by the surface area of the grain boundaries per unit volume SV or grain size d. The σ_i values were measured with various d in ferrite-cementite steel. However, the effect of SV on σ_i without precipitates has not been examined experimentally. The objective of this study is to clarify the relationship between σ_i and SV. To obtain various SV values for different specimens, heat treatment was conducted on pure copper tensile specimens. Two specimens were prepared for each condition of heat treatment. One of the two was for stress relaxation test to determine the σ_i value, and the other was for tensile test to obtain microstructure before stress relaxation. In the stress relaxation test, strain was

held for 3600s after the specimen was deformed to a nominal strain of 0.07. In the tensile test, the specimen was deformed to a nominal strain of 0.07. Then, the SV value was calculated with the intercept method, and the Vickers hardness in the grains HV were obtained by conducting the micro-Vickers hardness tests. The internal stress might be affected not only by grain boundaries but also by the dislocation density. However, as a result of this experiment, the HV values which have positive correlation with dislocation density were almost independent of heat treatment. In other words, the effect of dislocation density in the grain interior on σ_i was negligible in this experiment. Meanwhile, σ_i increased with the increase of SV between 7 to 80μm^{-1}. These results suggested that the σ_i values have positive correlation with the SV values.

17:35-17:55

Reflector Selection for the Indexing of EBSD Patterns via Dynamic Pattern Simulation

Stuart Wright, EDAX, USA; Marc De Graef, Carnegie Mellon University, USA; Saransh Singh, Lawrence Livermore National Laboratory, USA

Since it's automation, Electron Backscatter Diffraction (EBSD) in the Scanning Electron Microscope (SEM) has become an essential tool for the materials scientist for the characterization of polycrystalline materials. To determine the crystallographic orientation from an EBSD pattern, the bands in the pattern must be associated with the corresponding lattice planes. This "indexing"of the pattern requires a list of the planes producing the strongest bands in the pattern. One of the challenges associated with indexing EBSD patterns for a new crystal structure is selecting the optimal set of reflectors. The reflectors selected should correspond to the bands in the patterns mostly likely to be detected by the by the automated band detection algorithms (typically the Hough Transform). In early EBSD studies, reflectors were often chosen based on intensities listed in X-Ray powder diffraction tables. But X-Ray diffraction differs from electron diffraction and the reflectors selected in this manner are often inadequate. When the atom positions are known, a better set of reflectors can be constructed based on calculated structure factors from kinematic simulation of electron diffraction. Reflectors with the highest-ranking structure factors are selected as a starting set. However kinematical calculations provide an incomplete description of diffraction. Thus, in either case, this starting set of reflectors needs to be manually tuned against experimental patterns to get to an optimal set. For many materials, this can be a difficult process even for a skilled operator. To overcome this challenge, a ranking of reflectors based on dynamic simulations of EBSD is introduced. In this approach, we propose a beta factor analogous to the structure factors calculated assuming kinematical diffraction. The beta factor is determined by summing the diffraction intensities within the band width over the entire diffraction sphere as simulated for dynamical diffraction. Results for several crystal systems will be shown and comparisons with experimental patterns presented. These results also give insights into the relationships between the optimal set of reflectors and the diffraction conditions, material state and other indexing parameters.

17:55-18:15

Resolving the Hydrogen Effect on High Manganese Steel by Small-Scale Testing

Dong Wang, Xu Lu, Afrooz Barnoush, Norwegian University of Science and Technology, Norway

High manganese steels have received much interest in recent years due to their outstanding mechanical properties combining high strength and good ductility. However, this material group is susceptible to unexpected mechanical degradation when exposing to hydrogen containing environments due to hydrogen embrittlement. The volatile nature of hydrogen atoms and different existing states in metals makes hydrogen embrittle a complicated process that difficult to investigate. Therefore, we performed small scale mechanical tests in hydrogen containing environment to reveal the underlying mechanism. In this paper, we will present our novel studies of hydrogen embrittlement on Fe-22Mn-0.6C TWIP steel using in-situ electrochemical hydrogen charging nanoindentation and tensile test with in-situ scanning electron microscope (SEM) observation. Additionally, the characterization techniques of acoustic emission, high-resolution electron backscattered diffraction (EBSD) and electron channeling contrast imaging (ECCI) and simulation models were used to evaluate the effect of hydrogen.

For in-situ nanoindentation test, changes of the pop-in load and nanohardness were observed in the process of hydrogen charging and discharging. It was found that the introduction of hydrogen reduced the pop-in load, which is attributed to hydrogen-assisted homogeneous dislocation nucleation. The enhanced hardening behavior under the exposure of hydrogen is proposed due to the increased lattice friction between dislocations and hydrogen. Moreover, the pop-in load exhibited fast recovery, while the nanohardness showed a time-effect during anodic discharging. It was explained due to the different amount of residual hydrogen at the different affecting depths.

I. Composite Materials: II

Symposium Organizers:

Lin Geng, Harbin Institute of Technology, China; Boming Zhang, Beihang University, China; Junya Inoue, Tokyo University, Japan; Sang Bok Lee, Korea Institute of Materials Science (KIMS), Korea; Hao Wang, University of Southern Queensland, Australia; Rusty Gray III, Los Alamos National Lab, USA

Tuesday PM
August 20, 2019

Room: 307(3rd Floor)
Symposium: I

Chairs:
Hansang Kwon, Pukyong National University, Korea
Lujun Huang, Harbin Institute of Technology, China

13:30-14:00 Keynote

Improvement of High Temperature Performance of Titanium Matrix Composites by Constructing Hierarchical Microstructure

Lujun Huang, Lin Geng, Harbin Institute of Technology, China

The improvement of mechanical properties must be achieved by designing and constructing more suitable microstructure, such as hierarchical microstructure and nano microstructure. In order to significantly enhance the creep resistance of titanium alloys, one two-level hierarchical microstructure with micro-TiB whiskers (TiBw) and nano Ti_5Si_3 reinforcements were constructed to form the modified composites by powder metallurgy combining with in-situ synthesis and precipitation. The micro TiBw reinfrocement were in-situ synthesized around titanium matrix particles, which formed the first scale network microstructure. The nano Ti_5Si_3 particle were precipitated and distributed in the beta phase around alpha phase which formed the second network microstructure. The results showed that the high temperature strength has been significantly enhanced. The tensile strength at 550℃ for Ti6Al4V matrix composites is increased to 1050MPa. Moreover, the creep rate of the modified Ti_6Al_4V matrix composites was remarkably reduced by an order of magnitude compared with the conventional Ti_6Al_4V alloys at 550℃, 600℃, 650℃ under the stresses between 100MPa and 350MPa. Moreover, the rupture time of the composites increased by 20 times, compared with Ti_6Al_4V alloys at 550℃/300MPa. The superior creep resistance can be attributed to the two-level hierarchical microstructures and the two-scale reinforcements. The micro-TiBw reinforcement in the first network boundary contributed to creep resistance primarily by blocking grain boundary sliding, while the nano-Ti_5Si_3 particles in the second network boundary mainly by hindering phase boundary sliding. In addition, the nano-Ti_5Si_3 particles were dissolved to smaller-sized Ti_5Si_3 particles during creep deformation due to high temperature and external stress, which can further continually enhance the creep resistance. Finally, the creep rate during steady-state stage was unprecedentedly decreased, not stable or increased, which manifested superior creep resistance of the composites. The calculated results indicated that the dislocation climb is the dominant mechanism for the composites tested at 550℃/(250~350) MPa and 650℃/(100~250)MPa.

14:00-14:30 Keynote

Interface-Dominated Mechanical Behavior in Graphene-Reinforced Metal Matrix Composites

Qiang Guo, Zan Li, Lei Zhao, Zhiqiang Li, Di Zhang, Shanghai Jiao Tong University, China

When nano-scaled reinforcements ("nanofillers", such as carbon nanotubes and graphene) are incorporated into a metal matrix, the enhancement in mechanical properties may well exceed those predicted by the "rule-of-mixtures", owing to the rich interplay between the nanofiller and the various crystalline defects in the metal matrix. However, how the nanofillers and their interfaces with the matrix affect the deformation and failure mechanisms of the composites still remains elusive. In this study, using nanolaminated graphene-Al and graphene-Cu composites as model materials, we showed that the graphene incorporation into the metal matrix led to a significant strengthening effect, even if the graphene layers were not oriented in their load-bearing orientations. Further strain-rate dependence and stress relaxation measurements demonstrated that the graphene inclusion at the metal grain boundaries improved the dislocation storage ability in the metal grains and facilitated the dislocation-interface interactions, both of which resulted in elevated strain hardening capacity and subsequently a considerable increase in mechanical strength. This is the result of a substantially reduced grain boundary energy with graphene inclusion, as corroborated by both experiment and associated molecular dynamics similations. The easy control and general applicability of the grain boundary engineering by extrinsic nanofillers may open a new avenue for producing nanostructured metals with enhanced mechanical properties.

14:30-14:55 Invited

Mechanical Properties of Spark Plasma Sintered Graphene Nanoplatelet Reinforced Aluminum based Nanocomposites: Synergistic Strengthening Effect of Nano-Grained Aluminum and GNPs

Tapas Laha, Alok Bhadauria, Lavish K. Singh, Indian Institute of Technology (IIT) Kharagpur, India

Al-GNP nanocomposites with both microcrystalline and nanocrystalline matrices, were synthesized via

spark plasma sintering (SPS). Physio-chemically functionalized GNPs were mixed with microcrystalline and ball-milled nanocrystalline Al powders separately by a novel solution mixing method and further the powder mixtures were consolidated by SPS to develop the Al-GNP nanocomposites. The strengthening effects of (i) nanocrystalline Al matrix and (ii) GNP reinforcement have been systematically investigated. Identification of functional groups attached with functionalized GNPs was validated by Fourier transform infrared (FTIR) spectroscopy. Microstructural examination of Al powders, GNPs, sintered Al-GNP nanocomposites and Al-GNP interface was performed by carrying out scanning and transmission electron microscopy. Macro-scale mechanical properties such as yield strength, ultimate strength, ductility etc. were measured via tensile and compression tests. Nanocrystalline Al compact without GNP reinforcement, in comparison to the microcrystalline one, exhibited 57% and 53% improvement in yield strength (YS) and ultimate tensile strength (UTS). Addition of 0.5wt% physio-chemically functionalized GNPs in the nanocrystalline Al matrix resulted in further improvement in the YS and UTS by 85% and 44%, respectively. This is attributed to the homogenous distribution of the functionalized nano-sized GNPs with high elastic modulus and strength, resulting in very high densification (99%). Mechanical properties such as elastic modulus and nanohardness were measured via nanoindentation. The elastic moduli of the nanocomposites measured by nanoindentation were compared with the values estimated by applying micromechanics models. The strengthening mechanisms (load transfer effect, grain refinement and Orowan strengthening) involved in the NC Al reinforced with GNPs were comprehensively discussed and calculated. Load transfer strengthening mechanism showed highest (73%) contribution in enhancing the strength of the nanocomposite. Fractography analysis revealed that the mode of failure in microcrystalline Al compact was ductile. However, the fracture mode changed from ductile to mixed mode as the microcrystalline Al matrix was reinforced with the GNPs. The Al-GNP nanocomposite with nanocrystalline matrix exhibited completely brittle mode of fracture leading to decrease in the ductility.

14:55-15:15

Characterization of Aluminum(Al)-Copper(Cu) Composite Fabricated by Powder Metallurgy Process

Dasom Kim, Kwangjae Park, Hansang Kwon, Pukyong University, Korea; Kyungju Kim, The International Science Technology Research Center, Pukyong National University, Korea; Takagi Kenta, Hirayama Yusuke, The National Institute of Advanced Industrial Science and Technology (AIST), Japan

In this study, the aluminum(Al)-copper(Cu) composites were successfully fabricated by powder metallurgy process. To fabricate Al-Cu powder, sphere Al and Cu powder were used. A high content ratio of Al-20,50 and 80vol.% Cu composite powders were prepared through a mechanical ball milling process with 300 rpm rotation speed for 24 hours using heptane 20ml as process control agent(PCA) to realize each property of Al and Cu. In the results of observation with scanning electron microscopy (SEM) and field emission-electron probe microanalysis (FE-EPMA), it was shown that Cu particles were encapsulated by Al particles. Subsequently, the Al-Cu composites were fabricated by spark plasma sintering(SPS) process at 380, 390 and 400°C, pressured of 250MPa and held for 5min. Although the sintering temperature is 40% of Cu melting point, the composites have 100% relative density. The microstructures of Al-Cu composites were observed with field emission-scanning electron microscopy(FE-SEM) with energy dispersive X-ray spectroscopy (EDS). The intermetallic compounds(IC) produced by reaction between Al and Cu during SPS process were observed in the form of surrounding Cu. In the results of detection by the X-ray diffraction (XRD) patterns, the phases of IC were Cu_9Al_4 and $CuAl_2$. The mechanical and properties of Al-Cu composite could be improved by controlling the amount of produced IC, which is affected on composite powder and sintering conditions. The mechanical properties of Al-Cu composites were characterized by Vickers hardness test. The Vickers hardness values of Al-Cu composites were higher than the theoretical values calculated by rule of mixture. In addition, the thermal properties were analyzed using Laser Flash Thermal Conductivity Measuring System(LFA) at room temperature. the thermal conductivity of Al-Cu composites were higher than $200W \cdot m^{-1} \cdot K^{-1}$. The Al-Cu composites which have superior mechanical properties and thermal conductivity could be applicable in various industrial materials such as semiconductor components and electrical contact materials.

15:15-15:35

Multiscale 3D Investigation of Damage in Angle-Interlocked Ceramic Matrix Composite under In Situ Loading

Hrishikesh Bale, William Harris, Carl Zeiss Microscopy Inc, United States; Aly Badran, David Marshall, University of Colorado, United States; *Chunjie Cao*, Carl Zeiss (Shanghai) Co., Ltd., China

Textile composites with ceramic fiber tows woven into 2D/3D architectures in a ceramic matrix are important material options for many structural applications. These composites represent a new class of integrally woven ceramic-matrix-composites for high-temperature applications, where both strength and thermal conductivity are important. For high-performance and reliability, a key issue is irregularities and defects in the

textile reinforcement, which compromise strength and life. Environmental barrier coatings further expand the capabilities for extremely corrosive environments.
In recent years, high resolution X-ray imaging capabiliites that were previously only available atsynchrotron beamlines have been transferred to analogous laboratory-based instruments; using lab X-ray tubes but incorporating optical elements to achieve resolution and contrast comparable to many synchrotron experiments, and even adopting an increasing variety of imaging modalities. The lab X-ray tomography systems have benefited from ongoing development of various types of in situ and 4D imaging experiments, albeit at a different time scale than synchrotrons, presenting both unique challenges as well as opportunities to the researcher.
3D x-ray microscopy allows non-destructive imaging and enables subjecting samples simultaneously to in-situ mechanical loading under high-temperature and corrosive environments. We present results from a 3D multi-scale non-destructive investigation performed on a 3-layer angle-interlocked woven composite specimen subjected to in-situ mechanical loading. Results obtained through combination of in-situ image acquisition and image data analysis at the synchrotron and a lab microscope demonstrate the important aspects of CMC's that were investigated through in-situ testing.

15:35-16:10 Tea Break

16:10-16:30

The Microstructure and Wear Properties of TiC-Reinforced High Manganese Steel Matrix Composites Fabricated by Eutectic Solidification

Zhichao Luo, Jiapei Ning, Juan Wang, Kaihong Zheng, Guangdong Institute of Materials and Processing, China

High manganese austenitic steels are promising wear-resistant materials with a long history of more than one hundred years. Recently, numerous work has been done to further improve their wear performance by introducing the ceramic particles into the material as strengthening phases. However, the ceramic particles can be broken down and pulled out during the wear process due to the weak interfacial properties. In this work, high manganese steel matrix composites (SMC) with various volume fraction of TiC were designed and fabricated by eutectic solidification method. The microstructure, dry sliding wear and abrasive wear properties of these SMCs were examined. Our results show that grain size of SMCs are smaller than the single phase high manganese steel. After heat treatment, the TiC particles are homogeneously distributed in the matrix and the interface is clean. However, the particle clusters are formed and the particle size increases with increasing volume fraction. The results of dry sliding wear experiments show that the friction coefficient of SMCs are all higher than the matrix. Nevertheless, the wear rate has been reduced significantly with the introduction of TiC particles. However, the wear rate increases slightly with increasing volume fraction of TiC phase. Similar results were also found in the abrasive wear experiments. It demonstrates that the SMCs with excellent wear properties can be fabricated by the present eutectic solidification method. The wear mechanisms were investigated by using SEM, EBSD and TEM in this work. We found no interfacial failure during the all the wear processes. However, the large particles and particle clusters, which are formed in the SMC with higher TiC volume fractions, can be broken down and increase the wear rate. Furthermore, high dislocation density and deformation twins were observed under the wear surface and around the TiC particles, and no martensitic transformation was found. Therefore, the excellent wear resistance of present SMC can be attributed to the good interfacial properties, refined grain structure and intensive accumulation of dislocations and deformation twins under the wear surface and around the particles.

16:30-16:50

Deformation Mechanism of Titanium Matrix Composite with a Network Reinforcement Architecture at Elevated Temperature

Bin Chen, Huan Wang, Junying Yi, Huaxin Peng, Zhejiang University, China; Lujun Huang, Harbin Institute of Technology, China

The deformation behavior of a 3vol% TiBw/TA15 composite with quasi-continuous network microstructure fabricated by reaction hot pressing was investigated using in-situ SEM tensile testing at 700˚C. The in-situ observations elucidated different deformation regimes among the different phases including reinforcement, α phase and β phase of the matrix. With the increase in tensile deformation, a serial of cracks were almost simultaneously occurred along TiB whisker (the stiffest phase in this composite) and in the β phase of matrix (the softest phase). The cracks were inhibited when they propagated into α phase where slip bands were observed indicating plastic deformation of α phase. With further deformation, the cracks began to join up leading to fracture. The fracture mechanism of the composites is a mixture of fracture predominantly controlled by TiB whisker fracturing or debonding followed by the fracture of β phase and plastic deformation of α phase. The highly toughness of α phase will blunt the cracks occurred in TiB whiskers and β phase. With the increase of deformation, multiple cracks along TiB whisker and β phase occurred demonstrating the strengthening effect of the TiB which has been fully exploited.
The macroscopic fracture surface shows a honeycomb-like feature and it illustrates the cracks mainly propagated along the network boundary region. There is also few matrix fracture feature probably caused by the different way of cracks jointing up along matrix and reinforcement-rich boundary. Due to different

orientations of the TiB whisker, the pulling-out and fracture of TiBw and interfacial debonding between TiBw and matrix can be observed. These phenomena suggested that, at high temperature, the TiB whisker acts as the primary loading bearing phase during the tensile deformation and provides strengthening effect.

16:50-17:10

Processing and Mechanical Properties of Laminated Ti-Al Composites with the Gradient Structure

Xiong Wan, Tao Jing, Tsinghua University, China; Yanjin Xu, Baoshuai Han, AVIC Manufacturing Technology Institute, China

Metal-intermetallic laminate composites have been considered as the promising application in the aerospace industry for their high specific stiffness and strength. In this study, laminated Ti-Al composites with the gradient structure, and four compositional Ti-Al composites with different volume ratio between residual metal phase and intermetallic phases have been manufactured by Vacuum Hot Pressing (VHP) using pure Ti foils and Al foils with different thicknesses. Microstructural evolution and phase identification were conducted using scanning electron microscopy (SEM), energy dispersive spectroscopy (EDS) and X-ray diffraction (XRD). Mechanical properties were measured by three-point bend (TPB) under quasi-static and compression test under high strain rate. The results indicated that phases formed in all the composites are Ti, Ti_3Al, TiAl, $TiAl_2$, and $TiAl_3$ with Al foils completely consumed. Mechanical properties tests reveal that both flexural strength and dynamic compressive strength decrease with the increase of the thickness of Al foils when the thickness of Ti foils keep constant. Moreover, the flexural strength of the Ti-Al composites with gradient structure shows the apparent distinction between two different loading directions while the dynamic compression strength shows the little distinction. Therefore, this research provides a unique strategy to design the structure of laminated Ti-Al composites with the designate mechanical properties.

17:10-17:30

Effect of Magnesia Rich Spinel Adittion on Densification and Stabilization Behaviour of Monoclinic Zirconia by Different Sintering Methods

Mahmoud Abdelgawad, Shufeng Li, Xin Zhang, Deng Pan, Xi'an University of Technology, China; Emad Ewais, Central Metallurgical Research and Development Institute, Egypt; Safaa El-Gamal, Ain Shams University, Egypt

Monoclinic zirconia (m-ZrO_2) containing 5wt% Y_2O_3 and magnesia rich spinel (MMA) powders were used as starting materials, spark plasma sintering (SPS) technique was employed to fabricate high density ZrO_2 based composite ceramics. For comparison, conventional sintering (CS) samples with same composition also prepared meanwhile. Six different compositions were prepared in which the MMA content ranged from 0 to 50wt% with the increment of 10%. From the phase analysis and physical properties measurement, it was found that with the increase of the sintering holding time and temperature, the m-ZrO_2 was transformed and stabilized at the cubic form (c-ZrO_2) by the diffusion of Mg+2 and Al+3 ions at the expense of the magnesia and spinel (MA) phases. ZrO_2-MMA-SPS-1300˚c showed m- and c-ZrO_2 dual phases structure with a high relative density more than 99%. With the temperature increase to 1400˚c and MMA content increase to 50wt%, all the m-ZrO_2 was completely converted to c-ZrO_2. However, ZrO_2-MMA-CS-1600˚c composites showed dominant c-ZrO_2 structure with almost high density, while MMA-free composites maintained a high amount of m-ZrO_2 irrespective to the temperature and the sintering technique with a porosity of ~23% and ~3% at 1600˚c by CS and 1400˚c by SPS respectively. Compared to CS, the SPS proved to be a more powerful technique in densification and property of zirconia based ceramics.

J. Amorphous and High Entropy Alloys: Amorphous Alloys III

Symposium Organizers:

Weihua Wang, The Institute of Physics, Chinese Academy of Sciences, China; Zhaoping Lv, University of Science and Technology Beijing, China; Hidemi Kato, Tohoku University, Japan; Hojin Ryu, Korea Advanced Institute of Science and Technology (KAIST), Korea; Michael Ferry, New South Wales, Australia; Evan Ma, Johns Hopkins University, USA

Tuesday PM
August 20, 2019

Room: 405 (4th Floor)
Symposium: J

Chairs:
Jinwoo Hwang, Ohio State University, America
Tohru Yamasaki, University of Hyogo, Japan

13:30-14:00 Keynote

Plastic Deformation of Ni-Based and Zr-Based Alloys Having Amorphous and Nanocrystalline Dual Phase Structures

Tohru Yamasaki, University of Hyogo, Japan / Department of Materials and Synchrotron Radiation Engineering, Japan

Nanocrystalline and amorphous single phase alloys often exhibit low tensile ductility. However, the alloys with bimodal structures such as micrometer-sized grains embedded inside a matrix of nanocrystalline grains have exhibited high tensile strength and ductility. In

the Ni-based alloys, Ni-W alloys having nanocrystalline and amorphous dual phase structures with various W-contents of 15~18at.% have been prepared by electrodeposition. Ni-W dual phase alloys exhibited high tensile strength of about 2,000~3,000MPa and large plastic strain at fracture of about 1%~7%. This may be due to the nanocrystalline grain growth during plastic deformation, resulting the work hardening in the local plastic regions. Specimens having laminated structures of Ni-W and pure-Ni with each film thickness of 0.3~2 micrometer were also prepared by alternating Ni-W and pure-Ni electrodeposition. Tensile plastic strain at fracture depended on the laminated film thickness.
In the Zr-based alloys, Zr55Cu30Ni5Al10 (Zr55), Zr65Cu20Ni5Al10 (Zr65) and Zr65+xCu17-xNi5Al10M3 (Zr65+xM3, x = 0, 1.5 and 3at.%, M= Au and Pd) bulk metallic glasses (BMGs) have been prepared. By the Au/Pd addition, precipitation of an icosahedral quasicrystalline phase (I-phase) was observed. Compressive test was carried out at an initial strain rate of 5 x $10^{-4}s^{-1}$ at room temperature. The plastic strains at fracture of Zr55-, Zr65- and Zr65Au3/Pd3-BMGs were about 2%, 10% and more than 20%, respectively. In the Zr66.5Au3/Pd3-BMGs, stress-increasing like a work hardening during plastic deformation was observed until more than 5% of compressive strain. By the transmission electron microscopy of the Au/Pd-addition BMGs, precipitation of nanocrystallites having about 5~10nm in diameter was observed near the fractured surfaces of the compressive test specimens. So, the large increase of the plastic strain may be due to the work hardening by the dynamic precipitation of I-phase during plastic deformation.

14:00-14:20 Invited

Multiple Relaxations and Their Influences on Magnetic Properties of Metallic Glasses

Junqiang Wang, Ningbo Institute of Materials Technology and Engineering, CAS, China

Isothermal annealing is a very useful strategy in modulating the properties and structures of metallic glasses, which has been regarded as a single relaxation progress. In this talk, I will introduce our recent work on the enthalpy relaxation of Au- and Fe-based metallic glasses. An intriguing transition from β relaxation to α relaxation was confirmed during isothermal annealing. Energy landscape model is proposed to quantitatively explain how the relaxation modes transform. The magnetic properties are enhanced predominantly during b relaxation stage but don't change very much during a relaxation stage. The plasticity doesn't change very much during b relaxation stage but gets deteriorated during a relaxation stage. Based on this work, we propose an optimal relaxation strategy to obtain metallic glasses with the best soft magnetic properties and mechanical properties. The micro-structural origin of the influence of b relaxation on magnetic properties is studied. The evolution of nanostructure in stress field and the motion of domain walls under external magnetic field are studied. We find that the nanoscale fluctuation of structure is coupled with the motion of magnetic domain walls. It follows the magneto-elastic coupling theory. These results propose an optimum thermal annealing protocol to fabricate metallic glasses with both excellent magnetic properties and mechanical properties.

14:20-14:40

Polyamorphic Transition in a Transition Metal Based Metallic Glass under High Pressure

Xiongjun Liu, University of Science and Technology Beijing, China

Pressure-induced glass-glass transition (GGT) has been reported in a few rare-earth based and main-group metallic glasses (MGs), a process during which the compressibility decreases with the transformation from a low-density to a high-density amorphous state. Herein, we report an unexpected GGT behavior in Pd-based MGs under pressure, which is characterized by an anomalous increase in the compressibility with the pressure. State-of-the-art high-energy synchrotron technique, coupled with theoretical simulations, reveals that this unique
GGT behavior is primarily caused by the change in bonding characteristics, i.e., some covalent like atomic bonds in the as-prepared state change to metallic ones under high pressure, which also leads to the increase in the compressibility. Our current findings shed light on the understanding of the nature of polyamorphic transitions in MGs.

14:40-15:00

Fe-Based Bulk Metallic Glasses: Brittle or Ductile?

Shengfeng Guo, Southwest University, China

Fe-based bulk metallic glasses (BMGs) typically exhibit ultrahigh strength but a poor ductility at room temperature. To overcome the negligible plasticity, we have developed a series of Fe-based BMGs from structural and compositional design rules. I will describe our efforts in the development of Fe-based BMG matrix composite reinforced with ductile α-Fe dendrites and the monolithic Fe-based BMGs which exhibit a super large compressive plasticity at room temperature. Such a discovery is guided by understanding a composition-strength-ductility map, in which most of the Fe-based BMGs are classified into three types: FeC-based ones, FeB-based ones, and FeP-based ones. Among these BMGs, the FeP-based BMGs often possess a relatively lower glass transition temperature, a lower shear modulus, and a higher Poisson's ratio, resulting in a

very lower shear flow barrier and a higher plasticity. Our findings will provide a new insight into how to prevent the brittle failure and develop the high performance of Fe-based BMGs.

15:00-15:20

Ductile Co-Based Bulk Metallic Glasses with Ultrahigh Strength and Excellent Magnetic Properties

Qianqian Wang, Baolong Shen, Southeast University, China

Co-based bulk metallic glasses are promising structural and functional materials for engineering applications due to their superior mechanical properties, i.e., high fracture strength and high hardness, as well as excellent magnetic properties, i.e., high saturation magnetization, high effective permeability and low coercivity. A large number of Co-based bulk metallic glasses have been synthesized during the last several decades. The largest critical diameter of Co-based bulk metallic glasses reaches 5.5mm. However, the low room-temperature plasticity of Co-based bulk metallic glasses results in catastrophic brittle failure, which limits their large-scale industrial applications.
In this work, a novel Co-based bulk metallic glass with superior mechanical properties, i.e., ultrahigh fracture strength of 4770MPa, large plasticity of 5.5% and excellent soft magnetic properties, i.e., low coercivity of 1.33A/m and high saturation magnetization of 0.60T was successfully synthesized. Simultaneous improvement of the fracture strength and plasticity of Co-based amorphous alloy with Cu addition was also reported. For this Co-based bulk metallic glass with high fracture strength and large plasticity, the multiple shear bands formed on the rod surface (before failure) during compressive tests and the vein patterns observed on the fracture surface confirmed that the deformation was a ductile behavior. The serration flow during compressive tests of the Co-based bulk metallic glasses was thoroughly analyzed to reveal the dynamics of their mechanical behavior. It was found that the serration flow changed from chaotic state to self-organized critical behavior with proper Cu addition in these Co-based bulk metallic glasses. The structural heterogeneity induced by Cu addition verified by high-resolution transmission electron microscope and synchrotron radiation X-ray diffraction explains the improved plasticity. The enhanced strength is proposed to originate from the formed stiff Co-like clusters. Our findings provide a guideline in obtaining Co-based bulk metallic glasses with ultrahigh strength and large room-temperature plasticity, as well as excellent magnetic properties.

15:30-16:10 Tea Break

16:10-16:30

Internal Friction in the In-Situ Metallic Glass Matrix Composite

Jichao Qiao, Northwestern Polytechnical University, China

Owing to the amorphous-crystalline composite structure, metallic glass matrix composites (MGMCs) usually exhibit attractive physical, mechanical and chemical properties. In the present work, we report an unusual anomalous internal friction behavior in an in-situ dendrite reinforced Ti- and Zr-based MGMCs below the glass transition temperature Tg of its amorphous matrix. According to the high-resolution transmission electron microscopy (HRTEM) images, the compelling abnormal internal friction is mainly caused by the precipitation of nanocrystals in the crystalline dendritic phase and the formation of long-period ordered phase (LPOP) in nanocrystals. Consequently, the in-situ MGMCs shows a propensity of annealing-induced embrittlement. Through the combined efforts from mechanical spectroscopy testing, stress relaxation experiments and structural characterization, the physical and structural origin of the unanticipated internal friction behavior is explored. In addition, the mechanism of the annealing induced embrittlement of the Ti-based MGMC is discussed quantitatively based on the Eshelby's theory. The current research provides the key evidence that correlates the peculiar internal friction behavior of the in-situ MGMC with its mechanical properties, which is valuable to the development of the constitutive relations of MGMCs.

16:30-16:50

Anomalous Thermal Expansion in the Deep Super-Cooled Liquid Region of a ZrCuAlAg Bulk Metallic Glass

Qiang Hu, Jiangxi Academy of Sciences, China

An attractive advantage of bulk metallic glasses (BMGs) over traditional alloys is that it can be thermal-plastically formed in the super-cooled liquid region (SCLR), due to the viscous flow of the SCL. The viscous flow, however, brings along an unpleasant consequence when measuring the thermal expansion of BMGs using the mechanical thermal dilatation (DIL) method. i.e., sample softening, which essentially results in the DIL data look similar for different compositions, and thus featureless. It is reported that some BMGs have anomalous calorimetric signals in the SCLR, such as PdNiP, FeMoYB, ZrTiBe, CuZrAlY, etc. However, to the best of our knowledge, no anomalous expansion, especially a large expansion in the SCLR detected by the DIL method, during which a small amount of compressive load is applied on the sample, has been reported. On the other hand, BMGs shrink upon crystallization due to the amorphous materials with a disordered structure usually

having a lower density than the crystalline counterpart with an ordered structure. So far, only Pd40Ni40-xCuxP20 (x>30) alloys are reported to be less dense in the crystalline state than in the amorphous state.

Here in this work, surprisingly, a large expansion is reported occurring in the deep SCLR of a Zr47Cu37Al8Ag8 BMG, but without anomalous calorimetric signal. Nano-crystals are found precipitated during the anomalous expansion of Zr47Cu37Al8Ag8, but also in the SCLR of Zr43Cu41Al8Ag8 that exhibits a conventional softening. It is found that there is a steep composition and density change at the nano-crystals/amorphous-matrix transition region in the former alloy, and this transition region exerts a thermal stress of about 0.15MPa to the surrounding SCL and drives the soft SCL to expand severely. The novel phenomenon observed and the revealed mechanism behind it, provide new understanding to the effect of nano-crystal precipitation on the structure and properties of the SCL.

16:50-17:10

Cryogenic Thermal and Mechanical Processing of TiNi Based Crystalline/Amorphous Alloys

Jing Jiang, Hidemi Kato, Dmitri Louzguine, Institute for Materials Research Tohoku University, IMR Japan

Ti-Ni-Cu-Zr-Co-Y system crystalline/amorphous dual-phase materials containing an amorphous phase and two crystalline phases (B2 austenite and B19' martensite) studied here exhibit a good combination of high strength and plasticity. They undergo a martensitic transformation during deformation and exhibit the superelastic behavior and excellent mechanical properties: mechanical strength up to 2.5GPa and plasticity of more than 20%. Mechanical characteristics of the alloys revealed three deformation stages, which include elastic deformation, a martensitic transformation and "superelastic" type effect stage and plastic deformation process.

Structural changes induced by deformation during the loading/unloading cycles cause low cycle mechanical fatigue, i.e. increasing the residual strain and decreasing the critical stress for martensite transformation and decreasing the hysteresis area for each cyclic loop with increasing in the number of mechanical cycles. The amorphous phase acts as the sink for dislocation slip movement in austenite-martensite phase transition during the superelastic cycling and improve the low cycle mechanical fatigue compared to cP2 TiNi fully crystalline sample. The amorphous phase in BMGCs influences the dislocation slip process during loading and reduces the accumulation of irreversible strain and decelerates a decrease in martensite transformation inducing stress and, at same time promotes creation of new dislocation.

The Ti-Ni-Cu-Zr-Co-Y composite was also treated by the cryogenic thermal processing to improve the mechanical properties. Considering possible rejuvenation of amorphous phase by thermal cycling between room temperature (293K) and the liquid nitrogen temperature (77K), we found that the low cycle mechanical fatigue could be suppressed by the subsequent cryogenic thermal cycling. The results of compressive tests indicate that the martensitic transformation inducing stress, which is decreased upon the superelastic loading cycles, is recovered on the thermal treatment. The cryogenic thermal cycling effect on the microstructure of martensite phase associated with amorphous phase in the TiNi BMG composite that inducing the result to obstruct the dislocation movement and increase the critical phase transformation stress.

17:10-17:30

Ti-based Metallic Glass Matrix Composite

Yongsheng Wang, Taiyuan University of Technology, China

Nowadays, bulk metallic glasses (BMGs) have attracted attention as novel structural materials due to excellent mechanical properties. One of the remarkable properties is their superplastic behavior for the homogeneous deformation in supercooled liquid region, which provides opportunities for hot-working forming, near-net-shape processing. So, since 1970s, work in this field has been reported numerously. However, monolithic BMGs always show inhomogeneous deformation at low temperature (e.g. room temperature) lead to the limited plasticity or even brittle failure, which significantly restricts their possible application. Metallic glass matrix composites containing the in-situ β ductile dendrite phase have receiving intense attractions due to the combination advantages of BMGs and crystalline alloys. In the present work, mechanical property and deformation behavior of a Ti-based metallic glass matrix composite were investigated under the compression loading in supercooled liquid region temperatures. The overshoot behavior caused by the glassy matrix and the work-hardening character dominated by dendrite phase could be observed on the stress strain curves. The overshoot behavior and the work-hardening behavior were explored on the basis of the local uniformity and instability between the multiplied dislocations in the dendrite phase and the homogenous viscous flow of the glassy matrix. TEM results further uncovered that the plastic deformation of dendrite phase was achieved by lattice distortions and multiplications of dislocations, but

the viscous homogenous flow of the glassy matrix was constricted between the dendrites frame to coordinate superplastic deformation.

17:30-17:50

Zr-Based Metallic Glassy Particles Reinforced High-Strength Al Alloy Matrix Composites Obtained by Spark Plasma Sintering

Song Li, Wenliang Tan, Lanping Huang, Jun He, Central South University, China

Al-based metal matrix composites (MMCs) have attracted much attention and been widely used in aerospace, automotive manufacturing and electronics due to their excellent combined properties, such as low density, high elastic modulus, high strength, and excellent wear resistance. Among the MMCs, particle-reinforced MMCs exhibit some intrinsic advantages including nearly isotropic properties, easy and diverse processing, and the possibility to be post-processed by most existing processing methods such as hot forging, hot extrusion, rolling, and machining. Metallic glasses can be utilized as the potential reinforcement in MMCs due to their high strength and hardness, large elastic strain and excellent corrosion resistance. Recent studies on particle-reinforced MMCs have indicated that amorphous reinforcements, such as Fe-based, Mg-based and Zr-based metallic glasses, can significantly enhance the mechanical properties of the composites. However, the work on the MMCs reinforced with amorphous alloy particles has mainly focused on the introduction of various amorphous alloys into pure Al or Mg, but other aluminum alloys, especially Al-Zn-Mg-Cu alloys, are hardly used for the matrix materials. In this work, new high-strength aluminum alloy matrix composites reinforced with Zr55Al10Ni5Cu30 metallic glassy particles have been successfully fabricated by spark plasma sintering (SPS) combined with gas-atomization method. The highly dense bulk body is obtained by utilizing the viscous flow behavior of the glassy powder within the supercooled liquid region. The addition of amorphous reinforcing phase significantly increases the yield strength of Al alloys without obviously damaging the plasticity. It is confirmed that the mutual diffusion of elements takes place between Al alloy matrix and glassy reinforcement during SPS process. The imposed stress and temperature by SPS affect the mutual diffusion and elemental distribution at interface. The increased mechanical response is ascribed to the uniform distribution of the glassy particles and good interfacial bonding. The mechanical properties of such composites can be accurately described by the iso-stress model involving the matrix-strengthening mechanism.

17:50-18:10

Strain Hardening Behavior of Amorphous Alloys with Multiple Steps Crystallization under Tension at Elevated Temperatures

Hongwang Yang, Shenyang University of Technology, China

Strain hardening is one of the major strengthening approaches, which is crucial to avoid catastrophic failure for polycrystalline engineering metals and alloys under tension at room temperature. The imperfections in crystalline alloys act as dislocation movement barriers. The dislocations are effective dislocation movement stopper. This stain strengthening occurs because of dislocation movements and dislocation generation within the crystal structure of the material during plastic deformation. The plastic deformation mechanism changes with the rise of temperature. At room temperature, dislocation sliding dominates the plastic deformation in most metals and alloys, while grain boundaries contributes more deformation with the rise of testing temperature. The hardening phenomenon diminishes and even vanishes with the service temperature approaching 0.4 times the melting point (Tm). Monolithic amorphous alloys usually undergo brittle fracture at room temperature under both tension and compression conditions without confinement. For the amorphous alloys, super plasticity is achievable in the supercooled liquid region (SLR), but still lack of strain hardening, which is no helpful for high temperature applications avoiding catastrophic failure. We observed strain hardening behavior in aluminum based amorphous alloys and contributed the strengthening to dynamic crystallization during deformation. The strain hardening was also proposed to be attributed to high temperature elemental enrichment in the remaining amorphous matrix and precipitation strengthening behavior similar to crystalline materials. Strain hardening behavior was also observed in some Fe-based metallic glasses of primary crystallization. Both Al-based and Fe-based metallic glasses firstly precipitate pure Al crystals or a-Fe solid solution phase under thermal heat treatment. However, no strain hardening was reported in other metallic glass systems. We will represent a Zr-Ni-Nb-Co metallic glass with multi-step crystallization also processes remarkable strain hardening behavior at certain temperature and strain rates. In this presentation, we will discuss the universality of strain hardening of amorphous alloys with multiple steps crystallization and the mechanism of strain hardening of this type of metallic glasses.

J. Amorphous and High Entropy Alloys: High Entropy Alloys III

Symposium Organizers:

Weihua Wang, The Institute of Physics, Chinese Academy of Sciences, China; Zhaoping Lv, University of Science and Technology Beijing, China; Hidemi Kato, Tohoku University, Japan; Hojin Ryu, Korea Advanced Institute of Science and Technology (KAIST), Korea; Michael Ferry, New South Wales, Australia; Evan Ma, Johns Hopkins University, USA

Tuesday PM
August 20, 2019

Room: 303 (3rd Floor)
Symposium : J

Chairs:
Xinwang Liu, Huazhong University of Science and Technology, China
Koichi Tsuchiya, National Institute for Materials Science, Kobe University, Japan

13:30-14:00 Keynote

Microstructure Control in fcc High Entropy Alloys - SPD and Phase Transformation

Koichi Tsuchiya, Jian Qiang, Jein Lee, Ivan Guitierrez, Toshiji Mukai, Kobe University, Japan

High entropy alloys (HEAs) exhibit various attractive properties, such as pronounced work hardening and enhanced ductility at cryogenic temperatures, high fracture toughness, high fatigue resistance as well as the creep resistance comparable to nickel-base superalloys. The present talk will focus on fundamental metallurgical aspects of fcc-HEAs, such as i) nanostructure formation by severe plastic deformation (SPD), and ii) effect of stacking fault energy on phase transformation and mechanical properties.
Nanostructure formation by SPD: SPD by high-pressure torsion (HPT) was applied to an Al0.3CoCrMnNi alloy. After 3 rotations of HPT, grains were refined to about 50nm. Micro-Vickers hardness indicated high-work hardening rate compared to conventional fcc metals. Formation of fine lamellar structures by twinning or shear bands may be the key for the nano-scale grain formation. Process of nanograin formation will be compared with other low SFE materials.
Design of fcc HEA with improved strength-ductility balance: It has been demonstrated that CrCoNi HEA has improved strength at 77K over CrMnFeCoNi due to the formation of nanotwin-HCP lamellar. This suggests the possibility to further improve the low temperature toughness by controlling stacking fault energy (SFE) or relative phase stability of fcc and hcp phases. CALPHAD simulation revealed that FCC phase is stable in the Cr20Mn20Fe20Co40-xNix system and Gibbs free energy difference between HCP and FCC phases (ΔGHCP-FCC) decreases as the Ni content decreases, indicating the reduction of SFE. The improved mechanical properties were attributed to the deformation-induced twinning or phase transformation as seen in other low SFE alloys such as TWIP/TRIP steels.

14:00-14:25 Invited

Thermophysical Properties of Hexabasic AlxCoCrCuFeNi HEAs

Weili Wang, Lijun Meng, Bingbo Wei, Northwestern Polytechnical University, China

The hexabasic AlxCoCrCuFeNi (x=0.25, 0.5, 1, 2) HEAs were produced by doping the different mole fractions of Al element into the quinary CoCrCuFeNi alloy. The liquidus temperatures decrease with the increase of the Al mole fraction, here the Al mole fractions are less than 2. Once the Al mole fraction attains 2, the liquidus temperature increases rapidly and achieves 1659K. The analyzing of the solidified microstructures show that there are two kinds of phases at the different HEAs: a major high-entropy FCC phase together with a minor interdendritic Cu-rich FCC phase in the AlxCoCrCuFeNi (x=0.25, 0.5) HEAs, and a major high-entropy BCC phase and minor interdendritic Cu-rich phase in the AlxCoCrCuFeNi (x=1, 2) HEAs. The phase composition analysis shows that the elemental contents in high entropy phase have a curtain regularity and close to the original composition of HEAs for the AlxCoCrCuFeNi (x=0.25, 0.5, 2) HEAs, but the elemental contents in the AlCoCrCuFeNi HEA have the higher random where the Cr and Fe contents exceed the original composition. The relationships of the density and Vickers hardness display the opposite feature that the higher density has the lower Vickers hardness, meanwhile the FCC crystal has the lower Vickers hardness, and the BCC crystal has the higher Vickers hardness. Otherwise, the higher Al mole fraction in HEAs, the higher Vickers hardness and the lower density. The enthalpy and entropy of fusion, element segregation and lattice distortion affect the thermal diffusion coefficient in these HEAs. Otherwise, the enthalpy and entropy of fusion, crystal structure, lattice vibration and elemental segregation have the common effect on the thermal expansion coefficient.

14:25-14:45

Columnar to Equiaxed Transition and Grain Refinement of Cast CrFeCoNi High-Entropy Alloys

Xinwang Liu, Lei Liu, Zitian Fan, Huazhong University of Science and Technology, China; Gang Liu, Xi'an University of Technology, China; Easo George, University of Tennessee, USA

High-entropy alloys (HEAs) based on the CrMnFeCoNi system have attracted extensive attention during the

last decade and a half due to their excellent properties. Thermomechanical processing has been used to control the grain size/shape of the alloys and obtain excellent strength and ductility. However, in the cast state, the HEAs in many cases show coarse and anisotropic columnar grains, resulting in inferior mechanical properties. Although there is an extensive literature on grain refinement of dilute alloys (mainly based on binary systems), systematic studies of multi-principal-element alloys (MPEAs) are lacking. Due to their large number of constituent element (solute) species and their high concentrations, the solute effects linked to grain growth are different from those of dilute alloys, e.g., Al, Mg and Fe alloys. The solute effect has been considered to be the most important factor in most approaches of grain refinement. Here, we focus on solute effects on the columnar to equiaxed transition and grain refinement of the MPEAs, which involves the effect of the constituent elements themselves as well as those of externally added alloying elements, and further the interaction between solutes. The grain-refinement parameter related to the constituent undercooling induced by solutes was established for multicomponent alloys first. Then the CrFeCoNi system and its subsets were selected as model alloys to verify the applicability of the grain-refinement parameters by experiments. Based on these studies, several external solutes were high-throughput screened to predict and further verify the grain refinement effect. In the solute interaction paradigm, in addition to their individual effects, the strong mutual affinity between solutes rejected in front of the solid-liquid interface is utilized to restrict diffusion and facilitate constitutional undercooling to achieve finer grains. The results show that grain refinement leads to not only remarkable strengthening of the CrFeCoNi HEAs but also improvement of their isotropy (grain shape), which is significant for engineering applications.

14:45-15:05

Dynamic Mechanical Behavior and Microstructure Revolution of NbZrTiTa High-Entropy Alloy

Yu Tang, Ruixin Wang, Shun Li, Yuanlin Ai, Shuxin Bai, National University of Defense Technology, China

In recent years, high-entropy alloy (HEA), a novel design concept, has become a hotpot of metal and structural material due to the unique structure and characteristics. Unlike the traditional alloy design strategy and phase rule, HEA, which is composed of more than four elements, will form a simple solid solution structure with unordered atom occupation, and then HEA exhibits excellent properties including high corrosion resistance, high irradiation resistance, and excellent mechanical properties at extreme conditions, such as high temperature, low temperature and dynamic loading.

As most structural materials, HEA faces with the dilemma trading off between strength and ductility. Hence, the metastability engineering strategy, which has been widely used in high-Mn steels and titanium alloys, was introduced in HEAs. According to the metastability engineering strategy of HEA, the high-temperature structure of HEA is metastable, and the strain-induced transformation will be promoted during loading. The process of strain-induced transformation results in the uniform plastic deformation by delaying the onset of necking and releasing internal stress and the occurrence of the transformation-induced plasticity (TRIP) effect. Furthermore, the strength of HEA will be significantly enhanced by co-contribution from the interface hardening from the dual phases and the transformation hardening from the metastability (named as transformation-induced strength, TRIS). This combined increase in strength and ductility provides a useful guide for designing HEA.

In fact, the metastability engineering strategy has been successfully applied into the brittle refractory high-entropy alloy (RHEA), which was proposed as high-temperature structural materials. Huang and coworkers destabilized the high-temperature body-centered cubic (BCC) phase via reducing the Ta content in TaxHfZrTi system, which promotes the TRIP effect and work-hardening capability. Recently, Wang further explored the application of the TRIP effect in single-phase RHEA. As reported, in the NbZrTiTa RHEA with the single solid solution structure and uniform element distribution, two regions with different composition and phase stability forms during loading, due to the dislocation pipe diffusion and the low compatibility of elements. The increasing Ti and Zr content reduces the stability of BCC structure and leads to in-situ structure transformation in the TiZr-rich region. The co-contribution of various metastable-induced mechanisms distinguishes the strength and ductility of NbZrTiTa from those of all the reported refractory systems. Moreover, the risk that fracture has generated along brittle region in the HEA composited of ductile and brittle phases before the TRIP effect works could be effectively avoided in TRIP single-phase HEA. However, there is still more work to do for the application of TRIP HEA. For example, the structural materials bear not only static but also dynamic loads during service. It is known that the mechanical behavior of materials under dynamic loading is quite different from that under quasi-static conditions. During dynamic loading, the deformation mechanism is no longer limited to dislocation movement, other mechanisms, such as twinning and grain refining, will take part in too. Moreover, under high strain rate loading, the strain rate hardening effect, thermal soft effect, and adiabatic shear phenomenon also contribute to the deformation. Therefore, it is significant to study the mechanical behavior and the microstructure evolution of RHEA and explore the availability of metastability engineering strategy under dynamic conditions. But, there are only

two reports concerning the dynamic mechanical behavior of RHEA. In Ti20Hf20Zr20Ta20Nb20 system, the yield strength increases with increasing strain rate and the high dislocation density mainly results in the high flow stress at high strain rates. For the TRIP HfZrTiTa0.53 RHEA, although the TRIP and TRIS effects lead to great quasi-static mechanical properties, the appearance of thermoplastic instability and adiabatic shear band make the fracture strength and strain are just 1570MPa and 12.1% respectively under 2200s^{-1}.

In this work, the TRIP NbZrTiTa RHEA with the excellent quasi-static mechanical properties was selected. Its mechanical behavior and the microstructure evolution during dynamic compressions in a wide range of strain rates (10^{-3}~$10^{4}s^{-1}$) were systematically investigated. The deformation and strengthening mechanisms were revealed. Results showed that, at low and medium strain rate, the strength increased while ductility decreased resulting from the strain rate effect. However, at high strain rate, the strength and ductility increased simultaneously as a result of the co-contribution from TRIP effect, TRIS effect and grain refinement. On the other hand, the uniform microstructure and deformation of NbZrTiTa alloy could effectively delay the generation of adiabatic shear band. The adiabatic shear band occurs at a high strain rate of 5200s^{-1}, which is higher than those of other reported RHEA systems and conventional alloy. The true strain of NbZrTiTa at 6500 s-1 is greater than 103%, indicating a great potential for the application at high strain rate condition.

15:05-15:25

Novel MoxNbTaxTiZr Medium and High Entropy Alloys for Biomedical Implants-A Systematic Approach to Get a Combination of Mechanical Properties

Muhammad Akmal, Ho Jin Ryu, Korea Advanced Institute of Science and Technology (KAIST), Korea

In this research work, MoxNbTaxTiZr (x=0-1) medium and high entropy alloys have been investigated systematically in order to find an optimum alloy for biomedical implants. The arc melted alloys, homogenized at 1400˚C, have shown single-phase (bcc1) with a lower amount of Mo and Ta i.e., up to 0.6 molar fraction; however, higher content of Mo and Ta led another bcc phase appears named as bcc2. A logarithmic increase in the yield strength is observed as a function of Mo and Ta content because of immense solid solution strengthening imparted with the addition of Mo and Ta. Mo has the highest value of shear modulus and smallest atomic size among all other elements, hence it is most responsible for solid solution strengthening. Nonetheless, higher content of Mo and Ta incorporated the brittleness in the alloy. A linear increase in elastic modulus with respect to Mo and Ta was evaluated by using nano-indentation results. Potentiodynamic polarization results of all the compositions have shown tremendous passivation in the phosphate buffer solution. An excellent combination of strength, ductility, and elastic modulus was achieved in Mo0.2NbTa0.2TiZr alloy with strength reaching 1200MPa, plastic strain more than 30% under compression and elastic modulus close to 110GPa. This study accomplishes that the addition of Ta and Mo more than a critical value is not required for biomedical perspective as it enhances brittleness, elastic modulus and decreases the ductility of the system. It is, therefore, endorsed that single-phase Mo0.2Nb Ta0.2TiZr is the best candidate for biomedical implants because of its excellent strength and ductility combination in order to avoid any wear at the joint. Furthermore, this alloy has similar elastic modulus and corrosion behavior to commercial biomedical Ti-based alloys.

15:30-16:10 Tea Break

16:10-16:40 Keynote

Additive Manufacturing of Metallic Glasses and High Entropy Alloys: Challenges and Opportunities

Xiaopeng Li, The University of New South Wales, Australia;

Bulk metallic glasses (BMGs) and high entropy alloys (HEAs) are both important multi-component alloys with novel microstructures and unique physical and chemical properties, which make them promising for applications in many industries, e.g., aerospace, energy, healthcare and etc. However, certain hindrances have been identified in the fabrication of BMGs and HEAs by conventional techniques due to the intrinsic requirements of BMGs and HEAs. With the advent of metal additive manufacturing such as laser powder-bed fusion (LPBF) techniques, new opportunities have been perceived to fabricate geometrically complex BMGs and HEAs with tailorable microstructure theoretically at any site within the specimen, which are difficult to achieve using conventional fabrication techniques. After providing some background and introducing the conventional fabrication techniques for various BMGs and HEAs, this presentation will focus on the current status, development, and challenges in metal additive manufacturing of BMGs and HEAs including different additive manufacturing techniques being used (in particular electron beam melting and selective laser melting), microstructure design and evolution, as well as properties of the fabricated BMGs and HEAs. A few successful and pioneering examples will be given and discussed. A future outlook of metal additive

manufacturing of BMGs and HEAs will also be provided at the end.

16:40-17:05 Invited

Additive Manufacturing of an Equiatomic AlCoCrFeNi High-Entropy Alloy with Electron Beam Melting

Kenta Yamanaka, Hiroshi Shiratori, Yuichiro Koizumi, Akihiko Chiba, Tohoku University, Japan; Hiroshi Shiratori, Tadashi Fujieda, Kosuke Kuwabara, Hitachi, Japan

High-entropy alloys (HEAs) have been attracting much attentions because of their exceptional mechanical properties, such as high strength, good ductility, and superior fracture toughness at cryogenic temperatures. However, HEAs are not always ductile and some of these alloys show poor deformability due to the formation of brittle intermetallic compounds. Furthermore, from the viewpoint of future applications, it is important to explore methods for producing complex shaped products with HEAs. In this study, electron beam melting (EBM), a powder-bed-fusion additive manufacturing (AM) technology, was applied for an equiatomic AlCoCrFeNi HEA, and their microstructures, mechanical properties, and corrosion behavior were evaluated by comparing them with those of a conventionally cast specimen. Microstructural observations revealed that both cast and EBM specimens consisted of a nano-lamellar mixture of disordered body-centered-cubic (BCC) and B2 (ordered BCC) phases. Notably, the EBM process realized rapid cooling during fabrication, resulting in finer grains than those in the cast counterparts. Furthermore, the face-centered cubic (FCC) phase was identified at the grain boundaries of the B2/BCC matrix in the EBM specimen. The fraction of the FCC phase (approximately 30%) at the bottom part of the EBM specimen was higher than that at the top part. The preheating procedure, which is a process unique to EBM, is responsible for the precipitation of the FCC phase, because of the long-term exposure at elevated temperatures. As a result, the EBM specimen exhibited much higher plastic deformability than the cast specimen without significant loss of strength, suggesting that the FCC precipitates accommodate the stress concentration at grain boundaries. Furthermore, potentiodynamic polarization tests revealed a significant improvement in pitting corrosion resistance was identified in the EBM specimen. These results indicate that AM processes are promising for manufacturing as well as optimizing the microstructures of difficult-to-work HEAs.

17:05-17:25

Preparation of NbZrTiTa Refractory High-Entropy Alloy Powder with Uniform Element Distribution by Mechanical Alloying

Yating Qiao, Yu Tang, Yicong Ye, Shun Li, National University of Defense Technology, China

High-entropy alloy (HEA) is a novel metal material composed of more than four elements and possessing a unique single solid solution (SSS) structure and fully disorder atom occupation. The unique structure of HEA results in the special properties, such as high strength and high corrosion resistance. Among all reported HEAs, the refractory high-entropy alloy (RHEA) which is composed of refractory metal displays a great potential to as the special material working at an extreme environmental, such as high and low temperature structure material and energetic structure material, due to its element characteristics.

By far, the main route for fabricating RHEA is liquid mixing, including arc melting, electric resistance melting, inductive melting, etc. Due to the inherent compositional complexity and the huge difference in the melting points between the constituent elements, the liquid mixing is challenging. Significant elemental segregation occurs during melt solidification and cooling. Thus, compared to conventional alloys, the as-cast samples of RHEAs may have obvious casting defects, such as cracks, pores, and residual stresses along with compositional gradients and abnormal grain-size distributions.

In fact, solid mixing, which mainly contains the mechanical alloying and subsequent consolidation process, is another route for preparing HEA. Comparing with liquid mixing, solid mixing has an obvious advantage on preventing casting defects and formation of big and irregular sample. But the high melting point and low diffusion rate will delay the homogenization of refractory elements. According to the thermodynamics and high-entropy effect of HEA, the formation of SSS is mainly caused by the uniform distribution of constituent elements. Indeed, the increase of ball milling time can realize the homogenization of element distribution finally. But it also will lead to the increase of lattice defects and the decrease of crystallization degree. That is to say, the problem that element homogenization rate is lower than the defect increase rate makes the formation of RHEA powder with the uniform element distribution, SSS structure and high crystallization be difficult. Therefore, it is significant to find an effective way to speed up element diffusion and slow down defect generation during mechanical alloying process.

As it is known, the element diffusion will accelerate in the area without complete lattice. And the addition of liquid ball milling medium can increase grain refinement efficiency. The grain refinement will increase element diffusion rate through increasing grain boundary and reducing lattice completeness before the occurrence of cold welding, during which the element start to mutual diffuse. More important, the presence of liquid ball

milling medium will obstruct the direct contact between raw powders and lower the defect generation rate.
Thus, some ball milling mediums including liquid and solid were added during the prepare process of NbZrTiTa quaternary RHEA by mechanical alloying. The effect of different mediums on the element homogenization and the formation of SSS were investigated. An effective way to prepare RHEA powder with uniform element distribution and SSS structure was found.

17:25-17:45

Flexible High-Entropy Micro-Fiber for Niche Applications

Dongyue Li, Yong Zhang, University of Science and Technology Beijing, China

Increasing demands for stronger and more ductile structural materials have stimulated a vigorous search for novel alloys. The emergence of high entropy alloy is promising to breakthrough this general strength-ductility trade-off. Besides the widely studied bulk high entropy alloy ingots, low-dimensional and flexible high entropy fibers also have extremely broad prospects. In this work, we fabricated FCC-based Al0.3CoCrFeNi micro-fiber of 60μm in diameter by hot drawing. Additionally, appropriate heat treatment and coating can further optimize the performance of mechanical properties. This fiber will position the application of high entropy alloys in high-tech micro-devices. It provides support for the development of a new generation of the niche by precise processing and forming.

K. Nanocrystalline Materials, and Ultra-Fine Grained Materials: III

Symposium Organizers:

Yue Zhang, University of Science and Technology Beijing, China; Zhiyong Tang, National Center for Nanoscience and Technology, China; Nobuhiro Tsuji, Kyoto University, Japan; Jae-il Jang, Hanyang University, Korea; Kenong Xia, University of Melbourne, Australia; Nathan Mara, University of Minnesota, USA

Tuesday PM
August 20, 2019

Room: 309(3rd Floor)
Symposium: K

Chairs:
Glenn Sneddon, University of Sydney, Australia
Ning Wang, Hong Kong University of Science and Technology, Hong Kong, China

13:30-14:00 Keynote

Probing Electron Transport in Atomically Thin Semiconducting Transition Metal Dichalcogenides

Ning Wang, Hong Kong University of Science and Technology, Hong Kong, China

Atomically thin semiconducting transition metal dichalcogenides (TMDCs) such as MoS_2, $MoSe_2$, WS_2 and WSe_2 form a family of layered two-dimensional materials exhibiting novel electronic and optical properties. Probing the quantum transport in these TMDCs has been a long-standing challenge due to the low carrier mobility and the large contact resistance in their field-effect devices prepared by the exfoliation method. In this talk, I demonstrate our recent experimental study on quantum transport of few-layer MoS_2 and WSe_2, and their unconventional Landau levels (LLs) with strong interaction effects. We fabricate high-quality n-type MoS_2 and p-type WSe_2 devices by encapsulating these TMDCs in ultra-clean hexagonal boron nitride sheets which effectively eliminate impurity scattering and provide clean interfaces for making high-quality low-temperature ohmic contacts to these semiconducting TMDCs. Few-layer MoS_2 and WSe_2 field-effect devices with mobilities up to 30,000cm^2/Vs have been achieved at cryogenic temperatures. We observe interesting quantum Hall (QH) phenomena involving the Q valley, Γ valley and K valley, such as the Q valley Zeeman effect in all odd-layer MoS_2 devices and the spin Zeeman effect in all even-layer MoS_2 devices and highly density-dependent QH states of Γ valley holes in WSe_2. The predominant sequences of the QH states of Γ valley holes in few-layer WSe_2 alternate between odd- and even-integers with reducing the density. By tilting the magnetic field to induce Landau level crossings, we show that the strong Coulomb interaction enhances the ratio of Zeeman-to-cyclotron energy, giving rise to the even-odd alternation of the predominant sequences. For n-type MoS_2, we have studied the valley-resolved SdH oscillations relevant to the spin-valley locked massive Dirac electron LLs. With decreasing the carrier density in the conductance band (K valley), we observe LL crossing induced valley ferrimagnet-to-ferromagnet transitions and the enhancement of the valley Zeeman effect by Coulomb interactions. In n-type monolayer and trilayer MoS_2, we first detect the intrinsic valley Hall transport without any extrinsic symmetry breaking through measuring the nonlocal resistance that scales cubically with the local resistance. Such a phenomenon survives at room temperature with a valley diffusion length at the micron scale. We believe that the large intrinsic bandgap in MoS_2 contributes to maintaining a large amplitude of the Berry curvature, allowing to observe the valley Hall effects even at room temperature in monolayer MoS_2.

14:00-14:25 Invited

Direct Observation of the Dislocation Interaction with Grain Boundary in Ultrafine-Grained IF Steels by In-Situ TEM Technique

Seiichiro Ii, Hongxing Li, Takahito Ohmura, National Institute for Materials Science, Japan; Takahito Ohmura, Kyoto University / Kyushu University, Japan; Nobuhiro Tsuji, Kyoto University, Japan

Mechanical properties of polycrystalline materials are

often governed by their grain boundaries, which is well-known as Hall-Petch relation. In the Hall-Petch relation, the yield strength is linearly related to the inverse square root of the mean grain size and the slope of the relation is termed k, based on the concept of the interaction between dislocations and grain boundaries. For an improvement of the mechanical properties in the polycrystalline materials, the grain refinement is one of the effective ways. Ultrafine-Grained (UFG) materials, which are consisted of the fine grains of less than 1μm, exhibit high strength. Moreover, k value also becomes larger than that of coarse-grained one (>1μm). Even in the UFG metals, many researchers have discussed the plastic deformation mechanisms from the experimental and computational techniques. On the other hand, in-situ transmission electron microscopy (TEM) is known as one of the powerful techniques to directly clarify the microstructure change under the external field. Especially, recent in-situ straining TEM holder can obtain the mechanical data as well as microstructure change simultaneously. In this study, we investigated the dislocation interaction with grain boundary in the UFG IF steel fabricated by an accumulative roll-bonding process by the in-situ straining TEM technique. Micropillar specimens for in-situ observations were prepared by focused ion beam (FIB). The in-situ straining TEM was performed using an indentation TEM holder under compression with the displacement-controlled mode. Microstructure change during compression was recorded as a video using a CCD camera at 30 fps. We could directly observe that pre-existed dislocations in grain interior were moved during loading and those in the specific grain are absorbed into the grain boundary without piling up.

14:25-14:50 Invited

Atomistic Structural Characteristics of Amorphous B-Si-C-N based Coatings at Temperatures >1000℃

Jiechao Jiang, Efstathios I. University of Texas at Arlington, USA; J. Vlček, Physics Department, University of West Bohemia, Czech Republic

We present, in this talk, atomistic structure of B-Si-C-N and Hf-B-Si-C-N coatings at temperatures above 1000˚C and the high temperatures oxidation mechanism. The coatings were deposited by magnetron sputtering and are hard with an amorphous structure and exhibit superior high temperature oxidation resistance up to 1100˚C without any atomic structure changes. Annealing in air at temperatures from 1100˚C to 1500˚C transforms the amorphous coating structure into a two-layered structure comprising of an oxidized layer on the top followed by a non-oxidized bottom layer. The top oxidized layer possesses either a pure amorphous SiOx, or nanocomposite of HfO_2 nanoparticles dispersed in amorphous SiO_x matrix structure. The thickness of the oxide layer varies with the annealing temperature and coating composition. The non-oxidized bottom layer structure varies from amorphous to nanocomposite of HfB_2 and HfN nanoparticles separated by h-Si_3N_4 and h-BN boundaries depending on the annealing temperature. The oxide/bottom layer interfaces possess high population of either fine BN nanoparticles or fine HfO_2 nanoparticles surrounded by SiO_2 boundaries. The high-temperature oxidation resistance evolves either nanocomposite of BN nanoparticles and SiOx, or HfO_2 nanoparticles within a dense SiOx-based matrix and quartz SiO_2 in front of the bottom layer acting as a barrier for heat and O diffusion. This work was supported by the U.S. National Science Foundation under Award NSF/CMMI DMREF-1335502.

14:50-15:10

Designing Heterogeneous Ultrafine-Grained Metals and High-Entropy Alloys to Enable High Strength and High Ductility Simultaneously

Evan Ma, Johns Hopkins University, America

In a previous review, Materials Today 20 (2017) 323-331, we presented our perspective that heterogeneities intentionally introduced into a metal, such as a grain size distribution/gradient, or hierarchical defect structures, promote strain hardening and hence uniform tensile ductility. The result is a strength-ductility combination noticeably better than that known for conventional cold-worked or ultrafine-grained counterpart.

In this talk, we demonstrate that the properties achieved above still remain a trade-off between strength and ductility, albeit at a level better than that normally seen in conventional metals. This is true even for the most recent reports in 2018. In other words, there is plenty of room in the strength-ductility space yet to be reached. Very recent attempts, including in situ nanostructuring and hierarchical microstructures in multi-component multiphase alloys, have opened new opportunities that are not previously possible in those simple metals above.

We will discuss FCC high-entropy alloys and BCC high-entropy alloys to review what have been found over the past several years. These HEAs are strengthened via "multiple principal elements", together with easy storage of defects during tensile deformation due to their low stacking fault energy. The result is an added propensity for heterogeneous microstructure that promote strain gradient hardening. The most recent successes typically have a combination of gigapascal yield strength with >25% tensile strain, see, e.g., M. Yang et al., PNAS 2018, and Z. Lu et al., Nature in October 2018. The latter example used oxygen-(Ti,Zr) complexes (ordered local entities and not yet second phase) as heterogeneities to help increase the ductility of the base BCC high-

entropy alloy. Such chemical heterogeneities go beyond the structural heterogeneities in single-element metals. An exciting case, reported last month in Science by C.T. Liu's group, used a carefully crafted high-entropy intermetallic as the second phase. They achieved 50% uniform elongation, making the complex alloy as ductile as any single-element un-strengthened metal, at a yield strength above 1.5GPa (an order of magnitude higher than any single-element, un-strengthened metal). This extends the strength-ductility range to unprecedented territory. Note that previously, strength-ductility trade-off was claimed to have been "overcome" only by comparing with an already-strengthened low-ductility metal/alloy, or with alloys that have yield strength well below 1GPa.

Multi-component alloys also allowed the exploitation of in situ phase transformations, similar to the TRIP effect in steels. The Nature (2016) paper by Z. Li and D. Raabe for FCC HEAs, and the Advanced Mater. (2018) paper by Y. Wu et al. for BCC HEAs, followed this route. They have made use of martensitic transformation during the tensile deformation to elevate strain hardening, sustaining uniform elongation while strengthening the high-entropy alloy. This TRIP route towards strength-ductility synergy is interesting, as it adds a new twist to the known TRIP steels and takes advantage of the metastable nature of high-entropy alloys.

We advocate that multi-component, multiphase alloys are more effective in pushing the strength-ductility envelope, and constitute a fertile playground to be explored, especially with the advent of complex concentrated "high-entropy" alloys, a field that is emerging and attracting widespread attention recently.

15:10-15:30

Microstructural Characteristics and Dynamic Behaviour of Dislocations in Metal Nanowire under Tensile Process

Zhaoyang Hou, Xiao Qixin, Chang'an Uiversity, China; Rangsu Liu, Hunan University, China

The dislocation is an important microstructural configuration during the deformation process of nanocrystalline metals. The dynamic behaviour of dislocations play a crucial role in the mechanical properties and deformation mechanism of nanocrystalline metals. The dislocation atoms are usually regarded as disordered atoms, but its detailed microstructural characteristics are not completely understood. In this work, the microstructure characteristics and dynamic behaviour of dislocations in Au nanowire under the tensile process are investigated by molecular dynamic simulation. It is found the plastic deformation mechanism in Au nanowire is the emission, propagation and annihilation of Shockley partial dislocations, which is agree with the experimental results obtained by in situ high-resolution transmission electron microscopy. The microstructural configurations of the dislocation atoms are analysed by means of the microstructural analysis method--cluster-type index method (CTIM) proposed by us. It is found the dominating microstructural configurations of the dislocation atoms are the defective FCC clusters represented by the CTIM indexes (12, 2/1311, 1/1411, 9/1421), (11, 4/1311, 7/1421), (12, 8/1421, 2/1431, 2/1541), (13, 8/1421, 1/1441, 4/1541), and the defective BCC clusters represented by the CTIM indexes (14, 4/1441, 4/1551, 6/1661). During the propagation process of Shockley partial dislocations, a stacking fault with HCP atoms follows the dislocation. There are two different paths during the FCC→HCP transformation in term of tracing the evolutions of cluster structures.

15:30-16:10 Tea Break

16:10-16:35 Invited

Investigating Deformation in Nanocrystalline Materials Using In-Situ Transmission Kkuchi Diffraction

Glenn Sneddon, Vijay Bhatia, Julie Cairney, University of Sydney, Australia; Patrick Trimby, Oxford Instruments Nanoanalysis, England

Observations of strained nanocrystalline materials have shown that discontinuous grain growth can occur at room temperature with as little as 2% strain. Understanding such changes in nanocrystalline material properties at room temperature is vitally important and has, until now, required detailed TEM observations of the resulting microstructure and inferences regarding the processes involved.

Transmission Kikuchi diffraction (TKD) in the scanning electron microscope (SEM) has advantages in resolution over conventional electron backscatter diffraction that have resulted in a wide range of applications of TKD across the materials and earth sciences. However, to date TKD has not been applied to the study of dynamic processes, utilizing in-situ deformation. Here we present results from a prototype in-situ tensile deformation stage that has been custom modified for use with TKD, enabling the investigation of discontinuous processes on the nanoscale, such as grain boundary sliding, twinning and stress-assisted grain growth. The experiments were carried out using a Zeiss Ultra Plus field emission SEM equipped with an Oxford Instruments AZtec EBSD and TKD system, acquiring TKD data at discrete load steps for each sample. A variety of materials were analysed, including nanocrystalline copper films, surface treated stainless steels and steels undergoing stress-induced phase transformation.

We believe that this in-situ TKD technique can become an effective tool for understanding the complex nature of discontinuous stress-assisted grain growth, allowing us

to identify the exact nature of the grains and boundaries that are most affected by this mechanism.

16:35-16:55

Significantly Enhanced Wear Resistance of an Ultra-Fine Grained Edium Entropy Alloy CrFeNi at Elevated Temperatures

Fuzeng Ren, Dingshan Liang, Cancan Zhao, Weiwei Zhu, Pengbo Wei, Feilong Jiang, Yiwen Zhang, Southern University of Science and Technology, China

Metallic alloys for mechanical components involving sliding contacts in relative motion, particularly at the elevated temperatures, require not only good combination of strength and ductility, but also high sliding wear resistance. Thus, the design of novel metallic alloys with exceptional damage-tolerance for harsh environment is in great demand. In recent few years, new alloy design strategy with multi-principal elements have been developed, referring to as high/medium entropy alloys (HEAs or MEAs). Herein, we report a novel cost-effective equiatomic medium entropy alloy (MEA) CrFeNi consisting of an ultrafine-grained (UFG) face-centered cubic (fcc) matrix with a high density of nanoscale body-centered cubic (bcc) Cr-rich precipitates. Such a hierarchical structure offers an excellent combination of high tensile strength of 826 MPa and elongation of 26%. Remarkably, the alloy shows exponential decrease in wear rates and linear decrease in coefficient of friction (CoF) upon dry sliding against Inconel alloy 718 disk at elevated temperatures. Finally, we rationalized the formation of a hierarchical structure of the present UFG MEA CrFeNi, analyzed the origin for such an excellent high tensile strength-ductility combination, and explained the reasons for the significantly enhanced wear resistance at elevated temperatures. The results reported in our study provide deep insight into design of novel multi-principal element alloys with high strength and ductility, and particularly exceptional wear resistance at elevated temperatures for high temperature structural applications.

16:55-17:15

Mechanical Behavior of Ultrafine-Grained High-Entropy Alloy at 293K and 77K

Yanzhong Tian, Northeastern Univeristy, China

The strong desire for materials with high strength and good ductility in industrial applications is driving the development of new concepts in alloy design. In recent years, a new type of equiatomic or near equiatomic multicomponent alloys named high-entropy alloys (HEAs) intrigue a new strategy in developing alloys. Among the HEA systems, the HEAs with face-centered cubic (FCC) structure were widely studied because of the attractive properties, such as dynamic properties, fracture toughness and corrosion resistance. However, the yield strength of HEAs with FCC structure is insufficiently strong. In order to increase the yield strength of the HEAs with FCC structure, many efforts were conducted, such as grain refinement, precipitation and heterogeneous structure. Here, we introduce a new strategy to fabricate FCC HEA with superior strength and ductility. Bulk CoCrFeMnNi HEAs were prepared by magnetic levitation melting technique. The cast got was firstly hot forged into rods and further cold rolled into sheets 1mm thick with a nominal reduction in thickness of 95%. Ultrafine-grained (UFG) specimens with fully recrystallized microstructures were fabricated by cold rolling and subsequent annealing treatments. This novel UFG HEA is characterized with fine grains, high-fraction of high-angle grain boundaries and low dislocation density. Tensile properties were tested at room and cryogenic temperatures. Transmission electron microscope (TEM) and electron backscattered diffraction (EBSD) were used to characterize the microstructures. With decreasing the temperature, the yield strength, uniform elongation and strain-hardening capability were enhanced significantly. The enhanced yield strength is related strongly to the small grain size, and is originated from thermal and athermal contributions. The ductility and strain-hardening rate are enhanced by inhibiting the dislocation recovery and facilitating the deformation twins by lowering the temperature. Synchronous increase in strength and ductility is achieved in the present UFG HEA by decreasing temperature, which provide a strategy to design HEAs with adaptive mechanical properties.

17:15-17:35

Formation of Nanostructures in a γ' Precipitate Strengthened Ni-Based Superalloy Processed by Surface Mechanical Rolling Treatment

Yong Zhang, Hao Wu, Shengyun Yuan, Nanjing University of Science and Technology, China

Nanostructured materials have been widely investigated over the past twenty years due to its high strength, superior fatigue properties and so on. However, the fabrication of nanostructured Nickel-based superalloy has been few investigated before. In this study, a Nickel-based superalloy with high density of L12 structured γ' precipitates was processed by surface mechanical rolling treatment (SMRT). A gradient microstructure was formed along the depth from the treated surface, including nano-grained structure, nano-twins and stacking faults (SFs). The formation mechanisms of nanostructure in the topmost surface (<100mm) were systematically investigated by means of transmission electron microscopy (TEM), Super-X energy dispersive spectroscopy (EDS) and three-dimensional atom probe technology (3DAPT). TEM observations on the topmost

surface indicate that nano-grained structure has the face centered cubic (fcc) structure with an average size of ~15nm. However, the EDS scan perpendicular to the grain boundaries demonstrate that neiboring nano-grains exhibts similar elements partitioning tendency to the γ/γ' phase structure. The Ni, Ti and Al atoms tend to partition into one grain, while Co/Cr atoms into the neighboring grain, suggesting that the composition distribution in the nano-grains inherites from γ/γ' phase structure. TEM observations indicate that the deformation microstructure in the subsurface of SMRT processed sample are characterized by high density of nano-twins and stacking faults on two (111) planes. This suggested that the nanostructure on the topmost surface can be ascribed to the intersection of high density of nano-twins. The EDS analysis also indicate that the elemental partitioning tendency in the neighboring twin/matrix is quite similar to those in neighboring nano-grains, i.e., the neighboring twin/matrix exhibits enrichment of Ni, Ti and Al atoms and Co/Cr atoms alternatively. Therefore, the formation of the fcc structured nano-grains in the topmost surface can be attributed to shearing deformation exerted by the deformation twins on the γ/γ' phase structure, which leads to the fragmentation of γ' phase while preserving the composition.

L. Computational Design and Simulation of Materials: III

Symposium Organizers:

Tongyi Zhang, Shanghai University, China; Zhimei Sun, Beihang University, China; Shigenobu Ogata, Osaka University, Japan; Byeong-Joo Lee, Pohang University of Science and Technology (POSTCEH), Korea; Salvy Russo, RMIT, Australia; Saryu Fensin, Los Alamos National Lab, USA; Michele Manuel, University of Florida, USA

Tuesday PM
August 20, 2019

Room: 204 (2nd Floor)
Symposium: L

Chairs:
Asaph Widmer-Cooper, The University of Sydney, Australia
Yoshitaka Adachi, Nagoya University, Japan

13:30-13:55 Invited

Designing Crystallization in Phase-Change Materials for Universal Memory

Wei Zhang, Xi'an Jiaotong University, China; Evan Ma, Johns Hopkins University, USA

The global demand for data storage and processing has increased exponentially in recent decades. To respond to this demand, research efforts have been devoted to the development of non-volatile memory (NVM) technology. NVM combines the advantage of fast operation speed with non-volatile features (data are preserved in the absence of power supply) and holds great promises to simplify the current complex memory hierarchy for substantial improvements in computing and power efficiency. Chalcogenide phase-change materials (PCMs) are leading candidates for such application, and have become technologically mature with recently released competitive products, i.e. Intel Optane memory. In this talk, I will focus on the mechanisms of the crystallization dynamics of PCMs by discussing structural and kinetic experiments, as well as ab initio atomistic modeling and calculations. Based on the knowledge at the atomistic level, potential routes to improve the crucial parameters, such as switching speed, power consumption as well as cycling endurance of phase-change devices for universal memory are depicted by ab initio materials design.

13:55-14:20 Invited

Machine Leaning/Advanced Mathematics-Assisted Microstructure Quantification

Yoshitaka Adachi, Toshio Ogawa, Zhilei Wang, Nagoya University, Japan

This study will highlight advanced machine learning-based image processing and enhanced microstructure quantification. Various image processing methods were applied such as ML-based image segmentation, masked region with convolutional neural network(R-CNN), Segnet, U-net, etc. Microstructure were quantified by two ways; one is by extracting human-comprehensive features such as size, volume fraction, connectivity, etc., the other one is by deducing human-incomprehensive features such as distance in two-point correlation function, address in persistent homology, address in Gauss-mean curvature analysis, etc. Those enhanced image quantification modules were implemented in two types of material genome integration system; MIPHA which is a stand-alone version and shiny MIPHA which is a cloud version.
Microstructure descriptors obtained by these packages are input into direct analysis such as artificial neural network, support vector regression, random forest regression to correlate microstructure and property. Hype-parameters of those machine learning classifier were optimized by Bayesian optimization. Before direct analysis, important descriptors must be selected to suppress over fitting. Therefore, various sparse modeling methods were applied such as AIC, BIC, lasso, sensitive analysis, etc.
Subsequently, inverse analysis was performed by genetic algorithm or Bayesian optimization algorithm to suggest an ideal microstructure demonstrating the best property.

In the presentation, it will be demonstrated that above-mentioned machine leaning/advanced mathematics-assisted microstructure quantification followed by direct analysis and then inverse analysis were applied to optimize a steel and other materials.

14:20-14:40

A lattice BGK Scheme for Modeling of Dendritic Growth in Solidification of Alloys with Melt Convection

Dongke Sun, Southeast University, China; Hui Xing, Northwestern Polytechnical University, China

Dendritic growth is a commonly observed phase transition in nature andindustry, which influences microscopic structures and macroscopic properties of materials during solidification. A lattice Bhatnagar-Gross-Krook and phase field theory-based method is proposed to study dendritic growth of alloys with melt convection. It extends the BGK-Boltzmann equation to model the heat transfer, melt convection and liquid-solid phase transition by implementing a general streaming-relaxation steps based on the Chapman-Enskog expansion. Three sets of distribution function are adopted to describe the evolution of the temperature, flow and phase fields. The DnQd lattice vectors are used to describe advancement of solid-liquid interface, coupling with a convective-diffusion equation for heat transfer during solidification. It offers a simple and effective geometrical relationship between growing velocity and lattice spaces. The scheme is validated by simulating two classic examples of dendritic growth, i.e. the free dendritic growth into an undercooling melt in pure diffusion condition and the free dendritic growth in a square domain with melt convection. The simulated data shows good agreement with analytical predictions and benchmarks. It demonstrates that the present LB scheme is reliable and accurate to study dendritic growth with melt convection. The dendritic growth of binary alloys with melt convection have been investigated numerically. The results show that the present model provides an alternative numerical approach to study solidification of alloys with relatively fast efficiency, and it would like to facilitate the understanding the features of phase transition in a high-throughput way.

14:40-15:00

Ballistic Transport in Bent-Shaped Carbon Nanotubes

Zewen Wu, Beijing Institute of Technology, China / Hongzhiwei Technology (Shanghai) Co., Ltd. China; Yanxia Xing, Beijing Institute of Technology, China; Wei Ren, Shanghai University, China; Yin Wang, Shanghai University, China / Hongzhiwei Technology (Shanghai) Co., Ltd., China; Hong Guo, McGill University, Canada / Hongzhiwei Technology (Shanghai) Co., Ltd., China

We report theoretical investigations of ballistic transport properties of bent-shaped semiconducting single-walled carbon nanotubes (SWCNTs) in the form of NxN or PxP, where N and P stand for N-type and P-type doping, x takes N-type, P-type or intrinsic I-type. Our calculation is based on the state-of-the-art NEGF-DFT first principles approach, and rich physical phenomena is discovered due to the smooth bend.

The smoothly bent CNT induces a small electron redistribution on the CNT arc, which leads to three main transport differences between the NxN and PxP tubes. In particular, conductance G of NNN tubes does not change with the bending angle, as the redistribution does not affect the already heavily doped NNN tube. On the other hand, G of PPP tubes decreases with the bending angle, as the electron redistribution in the central region leads to a potential glitch at the source/central and central/drian interfaces. In addition, G of NPN and PNP tubes increases with the bending angle because the electron redistribution somewhat reduces the potential barriers at the source/central and central/drain interfaces. Finally, G of the PNP tubes varies with the bending angle in an oscillatory manner, due to quantum interference of the two scattering states at the Fermi level induced by the path difference.

The predicted conductance versus bent angle is useful for estimating how a flexible system may behave when strained and/or bent. The bent-shaped CNT changes propagating direction of the ballistic electrons, these electrons can perfectly negotiate - with no back-scattering, the smooth bent if the CNT is N-type (NNN). Therefore the NNN tubes are suitable for application as interconnect wires. The conductance of NPN or PNP tubes depends on the bent angle, as such they may play a role in electromechanic systems.

15:00-15:20

Modeling Microstructural Evolution during Selective Laser Melting Additive Manufacturing

Mohsen Eshraghi, Antonio Magana, Ryan Lenart, California State University, Los Angeles, USA

Further research is needed in order to understand the effect of process parameters on the development of solidification microstructure during powder bed fusion Additive Manufacturing (AM) processes. Controlling solidification microstructure in additively manufactured metallic components can play a game-changing role in the way engineering components are designed and fabricated. However, experimental analysis of the

melt pool is difficult because the size of the melt pool is very small and the heat source is moving very fast. Computational modeling of solidification microstructure can help to gain a better understanding of the kinetics governing microscopic features of the solidification process. Direct numerical simulation of the solidification microstructure formed during AM processes will provide a relation between macroscopically observable variables like cooling rate or temperature gradient and difficult-to-measure dynamic microscopic features like solute redistribution, columnar to equiaxed transition, and dendrite arm spacing. Although much observation has been done to examine the static microstructures during different stages of solidification, it has never been possible to capture and examine the dynamic response of these features in an evolving mushy zone. Several physical phenomena are involved during the solidification processes that make the simulation complex. In this study, a numerical model based on Discrete Element Method (DEM) is used to simulate the powder distribution and packing. Then a meso-scale thermo-fluid model is employed to simulate the molten pool geometry and dynamics. In addition, a numerical model based on the phase field and lattice Boltzmann methods is used to simulate the evolution of the solidifying microstructure in the melt pool. The multi-scale computational model is then used to investigate the effects of process parameters on the molten pool dynamics and solidification microstructure during selective laser melting of metallic alloys. Fundamental aspects of the mechanisms that regulate the formation of solidification microstructure during SLM will be discussed. The results can be adopted to enable location-specific grain structures and properties by tuning AM process parameters with minimal trial and error.

15:20-16:00 Tea Break

16:00-16:25 Invited

Colloidal Stability of Apolar Nanoparticles

Asaph Widmer-Cooper, The University of Sydney, Australia

Being able to predict and tune the colloidal stability of nanoparticles is of vital importance for technological applications, yet our ability to do so is poor due to a lack of understanding of how nanoparticles interact with one another. One area that has seen increased attention is the organic ligand shell that coats most inorganic nanoparticles dispersed in apolar solvents. This ligand shell is essential for keeping the particles from randomly aggregating in solution, but can affect the particle stability in subtle and surprising ways. In particular, the ligands can undergo a temperature-dependent order-disorder transition that switches the particle-particle interaction in solution from repulsive to attractive. As we have shown, the temperature of this transition is sensitive to a range of factors, including the particle dimensions, density of ligand coverage, and ligand length, often leading to non-linear trends that cannot be explained using conventional colloid theory.

In this talk, I'll explain how the ability of the ligand shell to order (or not) can make sense of a diverse range of surprising phenomena, including an inversion of the effect of ligand length on particle stability, solvent effects that run opposite to the rule of like-dissolves-like, and stabilities that increase by several orders of magnitude upon the addition of a single methyl group to the tail of the ligands. Our results for Au and CdSe nanoparticles, obtained from SAXS experiments and molecular dynamics simulations, provide a microscopic description of the forces that determine the colloidal stability of apolar nanoparticles and explain why classical colloid theory fails.

16:25-16:45

Machine Learning based on Local Composition-Structure Descriptors for Alloying Element Substitution in Superalloy

Yi Liu, Bin Xiao, Yuqin Wu, Shanghai University, China

Though various advanced data mining algorithm matters, for given data quality, the feature/descriptor engineering set up the accuracy limit of a machine learning (ML) model in materials science. The inherent relationship among "composition-structure-process-property" is deeply rooted in the heart of materials science. Therefore, we believe the good descriptors in ML model should contain the composition, structure, and process information. So far most early machine learning models used the elementary properties and composition information only. The large datasets are often required to achieve satisfied accuracy. The composition-structure based descriptors emerged to give better prediction. The current composition-structure descriptors are suitable for global structures and their associated global properties. In this work, we proposed a novel local composition-structure descriptor, dubbed "Center-Environment" (CE) model, to study the local energetic and geometrical properties of materials.

In alloy design, it is fundamentally important to clarify the preferential site occupancy of alloying elements to

elaborate the strengthening mechanisms. It is, however, a formidable task for first-principles (FP) calculations to explore the enormous potential doping configurations in the complex multi-component alloys. In this work, we first carried out high-throughput FP calculations systematically for several hundred alloy doping configurations in superalloy, considering ~10 alloying element substitution at multiple nonequivalent sites. The machine learning models can be used more efficiently for further prediction, reducing the cost of expensive FP calculations while maintaining the certain accuracy. We developed the machine learning models based on the high-throughput FP calculated data. Specifically, we designed a "Center Environment" (CE) descriptor model to construct descriptive features by combining elemental properties and local composition and structure information of both center and environment. It is shown that the CE descriptors can be used to predict both the substitution energy and local geometry of alloying elements in superalloy. By comparison we show clearly that the machine learning prediction using feature construction with both composition and structure information is more accurate and robust than that with composition only. Taking the advantages of the accuracy of first-principle calculations and efficiency of machine learning methods, such combined FP-ML approach becomes an emerging strategy to explore enormous configurations commonly required in computational materials simulations and design.

16:45-17:05

Tight-Binding Models for the Two-Dimensional Allotropes of Bismuth

Jackson Smith, RMIT University, Australia / Australian Research Council Centre of Excellence in Future Low-Energy Electronics Technologies, Australia; Qile Li, Chutian Wang, Yuefeng Yin, Nikhil Medhekar, Australian Research Council Centre of Excellence in Future Low-Energy Electronics Technologies, Australia / Monash University, Australia; Mykhailo Klymenko, RMIT University, Australia / Australian Research Council Centre of Excellence in Exciton Science, Australia; Jared Cole, RMIT University, Australia / Australian Research Council Centre of Excellence in Future Low-Energy Electronics Technologies, Australia / Australian Research Council Centre of Excellence in Exciton Science, Australia

Bismuthene is one of the two dimensional forms of bismuth, comprised of a single layer of atoms arranged in a honeycomb pattern. Electrical conduction at the edges of a bismuthene layer has been experimentally demonstrated by F. Reis et al. (Science 357, 287, 2017), but these measurements did not ascertain whether the observed edge states are topologically protected. In the same year, M. Bieniek et al. (J. Phys. Condens. Matter 29, 155501, 2017) used a semi empirical tight binding model for bulk bismuth to compute the electronic characteristics of a bismuth (111) bilayer. However it remains unclear whether tight binding parameters that have been derived for bulk bismuth can accurately reproduce the properties of the two dimensional allotropes of bismuth. Here we present new tight binding models for these allotropes that are derived from density functional theory using bases of maximally localised Wannier functions. This allows for the atoms in each of these structures to be relaxed from their bulk positions. The density functional calculations have been carried out using the software package VASP. Accurate models for the electronic structure of a bismuthene layer and the bismuth bilayers enable the topology of these systems to be probed through the simulation of quantum transport.

17:05-17:25

Mo Segregation at TiC-Ferrite Coherent Phase Boundary and Its Effect on H Trapping Behavior

Boning Zhang, Tsinghua University, China / Central Iron and Steel Research Institute, China; Hao Chen, Tsinghua University, China; Matthias Militzer, University of British Columbia, USA; Zhenbao Liu, Maoqiu Wang, Central Iron and Steel Research Institute, China

Hydrogen-trapping behavior of precipitations have attracted much attention due to the importance to take into account service degradation of high strength steels. By providing high density H traps, the contribution of two types of nanometer sized precipitates to improved hydrogen-embrittlement (HE) resistance, TiC and (Ti, Mo)C, have both been confirmed by literature results but not systematically compared. In the present work, the role of Mo addition in TiC carbide interphase precipitation steel on hydrogen-trapping characteristics was evaluated by a combination of density-functional-theory (DFT) calculations and thermal desorption analysis (TDA). The calculation results show that Mo atom is energetically not favorable to substitute Ti inside TiC carbide, while showing segregation trend towards the phase boundary. Interface boundary energy changed by Mo plays a major role for initial nucleation which indicates the formation of the so-called complex (Ti, Mo)C carbide is more of a kinetic process rather than thermodynamic equilibrium one. The binding energy of H at TiC-ferrite coherent interface trapping sites were

found to be around 0.27eV/atom. Compared with TiC, the interface for (Ti, Mo)C show reduced hydrogen trapping capacity and the binding energy decreases with increasing Mo content, supporting the experimental results that more diffusible H can be detected and higher HE sensitivity for the latter case under same H charging conditions. The reduced trapping energy derives mainly from the repulsive chemical interaction between Mo and H atoms. On the other hand, higher number density of carbides induced by Mo addition, may balance the disadvantageous effect stems from reduced trapping energy due to increased critical H concentration. The results suggest that for (Ti, Mo)C strengthened steels, a critical Mo concentration for hydrogen trapping may exist, and a better HE-resistance can be obtained by adopting prolonged time or higher temperature for isothermal holding while still retaining superior strength.

M: Renewable Energy Materials and Nuclear Materials: III

Symposium Organizers :

Min Zhu, South China University of Technology, China; Yuan Deng, Beihang University, China; Guanghong Lu, Beihang University, China; Tetsuya Uda, Kyoto University, Japan; Taek-Soo Kim, Korea Institute of Industrial Technology (KITECH), Korea; Dmitri Golberg, Queensland University of Technology, Australia; Assel Aitkaliyeva, University of Florida, USA

Tuesday PM
August 20, 2019

Room: 311(3rd Floor)
Symposium: M

Chairs:
Hongbo Zhou, Beihang University, China
Guanghong Lu, Beihang University, China
JongHyeon Lee, Chungnam National University, Korea
Jing Tang, University of Queensland, Australia

13:30-14:00 Keynote

Alternative Ways of Producing Group IV Metals Through a Liquid Copper-Aided Direct Reduction Process of Oxide Feedstocks

JongHyeon Lee, Sukcheol Kwon, Vladislav Ri, Wan-Bae Kim, Hwa-Young Woo, Gyu-Seok Lim, HanSik Ryu, Woo-Seok Choi, Hayk Nersisyan, Chungnam National University, Korea; Young Jun Lee. ZIRON TECH., Co., Ltd., Korea

Direct reduction could significantly simplify the isolation of group IV transition metals from their corresponding oxides (for example TiO_2, ZrO_2, and HfO_2). These metals are typically produced by the Kroll process, but the multiple stages, especially the chlorination step, reduces the effectiveness of the extraction, and increases the cost of the final product and the environmental impact. The main problem of conventional direct reduction of the group IV metal oxide is the higher impurity level than industrial standards, especially gas impurities due to their high oxygen and nitrogen affinities. Here, we report a metal production technology that lowers the oxygen content of Zr to meet the requirements for nuclear-grade metal.

In the first step, Zr-Cu alloy ingots were prepared from a Hf- free ZrO_2 precursor in a molten $CaCl_2$ medium by CaCu reducing agent. The CuZr alloy was further purified by a molten salt electrorefining process to recover pure nuclear-grade Zr in a LiF-Ba_2ZrF_8-based molten salt, the latter of which was fabricated from a waste pickling acid of a Zr clad tube. The purity of the recovered metal satisfied the ASTM B349 specifications for nuclear-grade Zr.

Also, this technology was successfully applied to the preparation of group IV transition metals such as Ti and Hf.

14:00-14:25 Invited

Novel Porous Carbon Produced by Elaborately Design of Metal-Organic Frameworks

Jing Tang, The University of Queensland, Australia / East China Normal University, China;Yusuke Yamauchi, Shahriar Hossain, Jeonghun Kim, The University of Queensland, Australia

Carbon is undoubtedly the most widely used material in all technologies due to its abundance and competitively outstanding properties. Metal–organic frameworks (MOFs) have been explored as the convenient and universal precursors for fabricating carbon composites with high specific surface areas, tunable and accessible nanopores, high degree of graphitization, and heteroatoms and/or metal-doping. Meanwhile, carbon-based materials with morphologies ranging from zero to three dimensions were also elaborately controlled to achieve better properties for electrochemical applications. Thus, it is important to elaborately design of MOF precursors to get novel porous carbon with desirable functionalities.

In this report, I will talk on the synthesis of MOF precursors with different composites and morphologies (Fig.1), as well as their derived porous carbon-based electrocatalyst for electrochemical applications. Core-shell structured MOF polyhedrons, tubular bimetallic MOFs, flake- or leaf-like bimetallic MOFs, MOF-based sandwich have been prepared as new precursors for synthesis of selectively functionalized porous carbon-based materials. Thanks to the adjustable dimensional,

structural, and compositional advantages of MOF-derived carbon, including the shorter pathways for mass transfer, accessible active sites, good electrical conductivity, the optimized MOF-derived carbon exhibit good performance in specific electrochemical applications. The relationships between the structural properties and electrochemical performances have been investigated carefully.

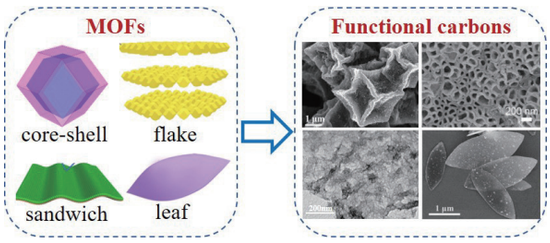

14:25-14:45

Non-Destructive Nanoscale 3D Characterization of Energy Materials

Stephen Kelly, Mansoureh Norouzi Rad, Robin White, Carl Zeiss Microscopy, LLC, Pleasanton, CA, USA; *Youli Hong*, Carl Zeiss Co, Ltd, Shanghai, China; Peter Attia, Jerry Liao, William Huang, Yi Cui, William Chueh, Stanford University, USA

While the discrete 3D microstructure of modern energy storage and conversion devices plays a critical role in device performance, capturing such features at appropriate length scales and with accessible imaging techniques has remained a challenge in the characterization and understanding of such heterogeneous materials. Image-based approaches provide not only an opportunity for direct insight into the complex structure and transport networks that exist, but also provide geometrical input to a host of performance models. Within this framework, non-destructive imaging becomes ideal because of the possibility to track the evolution of sample parameters (microstructure, chemistry, loads, etc) over several stages of processing or operational cycling and across multiple length scales. We present here results from non-destructive 3D imaging of two energy storage and conversion devices that provide valuable insight into the microstructural details that contribute to the device performance. Images were acquired via x-ray nano-CT in a laboratory instrument capable of resolving structures down to 50nm. First, we present an analysis on a Ni + ZrO_2:8%Y_2O_3 (8YSZ) / 8YSZ / $La_{1-x}Sr_xMnO_3$ (LSM) solid oxide fuel cell stack exposed to air to promote nickel oxidation. We analyze the pore and LSM size distribution in the cathode material, the connectivity of pores in the electrolyte layer, and plot the triple phase boundary in the anode. Second, we present results from imaging graphite Li-ion battery anodes after being subjected to extreme fast charging conditions. We observe a distinct surface layer in inactive portions of the anode via SEM, while x-ray nano-CT measurements show the surface layer extends ~10 µm into the electrode from the separator interface. These examples highlight the need for nanoscale 3D imaging in these materials, and the non-destructive nature of the approach opens the door to in situ or 4D measurements in the future.

14:45-15:05

Scale-Up Development of High-Performance Dielectric Films for Compact Capacitors

Daniel Tan, Guangdong Technion Israel Institute of Technology, China

Technology migration from research labs to commercial products has never been easy, which is especially true for transitioning a dielectric material to a compact capacitor that finds great promise in power electronics. This type of transition involves the development of high-performance materials and film processes as well as the scalability of films. The film scale-up processes along with the subsequent metallization and capacitor winding processes are crucial to the fabrication of a reliable capacitor component. A dozen programs were established in the past 10 years for addressing the polymer film requirements for high temperature, high energy density and compactness. Thickness is the third physical parameter in addition to the dielectric constant and the dielectric strength, that provides a satisfactory alternative pathway for the realization of a high-performance compact capacitor. It was found that every micron of film thickness reduction requires substantial technical efforts and cross-disciplinary coordination in the scale-up process. An overview of the developmental efforts on the dielectric materials and polymer films will be provided in this presentation. Several important attempts on scaling up dielectric films and capacitors recently supported by the US government and industry are described. The author' s scale-up efforts for high temperature polyetherimide films of various thicknesses via the melt extrusion process are illustrated. The successful demonstration of wrinkle-free PEI films in the thickness range of 4 to 10 microns in a commercial-scale is presented.

15:30-16:10 Tea Break

16:10-16:35 Invited

Towards Understanding the Influence of Re on H Dissolution and Retention in W by Investigating the Interaction between Dispersed/Aggregated-Re and H

Hongbo Zhou, Fangfei Ma, Fangya Yue, Yuhao Li, Guanghong Lu, Beihang University, China

Tungsten (W) and W alloys are considered as the most

promising candidates for plasma facing materials (PFMs) in future fusion reactors. Rhenium (Re) is not only the typical alloying element but also the main production of transmutation in W-PFMs. The microstructure and mechanical properties of W as well as the behaviors of impurities in W will be influenced by the presence of Re. The deuterium retention in damaged W-3%Re at 750K is two of magnitude lower than that in damaged Re-free W. Therefore, one can expect that Re should have significant effect on the behavior of H isotopes in W. However, little work has focused on this aspect so far.
Here, we have systematically investigated the effects of dispersed/aggregated Re on the behaviors of H in W as well as their interaction with point defects using a first-principles method in combination with thermodynamic models. It has been demonstrated that the influence of Re on H is strongly related to the distribution of Re in W. Re will aggregate and form clusters/ Re-rich precipitation phases under high energy ions/neutrons irradiation in W. The influence of Re clusters on H is extraordinary stronger than that of a single Re. The retention of H in W can be significantly suppressed by Re clusters, and their influences will be enhanced with the increasing of the number of Re atoms. On the contrary, it is found that the solution energy of H at most interstitial sites (> 80%) in W-Re sigma phase is much lower than that in pure W. Specifically, the H solution energy at most stable interstitial site in W-Re σ phase is only 0.47eV, ~ 54%lower than that in pure W. This can be attributed to that W-Re sigma phase provides the larger available volume for interstitial H than the pure W, weakening the W-H repulsive interaction. Consequently, our calculations reveal that the Re-rich precipitation can serve as the strong trapping centers for H in W, while dispersed-Re/small Re clusters can be used to suppress H retention. These results provide an important reference to evaluate the influence of Re and other alloying elements on the behaviors of H isotopes in W-PFMs under future fusion conditions.

16:35-16:55

The Recovery of Europium (II) Sulfate as Product of Recycling Waste Fluorescent Lamp Powder

Brajendra Mishra, Mark Strauss, Worcester Polytechnic Institute, United States

Europium is a required element for high technology application such as LEDs, cell phone screens, and laptop displays. The unique chemical properties of europium make it invaluable to these applications. This research shows a process to recovery europium (II) sulfate from waste lamp phosphors to create novel supply of europium. In this process, waste phosphor powder is chemically and physically beneficiated to produce yttrium and europium oxide concentrate. Next, europium (II) sulfate is separated from yttrium by selectively reducing Eu(III) to Eu(II) using zinc powder and precipitating it with sulfuric acid. Cursory experiments were performed to see the effect of pulp density, precipitation time, entrance pH, and stoichiometric ratio of europium to sulfate upon the grade and recovery of europium (II) sulfate. The ideal conditions to maximize grade and recovery of europium (II) sulfate were a 1 hour precipitation time, 10x the stoichiometric ratio of sulfate, 100g/L mixed REO, and the entrance pH equal to 3. The maximum grade of europium sulfate was 93%, and the maximum recovery was 78%. As a by-product of this separation process, yttrium is recovered by a precipitation step under controlled conditions of pH, temperature and organic to oxide ratio. Both Europium and Yttrium can be recycled into new phosphor production.

16:55-17:15

Thermoelectric Properties of Ag_8SiSe_6 Argyrodite Near Room Temperature Prepared with Different Quenching Conditions

Qinghui Jiang, Suwei Li, Junyou Yang, Jiwu Xin, Sihui Li, Huazhong University of Science and Technology, China; Haixue Yan, Queen Mary University of London, England

Argyrodite compounds, as promosing green thermoelectrics, received much attentations for their much low lattice themal conductivity which may be from low sound velocity, complex crystal structure, liquid-like ions, and lattice anharmonicity. There is a phase transition near 400K for Ag_8SiSe_6, a typical argyrodite compounds. At higher temperature, Ag_8SiSe_6 is face-center-cubic structure, where Ag^+ cations are fully disordered in $[SiSe_6]^{8-}$ anion sublattice which is composed of Se^{2-} anions and $[SiSe_4]^{4-}$ units. At lower temperature, Ag+ cations are localized partially, which leads to the decrease of the electrical conductivity and the increase of Seebeck coefficients. In this work, we first successfully fabricated Ag_8SiSe_6 alloys based thermoelectric bulks with high density (>95%). The processes include melting, annealing, milling and hot press sintering. We discussed the details of the effect of the parameters of these precesses on the phases and crystal structures. By controlling the cooling rates of the ingots, a remarkable improvement of power factor has been achieved in the sample quenched in water owing to the significant reduction in resistivity. In addition, a large amount of nano-precipitated particles and the

typical cladding structure confirmed by microstructure analysis may be responsible for the lower resistivity. The Seebeck coefficient, electric conductivity and thermal conductivity at different temperatures are also discussed in details. Its maximum ZT is over 0.7 near room temperature, which makes Ag-Si-Se alloys as a n-type thermoelectric material have a great commercial application instead of Bi_2Te_3 compounds in future.

17:15-17:35

Local Burnup Determination of Irradiated Fuel Using Atom Probe Tomography

Jian Gan, Mukesh Bahhav, Dennis Keiser, Jeffrey Giglio, Idaho National Laboratory, USA; Daniel Jadernas, Studsvik Nuclear AB, Nykoping, Sweden; Ann Leenaers, Sven Van de Berghe, SCK-CEN, Nuclear Materials Science Institute, Belgium

A novel approach is presented to determine the local U-235 burnup in irradiated fuels using isotopic quantification information obtained by Atom Probe Tomography (APT). Knowledge on burnup levels, composition along with distribution of isotopes and 3-D microstructural data of irradiated fuels is essential for nuclear fuel research and development. The microstructural evolution, radioactivity and the physical integrity of the irradiated fuel depend on burnup levels and thus its determination is critical to evaluate fuel performance. In this work, APT is used to quantify the isotopes of U-235, U-236, U-238, Pu-239 and Np-237 for burnup calculation in the irradiated U-7Mo dispersion fuel. This method provides local burnup analysis in the fraction of U-235 fissioned with unprecedented high spatial resolution based on isotopic ratios measured from as-received and irradiated fuels. APT analysis can also be applied to check uranium enrichment and its uniformity for fresh fuel for quality control of fuel fabrication, and the local fission product details in the irradiated fuel. This technique, combined with microstructural characterization using transmission electron microscopy, will help better correlating the local microstructural development with local burnup level. The capability of measuring local burnup is important for advanced characterization of irradiated fuels due to highly heterogeneous microstructure and technical challenges of in-pile irradiation test and post-irradiation examination of nuclear fuels.

N. Additive Manufacturing and Powder Metallurgy: Titanium & Titanium Alloy II

Symposium Organizers:

Huiping Tang, Northwest Institute for Nonferrous Metal Research, China; Yong Liu, Central South University, China; Yuichiro Koizumi, Osaka University, Japan; Kee-Ahn Lee, Inha University, Korea; Qian Ma, RMIT, Australia; Ed Herderick, Ohio State University, USA

Tuesday PM
August 20, 2019

Room: 402 (4th Floor)
Symposium: N

Chairs:
Xuezheng Yue, University of Shanghai for Science and Technology, China
Andrey Molotnikov, Monash University, Australia

13:30-13:55 Invited

Additive Manufactured TiTa Alloys for Biomedical Applications

Andrey Molotnikov, Monash University, Australia

Additive manufacture (AM) is emerging as a viable manufacturing method for creating bespoke implants. However, the majority of additively manufactured implants on the market are still made out of Ti-6Al-4V; an alloy which has not been designed for implant use and possesses drawbacks of containing toxic elements and much higher elastic modulus than bone. One promising alternative is β-titanium alloys, which can offer low elastic modulus (~ 40MPa) and high cycle fatigue strength (~800MPa).
In this work, fabrication of multiple compositions of TiTa alloys using selective laser melting (SLM) is reported. Tantalum is selected as not only a favourable β stabiliser, but also due to its promising biocompatibility and promotion of osseointegration for use in the orthopaedics applications. The optimisation of processing parameters to produce fully dense samples with a minimised volume fraction of unmelted Ta particles is discussed. The morphology of the resulting microstructures was analysed with scanning electron microscopy (SEM) and phase identification supported with x-ray diffraction (XRD) analysis. The material was then assessed for mechanical properties and microstructure, showing similar strength to SLM titanium with half the elastic modulus and an altered microstructure caused by the 'remelt' scanning strategy. The relationship between composition, microstructure and mechanical response of the TiTa alloy system will be elaborated.

13:55-14:15

Potential of Hydrogenated Powders for Manufacturing of Multicomponent Titanium Alloys by Blended Elemental Powder Metallurgy

Orest Ivasishin, G.V.Kurdyumov Institute for Metal Physics, Ukraine / Jilin University, China; Dmytro Savvakin, G.V.Kurdyumov Institute for Metal Physics, Ukraine; Yuanyuan Lee, Jilin University, China

The advanced approach based on using hydrogenated titanium as starting material has been earlier developed for blended elemental powder metallurgy (BEPM) processing of Ti-based alloys. In this approach hydrogen acts as temporary alloying addition for titanium, which activates chemical homogenization and sintering of powder blends, refines titanium powders from surface impurities and therefore, results in improved mechanical properties of sintered alloys. However, while BEPM processing multicomponent Ti-Zr-Nb and Ti-Zr-Nb-Ta (intended mainly for medical applications) even employment of hydrogenated titanium does not enable to achieve desirable microstructure and properties of the sintered materials because of low diffusivity of alloying elements. Generally, these alloys need post sintering thermomechanical treatment (HIP as an option) to minimize the porosity, unfortunately inevitable even after high temperature/long time sintering what certainly increases the cost of their BEPM processing.
In present study potential of various hydrogenated powders (zirconium hydride, hydrogenated tantalum and niobium, hydrogenated master alloys) was investigated to improve the BEMP processing of Ti-Zr-Nb and Ti-Zr-Nb-Ta alloys. Phase and structural transformations upon heating in vacuum of powder blends of several hydrogen containing constituents was analysed and their influence on mechanical characteristics of sintered products was established. It was shown that with proper selection of hydrogenated powders and optimization of processing parameters modified BEPM alloys reach the property level sufficient for medical applications without the post sintering treatment.

14:15-14:35

Numerical Simulation in the Absorption Behavior of Ti6Al4V Powder Materials to Laser Energy during Selective Laser Melting

Dongyun Zhang, Junyuan Deng, Long Zhang, Tai Zhang, Tingting Huang, Laser Engineering Research Institute of Beijing University of Technology, China

In the paper, the effects of porosities and average particle sizes of powder layer on light absorption during Selective Laser Melting process were investigated, in which closed-packing models based on Horsfieled's filling method were established and light absorption was simulated using ray tracing based on laser-material interaction mechanism. Corresponding to closed-packing models, the powder materials were prepared for absorption measurement using integrating sphere. The experimental results of light absorption verify the feasibility of the establishment of closed-packing models, the accuracy in calculation in the light absorption. The results show that the absorption of powder layer of Ti6Al4V alloy is higher than 70%. The decrease of porosity of powder layer benefits to improve the absorption, while the absorption tends to decrease if porosity decreases to a certain value due to the reflection. The decrease of average particle size of powder particles benefits also to improve the absorption. If the light irradiates at positions with different particle arrangements, the absorption behavior changes with irradiation condition whether there occurs the multi-reflection. As a conclusion, the above research provides theoretical basis for preparation of new powder materials, their parameter developing for SLM technology and even the properties regulation of Selective Laser Melting fabricated component.

14:35-14:55

Effect of Trace LaB_6 Additions on the Microstructure and Mechanical Properties of Ti-6Al-4V Manufactured by Electron Beam Melting

Min Liu, Chao Chen, Kecha Zhou, Powder Metallurgy Research Institute of Central South University, China

Ti-6Al-4V component modified by TiB and La_2O_3 particles was synthesized in electron beam melting (EBM) based on the reaction between Ti, LaB_6, and oxygen in the raw material. It was demonstrated that the added LaB_6 played significant roles on the microstructure and mechanical properties in the EBM fabricated Ti-6Al-4V alloys. Because of the cooling gradient parallel to the build direction, columnar prior β grains tended to grow along the build direction (preferred orientation) in both Ti-6Al-4V and Ti-6Al-4V-LaB_6 samples during the EBM processing. The acicular α' martensite and acicular α phase were obtained within prior β grains in as-built Ti-6Al-4V alloys, while with trace addition of LaB_6, the morphology of the Ti-6Al-4V-LaB6 were almost ultrafine lamellar (α+β) structures rather than α' martensite. The addition of LaB6 provided a high level of heterogenous nucleation sites for solidification and α phase formation. The width of columnar grains decreased significantly with LaB_6 additions. The texture intensity of α and β phase was reduced with the addition of LaB_6 in the EBM processed Ti-6Al-4V. Consequently, excellent tensile strength with considerable elongation were achieved in the EBM processed LaB6-Ti–6Al–4V, compared to the unmodified Ti-6Al-4V counterpart, due to the refined columnar prior-β grains and lamellar α laths.

14:55-15:15

Sintering of Titanium Alloys from the Core-Shell Structured Titanium@ Metal Powders

Yafeng Yang, Institute of Process Engineering, China

The conventional cold-compaction-and-sinter powder metallurgy (PM) approach is technically the simplest and economically the most attractive near-net shape manufacturing process, which allows making Ti with a poor machinability into complex parts at an affordable price. How to obtain the high sintering density and homogeneous microstructure has been the key issue of making high-performance titanium alloys by powder metallurgy technology. The traditional approach to making powder mixtures by mechanical blending hardly avoid the powder aggregation, which is thus one of the major reasons to produce these issues. In order to overcome these problems, a novel powder surface manipulation approach was developed to make the special multi-component composite powders with a core-shell structure through the fluidized bed chemical vapor deposition. A series of Ti-based multi-component core-shell powders, including Ti@Ni, Ti@Ni-B, Ti@Co, Ti@Co-B and Ti@Fe, have been successfully fabricated according to the designed compositions of titanium alloys. After the conventional sintering, a largely enhanced sintered densification was obtained while a homogenous microstructure was achieved. As a result, the sintered titanium alloys exhibited the superior mechanical properties compared with the traditional blended powder mixtures. This study will give a detailed discussion about the thermodynamic feasibility, processing parameter, the characterization of these core-shell powders and their sintering responses. This approach also provided popular additive manufacturing with some new inspiration of designing special functional powders that are not easily obtained by traditional approach.

15:15-15:35

Effect of Reducing Agents on the Direct Reduction of Titanium Dioxide during Combustion Synthesis of Titanium

Sang Hoon Choi, Korea Institute of Industrial Technology / In-Ha University, Korea; Jae Jin Sim, Jae Hong Lim, Kyoung-Tae Park, Korea Institute of Industrial Technology, Korea; Soong-Keun Hyun, In-Ha University, Korea

Commercially, gas atomization and hydrogenation-dehydrogenation processes are used to produce titanium powder from titanium ingot or titanium sponge. Titanium sponge is produced with Kroll process. Although Kroll process has advantages of mass production and high recovery of titanium, has bad impact on environment due to chlorination and it is complicated too. A quest to search for alternate ways of producing titanium is being researched actively. In this work, combustion synthesis (CS) route to produce titanium powder under direct reduction of titanium dioxide was adopted. Titanium dioxide was used as a raw material varying magnesium, calcium and aluminum as reducing agents. Comparison was drawn among combustion temperature (Tc), and the combustion velocity (Uc) for every reducing agent mixture with titanium dioxide by varying their molar ratios. It was found out that combustion temperature and combustion velocity decreased with the increase in molar ratio of reducing agents. By-products such as magnesium oxide, calcium oxide and aluminum oxide were removed by acid leaching under different leaching conditions. After leaching, the recovered titanium powder was collected, washed and dried. Detailed compositional analysis indicated that the final product satisfies the ASTM B299. In addition, structural and morphological characterization of obtained Ti powder was performed after each processing step, and the results were compared.

15:35-16:10 Tea Break

16:10-16:35 Invited

Controlling Microstructure In-Situ in Additively Manufactured Ti-6Al-4V by Selective Laser Melting

Wei Xu, Deakin University / RMIT University, Australia; Qi Chao, Francesco Ciaglia, Deakin University, Australia; Ma Qian, Milan Brandt, RMIT University, Australia

Achieving consistent mechanical performance is essential for the wider implementation of metal additive manufacturing (AM) but this remains far beyond the reach of current practice of selective laser melting (SLM). As the premier titanium alloy, Ti-6Al-4V made by SLM is strong but suffers from inconsistent anisotropic mechanical behavior as well as inferior ductility and fracture toughness. For instance, SLM Ti-6Al-4V can achieve yield strength over 1200MPa in the as-built state but has noticeably lower tensile ductility (< 10%), inferior fracture toughness and poor fatigue performance. More critically, mechanical properties attained in SLM Ti-6Al-4V are highly scattered, leading to greater uncertainty about the reliability of SLM parts. This lack of consistency is the most significant barrier to the adoption of SLM Ti-6Al-4V for fracture-critical structures.

Factors responsible for inconsistent properties include porosity, undesired microstructure and harmful residual stress. Porosity is a common defect that exists ubiquitously in SLM Ti-6Al-4V and adversely affects mechanical properties. With an optimized SLM process, porosity can be reduced to below 1% so that its negative

effect on mechanical properties is minimised. Compared to porosity, controlling microstructure is challenging due to complex thermal histories associated with the highly localised dynamic laser-powder interaction that involves simultaneous melting/solidification of the topmost powder layer and remelting/heat treatment of the underlying layers. Under such circumstance, the resulting microstructures are non-equilibrium and contain acicular alpha' martensites in columnar prior-beta grains. This kind of microstructure is problematic as it lacks capacity to sustain large deformation and exhibits strong anisotropy in mechanical properties. The propensity for brittleness and anisotropy is a major contributor to the inconsistent mechanical performance. This study has addressed this intractable challenge by developing a holistic thermal and microstructural control approach that allows the direct SLM manufacture of isotropic stress-relieved Ti-6Al-4V literally with minimal necessary post heat treatment. This newly developed approach leads to three in-situ transitions: transformation from columnar prior-beta grain structure to equiaxed, conversion of alpha' martensite into lamellar alpha+beta and simultaneous relief of residual stress.

16:35-16:55

Influence of Post-Sintering Thermomechanical Treatment on Microstructure and Properties of Ti-Zr-Nb Alloys Produced with Blended Elemental Powder Metallurgy

Orest Ivasishin, G.V.Kurdyumov Institute for Metal Physics, Ukraine/ Jilin University, China; Dmytro Savvakin, Denys Oryshych, G.V.Kurdyumov Institute for Metal Physics, Ukraine; Liang Chen, Elena Pereloma, University of Wollongong, Australia

Biocompatible low-modulus alloys of Ti-Zr-Nb system are attractive materials for medical applications. In the present study, two selected beta (body centred cubic (BCC)) phase alloys 55.5Ti-26Zr-18.5Nb and 29.5Ti-52Zr-18.5Nb, at.% which are promising candidates for medical implant production were synthesized by press-and-sinter blended elemental powder metallurgy (BEPM). The advanced manufacturing approach earlier developed for titanium alloys and based on using hydrogenated titanium as starting material was used in this project. In this approach, hydrogen acts as temporary alloying addition for titanium, which activates chemical homogenization and sintering of powder blends, refines titanium powders from surface impurities and therefore, results in improved mechanical properties of sintered alloys. However, even employment of hydrogenated titanium and hydrogenated zirconium powders in BEPM processing of multicomponent Ti-Zr-Nb alloys does not enable achieving the desirable microstructure and properties of these sintered materials. Generally, these alloys need post-sintering thermomechanical treatment to minimize the porosity. This is unfortunately inevitable even after high temperature/long time sintering, which results in the increased cost of the BEPM. Thus, the aim of this research was to apply thermomechanical post-processing to achieve the mechanical characteristics satisfying requirements for medical implant materials. The hot deformation behavior of Ti-Zr-Nb sintered alloys was studied using Gleeble 3500 thermo-mechanical simulator. The effects of deformation temperature and strain on reduction of residual porosity and microstructure were evaluated to improve mechanical characteristics. The influence of hot deformation regimes on microstructure peculiarities, hardness and tensile properties of sintered Ti-Zr-Nb alloys were determined and discussed.

16:55-17:15

Microstructural Characteristics of Electron Beam Melted Ti-6Al-4V Alloy

Nima Haghdadi, Ryan DeMott, Sophie Primig, UNSW Sydney, Australia; Simon Ringer, The University of Sydney, Australia

Additive manufacturing through Electron Beam Melting (EBM) is one of the promising methods to build final shape metallic products directly from computer-aided design. EBM usually produces a complex thermal history, with extreme temperature gradients that is expected to result in a graded microstructure. Multi-phase materials that go through phase transformations during heating/cooling cycles, such as Ti-6Al-4V, can have particularly complex microstructures. In the current work, the microstructure of a Ti–6Al–4V alloy manufactured by EBM has been studied. Three different electron beam scan paths were applied. It was found that the scan path has a profound impact on the general characteristics of the microstructure. Furthermore, a detailed EBSD analysis showed that microstructural characteristics such as alpha phase morphology, alpha variant selection as well as retained and prior beta orientation and morphology were highly varied across the height in each build. This was mainly arising from the change in the cooling rate. This study is a preliminary step towards understanding the complex relationship between the thermal history and microstructural properties of electron beam melted Ti-6Al-4V alloy.

17:15-17:35

Cost-Affordable Ti Powders for Additive Manufacturing Treated by Fluidized Bed

Gang Chen, Wangwang Ding, Qiying Tao, Mingli Qin, Xuanhui Qu, University of Science and Technology Beijing, China; Wei Cai, Stanford University, USA

HDH Ti powders were modified by fluidized bed. The properties and microstructures of the as-treated

Ti powders were investigated in terms of surface morphology, particle size distribution, flowability, oxygen level and surface oxidation behavior. The results showed that the modified particle size and morphology benefit its flowability after treatment. The Ti powders exhibit negligible oxygen increment after being treated at 450℃, while its flowability is effectively improved. The as-treated Ti powders were inspected by selective laser melting. The microstructure and mechanical properties of the as-built Ti components were also investigated. This study offers a promising approach to provide cost-affordable Ti powders for additive manufacturing.

O. Electronic and Spin Electronic Materials: III

Symposium Organizers :

Hongda Chen, Institute of Semiconductors, Chinese Academy of Sciences,China; Feng Pan, Tsinghua University, China; Rie Y. Umetsu(Ms.), Tohoku University, Japan; Joonyeon Chang, Korea Institute of Science and Technology (KIST), Korea; Lianzhou Wang, University of Queensland, Australia

Tuesday PM
August 20, 2019

Room: 312 (3rd Floor)
Symposium: O

Chairs:
Hongda Chen, Institute of Semiconductors, Chinese Academy of Sciences, China
Feng Pan, Tsinghua University, China
Rie Y. Umetsu, Tohoku University, Japan
Joonyeon Chang, Korea Institute of Science and Technology, Korea
Lianzhou Wang, The University of Queensland, Austraila

13:30-14:00 Keynote

Nickel-Iron Based Catalysts for Water Electrolysis

Chuan Zhao, University of New South Wales, Australia

The increasing demands for clean energy have triggered tremendous research interests on electrochemical energy conversion and storage systems with minimum environmental impact. Electrolytic water splitting holds the promise for global scale storage of renewable energy, e.g., solar and wind in the form of hydrogen fuel, enabling the continuous usage of these diffusive and intermittent energy sources when used together with fuel cells. Nevertheless, the widespread application of water splitting technology has been severely constrained by the use of precious metal catalysts, such as oxides of ruthenium and iridium for the anodic oxygen evolution reaction (OER), and platinum for the cathodic hydrogen evolution reaction (HER).

This presentation concerns our recent progress in developing low cost, Ni and Fe-based water splitting catalysts for OER and HER, as well as our strategies for enhancing the efficiency of these catalysts by nanostructuring to a level comparable to that of precious metal catalysts. The commercialisation of some our catalysts in water electrolysis industry also will be discussed.

14:00-14:25 Invited

Optoelectronic Characterisation of III-V Semiconductor Nanowire Structures and Devices

Ziyuan Li, The Australian National University, Australia

With excellent optical and electrical properties such as direct bandgap, large absorption coefficient and charge-carrier mobility, compound semiconductor nanowires (NWs) have shown great promises for electronic, optoelectronic and photovoltaic device applications. Nanowires can be fabricated by a variety of crystal growth techniques, among which the selective area epitaxy (SAE) growth has the advantages of accurate control of the position, geometry, uniformity and doping of NWs to achieve excellent and reproducible device performances. In this talk, we demonstrate the growth of high quality, stacking-fault-free and taper-free InP nanowires using selective-area metal-organic chemical vapour deposition (SA-MOCVD), as well as design, fabrication and characterization of a series of nanowire structures for optoelectronic device applications, including infrared photodetectors, THz detectors, solar cells and LEDs etc. With excellent optical and electrical properties such as direct bandgap, large absorption coefficient and charge-carrier mobility, compound semiconductor nanowires (NWs) have shown great promises for electronic, optoelectronic and photovoltaic device applications. Nanowires can be fabricated by a variety of crystal growth techniques, among which the selective area epitaxy (SAE) growth has the advantages of accurate control of the position, geometry, uniformity and doping of NWs to achieve excellent and reproducible device performances. In this talk, we demonstrate the growth of high quality, stacking-fault-free and taper-free InP nanowires using selective-area metal-organic chemical vapour deposition (SA-MOCVD), as well as design, fabrication and characterization of a series of nanowire structures for optoelectronic device applications, including infrared photodetectors, THz detectors, solar cells and LEDs etc. We show that while III-V semiconductor nanowires offer great potentials for optoelectronic device applications, in-depth understanding and optimisation of nanowire growth, structural, optical and electrical properties through combined simulation and nanocharactersation techniques are essential for achieving high performance nanowire optoelectronic devices.

14:25-14:45

Performance-Enhancing Selector via Symmetrical Multilayer Design

Yiming Sun, Jun Yin, Cheng Song, Fei Zeng, Feng Pan, Tsinghua University, China

Two-terminal selectors with high nonlinearity, based on bidirectional threshold switching behaviors, are considered as a crucial element of crossbar integration for emerging nonvolatile memory and neuromorphic network. Although great efforts have been made to obtain various selectors, existing selectors cannot fully satisfy the rigorous standard of assorted memristive elements and it is in great demand to enhance the performance. Here, a new type of Ag/TaOx/TaOy/TaOx/Ag (x < y) selector based on homogeneous trilayered oxides is developed to attain the required parameters including bidirectional threshold switching operation, a large selectivity of ≈1010, a high compliance current up to 1mA, and ultralow switching voltages under 0.2V. Tunable operation voltages can be realized by modulating the thickness of inserted oxygen-rich layer TaOy. All-TaOx-based integrated 1S1R cells, prepared completely by magnetron sputtering and no need of a middle electrode, exhibit a nonlinear feature, which is quite characteristic for the crossbar devices, avoiding undesired crosstalk current issues. The tantalum oxide based homojunctions offer high insulation, low ion mobility, and rich interfaces, which is responsible for the modulation of Ag conductive flaments and corresponding high-performance cation-based selector. These findings might advance practical implementation of two-terminal selectors in emerging memories, especially resistive random access memories.

14:45-15:05

Electric Field Control of Phase Transition and Tunable Resistive Switching in SrFeO2.5

Muhammad shahrukh Saleem, Tsinghua University, China

Complex oxides possess widely tunable oxygen stoichiometry that can host a variety of phases. For example, SrFeOx (SFOx) compound exhibits ionic conduction and oxygen-related phase transformation, having potential applications in solid-oxide fuel cells, smart windows, and memristive devices. The phase transformation in SFOx typically requires thermal annealing process under various pressure conditions, hindering their practical applications. Here we have achieved a reversible phase transition from brownmillerite (BM) to perovskite (PV) in SrFeO2.5 (SFO2.5) film through ionic liquid (IL) gating. The real-time phase transformation is imaged using in-situ high resolution transmission electron microscopy. The magnetic transition in SFO2.5 is identified by fabricating an assisted La0.7Sr0.3MnO3 (LSMO) bottom layer. The IL gating converted PV phase of SrFeO3-δ (SFO3-δ) layer shows a ferromagnetic-like behavior but applies a huge pinning effect on LSMO magnetic moments, which consequently leads to a prominent exchange bias phenomenon, suggesting an uncompensated helical magnetic structure of SFO3-δ. Whereas the suppression of both magnetic and exchange coupling signals for BM phased SFO2.5 layer elucidates its fully compensated G-type antiferromagnetic nature. We also demonstrated that the phase transition by IL gating is an effective pathway to tune the resistive switching (RS) parameters, such as set, reset and high/low-resistance ratio in SFO2.5-based resistive random access memory devices.

15:05-15:25

Effect of Cr Doping on Electronic and Magnetic Properties of Inverse Heusler Alloy Mn2CoGa

Gopi Chandra Kaphle, Sashi Nepal, Tribhuvan University, Nepal; Rambabu Roy, Hydra Research and Policy Center, Nepal

Heusler compounds have been found to exhibit interesting electronic properties and wide range of magnetic behavior. Many of Heusler compounds have been found to be half-metallic. In this work, we studied the electronic and magnetic properties of inverse Heusler alloy Mn2 CoGa and the effect induced by doping Cr on those properties. We used plane wave pseudo-potential method withing DFT framework implemented using Quantum ESPRESSO code. The calculation shows that Mn2CoGa exhibit weak half-metallicity as indicated by availability of tiny amount of states at fermi level below a gap for spin-down electrons. The calculated total magnetic moment is 2.01μB /cell which is very close to integral value and thus found to obey established Slater Pauling rule M = NV − 24 for inverse Heusler compounds. We performed doping at two different concentration. The empirical rule for atomic occupation established for Heusler alloys says that Cr will occupy D site, but Cr does not follow usual occupation rule and actually occupies A site. At 25% Cr concentration, calculation shows Mn2CoCr0.25Ga0.75 is a perfect half-metal with typical metallic behavior for spin-up electrons, but semi-conducting behavior with a gap at fermi level for spin-down electrons. This indicates we can have 100% spin polarization at fermi level. The calculated magnetic moment is 11.0μB /cell. Furthermore the calculation at 50% Cr concentration shows that majority of the channel in DOS still shows metallic nature where as electrons fermi level for the minority channel is slightly shifted into conduction band indicating the loss of half-metallicity.

15:30-16:10 Tea Break

16:10-16:40 Keynote

Fabricating Inorganic Materials with Structural Control

Rachel Caruso, RMIT University, Australia

Targeted enhancement of materials properties can lead to improved performance of the materials applied in a range of energy and environmental applications. Key materials properties, such as structure and composition, can be controlled during the synthesis process. We have applied hydrothermal/solvothermal processes, self-assembled and preformed templates and electrospinning approaches to vary the morphological features of inorganic materials, generally metal oxides. This results in variation of crystal size, pore size and overall structure as observed using X-ray diffraction, electron microscopy and gas sorption techniques.
For the application of such porous structures and films we have looked at energy conversion with studies on both dye-sensitized and perovskite solar cells, energy storage (lithium ion batteries), photocatalytic degradation of aqueous pollutants and adsorption of heavy metal ions. When considering these applications, the characteristics for enhancing the performancee of the materials specific to that application become important. For example, the total surface area of the materials and the pore size are important if reactions are taking place at the surface and diffusion to and from the active sites are important. An ability to manipulate light to enhance absorbance is key in photovoltaic and photocatalytic studies. The synthesis, characteristics and application of porous materials will be discussed in this presentation.

16:40-17:00

Structural Properties Optimization of Coal-Based Electrode Materials

Ting Su, Yonghui Song, Xinzhe Lan, Xi'an University of Architecture and Technology, China

The coal-based electrode materials were prepared from low rank pulverized coal (SJC) and coal direct liquefaction residuals (DCLR), the surface structure and properties of coal-based electrode materials were optimized by KOH activation of conventional pyrolysis, and the coal-based electrode materials have been applied to the treatment of cyanide wastewater by electrosorption. The surface morphology, composition and structure of coal-based electrode materials were characterized by SEM-EDS, FT-IR, XRD analysis. Conventional pyrolysis and KOH-HNO_3 activation experiments showed that the addition of KOH solution impregnation could effectively reduce the addition amount of KOH and improved its surface structure and composition under the premise of ensuring its compressive strength. The addition of KOH could improve the sensitivity of materials to temperature, promoted CO, inhibited the production of CH_4, and greatly improved the microporosity of coal-based electrode materials. When the addition of KOH was 20%, the micropore rate of coal-based electrode material reached 79.15%, the specific surface area was 452.08m^2/g, and the pore size distribution was mainly 1.5nm. At this time, the compressive strength was 2.75MPa, and the maximum adsorption value reached 835.16mg/g. The materials enjoy double-layer capacitance and good conductivity, and the minimum internal resistance is 0.8341Ω. Temperature was the key factor for the formation of micropores. The higher the temperature, the greater the micropore rate, but when the temperature rises to 800℃, the efficiency of the increase of micropore rate decreased. At high temperature, KOH promoted the development of micropores in the coal matrix intercalation in the form of K, and at 600~800℃, the accumulation of micropores increased at 0.65nm and 1.48nm, and the minimum pore size reached 0.25nm. At the same time, the addition of KOH lead to the increase of disorder in the microstructure of the material.

17:00-17:20

3D Atomic-Scale Insights into Advanced Materials

Rongkun Zheng, The University of Sydney, Australia

Atom Probe tomography have been applied to solve the critical questions in semiconductor and superconductor materials. We have demonstrated that, in the analysis of semiconductor nanowires epitaxially grown from a substrate, the presence of the flat substrate positioned only micrometers away from the analyzed tip apex alters the field distribution and ion trajectories, which provides extra image compression that allows for the analysis of the entire specimen. In InGaAs nanowires, we have revealed and explained: (i) Ga-rich core and In-rich shell structure was grown via different mechanisms; (ii) the decomposition rate of the group III precursors determines the In/Ga ratio in the core; (iii) The dimension of core increases from 45 to 65nm and the shape of the core changes from a hexagon to a rounded triangle from the top to the base of the nanowire; (iv) The In/Ga ratio and inhomogeneous distributions of group III atoms in the {112}. In order to unravel the magnetism of Co doped ZnO films, we have performed rigorous experiments on Co doped ZnO grown on α-Al_2O_3 and O-polar ZnO (0001) substrates. In both cases, atom probe tomography confirms a random distribution of Co ion even at the interface region. In the ZnO:Co on α-Al_2O_3 substrate, the interaction between high density of threading dislocation, dopants, native point defects holds the key to understand the hitherto puzzling ferromagnetism observed in wide variety of doped and undoped semiconductors. However, in the ZnO on the O-polar ZnO (0001) substrate, hydrogen plays a key

role in mediating magnetic ordering. Local fluctuations in the distribution of dopant atoms are thought to cause the nanoscale electronic disorder or phase separation in pnictide superconductors. Atom probe tomography has enabled the first direct observations of dopant species clustering in a K-doped 122-phase pnictide. First-principles calculations suggest the coexistence of static magnetism and superconductivity on a lattice parameter length scale over a wide range of dopant concentrations. Our results provide evidence for a mixed scenario of phase coexistence and phase separation, depending on local dopant atom distributions.

P. Dynamic Behaviour of Materials: II

Symposium Organizers :

Marc Andre Meyers, University of California, USA; Na Yan, Northwestern Polytechnical University, China

Tuesday PM
August 20, 2019

Room: VIP (1st Floor)
Symposium: P

Chairs:
Bingfeng Wang, Central South University, China
Pengfei Wang, University of Science and Technology of China, China

13:30-14:00 Keynote

Impact Resistant Natural Polymer Composites: Hooves and Horns

Wei Huang, Nicholas A. Yaraghi, David Kisailus, University of California, San Diego, USA; Alireza Zaheri, Horacio Espinosa, University of California, Riverside, USA; Wen Yang, Jae-Young Jung, Joanna McKittrick, Northwestern University, USA; Zezhou Li, Robert O. Ritchie, University of California, Berkeley, USA; Susan M. Stover, University of California, Davis, USA

Keratin is one of the most common natural structural biopolymers with remarkable mechanical properties that generate different functionalities in natural materials, such as in offensive weapons in sheep horns, defensive armor in pangolin scales and turtle shells, protective and energy absorptive layers in animal hooves and as environmental barriers in bird feathers and animal hairs. Energy absorption is one of the most important properties of keratin in tissues under extreme loadings. Although solely composed of polymer constitutes, keratin is one of the toughest natural materials. The toughness of keratin is greater than bone and wood, which are considered structural biological materials with desirable mechanical efficiencies. Bighorn sheep fight with each other, reaching speeds of ~9m/s with a deceleration of ~450g, which creates large amounts of impact energy. An unshod horse trotting at ~4m/s on an asphalt surface has a deceleration ~56g. Although sustaining less impact than horns, the high frequency of the contact with the surfaces also requires excellent energy absorption properties. Here we report on the structure and compressive static and dynamic mechanical properties of sheep horns and equine hooves samples oriented in different directions. High-resolution synchrotron x-ray micro-computed tomography and transmission electron microscopy, coupled optical and scanning electron microscopy were used to characterize the pristine and deformed samples. The major microstructural elements are tubules and cell lamellae. The lamellae consist of keratin cells, with a disc-shaped morphology, with an average thickness of ~2μm and diameter of ~20~30μm. The cells contain macrofibrils (~200nm diameter) composed of intermediate filaments (~12nm diameter), parallel to the cell surface. Samples subjected to high strain rate Hopkinson bar experiments showed energy-absorption mechanisms such as shear banding, lamellae buckling and delamination. We believe that our findings will provide inspiration for bioinspired designs of energy-absorbent synthetic structures and materials. This work is funded by a Multi-University Research Initiative through the Air Force Office of Scientific Research (AFOSR-FA9550-15-1-0009) and a National Science Foundation Biomaterials Grant (1507978).

14:00-14:25 Invited

Shear Localization and Microstructural Evolution in Dynamic Deformation Process

Na Yan, Northwestern Polytechnical University, China

Shear localization is a general failure mechanism of structural materials when subjected to dynamic loading. It occurs when thermal softening suppresses the strain-hardening and strain-rate hardening effect. The microstructure of the shear bands is modified significantly due to drastic thermal excursion and severe plastic deformation. Due to the excellent strain hardening of FCC alloys, special attention is paid to the dynamic behaviour of fcc Al0.3CoCrFeNi and CrMnFeCoNi high-entropy alloys (HEAs). These two kinds of single phase high-entropy alloys were subjected to dynamic impact to examine their dynamic properties, such as strength, and deformation mechanisms, especially focusing on shear localization.The dynamic behavior of single phase HEAs was investigated using a combination of Hopkinson bar experiments and hat-shaped specimens. The strain-hardening rate of FCC Al0.3CrFeCoNi HEA is significantly higher (above 1000MPa) than a coarse-grained pure Al and is retained in the dynamic regime. The combination of multiple strengthening mechanisms such as solid-solution hardening, forest dislocation hardening, as well as mechanical twinning leads to an excellent work-hardening rate in this alloy, which is significantly larger than that for pure aluminum. The

resistance to shear localization of this alloy was studied by dynamically-loading hat-shaped specimens to induce forced shear localization. However, no adiabatic shear band could be observed at a shear strain ~1.1. The formation of profuse mechanical twins near the inserted tip in the hat-shaped specimen indicates twinning-induced continuous strain-hardening, which suppresses shear localization in competition with the thermal softening effect. For CrMnFeCoNi HEA, only the specimen with a high shear strain of ~7 develops a shear band. The temperature inside the shear band can rise to the recrystallization temperature (~0.4 Tmelting), ~1550K. The formation of a narrow shear band is found with a width only about 10μm and nanostructured grains (100~300nm) inside the shear band. The elongated ultrafine-grained grains are proposed to be the first stage of severe shear deformation. Then, they break up into small ultrafine-grained grains and rotate to the equiaxed configuration according to the classical rotational dynamic recrystallization mechanism.

14:25-14:50 Invited

Investigation on the Adiabatic Shear Behavior of Heat-Treated Ti-6Al-4V Alloy under Different Strain Rates

Chunhuan Guo, Harbin Engineering University, China

Recently, the metal-intermetallic laminate (MIL) composite Ti/Al3Ti consisting of ductile metal (Ti-6Al-4V) and brittle intermetallic (Al_3Ti) is considered as a potential candidate in aerospace engineering and lightweight structural armor plating and has been widely researched and applied in recent years because of their low density, high strength, high stiffness and high modulus. As a new structural material, the mechanical response, fracture behavior, damage evolution, etc. have been investigated until now. However, many investigations are focused on the entirely deformed behavior except the unit of MIL composite, for example the behavior of ductile metal (Ti-6Al-4V). In order to understand the mechanical behavior of Ti/Al3Ti MIL composite and to supply essential material model used in finite element method, it is very significant to obtain the mechanical properties of ductile and brittle phases in MIL composite. Therefore, it is necessary to test the mechanical properties of each phase (Al_3Ti and Ti-6Al-4V). In this way, we test the mechanical behavior of Ti-6Al-V alloy under different loading condition using Instron testing machine and Hopkinson bar, which have the same heat treatment as the preparation process for MIL composite. The experimental results show that the occurrence of the serrated deformations is accompanied by the generation of adiabatic shear bands. The adiabatic shear effective became obviously with increasing strain rate. When the strain rate was higher than 1100/s, the compressive specimen was fractured along with 45 degree direction. For the fractured specimen, the adiabatic shear can be observed using the fracture. According to the SEM observation, the width of the adiabatic shear band has a linear relationship with the strain rate in a certain range. Based on the above results, the constitutive equation of heated Ti-6Al-4V alloy is obtained by the Johnson-Cook model, which can be used in the numerical simulations of MIL composite. The results attained in this work can help us to understand the deformation behavior and mechanism of MIL composite.

14:50-15:10

Elastoplasticity Properties of Alpha Keratin Bovine Hooves

Bingqian Zhou, Central South University, China

School of Materials Science and Engineering, Central South University, Changsha Bovine hoof with alpha keratin structure, as a biological structural material, has high toughness among the natural biological materials. As the interface between the ground and the skeleton, bovine hooves play an important role in preventing bony skeleton from impact and destroy, accounting for its structure and composition that can disperse pressure and reorient the crack propagation. Although, when comparing to metallic material, its physical properties such as stiffness, toughness and strength may not be outstanding, the low density and light weigh allow them to obtain some high specific applications. In order to find a way to understand the essence of bovine hooves and except to use feasible method and materials to achieve bionics, we choose bovine hooves to research mechanical properties and micro-structure evolution under the fracture experiments. We use an engineering fracture mechanical method to research the fracture toughness of bovine hoof, and apply the J-integral and Wei-bull distribution analysis methods to evaluate the fracture toughness, and also investigate microstructure of the bovine hoof by transmitted electron microscope and nanoindentation. Results show that it always reaches the peak values at 17wt% moisture content, and the mean Intergalactic of longitude orientation along the growth lines are higher than transverse orientation normal to the growth lines, and the longitude specimens are trended to crack redirect. On a more micro scale, the toughness of bovine hoof depends on many parameters, such as the volume fraction and orientation of the intermediate filaments (IFs), and the interface structures between inter-tubular materials and tubules are also thought to be of paramount importance. The IFs arrangement vary from about 0° to 90° against to tubule axis but not uniform distribution. This results in the different fracture characteristics of different layers of bovine hoof wall form inner toward to outer. Furtherly, we put forward a hypothetical mode to explain the structure of the alpha keratin bovine hoof. The fracture induced laminated keratinous structure could form extensive strain-transition interfaces and tubules play an important

role in re-orientating cracks propagation, which could absorb crack energy and make crack blunt.

15:10-15:30

Effects of Strain Rate on Mechanical Properties of FeCoNiCrAl0.1 High Entropy Alloy

Kun Jiang, Northwestern Polytechnical University, China

Unlike traditional alloys, which contain one and rarely two base elements, high-entropy alloys HEAs composed by multiple principal elements, generally contain more than four major elements in similar concentrations, ranging from 5 to 35at% for each element. In this work, the effects of strain rate on mechanical deformation of FeCoNiCrAl0.1 HEA with face-centered cubic (FCC) structure were investigated. Standard quasi-static and dynamic tensile/compression testing were performed at strain rate of $10^{-3}s^{-1}$ and $10^{3}s^{-1}$ using a universal testing machine (Instron5848, USA) and Split-Hopkinson Tension / Pressure Bar (SHT/PB) respectively to study the effect of strain rate on the properties of FeCoNiCrAl0.1 HEA, and dynamic compression testing was performed at both room temperature (298K) and liquid nitrogen (77K). Both pre- and post-deformation microstructures were studied using electron microscopes. The results show that this kind of HEA has excellent work-hardening rate and high strain-rate sensitivity of yield strength, as the strain rate increases from $10^{-3}s^{-1}$ to $2600s^{-1}$, the true tensile yield stress increases from 200MPa to 480MPa and its ductility is not reduced, these results may due to its low stacking fault energy and the existence of short-range order. SEM image show that the fracture modes of HEA are obviously different under quasi-static and dynamic conditions, a large number of dimples were found upon the appearance of fracture under dynamic conditions, which are not found under quasi-static conditions. Due to the different deformation mechanism under the quasi-static condition that compression deformed material show profuse mechanical twinning while the tensile deformed material did not exhibit any mechanical twinning. FeCoNiCrAl0.1 HEA exhibited significant tension/compression asymmetry in its work hardening rate and ductility. In addition, the dynamic mechanical properties of the FeCoNiCrAl0.1 HEA under low temperature was explored in this work. Low temperature environment can significantly improve the mechanical properties of HEA. Under the condition of dynamic compression, the true yield strength of FeCoNiCrAl0.1 HEA increased from 400MPa to 560MPa when the temperature decrease from room temperature to liquid nitrogen temperature under the strain rate about $4000s^{-1}$.

15:30-16:00 Tea Break

16:00-16:25 Invited

Temperature Rise Associated with Adiabatic Shear Band: Causation or Consequence

Yazhou Guo, Qichao Ruan, Shenxin Zhu, Haosen Chen, Yulong Li, Daining Fang, Northwestern Polytechnical University, China

One of the most important issues related to dynamic shear localization is the correlation among the stress collapse, temperature elevation and adiabatic shear band (ASB) formation. In this work, the adiabatic shear failure process of pure titanium was investigated by dynamic shear-compression tests synchronically combined with high-speed photography and infrared temperature measurement. The time sequence of stress collapse, ASB initiation, temperature rise and crack formation was recorded. The key characteristics of ASB, such as temperature, critical strain, propagation speed and cooling rate were systematically studied. The fraction of mechanical work converting into heat, i.e., the Taylor-Quinney factor, was derived to be 0.25 to 0.55 and it is also positively dependent on the loading rate. This experiment result indicates the commonly used values of 0.9~1.0 should be re-evaluated. The measured temperature rise at the maximum stress (or before ASB initiation) is in the range of 50~90℃, which by itself is not enough to outplay other strengthening mechanisms (such as strain rate hardening). Micro damage induced by the large shear strain should also be responsible for the stress drop. The measured temperature within the ASB is about 350~650℃, whereas the material close to the ASB is also heated. About 37μs after the stress collapse, the temperature reaches its maximum, which is due to the continuous development of the shear band until macro crack formation. The observed fact that temperature rise is quite behind ASB initiation suggests that it could not be the trigger for ASB formation. Therefore, the analytical and numerical analyses of ASB initiation based on temperature perturbation or thermal softening lose their foundation

16:25-16:50 Invited

Dynamic Behavior of Ultrafine-Grained and Noncrystalline Titanium at Cryogenic Temperature

Zezhou Li, University of California, San Diego, United States

The mechanical behavior of ultrafine-grained (500nm) and nanocrystallline (100nm) titanium was examined in the high strain-rate regimes. The stress of ultrafine-grained and nanocrystalline titanium increases significantly compared with coarse grained titanium due to the Hall-Petch effect. In compared with coarese-

grained titanium, the strain-hardening rate of the ultrafine-grained and nanocrystalline titanium is significantly lower due to the reduced dislocation activation volume. The strain-rate sensitivity of ultrafine-grained and nanocrysalline titanium does not change too much at both room and low temperature, in comparison with coarse-grained titanium, indicating no significant change of deformation mechanisms. The combinarion effect of low strain harndieng rate, general strain rate sensitivity and increased thermal softening effect made ultrafine-grained and naocrystalline titanium more prone to the shear localization. Dynamic deformation and failure mechanisms of ultrafine-grained and nanocrystalline titanium were studied by using a specimen geometry in which the forced shear was imposed into a narrow region at room and crogenic temperatures. The lower temperature can lead to the formation of narrower shear band under same strain and the strain-rate conditions. The combination effect of the decrease of the thermal conductivity, the decrease of the specific heat capacity and the increase of the thermal softening parameter can lead to the very narrow band of ultrafine-grained and nanocrystalline titanium at cryogenic temperature. The microstructure inside the adiabatic shear band consists of a mixture of elongated grains and equiaxed nanograins that are smaller than initial grains. Formation of equiaxed recrystallized grains inside the shear band was still caused by the classical rotational dynamic recrystallization mechanism in both titaniums. The dislocation density at grain boundaries decreases in a very short time during the cooling process of the well develpoed shear band, which results in the sharp boundary configurations as observed by the trasmission electron microscopy.The adiabatic shear bands were then subjected to the combined brittle and ductile failure.

16:50-17:10

Shear Localization in Near Beta Titanium Alloy

Xu Ding, Central South University, China

Near β Ti-5Al-5Mo-5V-1Cr-1Fe (Ti-55511) titanium alloy has high strength to weight ratios and very attractive combinations of toughness, corrosion resistance and superior fatigue resistance, and is widely applied in aerospace, biomedical and marine industries. Shear localization, also called adiabatic shear band, is a narrow zone in the specimen deformed under high strain rate loading conditions, and is a signal that the material has already lost deformation resistance. Shear localization is the main failure mechanism of the Ti-5Al-5Mo-5V-1Cr-1Fe titanium alloy deformed at a high strain rate. In the present work, an adiabatic shear band is generated in a hat-shaped Ti-55511 titanium alloy after dynamic deformation at cryogenic temperature 173K and room temperature 293K in Split Hopkinson Pressure Bar system. Double peaks appear on the curves of the strain and the stress during the shear localization process when the phase transformation occurs. Widths of the shear bands are affected by the nominal strain of the specimens and the treatment temperature. Microstructure and mechanical properties of a shear band are investigated by optical microscope, high resolution electron microscopy and nanoindentation, respectively. Results show that grains in the boundary of the shear band are highly elongated along the shear direction, and the core of the shear band consists of ultrafine equiaxed grains with sizes 0.1~0.5 microns and with low density of dislocations; and sizes of the grains in the shear band obtained at the cryogenic temperature are smaller than those in the shear band obtained at the room temperature. Strain rate sensitivity of ultrafine grains in the shear band is independent to deformation temperature and grain size, and strain rate sensitivity exponents are dependent on the loading strain rate and positive proportion with increasing the loading strain rate. Finally we find rotational dynamic recrystallization mechanism and phase transformation can take effect on the generation of the new ultrafine equiaxed grains in shear band by results analysis of experimental found and molecular dynamics simulation.

17:10-17:30

Effect of Loading Rate on Mode I Fracture Toughness of Carbon Nanotubes Reinforced Carbon Fibers / Epoxy Composites

Zhouyi Li, Northwestern Polytechnical University, China

Compared with traditional materials such as aluminum alloy and steel, carbon fiber reinforced resin-based materials have high specific strength, specific stiffness, and good fatigue resistance, so it is used more and more in the fields of aviation, weapons, electronics. However, fiber reinforced resin matrix composites have the disadvantages of low interlayer toughness and insufficient impact damage resistance, and need to improve interlayer toughness through some interlaminar toughening methods. Carbon nanotubes (CNTs) are ideal materials for strengthening and toughening of composite materials due to their large aspect ratio, high specific surface area, and excellent mechanical and electrical properties. In this study, the CNT films produced by the floating catalyst chemical vapor deposition method is interleaved between the layers of the carbon fiber resin-based composite material to improve the interlaminar fracture toughness of composite laminates. Carbon nanotube film was found to be porous by analyzing the SEM micrography, which is beneficial to resin infiltration. After hand-laying the preform, we use vacuum assisted resin transfer molding method to mold the composite laminates. We determined the Mode I interlaminar fracture toughness under different loading rate of the composites with different area densities CNT films. Double cantilever beam (DCB) test geometry

was employed for both quasi-static and dynamic fracture tests. The quasi-static test was performed on Instron 5848 tester, and the test method is accorded to ASTM 5528. The dynamic test was performed on a novel dual electro magnetic Hopkinson bar[5], which can achieve symmetric dynamic loading. The range of loading velocities is 10~30m/s. To determine the frature toughness, we use a hybrid experimental-numerical method. By analysis the test results, we can found that the interlayer of carbon nanotube film can enhance the interlaminar fracture toughness significantly compared with the neat composites. And there is a loading rate sensitivity can be found in the test.

17:30-17:50

Remarkable Strength Properties and Shear Fracture of (Al0.5CoCrFeNi)0.92(MoC)0.08 High Entropy Alloy under High Velocity Loading

Chu Wang, Central South University, China

High entropy alloys (HEAs) contain at least five elements in an equiatomic or near-equiatomic ratios and have excellent properties such as superb hardness, high heat resistance and strong corrosion resistance. As a broad category of high entropy alloy, AlxCoCrFeNi HEAs have aroused huge interests of researchers since the appearance of high entropy alloy. And they found that the Al0.5CoCrFeNi HEA has a face-centered cubic (FCC) plus body-centered cubic (BCC) solid solution structure and an excellent properties due to the strengthen of BCC structure on the well plastic FCC structure. Powder metallurgy is admitted as a cost effective preparation method and can produce uniform fine grain. Powder extrusion is one preparation method of powder metallurgy which includes the gas atomization and the following hot extrusion of pre-alloyed powder. We studied the mechanical properties of the (Al0.5CoCrFeNi)0.92(MoC)0.08 HEA prepared by hot extrusion under split Hopkinson pressure bar. Microstructure and mechanical behavior of the (Al0.5CoCrFeNi)0.92(MoC)0.08 HEA were investigated using optical microscope (OM), X-ray diffraction (XRD), electron probe microanalyzer (EPMA), and scanning electron microscope (SEM). Results show that the (Al0.5CoCrFeNi)0.92(MoC)0.08 HEA has a uniform FCC+BCC solid solution structure and an optimized grains about 0.5μm, and the yield strength is sensitive with the strain rate and the values increasing with the strain rates. The Johnson-Cook plastic model is obtained to describe the dynamic flow behavior. The hat-shaped specimens were used to investigate forced shear localization. However, the shear band does not be founded at the designed shear zone, and the cracks even propagate on the both sides of the shear zone. The failure of forming shear band can contribute to the high strain hardening rate, which makes the current HEA an excellent candidate for penetration protection application such as armors.

A. Advanced Steels and Processing: IV

Symposium Organizers :

Han Dong, Shanghai University, China; Zhigang Yang, Tsinghua University, China; Yoshitaka Adachi, Nagoya University, Japan; Dong-Woo Suh, Pohang University of Science and Technology (POSTCEH), Korea; Christopher Hutchinson, Monash University, Australia; Amy Clarke, Colorado School of Mines, USA

Wednesday AM Room: 205+206+207(2nd Floor)
August 21, 2019 Symposium:A

Chairs:
Yongjie Zhang, Tohoku University, Japan
Feng Liu, Northwestern Polytechnical University, China

8:30-9:00 Keynote

Preferred Morphologies of Phases in Steels—An Integrated Approach

Wenzheng Zhang, Tsinghua University, China

Reproducible morphologies characterized by preferred interfaces are a common feature of many phases in steels, such as Widmanstätten-ferrite, -austenite and -cementite, and lath martensite. In contrast, the crystallographic descriptions of the preferred interfaces and their interpretations are not commonly known. This presentation will report the major progress in our group over twenty years on understanding of the preferred interfaces in various steels. The key feature of a preferred interface is the singularity of the interfacial structure. A typical singular feature in a preferred fcc/bcc interface is the existence of an invariant line, a misfit-free direction, which often defines the long axis of the product phase. The habit plane (HP), the major preferred interface, between fcc and bcc phases often contains periodic dislocations parallel to the invariant line (O-line), as confirmed by numerous TEM images. The orientation relationship (OR) and interface orientation (IO) allowing such a singular dislocation structure are usually irrational. They can be calculated based on the O-lattice theory, with a free software. This presentation will discuss the constraints to the choices of the O-lines and invariant lines. It will also present the recent simulation results about the evolution of morphology and OR at the early stage, and about the migration of the HP. Migration of the HP together with the parallel dislocations is associated with a long-range strain, which may shed some light on the long-standing controversial issue of the surface relief effect. Precipitation of cementite from austenite represents a more complicated case, since the two lattices differ significantly. In this case, the singular structure in the

HP is characterized by parallel secondary dislocations associated with interfacial steps. Various examples from different steels will be provided. The calculated ORs, IOs, and the singular structures in the HP of different cases are fully consistent with the observations.

9:00-9:25 Invited

Concurring Kinetics of Phase Transition and Grain Growth in Nanostructured Alloy

Feng Liu, Northwestern Polytechnical University, China

Experimental observation and theoretical interpretation on the concurring kinetics of grain growth and phase transition in nanostructured Fe91Ni8Zr1 alloy were first presented. From in situ high temperature X-ray diffraction and differential scanning calorimetry, it can be confirmed that concomitant grain growth occurs and comes to a halt before phase transition is fully completed. From the currently kinetic description, grain growth not only adjusts the constitution of enthalpy change, but also influences the kinetics of phase transition. The present findings, offer a new behavior of phase transition owing to the size effect, and further, extend the understanding of the role grain boundary played in solid-state phase transition.

9:25-9:50 Invited

New Insights on Nucleation and Transformation Process in Temperature-Induced Martensitic Transformation

Wei Xu, State Key Laboratory of Rolling and Automation, China

Understanding mechanisms of the nucleation and transformation sequence is of critical importance to control temperature-induced martensitic transformations and hence retained austenite. In the present work, quasi-in-situ Electron Backscattering Diffraction (EBSD) and Transmission Electron Microscopy (TEM) were employed to investigate the nucleation and transition in a prototype SUS321 austenitic stainless steel. A new viewpoint was proposed, that temperature-induced martensitic transformation took place not only from pre-existing defects as assumed in the classical theory but also from newly formed potential sites such as faulted γ and stacking fault bundles formed during cryogenic treatment. Moreover, transformation follows both austenite→ε-martensite→α'-martensite and austenite→α'-martensite routes. In both, the martensite transformation was always trigged first by faulted γ and then by ε and stacking fault bundles as transitions, and eventually to the final α' transformation. Their associated mechanisms, and crystallographic characteristics were analysed. Despite the new nucleation mechanisms and different transformation sequences, the ε martensitic transformation followed the S-N relationship while the α' martensitic transformation obeyed the K-S relationship. Given the same nucleation behaviour, the newly formed potential nucleation sites can be directly considered along with pre-existing defects for modelling the transformation kinetics. These new insights could provide further guidelines for the optimization and modelling of martensitic transformation.

9:50-10:10

Phase-Field Modelling of the Formation of Ferrite and Widmanstätten Ferrite in Fe-C and Fe-C-Mn Alloys: an Emphasis on Morphology Transition and Alloying Element Effects

Luyao Fan, Zhigang Yang, Chi Zhang, Hao Chen, Tsinghua University, China

Austenite decomposition into grain boundary ferrite (GBF) and Widmanstätten ferrite (WF) has attracted significant attention from both academia and industry due to its great importance in the microstructure control of advanced high strength steels. It is well known that austenite could transform into GBF at relatively higher temperatures, while the transformation product switches into WF with decreasing transformation temperature. However, the mechanism of morphology change from GBF to WF was not fully understood. In this study, a phase-field model, in which the solute drag effects of substitutional elements, interface friction and the anisotropy of interfacial energy are all considered, was proposed to simulate the formation of GBF and WF in the binary Fe-C and ternary Fe-C-Mn alloys, and the mechanism of the transition from GBF to WF is discussed. The phase field model could predict a mixed-mode growth of GBF and WF, and the effects of interface mobility and solute drag on transformation kinetics can be well quantified. The kinetics of GBF and WF formation in Fe-C alloys simulated by the phase field model was firstly compared with experiments in order to obtain the value of interface mobility and the anisotropy of interfacial energy, which are used as inputs of the subsequent simulations for Fe-C-Mn alloys. The phase field model predicts that the addition of Mn could significantly reduce the kinetics of GBF and WF formation and lead to incomplete transformation phenomenon due to solute drag effects, which is in agreement with experiments. The sharpness of Widmanstätten plate tip was also predicted to increase with Mn addition. Based on the simulations for both Fe-C and Fe-C-Mn

alloys, the effects of the anisotropy of interfacial energy, solute drag, and interface mobility on the transition from GBF to WF was discussed in details. The anisotropy of interfacial energy and solute drag effects are found to play a dominant role in the transition from GBF to WF.

10:10-10:30

Investigation of the Roll Contour Effects on Strip Shape and Roll Contact Pressure in Hot Strip Rolling by 3D FE Simulation

Zhengyi Jiang, Haibo Xie, Lianjie Li, University of Wollongong, Australia; Tianwu Liu, Enrui Wang, Xu Liu, Hesteel Group, China

High-strength steel exhibits an excellent combination of high strength and high formability resulting from their high strain hardening capabilities. Strip profile control in cold rolling is a great challenge for high strength steel in cold tandem rolling. Because of the complex influence factors of plate shape and profile, shape detection and control technology have not been solved, especially for high strength steel rolling. The shape and flatness of the rolled strip will be affected by large roll deflection due to the high rolling force.

Roll contour plays an important role in strip shape control and also has significant influence on the roll wear induced by nonuniform contact pressure. In this study, a three dimensional elastic-plastic coupled thermo-mechanical finite element (FE) model is developed to simulate the complex hot strip rolling process. This model not only calculates the elastic deformation of rolls and plastic deformation of strip simultaneously, but also takes the effects of temperature variation into account. The roll contour effects of back-up roll (BR) and work roll (WR) are compared under different WR bending force and shifting value using this proposed in terms of strip crown, roll contact pressure and roll gap adjustment area. The results obtained provide valuable guidelines for roll contour design and optimization.

10:30-10:45 Tea Break

10:45-11:10 Invited

Data-Driven Properties-to-Microstructure-to-Processing Inverse Analysis for Steels Via Machine Learning

Zhilei Wang, Yoshitaka Adachi, Nagoya University, Japan

A traditional experimental approach is inefficient for designing novel materials with desired properties because of the complex combinations of processing conditions and chemical compositions in materials design. With the proposal of materials informatics, data science is now attracting increasing attention in the materials research field, which has led to achievements in predictions of phase diagrams, crystal structures, materials properties, and so on. In this study, a data-driven properties-to-microstructure-to-processing inverse analysis was proposed to design high-performance steels by using a machine learning approach. The quantitative microstructure information and employed algorithms in this work were extracted and implemented by two independently developed machine learning tools, Materials Genome Integration System Phase and Property Analysis (MIPHA) and rMIPHA (based on R programming environment). Since the commercial demands for highly strong and flexible steels are growing, a balanced property of tensile strength (TS) and total elongation (t_{EL}) TS × t_{EL} was inversely explored by using a genetic algorithm with a maximum search. The results indicated that a properties-to-microstructure / processing analysis approach identified a better model performance, and a microstructure comprised by Widmanstatten ferrite (WF), bainite (B) and martensite (M) phases was beneficial to a good balanced property. This study aimed to provide a new avenue in data-driven materials design and thereby accelerate the materials discovery process.

11:10-11:30

Effect of Isothermal Bainite Transformation Temperature on Microstructure and Mechanical Properties of a Low-Alloyed TRIP-Aided Steel

Jianeng Huang, Zhengyou Tang, Hua Ding, Hui Zhang, Linlin Bi, Northeastern University, China

The effects of isothermal bainite transformation (IBT) temperatures on microstructure and mechanical properties of cold-rolled Fe-0.2C-1.5Mn-1.5Si-0.025Nb transformation induced plasticity (TRIP) aided steel were studied. Microstructures were observed using scanning electron microscopy (SEM), transmission electron microscopy (TEM) and X-ray diffraction (XRD), and the tensile properties were also evaluated. The microstructure of the experimental TRIP-aided steel was mainly composed of polygonal ferrite, bainite and retained austenite (RA). The IBT temperature affects the volume fraction and stability of RA. With the increase of IBT temperature from 390 to 430˚C, the volume fraction of RA increased from 14.3% to 16.4%, then it decreased to 15.9% when the IBT temperature reached 450˚C. The RA stability decreased with the IBT temperature increasing from 390 to 410˚C, then it increased as the

IBT temperature increased to 450˚C. The austenite grain size and carbon content are the main factors for the RA stability. The RA fraction and stability are the keys to understand the phase transformation induced deformation behavior. The work hardening behavior of the experimental steel was studied to reveal the transformation behavior of RA during deformation, and the 390-sample exhibited three-stage strain hardening behavior, however, the 410-sample, 430-sample and 450-sample presented four-stage deformation characteristics. With IBT temperature increasing from 390 to 450˚C, the ultimate tensile strength (UTS) of the experimental steel decreased from 865 to 795MPa, however, the total elongation (TEL) increased to 28% then decreased to 22%. The variation in mechanical properties of the experimental sample was related to the constituent phases and TRIP effect. The best comprehensive mechanical properties of the experimental steel with the product of tensile strength and total elongation (PSE) of 23.5GPa% could be obtained when it annealed at 825˚C for 3min and austempered at 410˚C for 3min, which was mainly attributed to the TRIP effect.

11:30-11:50

Evaluation of Thermal Stability of Two Cr-Mo-V Hot-Work Die Steels by Simulation and Analysis of Microstructure and Hardness During Tempering

Ningyu Du, Chinese Academy of Sciences, China / University of Science and Technology of China, China; Hongwei Liu, Paixian Fu, Dianzhong Li, Chinese Academy of Sciences, China

Hot-work die steel refers to the alloy tool steel suitable for making the die for hot deformation of metal. Those steels are commonly used for tools subjected to thermal exposure and usually highly alloyed with strong carbide forming elements as Cr, V and Mo. During hot forming, the tools are exposed to thermal and mechanical loads that results in high temperatures or pressures. Therefore, it is required that the die materials have high strength, hardness, especially high thermal strength, thermal fatigue, toughness and wear resistance. Surely thermal stability, which is a crucial property for the hot working die steels, has to be considered before materials are used for engineering applications.

In this study, our aim is to evaluate the thermal stability of 4Cr5MoSiV1 and 5Cr5Mo2 during tempering at 600˚C for various time and explain the influencing mechanism. Rockwell hardness tester is used to test the hardness of samples with different tempering time. The microstructure characteristics of the 4Cr5MoSiV1 and 5Cr5Mo2 specimens were investigated by scanning electron microscopy (SEM) and transmission electron microscopy (TEM). The X-ray diffraction (XRD) analysis was performed to analyze the variation of dislocation density under different process conditions. Thermo-calc software is used to calculate and simulate the growth of precipitates.

The hardness test results show that the rate of hardness reduction of 5Cr5MoV is smaller than that of 4Cr5MoSiV1, and the value of hardness reduction is smaller after 60 hours of tempering at 600˚C. SEM results show that the martensite lath width of 5Cr5Mo2 is finer than that of 4Cr5MoSiV1 before and after tempering, and the carbides precipitated are smaller. TEM results show that the martensite recovering and carbide coarsening are efficiently inhibited in 5Cr5Mo2, however, it is obvious and serious in 4Cr5MoSiV1. Similarly, the simulation results show that carbide coarsening is slower in 5Cr5Mo2. XRD results show that the value of dislocation density of 5Cr5Mo2 decrease more slowly than 4Cr5MoSiV1. Overall, the thermal stability of 5Cr5MoV steel is better than that of 4Cr5MoSiV1 steel.

11:50-12:10

Microstructural Evolution in Carbon Steels

Dehai Ping, National Institute for Materials Science, Japan

In metals and alloys, most of the modern theories (martensitic transformation, hardening mechanism, deformation mechanism, etc.) are based on the studies on steels, particularly carbon steels. Thus, the exploration of martensitic substructure, which is a common microstructure in carbon steels, has been a fundamental research topic for more than one century. In Fe-C system, no matter how much carbon content, all microstructural evolution including the formation of cementite can be explained based on a compressive and logic theory, which has been built based on a newly uncovered ω-Fe metastable phase.

TEM characterizations have revealed that ω-Fe are 1~2nm ultra-fine particles with the lattice parameters dependent on its corresponding BCC partner, i.e. $a_\omega = a_{bcc}$, $c_\omega = /2\ a_{bcc}$. Unlike the ω-phase formed from BCC matrix phase, the ω-Fe particles distribute only at the BCC {112}<111>-type twinning boundaries in Fe-C martensite. The twin has been observed commonly as a martensitic substructure in any Fe-C alloys regardless of the carbon content.

Austenite with FCC structure initially transform into twinned martensite during martensitic transformation.

The matrix crystal and the corresponding twinned crystal are composed of ultra-fine α-Fe particles, which formed due to the martensitic transformation. After that, auto-tempering processing or de-twinning process immediately starts (for example, in low carbon alloy, the martensite transformation starting temperature is normally around 300 ~ 500℃. Below this temperature, those already formed martensite will suffer an un-avoided auto-tempering process during cooling). The ultra-fine α-Fe particles start to coarsen through recrystallization, and cementite particle also form through the coarsening of fine ω-Fe particles. Thus, various microstructures (lath, pearlite, etc.,) can be formed during auto-tempering.

12:10-12:30

Kinetic Transitions and Alloying Element Partitioning during Austenite Growth from a Ferrite-Cementite Mixture: Role of Heating Rate

Geng Liu, Zongbiao Dai, Zhigang Yang, Chi Zhang, Hao Chen, Tsinghua University, Beijing, China

Austenite formation from a ferrite-cementite mixture is a crucial step during the processing of advanced high strength steels (AHSS). The ferrite-cementite mixture is usually inhomogeneous in both structure and composition, which makes the mechanism of austenite formation very complex. In this contribution, austenite formation upon continuous heating from a designed spheroidized cementite structure in a model Fe-C-Mn alloy was investigated with an emphasis on the role of heating rate in kinetic transitions and element partitioning during austenite formation. Based on partition/non-partition local equilibrium (PLE/NPLE) assumption, austenite growth was found alternately contribute by PLE, NPLE and PLE controlled interfaces migration during slow-heating, while NPLE mode predominately controlled the austenitization by a synchronous dissolution of ferrite and cementite upon fast-heating. It was both experimentally and theoretically found that there is a long-distance diffusion of Mn within austenite of the slow-heated sample, while a sharp Mn gradient was retained within austenite of the fast-heated sample. Such a strong heterogeneous distribution of Mn within austenite cause a large difference in driving force for ferrite or martensite formation during subsequent cooling process, which could lead to various final microstructures. The current study indicates that fastheating could lead to unique microstructures which could hardly be obtained via the conventional annealing process.

A. Advanced Steels and Processing: V

Symposium Organizers :

Han Dong, Shanghai University, China; Zhigang Yang, Tsinghua University, China; Yoshitaka Adachi, Nagoya University, Japan; Dong-Woo Suh, Pohang University of Science and Technology (POSTCEH), Korea; Christopher Hutchinson, Monash University, Australia; Amy Clarke, Colorado School of Mines, USA

Wednesday AM
August 21, 2019

Room: 208+209+210(2nd Floor)
Symposium: A

Chairs:
Wei Xu, Northeastern University, China
Hao Chen, Tsinghua University, China

8:30-9:00 Keynote

Carbon Partitioning during Ferrite and Bainite Transformations in Low-Alloy Steels

Tadashi Furuhara, Goro Miyamoto, Tohoku University, Japan

Alloy partitioning at transformation interfaces is important in designing properties of high strength steels. Recently, it has been recognized that energy dissipation in interface migration plays critical roles on carbon enrichment into austenite. In this presentation, alloy partitioning behavior observed in low-alloy steels and effects of interface coherency are discussed in phase transformations in hypoeutectoid alloys.
Grain boundary ferrite (GBF), which is formed under low supersaturation, grows mainly by motion of incoherent interface. As temperature decreases, Widmanstätten ferrite (WF) and bainitic ferrite (BF) with partially coherent interfaces are formed. In alloyed steel, it has been repeatedly shown that GBF grows under local equilibrium with carbon partitioning. In Fe-C-Si alloys, carbon contents in austenite (γ) for GBF correspond well to negligible partitioning local equilibrium (NPLE) line whereas enrichment for WF is lower than the NPLE limit. It is thought that such deviation is caused by low interface mobility for high coherency. For BF, deviation is much larger than those for GBF and WF but also found to be smaller than the T0 line. In Fe-C-Mn, similar trends are also observed and deviation for BF becomes larger than the T0 line in alloys containing more than 2mass%Mn. Microalloying of Mo or Nb further enhances the deviation from local equilibrium.
During reverse transformation,it is well known that two major morphologies of reverted austenite are formed; granular (γ_G) and acicular (γ_A) ones. Growth of γ_G takes place by migration of incoherent interface but γ_A grows with partially coherent interface. In an Fe-C-Mn-Si alloy

intercritically annealed, it is seen that γ_G grows fast via the NPLE mode in early stages, followed by slower growth kinetics with Mn and Si partioning. For γ_A, on the other hand, Mn and Si partioning is seen in the early stage of growth. Such a difference in partitioning kineics also attributes to interface coherency of reverted austenite.
Effects of substitutional solute segregation on energy dissipation at the interface will be discussed based on nanoscale analyses.

9:00-9:25 Invited

Fast-Heating Enables Heterogeneous Microstructure and Upgraded Mechanical Properties of Q&P Steel

Hao Chen, Geng Liu, Chi Zhang, Zhigang Yang, Tsinghua University, China

Fast-heating technology was applied to processing the cold-rolled quenching and partitioning (Q&P) steels. Effects of heating rate on the kinetic interactions between cementite dissolution, ferrite recrystallization, austenite formation and elements diffusion upon heating were analyzed. It was found that fast-heating could induce explosive nucleation of austenite and yields heterogeneous austenite with an inhomogeneous distribution of elements, which significantly affects phase transformations and carbon partitioning during the subsequent Quenching and Partitioning process. In general, the microstructure of the fast heated Q&P steels was much finer than that of the conventional Q&P steels. Furthermore, retained austenite with various morphology and composition were experimentally identified by AES-EBSD in the fast-heated Q&P steels, which leads to a continuous transformation induced plasticity (TRIP) effect and thus improves work hardening behavior of the steels. The statistics of the ultimate tensile strength vs. total elongation of each sample under the orthogonal annealing conditions suggested that, compared with conventional Q&P steels, fast-heating could improve the strength with approximately 90MPa on average while the elongation was kept in the range of 17 to 27%. Fast heating technology opens up new routes to achieve unique microstructures and advanced mechanical properties in steels not accessible by the conventional heating technology.

9:25-9:50 Invited

Formation of Ultrafine Martensite from Ultrafine Ferrite Structure with Fine Dispersed Cementite Particle Including High Mn Content

Shiro Torizuka, Atsushi Ito, University of Hyogo, Japan

It is interesting and important to understand how austenite grain size refinement affects martensitic transformation. However, in the case of low carbon steels, austenite grain refinement promotes the formation of polygonal ferrite at austenite grain boundaries. In other words, because grain refinement makes it more difficult to obtain a purely martensite structure, researchers cannot easily examine relationships among austenite grain size, Ms temperature, microstructural morphology (packet, block, lath), and mechanical properties. We have recently been examining 0.1C-5Mn steel, reporting that this material offers excellent mechanical properties in comparison to common martensitic steels. The most notable feature of this steel is its 5% Mn content, which increases hardenability and enables 100% martensitic transformation even under air cooling. With low C-5Mn steel, it is possible to obtain a fully martensitic structure even from fine austenitic structures. This allows us to easily examine the mechanical properties of martensitic structures transformed from prior austenite with a wide range of grain sizes.
In this study, change in martensite structure in 0.1%C-2%Si-5%Mn steels with prior austenite grain size was investigated. Particularly it was focused whether single variant martensite formed when austenite grain size was reduced to which grain size. Fine austenite structure was produced by the reverse transformation from Ultrafine ferrite + fine dispersed cementite with high Mn content structure. When prior austenite grain size is from 150 to 24mm, multi-packets and multi-blocks martensite structure is formed. When prior austenite grain size is 7mm, single packet and multi-blocks martensite structure is formed. When prior austenite grain size is 2mm, single variant (single block) martensite structure is formed. Critical prior austenite grain size is 2mm to obtain single variant martensite. Tensile strength (1500MPa), uniform elongation (8%) and total elongation (14%) of single variant martensite are superior than those of multi-packets and multi-blocks martensite (TS=1350MPa, UEL=6% and TEL=13%). This is because strain hardening rate is enhanced by the structural change in martensite.

9:50-10:10

Characterization and Modification of the Compromise between Tensile Properties and Fracture Toughness in a Quenching and Partitioning Steel

Zhiping Xiong, Beijing Institute of Technology, China

The enhancement of the fracture toughness is essential for opening the possible range of applications of advanced high strength steels, while the focus is often put only on the strength-ductility compromise. A high fracture toughness is indeed needed for energy absorbing components as well as to limit the edge cracking sensitivity during part forming. This study investigates the tensile properties and the fracture toughness of various quenching and partitioning

microstructures. The fracture resistance is evaluated using double edge notched tension tests. While the uniform elongation continuously increases with the retained austenite (RA) fraction, the fracture toughness shows a maximum at intermediate RA content. For the highest amount of RA, the relatively low fracture toughness is mainly attributed to the formation of brittle necklace of fresh blocky martensite in the fracture process zone due to a high stress triaxiality, inducing an intergranular fracture mode. For intermediate RA fraction, the RA morphology evolves from blocky to film-type and the RA-to-martensite transformation contributes to a higher total work of fracture compared to tempered martensitic steel. A proper control of both amount and morphology of RA during microstructure design is thus essential to generate the best compromise between tensile properties and fracture toughness. As a general methodological conclusion, the present study, proves, once again, that it is very dangerous to generate conclusions about the cracking resistance of an alloy based only on uniaxial tension evidences. Fracture of materials must always be investigated through considering different stress states.

10:10-10:30

Effect of Retained Austenite on Some Service Performances of Quenched and Partitioned Steels

Zhenghong Guo, Jilan Yang, Zeng Zhen, Jianfeng Gu, Shanghai Jiao Tong University, China

In order to develop the high-strength martensitic steels without sacrificing the plasticity, the microstructural feature of retained austenite in quenched and partitioned (Q&P) steels and its role on the strengthening/toughening mechanism have received much attention in recent years. Comparing the traditional quenching and tempering (Q&T) steels, once the Q&P steels come into use in industry, the presence of the considerable amount of retained austenite in martensitic matrix may lead to the different service performances of manufactured parts. In addition to its amount and distribution, it may be true that the mechanical stability of retained austenite, and associated softening degree of martensitic matrix due to carbon depletion together, affect failure manner during service as well. Based on the experimental results, the present paper summarizes our initial achievements relating intrinsic properties of retained austenite with several kinds of service behaviors and failure manners of Q&P steels, mainly including dynamic compression, hydrogen embrittlement, corrosion in neutral environment and dry sliding wear property. Deep analysis indicates that, under the assistance of carbon-enriched retained austenite, the comprehensive factors referring to the deformability of carbon-depleted martensitic matrix result in the increase in service life of Q&P steels, they are but not limited to: (i) plastic deformation of retained austenite itself; (ii) improvement in harmonious deformation ability of martensitic matrix by other effects including blocking cracking propagation (BCP), dislocation absorption by retained austenite (DARA) and transformation induced plasticity (TRIP); (iii) relaxation of residual stress due to high amount of retained austenite and softened martensitic matrix caused by carbon depletion; (iv) enhanced resistance against hydrogen attack because of effective hydrogen trapping capability of retained austenite; (v) the low corrosion rate of martensitic matrix due to relatively high chemical potential of iron in retained austenite instead of in martensitic matrix; (vi) improved wear resistance by additional hardening from deformation-induced martensitic transformation. Besides, the further microstructural refinement by optimized thermomechanical processing is always favorable for better service security of Q&P steels.

10:30-10:45 Tea Break

10:45-11:05

In-Situ Neutron Study for the Effect of Ausforming on Phase Transformation Behavior During Q&P Process

Wu Gong, Kyoto University, Japan Atomic Energy Agency, Japan; Stefanus Harjo, Japan Atomic Energy Agency, Japan; Akinobu Shibata, Nobuhiro Tsuji, Japan Atomic Energy Agency, Japan; Yo Tomota, National Institute of Materials Science, Japan; Tomoya Shinozaki, Kobe Steel, Ltd., Japan

Ausforming, i.e. plastic deformation of austenite prior to phase transformation from austenite in steels, affects subsequent martensite or bainite transformations significantly. However, the effect of ausforming on phase transformation kinetics and carbon partitioning in the quenching and partitioning (Q&P) process is still not fully understood. It is well known that the kinetics of phase transformation and carbon partitioning in the Q&P process are the key to controlling the amount and stability of retained austenite in steels, which play crucial roles in mechanical properties of the product through a transformation-induced plasticity (TRIP) effect. In the present study, we conducted in-situ neutron diffraction experiments to examine phase transformation behaviors during Q&P process after ausforming in an 0.30C-2Mn-2Si (wt%) steel. Martensite transformation strart temperature was approximately 315˚C in the steel. In-situ neutron diffraction experiments were performed at the beam-line 19 TAKUMI in Japan Proton Accelerator Research Complex (J-PARC) with a thermomechanical processing simulator installed. Cylindrical specimens of the steel with height of 11mm and diameter of 6.6mm were prepared. The specimens were austenitized

at 900˚C for 300s, rapidly cooled down to 550˚C to carry out compression deformation (30% reduction in height), and then rapidly cooled to various temperatures (230˚C, 250˚C, 280˚C, 300˚C and 330˚C) for isothermal holding of 1.5 hours followed by quenching to room temperature. Kinetics of phase transformations and carbon partitioning behavior were tracked by neutron diffraction in real time. Microstructures of the specimens were analyzed by SEM and EBSD.

The neutron results showed that ausforming suppressed martensite transformation during quenching and subsequent isothermal holding, leading to larger amount of retained austensite than that in the process without ausforming. Carbon partitioning behavior was quantitatively evaluated from the change of lattice parameters. More efficient carbon enrichment in austenite was realized by ausforming than the process without ausforming. The kinetics of phase transformations and carbon partitioning behaviors at various quenching and partitioning temperatures in the processes with or without ausforming will be discussed in the presentation.

11:05-11:25

Atomistic Analysis on the C-Partitioning into κ-Carbides by Si Addition and Its Effect on the Deformation Mechanism

C*hiwon Kim*, Mathieu Terner, Jehyun Lee, Hyunuk Hong, Department of Materials and Science Engineering, Changwon National University, Korea; Joonoh Moon, Sungjun Park, Jaehoon Jang, Ferrous Alloy Department, Korea Institute of Materials Science, Korea; Bongho Lee, Center for Core Research Facilities, Daegu Gyeongbuk Institute of Science and Technology, Korea

Fe-Mn-Al-C lightweight steels have been investigated as the advanced high strength steels. It resulted from not only the excellent combination of specific strength and deformability but also high corrosion resistance. These steels have been developed from Transformation Induced Plasticity(TRIP) or Twinning Induced Plasticity(TWIP) steels with the addition of Al atoms for weight reduction. In the present research, the effect of Si addition in Fe-30Mn-9Al-0.9C-0.5Mo(-1Si) cast steel has been investigated. Si addition leads to the acceleration of κ-carbides precipitation during aging heat treatment which contributes to precipitation strengthening. Partitioning coefficients of alloying elements from γ-matrix to κ-carbides were calculated and the elements distribution was visualized by three dimensional atom probe tomography. Si addition let C atoms excessively partitioned into κ-carbides resulting in the increase of coherency strain and the probability of Al and C bonding formation which is expected to additionally block κ-carbides shearing. The first principles calculation confirmed that the energy which is required for κ-carbides shearing is higher in Si added steel(561mJ/m^2) than which of Si free(494mJ/m^2) steel because of excessive C partitioning. Not only Al and C bonding formation, but also additional atomic bonding with C and others lead to the gap of the energy required to shear κ-carbides. Therefore, the difference of the energy required for κ-carbide shearing leads to change of deformation mechanism from multi-directional to uni-directional shearband formation. Dislocations shear κ-carbides multi-directionally in Si free steel whereas shear κ-carbides uni-directionally in Si added steel due to the occurrence of significantly easy path after the first shearing of κ-carbides. Operative deformation mechanism was calculated as a function of precipitates volume fraction and size. The calculation implied that dislocations only shear and could not bypass κ-carbides as long as the radius of κ-carbides is smaller than 13.4nm which is a critical radius determining operative mechanism.

11:25-11:45

Effect of Cryogenic Treatment on Microstructure and Properties of Mn-Si-Cr Bainitic Steel

Zhunli Tan, Bo Gao, Ming Zhang, Bingzhe Bai, Beijing Jiaotong University, China

Effect of cryogenic treatment on the microstructure and properties of Mn-Si-Cr series bainitic steel and related mechanism was studied in the present work. The results showed that general properties can be improved to some degree by cryogenic treatment. Compared with conventional austempering-tempering treatment (AT), the hardness and wear-resistance properties are enhanced obviously after austempering-cryogenic-tempering treatment (ACT), keeping the same level of toughness and plasticity simultaneously. When cryogenic temperature changes from -80˚C to -196˚C, the strength and hardness are improved obviously and corresponding retained austenite volume fraction would decrease. After cryogenic holding time is prolonged from 12 hours to 24 hours, better general performances can be achieved, including higher strength, better impact energy etc. Tempering parameters in cryogenic treatment also have certain effect on final performances. These good results are correlated with retained austenite transformation and carbides precipitation in the processes. During cryogenic treatment, blocky retained austenite in the bainite/martensite microstructure would partially decompose, leading to higher stability itself. And the following tempering after cryogenic treatment contributes to fine carbide precipitation and some of these fine carbides distributes in martensite/austenite islands and ferrite base. These two aspects combine to be good to the enhancement of general properties for as-treated experimental steel.

11:45-12:05

Development of 850MPa Grade Nb-Ti-Mo Microalloyed Hot-Rolled High Strength Steel

Yajun Hui, Baoliang Xiao, Qian Du, Hui Pan, Kun Liu, Beijing key Laboratory of Green Recyclable Process for Iron & steel Production, Shougang Group, China; Kemin Wu, Kehao Xu, Beijing Shougang Co., Ltd. Manufacturing Department, China

Energy conservation and environmental protection have become an important direction for the sustainable development of the world economy. The rapid development of new energy buses in recent years meet the concept of green and low-carbon environmental protection. The battery is the most important energy source for electric vehicles, while the development of battery is not mature. The endurance capacity of electric buses mainly determined by its weight. The steel of new energy bus frame commonly used by carbon steel, such as Q235B、Q345C，which accounts for about 1/3 of the total weight. This work aims to develop 850MPa grade hot-rolled high strength square tube steel. The microstructure, properties and strengthening mechanism of the 850MPa grade Nb-Ti-Mo microalloyed hot-rolled high strength steel were investigated by utilizing optical microscope (OM), scanning electron microscopy (SEM) and transmission electron microscopy (TEM). The results show that the matrix of the steel is a fine ferrite single phase with a large number of ultra-fine precipitates. The size of the ferrite is fined to 1.8~2.6μm. There were there kinds of precipitates with obvious different sizes in ferrite matrix, one was some large particles with size of 100~150nm, which was compound carbonitride of Ti, Nb and C, S, these particles was distributed in the interior of ferrite grains. The other one was compound carbonitride of Ti, Nb and C with the size of 10~50nm, which distributed in the interior of ferrite grains, too. Another kind of precipitates was nanometer sized particles, which were smaller than 10nm, the composition of these particles was compound carbonitride of Ti, Nb, Mo and C, these particles precipitated in chains or dispersed in the interior of ferrite grains, which led to a strong precipitation hardening increment up to 300MPa. The steels mainly strengthened by grain refinement hardening and precipitation hardening. The variation of coiling temperature causes a significant difference in strength. The optimum mechanical properties obtained when the coiling temperature is 600℃, the yield strength, tensile strength and the elongation was 830, 875 and 22%, respectively.

12:05-12:25

Nanostructured Bainitic Bearing Steel

Zhinan Yang, Fucheng Zhang, Yanshan University, China

Bearing is the most important component for nearly all mechanical equipment, guaranteeing the steady running of the equipment, especially important for high-end equipment, such as high speed train, shield tunneling machine, et al. The requirement on the quality of bearing is increased with the fast development of technology. The manufacturing level of bearing directly reflects the level of steel metallurgy and machinery manufacturing of a country. The performance of bearing steel is the critical factor that determines the quality of bearing. Martensite, which is the traditional microstructure of the bearing, possesses high strength but low toughness. To improve the service life of the bearing used under impact load, the lower bainite bearing was developed. Developing new bearing steel with higher performance is the ambition of material researchers and expectation of manufacturing industry. Many famous bearing manufacturing enterprises are competing on developing the new generation of bearing steel. Nanostructured bainitic bearing steel, which is a newly developed bearing steel in recent years, not only possesses high strength and toughness, but exhibits excellent wear resistance and rolling contact fatigue resistance. In recent years, relevant achievements on nanostructured bainitic bearing steel in China have led significant progresses in this field. The nanostructured bainitic bearing steel has been first used in China to manufacture large-size bearings for wind turbines and heavy-duty bearings with excellent performance. Therefore, the relevant nanostructured bainitic bearing steel and its corresponding heat treatment process have been included in the national and industry standards for the first time. The bearing industry considers that the exploitation of nanostructured bainitic bearing steel is epoch-making, and named this kind of bearing as the second generation of bainitic bearing. This time, the development of nanostructured bainitic bearing steel is reviewed in detail, including its advantages and disadvantages. Moreover, the further research directions of the nanostructured bainitic bearing steel are proposed.

12:25-12:45

Study on Microstructures and Formability Enhancement Mechanism of Cold-Rolled DP590

Musheng Qiu, Shougang Group Co., LTD. Research Institute of Technology, China

The continuous annealing simulator was used to investigate the influences of annealing temperature and flash cooling temperature on mechanical properties of a DP590 steel. Base on these simulation process above, the key process for industrial production of formability enhanced DP590 has been established. The mechanical properties and microstructure of formability enhanced and traditional DP590 are analyzed, and the formability enhanced mechanism is discussed. The results shown that as the annealing temperature and the flash cooling temperature increases, the yield strength increases and the tensile strength decreases. The annealing temperature increased from 780℃ to 820℃, the maximum change occurred when the flash cooling temperature was 270℃, the tensile strength decreased from 662MPa to 629MPa, and the yield strength increased from 253MPa to 284MPa. The martensite of traditional DP590 is mainly distributed

along the ferrite grain boundary in a thin strip or granular distribution, the ferrite grain size is about 6~8μm, martensite fraction is 11.3%. However, the martensite of the DP590 with formability enhanced was diffuse distribution in the ferrite matrix with a volume fraction of 8.5%. In addition, the formability enhanced DP590 contains very fine dispersed granular martensite islands or retained austenite. The key difference of heat treatment process between formability enhanced and traditional DP590 is that the austenite cooling to the bainite region or martensite during cooling, and finally cooling to room temperature. During the flash cooling of the dual phase steel, the austenite is cooling to martensite below the martensite temperature point, so the final microstructure contains ferrite and martensite distributed in the ferrite matrix. However, The first stage of formability enhanced DP590 is cooling to bainite so that the final microstructure is mainly martensite, ferrite and a small amount of bainite or retained austenite, The fraction of retained austenite is about 2% quantified by XRD and EBSD. The retained austenite plays a key role in the improvement of the final product performance, and mass production performance has maintained good stability.

B. High Temperature Structural Materials: Processing and Alloy Design

Symposium Organizers:

Qiang Feng, University of Science and Technology Beijing, China; Shengkai Gong, Beihang University, China; Hyun Uk Hong, Changwon National University, Korea; Damon Kent, University of Sunshine Coast, Australia; Sammy Tin, Illinois Institute of Technology, USA; Hiroyuki Yasuda, Osaka University, Japan; Jun Zhang, Northwestern Polytechnical University, China

Wednesday AM
August 21, 2019

Room: 305 (3rd floor)
Symposium: B

Chairs:
Chengbo Xiao, Beijing Institute of Aeronautical Materials, China
Rajarshi Banerjee, University of North Texas, USA

8:30-9:00 Keynote

Microstructural Evolutions of Ni-Based Superalloys during High Temperature Straining

Yinong Liu[1], Haibo Long[2], Shengcheng Mao[2], Xiaodong Han[2]
1. The University of Western Australia, Australia
2. Beijing University of Technology, China

In this talk I will present a very brief overview of the microstructural and compositional designs of Ni-based single crystal superalloys in the past decades and then focus our most recent work on the complex and multifaceted microstructural evolutions of these alloys during high temperature straining. The main aspects discussed include: (i) Activities of dislocations. In this study we characterised the various movement manners of dislocations, such as sweep sliding, diagonal climbing and cross slip, their interactions with misfit of the γ/γ' interfaces, relationships between the full dislocations the γ phase and the partial dislocation pairs the γ' phases, formation and evolution of dislocation networks, and the modification of the Brooke formula. (ii) Formation of topologically close-packed (TCP) phases. In this study we clarified the morphologies and orientation relationships of the TCP phases with the matrix based on the minimum misfit criterion. We also discovered the progressive atomic shuffling for structure maturation after the formation of the TCP phases, revealing the atomistic processes of their formation. (iii) The evolution of secondary γ' phase precipitates. In this work we studied the continuation of secondary γ′ precipitate formation during high temperature straining, and discovered two different types of secondary γ′ precipitates formed inside the γ matrix and at nodes of dislocations networks, and explained their formation mechanisms and distinctive morphologies. (iv) Site preference of metallic elements in $M_{23}C_6$ carbide. In this study we used atomic resolution electron microscopy and super-EDS analysis to determine the atomic positioning of the alloying elements in $M_{23}C_6$ carbide precipitate in a Co-based superalloy. (5) Effect of pre-existing anisotropic dislocation networks on creep behaviour. Formation of dislocation networks and γ' phase rafting occur concurrently during creep testing. To delineate their effect on creep performance, we designed an innovative way to produce different anisotropic pre-existing dislocation networks without affecting the original γ' cuboidal structure. This study characterized their influences on the morphology of the rafted γ' phase and the creep properties of the alloys.

9:00-9:25 Invited

Residual Stress in Precipitation Hardening Superalloys Forgings

Hamish Fraser[1], Ben Georgin[1], Brian Welk[1], G B Viswanathan[1]
1.The Ohio State University, USA

The use of powder metallurgy to produce gas turbine components provides the possibility for enhancement of local properties by using different alloys in various locations. In this way, the performance of a given component may be optimized without having to accept design compromises when using a single alloy. The present paper describes a study in which hot isostatic pressing (HIP) has been employed to produce samples consisting of two couples of differing Ni-base superalloy powders, one being CMSX-486 and CM247LC, and

the other CMSX-486 and IN 718. The microstructures of the as-HIP'd couples, particularly the regions of the interfaces between the alloy combinations, have been characterized using optical metallography, scanning electron microscopy (SEM), and (scanning) transmission electron microscopy ((S)TEM). Thus, the degree of compositional intermixing has been determined. Also, it has been observed that at the interfacial regions, there is coarsening of the gamma prime (the $L1_2$ precipitate) phase, resulting from a discontinuous precipitation reaction. The superalloy couples have been subjected to a number of heat-treatments aimed at optimizing their mechanical performance. These samples have been tested in tension, and microstructure/property interrelationships have been determined. This study has been supported by CAMM.

9:25-9:50 Invited

Hot Isostatic Pressing of Dual Ni-Base Superalloys

Zhongnan Bi[1], Hailong Qin[1], Ruiyao Zhang[2], T L Lee[3], Xiaolong Liu[4], Vladimir Luzin[5], Jinhui Du[1], Hongbiao Dong[2], Ji Zhang[1]
1. Central Iron and Steel Research Institute, China
2. University of Leicester, UK
3. Rutherford Appleton Laboratory, UK
4. China Institute of Atomic Energy, China
5. Australian Center for Neutron Scattering, Australia

Residual stress is inevitable to generate during the quenching process for precipitation hardening superalloys forging such as turbine disk. It is relaxed during the following aging treatment, but not eliminated due to superalloys' low stacking fault energy and high creep resistance. Machining distortion could be caused by residual stress re-distribution and removed constraint, which may lead to significant re-working or additional operations. In addition, reduced but not negligible residual stresses of the final components plays an important role in determining service life. For these reasons, it has become increasingly important to know the mechanism of residual stress evolution and employ validated process models for prediction during and post manufacture, to optimize manufacture processes and improve the accuracy of life predictions. In the present work, residual stress evolutions behavior during heat treatments of disk-shape forgings have been studied by advanced detections such as in-situ neutron diffraction. Various commercial precipitation hardening superalloys (Inconel 718, Waspaloy, Udimet 720Li…) were employed to study the effect of precipitation behavior on the residual stress induced by heat treatments. It is shown that the quench-in residual stress is mainly generated by steep thermal gradients, which could reach the tensile strength level of the materials. The quench-in residual stress is partially relaxed during the ageing treatment as a result of plastic and creep deformation. The precipitation of γ' or γ'' plays an important role in the induction and relaxation of residual stress due to its significant effect on the plastic deformation behavior (such as tensile strength and creep rate) and expansion coefficient (volume shrinkage) at different temperatures. On the other hand, the precipitation behavior of γ' or γ'', such as nucleation rate and variant selection could be influenced by residual stress condition. Based on considering the interaction between residual stress evolution and precipitation reaction, a residual stress prediction model is carried out with experimental validation.

9:50-10:10

Hot Mechanical Behaviors for Alloy 800H Base and Weld Metals

Woo-Gon Kim[1], I.N.C. Kusuma[2], Injin Sah[1], Eung-Seon Kim[1], Seon-Jin Kim[2], Min-Hwan Kim[1]
1 Korea Atomic Energy Research Institute, Korea
2 Pukyong National University, Korea

A very high temperature reactor (VHTR) is one of the most promising Generation-IV reactors for the economic production of electricity and hydrogen. Alloy 800H, which is a modification of Alloy 800 developed for applications in which additional creep resistance is required, is the primary candidate for use a control rod system (CRS), a hot has duct (HGD), a core barrel, core supports, and a shutdown cooling system (SCS) in the VHTR system. This alloy was approved for use up to 760˚C under ASME Code Section III Subsection NH for nuclear applications. However, the data of mechanical behaviours for the weld metal (WM) are not available in the ASME code or elsewhere, although the data for the base metal (BM) are available in some reported documents. Therefore, to prepare the design data for Alloy 800H WM, the hot mechanical behaviors such as the tension, creep, and creep crack growth (CCG) data should be investigated and the mechanical tested database for the alloy should be established with various test data. In this study, the hot tension and creep behaviors for Alloy 800H WM fabricated by a gas tungsten arc welding (GTAW) procedure were comparatively investigated with those of the BM through the hot tensile tests from room temperature to 900˚C and a series of creep tests at 800˚C. And the hot-tensile curves for Alloy 800H BM and WM were modelled in comparison with the two models of the Ramberg-Osgood (R-O) model known as a typically strong tensile model and the General Atomic (GA) model proposed as a proper model herein. In addition, the CCG behavior for Alloy 800H BM was investigated in terms of C*-fracture parameter through a series of CCG tests at 800˚C. The equation for evaluating the CCG rate for Alloy 800H BM was proposed using the plot of da/dt vs. C*.

10:10-10:30

Dependency of Deformation Behavior on γ' Precipitates Formed by Various Heat Treatments in Haynes 282 Superalloy

Jin Hyeok Kim[1], Kyeong Yong Shin[1], Mathieu Terner[1], Byeong Ook Kong[1], Hyun Uk Hong[1]
1. Changwon National University, Korea

In this study, we investigated the microstructure features and the deformation mechanism of Haynes 282 superalloys in tension at 750˚C. The well-known strengthening phase in superalloy which is called γ precipitate was observed differently as various heat treatment conditions. We conducted the standard 2-step aging heat treatment (1010˚C/2h + 788˚C/8h) and modified 1-step aging treatment (800˚C/4h) which is more economical. Moreover, three different cooling rates were conducted to study mass effect which can occur in large scale products. All of the samples subjected different heat treatments were observed similar microstructure. However, the size distribution of γ precipitates was significantly different from each other. In all samples, about 20% of γ precipitates were precipitated with an average size between 12nm and 39 nm. The average γ precipitates size increased as the cooling rate from the solution temperature decreased. All four heat-treated alloys exhibited good mechanical properties at the high temperature of 750˚C with a yield strength in particular well over 620MPa. As it could be expected, the yield strength increased and the ductility decreased as the average γ' particles size decreased. All the alloys exhibited a mixed mode of deformation characterized by shearing and bypassing. However, the dominant deformation mechanism depended on the γ characteristics resulting from different heat treatment conditions. Only 1-step aged specimens with the largest γ particles of 39nm size, which was furnace-cooled from solution temperature, showed a plastic behavior typical of a dislocations shearing mechanism while the other alloys showed an Orowan dislocations bowing and looping mechanism behavior. To enhance theoretical approach, the strength increment was calculated to predict the major operative deformation mechanism based on the precipitation strengthening model. The theoretical calculation was well agreed with the results of observation.

10:30-10:45 Tea Break

Chairs:
Hamish Fraser, The Ohio State University, USA
Zhongnan Bi, Central Iron and Steel Research Institute, China

10:45-11:10 Invited

Materials Genome Initiative: Accelerated Ni-based Single Crystal Superalloy Design

Chengbo Xiao[1], Jingyang Chen[1], Xidong Hui[2], Zhenmin Du[2], Xuejing Shen[3]
1. Beijing Institute of Aeronautical Materials, China
2. University of Science and Technology Beijing, China
3. Central Iron and Steel Research Institute, China

Ni-based single crystal superalloys are key materials for hot section components of advanced aero engines and land based gas turbines. The successful experiences of General Electric (GE) and Pratt & Whitney (P&W) show that the use of Materials Genome Initiative (MGI) methods can accelerate the research and development of novel Ni-based superalloys. In the present study, the specific thermodynamic and kinetic database for Ni-based superalloys was founded preliminarily. The integrated design and screening of Ni-based single crystal superalloy composition were carried out combined with thermodynamic and kinetic calculations, machine learning technique and design experiences. High-throughput preparation and characterization was carried out using techniques such as multitarget carousel oblique angle deposition, variable cross-section creep testing and original position statistic distribution analysis combined with laser-induced breakdown spectrometry (LIBS-OPA). An integrated multi-scale design method for microstructure and property of novel Ni-based single crystal superalloys was established based on the MGI techniques. The above work lays the solid foundation for changing the traditional developing pattern of Ni-based single crystal superalloys as well as shortening the developing period and reducing the developing cost. The 2nd generation Ni-based single crystal superalloy DD489 for gas turbines with high temperature capacity, good hot corrosion resistance and microstructure stability was developed successfully.

11:10-11:35 Invited

Precipitate-Mediated Dislocation Transformation in Superalloys

Yunzhi Wang[1], Longsheng Feng[1], Mike Mills[1]
1. The Ohio State University, USA

High-temperature alloys in general and superalloys in particular are strengthened by ordered intermetallic phases that are relatively stable at elevated temperatures. Because of their low symmetry, these ordered intermetallic phases have rather complicated deformation mechanisms that are difficult to uncover by experiment alone. In this study we use a combination of ab initio calculation, phase field simulation and experimental characterization at individual dislocation level to illustrate how the interactions between dislocations and precipitates of a low-symmetry ordered

intermetallic phase such as gamma" ($D0_{22}$, tetragonal), the primary strengthening phase in IN718 superalloys, breed new particle dislocations, which may initiate twinning and other deformation modes. For example, two unstable stacking faults exist in gamma" phase, APB-like and CSF-like. These unstable stacking faults, once created, will transform spontaneously into nearby stable stacking faults on the generalized stacking fault (GSF) energy surface and generate new Shockley partial dislocations that do not exist in the system before the shearing events. Thus, the gamma" precipitates serve as a "dislocation-transformer" that transform incoming <110>/2 dislocations into Shockley partials (<116>/6) that are not part of the incoming full dislocations. By passing the same <110>/2 dislocation consecutively on one slip plane from an active Frank-Reed source, we found that, for each type of <110>/2 full dislocations, only one specific Shockley partial prevails in the system. This could be one of the reasons why extensive micro-twinning is observed in these alloys. Understanding this precipitate-mediated dislocation transformation mechanism can further spark new ideas on alloy design, especially for tailoring the twinning mode. This work is supported by US NSF under grant the DMREF program (Grant No. DMR-1534826).

11:35-11:55

High-Speed High-Throughput Thermodynamic Phase Equilibrium Calculation and Its Application in Phase Field Simulation

Shuanglin Chen[1], Dongke Sun[2], Weisheng Cao[1], Duchao Lv[1], Fan Zhang[1], Yunzhi Wang[3]
1. CompuTherm LLC, China
2. Southeast University, China
3. The Ohio State University, USA

Phase field method (PFM) has achieved increasing prominence in recent years for microstructure simulation. However, the PFM has not been utilized directly by designers for engineering applications since it has difficulties in being quantitative when applied to multi-component alloys. Any alloy-specific and quantitative phase field simulations require thermodynamic and phase equilibrium information as input for millions of different chemical compositions. Direct calculations of the required thermodynamic quantities for each composition from thermodynamic models are prohibitively expensive computationally, especially for multi-component and multi-phase alloys when the number of components is greater than four. To overcome this computational bottleneck, a thermodynamic data management system, PanDataNet, is developed to provide PFM with the required thermodynamic quantities. PanDataNet manages required properties by PFM on a net of temperature and composition grids. Properties on each grid are calculated only once from PanEngine (thermodynamic and phase equilibrium calculation engine) and only those grid points needed by PFM will be calculated. PanDataNet can save all calculated properties for future use. The speed to access PanDataNet is several orders of magnitude faster than the direct access to PanEngine. An example will be given for the direct coupling of PanDataNet and PFM in microstructure simulation of a multi-component alloy and the results demonstrate the computational efficiency of PanDataNet, a high-speed high-throughput thermodynamic data management system.

C1. Light Metals and Alloys-Aluminum: III

Symposium Organizers :

Baiqing Xiong, GRINM Group Co. Ltd., China; Yoshihito Kawamura, Kumamoto University, Japan; Young Min Kim, Korea Institute of Materials Science (KIMS), Korea; Jian-Feng Nie, Monash University, Australia; Diran Apelian, Worceste Polytechnic Institute, USA

Wednesday AM Room: Presidium Conference Room (4th Floor)
August 21, 2019 Symposium: C1

Chairs:
JaeHwang Kim, Korea Institute of Industrial Technology, Korea
Yong Jiang, Central South University, China

8:35-9:00 Invited

Formation Thermodynamics and Thermal Stabilities of Coherent L12 Nano-Precipitates in Al-RE Alloys

Yong Jiang, Chaomin Zhang, Fuhua Cao, Yiren Wang, Central South University, China

The thermal stabilities of nano-precipitates are critical in determining the service temperature of metallic alloys. Taking the Al-RE (rare earth) alloys as an exemplary case, we performed intensive first-principles investigations on solute segregation, coherent strains, and formation energies of L12 nano-phase bulks and interfaces. The following insights were obtained. Only matrix- dissolved solutes can strongly substitute the X sublattice sites in L12-Al3X. The Al3Er(L12)/Al3Zr(L12) or Al3Sc(L12)/Al3Zr(L12) interface has nearly zero formation energy. Zr segregation to the Al/Al3Er(L12) or Al/Al3Sc(L12) interface is in favor of forming a Zr-rich shell. Based on the classic nucleation theory, first-principles energetics results were further employed to evaluate the precipitation thermodynamics and relative stabilities of various possible complex structures of L12 nano-phases, revealing that ternary L12-Al3(ErxZr1-x) or L12-Al3(ScxZr1-x) precipitates tend to form the

Al_3Er-core+Al_3Zr-shell or the Al3Sc-core+Al_3Zr-shell structure with a sharp core/shell interface. The effects of temperature and the Er/Zr or Sc/Zr atom ratio on the relative stabilities of these L12-phase nano-structures in Al were also discussed. Finally, all the results were combined to establish the thermal stability advantage of core-shelled L12 nano-phases in Al alloys, which can provide the fundamental understanding of diverse experimental observations in the literatures.

9:00-9:20

Microstructural Evolution and Mechanical Properties of Mg Alloy Processed by Multi-Pass Caliber Rolling

Hui Yu, Saoda Fan, Xiaorui Dong, Hao Liu, Jianan Qin, Mingxu Yang, Fuxing Yin, Hebei University of Technology, China

Magnesium alloys are the lightest structural metals, and have good physical and mechanical properties that make them extremely attractive for applications requiring lightweight materials. The global market for magnesium alloys has steadily expanded in the past decade, stimulated by the strong demand from the automobile and electronic industries for lightweight magnesium components. In order to meet the demand of new high-performance alloys and overcome technical challenges, severe plastic deformation is becoming an effective way to manufacture high-performance and ultrafine-grained Mg alloy.

A promising process to produce high strength wrought magnesium bulk materials in a more cost-effective manner is multi-pass caliber rolling. Although this process has been used for many typical traditional alloys such as steel and titanium alloy, the caliber rolling of Mg alloy is relatively new.

In this study, the effect of various multi-pass reduction, caliber rolling temperature and rolling speed on the microstructure, texture evolution and mechanical properties of caliber rolling AZ31 magnesium alloys were systematically studied by means of OM, SEM/EBSD, TEM and tensile tests.

The results shown that the average grain size decreases with accumulated strain/increased pass. As a result, the tensile yield strength, the ultimate tensile strength and compressive yield strength improved significantly with reduction in anisotropy. However, the elongation was firstly increased and then decreased.

In addition, rolling speed has greater influence on the microstructure of AZ31 magnesium alloy rather than the rolling temperature. The smaller caliber rolling speed, the finer grain can be obtained. The optimal rolling parameters of AZ31 magnesium alloy are as follows: rolling temperature: 350˚C, the rolling speed: 0.2m/s, and the TYS, UTS, CYS and elongation were 320MPa, 356MPa, 321MPa and 13%, respectively.

Compared with other wrought AZ31 alloy with conventional fabrication methods such as ECAP, ARB, MDF and so on, the caliber rolling seems an idea approaching for achievement of high-performance commercial Mg alloys.

9:20-9:40

Understanding Corrosion Mechanisms of Magnesium Alloys from a Microstructure Perspective–A Review

Rongchang zeng, Shangdong University of Science and Technology, China

Magnesium (Mg) alloys with low density and high specific strength, have attracted great attention for potential applications in 3C (Computer, Communication and Customer electronic) products, aerospace, automobiles, high speed rail and biodegradable materials. However, they are susceptible to corrosion in aggressive environments due to the lower potential of Mg. The poor corrosion resistance of Mg alloys restricts their extensive applications. So far, understanding corrosion mechanisms of magnesium alloys have become a critical challenge. Alloying and subsequent processing lead to a change in microstructure and corrosion behaviour. This review reveals the cutting-edge advance in corrosion and protection of magnesium alloys. Particularly, corrosion types (i.e. galvanic corrosion, pitting corrosion, filiform corrosion, intergranular corrosion, exfoliation corrosion, stress corrosion and corrosion fatigue) and mechanisms of magnesium alloys are disclosed and discussed from a microstructure perspective. The discussion on the influence of microstructure (e.g. grain size and texture, the size, morphology and distribution of secondary phases or intermetallic compounds (quasi-crystals, long-period stacking ordered (LPSO) structure), and dislocations, twins as well on corrosion is stressed. The relationship between the formation and degradation mechanism of chemical conversion coating, layered double hydroxides (LDH), and micro-arc oxidation (MAO)/polymeric composite coating and the intermetallic compounds in Mg alloy substrates is also probed. The methods with multi-perspectives to characterize corrosion behaviour are proposed.

9:40-10:00

Underlying Mechanisms for the Enhanced Plasticity of Mg Alloys

Suqin Zhu, Simon P. Ringer, The University of Sydney, Australia

As the lightest structural metallic materials, Mg alloys have been attracting more and more attention in

science and engineering communities. However, the poor plasticity of the alloys greatly limits their industrial applications. We have developed a high strain-rate rolling (HSRR) process to effectively produce Mg alloys which possess attractive combinations of strength and ductility. During this thermomechanical process, the formability of Mg alloys is significantly improved, and untrafine-grained microstructure is obtained.

Underlying fundamental mechanisms for the formability and microstructure evolution has been investigated. Electron backscatter diffraction (EBSD), transmission Kikuchi diffraction (TKD) and conventional and high-resolution transmission electron microscopy (TEM) were used in the study, which provided both statistical and detailed atomic-level data for the same sample. In particular, the TKD and TEM observations were conducted at the same site of the specimen, enabling the integrated analysis of grain orientation and crystallographic defects.

The results shows that twinning and stacking faults play a critical role during the HSRR process. The key contribution to the enhanced plasticity is the formation of stacking faults in the high-intensity twin segments. The stacking faults interact with each other and form perfect glissile non-basal slip dislocations, which is the key contribution to the working hardening capacity and plasticity. Additionally, the leftover stacking faults nucleates low angle grain boundaries, and then contribute to the enablement of the dynamic recrystallisation, resulting in significant grain refinement.

10:00-10:20

A Pressure-Driven Mould Filling Model of Aluminium Alloy Melt/Semi-Solid Slurry Based on Rheological Behaviour

Zhen Ma, Huarui Zhang, Fangfang Wang, Hu Zhang, Beijing University of Aeronautics and Astronautic, China

Pressure-driven mould filling ability of aluminium alloy melt/semi-solid slurry is of great significance in pressure casting process such as low pressure die casting, high pressure die casting and squeeze casting, and the rheological behaviour of the alloy has a crucial effect on the mould filling ability according to fluid dynamics. In this paper, A356 alloy was employed as an example to clarify the rheological behaviour of aluminium alloy. The solid fraction and enthalpy change of A356 alloy during solidification was experimented by differential scanning calorimeter, and the rheological behaviour of the alloy in semi-solid state was investigated by rotational rheometry. The rheological behaviour of the alloy obeyed the power law model and was effected by temperature. The stop of mould filling was thought to be attributed to pressure loss caused by viscosity during flow of the melt/semi-solid slurry. The melt/semi-solid slurry stopped filling when the pressure loss was equal to the driving pressure. The steady-state rheological behaviour of the alloy in semi-solid state was modelled with shear rate and temperature as parameters. Pressure loss caused by viscous flow and heat transfer between the alloy and the mould was calculated and coupled during mould filling of the melt/semi-solid slurry. A pressure-driven mould filling model of aluminium alloy melt/semi-solid slurry was established based on steady-state rheological behaviour. The model was employed to predict the filling length of melt/semi-solid slurry in pressure casting process, and the results indicated that the model could provide a quantitative approach to characterize the pressure-driven mould filling ability of aluminium alloy melt/semi-solid slurry.

10:20-10:45 Tea Break

10:45-11:10 Invited

Role of Nanoclusters in Two-Step and Multi-Step Aging Behavior in Al-Mg-Si Alloys

JaeHwang Kim, Korea Institute of Industrial Technology, Korea

Weight reduction of automobile is required under consideration of CO_2 emission and enhancement of fuel efficiency. Al-Mg-Si alloys have been used for automobile panel due to their good age-hardening response. Generally, two-step heat treatment such as transportation at room temperature and baking process at around 170˚C for 1.2ks of Al sheets, is conducted for the production of Al panels. Nanoclusters formed during room temperature does not directly transform into the strengthening β" phase during two-step aging at 170˚C. This is called the negative effect of two-step aging behavior in Al-Mg-Si alloys.

In order to understand the effect of clustering during room temperature on two-step aging behavior, influence of natural aging time on two-step aging behavior is investigated. Not only harmful but also useful nanoclusters are formed during natural aging, resulting is 'three stages of two-step aging'. It is also confirmed that even though the harmful cluster is formed during natural aging, the positive effect during two-step aging is confirmed through the 'atomic rearrangement' during aging at 250˚C.

Effect of pre-aging and step-quenching on clustering formation and following artificial aging such as two-step and multi-step aging behavior is investigated since nanoclusters are competitively formed during low temperature aging. Detrimental clusters, Cluster (1) or Si-rich clusters, can be successfully suppressed by formation of Cluster (2). The two-step or multi-step aging behavior is discussed based on age-hardening phenomena.

11:10-11:30 Invited

Effects of Aging Treatment and Peripheral Coarse Grain on the Exfoliation Corrosion Behavior and Its Mechanism of 2024 Aluminium Alloy Using SR-CT

Shuangqing Sun, Fang Yi, Fengting Li, Xinyi Wang, Chunling Li, Songqing Hu, China University of Petroleum, China

2024 Al-Cu-Mg aluminium alloy has been widely utilized in aircraft and vehicles industries due to its excellent structural properties. However, 2024 aluminium alloy in certain aging states are vulnerable to exfoliation corrosion, which would greatly reduce its mechanical properties and shorten the integrated service life. In this work, the exfoliation corrosion behavior of 2024 aluminium alloy in different aging states was investigated through exfoliation corrosion test, together with SR-CT scan to achieve the 3D segementation of precipitated phases, corrosion cracks and corrosion products. The effect of aging treatment on exfoliation corrosion behavior were firstly studied. The results demonstrate that aging treatment has a significant effect on the distribution of the precipitated phase, and the precipitated phases continuously distributed along the grain boundary would contribute to IGC which is easily developed into exfoliation corrosion. The IGC and exfoliation corrosion sensitivity from high to low is in the order of peak-aged state, solution treated state and over-aged state. In addition, the effect of PCG structure on exfoliation corrosion behavior was discussed as well. The inner fine elongated grains structure was slightly corroded compared with the outer PCG structure, and the longest crack was located at the boundary between the two structures. The macro-galvanic corrosion due to the difference of electrochemical properties between the two structures is the main reason account for that phenomenon. This work may help us to understand the mechanism of exfoliation corrosion behaviour in 2024 aluminium alloy more intuitively.

11:30-11:50

Effects of Asymmetric Hot Rolling on Formability of 6061 Aluminium Alloy

*Mu Seob Jeon*g, Won Kee Chae, Jun Hyun Han, Chungnam National University, Korea; Ho Joon Park, Hyundai-steel, Korea

Because CO_2 gas contained in automobile exhaust gas causes global warming, CO_2 emission regulation for automobiles is strengthened. Therefore, aluminum alloy, which is a lightweight material, has attracted attention as a next-generation automobile plate.
Aluminum 6XXX alloy is widely used as automotive sheet material. It is made of Al-Mg-Si ternary system and small amounts of Ti and Mn are added for grain refinement. The aluminum 6XXX alloy has a low formability of 60%~70% compared to conventional automotive steel. Due to low formability, it is difficult to produce a complicated shape product. In addition, in order to improve the formability, Aluminum product is made by warm forming at about 300˚c . And the strength of the product is lowered. The age hardening to increase the strength lowered by warm forming raises the process cost.
After casting, the aluminum alloy has a low formability due to the strong development of <110>//ND texture. In addition, the average plastic strain ratio (r) of the cast aluminum 6xxx alloy is low as 0.7 to 0.8. Due to the low average plastic strain ratio, a defect called "earing" occurs during rolling. By applying shear stress, the average plastic strain ratio can be improved by developing <111>//ND texture. However, due to work hardening during rolling, the elongation will decrease. In this study, the effect of asymmetric rolling temperature on the texture of aluminum 6061 alloy is investigated. The formability of the alloy is evaluated. The texture of the rolled Al alloy sheet was analyzed by XRD.

11:50-12:10

Research on Heat Treatment Optimization of High Zn-Containing Al-Zn-Mg-Cu Alloy

Kang Du, Chinalco Group, China

The effects of single-stage, dual-stage solution treatment and retrogression re-ageing treatment on redissolution of alloying elements and mechanical properties change of high Zn-containing Al-Zn-Mg-Cu alloy were investigated in this paper. Microstructure evolution, conductivity change and tensile property comparison were occupied to optimize the solution treatment parameters. According to the OM, SEM and EDS analysis, the secondary phases existing in extrusion are mainly T(AlZnMgCu) phase and Al7Cu2Fe phase with a few of $MgZn_2$ phase. The melting point of the alloy is 476˚c by DSC test. According to the conductivity test and tensile property test results, dual-stage solution treatment lead to a better secondary phases solubility and better property stability than single-stage solution treatment. 460˚c /2h+470˚c /4h was recognize as optimal solution treatment parameter. The results also show that, dual-stage solution treatment has better solubility than single-stage solution treatment in the point of conductivity and AIMP view. The conductivity extremum could be as low as 15MS/m, and the AIMP value could goes down to 0.5J/g. RRA treatment leads to higher conductivity than traditional T6 heat treatment of the Al-Zn-Mg-Cu alloy. The highest tensile property in this alloy is 729MPa in ultimate strength and 10.3% in elongation. Dual-stage solution treatment also benefit the property improvement and stability for industrial production line than single-stage solution treatment.

C2. Light Metals and Alloys-Magnesium: III

Symposium Organizers :

Xianhua Chen, Chongqing University, China; Yoshihito Kawamura, Kumamoto University, Japan; Young Min Kim, Korea Institute of Materials Science (KIMS), Korea; Jian-Feng Nie, Monash University, Australia; Diran Apelian, Worceste Polytechnic Institute, USA

Wednesday AM
August 21, 2019

Room: 406 (4th Floor)
Symposium: C2

Chairs:
Bong Sun You, Korea Institute of Materials Science, Korea
Yuanding Huang, Helmholtz-Zentrum Geesthacht, Germany

8:30-8:55 Keynote

Texture Evolution of Ca-Containing Mg-Zn Alloys during Annealing

Nack J. Kim, Jae H. Kim, T.T.T. Trang, Jihyun Hwang, Postech, Korea; Byeong-Chan Suh, KIMS, Korea

Mg alloys have the lowest density among commercially available structural alloys, which can provide significant weight savings in automobiles. For the widespread application of Mg alloys, however, Mg alloys should overcome a critical shortcoming; poor formability at room temperature mainly originated from strong basal texture developed during thermomechanical processing. Although several Mg alloys show random/weak texture and accordingly good room temperature formability, most of such alloys rely on the usage of expensive rare earth elements. It has been recently reported that the addition of Ca to Mg-Zn alloys weakens and randomizes the texture, similar to the effect of RE addition on modifying the texture. The texture of these Ca containing Mg-Zn alloys can be described as the broadened angular distribution of basal poles along the transverse direction (TD) and split of basal poles along the rolling direction (RD) in as-rolled condition. However, a significant change in texture occurs after annealing process; splitting of basal poles toward the TD from the original RD in particular. Despite the weak texture intensity, their texture is less than ideal since one directional orthotropic texture developed during annealing would result in non-uniform deformation during stretch forming. However, the detailed mechanism of such texture evolution has not been clearly revealed yet. In the present work, an attempt has been made for having a better understanding of the texture evolution during annealing process of Ca containing Mg-Zn alloys. The details of their texture evolution have been analyzed by quasi-in-situ EBSD after various stages of annealing with particular emphasis on recrystallization and growth behavior.

8:55-9:20 Keynote

High Performance Magnesium Alloy Plate and Its Novel Process

Bin Jiang, Guangsheng Huang, Jiangfeng Song, Dingfei Zhang, Fusheng Pan, Chongqing University, China

Magnesium (Mg) alloys have attracted considerable attention for a promising application in the automotive and electronics owing to their high specific strength and high electromagnetic shielding. However, the application of wrought Mg alloys has been limited by poor room temperature ductility. It was ascribed to the large difference in critical resolved shear stresses (CRSS) between basal and prismatic slip in hexagonal close-packed (hcp) crystal structure in Mg alloy. This results in a lack of the active slips systems and can hardly offer an arbitrary shape change at the grain level. Conventionally extruded Mg alloy sheets possess poor mechanical properties due to the strong basal texture where c-axes of the grains are predominantly aligned parallel to the sheet normal. This brings about a poor deformation capability of sheet thinning and a stronger anisotropy and consequently results in limited number of available plastic deformation modes. In this work, a novel extrusion approach to get high strength magnesium alloy plates will be introduced through differential speed processing. A suitable constitutive model of differential speed extrusion is established to ameliorate the texture-dependent mechanical properties. The velocity evolutions of the extruded sheets at near-surface and mid-layer region are different due to the extra asymmetric shear deformation. This simple shear enforces the near-surface microstructure to exhibit more dynamically recrystallized grains having the c-axis tilted toward the extrusion direction.The yield stress of AZ31 alloy sheet has been increased from 161.2MPa to 179.9MPa and the elongation has been improved from 15.4% to 20.1%. Moreover, as for the high strength AZ61 alloy sheets, the ultimate tensile strength was increased from 387.9MPa to 427.1MPa and the yield stress was improved from 147.7MPa to 195.9MPa. Grain refinement and tilted weak basal texture obtained by differential speed extrusion process. This approach is an efficient substitute to increase the texture-induced softening and ductility and thus favorable for the thin sheet fabrication.

9:20-9:40 Invited

Searching for Stainless Magnesium Alloy – a First Principal Based Approach

Yang Guo, General Motors, USA; Mingfei Zhang, Liang Qi, University of Michigan, USA

A significant challenge for applications of Mg alloys is

their poor corrosion resistance and hence Mg alloys designs with built-in corrosion resistance are of significant interest. Corrosion can result from the coupling of anodic dissolution of Mg and cathodic reduction of water on impurities such as Iron (Fe)-rich second-phase particles. Experiments have shown that small quantities of Arsenic (As) or Germanium (Ge) can inhibit Mg corrosion, possibly slowing the hydrogen evolution reaction (HER) as the cathodic reaction on Fe surfaces. Since a broader experimental search across the periodic table for other Mg corrosion inhibiting elements is unavailable, we designed thermodynamic and HER criteria, and used high-throughput computations to search a pool of 68 elements including As and Ge that can segregate from bulk Mg to surfaces of Fe particles and impede the HER there. Our computational procedure predicts that six p-block elements meet these criteria, and they rank according to their ability to reduce H adsorption energies and the HER rate as follows: As > Ge > Si > Ga > P≈Al. Results for As, the most effective corrosion-inhibiting element, and Ge are in qualitative accord with recent experiments. While none of the 68 elements was found to enhance H adsorption, the six p-block elements reduce H adsorption via strong orbital overlap (Pauli repulsion) between their outershell orbitals and the s orbitals of H adsorbates. These p-block elements are also found to have the potential to reduce HER on surfaces of Ni second-phase particles in Mg according to the same criteria, but not on surfaces of Cu second-phase particles.

9:40-10:00 Invited

Carbon Nanomaterials Reinforced Mg Matrix Composites

Xiaojun Wang, Kun Wu, Harbin Institute of Technology, China

Carbon nanomaterils are considered as the ideal reinforcement for metal matrix composite, due to their ultra-high mechanical properties. However, CNTs were very chemically active and easy to get tangled. Thus, it is very difficult to fabricated CNTs reinforced metal matrix composite. In this paper, a novel liquid processing was developed to fabricate CNTs reinforced Mg matrix composites. The processing included pre-dispersion, semisolid stirring and ultrasonic vibration in Mg melts. And then the CNTs/Mg-6Zn composites were extruded. Pre-dispersion is necessary to obtain uniform dispersion of CNTs in CNTs/Mg-6Zn composites. In as-cast composites, the CNTs distribution was uniform. The good interfacial bonding between matrix and CNTs was observed. Moreover, Raman spectroscopy shows that the damage to CNTs was not evident during fabrication. Hot extrusion eliminated CNT segregation and improved CNT distribution. Compared with as-cast composites, the yield strength and ultimate tensile strength of the CNTs/Mg-6Zn composites were significantly enhanced. Graphene nanoplatelets (GNPs) reinforced magnesium (Mg) matrix composites were synthesised using the multi-step dispersion route. ell-dispersed but inhomogeneously distributed GNPs were obtained in the matrix. Compared with the monolithic alloy, the nanocomposites exhibited dramatically enhanced Young's modulus, yield strength and ultimate tensile strength and relatively high plasticity, which mainly attributed to the significant heterogeneous laminated microstructure induced by the addition of GNPs. With increasing of the concentration of GNPs, mechanical properties of the composites were gradually improved. Especially, the strengthening efficiency of all the composites exceeded 100%, which was significantly higher than that of carbon nanotubes reinforced Mg matrix composites. The grain refinement and load transfer provided by the two-dimensional and wrinkled surface structure of GNPs were the dominated strengthening mechanisms of the composites.

10:00-10:15

Effects of Twinning Deformation on Aging Precipitation and Hardening Response in AZ80 Mg Alloys

Renlong Xin, Feiya Liu, Chunpeng Wang, Qing Liu, Chongqing University, China

Mg17Al12 is the hardening phase in Mg-Al based alloys such as AZ80 and AZ91. It generally precipitates in two different forms: the coarse discontinuous precipitation and the fine continuous precipitation. The discontinuous phase may act as crack initiation and deteriorate the strength and ductility. The continuous precipitation is responsible for most of the age-hardening response. Obviously, promoting continuous precipitation is the key to enhance the mechanical properties of such alloys. Recently it has been found that the continuous precipitates prefer to nucleate within twins in Mg-Al based alloys. However, the effects of twinning deformation on the characteristic of precipitates and the subsequent age hardening response are not very clear. In this talk, we will present the effects of twinning, detwinning and multiple twinning on the size, morphology and distribution of precipitates in Mg-Al based alloys. Then the improvements in aging hardening and mechanical properties will be discussed. Moreover, it is known that Mg17Al12 is plate-like, formed on the basal plane of Mg matrix (named basal plates). These basal plates generally give poor strengthening compared to the prismatic plates formed in Mg-Y alloys. Currently, it is hard to promote prismatic plates in Mg-Al based alloys. Recently we found that the orientation of basal precipitates in AZ80 Mg alloy can be altered by coupling twinning, aging and detwinning processes. This gives the prismatic precipitates with their broad plane parallel to one of the {10-10} Mg. Such prismatic precipitates significantly improve the compressive and

tensile strength of AZ80 Mg alloys compared to the basal precipitates. This provides a new way to regulate precipitate orientation and hence its hardening response in Mg alloys.

10:15-10:30

Quasi-in-Situ EBSD Insight into the Role of Annealing in the Microstructure and Texture Behavior of Extruded Mg-Zn-Gd alloy

WASI ULLAH, Institute of Metal Research, CAS, China; Hong Yan, Rongshi Chen, Institute of Metal Research, CAS, China / University of Science and Technology of China, China

The present abstract reports a quasi-in-situ EBSD approach for studying the role of annealing in the microstructure and texture behavior of extruded Mg-1.58Zn-0.52Gd(wt%) bar alloy. The samples was annealed at 400˚c and increased the annealing time gradually to investigate the effect of annealing and annealing time on the microstructure. Based on quasi-in-situ EBSD the annealing temperature have significant influence on the microstructure and texture, it is seem to be static recrystallization (SRX) begins at the beginning of annealing treatment i.e 400˚c for 5 minutes. By increasing annealing time the average grain size increased from 16.9μm to 20.7μm as a result of merging the huge number of grains and some grains growth by increasing the annealing time. The texture is slightly converted from basal texture to rare earth texture. The rare earth texture favored the operation of both basal slip and {10-12} extensions twins, thus leading to improved strength of the alloy. It is hypothesized that the segregation of solutes atoms to the special boundaries greatly influences the recrystallization behavior and thus contributes to the formation of rare earth texture.

10:30-10:45 Tea Break

10:45-11:05 Invited

Research on High Performance Magnesium-Based Functional Materials

Xianhua Chen, Jingfeng Wang, Jian Peng, Yong Wang, Fusheng Pan, Chongqing University, China

The development and application of magnesium alloys have special important strategic significance, especially in solving the light weight problems of key equipment and important engineering. In the past ten years, the development and application of magnesium-based structural materials have made great progress, but the high-performance magnesium-based functional materials with great potential are relatively lagging behind. The key problem that restricts high-performance magnesium-based functional materials is that the functional properties and mechanical properties of magnesium alloys are difficult to achieve and even contradict each other. Aiming at the problems faced by magnesium-based functional materials, we carried out basic scientific research for improving the comprehensive performance of magnesium-based functional materials. The effects and mechanisms of purification, asymmetric deformation, second phase, solid solution atoms and surface modification on mechanical properties and functional properties of magnesium alloys such as electromagnetic shielding, damping, thermal conductivity, corrosion degradation and biocompatibility were clarified. New synergistic regulation criteria and theory for functional properties and mechanical properties of magnesium-based functional materials were constructed recently, and a series of new high performance magnesium-based functional materials and their preparation methods were developed. These high performance magnesium-based functional materials have achieved engineering applications in aerospace, railway vehicles, automotive, 3C products and other areas.

11:05-11:25 Invited

Development of High Performance Magnesium Base Metal Matrix Nano Composites for Aerospace Applications Using Powder Metallurgy Technology

Spartak Makovskyi, Vyacheslav Boguslayev, Volodymir Klochykhin, Volodymir Lukinov, MOTOR SICH JSC, Ukraine; Vadym Shalomeyev, Eduard Tzyvirko, MOTOR SICH JSC, Ukraine / Zaporozhye National Technical University, Ukraine

Application of lightweight high strength magnesium based materials in the contemporary aero engine manufacturing and rotorcraft industries plays an important role in attaining high performance characteristics, such as low specific fuel consumption, higher payload and low emissions level.

Cast magnesium alloys of Mg-Al-Zn system are widely used for the manufacture of structural parts of aero engines and rotorcraft gearboxes thanks to their low specific gravity, relatively high strength and high castability. However, this class has some disadvantages, such as low operation temperature (up to 150°) and susceptibility to internal porosity. Therefore, at present the development of lightweight magnesium based materials of a new generation with improved room temperature mechanical properties and high temperature capability via control of the structure is of great current interest in the aerospace industry.

The paper presents data on the development of a magnesium metal matrix nano composite (MMNC) on the basis of a magnesium cast alloy of Al-Mn-Zn system with the use of carbon nano particles as a reinforcement phase.

A series of experimental samples of MMNC has been

fabricated by the stir casting process using a magnesium casting alloy of Mg-Al-Zn system as a matrix. Incremental additives of carbon black and nanographite were added into the melt as a reinforcement phase in the form of consolidated pellets. In order to increase the inoculation effect of the carbon nanoparticles the chemical composition of the matrix alloy was tailored within the alloy specification ranges based on a thermodynamic calculation.

Preliminary a master alloy was produced by making a highly homogenous mix of the matrix alloy elements and the reinforcement by powder metallurgy processing route to obtain consolidated pellets.

Mechanical tensile tests of MMNC specimens demonstrated a unique set of improved properties; a 45% increase in the ultimate tensile strength has been attained as compared with a commercial magnesium alloy MJI-5 with simultaneous improvement in ductility. A higher stress-rupture strength at elevated temperature was also achieved. The new MMNC displayed a lower susceptibility to hot tearing.

Metallographic examination and the electron microprobe analysis of the MMNC showed a pronounced grain refinement effect, uniform distribution of Mg17Al2 on the grain boundaries and high homogeneity of the micro- and microstructure, which contributed to attaining more consistent mechanical properties of the material. Based on the results of the study a mathematical model of the new comm\position was developed and a mechanism of the influence of the carbon particles on the structure and mechanical properties has been put forward.

One of the key elements in the concept of the MMNC is the powder metallurgy technology, which ensures effective introduction of the carbon nano particles into the alloy and their uniform distribution. The new MMNC is a promising lightweight high strength material for a cost-efficient production of critical structural components of aero engines and rotorcraft assemblies.

11:25-11:40

Atomic-Scale HAADF-STEM Study of Tilt Boundaries in Magnesium Alloys

Yuman Zhu, Jian-Feng Nie, Monash University, Australia; Shiwei Xu, Baowu Steel Group Corporation, China

Mg alloys are the lightest structural metals that have tremendous potentials to improve energy efficiency and system performance in automotive, aerospace and electronics industries, as well as for rechargeable batteries and biomedical applications. Previous studies have shown that the addition of minor amounts of rare-earth (RE) or Ca alloying elements can produce appreciable effects on formability and mechanical properties of Mg. Furthermore, some recent work indicated that grain boundary characters play a critical role in determining these mechanical properties of Mg alloys. However, the related atomic-scale mechanisms remain poorly understood because direct experimental observations for local structures and chemistry of grain boundaries remain very limited. This situation has restricted the attempt to further improve the performance of existing magnesium alloys, and to develop new alloys. The high-angle annular dark-field scanning transmission electron microscopy (HAADF-STEM) has been proved to be a powerful technique in the study of Mg alloys. Especially, it can reveal the existence of distinct solute clusters in the matrix and the occurrence of a periodic segregation of solute atoms in different types of fully-coherent twin boundaries in Mg alloys. In this work, we will report our recent findings on the study of microstructures in the deformed and annealed Mg alloys using atomic-resolution HAAD-STEM imaging technique. It is found that the deformed microstructures of these alloys always contain many local areas which are made of nano-sized grains. These nanograins exhibit strong texture and a range of tilt boundaries are detected between these nanograins. Segregation of alloying atoms occurs in the tilt boundaries either with or without further annealing of the cold deformed sample. Also, these segregated atoms form a range of unique, chemically ordered patterns specific to different types of tilt boundaries. The results will provide a solid experimental basis for any further study of grain boundary characters, such as energy, mobility and stability, and eventually for the establishment of their relationships with the material performance.

11:40-11:55

Overview of Advancement and Development Trend on Magnesium Alloys based on 《Journal of Magnesium and Alloys》

Yan Yang, Xiaodong Peng, Tiancai Xu, Jiangfeng Song, Fusheng Pan, Chongqing University, China

Magnesium alloys are characterized by their low density, high strength, large modulus of elasticity, good heat dissipation, good shock absorption, greater ability to withstand impact load than aluminum alloys, good corrosion resistance to organic matter and alkalinity. According to the statistical analysis of literature data collected by Web of Science Core Collection, it can be found that the growth rate of publications on magnesium alloy during 2008-2018 is significantly higher than the overall growth rate of alloy research papers. In the past 11 years, the Web of Science Core Collection has collected 21440 papers on magnesium alloys, averaging nearly 2000 papers annually, of which 2768 papers were collected in 2018, an increase of 206% over 2008, accounting for more than one fifth of the total literature on alloy research. Magnesium alloys have become an important lightweight metallic structural material and have been widely studied worldwide. As the only journal focusing on magnesium alloy research which devoted to

the coverage and dissemination of global research on magnesium alloys. This article statistically analyzes all the academic articles published by Journal of Magnesium and Alloys from 2013 to 2018 and compares them with all the articles containing magnesium alloy in their titles on the Web of Science during this period. The development trends of magnesium alloys are summarized based on these articles, and the influence and academic value of the articles published by the Journal of Magnesium and Alloys are summarized as well. This paper hopes to better realize the value of JMA, help better spread the academic research of magnesium alloys, and promote the development of global magnesium alloy research.

D. Advanced Processing of Materials: IV

Symposium Organizers :

Wanqi Jie, Northwestern Polytechnical University, China; Jianguo Li, Shanghai Jiaotong University, China; Hideyuki Yasuda, Kyoto University, Japan; Myoung-Gyu Lee, Seoul National University, Korea; Huijun Li, University of Wollongong, Australia; Dan Thoma, University of Wisconsin- Madison, USA

Wednesday AM Room: International Reporting Hall (3rd Floor)

August 21, 2019 Symposium: D

Chairs:
Hongbiao Dong, University of Leicester, UK
Feng Liu, Northwestern Polytechnical University, China

8:30-8:55 Invited

Aplication of Non-Equilibrium Dendritic Solidification Model Considering Thermo-Kinetic Correlation in Twin-Roll Casting

Feng Liu, Northwestern Polytechnical University, China

Upon non-equilibrium solidifications, the dendritic growth, generally as precursor of as-solidified structures, has severe effects on subsequent phase transformations. Considering synergy of thermodynamics and kinetics controlling interface migration and following conservation of heat flux in solid temperature field, a more flexible thermo-kinetic modeling for the dendritic growth is herein developed for multi-component alloys, where, two inherent problems, i.e. correlation between thermodynamics and kinetics (i.e. thermo-kinetic correlation), and theoretical connection between dendritic model and real processing, have been successfully solved. Accordingly, both the thermodynamic driving force G and the effective kinetic energy barrier Q_{eff} have been found to control quantitatively the dendritic growth (i.e. especially the growth velocity, V), as reflected by thermodynamics-kinetics trade-off. Compared with previous solidification models, it is the thermo-kinetic correlation that guarantees quantitative connection between the realistic parameters and the currently theoretical framework, as well as more reasonable description for kinetic behaviours involved in the dendritic growth. Appling the present model into the vertical twin-roll casting (VTC), a good prediction for kiss point has been performed, which influences significantly alloy design and processing optimization. This work deduces quantitatively the thermo-kinetic correlation controlling the dendritic growth, and by proposing the parameter-triplets (i.e. G Qeff V), further opens a new beginning for connecting solidification theories with industrial applications, such as the VTC.

8:55-9:15

Solute Redistribution Ahead of Solidification Fronts and Rolling Deformation in Cu-Ag Eutectic Alloy

Jiehua Li, Montanuniversität Leoben, Austria

Solute partitioning and redistribution ahead of solidification fronts is one of the dominant factors affecting solidification microstructure. In this contribution, solute partitioning and redistribution ahead of solidification fronts in Cu-Ag eutectic alloys produced by directional solidification technique has been investigated in a multi-dimensional multi-scale manner by scanning electron microscopy, transmission electron microscopy and atom probe tomography. Furthermore, the ultra-strong magnetic field (0.5T, 1.0T) was also employed to elucidate the evolution of solidification fronts and thereby to reveal eutectic growth behaviours of Cu-Ag eutectic alloys. The obtained results were compared with classic eutectic growth modes under different solidification conditions. Finally, the directionally solidified Cu-Ag eutectic alloy was deformed by rolling in order to understand the role of heterophase interfaces on deformation behavior. During rolling, the initial <220> fibre texture was gradually shifted to a Brass type texure for both Ag and Cu phases. More interestingly, a similar path of texture evolution was observed for both the phases at all strain levels. The in-depth transmission electron microscopy analysis revealed that the Ag lamellae deformed by twinning, while the Cu lamellae deformed by twinning and dislocation slip. Furthermore, the special cube-on-cube and twin heterophase interfaces facilitated co-deformation and co-rotation of the adjacent Ag and Cu lamella due to a strong latent hardening effect, which stimulated a similar texture evolution for both phases. The correlation of microstructure and hardness of the rolled samples showed that interlamellar spacing (λ) plays a more important role in strengthening below λ < 100nm. This contribution provides a novel way to

produce the materials with lamella structure using directional solidification technique and elucidates the deformation mechanisms of the materials with lamella structure using rolling.

9:15-9:35

Thermophysical Properties and Microstructural Evolution of Highly Undercooled Ti-Ni Alloys

Pengfei Zou, Haipeng Wang, Chenhui Zheng, Liang Hu, Bingbo Wei, Northwestern Polytechnical University, China

The Ti-Ni alloys are common materials, which are widely used in aerospace, mechanism and biomedical industry due to its wonderful shape memory effect, good biocompatibility and mechanical properties. Many researches are focus on the technologies and heating process during solidification process, while the studies on the thermophysical properties and structure of the Ti-Ni liquid alloys are indeed important and necessary, which are great helpful for controlling he solidification process and computer simulation. And the microstructural evolution of the material is directly related to the final performance of the material. For the Ti-Ni alloys, Ti76Ni24, Ti50Ni50 and Ti39Ni61 were chosen to obtain the densities by both electrostatic levitation (ESL) technique and molecular dynamics (MD) simulation. A nonlinear relationship between density and temperature was found in liquid Ti50Ni50 alloy. And the densities of other liquid Ti-Ni alloys exhibit linear dependences on temperature. The liquid Ti-Ni alloys show strong negative excess volumes, and the dependence of excess volume on temperature of Ti50Ni50 alloy is different with other Ti-Ni alloys. Besides, the surface tensions of the three liquid Ti-Ni alloys were also measured by ESL combined oscillation drop technique. The surface tensions of the liquid Ti-Ni alloys increase with the decrease of undercooling. The good agreement of the liquid densities between experiments and simulations proves the reliability of the MD simulation. Thus, the structural information could be derived from the pair correlation function (g(r)) and static structure factors (S(q)). A split of the second peak of the partial pair correlation function suggests various clusters existed in liquid Ti-Ni alloys. And it is inferred that the tetragonal bipyramid structure may exist from the split position. Analyzing the Ni-Ni and Ti-Ni pair correlation function, the Ni-Ni bonds would like to transform to Ti-Ni bonds with the increase of Ni content. Furthermore, the microstructural evolution of the Ti50Ni50 alloy was investigated under electrostatically levitated condition. With the increase of undercooling, the growth velocity of the TiNi intermetallic compound rises monotonously. More importantly, the order-disorder transition is trigged in sufficiently undercooled state.

9:35-9:55

Liquid State Property and Solidification Mechanism of Zr-Ni Alloys Investigated under Electrostatic Levitation Condition

Lei Wang, Haipeng Wang, Bingbo Wei, Northwestern Polytechnical University, China

The crystallization behavior within undercooled metallic alloys has attracted much attention due to its significant influence on their physical and chemical properties. Several interesting phenomena have been discovered in alloy systems with intermetallic compounds, such as Zr-Ni, Cu-Zr and Fe-B alloys. The liquid and solid structures of compounds are much more complicated than those of pure metals and solid solution alloys. That means some unusual liquid state phenomena, like liquid-liquid transition may exist, which undoubtedly affects the subsequent nucleation and dendritic growth. In this work, the liquid state properties and solidification mechanisms of ZrNi, Zr_2Ni intermetallic compounds and Zr64Ni36 eutectic alloys were investigated by electrostatic levitation(ESL) technique. The superheating level was found to have a great influence on the solidification processes of both ZrNi and Zr_2Ni intermetallic compounds. For ZrNi alloy, there were two solidification pathways under different superheating levels. If the superheating was less than 150K, double-recalescence phenomenon occurred during solidification, which was the metastable solid phase transition from B2 to B33 structure. When the superheating was large enough, the undercooling reached 286K and only one recalescence occurred subsequently. The solid-liquid interface on the surface of the levitated sample displayed the characteristic of pentagonal symmetry. For Zr_2Ni alloy, the relation between liquid undercooling and superheating followed a sigmoidal curve, which was probably attributed to the liquid structure transition. Besides, the solidification kinetics and microstructure morphology were studied to explore the solidification characteristics of Zr-Ni alloys. Interestingly, for Zr_2Ni alloy, the dendritic growth velocity displayed a parabolic relation versus undercooling, which followed the diffusion-limited growth mechanism. In addition, the liquid state properties, such as density and viscosity, were measured to understand the solidification mechanism for Zr-Ni alloys.

9:55-10:15

Microstructure, Strengthening and Toughening Mechanisms for Ti-Zr-Nb Refractory High-Entropy Alloys

Xidong Hui, University of Sciecne and Technology Beijing, China

The concept of high-entropy alloys (HEAs), which is a brand new alloy design strategy, was first proposed in

the 1990s. The concentrations of all principle constituent in HEAs are usually near queal to each other and higher than traditional alloys. Ascribed to the "high-entropy effects" originated from the unique compositional characteritics, HEAs usually possess unique features, such as high pahse stability and sluggish diffusion. Using the concept of HEAs, refractory high-entropy alloys based on refractoty lements was proposed and have attracted increasing research interest.

Nevertheless, research of HEAs is still at an initial stage, and many scientific issues are urgently needed to be addressed. First of all, the previous reported refractory HEAs usually contained large amounts of high-cost and high density elements, resulting in costly and high density alloys, and hence hindering their industrial applications. Secondly, the researches on predicting thermodynamic and mechanical proterties for refractory HEAs from computational simulation are rarely reported, and the correlation between phase formation and mechanical properties needs more investigation. Finally, the existing refractory HEAs usually showed only compression properties, but the tensile properties are much more important in industrial applications. Thus, the development of refractory HEAs which possess excellent tensile properties and investigate the ductilization and toughening methods is very important for further development of refractory HEAs. In this presentation, the microstructure, strengthening and toughening mechanism of Ti-Zr-Nb based HEAs have been systematically studied. Reliable random solid solution structure was constructed for TaNbMoW and TiZrNbHf quarternary alloys. The phase structure, thermodynamics and elastic properties have been calculated by using first-principle calculations. These calculations are hopeful to provide theoretical guidance for the compositional design and development of novel refractory HEAs. Ti-Zr-Nb-Mo-V HEAs with high specific strength and Ti-Zr-Nb-Hf HEAs with excellent tensile strength and ductility were fabricated. And the strengthening and toughening mechanisms for these HEAs were investigated. The results indicate that TiZrNbHf HEAs may be a promising prototype alloy system for further development of refractory HEAs for high temperature applications.

10:15-10:35

On the Prediction of Casting Defects: from Macrosegregation to Multi-Defects Modelling

Jun Li, Shanghai Jiao Tong University, China / University of Leicester, UK; Hongbiao Dong, University of Leicester, UK; Jianguo Li, Shanghai Jiao Tong University, China

Casting defects, including macrosegregation, shrinkage cavity, porosity, and inclusion, seriously affect the materials performance and even lead to the failure of the component that made of the casts. It is very important to study the formation processing and mechanism of these defects. The formation of these defects which result from the combined action of multi-physics filed is a complex process. These process including the nucleation, growth, floating (or settling) of both inclusion and equiaxed crystals; growth and fragmentation of dendritic crystals; solidification shrinkage; solute redistribution and migration; etc. It is a multiphase, multi-physic field and multi-scale subject. Therefore, it is a big challenge to predict these defects together in one model.Based on the dendritic-equiaxed & columnar macrosegregation model which we have established previously, a four-phase solidification model that further consider the gas phase, which supplements the volume reduction of solidification shrinkage, has been established to realize the prediction of shrinkage cavity in metal solidification process. For the prediction of inclusion, in order to distinguish the difference between exogenous and endogenous inclusions, two models had been established respectively: i) for exogenous inclusions, the coupling of Discrete Phase Model (DPM) and four-phase solidification has been considered, which has the possibility to track the moving of inclusion particle; ii) for endogenous inclusions, inclusion-combined macrosegregation model, which coupling the inclusion growth theory with the multicomponent four-phase solidification model, has been established.After the verification by the experimental results in terms of macrosegregation, this multi-defects model has been implemented on the solidification process of steel ingot to investigate the formation process of macrosegregation, shrinkage cavity, porosity, and inclusion defects. Typical defects such as negative segregation in the bottom region, positive segregation in the top region, and A-segregation have been observed. The strong interaction behaviors between the shrinkage cavity, inclusion and macrosegregation had been observed.

10:35-10:45 Tea Break

10:45-11:10 Invited

Using Deep Neural Network with Small Dataset to Predict Solidification Defects

Hongbiao Dong, Shou Feng, Huiyu Zhou, University of Leicester, UK

Deep neural network (DNN) exhibits state-of-the-art performance in many fields including microstructure recognition where big dataset is used in training. However, DNN trained by conventional methods with small datasets commonly shows worse performance than traditional machine learning methods, e.g. shallow neural network and support vector machine. This inherent limitation prevented the wide adoption of DNN in material study because collecting and assembling big dataset in material science is a challenge. In this

study, we attempted to predict solidification defects by DNN regression with a small dataset that contains 487 data points. It is found that: Fully connected DNN which consists of 3 or more hidden layers shows its advantage over shallow neural network and support vector machine in that it can achieve higher prediction accuracy and better generalization performance. Through DNN regression, vast scattered experimental data in the literature can produce simple quantitive expression of specific material property as function of chemistry composition and processing parameters, etc. The derived mathematical expression can be used in the material defects prediction, new alloys development, and comparison with experimental results.Though DNN with big datasets is the best choice, DNN with small datasets and pre-training can be a reasonable choice when big datasets are unattainable. In material science, small datasets are common, and the problems to be solved have fewer input variables than that in image recognition. Thus, deep and narrow (neuron number in each hidden layer is small) neural network are suitable for material problems, such as solidification cracking susceptibility prediction in this paper, and pretraining using stacked auto-encoder is effective and necessary in the DNN regression of numerical small datasets. Study in this paper demonstrate that small/narrow DNN with small dataset and special training methods has huge potential for extensive applications in material study, especially for those multivariable nonlinear problems.

11:10-11:30

Distribution and Recovery of Cobalt through Copper Industry

Daiwei Feng, University of Science and Technology Beijing, China

Cobalt is an important metal which could be produced as byproduct from copper and nickel industry. Cobalt has significant applications in high-temperature alloys, cemented carbides, rechargeable batteries as well as catalysts. The demand for cobalt is growing rapidly in last decades. However, environmental management is an issue of interest concerning cobalt, particularly in Europe. The Swedish Environmental Protection Agency lists cobalt, together with cadmium, lead, and mercury, as a metal of concern in the environmental context. However, its distribution during the production process is not well established. In this study, the matte and slag of copper matte smelting have been characterized through XRD and SEM, in order to determine their mineral compositions and occurrence states. It indicates that copper is primarily lost in slag in the form of sulfide, while cobalt is mostly lost in the form of oxide. Based on the experimental results and available thermodynamic data, the activity coefficients of CoS in the matte were estimated as a function of mole fraction of FeS in the matte at 1250˚C. The distribution coefficients of cobalt between the matte and slag has been calculated based on experimental work.Since the distribution behavior of minor elements between matte and slag during the pyrometallurgical treatments of nickel-copper sulfide concentrates will affect the quality of the final products and the revenues gained from byproducts, the distribution study in the matte-slag system is necessary to achieve desirable control of minor elements. For example, cobalt loss to the slag phase during the smelting and converting processes is high and there is only 30 to 60pct of recovery to the matte phase. An increased understanding of the fundamental mechanisms governing these losses could help further improve production efficiencies. A number of investigations have been carried out for the distribution of minor elements both between molten metal and slag and between matte and slag during copper sulfide smelting and converting processes. However, only few studies were conducted on nickel-copper matte and the slag system. In this paper, the mineral characterization of matte and slag were performed to identify the mineral composition and occurrence state of copper and cobalt. The distribution behavior of cobalt between matte and slag during copper smelting was investigated using a high temperature equilibrium method as well as comprehensive phase analysis. Much effort has been made to recover valuable metals from copper slag, for instance by using beneficiation process, hydrometallurgical process, or pyrometallurgical process. The beneficiation process is considerable successful to recover copper from slow-cooled copper slag by flotation. However, this method requires a large occupation of land and high investment. On the other hand, significant amounts of gangues are present in the matte–slag mixture, so the acid consumption is large and the purification process is complex in the hydrometallurgical method. Recently, hydrometallurgical processes for cobalt recovery from slag by selective leaching of metal values were reported. For low content of cobalt in converter slag, however, plentiful slag is put through the entire process, resulting in high capital and operating costs for a practice process. Pyrometallurgy, in particular, is a widely used technology for recovering valuable metals from copper and cobalt slag. A reduction study was conducted by Zhai et al., in which activated carbon acted as the reductant and TiO_2 as the slag modifier to recover cobalt and copper from converter slag. Under the optimal conditions, the contents of copper and cobalt in depleted slag were 0.97 and 0.025pct, respectively. Besides the reducing agent, pyrite (FeS_2) or some other sulfides were also used as a vulcanizing agent and collector to reduce the content of valuable metals in slag.

E: Thin Films and Surface Engineering: IV

Symposium Organizers :

Chuang Dong, Dalian University of Technology, China; Hongbo Guo, Beihang University, China; Hiroshi Masumoto, Tohoku University, Japan; Ho Won Jang, Seoul National University, Korea; Mingxing Zhang, University of Queensland, Australia

Wednesday AM
August 21, 2019

Room: 312 (3rd Floor)
Symposium: E

Chairs:
Yue Zhao, University of Wollongong, Australia
Young-Rae Cho, Pusan National University, Korea

8:30-8:55 Invited

Application of Transition Metal Sulfides Synthesized by $(NH_4)_2MeS_4$ Precursors (Me: Metal)

Soo Young Kim, Chung Ang University, Korea

Recently, transition metal dichalcogenides (TMDs) including MoS_2 and WS_2 have attracted increasing attention because of their great potential as semiconductors of electronic devices such as field-effect transistors, organic photovoltaics, memory, logic, and energy storage devices.
First, TMDs were used in order to enhance the stability in air comparing to poly(3,4-ethylenedioxythiophene): poly(styrenesulfonate) (PEDOT: PSS). TMD layers with a polycrystalline structure were synthesized by a chemical deposition method using uniformly spin-coated $(NH_4)MoS_4$ and $(NH_4)WS_4$ precursor solutions. Organic light emitting diodes (OLEDs) and organic photovoltaic cells based on TMD showed two to six times longer stability in air compared with PEDOT: PSS based devices. Second, TMD layers were applied as the hole transport layer as well as the template for highly polarized OLEDs. The MoS_2 nanosheets were patterned by rubbing/ion-beam treatment. The use of patterned MoS_2 nanosheets not only tuned the polarization of the OLEDs but also dramatically improved the device performance as compared with that of devices using untreated MoS_2. Third, TMD nanosheets are used as efficient catalysts for hydrogen evolution reaction, which can potentially replace the expensive platinum catalyst. Finally, tungsten trioxide (WO_3) films synthesized by using TMD precursors, $(NH_4)_2WS_4$, was applied to electrochromic (EC) devices. It is shown that Au-doped WO_3 films are great candidates for the development of smart windows with high EC performance. This presentation will show us many applications of TMD materials.

8:55-9:20 Invited

Tunneling Magneto-Dielectric (TMD) Effect: Recent Advances and Future Perspectives

Yang Cao, Hiroshi Masumoto, Tohoku University, Japan

Single-phase material with multifunctional properties, such as combining both electronic and magnetic properties, holds potential for both fundamental science and device application [Nature 442, 759 (2006).]. In the case of granular ME composites, a BaTiO3/Ni ME compacted composite by virtue of elastic interactions between piezoelectric (Ba_2) and magnetostrictive (Ni) phases, wherein the strain arising from the magnetostrictive phase passes on the piezoelectric phase and generates an electric field. Similar ME effect was also observed in annealed $BaTiO_3$/Co thin films [Appl. Phys. Lett. 92, 062908 (2008).].
Different from the aforementioned strain-mediated MD effect, we recently discovered a kind of MD effect in FeCo-MgF granular nanocomposites, wherein superparamagnetic FeCo granules with sizes of 2~5nm are homogeneously distributed in MgF insulating matrix [Nat. Commun. 5, 4417 (2014).]. This dielectric enhancement is caused by the charge tunneling through the MgF barrier in each granule pair, whereby the tunneling rate depends on the relative orientation of the magnetic moments between two magnetic granules, i.e., the spin-dependent tunneling. By analogy with tunnel-type magnetoresistance (TMR) in granular films, we termed the tunnel-type MD (TMD) effect. These granular films have the practical advantage of thermal stability and do not require any additional treatment, such as binding, compaction, or annealing.
In this presentation, we reviewed the recent advances of this TMD effect and give future perspectives. We first clarified how the granular content determined the frequency dependence of the TMD response and the inter-granular distance play a crucial role in regulating the frequency response of the TMD effect [Appl. Phys. Lett., 111, 122901 (2017).]. From this perspective, the frequency response of the TMD effect was artificially controlled by in-situ insertion of several insulator layers [Appl. Phys. Lett., 113, 022906 (2018).]; this verified the important role of granular distribution played in the regulation of TMD response. Second, to improve the low-field TMD response, we fabricated a two-dimensional (2D) granular heterostructures, wherein a mechanism based on a balanced control of ferromagnetic and super-paramagnetic components has been proposed [Appl. Phys. Lett., 110, 072902 (2017).]. Our recent results have shown that the variation of CoFe granules has induced the high TMD responses $(\Delta\varepsilon'/\varepsilon'_0)$ from 2.3% to 4.3%, the enhanced effect was briefly discussed based on the variation in the spin polarization (PT) of magnetic Co-Fe alloy granules.

Theoretical prediction gives its maximum TMD limit of over 20% as if using the high spin-polarized materials with PT =1, e.g. half-metallic compound. The discovery of room temperature TMD effect would offer a new avenue to achieve the magnetoelectric response, as well as potential applications in magnetoelectric devices.

9:20-9:40

Preparation and Characterization of TiO_2 Nanoparticles by Two Various Precipitations

Shimin Liu, Zhinuo Wang, Yu Guo, Dongdong Liang, Weiwei Jiang, Chaoqian Liu, Hualin Wang, Nan Wang, Wanyu Ding, Dalian Jiaotong University, China

TiO_2 has become the most studied photocatalyst which has been widely used in wastewater treatment, photocatalytic degradation of organic pollutants, photolysis of water and other fields due to its high efficiency, low cost, stable physical and chemical properties. It is well known that the polymorphs of TiO_2 can be divided into anatase, rutile and brookite. Generally, TiO_2 is prepared either from minerals or from a solution of salts or alkoxides by such as the sulfate, chloride and one of the various processes including hydrothermal, coprecipitation, and sol-gel Understanding the nature of crystallization in nanoscale TiO_2 is important for its use in photocatalysis applications. This paper presents the preparation of TiO_2 nanoparticles by precipitation method using titanium tetrachloride and titanium oxalate as raw materials, respectively. The effects of calcination temperature on the structure, crystal size, morphology, energy gap and photocatalytic properties of TiO_2 nanoparticles were investigated. The obtained samples were characterized by thermogravimetry-differential scanning calorimetry, X-ray diffractometry, transmission electron microscopy, and ultraviolet visible spectrophotometer. The results show that with the increase of temperature, the crystal structure of TiO_2 nanoparticles gradually changed. The crystallization temperature of TiO_2 nanoparticles was 250˚C when titanium chloride was used, while it was 450˚C when titanium oxalate was used. TiO_2 powders began to form rutile phase at 450˚C when titanium chloride was chosen. Nevertheless, TiO_2 powders began to form rutile phase at 850° C when titanium oxalate was selected. With the increase of calcination temperature, the particle sizes of the two prepared TiO_2 nanoparticles increased. The grain size of TiO_2 powders obtained using the titanium oxalate was significantly larger than that using the titanium tetrachloride as raw materials heat treated at the same temperature. Lastly, the degradation of methyl orange by TiO_2 powders using the titanium chloride as raw material is as high as 90%, but the maximum degradation was only 39% when titanium oxalate was used.

9:40-10:00

Electrical-Resistivity Properties of Al-Co-Cr-Fe-Ni High-Entropy Alloy Thin Films

Chenyu Wang, Xiaona Li, Linxia Bi, Qing Wang, Chuang Dong, Dalian University of Technology, China; Peter Liaw, The University of Tennessee, USA

High-entropy alloys (HEAs) possess some basic electrical-resistivity characteristics [such as high resistivity values and low temperature coefficients of resistivity (TCRs)] of concentrated disordered solid-solutions due to their properties of highly chemical-disorder. However, the resistivity properties of HEAs still need more comprehensive and in-depth investigation, and the application potential of HEAs as thin-film resistive materials is also worth assessing. In the present work, the AlxCoCrFeNi (x=0.7,1) HEA films were prepared by magnetron sputtering. The resistivity properties of the HEA films from room temperature to 1078K were thoroughly analyzed and compared to the bulk AlxCoCrFeNi HEAs with similar compositions. Results showing: The AlxCoCrFeNi HEA films are consisted of face-centered-cubic (fcc) and body-centered-cubic (bcc) phases, which are more disordered than the bulk HEAs mainly with the B2 (ordered bcc) phase. Differences between the phase structures of the film and bulk AlxCoCrFeNi HEAs is the main reason for their different changing behavior of resistivity with temperature. The large decline of resistivity appeared at around 565K of the HEA films is attributed to their ordering transitions of the bcc to B2 phases, while this phenomenon does not exist in the bulk HEAs. On the premise of considering the s-d scattering effects (additional scattering occurred in transition metal alloys when electrons from the s band transfer to the d band), the parts of the resistivity curves before phase transitions of the HEAs are described. Important characteristics of the resistivity properties of AlxCoCrFeNi HEAs were also investigated, the high resistivity is mainly attributable to the severe lattice distortion (caused by the chemical disorder) and the s-d scattering effects, and the generalized diffraction model can be used to explain the near-zero TCRs. After comparing with the conventional thin-film resistive materials, the multiple-components advantage of HEAs shows contributions to the wider resistivity range of AlxCoCrFeNi films as well as their near-zero TCRs.

10:00-10:20

Theoretical Investigation of the Catalytic Activity of Goethite (α-FeOOH) for the Electrochemical Water Oxidation

Zhumin Li, Xiaona Li, Nanjun Li, Chuang Dong, Dalian University of Technology, China

In many applications (mold's internal), copper and

copper alloys not only pursue good conductivity and thermal conductivity, but also require its surface to have high hardness, good thermal conductivity and high temperature corrosion resistance. The surface strengthening method can be used to improve the surface properties while keeping good thermal and electrical conductivity of copper substrate. According to the strengthening theory of Ni-based alloys, the r'-Ni3A1 phase still has the advantage of long range order under high temperature, and good creep performance. Therefore, this article aims to prepare (r'+r) phase precipitation strengthening films on pure Cu surface to improve the mechanical and heat resistance properties of material surface. To obtain r'-Ni3A1 phase, a series of Cu-Ni-Al ternary films were prepared by magnetron sputtering with Ni/Al ratio close to 3. After the initial microstructure and performance characterization, the experimental results showed that r'-Ni3A1 phase existed in the sputtered Cu-Ni-Al films and embedded in the matrix r with nano-state. By this stage, the film has a high hardness, and gradually increases with increasing of the Ni and Al content. The reasons are as follows: first, the solid solution of alloying elements into Cu lattice leads to the strengthening effect of solid solution; The other is the precipitation enhancement caused by the precipitation phase of r'-Ni3A1; The third is the fine grain strengthening effect caused by the uniform nanometer columnar crystal. After annealing 723K for 20h, the hardness of pure Cu film decreased significantly, while Cu-Ni-Al films still maintain a high level, indicating good stability of the films. It also suggests that precipitation strengthening deriving from r'-Ni3A1 phase can partially offset the weakening of the fine grain strengthening due to grain consolidation and solid solution strengthening causing by alloying elements during the annealing process.

10:20-10:40

Comprehensive Study on Morphology Control of TiO_2 Nanorods on Foreign Substrates by Hydrothermal Method

Jongseong Park, HoWon Jang, Seoul National University, Korea

The hydrothermal method is a facile route for the synthesis of TiO_2 nanostructured materials, but it requires accurate process optimizations and adjustments to circumvent the undesirable morphology products. In this study, systematically controlled experimental studies are carried out under thermodynamic and kinetic considerations to understand the formation of the well–aligned TiO_2 nanorods during the hydrothermal reaction. In this regard, TiO_2 nanorods are synthesized on various types of substrates, including single crystal TiO_2 and sapphire, fluorine doped tin oxide, and silicon. Variable growth parameters are classified and investigated for their effects on the morphological evolution of TiO_2 nanorods. The preferred morphology of TiO_2 nanorods with {110} facet is confirmed based on the crystallographic results for TiO_2 nanorods acquired by extensive transmission electron microscopy studies during the entire growth processes. The presence of the seeds on the substrates is found to be mandatory for the formation, growth and strong adhesion of the TiO_2 on the applied foreign substrates. The results elucidate that the growth kinetic of the process is significantly governed by the amount of the applied HCl concentration, which is highly influential on the morphology of the synthesized TiO_2 nanorods. Accordingly, the growth mechanism for the preferential growth maintaining the rod shape is derived.

F. Biomaterials: Biomedical Titanium and Zirconium Alloys

Symposium Organizers :

Yufeng Zheng, Peking University, China; Luning Wang, University of Science and Technology Beijing, China; Takayoshi Nakano, Osaka University, Japan; Seung-Kyun Kang, Korea Advanced Institute of Science and Technology (KAIST), Korea; Cuie Wen, RMIT University, Australia; Marc Meyers, University of California, San Diego, USA

Wednesday AM
August 21, 2019

Room: 306 (3rd Floor)
Symposium：F

Chairs:
Takayuki Narushima, Tohoku University, Japan
Cuie Wen, RMIT University, Australia

8:30-9:00 Keynote

Preparation of Bioceramic Coatings on Ti and Its Alloys by Dry Processes and Their Antibacterial Activity

Takayuki Narushima, Tohoku University, Japan

The benefits of Ti and its alloys are widely recognized in the orthopedic and dental fields as implants due to their excellent specific strength, high corrosion resistance, hypoallergenic property, and unique osseointegration property. However, in hard tissue replacement surgery, such as artificial joints and dental implants, the risk of surgical site infection (SSI) is high because of the large incision required and use of artificial implants. It has been reported that SSI occurs at a rate of several to 30%, which increases further for revision surgery, although these rates depend on the surgical site. Implant surfaces are preferred sites for bacterial adhesion and microbial contamination. In dental implants, peri-implantitis within 5 years of implantation occurs at a rate of 14%, which increases for long term implantation. Therefore, the addition of antibacterial agents to the surfaces of implants is required to prevent such infections.

We studied bioceramic coatings, such as photocatalytic active TiO_2 and Ag-added amorphous calcium phosphate (ACP) layers on Ti substrates, formed by dry processes, to impart antibacterial activity to Ti and its alloys. The thermal oxidation of Ti has been used for the preparation of photocatalytic active TiO_2 layers, resulting in high crystallinity and excellent adhesion to the Ti substrates. We developed a two-step thermal oxidation process for forming an anatase-type TiO_2 layer, consisting of a first carburization step under a CO-containing atmosphere and a second step of air oxidation. The TiO_2 layer formed by two-step thermal oxidation exhibited organic decomposition under visible-light irradiation because of the introduced carbon in the anatase-type TiO_2 layers. This process was applied to the practical materials of dental implants, commercially pure (CP) Ti, Ti-6mass%Al-4mass%V alloy, and Ti-6mass%Al-7mass%Nb alloy, for the preparation of anatase-containing TiO_2 layers. Excellent antibacterial activity against E. coliwas observed in the TiO_2 layers with high anatase fractions and high contents of dissolved carbon, which were achieved by adjusting the temperature of the second step. The use of Ti-Au alloys as substrates enabled the preparation of visible-light-active TiO_2 layers, consisting primarily of rutile, by a simple air oxidation process. The visible-light activation was attributed to the surface plasmon resonance of the metallic Au nanoparticles and/or a decreased band gap energy due to the dissolved Au ions in the TiO_2 layers. Electron spin resonance (ESR) analysis under visible-light irradiation indicated hydroxyl radical formation from the anatase-rich TiO_2 layers with added carbon and Au-incorporated TiO_2 layers on Ti and its alloys, which significantly contributed to their antibacterial activity.

For the formation of Ag-added ACP layers, RF magnetron sputtering was used, which formed uniform and dense ceramic layers on the metallic substrates. ACP possesses resorbability under biological conditions and can be used as a carrier of antibacterial agents such as Ag. The Ag-added ACP layers on the Ti substrates released Ag ions in Hanks' solution and their antibacterial ability against E. coliwas confirmed. The co-addition of Nb+Ag or Ta+Ag suppressed Ag-ion release from the ACP layers, indicating that the resorbability of the ACP layers can be controlled.

Thus, these bioceramic coatings, composed of TiO_2 and ACP layers, are both expected to improve bone compatibility and to lower the risk of infection of Ti implants.

9:00-9:25 Invited

CP-Ti Gyroid Scaffolds Manufactured by Selective Laser Melting for Bone Implant Applications

Cuie Wen, Arash Ataee, Yuncang Li, RMIT University, Australia

Applications of titanium and its alloys have increased in the biomedical industry over the past few decades. In particular, commercially pure titanium (CP-Ti) and Ti-6Al-4V (Ti64) have been widely used in bone implant applications due to their good biocompatibility, high specific strength and corrosion resistance. While Ti64 has been the material of choice for load-bearing applications, CP-Ti, on the other hand, shows lower strength and wear resistance compared to Ti64, which limits its application where combined high strength and wear resistance are required. However, the use of CP-Ti has some advantages over alloyed titanium. Firstly, CP-Ti is entirely biocompatible and free from any potentially hazardous or toxic alloying elements such as aluminum (Al) or vanadium (V) that can cause adverse tissue reactions over time. Secondly, CP-Ti shows higher ductility than Ti64 and, in specific applications such as skull implants or bone plates, this could be a significant advantage when implant deformability is desirable in order to better fit into patient-specific bone defect during surgery.

In this study, CP-Ti gyroid scaffolds with interconnected pores and high porosities ranging from 68% to 73% and three different unit cell sizes of 2, 2.5, and 3mm were manufactured by selective laser melting (SLM) for bone implant applications. The microstructure and mechanical properties of the scaffolds with different unit cell sizes and sample orientations were evaluated. The as-built struts consisted of a massive structure, and lath-shaped or acicular alpha prime. The average microhardness of the struts was 2.28GPa, which is ~50% higher than that of dense cast CP-Ti. The elastic modulus and yield strength of the as-built scaffolds ranged from 1465 to 2676MPa and from 44.7 to 56.5MPa, respectively, values which are close to the modulus of trabecular bone and presumably strong enough to bear the physiological loading. The as-built scaffolds exhibited excellent ductility up to 50% strain and no sign of fracture up to 20%~30% strain under compression. The dominant compressive response of the scaffolds was observed in formation of plastic hinges followed by formation of local shear band on each struts. The SLM-manufactured gyroid CP-Ti scaffolds exhibited a significantly enhanced hardness and an elastic modulus close to that of trabecular bone.

9:25-9:50 Invited

Dynamic Precipitation Softening in Beta-Titanium: Phase Stability and Al Addition Effects

Pan Wang, Osaka University, Japan / Singapore Institute of Manufacturing Technology, Singapore; Mitsuharu Todai, Takayoshi Nakano, Osaka University, Japan

In the past years, our group has been promoting the single-crystalline beta (β) titanium (Ti) alloy as an implant material by designing bone-like elastic modulus with large crystallographic elastic anisotropy. These

newly developed single-crystalline β-Ti alloys are metastable and may suffer some phase transformations during deformation. Therefore, the fatigue properties of them must be clarified for the practical application since the hard tissue replacements are usually used under cyclic loading conditions. Here, we design a series of binary Ti-Nb single crystals with different β phase stability and ternary Ti-Nb-Al single crystals with Al doping. The monotonously compressive deformation behavior and tension-compression cyclic deformation behavior have been systemically investigated. Results reveal that the deformation behaviors are dependent on the β phase stability and the doping of Al. Unusual precipitation of a single variant of ω-phase that is caused by the to-and-fro motion of the dislocation and results in "dynamic precipitation softening" is found in a suitable β phase stability range of binary Ti-Nb single crystals. Out of this range, a sharp cyclic hardening with four variants of ω-phase and a normal cyclic hardening without precipitation are observed in the low and the high β phase stability Ti-Nb single crystals, respectively. Doping of Al can suppress both the athermal ω-phase and the deformation-induced ω-phase, which make the dynamic precipitation softening no longer appear in the ternary Ti-Nb-Al single crystals, regardless of the β phase stability. These findings break through the understanding that formation of ω-phase induces significant hardening of β-Ti alloys, which is useful for developing the "single-crystalline β-Ti implant material" with advanced mechanical performance beyond the usual trade-off relationship between strength, Young's modulus, and ductility via the appropriate crystal orientation control.

9:50-10:10

New Zirconium Alloy with Large Strength to Decrease MRI Artifact

Takao Hanawa, Maki Ashida, Yusuke Tsutsumi, Peng Chen, Tokyo Medical and Dental University, Japan; Noumura, Naoyuki , Tohoku University, Japan

Metals implanted into the human body have sometimes higher magnetic susceptibility than the tissues. Therefore magnetic resonance imaging (MRI) diagnosing is disturbed by artifacts appearing on the MR images. In our previous study, Zr-1Mo alloy with low magnetic susceptibility is developed and generates much smaller artifact than Ti-6Al-4V ELI alloy. In this study, with d-electron alloy design method, Zr alloy is designed and in the resultant composition alloy mechanical properties, magnetic susceptibility, corrosion resistance, and cytocompatibility are evaluated.

Employing d-electron alloy design method, Composition of alloys were decided. The designed ally was fabricated by induction skull melting. The ingot was forged at 1050℃. A rod with ϕ5mm was obtained through electrical discharge machining. Then, cold swaging was performed to 56% and 97%. In addition, heat treatment was performed to all specimens: heated at 400℃ for 45min and quenched in iced water. The crystal phase structure was characterized using XRD and TEM. Mechanical property was evaluated by tensile test and Vickers hardness test. Moreover, corrosion resistance and cytocompatibility were evaluated.

According to d-electron alloy design method, composition of alloys were determined as Zr-14Nb-5Ta-1Mo (mass%). There is no macro-segregation in the ingot of the alloy. Hot forging and cold swaging are performed without any fracture of the specimen. The alloy was constituted of β phase with a small amount of α phase and/or ϖ phase. In the case of 97% cold swaging, tensile strength was 1054MPa, 0.2% proof strength was 1011MPa, elongation to fracture was 16%, Vickers hardness was 258, and Youngs' modulus was 67GPa. The mass magnetic susceptibility was 18.1×10^{-9} m3kg^{-1}. After heat treatment, Tensile strength 0.2% proof strength, and Vickers hardness increased remaining Youngs' modulus and magnetic susceptibility. In addition, this alloy did not show any cytotoxicity.

Zr-14Nb-5Ta-1Mo alloy has excellent balance of mechanical property with low magnetic susceptibility, high corrosion resistance, and no cytotoxicity. This alloy achieves large strength and elongation with small Youngs' modulus that is not acquired in conventional titanium alloys. In addition, magnetic susceptibility was half of titanium alloys. Therefore, Zr-14Nb-5Ta-1Mo alloy is a useful metallic materials for medical use.

10:10-10:30

Low Cost Titanium Alloys for Biomedical Implant Applications

Damon Kent, Shima Ehtmam Haghighi, University of the Sunshine Coast, Australia / The University of Queensland, Australia / ARC Research Hub for Advanced Manufacturing of Medical Devices, Australia; Hooyar Attar, The University of Queensland, Australia; Matthew Dargusch, The University of Queensland, Australia / ARC Research Hub for Advanced Manufacturing of Medical Devices, Australia

Titanium (Ti) and its alloys are used extensively for biomedical applications due to their outstanding combination of properties. In comparison to other conventional metallic biomaterials such as 316L stainless steel and cobalt-chromium alloys, they possess higher specific strength, lower elastic modulus, better corrosion resistance and superior biocompatibility. Among Ti-based alloys, commercially pure Ti (CP-Ti) and Ti-6Al-

4V are the most commonly used biomaterials. However, they present some concerns such as the release of Al and V ions from the Ti-6Al-4V alloy which may have long-term health consequences. Additionally, the elastic modulus mismatch between the implant and that of the surrounding bone (10~30GPa) can cause stress shielding, leading to bone resorption and premature failure of the implant. Therefore, in recent years, attention has been directed toward development of new, more biocompatible Ti alloys with mechanical properties better suited to implant applications. These new Ti alloys are predominantly β-type alloys which typically include significant proportions of expensive and scarce alloying elements such as Ta, Zr, Nb and Hf with high melting points and high densities. The high melting points of these alloying elements introduces increased difficulty to the processing and make the alloys more prone to compositional segregation which is detrimental to their mechanical properties and performance. Additional post-fabrication processes such as high temperature homogenising heat treatments and/or thermoplastic processing are required to alleviate or eliminate segregation. Thus, increasing attention has been paid to development of Ti alloys containing greater proportions of common low-cost, low melting points elements such as Mn and Fe. Mn and Fe are also essential elements in the body. Niobium is another important biocompatible β-stabiliser and its addition to Ti alloys contributes to reducing their elastic modulus. Therefore, there is potential to utilise Mn and Fe in conjunction with Nb to develop low modulus, lower cost Ti alloys for biomedical implant applications. This talk will present research into the development of new Ti-Mn-Nb and Ti-Fe-Nb based alloys prepared by conventional powder metallurgy (PM) from blended elemental powders. As a near-net shape process, PM offers considerable cost savings compared to other conventional processing techniques. This study demonstrates that the Ti-Mn-Nb and Ti-Fe-Nb based alloys are suited to press and sinter PM fabrication of lower cost biomedical implants with excellent mechanical properties.

10:30-10:45 Tea Break

10:45-11:10 Invited

Recent Development of Biomedical Ti-Zr-Nb Shape Memory Alloys

Yan Li, Beihang University, China

Microstructure, mechanical properties, superelasticity and biocompatibility of a Ti-Zr-Nb-Fe alloy are investigated. X-ray diffraction spectroscopy and transmission electron microscopy observations show that the as-cast Ti-Zr-Nb-Fe alloy is composed of α' and β phases, but only the β phase exists in the as-rolled and as-quenchedalloys. The tensile stress–strain tests indicate that the as-quenched alloy exhibits a good combination of mechanical properties with a large elongation of 25%, a low Young's modulus of 59GPa and a high ultimate tensile stress of 723MPa. Superelastic recovery behavior is found in the as-quenched alloy during tensile tests, and the corresponding maximum of superelastic strain is 4.7% at the pre-strain of 6%. A superelastic recovery of 4% with high stability is achieved after 10 cyclic loading–unloading training processes. Potentiodynamic polarization and ion release measurements indicate that the as-quenched alloy shows a lower corrosion rate in Hank's solution and a much less ion release rate in 0.9% NaCl solution than those of the NiTi alloys. Cell culture results indicate that the osteoblasts' adhesion and proliferation are similar on both the Ti-Zr-Nb-Fe and NiTi alloys. A better hemocompatibility is confirmed for the as-quenched Ti-Zr-Nb-Fe alloy, attributed to more stable platelet adhesion and small activation degree, and a much lower hemolysis rate compared with the NiTi alloy. Therefore, the Ti-Zr-Nb-Fe alloy has shown promising potential as an excellent material candidate for biomedical implants.

11:10-11:35 Invited

Microstructure and Mechanical Properties of Low Magnetic Zr-1Mo Alloy for Biomedical Applications

Naoyuki Nomura, Xiaohao Sun, Weiwei Zhou, Keiko Kikuchi, Akira Kawasaki, Tohoku University, Japan; Yusuke Tsutsumi, Takao Hanawa, Tokyo Medical and Dental University, Japan

Magnetic resonance imaging has become popular for medical diagnosis. However, when metallic implants exist in the human body, artifact formes around the implant due to the magnetic susceptibility difference between human tissue and metals. In order to solve the artifact ploblem in magnetic resonance images, a low magnetic Zr-1Mo alloy was developed and fabricated by thermo-mechanical treatment and powder bed fusion process with fiber laser (L-PBF). In this study, we compared microstructure, magnetic and mechanical properties of Zr-1Mo alloy fabricated with different process. Microstructure was observed by OM, SEM, and TEM. Phase constitution was analyzed by X-ray diffraction. Magnetic susceptibility was measured by magnetic susceptibility balance. Mechanical properties were evaluated by tensile test. In the swaged Zr-1Mo alloy, thin layered microstructure was bended and rolled as swaging process proceeded. Fiber {10-10} texture was confirmed along the longitudinal direction. TEM

observation revealed that the layered structure consisted the alpha and beta phase. On the other hand, texture formation was not observed for the as-built Zr-1Mo alloy consisting acicular alpha prime phase. Magnetic susceptibility of the swaged alloy was higher than that of the as-built alloy. This difference was considered to be due to the texture formation and may possibly influence the artifact volume depending on the direction, because the volume was proportional to the magnetic susceptibility. Mechanical properties difference would be also discussed.

11:35-12:00 Invited

Mechanical Properties and Biocompatibility of β Ti35Zr28Nb Alloy Scaffolds Manufactured Using Selective Laser Melting

Yuncang Li, Khurram Munir, Cuie Wen, RMIT University, Australia

Selective laser melting (SLM) was used for the fabrication of a new β Ti35Zr28Nb alloy and its scaffolds for biomedical applications. The SLM-manufactured porous scaffolds included an FCCZ structure (face centered cubic unit cell with longitudinal struts) and an FBCCZ structure (face and body centered cubic unit cell with longitudinal struts), exhibiting porosity values of 83.2% and 49.9%, respectively. The SLM-manufactured bulk samples showed a very similar elastic modulus in the longitudinal and transverse directions, but significantly higher yield strength in the transverse direction than in the longitudinal direction. However, both porous FCCZ and FBCCZ structures exhibited significantly higher elastic modulus and plateau strength in the longitudinal direction than in the transverse direction. The FCCZ scaffolds showed a longitudinal elastic modulus of 1.1GPa and plateau strength of 27MPa, and a transverse elastic modulus of 0.7GPa and plateau strength of 8MPa; while the FBCCZ scaffolds showed a longitudinal elastic modulus of 1.3GPa and plateau strength of 58MPa, and a transverse elastic modulus of 1.0GPa and plateau strength of 45MPa. These mechanical properties of the SLM-manufactured porous structures fall within the ranges of the mechanical properties of trabecular bone. The SLM-manufactured β-Ti35Zr28Nb alloy showed good corrosion properties. The MTS assay revealed that both the FCCZ and FBCCZ scaffolds displayed cell viability at the same level as that of the control. SEM observation indicated that osteoblast-like cells attached, grew, and spread in a healthy way on the surfaces of both the FCCZ and FBCCZ scaffolds, demonstrating the excellent biocompatibility of these materials. Overall, the SLM-manufactured Ti35Zr28Nb scaffolds possess promising potential for use as hard-tissue implant materials due to their appropriate mechanical properties, good corrosion resistance, and biocompatibility.

G. Smart and Magnetic Materials: Magnetocaloric and Elastocaloric Materials

Symposium Organizers :

Shaoxiong Zhou, Center Iron & Steel Research Institute, China; Chengbao Jiang, Beihang University, China; Satoshi Sugimoto, Tohoku University, Japan; Haein Yim, Sookmyung Women's University, Korea; Sean Li, New South Wales, Australia; Bob Shull, National Institute of Standards and Technology, USA

Wednesday AM Room: Yulan Hall-220 (2nd Floor)
August 21, 2019 Symposium: G

Chairs:
Dunhui Wang, Nanjing University, China
Hong Yang, The University of Western Australia, Australia

8:30-9:00 Keynote

Multicaloric Effect in Magnetic Refrigeration Materials

Fengxia Hu, Jing Wang, Jirong Sun, Baogen Shen, Institute of Physics, Chinese Academy of Sciences, China; Qingzhen Huang, NIST Center for Neutron Research, National Institute of Standards and Technology, USA

Solid state refrigeration based on magnetocaloric, electrocaloric, mechanocaloric effect (multicaloric effect) has attracted world-wide attention for its environmental-friendly and energy-saving superiority over the conventional vapor compression technique.

Here, we report our recent progress on multi-field modulated hysteresis loss and multicaloric effect for the materials with various magnetostructural transitions, such as $La(Fe, Co, Si)_{13}$, FeRh, Ni-Mn-In, and Ni_2In-type MM'X materials. For a room temperature $La(Fe, Co, Si)_{13}$ magnetocaloric material, enhanced magnetocaloric effect (MCE) by hydrostatic pressure has been demonstrated by magnetic measurements under pressure. To understand the origin, we performed neutron powder diffraction (NPD) studies on the crystal and magnetic structures as a function of temperature under different pressures. The change of atomic local environments and 5 kinds of Fe-Fe bonds (B1-B5) with pressure were illustrated. Detailed analysis indicated that the sensitivity of intra-icosahedron Fe-Fe bonds (B1, B2, B3) to hydrostatic pressure is mainly responsible for the change of magnetic properties. Moreover, we found that the change of lattice volume $\Delta V/V$ across Curie temperature TC becomes significantly larger with increasing pressure. Accordingly, lattice entropy change was estimated by Debye approximate. The results indicate that the contribution of entropy change from

lattice increases by ~40% as the pressure increases to 11.3kbar. This result indicates that hydrostatic pressure is an effective way to dig the lattice contribution. Moreover, the contribution from interplay between spin and lattice, the so-called coupled caloric effect, plays an important role in multicaloric effect driven by multi-field in materials with magneto structural transition. We firstly carried out experimental studies on the coupled caloric effect of metamagnetic Heusler Ni-Mn-In alloys. On the other hand, hysteresis loss is a longstanding problem harming refrigeration efficiency, which exists in most of giant magnetocaloric materials. Here we report a new way to reduce hysteresis loss by taking FeRh as a model material. Utilizing strain memory effect to engineer the magnetization process of FeRh film, a nonvolatile large reduction of hysteresis loss was firstly demonstrated. As a result, effective refrigeration capacity increases to a new height through introducing external mechanical work in a designed magnetic refrigeration cycle. The feasibility of proposed refrigeration cycle with the cooperation of strain memory effect not only helps rescuing the FeRh as a magnetic refrigerant but also paves a new way to solve large hysteresis loss for similar caloric materials.

This work was supported by the National Key Research and Development Program of China (2017YFB0702702, 2018YFA0305704), and the National Natural Sciences Foundation of China (51531008, 51771223, 51590880).

9:00-9:30 Keynote

Toward Realization of Reliable High-Performance Magnetic Refrigerants Based on La(Fe,Si)$_{13}$ – Variants

Asaya Fujita, National Institute of Advanced Industrial Science and Technology, Japan

Materials having a large magnetocaloric effect (MCE) are considered as candidates for magnetic cooling/heat-pump applications. Hydrogenated La(Fe, Si)$_{13}$-based system is one of the realistic candidates material for room-temperature magnetic refrigerants. Hydrogenation is indispensable in controlling the transition temperature TCup to room temperature. Meanwhile, the hydrogenation technique runs into the hydrogen re-distribution problem. Namely, hydrogen atoms move between the ferromagnetic and paramagnetic portions coexisting during the phase-transition process. One of the workarounds is a full-charge of hydrogen up to the maximum concentration (y_max).

To establish compatibility in the control of TCwith a suppression of the re-distribution, the complex substitution by Ce and Mn in La(Fe, Si)$_{13}$Hy_maxhas been proposed. In this case, sample quality strongly influences the MCE, and a local chemical disorder strongly damages the MCE performance. Our recent improvements of homogenization bring about recover of the MCE, and a large entropy change DSMbeyond 20J/kgK at 1T was observed in (La, Ce) (Fe, Mn, Si)$_{13}$Hy_maxaround room temperature. Also, we have found an indication that the re-distribution (suppression) magnitude is related to the crystalline grain size distribution. To obtain the relation between the transition progress and the crystalline grain pattern, we have carried out microscopic observations under the metallographic and magneto-optical conditions, and a grain-pattern dependent nucleation mode, which is considered to be a source of the hydrogen distribution path, was captured.

9:30-9:55 Invited

Magnetocaloric Studies to Identify First-Order Phase Transitions

Jia Yan Law, Victorino Franco, Alejandro Conde, Sevilla University, Spain

The usual techniques to determine the order of phase transitions depend on interpretations based on qualitative data features, thus jeopardized by misinterpretations or extensive calculations. Among them, the universal scaling of magnetocaloric effect is the only one that is model-independent to identify the order of phase transition, simply based on the collapse of rescaled data. However, its identification of first-order phase transition via the absence of a feature (collapse) also introduces the earlier-mentioned handicap of arising subjective interpretations.

In this talk, we show that using the field dependence of isothermal entropy change (magnetocaloric effect), $\Delta ST \ \alpha \ Hn$, the order of the phase transition can be quantitatively determined: an exponent n larger than 2 at the transition constitutes the fingerprint of first-order thermomagnetic phase transition. This newly proposed alternative to identify the order of thermomagnetic phase transitions will be applied to various series of magnetic materials, including alloys, oxides and multiphase composites. With the successful application to both experimental data and simulations, the method implements a quantitative fingerprint of first-order thermomagnetic phase transitions that provides objective interpretations and is general to use. Furthermore, the use of this new criterion can further uncover the alteration in the order of thermomagnetic phase transition by very minor compositional changes despite retaining the crystal structure. This technique could outdo the accuracy of the typical methods used for identifying the order of magnetic phase transitions, in particular for compositions very near to the critical point of second-order phase transition. Furthermore, we will also show that the criterion aids in the analysis of intricate character of concurrent phase transitions whereby their respective transition temperatures are very close to each other.

Supported by AEI/FEDER-UE (project MAT-2016-77265-R) and the PAI of the Regional Government of Andalucía.

9:55-10:15

Modulation of Martensite Transition and Exchange Bias Behavior in Ni-Mn-In Alloy

Yao Liu, Tianyu Ma, Xi'an Jiaotong University, China

The Heusler alloy NiMn-X is a kind of well-known multifunctional materials. Superelasticity, shape memory effect, magnetocaloric effect and barocaloric effect can be generated under the stimulation of magnetic field, stress and temperature. These effects could be ascribed to magneto structural (Ms) coupling of the alloy. Hence, the modulation of the martensitic transition is very important to tune and promote the multi-function of the alloy. The martensitic transition temperature of the alloy is very sensitive to the alloy composition, atomic order, residual stress and extrinsic magnetic field, pressure and thermal activation.

In the present study, the influence of intrinsic atomic order and extrinsic hydrostatic pressure on the martensitic transition and exchange bias behavior has been studied in Ni-Mn-In alloy ribbons. Ni50Mn35In15 melt-spun ribbons with different atomic order were fabricated using melt spinning technique with different spinning speed. The magnetization dependence on temperature (M-T) of all the ribbons displays a large thermal hysteresis, implying a magneto structural coupling. The transition temperature determined from the M-T curves denotes an increasing behavior with reducing atomic order. The mechanism is analyzed, and could be ascribed to the tuning of the Gibbs free energy of the parent phase through the influence on the magnetic behavior.

The previous research has shown that the low temperature martensitic state mixing ferromagnetic and anti-ferromagnetic phases. This fact results in the emergence of exchange bias behavior in the alloy as there exists ferromagnetic-antiferromagnetic interface. The alloy ribbons studied here, as expected, display an exchange bias effect. The present study shows that the exchange bias field could be tuned by the atomic order, which, in essence, adjust the AFM-FM phase ratio. Specifically, the exchange bias field could be increased through reducing atomic order.

Furthermore, hydrostatic pressure of 1.21GPa was applied on the alloy ribbons, its influence on the Ms transformation and exchange bias behavior were studied. The application of 1.21GPa pressure drives the Ms transition temperature from 260K to 283K, while the exchange bias field, simultaneously, increases to 280Oe. The pressure could tune the volume and atomic distance of the alloy. The decrease of the alloy volume could stabilize the martensitic phase thus driving the Ms transition temperature higher. The Mn-Mn distance is very crucial to the magnetic state of the alloy. We infer that the pressure could tune the Mn-Mn distance, and further the AFM-FM ratio in the martensitic state. The exchange bias behavior, which is related to the AFM-FM interface, is thus modulated by the pressure applied.

10:15-10:45 Tea Break

10:45-11:05 Invited

Ultrahigh Cyclability of a Large Elastocaloric Effect in Multiferroic Phase-Transforming Materials via Strengthening Grain Boundary

Zhi Yang, Daoyong Cong, Yandong Wang, University of Science and Technology Beijing, China

Refrigeration is becoming increasingly important to industry, transportation and households and it accounts for a considerable fraction of the global energy consumption. Elastocaloric refrigeration is an environment-friendly and high-efficiency solid-state cooling technology that can potentially replace the traditional vapor-compression-based one. Cyclability of elastocaloric effect, which determines the service life of refrigerants, is of utmost importance to elastocaloric refrigeration. Intriguing elastocaloric, magnetocaloric and barocaloric effects have been discovered in the prototype Ni-Mn-based multiferroic phase-transforming alloys, opening the opportunity for harnessing multicaloric effects, but these alloys are brittle and demonstrate poor cyclability of elastocaloric effect, which remains a major challenge for exploiting more efficient multicaloric refrigeration. In the present work, by employing the strategy of simultaneously strengthening grain boundary and refining grains, the cyclability of elastocaloric effect in the Ni-Mn-In-based multiferroic magnetic shape memory alloys is strikingly enhanced by two orders of magnitude. High cyclic stability of a large elastocaloric effect is achieved in the boron-microalloyed (Ni51Mn33In14Fe2)99.4B0.6 alloy: the high adiabatic temperature change of ~5.6K remains stable for 2700 cycles of loading and unloading. This high cyclability of elastocaloric effect far exceeds that reported in other polycrystalline magnetic shape memory alloys. The strengthening of grain boundary resulting from boron microalloying was evidenced by the transgranular fracture in the boron-doped alloys, which is in contrast to the intergranular fracture in the boron-free alloys. The possible mechanism for the grain boundary strengthening by boron microalloying was also investigated. Furthermore, the same strategy was demonstrated to be effective in Ni-Mn-Sn-based magnetic shape memory alloys. This not only paves the

way for exploiting multicaloric effects for more efficient cooling, but also provides a strategy for overcoming the cyclability issues in the ubiquitous brittle intermetallic phase-transforming materials.

11:05-11:25

The Structural Transition in Typical Fe-Based Glass-Forming Alloy Melts

Bangshao Dong, Shaoxiong Zhou, Jiangsu JITRI Advanced Energy Materials Research Institute Co., Ltd., China

The evolution of liquid metal at high temperature is known much less than their solid states. This is partially due to that the message concerning clusters, metastable phase or heterogeneity in liquid is usually too slight to be traced. Here, we shed some light on the nature of structural evolution of Fe-based glass-forming alloy. The viscosity-temperature relation of several typical Fe-based amorphous ribbons (Fe80Si9B11, Fe82Si4B13C1 and Fe73.5Cu1Nb3Si15.5B7) and their ingots was investigated by rotational vibration-type high-temperature melt viscometry and ab initio molecular dynamics simulation. Experimental results have shown that the viscosity decreases suddenly at approximately 1400˚C with increasing temperatures during the heating process, demonstrating that a structural transition occurs at this point. However, the viscosity-temperature curve is completely reversible when the heating temperature is below 1400˚C. Moreover, the structural transition phenomenon disappears during the following second thermal cycling. A proper heat treatment at a temperature higher than the needed disintegration energy can eliminate this transition. This structural transition around 1400˚C was confirmed by the results from differential scanning calorimeter (DSC). The viscosity curves of all samples during cooling processes can be well described by the Arrhenius equation. The activation energy of viscosity is inverse proportional to the Fe content for the studied alloys. The simulation results were pointed that Fe2B-like clusters was of higher total energy, higher melting point and larger size than that Fe3B-like clusters. Combining these results with Fe-Si-B ternary phase diagram and the melting characteristics of Fe-B compounds, the nature of the structural transition could be due to the transformation from Fe2B-like clusters to Fe3B-like clusters. The observation probably offers a reference for the preparation and property control of amorphous alloys in the fields of materials science and metallurgy.

H. Materials Characterisation and Evaluation: IV

Symposium Organizers :

Zhiwei Shan, Xi'an Jiaotong University, China; Xiaodong Han, Beijing University of Technology, China; Satoshi Hata, Kyushu University, Japan; Ju-Young Kim, Ulsan Institute of Science and Technology (UNIST), Korea; Jin Zou, University of Queensland, Australia; Jennifer Carter, Case Western Reserve University, USA

Wednesday AM
August 21, 2019

Room: 308 (3rd Floor)
Symposium: H

Chairs:
Yong Wang, Zhejiang University, China
Shunsuke Muto, Nagoya University, Japan

8:30-9:00 Keynote

Mining Physical/Chemical Properties from Nano-Scale Areas Using STEM Spectroscopic Methods and Informatics Techniques

Shunsuke Muto, Nagoya University, Japan

Scanning transmission electron microscopy (STEM) equipped with analytical instruments (EDS, EELS, CL and others) is now one of the most indispensable analytical tools in materials science. A set of microscopic image/spectral intensities collected from many sampling points in a 2D region of interest should be a rich source of material information, in which multiple physical/chemical components may be spatially and spectrally entangled. To unfold such entangled image information/spectral features to the individual pure components involved, statistical treatments based on informatics/mathematics are necessary, and such computer-aided schemes or techniques are called as neural network, blind source separation (BSS) and hyperspectral image analysis, depending on their application fields as a part of machine learning-related fields. We have developed such unfolding techniques and applied them to solve a wide variety of materials problems, particularly using STEM-EELS/EDS. The present scheme is powerful for a wide range of applications, from soft to hard materials, to solve the nanometric materials analysis problems.
The present talk focuses on briefly introducing the methodology and then recent application examples such as degradation analysis of lithium ion battery electrode materials, chemical state analysis of heterophase interfaces and measurement of magnetic moments at nanometric scale. We also discuss the future prospects of this field.

9:00-9:25 Invited

Interpretation of Stretch-Flangeability Using Nanoindentation and In-Situ Fracture Observation in Dual-Phase Steels

Jung-Gu Lee, University of Ulsan, Korea; Ju-Young Kim, Ulsan National Institute of Science and Technology (UNIST), Korea; Jong-Bae Jeon, Korea Institute of Industrial Technology (KITECH), Korea; Bong-June Park, Hyundai Steel Co. Korea

Ferrite/martensite dual-phase steels with high tensile strength up to 980MPa or higher have received great attention in automotive industry because of their characteristic mechanical properties. Although dual-phase steels have such an excellent combination of high strength and large elongation, their stretch-flangeability estimated as hole expansion ratio is frequently a critical property to avoid fractures in actual parts forming. In this study, the deformation and fracture behaviors during hole expansion testing were interpreted based on nanoindentation and in-situ fracture observation in order to capture the stretch-flanging phenomenon and to improve the stretch-flangeability of high strength dual-phase steels. Nanoindentation hardnesses were correlated with tensile properties and hole expansion ratio values to assess the importance of the individual constituent properties in the ferrite and martensite phases. Subsequently, microscopic deformation and fracture mechanisms were investigated by in-situ fracture observation in a scanning electron microscope to clarify how the individual constituent properties affect the crack initiation and propagation during hole expansion testing. This combined analysis suggests that the degree of plastic localization in the ferrite phase is the dominant factor for determining the stretch-flangeability of high strength dual-phase steels. The severe plastic localization caused brittle crack propagation through the highly deformed ferrite area, which was mainly attributed to the large difference in hardness between the ferrite and martensite phases. When the difference in hardness was not so large, on the other hand, the martensite phase could be deformed considerably together with the ferrite phase, thereby inducing crack blunting and delayed crack propagation. Owing to such deformation and fracture behaviors observed, the hole expansion ratio decreased with an increase in the martensite hardness and increased with a decrease in the martensite-to-ferrite hardness ratio, indicating that hardening the ferrite phase and softening the martensite phase is a proper approach to improve the stretch-flangeability of high strength dual-phase steels.

9:25-9:50 Invited

3DAP Analysis of Solute Segregation at Ferrite or Bainite / Austenite Interface

Goro Miyamoto, Kentaro Yokoyama, Tadashi Furuhara, Tohoku University, Japan

It has been long known that segregation of solute atoms at ferrite / austenite interface induces solute drag effect (SDE), which delays growth kinetics of ferrite or bainitic ferrite. Therefore, additions of solute elements having strong segregation tendency, such as Mo or Cr, Mn etc, are widely used to improve hardenability of steels. However, details of segregation behavior, such as amount of solute segregated at interface and its interface character dependence, energy dissipation due to SDE, are not well clarified because interface segregation occurs in nano-scale and its quantitative investigation had been difficult. Recent development of three-dimensional atom probe (3DAP) technique coupled with site-specific sampling using focused ion beam (FIB) makes quantitative analysis of solute segregation at interface or grain boundary possible. In this study, we aim to clarify Mo segregation at ferrite / bainite and austenite interfaces by means of 3DAP and resultant SDE on transformation kinetics in Fe-0.4C-0.5Mo alloy transformed at various temperatures. Needle specimen for 3DAP measurements are prepared by FIB from interfaces whose orientation relationship was characterized using electron backscattering diffraction method (EBSD).
0.5%Mo addition delays transformation kinetics both in ferrite and bainite transformations. Energy dissipation evaluated from interfacial carbon content increase with lowering transformation temperature, that is, the dissipation for bainite transformation is larger than that for ferrite. 3DAP analysis reveals that amount of Mo segregation in allotriomorphic ferrite formation is more significant at interfaces without having K-S orientation relationship than that at interfaces having near K-S OR. Observed Mo segregation and energy dissipation for ferrite transformation can be rationalized by solute drag theory. On the other hand, Mo segregation at bainite / austenite interface is negligibly small in spite of large energy dissipation. Therefore, the large energy dissipation in bainite transformation should not be originated from SDE but from other factors such as transformation strain or finite mobility of bainitic ferrite / austenite interface.

9:50-10:10

STEM-EDS Investigations of Doping Atoms' Positions in η-Cu6Sn5

Wenhui Yang, Tomokazu Yamamoto, Xuan Quy Tran, *Syo Matsumura*, Kyushu University, Japan; Kazuhiro Nogita, University of Queensland, Australia

Due to environmental concerns, Pb-free Sn-based alloys have been widely used for solder interconnects in electronics packaging applications. It is also well known that the Cu6Sn5, which forms between Cu substrates and Sn-based solders during the soldering process, is detrimental to the structural stability of solder joints due to the significant volumetric change

associated with its polymorphic phase transformation (η → η') when cooling below 186˚C. In previous studies, researchers have found that Au, Ni and Zn doping show a remarkable effect on stabilizing the high temperature η-Cu6Sn5 even down to room temperature, thus leading to significant improvement on the reliability of solder interconnects. However, the underlying mechanisms on the role of these dopants still remain unclear and their atomic locations within the Cu6Sn5 have not yet been experimentally determined.
In the current study, we directly identify the atomic positions of Au, Ni and Zn at the Wyckoff sites Cu1, Cu2 and Sn of η-Cu6Sn5, respectively, via atomic-scale Energy Dispersive Spectroscopy (EDS) maps utilizing advanced Cs-corrected Scanning Transmission Electron Microscopy (STEM). Due to the low concentrations of dopant atoms (Au: 5at.%, Ni: 5at.%, Zn: 5at.%), a Poisson Non-Local Principal Component Analysis (Poisson NLPCA) algorithm was also employed to reduce the Poisson background noise in the acquired EDS maps, thereby effectively improving the signal-to-noise ratios. In addition, these findings are in agreement with our calculations based on Density Functional Theory (DFT) where the dopants are found more energetically favourable at these positions.

10:10-10:30

Mapping Grain Morphology and Orientation by Laboratory Diffraction Contrast Tomography

Jun Sun, Jette Oddershede, Florian Bachmann, Christian Holzner, Erik Lauridsen, Xnovo Technology Aps, Koege, Denmark; Hrishikesh Bale, Steve Kelly, William Harris, Carl Zeiss X-ray Microscopy Inc, Pleasanton, CA, USA

The majority of engineering materials are polycrystalline. Their properties and performance strongly depend on the 3D microstructure in a sense that the individual grains, their crystallographic orientations, their size and shape as well as their spatial distribution ultimately determine the material's behaviour under use. Characterizing such microstructure through x-ray diffraction contrast tomography was for a long time only possible at large-scale synchrotron facilities; involving both intricate data acquisition schemes and demanding data analysis and reconstruction approaches.
The novel lab-based diffraction contrast tomography (LabDCT), operating on a commercially available x-ray microscope, made it possible to map 3D grain morphology and orientation non-destructively in the home laboratory. In addition, the highly demanding analysis and reconstruction requirements were made accessible in a straightforward workflow, enabling non-expert users for this advanced imaging modality. Combination of LabDCT with conventional absorption microCT allows simultaneous characterization of both the 3D grain structure and a wide range of other microstructural features such as particles, cracks and porosity.
Permitting wide accessibility and routine use of diffraction contrast tomography allows for non-destructive, time-evolution studies of dynamic microstructural evolutions and materials characterization. Aside from introducing the fundamentals of the technique and its implementation on a laboratory scale, we will present a selection of LabDCT applications with particular emphasis on how its non-destructive operation can facilitate a better understanding of the relation between structure and property for advanced materials.

10:30-10:45 Tea Break

10:45-11:10 Invited(1232901)

In-Situ TEM Studies of Nanocatalysts under Gas Environment

Yong Wang, Zhejiang University, China

The environment, such as temperature, gas and pressure, has a significant impact on the catalyst surfaces, which may result in structural and electronic changes during reactions. It is therefore essential to investigate the structural evolution of nanocatalysts during real reaction conditions to understand how the environment affects the catalytic nanocrystals and the catalytic mechanism at the atomic scale. In this talk, I will report our recent progress in studying the dynamic behaviors of catalytic nanocrystals under gas environment using advanced environmental TEM in low pressure and gas cell system up to atmospheric pressure. The effect of environment on the surfaces and interfaces of supported catalysts will be discussed.

11:10-11:35 Invited

Synthesis of Platinum Silicide at Platinum/Silicon Oxide Interface by Photon Irradiation

Kazuhisa Sato, Hidehiro Yasuda, Shuhei Ichikawa, Hirotaro Mori, Osaka University, Japan; Masaki Imamura, Kazutoshi Takahashi, Saga University, Japan; Satoshi Hata, Syo Matsumura, Kyushu University, Japan; Satoshi Anada, JFCC, Japan; Jung-Goo Lee, KIMS, Japan

Materials modification by high-energy particle irradiation can be achieved by two different routes, namely atom displacement caused by knock-on of primary particles, and processes caused by electronic excitation. However, our understanding of electronic excitation in materials modification is still insufficient, in contrast to the deeper understanding of knock-on atom displacement. Consequently, it is of primary importance to improve our understanding of the effects of electronic excitation on materials modification. In this study, the synthesis of platinum silicide at a Pt/SiOx interface by

photon irradiation was investigated using transmission electron microscopy (TEM) and electron diffraction. To elucidate the mechanism behind the synthesis reaction, we used photon irradiation, with which energy-selective excitation of electrons can be achieved more accurately than with conventional electron irradiation.

Pt particles were epitaxially grown on cleaved NaCl(001) substrates, kept at 573K, by DC sputtering of a Pt target. The Pt particles were then backed with an amorphous (a-) SiOx film, which was vapor deposited onto the Pt particles on the NaCl. Pt/SiOx films prepared on NaCl were then floated on distilled water and mounted on copper grids with a single hole of ϕ0.3mm in their center for photon irradiation experiments and subsequent TEM observations. The Pt/SiOx films on copper grids were irradiated with photons of energies 680, 140, and 80eV with beam line BL13 in the Saga Light Source. The irradiation temperature was room temperature. In the TEM studies, bright-field images, the corresponding selected area electron diffraction patterns, and high-resolution electron microscopy images were obtained using a 200kV-TEM (JEM-ARM200F).

A platinum silicide, α-Pt2Si, was successfully formed at the Pt/SiOx interface by irradiation with 680 and 140eV photons, but not by irradiation with 80 eV photons. These results indicate that excitation of the valence band (VB) electrons only was insufficient to induce silicidation, and that at least excitation of electrons in the Si_2p level (2p1/2: 100eV、2p3/2: 99eV), i.e., electrons in the highest-lying Si core level below the VB, was necessary for silicidation to occur. Silicide formation was also induced by irradiation with electrons of energy 75keV. The amount of silicide formed by photon irradiation was lower than the amount obtained by electron irradiation. Silicide formation by both photon and electron irradiation was accompanied by Si depletion in amorphous SiOx. The experimental results indicate that silicide formation is induced by electronic excitation. It is envisaged that a core-hole Auger decay mechanism (i.e., Auger decay of a hole in Si_2p) is responsible for decomposition of SiOx and Pt_2Si formation. A possible mechanism of silicide formation by electronic excitation is proposed on the basis of the experimental results.

11:35-11:55

Study on Test Method of Adhesion of Corrosion Products in High Temperature and High Pressure Heat Exchange Tube

Aijun Yan, Yue Qiao, Zhidong Fan, Xi'an Thermal Power Research Institute Co., Ltd., China

The corrosion of high temperature steam oxidation in fossil fuel power plants is the main cause of the accident of superheater, reheater oxide exfoliation, blockage, tube-burst and solid particle erosion (SPE), which is still one of the main hazards to the safety of the power industry, and results in huge economic loss. Unfortunately, this problem has not yet been solved thoroughly. With the increasing proportion of larger capacity, higher parameter units and frequent deep peak-regulating operation, problems caused by high temperature steam oxidation corrosion are further aggravated. Exfoliation of the corrosion products of high temperature steam oxidation, is the immediate cause of such accidents, but up to now, there is no method to detect and evaluate its adhesion.

In this paper, methods of adhesion testing of both domestic and overseas standards are compared and studied, and a scribed spiral method is proposed to test the adhesion of corrosion products of high temperature and high-pressure tubes, which had been used in the adhesion evaluation test of more than 100 tubes in the laboratory. Based on the tests, the effect factors to adhesion of corrosion products are analyzed. The results show that he thickness of oxide skin and the distance between helixes are important factors affecting adhesion. Furthermore, a new image recognition method is proposed to replace the appearance observation grading method for the evaluation and representation of test results.

11:55-12:15

Anisotropic Elastic-Plastic

Jason Scharff, Gerald Stevens, Brandon La Lone, William Turley, Nevada National Security Site, USA

High-fidelity strength and damage model development and implementation remains a high priority to modern hydrocode development and for predictive material modeling capabilities. Prior work has focused on controlling the internal microstructure (grain size, texture, anisotropy) of polycrystalline metal through processing methods such as annealing and hot/cold rolling. However, very little experimental effort has been devoted to clarifying inelastic deformation mechanisms and understanding plastic flow in dynamically compressed single crystalline metals.

The measured loading and unloading particle velocity time histories in shocked polycrystalline metals exhibit well known deviations from typical elastic-plastic response models that are often used to describe shockwave behavior in metals. For example, shock and release wave measurements in polycrystalline metals demonstrate significant departure from the ideal elastic-plastic response upon release in particular, that shows a gradual transition from elastic behavior to fully plastic behavior, an indication that some amount of plastic deformation is occurring along the entire release path as the material unloads. It has been hypothesized that dislocations pile up at grain boundaries during the loading process creating a back-stress.

Decades of research have established that metals exhibit rate dependent stress-strain behavior due to the irreversible motion of crystal lattice defects called

dislocations. As the material unloads, the dislocations reverse motion, giving rise to the observed quasielastic unloading response. The use of polycrystalline metal simplifies the experiment but complicates theoretical analysis due to the random orientations of slip planes and Burgers vectors, which are required to define the kinematics of crystal plasticity. The distribution crystalline grains that occurs in polycrystalline metals gives the perception that the plastic response is isotropic. Ideally for polycrystalline metals, this means the microstructural origins of strength and plastic deformation should be determined as a function of crystallographic orientation under conditions of shock compression. However, single crystals are strongly anisotropic in their plasticity.
We will present particle velocity time histories obtained during dynamic experiments on individual single crystals of β-Sn impacted along varying orientations and varying thicknesses. Our experiments show orientation-dependence to the HEL and plastic flow.

I. Composite Materials: III

Symposium Organizers:

Lin Geng, Harbin Institute of Technology, China; Boming Zhang, Beihang University, China; Junya Inoue, Tokyo University, Japan; Sang Bok Lee, Korea Institute of Materials Science (KIMS), Korea; Hao Wang, University of Southern Queensland, Australia; Rusty Gray III, Los Alamos National Lab, USA

Wednesday AM
August 21, 2019

Room: 307(3rd Floor)
Symposium: I

Chairs:
Bolv Xiao, Institute of Metal Research, China
Qiang Guo, Shanghai Jiao Tong University, China

8:30-9:00 Keynote

Characteristics of Boron Carbide Reinforced Aluminum Matrix Composites

Seungchan Cho, Donghyun Lee, Sang-Bok Lee, Sang-Kwan Lee, Korea Institute of Materials Science (KIMS), Korea; Ilguk Jo, Dong-Eui University, Korea; Ki Hyeon Kim ,Yeungnam University, Korea

Aluminum matrix composites (AMCs) have drawn much attention over the past few decades and are most promising materials to meet the increasing demand of modern day technology, due to their excellent properties such as light weight, high strength, elastic modulus, good damping characteristics, and excellent wear resistance. Especially, boron carbide (B4C) possesses high hardness, low density (2.51g/cm^3), good hardness and good neutron absorbing ability. The average natural abundance of 10B in B4C is 19.9%, and its thermal neutron absorption cross-section is 3837b. Due to the high neutron absorption cross-section of 10B for a wide energy range of neutrons, B4C has been increasingly used as a neutron absorber material in nuclear industry. However, it is difficult to fabricate B4C thin plates due to their brittleness. Alternatively, many attentions have been paid to B4C reinforced aluminum (Al) matrix composites. Studies on the neutron shielding ability of B4C-Al composites have been carried out and mainly focus on high B4C content.In this study, B4C reinforced Al6061 composites were produced by stir casting and rolling process. B4C particles with the average particle size of 40μm used as the reinforcement material. 5, 10, 20vol% B4C-Al6061 composites fabricated by stir casting were pre-heated and rolled for fabricating B4C-Al6061 plate with 1~2mm thickness. Microstructure of composites specimen was investigated by optical microscopy, transmission electron microscopy (TEM) and scanning electron microscopy (SEM). The density of the prepared metal composite material was measured using the Archimedes principle. Tensile tests were performed using an Instron 5882 machine. Thermal neutron shielding ability of the B4C-Al6061 composites were also analyzed using Am-Be source ($1.227 \times 10^7 s^{-1}$). Thermal conductivity and coefficient of thermal expansion of the B4C-Al6061 composites also evaluated by laser flash apparatus and dilatometer, respectively. These achievements strongly suggest that B4C-Al6061 composites fabricated by the stir casting and rolling process are expected to play a promising neutron absorbing materials in nuclear industry.

9:00-9:25 Invited

Wettability and Reactivity between Molten Aluminum and Carbon Nanotubes

Ping Shen, Jilin University, China

The wettability and reactivity between molten aluminum (Al) and carbon nanotubes (CNTs) is a key issue in the preparation of CNTs-reinforced Al-matrix composites using a solidification route. In this work, we measured the wetting of randomly aligned multi-walled carbon nanotubes (buckypaper) by molten Al at 973~1173K in a high vacuum using a modified sessile-drop method and examined their interactions using a droplet-retraction technique. The wettability between Al and CNTs is even worse than that of the Al/graphite system. The contact angles are basically larger than 140° and only show a sluggish decrease with time during isothermal dwelling. The chemical stability of CNTs in contact with Al is closely related to their structural integrity. The CNTs with good crystallinity and structural integrity have high chemical stability and exhibit only a weak interfacial reaction with Al even at 1173K. However, the stability of structural defects is much lower. The open end of the CNTs slowly dissolves in molten Al at a low temperature (973K) while the tubular structure is not seriously damaged in a relatively short time (10 minutes). At higher temperatures (T≥1073K), the defective portions

of the CNTs such as both ends of the tube, the gaps at the tube wall and the areas of large curvature are readily eroded by molten Al, leading to the fragment of the CNTs. These CNT segments having an open tubular structure are then rapidly dissolved in molten Al in the axial and radial directions. The diameter of the CNT tube becomes smaller and the length shorter. Simultaneously, a large amount of Al_4C_3 is formed at the interface.

9:25-9:45

Dynamic Compressive Properties of Glass/Tungsten Composites at Elevated Temperatures

Chong Gao, Yingchun Wang, Xueya Ma, Beijing Institute of Technology, China

Uniform and compact glass matrix composites with tungsten volume fraction of 40%, 45% and 50% were prepared by powder metallurgy technology with hot-pressing sintering procedure. The dynamic compressive testing was accomplished at temperatures in the range from 450˚C to 750˚C at the strain rate of $3\times10^{3}s^{-1}$ by using a split Hopkinson pressure bar with a synchronous device. The results show that the influence of temperature on dynamic compressive properties of glass matrix composites with different volume tungsten presented a similar trend. At low temperatures such as 450˚C, composites are brittle and the stresses decline sharply after the peak stresses. With the temperature rising, the stresses decrease slowly with strain further increasing after the peak values and the fracture strains increase to 0.3 gradually with the occurrence of the brittle-to-ductile transition. Composites exhibit a high flow stress when the testing temperature reaches 750˚C. When the temperature is below 600˚C, the compressive strength of the composites decreases with the increase of tungsten content, but at relative high temperatures, the trend is the opposite, the more the tungsten content, the higher the strength. With the tungsten content increases from 40 to 50vol.%, the brittle-ductile transition temperature reduces from 505 to 460˚C. Under dynamic loading, adiabatic shear bands appear in the composites, the amount of which decreases with the temperature rising and the tungsten content reduce. Under the experimental conditions, Crack initiation in the composites occurs at the fracture of tungsten particles and the interface separation of the glass and tungsten particles caused by the stress concentration due to the inconsistent deformation of the two phases and disappears in the place where there are many trans-granular fractures of the tungsten particles. In the crack propagation path, the glass tearing, separation of the interface and the splitting of some tungsten particles can be observed.

9:45-10:05

Characterization of Al-Si-SiCp FGMMCs Cast Through Centrifuge Technique

Kiran Aithal, Chethan KS, Nitte Meenakshi Institute of Technology, India; Nareandranath S, Vijay Desai, Nitk Surathkal, India

FGM is a material that shows change in magnitude of property values from one end of a specimen or component to the other end. FGM has an intermediate layer whose structure, composition and morphology vary smoothly from one end of the specimen to the other end. The present work was carried out through centrifuge technique developed by the author to produce FGMs in order to meet the wide range of and also suitable mechanical and tribological properties for specific thermal and mechanical engineering applications. Taking into consideration the advantages such as high wear resistance, controlled thermal-expansion coefficient, good corrosion resistance, and improved mechanical properties over a range of temperatures that Al-Si composites can provide, in this work Al-Si-SiCP FG composites have been produced Al-17%Si and Al-12% Si as matrix with SiCP as reinforcement. Three different volume fractions of SiCP were used to produce FG composites. The FG composites were produced using 900˚C pouring temperature with preheating the mold at 180˚C under 200, 300, 400rpm mold rotational speed. The structure and properties of the FG Composites are studied to understand the effect of different process parameters. It is found that the FG Composites are produced successfully using centrifuge technique. In the Al-Si-SiCP system the gradation occurred in terms of the reinforcement as well as the alloying element. The cast specimen showed the segregation of SiCP at the bottom while Si at the top. The segregation and movement of SiCP to the bottom and Si to the top is influenced by the mold rpm. Higher the rpm better the gradation at the both the ends of the casting. Further the pattern in gradation remained same for all percentages of SiCP and only the percentage segregation increased with increase in weight percentage of SiCP.The experimental findings of hardness and the wear tests provide adequate proof on the gradation characterization in terms of % volume fraction of primary Si and % volume fraction of SiCP carried using microstructural studies.

10:05-10:25

Study on High Temperature Characteristics of TiC Particle Reinforced Stainless Steel

Yeong-Hwan Lee, Seongmin Ko, Hyeonjae Park, Ilguk Jo, Sang-Kwan Lee, Sang-Bok Lee, Seungchan Cho, Korea Institute of Materials Science (KIMS), Korea; Yangdo Kim, Pusan National University, Korea

In the aerospace and transportation industries, there is a

continuing need to develop materials that are lighter and have better mechanical properties in order to improve product performance and reduce costs. When a ceramic reinforcing material is added to an Fe-based alloy base, a metal composite material can be made lighter and more excellent physical properties can be obtained. Of the various ceramic-based reinforcements, TiC has low density and high mechanical properties, and has excellent wettability with metal base, making it highly useful as a reinforcement material for Fe-based metal composite materials.

In this study, we propose the weight reduction and improved high temperature characteristics of SUS 431 alloy by preparing TiC-SUS431 metal matrix composites (MMCs). TiC reinforced stainless steel matrix composites were successfully fabricated by a liquid pressing infiltration process (LPI process) and research was subsequently conducted to investigate the composite's oxidation resistance. The TiC particles are homogenously distributed in the SUS431 matrix and no apparent pores are found in the composites.

The composites were 25.5% lighter than conventional SUS431 alloy.

The microstructures of the composites were analyzed by SEM / EDS, TEM and EPMA analyzes, and high temperature properties were evaluated through high temperature tensile and high temperature compression tests. The high temperature mechanical properties were evaluated through high temperature tensile and high temperature compression tests and the oxidation behavior of the composite at high temperature was analyzed by oxidation resistance test. The oxidation resistance test was conducted through an isothermal oxidation test for 50 hours in an atmospheric environment at 700 degree. The mass gain of the tested TiC 1μm–SUS431 composite held at 700 degree for 50 h in an air environment decreased by about 90%, versus that of TiC 3μm–SUS431composite, which indicates improved oxidation resistance. Improved oxidation resistance of the TiC–SUS431 composite originates from uniformly reinforced TiC, with a phase transition to thermodynamically stable, volume-expanded TiO_2.

10:25-10:45 Tea Break

10:45-11:05

Study on the Microstructure and Mechanical Properties of High Volume Fraction TiB_2-Al Composites

Seongmin Ko, Hyeonjae Park, Yeong-Hwan Lee, Sangmin Shin, Donghyun Lee, Ilguk Jo, Sang-Bok Lee, Sang-Kwan Lee, Seungchan Cho, Korea Institute of Materials Science (KIMS), Korea

In recent years, there has been an increasing interest in high-performance lightweight materials for cost reduction, environmental improvement, and performance enhancement in various fields such as aerospace, transportation, and defense. In order to produce lightweight materials, aluminum (Al) is generally used which has a low density. Although Al is a very light metal with a density of 2.7g/cm^3, the low strength and elastic modulus of Al compared to iron limits the application of Al. In order to overcome these disadvantages, studies have been conducted on the fabrication of Al-based metal composites with ceramic reinforcements such as SiC, B4C, TiB_2, TiC, and Al_2O_3. Especially, TiB_2 ceramic particles, which have high melting point (2790˚c), high hardness (960HV), high elastic modulus (530 × 10^{3}GPa), excellent abrasion resistance, corrosion resistance and thermal stability with excellent Al wettability at high temperature, are suitable as a reinforcement for Al composite materials. In this study, high volume fraction TiB_2-Al composites were fabricated by liquid pressing infiltration (LPI) process using TiB_2 powder (purity: 99.84%, average grain size: 2~3μm) and Al1050, Al6061 and A356 alloys. The LPI process has been developed to infiltrate molten metal into a ceramic preform using hydrostatic pressure, which leads to a uniform dispersion of reinforcements inside the metal matrix. TiB_2 powders were compressed under a uniaxial pressure of 80MPa, and were sintered at 1200˚c for 60min under argon atmosphere for fabricating a TiB_2 preform. The TiB_2 preform was heated to 1000˚c in an MgO mold in the LPI chamber. The molten Al alloys were infiltrated in the pre-heated TiB_2 preform, and was then pressurized with the argon pressure of 10bar. The density of the TiB_2–Al composite was measured by the Archimedes method. The microstructure of the composite is investigated in detail using a scanning electron microscope (SEM; JSM-6610LV, JEOL). Tensile tests were performed using an Instron 5882 machine.

11:05-11:25

Study on Thermal and Mechanical Properties of SiC-Al Alloy Metal Matrix Composites Fabricated by Casting

Hyeonjae Park, Seongmin Ko, Donghyun Lee, Sangmin Shin, Yeong-hwan Lee, Sang-Bok Lee, Seungchan Cho, Sang-Kwan Lee, Ilguk Jo, Korea Institute of Materials Science (KIMS), Korea; Dooho Choi , Dong-Eui Unicersity, Korea

According to European Union (EU) regulations on automotive gas emissions, the automotive industry is improving fuel efficiency, and reducing gas emissions by reducing the weight of vehicle. When the weight of the vehicle is reduced by 100kg, the CO_2 emissions are reduced by 9.7g/km. Aluminum alloys are lightweight(2.71g/cm^3) and have excellent mechanical properties. However, there are limitations in applying them to automotive parts (brake disc, brake pads, engines as piston) due to the relatively lower specific

strength at the elevated temperature. In order to produce lightweight part, many researches are being conducted on lightweight and high-strength Al based metal matrix composites (Al-MMCs) which reinforced with ceramic reinforcements such as SiC, Al_2O_3, B4C. Al-MMCs with their high-temperature capability, high thermal conductivity, low coefficient of thermal expansion (CTE), and high specific strength provide the necessary characteristics to produce lightweight automotive parts for harsh conditions. In this study, Al alloy which has excellent mechanical properties such as high strength and high hardness was used as a matrix. For the reinforcement, SiC particle was used due to the thermal stability, superior mechanical properties and good interfacial bonding with Al. SiC-Al metal matrix composites were fabricated by casting process and their microstructure, mechanical properties and thermal properties were characterized. Optical microscopy (LV100ND, NIKON) and scanning electron microscope (JSM-6610LV, JEOL) were used to analyze the microstructures of the SiC-Al composites. The density of the prepared SiC-Al metal matrix composites was measured using the Archimedes principle. To evaluate mechanical properties, tensile strength at room temperature was measured by using a universal material testing machine (5882 model, Instron) and the hardness was measured 5 times using Vickers hardness tester (HR-210MR, mitutoyo) and the average value was calculated. The coefficient of thermal expansion (CTE) of the SiC-Al composite material was measured using a Dilatometer (DIL 402C).

11:25-11:45

Preparation and Properties of Metal-Ceramic Hollow Spheres and Their Composite Foams

Mengxin Cao, Chunhuan Guo, Fengchun Jiang, Chunhe Wang, Tianmiao Yu, Harbin Engineering University, China

Composite metal foams (CMFs) are a kind of novel cellular and porous materials with low density, high specific strength, great thermal insulation, energy absorption and radiation shielding capabilities. There are many processing methods to fabricate CMFs materials. Using the traditional method, the porous composite with different size and non-uniform distribution may be prepared. In order to improve above limitations. The metal hollow spheres are proposed. Metal hollow spheres as a new phase are embedded in different metal substrate by various methods to create close porous composite with the same size and uniform distribution, which can effectively manufacture heat transfer barriers and prolong the heat transfer path. Small diameter of metal hollow spheres reduce gas convection and heat conduction inside the hollow sphere structure. Therefore, a sufficient number of interfaces between metal spheres and matrix can affect the thermal radiation decreasing. As we all know that the thermal conductivity of hollow sphere wall made of metal is still high. In order to further improve the thermal insulation properties of metal hollow spheres and their composite material, ceramic was added to the hollow spheres utilizing the thermal shielding advantage of ceramic. Metal-ceramic hollow spheres with 3~5mm diameter of inner ceramic and outer metal were produced by coating and sintering. Based on the production of hollow spheres above, combine them with lower melting point metals to prepare composite materials. Their composite metal foams were produced by powder metallurgy (PM). The microstructure, interface combination and properties of metal-ceramic hollow spheres and their composite metal foams were studied. As for metal-ceramic hollow spheres, inner ceramic may further enhance the thermal insulation performance of composite foams, and plays a supporting role on each hollow sphere as well. While the outer metal can also increase the strength and toughness of the ceramic hollow sphere. These metal-ceramic hollow spheres and their composite foams can combine the advantages of hollow sphere structure and ceramic in terms of thermal insulation. At present, there are some investigations on metal hollow spheres and their composite materials. Some works has focused on thermal insulation and other functional performances of composite metal foams. This study applies composite ideas to the scale of single metal hollow spheres, which combine ceramic and metal on the wall. These may help solving some thermal insulation and radiation shielding issues in some engineering fields.

11:45-12:05

Multifunctional Properties of Geopolymer Composites

Liying Zhang, Donghua University, China

Geopolymer belongs to a new class of inorganic polymers obtained through polymerization of aluminosilicates and alkaline solution with significantly reduced greenhouse gas emission during production. It can be easily processed at low temperature, and possess mechanical performance comparable to conventional ceramics and alumina alloy. Other merits include low density, high thermal stability, fire and acid resistance. Owing to its many excellent properties, geopolymer has been considered a promising structural material to replace Portland cement for construction applications. However, geopolymers suffer intrinsic brittleness and inherent stable similar to conventional concrete and ceramic materials. In this work, the geopolymer nanocomposites were prepared based on the unique behaviors of SiO_2 coating on CNTs in the geopolymer matrix. The SiO_2 layer on CNTs was partially or fully removed during the fabrication process to restore the conductive nature of

CNTs, facilitating the dispersion of CNTs and forming well connected 3D electrical conductive networks. This unique interface engineering on chemistry and materials science aspects enabled us to prepare geopolymers composites not only with high strength and fracture toughness, but also with multifunctional properties such as self-stress sensing and EMI shielding properties. The obtained geopolymer composites with enhanced strength and toughness allow for applications requiring high load capacity. Integrating functional properties of geopolymers fulfills the strict requirements for advanced applications, especially the combination of good mechanical properties.

J. Amorphous and High Entropy Alloys: Amorphous Alloys IV

Symposium Organizers:

Weihua Wang, The Institute of Physics, Chinese Academy of Sciences, China; Zhaoping Lv, University of Science and Technology Beijing, China; Hidemi Kato, Tohoku University, Japan; Hojin Ryu, Korea Advanced Institute of Science and Technology (KAIST), Korea; Michael Ferry, New South Wales, Australia; Evan Ma, Johns Hopkins University, USA

Wednesday AM
August 21, 2019

Room: 405 (4th Floor)
Symposium: J

Chairs:
Ye Pan, Southeast University, China
Lin Liu, Huazhong University of Science and Technology, China

8:30-8:55 Invited

Single-Element Metallic Glasses

Scott Xingyuan Mao, University of Pittsburgh, USA

It has long been conjectured that any metallic liquid can be vitrified into a glassy state provided that the cooling rate is sufficiently high. Experimentally, however, vitrification of single-element metallic liquids is notoriously difficult. True laboratory demonstration of the formation of monatomic metallic glass has been lacking. Here we report an experimental approach to the vitrification of monatomic metallic liquids by achieving an unprecedentedly high liquid-quenching rate of 1014Ks. Under such a high cooling rate, melts of pure refractory body-centred cubic (bcc) liquid tantalum and vanadium, and fcc Ni under H_2 environment are successfully vitrified to form metallic glasses through liquid/solid interface driven process. Combining in situ transmission electron microscopy observation and atoms-to-continuum modelling, we investigated the formation condition of the monatomic metallic glasses as obtained. The availability of monatomic metallic glasses, being the simplest glass formers, offers unique possibilities for studying the structure and property relationships of glasses. The interface-driven technique also shows great control over the reversible vitrification–crystallization processes, suggesting its potential in micro-electromechanical applications. The ultrahigh cooling rate, approaching the highest liquid-quenching rate attainable in the experiment, makes it possible to explore the fast kinetics and structural behaviour of supercooled metallic liquids within the nanosecond to picosecond regimes.

8:55-9:20 Invited

Manufacturing of Metallic Glasses

Lin Liu, Huazhong University of Science and Technology

Metallic Glasses (MGs) and bulk metallic glasses (BMGs), as a novel type of metals with disordering atomic structure, exhibit a set of unique properties, including high strength, high elasticity, good wear and corrosion resistance, as well as excellent magnetic properties (For Fe-based MGs), thus have attracted increasing attention in recent years. However, the inherent brittleness and manufacturing difficulty block the application of MGs/BMGs as structural materials. The development of appropriate manufacturing techniques is the key to break through the bottleneck of the application of these materials. This report will introduce the recent progress in manufacturing of metallic glasses in the author's team in recent years, including thermoplastic microforming, thermal spray and laser-based 3D printing. The principle of each technique and the effect of manufacturing process on microstructure and properties of metallic glasses are addressed.

9:20-9:45 Invited

Consolidation of the Ni-Cr-Nb-P-B Metallic Glass Powder

Kenji Amiya, Tohoku University, Japan; Yasunori Saotome, MGA Research Laboratory, Japan; Noboru Shimada, Porite Co., Ltd., Japan

A large number of Ni-based metallic glasses (MGs) such as Ni-X-P-B and Ni-X-Nb-Zr multi component alloy have been developed. The Ni-Cr-Nb-P-B MG exhibit high yield strength, large elastic strain limit and high corrosion resistance with high glass forming ability. We are investigating the application using the high corrosion resistance property of Ni-Cr-Nb-P-B MG. However, there is a problem of the crystallization with heterogeneous nucleation in the casting material of Ni-Cr-Nb-P-B alloys. Therefore, the powder consolidation is a good method of improving preparation of the parts of Ni-Cr-Nb-P-B bulk MG. The powder consolidation of Ni-Cr-Nb-P-B MG powder was carried out.
Ni69Cr9Nb2P16B4 ($Ni\text{-}Nb_2$) MG exhibits larger super-

cooling liquid region and higher elongation compared to Ni65Cr11Nb4P16B4 (Ni-Nb_4) MG. There were no crystalline peaks in the X-ray diffraction pattern of the Ni-Nb2 powders with diameter below 250μm. However, a few crystalline particle were seen on the cross-section of Ni-Nb_2 powders with diameter below 38μm and by a differential interference contrast microscope. No crystalline particles were observed in the gas atomized Ni-Nb_4 MG powders with diameter below 53μm. In order that back extrusion and consolidation process might give large shearing to powder, the Ni-Nb_4 MGs are indicated good consolidation. Furthermore, the high-rates powder consolidation sequential system for MGs with no vacuum was also developed, and can carry out consolidation of 60 parts per hour of Ni-based MG. The miniature bearing made from Ni-Nb_4 MG was demonstrated as the results of above development.

9:45-10:05

Investigations on New Bulk Metallic Glasses Alloys Fabricated by High-Pressure Die Casting Based on Industrial Grade Zr

Tao Zhang, Guangdong University of Technology, China / Institute of Eontec New materials Co., Ltd., China; Chengyong Wang, Xianna Meng, Guangdong University of Technology, China; Lugee Li, Kuan Gao, Xuguang Zhu, Institute of Eontec New materials Co., Ltd., China; Yong Zhang, University of Science and Technology Beijing, China

Low-cost Zr65.31Ti3.27Cu15.51Ni11.69Al3.68Y0.4 and Zr68.84Nb4.59Cu12.99Ni9.76Al3.66Y0.5 BMGs were successively designed and fabricated by high-pressure die casting with industrial grade sponge Zr material with minor Y addition, with 1mm-5mm in diameter. The glass forming ability, critical size, microstructures were investigated, in association with mechanical property measurements. The results show that Y addition effectively eliminates the residual O-concentration of BMGs, and improve the glass forming ability. The critical sizes of both BMGs reach several millimeter (less than 5mm). The compressive stress-strain curves of Zr65.31Ti3.27Cu15.51Ni11.69 Al3.68Y0.4and Zr68.84Nb4.59Cu12.99Ni9.76Al3.66Y0.5 BMGs with a strain rate of $5\times10^{-5}s^{-1}$ were obtained at room temperature. The fractured surfaces of fractured BMGs were characterized by SEM and EDS. The effective activation energy E for the crystallization under continuous heating conditions was determined. The Zr68.84Nb4.59Cu12.99Ni9.76Al 3.66Y0.5 BMG shows the higher glass forming ability, thermal stability, compressive strength and ductility when compared with the Zr65.31Ti3.27Cu15.51Ni11. 69Al3.68Y0.4 BMG due to its higher △Tx, Trg, γ and Ec values. However, both the BMGs show good glass forming ability and compressive strength, and have excellent potentials of industrial application. Meanwhile, the present work provides good guidance effects for the design and preparation of low-cost BMGs.

10:05-10:25

Tailoring Phase Selection and Microstructure through Controlled Synthesis of Al-Sm Metallic Glasses

Fanqiang Meng, Yang Sun, Matthew Kramer, Ryan Ott, Ames Laboratory (USDOE), USA

The importance of short-and medium-range ordering as precursors for phase and structural formation during devitrification of metallic glasses is well-known. It is less clear, however, how the structural ordering in the starting amorphous structure can be controlled, and thus, the subsequent phase selection tailored. For example, Al-Sm metallic glasses synthesized via melt spinning show very different devitrification behavior, which is presumably due to the difference in cooling rates through the thin ribbons. A metastable phase with a large hexagonal structure, usually present in sputtered thin film, was formed at wheel-side of the ribbon coupled with fcc-Al phase. Meanwhile, the grain size of primary cubic phase with large unit cell shows an abnormal change as a function of distance from wheel-side. The minimum grain size was found at the location about 4~5 micrometer away from wheel side. Using a combined experimental and modeling approach, we have investigated the importance of different cluster structures in controlling the phase selection and morphologies during devitrification. <16661> short-range ordering cluster in supercooled liquid was regarded as a key factor to decide the different phase selection and abnormal evolution of grain size is possible related to the competition between growth of quenched-in and newly formed nuclei. The implications for controlling subsequent phase selection in these amorphous alloys via smart synthesis are discussed.

10:30-10:45 Tea Break

10:45-11:10 Invited

Controlled Microstructures and High Photocatalytic Efficiency of Metal Oxides Synthesized by Amorphous Alloys

Ye Pan, Ning Wang, Tao Lu, Southeast University, China

Amorphous alloys have recently attracted the most attention not only due to their outstanding mechanical properties, but also thermodynamically metastable and highly homogeneous composition which makes synthesize high performance functional materials effectively. The photocatalytic techniques, such as dye

degradation by metal oxides, are efficient and practical approach used for wastewater remediation in the case of increasingly serious resource scarcities, energy shortages and environmental problems nowadays. Active radicals produced in these processes can effectively degrade organic dyes due to their strong oxidizing. In order to obtain high photocatalytic efficiency, the microstructure controlled metal oxides have been fabricated by using the precursors of Cu-based amorphous ribbons in this work. Nano-TiO_2 photocatalytic materials were synthesized by dealloying Cu-Ti amorphous ribbons in the corrosion system of nitric acid. The microstructure and catalytic activity of the corrosion products of Cu70Ti30 amorphous ribbons can be tuned by the addition of surface active agent in the corrosion process, the active element substitution in amorphous alloys and heat treatment for corrosion products. The results showed that the addition of surface active agent (K_2SO_4) adjusted the preparation period of nano-TiO_2, thus achieving the goals of crystal structure control of TiO_2. Interestingly, the active element (Y) substitution not only shortened the preparation period of nano-TiO_2, but also refined its microstructure and improved the photocatalytic activity. Besides the preparation of nano-TiO_2, SnO_2-TiO_2 solid solution and composites were fabricated by dealloying Cu60Ti30Sn10 amorphous ribbons in nitric acid solution. The rutile TiO_2/Sn0.42Ti0.58O_2 exhibited enhanced photodegradation activity towards RhB compared to rutile TiO_2 and Sn0.42Ti0.58O_2. The high photocatalytic activity is mainly attributed to the formation of TiO_2/Sn0.42Ti0.58O_2 heterojunction, which can provide a driving force for the migration of photogenerated carriers to the catalyst reaction interface. Thus, the separation of photogenerated electrons and holes is promoted, and the photocatalytic activity is improved. Our findings not only provide the new highly photocatalytic hybrid metal oxides, but also extend the functional applications of amorphous alloys.

11:10-11:35 Invited

Preparation High Entropy Bulk Metallic Glass with High Glass Forming Ability

Takeshi Wada, Hidemi Kato, Tohoku University, Japan

High-entropy alloys (HEAs) are recently attracting great attention in the material science research. It is a multicomponent alloy with single of multiphase solid solution with simple crystalline structure such as BCC, FCC or HCP. The HEAs exhibit excellent properties such as high strength, ductility, thermal stability, creep resistance, corrosion resistance that originate from four core effects, namely, high configurational entropy, sluggish diffusion, lattice distortion and cocktail effect. The bulk metallic glass, on the other hand, is also known to have attractive properties such as high strength, excellent corrosion resistance, and viscous workability. By introducing high entropy effect to the BMGs, one can expect novel properties that are different form the conventional BMGs or crystalline HEAs. To date, the HEBMGs have been developed mainly in the equimolar alloy compositions such as Ti20Zr20Hf20Cu20Ni20, Zn20Ca20Sr20Yb20, Pd20Pt20Cu20Ni20P20, Sr20Ca20Yb20Mg20Zn20, Sr20Ca20Yb20Mg20Zn10Cu10, Er20Tb20Dy20Ni20Al20, Zr20Ti20Cu20Ni20Be20 and Ti16.67Zr16.67Hf16.67Cu16.67Ni16.67Be16.67. However, these HEBMGs generally have lower glass-forming ability than that of their parent alloy. These previous works clearly indicate that the composition that maximizes configuration entropy is not necessarily the composition that maximizes glass-forming ability. Accordingly, there is a possibility of finding a high glass-forming ability HEBMG in the non-equimolar composition.

In this research, we aim to develop new HEBMGs with high glass-forming ability. We search for the senary and septenary eutectic alloy within the composition range that satisfies the widely accepted definition of HEA, that is, (i) more than 5 components, (ii) concentration of components between 5 to 35at.% and (iii) configurational entropy of alloy is more than 1.5R. We started from a ternary eutectic Zr-based alloy and it was modified by heavy doping of other components such as Hf, Ti, etc. Based on the microstructural, compositional and calorimetric analyses of the alloys, the composition was optimized close to the eutectic point. As a result, a septenary near-eutectic Zr-Hf-Ti-Al-Co-Ni-Cu alloy with a high glass-forming ability up to 18mm diameter by copper mold casting was discovered. In the presentation, the entropy effects on the glass forming ability, crystallization and mechanical properties, etc. will be discussed.

11:35-11:55

U-Based Binary Strong Glass Forming Systems

Huogen Huang, Haibo Ke, Pei Zhang, Pengguo Zhang, Institute of Materials, China Academy of Engineering Physics, China

Fundamental issues of U-based binary metallic glasses have been scarcely studied due to their low thermostability and glass forming ability. In this work, the glass formation in U-Fe, U-Co and U-Ni alloy systems was re-examined. A series of alloys in these systems were designed and then melted. After melting, they were prepared into ribbon samples by melting-spinning technique. The structures and thermal

stabilities of the assembling ribbons were studied by means of X-ray diffraction and differential scanning calorimetry. It is found that amorphous phase can be obtained in all these alloys. The glassy alloys in U-Ni system show a pronounced thermal glass transition feature at the usual heat rate of 20K/min for the first time among binary U-based alloy systems, and also have a relatively high glass transition temperature (Tg) above 600K and a comparatively high reduced glass transition temperature (Trg) of 0.597. Meanwhile, the metallic glasses in U-Fe and U-Co systems show the Tg feature only at high heating rates of >80K/min, and have lower Tg and Trg values than those in U-Ni system at the same heating rate. The Tg presence contributes to the evaluation of their glass transition activation energy, liquid fragility, viscosity as well as the Kauzmann temperature. For a typical alloy in U-Ni system, the glass transition activation energy can reach about 226kJ/mol, the fragility value is close to 20, and the Kauzmann temperature is about 450K. But for U-Fe and U-Co systems, the fragility values are less than 20, despite the glass transition activation energies are above 226kJ/mol. The low fragility behavior illustrates that these three systems belong to strong glass forming systems. The reasons for the remarkable Tg presence in U-Ni system and low fragility together with the GFA level of binary and ternary U-based glass systems are discussed from the structural, thermodynamic and kinetic viewpoints.

11:55-12:15

Die-Imprinting of Metallic Glasses and Its Potential Applications

Xue Liu, Institute of Materials, China Academy of Engineering Physics, China / Tsinghua University, China; Jinfeng Li, Guomin Le, Institute of Materials, China Academy of Engineering Physics, China; Kefu Yao, Tsinghua University, China

Metallic glasses (MGs) possess not only superior mechanical and functional properties but also excellent net-shape forming ability, which could be used for fabricating structures and devices in nano-micro scale. In order to overcome the drawback of the commonly used free-imprinting technique, where the stress decreasing along the radial direction of the imprinting surface, a die-imprinting technique has been developed, which can effectively enhance the uniformity of the stress within the supercooled liquid of the glassy alloys. In the present work, the preparation, characterization, morphology evolution and the potential applications of the die-imprinted nano-micro structures were systematically studied. The prepared MG nanowire arrays possess high uniformity and exhibit reproducible surface enhanced Raman scattering activity. The prepared MG sub-micro photonic crystals exhibit uniform structural colors. The MG micro optical devices could serve as inexpensive and durable mould inserts for precise embossing of polymer micro devices in large scale. Besides that, a new type of Ni-based MG was developed for the die-imprinting application. The present work provides important insights into the experimental fundaments for the die-imprinting processing, and can greatly promote the further applications of MGs.

12:15-12:35

CuZrY Metallic Glass: An Energetic and Controllable Precursor for Preparing Oxide Hetero-Junction

Yinan Zhu, Southeast University, China

Photocatalytic technology is widely considered to be a promising approach toward overcoming the problems of increasing environmental pollution and worldwide energy shortage. Transition metal oxides with suitable band structure and strong optical absorption, which avoid the light corrosion and instability of the traditional sulfide, have been an important direction for designing and fabricating new visible-light responsive photocatalysts. Most synthetic processes in the previous studies focused on liquid-phase chemistry that is typically associated with waste liquid and gas, so that this is not friendly to the environment and new green routines are necessary to be developed. The metallic glass is obtained at an extremely high cooling velocity, which makes it a thermodynamically metastable state that a tiny amount of energy could ignite the metal ribbon. What determines the possibility of a metallic glass to be ignited actually is the metal to oxygen chemical-bond energy and the density of the oxides. In this work, metallic glasses, such as Cu60Ti40, Cu60Zr40 and Cu60Zr40-xYx (x=5, 10, 15) were prepared by the melt-spinning method. It was found the Cu60Ti40 metallic glass is burning-resistant while the rest metallic glasses are self-sustaining. Compared with the results of the calculation and experiments, the combustion violence of the metallic glasses can be efficiently regulated by replacing Zr with Y in Cu60Zr40. It also reveals that the optimal doping of yttrium in precursors was approximately 10at%, and the corresponding sample possesses bandgap energy of 2.61eV and the most outstanding photocatalytic ability in degrading Methylene Blue (MB). The result above could be attributed to the important role of Y_2O_3, which stabilizes the ZrO_2 phase and reduces the bandgap of the ZrO_2 in the hetero-junction, thus significantly prolongs the lifetime of electron-hole pairs and improves solar energy utilization ratio. This work opens up a new window to use this facile approach to synthesize composite materials in the area of photocatalysis.

J. Amorphous and High Entropy Alloys: High Entropy Alloys IV

Symposium Organizers :

Weihua Wang, The Institute of Physics, Chinese Academy of Sciences, China; Zhaoping Lv, University of Science and Technology Beijing, China; Hidemi Kato, Tohoku University, Japan; Hojin Ryu, Korea Advanced Institute of Science and Technology (KAIST), Korea; Michael Ferry, New South Wales, Australia; Evan Ma, Johns Hopkins University, USA

Wednesday AM
August 21, 2019

Room: 303 (3rd Floor)
Symposium: J

Chairs:
Yuan Wu, University of Science and Technology Beijing, China
Weili Wang, Northwestern Polytechnical University, China

8:30-9:00 Keynote

Computational Design of High Entropy Alloys

Byeong-Joo Lee, Won-Mi Choi, Pohang University of Science and Technology (POSTECH), Korea

High-entropy alloys (HEAs) are attracting an academic interest for their promising and unique properties as structural materials. Particularly, the equiatomic CoCrFeMnNi HEAs have been reported to possess a wide-range of promising properties such as good high temperature structural stability and an excellent balance between strength and ductility, particularly at cryogenic temperatures, typically 77K, the liquid nitrogen temperature. Even though most HEAs have equiatomic or near equiatomic compositions, it is believed that the equiatomic composition would not be the optimum composition for a wide range of material properties. To improve a specific material property, one may have to change the alloy composition from the equiatomic composition. Indeed, there have been many efforts to improve the face-centered cubic (fcc) single-phase stability or mechanical properties of the CoCrFeMnNi HEAs by adjusting the composition or introducing new elements. However, for an efficient alloy design, one would need to understand the reason for the typical HEA properties and the effect of individual elements on them. In the present talk, an alloy design procedure to improve the strength of the alloy will be outlined. The CALPHAD computational thermodynamics technique is used to predict the fcc single phase region and the relative stability of the fcc phase over body-centered cubic (bcc) or hexagonal close-packed (hcp) phases in multicomponent systems. Atomistic simulation based on a newly developed (semi-)empirical interatomic potential is used to estimate the effect of individual elements on the critical resolved shear stress of the multicomponent fcc crystal as well as to understand fundamental materials properties of the fcc HEAs (deformation mechanism, diffusion behavior, etc.). An experimental validation of the computational approaches will be presented. Some examples of the application of the computational approaches to alloy design of HEAs with fcc single phase microstructure, with transformation-induced plasticity (TRIP), twinning-induced plasticity (TRIP) and with optimum amount of second phase will also be presented together with experimental results.

9:00-9:25 Invited

A Combinatorial Study of BCC High Entropy Alloys for Heat Resistant Applications

Ho Jin Ryu, Owais Waseem, Korea Advanced Institute of Science and Technology, Korea

Refractory high-entropy alloys based on the BCC structured matrix are promising for high temperature applications because of their unprecedented high temperature strength. However, their brittleness at room temperature and poor oxidation resistance hinder the progress of the development for heat resistant high entropy alloys. A combinatorial alloy design approach was used to explore the microstructure evolution and mechanical properties of refractory high entropy alloys containing Al, Cr, Mo, Nb, Ti, and Zr. By changing the compositions of Al, Cr, Mo, Zr, the constituent phases, room temperature failure strain, high temperature yield strength were characterized by using electron microscopy and compression testing, respectively. AlxCryMozNbTiZr and AlaCrbMocNbTiZr0.5 systems were prepared by arc melting. The effects of annealing were tested by changing the annealing temperature and cooling rate of samples. The specific compositions having a high yield strength greater than 1000MPa at 1000˚c were selected and investigated their high temperature deformation behavior. Oxidation resistance of the high entropy alloys were characterized by thermogravimetry and long term air oxidation tests. Specifically the effects of the composition of Al, Cr, Mo were characterized in the AlxCryMozNbTiZr system and in the Al0.5CrMoxNbTiZr0.5 system, respectively. The combinatorial approach of BCC-based high entropy alloys with the high temperature strength and oxidation resistance was useful to select promising alloy systems and investigate the strengthening mechanisms resulting in extraordinary yield strengths at high temperature.

9:25-9:50 Invited

Fabrication of Nano-Structure AlCoCrFeNi High Entropy Alloy Through Shock Consolidation and Mechanical Alloying

Ali Arab, Pengwan Chen, Beijing Institute of Technology, China

HEAs are usually fabricated using arc melting which has the disadvantages of diseconomy, and the limitations in the shape and size of final products. However, recently,

quite a large number of researches have carried out to find the new fabrication techniques to fabricate HEAs with better properties such as mechanical alloying and rapid solidification. AlCoCrFeNi high entropy alloy is fabricated by different fabrication techniques. In this paper, AlCoCrFeNi high entropy alloy is successfully fabricated by the shock consolidation technique. In this method, the starting powders were mixed by the mechanical alloying, and then, the shock wave was imposed to the compacted powders by explosion. The shock consolidation experiments were carried out in a set up with a cylindrical configuration, the steel tube was filled with the mixed powders which was uniaxial pressed in order to attain a 70% of theoretical density, and closed at both ends. The steel tube was surrounded by powder explosive named expanded Ammonium Nitrate with a detonation velocity of 2300m/s. The microstructure of the sample was examined by the XRD, SEM and EBSD. Body Center Cubic (BCC) and Face Center cubic (FCC) Crystal structures are identified in both milled and shock consolidated samples. The microstructure of the fabricated sample shows that the nano-size grain (average grain size of 26nm) is formed in the sample. Fabricated HEA has high hardness (550.7HV) as well as high density.

9:50-10:10

Nanoporous High-Entropy Alloys Overcome the Thermally-Induced Coarsening

Soo-Hyun Joo, Takeshi Wada, Hidemi Kato, Tohoku University, Japan

Controlling the size of nanomaterials is essential to apply these unique materials for the various applications such as catalyst, sensor, and capacitor which need a high specific surface area. Among diverse categories of nanomaterials, three-dimensional bicontinuous nanoporous (3DNP) materials produced by chemical dealloying have outstanding electrochemical properties because of its unique structure with open porous networks constructed by nanoscale interconnected ligaments. The sizes of produced features such as ligament and pore are dependent on processing conditions like dealloying temperature and time. However, the coarsening behavior, which is the surface-diffusion-driven phenomenon regarded as an intrinsic property of a material to reduce the surface energy, degrades physical properties of nanomaterials even at ambient temperature. The conventionally treated alloying concepts do not overcome the universal relationship in an empirical correlation with homologous temperature (T melting /T dealloying or annealing) because the matured ligament size is inversely proportional with a melting point. Here we present a multi-principle alloying strategy for designing 3DNP material. High-entropy alloys (HEA) with compositionally equivalent phase demonstrates high phase stability through entropy maximization, and sluggish diffusion kinetics is the reason for the exceptional high strength and structural stability at high temperatures.

To attain the multi-principle nanoporous alloy, we utilize liquid metal dealloying (LMD) process which is the unique technique to fabricate non-noble porous materials by preventing oxidation in a metallic melt. We increase the structural stability of nanoporous materials by suppressing surface diffusion to achieve a key benefit in maintaining ideal physical properties even at high-temperature applications. Our achievement, remarkably tiny ligaments, is one order of magnitude smaller than other general porous materials in the empirical correlation. This strategy to synthesize the stable nanoporous structure will guide to improve mechanical, physical and hybrid properties by tuning the pore size down to even at high temperatures. Therefore, our findings will shed light on studies to enhance and maintain the properties of nano-materials.

10:10-10:30

Experimental Investigation and Phase Diagram of CoCrMnNi–Fe System Bridging High-Entropy Alloys and High-Alloyed Steels

Nokeun Park, Ibrahim Ondicho, Yeungnam University, Korea; Won-Mi Choi, Byeong-Joo Lee, Pohang University of Science and Technology, Korea; Jong Bae Jeon, Korea Institute of Industrial Technology, Korea; Hamidreza R. Jafarian, Iran University of Science and Technology, Iran; Sun Ig Hong, Chungnam National University, Korea

High-entropy alloys (HEAs) constitute a unique class of alloys that has attracted significant attention from material scientists. It has been reported that their high-configurational entropy favors the formation of solid solution phases such as face-centered cubic (fcc), body-centered cubic (bcc), and hexagonal closed-packed (hcp) crystal structures against the expected intermetallic phases according to existing physical metallurgy principles. An investigation of equiatomic and non-equiatomic high-entropy alloys (HEAs) and medium-entropy alloys (MEAs) was carried out by performing both thermodynamic calculations and experiments. The design strategy of the alloys was based on a constant valence electron concentration (VEC) of 8 while varying the content of Fe in a Fex(CoCrMnNi)100−x where x = 00, 20, 40, and 60.

A phase diagram of CoCrMnNi-Fe system was presented. According to this phase diagram, increasing the Fe content reduces the melting temperature and the onset temperature of the undesirable σ phase, with Fe50 having a single phase fcc, even at 600℃. The alloys exhibit a single-phase fcc structure after annealing at 900℃. Additionally, the probability of the formation

of a bcc phase increases with the increase in the Fe content. Our experimental results confirmed that Fe20, Fe40, and F60 have a single-phase fcc, which is in good agreement with the results of the thermodynamic calculations.
The tensile test results revealed that both the yield strength and ultimate tensile strength decrease as the amount of Fe is increased but the uniform elongation increases. Additionally, the strain-hardening rate is significantly enhanced at higher Fe concentrations due to the activation of deformation twinning as an additional deformation mechanism. Interestingly, the critical twinning stress is significantly reduced as the Fe content is increased from Fe00 to Fe60. As a result, the deformation twins were easily activated in a specimen deformed up to a true strain of 20% for Fe60, unlike the other alloys, which exhibited no deformation twinning at the same true strain. Furthermore, it was revealed that the frequency of deformation twinning increases proportionally with increase in the Fe content.

10:30-10:45 Tea Break

10:45-11:10 Invited

Material Wear Map for High Entropy Alloys

Nima Haghdadi, UNSW Sydney, Australia; Nima Haghdadi, Tingting Guo, Alireza Ghaderi, Peter Hodgson, Matthew Barnett, Daniel Fabijanic, Deakin University, Australia

The intrinsic scratch resistance of as-cast Al1.0CoCrFeNi (BCC) and Al0.3CoCrFeNi (FCC) in the as-cast, homogenized and recrystallized conditions was investigated using tip radii of 25μm and 0.8mm. Through analyzing the geometry of the grooves, the wear mechanism and total material loss were measured. For the FCC material in all conditions, the wear mechanism was almost the same. The wear rate increased with increasing load, and the fraction of material removed from the groove fell in the range of 0.2~0.7. A significant decrease in the wear rate was observed for the BCC material mainly due to its high hardness. The fraction of material removed from the groove for the BCC material was in the range of 0.7~0.9, which implies dominance of the cutting wear mechanism. A wear map based on 'scratch hardness' and 'scratch ductility' was constructed to enable comparison of the wear performance of materials under different loading conditions. The map was analogous to those frequently used to compare the strength and ductility of structural metals. It was found that the importance of hardness in wear is highly dependent on load. At high loads the wear performance of alloys highly depends on the scratch hardness. For low loads, however, the combination of hardness and scratch ductility dictates material total loss.

11:10-11:35 Invited

Reinforcement of HEAs via Stress-Induced Phase Transformation

Yuan Wu, Zhaoping Lu, Hui Wang, Xiongjun Liu, Hailong Huang, Fei Zhang, University of Science and Technology Beijing, China

High-entropy alloys (H E A s) which are composed of equiatomic or near-equiatomic elements have attracted extensive attentions for their continuously revealed novel physical, chemical and structural properties. Body-center-cubic (bcc) H E A s, particularly those based on refractory elements are promising for high-temperature application but generally fail by early cracking with limited plasticity at room temperature, which limits their malleability and widespread uses. In this work, we clearly demonstrated that these brittle bcc HEA s can be successfully ductilized and toughened by exploiting the "metastability-engineering" strategy. We controlled the thermodynamically and mechanical stability of bcc phase via tuning the content of bcc stabilizer Ta in the prototype TaHfZrTi, rendering the formation of composite structure of interlaced hcp and deformation-transformable bcc phases. The destablized H E A s exhibited pronounced ductility (from 4.0 ± 1.7% to ~30%) and work-hardening ability. The enhancement of comprehensive mechanical properties was attributed to collaborative transformation-induced plasticity (TRIP) and dynamic interface hardening effect. This work not only sheds new insights on development of HEA s with excellent combination of strength and ductility, but also has great implications on overcoming the long-standing strength-ductility tradeoff of metallic materials in general.

11:35-11:55

Effect of High Pressures on the Phase Transition of MoxCrFeCoNi High Entropy Alloys

Wei-Hong Liu, Yang Tong, Hong-Hui Wu, Tao Yang, Xunli Wang, J. J. Kai, C. T. Liu, City University of Hong Kong, Hong Kong, China; S. W. Chen, National Synchrotron Radiation Research Center, Taiwan, China; Xingjun Liu, Harbin Institute of Technology (Shenzhen), China

The pressure-induced face-centered cubic (fcc) to hexagonal close-packed (hcp) athermal martensitic transition in CrMnFeCoNi has drawn a great attention in high-entropy alloys (HEAs) research community, as it not only demonstrates a new paradigm to tune their structures and properties but also inspires new understanding of the intrinsic stability of the two close-packed structures. However, the key factor in determining the occurrence of this pressure-driven transition is still unclear, here, we demonstrate that the

alloying of Mo with a relatively low d-band occupation into CrFeCoNi could destabilize the initial fcc structure and accelerate the pressure-induced fcc-to-hcp transition, this suggesting that the contribution of d electrons to valence states of the starting materials determines whether the transition takes place or not. Furthermore, a full recovery to the fcc phase was observed by high resolution transmission electronic microscope in Mo0.23CrFeCoNi after releasing from a high-pressure of 20GPa, at this pressure about 25% the hcp phase was detected by synchrotron radiation X-ray diffraction. This result evidently demonstrates that the fcc structure is more stable than the hcp structure at least above 298 K at ambient pressure in Mo0.23CrFeCoNi.

K. Nanocrystalline Materials, and Ultra-Fine Grained Materials: IV

Symposium Organizers :

Yue Zhang, University of Science and Technology Beijing, China; Zhiyong Tang, National Center for Nanoscience and Technology, China; Nobuhiro Tsuji, Kyoto University, Japan; Jae-il Jang, Hanyang University, Korea; Kenong Xia, University of Melbourne, Australia; Nathan Mara, University of Minnesota, USA

Wednesday AM
August 21, 2019

Room: 309(3rd Floor)
Symposium: K

Chairs:
Pingheng Tan, Chinese Academy of Sciences, China
Hua Zhang, City University of Hong Kong, HongKong, China

8:30-9:00 Keynote

Phase Engineering of Novel Aanomaterials

Hua Zhang, City University of Hong Kong, Hong Kong, China; Nanyang Technological University, Singapore

In this talk, I will summarize the recent research on the phase engineering of nanomaterials in my group. It includes the first-time synthesis of hexagonal-close packed (hcp) Au nanosheets (AuSSs) on graphene oxide (GO), the first-time synthesis of 4H hexagonal phase Au nanoribbons (NRBs), the synthesis of crystal-phase heterostructured 4H/fcc Au nanorods, the epitaxial growth of metal nanostructures with novel crystal phases on the aforementioned Au nanostructures, and the synthesis of amorphous/ crystalline hetero-phase Pd and PdCu nanosheets. In addition, the first-time synthesis of 1T'-MoS_2 and 1T'-$MoSe_2$ crystals have been achieved. Moreover, the phase transformation of transition metal dichalcogenide (TMD) nanomaterials during our developed electrochemical Li-intercalation method will also be introduced. Interestingly, the lithiation-induced amorphization of $Pd_3P_2S_8$ is also achieved. Currently, my group focuses on the (crystal) phase-based nanomaterial syntheses, property studies, and applications in catalysis, surface enhanced Raman scattering, waveguide, photothermal therapy, chemical and biosensing, clean energy etc., which we believe are quite unique and very important not only in fundamental studies, but also in practical applications. Importantly, the concepts of crystal-phase heterostructures and hetero-phase nanomaterials are proposed. We believe the phase engineering of novel materials will become one of the hottest research topics in materials science and chemistry in the near future.

9:00-9:30 Keynote

Peculiar Electron Phonon Coupling in Van Der Waals Two-Dimensional Heterostructures

Pingheng Tan, Institute of Semiconductors, Chinese Academy of Sciences, China

Two-dimensional materials (2DMs) have been under intensive investigation. The rapid progress of research on graphene is now stimulating the exploration of different types of 2DMs, such as monolayer and multilayer 2DMs, 2D alloy, 1D nanoribbon, 0D nanocrystal and van der Waals heterostructures (vdWHs). Raman spectroscopy can reveal information on the crystal structure, electronic structure, lattice vibrations and flake thickness of 2DMs, and can be used to probe the strain, stability, charger transfer, stoichiometry, and stacking orders of 2DMs. In this talk, we will discuss that Raman spectroscopy of vdWHs can be modulated by the excitonic resonance effects, which demonestrates peculiar electron phonon coupling. Due to this peculiar electron phonon coupling, the intensity of some Raman modes is significantly enhanced when the excitation energy matches the energy of excitonic absorption peaks. These excitonic resonance effects in Raman spectra of vdWHs make many interesting results be revealed.

9:30-10:00 Keynote

Nanostructured Semiconductor Photoelectrodes for Solar Energy Conversion

Lianzhou Wang, The University of Queensland, Australia

Semiconducting materials hold the key for efficient photocatalytic and photoelectrochemical water splitting. In this talk, we will give a brief overview of our recent progresses in designing semiconductor metal oxides materials for photoelectrochemical energy conversion including photocatalytic solar fuel generation. In more details, we have been focusing the following

a few aspects; i) band-gap engineering of layered semiconductor compounds including layered titanate, tantalate and niobate-based metal oxide compounds for visible light phtocatalysis, and ii) facet-controlled TiO_2, Fe_2O_3, WO_3, $BiVO_4$ as building blocks for new photoelectrode design, and iii) the combination of a high performance photoelectrode $BiVO_4$ with perovskite solar cells can lead to unassisted solar driven water splitting process with unassisted solar-to-hydrogen conversion efficiency of >6.5% (Fig.1); The resultant material systems exhibited efficient photocatalytic performance and improved power conversion efficiency in solar cells with record high efficiency, which underpin important solar-energy conversion applications including solar fuel and solar electricity generation.

10:00-10:20

Asymmetric Cyclic Response of Pretensioned Cu with Highly Oriented Nanoscale Twins

Qingsong Pan, Qiuhong Lu, Lei Lu, Institute of Metal Research, Chinese Academy of Sciences, China; Haofei Zhou, Zhejiang University, China; Huajian Gao, Haofei Zhou, Brown University, USA

Pre-deformation of metallic materials generally induces high density dislocations and irreversible microstructural change, thus strongly influencing their subsequent cyclic behavior and causing obvious cyclic softening. In this study, to deepen the understanding of cyclic deformation in nanotwinned (NT) structures, small levels of pre-tension strains were applied on NT-Cu, followed by strain-controlled symmetric tension-compression cyclic tests. Distinct from the symmetric cyclic response of as-deposited NT-Cu, the magnitude of the maximum stress in tension is much larger than that of the minimum stress in compression, indicating that the cyclic response of pre-tensioned NT-Cu is highly asymmetric. The degree of its cyclic asymmetry gradually decays as the number of cycles or the plastic strain amplitude is increased. The pre-tensioned NT-Cu recovers to its symmetric cyclic response after cyclic deformation at sufficiently large plastic strain amplitude, analogous to that detected in as-deposited NT counterparts. Molecular dynamics simulations and microstructural observations revealed that the observed asymmetric cyclic response is mainly related to the activation and movement of threading dislocations with extended misfit dislocation tails lying on the twin boundaries (TBs) during pre-tension deformation. During cyclic deformation, threading dislocations in adjacent twin interiors tend to link their long tails with one another to form correlated necklace dislocations (CNDs) with a symmetric structure. The CNDs move back-and-forth along the twin boundaries without directional slip resistance, contributing to the transition from asymmetric to symmetric cyclic response of NT-Cu.

10:30-10:45 Tea Break

10:45-11:10 Invited

Increasing Photoluminescence Quantum Yield by Nanophotonic Design of Quantum-Confined Halide Perovskite Nanowire Arrays

Zhiyong Fan, Daquan Zhang, Yuanjing Lin, Leilei Gu, Hong Kong University of Science and Technology, Hong Kong, China

Metal halide perovskite materials have demonstrated many appealing properties that can be harness for high performance optoelectronics. Among them, high photoluminescence quantum yield (PLQY) is required to reach optimal performance in solar cells, lasers and light-emitting diodes (LEDs). Typically, PLQY can be increased by improving the material quality to reduce the non-radiative recombination rate. It is in principle equally effective to improve the optical design by nanostructuring a material to increase light out-coupling efficiency and introduce quantum confinement, both of which can increase the radiative recombination rate. However, increased surface recombination typically minimizes nanostructure gains in PLQY. Here a template guided vapor phase growth of perovskite nanowire (NW) arrays with unprecedented control of NW diameter from the bulk (250nm) to the quantum-confined regime (5.7nm) is demonstrated, while simultaneously providing a low surface recombination velocity of 18cm s^{-1}. This enables an obvious PLQY enhancement from 0.33% up to 42.6% for $MAPbI_3$ quantum wires, and up to ~90% for $MAPbBr_3$ quantum wires, exclusively using nanophotonic design, which will be promising for LEDs applications with high external quantum efficiency (EQE). The simple extension of this technique to a wide variety of semiconductors and the ultra-high density of vertical QWs may also provide interesting opportunities in quantum transport, electronics and memory devices in the future.

11:10-11:30

Atomically Thin Homogeneous MoS_2 Logic Inverter via Solution-Processable Defect Engineering

Li Gao, University of Science and Technology, China

Ultrathin molybdenum disulfide (MoS_2) presents ideal properties for building next-generation atomically thin circuitry because of their atomic-level thickness, superior theoretical mobility, moderate band gap, and stable structure. However, it is difficult to construct a logic unit of monolayer MoS_2 using traditional silicon-based doping schemes, such as atomic substitution and ion implantation, to cause lattice disruption and doping

instability. Nevertheless, defects, which customarily act as negative components, may play a stable and positive role in modulating the electronic structure of MoS_2 to build atomically thin logic devices. Here, a facile, feasible and novel electronic structure modulation strategy of a defect is proposed to construct an in-plane monolayer MoS_2 logic inverter. By utilizing the energy-matched electron induction of the solution process, numerous pure monosulfur vacancies (Vmonos) with lattice stability are introduced to modulate the electronic structure of monolayer MoS_2 via a trapping effect. The resulting modulation effectively reduces the electronic concentration of MoS_2 by one hundred times and improves the work function by approximately 100 meV. Under modulation of Vmonos, an atomically thin homogenous monolayer MoS_2 logic inverter with a voltage gain of 0.34 is successfully constructed. This research highlights a new and practical design route for circuit development of 2D ultrathin materials.

11:30-11:50

Hetero-Contact Microstructure to Program Discerning Tactile Interactions for Virtual Reality

Xinqin Liao, Weitao Song, Xiangyu Zhang, Yuanjin Zheng, Nanyang Technological University, Singapore

Helping to reconstruct and restore tactile perception motivates the continuous development of functional materials, sensing structures, and manufacturing strategies. Functional materials including micro/nanoparticles, one- or two-dimensional materials, and their composites with the capabilities that provide the electromechanical signal conversion of exteroceptive stimulus play a considerable role in the reconstruction and restoration of tactile perception, and thus enable the dexterous manipulation of objects and the discerning interaction of apparatus. Efforts of sensing devices are mainly based on homo-contact microstructure (HoCM) that utilizes the microstructural contact between the same materials or within a single material as the sensing contact for the scientific and engineering researches of artificial tactile perception. However, the sensing mechanism of hetero-contact microstructure (HeCM) that bases on the microstructural contact between different types of materials is seldom reported where the influence on device's sensitivity and sensing range has yet to be studied.

Here we propose the HeCM to fabricate tactile sensors inspired by the synergistically sensory mechanism of mammalian tactile mechanoreceptors. The synergistically perceiving of HeCM enables the mechanosensational range of the tactile sensor to be significantly enhanced by >100% compared to the one of the counterpart based on the HoCM. The as-designed HeCM tactile sensor characterizes fast, stable, and reproducible electromechanical properties to identify static and dynamic external pressure changes. Wearable three-dimensional tactile panel with auxiliary analog-to-digital conversion circuit demonstrates the fascinating application of the HeCM tactile sensor in the field of human-machine interactions. Noteworthily, the coding and use of the mechanotransduction signal from the HeCM tactile sensor do not need any denoise processing or signal amplification that significantly reduces the difficulty of circuit design specially for multiple units integrated system and makes the competitive advantage compared to other sensors. As a proof-of-concept, the HeCM tactile sensor is served as the functional sensing medium of a data glove to turn actual fingertip events into specified interactions of virtual reality system, where precise and free control of virtual navigation is realized.

11:50-12:10

In Situ Exploration on the Structure-Property Correlation for Low-Dimensional Inorganic Materials

Qi Zhang, Xing Zhou, Xin Li, Bao Jin, Zhiwei He, Minxuan Xu, Chengchao Jin, Hangzhou Dianzi University, China; Xing Zhou, Huazhong University of Science and Technology (HUST), China

The widespread availability of nanostructures and nanodevices toward next-generation optoelectronic systems has placed strict requirements on their comprehensive characterization. To this end, pursuing clear "structure-property" correlations become significantly challenging for the correct and impersonal assessment on the interaction and coupling between photons and electrons within the optoelectronic nanostructures, a key issue for the precise control over the photoelectric conversion dynamics. However, most of the currently available property measurements are ex situ approaches that have no direct access to the material internal structures and are thus unable to uncover the precise structure-property relationships. This article aims at in situ characterizing low-dimensional optoelectronic nanostructures by employing a probe-based system established on the optical or scanning electron microscope, allowing full and direct access to the true evolution on the structural dependent properties. The connection with spectrometer, semiconductor analyzer, laser etc. through the nanoprobes along with micro/nanofabrication technologies offers a powerful real-time tool to explore the effect of microstructures such as geometry configuration, crystal and electronic band structure and device design, on the optoelectronic

features including waveguide, electron transport, photon absorption, barrier and photocoupling process. Based on the true access to the structure-property relationships in low-dimensional systems, diverse optoelectronic devices, including photodetector, light emitting, photovoltaic transducer and waveguide have been achieved with impressive performance. The high information throughput gained from in situ studies, in the form of video streams along with the quantitative and analytical information, will pave the way to explore new nanoworld features, thus uncovering more details of the macroworld we live in.

L. Computational Design and Simulation of Materials: IV

Symposium Organizers :

Tongyi Zhang, Shanghai University, China; Zhimei Sun, Beihang University, China; Shigenobu Ogata, Osaka University, Japan; Byeong-Joo Lee, Pohang University of Science and Technology (POSTCEH), Korea; Salvy Russo, RMIT, Australia; Saryu Fensin, Los Alamos National Lab, USA; Michele Manuel, University of Florida, USA

Wednesday AM
August 21, 2019

Room: 204 (2nd Floor)
Symposium: L

Chairs:
Yunjiang Wang, Institute of Mechanics, Chinese, Academy of Sciences, China
Tiffany Walsh, Deakin University, Australia

08:30-09:00 Keynote

Molecular Modelling of Bio/Nano Interfaces: Materials for Bio-Sensing, Energy, and Catalysis

Tiffany Walsh, Deakin University, Australia

An in-depth appreciation of how to control the interaction between biomolecules and solid surfaces, including nanoparticles, at the molecular level, is central to advancing application areas such as self-organised metamaterials for photonics and plasmonics, biosensing, catalysis, energy generation and harvesting, and nano-medicine. Exploitation of materials-selective binding of biomolecules is key to success in these areas; i.e. by realising preferrential adsorption of a biomolecule onto a surface comprising one materials composition over another, one materials facet over another of the same material, or one materials polymorph over another of the same material. Structural characterisation of the surface-adsorbed biomolecules is essential for establishing the required structure/property relationships in these systems, but this can be challenging to accomplish via experimental approaches alone. In partnership with experimental characterisation, molecular simulations can bring complementary insights into the molecular-scale origins of this selectivity, and suggest routes to manipulating these phenomena for realising new types of hybrid materials. Our team specialise in the development and deployment of interfacial force-fields and molecular simulation techniques for the purpose of elucidating these insights at biomolecule/materials interfaces. In this contribution I will overview our developments and applications of advanced molecular simulation approaches for investigating these challenging interfacial systems, and highlight our findings for manipulating the adsorption of biomolecules at the aqueous interface for bio/nano applications in bio-sensing, catalysis, and energy applications.

09:00-09:20

Simulation of Light Scattering in Stereolithography Ceramic Manufacturing

Chuchu Qian, Shuji Zhao, Kehui Hu, Zhigang Lv, Peijie Li, Xinyi Li, Tsinghua University, China

In the process of stereolithography ceramic manufacturing, the erroneous curing caused by multiple scattering of light in the suspension will lead to the expansion of the part which seriously affect the precision of the green part and then influence the prediction of the curing shrinkage. The classic Mie Theory is not applicable here and needs to be corrected which has complicated theoretical calculation. In this paper, we simulated the curing process based on Comsol software. The distribution of light field intensity under various Gaussian light beam illumination with different partice sizes is compared. The critical exposure energy is calculated based on Beer- Lambert theory and the relationship between light intensity and conversion rate is established by infrared spectroscopy. The simulation gives the erroneous curing range of the regular quadrilateral plane under the single-layer exposure, and the distribution of ceramic slurry conversion in the erroneous curing zone with different particle sizes. Besides, the possibility of double exposure of the cured layer is verified according to the results. The study in this paper have an important guiding role in the precision control of ceramic light-cured 3D printing, and also provide important data reference for the research of double exposure of cured layer.

09:20-09:40

Evaluations of Cross-Slip Activation Energy Considering the Geometrical Effect of Bow-Out on Line Tension

Hui Liu, Jianxing Mao, Beihang University, China; Rongqiao Wang, Dianyin Hu, Beihang University, China / Collaborative Innovation Center of Advanced Aero-Engine, China / Beijing Key Laboratory of Aero-Engine Structure and Strength, China; Jun Song, McGill University, Canada

Cross-slip, a stress assisted and thermally activated process where a screw dislocation changes its glide

plane, plays an important role in the work hardening, dynamic recovery, fatigue, and creep of metallic materials. The line tension model (LTM) has been one of the most widely used models for studying cross-slip. For LTM to provide a good description of the cross-slip process (e.g., activation energy), an accurate value of line tension is essential. However, previous studies usually assumed a line tension on the basis of small bow-out of straight dislocations and neglected the long-range interaction between dislocation segments, which failed to give satisfactory predictions of the absolute value and stress dependence of cross-slip activation energy. The purpose of this study is to answer the question: What is the accurate form of line tension to predict the cross-slip activation energy precisely? First, we generalized the original Escaig's LTM to eliminate the isotropy constrain of ν=1/3 and proposed a numerical method to solve the LTM in order to avoid the assumptions made by Escaig. On top of that, we introduced several formulas of line tension corresponding to different bow-out geometries into the generalized LTM. Then, the cross-slip activation energy under applied stress components (i.e., Escaig and Schmid stresses) was obtained using different line tension formulas. In addition, through the climbing image nudged elastic band (CI-NEB) method, atomistic simulations in face-centered cubic (FCC) nickel (Ni) were carried out as well. By comparing the predictions of LTM with atomistic results, it was found that the uncertainties of LTM in predicting the cross-slip activation energy were attributed to the arbitrary cut-off radius and core energy in elastic theory. Besides, the line tension model with different line tension agreed qualitatively with each other on the general trend in the stress dependence of the cross-slip activation energy, but the predicted relative effectiveness of stress components in reducing the activation energy was very sensitive to the chosen formula of line tension, i.e., the geometry of bow-out.

09:40-10:00

Theoretical Understanding of Crystal-Melt Interface Kinetic Coefficients: From Pure Metals to Molecular Crystals

Xianqi Xu, Yang Yang, Physics Department, School of Physics and Material Science, China

The crystal-melt interface kinetic coefficient of pure material, is the proportionality between the crystal growth velocity and undercooling, within the linear regime near its melting point. The magnitudes and crystalline anisotropies of this property play vital roles in the solidification rates and growth morphologies. Accurate values for the kinetic coefficient is critical for quantitative modeling of solidification microstructure, while it has been challenging to measure experimentally. Over the past two decades, atomistic simulations have been extensively employed to the investigations of kinetic coefficients for simple model systems and pure metals. In this talk, we will first review insights regarding the magnitude and the anisotropy of the kinetic coefficients reported in previous theoretical and simulation studies. We then present our recent molecular dynamics (MD) simulation study of crystal growth from the melt, and research focuses on fcc crystal consist of molecules modeled by extended point dipole model. Non-equilibrium MD simulations of crystal growth for systems modeled with different magnitude of molecular dipole moments, yield the measurement of kinetic coefficients vs. the molecular dipole moments for the (100) and (110) interfaces. The kinetic coefficients determined by the MD simulations will be compared quantitatively to the prediction of existing kinetic theories, i.e., kinetic theory by Mikheev and Chernov and a time-dependent Ginzburg-Landau (TDGL) kinetic theory. We find that the kinetic coefficient predicted from the TDGL theory agree well with the MD calculation for (100) interfaces at low dipole moment systems, but failed in high dipole moments systems where spontaneous polarization showed up in crystal phase or/and even in the melt phase. Possible improvements in the applicability of the TDGL kinetic theory to better reproduce MD data will be discussed in the final part of this talk. It is hoped that the current study could elucidate the trend of the kinetic coefficient with inter-molecular interactions and shed light in the crystal growth for materials beyond metals, e.g., ferroelectric molecular crystal and Janus colloidal crystal.

10:00-10:20

A Statistics-Based Analysis of the Combined Effect of Strain Hardening and Precipitation Strengthening

Rafael Schouwenaars, Universidad Nacional Autónoma de México, USA

Precipitation strengthening is an efficient way to increase the strength of aluminium, which in its pure state is a very soft material. Also, in Mg alloys and HSLA steels, precipitation is an important way to increase hardness. In its simplest form, ageing is applied after a homogenisation treatment, which generally has the consequence that pre-existing dislocation networks are eliminated by recrystallisation or advanced recovery. However, under certain conditions, such as friction stir welding or strain-enhanced ageing, complex interactions between strain hardening and precipitation may occur. The resulting strength of the alloy is then often approached by empirical modifications of the classical

Taylor equation. The latter predicts that the yield stress is proportional to the dislocation density.

Although the Taylor equation is generally considered to be empirical, it can be obtained in a mathematical way by using geometrical statistics. Moving dislocations are considered to bow out between the junctions formed by forest dislocations, which are assumed to be randomly distributed in the slip plane. By calculating the number of bow-out events before the entire dislocation loop is stored, one obtains a differential equation describing the relationship of yield stress to dislocation density. The solution to this differential equation is the Taylor equation . Further analysis of these results has pointed out that, in presence of a fixed number of additional obstacles for dislocation movement, the Taylor equation no longer solves the evolution equation mentioned above. This point was not explored further but will be analyzed here. This paper presents a brief summary of the theoretical background required to obtain the evolution equation for dislocation density as a function of stress, in presence of precipitates. This equation has not been solved analytically. An important issue for its numerical solution is the proper determination of the initial condition, which states that, at zero strain, the strengthening of the material is due only to precipitates and that the strain hardening rate is positive. This analysis already gives important information with respect to the mathematical form of the solution. Numerical solutions are then presented for different precipitate densities, showing that existing empirical approaches overestimate the slope of the stress-dislocation density curve and predict a combined strengthening effect which is higher than what is obtained by the statistical approximation. Possibilities to further extend this method will be discussed at the end of the paper.

10:20-10:40 Tea Break

10:40-11:05 Invited

Understanding the Collective Diffusion of Amorphous Solids: an Accelerated MD Study

Yunjiang Wang, Institute of Mechanics, Chinese Academy of Sciences

The nature of collective diffusion in amorphous solids is in strong contrast with diffusion in crystals. However, the atomic-scale mechanism and physics of collective motion remains elusive in disorder materials. Here the free energy landscape of collective diffusion triggered by single atom jump in a prototypical CuZr model metallic glass is explored with the recently advanced well-tempered metadynamics which significantly expands the observation time-scale of diffusion process at atomic-scale. Metadynamics samplings clarify a long-standing experimentally suggested collective diffusion mechanism in the deep glassy state. The collective nature is strongly temperature-dependent. It evolves from string-like motion with participation of only several atoms to be large size collective diffusion at high temperature, which would remarkably promote the atomic transport upon glass transition. We also proposed a mechanism of sequential diffusion if heterogeneity of dynamics with wide distribution of energy barriers are considered, while the parallel diffusion mechanism would overestimate diffusivity. The findings indicate the complex topolocial strcuture of amorphous diffusion. The temperature and pressure dependence of collective diffusion are further quantified with big activation entropy and small activation volume of half atom volume, which both agree quantitatively with experiments. Direct atomic-scale simulations of diffusion at laboratory time-scale brings several physical insights into the nature of collective diffusion in amorphous solids which is beyond the knowledge established in diffusion of crystals.

11:05-11:25

Atomistic Simulation Study of In-Plane Structural and Thermodynamic Properties for Steps at Chemically Heterogeneous Solid/Liquid Al-Pb Interfaces

Hongtao Liang, Yang Yang, East China Normal University, China; Brian Laird, University of Kansas, USA; Mark Asta, UC Berkeley, USA

Steps play important roles in crystal morphology and many interfacial processes, including surface roughening and faceting transitions, the collective fluctuations among neighboring vicinal steps, layer-by-layer growth process in solidification from of the melt, as well as VLS nanowire growth and homoepitaxial growth. Thermodynamic and structural properties of the steps govern the nucleation rate and the island growth during crystallization. In addition, they determine the equilibrium shape and Brownian motion of small liquid Pb inclusions embedded in an Al crystal matrix. Understanding these one-dimensional defects, in terms of their fundamental properties, is crucial for developing theories of phase nucleation at interfaces.

We present a methodology for studying steps at faceted chemically heterogeneous solid/liquid interfaces based on molecular-dynamics simulations. The methodology is applied to a faceted Al(111)/Pb(liquid) interface yielding a direct calculation of step free energy and extensive atomic-scale characterization for the interfacial layer

containing the step.

We characterized the step by calculating the in-plane density, potential energy, pressure components and stresses profiles. Main findings include: i) Calculated step free energy is in good agreement with TEM experimental measurement. ii) The step is connecting the interface liquid under tension and the interface solid under compression. iii) Fundamental properties of interface solid and interface liquid show orders of magnitudes difference in comparing with those predicted from the bulk Al-Pb alloy phase diagram. The in-plane profiles give a new level of understanding of the thermodynamical and mechanical conditions for solid/liquid interfacial step. Prosperities calculated for the interfacial liquid and interfacial solid coexistence are essential to the development of a detailed thermodynamic theory for faceted solid/liquid interfaces. It is hoped that the methodology is extendable to the exploration of complexion equilibria/transitions at grain boundaries.

11:25-11:45

Two-Dimensional Magnetic Semiconductors

Naihua Miao, Beihang University, China

Atomically thin two-dimensional (2D) ferromagnetic materials with the combination of large spin polarization and high Curie temperature (TC) are of particular importance and interest for nanoscale spintronic devices. However, although plenty of 2D crystals have been widely explored, most of them are lacking of intrinsic polarization or ferromagnetic ordering, which greatly hinder their direct applications in spintronics. To this end, 2D ferromagnetic materials with desirable magnetic and electronic properties for nanoscale spintronic devices are highly sought. In this talk, by means of ab initio calculations, molecular dynamics, and Monte Carlo simulations, we reported a alternative promising way to create 2D intrinsic ferromagnetism from bulk van der Waals antiferromagnets, as realized in the single-layer CrOX semiconductors, which can be easily exfoliated from their bulk counterparts. These CrOCl and CrOBr monolayers show excellent stability and much higher TC than the recently reported 2D CrI3 and $Cr_2Ge_2Te_6$, indicating their great potential for nanoscale spintronics. Our findings on the intrinsic ferromagnetism of 2D CrOX crystals open new pathway to develop 2D semiconducting intrinsic ferromagnets from antiferromagnetic bulk crystals and also provide new opportunities for future spintronic investigations and applications at atomic thickness.

M. Renewable Energy Materials and Nuclear Materials: IV

Symposium Organizers :

Min Zhu, South China University of Technology, China; Yuan Deng, Beihang University, China; Guanghong Lu, Beihang University, China; Tetsuya Uda, Kyoto University, Japan; Taek-Soo Kim, Korea Institute of Industrial Technology (KITECH), Korea; Dmitri Golberg, Queensland University of Technology, Australia; Assel Aitkaliyeva, University of Florida, USA

Wednesday AM
August 21, 2019

Room: 311(3rd Floor)
Symposium: M

Chairs:
Renzong Hu, South China University of Technology, China
Xiaoqiu Ye, China Academy of Engineering Physics, China
Tiejun Zhu, Zhejiang University, China
James Stubbins, University of Illinois at Urbana-Champaign, United States

8:30-9:00 Keynote

Defective Half-Heusler Thermoelectric Compounds

Tiejun Zhu, Zhejiang University, China

Typical 18-electron half-Heusler (HH) compounds, ZrNiSn and NbFeSb, have been identified as promising high temperature thermoelectric materials. NbCoSb with nominal 19 valence electrons, which is supposed to be metallic, has recently been reported to also exhibit thermoelectric properties of a heavily doped n-type semiconductor. In this talk we experimentally demonstrate that the nominal 19-electron NbCoSb is actually the composite of 18-electron Nb0.8CoSb and impurity phases. Single phase Nb0.8CoSb with intrinsic Nb vacancies possesses improved thermoelectric performance. The similar phenomenon has also been observed in some of other defective 19-electron HH compounds. They all display abnormally low thermal conductivity compared to the normal 18-electron HH. TEM observation indicates a complex and interesting crystal structure, in which the short-range order of vacancies coexists with long range atomic order. This new finding provides important insights into the intrinsic nature of defective HH compounds.

9:00-9:25 Invited (1222513)

Development of Austenitic Oxide Dispersion Strengthened Alloys for Nuclear Applications

Yinbin Miao, Materials Scientist, Chemical and Fuel Cycle Technologies Division, Argonne National Lab, Lemont, USA; Xiang Chen, Research Associate, Advanced Post-Irradiation Examination Department, Idaho National Lab, Idaho Falls, USA; *James Stubbins*, Donald Biggar Willett Professor, Department of Nuclear, Plasma and Radiological Engineering, University of Illinois at Urbana-Champaign, Urbana, USA

There has been a continuing effort to develop enhanced versions of several types of engineering alloys by strengthening them with a very high number density of very small oxide particles. Most of the recent work has concentrated on ferritic / martensitic ODS alloy development and performance. It is clear that the addition of a fine distribution of nano-oxide dispersoids will provide major improvements in material strength especially at very high temperatures and extend the application temperature range to levels appropriate for advanced nuclear systems. Since the oxide particles are actually ceramics, they should maintain their stability and strengthening capabilities even at very high temperatures. For nuclear applications where atomic displacement damage takes place, the particles also offer a very large amount of internal surface area which can potentially absorb irradiation-induced defects to reduce radiation damage effects.

This process of making metal alloys with dispersed oxide particles has been attempted in a wide variety of metal systems with some success. The current heavy emphasis on developing ODS F/M steels has resulted in a nearly negligible interest in the development of ODS stainless steels. This talk will discuss the possibilities for the development of ODS austenitic steels. Since austenitic stainless steels are currently used for a wide variety of applications in current nuclear reactors and are slated for use in a number of advanced nuclear fission and nuclear fusion reactor systems, the development of ODS austenitic alloys should be of considerable interest. The research work discusses the oxide dispersoid microstructure and mechanical behavior of this class of new alloys for nuclear applications. The talk will also cover recent results on the irradiation behavior of ODS particles and other microstructural features in the ferritic alloys.

9:25-9:50 Invited

In-Situ Investigation of Hydrogen Induced Corrosion of Titanium

Xiaoqiu Ye, Xuefeng Wang, Jiliang Wu, Changan Chen, China Academy of Engineering Physics, China

Titanium(Ti) and its alloys have many industrial applications thanks to their excellent corrosion resistance and high specific strength. However, they are potentially susceptible to hydrogen-induced cracking as a consequence of hydrogen absorption. To ensure long term use, a predictive model of hydriding behaviour is desirable and requires detailed understanding. Unlike widely studied thermodynamic properties of the titanium-hydrogen systems, in-situ investigation of hydrogen induced corrosion of titanium was carried out in the present work by pressure-volume-temperature (PVT) method and hot-stage microscope (HSM) technique. The results show that hydrogen absorption rate of Ti foil at room temperature is very slow, no more than 0.2 H/Ti ratio for 1h. However, when the temperature increasing to 550˚C, the hydrogen absorption rate increased abruptly, with the morphology of Ti foil changing surprisingly: cracks firstly formed on the edge of the sample, and then progresses to the centre part. Thermal stabilities of the surface passivation layers on Ti foil under UHV were investigated using X-ray Photoelectron Spectroscopy (XPS). XPS results show that the C, N and O species on the surface of Ti reduce significantly or even disappear when heated to 700˚C in ultra-high vacuum condition(UHV), thus inducing an appearance of "active" surface with clean metal; while heated to lower than 300˚C the oxygen content on the surface will further increase and the corresponding carbides or nitrides are formed. Among these species, TiO and TiN decompose at 600˚C due to the underlying metal, while TiC decompose at 700˚C. The active surfaces of Ti obtained at 700˚C can be contaminated by oxygen again when cooled down to room temperature in the UHV. The active surface of Ti with clean metal can also be obtained by Ar ion gun sputtering at room temperature. Possible mechanisms of hydrogen induced corrosion of Ti during heating was discussed.

9:50-10:10

The Effect of Location on the Microstructure and Mechanical Properties of Wire Arc Additively Manufactured Nuclear Grade Steel

Chuang Gao, Chuanchu Su, Xizhang Chen,Wenzhou University, China; Xiao Chen, Wenzhou University / Liaocheng University, China

The Wire and arc additive manufacturing (WAAM) is a promising process for the fabrication of complex and larger size 9Cr ferritic/martensitic nuclear grade steel components, which are used in the power industries/ nuclear reactor due to good high-temperature performance and excellent corrosion resistance. For this new study, using cold metal transfer (CMT) welding as heat source, 9Cr ferritic/martensitic nuclear grade steel is fabricated by the WAAM technology for the first time. This paper investigated the microstructure and mechanical properties of the additively manufactured

9Cr ferritic/martensitic component in the different locations. The microstructure mainly consists of untempered martensite. As the height of the deposited wall increases, the microstructures exhibit differences. Positions at different heights have no significant influence on micro hardness and tensile testing results. However, the tensile properties and impact toughness of samples show anisotropy both perpendicular to the build direction and parallel to the build direction. The microstructure variation, defects, the differences of mechanical properties and fracture behavior of samples are also analyzed carefully. The obtained experimental results show that although there are still some shortcomings, it is feasible that using the new additive manufacturing process fabricates 9Cr ferritic/martensitic steel component.

10:10-10:30

Aqueous Asymmetric Supercapacitors Based on Conducting Polymers

Jinzhang Liu, Yi Zhao, Beihang University, China

Supercapacitors are distinguished from ionic batteries for their high power density, yet their drawback is the low energy density, which is about one order of magnitude lower than that of Li-ion battery. The voltage window of a supercapacitor is an important issue determing the energy density. Hence the asymmetric design by using two dissimilar materials as the negative and the positive electrodes, respectively, has received much attention. We have been focusing on redox-active organic molecules, which can be exploited to make supercapacitor electrodes with strong pseudocapacitance. Amino-contained aromatic molecules are electropolymerized and combined with porous activated carbon to make asymmetric supercapacitors with both high specific capacitance and wide voltage window, thus achieving high energy densities. In particular, the electrodeposited poly(diaminonaphthalene) used as the negative electrode shows excellent cycling stability, with a capacitance retention of 103% over 10000 cycles. We studied several newly-syntghesized conducting polymers as the positive electrodes, and performances of different asymmetric cells are investigated. High energy densities up to 55Wh/kg are achieved. To demonstrate the practical application, several cells in series are used to power LEDs or a mini electric fan.

10:30-10:45 Tea Break

10:45-11:10 Invited

Advanced Sn-Based Anode Materials for Li Storage

Renzong Hu, Min Zhu, South China University of Technology, China

The energy density of LIBs is mainly determined by the voltage difference (V) between the cathode and anode, and in particular, the specific capacity (mAh $\cdot g^{-1}$ or mAh$\cdot L^{-1}$) of the electrode materials in suitable potential window. Thus, intense efforts have been devoted to developing high-voltage cathode materials and exploring new high-capacity anode materials to replace the commercial graphite anode that has a low theoretical specific capacity of 372mAh$\cdot g^{-1}$.

The application of a ternary Sn-based alloy (Sn-Co-C) anode has contributed an 30% increase in capacity, and 20% increase in volumetric energy density in Sony's Nexelion battery which introduced firstly in 2005 and then updated in 2011. The reversible specific capacity of the Sn-Co-C ternary anode was around 600mAh$\cdot g^{-1}$, which could be further increased when the Sn (with theoretical capcity of 994mAh$\cdot g^{-1}$) is replaced with SnO_2 (1494mAh$\cdot g^{-1}$). Thus we designed a series ternay SnO_2-M-graphite (M: transition metal, Fe, Co, Mn, Cu, etc) composite. However, two major challenges must be faced for the realization of the full capacity of SnO_2-based anodes. The first one is capacity fading and the short lifetimes induced by large volume changes and particle aggregation upon continued lithiation/delithiation. The second one is the unsatisfactory initial Coulombic efficiency and large irreversible capacity loss, which has to be minimized because it is detrimental to the potential energy density and the cost of LIBs.

In this work, we demonstrate that the nanosize transition metal Mn additives inhibit Sn coarsensing in lithiated SnO_2, resulting in fast interdiffusion kinetics of interdiffusion between Sn and O in the Sn/Li_2O interfaces and thus enabling highly reversible conversion, superior round-trip efficiency, large capacity and long lifetime. We hope that this new ternary SnO_2-based composite could be an alternate high capacity anode material for the current ternary Sn-based alloy anode.

11:10-11:30

Keys for Radiation Tolerance of ODS Steels for Advanced Nuclear Systems

Akihiko Kimura, Peng Song, Jim Gao, Yenjui Huang, Kiyohiro Yabuuchi, Yuuki Yamasaki, Daniel G. Morrall, Kyoto University, Japan; Takanari Okuda, KOBELCO, Japan; Naoko Oono, Hokkaido University, Japan; Yoosung Ha, JAEA, Japan; Peng Dou, Chongqing University, China; Sanghoon Noh, KAERI, Japan

Materials development is essential for realization of advanced nuclear systems where radiation tolerance is demanded for the structural materials to keep their performance during a long term operation. Among the several candidate structural materials of the nuclear systems, oxide dispersion strengthened (ODS) steels, which consist of nano-scaled oxide particles in a high number density and sub-micron sized grains, have been considered to be promising for advanced nuclear systems.

There are several sorts of ODS steels with different Cr contents: (9-12)Cr-ODS ferritic/martensitic steels and (14-16)Cr-ODS ferritic steels with and without Al addition. The former group of ODS steels were developed for applications to sodium cooled fast reactors and fusion reactors, and the latter of ODS steels were for so-called Generation IV nuclear systems. More recently, accident tolerant fuel R&D is progressing to apply high Cr/high Al ferritic ODS steels to fuel cladding of light water reactors because of "Fukushima Incident". It has been considered that the replacement of zirconium alloys cladding with high-performance ferritic steel one may retard the hydrogen generation at a severer accident of nuclear reactors, resulting in a large time lag up to hydrogen explosion.

In this presentation, radiation tolerance mechanisms of ODS steels are introduced in terms of trapping capacity and dislocation sources. Oxides trap radiation defects at the interfaces of nano-scaled ultra-fine oxide particles and matrix and at grain boundaries of sab-micron sized grains. The tolerance to void swelling and He-embrittlement may owe it to this mechanism. As for no loss of elongation mechanism, the suppression of localized deformation can be considered to work as a mechanism, where sub-micron sized grains supply a large number of dislocation sources at grain boundaries as triple points. This mechanism may be workable in most of the cases where embrittlement is accompanied by hardening, like irradiation embrittlement and aging embrittlement.

11:30-11:50

Flexible and Self-Supported Sulfur Cathode for High-Energy-Density Lithium-Sulfur Batteries

Jun Liu, South China University of Technology, China

Lithium–sulfur (Li-S) batteries have attracted much attention in the field of electrochemical energy storage due to their high energy density and low cost. However, the 'shuttle effect' of sulfur cathode, resulting in the poor cyclic performance of batteries, is a big barrier for the development of Li-S batteries. It is critical to design and synthesize novel materials as the sulfur cathode host for Li-S batteries which has high electrical conductivity, large sulfur loading and strong absorb interactions of polysulfides to prevent the 'shuttle effect'. Self-supported nanoarrays with hierarchical voids and rich reaction sites are promising for advanced electrodes of high-performance Li-S batteries. Herein, we have designed a novel sulfur cathode of integrating sulfur, flexible carbon cloth, and metal-organic framework (MOF)-derived N-doped carbon nanoarrays with embedded CoP. These unique flexible nanoarrays with embedded polar CoP nanoparticles not only offer the enough voids for volume expansion to maintain the structural stability during the electrochemical process, but also promote the physical encapsulation and chemical entrapment for all sulfur species. Such designed CC@CoP/C cathodes possess high sulfur loadings (as high as 4.17mg/cm^{-2}) and exhibit large specific capacities at different C-rates. Specially, an outstanding long-term cycling performance could be reached. For example, an ultra-low decay of 0.016% per cycle during the whole 600 cycles at a high current density of 2C is displayed. The current work provides a promising design direction for high-energy-density Li-S batteries.

N. Additive Manufacturing and Powder Metallgufy: Medium/High Entropy Alloy

Symposium Organizers :

Huiping Tang, Northwest Institute for Nonferrous Metal Research, China; Yong Liu, Central South University, China; Yuichiro Koizumi, Osaka University, Japan; Kee-Ahn Lee, Inha University, Korea; Qian Ma, RMIT, Australia; Ed Herderick, Ohio State University, USA

Wednesday AM
August 21, 2019

Room：402 (4th Floor)
Symsposium：N

Chairs：
Bin Liu, Central South University, China
Lijuan Zhang, National Innovation Institute of Additive Manufacturing, China

8:30-9:00 Keynote

PM Materials and New Technologies in Automotive Industry

Xiang Xiong, Yong Liu Central South University, China

Compared to other manufacturing processes, PM technology has the highest raw material utilisation and the lowest energy requirement per kg of finished parts.With the development of automobile industry, opportunities to PM, such as cost-effective materials with high performance, light weight materials and advanced processing, will emerge .

Ferrous alloys, which include parts used in the body & chassis, pumps & hydraulics engine, exhaust transmission and drive train, are dominant in automotive PM alloys. Lean-alloys, free of Ni and Mo, become attractive in ferrous parts. Al alloys have been widely used in automobiles due to their unique properties of low density, excellent formability, machinability and corrosion resistance. Sintering is regarded as the most critical step in the aluminum PM manufacturing process. The best sintered properties of aluminum-based compacts are achieved by sintering in dry nitrogen and magnesium can concentrate on the surface of Al powder particles and enhances sintering by local reduction of Al_2O_3. Due to consideration of complexity and economy of parts, MIM has expanded its application from 3C to auto industry. MIM makes designs more flexible

and complex-shaped parts originally separately made of several pieces can be injected into an integrated whole by a single step. Products by MIM have been widely and maturely applied. Additive manufacturing (AM) technique has been used for fabricating a wide range of structures and complex geometries from three dimensional (3D) model data. More and more attention of major car-makers has been drawn by AM technique. It is concluded in automobiles that ferrous parts will still be the major PM products, PM Al alloys will see more and more applications, MIM parts will take over quite a large portions of conventional press-sintered parts and AMed alloys will be applied widely especially for large and complex-shaped parts.

9:00-9:25 Invited

Manufacturing Complex-Component Alloys by Using Powder Metallurgy

Yong Liu, Central South University, China

Complex-component alloys (MMAs), including high entropy alloys (HEAs), are a kind of new materials consisting of multi-elements with almost equal-atomic ratio. Compared with conventional single-element alloys, MMAs have outstanding properties, for example, simultaneous high strength and high ductility, and high corrosion and wear resistance. Compared with ingot metallurgy (IM), powder metallurgy (PM) can produce homogeneous MMAs with high performance more conveniently. This talk introduced our recent work on producing MMAs, and the study concerning the relationship between microstructures and mechanical properties of powder metallurgical MMAs. Both hot extrusion and selective laser sintering methods were extensively studied, and much better mechanical properties compared with alloys of the same compositions made by IM were obtained. Both the gas atomization and mechanical alloying were used to synthesize HEA powders, and then the powders were spark plasma sintered, hot extruded or selective laser sintered to bulk alloys. It indicates that the powder metallurgical HEAs cannot be fully consolidated without primary particle boundaries and residual porosities due to the complex alloy systems. Hot extrusion leads to a fully recrystallized equiaxed microstructure, but it is difficult to obtain complex-shaded parts. Finally, selective laser sintering was conducted. For example, a C-containing FeCoCrNi high entropy alloy with full density was successfully fabricated using selective laser melting (SLM). The density of HEA is dependent on the SLM processing parameter. The increase of the SLM scanning power or the decrease of the scanning speed leads to the increase of the density of HEA. The grain size reduced when the high scanning power or the low scanning speed was used. The C-containing HEAs with full density has a yield strength of 650MPa, which is nearly doubled than the same alloy made by casting. The HEA has unique cellular and columnar subgrain structures. The subgrain boundaries are made of dislocation networks decorated by the segregation of Cr element and nanosized M23C6-type carbides, and thus, are the main strengthening factor for the C-containing HEA. The improvement of mechanical properties MMAs is caused by the solid solution strengthening, grain boundary strengthening and the homogenous microstructure, which increases the work hardening ability. In general, powder metallurgy can be considered as a promising way for preparing large-sized and complex-shaped MMAs with high mechanical properties.

9:25-9:50 Invited

Additively Manufactured CoCrFeNiMn-xTi High-Entropy Alloy Via Electron Beam Melting

Pan Wang, Mui Ling Sharon Nai, Wai Jack Sin, Jun Wei, SIMTech, Singapore

To explore the electron beam melting (EBM), new alloys development is High Entropy Alloys (HEAs) have attracted significant research interest in recent years due to the novelty of the underlying alloy design principle as well as their promising mechanical properties, such as good corrosion resistance, excellent wear resistance, high strength, and exceptional ductility, of the massive solid solution microstructure. Here, we detailed characterize the equiatomic CoCrFeNiMn HEA powder produced by gas atomization. It is revealed that gas atomized HEA powder is suitable for additive manufacturing (AM). The printability of the pre-alloyed CoCrFeNiMn and mixed CoCrFeNiMn-x ($0 < x < 2$) is investigated by electron beam melting (EBM), which is one of powder-bed-fusion AM. For the pre-alloyed CoCrFeNiMn powder, the processing window narrow and the EBM-built parts exhibit comparable mechanical properties to their conventional cast counterparts. For the mixed CoCrFeNiMn-xTi powder, the chemical composition parts are obtained by EBM and the in situ formed precipitates enhance the strength. The microstructure and deformation mechanism of the EBM-built HEAs are presented and the formation of caused by the in situ reaction during the process is also discussed. These findings are expected to be usefully for understanding the relations between the AM part quality and the feedstock powder, the AM part deformation mechanism, and the role of cellular sub-structure on the AM part mechanical properties.

9:50-10:10

Additively Manufactured Medium Entropy Alloy (MEA) Via Selective Laser Melting (SLM)

Heng Duan, Bin Liu, Yong Liu, Ao Fu, Central South University, China

Medium entropy alloys (MEA) exhibite high tensile strength and ductility over a wide temperature range

(-196℃ to 400℃), which are believed to come from the deformation mechanism of a dislocation slip coupled with deformation nano-twinning. Additive manufacturing (AM) technology is now widely used to study complicated metallic parts from a computer aided design, as a beneficial supplement to the traditional forming methods of metal materials. However, there are few reports on the study of AM-MEA. In this work, a bulk FeCrNi MEA was successfully fabricated by SLM. The laser power in a range of 200~400W and the scanning speed in a range of 800~2000mm/s were employed. The effects of process parameters on microstructure and mechanical properties were discussed. The results show that, as the energy density increases, the relative density first increases and then decreases. The grain size increases when high scanning power or low scanning speed is used. High temperature gradients and cooling rates in SLM processes result in unique cellular microstructures. Due to the unique dislocation cell structure formed in SLM manufacturing process, SLM manufactures FeCrNi MEA shows good mechanical properties. The room temperature yield strength and the tensile elongation of the SLM FeCrNi MEA are760±20MPa and 36±3%, respectively.

10:10-10:30

Development of Powder Metallurgy High Strength-Ductility Medium Entropy Alloy

Bin Liu, Central South University, China / Hunan University, China; Yong Liu, Ao Fu, Central South University, China; Jia Li, Qihong Fang, Hunan University, China

The combining of high strength and good ductility is a crucial challenge for developing structural materials. Deformation induced twinning and deformation induced phase transformation can achieve a desirable strength ductility combination. Here, we present a novel FeCrNi based medium entropy alloys (MEAs) with high strain hardening and excellent strength ductility combination. The FeCrNi based MEA was prepared through powder metallurgy (P/M) method. The P/M process includes a gas atomization (GA) and a hot extrusion (HT) of pre-alloyed MEA powder. Microstructures and mechanical properties were characterized using scanning electron microscopy (SEM), electron backscattered diffraction (EBSD), high resolution transmission electron microscope (HRTEM) and tensile tests. Atomic-scale structural characterization and molecular dynamics simulation are utilized to reveal the microstructural evolution during tensile deformation. The results indicate that the P/M MEA has a equiaxed single face centered cubic (fcc) microstructure. No obvious porosity and brittle intermetallic phase was found. The MEA possesses an excellent strength-ductility combination, represented by yield strength (YS) of ~644MPa and ultimate tensile strength (UTS) of ~1034MPa with an elongation of ~54%. The outstanding mechanical properties are contributed to the twinning induced plasticity (TWIP) and transformation induced plasticity (TRIP). The current work provides a guideline for designing high-performance mechanical materials via the multiple deformation mechanisms.

10:30-10:45 Tea Break

10:45-11:10 Invited

Properties and Heat-Treatment of High Entropy Alloy CoCrFeMnNi Manufactured in SLM Process

Lijuan Zhang, Bowen Wang, National Innovation Institute of Additive Manufacturing, China

In this study SLM process is used to fabricate bulk high Entropy Alloy CoCrFeMnNi through optimized processing parameters and element powders. The mechanical properties are assessed and compared with the alloys produced in conventional processes. It is noticed that the properties of the alloys manufactured in this study are better than those made both in conventional processes and other reported additively manufactured. The microstructure of the alloys are characterized through XRD, SEM and EBSD in order to correlate the processing parameters with the microstructure, so that to understand the effects of mechanical property dependence of the processing parameters. The results show that the strength and plasticity at low temperature are improved with the decrease of test temperature, also superior to the currently used low temperature materials. In addition the heat treatment conditions are selected as 800℃、900℃ and 1000℃ respectively for 1h. The effects of heat treatment conditions on the mechanical properties and the formation of defects such as micro-cracks and pores are also studied. This study discovers a new manufacturing method for the high entropy alloys and indicates a potential application for this group of alloys at extreme conditions.

11:10-11:30

Laser Metal Deposition Process and its Advances

Nazmul Alam, CSIRO, Australia

High power industrial laser system started as an advanced hardfacing processing tool where a thin coating of noble metals were deposited track by track over a surface area. This process commonly known as laser metal deposition (LMD) provides all the metallurgical benefits including low dilution, low distortion, narrow HAZ, ultrafine microstructures, and others. This novel coating technique has tremendous potential in wider applications despite many other technical challenges including cracking at the interface, formation of intermetallic, distortion and other issues. In recent times the high power industrial laser systems

have been adapted to produce 3D printing objects.
This paper is based on many years of experience in the use of LMD process in various fields of applications. Different types of industrial lasers used for materials processing will be discussed. The work is mostly based on solid state high power fiber delivery industrial laser systems utilizing blown powder deposition technique, and its application on ferrous based alloy bodies of different grades. It will analyze and describe some of the attributes of the LMD process and its successes and failures in applications where understanding of material types is crucial. It will also discuss the future directions of this process for remote applications.

11:30-11:50

Effect of Pressure on the Solid-State Transformations in Powder Metallurgy High Entropy Alloy FeCoCrNiMo0.15 during Spark Plasma Sintering

Wei Zhang, Mingyang Zhang, Yingbo Peng, Yong Liu, Li Wang, Songhao Hu, Central South University, China

A novel graded material of a powder metallurgy high-entropy alloy (HEA) FeCoCrNiMo0.15was fabricated by spark plasma sintering(SPS) processing. After SPS, the HEA specimens consisted of a single face-centred cubic (FCC) phase in the centre, but dual FCC and a tetragonal structure σ phase near the surface. Surprisingly, the sintering pressure was sufficient to influence the proportion of phases, and thus, the properties of HEA samples. The hardness of the specimen sintered under a pressure of 30MPa increased gradually from 167HV in the centre to 634HV near the surface due to the gradual increase in the fraction of the transformed σ phase. The σ phase being the complex hard intermetallic particles to manipulate the properties of fcc-type HEA systems, which could be influenced by pressure indicated a major possibility for designing gradient HEA materials. The mechanical properties of the FeCoCrNiMo0.15HEA exhibited a significantly gradual change because of gradient distribution of the mixed FCC and σ phase structure. This gradient distribution was mainly caused by the sintering pressure. It was found that the alloying of Mo into the CoCrFeNi HEA system generated precipitation of brittle but extremely hard σ intermetallics in the FCC matrix. The hard, Cr-rich σ phase was homogeneously distributed throughout the FCC matrix, and the volume fraction of the σ structure increased from the centre to the surface of the SPS sample like it would for gradient materials. The volume fraction of transfromed σ structure can be easily adjusted by sintering pressure. The implication for control of properties via changing the phase balance in HEAs will provide a strong technical base for the potential applications of a novel gradient material.

11:50-12:10

Precipitation Behavior and Mechanical Properties of a Powder Metallurgy TiNbTa0.5ZrAl0.5 Refractory High Entropy Alloy

Yuankui Cao, Bin Liu, Yong Liu, Central South University, China

Refractory high entropy alloys (RHEAs) have attracted much attention due to their high temperature properties. Precipitation strengthening act as an important role in RHEAs. But, most of RHEAs were prepared by casting method, and have a coarse dendritic microstructure. The coarse microstructure and the segregation of components weak the strengthening effects of precipitation in RHEAs. To carry out the effects of precipitation on mechanical properties of RHEAs, a fine microstructure with homogeneous distribution of components is expected. Powder metallurgy has positive effects on refining microstructure and homogenizing components. In the present work, a TiNbTa0.5ZrAl0.5 refractory high entropy alloy was prepared by powder metallurgy and subsequently subjected to hot forging. The microstructural evolution, precipitation behavior and strengthening mechanism were studied. Results show that the as-sintered TiNbTa0.5ZrAl0.5 alloy has a single BCC phase. The residual pores of the as-sintered RHEA have been fully eliminated after being hot forged to a strain of 50%, and the grain size is refined from 50 μm to about 1 μm. The initial BCC phase is thermodynamically instable, and decomposes into two phases, the BCC matrix and the HCP (Zr, Al)-rich precipitates after hot forging. The precipitates are much harder than the matrix, and have significant effects on the mechanical properties of the refractory high entropy alloy. At room temperature, the deformed TiNbTa0.5ZrAl0.5 alloy has a high compressive yield strength of 174 MPa with a considerable compressive strain of 12%. The precipitation strengthening contributes about 51% while the grain-boundary strengthening contributes 35% to the increment of yield strength. At high temperatures, however, the deformed TiNbTa0.5ZrAl0.5 alloy shows mediocre strength. Precipitation strengthening acts as the dominant strengthening mechanism, while grain boundary sliding and dynamic recrystallization are responsible for the softening.sensing, catalysis, and energy applications.

12:10-12:30

Microstructures and Properties of an Equimolar AlCoCuFeNi High Entropy Alloy Printed by Selective Laser Melting

Tie Zhu, Hong Wu, Central South University, China

In this paper, the equimolar AlCoCuFeNi HEA powder was printed by SLM, with emphasize on its densification, phase identify, microstructure evolution,crystallographic

texture, micro-hardness and correction resistance. The density of SLM samples increase gradually with the increase of volumetric energy density (VED) with the maximal relative density 98.6%. The as-fabricated AlCoCuFeNi sample predominantly consisted of a single B2 solid solution structure with homogeneous chemical distribution, due to the rapid solidification during SLM and the sluggish diffusion in HEAs. The BCC(B2) matrix was rich in Al and Ni.Fine columnar sub-structures with strong <001> texture parallel to the building direction were present in the as-fabricated sample due to the temperature gradient and epitaxial growth during the SLM process.The micro-hardness and the corrosion resistance are gradually improved as the VED rises and the maximum micro-hardness rises to 610.8HV, which is much higher than that of the samples fabricated by other methods (> 100Hv). Owing to the fast cooling rate, a finer microstructure and B2 phases are formed. Because that the B2 (Ni-Al) phase are mainly distributed along the columnar grains, it has the best corrosion resistance.The main reason is that the higher VED results in the much more rapid cooling rate and the formation of more B2 phases.

N. Additive Manufacturing and Powder Metallgufy: Other Preparation Methods

Symposium Organizers :

Huiping Tang, Northwest Institute for Nonferrous Metal Research, China; Yong Liu, Central South University, China; Yuichiro Koizumi, Osaka University, Japan; Kee-Ahn Lee, Inha University, Korea; Qian Ma, RMIT, Australia; Ed Herderick, Ohio State University, USA

Wednesday AM Room: 313 (3rd Floor)
August 21, 2019 Symposium: N

Chairs:
Dong Qiu, RMIT University, Australia
Naoyuki Nomura, Tohoku University, Japan

8:30-9:00 Keynote

The Needs for 3D-Printed Bone Replacement and Repair in Australia and Technical Challenges

Ma Qian, Royal Melbourne Institute of Technology (RMIT University), Australia

In Australia about one in every 200 people each year undergo a hip, knee or shoulder replacement surgery. With a growing and ageing population worldwide, it is expected that the number of primary replacement or repair surgeries will continue to rise, and so will the number of revision surgeries. Hence there is an increasing need to design and manufacture orthopaedic implants that can facilitate robust osseointegration for long-lasting healthy services.
The actual clinical application determines the design and property requirements for implants, e.g., femoral implants call for superior compressive and tensile strengths while dental implants require high fatigue life and wear resistance. In addition, implants are expected to serve a lifetime without failure or revision surgery. Titanium and its alloys are premier orthopaedic implant materials due to their excellent biocompatibility, corrosion resistance and mechanical properties. Of them, Ti-6Al-4V has long been used as a key implant alloy for orthopaedic applications. This situation is well expected to continue in the foreseeable future. For example, 3D-pritned Ti-6Al-4V implants have found significant applications globally since 2007.
The first part of this paper reviews the current needs for human bone replacement and repair in Australia, with a special focus on young Australians aged between 15 and 24 years old. This is followed by a review of the essential properties of human bones. On this basis, design criteria are proposed for human bone-mimetic replacement and repair by 3D printing or additive manufacturing. The fourth part of this talk discusses the current status of 3D-printing enabled bone replacement and repair using Ti-6Al-4V alloy lattice implants as an example. Finally, the outstanding challenges for design and 3D printing of human bone-mimetic replacement and repair prostheses are identified and discussed. It is shown that some of the identified challenges can be substantially significant, which would require relentless innovation in implant design, material development and 3D printing processes.

9:00-9:25 Invited

Developing Low-Cost, High-Strength Ti-Cu Alloys Through Laser Metal Deposition

Dong Qiu, Duyao Zhang, Mark Easton, RMIT University, Australia

Titanium alloyed with a certain amount of copper is reported to have excellent anti-bacterial properties, good biocompatibility and corrosion resistance for dental applications. However, conventionally cast Ti-Cu alloys are not strong enough even after artificial aging. Given the unique advantages of very high cooling rates and multiple thermal cycles, additive manufacturing (AM) opens a new opportunity to produce low-cost, high strength Ti-Cu alloys. In this study, a series of Ti-xCu binary alloys (4≤x≤10wt. pct.) were produced by direct laser deposition (DLD). Elemental Ti and Cu powders with the particle size between 45μm and 90μm were mixed according to the designated composition. Both small cubes and large plates were printed on a TRUMPF Trulaser 7020 for microstructure characterization and

mechanical properties test respectively. It was found that the addition of copper can eliminate the columnar prior β-Ti grains that were commonly observed in other AM Ti alloys, in particular AM Ti-6Al-4V. The higher addition level of Cu resulted in the smaller equiaxed grains. The prior β-Ti grain size is as small as 10 μm in average in the as-built Ti-10Cu alloy. Meanwhile, very fine pearlite microstructure was observed with the interlamellar spacing of eutectoid Ti_2Cu as small as 40nm in the as-built Ti-10Cu alloy. In order to understand the microstructure evolution during the DLD process, the temperature history of a fixed location at the first layer was recorded by a pyrometer. It was found that the first layer has experienced at least 10 thermal cycles that converted the original martensite to the final fine pearlite microstructure. The small grain size and fine pearlite microstructure in the AM Ti-10Cu alloy resulted in similar tensile strength with commonly used Ti-6Al-4V at a much lower cost. The performance of AM Ti-Cu alloys was also compared with their cast counterparts in terms of the mechanical properties and anti-bacterial capability.

9:25-9:50 Invited

In-Situ Alloying with Twin Wire Arc Based Additive Manufacturing

Huijun Li, University of Wollongong, Australia

Additive manufacturing (AM) builds up a component through the deposition of materials layer-by-layer instead of starting with an over dimensioned raw block and removing unwanted materials, as practised in conventional subtractive manufacturing. With the development of AM technology, the current focus has shifted to producing functional metal components of complex shape that can meet the demanding requirements of aerospace, defence, and automotive industries. Wire and Arc Additive Manufacturing (WAAM) is by definition a wire-feed and arc-based additive manufacturing that uses either the gas tungsten arc welding (GTAW) or the gas metal arc welding (GMAW) process has drawn the interest of the research community in recent years due to its high deposition rate. This technique has been presented to the aerospace manufacturing industry as a unique low cost solution for manufacturing large thin-walled structures through significantly reducing both product development time and "buy-to-fly" ratios.

Intermetallic alloys such as aluminides of titanium, nickel and iron exhibit an attractive combination of physical and mechanical properties such as high melting point, low density, high strength, good oxidation, and creep resistance, due to their strong internal order and mixed bonding. However, the properties of these materials are often obtained at a cost in terms of ease of manufacturing. In recent years the WAAM process has been successfully applied to in-situ produce TiAl and Fe3Al intermetallic components with designed chemical compositions. One of the major concern is residual stresses (RS) distribution in the WAAM fabricated components as it not only influences the part tolerance but also cause premature failure.

The neutron diffraction technique has been recoganised as the most precise and reliable method of mapping sub-surface RS in components for both academic and industrial-economic relevance. Considering the outstanding capability of obtaining RS non-destructively deep within the interior of components, our study utilised neutron diffraction technique to conduct RS measurement by the angular scanning instrument KOWARI. Furthermore, an averaging method has been developed for the WAAM multi-bead buildup intermetallic alloys with large grain size. With the averaging method applied during experimental setup and data processing, reasonable residual stress results have been obtained from the acquired neutron diffraction data.

9:50-10:10

Application and Development of Laser Cladding Technology in Iron and Steel Industry

Yong Zhang, Sihua Cheng, Jiamin Luo, Qisong Sun, Jie Zhou, Xianglin Mu, Technical Research Institute of Shougang Group Co., Ltd., China

Laser cladding technology is a process in which a high-energy density laser beam is used as a heat source to rapidly heat and melt the powder to rapidly form a high-strength metallurgical bond with a small range of the substrate. It has been successfully applied to the dynamic and static blades of the blast furnace TRT unit in the steel industry, the flying shear drum flat head, the universal joint bearing hole, the main drive shaft of the rolling mill and the rolling mill arch. Laser cladding technology greatly extends the life of these components. For example, a steel company repaired the dynamic and static blades of the "one-to-two" TRT unit of the blast furnace turbine. The two repaired units have been put into production and service, and they are running smoothly and reliably. Moreover, all the moving and static blades of the two units after repair can increase the service life by 50%~100% compared with the new blades originally designed and manufactured. After repairing the two equipments, it can save about 5 million RMB in maintenance funds. In addition, nearly 95% of the steel companies in Baosteel, Angang, Shougang, WISCO, Tanggang, Tisco, etc. use laser cladding technology to repair and transform a large number of turbine rotating equipment, especially various imports. Key components. This not only ensures the normal operation of the equipment, but also increases the service life of the equipment. At present, laser cladding technology is gradually developing towards

high-power rapid cladding, small-scale movability, and various cladding heads, such as the Fraunhofer Institute for Laser Technology (Fraunhofer ILT) and the RWTH-Aachen University of Technology (RWTH-Aachen). An ultra-high speed laser cladding technology and equipment have been developed and introduced by a domestic enterprise. Another example has been the invention of a retractable inner hole cladding head at home and abroad, which solves the problem of inner hole cladding. At the same time, more and more kinds of powder materials for cladding have been developed. Laser cladding has gradually evolved from the simple repair parts of the past to the coexistence of the repair of old parts and the surface strengthening of new parts. This further promotes the application of laser cladding technology in the steel industry.

10:10-10:30

Research for Surface Characteristics of Aluminum Mirrors Made by Laser Additive Manufacturing

Xiao Han, Jianchao Jiao, Nan Kang, Beijing Key Laboratory of Advanced Optical Remote Sensing Technology, China

Additive manufacturing (AM) enable new and innovative design forms that cannot be produced by conventional manufacturing methods. Space optical instruments are precision systems that require high resolution, light weight, low cost and short schedule. Metal AM technology is becoming more adept at intricate mirror substrates and complex support structure shapes, enabling lightweight. Using the same material for both optical mirror and mechanical structure can make the instrument insensitive to temperature changes. In this study, selective laser melting (SLM) technology were utilized to create workpieces. The AlSi10Mg mirror blanks were fabricated with metallic powder bed fusion. Post annealing process was performed to relieve internal stresses. The microstructure of AlSi10Mg produced by SLM is compact, and the mechanical properties are much higher than the alloy formed by conventional casting. The single point diamond turning (SPDT) was been applied to deliver optical quality surface with the 5nm RMS and 1/20 λ PV. A high and low temperature cycle test was designed to measure the change of surface shape. The results show that the surface quality of mirror deteriorate after 3 cycles. The processing of 3D printed aluminum mirror must be improved for high-quality optical surfaces. This research can be used for the manufacturing of lightweight space optical mirrors and improve overall process efficiency.

10:30-10:45 Tea Break

10:45-11:10 Invited

Microstructure and Mechanical Properties of Cu-Cr-Zr Alloy Builds Fabricated by Powder Bed Fusion Process Using Fiber Laser

Naoyuki Nomura, Takato Kosaka, Keiko Kikuchi, Akira Kawasaki, Tohoku University, Japan; Shinichi Moriya, Japan Aerospace Exploration Agency, Japan; Takayuki Nakamoto, Takahiro Kimura, Osaka Research Institute of Industrial Science and Technology, Japan

The Cu-Cr-Zr alloys have been used in the regeneratively cooled combustion chamber of a liquid rocket engine due to their high yield strength and thermal conductivity. The inner wall of the combustion chamber, which is exposed to high-temperature combustion heat, is cooled with liquid fuel flowing through internal cooling channels. To obtain this structure, multi-step and complex processes are required to obtain internal cooling channels and it takes long time for completion. Recently additive manufacturing has been received great attention due to both the simplification of processing and fabrication of complex geometry. However, Cu shows low laser absorptivity around the fiber laser wave length. In this study, we tried to fabricate Cu-Cr-Zr alloy by laser powder bed fusion process (L-PBF). The effects of Zr content and post treatment on the microstructures and mechanical properties were investigated. The characteristics of gas-atomized Cu-Cr-Zr alloy powders were evaluated from the point of apparent and tap densities, flowability, and laser absorptivity. The builds were fabricated using EOS M280 with Yb fiber laser in N_2 atmosphere. Microstructure was observed by OM, SEM and TEM. Mechanical properties were evaluated by tensile test. Laser absorptivity of the powder with higher Zr content was higher than that with lower Zr content. When the builds were fabricated with the same building parameters, relative density of the builds with higher Zr was higher than that with lower Zr. This may be attributed to the laser absorption difference. In addition, the higher yield strength and elongation were obtained in the builds with higher Zr content. TEM observation revealed that fine Cr precipitates were confirmed in the matrix. Effect of hot isostatic pressing on the microstructure and mechanical properties would be also discussed.

11:10-11:30

Cold Spray Additive Manufacturing of Biocompatible Structures

Guang Zeng, Xiaobo Chen, Ivan Cole, RMIT University, Australia; Saden Zahiri, Stefan Gulizia, Commonwealth Scientific and Industrial Research Organisation (CSIRO), Australia

Titanium (Ti) and its alloys are widely used for load-bearing implants, however, slow but continuing

release of toxic metal ions and wear debris may incur undesirable side-effects. Tantalum (Ta), as an emerging metallic biomaterial, exhibits high corrosion and wear resistance in vivo, but the extremely high melting temperature of Ta (3017˚C) is a critical technical challenge for manufacturing fully dense structures through conventional processing approaches. As such, new and feasible manufacturing techniques for Ta-based implant materials are highly desired. Cold Spray (CS), an emerging technology of additive manufacturing provides a promising solution to depositing metallic coatings on Ti implants with a variety of benefits, including low-temperature and solid-state process with no phase transitions in Ti/Ta mixture. In this study, Ti-Ta composite coatings on Ti-based substrates (Ti-6Al-4V) were developed via CS. Chemical and physical features were examined through electron microscopy, EDX (Energy Dispersive X-ray Detector) and XRD (X-ray diffraction). Mechanical properties were measured by hardness tests. Corrosion resistance was analysed by potentiodynamic polarisation curves. In particular, in vitro biocompatibility was evaluated by cell culture in Dulbecco's Modified Eagle's Medium (DMEM). Results illustrated that CS is able to create unique biocompatible structures of pure Ta and a mixture of Ta and Ti. Vickers microhardness showed CSed Ti-Ta coatings were softer than Ti-6Al-4V substrate. Corrosion resistance of Ti-6Al-4V substrate and CSed Ti-Ta coating were similar. In vitro biocompatibility study indicated excellent cellular adherence and growth with abundant extracellular matrix formation on CSed coatings compared with Ti-6Al-4V substrate. Higher cell viability was observed on CSed Ti-Ta coatings. Such outcomes hold a promise for practical applications of CS coating in biomedical industry and implantable medical devices.

11:30-11:50

Metal Additive-Manufacturing Process and Residual Stress Modeling

Mustafa Megahed, ESI Software Germany GMBH, China

Additive manufacturing (AM), widely known as 3D printing, is a direct digital manufacturing process, where a component can be produced layer by layer from 3D digital data with no or minimal use of machining, molding, or casting. AM has developed rapidly in the last 10 years and has demonstrated significant potential in cost reduction of performance-critical components. This can be realized through improved design freedom, reduced material waste, and reduced post processing steps. Modeling AM processes not only provides important insight in competing physical phenomena that lead to final material properties and product quality but also provides the means to exploit the design space towards functional products and materials. The length- and timescales required to model AM processes and to predict the final workpiece characteristics are very challenging. Models must span length scales resolving powder particle diameters, the build chamber dimensions, and several hundreds or thousands of meters of heat source trajectories. Depending on the scan speed, the heat source interaction time with feedstock can be as short as a few microseconds, whereas the build time can span several hours or days depending on the size of the workpiece and the AM process used. Models also have to deal with multiple physical aspects such as heat transfer and phase changes as well as the evolution of the material properties and residual stresses throughout the build time. The modeling task is therefore a multi-scale, multi-physics endeavor calling for a complex interaction of multiple algorithms. This paper discusses models required to span the scope of AM processes with a particular focus towards predicting as-built material characteristics and residual stresses of the final build. Verification and validation examples are presented, the over-spanning goal is to provide an overview of currently available modeling tools and how they can contribute to maturing additive manufacturing.

11:50-12:10

Metallurgical Defect Control and 3D Printing Alloys Development:Case of Al, SMA, HEA

Ruidi Li, Tiechui Yuan, Yong Liu, Central South University, China

Laser 3D printing usually accompany metallurgical defects, such as pores and hot-crack. We proposed several methods to solve the crack problem. These methods contain surface plastic deformation, adding alloying element to adjust solidification path, stress inducing phase transformation, etc. On above basis, a high strength Al-Mg-Sc alloys for 3D printing was developed without crack, because the interest of additive manufacturing (AM) Al and Ti-base alloys for lightweight applications is growing. The microstructure exhibits alternately coarse and fine grain. The fine grained band is beneath the weld pool while the coarse epitaxial columnar grains locate at the central zone of weld pool above the fine grain band, which is caused by the segregation of $Al_3(Sc,Zr)$ particles in weld pool boundary. The tensile strength of the optimized alloy system surpasses 460MPa. After heat treatment, the tensile strength is close to 530MPa. The crack inhibiting mechanisms and strengthening mechanisms were discussed. We also developed 3D printing shape memory alloy and high entropy alloy. The microstructure, property and metallic parts were also introduced.

12:10-12:30

RINA CSM Role in AM – Powder Production Yield Increase Case Study

Alessandro Colaneri, RINA Consulting CSM, Italy

RINA CSM has been involved in the study and

development of powder metallurgy for over fifteen years. Over the years, RINA CSM has developed its experience in the production of metal powders using VIGA (Vacuum Inert Gas Atomizer) for applications in coating and additive manufacturing (AM). RINA CSM has followed the increase in market interest in this innovative technology, thanks to its participation in many research projects. The entire metal powder production chain takes place within the company's own facilities. This allows to produce high quality powders starting from alloy design, VIGA atomization and chemical, rheological and particle size analysis. Moreover, the knowledge of the production plants allows RINA CSM to have a wide vision on the realization and the characterization cost of the powders. The study in analysis focuses on the reduction of the production cost of aluminum powders, increasing the yield of an atomizer in the particle size range suitable for AM applications, from less than fifty percent up to 65%, by the choice of process parameters.

O. Electronic and Spin Electronic Materials: IV

Symposium Organizers :

Hongda Chen, Institute of Semiconductors, Chinese Academy of Sciences, China; Feng Pan, Tsinghua University, China; Rie Y. Umetsu(Ms.), Tohoku University, Japan; Joonyeon Chang, Korea Institute of Science and Technology (KIST), Korea; Lianzhou Wang, University of Queensland, Australia

Wednesday PM
August 21, 2019

Room: Room VIP (1st Floor)
Symposium: O

Chairs:
Hongda Chen, Institute of Semiconductors, Chinese Academy of Sciences, China
Feng Pan, Tsinghua University, China
Rie Y. Umetsu, Tohoku University, Japan
Joonyeon Chang, Korea Institute of Science and Technology, Korea
Lianzhou Wang, The University of Queensland, Austraila

8:30-8:55 Invited

Spin Generation from Ultrafast Perturbation of Magnetization

Gyung-Min Choi, Sungkyunkwan University, Korea

Manipulating magnetization by a spin current rather than a magnetic field is a fundamental issue in spintronics. Conventionally, spin currents have been generated from charge currents by spin filter effect or spin Hall effect. In this presentation, I will show that spin currents can be generated from ultrafast perturbation of magnetization. The ultrafast perturbation could be either a decrease of magnetization (demagnetization) or magnetic phase transition. For the ultrafast demagnetization, I will show the spin generation results with metallic ferromagnets and ferrimagnets. For the magnetic phase transition, I will show the spin generation results with metallic antiferromagnets. These results demonstrate novel mechanisms for the spin generation by exchange of energy and angular momentum among electrons, magnons, and phonons on various magnetic materials on a short timescale.

8:55-9:20 Invited

Voltage Control of Interfacial Magnetism in Multiferroic based Spintronic Devices

Ming Liu, Xi'an Jiaotong University, China

One of the central challenges in realizing magnetoelectric (ME) devices lies in finding a deterministic way to modulate magnetism in integrated circuits with a circuit-operation voltage. Ionic liquid (IL) gating on magnetic thin films with abundant electronic, chemical and magnetic interactions at the interface has become an emerging technology for controlling magnetism in a fast, compact and energy-efficient way. Compared with conventional strain effect dominated piezo/ferroelectric layer multiferroics, IL gating method has advantages like small gating voltage (V_g<5V), easy-to-integration and compatibility with varied substrates such as Si, flexible substrates etc. In additional, unlike the oxide structures require a high temperature to overcome the oxidation energy barrier, the IL gating control process can be operated at room temperature, suitable for applications in room temperature environment. Here, we will summarize our recent progresses of IL gating control of magnetism in varied magnetic heterostructures, as well as in dfferent manners. As IL gating process, proven to be a truly powerful and compatible gating method, enables giant ME tunability in different heterostructures and provides a tremendous potential in next generation of voltage-tunable spintronics/electronics.

9:20-9:45 Invited

Spin Pumping during the Antiferromagnetic-Ferromagnetic Phase Transition of FeRh

Yuyan Wang, Beihang University, China; Lin Chen, Technical University of Munich, Germany; Xianzhe Chen, Cheng Song, Tsinghua University, China; Christian H. Back, Technical University of Munich, Germany

As a promising candidate for thermally-assisted magnetic recording and antiferromagnetic (AFM) spintronics, FeRh attracts intensive interest due to its

first-order phase transition between the AFM and the ferromagnetic (FM) phase, which is unique for exploring spin dynamics in one material with coexisting phases. In this work, we focus on the spin pumping during the phase transition of FeRh. Ultrathin FeRh films of 5nm and 10nm capped with 4 nm Pt or Al were investigated via inverse spin Hall effect, using a coplanar waveguide. Here we mainly report the lateral spin pumping by which angular momentum is transferred from FM domains into the AFM matrix of FeRh during its phase transition. In addition, vertical spin pumping from FM-FeRh into Pt as well as from Py into AFM-FeRh is probed electrically by the inverse spin Hall effect. A dramatic enhancement of damping related to AFM-FeRh is observed during the phase transition, which is proved to be dominated by lateral spin pumping across the FM/AFM interface. The discovery of lateral spin pumping provides new insight into the spin dynamics of magnetic thin films with mixed-phases, and the significantly modulated damping during the phase transition advances its potential for practical applications such as ultrafast spintronics.

9:45-10:10 Invited

Spin-Orbit Torque Switching in Antiferromagnets

Cheng Song, Feng Pan, Xianzhe Chen, Xiaofeng Zhou, Tsinghua University, China

Antiferromagnets with zero net magnetic moment, strong anti-interference and ultrafast switching speed have potential competitiveness in high-density data storage. Electrical switching of antiferromagnets is at the heart of their device application. The antidamping torque-induced switching of Néel order is attained in a biaxial antiferromagnetic insulator NiO, which is manifested electrically via spin Hall magnetoresistance in NiO (100)/Pt bilayers. The antiferromagnetic moments are switched towards the current direction, different from the vertical configuration in the fieldlike torque scenario (e.g., CuMnAs and Mn2Au). On the other hand, electric field is used to switch the magnetic moment of Mn2Au films grown on piezoelectric Pb(Mg1/3Nb2/3)0.7Ti0.3O3 (PMN-PT) (011) substrates. When the electric field is swept, the easy axis of Mn2Au is switched between [100] and [ ] directions of PMN-PT (011) at room temperature, exhibiting a butterfly-like swithing feature. This feature indicates that the underlying mechanism is the electric field-induced ferroelastic strain. Such a transition of the easy axis leads to the change of threshold current for the field-like torque switching of Mn2Au. Electrical switching of antiferromagnetic moments pave the way for all-electrical writing and readout in antiferromagnetic spintronics. I am grateful to the theoretical contribution by Prof. Yaroslav Tserkovnyak, Dr. Jia Zhang, and Dr. Ran Cheng.

10:10-10:30

Electrical Control of Anisotropic Ferromagnetic Domains during Antiferromagnetic-Ferromagnetic Phase Transition

Xianzhe Chen, Cheng Song, Feng Pan, Tsinghua University, China; Hao Liu, Lifeng Yin, Fudan University, China

The rotation or propagation of magnetic domains is generally involved in the magnetization process. The magnetization switching of individual magnetic nano-elements, such as magnetic tunnel junction, was used to build novel magnetic memory and logic devices. The domain walls (DWs) motion driven by large current in magnetic racetrack provides an alternative way for the information storage, named racetrack memory, which has been proposed as an innately three-dimensional memory-storage device. Therefore, the current-driven ferromagnetic DWs motion has attracted intensive attention due to its rich physics and promising implement in racetrack nonvolatile memory. However, the interplay between antiferromagnetic / ferromagnetic (AFM/FM) phase boundaries and current has been remained elusive. Here we investigate the electrical control of anisotropic FM domains in AFM domains during the antiferromagnetic–ferromagnetic phase transition of Pd-doped FeRh films. For the as-grown state, the AFM/FM phase boundaries initially prefer to be aligned along [100] axis with weak anisotropy. A stronger anisotropy is introduced by applying a current with the density of ~106A/cm2. Moreover, the phase boundaries can be reversibly oriented by the applied (writing) current, giving rise to the orthogonal alignment between the phase boundaries and the current. Such alignments of anisotropic FM domains as a function of applied current generate multilevel resistance. Our finding not only fulfills the electrical control of domains in magnets, but also provides an alternative way for multilevel memories.

10:30-10:50

Field-Like Torque Switching and Antidamping Torque Switching in a Biaxial Metallic Antiferromagnet

Xiaofeng Zhou, Xianzhe Chen, Fan Li, Feng Pan, Cheng Song, Tsinghua University, China; Jia Zhang, Huazhong University of Science and Technology, China

Antiferromagnets with strong anti-interference and ultrafast switching speed have potential competitiveness in reliable high-density information storage with fast operation speeds. Antiferromagnet Mn2Au with opposite spin sub-lattices is a unique metallic material with huge anisotropic magnetoresistance and it has been proved that Edelstein effect can induce field-like torque switching the magnetic moments. Recently, antidamping

torque induced magnetic moments switching was observed in biaxial antiferromagnetic NiO(001)/Pt heterostructure. The spin current from spin hall effect of platinum is expected to induce antiferromagnet (AFM) magnetic moments switching, which has not been realized in metallic antiferromagnets. As previous researches have shown in pure Mn2Au film, the Hall resistance first increases and then decreases. When the current passes the pure Mn2Au film, the Néel spin orbit torque manipulates AFM spins perpendicular to current direction. Interestingly, when 7nm Pt deposited on top of Mn2Au film, the Hall resistance first decreases and then increases, which is opposite to the change direction in pure Mn2Au film, illustrating that the AFM spins switch different direction in Pt/Mn2Au comparing to pure Mn2Au. So in the Pt/Mn2Au heterostructure, the AFM spins prefer switching to the direction parallel to current direction. When the writing current flow through bilayer films, the spin-orbit coupling of heavy metal platinum produce spin current inject into Mn2Au, which induces antidamping torque switching the magnetic moments of Mn2Au and detected by AMR through reading current. The opposite magnetic moment switching models in pure Mn2Au film and Pt/Mn2Au bilayer structure is not only a typical feature for field-like and antidamping torque of SOT in metallic AFM from the fundamental viewpoint, but also provides a multifunctional candidate for antiferromagnet spintronics.

A. Advanced Steels and Processing: VI

Symposium Organizers :

Han Dong, Shanghai University, China; Zhigang Yang, Tsinghua University, China; Yoshitaka Adachi, Nagoya University, Japan; Dong-Woo Suh, Pohang University of Science and Technology (POSTCEH), Korea; Christopher Hutchinson, Monash University, Australia; Amy Clarke, Colorado School of Mines, USA

Wednesday PM — Room: 205+206+207(2nd Floor)
August 21, 2019 — Symposium: A

Chairs:
B.Cem TASAN, Massachusetts Institute of Technology, USA
Wei Li, Shanghai Jiao Tong University, China

13:30-13:55 Invited

A Self-Decarburized Layer on Nanostructured Bainitic with Excellent Resistance to Hydrogen Embrittlement

Wei Li, Binggang Liu, Pengwei Zhou, Xuejun Jin, Shanghai Jiao Tong University, China

A decarburized surface layer was introduced to nanostructured bainitic steel to improve its resistance to hydrogen embrittlement. The results showed that total elongation loss dropped from 44% to 5% but with few strength loss after decarburizing at 1223K for 20min. Furthermore, the DC-NB(decarburized nanobainite) sample showed a hydrogen diffusion rate two orders of magnitude lower compared with that in the untreated bulk material. Thermal desorption spectroscopy (TDS) results showed that there are three hydrogen desorption peaks in DC-NB sample. The desorpted H content was 0.284wppm in the NB sample, but 0.943wppm in DC-NB sample. It could be deduced that the decarburization layer could provide amount of hydrogen trappings to store the hydrogen. In addition, it showed that only one peak(~ 250˚C) left when 40μm-thick decarburization layer was removed in sample DC-NB-40. The peak of carbides appeared at 500˚C with superior trapping capacity, which meant that the carbides in decarburization layer were strong hydrogen trap sites with a higher binding energies compared to the grain boundaries or dislocations. In decarburization layer, the twinned boundaries with ε-carbides, and dispersed fine carbides acted as effective hydrogen traps. The decarburization layer covered on the surface of nanostructured bainitic steel could act as a protective barrier to hindering the H diffusion effectively, which improve the HE resistance greatly.

13:55-14:15

Microstructure and Mechanical Properties of Austenitic FeMnAlC Lightweight Steels and the Effects of Alloying Elements

Joonoh Moon, Seong-Jun Park, Chang-Hoon Lee, Jae Hoon Jang, Sung-Dae Kim, Tae-Ho Lee, KIMS, Korea; Bong Ho Lee, DGIST, Korea; Heung Nam Han, Seoul National University, Korea; Hyun-Uk Hong, Changwon National University, Korea

The effects of alloying elements on the microstructure and mechanical properties of austenitic FeMnAlC lightweight steels were investigated. For this purpose, several Fe-30Mn-10.5Al-1.1C based lightweight steels with an addition of different Mo, Cr and Si contents were prepared by vacuum induction melting and hot-rolling process. In order to make base metals having austenite matrix, the hot-rolled samples were solution-treated at 1050˚C. The microstructures were identified through transmission electron microscopy (TEM) and atom probe tomography (APT) analyses. The microstructure of solution-treated samples consisted of austenite and κ-carbide. In addition, Mo-enriched M6C and $M_{23}C_6$ carbide were additionally precipitated in samples containing high Mo during solution treatment, and DO3 ordered phases were precipitated in samples containing high Cr. Tensile properties and deformation behavior of the solution-treated samples were evaluated by tensile tests. In addition, the intrinsic properties of austenite

matrix were investigated through nanoindentation experiments. The results clearly indicated that the addition of Mo and Cr decreased the intrinsic strength of austenite, while Si increased it. These results were closely related to the precipitation behavior of κ -carbide. Finally, the changes of microstructure with an addition of alloying elements and its effects on the mechanical properties and deformation behavior were carefully discussed through TEM analyses, thermodynamic calculations and first-principles calculations.

14:15-14:35

Effect of Martensite Morphology on Damage Initiation of Dual Phase Steels under Dynamic Tensile Strain

Huasai Liu, Yun Han, Chunqian Xie, Yinghua Jiang, Shougang Group Co., Ltd, China

Ultra-high strength steels especially dual phase steels are used as structural components more and more in automobile industry, and sometimes for energy absorption parts to protect passengers when vehicle crash happens. While the dynamic tensile performance of the steels directly affects vehicle crash safety, the appropriate steels suit for energy absorption should be careful. It was known that the formation of microcracks and voids at the ferrite/martensite interface was the main failure mechanism under dynamic tensile strain, but for steels with different martensite morphology at the same strength grade, maybe the fracture behaviours of the steels are not the same. In this study, two different DP780 steels with different martensite morphology were studied using dynamic tensile testing machine under different strain rates at room temperature. One of DP780 steel is traditional C-Si-Mn-Cr system steel, which has bulk martensite island distributed in ferrite matrix, and another DP780 steel is Ti micro-alloyed C-Si-Mn-Cr-Mo system steel, which has a much finer martensite island. For revealing the deformation mechanism and failure processes and understanding the energy absorption ability of the steels with different martensite morphology, the deformation and fracture behaviors were investigated using SEM and TEM, and the observation areas were near the fracture surface. The results indicate that both DP780 steels have significant strain rate sensitivity when strain rates are between $1s^{-1}$ and 1000s-1, and area under tensile curves indicate the different energy absorption ability of the two DP780 steels. It can be seen big and small dimples are on the fracture surfaces of the two DP780 steels under different strain rates, but the number of voids and void density of the DP780 steels are quite different, and it is explained why DP780 steel with fine martensite island has a much better energy absorption ability than DP780 steel with bulk martensite island.

14:35-14:55

Very High Cycle Fatigue Properties of Hot Rolled Bearing Steel with Rare Earth Addition

Chaoyun Yang, Yikun Luan, Dianzhong Li, Chinese Academy of Sciences, China / University of Science and Technology of China, China; Yiyi Li, Chinese Academy of Sciences, China

This study mainly aims to clarify the effect of rare earth (RE) on the fatigue property of hot rolled high-carbon chromium bearing steel together with crack initiation and propagation behavior induced by long strip type inclusions in the very high cycle fatigue (VHCF) regime. For this purpose, ultrasonic tensile-compression fatigue tests were carried out on transverse and longitudinal fatigue specimens extracted from hot rolled bearing steels with and without RE addition, and the corresponding fracture surfaces having inclusions with different length-width ratios at fatigue source were analyzed. As a result, complex inclusions, usually containing inner oxide and peripheral oxide-sulfide duplex inclusion as well as (Ca, Mn)S inclusion, dominate the fatigue property of high clean bearing steel although MnS inclusions may lead to fatigue failure of transverse specimens and contribute to fatigue anisotropy. RE addition can better improve longitudinal fatigue property of hot rolled bearing steel than transverse fatigue property by modifying MnS and common complex inclusions into complex RE inclusions, which deform easily during hot rolling to reduce the effective inclusion size at fatigue source, especially for longitudinal fatigue specimens. In contrast with fatigue failure caused by inclusion particle indicating almost synchronous crack propagation in all directions from inclusion particle, the width of inclusion strip and instant crack plays a dominating role in crack initiation and propagation process for fatigue failure induced by long strip type inclusion. Fine granular area (FGA) only exists on both sides of the wider part of inclusion strip, and the length-width ratio of instant crack may continuously decrease with crack propagation, whether the crack propagation speed near the direction of crack width is higher than that near the direction of crack length or not. Effective inclusion area and corresponding effective inclusion size can be determined from the perspective of crack initiation and propagation in the VHCF regime. For VHCF fracture surface with FGA, the effective inclusion area corresponds exactly to the inclusion area included in FGA.

14:55-15:15

Micro-Alloying of Mo, Cr, RE and Ag in Gray Iron Cast

Xintong Lian, Han Dong, Shanghai University, China

Gray cast iron is widely used in industrial production,

due to its low cost and excellent performance in wear resistance and shock absorption. Adding moderate amounts of alloying elements not only controls the content of pearlite and the graphite morphology, but also improves the comprehensive performance by the reinforcement of micro-alloying. This paper studied the effect of Mo, Cr, RE and Ag on the microstructure and mechanical properties of HT200 gray cast iron. The matrix, graphite, pearlite content, element distribution and mechanical properties were analyzed in depth. The results show that the size of grain is refined obviously in the alloy of HT200 after micro-alloying. The average length of graphite also decreases from 249 mm to 212mm. The content of pearlite decreases from 98% to 92%. Mo and Cr are solutioned in the ferritic matrix and even enriched in cementite. RE and Ag segregate towards grain boundaries. The mechanical properties also vary a lot because of the change of microstructure. The hardness of HBS increase from 150 to 185. The tensile strength and yield strength at room temperature and 700℃ both increase respectively, while the elongation also enhances. It is known that the strength of pearlite is higher than that of ferrite. Although the proportion of pearlite decreases, the strength of alloy still increases, which is caused by multiple reasons. Firstly, A type graphite after micro-alloying is more short and thinner than as-cast alloy. Graphite distributes dispersively, which makes the matrix keeping good continuity. Short graphite is helpful to reduce the stress concentration and improves the strength of the matrix. Furthermore, the solution strengthening effect of Mo and Cr in the matrix is also beneficial for enhancing the strength, especially in the ferrite and cementite. Finally, the segregation of RE and Ag atoms towards grain boundaries may enhances the binding force of grain boundaries. The ability of micro-alloyed matrix against nital corrosion and heat corrosion also increases.

15:15-15:35

Interfacial Morphologies and Corrosion Behaviors of Fe-B Alloy and T91 Steel in Liquid LBE at 500℃

Shengqiang Ma, Jingyi Liang, Jiandong Xing, Ping Lyu, Zongliang Lu, Xi'an Jiaotong University, China

The present work investigated the static corrosion behaviors of Fe-B alloy and T91 steel in liquid Lead-bismuth eutectic (LBE) environment. The results show that the corrosion rate of Fe-B alloy is proximate to T91 steel, they are both around $0.23\times10^{-3}mm\cdot h^{-1}$, the corrosion rate of T91 steel is higher than Fe-B alloy in the stable corrosion stage at 500℃. The corrosion process of Fe-B alloy in liquid LBE mainly includes Fe element dissolution from Fe-B alloy into LBE. Meanwhile, liquid LBE can penetrate into Fe-B alloy through destructible phase boundaries of α-Fe and Fe_2B, thus leading to the combination of the dissolved Fe with O and Pb atoms to form a stable oxide layer which is a mixture of Pb2Fe10O17、Fe_3O_4 and PbO. Cracks are produced around the damaged phase boundaries around Fe_2B. The failure mechanism of Fe_2B phase is mainly caused by the crack initiation and propagation because of the penetration of Pb and Bi. The Fe and Cr in T91 steel can also dissolve into LBE. LBE could penetrate into T91 steel through grain boundaries to produce an IOZ（Inner oxidation zone）at subsurface of T91 steel matrix. There will be a double-deck oxide layer at the interface between T91 and LBE which formed by an inner $FeCr_2O_4$ layer and outer Fe_3O_4 layer. The higher corrosion resistance of Fe-B alloy in liquid LBE at 500℃ is attributed to the barrier effect of Fe_2B in this alloy compared to the T91 steel. The inhibition of α/Fe_2B phase boundary may further improve the corrosion resistance of Fe-B alloy in liquid LBE. In addition, the results show that the penetration of LBE mainly occurs at large angle grain boundaries of α, especially at its trigeminal grain boundaries. Therefore, the effective inhibition of large angle grain boundary and interphase corrosion of Fe-B alloy plays an important role for the improvement of the corrosion resistance in liquid LBE.

15:30-16:10 Tea Break

16:10-16:35 Invited

In-Situ SEM Characterization of Wear and Fracture in Martensitic Blades

Cem Tasan, Gianluca Roscioli, MIT, America

Steels for razor blade applications typically have tempered martensitic microstructure with high carbide content, to have high hardness and wear resistance. However, these steels are deformed to the point of fracture upon interacting with a material that is more than an order of magnitude softer: human hair. Despite its practical relevance, the underlying physical reasons of this surprising damage and failure phenomena resulting from the interaction of these two dissimilar materials are not fully understood. The challenge in developing an improved understanding is partially due to the multi-scale nature of this deformation process, and the complex boundary conditions that are difficult to realize in controlled experiments. In order to address this problem, we developed a novel multi-scale experimental methodology that utilized: (i) in-situ SEM shearing experiments employing a miniaturized tensile stage; and (ii) micro-mechanical tests employing an in-situ SEM picoindenter. These experiments, and post-mortem microstructure analyses using ECCI and EBSD, revealed crack nucleation and propagation mechanisms and how they relate to microstructural heterogeneities in ferrous martensite. Based on these observations, a phenomenological model for crack

nucleation and growth is proposed, which is further confirmed with elasto-plastic finite element simulations. These investigations also provide key insights on how to design wear-resistant steels.

16:35-16:55

Effect of Texture Evolution on Hydrogen Embrittlement Susceptibility in Stable 18Cr-10Ni-2Cu Austenitic Stainless Steel

Hyung Jun Cho, Han Seop Noh, Sung Joon Kim, POSTECH, Korea.

A growth of attention has been paid to hydrogen as an environmentally friendly alternative energy. The need for structural materials in hydrogen facilities has been increased as well. In hydrogen environment, ferritic steel has been frequently experienced a drastic elongation and toughness reduction owing to its large H diffusivity and low H solubility, which is called as hydrogen embrittlement. Thus, stable austenitic stainless steel has been mostly used in hydrogen facilities due to its low H diffusivity, high H solubility and resultant superior hydrogen embrittlement resistance. In this work, stable 18Cr-10Ni-2Cu austenitic stainless steel was investigated to elucidate the relationship between texture and hydrogen embrittlement susceptibility. Different types of texture could be obtained by 30% cold-rolling and 30% tension tests. The present austenitic stainless steel preferred to evolve Goss, Copper twin and Brass components by cold-rolling, and Copper and components by tension without any a'-martensitic transformation. The two tensile specimens containing different types of initial texture were electrochemically pre-charged with hydrogen, and their hydrogen embrittlement susceptibility was evaluated by slow strain rate tensile testing. The elongation loss of 30% cold-rolled specimen was larger than that of 30% interrupt tensile one, which indicated that hydrogen embrittlement susceptibility of stable austenitic stainless steel was dependent on initial texture evolution. In thermal desorption analysis, the same total amount of desorbed hydrogen was confirmed regardless of initial texture difference. However, a different fracture morphology was observed after slow strain rate tensile testing. Thus, the initial texture difference in stable austenitic stainless steels was assumed to affect H behavior and initiation as well as propagation of microcracks during slow strain rate tensile testing, which caused a different hydrogen embrittlement susceptibility in 30% cold-rolling and 30% interrupt tensile testing specimens. Finally, detailed hydrogen embrittlement mechanism depending on texture evolution will be discussed in the following presentation.

16:55-17:15

Minor Ce Element Addition and Microgravity Solidification of 13Cr Steel

Ying Ruan, Qingqing Wang, Bingbo Wei, Northwestern Polytechnical University, China

The 13Cr martensitic stainless steel with lower C content and controlled Ni and Mo contents has been mainly applied in ship, petroleum and natural gas industries owing to its excellent strength, toughness and corrosion resistance. If a sort of rare earth (RE) element is added into 13Cr steel, the interaction between the RE and other elements during solidification contributes to the variation of both phase and microstructure characteristics, consequently influencing its performances. Here, we added the Ce element with its content less than 0.1at.% on 13Cr martensitic stainless steel, aiming at investigating the effect of minor Ce content on the solidified microstructure and mechanical properties of 13Cr steel by arc melting and drop tube processing methods. As the Ce content increased from 0 to 0.09at.%, the microstructure composed of martensite with lath shape and a small amount of feathery bainite refined, and the volume fraction of the latter enlarged. Meanwhile, the impurities in the steel varied, and the hardness and yield strength dropped slightly. The rapid solidified steel droplets in the drop tube were confirmed to be consisted of lathy martensite and cluster-shaped ferrite. Their hardness values rose with the increase of both cooling rate and undercooling regardless of Ce content.

17:15-17:35

Formation of Segregation Causing Cracks in High-Quality Crankshaft Steel

Rensheng Chu, Yue Ma, Jingang Liu, Zhanjun Li, Ning Hao, Shougang Group Co., LTD., Research Institute of Technology, China

It is innovative to use the continuous casting slab to produce high quality crankshaft steel forgings for reducing cost at the same time with the formation of green production process. However, slab quality is hard to control, especially cracks can be generated during the process. The segregation of C, S, Cr, and Mo along the crack is analyzed by EPMA and SEM. The magnetic particle inspection is used for defects analysis with the continuous casting process for the production of high quality crankshaft steel forgings. The result shows that from the overall crack direction, the main crack is along the segregation zone expansion. Segregation zone shows obvious lath structure, or martensitic(M) or bainitic(B) structure. When the crack expands in the segregation zone, almost no transition occurs inside the slat bunch but the transition occurs when passing through the slat bunch interface. The M/B structure

fragility is much higher than the ferrite(F)+ pearlite(P) structure. When the crack propagates in the F+P microstructure, the F phase has a certain crack-arresting toughness and it is terminated for the propagation of the crack in the ferrite phase. Between the brittle M/B structure and the normal transformed F+P structure, there is a significant structure stress that causes brittle M/B structure cracking under superposition with residual internal stress in the forging process. In the crack, the segregation of C is serious with the maximum and the minimum levels of, respectively, 1.8% and 0.28%. The maximum and minimum values of S segregation are 1.73% and 0.01%m respectively. The segregation of Cr is relatively serious with the maximum and minimum contents of 8.14% and 1.26%, respectively. The higher contents of C, S and Cr in cracks compared with those in steel provide thermodynamic driving force for the formation of M/B hard phase.

A. Advanced Steels and Processing: VII

Symposium Organizers :

Han Dong, Shanghai University, China; Zhigang Yang, Tsinghua University, China; Yoshitaka Adachi, Nagoya University, Japan; Dong-Woo Suh, Pohang University of Science and Technology (POSTCEH), Korea; Christopher Hutchinson, Monash University, Australia; Amy Clarke, Colorado School of Mines, USA

Wednesday PM
August 21, 2019

Room: 208+209+210(2nd Floor)
Symposium: A

Chairs:
Zhilei Wang, Nagoya University, Japan
Mingxin Huang, University of Hong Kong, China

13:30-14:00 Keynote

Developing Advanced High-Performance Metallic Materials Via Engineering Ordered Nanostructures

Zhaoping Lu, University of Science and Technology Beijing, China

Advanced metallic materials with high strength, large ductility and high damage tolerance are urgently required for implementation of the "National Major High-tech Projects" and "Made-in-China 2025" plan in the fields of aerospace, transportation and nuclear energy where materials suffer from the most challenging service environments. Strengthening and toughing of the structural materials, which tend to be mutually exclusive, are therefore the eternal topic and critical scientific issue for both academia and industry. In this work, a novel alloy design strategy was proposed to overcome the long-standing strength-ductility tradeoff, especially in ultrahigh-strength regimes through formation of coherent nanostructures with strongly ordered lattices. A new grade of ultrahigh strength steels and refractory high-entropy alloys with superior mechanical performances were developed via tailoring the ordered nanostructures in the different matrices. The unique deformation behavior and the underlying strengthening mechanism responsible for the outstanding properties was also discussed

14:00-14:25 Invited

Dislocation Engineering for Designing High Strength Steel with Improved Ductility

Mingxin Huang, The University of Hong Kong, China

The Materials Science community has spent tremendous efforts on developing ultrahigh-strength steels with good ductility for lightweight structural application. However, improving the strength of steels frequently results in a reduction in ductility, which is known as the strength-ductility trade-off in materials. Current design methodology for improving the ductility of ultrahigh-strength steels mainly focus on the selection of steel composition (atomic length scale) or manipulating ultrafine and nano-grained microstructure (grain length scale). The intermediate length scale between atomic and grain scales is the dislocation length scale. A new steel design concept based on such dislocation length scale, namely dislocation engineering, is illustrated in the present work. This dislocation engineering concept has been successfully substantiated by the design and fabrication of a deformed and partitioned (D&P) steel with a yield strength of 2GPa and an uniform elongation of 16% published in Science. In the D&P steel, high dislocation density can not only increase strength but also improve ductility. In addition to the D&P steel, the present work shows that the dislocation engineering concept can be also successfully applied to some other quenching & partitioning steels.

14:25-14:50 Invited

Development of Nanoprecipitate-Strengthened High-Toughness Steels via Multistage Heat Treatment

Qingdong Liu, Wei Hou, Jianfeng Gu, Shanghai Jiao Tong University, China; Wenqing Liu, Shanghai University, China

The combination of high-strength and high-toughness not only reduces section of heavy components (low-cost) but also lower the possibility of risk from failures due to corrosion, fatigue, or their coupling effect for the transportation engineered systems such as advanced ship, offshore platform etc., particularly in the cryogenic condition or corrosive environment. Nanoscale Cu-

rich precipitates (CRPs) and reversed austenite (RA) are important strength and toughness contributors, respectively, which render the steels desired strength-toughness balance by forming so-called hierarchical and nanolaminated microstructures consisting of metastable RA and tempered martensite matrix. In addition, compared to conventional quench-temper (QT) treatment, flexible multistage heat treatment opens an advisable way to realize maximum strengthening and toughening effects at the same time. Therefore, it is important to broaden the property-limit for alloyed steels with given compositions via optimization of processing schedules, but which require in-deep knowledge on the related precipitation reaction and phase transformation at atomic scale, as well as the responses of microstructural constituents to the crack initiation and propagation during fatigue or stress corrosion.

We mainly focus on the nature of Cu precipitation and austenite reversion, particularly on the co-precipitation and competitive formation of various nanoscale precipitates (CRPs, NiAl phase and alloyed carbide) as well as RA in Ni-Cu-Al-Mn-containing steels that subjected to multistage heat treatment, utilizing the multiscale analytic methods of EBSD, TEM and atom probe tomography (APT). The temper-induced CRPs in hierarchical martensitic structure along with the concurrent formed NiAl phase and alloyed carbide are responsible for extremely high strength but degraded impact cryogenic toughness, especially when these precipitates are small and high-dispersed distributed. However, the metastable RA or the secondary martensite formed during intercritical tempering will partly compensate the toughness loss. A novel multistage heat treatment, which proves to benefit from the almost maximum effect of alloying elements added, endow the present multicomponent steel with fine laminated multiphase microstructures and, therefore a yield strength over 1700MPa together with a moderate impact toughness at -196˚C. In addition, the corrosion fatigue of the plate steel with different microstructures (or processing schedules) is comparatively estimated in simulated sea water of 3.5% NaCl solution.

14:50-15:10

Effect of Microstructure on the Strength of Low Alloy Martensite Steel

Chen Sun, Paixian Fu, Dianzhong Li, Hongwei Liu, Hanghang Liu, Chinese Academy of Sciences/ University of Science and Technology of China, China

Lath martensite is one of the most important constituent phase in numerous high strength and ultra-high strength steel. The current view of the lath martensitic structure is that a prior austenite grain is divided into packets of parallel laths, containing extended parallel blocks, and that block is further subdivided by laths, among which are low-angle boundaries while the packet and block boundaries are at high angles. It is of great importance to study the substructure of lath martensite since it is closely related to the strength and toughness of steel.

The early work by Grange indicated that the yield strength follows the formula of Hall–Petch with the prior austenite grain size. The Hall–Petch linear relation between the yield strength and the martensitic packet size was also presented by Swarr and Krauss in a Fe–0.2C alloy, Roberts in an Fe-Mn alloy, and Wang et al. in a 17CrNiMo6 steel. The martensitic packet size was further regarded as the primary microstructural parameter dominating the yield strength by Tomita and Okabayashi. On the other side, with the use of EBSD S. Morito et al. revealed that the block in the Fe-0.2C and the Fe-0.2C-2Mn alloys is the key structure controlling the yield strength of lath martensite. Moreover, Norstrom attributed the change in strength mainly to the packet size, while the lath width makes little effect on the strength. This observation is quite different from that of the early work by Smith and Hehemann and Naylor. They found that the strength increases with the refinement of martensitic lath.

Therefore, there are still plenty of controversies about the structure of lath martensite dominating the yield strength. The present work aims to provide an model for further understanding the microstructure-property relationship in lath martensitic steel. The microstructures of lath martensite in 42CrMo4 steel quenched at 820~940˚C for 5h were characterized by optical microscope (OM), electron backscattering diffraction (EBSD) and transmission electron microscopy (TEM). The result showed that with the quenching temperature increased, the prior austenite grain size (PAGs) increased, the martensitic block width increased, the lath width decreased and the yield strength increased. According to the result, a new model was established, as shown in Fig.1. In this model, the martensite lath determined the yield strength by controlled the area of the slip plane. The model combined the martensite block width and the martensite lath width, which could explain why previous studies pointed to different results. Based on this model, martensite lath was the structural unit that determined the yield strength of martensite steel.

15:10-15:30

Maraging Steels–Modelling of Microstructure and Properties

Zhanli Guo, Sente Software ltd, UK

Maraging steels are a special class of ultrahigh strength steels that differ from other martensitic steels in that they are not hardened by carbon. Instead of relying on

carbide precipitation, these steels are hardened by the precipitation of intermetallic compounds. Quantification of precipitation hardening in maraging steels is a challenging subject as it demands combined knowledge of precipitation kinetics and strengthening mechanisms. The effective hardening phases are of many types, the three most common ones being B2-NiAl, bcc-Cu and Eta-Ni3(Ti, Mo), either singly or simultaneously occurring. Moving on to precipitation strengthening mechanisms, there are dislocation looping mechanism and various shearing mechanisms.

Hardening and strengthening of maraging steels are produced by heat-treating (ageing) for several hours at temperatures typically around 400~600˚c. Martensite is easily obtained in these steels due to the high nickel content, and for the same reason austenite is a stable phase at room temperature for maraging steel compositions. Austenite reversion, or the prevention of it in most cases, has been an important issue for maraging steels. In addition, although carbides are not desirable phases in maraging steels, they may still appear due to carbon impurities. Therefore, the precipitates considered in the current model include B2-NiAl, bcc-Cu, Eta, Delta and Laves, as well as carbides M3C, M(C,N), M2(C,N), M7C3, M23C6 and M6C, whereas the martensitic matrix transforms gradually to ferrite and austenite.

The model is first checked against experimental data of systems with one dominant phase, during which the evolution of precipitate type, size and amount, austenite reversion, and strength/hardness has been validated. The model is then applied to alloy systems with more than one strengthening phase. The assessment covers most of the commercial maraging grades, including the 18Ni types and their Co-free counterparts. The limitations of the current model are discussed as well.

15:30-16:10 Tea Break

16:10-16:30

Carbide Clusters and Precipitates in Ti-Mo Microalloyed Steels

Jiangting Wang, Ilias Bikmukhametov, Hossein Beladi, Peter Hodgson, Ilana Timokhina, Deakin University, Australia

Precipitation hardening is an important strengthening mechanism for producing advanced high-strength steels (AHSSs). Carbide cluster and nano-precipitate have been successfully introduced in Ti-Mo microalloyed steels to strengthen the ferrite phase while maintaining good ductility and flangeability. However, the lack of fundamental understanding on carbide clusters has hindered the development of precipitation mechanism. The link between carbide cluster and nano-precipitates are still unclear.

In this work, we've characterized the carbide cluster and nano-precipitates in a Ti-Mo microalloyed steel using atom probe tomography (APT) and transmission electron microscopy (TEM). Their crystal structure, chemical composition, and size distributions have been systematically analysed at the atomic-scale. The APT results shows that the carbide clusters and nano-precipitates are composed of (Ti, Mo)C, and their chemical compositions do not change with particle size. High-resolution scanning electron microscopy (HR-STEM) results show that carbide clusters are disc-shaped particles of 2~6nm in diameter and several atomic layers in thickness, having the same lattice structure as ferrite matrix. It also reveals that the precipitate growth mechanism consists of three stages, i.e. embryo cluster -> GP cluster -> nano-precipitates. Furthermore, hot-deformation at 890˚c are applied to modify the ferrite microstructure and precipitation characteristics. The effects of hot-deformation on carbide formation and distribution are investigated for both ferrite grain interior and grain boundary regions.

16:30-16:50

Effect of Niobium on the Microstructure and Mechanical Properties of a Mn-Si Series Bainite Steel

Min Zhang, Bo Gao, Xinxin Zhang, Zhunli Tan, Beijing Jiaotong University, China; Benqian Gao, Beijing Jiaotong University China / Shandong Shuangyi Science and Technology Co., China

As a simple process and new technology of high economic benefit, Nb microalloying technology shows good market prospect. Mn-Si based bainite steels have received intensive interest in wide applications, especially in the form of thick and heavy steel pieces. In order to further improve the mechanical properties and enlarge the applicable area of bainite steel, we extends Nb microalloying method to provide more studies on the microstructures and mechanical properties survey of a common Mn-Si series bainite steel. The nominal chemical composition of the experimental bainite steel is 0.2C-2.0Mn-1.8Si-0.6Cr-0.07Nb(wt.%). The characteristic phase transformation temperatures are determined by adopting dilatometer. The addition of Nb elevates the critical temperatures of Ac1, Ac3 and Ms of the present steel. Different quenching mediums and heat treatment processes are applied to the present steels.The microstructures and mechanical properties, including wear-resisting property of the present steel

and its comparative component steel with no Nd addition are analyzed. Nd micro-alloyed Mn-Si bainite steel shows better combination of mechanical properties. The average original austenite grain size is effectively refined from 29 μm to 18 μm. Fine precipitates of Nb compounds less than 20nm are observed to distribute evenly in the matrix. The present work will devote to the Nb microalloying technology and extend practical application area of Mn-Si series bainite steels.

16:50-17:10

Design of High-Strength Steels Strengthened by Nanoparticles

Zengbao Jiao, The Hong Kong Polytechnic University, China

Advanced high-strength steels are highly desirable for a wide range of engineering applications, such as automotive, marine, energy, and constructions. Nanoscale precipitation strengthening in steels has received increasing attention in recent years and becomes a new cornerstone for the development of advanced steels with superior combination of mechanical and welding properties. Recent studies have demonstrated that bcc-type steels are perfect metallic materials for coherent nanoparticles strengthening, which can precipitate on a sufficiently fine scale (less than 5nm in diameter) to provide an extremely high strengthening response. In this talk, we will present our recent study on the development of ultrahigh-strength steels strengthened by a group of nanoparticles, including bcc-type Cu nanoclusters, B2-type NiAl intermetallics, and L21-type Ni_2AlMn Heusler nanoparticles. The alloy design strategy, nanostructural features characterized by 3D atom probe tomography, and mechanical properties of this class of materials will be discussed. In particular, the precipitation mechanism of Cu and NiAl co-precipitates will be analyzed. In steels with high Cu contents, the Cu nanoparticles nucleate first from the supersaturated solid solution, whereas Ni and Al segregate at the Cu-particle/matrix interface, the enrichment of which leads to the heterogeneous nucleation of NiAl nanoparticles, resulting in the formation of Cu/NiAl co-precipitates. In steels with low Cu contents, NiAl nanoparticles, enriched in Ni and Al together with a significant amount of Cu, nucleate first from the supersaturated solid solution. As the precipitation reaction proceeds, the first formation of NiAl-based nanoparticles leads to the rejection of Cu solutes toward the nanoparticle surface, resulting in the heterogeneous precipitation of Cu nanoparticles on the outer surface of NiAl nanoparticles, thus forming Cu/NiAl co-precipitates. In addition, mechanical and welding tests indicate that this class of nanostructured steels exhibit a unique combination of high strength, high ductility, and good weldability, which makes them attractive for future structural applications.

17:10-17:30

Research and Development of 900MPa Ultra-High Strength Rim Sheet Steel

Chang Song, Jia Feng, Yulai Song, Haihe Luo, Jiqing Chen, Wuhan Branch of Baosteel Central Research Institute, China

The rotor yoke is a key component of the hydro-generator. With the large-scale development of hydropower units, higher strength with good toughness and magnetic properties were needed, According to the characteristic and demand of high strength rim sheet, the Nb-Ti-Mo microalloying chemical composition design and TMCP technology for 900MPa grade rim sheet steel were introduced. The microstructure and the distribution of precipitation were observed. The results show that the tensile and magnetic properties of this steel are good enough for rim sheet needed. The analysis results show that the main strengthening method in the yoke steel is precipitation strengthening, the fine-grain strengthening and transformation strengthening. The rotor yoke is a key component of the hydro-generator. With the large-scale development of hydropower units, higher strength with good toughness and magnetic properties were needed, According to the characteristic and demand of high strength rim sheet, the Nb-Ti-Mo microalloying chemical composition design and TMCP technology for 900MPa grade rim sheet steel were introduced. The microstructure and the distribution of precipitation were observed. The results show that the tensile and magnetic properties of this steel are good enough for rim sheet needed. The analysis results show that the main strengthening method in the yoke steel is precipitation strengthening, the fine-grain strengthening and transformation strengthening. The rotor yoke is a key component of the hydro-generator . With the large-scale development of hydropower units, higher strength with good toughness and magnetic properties were needed, According to the characteristic and demand of high strength rim sheet, the Nb-Ti-Mo microalloying chemical composition design and TMCP technology for 900MPa grade rim sheet steel were introduced, The microstructure and the distribution of precipitation were observed, The results show that the tensile and magnetic properties of this steel are good enough for rim sheet needed, The analysis results show that the main strengthening method in the yoke steel is precipitation strengthening, the fine-grain strengthening and transformation strengthening.

B. High Temperature Structural Materials: Novel Concepts

Symposium Organizers:

Qiang Feng, University of Science and Technology Beijing, China; Shengkai Gong, Beihang University, China; Hyun Uk Hong, Changwon National University, Korea; Damon Kent, University of Sunshine Coast, Australia; Sammy Tin, Illinois Institute of Technology, USA; Hiroyuki Yasuda, Osaka University, Japan; Jun Zhang, Northwestern Polytechnical University, China

Wednesday PM
August 21, 2019

Room: 305 (3rd floor)
Symposium: B

Chairs:
Jian Zhang, Institute of Metal Research, Chinese Academy of Sciences, China
Pyuck-Pa Choi, Advanced Institute of Science and Technology, Korea

13:30-13:55 Invited

Gamma–Gamma Prime based Precipitation Strengthenable High Entropy Alloys

Rajarshi Banerjee[1], Bharat Gwalani[1], Sriswaroop Dasari[1], Abhinav Jagetia[1], Rajiv Mishra[1]
1. University of North Texas, USA

While high entropy alloys (HEAs), based on single phase concentrated solid solutions, have attracted a lot of worldwide attention, their potential application as real engineering alloys is rather restricted, especially for high temperature applications. Furthermore, often the experimentally observed single phase HEA is the result of second phase precipitation constrained by thermodynamic and kinetic factors. This presentation will focus on designing HEAs strengthened using a second (or more) phases. Al0.3CoCrFeNi will be discussed as a model HEA, to investigate second phase precipitation as a function of different thermo-mechanical treatments. This includes refined $L1_2$ (γ') precipitation as well as B2 precipitation in this alloy leading to substantial improvements in yield and tensile strength while maintaining substantial ductility. Subsequently, using a CALPHAD based solution thermodynamic approach, another novel precipitation strengthened fcc based HEA has been developed with the objective of maximizing the phase fraction and solvus temperature of $L1_2$ (γ') precipitates. Detailed microscopy using transmission electron microscopy (TEM) and atom probe tomography (APT) was carried out to characterize the alloy in various conditions. Hall-Petch strengthening coupled with precipitation resulted in a high tensile yield strength of 1600MPa with a reasonably good ductility of ~15%. These results hold promise for the development of precipitation strengthened HEAs for high temperature applications.

13:55-14:20 Invited

Design of γ'-Strengthened Co-Base Alloys Based on Multi-scale Characterization

Choi Pyuck-Pa[1], Im Hyeji[1], Yoo Boryung[1]
1. Korea Advanced Institute of Science and Technology, Korea

In this research we have explored Co-Ti-based alloys forming a two-phase gamma/gamma' microstructure with cuboidal gamma' precipitates of 60%~70% volume fraction and 0.5%~1.0% lattice misfit. Such a microstructure is well known from modern Ni-based superalloys, used in aerospace and land-based gas turbine applications, and is reported to be beneficial for high-temperature strength and creep resistance. However, the simple binary Co-Ti system cannot meet the above-mentioned criteria for the gamma/gamma' microstructure, and hence, the aim of this work is to identify novel multicomponent Co-Ti-based alloys forming the desired microstructures. We have investigated the binary Co-Ti reference system as well as ternary Co-Ti-X (X=Cr, V, Mo, W) and quaternary Co-Ti-X-Y (X=Mo, W, Y=Cr, Al) alloys with respect to their microstructure and high-temperature properties. Aged alloys were characterized using scanning electron microscopy, X-ray diffraction, and atom probe tomography (APT). APT analyses were performed to elucidate the elemental partitioning and site-occupation behavior of specific alloying elements and to understand the changes in gamma' volume fraction and morphology upon alloying. We found that Co and Cr partition to gamma, whereas Ti, Mo, W, and Al partition to gamma'. Additions of third elements to the reference Co-Ti system lead to significant increases in gamma' volume fraction. Elemental spatial distribution maps of the $L1_2$-ordered gamma' phase reveal that the third elements preferentially replace Ti on its sub-lattice. Some of them also affect the Ti solubility within gamma. The remaining excess Ti is available for formation of additional gamma', resulting in enhanced gamma' volume fractions and phase stability. In addition to microstructural characterization, we performed differential scanning calorimetry measurements to determine phase transition temperatures such as gamma-prime solvus, solidus, and liquidus temperatures. By combining the above-mentioned characterization techniques, we could elucidate the role of the alloying elements on the gamma/gamma' microstructure and the stability of the gamma' phase.

14:20-14:40

Thermal Stability and Strenghening Effects of Nano-Precipitated Ni_3Al Phase in CrCoNi Alloys

Ning An[1], Jianjun Tian[1], Yongji Niu[1]
1. Beijing Beiye Functional Materials Corporation, China

The single-principal alloy is mainly constituted of one metal or intermetallic compound, then optimized by alloying and processing to achieve optimum performance. However, the arisen multi-principal alloy design subverts the classic design. Multiple principal elements could lead to more composition design choices, together with reasonable heat treatment and deformation treatment, which can meet different engineering requirements. CrCoNi alloy is a single-phase solid solution with FCC structure. If there are only Cr, Co, and Ni components, CrCoNi alloy do not have precipitates; However, the addition of other microalloying elements, there can precipitate some super-lattice structure phases in CrCoNi alloy. It is well known that the proper addition of Al and Ti elements can facilitate to precipitate a large number of $L1_2$ type γ' phase (Ni_3Al) and DO_{24} type Ni_3Ti phases in Ni-based alloys. With the increase of Al and Ti content, these precipitates can grow rapidly from nanometer to micron in size. That could significant improve high temperature creep properties. In this study, the effects of Al and Ti additions on the microstructure and properties of CrCoNi alloys were investigated by means of X-ray diffraction analysis, differential scanning calorimetry, scanning electron microscopy, transmission electron microscopy and Thermo-calc; And the microstructure and strengthening and toughening mechanism of Ni_3Al phase precipitation strengthening CrCoNi multi-principal alloy were explored too. The results presented that the addition of Al and Ti significantly reduced the solidus and liquidus temperatures of CrCoNi multi-principal alloys, and enlarged the solidification interval. The Al/Ti ratio has a significant effect on the type and precipitation order of precipitated phases. The results of tensile and microscopic analysis presented that the deformation-induced three-dimensional structure of nano twins could play a significant role in strengthening and toughening. The multi-layer nanostructures with nanocrystalline, nano twin nanocrystalline, nano Ni_3Al precipitates and microcrystals can be regulated and controlled by adjusting the composition and process. The microstructure stability and toughness of CrCoNi multicomponent alloy can be improved significantly. There are superior oxidation resistance and corrosion resistance in CrCoNi alloy. With improvement of creep resistance at high temperature, it is very promising to broaden the application range of CrCoNi alloy, which can be more widely used in high temperature structural parts.

14:40-15:00

Studies of Discontinuous Precipitation in Ni-Co-Al Ternary Alloy System

Yang Zhou[1], Jun Wang[1], Zhou Fei[1], Philip Nash[2]
1. Shanghai Jiaotong University, China
2. Illinois Institute of Technology, USA

Discontinuous precipitation (DP) produces precipitate lamellars that have a distinct orientation relationship with the matrix and nanoscale widths and spacings. The major effects of discontinuous precipitation on the microstructure and mechanical properties in Ni-Co-Al alloy system were investigated in this work. 1) We proposed a novel technique for the large-scale synthesis of aligned-plate nanostructures that are self-assembled and self-supporting, which involves developing nanoscale two-phase microstructures through discontinuous precipitation followed by selective etching to remove one of the phases. This technique is demonstrated in Ni-Co-Al ternary alloy system using the discontinuous precipitation of a γ' phase, $(Ni, Co)_3Al$, followed by selective dissolution of the γ matrix phase. The method could be applied to any alloy system in which the discontinuous precipitation transformation goes to completion. The resulting structure may have many applications in catalysis, fltering and thermal management depending on the phase selection and added functionality with the retained phase. 2) The mechanical properties of Ni-Co-Al alloy samples with DP structure were investigated. The results imply that the presence of large volume fraction of DP transformed structure increases the hardness, ultimate tensile strength and yield strength significantly while decreasing the ductility. Higher aging temperature favors the occurrence of continuous precipitation and decreases the driving force for discontinuous precipitation.

15:00-15:20

Effect of $L2_1$-Co_2Al(Ti, V) Precipitates on Deformation Behavior of Fe-Al-Co-Ti-V Single Crystals

Hiroyuki Yasuda[1], Yuki Yasunishi[1], Ryota Kobayashi[1], Ken Cho[1]
1. Osaka University, Japan

Recently, ferritic heat-resistant alloys strengthened by the intermetallic precipitates such as B2-type NiAl and $L2_1$-type Ni_2AlTi have attracted much attention due to high strength at high temperatures. The CoAl precipitates with the B2 structure are also found to be effective in increasing high temperature strength of ferritic Fe-Al based alloys. The CoAl phase is precipitated in the bcc matrix with cube-on-cube orientation relationship with small misfit strain. If the precipitates are sheared by the dislocations in the bcc matrix, the precipitates strongly suppress the dislocation motion due to the

difference in primary slip system between the matrix and the precipitates, resulting in high strength. We call the precipitation hardening mechanism "slip frustration hardening". However, if the B2 precipitates dissolve into the bcc matrix above 973K, the yield stress decreases steeply. Small amount of Ti addition leads to the formation of the Co_2AlTi precipitates with the $L2_1$ structure. The $L2_1$ precipitates demonstrates a high dissolution temperature, which is favorable for high temperature strength. However, the dislocations in the bcc matrix bypass the coarse $L2_1$ precipitates with large misfit strain, resulting in low strength. On the other hand, if small amount of V is doped, the Co_2AlV phase with the $L2_1$ structure is precipitated in the bcc matrix with small misfit strain. The precipitates are sheared by the dislocation in the bcc matrix, resulting in high strength. However, V doping is not effective in increasing the disolution temperature of the precipitates. Co-doping of Ti and V leads to the fromation of the $L2_1$-$Co_2Al(Ti,V)$ precipitates and is effective in decreasing misfit strain between the bcc matrix and the precipitates and increasing the dissolution temperature. As a result, the $L2_1$ precipitates can be cut by the dislocations, resulting in high yield stress above 500MPa even at 1023K. The precipitation hardening mechanism was examined using the Fe-Al-Co-Ti-V single crystals.

15:20-16:10 Tea Break

Chairs:
Hongbo Guo, Beihang University, China
Hideyuki Murakami, National Institute for Materials Science, Japan

16:10-16:35 Invited

β-NiAl Based Protective Coatings for Advanced Single Crystal Superalloys

Hongbo Guo[1], Jian He[1], Liangliang Wei[1], Hui Peng[1], Shengkai Gong[1]
1. Beihang University, China

β-NiAl based coatings have seen promising potential application as protective coatings over superalloys or as the bond coats in thermal barrier coating (TBC) system due to their capability of forming an α -Al_2O_3 oxide scale above 1150˚C. However, the oxide scale on the β-NiAl based coating spalls readily during high-temperature cyclic oxidation. In this work, more than 10 reactive elements (REs) were investigated to improve the cyclic oxidation performance. The effects of different REs on the adherence of Al_2O_3/NiAl interface were investigated by first principles theory calculations and experiments. We find that the solubility of the REs in NiAl alloy arrive at an order of Hf >Zr>Dy>Y>La. All the REs exhibit an affinity for sulfur, with an order of La>Dy>Y>Zr>Hf, whereas effects of the REs on the Al_2O_3/NiAl interface exhibit an order of Hf>Y>Hf>Zr>clean interface>La. Combined with experimental results, we provide some suggestions on how to choose appropriate REs. Meanwhile, co-doping of congeneric REs such as Hf+Zr or Dy+Y is more effective than single RE doping in improving the oxidation behavior due to the synergistic effect of co-segregation of RE ions. Some strategies on inhibiting interdiffusion between the β-NiAl coatings and advanced single crystal superalloys were discussed to constrain the formation of secondary reaction zone (SRZ) and needle TCP phases in the superalloys.

16:35-17:00 Invited

Application of Pt-Ir Paste Coating for Ni-Based Superalloys

Hideyuki Murakami [1, 2]
1. National Institute for Materials Science, Japan
2. Waseda University, Japan

Ni-based single crystal superalloys with good high temperature strength and creep resistance can be used in the hottest section of gas turbines such as turbine blades. For further protection against oxidation and hot corrosion, thermal barrier coating (TBC) systems were developed. Basically, TBCs consist of a ceramic top coat which provides thermal insulation and a metallic bond coat, which not only supports the bonding between the TC and a substrate material but also works as an Al reservoir to form a TGO layer during high temperature exposure. Recently, a Pt diffusion coating with the γ-γ' microstructure, which is similar to that of the substrate has been proposed as a BC. It has been reported to reduce rumpling and suppress the precipitation of brittle TCP phases. To further improve the performance of bond coats, addition of iridium was focused, because it exhibits the highest melting temperature, high tensile strength at room temperature, excellent chemical stability and lower diffusivity into Ni-based alloys than Pt. It can thus be expected that the addition of Ir into Pt diffusion coating may result in better thermal properties and prolong the life of coated materials. The authors' research group has investigated Pt-Ir-modified aluminide coatings and reported that Ir addition can improve the high temperature oxidation resistance of the Pt-modified aluminides. Then the next step is to further improve the oxidation resistance of Pt diffusion coating by the Ir addition. In this study, the microstructure and oxidation resistance of Pt-Ir diffusion coating on single crystal Ni-based superalloy were investigated. Indeed, Yasui et. al. reported that in the electrodeposition process, addition of Ir to Pt-diffusion coating suppresses the formation of voids in the substrate but oxidation resistance of the coating is dependent on the quality of Pt-Ir films deposited, which is affected by substrate surface finishing and composition. To minimize this problem, a new route to fabricate Pt and Pt-Ir coating, i.e., a paste coating, was introduced in comparison with the electroplating method. The phase transformation and cyclic oxidation

behaviors of the Pt and Pt-Ir coatings at 1423K by both paste and electroplating methods were discussed. Some Ni-based single crystal superalloys were used as the substrate materials. The Pt and Pt-Ir films were deposited on the surface of specimen by two methods: electroplating and paste coating. All the electroplated coatings were diffusion heat treated for 1 hour at 1373K in flowing Ar to protect coatings from oxidation, whereas paste-coated specimens were eat treated at 773K for 2.5 hours to evaporate the binding elements and diffusion heat treated for 1 hour at 1373K in flowing Ar. The cyclic oxidation tests were carried out in a programmable muffle furnace at 1423K in still air. Each thermal cycle consisted of three periods: i) putting the specimens into the furnace to rapidly increase the temperature of specimens to 1423K (the temperature of furnace), ii) holding the specimens in furnace at 1423 K for 1 hour, and iii) removing the specimens from the furnace for 20 minutes air-cooling. The surface and morphologies and element concentration profiles along the cross section of the coating were analyzed by an FE-SEM equipped with EDS. In addition, the crystal structure of the coatings was identified by an x-ray diffractometer. The paste coating by a simple spray method was successfully applied to synthesize Pt and Pt-Ir diffusion coatings. It was found that Ir addition retards the formation of voids, and the pasted Pt-20Ir coating shows the promising features as the bond-coat: with no cracks, less voids and stable protective Al_2O_3 formation on the surface.

17:00-17:20

Research on the Interface Reactions and Wettability between a Y-Containing Superalloy Melt and Ceramic Materials

Yun Zi[1,2], Jie Meng[1], Yizhou Zhou[1]
1. Institute of Metal Research, Chinese Academy of Sciences, China
2. University of Science and Technology of China, China

In this paper, the interface reactions and wettability between a Y-containing supperalloy melt and ceramic materials were studied by means of sessile drop tests. The microstructural characterization of the alloy-ceramic interface and the elemental composition of reaction products were performed by SEM/EDS analysis and EPMA analysis, the phases of reaction products were identified by XRD analysis, and the surface analysis of reaction products was carried out by XPS. The results showed that Al and Hf in the alloy melt reacted with SiO_2 in the ceramic mould when Y content was 0.011wt%, and the reaction products were Al_2O_3 and HfO_2, with little change in the wetting angle. However, when Y content was higher than 0.011wt%, Y and Al reacted with SiO_2 in the ceramic mould, and the wetting angle decreased significantly. The reaction products of 0.1Y alloy were $Y_3Al_5O_{12}$ and $Y_4Al_2O_9$, and the reaction products of 0.5Y alloys were double reaction layer composed of Y_2O_3 and $Y_3Al_5O_{12}$. For the alloy-ceramic core system, when Y content was 0.011wt%, the reaction products were Al_2O_3, HfO_2 and ZrO_2, and the wetting angle dropped slightly. However, when Y content was more than 0.011 wt%, Y, Al, Hf and Ta both reacted with SiO_2 in the ceramic core, the reaction products of 0.1Y alloy were $Y_3Al_2(AlO_4)_3$, $Y_4Al_2O_9$, HfO_2 and ZrO_2, and the reaction products of 0.5Y alloy were Y_2O_3, TaO, HfO_2 and ZrO_2. $ZrSiO_4$ in the ceramic core partially decomposed to form ZrO_2 at high temperature.

17:20-17:40

Experimental and Numerical Investigation of Compressive Creep in 3D-Woven Ni-Based Superalloys

Hoon-Hwe Cho[1], Dinc Erdeniz[2], Keith W. Sharp[3], David C. Dunand[2]
1. Hanbat National University, Korea
2. Northwestern University, China
3. TexTech Industries, Inc. Korea

Micro-architectured Ni-based superalloy structures, with Ni-20Cr-3Ti-2Al (wt.%) composition and r/r'-microstructure, are created by a multi-step process: (i) non-crimp orthogonal 3D-weaving of ductile, 202 mm diameter Ni-20%Cr wires, (ii) gas-phase alloying with Al and Ti, (iii) simultaneous transient-liquid phase (TLP) bonding between wires and homogenization within wires via interdiffusion, (iv) solutionizing to create a single-phase solid solution, and (v) aging to precipitate the r' phase. The creep behavior of these 3D-woven r/r' nickel-based superalloys is studied under uniaxial compression via experiments at 825˚C and via finite element (FE) analysis, using a 3D model of the woven structures obtained through X-ray micro-tomography. The creep strain rate for the woven Ni-based superalloy is higher than that for the bulk superalloy due to the lower solid volume fraction of the woven structure, while the creep exponents are identical. The compressive creep behavior is sensitive to the geometry of the woven structures: fewer wires perpendicular to the load and fewer bonds between wires cause lower creep resistance of the woven structure, due to a reduction in load transfer from the longitudinal wires (which are primarily load-bearing) and the perpendicular wires. Creep buckling of longitudinal wires drastically reduces creep resistance of the woven structure, confirming the importance of maintaining longitudinal wires vertical and parallel to the uniaxial compression direction. Finally, reducing wire cross-section, e.g., via oxidation, reduces creep resistance. The oxidation kinetics of the wire structures at 750, 825, and 900˚C displayed parabolic rate constants comparable to commercial Ni-based superalloys, but indicates that up to 35% of the wire cross-section is oxidized after 7 days at 825˚C , such that oxidation-resistant coatings are needed for long-term use in oxidative environment.

C1. Light Metals and Alloys-Aluminum: IV

Symposium Organizers :

Baiqing Xiong, GRINM Group Co. Ltd., China; Yoshihito Kawamura, Kumamoto University, Japan; Young Min Kim, Korea Institute of Materials Science (KIMS), Korea; Jian-Feng Nie, Monash University, Australia; Diran Apelian, Worceste Polytechnic Institute, USA

Wednesday PM Room: Presidium Conference Room (4th Floor)
August 21, 2019 Symposium: C1

Chairs:
Shinji Muraishi, Tokyo institute of technology, Japan
Cheng Liu, CHINALCO Materials Application Research Institute, China

13:30-13:55 Invited

Prediction and Evaluation of Residual Stress in Aircraft 7050 Thick Plates

Cheng Liu, J. Q. Wang, H. L. Cao, G.M. Niu, CHINALCO Materials Application Research Institute, China

To meet increasing demand on weight reduction and structure performance, a large amount of integral structures are used in modern aircrafts. The integral structures are manufactured by machining aluminum thick plates. Residual stress in the aluminum thick plates could cause unacceptable structure distortion during and after machining. To get a better control on the residual stress in thick plates, we have worked on the following aspects: predicting residual stress evolution in key production steps including quenching and stretching, developing and selecting on-site fast residual stress measurement method and setting-up a residual stress internal control standard. Firstly a FEM model was constructed to establish the relation among process parameters, residual stress and distortion. After validation, the model was used to generate a database containing key process parameters, residual stress and distortion. Based on the database, a software tool was developed being able to in-line predict the residual stress based on actual process parameters. Based on the database, a very accurate residual stress measurement method was designed. In addition, ultrasonic method was also evaluated for suitability for the onsite measurement. Then both methods were used to measure a large number of thick plates as well many imported 7050 ones. From these measurements a company internal residual stress standard was set-up for quality control purpose.

13:55-14:15

Effect of Heat Treatment on Hydrogen Embrittlement of an Al-10Zn-2.6Mg-1.6Cu-0.2Cr Alloy

Toshiaki Manaka, Mitsuharu Todai, National Institute of Technology, Niihama College, Japan

Al-Zn-Mg-Cu alloys have been used as structural components due to their high strength. Large amounts of Zn and Mg elements additions increase strength, but stress corrosion cracking (SCC) susceptibility also increase. Crack propagation of SCC in the Al-Zn-Mg-Cu alloys is caused by hydrogen embrittlement. The peak-aged Al-Zn-Mg-Cu alloys show a degradation of ductility in humid air (HA) compared to dry nitrogen gas (DNG) when tensile testing is conducted at a slow strain rate. In humid air, hydrogen uptake occurs resulting from the reaction of water vapor with aluminum fresh surface. Although many studies have been carried out to improve SCC susceptibility of these alloys, the mechanism of hydrogen embrittlement has not been elucidated yet. In the present study, effect of heat treatment on hydrogen embrittlement of an Al-Zn-Mg-Cu alloy with high Zn content was investigated by tensile testing at various strain rates from $10^{-6}s^{-1}$ to $10^{-3}s^{-1}$ in humid air and dry nitrogen gas. The tensile test pieces were solution-treated at 470˚C for 1h, water-quenched and followed by different aging treatments, natural aging, peak aging and overaging. The tensile strength in peak-aged sample was ~650MPa, larger than that of the commercial high strength 7075 aluminum alloy. The elongation of specimens in any aging condition at a strain rate of $10^{-6}s^{-1}$ was smaller in HA than in DNG due to hydrogen embrittlement. Fracture surface observation revealed that intergranular fracture resulted in a loss of elongation in naturally aged and peak-aged specimens, while quasi-cleavage fracture was observed in over-aged specimens. Moreover, in naturally aged and peak-aged specimens, elongation decreased due to hydrogen embrittlement even at a strain rate of $10^{-3}s^{-1}$.

14:15-14:35

Effect of Ti Addition on Microstructure Evolution, Precipitation and Mechanical Properties of Al-Zn-Mg-Cu-Zr Alloy

Sang-Hwa Lee, Korea Institute of Materials Science (KIMS), Korea / Yonsei University, Korea; Jae-Gil Jung, Min-Seok Kim, Kwangjun Euh, Korea Institute of Materials Science (KIMS), Korea; Se-Hun Kim, Korea Automotive Technology Institute (KATECH), Korea; Sung-Hyuk Park, Kyungpook National University, Korea; Young-Kook Lee, Yonsei University, Korea

We investigate the effects of Ti addition on the microstructure evolution, precipitation and mechanical

properties of high strength Al–7.6Zn–2.6Mg–2.0Cu–0.1Zr alloy during casting, extrusion and heat treatment. The microstructure evolutions of the alloys were examined using scanning electron microscope (SEM), electron back-scattered diffraction (EBSD), and transmission electron microscope (TEM), and their mechanical properties were evaluated by hardness and tensile test at room temperature. The addition of Ti causes the refinement of Al grain and agglomerated eutectic phases in the as-cast alloy. The Ti addition increases the number of η -phase bands aligned along extrusion direction by reducing their length and spacing. The Ti addition also causes the refinement of η-phase particles present between the η-phase bands. In addition, the Ti addition increases the area fraction of dynamically recrystallized (DRXed) grains formed during extrusion, while it decreases the size of DRXed grains. During solution treatment of the extruded alloy at 450˚C, the addition of Ti causes the refinement of L12-structured dispersoids by changing the chemical composition from Al_3Zr to $Al_3(Zr,Ti)$ as well as the formation of new $Al_{18}Mg_3Ti_2$ dispersoids. The $Al_{18}Mg_3Ti_2$ dispersoids act as preferential nucleation sites of η precipitates during artificial aging at 120˚C. The kinetics of η' precipitation in the matrix is accelerated by the addition of Ti. The Ti-induced changes in the microstructure, dispersoids and precipitates improve the strength and ductility of T6-treated extruded alloy.

14:35-14:55

Influence of Pre-Aging and Natural Aging on Mechanical Property of SiC/6xxxAl Composite

Shize Zhu, Shenyang National Laboratory for Materials Science, Institute of Metal Research, Chinese Academy of Sciences, China / School of Materials Science and Engineering, University of Science and Technology of China, China; Dong Wang, Bolv Xiao, Zongyi Ma, Shenyang National Laboratory for Materials Science, Institute of Metal Research, Chinese Academy of Sciences, China

Some aluminum matrix composites based on heat treatable aluminum alloys, with poor ductility at artificial aging (AA) state, could be cold worked at natural aging (NA) state and service after AA. However, the cluster behavior during NA will increase the strength of NA composites and impair the hardening response during AA, which are adverse for the above strategy. In this study, the pre-aging (PA) treatment was used to inhibit the adverse influence of NA. The composite, with a nominal composition of Al-1.2Mg-0.6Si-1.0Cu (in weight fraction) and 17% (in volume fraction) SiC particles, was fabricated by powder metallurgy (PM) process then hot extruded to the bar. The extruded bar was solution treated at 540˚C then water quenched to room temperature (RT). The quenched specimens were subjected to two aging process: (i) NA at RT for two weeks. (ii) Pre-aging at various temperature and time, then NA at RT for two weeks (named as PA-NA). Next, the two kinds of NA specimens were AA at 170˚C for 6h (named as NA/AA, PA-NA/AA, respectively). The unreinforced alloy was fabricated and heat treated by the same method for comparison. Results from the hardness and tensile test showed that the hardening response in PA-NA specimens was weaker than that in specimens without PA. Moreover, the strength of PA-NA/AA specimens was higher than that of NA/AA specimens, and this phenomenon is more obvious in the composite than in the unreinforced alloy. The most suitable PA process is 150˚C, 10min. Transmission electron microscopy results reveal that the size of precipitates in NA/AA composite was larger than that in PA-NA/AA composite. Calculation based on Orowan strengthening mechanism showed that the smaller precipitates size and higher precipitates density in PA-NA/AA composite could be responsible for higher strength. The phase transformation activation energy was calculated according to the Avtami-Johnson-Mehl (AJM) theory based on differential scanning calorimetry. Results show that the dissolution activation energy of clusters was much larger, but the precipitation activation energy was lower in PA-NA specimens than in NA specimens, which indicates that clusters formed during PA is more stable and can become favorable nucleation sites for precipitates during AA, resulting in higher strength in PA-NA/AA specimens. The difference of phase transformation activation energy between PA-NA specimens and NA specimens was more obvious in the composite than that in the unreinforced alloy, leading to the larger increment in strength between PA-NA/AA specimens and NA/AA specimens in the composite.

14:55-15:15

Effect of Excess Si on Age-Hardening Behaviour in Al-Mg_2Si Cast Alloy Aged at 473K

Taiki Tsuchiya, Yuki Makita, Seungwon Lee, Seiji Saikawa, Susumu Ikeno, Kenji Matsuda, University of Toyama, Japan

Al-Mg_2Si alloy is age-hardening alloy and used for structural materials. Metastable phase affects hardening in this alloy. The alloy having higher Si content than quasi-binary Al-Mg_2Si alloy is called as excess Si type alloy. This alloy has higher peak hardness than quasi-binary Al-Mg_2Si alloy by aging heat treatment. In our previous work, we researched age-hardening behavior in excess Si type aluminum alloy to know precipitation sequence. And recently, we are investigating age-hardening behavior in Al-7mass%Si-0.3mass%Mg cast alloy to know precipitation sequence. Al-7mass%Si-0.3mass%Mg alloy is considered to Al-0.5mol%Mg_2Si-6.4mol%Si alloy. So the aim of this work is to investigate the effect of excess Si contents on age-hardening

behavior and microstructure evolution in Al-Mg_2Si cast alloy. The samples with basic composition Al-0.5mol%Mg_2Si were casted into iron mold. Then we measured temperature in cast and quenched into iced water when that temperature reached under 773K. The amount of Si addition in excess were 0.2mol%, 0.4mol%, 0.8mol%, 1.6mol%, 3.2mol% and 6.4mol%. We called samples as Base alloy, 0.2Si alloy, 0.4Si alloy, 0.8Si alloy, 1.6Si alloy, 3.2Si alloy and 6.4Si alloy, respectively. The samples were cut by diamond-cutter and polished. We measured hardness of as-cast using micro-vickers hardness measurements (load:0.98N, holding time 15s) and after that the samples were aged at 473K. The effect of excess Si addition on microstructures were researched using transmission electron microscopy (TEM, Topcon EM-002B).
Result of hardness tests, hardness of as-cast and peak-hardness increased with increasing Si content.
We performed TEM observation in Base alloy from [001]Al direction. There were two regions. One is small amount of precipitates region, another is large amount of precipitates region. Rod-shape precipitates along <100> direction were observed in both region. We observed cross section of rod-shape precipitates more higher magnification. We measured lattice spacing and internal angle of precipitates. It was confirmed that precipitates was β'. We will report other observation results on the day.

15:30-16:10 Tea Break

16:10-16:35 Invited

Micromechanics Based Precipitation Hardening Analysis in Aluminum Alloys

Shinji Muraishi, Jianbin Liu, Tokyo Institute of Technology, Japan

Fine misfit precipitates in age-hardenable aluminum alloys has important roles in their excellent age-hardening ability by their interaction with dislocations, so the design of precipitation microstructure has attracted much attention in many decades. Typical precipitation microstructure in peak hardness consists of GP-zones and meta-stable phase on certain habit planes in aluminum alloys, e.g. {001} GP zones and θ" plates in Al-Cu alloys, {001} β" needles in Al-Mg-Si alloys, spherical GP-zones and {111} η" in Al-Zn-Mg alloys, etc.
Present study focused on the internal stress field of precipitates with various different shapes and misfit strains to evaluate their roles in dislocation cutting and by-pathing manners in terms of numerical computation based on micromechanical Green's function method. Stress field of misfit precipitates on certain habit plane is reconstructed by homogeneous misfit strain (eigenstrain) in precipitate (Eshelby inclusion method), and dislocation motion vector on primary slip and cross-slip planes are predicted by force acted on the dislocation by Peach-Koehler formula. According to simulation results, dislocation interaction strongly depends on the stress field and geometry of misfit precipitates, repulsive and attractive force are operated on the dislocations laying on the primary slip plane, and simultaneous climb force becomes significant when dislocation approaching toward the misfit precipitates. Hardening ability of precipitate is discussed in terms of energy dissipation associated with dislocation motion

16:35-16:55

Microstructural Characteristics of the Stir Zone for Friction Stir Processed 5083 Aluminum Alloys

Tsutomu Ito, Toyama Prefectural University, Japan; Takashi Mizuguchi, Ehime University, Japan

The mechanical properties of crystalline metallic materials can be enhanced by strengthening the grain interior and grain boundaries, as described by the Hall-Petch relationship. The strengthening mechanisms for the grain interior include solid-solution strengthening, precipitation/dispersion-strengthening, and work hardening; and the strengthening mechanism for the grain boundaries of the materials is grain boundary strengthening, which depends on the grain sizes. Material strengthening is expected to affect weight saving of various structural members by decreasing the thickness of the materials. Therefore, development of microstructure refinement processes through severe plastic deformation (SPD) techniques such as equal channel angular pressing (ECAP), high pressure torsion (HPT), and accumulative roll bonding (ARB) have been recently conducted in the laboratory scale. This study attempts to use friction stir processing (FSP) as a microstructure refinement process. FSP is a microstructure refinement process that employs the principles of friction stir welding (FSW), which is a solid-phase bonding process developed by the welding institute (TWI) in the United Kingdom (UK) in 1991; this process can be used to obtain fine-grained microstructures of sizes $\leqslant 10\mu m$ through very few operations. The practical uses of FSW in various fields such as civil engineering, construction, railway, automotive, and aerospace have been demonstrated. However, FSP, which is based on the principles of FSW, is required the something ideas such as the increasing method of microstructural refining volume or use as selectively microstructural refinement because the volume permitted by microstructural refinement depends on the tool geometry. Therefore, this study conducted a single-pass FSP using various FSP conditions for the solid-solution strengthening type 5083 aluminum alloy. This paper briefly reports the microstructural characteristics formed in the stir zone, and the area of stir zone.

16:55-17:15

Online Prediction of Mg Alloys Melt Structure under Temperature and Electromagnetic Field Inducement by Electrical Resistivity and Thermoelectric Power

Qing Lan, Qichi Le, Ruizhen Guo, Jianfeng Zhang, Northeastern University, China

In this paper, temperature-induced the electrical resistivity and thermoelectric power variation of Mg-Gd binary alloys melt have been studied with four-point probe technique, as well as the thermoelectric power of these two alloys melt at constant temperature induced by alternating current (AC) electromagnetic fields. It should be noticed that online electrical resistivity and thermoelectric power provide the real-time and continuous measurement for the melt structure during the temperature inducement or electromagnetic field treatment process. In our research, the heating or cooling melt temperature is in the range of 580~720˚C , and the melt is respectively under the liquid-solid mixed stae, semi-solid stae and absolute liuqid stae. Both electrical resistivity and thermoelectric power show the invertibility during the heating and cooling process. The results also indicate that temperature-induced thermoelectric power and electrical resistivity change occurs in the semi-solid state, and temperature-induced change point attributes to Gd content in magnesium alloys.

On the other hand, the experimental constant temperature during the electromagnetic fields treatment is above the liquidus (640~730˚C). The results show that the thermoelectric power is strongly sensitive to the electromagnetic field, showing the sharp increment. Then thermoelectric power gets back to the initial value after turning off the electromagnetic field. Some characteristic parameters of thermoelectric power are extracted to indicate the melt structure variation degree under the electromagnetic fields. The results show that the electromagnetic field induced the characteristic parameters change occurs at different experimental temperature, which attributes to the Gd content in magnesium alloys. Furthermore, the effects of electromagnetic field condition, such as the electrical current, electromagnetic field frequency and duty cycle, on the thermoelectric power of melt have also researched further.

17:15-17:35

TEM Observation of Al-2.5wt%Li(-2.0wt%Cu) (-2.0wt%Mg) Alloys Deformed by HPT (High Pressure Torsion)

Seungwon Lee, Yuhei Haizuka,Taiki Tsuchiya, Seiji Saikawa, Kenji Matsuda, Susumu Ikeno, University of Toyama, Japan; Zenji Horita, Kyushu University, Japan; Shoichi Hirosawa, Yokohama National University, Japan

Severe plastic deformation (SPD) processes attracted attention in recent years as a method of grain refinement. High-pressure torsion (HPT) process can introduce a large amount of strain continuously compared to other SPD processes. Al-Li alloys have low density and are strengthened by dispersed fine precipitates through an aging treatment, traditionally. They have been used as aircraft materials. The intention of this research is to investigate the effect of Cu and Mg on Al-Li alloys on grain refinement using HPT process and aging behavior using aging treatment.

In this research, three kinds of alloys (Al-2.5%Li, Al-2.5%Li-2.0%Cu, Al-2.5%Li-2.0%Mg alloy in wt.%) were prepared by casting. Alloys were subjected to a homogenization treatment at 808K for 12h, then, they were undergone hot-rolling to the thickness of 1.2mm. Disks with 10mm diameter were cut from the sheets using an electrical discharge machine (EDM). The discs were solution treated at 833K for 3.6ks at Ar atmosphere, then quenched into ice water. The solution treated discs were subjected to HPT process under an applied pressure of 6GPa for 5 revolutions with a rotation speed of 1rpm at room temperature. Aging treatments were conducted on the HPT-processed alloys at 423K for a total time period of up to 600ks.

The Micro Vickers hardness measurement was conducted on a mechanically polished surface of the disks. Each hardness measurement was performed by using a load of 100g for 15s. After HPT process, hardness increased significantly compared to as-quenched (asQ). During aging treatment, Al-Li-Cu and Al-Li-Mg alloys reached peak aging at 0.48ks (8min), however, Al-Li alloy did not change the hardness level at the initial stage of aging, then hardness started to decrease.

The microstructures of the disks were observed using a TOPCON EM-002B transmission electron microscope (TEM) operating at 120kV. The samples were thin disks electrochemically polished with a solution of 75vol.% methanol and 25vol.% nitric acid. In as-HPT sample, i.e. no aging treatment, δ' (Al_3Li) phase was observed. With an increase of aging time, it was possible to observe the coarsened δ' phase in all alloys and T_1 phase in Cu added alloy.

17:35-17:55

Integrated Development "High Entropy" Aluminum Alloys

Yu Zhong, Mohammad Asadikiya, Songge Yang, Libo Wang, Diran Apelian, Worcester Polytechnic Institute, USA

High entropy alloys have been greatly investigated in recent fifteen years due to their superior properties such as high strength, high hardness, high temperature softening resistance, etc. Meanwhile, the traditional

aluminum alloys have attractive properties including light weight, high corrosion resistance, and high thermal conductivity, etc., it would be beneficial if a new alloy can be developed with the excellent properties of High entropy alloys and aluminum alloy combined. Especially, an "high entropy" concept alloy with the aluminum fcc matrix will be of great interests.

In this project funded by Advanced Casting Research Center (ACRC) at Worcester Polytechnic Institute (WPI), the calculation of phase diagrams (CALPHAD) is combined with the experiments to design a multicomponent "high entropy" aluminum-rich alloy with fcc matrix. The "high entropy" concept borrowed from High entropy alloys shows a totally new composition region which has much higher entropy of mixing (delta Hmix) than the traditional aluminum alloys. In addition, the casting and heat treatment experiments with the CALPHAD proposed compositions are carried out. Especially the multiple-stage solutionization is carried out, which successfully avoided the commonly existed incipient melting phenomena. The final candidates show promising yield strength and ductility behavior.

C2. Light Metals and Alloys-Magnesium: IV

Symposium Organizers :

Xianhua Chen, Chongqing University, China; Yoshihito Kawamura, Kumamoto University, Japan; Young Min Kim, Korea Institute of Materials Science (KIMS), Korea; Jian-Feng Nie, Monash University, Australia; Diran Apelian, Worceste Polytechnic Institute, USA

Wednesday PM
August 21, 2019

Room: 406 (4th Floor)
Symposium: C2

Chairs:
Bin Jiang, Chongqing University, China
Xiaobo Chen, RMIT University, Australia

13:30-13:55 Keynote

Research on Hydrogen-Chromic Magnesium-Based Thin Films

Liming Peng, Juan Chen, Yue Liu, Nanxiang Deng, Wenjiang Ding, Shanghai Jiao Tong University, China

As a new functional material, hydrogen-chromic film is mainly composed of a core composite film with reversible hydrogen storage property. It converts between transparent and reflective states through hydrogenation and dehydrogenation, regulates light at the visible and infrared spectrum intelligently. Therefore, it is widely used in smart switchable energy-saving window and hydrogen sensor. Magnesium has high hydrogen storage capacity and abundant output, then it is easy to be combined with various elements, these characteristics make magnesium-based materials play an important role in hydrogen energy application. For the past two decades, the reported magnesium-based gasochromic switchable mirrors have been limited to magnesium alloys. Herein, inspired by the excellent catalytic property of some transition metal oxides (TMO) for the magnesium-hydrogen reaction, we fabricated the novel gasochromic switchable mirrors based on Pd/Mg-TMO films by magnetron sputtering method. The results show that the mirror based on Pd/0.9Mg-0.1TiO2 film exhibits larger optical dynamic range at visible wavelengths and excellent structural recovery even after 100 cycles of hydrogenation and dehydrogenation compared with Pd/Mg film. The brookite TiO_2, crystalline Mg and some amorphous phases coexist in the Mg-TiO_2 layer of Pd/0.9Mg-0.1TiO_2 film with no trace of Pd. Interestingly, the TiO_2 nanocrystal clusters are distributed in stripe among Mg matrix. In contrast, the Pd/0.63Mg-0.37TiO_2 film consists of crystalline Mg and $MgTi_2O_5$ phase, where $MgTi_2O_5$ phase is derived from the reaction of superfluous TiO_2 with a part of Mg and deteriorates the optical properties of the mirror dramatically. In addition, the Pd/Mg-Nb_2O_5 and Pd/Mg-V_2O_5 films have better performances on reflectance conversion range and optical dynamic range, respectively. In summary, the optical performance of Mg-based switchable mirrors can be improved by introducing transitiom metal oxides into switchable layer.

13:55-14:20 Keynote

Solute Effects of Rare Earth Elements on Deformation Behaviors and Mechanical Properties of Mg

Jing Zhang, Fusheng Pan, Chongqing University, China

The application of magnesium alloys for lightweight structural components in microelectronics, aerospace, and automobile industries has significantly increased during the last decade. However, the potential use of magnesium alloys in wrought forms, such as sheets and extrusions, is still limited due to their poor ductility and strong directionality of properties. Alloying is known to be one of the most effective approaches to improve materials properties; among them, rare earth elements have attracted the most scientific attention. Taking rare earth elements for example in this presentation, the solute effects of alloying elements on the deformation behaviors and mechanical properties of Mg are evaluated from the perspective of the interaction between solute and basal dislocation, the solute segregation and pinning at twin boundary, and the activation of <c+a> slip system

and its competition with crack propagation on {0001} cleavage plan, by using first-principles calculations and molecular dynamics simulation. The underlying mechanism are proposed and design maps based on alloying effects are constructed which could serve as the basis for the design of high-ductility Mg alloys. The results are not only helpful to deepen our understanding of alloying effects in Mg, but also essential to develop new Mg alloys with better combined properties.

14:20-14:40 Invited

Development of a Magnesium Metal Production Process Using North Korean Magnesite

Jungshin Kang, Tae-Hyuk Lee, Hyung-Kyu Park, Jin-Young Lee, Korea Institute of Geoscience and Mineral Resources, Korea

In order to produce high-purity magnesium metal from North Korean magnesite ($MgCO_3$), the conventional process involving the electrolysis of anhydrous $MgCl_2$ produced from $MgCO_3$ and a novel and environmentally sound process using the electrolysis of MgO were investigated. Anhydrous $MgCl_2$ was prepared with combination of HCl leaching of $MgCO_3$ at 343 K, removal of impurities in the $MgCl_2$ solution by precipitation using MgO and H_2O_2, condensation at 373K after dissolving NH_4Cl in the $MgCl_2$ solution, and dehydration of $NH_4Cl{\cdot}MgCl_2{\cdot}6H_2O$ at 593K under Ar gas atmosphere. As a result, 99.3% pure anhydrous $MgCl_2$ was produced. To produce Mg metal, the electrolysis of $MgCl_2$ was conducted at 973~1040K using molten salt consisting of $MgCl_2$, NaCl, $CaCl_2$, and CaF_2. By applying voltage of 7.0V between an iron cathode and a graphite anode, Mg metal with purity of 99.8% was obtained, and the current efficiency was 81.2%~83.9%. In spite of high efficiency of the conventional electrolytic process, it incurs an environmental burden because chlorine gas is generated at the anode. Therefore, a novel Mg production process involving the electrolysis of MgO using a liquid metal cathode and vacuum-distillation of Mg alloy was investigated. In this process, copper, silver or tin for the cathode and graphite or platinum for the anode were immersed in molten CaF_2-MgF_2-NaF at 1273K or MgF_2-LiF at 1083K. When 3.0V was applied between electrodes, Cu-Mg, Ag-Mg, or Sn-Mg alloy was obtained depending on the cathode material, and the current efficiency was 75.8%~85.6% under certain conditions. Vacuum-distillation was conducted at 1100 ~1400K with the Mg alloy obtained, and Mg metal with high-purity of 99.97% was obtained. Therefore, the feasibility of the novel electrolytic process was demonstrated for the production of high-purity Mg metal from $MgCO_3$.

14:40-15:00 Invited

Development of Room Temperature Reciprocally Bendable Magnesium Sheets in China Baowu

Shiwei Xu, Yu Xie, Weineng Tang, Yun Qin, China Baowu Steel Group Corporation Limited, China; Jianfeng Nie, Monash University, Australia

In this presentation, the recent industrial application of magnesium alloy in China Baowu will be firstly introduced. From 2015 to 2018, China Baowu has developed two types magnesium instrument panel beams for China's domestic cars and five types magnesium alloy parts for China's high-speed trains, which significantly boosts the industrialization of magnesium alloys. Since the beginning of 2019, China Baowu has became the shareholders of sever scale magnesium enterprises through commercial cooperation.

The recent research progress of high-performance magnesium sheets in China Baowu will be then introduced. Several kinds of non-rare-earth-containing magnesium alloy sheets with the thickness from 0.5 to 1.5mm were successfully developed, which could be manually bent at room temperature by 180 degrees over and over again without cracking. It should be emphasized that this remarkable phenomenon was hardly achieved in industrial products that were manufactured merely by one pass optimized extrusion process and the following two or three passes rolling. These findings provide a new pathway for designing and developing magnesium alloy products with high formability at room temperature, compared to those traditionally difficult to form at room temperature. After heat-treatment, some sheets exhibit a tensile 0.2% proof stress of 228 MPa along the rolling direction (RD) and of 234MPa perpendicular to the RD with an elongation to failure more than 20% in both directions. It means that these sheets show no anisotropy. The microstructure evolution in these sheets during three-point bending tests were also systematically investigated by the in-situ electron backscattering diffraction (EBSD) analysis and transmission electron microscopy (TEM).

15:00-15:15

In-Situ High-Energy X-Ray Characterization of LPSO Reinforced Mg Alloy under Tensile Deformation

Jie Wang, Leyun Wang, Gaoming Zhu, Xiaoqin Zeng, Shanghai Jiao Tong University, China

Mg alloys containing long period stacking ordered (LPSO) phases often display excellent mechanical properties. The underlying mechanism is yet unclear. In this work, in situ synchrotron X-ray diffraction was employed to study the tensile deformation of a Mg97Y2Zn

alloy that contains 18R-type LPSO phase. The material showed a high strength and good ductility at both room temperature and 200℃, but the strength dropped a lot when the temperature increased to 330℃. From lattice strain measurement, it is found that the LPSO phase has a similar elastic modulus as Mg. After material yielding, lattice strain in the Mg phase decreased, while lattice strain in the LPSO phase increased further. This load transfer effect from Mg matrix to LPSO can maintain up to 200℃, while it disappeared when the temperature up to 330℃. The lose strengthening effectiveness of LPSO at higher temperature have been examined elaborately. Fiber LPSO phase is no more thermal-stable and broke into small particles during the tensile deformation at a higher temperature. Due to the diffusion of Zn and Y tends to concentrate into the defects, stress in the local areas are high and microcracks are easily nucleated in the vicinity of stacking faults (SF). By analyzing the lattice strain evolution of different Mg peaks, deformation mechanisms at different temperatures have been concluded. That is, basal slip and deformation twinning are identified as the dominant deformation mechanisms at room temperature, while non-basal slip and grain boundary slide are active at elevated temperatures. These findings are further confirmed by ex situ electron microscope techniques (e.g. surface slip trace analysis using electron backscattered diffraction (EBSD) and TEM examination of the postmodern samples). Additional analysis of diffraction peak broadening indicates a diverse microstructure evolution (e.g. dislocation density) at different temperatures during the tensile deformation. Based on the above results, the origin of the high strength and good ductility in LPSO-containing Mg alloys is elucidated.

15:15-15:30

Effect of Stress State on Microstructure Evolution of AZ31 Magnesium Alloy during Bending Process

Yuanping Jin, Lili Chang, Yaru Zhao, Jing Guo, Shandong University, China

The present study aims to investigate the twinning behavior and texture evolution of the as-rolled commercial AZ31 magnesium alloy using three kinds of three-point bending tests (bending ,flattening and rebending with a reversal loading). Microstructure evolution after the bending, flattening and rebending processes was characterized by an electron back-scatted diffraction (EBSD) technique. Meanwhile, a three-dimensional finite element (FE) model of the bending processes was set up using ABAQUS/Standard to theoretically predict the stress state during bending. The experimental results revealed that deformation mode remarkably influenced twinning development and {10-12} tension twin was the main twin type in the bent samples. EBSD maps and pole figures showed twinning, detwinning and retwinning processes. For the case of the region close to punch and the center region, {10-12} tension twin could be found after the bending process, while detwinning appeared in the flattening process and retwinning happened in the rebending process. Twinning occurred in the region away form punch of the sample during the bending process, then detwinning could be found in the flattening process, and retwinning could be observed in the rebending process. Numerical simulation results showed the contours of Von Mises stress and the contours of the stress components corresponding to the longitudinal (σ11), width (σ22), and thickness (σ33) directions developed in the bent samples following bending process, flattening process and rebending process. In addition, analysis results showed the evolution of stress components developed at three points (point close to punch, center point and point away from punch) of each sample in the three bending processes. The Von Mises stress contour revealed that the stresses increased with increasing the displacement from the center region to the region close to punch and the region away from punch during the three bending processes. Stress components analysis for all three bent samples revealed that the region close to punch was under compression while the region away from punch was under tension.

15:30-16:00 Tea Break

16:00-16:20 Invited

Strengthening of Mg-based Long-Period Stacking Ordered (LPSO) Phase Alloys Induced by the Formation of Deformation Kink Band

Koji Hagihara, Takayoshi Nakano, Osaka University, Japan; Michiaki Yamasaki, Yoshihito Kawamura, Kumamoto University, Japan

The LPSO phase is expected as a suitable strengthening phase of Mg alloys. The recent hot topic found in Mg-alloys containing large amount of long-period stacking ordered (LPSO) phase is the unusual increase in the strength by the extrusion. Recently we clarified the mechanisms which induce the drastic strengthening of the LPSO-phase alloys by extrusion, on the basis of the quantitative analysis. In this presentation, the details of this are discussed. In order to achieve this, the temperature and loading orientation dependence of the deformation behavior of the Mg88Zn4Y7 extruded alloy which contains a ~86vol.% of LPSO-phase were examined, in addition to the test using the directionally solidified (DS) LPSO-single-phase crystals.
Using several extruded alloys with different extrusion ratio, the influence of extrusion ratio to the microstructure formation and the following mechanical properties were examined. Rectangular specimens were cut by electro-discharge machining from the as-cast ingot

and extruded alloys, and the mechanical properties of them were examined by compression tests. The tests were conducted in a temperature range between the room temperature and 400℃ in a vacuum. Two loading orientations were selected for the compression test; one is parallel to the extrusion direction (0° orientation), and the other is inclined at an angle of 45° from the extrusion direction (45° orientation), to clarify the anisotropic mechanical properties of the extruded alloys. As a result, the yield stress of the LPSO phase alloy was found to exhibit a strong orientation dependence varied with the extrusion ratio. Especially, the yield stress of the extruded alloy with the reduction ratio of 10 showed an extremely high value of ~460MPa when loaded at 0° orientation, while it was largely reduced when loading at 45° orientation. This strong anisotropy of the plastic deformation behavior was considered to be derived from the variation in the deformation mechanisms depending on the loading orientation because of the development of strong {10-10} fiber texture along the extrusion direction. Basal slip was found to govern the deformation behavior at 45° orientation, while the predominate deformation mechanism varied from basal slip to the formation of deformation kink band at 0° orientation, as increasing in the extrusion ratio. In addition, it was found that the introduction the deformation kink band boundary during the extrusion process effectively act as strong obstacles against the motion of basal slip. That is, "the kink band strengthening" was first quantitatively elucidated, which contributes to the drastic increase in the yield stress of the extruded LPSO-phase alloys in the wide temperature range below 400℃. The further details on this "kink band strengthening" will be discussed on the basis of the new results obtained by using the DS crystals.

16:20-16:35

The Effect of Twin Boundary on Precipitation Crystallography in Magnesium Alloy

Xinfu Gu, University of Science and Technology Beijing, China

Precipitation on deformation defects is essential for enhancing mechanical properties of age-hardenable alloys. The deformation defects act as heterogeneous nucleation sites and promote precipitation; in turn, these precipitates pin the movement of efects and improve the mechanical properties. Similar to other alloy systems, the precipitates in magnesium alloy also often exhibit preferred crystallographic features, such as specific orientation relationship (OR) between precipitates and matrix, interfacial orientation, morphology, and growth direction. These crystallographic features are one of the determinant factors of mechanical properties.Therefore, the understanding of precipitation crystallography at deformation defects in magnesium is indispensable in controlling the mechanical properties, but the related studies are limited.

The crystallographic restriction of deformation defects on precipitation was studied in the alloy systems mostly with cubic matrix due to the importance of steel, titanium alloy, etc. In magnesium alloys, twinning is an important deformation mode to accommodate the deformation strains due to limited slip systems. Therefore, it is important to study the effect of the twin boundary (TB) on the precipitation process.

In this work, we revealed how TB influences precipitation in Mg-Al-Zn alloys. As-cast Mg-9Al-1Zn (AZ91) alloy was homogenized at 415℃ for 24 hours and subsequently quenched by water. Compression samples with outer diameter of 10mm and height of 15mm were cut from the solution-heat-treated sample and then compressed at room temperature with ~ 4pct strain to introduce the proper amount of deformation twins. Finally, the samples were aged at 300℃ for 2 to 6 hours. The method for preparing TEM specimens was prepared by ion milling. The TEM observation was carried out with Talos F200 (200kV, FEI, OR, USA), and the statistic study of the crystal orientation was based on EBSD (Oxford Instruments, Oxfordshire, England).

It is shown that the precipitates on the TBs are different from those in matrix. Most precipitates hold the reproducible OR only with twin or matrix. Moreover, certain precipitate variants are absent and a new rule for variant selection on TB is proposed.

16:35-16:50

Effects of Solution Temperature on Microstructure and Mechanical Properties of a Sand Cast Mg-Gd-Y Magnesium Alloy

Bo Zhou, Institute of Metal Research, Chinese Academy of Sciences, China / University of Science and Technology of China, China; Di Wu, Rongshi Chen, Enhou Han, Institute of Metal Research, Chinese Academy of Sciences, China

Solution treatment at different temperatures ranging from 475℃ to 545℃ and subsequent aging treatment were performed to investigate the microstructure evolution during solution treatment and the effects of solution temperature on the mechanical properties of sand cast Mg-6Gd-5Y (GW65) Mg alloys. The microstructure of as-cast samples consists of α-Mg, eutectic Mg24(Gd, Y)5 phase and sparse cuboid phase. After solution treatment, the eutectic Mg24(Gd, Y)5 phase is almost completely dissolved into the matrix, and a large amount of cuboid phase is observed mainly in grain boundaries and with small amount within grains. In addition, the grain size increases and the fraction of cuboid phase decreases gradually with increasing the solution temperature. Quasi in-situ examination shows that clusters of cuboid phase are observed probably due

to the decomposition of coat and surround of Mg24(Gd, Y)5 phase. Interestingly, there is almost no appreciable difference of hardness (varying from 125HV to 130HV) in peak-aged samples with different solution treatments. All samples exhibit similar age hardening response in spite of the solution temperature variations. The best comprehensive mechanical properties are obtained in cast-T6 samples with previous solution treatment at 500˚C. It is mainly because of the moderate grain size and relatively small amount of cuboid phase left in matrix.

16:50-17:05

Heat Resistance Improvement in Mg-Al-Si System Alloy AS31 with tin Addition

Seiji Saikawa, Satoru Ishihara, University of Toyama, Japan

The vehicle weight reduction is needed to achieve high fuel efficiency. Therefore, aluminum and magnesium high-pressure die-casting (HPDC) is applied for automobile parts because of high productivity, good dimension accuracy and relatively low cost. Magnesium alloy components produced by HPDC, which have the characteristic with high specific strength and lightweight property, it is widely used for auto mobile industry. Heat-resistant magnesium alloy is focused as a suitable material for weight reduction of the engine and power train parts in automotive field. Recently, heat-resistant magnesium alloy in automobile field, Mg-3mass%Al-1mass%Si system alloy AS31 is the most expected and mass-produced alloy, because of good castability and mechanical property after as-cast (as-HPDC) . However, this alloy had the problem that heat resistance was not so high compare with special elements contained one's. In this study, microstructure and heat-resistant property in Mg-3mass%Al-1mass%Si alloy with containing large amount of Sn(tin). The alloys produced by permanent mold casting were investigated by optical microscope (OM), scanning electron microscopy (SEM) and measuring of bolt load retention at 423K. In based alloy AS31, BLR value is lowest in all alloy. However, the heat resistance properties are improved by adding more than 6 - 10mass% of Sn in this alloy, and the heat- resistant level improves remarkably from around 10% to 50%. The reason of such a remarkable heat-resistant improvement, when Sn increases to 10%, is the crystallization of new Mg_2Sn Phase. The cause that heat resistance decreased in Sn addition of more than 13% is because Mg_2Si phase begins to be crystallized as primary phase. The heat-resistant property of Mg-3mass%Al-1mass%Si alloy with containing 6-13masss%Sn was higher compared with Sn free alloy and conventional magnesium alloys (e.g. AZ91 and AM60 alloys). We have successfully developed a superior alloy with castability and heat-resistability. The most suitable addition of the Sn is around 6%, but it still have a problem that specific gravity rises up to 2.0g/cm^3.

17:05-17:20

Analysis on Edge Failures and Construction of Edge Cracks Pre-Criterion Model of AZ31 Magnesium alloy Plate

Fangkun Ning, Qichi Le, Northeastern University, China

Edge failure of AZ31 plate during hot rolling, including damages and cracks, would increase the edge cutting amount, reduce yields and also destroy the production continuity. The meso- or micro-failure called damage would induce the cracks growing when it is cumulated to some extent. In this paper, morphologies and types of edge damages or cracks during the rolling under various initial rolling temperatures and rolling reductions were compared and analyzed. Based on normalized C-L criterion, FE simulation was carried out and hot rolling experiments under a temperature range of 200~350˚C, the rolling reduction rate of 25%~40% and rolling speed from 7~21r/min were implemented. The microstructure was observed by optical microscope and damage values of simulation results were contrasted with the length of cracks on diverse parameters. The results showed that there were no obvious cracks but the 1~2mm damage scopes distanced from the edge during the 200~350˚C rolling with a small rolling reduction. Nevertheless, edge cracks depth were approximate 10mm with a larger rolling reduction under various initial rolling temperatures. With the increase of the reduction, the depth of cracks increased. At the same temperature, the depth of chevron cracks was shallow than slash cracks and the amounts of slash cracks were less than chevron cracks. The plate generated fewer edge cracks and the microstructure emerged slight shear bands and fine dynamic recrystallization grains rolled at 350˚C, 40% reduction and 14r/min. The edge cracks pre-criterion model was obtained combined with the Zener-Hollomon equation and deformation activation energy.

17:20-17:35

Active Corrosion Protection by a Smart Coating Based on Layered Double Hydroxide on Mg Alloy

Liang Wu, Gen Zhang, Xingxing Ding, Aitao Tang, Fusheng Pan, Chongqing University, China

The fabrication of traditional LDHs films usually involves the introduction of foreign metal ions. In this study, it was found that micro-arc oxidation coatings or anodic oxide films contains magnesium and aluminum oxides, when it was carried out in the bath containing aluminum

element. Mg-Al LDHs films can be fabricated by using Mg-Al mixed oxides, which can provide a source of Mg^{2+} and Al^{3+} for the transformation. In addition, the films can load inhibitors through ion exchange to improve their corrosion resistance. The structure and composition of Mg-Al LDHs conversion coatings are investigated by scanning electron microscope (SEM), energy dispersive spectrum (EDS), X-ray diffraction (XRD), and Fourier transform infrared (FT-IR), respectively. Furthermore, the corrosion resistances of Mg-Al LDHs films are investigated by potentiodynamic polarization, electrochemical impedance spectroscopy (EIS), and Scanning Vibrating Electrode Technique (SVET), respectively. The results show that Mg-Al LDHs films can be formed directly by the conversion of anodic oxide films, without the introduction of other ions. The corrosion resistance mechanism of Mg-Al LDHs films have two aspects: (i) The pores of the micro-arc oxidation coating or anodic oxide films were sealed by LDHs nanosheets, which can act as a good physical barrier to prevent chloride ion erosion; and (ii) as a kind of nano-container, LDHs can store and release inhibitors to protect the substrate actively.

17:35-17:50

Fabrication and Properties of Lotus-Type Porous Mg-2wt.%Mn Alloy by Gasar Process

Canxu Zhou, Yuan Liu, Tsinghua University, China

Lotus-type porous Mg-2wt.%Mn alloys distributed with elongated pores were fabricated by a novel Gasar process. By incorporating the Bridgman technique into the mold casting, the newly designed mold casting technique showed the capability to improve the pore straightness and parallelism. The porous structures of the ingots could be controlled through adjusting and optimizing the withdrawing rates during the processing. Also, the porosity, pore diameter, and pore length could be modified by changing the solidification speed and the hydrogen pressure. The porosity of the ingots was nearly constant under different solidification speeds, but decreased with the increase of the hydrogen pressure. The pore growth direction bended outward when the withdrawing speed was lower than 1.75mm/s. However, when the withdrawing speed increased above 2mm/s, the pore growth direction started to bend inward. With the increase of the hydrogen pressure from 0.1MPa to 0.6MPa, the average porosity of the ingots decreased from 53.6% to 38.4%, and the average pore diameter decreased from about 2512μm to 327μm. The phase constitution of Mg-2wt.%Mn ingots was the α-Mg matrix and the α-Mn precipitates. The compressive properties and corrosion resistance of the porous Mg-2wt%Mn alloys were studied. The yield strength of the porous Mg-2wt.%Mn alloys was varied with increasing the angle between the pore axis and the compressive direction. Meanwhile, the electrochemical polarization curves exhibited that the self-corrosion potential of the Mg-2wt.%Mn alloys was influenced by the porosity and pore diameter. Moreover, based on a model for estimating activity coefficient of multi-component molten alloys, the hydrogen solubility in molten alloys was calculated, and the calculated results showed good agreements with the experimental results. All the work above was to evaluate the structures and properties of the Mg-2wt.%Mn alloys including their microstructure, porosity, pore size, mechanical properties and corrosion resistance, aiming to investigating the possibility of being considered as a biomaterial candidate.

17:50-18:05

The Effect of Sn and Ca Addition on Microstructural Evolution and Mechanical Properties of Magnesium Alloys Subjected to Direct Extrusion Process

Young Min Kim, Yohan Go, Joung Sik Suh, Bong Sun You, Korea Institute of Materials Science, China

Magnesium alloys are recognized as promising materials for lightweight transportation vehicles due to the lightest density and good specific strength among structural metallic materials. Particularly in aircraft application, where safety and high strength are required, magnesium alloys must have both high ignition resistant and high absolute yield strength. We have recently reported that the addition of Ca and Y greatly improves ignition resistance and corrosion resistance of magnesium alloys. For further improvement in yield strength, Sn is known to be an effective element leading to precipitation hardening through the formation of fine Mg_2Sn. In this study, it was found that Sn addition led to complete dissolution of Mg17Al12 eutectic phase into Mg matrix and greatly improved the yield strength through the formation of fine precipitates. On the other hand, when a large amount of Sn and Ca was added, the ductility of the magnesium alloys greatly decreased by the formation of coarse Mg-Sn-Ca eutectic phase, of which influence on mechanical properties was not been fully understood. In this study, the microstructural evolution, especially the formation of second phases, during solidification in Mg-9Al-1Zn-0.2Y-Ca-Sn alloys was systematically investigated, and the optimization of chemical compositions and extrusion process parameters for the application to an aircraft interior component was also carried out.

D. Advanced Processing of Materials: V

Symposium Organizers :

Wanqi Jie, Northwestern Polytechnical University, China; Jianguo Li, Shanghai Jiaotong University, China; Hideyuki Yasuda, Kyoto University, Japan; Myoung-Gyu Lee, Seoul National University, Korea; Huijun Li, University of Wollongong, Australia; Dan Thoma, University of Wisconsin- Madison, USA

Wednesday PM Room: International Reporting Hall (3rd Floor)
August 21, 2019 Symsposium: D

Chairs:
Jiehua Li, Montanuniversität Leoben, Austria
Abu-Zahra Nidal, University of Wisconsin-Milwaukee, USA

13:30-13:50

Rapid Solidification of undercooled Alloys by electrostatic Levitation Method

Haipeng Wang, Bingbo Wei, Northwestern Polytechnical University, China

Electrostatic levitation Method is a containerless processing for metallic material, which allows that the sample levitates between the top and bottom electrodes by the coulomb force and does not contact with containers. As a result, the material with high undercooling could be obtained. For the reason that the sample is steadily levitated and the observing environment is good enough to use various detectors to obtain the different information during the heating and solidification process, there are many researches that could be achieved with the electrostatic levitation method. Firstly, the thermophysical properties of the liquid alloys are important and necessary for improving the manufacture of the material, the theory of the solidification and the computer simulation. The dates of the thermophysical properties of the liquid alloys are not accurate if they are measured by traditional methods. While many thermophysical properties could be accurately determined by electrostatic levitation method combined the digital image processing and drop oscillation method, such as density, surface tension, specific heat and viscosity in a wide temperature range.Secondly, the oscillation of the high temperature drop with large surface tension are investigated by electrostatic levitation method. It is difficult to study the oscillation of the melt without electrostatic levitation method because of its high activity. The second- and third- order zonal oscillations were observed with the change of the sample size. Furthermore, the formula of melt oscillation between the density and surface tension was established, which is of great help for the chosen of the material that promises to be levitated in a larger size. Thirdly, the alloys solidified in the electrostatic levitation are different with that solidified in equilibrium state, which makes it possible that we could obtain the desired material. With the increase of undercoolings, the grains will refine and the segregation degree decreases. In the high undercooling, the typical peritectic reaction is restrained and the final solidification microstructure is only consisted of peritectic phase, which is hard to obtain the microstructure of whole peritectic phase in equilibrium state.

13:50-14:10

The Density Determination and the Undercooling Capacity Exploration of Metastable Liquid Zr-24at.%Fe by Electrostatic Levitation Method

Chenhui Zheng, Pengfei Zou, Haipeng Wang, Liang Hu, Northwestern Polytechnical University, China

The accurate densities of the alloys are indispensable, especially the densities in liquid state are closely related to the mass transfer, solute macrosegregation, atomic distribution and so on, which have strong influences on solidification process, so density has great effect on the alloys production. Zr-Fe alloys are vital for nuclear industry due to their excellent mechanical properties, low neutron absorption cross section and good corrosion resistance for high temperature water. Because of the danger of the nuclear reactor and the radiation, it is difficult to experimentally test whether the cladding materials of Zr-Fe alloys are suitable for the nuclear reactor or not. And for the investigation of the danger accident that may happened, the simulation for understanding dynamic behavior of molten liquid Zr-Fe alloy, which was part of the cladding materials, was also needed. So the accurate densities are necessary for accurate simulation test to ensure insure that no impediment shall arise. The density of liquid Zr-24at.%Fe was experimentally measured by electrostatic levitation technique combined with digital image processing. The density of liquid Zr-24at.%Fe shows linearly dependence with temperature and increases with the decrease of temperature in both superheated and undercooled ranges. Because of the high vacuum and containerless environment created by the electrostatic levitation method, the molten droplet was easily to reach undercooling state, which was a metastable state and has greatly influence to the solidification process. The largest undercooling realized during the density measurements for Zr-24at.%Fe was 178K. Furthermore, some explorations of undercooling capacity of Zr-24at.%Fe were done. And it can be seen that except the content influence, the super heating temperature

and the holding time during the super heating process may influence the undercooling capacity of liquid Zr-24at.%Fe under electrostatic levitation. The stability of levitation position and molten droplet itself also have influence to the undercooling that finally reached.

14:10-14:30

Tuning Mechanism for Heterogeneous Nucleation of Metallic Crystal

Mingxu Xia, Jianguo Li, Shanghai Jiao Tong University, China

For liquid metal, heterogeneous nucleation is main channel towards the formation of solid crystal. Fine tuning of nucleation means an optimized solidification structure, and consequently promises tailored properties for application. There are a few extensively used industrial practices for nucleation tuning, as AlTiB catalyzed grain refining in Al alloys, silicon modification for AlSi alloys, spheroidization of graphite in cast iron, and so on. In new energy storage area, the nucleation control is also important for high energy lithium-ion batteries. An unexpected nucleation of lithium leads to infinite relative volume expansion presenting low cycling efficiency and even safety hazards in batteries with lithium metal electrodes. The nucleation potential of a new crystal on substrate was believe to be a function of lattice misfit between new crystal and substrate as stated by conventional nucleation theory. But as we understood, solidification is a liquid/solid transition rather than solid/solid transition, thus the lattice misfit between two crystals are hardly to elaborate the real scenario of nucleation process. The state-of-the-art analytical techniques offer the opportunities tracking the atomic structural evolution adjacent to solid-liquid interface which makes the in situ observation on heterogeneous nucleation possible. Here we report up-to-date results on in situ observed heterogeneous nucleation of a few metals on different substrates. The results indicates that the nearest neighbor distance of liquid atoms and their coordination number can be tuned by the alloying element or substrate. The prenucleated ordering structures in the liquid have a tendency to be aligned in a preferred orientation, which is templated by the lattice structure of the substrate. This prenucleated ordering structure with preferred orientation will match the atomic structure of the substrate forming new crystals. That's the reason why the lattice mismatching, a parameter describing the matching of new crystal with substrate, is still able to predict the nucleation potential of the substrate in a given liquid. The alloying element can be used to tune the lattice mismatching at the interface through interfacial structural tuning to enhance heterogeneous nucleation in the liquid. This findings will extend the understanding on heterogeneous nucleation leading to more effective nucleation tuning approaches in casting foundries, epitaxial growth of functional metal film or even more extensive application as energy storage area.

14:30-14:50

Effect of Preform's Wetting Pretreatment on the Structure of Open Cell Aluminum Foam

Tan Wan, Yuan Liu, Tsinghua University, China

The degree of pore opening and porosity of the open cell aluminum foams are important parameters of structure relating to their properties. In the process of preparing open cell aluminum foam by infiltration casting, the connectivity between the space holders of the preform affects the removal performance of them after the infiltration of the melts followed by solidification, which finally determines the degree of pore opening and porosity of the resultant aluminum foam.

There are two main ways to improve the connectivity between the space holders. The first is to make the space holders be together by sintering before infiltration, and the other is to bond the space holders together by binder. Both methods can increase the contact areas between the space holders and ensure the permanent contact among them. However, it is not easy to control the process of particle sintering, and, the binder is generally not resistant to infiltration temperature, which is only suitable for high-pressure rapid casting. Thus, these two methods cause a lot of difficulties to fabricate the open cell aluminum foam via infiltration casting. To solve with this problem, a new preform treatment method is proposed in this paper.

Spherical $CaCl_2$ particles with diameter ranging from1.25~1.6mm and 2~3mm were used as space holders in this experiment. Affected by its naturality, $CaCl_2$ particles perform strong hygroscopicity. Inspired by this, after being simply treated such as homogenization wetting with water, stacking and drying, good connections were formed between the space holders due to the diffusion. When wetted space holders were pressed by weigh for a period of time, the connectivity between the space holders was further improved, which meant easier removal of the $CaCl_2$ particles during the leaching process. The pore structures of the resultant open cell aluminum foam with spherical pores were characterized in the present study. The results showed that the number of opening pores between the cells increased significantly after the wetting treatment of the space holders, which resulted in the higher degree of pore opening and porosity of the resultant aluminum foam.

14:50-15:10

The Heterogeneous Nucleation of Al Alloy on MgO and $MgAl_2O_4$ Substrates

Lin Yang, Lu Wang, Jiangsu University of Technology, China

Grain refinement using oxide addition is commercially feasible and eco-friendly. The manufacturing process involves combining two or more compounds in both the solid and liquid phase. The solidification of alloy on oxide substrates MgO and $MgAl_2O_4$ has been studied in terms of the chemistry and mechanics of wetting, the influence of particles size on nucleation, the growth and lattice distortion of the alloys with other element reinforcements, and chemical reactions at the liquid/solid interfaces in this paper. MgO and $MgAl_2O_4$ have the similar lattice structure and small lattice misfits with Al, both of them are common oxides of Al especially Al-Mg alloys. However, the substrates can be effective nucleation cores only when they are micron-size and homogeneous bulk distribution. Orientation relationship of endogenous oxide films and Al have been determined by high resolution transmission electron microscopy (HRTEM). The film can be broken into dispersed particles with external mechanical forces, such as shearing or ultrasonication. The particles were identified in grain boundaries and interdendritic regions and enhanced further grain refinement as effective heterogeneous nucleation core. Relatively, the substrates have low nucleation ability and easy to form alumina which hinder nucleation when the substrates were not endogenous but additional. The thickness of alumina reacted at the interface is determined by temperature and heating duration. In this situation, interfacial tuning through addition of alloying elements such as Mg, Ti or Cu, is an effective way to improve nucleation ability of the substrates. On the one hand, alloying elements can be effective surfactant to liquid aluminum, which has a high concentration at the surface of liquid alloys by the work of adhesion and can reduce the interface energy to assist nucleation. And on the other hand, a solid-solution effect of alloying elements on lattice distortion of Al matrix is another origin for enhancing nucleation efficiency through reducing the interface lattice mismatch.

15:10-15:30

Nano Metallurgy: Thermodynamics-based Predictive Fabrication of Functional Nanomaterials

Young-Chang Joo, Wonhyo Joo, Jiyong Kim, Seoul National Universrtiy, Korea

Through the development of computational materials science including 'Materials Genome Projects,' there have been many progresses in predicting what to make for the best performance. However, the key challenge still remains in how to make it. We have demonstrated that such challenge could be achieved through applying thermodynamics into nanoscale functional materials, so called "predictive fabrication." Inspired by well-developed and widely used principle which mankind has used to refine metals from the ore, extractive metallurgy, we developed a new approach to the synthesis for nanomaterials. A new nanomaterials fabrication technology for efficient structure and phase control of the functional materials via gas-solid reactions has developed. Diversely structured metal compound nanomaterials can be fabricated by modulating redox reactions during the calcination through thermodynamics and kinetics prediction. From the understanding of how the redox reactions between elements, we could make precisely controlled nanostructures from pure metal to oxide, nitride and sulfides. This work can open a new standard synthetic route which enables the fabrication of various nanostructures for wide applications such as batteries, catalysts, and sensors. As a demonstration, Cu_2O nanofibers for CO_2 reduction catalyst are discussed. Bandgap difference according to the oxidation states of Cu oxide determines the performance of water splitting and CO_2 reduction in aqueous media. The oxidation path designed calcination can successfully make mono-phase Cu_2O nanofibers, which produced methanol with high Faradic efficiency over 90%. Furthermore, with these rationales, we successfully fabricated NiP_2 embedded in carbon nanofibers, using successive oxygen partial pressure controlled carbonization for structure refinement and phosphorus partial pressure controlled phosphidation for target phase. Furthermore, using the thermodynamics of defect formation by gas-solid reaction, we can make highly sulfur-deficient MoS_2 in carbon nanofiber system and induce polymorphic transition of $2H^-$ to 1T-MoS_2. We believe that this approach can provide a rational direction to fabricating reliable & functional nano-materials from earth abundant elements.

15:30-16:10 Tea Break

16:10-16:30

Preparation of AlMg35-TiH_2 Composite Foaming Agent for Small Pore size Aluminum Foam Fabrication

Xu Zhou, Yanxiang Li, Ying Cheng, Xiang Chen, Lei Hu, Guangzhao Yuan, Tsinghua University, China

In the liquid state processing of aluminum foams, titanium hydride (TiH_2) is added (typically1.6wt%) to aluminum melt and serves as a blowing agent by

releasing hydrogen gas in the hot viscous liquid. In fact, hydrogen release from TiH_2 starts around 400˚C, early decomposing and poor dispersing of foaming agent always make troubles, and it is difficult to disperse small TiH_2 particles. The porosity of aluminum foams produced this way ranges from 67% to 89%, corresponding to densities between 0.30g/cm^3 and 0.89g/cm^3, with an average pore size ranging from 2 to 10mm. In this study, in order to obtain small pore foam structure, an AlMg35-TiH_2 composite foaming agent was prepared by the method of liquid dispersion. The composite foaming agent was fabricated by pre-dispersing the blowing agent (oxidizing treated TiH_2) into a low melting point master alloy (AlMg35) melt. Microscopic distribution and composition of the foaming agent in the preparation process was explored, and the suitable dispersing parameters were obtained. Aluminum foams, with better porous structure uniformity and good process controllability, were manufactured. The foam structure showed a good fine cell size distribution. Pore size ranges from 0mm to 4mm, compressive strength reaches 36MPa and energy absorption ability reaches 20MJ/m^3.

16:30-16:50

Sub-Micron Sized Bare FeCo Single Crystalline Alloy Powder Prepared by Induction Thermal Plasma

Hirayama Yusuke, Takagi Kenta, National Institute of Advanced Industrial Science and Technology, China

The induction thermal plasma process is one of the promising bottom-up processes for the preparation of submicron-sized powder, especially for the metals and ceramics with high melting/boiling temperature. In the case of oxidizable metals, however, the usage of this process is limited because of the difficulty to handle the fine metal powder in the air. Recently, we developed a new set up to prepare the submicron-sized bare metal powder using low oxygen induction thermal plasma (LO-ITP) system. In this work, we focus on the magnetic material of binary FeCo alloy since magnetic properties are sensitive to the surface oxidation and prepared "bare" fine binary alloy of Fe-Co system by the LO-ITP system and evaluate the particle size, the distribution of the composition of Fe and Co and their magnetic properties.

The ITP of TP-40020NPS (JEOL Co., Ltd.) and the powder feeding system of TP-99010FDR (JEOL Co., Ltd.) were used. The power of the RF generator is 6 kW with 13.56MHz. We used two kinds of powders with the following characteristics: particle size of ~3 micron, purity 99.9% for Fe and particle size of ~5 micron, purity 99% for Co. These powders were mixed in the atomic ratio of Fe : Co = 1-x : x (x = 0, 0.3 and 0.5) and then used as starting powders. For thermal plasma process, the process pressure of 100kPa was used. The feed rate of the powder is ~ 0.3g/min. A G1 grade argon gas was used as a plasma and carrier gas and their flow rate were 35 and 3L/min., respectively. Then, the processed powder was collected from the wall of the main chamber. Since the metal fine particle is easily oxidized, the powder collecting atmosphere of oxygen level below 0.5ppm and due point below -80˚C was controlled. Moreover, XRD and SEM were carried out without atmospheric exposer.

The particle diameters of processed FexCo1-x were around 100nm, which is estimated by SEM images. There are no unprocessed particles since only peaks from BCC structure were found in XRD profiles for x = 0.1, 0.3 and 0.5 samples, and note that no oxide signal was detected from all XRD profiles. The calculated lattice parameter is started at 0.2868 nm for Fe, reached a peak of 0.2869nm at the composition of x = 0.1, and decreased thereafter as Co content increased. This behavior does not follow the Vegard raw, which is consistent with the behavior of the bulk Fe-Co. The saturation magnetization values are on the Slater-Pauling curve, indicating that the distribution of the composition is narrow and also the oxide layer of the Fe1-xCox surface is thin enough not to influence on the magnetization. Therefore, the bare Fe1-xCox alloys were obtained by the LO-ITP system successfully.

16:50-17:10

Novel Perovskite Materials with Excellent Dielectric Properties Obtained by Engineering in Twins, Domains, and Antiphase Boundaries

Huiqing Fan, Shenhui Lei, Northwestern Polytechnical University, China

With the widespread dielectric application, engineering of perovskite materials in microstructures, domains, twins, and antiphase boundaries (APBs) is attracting significant attention. However, the origin of the domains, especially in the paraelectric phase, as well as the mechanism of variation in twins or domains and their relationship are still not clear. Generally, these structures are recognized as one of the key origins of intrinsic loss. Our studies reveal that the formation of twins is closely related to the asymmetry of the crystal structure. With the introduction of a lattice blockage-trigonal $NdAlO_3$ phase, the increase in the symmetry of the $CaTiO_3$ tetragonal phase results in a transformation

from the (110)-oriented twins to the (111)-oriented twins. Then, it forms a new ordered structure. With the help of peak-differentiation and imitation of the Raman spectra, the A-site in the perovskite structure is found to be a dominant factor in lattice energy and performance. By designing an A-site displacement, i.e., Sr^{2+} or Ba^{2+} substitution into Ca^{2+} , we created a controllable structure of twins by symmetry regulation and APBs by introducing ferroelectric spontaneous polarization. Via selected area electron diffraction patterns (SAED) and variable temperature electric field piezoresponse force microscopy (PFM) images, we found that 180° and 90° domains could coexist in the grains of ceramics. Interestingly, the 90° domains and twin boundaries (TB) play more important roles in the anisotropic resistance to the electron/hole transfer. Our studies prove that the defect engineering can realize a controllable enhanced dielectric performance by defect regulation within the host lattice. These may pave a possible way for the design of the microstructure of the defects to achieve better predictable performances of the dielectric materials.

17:10-17:30

Mouldable Electro-Active Material based on Vitrimer

Zhen Li, Pengfei Wang, Qian Xuesen Laboratory of Space Technology, China

Dielectric elastomer (DE) is a class of smart material which can convert electric energy into large-scale shape deformation and output electric signal under mechanical stimuli. Due to such capabilities and other remarkable physical characteristics such as softness, lightweight, transparent and so on, DE have been proposed as a promising candidate material for the application of smart devices and soft robots.

So far, scientists have done a lot of work on physical model, material design and device fabrication of DE. However, there are still some limitations to its further application. Firstly, the chemical structure of DE is mostly cross-linking network, which makes their permanent shape cannot be changed after forming. Therefore, it can only perform deformation in the direction of its inherent geometry (usually thin film) under the electric field, such as elongation-shortening or expansion-contraction. More complex deformation, such as curling and bulging, are difficult to achieve. Secondly, devices usually exhibit special three-dimensional structures, which are difficult to achieve from one-step mould. Currently, most of the smart devices based on DE are based on plane pre-strain film. And the DE devices with complex structures, such as multilayer and pattern electrode coating, face the problem of slippage between DE layers and DE-electrode interface. Although the introduction of glue can enhance the adhesion strength, it will affect the mechanical behavior of the actuation. Recently, the appearance of the concept of glass-like polymer (Vitrimer) has made it possible to realize the plasticity of covalent-crosslinking thermoset networks. This class of materials consist of dynamic chemical bonds, which can be rearranged at a certain temperature, so that the materials can be re-moulded, welded and repaired. More importantly, Vitrimer can maintain stable cross-linking structure at high temperature without melt down, which allows the post- Assembly of the material into complex structure. Due to this advantage, Vitrimer is attracting more and more research interests and become to be applied in the field of smart materials. However, till mow there are no research which apply Vitrimer into DEs.

In this paper, we prepared a DE Vitrimer material, which combines both the advantages of Vitrimer and DE material. The dynamic covalent Silicone-oxygen bond was introduced into a silicone rubber based DE materials. The resultant material performs some new characteristics, which may be beneficial for practical application. Firstly, this material can be easily prepared into film via simply hot pressing and the thickness can be accurately controlled by thin metal mold. The thickness from 100μm to 2mm were achieved. The resultant film can bear over 500% strain and perform deformation under electro-stimuli. Moreover, benefit from the dynamic covalent bond, the materials can be easily welded, which makes it possible to assemble materials with different composition together. In this way, several kinds of 3D structure were achieved. Instead of plane expansion-contraction, a raise and lay actuation were demonstrated. Furthermore, the dynamic covalent bonds allow the resultant materials to be repaired and recycled. The experiment results showed that the crack of the damage can be healed in 10min with 90 heating, and the material that broken into pieces can be recycled by hot pressing for 3 times without the change of mechanical properties.

In summary, we design and prepare a Vitrimer based DE material. This material consists of dynamic covalent bonds and are re-mouldable, weldable, repairable and recyclable. Three dimensional can be achieved by the assembly of materials. This approach can be extended to lots of other DEs, which offers new possibilities in future applications of DEs.

F. Biomaterials: Interface

Symposium Organizers :

Yufeng Zheng, Peking University, China; Luning Wang, University of Science and Technology Beijing, China; Takayoshi Nakano, Osaka University, Japan; Seung-Kyun Kang, Korea Advanced Institute of Science and Technology (KAIST), Korea; Cuie Wen, RMIT University, Australia; Marc Meyers, University of California, San Diego, USA

Wednesday PM
August 21, 2019

Room: 306(3rd Floor)
Symposium: F

Chairs:
Nicolas Voelcker, Monash Institute of Pharmaceutical Sciences, Australia
Poyu Chen, National Tsing Hua University, China

13:30-14:00 Keynote

Ordered Silicon Nanowire Arrays: Opportunities for Biointerface Control

Nicolas Voelcker, Monash Institute of Pharmaceutical Sciences, Australia

Engineered cell–nanostructured interfaces driven by vertically aligned silicon nanowire (VA-SiNW) arrays have become a promising platform for orchestrating key cell function, behaviour, and fate conversion. The key advantage of ordered VA-SiNW arrays lies in their enhanced interaction at the interface between cells and NWs due to their nanoscale dimension, enabling the bidirectional informational flow – biochemical/biophysical signals from or to the intracellular environment. The NW–cell interface open possibilities for implementing applications in biological applications such controlling cell behaviour or gene delivery. We have recently developed a suite of low-cost and easily implemented methodologies to fabricate VA-SiNW arrays with adaptable and programmable designs. Our study has the goal: to establish NW-mediated gene delivery that may ultimately have implications for therapeutic approaches. This talk will present the materials science approaches underpinning the generation of VA-SiNW arrays using a range of lithography and micro/nanofabrication tools. The talk will also present results in relation to delivery of DNA plasmids, siRNA and proteins into cells and characterise the interface between the nanowires and the cellular sub-structures using electron microscopy and confocal microscopy techniques. Finally, the talk will highlight gene delivery applications for example in relation to the generation of CAR T cells and genetic modification of hard-to-transfect stem cells.

14:00-14:25 Invited

Lightweight Yet Tough Bio-Inspired Cellular Materials: Multi-Scale Modeling, Characterization, Mechanical Testing, and Optimization

Poyu Chen, Chengche Tung, National Tsing Hua University, Taiwan, China

Cellular structures provide lightweight, high material usage efficiency, specific strength, toughness and energy absorption capability and are widely adopted in Nature. The mechanical properties of natural cellular materials are often optimized by apposite porous arrangements and wall designs. In this study, several bio-inspired cellular structures were investigated by multi-scale structural characterization, mechanical testing, modeling and optimization. Voronoi tessellation, often appears in cells and bone microstructure generation modeling, was used to partition a plane into several pores after the distribution of pore centers were calculated. The Fibonacci sequence divides planes or spaces regularly, often found in nature such as sunflowers, pinecones, etc. The Poisson-disc sampling mimics cells growth distribution in two-dimensional plane. The hexagon model is proposed to tile the plane in highly symmetric situation. The regular model and Monte Carlo sampling correspond to a completely regular and completely random distribution models. The porosity variance of specimens was controlled by changing the distribution and quantity of the porous. A series of polymer-based specimens were produced by additive manufacturing. The numerical models were systematically simulated to verify the stress-strain behaviors under tensile and compressive tests. The lattice spring model was used to simulate micro-cracks generation and propagation. We found when the porosity was kept at 40%, the Poisson-disc and the Fibonacci sequence samples have higher elongation at fracture (20% enhancement), ultimate tensile strength (15% enhancement), and toughness (35% enhancement) than other models. Toughening mechanisms such as crack deflection/tortuosity and uncrack ligament bridging were observed and validated. This research proposes a feasible analysis of lightweight structures and developed bio-inspired structural materials that can be potentially applied to structural engineering, civil engineering, and aerospace technology.

14:25-14:50 Invited

2D Patterning of Cells on Titanium Dioxide by Light Irradiation

Masato Ueda, Masahiko Ikeda, Kansai University , Japan

Several techniques have been employed to attach/detach cells to/from a substrate. Cells cultured on a substrate are generally detached from the substrate into a sheet

by the destruction of protein between the cells and the substrate using enzymes. However, it also damages the adhesion molecules among the cells. Titanium dioxide (TiO_2) is an n-type semiconductor with an energy band gap of 3.2eV, which displays a photocatalytic activity under UV. The purpose of this work was to fabricate photo-responsive cell culture vessel using TiO_2 film and to investigate adhesion behaviour of cells on it.

TiO_2 films were prepared on SiO_2 plates by a sol-gel method using titanium tetraisopropoxide, or a conventional RF sputtering using pure Ti target. Primary osteoblasts were seeded on the vessels and then incubated at 37˚c. During the incubation, UV irradiation was performed previously or continuously from back-side of the vessels.

Colourless and transparent films could be uniformly synthesised on SiO_2 plates by the present methods. The film showed high transparency in the visible range of 400~800nm. However, the UV light was completely absorbed by the TiO_2 thin layer. It is attributed to a fundamental absorption in semiconductor of TiO_2 with an energy band gap of 3.0~3.2eV. Basically the number of cells monotonically increased with incubation periods under darkness. Previous light irradiation promoted the cell adhesion on the surface. The formation of Ti-OH groups on the TiO_2 seems to be facilitated by the UV irradiation. In contrast, the cells decreased under continuous light irradiation. The cells were not exposed to UV in the vessels as mentioned above. It might be due to generated photocurrent or hydroxyl radicals on the TiO_2 surface. These results imply that the adhesion/proliferation/detachment behaviours of cells can be controlled by the photocatalytic reaction of TiO_2 and the irradiation patterns.

14:50-15:10

The Use of Biocompatibility Assessment Techniques in the Development of Novel Biomaterials: Strengths, Limitations, and Common Pitfalls

Arne Biesiekierski, Yuncang Li, Cuie Wen, RMIT University , Australia

The development of novel biomaterials, devices and structures is a complex and multidisciplinary field, driven by numerous intersecting and competing requirements. It is dominated most notably by achieving a combination of satisfactory structural performance while simultaneously optimising the biological suitability of the biomaterial. Unfortunately, these constitute two widely differing skillsets, that of the materials scientist, and the physiologist. While it may be tempting for a nascent biomaterials scientist to focus first on their specialty, working sequentially (e.g. to create satisfactory structural properties and only then considering biocompatibility) risks unforeseen issues leading to wasted time, funds and effort.

As such, it is necessary for a materials scientist in the biomaterials field to be able to critically examine existing literature regarding the biocompatibility of the prospective biomaterial, and to assess the physiological response in a preliminary manner throughout the development process. Still further, one must be able to correctly interpret and report these findings. Therefore, it is incumbent on this scientist to be familiar with common methods for assessing the physiological response, and to understand the specifics of what these assays report. To this end, this talk will summarise a published review of common preliminary toxicological assays, and highlight the strengths and limitations of the information obtained therefrom. In particular, this talk will be targeted towards those coming from materials engineering, rather than bioscience, backgrounds.

15:10-15:30

Study on the Toughening Mechanisms of Collagenous Materials by Using Real-Time X-Ray Characterization and Imaging

Wen Yang, University of California, San Diego, America / Lawrence Berkeley National Laboratory, America; Haocheng Quan, Marc Meyers, University of California, San Diego, America; Eric Schaible, Lawrence Berkeley National Laboratory, America; Robert Ritchie, Lawrence Berkeley National Laboratory, America / University of California, Berkeley, America

Nature designs organisms using primarily minerals and proteins as the structural components. Collagen is the most common protein for nature to architect the structures for diverse functions; among these architectures, there are a wide of variety of hierarchical designs with different toughening mechanisms. In this work, the toughening mechanisms and the illustration on how nature uses the hierarchical structures to give different functions to the organisms from nano-, micro- to macro-levels are studied by using the real-time small angle X-ray scattering and structural imaging on non-mineralized collagenous materials – skin, mineralized collagen materials - arapaima, carp and the "living fossil" coelacanth fish scales. Detailed analysis will be discussed in the presentation according to the various complicated hierarchical structures of biological collagenous materials. The deformation of skin in terms of four mechanisms of collagen fibril activity under tensile loading virtually eliminates the possibility of tearing in pre-notched samples: fibril straightening, fibril reorientation towards the tensile direction, elastic stretching and interfibrillar sliding, all of which contribute to the redistribution of the stresses at the notch tip; the Bouligand-type structure in arapaima and carp fish scales allows the lamellae to reorient in response to

the loading environment; remarkably, most lamellae reorient towards the tensile axis and deform in tension through stretching/sliding mechanisms, whereas other lamellae sympathetically rotate away from the tensile axis and compress, thereby enhancing the scale's ductility and toughness to prevent fracture; distinct from the Bouligand structure of elasmoid scales, the collagen fibrils in double Bouligand structure of the coelacanth fish scales form bundles which are embedded in a matrix comprising fibers arranged perpendicular to the layered structure that provide added rigidity and resistance to deformation. The hierarchical structural assemble information as well as the toughening mechanisms are provided to artificial processing and engineering.
Nature designs organisms using primarily minerals and proteins as the structural components. Collagen is the most common protein for nature to architect the structures for diverse functions; among these architectures, there are a wide of variety of hierarchical designs with different toughening mechanisms. In this work, the toughening mechanisms and the illustration on how nature uses the hierarchical structures to give different functions to the organisms from nano-, micro- to macro-levels are studied by using the real-time small angle x-ray scattering and structural imaging on non-mineralized collagenous materials – skin, mineralized collagen materials - arapaima, carp and the "living fossil" coelacanth fish scales. Detailed analysis will be discussed in the presentation according to the various complicated hierarchical structures of biological collagenous materials. The deformation of skin in terms of four mechanisms of collagen fibril activity under tensile loading virtually eliminates the possibility of tearing in pre-notched samples: fibril straightening, fibril reorientation towards the tensile direction, elastic stretching and interfibrillar sliding, all of which contribute to the redistribution of the stresses at the notch tip; the Bouligand-type structure in arapaima and carp fish scales allows the lamellae to reorient in response to the loading environment; remarkably, most lamellae reorient towards the tensile axis and deform in tension through stretching/sliding mechanisms, whereas other lamellae sympathetically rotate away from the tensile axis and compress, thereby enhancing the scale's ductility and toughness to prevent fracture; distinct from the Bouligand structure of elasmoid scales, the collagen fibrils in double Bouligand structure of the coelacanth fish scales form bundles which are embedded in a matrix comprising fibers arranged perpendicular to the layered structure that provide added rigidity and resistance to deformation. The hierarchical structural assemble information as well as the toughening mechanisms are provided to artificial processing and engineering.

15:30-16:10 Tea Break

16:10-16:45 Invited

The Interplay between Cells and Multiscale 3D Printed Scaffolds

Cynthia S. Wong, David Forrestal, Naomi C. Paxton, Matthew Lanaro, Maria A. Woodruff, Queensland University of Technology, Australia

Scaffold fabrication for biomedical applications has evolved significantly in the last decade and with increased understanding of the interaction between cells and scaffold designs, its development has progressed even further. The ability to create nanostructures resembling extracellular matrix of tissues to enhance cell attachment and proliferation has been made possible with fabrication techniques such as electrospinning. The advancement of additive manufacturing techniques (3D printing) has enabled scaffolds with complex geometry to be manufactured so that the fabrication of scaffolds can now be patient-specific. Melt electrowriting is a manufacturing technique that combines electrospinning and 3D printing to produce scaffolds with micron-sized fibres and highly accurate and ordered microstructures. The ability to control the deposition of fibres with great precision allows for the production of scaffolds with customised mechanical properties as well as those with complex structures. Additionally, the incorporation of biomolecules can be strategically placed within the scaffolds to impart biological functions such as enhanced cell proliferation and/or controlled release of growth factors and antibacterial agents. While the microstructures of scaffolds play a role in cell behaviour, in order for these scaffolds to be applicable for biomedical use, there is a need to scale up the size of the scaffolds. However, cell growth in large scaffolds using the standard culture methods are met with limitations such as restricted nutrient and gas exchange, which present with adverse effects for the cells. Our group has created a system that is designed specifically for growing cells on large scaffolds with complex human anatomical structures. This talk will present work that demonstrates the influence of scaffold designs on cell behaviour on both small and large scale, and the potential of using these scaffolds for cardiovascular and bone regeneration applications.

16:45-17:10 Invited

Modelling Bone Fracture Healing under the Locking Compression Plate System

Lihai Zhang, The University of Melbourne, Australia

Osteoporotic fractures lead to chronic pain, disability, loss of independence and even premature death. The total cost of fracture management in community health programs, aids and appliances, and indirect costs, such as lost earnings, is projected to rise to US$131 billion worldwide by 2050. The stiffness of a fracture fixation

construct, such as the locking compression plate (LCP) system, has to be increased as osteoporosis decreases the mechanical properties of bone. However, an overly stiff fixation construct may lead to impaired micromotion at the fracture site which inhibits callus formation, which may lead to potential delayed healing or non-union. To date the influnce of the flexibity of LCP on healing outcomes has not yet been fully understood and clinical evidence is still lacking. The focus of this research is to investigate the influence of the mechanical stiffness of fixation on bone healing. Our results show that the stiffness of locking plate fixations can be modulated by plate type (i.e. plate size and material) as well as configuration of locking plate fixation [bone-plate distances (BPD), and the increase of BPD could result in a more uniform IFM could be achieved across the fracture gap resulting in enhanced callus formation and better healing outcomes.

17:10-17:30

High Strength and High Ductility in a Biomedical Co-20Cr-15W-10Ni Alloy Having Bimodal Grain Structure Achieved by Static Recrystallization

Chenglin Li, Wuhan University, China / Korea Institute of Materials Science, Korea; Chan Hee Park, Jong-Taek Yoem, Korea Institute of Materials Science, Korea; Qingsong Mei, Wuhan University, China

Co–Cr-based alloys have been extensively used as implant materials in dentistry, orthopedics, and cardiology owing to their biological/mechanical compatibility and excellent corrosion resistance. In particular, Co-20Cr-15W-10Ni (also known as L-605, Haynes 25, or ASTM F90) is of particular interest for stent applications where both a high strength and high ductility are important to enable thinner wall design and higher fatigue life and to improve stent deliverability and expandability. The strength–ductility behavior of a metallic material strongly depends on the average grain size and, grain size distribution as well. Generally, a fine-grained structure enhances the strength by the Hall–Petch relation but limits the ductility, whereas the coarse-grained structure improves the ductility but reduces the strength. One effective approach for overcoming this strength–ductility trade-off is to produce heterogeneous structures such as heterogeneous lamella structure, gradient grains, or grains containing different density/types of crystal defects or grain size distributions.
In this study, two kinds of bimodal structures were tailored in a biomedical Co-20Cr-15W-10Ni alloy via medium cold rolling (area reduction of 50%) followed by short-term annealing (15min) at temperatures of 800~1100˚C. The medium cold rolling induced a heterogeneous microstructure featuring the coexistence of severely deformed regions and weakly deformed domains. With short-term annealing at low temperatures (800~900˚C), recrystallization preferentially occurred in the severely deformed domains, which resulted in a partially recrystallized structure consisting of recovered grains with high-density dislocations and recrystallized grains free of dislocations. At higher temperatures (950~1100˚C), however, fine and coarse grains were preferentially recrystallized in severely deformed regions and weakly deformed domains, respectively, resulting in a bimodal grain structure that consisted of fine grains (~1~2μm) and coarse grains (~10~20μm). The first one obtained at 800~900˚C resulted in super high strength (ultimate tensile strength of 1315~1550MPa and yield strength of 888~1245MPa) and lower ductility (total elongation of 13%~40%). However, the second one obtained at 950~1100˚C provided a well-balanced strength–ductility behavior with an ultimate tensile strength of 1200~1300MPa, a yield strength of 700~800MPa, and an elongation to fracture of ~40%~60%, making the alloy suitable for surgical implant and stent applications where the strength and ductility are both important to ensure mechanical reliability in a human body.

G. Smart and Magnetic Materials: Shape Memory Materials

Symposium Organizers :

Shaoxiong Zhou, Center Iron & Steel Research Institute, China; Chengbao Jiang, Beihang University, China; Satoshi Sugimoto, Tohoku University, Japan; Haein Yim, Sookmyung Women's University, Korea; Sean Li, New South Wales, Australia; Bob Shull, National Institute of Standards and Technology, USA

Wednesday PM Room: Yulan Hall-220 (2nd Floor)
August 21, 2019 Symposium: G

Chairs:
Fengxia Hu, Institute of Physics, Chinese Academy of Sciences, China
Jia Yan Law, Sevilla University, USA

13:30-14:00 Keynote

Confined Martensitic Transformation and Related Anomalous Functional Behavior

Yandong Wang, University of Science and Technology Beijing, China

Recently a kind of new type martensitic transformation called as confined martensitic transformation (CMT) in shape memory alloys with the transformation kinetics obviously different from that found in traditional martensitic transformation (TMT) has been experimentally evidenced. For the TMT, the collective motion of martensitic variants controls the transformation kinetics, while both nucleation and growth of martensite

is confined for the materials subjected to the CMT due to the nano-scale heterogeneity in the distribution of chemical elements or crystal ordering. This talk will summarize our new experimental findings on new functional behaviors in some shape memory alloys exhibiting CMT and in-situ experimental investigations on evolution of the complex crystallographic structures and transformation kinetics by the high-energy X-ray and neutron diffraction techniques. The in-depth understanding of the new physical mechanisms on CMT and superelastic behavior in the above-mentioned interesting alloy systems will be also presented.

14:00-14:25 Invited

Broadening Refrigeration Temperature Regions in Ferromagnetic Shape Memory Alloys

Dunhui Wang, Nanjing University, China

Magnetic refrigeration based on magnetocaloric effect has attracted more and more attention since it is environmentally friendly and possesses higher cooling efficiency. Consequently, it is regarded as the most promising candidate to replace traditional vapor-compressing refrigeration technology. Many of Ni-Mn based ferromagnetic shape memory alloys exhibit large magnetocaloric effects, but their refrigeration temperature regions are usually in a limited scale due to the narrow magnetic phase transition regions, which has been a key drawback for the practical applications. In this work, we will demonstrate some alternative methods to broaden the magnetic refrigeration temperature regions. First, we fabricate a laminated structure consisting of a Ni-Mn-Co-In ribbon and a piezoelectric substrate (1-x) Pb(Mg1/3Nb2/3)O3-xPbTiO3 (PMN-PT). Since the martensitic transformation is very sensitive to the stress, by using the electric-field-induced stress of PMN-PT, the magnetic phase transition of Ni-Mn-Co-In alloy can be shifted. As a result, a broadened refrigeration temperature region is obtained. One the other hand, the multiferroic Ni-Mn-Ga alloys can show magnetocaloric effect and elastocaloric effect simultaneously. Since the working temperature regions of these caloric effects are adjacent, by combining the magnetocaloric effect and elastocaloric effect, a wide refrigeration temperature region with more than 100K can be realized in the Ni-Mn-Ga alloy.

14:25-14:50 Invited

Magnetic-Field-Induced Austenitic Transformation and Large Reversible Magnetostrain Effect

Jingmin Wang, Qijia Yu, Hui Hua, Chengbao Jiang, Huibin Xu, Beihang University, China

In recent years magnetic shape memory alloys featured by large magnetostrain effect have attracted as excellent smart materials potentially used in sensors, actuators and harvesters. At early development stage of magnetic shape memory alloys the large magnetostrain over 10% can be produced by magnetic-field-induced twin variants reorientation, but the magnetostrain is irreversible and the output stress is only 1~2MPa. Later, it was reported that large magnetostrain with output stress over 100MPa could be realized by magnetic-field-induced phase transformation. However, up to date the reported reversible magnetostrain is less than 0.5%, which is much lower than the theoretical value of about 6%. Recently based on the typical NiMnGa alloys we have developed Ni(CuCo)MnGa alloys. By tailoring the phase transition sequence and magnetism, the magnetostructural transition from paramagnetic martensite to ferromagnetic austenite was realized. The magnetization change across the transition is up to 100emu/g. Thus reversible magnetic-field-induced austenitic transition was realizedover wide composition range and wide temperature window. Further, we have investigated the magnetostrain effect of the magnetic-field-induced austenitic transformation. By tailoring the twining microstructure, preferential orientation of twin variants was realized during the magnetic-field-induced austenitic transformation. Large reversible magnetostrain was obtained. The associated mechanism was also discussed by checking the microstructure.

14:50-15:10

Driving Remarkable Metamagnetism in a Metallic Helical Antiferromagnet

Shengcan Ma, Kai Liu, Xiaohua Luo, Changcai Chen, Zhenchen Zhong, Jiangxi University of Science and Technology, China

The MnNiGe-based compounds have attracted increasing interest due to the excellent magneto-functional properties across the martensitically magnetostructural transformation (MMST) from paramagnetic (PM) austenite to ferromagnetic (FM) martensite. The key to achieve this MMST is the antiferromagnetic (AFM)-FM conversion in TiNiSi-type martensite, which is just realized by the Fe/Co substitution to date. Here, the AFM-FM conversion and accordingly a striking magnetic-field-driven MMST is achieved in the Ni-substituted and especially Mn-substituted MnNiGe alloys upon indium, a non-magnetic and large-sized main group element. Resultantly, a giant magnetocaloric effect such that a twofold increase of the magnetic entropy change in MnNi0.92GeIn0.08 (~29Jkg^{-1}K^{-1}) and even almost threefold increase in Mn0.92NiGeIn0.08 (~38Jkg^{-1}K^{-1}) alloy due to the more remarkable metamagnetism is obtained with respect to Ge-substituted alloy (~15Jkg^{-1}K^{-1}) under the field change $\mu_0\Delta H$=0~8.5T. The Mn moment and interatomic distance, especially the nearest and next-nearest Mn-Mn separation, are calculated and

analyzed from the first-principles calculations and X-ray absorption spectroscopic measurements. The strong magnetoelastic coupling should be responsible for the internal establishment of FM order and resultantly striking metamagnetism, and further the enhanced magnetocaloric effect in Ni- and particularly Mn-substituted compounds upon indium.

15:10-15:30

Investigation on Porous Magnetic Shape Memory Alloys Fabricated Using Sintering Method

Ping Gao, Bing Tian, Yunxiang Tong, Feng Chen, Li Li, Harbin Engineering University, China

Magnetic shape memory alloys (MSMAs) have attached much attention due to the large reversible magnetic-field-induced strain (MFIS). Ni–Mn–Ga MSMA single crystals display MFIS of up to 10%. But the preparation of single crystalline Ni-Mn-Ga alloy is difficult and high cost. Polycrystalline materials are much easier to be prepared but display a small MFIS because twinning of neighboring grains introduces strain incompatibility. It has been reported that introducing pores in polycrystalline Ni–Mn–Ga alloy by casting replication technique reduce these strain incompatibilities between grains and thus increase the MFIS. After proper training (thermo-magneto-mechanical cycling) porous Ni–Mn–Ga alloy exhibits MFIS as high as 8.7%. However, the casting replication preparation process is complicated, and the molding temperature is high (>1200˚c) due to that the alloy needs to be melted and pressed into the preform. In addition, the process of pickling to remove the preform corrode the magnetic memory alloy to varying degrees, and the ultrasonic vibration can easily cause many fine microcracks in the alloy, which will adversely affect the stability of the alloy properties.
Here, we reported a relatively simple approach to prepare porous Ni-Mn-Ga and Ni-Co-Mn-In alloys by powder sintering from a mixture of ball milled Ni-Mn-Ga (Ni-Co-Mn-In) particles and gas atomized Mg powders (50/50vol% and 60/40vol%). Ni-Mn-Ga and Ni-Co-Mn-In samples were sintered at 900˚c and 850˚c, respectively. The Mg was removed during sintering to reveal a porous skeleton of the alloys. The pore distribution of Ni-Mn-Ga alloys was relatively uniform, but the pore size was different. Black holes, dark gray parts and white matrix were observed in the SEM photograph. EDS analysis showed that the dark gray parts were Ni-Mn-Ga particles with less Mg element, the white matrix was the interfacial reaction products of Ni-Mn-Ga and Mg particles. The microstructure of Ni-Co-Mn-In porous alloys was roughly the same as that of Ni-Mn-Ga. The 50vol% alloys had more dark gray parts than the 60vol% alloys. 50vol% Ni-Mn-Ga porous alloy exhibited a certain martensitic transformation and curie transformation behavior, but they were weaker than the phase transformation of Ni-Mn-Ga powder. The phase transformation of 60vol% Ni-Mn-Ga, 50vol% Ni-Co-Mn-In and 60vol% Ni-Co-Mn-In porous alloys was not observed. The occurrence of severe interfacial reaction could lead to weakening or even disappearing of the phase transformation. With the increase of the MSMA particles content, the compression mechanical properties of porous alloys were enhanced. However, the fracture stress of all porous alloys were all under 60MPa due to the introduction of pores.

15:30-16:10 Tea Break

16:10-16:35 Invited

Generating Large Elastic Strains in Functional Metallic Thin Films by a Phase Transforming Substrate

Hong Yang, Fakhrodin Motazedian, Junsong Zhang, The University of Western Australia, Australia; Daqiang Jiang, Lisan Cui, Yinong Liu, China University of Petroleum Beijing, China; Zhigang Wu, Guangzhou University, China

Elastic strain engineering is a novel concept that utilizes elastic strains to create, modify or enhance the physical and chemical properties of functional materials. However, in conventional solids the elastic strains are typically limited to <0.5% and it is challenging to generate large enough elastic strains in solids to have significant effects on these properties. This study presents a novel 'thin film on substrate' system that is capable of inducing large elastic strains in thin films well beyond what may be achieved in conventional materials. This is achieved by using a 'martensitic phase transforming substrate' which upon deformation produces a uniform lattice distortion via a diffusionless crystallographic phase transformation. This uniform lattice distortion can induce large elastic strains in the functional thin film atop the substrate following a principle known as 'lattice strain matching'.
In this work, we used a NiTi shape memory alloy substrate, which is capable of producing large pseudo-elastic strains of 6%~8% via its martensitic phase transformation. Two deformation modes of the substrate were utilized to investigate the strain transfer behaviour from the substrate to the thin film. Mode-1 utilizes the stress induced martensitic transformation of the NiTi to induce a large tensile strain in the thin film deposited on it. Mode-2 utilizes the martensitic reorientation of the NiTi to generate elastic strain in the thin film.
Using this system we are able to induce large elastic stains in metallic thin films. This talk presents experimental results of Nb thin film on NiTi substrate, which has shown to achieve a tensile elastic strain of greater than 5%.
In addition, this talk also presents a new method we have

developed to determine the stress/strain state of thin film on substrate using combined XRD data obtained from both Bragg-Brentano and asymmetrical x-ray diffraction configurations. This method eliminates the need to have specialized XRD facilities such as polycapillary lens and tilting sample stage in order to determine stress/strain of thin film samples by XRD measurements.

16:35-16:55

Research on Abnormal Thermal Expansion and Correlated Magnetic Properties of Antiperovskite Mn_3XN Compounds

Ying Sun, Cong Wang, Beihang University, China

Antiperovskite structured Mn_3XN (X=Ga, Zn, Cu, Sn, etc.) have attracted great attentions due to their rich physical properties and important applications, such as negative thermal expansion(NTE), giant magnetoresistance, near zero temperature coefficient of resistance, and so on. Associated crystallographic and magnetic properties of the materials are highly intriguing in connection with mutual interactions among those freedom of lattice, spin, and charge. The band structure of Mn_3XN is significantly mediated by chemical bonding of MnN_6 octahedra, which forms a relatively narrow band. This probably results in rich varieties of electronic structure and physical properties of the materials because the conduction band of X highly overlaps with the narrow band.

In Mn_3XN, Γ5g AFM magnetic structure plays an important role in the near zero thermal expansion properties of Mn_3ZnN, Mn_3GaN, and Mn_3NiN. The mechanism will be discussed in detail about how to precisely control the zero thermal expansion of a single compound by achieving the special Γ5g magnetic phase of Mn atoms. In addition, the pressure effect of Γ5g AFM magnetic structure induced the baromagnetic effect in antiperovskite Mn3Ga0.95N0.94. The macroscopic baromagnetic effect is 0.63 μB (f. u.)$^{-1}$ at 130K by the hydrostatic pressure of 750MPa. In this work, neutron diffraction technique combined with Rietveld refinement to clarify the origin of the particular properties referred above, i.e. near zero thermal expansion, baromagnetic effect, and so on.

16:55-17:15

Spin Cluster Size Dependence of Exchange Bias Effect in Mn50Ni40Ga10 Heusler Alloys

Fanghua Tian, Yin Zhang, Jianing Li, Qizhong Zhao, Sen Yang, Xi'an Jiaotong University, China

The technique based on exchange bias effect is believed to play a significant role in next-generation spin-involved magnetic devices. However, 60 years after the discovery of the exchange bias, it remains unclear about origin and influencing factors of exchange bias. In this study, a giant exchange bias field of 5132 Oe was introduced in Mn50Ni40Ga10 Heusler alloys at 2K with a cooling field of 10kOe. Magnetic measurements showed that the giant exchange bias effect at lower temperature originates from the coupling between super spin glass and antiferromagnetic matrix. Different from previous reports, we elaborated on the issue of cooling field dependence from the perspective of size effect. The size effect was further demonstrated by calculating and comparing the relaxation time of super spin glass under different cooling fields. Although the relationship between particles sizes and relaxation time yet requires further validation, the current proposal can be applied to most exchange bias in Heusler systems. The EB is attributed to the exchange coupling between SSG and AFM matrix, since short-range ordered FM clusters are assumed to be formed in SSG during application of external field in cooling process. Critically, a size effect model, in which SSG clusters are tailored by external cooling magnetic field, serves as a supplement to dependence of cooling field on conventional EB effect, and additionally implies a novel approach to enhance EB.

H. Materials Characterisation and Evaluation: V

Symposium Organizers :

Zhiwei Shan, Xi'an Jiaotong University, China; Xiaodong Han, Beijing University of Technology, China; Satoshi Hata, Kyushu University, Japan; Ju-Young Kim, Ulsan Institute of Science and Technology (UNIST), Korea; Jin Zou, University of Queensland, Australia; Jennifer Carter, Case Western Reserve University, USA

Wednesday PM
August 21, 2019

Room: 308 (3rd Floor)
Symposium: H

Chairs:
Sam Yang, CSIRO, Australia
Akira Taniyama, Nippon Steel Corporation, Japan

13:30-14:00 Keynote

Advanced Material Characterization Techniques in Development of Steel Products-Current Topics and Future Anticipation in Industrial Application

Akira Taniyama, Advanced Technology Research Laboratories, Nippon Steel Corporation, Japan

Recent steel products have complex microstructure and chemical composition due to their high strengthening and high functionality. Therefore, material characterization with microstructure analysis techniques is one of important process in research and development of the

steel products to reveal and understand metallurgical phenomena in the products. Conventional techniques such as X-ray diffraction, SEM, and TEM have been widely used and have provided macroscopic and microscopic information about the crystal structure, the crystal orientation, the lattice defects, the precipitates, and segregation of the composition, in the steel products. Recently, advanced techniques such as synchrotron radiation and ultra-high resolution microscopy have been applied to reveal more detailed phenomena in sub-nano and atomic scale. Furthermore, advanced techniques such as in-situ observation and 3D characterization also has been required to understand dynamic behavior of the structural arrangement, of the shapes of defects such as voids and cracks, and of the crystallographic grain structure, in the steel products during production processes such as rolling and thermal treatment.
In this talk, internal structure analysis utilizing X-ray diffraction with synchrotron radiation, in-situ observation, and 3D characterization will be presented as examples of industrial application of advanced material characterization techniques. Additionally, future anticipations of new characterization techniques in industrial application will be discussed.

14:00-14:25 Invited

Quantum Characterization for Functional Materials Using High-Energy X-Ray Compton Scattering

Kosuke Suzuki, Gunma University, Japan

High-energy X-ray Compton scattering is a unique technique for characterizing the active species in functional materials in operando. The features of this technique are high-energy X-rays which have high-penetration power to the material are used. Hence, this technique allows non-destructive and bulk sensitive measurements. Moreover, a Compton scattered X-ray energy spectrum, so-called Compton profile, which directly links to the wavefunction of the electrons can be probed the orbital characters and occupations of chemically active electrons. In this talk, we present our recent studies for a VL2020 lithium rechargeable coin battery and cathode materials using high-energy X-ray Compton scattering technique which carried out at BL08W of SPring-8 of synchrotron facility in Japan.
In the studies of a VL2020 coin battery, we developed quantitation method of lithium from the change of Compton scattered X-ray energy spectrum and successfully obtained lithium concentration at cathode and anode during the charge-discharge cycle. Moreover, we revealed the dependency of the charge-discharge rate in lithium reaction distribution.
In the studies of cathode materials, we applied Compton scattering technique to cathode material of $Li_xMn_2O_4$ with $0.5 < x < 1.2$. By combining with first-principle calculation we clarify the active orbital involved in lithium insertion and extraction process is mainly the oxygen 2p orbital and Mn 3d electrons control structural stability of MnO_6 octahedral in the reduction-oxidation reaction mechanism of $Li_xMn_2O_4$ cathode materials.
The above demonstrations based on quantum mechanical approach paves the way for advanced characterization of the functional materials.

14:25-14:50 Invited

Application of EBSD on the Classification of Microconstituents in Advanced High-Strength Steels

Jun-Yun Kang, Seong-Jun Park, Korea Institute of Materials Science, Korea; Soon Woo Kwon, Minwoo Kang, Chung-an Lee, Seung-Hyun Hong, Hyundai Motor Group, Metallic Material Research Lab. Korea

Modern high-strength steel products are frequently designed to have multi-constituent (or phase) microstructures in order to meet demands for various properties as well as high strength. The constitution of microstructure, i.e. the fraction of microconstituents has a key influence on the properties and performances of these products. Therefore, phase discrimination and quantification should have a considerable contribution to the prediction of their properties and performances, and to the development of new products. However, there have been difficulties in the classification of the product phases by austenite decomposition. Conventional macro-diffraction techniques barely have ability to discriminate them due to their overlapping crystallographic characters, while microscopic image analysis by a human expert is much labor-intensive and lacks consistency.
The orientation mapping by electron backscatter diffraction (EBSD) has many benefits in this task, because it provides much richer features of microstructures which are morphologic as well as crystallographic than other conventional macro-diffraction or image-based techniques. In this study, traditional applications of EBSD to this task were reviewed and the feasibility of recent ones by machine learning approach were discussed for the application to an advanced high-strength steel sheet.
A hierarchical discrimination scheme which used various parameters from an EBSD mapping was designed and examined on the microstructure of ferrite-bainite matrix with austenite-martensite dispersion. This presented successful segmentation of the raw maps according to the microconstituents. Although this greatly reduced the inconveniences of the traditional image analysis, it still required some user-input values for the discriminants. Thus, inconsistency could not be resolved and this

can be significant when the phase contrast, especially between the matrix constituents were weak. A convolutional neural network model which was trained on several thousand of the matrix constituents solved this problem. This presented sound reconstruction of phase maps for the test microstructures and exhibited excellent flexibility with the variation of phase contrast.

14:50-15:10

The Study of Current Density on the Tinplate Passivation Film by X-Ray Photoelectron Spectroscopy

Feifan Xu, Shougang Research Institute of Technology, China

Tinplate is a kind of non-homogeneous material with a stratified structure, basically consisting of a thin sheet of low carbon steel with two layers of commercial pure tin on both sides. By virtue of it being non-toxic, strong, light in weight, and corrosion resistant, the largest application of tinplate is in packaging. Through produces a protective surface layer, the chromium-based treatments are currently used for the passivation of tinplate. The passivation film is effective against the formation of tin oxides and corrosion by food media, offering a good substrate for the adhesion of lacqure. Because of the significances of the tinplate surface passivation, many researchers in this area have organized relevant studies. However, the relationship between passivation process parameters and film structure is not sufficiently studied. For example, the current density has a great effect on the thickness and composition of the passivation film, which are directly related to the corrosion resistance of the tinplate. In the aspect of chromium element analysis, there is also a lack of explanation on the relative content of chromium compounds in different valence states. Therefore, it's great significance to analyze the influence of current density on the thickness, composition and the state content of chromium in the passivation film.

Influence of tinplate passivation film's structure caused by current density has been studied; X-ray photoelectron spectroscopy (XPS) was used to analysis the thickness, component and valence state of chromium in the film. Results have showed that with the current density changed from 3A/dm^2 to 0.5A/dm^2: Thickness of passivation film is thinning, contents of Sn element in the film increasing while Cr element decreasing; Chromium element in the film was consisted by Cr, Cr_2O_3, and $Cr(OH)_3$ while the relative content of each valence components changed, content of low state Cr decrease and high state Cr increase; Tinplate passivation film was rendering layered distribution, the dominant composition of the outermost film is $Cr(OH)_3$ while the middle and innermost mainly is Cr_2O_3.

15:10-15:30

Recent Advances in Real-Time Studies of the Fundamentals of Solidification Processing of Advanced Materials

Jiawei Mi, University of Hull, UK

In the 1990s and early 2000s, Professor John Campbell's Casting Research Group at the University of Birmingham UK was among the first in the world to use real-time X-ray video radiography to study liquid metal flow during the mould filling processes with the focus on investigating the entrainments of air bubbles and oxide films, and the formation of casting defects. In the late 1990s, Professor Ragnvald Mathiesen and Lar Arnberg of Norwegian University of Science and Technology started the pioneer work of using the coherent and monochromatic synchrotron X-rays available at the beamlines ID22 and ID18 of ESRF to study in-situ the cellular and dendritic solidification of metal alloys. The spatial and temporal resolutions achieved at that time were ~2.5μm and ~0.7s respectively in a field of view of up to 1mm^2. Since then, worldwide research on using Synchrotron X-rays to study the solidification processes has taken off. Systematic studies were made to visualise directly the dynamic evolutions of dendrites and other phases in conventional solidification conditions, under ultrasonic wave, electric current and pulse electromagnetic field, and in semisolid state. These studies provided much more insights into how dendrite morphology evolves and adapts according to the coupled physics of heat/solute transfer, fluid flow and external fields. However, almost all such experiments were conducted using thin metal samples of thickness of 100~200μm encapsulated inside thin cells. Hence, only 2D spatial information was obtained, which normally cannot represent the 3D spatial environment in which dendrites experience in most practical solidification conditions. In the past 10 years or so, the studies of dendritic morphology evolutions moved onto three spatial dimensions and more recently into fourth dimensional domain when time is included. Recently, extensive research has been carried out in Professor Peter Voorhees' research group in Northwestern University USA on studying time-evolved 3D interfacial morphologies of dendrites. While approximately at the similar time, Professor Peter Lee's group at Manchester University made a systematic study on the deformation of semisolid melt mixed with dendritic grains. In parallel

to those activities, researchers in the author's group has concentrated on studying the dynamic evolutions of dendrites and intermetallic phases in highly dynamic solidification environments, i.e. under ultrasonic waves and pulse electromagnetic fields. Most of those real-time and in-situ experiments were made in the 3rd generation Synchrotron X-ray facilities, for example, the European Synchrotron Radiation Facility in Grenoble, France, the Advanced Photon Source at Argonne National Laboratory, and SPring-8 in Harima Science Garden City in Hyogo prefecture, west of Osaka, Japan. In addition to the coherent and high brilliance X-ray sources, numerous special beamlines and dedicated instruments have been also built gradually over the years and added at those synchrotron X-ray facilities. Some of those are designed for studying the structures of materials and the dynamic responses to the thermomechanical forces in a spatial and temporal resolution previously impossible. This opens a new era for the solidification science. This paper gives an overview on the recent development in this field and the new sciences concerning the solidification processes discovered by using those advanced real-time characterisation techniques.

15:30-16:10 Tea Break

16:10-16:30 Invited

Understanding Fatigue Crack Nucleation in Some Ni Systems

Ben Britton, Jun Jiang, Bo Chen, Zichao Peng, Yongjun Guan, Jie Yang, Fionn Dunne, Imperial College London, UK

Understanding fatigue crack nucleation remains a challenge for predicting component life in engineering systems, especially for disc alloys used in aerospace applications. In this work, we develop understanding using an integrated approach of experiment and model to develop our hypothesis that we can predict fatigue crack nucleation sites using an energy based criterial. We combine mechanical testing of single crystal, directionally solidified, and polycrystalline Ni-alloys with inclusions, together with high resolution electron backscatter diffraction, high resolution digital image correlation, to reveal full field strain and damage fields. We use these measurements to develop a physically based crystal plasticity model and use this to predict the initiation sites of cracks.

16:35-16:55

Non-Destructive Multi-Scale Characterization of Material Microstructure and Properties

Sam Yang, Clement Chu, Tony Murphy, Christophe Comte, Miao Chen, Yi Yang, Tony Hughes, David Molenaar, Ben Clennell, Shakil Ahmed, Peter King, Darren Fraser, Sherry Mayo, Adrian Trinchi, Vu Nguyen, Darren Thompson, Stefan Gulizia, Daniel East, Adam Best, Leon Prentice, Australia; Haipeng Wang, Jianli Li, Shanxi University, China; Keyu Liu, Tongcheng Han, China University of Petroleum, China; Barrie Finnin, Amaero Engineering, Australia; Trevor Layzell, HRL Technology, Australia; Neil Wilson, Alan Lipman, Romar Engineering, Australia; Glenn Frankish, Lockheed Martin, Australia; Brian Rosenburger, Lockheed Martin, USA; Jing Zou, Tianjin University, China; Ying Xu, Sanying Precision Instruments, China; Jing Zou, Sun Yat Sen University, China; Ivan Cole, RMIT, Australia

The properties of materials are related to their internal structures at multiple length scales. X-ray CT has been widely used for non-destructive 3D microstructure characterization. However, the mainstream image analysis techniques have limitations when resolving spatial features that are smaller than 10^{-3} times the sample size, and in discriminating of material phases at microscopic length scales. By integrating statistical physics and quantitative X-ray CT imaging, the data-constrained modelling (DCM) approach has been able to address these limitations. It opens the possibility of non-destructive quality evaluation of parts produced by metal additive manufacturing (AM), for which the lack of an efficient and convenient technology for non-destructive quality evaluation is one of the major barriers to broader industrial adoption. DCM has also found applications in several other disciplines including metal corrosion protection, metal extraction from minerals, microstructure characterization for unconventional oil and gas reservoir rocks, coal and soil clay. The approach will be demonstrated using metal AM components and other materials.
The DCM technique has been implemented as a DCM software which is a Microsoft Windows™-based application for 3D microstructure characterization, modelling and visualization. The DCM software is available for download at https://data.csiro.au. A tutorial introduction is available at http://dx.doi.org/10.1063/1.4937523. Additional information is available at http://research.csiro.au/dcm.

16:55-17:15

Comparison of the Hardness Reduction Behavior by Various Residual Stress Improvement Methods

Lina Yu, Kazuyoshi Saida, Kazutoshi Nishimoto, Osaka University, Japan; Naoki Chigusa, The Kansai Electric Power Co., Inc., Japan

Stress corrosion cracking (SCC) is a significant aging

degradation problem for the alloy 600 components of pressurized water reactors (PWRs). In order to prevent SCC, various methods have been developed to introduce compressive stresses at the surfaces, such as water jet peening (WJP), laser peening (LP), surface polishing and so on. However, it has been reported that compressive residual stress would relax during the actual operation, because of high temperature environment. Since there is a correlation between the compressive residual stress relaxation and the decrement of hardness, the hardness reduction behavior in the thermal aging process after LP, Buffing and WJP have been investigated, and the behavior of the compressive residual stress relaxation of the three methods analogized each other. It is found that hardness of the sample produced by WJP, LP and Buffing has reduced after thermal aging, and the hardness reduction was confirmed only near the sample surface. Even after thermal aging, the sample produced by LP keeps the highest hardness, while that of Buffing continues the lowest hardness. Therefore, LP seems to cause the best stress improvement even after aging. Though the kinetic analysis of the hardness reduction behavior, it was found that the Johnson-Mehl equation fit all the hardness reduction behavior for WJP, LP and Buffing. From the value of the activation energy obtained, the mechanism of the hardness reduction after aging is considered to be caused by the recovery of plastic strain. Furthermore, heat recovery would occur during LP and Buffing process, which caused the low hardness reduction rate during the thermal aging process. However, the heat recovery would not occur during WJP process, thus the hardness reduction rate during thermal aging process after WJP is much higher than that after LP and Buffing. It is considered the reason for the difference in the hardness reduction rate.

17:15-17:35

Advancements in Laboratory X-Ray Characterization of Materials & Systems

Wenbing Yun, Jeff Gelb, David Vine, Benjamin Stripe, Xiaolin Yang, Srivatsan Seshadri, Ruimin Qiao, SH Lau, Sigray, Inc.

The past decade has witnessed a remarkable increase in both the development and usage of x-ray techniques for characterization of materials. Owing to the high penetrating power of x-rays and flexible analysis environments (e.g., air or vacuum), researchers worldwide have begun capitalizing on the power of these techniques for non-destructive and/or volumetric characterization.

X-rays allow features below the surface of a material to be identified, inspected, visualized, and understood with high sensitivities and high spatial resolutions. Furthermore, x-rays are able to provide this information without additional sectioning or complex specimen preparation, making the techniques highly approachable and preserving the specimen for further analysis with correlative microscopy protocols. This has opened the door to so-called "4D" analysis, where 3D volumetric representations may be achieved in an iterative manner, subjecting the specimen to a particular stimulus and observing the 3D response non-destructively. The unique experimental methods enabled by x-ray analyses continue to grow as the instrumentation becomes more refined, with advanced x-ray facilities recently becoming available across all continents of the world.

While the power of x-ray techniques is well-accepted, there remains a divide between laboratory-based approaches and those available in synchrotron facilities. The beamlines available at synchrotrons are often the best representation of what x-rays can do, but synchrotrons are often oversubscribed and competition is correspondingly high for time on the system. Nevertheless, researchers continue to struggle for a few days per year of access to a synchrotron facility, for example to perform X-ray absorption spectroscopy or energy-selective nano-scale X-ray tomography. Laboratory systems for these techniques are not widely available and tend to be unacceptably slow or limited in their capabilities as compared to their synchrotron counterparts. Efforts from the instrumentation industry have largely reached their fundamental limitations and it is clear that several new advancements need to be made in order to migrate these techniques back into the laboratory.

In our research, we have worked extensively to redefine what is possible in the laboratory by making several key advancements in laboratory x-ray science. This work began by re-imagining the conventional x-ray source, starting from basic principles. While most x-ray sources on the market operate by impinging an electron beam onto a solid target of metal, the brightness of these sources is fundamentally limited by the thermal conductivity of the metal target itself. In order to correct this and enable substantially higher brightness x-ray sources, we designed a microstructured target array with the tiny metal targets embedded in diamond. The diamond acts as a much more thermally-conductive substrate, aiding in heat dissipation and enabling more photon flux from the x-ray source. In addition to this, we have embedded a variety of target materials inside the new x-ray source, allowing fast & easy switching between materials of vastly different spectra and enabling different characteristic emission lines to be swapped on an as-needed basis. Further to the x-ray source, we have produced highly-efficient twin paraboloidal x-ray mirror lenses with double the numerical aperture of conventional single-reflection optics and, correspondingly, four times higher flux output. Combining these advancements with continued improvements in Fresnel zone plates, novel x-ray detection schemes, and meticulous thermal management solutions for stable instrumentation environments, many new possibilities have been opened for advanced x-ray instrumentation.

In this presentation, we will review the progress we have

made with developing the new x-ray source and x-ray optical systems, and discuss how these components fit together to make flexible, high-throughput x-ray measurement equipment. We will show how the source and optics together have produced a high-sensitivity micro x-ray fluorescence spectrometer (uXRF), capable of providing elemental identification in the parts-per-billion (attogram) regime, as well as how these same components have allowed us to develop a laboratory x-ray absorption spectrometer, capable of producing similar results as synchrotron-based analysis with sub-eV energy resolution in a compact laboratory package. Furthermore, we will discuss our progress in developing a nano-scale 3D X-ray microscope with record-setting 40nm resolution, multi-energy scan capabilities, and an approachable user interface to facilitate novice users learning to collect tomography. In addition to describing the system, we will illustrate a few key examples of how these instruments have enabled new characterization workflows, including both basic and complex systems from glasses to geological specimens.

17:35-17:55

Microstructural Optimization of High Strength Pipeline Steel Using TMCP Simulation Technique

Liangyun Lan, Northeastern University, China

High performance pipeline steels as a potential candidate is expected to be used to transport the natural gas and oil. However, their mechanical properties face to a new challenge because of serious service environment, such as deep ocean, permafrost and the area that earthquake frequently occurs. In this work, a thermomechanical simulator was used to simulate the thermomechanical control process (TMCP) that is always applied to produce the pipeline steel plates. Various TMCP parameters were tuned to optimize the microstructure, e.g. refining effective grain size that is considered as a most effective parameter to improve the strength and toughness at the same time. The microstructural observation was conducted on an optical microscope and scanning electron microscope equipped with electron backscattering diffraction technique. The results showed that the main microstructure formed in sequence is granular ferrite, acicular ferrite and bainitic ferrite with increasing cooling rate. The reduction schedule seems have an insignificant effect on the microstructure evolution. The second particles such as MA constituents become small and dispersive with cooling rate. The optimal effective grain size can be obtained about 4.1~4.4μm when the acicular ferrite acts as a main microstructure with the cooling rate ranged from 12 to 25℃/s and finish cooling temperature of 500℃.

I. Composite Materials: IV

Symposium Organizers :

Lin Geng, Harbin Institute of Technology, China; Boming Zhang, Beihang University, China; Junya Inoue, Tokyo University, Japan; Sang Bok Lee, Korea Institute of Materials Science (KIMS), Korea; Hao Wang, University of Southern Queensland, Australia; Rusty Gray III, Los Alamos National Lab, USA

Wednesday PM — Room: 307(3rd Floor)
August 21, 2019 — Symposium: I

Chairs:
Seungchan Cho, Korea Institute of Materials Science (KIMS), Korea
Ping Shen, Jilin University, China

13:30-14:00 Keynote

Effect of Cu/Mg Ratio on Mechanical Properties and Fracture Behavior of SiCp/Al-Cu-Mg Composites

Bolv Xiao, Institute of Metal Research, Chinese Academy of Sciences, China

Particle reinforced aluminum matrix composites (PRAMCs) are increasingly used for structural applications in the aerospace and automotive industries, since they offer a number of advantages such as a 15%~40% increase in strength, a 30%~100% increase in stiffness and superior wear resistance compared with the un-reinforced aluminum alloys. In the past decades, the influence of reinforcing phases (particle size, aspect ratio and volume fraction) and matrix (composition, heat treatment condition, etc.) on the mechanical properties of the PRAMCs were extensively investigated. However, the fracture behavior of the composites in the entire fracture process was still not very clear. In this study, we fabricated 20vol.%SiCp/2009Al composites by powder metallurgy (PM) technique, and the combining effects of particle size and aging treatment on the strength and fracture behavior of the composites were detailed investigated. The aim of this study is to elucidate the relationship between fracture behavior and microstructures of the forged PRAMCs.
20vol.% SiCp/2009Al composites reinforced with particles 7 and 20μm, respectively, in size were fabricated through hot pressing and subsequent forging. The composites were naturally aged (T4) and artificially aged (T6), respectively, after solid solution treatments. Tensile test indicated that the yield strength (YS) and the ultimate tensile strength (UTS) of the composites decreased and the elongation increased as the particle size increased from 7 to 20μm under both T4 and T6 tempers. The YS increased substantially for the two composites when the aging process changed from T4 to T6. However, the UTS did not increase almost for the composites reinforced with 7μm SiC, while the corresponding increase was 43MPa for the composites

reinforced with 20μm SiC. Observations of the fracture surfaces and the longitudinal sections of the fractured specimens indicated that the influence of the aging treatment on the fracture behavior was dependent on the particle size.

14:00-14:25 Invited

The Modulation Mechanism of the Electron Distribution at Al_2O_3/Al Interface on the Interface Interaction and Its Tensile Properties

Enzuo Liu, Yongtao Chen, Tianjin University, China

In order to regulate the interface interaction and reveal the interplay between the interface bonding mechanism and mechanical performances of metal matrix composites in microscale, in this study, the structure, stability, and bonding characteristics of the Al (111)/Al_2O_3 (0001) interface are studied based on the first-principles calculations. It is found that the Al-terminated Al2O3 surface has the lowest surface energy, which is used to construct the interface with Al (111). The most stable stacking model and the interface bonding characteristic are determine through the investigation of the work of adhesion and interface energy, as well as the electronic structure at the interface. Based on the first principles total-energy calculations, the tensile simulation is performed, and the tensile strength and elongation are calculated. Several alloying elements such as Mg, Sc, Zn, Co, Ti, Cu, Ta, and Cr are selected to be doped at the interface to regulate the interface interaction. The stable doping configurations are determined, and the influences of the addition of alloying elements on the work of adhesion and interface energy are investigated. It is revealed that there are no correlations between the mechanical property and the work of adhension or the interface energy. However, we found that the different alloy elements doped at the interface have totally different effect on the interface bonding and mechanical properties. When Mg, Ti, and Cu are doped at the interface, the interface exhibits both enhanced tensile strength and high ductility. In combination with the study on the electronic structure at the interface, we have deeply investigated the mechanism of the interface bonding and mechanical fracture to reveal the interplay between the interface microstructure and mechanical properties. It is found that the incorporation of alloying elements will redistribute the electrons at the interface, and the electronic gradient distribution benefits the tensile strength and elongation.

14:25-14:45

The Relationship between the Effective Thermal Conductivity and the Orientation of Graphite Flakes in Al Matrix Composites

Yan Zhao, Kenjiro Sugio, Yongbum Choi, Sasaki Gen, Zhefeng Xu, Jinku Yu, Hiroshima University, Japan; Jinku Yu,Yanshan University, China

The effective thermal conductivity (ETC) of Al-Graphite flakes (Gf) composites were affected by the orientation of Gf and the interfacial thermal resistance (IFTR) at the interface of Al/Gf. In this study, the effect of the Gf orientation and the IFTR was investigated. The Al-Gf composites were fabricated by spark plasma sintering method, and the relative density of Al-10%vol.Gf and Al-20%vol.Gf composites were 99.4% and 99.2%, respectively. The measured ETC of Al-10%vol.Gf and Al-20%vol.Gf composites were 220$Wm^{-1}K^{-1}$ and 273$Wm^{-1}K^{-1}$, respectively. The microstructure observation of the composites was conducted by OM, SEM and EPMA. The Gfs were dispersed homogeneously, and the overall orientations of graphite flakes were uniform, except for a few local orientations of the graphite flakes that remained disordered. The simulations based on the obtained microstructures were conducted by a new developed code which can consider the effect of the orientation of Gfs on the ETC of the composites. The results showed that the ETC of composites increased when the angle (between the Gf basal plane and heat flux direction) was less than 62 degree. On the other hand, that also showed that the effect of the orientation of graphite in the Al-matrix on the ETC can be neglected when the angle was less than 10 degree. The simulated ETC of Al-10%vol.Gf and Al-20%vol.Gf composites were 270$Wm^{-1}K^{-1}$ and 310$Wm^{-1}K^{-1}$, respectively, which were still larger than the experimental values. The new developed code can also consider the effect of the IFTR on the ETC, and IFTR at the interface of Al/Gf was estimated.

14:45-15:05

Selective Laser Melting Graphene Reinforced Nickel Matrix Nanocomposites

Zhen Chen, Pei Wei, Shuzhe Zhang, Xigang Yang, Bingheng Lu, Xi'an Jiaotong University, China; Lijuan Zhang, Dongguan University of Technology, China

In this work, graphene reinforced K418 Nickel matrix nanocomposites (GNPs/K418-MMC) were successfully fabricated by selective laser melting (SLM), with uniform dispersion of graphene nanoplatelets in the K418 superalloy by ultrasonic vibration in anhydrous ethanol and dielectric barrier discharge plasma (DBDP)-assisted milling. The influence of phase formation, distribution and interfacial reaction on the microstructure and properties of SLM processed GNPs/K418-MMC samples was studied, and its strengthening and toughening mechanism was revealed by Materials Studio numerical simulation and experiments. Microstructures and composition of SLM processed GNPs/K418-MMC samples were investigated by scanning electron microscopy (SEM) and transmission electron microscopy (TEM), energy dispersive spectrometer (EDS), X-ray

diffraction (XRD) and Raman spectroscopy. The results show that some of the graphene interfacially reacted to MC dispersed in the grain boundary and inside the interior of ultrafine-grained γ crystal. Strengthening-toughening mechanisms of graphene in K418 were load transfer, dislocation density enhancement, Orowan strengthening, and fine-grain strengthening mechanism. The hardness and mechanical properties at room and e levated temperatures of SLM processed GNPs/K418-MMC samples are significantly improved than that of the as SLM-ed ones. Compared to the SLM-ed K418 superalloy, the room and high temperature mechanical strength was increased by 11.72%, the ductility at room and high temperature of the GNPs/K418 were increased by 44.46% and 20%~45%, separately.

15:05-15:25

Reinforcement of Cyclosiloxane Hybrid Polymer and Sintered Black Glass

Yujie Song, Ningbo Institute of Materials Technology & Engineering, CAS, China

Cyclosiloxane Hybrid Polymer (CHP) is a highly crosslinked polysiloxane polymer and was pointed to be a unusual materials for multiple applications. CHP has outstanding thermal stability in both nitrogen and air, but it suffers from cracking due to highly crosslinked structure. The structure of CHP was identified as a nacre-like structure at the nanoscale but isotropic in bulk. Through design of the structure, CHP was reinforced by modified graphene sheets and vinyl terminated PDMS, achieving dramatic improvement in toughness with extremely low loading of graphene or PDMS. 153% improvement in toughness with 0.08wt% graphene and 200% improvement in toughness with 0.2wt% PDMS were observed. For graphene reinforced CHP, 25% improvement in thermal conductivity with only 0.1wt% loading of graphene was observed. 'Double sided tape' was proposed to explain the reinforcement of CHP by graphene nanosheets. For PDMS toughened CHP, simultaneous improvements in both toughness and strength were observed and 'molecular stitching' was proposed to explain the reinforcing effect. CHP was further investigated as a preceramic polymer for SiCO through low temperature sintering in argon. The resulting amorphous SiCO ceramic was thermally stable in air and inert gas at high temperature, indicating possible candidate for harsh environment applications.

15:25-16:10 Tea Break

16:10-16:30

The Microstructure Evolution of Prior β Phase during the Hot Working Processing in TiBw/Ti60 Composites

Bo Wang, Shanghai University of Engineering Science, China

The present work was inspired to understand microstructure evolution of the TiBw/Ti60 composites and its effects of hot working parameters in single β phase region, which is processing window of this kind of the composites. The microstructure evolution of TiBw/Ti60 composites has been investigated during isothermal compression in the temperature range of 1040~1200˚C and strain rate range of $0.001^{-1}s^{-1}$. Substructure evolution and deformation mechanism have been further investigated by electron backscatter diffraction (EBSD). According to the Burgers orientation, the prior β phase were reconstructed using the orientation of the α lath, which were measured by electron backscatter diffraction (EBSD). The analysis of reconstructed prior β grains showed that the recrystallized β grains formed gradually from subgrains by continuous recrystallization. With increasing the deformation temperatures, dynamic growth of the prior β grains occurred, which may lead to coarse macro α grains during the cooling processing. Moreover, at high strain rates, TiBw were seriously broken and TiBw were surrounded by lots of LAGBs. At low strain rate, DRX of β phase occurred prior near TiBw region due to providing the nucleation site for DRX and strain accumulation respectively. At proper deformation parameters, the fine and equiaxed prior β grains can be obtained.

16:30-16:50

Comparison of TiB_2/ZK60 Composites Fabricated by In-Situ Synthesis Reaction and Ex-Situ Method

Jian Liu, Shuwen Guan, Wuxiao Wang, Xi'an University of Technology, China

For particles reinforced metal matrix composites (MMCs), the uniform distribution, strong interfacial bond and good wettability of reinforcements are critical factors for obtaining desirable mechanical properties. Compared with conventional ex-situ methods, in-situ reaction synthesis is a relatively new processing method, wherein the reinforcements are directly synthesized in the metallic matrix by chemical reactions between elements or between elements and compounds. The obtained reinforcements are generally thermodynamically stable with clean reinforcement-matrix interfaces, thus in-situ MMCs usually exhibit excellent mechanical

properties. However, it is a challenge to obtain fine and uniform reinforcements during intense chemical reactions, especially to generate nanoparticles in-suit. In present study, Mg-TiB_2 master alloys were fabricated by in-situ synthesis from Mg-Ti-B system in a vacuum sintering furnace firstly, in which TiB_2 particle is a potent nucleating substrate for primary Mg, thus can act as the grain refiner of magnesium alloy theoretically. During the fabrication of composites, preheated master alloy was introduced into molten Mg alloy, after complete dissolution, the molten mixture was cooled to semi-solid state and mechanically stirred to disperse the TiB2 particles preliminarily. After that, the melt was reheated above melting point, and then ultrasonically processed for 10~20min. At last, the composite melt was cast into a steel mould. Samples sectioned from the ingots were subjected to a solution treatment at 420˚C for 8h in order to characterize the morphology of grain and TiB_2 particles. Compressive strength of the composites were measured after aging treatment (200˚C × 4h) followed by air cooling. For comparison purpose, ex-suit TiB_2 nanoparticles reinforced magnesium matrix composites were prepared by the same stir casting assisted with ultrasonic vibration, and microstructure characterization, heat treatment and compression tests were also carried out under the same condition.

16:50-17:10

Microstructure Observation of Bronze Processed Nb_3Sn Multifilamenary Wires Fabricated by the Cu-Sn-Zn Ternary Bronze Alloy

Daichi Kawamukai, University of Toyama, Japan

The bronze processed Nb_3Sn multifilamentary wires is applied to the toroidal field (TF) and the center solenoid (CS) coils on the ITER (International Thermonuclear Experimental Reactor) to confine fusion plasma with high performance. Nb_3Sn has excellent high magnetic field characteristics and relatively good wire workability, however, the deterioration of critical current density on Nb_3Sn wire by the thermal and mechanical strain effect was confirmed. This deterioration was hardly serious problem for an advanced fusion reactor. Therefore, the mechanical strengthening of Nb_3Sn would become the most important key issues to apply for the future fusion reactor. Recently, the bronze matrix strength method using Cu-Sn-Zn ternary alloy due to the solid solution hardening was reported by Hishinuma et al. We proposed to understand the high mechanical strength mechanism due to the solid solution hardening of the matrix material after Nb_3Sn formation heat treatment.
In this study, the prepared observation samples were various Nb/Cu-Sn-Zn-(Ti) multifilamentary wires before and after Nb_3Sn synthesis heat treatment, and these samples were embedded in U alloy (Bi-Sn-In alloy). The cross section of the embedded sample wire was ground mirror-like surface by buffing after water-resistant polishing. Microstructure observation of the cross section of the Nb_3Sn multifilamentary wire was carried out by SEM and TEM. Detailed quantitative analysis and microstructure observation were performed on the central part of the Nb filament, the Nb_3Sn layer, and the matrix material.

J. Amorphous and High Entropy Alloys: Amorphous Alloys V

Symposium Organizers :

Weihua Wang, The Institute of Physics, Chinese Academy of Sciences, China; Zhaoping Lv, University of Science and Technology Beijing, China; Hidemi Kato, Tohoku University, Japan; Hojin Ryu, Korea Advanced Institute of Science and Technology (KAIST), Korea; Michael Ferry, New South Wales, Australia; Evan Ma, Johns Hopkins University, USA

Wednesday PM
August 21, 2019

Room: 405 (4th Floor)
Symposium: J

Chairs:
Junqiang Wang, Ningbo Institute of Materials Technology and Engineering, CAS, China
Yongjiang Huang, Harbin Institute of Technology, China

13:30-13:55Invited

Impact Damage Mode in Fe-Based Amorphous Coatings

Jianqiang Wang, Hui Guo, Institute of Metal Research, CAS, China

Bulk metallic glasses (BMGs) continue to draw significant attention because of their unique structure and properties. However, BMGs face limitations during the industrial application because of their intrinsic brittleness, limited glass forming ability and high production cost. Amorphous metallic coatings have been recognized as an attractive and efficient way to overcome these drawbacks. The aim of this work is therefore to investigate the impact behavior of the Fe-based metallic glass coatings in detail.
The impact behavior was investigated systematically in HVAF sprayed Fe-based metallic glass coatings with various thicknesses via 3D-XRT. The results showed that the impact damage occurred principally by cracking in the coating and plastic deformation in the substrate, along with the delamination at the coating/substrate interface. It was found that the size of the interfacial delamination was a nonlinear function of coating thickness t_c. Three

thickness regions of distinctive damage modes were identified: thin coating region (t_c < 400μm), intermediate-thickness region (400 < t_c < 600μm), and thick coating region (t_c> 600μm). For t_c < 400μm, no delamination appeared in the coating/substrate interface. With an increase of coating thickness from t_c = 400μm to t_c = 600μm, the extent of interfacial delamination increased quickly and reached a maximum. Finally, when t_c > 600μm, the extent of delamination decreased when tc increased. An agreement with the Hertz theory was identified in the case of interfacial damage: significant delamination was observed on the 600μm coating where the maximum shear stress was close to the coating-substrate interface. Similarly, the damage mode transition was also found in crystalline stainless steel coating. This finding needs to be borne in mind when designing coated systems for use in applications where impact resistance is required.

13:55-14:20 Invited

Biocompatible Ti-Based Bulk Metallic Glasses and the Composites

Guoqiang Xie, Harbin Institute of Technology (Shenzhen), China / Tohoku University, Japan; Zhenwei Wu, Harbin Institute of Technology (Shenzhen), China; Hiroyasu Kanetaka, Tohoku University, Japan; Wei Wang, Tokyo Medical and Dental University, Japan

Owing to the excellent mechanical properties, high corrosion resistance and good biocompatibility, Ti-based bulk metallic glasses (BMGs) have attractive potential for functional applications such as biomedical materials. Many Ti-based BMGs have been developed in the framework of the Ti-Ni-Cu, Ti-Zr-Be and Ti-Zr-Cu-Ni alloy systems. However, the presence of toxic elements such as Ni and Be, which are not suitable to be in contact with human body, limits the applications in biomedical fields. We developed Ni- and Be-free Ti-based BMGs with high glass-forming ability (GFA), high strength and good corrosion resistance, and prepared Ni- and Be-free Ti-based BMGs and the composites with the diameter over 15mm by using spark plasma sintering (SPS) process. We also produced the porous Ti-based BMGs with a large size. The porous Ti-based BMG samples having high strength and low Young's modulus approximating to that of natural bone were obtained. The biocompatibility of these developed Ti-based BMGs had been in vivo evaluated by implantation the Ti-based BMG samples under the skin and in the bone of rats. The Ti-based BMG samples exhibited excellent biocompatibility in both soft tissue and hard tissue. It also showed nice osteoconductivity when implanted in bone tissue, and no metal ion diffusion was detected up to three months after operation.

14:20-14:40

Ion Irradiation of Metallic Glasses and Their Composites

Yongjiang Huang, Jianfei Sun, Harbin Institute of Technology, China

Due to their unique metastable structural feature of long-range disorder and short-range order, metallic glasses (MGs) often demonstrate promising mechanical, physical and chemical properties like high hardness, superb strength approaching the theoretical limit, high elastic limit, and superior wear and corrosion resistance. Taking advantage of such exceptional properties, MGs are attractive for structural and/or functional applications in various fields such as sports and luxury goods, micro-electromechanical systems, medical devices, and national defense. Especially, MGs are a proper candidate for use in radiation environments (for example, fusion, and spallation sources) due to their lack of crystalline defects, such as dislocations and grain boundaries, which prohibits the formation of conventional radiation defects including vacancy-interstitial Frenkel pairs and dislocation loops that occur in crystalline solids. Therefore, it is of essence to study in-depth the effect of ion irradiation on the microstructure and related properties of MGs.

Here, the effect of ion irradiation on the structure and mechanical properties of a Ti-, and Al-based metallic glasses, and CuZr-based metallic glass matrix composite has been studied. The Ti-based glassy sample maintains amorphous nature after ion irradiation. The irradiated Ti-based glass exhibits higher hardness and Young's modulus, and higher indent load at first pop-in event, which can be interpreted from the perspective of atomic-scale structural evolution. Ion irradiation induced crystallization can be observed in the studied Al-based metallic glass. The surface morphologies have been also examined by atomic force microscopy prior to and after ion irradiation of Al-based glass. The nanohardness and Young's modulus of metallic glass increase after ion irradiation, which can be attributed to the formation of crystalline phases. For the studied CuZr-based metallic glass matrix composite, Ion irradiation increases the disorder near the surface, as probed by neutron diffraction, and, moreover, causes the phase transformation from B2 CuZr to B19' CuZr martensitic phase in the studied BMGC. The tensile plasticity of the BMGC is dramatically improved after ion irradiation, which results from multiple shear banding on the surface and the martensitic transformation of the B2 to B19' CuZr martensitic phase. The results obtained here indicate that ion irradiation can be considered as a powerful method to finely tune the microstructure and properties of metallic glasses and their composites.

14:40-15:00

Corrosion Behavior of Plasma Sprayed Cost-Effective Fe-Cr-B-P-C Amorphous/ Nanocrystalline Coating

Tapas Laha, Anil Kumar, Sapan Kumar Nayak, Indian Institute of Technology, Kharagpur, India; Atanu Banerjee, Research and Development Division, Tata Steel, Jamshedpur, India

This work reports the corrosion behavior of cost-effective Fe-based amorphous/ nanocrystalline coatings deposited by plasma spraying technique at various spraying power. A water-atomized Fe-based feedstock powder of novel composition (Fe-10Cr-4B-4P-2C, wt.%) was sprayed. The effect of heat input on porosity content and degree of crystallization in the coatings, and its correlation with the corrosion behavior was investigated. Microstructural studies revealed that elevated plasma power led to decrease in the porosity content as well as higher devitrification. The corrosion behavior of the coatings was evaluated by potentiodynamic polarization test and electrochemical impedance spectroscopy in 3.5wt.% NaCl solution. Coating deposited at moderate plasma power displayed the best anti-corrosion behavior among various plasma sprayed coatings which was attributed to the lower porosity and higher retained amorphous content. This coating demonstrated crack-free surface after corrosion (investigated by SEM) and comparatively lower intensity of lepidocrocite (γ-FeOOH, investigated by Raman analysis) on the rusted surface, which further validated its better corrosion resistance. Additionally, corrosion resistance of the Fe-based amorphous/ nanocrystalline coatings were compared with the plasma sprayed SS316L coating. The corrosion resistance of the amorphous/ nanocrystalline coatings was superior to that of SS316L coating.

15:00-15:20

Fabrication of L10 FeNi Hard Magnetic Alloy by Annealing Amorphous Alloys

Yaocen Wang, Ziyan Hao, Chongde Cao, Northwestern Polytechnical University, China; Yan Zhang, Xiaoyu Liang, Tohoku University, Japan

Hard magnetic material is a very important kind of functional material that could be used in electric power, data storage, electronics, mechanical engineering and other related application fields. In the past several decades, rare-earth elements appeared to be unreplaceable additives in the currently used high performance hard magnetic materials such as Nd-Fe-B and Sm-Co classes.

The chemically ordered L10 FeNi is one of the most promising alternative high performance hard magnetic materials to relieve the heavy dependence and consumption of rare-earth elements. As crucial parameters to describe the magnetic hardness, the uniaxial magneto-crystalline anisotropy of L10 FeNi could reach 1.3×10^{7}erg/cm^{3}, and the maximum energy product reaches 42 MGOe, comparable to those of the popularly used Nd-Fe-B alloys.

However, unlike the production of Nd-Fe-B hard magnets or other L10 hard magnetic material such as FePt, the formation of L10 FeNi appears to be considerably difficult since the chemically order-disorder transition temperature of the equimolar FeNi alloy lies in 320℃, too low for the Fe/Ni atoms to rearrange. Thus, the disordered soft magnetic A1 FeNi formed at high temperature can hardly be processed into L10 phase.

In this presentation, we will report the research progress in a new fabrication method of L10 FeNi by initiating crystallization of the Fe-Ni-based amorphous alloys (Fe42Ni41.3Si8B4P4Cu0.7 as suggested by Makino's group). This study gives a new direction to the application of the amorphous alloys.

Currently, the processed alloy ribbons exhibit coercivity up to 860 Oe. Although the magnetic hardness is still much lower than the rare-earth containing hard magnets, it appears to be a promising idea for the fabrication of application worthy L10 FeNi in the future.

Deep study on the crystallization mechanism has been performed. Unlike been described in the previous articles, the former stage in the two crystallization stages should have merely little effect on the L10 FeNi formation. The slow undergoing second stage crystallization contributes the major part of L10 phase. Moreover, just as been expected, it is shown that the crystallized A1 FeNi phase show no sign of turning into L10 phase, and the early precipitated α-Fe grains are also not beneficial. Therefore, the inclusion of Cu which helps α-Fe formation should be removed from the alloy system, and the concentration of Fe should be reduced to prevent the precipitation of α-Fe which is futile to for fabrication of L10 FeNi.

Next stage of research on Ni richer Fe-Ni-Si-B-P amorphous alloy and its crystallization behavior is being conducted. The up-to-date progress will be shown in the presentation.

15:20-15:40

Enhanced Oxidation Resistance by Stabilizing Amorphous Oxide Structure in Metallic Glasses

W.T. Kim, Cheongju University, Korea; Y.J. Kim, D.H. Kim, Yonsei University, Korea

Metallic glasses(MGs) experience glass transition into a supercooled liquid (SCL) before crystallization at a higher temperature, enabling rapid softening and superplastic behavior. Utilizing the rapid softening and viscous flow in the SCL region, various functional applications of MGs have been reported. MG frits has been developed for application as a binding agents in

Ag paste. Thermoplastic forming processes have been used to fabricate various types of complex micro-part and surface patterning in a cost effective way. Oxidation of MG is commonly accompanied during these applications of viscous flow in the SCL region due to high temperature exposure. Therefore the oxidation resistance of MG especially in the SCL region is important. During oxidation of MG, amorphous oxide film appears first on surface and becomes thicker with proceeding oxidation. Then the amorphous oxide transforms into a mixture of crystalline oxides. The amorphous oxide films in general yield enhanced oxidation resistance since they do not provide fast ion diffusion paths such as grain boundaries and ion vacancies. Therefore the stability of amorphous oxide can play an important role on the enhancement of oxidation resistance of metallic glass. Due to the complex alloy composition, required for high glass forming ability, there are wide spectrum in the stability of amorphous oxides. In this talk we will show that the stability of the amorphous oxide film can be enhanced by the formation of complex oxide consisted with cations having large difference in size and valence state.

15:40-16:10 Tea Break

16:10-16:30

The Degradation of Petroleum Wastewater by Fe78Si9B13 Amorphous Ribbon

Keqiang Qiu, Xiaochen Xu, Zhongling Shi, Shenyang University of Technology, China

Amorphous alloys do not have defects such as grain boundaries, dislocations, and segregation. The atoms are connected by metal bonds in short-range order and long-range disorder structure characterized the homogeneity of structure. The disorder state between them makes it present in the catalytically active center that the crystalline alloy does not possess in a highly coordinated unsaturated state. Therefore the amorphous alloy has a high catalytic activity, and is an ideal catalyst. Now amorphous alloys can be used to degrade dyestuff wastewater, pesticide wastewater and so on, but whether they can degrade petroleum wastewater has not been reported. In this work, the electro-Fenton oxidation method was used to degrade the petroleum wastewater to avoid the limitations which includes the high COD contained effluent and the high consume of H_2O_2 in the traditional Fenton progress. The effects of initial pH value, current density, initial oil content (O&G) and initial COD concentration on the degradation rates of petroleum wastewater were investigated by using Fe78Si9B13 amorphous ribbon and graphite plate as anode and cathode respectively. The results show that the COD removal rates increase with the increase of current density. A suitable pH value for the best degradation rate is between 2.5~3.5. The higher the initial COD or O&G concentration, the higher the reaction rate as well as the higher the COD or O&G concentration in the effluent. It was found that the removal rates of COD and O&G are up to 89.6% and 83.3%, respectively, under the optimal parameters and a time duration of 100min. After recycling for 3 times and each time duration of 60min, the anode remains an amorphous nature and COD remove rate can reach up to 86.3% in the same load wastewater. Compared to the traditional Fenton method, it is obvious that the electro-Fenton method shows obvious superiority in reducing the consumption of H_2O_2 and obtaining higher COD removal rate.

16:30-16:50

New Soft Magnetic FeCoNi(P, C, B, Si) High Entropy Bulk Metallic Glasses

Yanhui Li, Wei Zhang, Dalian University of Technology, China

In the recent past, high entropy alloys (HEAs) or called multi-principal component alloys have emerged as a new type of advanced materials, and received increasing attention due to their unique composition characteristic and excellent properties including high strength and hardness, and good wear and corrosion resistance. In addition to simple solid solution type of HEAs, high entropy bulk metallic glasses (HE-BMGs) with a glassy structure have also been discovered in some specific alloy systems, which might provide a novel and effective approach for the design and synthesis of new bulk metallic glasses (BMGs). Although series of HE-BMGs have been developed, they are actually derived from the very limited BMG formers with high glass forming ability (GFA). Exploration of new HE-BMGs in broader alloy systems is still an unmet challenge. In addition, the existing work of the HE-BMGs mainly focus on the mechanical properties, the study referring to the functional properties of the HE-BMGs, such as magnetic properties, is still limited. In this work, we will report new metal-metalloid FeCoNiM HE-BMGs with high GFA and excellent soft magnetic and mechanical properties, where M represents a combination of 2~4 elements in (P, C, B, and Si). The FeCoNiM HE-BMGs can form fully glassy rods with a diameter of ~2.0mm by copper mold casting method, and exhibit wide supercooled liquid region of ~56K, high saturation magnetization of ~0.87 T, low coercivity of ~1.1A/m, combined with high yield strength of ~3624MPa and distinct compressive plastic strain of ~3.1%. The mechanisms of the high GFA, good thermal stability of supercooled liquid, and superior magnetic softness of the HE-BMGs will be discussed.

16:50-17:10

Nanocrystalline FeBPCCu Soft Magnetic Alloys

Xingdu Fan, Southesat University, China

Over the past three decades, nanocrystalline soft magnetic alloys of FeSiBNbCu, FeZrB(Cu) and FeCoZrBCu under the trade name of FINEMET, NANOPERM and HITPERM have been successively developed. The research and application of nanocrystalline alloys have greatly promoted the development of modern power electronic industry. However, with starting the problems of energy shortage and environmental pollution, more requirements are put forward on nanocrystalline alloys, and it becomes a noticeable topic to develop nanocrystalline alloys combined with high saturation magnetic flux density (Bs), low coercivity (Hc), low core loss, as well as low materials cost. The traditional nanocrystalline alloys cannot meet the above requirements anymore.

From 2009, nanocrystalline FeSiBPCu alloy (NANOMET) has attracted great attention due to its high Bs of more than 1.8T, low Hc of less than 10A/m and low material cost. However, the relatively low amorphous forming ability (AFA), by which the ribbon thickness must be suppressed to 20μm or less, constrains its application. Therefore, how to increase the AFA has become the crucial problem for NANOMET alloy.

It has been reported that flux melting is an effective way to improve the AFA. The fluxing purification by B_2O_3 and CaO has been proved feasible to increase the AFA in high Bs FeSiBPC amorphous alloy because it can suppress the surface crystallization and alleviate the effect of detrimental impurity such as oxide and sulfide. But the complex fluxing process increases the manufacturing cost. Recently, it is found that a proper amount of Co substitution for Fe in NANOMET-type alloys is effective to increase the AFA without losing high Bs because the addition of Co decreases the liquidus temperature which facilitates the amorphous phase formation. However, noble metal elements such as Co compared to others present in the alloy detract the commercialization. Recent researches suggest that minor C addition is effective to obtain good soft magnetic properties (SMP) in thicker ribbons. The enhancement of AFA by C addition is owing to the small size of metalloid atom which disrupts the short-range order, the formation of competition complex phases which impedes the devitrification as well as the approach of deep eutectic point. Nevertheless, the above researches are only based on a small amount of C addition with less than 1at%. Meanwhile, it is worth mentioning that P plays a crucial role on AFA and SMP of NANOMET alloys as there are previous reports revealing that the Cu_3P like clusters are easily formed due to the strong attractive interaction between P and Cu atoms, which possibly act as nucleation sites for α-Fe phase in the as-quenched state and consequently lead to the formation of the hetero-amorphous structure. Therefore, with the aim of synthesizing a novel NANOMET-type alloy with higher AFA, good SMP as well as low cost, we developed the Fe83.3Si4B8P4-xCxCu0.7 (x =0, 1, 2, 3, 4) alloys. The influence of C substitution for P on amorphous forming ability, crystallization behavior, microstructure and soft magnetic properties in FeSiBPCCu alloys was investigated.

Microstructure analysis revealed that the substitution of C for P inhibited the precipitation of α-Fe phase during the quenching process hence increased the AFA. The critical thickness increased from 18μm for the alloys with composition of x = 0 to 43μm for x = 4, respectively, owing to the decrease in the melting entropy (ΔSm), the approach of eutectic point and micro-alloying effect. Saturation magnetic flux density (Bs) increased obviously after proper annealing with increasing C substitution due to the increase in volume fraction of α-Fe nanocrystals, while excessive C content leaded larger coercivity (Hc) but improved the frequency and DC superposition performance. The Fe83.3Si4B8P2C2Cu0.7 nanocrystalline alloy was successfully synthesized with high Bs of 1.84T, low Hc of 4.8A/m and high effective permeability (μe) of 13540. The combination of high Bs and high resistance to DC bias promises potential material in DC superposition application.

17:10-17:30

Effects of Magnetic Field on the Microstructure and Magnetic Behavior in FeCoSiBPC Amorphous Alloy

Chengliang Zhao, Chuntao Chang, Dongguan University of Technology, China; Anding Wang, City University of Hong Kong, China

Fe-based amorphous alloys have been drawing scientific and industrial attentions for their excellent soft-magnetic properties and energy-saving application in magnetic devices. Co-doped Fe-based amorphous alloys were specially noticed for their usually exhibiting higher saturated magnetization comparable with Si-steels and better magnetic thermal stability. In our previous work, Co-doped FeSiBPC amorphous alloy show high Bs up to 1.74T and relatively high coerecivity of ~20A/m after normal annealing. It has been reported that magnetic field annealing can be greatly improved the soft magnetic properties compared with samples after normal annealing especially effective in FeCo-based amorphous alloy. The effects of magnetic field on

nucleation and crystallization kinetic were shown that the high magnetic field (10 Tesla) could greatly increase the nucleation and crystallization. However, how small magnetic field affect the microstructure is still not surely known.

Through our research, soft magnetic properties can be significant improved through longitudinal magnetic field. In our research the small magnetic field of about 200 Oe was applied and the soft magnetic properties was greatly softened to about 1A/m. Soft magnetic properties including Bs, coerecivity, permeability and loss (at 1.0T and 50Hz) were systematically researched. The microstructure evolution and the magnetic properties was correlated. The mechanism of magnetic field on the microstructures was also discussed.

K. Nanocrystalline Materials, and Ultra-Fine Grained Materials: V

Symposium Organizers :

Yue Zhang, University of Science and Technology Beijing, China; Zhiyong Tang, National Center for Nanoscience and Technology, China; Nobuhiro Tsuji, Kyoto University, Japan; Jae-il Jang, Hanyang University, Korea; Kenong Xia, University of Melbourne, Australia; Nathan Mara, University of Minnesota, USA

Wednesday PM
August 21, 2019

Room: 309(3rd Floor)
Symposium: K

Chairs:
Eric Hintsala, Bruker Nano Surfaces, America
Irene Beyerlein, University of California at Santa Barbara, America

13:30-14:00 Keynote

Understanding Interface-Driven Mechanisms in Biphase Nanolaminates

Irene Beyerlein, University of California at Santa Barbara, America

Nanolayered materials are a material class gaining much attention due not only to their ten-fold enhancement in strengths higher over those of its constituents, but also the tunability of this exceptional strength with layer thickness and interface engineering. They have also demonstrated high radiation damage tolerance, shock resistance, and thermal stability. Approaches to fabricate them include physical vapor deposition (PVD), electrodeposition (ED) for small-scale laboratory size samples and accumulative roll bonding (ARB) for larger-scale bulk size samples. While the positive layer size scaling with decreasing layer thickness applies to many nanolayered material systems, such as nanotwinned materials and bimetallic nanolayered composites (MNCs), its origins are not well understood, hindering exploitation of this material class in broad application. We present and apply a crystal plasticity based computational method to predict the plastic response and underlying deformation mechanisms of nanotwinned metals and MNCs. Interface-driven mechanisms, such as confined layer slip, pseudomorphic phase transformation, and interface dislocation emission, are introduced. Calculations are applied to Cu/Nb, Cu/Ta, Zr/Nb, and Mg/Nb nanolaminates and compared to measured strengths over a wide range of layer thicknesses, plastic anisotropy, texture evolution, and/or transmission electron microscopy analyses. We discuss the origins of size effects in strength identified by the model and effective ways to tune the microstructure.

14:00-14:25 Invited

Two Dimensional Lateral Complicated Struture

Xidong Duan, Hunan University, China

Two-dimensional layered materials such as garphene, MoS_2 and WSe_2 have attracted considerable interest in recent times as semiconductor after Si and becoming an important material platform in condensed matter physics and modern electronics and optoelectronics. The studies to date however generally rely on mechanically exfoliated flakes which always be limtited to simple 2D materals, especially 2D lateral complicated structure can not be perpared through exfoliation strategy. Much like the traditional semiconductor technique, complicated structure such as controlling the space distribution of composition and electronic structure of two dimensional semiconductor material is essential to copnstruct all modern electronic and optoelectronic devices, including transistors, p–n diodes, photovoltaic/photodetection devices, light-emitting diodes and laser diodes. And many physics phenomenon can only appear in more complicated structure. To fully explore the potential of this new class of materials, it is necessary to develop rational synthetic strategies of two dimensional lateral complicated struture,such as lateral heterostructure,multiheterostructure, superlattice, quantum well, etc.With a relatively small lattice mismatch (~4%) between MoS_2 and $MoSe_2$ or WS_2 and WSe_2, it is possible to produce coherent MoS_2-$MoSe_2$ and WS_2-WSe_2 heterostructures through a lateral epitaxial process (Fig.1a). Our studies indicate that simple sequential growth often fails to produce the desired heterostructures because the edge growth front can be easily passivated after termination of the first growth and exposure to ambient conditions. To retain a fresh, unpassivated edge growth front is important for successive lateral epitaxial growth. To this end, we have designed a thermal CVD process that

allows in situ switching of the vapour-phase reactants to enable lateral epitaxial growth of single- or few-layer TMD lateral heterostructures. We used this technique to realize the growth of compositionally modulated MoS_2-$MoSe_2$ and WS_2-WSe_2 lateral heterostructures. From the Fig.1 b, c, d, e we can see the formation of WS_2-WSe_2 lateral heterostructures clearly. The WS_2-WSe_2 lateral heterostuctures with both p- and n-type characteristics can also allow us to construct many other functional devices, for example, a CMOS inverter. Fig. 1g is the optical image of the invert constructed using the WS_2-WSe_2 lateral heterostuctures and the curves of the output–input and the voltage gain. The voltage gain reaches as large as 24.

In a typical sequential-growth process for 2D lateral heterostructure, the excessive thermal degradation or uncontrolled nucleation during the temperature swing between sequential growth steps represents the key obstacle to reliable formation of monolayer heterostructure or other lateral complicated structure .We designed a modified CVD system. We used a reverse flow from the substrate to the source during the temperature swing between successive growth steps A forward flow fromt he chemical vapor source was only applied at the exact growth temperature. With such reverse flow, the existing monolayer materials will not exposure to high temperature and chemical vapor source at the tempreture increasing and decreasing steps to minimize thermal degradation and eliminate uncontrolled homogeneous nucleation. With a high degree of controllability in each step, the integrity and quality of monolayer heterostructures can be well preserved after multiple sequential growth steps. We used our approach initially for the general synthesis of a wide range of 2D crystal heterostructures. We also grew more complex compositionally modulated superlattices or multiheterostructures, the number of periods and repeated spacing can be readily varied during growth. HADDF-STEM analysis of the atomic structure of the lateral heterostructures and Multiheterostructures show the atomically sharp interface can be clearly observed.

14:25-14:50 Invited

Direct Growth of Single Crystalline Graphene Film on Germanium Substrate

Zengfeng Di, Shanghai Institute of Microsystem and Information Technology, Chinese Academy of Sciences, China

Graphene has been predicted to play a role in post-silicon electronics due to the excellent electrical performance. Chemical vapor deposition (CVD) of graphene on transition metals has been considered as a major step towards commercial realization of graphene. However, fabrication based on transition metals involves an inevitable transfer step which can be as complicated as the deposition of graphene itself. By ambient-pressure CVD, we demonstrate large-scale and uniform depositon of high-quality graphene directly on a germanium (Ge) substrate. In addition, on both Ge (110) and off-cut Ge (100) substrate, the nucleated graphene domains are inclined to align along the identical direction, thus merging into the continuous graphene film without grain boundary, i.e., wafer-scale single crystalline graphene.

14:50-15:10

Numerical Study of Three-Body Diamond Abrasive Nanoindentation Single-Crystal Si by a Molecular Dynamics Simulation

Fa Zhang, Guizhou University, China

With the development of technology and industry, because of the high physical strength, wear resistance, high temperature resistance, corrosion resistance, oxidation resistance and other physical and mechanical properties of hard and brittle materials such as silicon germanium semiconductors, they can withstand the harsh working environment in which polymer materials and metal materials are difficult to handle. At the same time, exploring the indentation effect and accuracy of nanoindentation on materials has always been a key issue in material properties research. Most scholars use a two-body indentation model, but the actual operation tells us that the abrasive particles are rigid bodies of three-body motion (self-rotation of abrasive grains). We used molecular dynamics (MD) simulation to study the nanoindentation mechanism of three-body diamond abrasive grains rotating at different speeds on single crystal silicon materials. In-depth study of three-body diamond abrasive nanoindentation single crystal silicon process, indentation stress, dislocation, crack propagation, coordination number, defect atom, load, nanoindentation zone temperature and potential energy changes. The results show that the smaller the rotational speed of the three-body abrasive particles, the greater the stress in all directions, the more dislocations are easily observed in the workpiece, and the brittle-ductile transition is produced. In addition, the greater the rotational speed of the abrasive particles, the less the number of Si-II phase transitions in the workpiece, and the number of defective atoms inside the workpiece after the three-body abrasive nanoindentation is greater than the amount between the two. In addition, the faster the abrasive grain rotation speed is, the higher the temperature of the nanoindentation zone of the workpiece is, the larger the potential energy is, the more obvious the atomic displacement movement in the workpiece is, and the more atomic motion inside the atom. The workpiece is biased in the direction of rotation. In addition, the faster the grain rotation speed of the three-body nanoindentation, the smaller the average load on the workpiece.

15:10-15:30

Programmable and Multilevel Memory based on Graphdiyne-MoS_2 Heterostructure

Jialing Wen, Zheng Zhang, Yue Zhang, University of Science and Technology Beijing, China

High-capacity storage is a pivotal component for integrated circuits as reducing the cost of constructing integrated circuits are more challenging and urgent nowadays with constrain of lithography technique and ever-growing amount of data. Two-dimensional materials with atomic-thickness, transparency, flexibility, startling physical and chemical properties are therefore being explored as multilevel memory. Multilevel memory is expected to enlarge capacity and realize low cost at the same time and the performance of two-dimensional memory is still under study. Graphdiye (GDY), a new carbon allotrope with three hybridization states and various chemical bonds, is able to provide carrier trapping sites in memory devices. Herein, a switchable multilevel bilayer memory device with GDY and MoS_2 is constructed. This hetero-bilayer memory with GDY enabling efficient and reversible charge trapping states for MoS_2 channel is based on field effect transistor and shows large memory window (100V), high degree of modulation (on/off ratio more than 10^4), and programmable multilevel states (9 levels or 5 levels under different procedures). Significantly, the memory device exhibits ultralong retention time at its off states at 10~12 A. Eventually, this GDY/MoS_2 memory transistor provides a novel application of GDY material and promotes process to deduce both power consumption and production cost of integrated circuits.

15:30-16:10 Tea Break

16:10-16:35 Invited

Evaluating Microstructures and Interfaces by High Speed Nanoindentation Mapping

Eric Hintsala, Douglas Stauffer, America Youxing Chen, University of Minnesota University of North Carolina, America; Daniel Sorensen, Ohio State University, America; Joseph Stevick, Liquidmetal Technologies, America

Recent advancements in high speed nanoindentation mapping have many potential applications, but it can be argued that exploring mechanical properties distributions at materials interfaces is the most impactful. Not only are the strongest property variations typically observed at interfaces, but they are also crucial to performance of the bulk material or component. In some cases, they are introduced purposefully to enhance properties, but can also represent a common failure point. Owing to relatively easy sample preparation compared to the amount of testable area, these techniques can also be considered high throughput and can be adapted to exploring a variety of interfaces through control of the indent spacing, tip geometry and force/depth of the test. Furthermore, the technique can also be applied at elevated or cryogenic temperatures, and in controlled environments to limit problematic contamination or oxidation. Several examples will be presented and discussed that help illustrate the potential. One example is that of laser welding of bulk metallic glasses to titanium alloys for medical devices, an exotic materials joining problem where a variety of brittle intermetallics could form. Here, nanoindentation mapping was used as a critical input alongside structural characterization to optimize welding conditions by establishing statistical significance to the different processing conditions (primarily laser settings). Another example is that of evaluating potential nuclear materials at high temperature, such as additively manufactured and high entropy alloys with enhanced tolerance for absorbing radiation defects. Here, evaluating the stability of mechanical properties at elevated temperatures is possible, and, through use of correlated EBSD, these can be separated by the microstructurally constitutive phases. Looking towards the future, with the increasing ability and desire to link nanoscale properties to bulk performance, such techniques have great potential to deliver large datasets needed for evaluation and refinement of modelling efforts.

16:35-17:00 Invited

Structural and Functional Properties of Ultrafine-Grained Si Produced by High-Pressure Torsion

Yoshifumi Ikoma, Zenji Horita, Kyushu University, Japan

The application of severe plastic deformation (SPD) to semiconductor materials is of great interest for exploring novel properties associated with the formations of nanograins and metastable phases. Among various SPD techniques, high-pressure torsion (HPT) is applicable to brittle materials such as intermetallics, ceramics and semiconductors. We have applied HPT to crystalline Si, and found the formation of nanograins including diamond-cubic Si-I and metastable phases such as body-centered-cubic Si-III and rhombohedral Si-XII as well as amorphous phase. The formation of metastable phases was enhanced by imposed shear strain. The electrical resistivity increased after compression without anvil rotation, while it decreased after HPT processing for 10 revolutions due to the formation of metastable phases, especially semimetallic Si-III. Photoelectron spectroscopy measurements revealed that the valence band (VB) spectra corresponded to a mixture of Si-I, Si-III and Si-XII, and the VB edge was located at ~0.3eV. After annealing at 200˚C , the VB spectra changed to a mixture

of Si-I and hexagonal-diamond Si-IV, and the VB edge shifted by ~0.4eV. It was found that the Si-III/XII phases in the HPT-processed samples have a smaller bandgap than that of Si-I. No appreciable photoluminescence (PL) was observed from the HPT-processed samples because of a high density of lattice defects. A broad PL peak in the visible light region appeared after annealing at 600℃. Since high-resolution transmission electron microscopy observations revealed that Si-III and Si-XII phases disappeared and Si-I nanograins remained after annealing, the observed PL was due to a quantum confinement effect. These results conclude that the HPT processing is promising for the development of various functional properties of Si.

17:00-17:20

The Effect of Gradient Order on Mechanical Behaviors of Gradient Nanotwinned Cu

Zhao Cheng, Institute of Metal Research, Chinese Academy of Sciences, China / University of Science and Technology of China, China; Lei Lu, Institute of Metal Research, Chinese Academy of Sciences, China

Gradient structures, such as gradient nanotwinned structures and gradient nano-grained structures, possessing unique strengthening and work hardening, have opened an avenue towards understanding the gradient structure-related mechanical behavior. Gradient nanostructured metals with a normal gradient order (hard surfaces and soft core) or the reverse gradient order (soft surfaces and hard core) were often believed to possess superior mechanical properties with respect to their homogeneous counterparts due to the extra incompatible plastic deformation along the gradient depth. However, quantitative understanding the effect of gradient order on the mechanical behavior of the gradient metals remains unclear.

In this study, we designed and fabricated two gradient nanotwinned Cu with reverse gradient orders but the same structural gradient, including GNT-I with a normal gradient order (hard surfaces and soft core) but GNT-II with the reverse one. Tension tests indicated that GNT-I exhibits a higher strength and a lower surface roughening during deformation than GNT-II. Interestingly, GNT-I has the faster elastic-plastic transition than GNT-II, which is demonstrated by much steeper tensile curves and work hardening-true strain curves at small strains.

The systematic study on lateral deformation of GNT tensile samples reveals that the normal gradient order offsets but the reverse order aggravates the surface effect that the plastic deformation starts at the surface and then extends into the sample core due to the less constraint of grains near surface. Such a stronger constraint is therefore generated in GNT-I and may postpone the yielding of the soft core and accelerate the progressive yielding from soft core to the hard surface, both of which lead to the faster elastic-plastic transition in GNT-I. The larger strain gradient detected in GNT-I is consistent with the mechanical properties that higher yield strength according to the classic theory of strain gradient plasticity. Besides, the finer grains and thinner twin lamellae at the hard surfaces are responsible for the lower surface roughening in the GNT-I during the tensile deformation. This study exploring deformation behaviors related to the gradient order in GNT metals will afford a guide for architecting gradient structures in metals for superior mechanical properties.

L. Computational Design and Simulation of Materials: V

Symposium Organizers :

Tongyi Zhang, Shanghai University, China; Zhimei Sun, Beihang University, China; Shigenobu Ogata, Osaka University, Japan; Byeong-Joo Lee, Pohang University of Science and Technology (POSTCEH), Korea; Salvy Russo, RMIT, Australia; Saryu Fensin, Los Alamos National Lab, USA; Michele Manuel, University of Florida, USA

Wednesday PM
August 21, 2019

Room: 204 (2nd Floor)
Symposium: L

Chairs:
Ying Chen, Tohoku University, Japan
Riccardo Mazzarello, RWTH Aachen University, Germany

13:30-13:55 Invited

First-Principles Investigation of Ultrathin Films of Phase-Change Materials

Riccardo Mazzarello, RWTH Aachen University, Germany

Chalcogenide phase change materials such as GeTe and GeSbTe are capable of switching between the crystalline and the amorphous state on a nanosecond time scale at elevated temperatures. At room temperature, however, the two phases are very stable. Furthermore, they exhibit a large optical and electrical contrast, which is exploited in rewritable optical discs and novel storage-class memory devices. The continuous miniaturization of electronic memory devices requires an understanding of the structural and electronic properties of these compounds in the quasi two-dimensional limit. Besides, few-layer crystalline films of GeTe and similar monochalcogenides have recently drawn attention because they display peculiar properties, which include large ferroelasticity and piezoelectricity, and in-plane ferroelectric polarization tunable by strain-engineering. In this work, thin layers of selected chalcogenides -

namely GeTe, SnTe, GeSe and SnSe - with thickness varying from a single bilayer to 15 bilayers are investigated by first principles calculations based on density functional theory. Structural and electronic properties, including band gaps, dielectric constants, Born effective charges and polarization, are computed as a function of film thickness and compared to the bulk values. The dependence of these properties on the film thickness and the composition is rationalized in terms of bonding mechanisms and effects of depolarizing fields.

13:55-14:20 Invited

Density Functional Study on Energy Materials: Possibilities and Prediction

Koushik Biswas, Indian Institute of Technology Kharagpur, India

Density Functional Theory (DFT) can be employed to identify suitable and efficient materials in terms of structural stability, electronic conductivity, energy density and electrochemical properties for Li ion battery, magnesium hydride and solid oxide fuel cell electrode.
Simulation studies regarding structural and electronic properties, effect of ion insertion-extraction during charge-discharge on structure, electronic states and electrochemistry of Li_2FeSiO_4, Li_2FeVO_4 and $LiFeTiO_4$ prior to experimentation, would give an insight on functional material properties relating to electrode application and on the basis of that oxide materials can be selected for further experimental evaluation through device application. Material property studies and electrochemical analysis of $LiFeTiO_4$ and Li_2FeTiO_4 would help to provide an identification of efficient electrode material for energy storage application. DFT analysis has provided insight into structural details and stability, Density of state (DOS) calculation and band gap estimation, electrode characteristics (intercalation-deintercalation voltage) estimation.
For hydrogen storage material MgH_2, DFT can very well define the structure-property correlations and the effect of several dopants (including RE and light atomic number elements) on Hydrogen desorption efficiency in MgH_2. Pr, Nd, Gd and Dy doped MgH_2 have been studied for de-hydrogenation efficiency and volumetric and gravimetric capacity. It is seen that volumetric capacity will follow the decreasing trend in accordance with Dy>Gd>Nd>Pr. This is due to the increment in volume of doped MgH_2 in the same trend. The gravimetric storage capacity follows the opposite trend in accordance with the increment of mass of the dopants. In density of states analysis, part of H-s states across Fermi energy are seen for H atoms which are nearest neighbor of the dopants only, while no H-states can be seen for H-atoms which remain away from dopant. This is happened due to the shorter Mg-H bond length, leading to delocalization of H-s states, while the connected H is a part of dopant-H bonding and also due to the superposition and polarization of H-s states across Fermi energy with the f-orbital of RE elements. This leads to easier electron transfer from H-atoms and hence de-sorption of H-atoms from nearest neighbor of dopant atoms only. Simulation of H_2 de-sorption energy showed that Pr and Nd doped MgH_2 will exhibit H_2 desorption at lower temperature than that can be achieved in pure MgH_2 and in a very similar temperature as found in La and Ce doped MgH_2, while, Gd and Dy doped MgH_2 will exhibit higher desorption temperature than even pure MgH_2. In this regards, among rare earth elements, doping of only La, Ce, Pr and Nd will be fruitful while doping of Gd and Dy can be negated.
To predict the conductivity, activation barrier and ion transport in SOFC component materials, DFT has provided a greater insight of mechanism of ionic transfer and fundamental origin of higher conductivity in LSGM or LSBGM materials. DFT calculations optimized structure for various levels of Barium doping in $LaSrGaMgO_{4-x}$ system and transition state search provides the activation energy for oxygen migration in these structures. Volume expansion was observed to be increased with increase in Ba doping from 0% to 8% in LSGM structure. Oxygen migration will lead to long-range diffusion once a significant concentration of vacancies exists in LSBGM. The minimum energy pathway for oxygen migration in LSBGM using the CI-NEB method is O1-O2. The curved migration pathway confirmed previously predicted in both experimental and computational results. The migration barrier for the undoped LGO structure comes to be 2.76eV. Compared to this the energy barrier for LSBGM structures are lower and in the range 0.8~0.95eV.

14:20-14:40

Novel Material Screening Based on High-Throughput Calculations

Jiong Yang, Shanghai University, China

In recent years, high-throughput (HT) material screenings, represented by the materials genome initiative proposed in 2011, have been ever important in the search of novel functional materials. The key issues of successful HT prediction are two-fold, one is the construction and/or utilization of HT infrastructures, the other is the proper HT algorithm for predicting functional properties. In Shanghai University, we created the Materials Informatics Platform (MIP) with the ability of automated first-principles calculations. Over 80,000 three-dimensional entries and 2,000 two-dimensional entries have been included in MIP. Modules for electronic structures, electrical transport properties, and elastic properties are integrated. Based on MIP, HT screenings on various functional materials have been performed. In thermoelectrics, several diamond-

like compounds with high thermoelectric performance have been predicted. Some of the predictions have been verified in experiments. The ABO_3 perovskites and other structural types have been screened for new thermal barrier coating materials with new compositions proposed. Besides the screening of novel materials, two examples for HT search for proper dopants in two types of materials will also been presented. One is in the Rashba spin splitting system BiTeI, where suitable dopants maximize the thermoelectric properties. The other one is for the rightful doping elements in LLZO which maintain the interface stability.

14:40-15:00

Atomistic Understanding on Friction Mechanism of Amorphous Carbon Films with Surface Hydrogenated Modification

Xiaowei Li, Korea Institute of Science and Technology, Korea / Ningbo Institute of Materials Technology and Engineering, CAS, China; Aiying Wang, Ningbo Institute of Materials Technology and Engineering, CAS, China; Kwang-Ryeol Lee, Korea Institute of Science and Technology, Korea

Hydrogenated a-C (a-C:H) film is a strong candidate as solid lubricant for the engineering applications due to its excellent anti-friction property. However, when only the a-C surface is hydrogenated, the effect of H-induced surface passivation degrees on the structural properties of friction interface is still not fully elucidated yet. Hence, in the present work, friction behavior of self-mated amorphous carbon (a-C) films with hydrogenated surface were investigated by reactive molecular dynamics simulation using ReaxFF, and the dependence of structural transformation on surface passivation degree under different contact pressures were explored systematically to disclose the underlying mechanism. Results revealed that compared to the H-free case, hydrogenating the a-C surface improved the friction property drastically without the deterioration of the intrinsic properties of a-C films and especially showed great potential to achieve better anti-friction properties than oil-lubricated cases by tailoring the surface H content. Although the variations of friction coefficient with the surface H content were similar to those in hydrogenated a-C cases, there were no layered graphitic structures generated, while the competitive relationship between the stress state of H atoms and interfacial passivation caused by H and C-C structural transformation accounted for the evolution of friction coefficient with surface H content. This work sheds light on the friction mechanism of a-C with surface hydrogenated modification, but most importantly, enables a simple and effective approach to functionalize the carbon-based films for combined tribological and mechanical properties.

15:00-15:20

Data-Driven Formula Discovery: Peak Current Density in Cyclic Voltammetry

Sheng Sun, Tongyi Zhang, Shanghai University, China

Materials informatics is developing extremely fast by applying artificial intelligence and machine learning in the innovation of materials science and engineering. Symbolic regression is vigorous in the data-driven discovery of analytic formulas for complex systems with multiple variables. Cyclic voltammetry test and cyclic voltammogram (CV) are essential and popular in the electrochemical study of complex redox reactions at electrode/electrolyte interface. The peak current density (Ip) in a CV is a function of many parameters involved in the redox reaction, thereby being an indicator of the reaction mechanism. Although the Randles-Sevcik equation gives the analytic expression of Ip for reversible and irreversible reactions, no analytic formula has been reported yet covering the entire reaction spectrum. The present work demonstrates the success of data-driven discovery of two simple and analytic formulas of Ip for the entire reaction spectrum by using symbolic regression combining with sparse regression, where the data are generated from high-throughput calculations of the Butler-Volmer equation combined with diffusion equations. The two formulas are discovered respectively with and without expert knowledge. Without expert knowledge, the discovered formula is not able to directly and explicitly illustrate the reaction mode: reversible, irreversible or quasi-reversible. On the other hand, the discovered formula with expert knowledge shows the reaction mode clearly and the formula is more compact than that without expert knowledge. The present results demonstrate that symbolic regression with expert knowledge is powerful in the development of analytic formulas for complex electrochemical kinetics once sufficient data are available.

15:25-16:00 Tea Break

16:00-16:25 Invited

Fermi Surface Stability Analysis in Fe-Rich Si Alloy

Ying Chen, Arkapol Saengdeejing, Tetsuo Mohri, Tohoku University, Japan

Fe-Si alloy has a variety of applications due to its excellent magnetic and mechanical properties. Some drastic change in mechanical properties as Si concentration is increased to 9~10at.% has been intriguing since a long time ago. We have conducted an integrated study on elastic properties in Fe-rich Si alloy based on the electronic structure calculations incorporated with phonon vibration effect and thermal electrons

excitation for a Si-doped bcc-Fe alloy up to 12.5at.%Si. Our calculations reproduced a non-monotonic change of the elastic properties with Si concentration, further revealed that the Si concentration dependence of the elastic properties is originated from joint effects of the magnetovolume at the low Si concentration up to 8.0at.%, the D03 ordering on the recovery of elastic properties at Si concentration being over 10.9at.%, and the instability of density of states at the Fermi energy right at the Si concentration with drastic degradation of elastic properties. The present work aims at a thorough understanding on this Fermi level instability. We calculated the Fermi surfaces at 8.3 and 10.9at.%Si, as well as 10.9at.%Si with Ni-doping. It has been found that at 10.9at.%Si, the Fermi surface just touches the boundary of the Brillouin Zone (BZ) which leads to a high electron density at Fermi level, which associates to a degradation of elastic properties, while re-distribution of band structure with Ni-doping results in a recovery of elastic properties. This founding suggests that the Fermi lever stability/instability might be the electronic structural origin of the drastic change of the mechanical properties at some subtle Si concentrations in Fe-rich Si alloy.

16:25-16:45

MoS_2 Transistor with Atomic Level Gate Length: A First Principles Study

Junjun Li, Shanghai University, China / Hongzhiwei Technology (Shanghai) Co., Ltd., China / Harbin University of Science and Technology, China; Yin Wang, Shanghai University, China / Hongzhiwei Technology (Shanghai) Co., Ltd., China; Wenze Xie, Hongzhiwei Technology (Shanghai) Co., Ltd., China; Wei Ren, Shanghai University, China; Guiling Zhang, Harbin University of Science and Technology, China

As the rapid development of the semiconductor industry, the scaling limit of metal-oxide-semiconductor field-effect transistor (MOSFET) fabricated by traditional top-down method is approaching mainly due to the short channel effects. The seeking for emerging device architectures and new electronic materials is continuous in the past years to pursuing the Moore's Law. Using first principles quantum transport calculation method based on a four probe model, we calculated the MoS_2 junctionless transistor with an atomic level physical gate length using polysilanes (PSi) as the gate electrode. In our calculations, the atomic details of the gate material and the influence of the gate material to the transport properties of the device are considered self-consistently from first principles for the first time. Results show that the N-type MoS_2 junctionless transistor has a much bigger On/Off ration up to around 500 than that of the P-type MoS_2 junctionless transistor. In addition, due to the influence of the PSi gate, the transmission of the P-type transistor at zore gate bias is much small than that of the system without PSi, with adding negative gate bias the transmission of P-type transistor increase first and then decrease. Further scattering states, electrostatic potential and charge distribution analysis reveal the detailed physics of transistor. Our results suggest a potential fabrication and application of the ultimate short gate using the molecules in future nano-electronics devices.

16:45-17:05

High Thermoelectric Performance of Few-Quintuple Sb_2Te_3 Nanofilms

Zhen Li, Naihua Miao, Jian Zhou, Zhimei Sun, Beihang University, China

Conversion efficiency of thermoelectric materials is determined by the figure of merit (ZT), which is related to the Seebeck coefficient, electrical conductivity, temperature, lattice thermal conductivity, and electronic thermal conductivity. It is nearly a mission impossible to tune these parameters independently and maintain a high power factor and low thermal conductivity simultaneously to achieve high performance. Considering research and development of the state-of-the-art materials, the most widely used thermoelectric materials are alloys of Bi_2Te_3 and Sb_2Te_3 due to their small band gaps, complex crystal structures, and the presence of heavy elements. However, at room temperature (300K) Sb_2Te_3 has a low Seebeck coefficient and thus a low ZT value, whereas the p-type compositions with dopants (e.g., near Sb1.6Bi0.4Te3) can possess the figure of merit up to 1. In this talk, taking advantage of nano-structures and topological insulators (TIs), we report that high ZT values of larger than 2 can be achieved in one quintuple-layer (QL, ZT ≥ 2.1) and 4 QLs (ZT ≥ 2.2) of Sb_2Te_3 at room temperature, while the ZT value for bulk is around 0.5. For 1 QL, Seebeck coefficient has been greatly enhanced due to the increase in the number of band extrema by virtue of the twelvefold valley degeneracy from surface states. For 4 QLs, the high ZT value is attributed to the much longer surface relaxation time associated with the robust nature of the topological surface states. Moreover, the ZT values and the TI character of few-quintuple Sb_2Te_3 nanofilms demonstrate thickness(layer)-dependent behaviors. Our results offer significant clues for future applications and investigations of Sb_2Te_3-related quintuple layers as promising p-type thermoelectric materials and quasi-2D topological insulators for nanoelectronics.

17:05–17:25

Deformation Mechanisms of Mechanically Induced Phase Transformations in Iron by Molecular Dynamics Simulations

Xiaoqin Ou, Min Song, Central South University, China

In the present study, effects of different uniaxial tensile

directions on the phase transformations in a nano-sized (about 30nm×30nm×30nm) face centred cubic (fcc) crystal in pure iron were studied by molecular dynamics simulations. Three simulations were performed at a constant strain rate of $0.01ps^{-1}$ with tensile directions parallel to the <112>, <110> and <111> directions of the fcc phase, respectively. Periodic boundary conditions were applied in x, y and z directions. The simulation results show that externally applied loading induced phase transformations from fcc phase to body centred cubic (bcc) phase, and variant selection took place depending on the tensile direction relative to the crystallographic orientation of the fcc crystal. For the loading on the close packed fcc plane, the uniaxial tensile direction perpendicular to the close packed direction led to the formation of flat-ellipsoid bcc nuclei composed of {011} twinning martensite following the Nishiyama-Wassermann orientation relationship, while that parallel to the close packed direction resulted in zigzag bcc plates with the {112} twinning sub-structure following the Pitsch orientation. The variant selection conformed to the Schmid's rule. There are 12 slipping systems in the fcc crystal. Given a specific loading direction, slip occurs when the resolved shear stress acting in the slip direction on the slip plane reaches a critical value. The slip systems with the higher Schmid factors prefer to slip, which further induces phase transformation. When the tensile loading was perpendicular to the close packed fcc planes, a number of stacking faults in the hexagonal close packed (hcp) structure as a result of the movement of Shockley partial dislocations appeared temporarily in the shape of "funnels", which distorted the fcc lattices severely before it transformed into the bcc phase. The deformation mechanisms of the mechanically induced phase transformations through twinning or dislocations revealed in the present study may provide clues to develop iron or iron-based alloys with both high strength and good ductility.

17:25-17:45

Phase Field Crystal Simulation of Void Growth by Dislocation Emission during Deformation

Qianqian Deng, Yingjun Gao, Zongji Huang, Yixuan Li, Zheyuan Liu, Guangxi University, China; Zhirong Luo, Yulin Normal University, China

The creep process involves void defect evolution in late stage in metal. When the stress is high, the creep damage manifests the voids grow, join, and finally fracture occur. The deformation process of a square lattice sample containing void in two dimensions is simulated by using phase field crystal. During the deformation process, it is found that the void changes its shape with the applied strain. Subsequently, a pair of dislocations is generated on each of the sides of the void. After the two dislocation pairs are emitted from the void, they are in a climbing motion instead of sliding motion. Finally, this dislocation pair is broken down into two sliding dislocations. Using the dislocation emission model of the void, the condition of the force of the void and the distance between the void and dislocation during the deformation process can be well be analyzed, which can be used to explain the mechanism of the void growth caused by the dislocation emission. The dislocation pair emitted from the void is for the climbing movement, causing local stress concentration and result in the dislocation pair to decompose, and then the local strain energy is released in order that the system becomes more stable. The theoretical results have been validated by the experimental ones and are helpful to reveal the mechanism of initiation of nano-holes and fracture in the late stage of metal creep.

M. Renewable Energy Materials and Nuclear Materials: V

Symposium Organizers :

Min Zhu, South China University of Technology, China; Yuan Deng, Beihang University, China; Guanghong Lu, Beihang University, China; Tetsuya Uda, Kyoto University, Japan; Taek-Soo Kim, Korea Institute of Industrial Technology (KITECH), Korea; Dmitri Golberg, Queensland University of Technology, Australia; Assel Aitkaliyeva, University of Florida, USA

Wednesday PM
August 21, 2019

Room: 311(3rd Floor)
Symposium: M

Chairs:
Young-Joo Eo, Korea Institute of Energy Research, Korea
Ajayan Vinu, University of Newcastle, Australia

13:30-14:00 Keynote

TiFe and Related Alloys for Energy Storage

Etsuo Akiba, Rika Hayashi, Haiwen Li, Makoto Arita, Zenji Horita, Kaveh Edalati, Kyushu University, Japan

TiFe was reported in 1974 by Reilly and Wiswall. The alloy has the appropriate hydrogen equilibrium pressure at room temperature that is almost same as that of LaNi5. The hydrogen capacity is 1.8~1.9wt% that is higher than LaNi5. For stationary applications the cost is the critical issue. TiFe is the least expensive hydrogen absorbing alloy as far as the authors know. However, initial activation of TiFe needs hydrogen pressure of 30MPa and temperature at 400˚C at the same time. This is the serious roadblock to apply realistic applications, especially large-scale hydrogen storage.

There have been various attempts to solve this roadblock. We have already been very much successful in introducing super plastic deformation to TiFe.

Diffusion of surface elements of TiFe makes hydrogen pass through the surface oxide layers. Of course, huge defects are introduced and they are also thought to contribute for easy activation.
In this paper, we showed the effect of the third element addition to the TiFe. TiFe0.8x0.2 (x= V, Cr, Mn, Co, Ni, Zr, Nb, Sn) are prepared using the arc melting method. Evacuation at 150˚c for 2 hours was enough for activation for every TiFe0.8x0.2 alloy. However, the heat of 150˚c is almost impossible for large scale application considering the cost and design of heat exchanger. It was found that some of the alloys could be activated by evacuation at 30˚c for 2 hours but some could not. The surface analysis using XPS has been done with heating from room temperature to 150˚c under vacuum. The surface was covered by carbon but carbon existed just on the surface. The alloy that could not be activated at 30˚c has thicker oxide layers, which is one of the reasons for difficulty in activation. The alloy TiFe0.8Co0.2 that could not be activated near room temperature is pseudo-binary alloy. In other words, it is pure solid solution. TiFe0.8Cr0.2 consists of three phases such as TiFe, Ti and the Laves phase. Co-existence of the active phase near the surface to decompose hydrogen molecule to atoms is other reason of easiness of activation.

14:00-14:25 Invited

Advanced Nanoporous Nitrides for Energy and Environmental Applications

Ajayan Vinu, University of Newcastle, Aaustralia

Mesoporous carbon nitrides (MCN) with large surface areas and uniform pore diameters are unique semiconducting materials and exhibit highly versatile structural and excellent physicochemical properties which find them applications in diverse fields such as metal free catalysis, photocatalytic water splitting, energy storage and conversion, gas adsorption, separation, and even sensing. Although there have been series of mesoporous boron nitride or carbon nitride materials with C_3N_4 stoichiometry reported, only a little attention has been given to the mesoporous materials with C_3N_5, C_3N_6, C_3N_7, etc even though they have unique band structure. In this talk, I will present the preparation, structural and morphological control, and the functionalization of highly ordered and graphitic carbon nitride materials with tunable nitrogen contents. The relation between the structural parameters and the performance of these materials in various applications including catalysis, sensing, and carbon capture and energy storage will be demonstrated. In the second part of the talk, the fabrication of various nanoporous films including carbons, nitrides, semiconducting nanostructures, and biomolecules with tunable macroporosity, thickness, and morphology will be presented. These porous films have been fabricated by using P123 block copolymer and polystyrene spheres as templates, and utilized for sensing. For example, nanoporous CN film offers the superior affinities for toxic acid molecules but the selectivity can be totally reversed for basic molecule after treatment with UV. The application of these fascinating materials for carbon capture, water splitting, oxygen reduction reaction will also be presented.

14:25-14:50 Invited

Development of Commercialization Technology of CIGS Thin Film Solar Cell at KIER

Young-Joo Eo, Korea Institute of Energy Research, Korea

Solar energy has attention as a renewable and alternative energy source for the further sustainable development. A silicon solar cell producing electricity from solar energy has been conventionally used, however the material cost has been still the first problem for the supply of global energy demand. A chalcogenide Cu(In, Ga)Se_2 (CIGS) solar cell is one of the most promising alternatives due to the potential of low-cost fabrication technique and high efficiency among all the thin film solar cells. The technological development of fabrication method for CIGS solar cell has resulted in record-breaking efficiency improvement, which can realize the highest efficiency of 23% in polycrystalline thin film CIGS solar cells by a three-stage vacuum-based process. However, since it is the complicated and expensive method for commercial fabrication, the simple process with low cost are required as well as high efficiency. To address these concerns, commercialization technology of CIGS thin film solar cell has been researched at KIER (Korea Institute of Energy Research) for the last 10 years and achieved many promising results. Here, we introduce the recent development of large area of CIGS thin film solar cell at KIER including Roll to Roll equipment and process, and its application toward building integrated photovoltaics (BIPV).

14:50-15:10

Materialization of High Grade Tantalum Metal from End of Life Ta Scrap

Kyoung-Tae Park, Taek-Soo Kim, Korea Institute of Industrial Technology, Korea; Jae-Hong Lim, Korea Institute of Industrial Technology / Kroea University, Korea; Bon-Woo Koo, Eco-Recycling Co., Korea; Soong-Ju Oh, Kroea University, Korea

Tantalum (Ta) is a refractory metal with atomic number 73, atomic weight of 180.95g/mol, density of 16.6g/cm^3 and a high melting point of 3017˚c. From refractory characteristics, it shows excellent chemical and physical stability at elevated temperatures. Demand of Ta metal and related compounds is growing with the growth of the electronics and chemical industries. However, Ta ores are classified as conflict minerals due to which Ta production is strictly regulated. To ensure smooth supply demand

balance, it is necessary to recycle Ta from the currently available Ta end of life products.

This work consists of two parts; in which first part deals with the extraction of Ta from Ta end of life springs and the later part deals with its materialization. Ta was first converted to K_2TaF_7 by hydrometallurgical process followed by metallothermic reaction to obtain pure Ta powder. Later, Ta ingot, TaCu and TaC were manufactured from extracted Ta powder using electron beam melting (EBM), spark plasma sintering (SPS), and self-propagating high temperature synthesis (SHS) respectively. Detailed microstructural, structural and compositional analysis of all extracted and materialized Ta products were performed. Moreover, the ideal conditions necessary for the extraction of Ta from Ta scrap and its materialization are also discussed in detail.

15:10-15:30

Retarded Recrystallization of Helium-Exposed Tungsten

Wangguo Guo, Shiwei Wang, Long Cheng, Yue Yuan, Guanghong Lu, Beihang University, China; Gregory De Temmerman, ITER Organization, China

It has been recognized that impurity such as helium (He) from fusion edge plasma could affect recrystallization kinetics. In view of ITER operations, where recrystallization poses serious issues, it is important to understand the necessary conditions for retarded recrystallization to occur and identify the mechanisms at play. In this work, a combined experimental and modelling approach is used to study the effect of He plasma and ion implantation on the recrystallization kinetics of W.

He plasma exposure was observed to have a moderate retarding effect on recrystallization of W. The recrystallization temperature of W was increased by about 50K after He plasma exposure. And He ion implantation showed a significant retarding effect on recrystallization of W. The recrystallization temperature of W was increased by more than 400K. The retarding effect requires only tens of appm He and it is suggested that a deeper He distribution in W bulk is favourable for the retarding effect. The affected depth was limited to He range.

The retarding effect is attributed to the pinning effect of He bubble or cluster on grain boundary migration and is confirmed by transmission electron microscope observation. Molecular dynamics simulation shows that grain boundary migration could be impeded by a cluster of few He atoms at elevated temperatures.

This study demonstrates that He in W leads to significant changes in the kinetics of recrystallization and grain growth. The implications of plasma and particle induced retarded recrystallization on the operational budget of the ITER divertor will be discussed.

N. Additive Manufacturing and Powder Metallgufy: Materials Characterization & Properties

Symposium Organizers :

Huiping Tang, Northwest Institute for Nonferrous Metal Research, China; Yong Liu, Central South University, China; Yuichiro Koizumi, Osaka University, Japan; Kee-Ahn Lee, Inha University, Korea; Qian Ma, RMIT, Australia; Ed Herderick, Ohio State University, USA

Wednesday PM
August 21, 2019

Room: 402(4th Floor)
Symposium: N

Chairs:
Hong Wu, Central South University, China
Makoto Watanabe, National Institute for Materials Scinece, Japan

13:30-13:55 Invited

Development of Crystallographic Texture with Scanning Strategy in Selective Laser Melting

Shihai Sun, Koji Hagihara, Takuya Ishimoto, Takayoshi Nakano, Osaka University, Japan

We successfully achieved different types of crystallographic texture via scanning strategy control in the alloys (e.g. Ti-15Mo-5Zr-3Al alloy, Ni-25at.% Mo alloy, Stainless Steel 316L, and $MoSi_2$) with different crystal structures in selective laser melting. In bidirectional scanning along one axis (X-scan), single-crystalline-like texture or "crystallographic lamellar microstructure" (CLM), in which two differently oriented grains appear alternately, can be obtained in the alloys with high crystal symmetry (CS) (i.e. BCC, FCC) according to the melt mode. X-scan was found to be significantly effective for controlling the crystallographic texture in the alloy with low CS (e.g. $MoSi_2$ with C11b structure). In bidirectional scanning with a 90° rotation in each layer (XY-scan), single-crystalline-like texture can also be obtained in the alloy with high CS, which was rotated along the x-scanning direction by 45° with respect to the one formed in the X-scan. However, in bidirectional scanning with a 67° rotation (Rot-scan), only fiber texture can be formed. It is possible to control the crystallographic texture arbitrarily from single-crystalline-like and CLM to random, including the fibered one via controlling the other build parameters such as power and scanning speed, beside scanning strategy. The aligned crystal orientation along the build direction can be varied by the scanning strategy in the alloy with high CS; <001> was preferred in the XY- and Rot-scan specimens, while <101> was preferred in the X-scan specimens with single-crystalline-like texture. The major and minor grains were aligned along the <101> and

<001> in the build direction of X-scan specimens with CLM, respectively. Control of the growth behavior of the columnar cells in the melt pools via scanning strategies contributes to the generation of such different textures. The development of texture in the materials fabricated by selective laser melting was found to be an effective approach to largely improve the material properties such as lowering the Young's modulus, and increasing the strength and corrosion resistance.

13:55-14:15 Invited

Image Analysis for Microstructure and Property Evaluations on SLM Ti-6Al-4V Alloy

Makoto Watanabe, National Institute for Materials Scinece / The university of Tokyo, Japan; Masahiro Kusano, Shiho Miyazaki, Satoshi Kishimoto, Dmitry Bulgarevich, National Institute for Materials Scinece, Japann

The selective laser melting could be employed in fabrication of near-net shape products for airplane and biomedical applications from high performance titanium alloys such as Ti-6Al-4V. In this process, since the high-power laser beam in SLM scans on metal powder layer, the material melts and solidifies rapidly. Such localized laser irradiation occurs continuously layer by layer and unique microstructure is formed. In addition, it was found that materials processed by SLM exhibit a non-equilibrium structure. For example, a fine acicular martensitic structure was reported for Ti-6Al-4V due to martensitic transformation with high cooling rate. Besides, Ti-6Al-4V could form other various types of microstructures such as martensite, lamellar, equiaxial, and bi-modal ones. These microstructures can be changed significantly by laser irradiation and heat treatment, and they have an important role in governing of the mechanical properties such as alloy strength, creep resistance, fracture toughness, etc. Although the microstructure of the Ti-6Al-4V greatly affects its mechanical properties, the researches on quantitative evaluations of the corresponding relation are limited. For example, the correlation between mechanical properties and averaged width of the α lath structure had been reported by H. Galarraga et.al., but without sufficient analysis of complex microstructure patterns and based on limited number of α particles, which could affect the evaluation accuracy. Nevertheless, it showed the potential of image analysis for microstructure quantitative evaluations, corresponding correlations with the mechanical properties, and possibilities of predictions of such properties for samples fabricated by novel SLM processes.

In this study, the effects of heat treatments on mechanical properties of Ti-6Al-4V samples produced by selective laser melting are discussed based on quantitative analysis of microstructures with image processing and machine learning tools. It was found that microstructures of heat-treated samples retained their original morphologies and secondary α phase precipitated regularly at β grain boundaries with increased treatment time. These microstructures were appropriately segmented and classified. Each α particle geometrical characteristics were successfully extracted and evaluated by image analysis. Importantly, the hardness of the heat-treated samples was lower compared to that of as-built ones and it tended to increase with the area fraction of α phase, the α particle width, and the nearest neighbor distance between α particles.

14:15-14:35

Dimensional Comparison of Additive Manufacturing Technologies

Muammer Koc, Younss Mou, HBKU, QF, Qatar

This paper presents a comparative and experimental investigation on three different Additive Manufacturing (AM) technologies (i.e., FDM, SLA, MJ) in terms of their dimensional accuracy, surface roughness and surface finish. This paper offers a comprehensive understanding of the dimensional accuracy, repeatability and surface finish of commonly used AM technologies. It is aimed that our results will be useful for other studies in selecting an optimal technology and equipment for a given AM application.

A benchmark model with several common features was designed and printed repeatedly using four different equipment of three different AM technology. The dimensional accuracy of the AM parts was measured using non-contact digital measurement. The surface roughness was evaluated using a digital profilometer. The surface quality and edge sharpness were evaluated under a reflected light microscope.

In this work, three different 3DP technologies, namely, FDM (Fused Deposition Modeling), SLA (Stereolithography), MJP (MultiJet Printing) are compared for their resulting dimensional accuracy and surface finish for the same part geometry containing a variety of common product features such as a round protrusion with an internal hole, a wide flat surface, vertically oriented short micro ribs and long micro-channels

Final results indicate that the FDM technology results in quite rough surface and loose dimensional accuracy although it is the most commonly used and affordable AM technology. The SLA produced smoother surface but led to distortion of thin features (<1mm). MJP produced reasonably smooth surface roughness and tight dimensional accuracy. ProJet MJP 3600 resulted in sharper edges when compared to the Objet 260 with produced round edges.

Our result showed significant differences between the dimensional performance of FDM, SLA, and MJ 3DP

technologies. FDM stands out be the right choice for applications that do not require superior surface finish and tight dimensional accuracy at low costs. In contrast, SLA can be employed in applications where surface finish is needed such as micro-fluidic applications. Finally, MJP printers can be an appropriate choice for application that require both low surface roughness and dimensional accuracy especially applications comprising thin features. However, care must be taken when choosing the MJP printer as shown in this study not all printers are equally effective.

14:35-14:55

X-Ray Microscopy for 3D Characterization and Qualification of AM Materials

William Harris, Hrishikesh Bale, Stephen Kelly, Liu Nan, Carl Zeiss Microscopy, United States

Additive manufacturing holds the promise to produce geometrically complex parts with a variety of materials; particularly irregular three dimensional structures not achievable by conventional manufacturing techniques. This brings new opportunities for prototype or customized parts, as well as functionally graded structures along with their unique properties.

The performance and reliability of these parts, and therefore qualification of their service, can be highly dependent on the material microstructure, especially in high stress applications. Therefore it is critically important to understand the effects that feedstock powder characteristics, build process parameters, and post-build treatments have on discrete microstructural features in 3D.

X-ray computed tomography and 3D X-ray microscopy (XRM) provide nondestructive, three-dimensional mapping of the internal structure of objects. Complimenting other relevant microscopy methods like optical and electron microscopy, 3D tomography can be applied to evaluate many such features including solidification and lack of fusion defects, voids or gas pores, entrapped powder, delamination or stress cracks, foreign inclusions/particles, grain structures, internal surface roughness, and dimensional accuracy. In this talk, application of high resolution XRM to different steps of the AM process from powder characterization to analysis of as-built parts will be examined. Material systems will focus on metals, including Ti6Al4V, Al, and CoCr, but also touch on the opportunities in polymers and ceramics.

In addition, the new XRM modality of diffraction contrast tomography (DCT) will be discussed, for use in 3D grain mapping of polycrystalline samples. An example of DCT will be shown, following the sintering and grain growth of copper particles through a series of heat treatment steps.

14:55-15:15

Crack Propagation Behavior of an Inhomogeneous Laminated Ti-Nb Metal-Metal Composite: In-Situ SEM Investigation

Dapeng Zhao, Xiaogang Wang, Hunan University, China; Wenjuan Cheng,Bin Liu,Yanni Tan, Hanchun Tang,Yong Liu, Central South University,China

Developing strong and ductile metallic materials is usually a great challenge, because the strength and ductility are mutually exclusive in most cases. One of the effective strategies is to achieve the inhomogeneous microstructures. Spark plasma sintering (SPS) provides an effective way to fabricate almost full-densed materials with high flexibility to obtain unique inhomogeneous microstructures. In the present work, a Ti-18Nb (at. %) metal-metal composite with brittle/ductile laminated structures was prepared by using SPS, followed by hot-rolling, annealing quenching. Scanning electron microscopy (SEM), energy dispersive spectroscopy (EDS) and micro-region X-ray diffraction (MRXRD) analyzer were applied for microstructural analyses and phase characterization. The results show that the MMC consists of Ti-enriched zones, diffusion zones and Nb-enriched zones, and the sharp Nb gradient across different zones leads to an inhomogeneous distribution of phase and mechanical properties. An in-situ scanning electron microscopy tensile testing system was applied to record the real-time crack initiation and propagation, which allows characterization of the fracture toughness of different zones by measuring the crack-tip-opening angles (CTOA). A remarkable finding is that the diffusion zones not only enable the cooperative deformation between the brittle Ti-enriched zones and the ductile Nb-enriched but also act as crack-arresters to prevent the local cracks in the Ti-enriched zones from further propagating across the composite.

15:15-15:35

Electron Beam Melting Process of Tantalum and Titanium Alloy: Microstructure and Mechanical Properties

Ahu Celebi, Stefan Gulizia, Darren Fraser, Christian Doblin, Leon Prentice, Commonwealth Scientific and Industrial Research Organisation (CSIRO), Australia

Electron beam melting (EBM) is a powder bed fusion additive manufacturing (AM) technique that produces three-dimensional (3D) parts by fusing metallic powders with a high-energy electron beam. Additive manufacturing of tantalum is challenging due to the material's high melting temperature and ease of oxidation and contamination. In our early stages of process development for AM tantalum, process-induced porosity was identified in AM tantalum cubes by the presence of

un-melted powder inside the pores. In this study; The CP Ti powder (Grade 2 ASTM B348, AP&C) is spherical in shape and has an average particle size of 75μm. The tantalum powder (H.C.Starck Ltd) is irregular in shape and has average particle size of 29μm. Ta-40Ti, Ta-60Ti, Ta-80Ti was a blend of tantalum and titanium powders. The titanium powder particles remained spherical after the mixing, which is important for the flowability of the powder mixture. Flowability tests were conducted on the CP Ti, tantalum and Ta-Ti powders using PMT as well as the Hall flow meter. The blend of powder was characterized in terms of the particle size distribution (PSD), apparent density, tap density, X-ray diffraction analysis (XRD), chemical analysis (LECO) and particle morphology. In addition, a universal powder bed (UPB) system was used to characterize the powder behaviour after raking. Fabrication of all samples was carried out on an EBM machine (EBM® A1, ARCAM EBM). The EBM tantalum alloy material was built on top of a solid stainless steel substrate in a vacuum atmosphere. After production, the samples were removed from the substrate. The densification, microstructure and mechanical properties in terms of hardness, tensile strength and surface roughness of the EBM-processed Ta-Ti alloys were investigated. This study shows that TiTa alloys can be formed in-situ successfully using EBM.

15:35-16:10 Tea Break

16:10-16:30

Development of High Performance Powder Metallurgy Aluminum Alloys and Aluminum Matrix Composites

P.Y. Li, P.J. Tang, AECC Beijing Institute of Aeronautical Materials/ Beijing Engineering Research Center of Advanced Aluminum Alloys and Applications/ National Key Laboratory of Advanced Composites, China; W.D. Zheng, AECC Beijing Institute of Aeronautical Materials/ Beijing Engineering Research Center of Advanced Aluminum Alloys and Applications, China

Powder metallurgy (P/M) aluminum alloys, P/M aluminum matrix composites, and additive manufactured aluminum alloys have received great attention in recent years, because they possess high specific strength, high specific elastic modulus, good fatigue strength or/and good heat resistance, exhibiting great potential of applications in aerospace and automotive for weight reductions.
Beijing Institute of Aeronautical Materials (BIAM) has been active in research and development of the rapidly solidified aluminum alloy powders by ultrasonic gas atomization process for nearly thirty years. A small ultrasonic gas atomization unit with capacity of 5kg-Al was first established in the late 1980's. Then, another large ultrasonic gas atomization furnace with capacity of 50kg-Al was built in 2003, increasing the annual capacity of the aluminum alloy powder products to about twenty tons per year. Up to now, the ultrasonic gas atomization process for powders of 2XXX, 6XXX, 7XXX and 8XXX series aluminum alloys, together with suitable P/M process, have matured for producing high performance aluminum alloys and aluminum matrix composites. In addition, powders of AlSi10Mg, AlSi7Mg, and other high-strength aluminum alloys for additive manufacturing have also been produced by ultrasonic gas atomization process in recent three years.
This paper presents the main BIAM's advancement of development of P/M aluminum alloys, P/M aluminum matrix composites and aluminum alloy powders for additive manufacturing. First, the BIAM's P/M aluminum technology is outlined, which includes powders preparation by ultrasonic gas atomization, powder treatment, canning/degassing, and hot working. Then, the typical compositions and characteristics of the developed P/M aluminum alloys, P/M aluminum matrix composites and aluminum alloy powders for additive manufacturing are described. Third, some examples of available products of these alloys and composites in the form of extrusions, forgings and powders are provided. Their microstructures and properties are also presented. Finally, the potential applications and future research directions for these alloys and composites are discussed.

16:30-16:50

Consolidation of Aluminum Nanopowders without Surface Oxide

Kenta Takagi, Yusuke Hirayama, National Institute of Advanced Industrial Science and Technology, Japan; Dasom Kim, Hansang Kwon, Pukyong National University, Japan

Processing of aluminum with powder metallurgical approaches is often used to produce metal matrix composites. However, surface oxide films of Al powders are always bottleneck in terms of properties of resulting sintered products as well as sintering densification. It is very difficult to remove surface oxide films of Al powder by both chemical and mechanical approaches, because they are generally dense, strong and chemically stable. The problem of oxide films naturally becomes much serious for nanopowder. Therefore, we are trying to create Al nanocomposites from nanopowder without surface oxide films. For fundamental understanding of this purpose, the present study examined consolidation of bare Al nanopowders without inclusion and electrical and mechanical properties of resulting compacts in order to understand the influence of surface oxide films. Al nanopowders were prepared by our developed low-oxygen induction thermal plasma (LO-ITP) system. This system is capable of producing non-oxidized metal nanopowder in the particle size range from several tens to a few hundred nanometers. In this study, commercial Al powder with the diameter of several tens

of micrometers was used as a raw material. Two kinds of Al nanopowders with different particle sizes were prepared in order to investigate an influence of particle size. In addition, portions of the two powders were gently oxidized to investigate an influence of surface oxide film. These four types of powders were consolidated at various temperatures of 20, 200, and 450˚C with an uniaxial press by using current sintering apparatus. Electrical and mechanical properties of the obtained compacts were evaluated by four-terminal method, hardness test, tensile test, and so on. Microstructure of the compacts was characterized by field-emission scanning electron microscopy and transmission electron microscopy.

LO-IPT system was successful in producing two kinds of low-oxygen Al powders consisting of spherical particles with diameters of around 100nm and submicrometer. The powders were uniaxially compacted in the temperature range from room temperature to 450˚C. Green density of the nano-sized powder was not dependent on the compacting temperature, while one of the submicron-sized powder depended on the temperature. The important thing was that the compacts derived from the low-oxygen powders were robust and ductile, while ones of the surface-oxidized powders were brittle. Furthermore, the compacts of low-oxygen powders showed much higher electrical conductivities than ones of surface-oxidized powders, which was equivalent to pure Al bulk formed by casting. These results proved that the suppression of surface oxide film is significantly important for powder metallurgy process of Al materials. The Al nanopowders without surface oxide film are believed to be very effective for creation of desired Al nanocomposites.

16:50-17:10

Microstructure and Mechanical Properties of Wire and Arc Additive Manufactured 4043-Al Alloy

Xuewei Fang, Lijuan Zhang, Jiyuan Zhao, Bingheng Lu, National Innovation Institute of Additive Manufacturing/ Xi'an Jiaotong University, China; Ke Huang, Chaolong Li, Hui Li, Guopeng Chen, Longfei Zheng, Jianlong Wang, Xiaofeng Dang, Xi'an Jiaotong University, China

In the paper, the bead geometry, macro-microstructure, microstructure and mechanical properties of 4043-Al alloy fabricated by wire and arc additive manufacturing (WAAM) have been investigated. The CMT based AM process with four different arc modes were used to systematically explore the most suitable mode for depositing 4043-Al. The CMT, CMT-P, CMT-ADV and CMT-PADV were chosen to deposit 4043-Al parts. The result indicated that porosity, microstructure and mechanical property were significantly influenced by the by different arc modes and processing parameters in the CMT process. It was found that the CMT-ADV and CMT-PADV arc modes have a wide depositing speed range which can go up to 7.5m/min. For the CMT-P arc mode, the maximum speed was limited to 5m/min since the heat input was higher in CMT-P process. To ascertain the suitable arc modes for welding 4043-Al, the effect of different arc modes on the layer width and height were studied. The porosity and microstructure analysis proved that CMT and CMT-P arc modes had good performance with small and uniform pores size of less than 20μm in both horizontal and vertical directions. The average second dendrite arm spacing values for the CMT, CMT-P, CMT-ADV, CMT-PADV arc mode were 7.10μm, 7.24μm, 8.05μm and 7.80μm respectively which also indicated that CMT and CMT-P process were more suitable for manufacturing 4043-Al parts. Besides, the mechanical property comparative analysis proved that the CMT-P arc mode generates the most stable mechanical properties. What's more, different types of 4043-Al metal parts with good apparent quality were fabricated by CMT-P arc mode which also demonstrated that the CMT-P arc mode was more suitable for deposition of 4043-Al parts. It can be concluded that with proper control of the heat input and under good protection the CMT-P arc mode can build 4043-Al with no porosity and good mechanical properties can be achieved for certain industrial applications.

17:10-17:30

Effect of Si Content on Microcrack Generation in Selective Laser Melted Al–Si Binary Alloys

Takahiro Kimura, Takayuki Nakamoto, Osaka Research Institute of Industrial Science and Technology, Japan; Kazuki Sugita, Masataka Mizuno, Hedeki Araki, Osaka University, Japan

The effects of Si content on the relative density and mechanical properties of Al–Si binary aluminum alloys (Al–0~20Si) processed by selective laser melting (SLM) were systematically studied.

Pure Al and Al–4~20Si SLM specimens were densified by optimizing the laser scan parameters. However, the only Al–1Si SLM specimen contained many microcracks generated along the stacking direction, due to which the strength and elongation significantly decreased.

To investigate the generation mechanism of the microcracks, verification experiments and microstructural analyses were conducted. Comparison of single beads with pure Al and Al–1Si alloy formed by a single-line laser scan suggested that microcracks occurred in the single bead state only in the Al–1Si alloy. This indicated the extremely brittle characteristics of the Al–1Si alloy melt during laser-melting. Electron backscatter diffraction (EBSD) analysis of a vertical cross section of the Al–1Si SLM specimen indicated that the cracks were generated at the grain boundaries, and the crystallographic directions on either side of the cracks were different. Additionally, the fracture surfaces of the Al–1Si tensile

SLM specimen showed the characteristic morphology of solidification microstructures. These microstructural features suggested that the microcracks were generated before solidification was complete (namely, in the solid–liquid coexisting state).

From these results, the microcracks originated from solidification cracks (otherwise called "hot cracks"). That is, the Al–1Si SLM specimen in the solid–liquid coexisting state was brittle, and no healing of cracks by infiltration of the liquid phase occurred, leading to the generation of microcracks due to thermally induced tensile stresses by solidification shrinkages. Considering the generation mechanism of the solidification cracks, the microcrack generation of aluminum SLM materials can be typically estimated by a semisolid-state temperature range in the alloys.

Microcrack generation is a critical issue for aluminum SLM materials. These results provide insight for the design of aluminum SLM alloys.

17:30-17:50

Microstructural Characteristics of Lattice Structured AlSi10Mg Alloy Fabricated by Selective Laser Melting

Mulin Liu, Asuka Suzuki, Naoki Takata, Makoto Kobashi, Nagoya University, Japan

Cellular metals are also called porous materials that exhibit several unique physical and mechanical properties including low density, low thermal conductivity, high specific stiffness, high gas permeability and high impact energy absorption. These materials can be used in a wide range of applications such as thermal insulators, lightweight structures and shock absorbers. In particular, Al alloy lattice structure which consists of interconnected struts and nodes with a repetitive arrangement is a new category of cellular metals. Al alloy lattice structures are candidate for using in the crumple zones of automobile or impact absorbing materials of spacecraft. Selective laser melting (SLM) is one of additive manufacturing (AM) technologies combined with a powder-bed system. The SLM process has been widely used to fabricate lattice structures from AlSi10Mg alloy, which is the most commonly used Al alloy for AM technology. Several studies have investigated the mechanical properties and microstructures of bulk Al alloys fabricated via SLM. However, little information is available about the microstructure of the Al alloy lattice structures.

In order to understand the microstructural characteristics of SLM-fabricated Al alloy lattice structures, Body-Centered Cubic type (BCC-type) lattice structure was fabricated from AlSi10Mg alloy. In the present study, we observed the microstructures in node portion and strut portion of BCC-type lattice structure by using optical microscope (OM), SEM, EBSD and TEM. Vickers micro-hardness tests were performed to investigate the mechanical property of SLM-fabricated BCC-type lattice structure.

In both node portion and strut portion, microstructures comprising melt pools were observed by using OM and fine cellular structures consisting of columnar prime a-Al phases surrounded by fine eutectic Si particles were observed in melt pools by using SEM. From the result of EBSD analysis, several columnar a-Al phases exhibited <001> orientations along the long axis direction of the columnar a-Al phases, resulting in a {001} texture. However, in the strut portion, the long axis direction of the columnar a-Al phases elongated along the direction of strut, reducing the formation of {001} texture. This finding is more significant in a region near the bottom surface of strut portion. Similarly, in the node portion of the lattice structure, the microstructure is different depending on the location: the α-Al phases observed near the bottom surface appeared coarser and more equiaxed compared with those near the top surface. Several fine particles (less than 100nm) were observed within the α-Al phases by using TEM in both node portion and strut portion. The Vickers hardness values are also different depending on the location because of the inhomogeneous microstructures. Based on the results obtained, we discuss the dominant factor leading to the observed inhomogeneity of the microstructure of AlSi10Mg alloy lattice structure fabricated via SLM.

17:50-18:10

Effect of Laser Parameters on Microstructure, Metallurgical Defects and Properties of AlSi10Mg Fabricated by Selective Laser Melting

Hong Wu, Junye Ren, Yaojia Ren, Ruidi Li, Central South University, China; Shifeng Liu, Xi'an University of Architecture and Technology, China; Xin Yang, Xi'an University of Technology, China

AlSi10Mg alloy has been widely used in selective laser melting (SLM). However, the formation of metallurgical defects in this material during SLM process has not been studied sufficiently. In this work, different laser parameters were adopted to fabricate the specimens. The effects of volumetric energy density (VED) on the metallurgical defect, densification, phase composition and mechanical property were also comprehensively analyzed. At low VED of 37.39J/mm^3, the SLM printed density was 2.602g/cm^3, nearly full dense. While with the increase of VED, the formation of the micro-pores increased. The spherical micro-pores were gas pores, which were dissolved out from the melt during the solidification process because of the hydrogen evolution. The other pore was formed by keyhole in high laser energy density. There are no significant differences in the phases observed in the SLM processed parts at various VEDs: they all demonstrated a major α-Al phase and Si phase. However, when the VED reached a very high level of 92J/mm^3, the diffraction peaks of Al_2O_3 appeared, suggesting significant oxidation

at high VED. The sample with maximal tensile strength of 475MPa can be printed. While with the increase of VED, the ultimate tensile strength decreases due to the formation of micro-pores. The formation mechanisms of micro-pores including gas pores and keyhole-induced pores were disclosed from the angle of alloy smelting. Better understanding of the influence mechanisms of the laser parameters on the formation of metallurgical defects is beneficial for the production of high performance SLM parts.

N. Additive Manufacturing and Powder Metallgufy: Composites

Symposium Organizers :

Huiping Tang, Northwest Institute for Nonferrous Metal Research, China; Yong Liu, Central South University, China; Yuichiro Koizumi, Osaka University, Japan; Kee-Ahn Lee, Inha University, Korea; Qian Ma, RMIT, Australia; Ed Herderick, Ohio State University, USA

Wednesday PM
August 21, 2019

Room: 313 (3rd Floor)
Symposium: N

Chairs:
Yafeng Yang, Institute of Process Engineering, Chinese Academy of Sciences, China
Kee-Ahn Lee, Inha University, Korea

13:30-14:00 Keynote

Progress in Bimodal Metal Nanopowder Processing

Jai-Sung Lee, Hanyang University ERICA, Korea

Powder Metallurgy (PM) processing of nanoscale metal powders has been of great interest in that it can realize fabrication of high performance PM parts with saving process-energy and using cost effective materials. Among many expecting properties of PM materials the grain refinement relating material properties is important. However, these hopeful expectations are only possible when proving the following requirements are fulfilled; i) feasibility of nanopowder processing by conventional PM process, ii) compaction and shaping, iii) homogeneity in sintering consolidation and fine microstructure. Among these prerequisite demands, first the compaction or shaping of nanopowder is the most important issue in processing PM nanomaterials by conventional PM technology. Despite great efforts for solving this issue, however, a breakthrough is not yet reported.

The first part of this presentation overviews our recent works on progress in the compaction and shaping of metal nanopowder by using iron bimodal nanopowder. Especially, the die compaction and powder injection molding of Fe nanopowder are discussed in terms of microstructure, sintering behavior and mechanical property.

The second part of the presentation introduces our researches on finding a breakthrough how to process a high strength iron PM parts using Fe nanopowder. The most important issue is a question; "Is it possible to achieve a high strength pure iron PM parts only by grain refinement effect without alloying treatment?" To solve this problem, our researches have been focused on understanding the sintering mechanism of bimodal nanopowder compacts. It was experimentally found that the bimodal nanopowders underwent a full densification and slow grain growth during compaction and sintering. The key idea of these studies is based upon the optimization of structure design and full density process of micro-nano or nano-nano type bimodal powder mixtures into fine-grained Fe PM parts. Especially understanding the roles of hierarchical interfaces in nanopowder agglomerates on densification and grain growth during sintering is stressed.

14:00-14:25 Invited

Microstructure and High Temperature Mechanical Properties of Particle Reinforced 316L Stainless Steel Composites Manufactured by Selective Laser Melting Process

Kee-Ahn Lee, Young-Kyun Kim, Min-Seok Baek, Inha University, Korea; Bandar AlMangour, Harvard University, USA

316L stainless steel possesses superior ductility and corrosion resistance. However, its poor wear resistance and low strength cause problems for applications in harsh environment. Dispersing harder and stiffer ceramic reinforcement particles into a matrix of steel would improve not only its strength and wear resistance, but also its thermal properties, making it more attractive for high-performance applications. Selective laser melting (SLM), one of the powder-based additive manufacturing technology processes, fabricates a desired 3D shape by the incremental addition of materials in a layer-by-layer manner to a substrate. This study investigates the manufacturing, microstructure and room high temperature mechanical properties of particle (TiC, TiB_2)-reinforced 316L stainless steel composites developed by selective laser melting process. Gas-atomized spherical 316L stainless steel powder was mixed with TiC and TiB_2 particles. The composite powders were then used as feedstock to process composite samples using SLM The composite powders were prepared via mechanical alloying inside a high-energy planetary ball mill. The microstructures obtained with various contents of reinforcements were observed using electron microscopy and electron backscatter diffraction, while the room- and high-temperature mechanical properties were evaluated by compression tests. Directionally columnar grains were observed in the SLM-processed stainless steel. Cellular dendritic structures were homogenously distributed in the SLM-processed parts; significant reductions in both cellular and grain sizes were noticed

after the TiC and TiB_2 addition. Interestingly, the addition of particle reinforcements to the steel matrix significantly reduced the grain sizes of the matrix and disrupted the established directional structures relative to those of pure 316L. The mechanical properties of the SLM-processed 316 stainless composites were sensitive to the initial particle size and particle fraction. The TiC and TiB2 added metal matrix composites exhibited greater room- and high-temperature compressive yield strengths than unreinforced steel mainly because of combined effects of grain-boundary strengthening and Orowan strengthening. New strengthening mechanism was elaborated, and a correlation between the novel microsegregation phenomenon and the enhanced mechanical properties was suggested. These high-performance metal matrix composites (MMCs) demonstrate the potential of selective laser melting as an additive fabrication method.

14:25-14:45

In-Situ Synthesis of a High Strength Oxide Dispersion Strengthened Alloy by Selective Laser Melting

Chunlei Qiu, Beihang University, China

High oxygen content is usually harmful for metals and alloys. Powder materials usually contain higher oxygen level as compared with their cast ingot counterparts. In this study, by selective laser melting (SLM), we successfully transform a Fe-Ni alloy powder that contains a high oxygen level of 3000 ppm into a nano-oxide dispersion strengthened (ODS) alloy. The as-fabricated samples were characterized by using scanning electron microscopy (SEM) and transmission electron microscopy (TEM) together with energy dispersive X-ray spectroscopy (EDX). Some of the samples were heat treated at different temperatures to understand the microstructural stability. Their mechanicl properties were evaluated by tensile testing and the fracture surfaces examined by using SEM. TEM and EDX examination demonstrates that the nano-oxides dispersed in the as-fabricated sample are face-centred cubic Fe_3O_4 and are entangled with dislocations. Tensile testing demonstrates that the as-fabricated samples exhibit excellent tensile strengths and ductility as well as a highly ductile fracture mode. TEM imaging shows that during tensile deformation dislocations tend to bow around these particles, suggesting that the oxides have acted as effective dislocation barriers, which accounts for the enhanced strengths in the current sample. Heat treatments at or above 950°C were found to have caused depletion of oxides within grain interior and segregation of oxides along grain boundaries (GBs), resulting in significant reduction in both strengths and ductility as well as an intergranular fracture mode. TEM study reveals that at increased temperatures dislocations tend to become highly oriented, either perpendicular to or in a slanted angle against the GBs. Meanwhile, they have either cut into or stayed in contact with the oxides, acting as bridges between the oxides and grain boundaries. This is believed to have promoted dissolution of oxides in grain interior and nucleation and coarsening of oxides at GBs at high temperatures. The findings open up a new way of synthesizing high performance ODS alloys, i.e., by increasing oxygen level in an alloy powder that contains strong oxide formers followed by additive manufacturing. The current study also gives a strong implication that the precipitate-dislocation interaction plays a significant role in microstructural evolution during annealing.

14:45-15:05

The Fabrication of (Fe-10Ti)–30%TiB_2 Composites with both High Thermal Conductivity and Hardness by SPS

Yujiao Ke, Kazuhiro Matsugi, Zhefeng Xu, Yongbum Choi, Hiroshima University, Japan; Yu He, Mingzhi Wang, Jinku Yu, Yanshan University, China

Fe-TiB_2 composites as a new generation of novel materials show the great potential in hot work steel tools (HWSTs) usage. Compared with the traditional HWSTs, the new generation materials are focused on improving both thermal conductivity and wear resistance. In this work, (Fe-10 at.%Ti) -TiB_2 composites with both high thermal conductivity and high hardness were fabricated by spark plasma sintering. Fe-10at.%Ti alloy powder was used to suppress the Ti atoms from TiB2 diffusing into Fe. Therefore, Fe and Ti powder were first mixed and then mechanically alloyed for 108ks in order to synthesize Fe-10at.%Ti alloy powder. Thereafter, (Fe -10at.%Ti) - 30 vol.%TiB_2 composites sintered at 1323, 1373K for 0.6ks were obtained. Main phase composition of the two compacts are α Fe, TiB_2 and basically no Fe2B is found according to the results of XRD and BSE images. Besides, the volume fraction of TiB2 in sintered compacts predicted by image analysis is close the 30vol.% in both compacts, proving that the TiB_2 was barely decomposed during the sintering process and thus, thermal and chemical stability of TiB_2 in Fe are successfully achieved. More importantly, TEM image obtained at the Fe/TiB2 interface characterizes an excellent interface cohesion between Fe and TiB_2 particles, which may contribute to a good mechanical properties in the future tests. The thermal conductivity and Vickers hardness of compacts sintered at 1323, 1373K for 0.6ks are 32.7W·m^{-1}K^{-1}, 686.7HV and 38.2W·m^{-1}K^{-1}, 727.5HV, respectively. This work provides a new method for fabricating Fe-TiB_2 composites by powder metallurgy with both improved thermal conductivity and hardness in the usage of HWSTs.

15:05-15:25

New Composites for Additive Manufacturing

Dan Batalu, Anamaria Bunescu, University Politehnica of Bucharest, Romania; Petre Badica, National Institute of Materials Physics, Romania; Zhen Xiang, Wei Lu, Tongji University, China

Introduction: Additive manufacturing has known a boom in recent years, being an important component of the fourth industrial revolution. There are two main directions of additive manufacturing: (i) developing new technologies, along with improved accuracy and advanced customized software, and (ii) developing new materials for special applications. New materials should fulfil various criteria such as eco-friendly, recyclability, biocompatibility or antibacterial properties for medical applications, functional characteristics (e.g. magnetic/electric properties, working in extreme conditions, etc). Design of new materials should also consider the technology requirements, beside those of the 3D printed product, such as electromagnetic, optical, medical properties, esthetical, etc. In our work we proposed new composite with polymeric matrix (PM: ABS, PLA), and inorganic additions (IA).
Materials and methods: Commercial ABS and PLA were dissolved in solvent, mixed with inorganic additions, and dried by evaporation. The solid mixture was cut in small pieces and extruded at 200~215℃ into filaments with constant diameter, in the range of 1.4~1.7mm. The obtained filament was used for printing bulk samples.
Results: We obtained a composite filament of PM+IA. First filaments show high porosity due evaporation of remnant solvent. The filament was cut in small pellets and extruded for the second time. The new filament was more compact, and the powder was homogenous distributed. The 3D printing parameters were selected as for commercial polymers ABS or PLA.
Conclusions: In our work we produced composite filament of PM+IA. The resulted filaments can be successfully 3D printed. The obtained composites can be used for applications in medical field or magnetic applications. For better 3D printing results, working parameters require optimization.
Acknowledgements: This work was supported by (i) grants of the Romanian Ministry of Research and Innovation, CCCDI - UEFISCDI, project number PN-III-P3-3.1-PM-RO-CN-2018-0113 / 17 / 2018, within PNCDI III, and project number 74/2017 COFUND-M-ERA.NET II-BIOMB, within PNCDI III, and by (ii) grants of China-Romania Inter-Governmental Science and Technology Cooperation (project number 2018-43-17), the National Natural Science Foundation of China (Grant No 51671146), and the Fundamental Research Funds for the Central Universities of China (22120180096).

15:30-16:10 Tea Break

16:10-16:35 Invited

Designing Core-Shell Structured Composite Powders for Making High-Performance Titanium Matrix Composites

Yafeng Yang, Shaofu Li, State Key Laboratory of Multiphase Complex Systems, Institute of Process Engineering, Chinese Academy of Sciences, China

Titanium metal matrix composites (TMCs) possess a good balanced mechanical properties and therefore have a big potential of being widely applied in the aerospace industry. Ceramic particle and carbon nanotubes (CNTs) are always selected as the reinforcements due to their high hardness, good wear resistance, excellent creep resistance and high temperature mechanical properties. However, how to obtain the homogenous distribution of these reinforcements in the matrix is a key question to make high-performance TMCs. Traditionally, the reinforcements were introduced by mechanical blending of reinforcement and titanium powder mixtures (ex-situ) or pure ceramic reactants and titanium powder mixtures (in-situ), followed by conventional powder consolidation technologies. Both approaches can not essentially resolve the inhomogeneous dispersion of these reinforcements, but along with the contamination at the interface of reinforcements and matrix and the damage on the structural integrity of CNTs. In order to overcome this problem, a novel powder surface manipulation approach was developed to make carbon and/or CNTs coated titanium metal powder by fluidized bed chemical vapor deposition. Particularly, trace iron impurity solid solute in titanium alloys powders were activated to act as an effective catalyst to in situ synthesize CNTs by which CNTs were planted within the titanium alloy powders. This type of powders can be directly consolidated by hot pressing and/or spark plasma sintering. Microstructure observation indicated that nano-sized TiC precipitates and CNTs had a uniform distribution in the matrix. This TMCs exhibited the superior mechanical properties to those fabricated by traditional process. Moreover, this powder manipulation technology was also demonstrated to be effective in making high-quality 3D printing metal matrix composites powders with a spherical morphology.

16:35-16:55

The Preparation of Metallic Glasses/Crystalline Composite Coatings by Laser Cladding with Enhanced Wear and Corrosion Resistance

Xue Liu, Guomin Le, Jinfeng Li, Institute of Materials, China Academy of Engineering Physics, China

Metallic glasses (MGs) exhibit excellent wear resistance

and corrosion resistance due to their unique short-range order and long-range disordered structure. However, it is difficult to obtain large-sized MG due to their amorphous forming ability. Laser cladding technology can prepare coatings with tunable compositions, and the rapid solidification conditions in the cladding process are favorable for the formation of MG. Therefore, the MGs and their composite coatings may be prepared by laser cladding. In this study, low-cost Fe-based and Zr-based MG with strong MG forming ability were selected as the research alloys. Dense Fe-based coatings and Zr-based amorphous/crystals coatings were prepared by laser cladding. The effect of cladding parameters on the microstructure and wear and corrosion resistance of the coating was investigated. It is found that the Fe-Si-Al coating consists of a single solid solution phase, and its wear resistance is mainly controlled by grain size. The Fe-Si-B coating consists of (Fe, Si) solid solution and (Fe, Si) and Fe_2B eutectic structure, and its wear resistance is mainly dominated by the distribution of Fe_2B. Columnar crystal to equal crystal transformation occurres in both of the two Fe-based coatings, and the wear resistance was more than 10 times higher that of the matrix. Similar to the Fe-based coating, the grain in the Zr-Cu-Ni-Al-based composite coating also first epitaxially grows at the front of the fusion line, but then transforms into dendrites dispersed in the MG matrix. The MG content in the coating increases with the decreasing laser power. The Zr-Cu-Ni-Al-based composite coating exhibits obvious passivation phenomenon in the 3.5 wt.% NaCl solution, which is rare to found in other Zr-Cu-Ni-Al-based composite coatings. It was found that the increase of the amorphous phase can significantly promote the formation of the passivation film in the electrochemical corrosion process, thereby improving the corrosion resistance of the coating. The formation of the passivation film is closely related to the enrichment of Zr, Ni and Al. This work provides important insights into the structural evolution as well as the wear and corrosion mechanism of MG/crystalline composite coatings.

16:55-17:15

A Simple Two-Step Fabrication Route for Cu Composite Reinforced by Three-Dimensional Graphene Network

Xue Li, Byung-Sang Choi, Chosun University, Korea

Recently, many projects have been carried out for the synthesis of graphene-metal composites utilizing various methods of dispersing carbon materials into the matrix. An example is the use of powder metallurgy to resolve the density difference between metal and carbon materials such as CNTs or graphene flakes. The method involves three steps: mixing of metal powder with CNTs or graphene flakes (or both) and additives, compacting the mixture into a certain shape, and lastly sintering it at an appropriate temperature. However, this method has several drawbacks: i) it is economically inefficient, ii) unavoidable contaminations occurs during the mixing process, and iii) most importantly it is not easy to obtain uniform distribution of carbon materials in the metal matrix.

In this study, therefore, a simple process is introduced to fabricate a graphene-Cu composite, i.e., Cu grains reinforced by a uniform three-dimensional (3D) graphene network. The process involves only two simple steps: compaction of Cu powder without any additives, and then chemical vapor deposition (CVD) to fabricate graphene among Cu grain boundaries, leading to 3D graphene network. This 3D graphene network reinforced Cu (3DGR-Cu) composite is expected to show chemical and physical properties similar to or better than OFHC Cu in some aspects. Thus, 3DGR-Cu will be able to replace the expensive OFHC Cu currently being used in various industrial applications if mass production is possible with high quality control. Relatively inexpensive Cu powder (purity 99%) was used to synthesize 3DGR-Cu composite. The simple way to synthesize the 3DGR-Cu composite is presented herein, along with a possible explanation for and characterization of the formation of graphene or graphite. In addition, physical properties of Cu composite were studied by various spectroscopic (μ-Raman, EPR, and thermal conductivity) and microscopic (SEM and TEM) methods. Lastly mechanical and physical properties such as thermal and electrical conductivities of 3DGR-Cu will be presented.

17:15-17:35

Effect of WC and Ti(C0.7N0.3) Content on the Microstructure and Mechanical Properties of NbC Matrix Cermets

Shuigen Huang, Jozef Vleugels, Jinhua Huang, Bert Lawers, Jun Qian, KU Leuven, Belgium; Hardy Mohrbacher, NiobelCon bvba / KU Leuven, Belgium; Jacob Sukumaran, Patric De Baets, Ghent University, Belgium; Eduardo Cannizza, EHT-Engineering Consulting Ltd, Belgium; Mathias Woydt, BAM, Federal Institute for Materials Research and Testing, Belgium

As a refractory carbide, NbC has a low density of 7.79g/cm^3, a good chemical stability, high melting point of 3600˚C and high hardness of 19.6GPa. In this study, NbC-7Co-7Ni-52(Ti(C0.7, N0.3)-xWC)-4Mo_2C(wt%) based cermets with x varying from 12 to 52wt% were prepared by conventional pressureless liquid phase sintering in vacuum for 90min at 1390˚C, 1420˚C or 1450˚C. Detailed microstructural investigation was performed by SEM, EPMA and XRD and the phase constitution was compared with thermodynamic modelling. The WC and Ti(C0.7, N0.3) content in the NbC cermets had a significant effect on the (Nb, W, Ti, Mo)(C,N) matrix grain growth, the constituent phases, and mechanical properties of the fully densified NbC-based cermets. The Ti(C0.7, N0.3)-free NbC cermet was composed of homogeneous (Nb,W)C grains

with a Ni-Co based binder as well as undissolved or reprecipitated WC grains, whereas core-rim structured NbC-based grains were observed in all cermets with Ti(C0.7, N0.3) addition. All cermets with =< 32 wt% WC were composed of a fcc Co + Ni solid solution binder and a cubic core-rim (Nb, W, Ti, Mo)(C,N) phase with a W-rich core and a Ti-rich rim, as well as a rimless Ti(C, N) phase. Thermodynamic analysis indicated that both the composition of the cubic NbC and Ti(C, N) based solution phases are closely related to the WC content, i.e., the higher the WC content the higher the nitrogen concentration in the Ti(C,N) phase. A good combination of 1500 ~ 1600 kg/mm^2 Vickers hardness (HV30) and indentation toughness of 8 ~ 9 MPa.m$^{1/2}$ were obtained for the NbC cermets with 20 to 32wt% WC.

17:35-17:55

Fabrication of in Situ Al_4C_3/Al Composites via Laser Additive Manufacturing

Weiwei Zhou, Keiko Kikuchi, Naoyuki Nomura, Akira Kawasaki, Tohoku University, Japan

Due to their strong, lightweight, and cost-effective properties, Al matrix composites (AMCs) can improve the energy efficiency in many applications that place demands on high-specific-strength materials, such as those in the aerospace and automobile industries. In general, AMCs have been produced by traditional routes, in which the reinforcements were directly incorporated to molten- or powder-formed Al. However, in such a fabricated ex situ composite, the interfacial bonding between the reinforcement and Al is usually weak. Moreover, conventionally manufactured AMCs need time- and energy-consuming post-processing for practical use. Thanks to its flexibility in materials and processing, laser powder bed fusion (L-PBF) provides new technological opportunities for producing high-performance composites with tailored structures. More importantly, the highly nonequilibrium and completely melting nature of L-PBF allows the possibility of creating in situ AMCs. In situ fillers are thermodynamically stable, having interfaces with the matrix that are clean and compatible; thus, they are deemed to be superior to ex situ fillers for strengthening. In this work, a novel in situ Al_4C_3/Al composite was synthesized from graphene oxide (GO)/Al mixed powders via L-PBF. GO sheets containing 3~5 layers of graphene monolayer were uniformly mixed with Al powders without changing the powder features. After subsequent L-PBF processing, GO was reacted with Al atoms in molten pools and completely transformed to Al_4C_3 nanorods, showing a higher aspect ratio than that produced by powder metallurgy. In addition, the Al_4C_3 nanorods were well distributed, and intimately contacted with the Al matrix, giving rise to an improvement in the Vickers hardness of the composite. This work offers a simple approach to synthesizing in situ reinforcements with excellent strengthening effects via L-PBF.

A. Advanced Steels and Processing: VIII

Symposium Organizers:

Han Dong, Shanghai University, China; Zhigang Yang, Tsinghua University, China; Yoshitaka Adachi, Nagoya University, Japan; Dong-Woo Suh, Pohang University of Science and Technology (POSTCEH), Korea; Christopher Hutchinson, Monash University, Australia; Amy Clarke, Colorado School of Mines, USA

Thursday AM
August 22, 2019

Room: 205+206+207(2nd Floor)
Symposium: A

Chairs:
Hongshan Zhao, Shanghai University, China
Haiwen Luo, University of Science and Technology Beijing, China

8:30-8:55 Invited

Simulation on the Evolution of Inhibitors During High Temperature Annealing of Grain-Oriented Silicon Steel

Haiwen Luo, University of Science and Technology Beijing, China

We studied the evolution of inhibitors in the grain-oriented silicon steel sheet during high temperature annealing, before which it was subjected to nitriding for the acquired inhibitors. Microstuctures, including nitirides particles, were examined on the samples that were extracted from the high annealing tests interrupted at different temperatures. Many nitride particles, including both silicon nitride and AlN, were observed near surface when the annealing temperature increased to more than 1000℃; whilst an inhibitor-poor layer was revealed at subsurface; moreover, the density of inhibitors was found to increase from subsurface towards the center of silicon steel sheet. Such extraordinary phenomena were first discovered in the grain oriented silicon steel. A kinetic model was established to simulate the evolution of precipitates during the high temperature annealing, in which the nitriding microstructure was set as input. The evolution of nitride inhibitors were calculated across the thickness of silicon steel sheet according to the real high temperature annealing profile. We conclude that such an evolution is due to the diffusion of N in the near surface of steel sheet to both atmosphere and the center of steel sheet, and the diffusion of Al to glass film, the latter is coated on the silicon steel sheet. The established numerical simulations based on diffusions of solute elements have successfully reproduced the observed distribution of inhibitors varying during the high temperature annealing process.

8:55-9:15

X-Phase Precipitation in 6wt.%Si High Silicon Austenitic Stainless Steels

Sihan Chen, Tian Liang, Yangtao Zhou, Chengwu Zheng, Yingche Ma, Kui Liu, Institute of Metal Research, Chinese Academy of Sciences, China

As is known to us all that X-phase is a kind of intermetallic compound or a kind of carbide as type M18C with a lattice parameter between 0.88nm to 0.89nm. The composition of it is usually consists of Fe, Cr and Mo. The existence of X-phase can results in severely negative effect on mechanical properties. It is mainly occurrence in duplex, austenitic and ferrite stainless steels or in ternary Fe-Cr-Mo and quaternary Fe-Cr-Ni-Mo systems. However, few reports can be found about the precipitation of X-phase occurs in high silicon stainless steels. The characteristic of X-phase has a significance influence on the properties of the steel, which may lead to cracks during the mechanical process, as a result, getting information of X-phase is essential. The X-phase precipitation mechanism of 6%Si high silicon austenitic stainless steel after different aging treatment temperature was investigated by means of OM, SEM, XRD and TEM in this work. The samples were first treated at 1150 for 2h, to dissolve the phase into the matrix, and then preformed at 600~1000℃ for 24h aging treatment, followed by air cooling. The results showed that χ-phase precipitates during the aging process and exists between the temperature of 600℃ to 1000℃, rich in Fe, Cr, Ni, Si and Mo elements. The amount of the phase increase firstly and decrease after 800℃.The phase precipitates along the grain boundaries initially, the size is below 2μm. Then with the increasing of the temperature (700~1000℃), the phase precipitates both inside and along the grain boundaries. The tensile test at room temperature shows that the highest strength of extension is 802MPa, whereas the elongation is only 4.8%. From the fracture morphology, it can be observed that the fracture mode of the samples is brittle fracture and the cracks extension through the phases. We can conclude that X-phase is a kind of brittle phase, which may become the cracking sources when under forces.

9:15-9:35

Grain Refinement and Strengthening Mechanism of Austenitic Stainless Steel and Relationship with Grain Size

Renbo Song, Yang Su, Tianyi Wang, University of Science and Technology Beijing, China; Hengjun Cai, Jian Wen, Lianzhong (Guangzhou) Stainless Steel Corporation, China; Ke Guo, University of Science and Technology Liaoning, China / Angang Group Mining Design and Research Institute Co. Ltd., China

In this study, 20LH5 Chromium-Manganese austenitic stainless steel is used as experimental material. The new stainless steel replaces nickel in traditional nickel-chromium stainless steel with manganese and nitrogen to reduce cost. The comprehensive modification of chromium-manganese-nickel stainless steel has great influence on its mechanical properties and strain hardening properties. To evaluate the potential application value of the new steel, the strengthening and toughening mechanism of grain size in tensile process was studied. The fine-grained austenitic stainless steel was obtained by large reduction cold rolling and solid solution treatment based on phase reversion. The microstructure evolution and mechanical properties of the fine-grained austenitic stainless steel were compared with those of coarse-grained austenitic stainless steel during tensile test, and the internal relationship between deformation mechanism and austenite stability was analyzed. In the process of research, mechanical properties of austenitic stainless steels with different grain sizes were obtained by tensile test and phase analysis was carried out by electron backscatter diffraction (EBSD), then deformation structure was observed by transmission electron microscopy (TEM) and fracture characteristics were observed by scanning electron microscopy (SEM), finally the relationship between mechanical properties, morphology and grain size was studied. It is found that the evolution of microstructure plays a determined role in material properties during plastic deformation. TRIP or TWIP effect will occur in metastable austenite of austenitic stainless steel under external stress, so good tensile strength and high plasticity can be obtained. The results show that the grain size of austenitic stainless steel is refined from coarse grains, and the strength and plasticity of fine grained austenitic stainless steel are improved significantly. At the same time, fine grained austenitic stainless steel obtains excellent plasticity mainly through deformation twinning (TWIP), while coarse grained austenitic stainless steel obtains good plasticity mainly through strain induced martensite effect (TRIP). The deformation mechanism from deformation twins to strain induced martensite in the coarse-grained structure is owing to the increased stability of austenite with grain refining.

9:35-9:55

Effect of Gadolinium on the Microstructures and Mechanical Properties of Super Duplex Stainless Steels

Ji-Ho Ahn, Sang-Wook Lee, Byung-Moon Moon, Hyun-Do Jung, Korea Institute of Industrial Technology, Korea

Super duplex stainless steels with good corrosion resistance and tensile strength serve as the attractive metals in various industries. However, improvements in their mechanical properties such as toughness and

ductility are required in severe environments. In this study, A890 grade 7A super duplex stainless steels were modified by gadolinium, a kind of rare earth metal, with using a normal casting method. The grain size and non-intermetallic inclusions size in the alloy decreased from 684μm to 598μm and from 7.01 to 5.70μm upon gadolinium addition, respectively. It is noted that the ultimate tensile strength and elongation of the as-cast alloy after gadolinium addition remarkably increased from 920 to 970MPa and from 24.8% to 28.4%, respectively. The hardness of the as-cast alloy with gadolinium marginally increased from 24 to 25HRC. Compared with control without gadolinium, modified super duplex stainless steel exhibited a higher absorbed energy, including the lower shelf energy and upper shelf energy, and the lower impact transition temperature. Specifically, the ductile-to-brittle transition temperature analyzed by fracture appearance transition temperature decreased by 22.5℃ after the addition of gadolinium. This approach to improve microstructure and mechanical properties of super duplex stainless steels was successfully performed. Accordingly, the modified super duplex stainless steels by the addition of gadolinium have a great potential for industrial applications under some severe conditions.

9:55-10:15

The Research and Application of Heavy Gauge Steel Plate with High Toughness

Yongda Yang, Yanfeng Wang, Changwen Ma, Longteng Ma, Shougang Group Co., Ltd. Research Institute of Technology, China; Chengliang Han, ShouGang Jingtang United Iron & Steel Co.,Ltd,China

Currently, the impact toughness of heavy gauge steel plates can hardly reach the requirement of related standards. In the study, the reason for low impact energy of heavy gauge steel plates were experimentally analyzed. These plates with the low carbon and Nb/Ti addition were produced by TMCP process. Samples for metallographic observation and impact toughness tests were taken along the thickness direction per 10mm from the plate surface to the center. The impact tests were conducted at -20℃, -40℃, -60℃, and -80℃. The results indicated that the microstructure as well as the toughness values varied greatly from the plate surface to the center. Impact tests results revealed that samples from 20 to 30mm below the surface had worst impact toughness, for reason of numerous large size of granular bainite, which shows poor crack-resistant performance. Additionally, the worse impact energy of samples from 30mm to 60mm below the surface could be attributed to large amount of pearlite, which has poor deformability and easy to trigger micro-cracks. At last, samples from the surface to 20mm had excellent impact toughness because of a large mount of polygonal ferrite and acicular ferrite. Polygonal ferrite with good deformation and acicular ferrite with excellent crack-resistant performance significantly improve impact toughness. In consequence, the aim of microstructure optimization was determined to improve the impact energy of heavy gauge plates. Through modifying the parameters of TMCP process, large size of granular bainite and pearlite could be effectively avoided or suppressed hence the impact toughness was improved immensely. Besides, results of welding tests indicated that the strength and impact energy of welding joints meet the requirements, ensuring the need of domestic large scale steel structure for heavy gauge steel plates. The heavy gauge plates applied this technique show superb toughness and have been widely used in steel bridges as well as high-rise buildings.

10:15-10:35

Development and Application of Thin Gauge Ultra Fast Cooling Process Wear-Resistant Steel

Yayuan He, Wuhan Branch of Baosteel Central Research Institute, China

The production of thin gauge steel for construction machinery, especially high strength wear resistant steel, is limited because of the lack of heat treatment production line for sheet metal in WISCO. Under this background, it is necessary to develop the ultra fast cooling technology for high strength wear resistant steel by utilizing the 2250mm hot strip rolling line and its ultra fast cooling equipment of WISCO, which can cancel the offline quenching and tempering process for traditional wear resistant steel, so as to quickly seize the market with the advantages of high performance cost ratio. The stage achievement is illustrated in this paper.

Based on the progressiveness of ultra fast cooling technology and the production dilemma of high strength wear resistant steel in WISCO, the thin gauge wear resistant steel has been successfully developed by reasonable composition design (CE is below 0.5%), smelting, continuous casting, controlled rolling and controlled cooling especially ultra fast cooling process. The microstructure is fine and uniform lath martensite, and retained austenite (content 1%~2%). Retained austenite can effectively reduce the yield-strength ratio and obtain excellent workability, cold bending performance and low temperature toughness products. The properties are excellent, strength and toughness, hardness and cold bending performance reach even far beyond the technical requirement, fully meet the requirements of welding and processing in the downstream engineering machinery industry. For example, the hardness reaches 430~450HBW, the center hardness reaches 103% of the surface, while the longitudinal impact energy of -20℃ is above 37J (sample size: 7.5mm×10mm×55mm), the transverse

cold bending property can bend beyond 120° without crack at the condition of diameter equaling 4 multiply by thickness.
In conclude, the effect of water instead of alloy has been realized through ultra fast cooling process, the production cost is significantly reduced, and labor productivity is significantly improved.

10:30-10:45 Tea Break

10:45-11:05

Development of the High Performance Steel Plates with Grain Refined Surface Layers

Ae-Young Cho, Il-Cheol Yi, Hwan-Gyo Jung, Gwangyang-si, Technical Research Laboratory, POSCO, South Korea

Toughness, strength, ductility and fatigue properties can be improved with a finer grain microstructure. However in other to get fine microstructure, it becomes necessary to have additional mechanical or thermal process like severe rolling, inter-critical annealing and others. Also they require more cost but we should minimize it for commercial productions. When we produce plate steel products, it becomes more difficult because their large thickness require hard reduction in rolling and longer time in heat treatment. POSCO recently has developed the plate steels with grain refined surface layers. The grain refined surface layers can improve mechanical properties even in thick plates. The surface area of plate is exposure to air or water during rolling and cooling. This causes the temperature gradient along its thickness. Usually, surface has lower temperature and center has higher temperature because the TMCP is on cooling to room temperature from reheating temperature. The temperature gradient can be changed to more stiff during water cooling temporary but it would be recovered to stable state immediately. The plate steel with grain refined surface layer which is developed by POSCO is using this recovering of temperature gradient. During rolling process, the difference of temperatures between surface and center of plate is controlled and only surface layer is inter-critical annealed without an additional heat treatment. The microstructure and its properties would be discussed in detail.

11:05-11:25

Research and Application of Surface Control Technology of Battery Shell Steel Based on Two-Stand Skin Miller

Yongqiang Wang, Meng Yu, Jie Wen, Shougang Research Institue of Technology, China

With the rapid development of domestic new energy vehicles, demand for new materials is rapidly expanding. In particular, the battery shell steel not only needs good deep drawing performance, but also has very high surface quality requirements, and its production is very difficult. Surface quality is one of the most important indicators of battery shell steel. The surface quality of battery shell steel is not only the requirement of surface roughness, but also has certain requirements on its surface compactness. By analyzing the surface characteristic parameters, the first proposed RPC value is the main parameter affecting the compactness of the strip surface. The larger the RPC value, the finer the macroscopic appearance of the strip surface, the lower the RPC value, the rougher the strip surface looks. Because the research on the roughness and RPC value control of the two-stand Skin Miller is relatively small, it is of great significance to study it, since there are two stands in the two-stand skin miller, it is difficult to study the roughness replication law and surface topography. Development of battery shell steel based on a two-stand Skin Miller in a factory, through the experiment, the three-dimensional shape analysis of the strip surface was carried out, and the formation law of the surface roughness of the strip during the rolling process of the Two-stand Skin Miller was revealed by industrial experiment. Based on the actual data, the roughness prediction model of the two-stand tempering machine was obtained by mathematical method. Studying the Two-stand Skin Miller process strategy and setting parameters that meet the surface requirements of the Battery Shell Steel, a set of surface control technology for Battery Shell Steel was formed. Applying this technology to the actual production process solves the problem that the surface roughness of the battery shell steel cannot meet the customer's use, Bring huge economic and social benefits.

11:25-12:45

Effect of Quenching and Partitioning on Microstructure and Mechanical Properties of Medium Manganese Wear Resistant Steel

Jie Deng, Xinjun Sun, Xinli Song, Xiaokai Liang, Zhidong Xiang, Wuhan University of Science and Technology, China; Tao Zhang, Ansteel Group Iron and Steel Research Institute, China

The influence of quenching temperature and partitioning treatment on microstructure and mechanical properties of medium manganese wear resistant steels were researched. The results showed that the microstructure was composed of primary martensite and retained austenite and secondary martensite. The filmy and blocky retained austenite distributed between the martensite lath and the martensite lamellar bundle group respectively. The width of filmy retained austenite was 100nm to 300nm. The volume fraction of retained austenite of the steels after quenching and partitioning increased first and then decreased with increasing the

quenching temperature. The maximum volume fraction of retained austenite was 19.5% for the steel quenching at 220˚C and partitioning at 350˚C for 10min.The carbon concentration in the retained austenite decreased from 1.0276wt.% to 0.974wt.% with increasing the temperature from 195˚C to 280˚C. The tensile strength increased from 867MPa to 958MPa and the tensile strength increased from 1392MPa to 1571MPa, the elongation changed from 14% to 16.11% with increasing the quenching temperature from 195˚C to 280˚C. The content of retained austenite decreased from 19.6% to 6% or so after the steel was tensile failure. The retained austenite transformed into martensite under the tensile stress and contributed to the high strength and high elongation of the quenching and partitioning medium manganese wear resistant steels.

11:45-12:05

Effect of Mo on Formation of Coarse Austenite During Cooling after Hot Forging in Case Hardening Steels

Takeshi Miyazaki, Takeshi Fujimatsu, Goro, Sanyo Special Steel, Japan; Miyamoto, Tadashi Furuhara, Tohoku University, Japan

Case hardening steels are widely used for gears and shafts for automotive and industrial components. Normally, hot forging is employed to fabricate these parts. Formation of coarse austenite grain during cooling from forging temperature often causes abnormally coarse pearlite and bainite microstructure. Since this microstructure deteriorates grain stability in the following carburizing process, it is of industrial importance to avoid coarse austenite.

In the present study, the effect of Mo on formation of coarse austenite grain during cooling was investigated by a thermomechanical simulator for JIS SCM420 (Fe-0.2C-0.3Si-0.8Mn-1.0Cr-0.2Mo in mass%) and SCr420, both of which are often used for gears and shafts. Difference between SCM420 and SCr420 is presence or absence of Mo addition. Specimens were austenitized at 1200˚C, followed by compression by 65% at 1100˚C at strain rate of $10s^{-1}$. Subesquently, small compression by 5% was applied at the same temperature and strain rate. After these compressions, the specimens were cooled down at slow cooling rate of 0.05˚C/s to 900˚C and quenched. It was found that abnormally coarse austenite grains evolved during cooling in SCM420, while normal grain growth was observed in SCr420.

In order to clarify the formation mechanism, the parent austenite orientation map was reconstructed for specimens quenched just after small compression, utilizing martensite orientation map obtained from EBSD. Grain orientation spread (GOS, a measure of plastic deformation to which austenite grain is subjected) was used to discuss formation of coarse austenite grain. According to the GOS maps, it was clear that strain was introduced in homogeneously in austenite in SCM420, while strain in SCr420 was relatively homogeneous. It was inferred that strain energy difference in SCM420 might cause abnormal grain growth. This result suggested that Mo addition might induce inhomogeneous strain distribution in austenite during small compression and was related to formation of coarse austenite during cooling.

B. High Temperature Structural Materials: Casting and Manufacturing

Symposium Organizers:

Qiang Feng, University of Science and Technology Beijing, China; Shengkai Gong, Beihang University, China; Hyun Uk Hong, Changwon National University, Korea; Damon Kent, University of Sunshine Coast, Australia; Sammy Tin, Illinois Institute of Technology, USA; Hiroyuki Yasuda, Osaka University, Japan; Jun Zhang, Northwestern Polytechnical University, China

Thursday AM Room: 305 (3rd floor)
August 22, 2019 Symposium: B

Chairs:
Jun Zhang, Northwestern Polytechnical University, China
Paraskevas Kontis, Max-Planck-Institut für Eisenforschung GmbH, Germany

8:30-8:55 Invited

Research Statues and Progress of Solidification Structure and Grain Defects in Nickel-Based Single Crystal Supealloys

Lin Liu[1], Jun Zhang[1], Hengzhi Fu[1]
1. Northwestern Polytechnical University, China

With the alloy development and size and structure diversification of engine blades, two aspects of single-crystal superalloy development have increased the likelihood of solidification defects forming in industrial practice. First, refractory element additions, to enhance the creep performance and alloy stability in service, have a detrimental effect on their casting characteristics. This has led to difficulties in controlling the single crystal orientation and to an increased occurrence of stray grains and freckle chains. Second, thermal conditions in producing large castings for industrial gas turbines are quite different from those experienced in the manufacture of turbine blades for aero-engines. In particular, the critical solidification parameters, temperature gradient and solidification rate are significantly reduced and the solidification front tends to be macroscopically curved, rather than planar. These factors combine to produce conditions

where solidification defects are more likely to occur. The present presentation initially introduces some typical casting defects frequently encountered in casting practices in single crystal superalloys, In order to establish physical basis for defect formation, solidification characteristics, dendritic orientation and growth competition for single crystal superalloys are analyzed. The grain selection process during single crystal casting both in with bottom seeding and spiral grain selection is simulated by a macro-scale ProCAST coupled a meso-scale Cellular Automaton Finite Element (CAFE) model. The microstructure evolution of grains with different orientations during directional solidification is investigated also by the phase-field method. An in depth analysis is presented of formation mechanisms, effect of processing parameters/composition, and possible control technique for distinct defect. We emphasis on the effect of solidification characteristics of alloys, crystal growth orientation, thermal and solutal fields on the defects, try to reveal nature of defect formation. The key developments and future challenges in this field are summarized. The overall objective is to establish defect formation criterion and a relationship between alloy chemistry, process and defect-free single crystal superalloy components.

8:55-9:20 Invited

A Phenomenological Analyses of Freckling in Directional Solidification of Ni-Base Alloys

Hongbiao Dong[1], Fu Wang[2], Zihui Dong[1], Dexin Ma[3]
1. University of Leicester
2. Xi'an Jiao Tong University
3.Shenzhen Wedge Central South Research Institute, China

Freckles have been of interest for many researchers for around 50 years, due to their deleterious detrimental effects in the advanced directional solidification (DS) and single crystal (SC) castings of superalloys. Freckles appear as long trails of equiaxed grains aligning roughly parallel to the direction of gravity. And they were often found on the surface of DS/SC superalloy castings. It is now generally agreed that freckles are associated with thermosolutal convection originating in the interdendritic liquid during solidification, which is driven by a density inversion occurring in the mushy zone as a result of interdendritic segregation. Besides the alloy chemistry the occurrence of freckles is known to be mainly dependent on the solidification parameters and casting size. A lower temperature gradient G and solidification velocity V result in the larger dendrite spacing and higher permeability. The occurrence of freckles was rarely taken geometrical factor of castings into account. In this work, the freckle formation in complex geometry superalloy components was analysed. According to new features of freckle appearance, freckle is subject to edge and the curvature effects. In polygonal casting sections, freckles are formed preferably on the convex edges. In the components with curved contour, freckles were exclusively found on the outward curving surface having positive curvature. Two effects can be attributed to the overlapping or divergence of the surface effect, which can more effectively affect the freckle formation than the local thermal conditions.

9:20-9:45 Invited

Formation and Evolution of Casting Defects in Single Crystal Nickel Based Superalloys

Jian Zhang[1],
1. Institute of Metal Research, Chinese Academy of Sciences, China

Single-crystal (SX) nickel-based superalloys have been widely used in turbine blades for their excellent high-temperature capabilities. However, casting defects, such as slivers, freckles, and micro-pores, limit the performance of SX superalloys. The formation and evolution of sliver and micro-pores in SX superalloy are discussed in the present talk. Ex-situ X-ray computed tomography (XCT) characterization combined with microstructure observation and electron backscattered diffraction (EBSD) revealed that sliver generally generated from one or two deformed dendrites. The misorientation between sliver and matrix did not change during directional solidification, although the orientation of both sliver and matrix may rotate according to the geometry of the casting. The role of micro-pores during solidification, heat treatment, creep and fatigue tests was also discussed. For example, large casting pores generated during directional solidification may induce deformation of regular dendrite arms. Sliver developed from the deformed dendrites. Some of the casting pores grew up in situ during solution heat treatment. New pores also generated during solution. It is believed that the growth behaviors of both solidification-pores and solution-pores can be related to the vacancy formation and diffusion during heat treatment. Size and volume fraction of most micro-pores was unchanged during low cycle fatigue (LCF), but micro-pores near the surface may play an important role in LCF.

9:45-10:05

High Temperature Mechanical Behavior of Ceramic Core for Directional Solidification of Turbine Blades

Jiangwei Zhong[1], Zilin Xu[1], Qingyan Xu[1], Baicheng Liu[1]
1.Tsinghua University, China

The high temperature mechanical behaviors of SiO_2-based cores for the directional solidification of turbine hollow blades were investigated. Isothermal uniaxial

compression tests of ceramic core samples were conducted on a Gleeble-1500D mechanical simulator with an innovative auxiliary thermal system. This thermal system was established to measure the high-temperature mechanical properties of non-conductive materials. The measured temperature can reach 1600℃. The temperature control accuracy is ±4℃. The stress-strain results, macro- and microstructures of SiO_2-based ceramic cores were investigated experimentally. The microstructures were characterized by the scanning electron microscope (SEM). The elastic moduli of ST25, ST700, ST1100, and ST1400 are 2726.39MPa, 2259.19MPa, 2316.82MPa, and 1441.87MPa, respectively. With the increase of the temperature, the elastic modulus of the SiO_2-based ceramic core shows a decreasing trend. There is a small change in the range of 25~1100℃, while the elastic modulus decreases rapidly at the range of 1100~1400℃. The stress-strain curve of ST1400 at the viscoplastic stage is narrow, indicating that the high-temperature experimental result achieves high repeatability and reproducibility. However, the overall high-temperature mechanical property of the sample ST1400 decreases significantly. The SiO_2-based ceramic core samples are all brittle fractures, but when the temperature exceeds 1400℃,there are almost no cleavage fractures in SiO_2 particles of the ST1400 fracture, and there are some dimple-like $ZrSiO_4$ sections. The mechanical behavior of the SiO_2-based ceramic cores is characterized by thermo-viscoelastic and viscoplastic property. In the high temperature environment of 1400℃, the main reason for the viscous slip of the SiO_2-based ceramic core samples is that the surface of the fine SiO_2 particles is initially melted, which plays a role in lubrication between large particles. The SiO_2, which is initially melted at a temperature of 1400℃, adheres to the surface of the large SiO_2 particle. When the temperature drops further to the room temperature, it combines with the large particles to form a unitary body.

10:05-10:25

Application of Combined HIP and High Pressure Heat Treatment for Superalloy Post Processing

Chuanlong Hao[1], Anders Eklund[1], James Shipley[1]
1. Quintus Technology, China

Since the middle of the 20th century, due to the increase of the operating temperature of the aero-engine, high temperature properties of the turbine blade and turbine disk alloys has been further demanded. High temperature properties like fatigue, creep, fracture toughness, damage tolerance and reliability become more and more important. The mechanical properties of superalloys depend strongly upon the state of microstructure, which, in turn, is controlled by the chemical composition and the processing conditions. The volume of strengthening phase like gamma prime, double gamma prime phase etc. Of the service alloys has been increasing as alloying continuously increased. Meanwhile, forming problems arise as well as the data scatter increases. Investment casting and additive manufacturing in place of forging becomes a tendency for those critical components. These forming methods may have defects such as porosity, segregation, shrinkage, and microcracking. Hot Isostatic Pressing (HIP) is a technology that has been around for 60+ years. By using high temperature and high gas pressure, defects like porosity, shrinkage and microcracks will be elimilated. Later developments include rapid cooling and rapid quenching to enable higher productivity and high pressure heat treatment (HPHT). A modern HIP system today has a great flexibility and can cool with up to 4500℃/min under pressures up to 200MPa. These capabilities make it possible to heat treat a great array of different materials and alloys. In this presentation, the combination of hot isostatic pressing and high pressure heat treatment with fast quenching in one cycle for the alloy 718 and ERBO-1 shows defects like porosity, shrinkage has been eliminated, microstructure and mechanical properties improved. In the case of alloy 718, Inconel 718 was fabricated by selective laser melting (SLM) and subsequently subjected to different heat treatments. The one with HIP plus treatment eliminate the porosities and satisfied the properties required by the specification of their corresponding forged and casted parts. In the case of ERBO-1, the application of hot isostatic pressing for heat treatment of the single-crystal Ni-base superalloy ERBO/1. An integrated heat treatment consisted of solutioning and aging in the HIP incorporation of quenching, was successfully applied. It led to smaller γ'-particle sizes and narrower γ-channels compared to the conventionally heat-treated material and almost no porosity. It is thus proved that the combination of hot isostatic pressing plus heat treatment is a good way for post processing for those alloys.

10:30-10:45 Tea Break

Chairs:
Qiang Feng, University of Science and Technology Beijing, China
Sammy Tin, Illinois Institute of Technology, USA

10:45-11:10 Invited

Microstructural Evolution of Ni-Based K403 Alloy During Thermal Exposure

Jiehua Li[1]
1. Montanuniversität Leoben, Austra

The microstructure evolution of Ni-based K403 superalloy as a function of thermal exposure temperature and time has been investigated by a correlative characterization

mehtod, including scanning electron microscopy, electron backscatter diffraction, transmission electron microscopy, high-angle angular dark-field scanning transmission electron microscopy (HAADF-STEM) imaging and electron energy loss spectroscopy (EELS) as well as atom probe tomography. The as-cast microstructure shows a typical dendritic structure and consists of a γ solid solution, γ' phase, (γ + γ') eutectic phase and a metal carbide (MC) phase. After thermal exposure at 800˚C or 950˚C for up to 200h, the typical dendritic structure was still observed. However, the MC carbides were partially decomposed and further transformed to the M_6C phase and $M_{23}C_6$ phase. Furthermore, the size of γ' was increased from 302.88 ± 20.49nm to 374.75 ± 29.76nm (800˚C, 50h) and 751.73 ± 123.14nm (950˚C, 50 h), respectively. The morphology of γ' was changed from cubic to triangular or round. A topologically close-packed (TCP) σ phase was observed after thermal exposure at 800˚C for 100h or 950˚C for 50h. More interestingly, an in-situ phase transformation of the σ phase to other TCP phase (i.e. P phase) was also observed after thermal exposure at 950˚C for 50h. The present investigation provides a better understanding on the high temperature performance of the Ni-based K403 superalloy, which is essential to predict the failure and thereby enhance the reliability and service life of the K403 Ni-based superalloy.

11:10-11:30

Design of Ni-Base Superalloys for Additive Manufacturing

Sammy Tin[1]
1. Illinois Institute of Technology, USA

Additive manufacturing techniques can now be utilized as innovative tools that provide unlimited design flexibility for the fabrication of geometrically complex metallic structures. For production of Ni-base superalloy components used in advanced gas turbine engines, these techniques may enable transformational design concepts and contribute to the development of ultra-efficient power systems for aerospace propulsion, space exploration and power generation. One of the major challenges associated with additively manufactured Ni-base superalloy components is that the extreme temperature gradients encountered during processing negatively impact the underlying microstructure and mechanical properties of the material. Although the macroscopic shape and chemistry of the additively fabricated part may be identical to the conventionally manufactured part, the resulting properties are usually compromised. In an effort to make Ni-base superalloys more amenable for processing via additive manufacturing, varying levels of benign inoculants that promote heterogeneous grain nucleation were blended into IN718 powder feedstock and used for powder bed selective laser melting (SLM) trials. For nominally identical processing conditions, varying levels of metal, intermetallic and reactive oxide particles comprised of elements common to Inconel 718 were systematically blended with the powder feedstock and used to additively build structures in a directed metal deposition (DMD) system. The effectiveness of these inoculants on modifying the resulting grain structure of the fabricated structures was evaluated using advanced characterization techniques. Selected inoculants were found to reduce the average grain size and grain size distributions in as-fabricated specimens. The effectiveness of these inoculants on modifying the resulting grain structure during additive manufacturing will be discussed.

11:30-11:50

Characterization of High-Entropy-TLP Joints of a Single Crystal Superalloy

Lu Chai[1], Jinbao Hou[1]
1. AVIC Manufacturing Technology Institute, China

When the misorientation angle of base metal was more than 10° , there would be second-phase particles distributed in grain boundaries, and thus resulting in poor mechanical property of joint; moreover, the characteristics of joint did not change with base metal misorientation in this case. In order to reduce the detrimental effect of base metal misorientation on the performance of a nickel-based single crystal TLP joint, the insert metal composition and bonding process for the purpose of obtaining high-entropy-TLP joints were designed. Microstructural and compositional analyses were performed using a scanning electron microscopy (SEM). Electron back scattering diffraction (EBSD) approach was applied to determine the crystallographic orientation of the joints. The results show that, there are also high-angle grain boundaries and compounds at the joint center. Under the condition of random base metal misorientation, with the newly designed insert metal and bonding process for joining, joints with significantly improved performance can be obtained. The high entropy component reduces the formation of the compound to a certain extent, and significantly weakens the detrimental effect of grain boundary and compounds on joint performance. Mechanical property tests at elevated temperatures have been done to determine the joints' quality. High temperature creep rupture strength (for 100h at 980˚C) could achieve no less than 150Mpa, and tensile strength (at 980K) of the joints could attain 670MPa.

11:50-12:00

Best Poster Award Ceremony

12:00-12:05

Closing Remarks

C1. Light Metals and Alloys-Aluminum: V

Symposium Organizers :

Baiqing Xiong, GRINM Group Co. Ltd., China; Yoshihito Kawamura, Kumamoto University, Japan; Young Min Kim, Korea Institute of Materials Science (KIMS), Korea; Jian-Feng Nie, Monash University, Australia; Diran Apelian, Worceste Polytechnic Institute, USA

Thursday AM Room: Presidium Conference Room (4th Floor)
August 22, 2019 Symposium: C1

Chair:
Kenji Matsuda, University of Toyama, Japan

8:35-9:00 Invited

Existence of Two Phases in Al-Zn-Mg Alloys Containing Cu

Kenji Matsuda, University of Toyama, Japan

We have proposed the existance of the universal clusters in age-hardenable aluminum alloys, for example, Al-Cu-Mg, Al-Mg-Si, and Al-Zn-Mg alloys. The effect of Cu-addition on age-hardening and precipitation in Al-Zn-Mg alloys has been investigated by hardness measurement, tensile test, High Resolution Transmission Electron Microscopy (HRTEM) and Annular Dark Field Scanning Transmission Electron Microscopy (HAADF-STEM) techniques. Higher hardness, strength, and lower elongation were caused by increasing amount of Zn + Mg because of increased number density of precipitates. Cu addition also provided even higher peak hardness, strength, and lower elongation. The alloy containing highest Cu content had fine precipitates of GPB-II zones or the second clusters which we proposed, in the precipitate free zones (PFZs) and the matrix, together with η'/η in the matrix from the early stage of aging. Two regions have been confirmed as the PFZs: (i) nearest to grain boundary about 70nm in width and (ii) conventional PFZ about 400nm in width which can be confirmed by conventional TEM. The conventional PFZ contains fine precipitates consisting of GPB-II zones or the second clusters, even for 2 minutes of aging at 473K which were not present in the PFZ nearest to grain boundaries. The fine precipitates, GPB-II zones or the second clusters in the conventional PFZ and the matrix disappeared at overaged condition.

9:00-9:20

Role of Subgrain Stripe in the Exfoliation Corrosion Behavior of Al-4.6Mg-3.1wt%Zn Alloy

Qingwei Ding, Di Zhang, Jishan Zhang, University of Science and Technology Beijing, China; Linzhong Zhuang, University of Science and Technology Beijing, China / TaTa Steel, 1970 CA Ijmuiden, Canada

As a kind of inhomogeneous microstructure generated during dynamic recovery after plastic deformation, subgrain stripe has a significant effect on the properties of high alloying aluminum alloys. However, few attentions have been paid on the effect of exfoliation corrosion (EXCO) behavior. In this study, the effect of subgrain stripe on the EXCO behavior of Al-4.6Mg-3.1wt%Zn alloy has been elucidated. The studied alloy sheets have been solid solution treated at 495℃ for 50min and 1440min before artificial aging treatment respectively to obtain the microstructures with different volume fractions of subgrain stripe. Then the EXCO test of both status samples were carried out in the test solution for different immersing times. The observations showed that both samples were suffered with corrosion, but the corrosion rate of the sample with abundant subgrain stripes in its microstructure was much faster than the other sample with lower volume fraction of subgrain stripes, so that the final EXCO rating was much higher after 48h corrosion. These phenomena were also proved by the electrochemical analysis that the sample with higher volume fraction of subgrain stripe in its microstructure has more than twice of the corrosion current compared to the other sample. To reveal the mechanism of the difference mentioned above, the interfaces of the samples after EXCO test were divided into two groups and observed under electron backscattered diffraction and transmission electron microscopy respectively. One is the normal grain boundary and the other special interface is defined as the interface between subgrain stripe and the normal grain. It was proposed that the higher residual stresses and strains were generated at the special interface than that of normal grain boundary in the studied alloy. This kind of special interface acted as a fast track for the propagation of corrosion during the EXCO test, which accelerated the corrosion rate of the alloy.

9:20-9:40

Differences in Microstructure and Mechanical Characteristics of Al Alloy Sheet Containing RE Element Produced by Strip and Direct Chill Casting

Seonghyeon Yoo, Heon Kang, Hojun Park, Namhoon Goo, Hyundai-steel, Korea

Aluminum alloy has been spotlighted as a light-weight

structural material in automotive industry and its application to sheet material for vehicle has recently been expanded due to environmental regulation and reduction weight of automotive. Among the Al alloys, heat-treatable Al 6000 series alloy has been most studied for vehicle because it has sufficient ductility after solution treatment and high strength after a baking process. The Al 6000 series alloy sheet requires high plasticity and uniform formability to form complex shape and alloy design and processes are being studied to satisfy these properties.

Recently, rare earth metals (RE) which were mainly used in Mg alloys, are used as the Al alloy element because the RE element can improve the strength and plasticity of Al alloy by refinement and sphericalization of eutectic and secondary phases. The general methods of producing aluminum alloys are D.C (direct chill) casting and strip casting. For D.C casting, the Al alloy sheet produced through many process such as casting, grinding, heat-treatment, hot rolling and cold rolling. In other hand, the strip casting has several advantages such as low process cost and minimized hot rolling process result that it is possible to control the texture rather than D.C casting.

In this study, the Al alloy containing RE element (Ce, La) with high formability were designed for automotive sheet in lab-scale. Furthermore, the Al alloy sheet also produced using the conventional D.C casting and strip casting in pilot-scale. The microstructure and texture of produced Al alloy sheets by lab and pilot-scale processes analyzed using a OM (optical microscope), SEM (scanning electron microscope) and EBSD (electron backscattered diffraction). The tensile test conducted using a UTM (universal testing machine) based on ASTM standards. The mechanical properties of the produced Al alloy sheet improved compare to conventional Al alloy. The strengthening mechanism of the RE element and effects of strip and D.C casting processes on mechanical properties and texture of Al alloy sheet will be more detail discussed.

9:40-10:00

The Correlation between Stored Energy on Localized Corrosion Development of Aluminium Alloys

Xinxin Zhang, Huazhong University of Science and Technology, China / University of Manchester, United Kingdom; Zehua Dong, Huazhong University of Science and Technology, China; Xiaorong Zhou, University of Manchester, United Kingdom

High strengthen aluminium alloy was widely used as structural components of transportation industry due to its high strengthen weight ratio and low manufacturing cost. However, high strengthen aluminium alloys were not immune to localized corrosion, especially in chloride-containing environment, which could lead to catastrophic result. Therefore, extensive attention was attracted to advance the understanding of localized corrosion behaviour in aluminium alloys to ensure the transportation safety.

In the present work, the correlation between stored energy distributions with localized corrosion development in AA2024-T351, 2A97-T8 and AA6082-T6 aluminium alloys was investigated. Scanning and transmission electron microscopes were employed to characterize the corrosion morphology of aluminium alloys. Electron backscatter diffraction analysis was conducted at the localized corrosion site to correlate stored energy distribution to the development of localized corrosion. It is revealed that localized corrosion occurs in aluminium alloys in forms of intergranular attack and crystallographic pitting, which tends to occur in the regions with higher levels of stored energies in all three alloys, suggesting that region with higher stored energy exhibiting higher localized corrosion susceptibility and vice versa.

The correlation between stored energy distribution and localized corrosion development may be associated with the combined effect between thermodynamic stability and precipitation behaviour during the thermomechanical process of aluminium alloys.

10:00-10:20

Liquid Phase Separation of Ternary Al-Sn-Cu Immiscible Alloy within Three Orthogonal Ultrasounic Field

Wei Zhai, Bingbo Wei, Northwestern Polytechincal University, China

Applying power ultrasound during solidification has proven to be an effective way to improve the microstructure and enhance the mechanical properties of metal alloys. The most popular way for introducing ultrasound is to insert a vibrating ultrasonic horn into the solidifying liquid alloys. However, the disadvantage of this one dimensional ultrasound method is that the ultrasonic effects are always confined to a limited volume, beyond which weak or even no influence on the microstructures takes place.

To overcome the disadvantage of one dimensional ultrasound, in the present work, we propose firstly by numerical simulation that the employment of three orthogonal ultrasounds can greatly enhance the sound pressure level and enlarge the cavitation volume which may strengthen the effect of ultrasounds on the resultant microstructure. Then, we experimentally apply three orthogonal ultrasounds during the liquid phase separation process of ternary Al71.9Sn20.4Cu7.7 immiscible alloy. In contrast to the layered structure caused by the large density difference between the two immiscible liquid (Al) and (Sn) phases, a uniform microstructure consisting of

fine secondary (Sn) phase dispersed on Al-rich matrix is fabricated in the whole alloy sample with a large size of 30mm×30mm×100mm. Theoretical analyses indicate that the coupled effect of three ultrasounds promotes the sound pressure level and consequently enlarges the cavitation zone within the alloy melt. The strong shockwaves produced by cavitation prevent the (Sn) droplets from coalescence, and keep them suspended in the parent Al-rich liquid phase. This accounts for the formation of homogeneous composite structures. Thus the introduction of three orthogonal ultrasounds is an effective way to suppress the macrosegregation caused by liquid phase separation and produce bulk immiscible alloys with uniform structures.

10:20-10:45 Tea Break

10:45-11:05

Interfaces in Graphene Reinforced Aluminum Matrix Composites

Haiyan Gao, Min Li, Jun Wang, Baode Sun, Shanghai Jiao Tong University, China

Facing with the urgent demand for conductive materials of high strength, high electrical conductivity and light density, graphene reinforced aluminum matrix composites has attracted great attention in recent years due to the excellent mechanical and electrical performance of graphene. Aluminum matrix composites reinforced with graphene nanoplatelets (GNPs) were prepared by continuous casting and subsequent rolling. The ultimate tensile strength of Al-0.2wt.% GNPs composites was about 36.8% higher than that of pure Al with the same casting and rolling process with the conductivity of the composites decreased slightly, indicating that interface scattering between Al and GNPs is very limited. The investigation results show that Al-GNPs composite is potential for high strength and high conductivity application. Better understanding of the interface is the key to achieving graphene/Al composites with superior performance. To investigate the phase composition and interface bonding between Al matrix and GNPs and evolution of interface structure during deformation, graphene nanoplatelets and Al matrix in Al-GNPs composites prepared by ball milling, spark plasma sintering (SPS) and subsequent hot extrusion. High resolution transmission electron microscopy (HRTEM) was used for interface observation. Tensile tests were carried out on as-SPSed and as-extruded GNPs/Al composites to evaluate the interface strength. 5-layered interfaces Al/Al_2O_3/GNPs/Al_2O_3/Al were observed in the as-SPSed composites and some fresh GNPs/Al interfaces formed after hot extrusion and led to the formation of 7-layered interfaces Al/Al_2O_3/GNPs/Al/GNPs/Al_2O_3/Al. No evidence of Al_4C_3 were found in the interface. However, stacking faults were observed in the Al matrix near the interfaces resulted from high stress formed during SPS. Individual GNPs engulfed inside the Al grains was observed after extrusion, indicating the good wetting between Al with amorphous Al_2O_3 layer on the surface and GNPs. The composite deformation and load transfer across the interfaces contributed by the multilayered structure were confirmed by strengthening analysis.

11:05-11:25

High Strength, High Ductility 7xxx Series Aluminum Alloys

Hojun Park, Heon Kang, Seonghyeon Yod, Nam Hoon Goo, Hyundai-Steel, Korea

Aluminum demand for automobile industry has been rising recently due to the increasing demand for light weight of automobile bodies. Technological developments have been actively carried out to overcome the limitations of mechanical properties and productivity of automobile aluminum sheets and to secure economical applicability. In the case of automobile bumper beams, 6xxx series and 7xxx series aluminum alloys are mainly used. In recent years, study has been carried out to increase the productivity through the rolling process by improving the formability of alloys due to the preference of 7xxx series (Al-Zn-Mg) alloys with higher yield strength. Al-Zn-Mg has a disadvantage in that it has difficulty in cold forming because of its high strength but lack of ductility. In this study, by adding Cu and Si elements to Al-Zn-Mg alloy, the alloys with yield strength of 340MPa or more and elongation of 15% or more were developed under T6 condition to secure high strength and high ductility. Through the thermodynamic simulation, the phase composition, amount and the solidification behavior were predicted, and the sheet was fabricated through rolling process after gravity casting. The effects of additive elements on the microstructure of homogenization, solution treatment and artificial aging were analyzed and mechanical properties and formability were evaluated. Optimum heat treatment conditions for improving the yield strength and elongation were derived by controlling the precipitation behavior of the $MgZn_2$, Al_2Cu, Mg_2Si and other phases and the microstructures such as grain size and crystal structure. In addition, Alloys were fabricated by twin roll casting (TRC) process and direct chill cast (DC) process, and the properties and microstructure were compared and evaluated. The mechanical properties were evaluated by tensile strength and the microstructure was analyzed by optical microscopy (OM), scanning electron microscopy (SEM), X-ray diffraction (XRD), electron backscattered diffusion (EBSD) and transmission electron microscopy (TEM) .

C2. Light Metals and Alloys-Magnesium: V

Symposium Organizers:

Xianhua Chen, Chongqing University, China; Yoshihito Kawamura, Kumamoto University, Japan; Young Min Kim, Korea Institute of Materials Science (KIMS), Korea; Jian-Feng Nie, Monash University, Australia; Diran Apelian, Worceste Polytechnic Institute, USA

Thursday AM
August 22, 2019

Room: 406 (4th Floor)
Symposium: C2

Chairs:
Daisuke Ando, Tohoku University, Japan
Xianhua Chen, Chongqing university, China

8:30-8:45

Forming Characteristic of Wrought Magnesium Alloy Sheet during Cold Roll Forming

Hisaki Wwtari, Ryohei Suzuki, Harunori Kobayashi, Toru Shimizu, Tokyo Denki University, Japan; Yuji Kotan, Gunma Industrial Research Centre, Japan

In recent years, expectation to innovate lightweight technologies for reducing carbon dioxide emission has been gradually increasing. Under such circumstances, lighting technologies which can reduce products weights by using light metals such as aluminum alloys and magnesium alloys has been attracting much attention. However, there are few practical examples of magnesium alloy products in automotive industries although the magnesium alloy can be recognized that it can contribute to reduce product weight dramatically because the specific weight of magnesium alloys are two third of aluminum alloys. There are three barriers in practical use of the magnesium alloys. The following three reasons are considered to be main problems for overcoming the difficulties of magnesium alloys, namely, (i)The prices of magnesium alloys for plastic working (wrought magnesium alloys) are normally very expensive. (ii)Magnesium alloys have poor workability at room temperature due to its crystal structure (hexagonal closed pack). (iii)There are not so much established manufacturing technologies in forming magnesium alloys when in considering large scale production at room temperature, die casting is only practical process for large scale production at high temperature. Over the past years, although the production of magnesium has gradually increased, the production of magnesium alloy plates (wrought magnesium alloy sheet) has remained at a very low level at practical level, which is far from the recent dramatic change in automotive manufacturing industries.
One of the authors has been investigating into possibilities magnesium alloy sheets (wrought magnesium alloy sheet) by using cold roll forming process while considering future possibilities of cold roll forming of wrought magnesium alloys. If cold forming of the magnesium alloy is possible, it can greatly contribute to establishing the manufacturing process which can reduce the product weight while maintaining the strength of the product.
The aim of the present work is to establish the roll forming of wrought magnesium alloys, which have complicated stress-strain curves of tension–compression asymmetry. Firstly, a three-dimensional elasto-plastic analysis in simple V bending process by finite element method has been conducted to investigate into effect of stress-strain curves in tension and compression on simple V bending process. Secondary, after the testing of the V-bending simulation which can consider different stress-strain curves in tension and compression state, a finite element analysis for V-section during cold roll forming of a wrought magnesium alloy has been performed. A simple V-sections were formed by a tandem six stands roll forming machine to demonstrate effectiveness of the proposed simulation method which can consider stress-strain curves of tension–compression asymmetry. The variation of longitudinal strain as well as bending strain in width direction at bent corner were shown by suing finite element simulation. Spring back analysis has been conducted to investigate exact cold roll forming phenomenon for wrought magnesium alloy sheets.

8:45-9:00

Four-Point Bending Behaviour of Hot-Rolled Mg-0.8Zn-0.4Ca Alloy

Kourosh Tavighi, Chris H. J. Davies, Monash University, Australia

Complex stress states are a feature of engineering applications. We studied the effects of grain size on the four-point bending behaviour of hot-rolled Mg-0.8wt.%Zn-0.4wt.%Ca strips with a thickness of 0.9mm. Microstructural evolution was examined in the through-thickness direction of the strip because the stress state changes from tension to compression through the thickness when subjected to bending. Grain sizes were selected to give ratios of sample thickness to grain size over two orders of magnitude. Strips were heat treated at 400˚C, 470˚C and 490˚C for 2 hours, leading to grain sizes of 11.7μm, 29.4μm and 76.1μm, so there are 80, 30 and 10 grains at the strip wall approximately. The original material has a grain size of 6.2μm resulting in the presence of 145 grains at the wall.
This work explores the relationship between increasing grain size (decreasing thickness to grain size ratio), microstructural evolution, and mechanical response of the alloy using electron backscattered diffraction metallography of areas close to the tensile surface, near the neutral axis, and close to the compressive surface of the strip. Implications are explored for the design,

manufacture, and deployment of magnesium alloy thin-walled structures, with particular reference to cyclic loading conditions.

9:00-9:15

Atomic and Electronic Basis for the Solutes and the Planar Faults Strengthened Mg Alloys

Yi Wang, Bin Tang, Jun Wang, Hongchao Kou, Jinshan Li, Northwestern Polytechnical University, China; Shunli Shang, Yi Wang, Zikui Liu, Pennsylvania State University, USA; Laszlo J. Kecskes, Johns Hopkins University, USA; Suveen N. Mathaudhu, University of California, USA; Xidong Hui, University of Science and Technology Beijing, China

Mg alloys, being the lightest metallic structural materials, are particularly attractive for transportation applications such as automobiles and aircrafts for weight reducing and higher fuel efficiency and biocompatible and biodegradable features ideal for implant applications. The improvement of both the strength and the ductility is still a challenge in the development of advanced Mg alloys. Recent works have shown that the fault layers enriched of solute atoms could stabilize the long period stacking ordered (LPSO) structures described by a common structural unit composed of local FCC-type stacking sequence and improve the mechanical properties of Mg alloys. Here we show the strategies to strengthen Mg alloys through modifying the matrix by planar faults and optimizing the local lattice strain by solute atoms. The anomalous shifts of the local phonon density of state of stacking faults (SFs) and long periodic stacking ordered structures (LPSOs) toward the high frequency mode are revealed by HCP-FCC transformation, resulting in the increase of vibrational entropy and the decrease of free energy to stabilize the SFs and LPSOs. Through integrating bonding charge density and electronic density of states, electronic redistributions are applied to reveal the electronic basis for the "strengthening" of Mg alloys.
Moreover, the atomic and electronic basis for lattice-distortion-mediated formation of stacking faults, i.e., localized face-centred-cubic (FCC) structures, within a Mg-Zn-Y alloy with a hexagonal close-packed (HCP) structure. The atomic motion trajectories from ab-initio molecular dynamic simulations show that the Mg atoms occupying the nearest neighbour positions of Zn and Y solute atoms undergo a local HCP-to-FCC transition. It is revealed that a local lattice distortion caused by the solute atoms enables the Mg atoms to move and rearrange into a local FCC configuration, which is validated by high resolution scanning transmission microscopy and in-situ synchrotron X-ray diffraction. Our simulations provide profound insight into the formation mechanism of stacking faults in HCP Mg and their physical nature of phase transformations; this is not only critically important because conventional defects, such as dislocations and vacancies, are important to deformation are rare for Mg and its alloys, but also because they serve as a potential new approach to the design of advanced Mg alloys when defects are actually phase transformations.

9:15-9:30

Microstructure Observation of Sc Added Mg-Y Alloy with Aging at 473K

Tomoya Hiragi, Taiki Tsuchiya, Seungwon Lee, Susumu Ikeno, Kenji Matsuda, University of Toyama, Japan

Magnesium (Mg) has been widely used as structural materials, for example, frame of electrical devices, parts of automobile, due to its light weight. Several reports are available about addition of rare-earth element (RE) on Mg, and Mg alloys show precipitation hardening by aging treatment of super saturated solid solutions (S.S.S.S.). Lorimer et al. reported the precipitation sequence in Mg-Y alloys aged at 473K as S.S.S.S. → β"(D019) → β'(cbco) → β(Fm-3m). Scandium (Sc) addition on Mg alloy is known that it enhances a heat resistance.
This study uses high-resolution transmission electron microscopy (HRTEM), selected-area electron diffraction (SAED) pattern and energy-dispersive X-ray spectroscopy (EDS) to identify the crystal structure of a metastable phase in a Sc-added Mg-Y alloy, which we compared with the crystal structure of the β' phase in binary Mg-Y alloy.
Mg-3.6at.%Y and Mg-3.5at.%Y-0.9at.%Sc used in this study were prepared by casting using 3N Mg ingot, 3N Y and 2N Sc chips. The fabricated alloys were homogenized at 773K for 43.2ks and then hot-rolled at 773K. The hot-rolled sample were subjected to solution heat-treated at 773K for 3.6ks in an argon gas atmosphere. Then, quenched into water of 293K, and aged using a silicone oil bath at 473K. TEM samples were thinned by the twin-jet electro polishing technique using a solution of 10% perchloric acid-ethanol at 253K. For HRTEM observation was conducted using TOPCON EM-002B, under the applied voltage of 120kV. HRTEM simulation images were calculated using the multi-slice method. Simulation images are obtained for each defocus and TEM sample thickness. The model used for the HRTEM simulation using a rectangular cell of 1.92nm x 2.22nm x 0.52nm including 96 atoms based on the hcp structure of Mg by MacTempasX. HRTEM images and HRTEM simulation images contrast were measured using Gatan Digital Micrograph software.
In HRTEM observation, zig-zag structure and pre-β" were observed. Also, both precipitates were confirmed in SAED pattern as diffuse spots in the early stage of aging. SAED and HRTEM images of the β' phase in the Sc added Mg-Y alloy were similar to those of the β' phase in the binary Mg-Y alloy. However, Sc-added alloy, β' showed different lattice parameter with close

inspection of SAED and HRTEM images. Also, first principle calculation and HRTEM simulation were conducted to understand the effect of Y and Sc addition on precipitates.

9:30-9:45

Study on Microstructure and Creep Behavior of T6 State Mg-15Gd Metal Mold Casting Alloy

Shuxia Ouyang, Guangyu Yang, Wanqi Jie, Northwestern Polytechnical University, China

Microstructure and creep behavior of T6 state Mg-15Gd metal mold casting alloy were studied. The experimental alloy was composed of α (Mg) matrix, short rod-like MgGd phase, lath β' precipitates, square shaped GdH2 phase and a small amount of undissolved Mg5Gd phase. It was found that the creep strain and the creep rate of the experimental alloy increased but the creep life decreased with increasing the creep temperature and the applied stress. At a fixed creep temperature of 260℃, when under the low applied stress range of 50~80MPa, the calculated n value is about 2.6, indicating the creep deformation may be controlled by dislocation slip; when under the high applied stress range of 80~90MPa, the calculated n value is about 4.8, indicating the creep deformation may be controlled by dislocation climb. Meanwhile, under a defined creep stress of 50MPa, when in the low temperature range of 235~260℃, the calculated Qc value is about 80KJ·mol^{-1}, which is close to the grain boundary diffusion activation energy (60~80KJ·mol^{-1}), suggesting that the grain boundary sliding may be a dominant affecting factor; when in the high temperature range of 260~300℃, the calculated Qc value is about 141KJ·mol^{-1}, which is close to the self-diffusion activation energy (130~135KJ·mol^{-1}), suggesting that the dislocation climb may be a dominant affecting factor. Furthermore, not only the α (Mg) grain size but also the quantity and the size of precipitated phases of the experimental alloy increased with the increase of the creep stress, the creep temperature and the creep time.

9:45-10:00

Achievement of Excellent High-Strain-Rate Superplasticity and Low- Temperature Superplasticity through Low-Angle Boundary Formation in a Mg-Y-Zn Alloy with the Icosahedral Phase

Taejin Lee*, Woojin Kim*, Hongik University, Korea

Severe plastic deformation by high-ratio differential speed rolling (HRDSR) with different roll speed ratios (2 and 3) was applied to cast Mg-Y-Zn alloys with the icosahedral phase (I- phase) at low temperatures. During the HRDSR process, the I-phase network structure was fragmented. The roll speed ratio of 3 provided a higher degree of refinement and dispersion of the I-phase than the roll speed ratio of 2, but a high portion of the refined I-phase particles were agglomerated along the rolling direction. Two types of microstructures with ultrafine grains (~ 1m) were obtained, depending on the roll speed ratio. The material with the first type of microstructure (produced at the roll speed ratio of 2), which consists of ultrafine grains with low-angle boundaries, showed both low-temperature superplasticity (LTSP) at temperatures below 0.5Tm (Tm: melting temperature) and high-strain-rate superplasticity (HSRS) above 0.5Tm. The material with the second type of microstructure (produced at the roll speed ratio of 3), which consists of ultrafine grains (~ 1m) with a high portion of high- angle boundaries (i.e., a mixture of low- and high-angle boundaries), showed a better LTSP than the material with the first type of microstructure but did not show HSRS at temperatures above 0.5Tm. At low temperatures, grain boundary sliding occurred more readily along the high-angle grain boundaries than along the low-angle grain boundaries, leading to a better LTSP in the material with the first type of microstructure. At high temperatures, suppressing grain growth during the sample heating and holding stages for tensile testing or during tensile deformation was important in achieving HSRS. Rapid grain coarsening occurred in the material with the first type of microstructure during the sample heating and holding stages at temperatures above 0.5Tm, leading to the loss of HSRS. In the material with the second type of microstructure, however, the fine-grained microstructure could be maintained during the sample heating and holding stages. This was because low angle boundaries have a lower energy compared to high angle boundaries, such that the formers have a reduced driving force for grain growth. The dispersion of agglomerated I- phase particles into the matrix during deformation, which was promoted by grain boundary sliding, was also equally important in achieving HSRS from the material with the second type of microstructure. This was because as the fine I-phase particles were dispersed during deformation, the pinning effect of I-phase particles increased, resulting in an effective suppression of dynamic grain growth of the fine grains.

10:00-10:15

Evolution of Texture and Microstructure during Deep Drawing of Magnesium Alloys

JaeHyung Cho, Geon Young Lee, SangHo Han, Korea Institute of Materials Science, Korea

Ingot and twin-roll casted Mg-Al-Mn magnesium sheets were characterized in detail using EBSD and TEM and deep drawing was carried out at elevated temperatures. Initial sheets fabricated by twin-roll casting possessed smaller particles than those fabricated by the ingot-casting method. The twin-roll casted sheets possessed smaller grain sizes and weaker basal intensity levels than the ingot-casted sheets. Strength and elongation

at room temperature for the twin-roll casted sheets were greater than those of the ingot-casted sheets. At an elevated temperature, the ingot-casted sheets showed better elongation than the twin-roll casted sheets. Working temperatures and deformation rates during the deep drawing process were 225℃ to 350℃ and 30mm/min to 50mm/min, respectively. During deep drawing, most thinning of the drawn cups was observed near the bent areas, and most thickening occurred near the top flange. At working temperatures between 225℃ and 350℃, IC sheets revealed a better drawability than TRC sheets. Twinning and dynamic recrystallization were frequently found in the top flanges of the cups. The deformation rate is important to activate tensile twins both near bent and flange areas. The working temperature is important to produce the refined grain structure caused by DRX in the flange.

10:15-10:30

Low Cost Preparation of Ultrafine AZ31 Magnesium Alloy

Peng Peng, Aitao Tang, Jia She, Xiaoxi Mi, Fusheng Pan, Chongqing University, China

Grain refinement is very important to magnesium alloys due to the higher k value in Hall-Petch relationship compares to the Fe, Al alloys. The severe plastic deformation methods to fabricate ultrafine grain structure (UFG) structure are complicated and high cost. To date, preparation of UFG structure in a common extruder is still a great challenge. In this work, double strain was achieved by reducing the billet diameter during the extrusion process, and this novel extrusion process was called continuous forging extrusion (CFE). After CFE, with the increment of equivalent strain, the average grain size of Mg–3Al–1Zn (AZ31) alloy was successfully refined to submicron scale (~0.6μm). The UFG AZ31 alloy exhibited an excellent combination of yield strength of 307MPa and ductility of 26.3%. The formation of submicron grains were attributed to the accelerated dynamic recrystallization process. The CFE process was easy to achieve because the manufacturing equipment was only a common extruder. The low cost process could be industrialized both readily and economically.

10:30-10:45 Tea Break

10:45-11:00

Precipitation and Hardening in Mg-Gd-Y-TM Alloys

Zhenyang Liu, Bin Chen, Xiaoqin Zeng, Shanghai Jiao Tong University, China; Zongrui Pei, Oak Ridge National Laboratory, USA

Mg-Gd-Y-TM (TM, transition metal, here refers to Zn, Ni, Ag) alloys are commonly researched for their superior strength and ductility. One representative Mg-Gd-Y-TM alloy is Mg-Gd-Y-Zn-Zr alloy with its tensile strength above 500MPa with adequate elongation after hot extrusion and aging. On the basis of this alloy, Mg-Gd-Y-Ag-Zr, Mg-Gd-Y-Zn-Ni-Mn and Mg-Gd-Y-Zn-Mn alloys have been developed, in which Ag and Ni replacing Zn totally or partially and/or Mn replacing Zr as grain refiner. Since some solution-treated and aged alloys consisting of solute clusters and early stage precipitates are still not to be fully understood, a clarification could be obtained with the application of Cs-corrected high angle annular dark field - scanning transmission electron microscopy (HAADF-STEM). Here in our work by using this technique these alloys have been characterized at atomic level. Atomic-scale images of Guinier-Preston (G.P.) zone, γ" phase, γ' phase and β' phase have been captured for different states (as-casted, solution-treated, aged) of alloys. Ag was found to promote the formation of γ" phase, which was perpendicular to β' phase in Mg-Gd-Y-Ag-Zr alloys. Inconsistent with previously reported results, Ni turned out not to participate in forming the long period stacking ordered structure (LPSO) in Mg-Gd-Y-Zn-Ni-Mn alloys. Confirmed by first-principle calculation, γ" phase could be distinguished from G.P. zone by their different extents of Mn segregation in as-casted Mg-Gd-Y-Zn-Ni-Mn alloy. As for γ" phase, compared to its rare occurrence in as-casted Mg-Gd-Y-Zn-Ni-Mn alloys its prevalence in long-time aged Mg-Gd-Y-Ag-Zr alloys implied that it was a stable phase rather other a phase formed prior to γ' phase. Isothermal ageing curves showed hardness plateau resulting from the predominance of γ"/γ' phase than β' phase in all the alloys. Our findings deepens the understanding of formation of these phases and effects of TM alloying, which contributes to the development of Mg alloys with better properties.

11:00-11:15

Influence of Continuous Pulsed Current Treatment on the Dynamic Response of Mg/Al Composite Plate Fabricated by Explosive Welding

Xiaoqing Cao, Xuewen Zhang, Xinxiao Zhu, Xiaolei Cui, Peng Lin, Taiyuan University of Technology, China

In recent decades, the research and preparation of laminated metal composite plates have attracted wide attention of scholars and experts due to their excellent physical, chemical and mechanical properties by taking into account the characteristics of its member metal materials. The preparation of Mg/Al laminated composite plates with lightweight, high strength and

corrosion resistance which has both advantages of components metals and achieves the complementary and optimum properties has attracted much attention. Explosive welding has high bonding strength, relatively thin diffusion layer, no porosity and other defects. But there is a little work reported on the dynamic behavior of Mg/Al composite plates especially the one fabricated by explosive welding. In this study, Mg/Al composite plate was prepared by explosive welding with good bonding strength. After explosive welding, Mg/Al composite is usually heat treated (annealing) to eliminate high residual stress from explosive wave, but this process will cause brittle intermetallic compounds between magnesium alloy and aluminum alloy and damaged the property of the composite plate. Continuous pulse current treatment is a useful way which could reduce the detriment according some researchers' work. The magnesium plate and Mg/Al composite plate fabricated by explosive welding were treated by continuous pulsed current with different current density respectively, and their dynamic behavior under different strain rates were tested by Hopkinson pressure bar test system to indicate the effect of pulsed current treat. To clarify the mechanism of pulsed current treat, the microstructure change before and after continuous pulsed current treatment of magnesium and Mg/Al composites were observed by OM, SEM, EBSD. The results showed that Mg/Al composite plate by explosive welding has better response under dynamic condition compared with magnesium plate under both conditions, i.e. with and without continuous pulsed treatment. The results will help to widen the use of magnesium alloy in collision condition such as automobile buffer beam and weapons.

11:15-11:30

Hot Forging Formability of Continuous Cast Mg-Al-Ca-Mn Alloys

Hisaki Wtari, Tokyo Denki University, Japan; Sueji Hirawatari, Fukushima University, Japan; Shiichi Nishida, Gunma University, Japan; Mayumi Suzuki, Toyama Prefectural University, Japan;Toshio Haga, Osaka Institue of Technology, Japan;

The movement that banning the sale of gasoline cars and diesel vehicles especially in Europe and allowing only electric cars for passenger's cars has been accelerated. For examples, Germany's federal council, the Bundesrat, has passed a resolution calling for a ban the sale of new cars with internal combustion engines by 2030. In Norway, until 2025 there is a movement to legislation prohibiting the registration of new cars for passenger car gasoline and diesel cars. Beginning in 2025 in the Netherlands, a bill to prohibit the sale of new cars for gasoline and diesel vehicles was submitted to ongress, ban the sale of new cars with internal combustion engines.

Recently, the European Union (EU) summarized a regulation to reduce carbon dioxide (CO_2) emissions of automobiles in 2030 by 37.5% from 2021 years. Although it is plan to decide concrete reduction width for each car manufacturer in the future, it is considered to be difficult to achieve by improving fuel economy of gasoline cars and hybrid cars. It is considered that manufacturers need to replace about one-third of new cars with electric vehicles (EV) . Under the circumstances, the growing demand for light weight products for automotive industries has been accerelated due to global trend of environmental preservation. Reducing to total weight of cars is one of the solution to achieve the regulation to reduce carbon dioxide (CO_2) emissions.

Reducing total weight of cars is one of the solution to achieve by replacing materials for car bodies from steel to lightweight materials, for examples, aluminum alloys, carbon fiber reinforced plastics (CFRP)and magnesium alloys.

In recent several years, although production of magnesium has risen dramatically, production of magnesium alloy sheet remains still at a very low level in practical use. The major barrier to greatly increased magnesium alloy use has been in still primarily high manufacturing cost as well as poor workability of magnesium alloys. Moreover, it has been recognized that higher strength as well as better corrosion resistance are needed for magnesium products when in practical use for car components. One of the author has been investigating into twin-roll casting (TRC) technology to adopt magnesium alloys into practical use, however detailed forming characteristics during hot forging of high aluminum content magnesium alloys has not been clarified.

The aim of the study is to confirm possibilities of practical use of cast magnesium alloy by continuous cast materials during hot forging with a servo press machine (SDE 1522 by AMADA Corp.) which can apply back pressure during forging. A simple compression test of continuous cast materials was performed to obtain exact stress strain relation in terms of forming temperatures. Double-ringed typed forming products were hot forged at 623K by using a servo press machine. Optical crystal observation as well as Vickers hardness test have been conducted to confirm the recrystallization and material flow. It has been found that manufacturing magnesium products could be possible when in selecting an appropriate manufacturing condition by using a servo press machine.

C3. Light Metals and Alloys: Ti and Others III

Symposium Organizers :

Yongqing Zhao, Northwest Institute for Nonferrous Metal Research, China; Yoshihito Kawamura, Kumamoto University, Japan; Young Min Kim,Korea Institute of Materials Science (KIMS), Korea; Jian-Feng Nie, Monash University, Australia; Diran Apelian, Worceste Polytechnic Institute, USA

Thursday AM | Room: 304 (3rd Floor)
August 22, 2019 | Symposium: C3

Chairs:
Qiaoyan Sun, Xi'an Jiaotong University, China
Lei Li, Northwest Institute for Nonferrous Metal Research, China

8:30-8:55 Invited

Effect of Calcium Treatment on the Control of Inclusions in Al Deoxidized Special Steel

Qiaoyan Sun, Pei Li, Lin Xiao, Jun Sun, Xi'an Jiaotong University, China

Strength and ductility of Ti-55531 (Ti-5Al-5Mo-5V-3Cr-1Zr) alloy with two different microstructures was investigated. The super-refined a precipitates together with grain boundary alpha file from beta solid solution and double aging (M1) and bimodal microstructure (M2) from alpha+beta solid solution and double aging were characterized using transmission electron microscopy, scanning electron microscopy and image analysis software. The results indicate that the samples with M1microstructure show brittle fracture in tensile tests. While the samples with M2 microstructures exhibits ductile fracture in tensile tests. The heterogeneous plastic deformation takes place within different morphology of α during deformation. The grain boundary alphas are softer than the precipitation hardened beta matrix. As a consequence, strain localizes in the beta grain boundary alpha severely and brings about crack and supply a low energy path for crack propagation, which leads to intergranular fracture. The microstructure (M2), including primary α phase together with alpha precipitates in beta matrix and grain boundary alpha, improves the ductility of samples in tensile tests. Slip is the dominant deformation mode in the equiaxed primary alpha in tensile deformation and occurrence of the multiple slip systems release the stress concentration at the equiaxed primary alpha /betatrans interface which delay crack formation. The cracks are difficult to grow in the beta matrix hardened by finer alpha precipitates due to high strength or connect each other because of scattered primary alpha. Therefore, Ti-55531 alloy with equiaxed primary alpha shows trans granular fracture and improvement in ductility is observed.

8:55-9:15

Increasing Mechanical Compatibility of Ti-13Nb-13Zr Utilizing Cold Caliber-Rolling

Taekyung Lee, Pusan National University, South Korea; Chan Hee Park, Korea Institute of Materials Science, South Korea

Good mechanical properties and biocompatiility of Titanium alloys leads to their wide applications in the biomedical industry as bone plate, bone screw, hip joint, and dental implant fixture. Ti-13Nb-13Zr alloy, developed at the early 90s, is an ASTM-registed material for implant applications (ASTM F1713). The developed thermomechanical processing route of this alloy gives rise to an elastic modulus of either 65GPa (after solution treatment) or 80GPa (after solution treatment and subsequent aging). Although these numbers are lower than conventional implant alloys, such as Co-Cr-Mo (227GPa) and Ti-6Al-4V (115GPa), they are still higher than an elastic modulus of human bone (20~40GPa) as well as those of recently developed β-phase Ti alloys including Ti-Nb-Ta-Zr alloy. We propose a novel thermomechanical process to significantly decrease an elastic modulus of Ti-13Nb-13Zr, which is denoted as a cold caliber-rolling (CCR). The solution-treated alloy was subjected to CCR up to 12 passes of deformation to obtain fine-grained microstructure and bulk dimension (>1m). Interstingly, the entire CCR samples showed lower elastic moduli than those fabricated via the ASTM procedure. Furthermore, the value kept decreasing with an increasing number of CCR passes. Such a tendency has been doubly confirmed using an uniaxial tensile test (to caculate the slope of elastic range) and ultrasonic measurement. It should also be noted that the suggested method also enhanced mechanical strength of Ti-13Nb-13Zr alloy to ~1GPa. As a result, the parameter of mechanical compatibility, defined as the ratio of yield strength to elastic modulus, significantly increased after applying the CCR process. This result had not been found in our previous study which utilized a warm caliber-rolling instead of CCR, suggesting that the temperature would play a key role in the enhanced mechanical compatibility. The mechanisms were investigated in light of grain refinement, dynamic recrystallization, texture development, and phase transformation.

9:15-9:35

Microstructure and Properties of Low-Ti Nitinol Powder manufactured by Supreme-Speed PREP

Xiaohao Zhao, Shujin Liang, Yunjin Lai, Qingxiang Wang, Chen Wang, Sino-Euro Materials Technologies of Xi'an Co., Ltd., China

Nitinol, mainly consisting of titanium and nickel, is

categorized as a shape memory alloy that attracts interests in the vast industries of engineering such as aerospace, bio-medical and other basic industries. The characteristics of Nitinol like shape memory property, bio-compatibility, and pseudo-elasticity make it ideal for making medical implants and aerospace additive manufacturing (AM) components. SS-PREP spherical powder is an effective assistance for intricate AM geometric structure, which are impossible to prepare by conventional machining. In this paper, the characteristics (including fluidity and apparent & tap density) and microstructures of three different particle sizes' powders were investigated, including 15~53 μm, 53~106 μm, and 106~150 μm. Owing to various effect of particle size, shape and surface roughness, 53~106 μm powder has best Hall fluidity with 13.97s/50g, apparent densitywith 3.92g/cm^3 ,and tap density with 4.34g/cm^3. Scanning electron microscopy (SEM) photos indicates the coarser particles are, the better sphericity them have. On the contrary, the finer particles were tend to reach egg-like shape. The molten droplet is prone to form dendritic microstructure when its cooling rate is $<2.74\times105K\cdot s^{-1}$ (particle size above 53 μm), while some droplets tend to form smooth martensitic structure when its cooling rate is above $2.74\times105K\cdot s^{-1}$ (particle size under 53 μm). With the increase of particle size distribution from 15~53 μm to 106~150 μm, the tested microhardness reduces from 322.9HV to 286.5HV.

9:35-9:55

TRIP and TWIP as Well as the Influence of ω Phase on These Two Phenomena in a Metastable β Ti Alloy

Minjie Lai, Northwestern Polytechnical University, China; Dierk Raabe, Max-Planck-Institut für Eisenforschung GmbH, Germany; Tong Li, Institute for Materials & ZGH, Ruhr-Universität Bochum, Germany

Metastable β titanium alloys are of particular interest for structural applications in aerospace and biomedical industries. Here, we have investigated the twinning-induced plasticity (TWIP) and transformation-induced plasticity (TRIP) as well as the influence of ω phase on these two phenomena in a metastable β-type Ti–25Nb–0.7Ta–2Zr (at.%) alloy. We set off with two starting states: one is ω-free and the other one contains a high number density ($(3.20\pm0.78)\times1024m^{-3}$) of nanometer-sized (~1.23nm) ω particles. Deformation experiments demonstrate that the plastic deformation of the ω-free alloy is mediated by stress-induced β →α" martensitic transformation, {332} twinning and dislocation slip, where the former two induce joint TRIP and TWIP effects and the latter one carries the majority of the plastic strain. In the ω-enriched alloy, the ω particles fully suppress the TWIP and TRIP effects and promote localization of dislocation plasticity into specific ω-devoid channels. Atom probe tomography analysis reveals that the elemental partitioning between β and ω results in only subtle enrichment of solutes in the β matrix, which cannot sufficiently stabilize the matrix to prevent martensitic transformation and twinning. A new mechanism based on the shear modulus difference between β and ω is proposed to explain the suppression of TRIP and TWIP effects by ω particles.

9:55-10:15

Trace of Yttrium Addition on Refining Prior-Beta Grains of Ti-6Al-4V Alloy

Duyao Zhang, Dong Qiu, Mark Easton, Royal Melbourne Institute of Technology, Australia; David StJohn, University of Queensland, Australia; Mark Gibson, CSIRO, Australia

Grain refining titanium and its alloys during solidification can significantly reduce casting defects, enhance mechanical properties and improve formability in the subsequent thermomechanical process. The potent grain refiner also plays a key role to convert columnar grains to equiaxed grains in additively manufactured Ti components. However, potent grain refiner for Ti alloys is limited in types. In this paper, we will present our recent work on refining prior-β grain of as-cast Ti-6Al-4V alloy though trace additions of yttrium. Pre-mixed elemental yttrium and Ti-6Al-4V powders was cold compacted and then arc melted to button ingot. Microstructures analysis revealed that columnar-to-equiaxed transition (CET) of prior-β grains occurs at certain amount of yttrium additions. The grain refining mechanisms of yttrium inoculation include (i) the grain growth restriction effect from in situ formed nano sized yttria particles, (ii) possible heterogeneous nucleation of β-phase around the micro-sized yttria particles and (iii) superior constitutional supercooling delivered by solute yttrium during solidification. In addition, laser surface remelting was applied on the button ingot and much smaller equiaxed prior beta grains were observed in the melt pool compared to the as-cast sample. It suggests that yttrium could be an efficient β-Ti grain refiner for Ti-6Al-4V alloy for additive manufacturing.

10:30-10:45 Tea Break

10:45-11:05

Quantitative Evaluation of Synergetic Strengthening Mechanisms in Carbon Nanotubes Reinforced Titanium Metal Matrix Composites

Khurram Munir, Cuie Wen, Yuncang Li, RMIT University, Australia

Carbon nanotubes (CNTs) are considered as promising

reinforcement materials for metal matrix composites (MMCs) because of their unique mechanical properties. However, their dispersion in MMCs is challenging because of their tubular morphology, high surface areas, and nano-scale dimensions. Powder metallurgy has emerged as an excellent technique to effectively disperse these CNTs in MMCs. Despite the effective dispersion of CNTs in the MMCs, harsh milling conditions damage the CNTs and eventually CNTs lose their unique properties. In this work, titanium (Ti) metal matrix composites (TMCs) reinforced with multi-walled carbon nanotubes (MWCNTs) were fabricated by powder metallurgy. MWCNTs (0.5wt.% and 1.0wt.%) were dispersed into Ti powders through two different dispersion processes; (i) high energy ball milling (HEBM), and (ii) solution ball milling (SBM) process. The solid-state interfacial reactions between MWCNTs and Ti were controlled through optimizing the dispersion processing conditions. The Ti-MWCNTs powder mixtures were consolidated and sintered at 1100˚C in a vacuum furnace. The graphitization induced strengthening efficiency and various strengthening modes in the fabricated composites were quantitatively characterized. The relationships between the graphitization and the key synergetic strengthening modes were established. The Ti-0.5wt.% MWCNTs composites with in situ formed titanium carbide (TiC) nanorods during HEBM and debundling of MWCNTs during SBM processes exhibited compressive yield strength of 882MPa and 920MPa which demonstrated 18% and 32% increase compared to commercially pure titanium (CP-Ti), respectively. The key strengthening modes included grain refinement, dispersion strengthening of homogenously dispersed MWCNTs and in-situ TiC particles, solid solution strengthening of carbon, oxygen and nitrogen in Ti matrix, and load-bearing strengthening in TMCs.

11:05-11:25

Microstructure Effect on Fatigue Stability and Fatigue Damage Mechanism of a Near β Titanium Alloy Ti7333

Zhihong Wu, Hongchao Kou, Wei Chen, Jiangkun Fan, Bin Tang, Jinshan Li, Northwestern Polytechnical University, China; Xiaoning Han, Ying Deng, AVIC Manufacturing Technology Institute, China

Due to its excellent mechanical and physical properties, including high specific strength, excellent corrosion resistance and high temperature strength, the near β titanium alloy has been widely used in aviation and aerospace fields. For aerospace structures to withstand alternating loads, high cycle fatigue failure is one of the main failure modes. Near β titanium alloys exhibit high fatigue performance causing increased interest in studying the microstructure-fatigue stability relationship and the underlying fatigue damage mechanisms. The material selected for this work is a new near β titanium alloy, Ti-7Mo-3Nb-3Cr-3Al. The thermomechanical processing routes were designed to produce different volume fractions of globular primary-α particles distributed in a matrix of transformed-β structure consisting of very fine secondary-α precipitations. Axial loading fatigue tests were conducted on smooth hour-glass specimens (K_t=1). The tests were run in load-controlled at RT and a lab-air environment, using a sinusoidal waveform with an R ratio of 0.1. A frequency of around 120Hz were used. Results show that the solution aged microstructure renders the alloy with a significantly higher fatigue strength of 927MPa. Besides, the fatigue stability increase with increasing of α_p percentage. The fracture morphologies pointed to at least five categories of fatigue crack-initiation modes: (i) β (isolated α_p) facets; (ii) β (several isolated α_p) facets; (iii) isolated α_p facet; (iv) several isolated α_p facets; and (v) isolated β facet. Furthermore, the formation of compound α / β facets is due to the cleavage fracture of α grains, then the crack propagate to the β grain boundary. In addition, α facets form on or very near basal planes, and β facet form on (110) plane with the maximum Schmid factor.

11:25-11:45

Effect of β Solutiuon Treatment on Microstructure and Dynamic Mechanical Properties of Ti-6Cr-5Mo-5V-4Al Alloy

Yang Yu, Wenjing Zhang, Wenjun Ye, Songxiao Hui, GRINMAT Engineering Institute Co, Ltd. Beijing, PR. China

Beta titanium alloys are attractive candidates for aerospace, automobile, orthopedic implant and down-hole service applications due to their unique combination of high specific strength, excellent hardenability, good fatigue performance, and excellent corrosion resistance. Ti–6Cr–5Mo–5V–4Al alloy is a new metastable beta alloy developed by BaoTi Group as thick-section structural materials for aerospace applications. Its design was to achieve an excellent combination of high strength and good ductility based on multicomponent strengthening.
In this work, we have studied the microstructure and dynamic mechanical properties of a Ti-6Cr-5Mo-5V-4Al alloy bar with 300mm in diameter. The samples were solution treated above the β transformation temperature. The result showed that the grain size increased with prolonging solution time when the alloy was solution treated at 890˚C . In addition, the acceleration of the grain growth occurred when solution time is more than 60min. When the alloy is solution treated at 890˚C , the function of grain growth followed by an equation = 165t 0.449. When the alloy was solution treated for 60min, grain size increased with increasing the solution temperature, and grain coarsening occurred at temperatures above

890℃. Within the ranges of the solution temperature and time in the present study, the grain size was more sensitive to the solution temperature than the solution time. In order to avoid grain growth and coarsening, the suggested solution treatments for the Ti-6Cr-5Mo-5V-4Al alloy is 800~900℃ for 15~60min. The true stress-strain curve of the β phase exhibited significant strain softening under dynamic loading. The samples with the finest grain size exhibited the best performance under dynamic loading. With increasing the grain size, there is a slight deterioration in their dynamic performance. However, the uniform plastic strain and the maximum absorbed energy did not decrease significantly. Twin related structures were observed inside the β grain of the samples after dynamic compression deformation, indicating that twinning occurred during dynamic loading. The occurance of twinning had no significant influence on the values of the average stress, while improved the values of uniform plastic strain and maximum absorbed energy.

F. Biomaterials: Bioactive Materials

Symposium Organizers:

Yufeng Zheng, Peking University, China; Luning Wang, University of Science and Technology Beijing, China; Takayoshi Nakano, Osaka University, Japan; Seung-Kyun Kang, Korea Advanced Institute of Science and Technology (KAIST), Korea; Cuie Wen, RMIT University, Australia; Marc Meyers, University of California, San Diego, USA

Thursday AM
August 22, 2019

Room: 306 (3rd Floor)
Symposium: F

Chairs:
Yan Li, Beihang University, China
Shuilin Wu, Tianjin University, China

8:30-9:00 Keynote

Fundamentals of the Theory of Biodegradable Metals

Yufeng Zheng, College of Engineering, Peking University, China

Biodegradable polymers and inorganic materials for biomedical application have been developed for decades, and formed matured theory. Since 2001, there have been over one thousand of publications on the research and development of biodegradable metals, with magnesium alloys at the dominant position, as well as Fe-based alloy, Zn-based alloys, Ca-based alloys, and so on. Recently, WE43-modified stent, WE43-based bone staple, Mg-Ca-Zn alloy bone staple and HP Mg staple had been clinically trailed in Europe, South Korea and China. However, no fundamentals of the theory or strategy which can guide the R&D of biodegradable metals have ever been set. More specifically, some important questions need to be clarified, including: (i) which kind of metallic element in the periodic table belongs to the category of biodegradable metals? What are the criteria for metals and alloys being regarded as biodegradable metals for medical application? (ii) Which kind of metallic elements and nonmetallic elements can be incorporated into biodegradable metals as alloying element/additive phase? (iii) Among all these elements that can be used to fabricate biodegradable metals, which elements are the best choice for alloying design, and what is their optimal addition content in consideration of mechanical performance and biodegradation behavior? (iv) What should be considered for the fabrication of the medical device made of BMs? The aim of the present work is to construct the frame of the fundamental theory of biodegradable metals, with the definition, biodegradability and biocompatibility criteria and the guidance on material design as core contents. In this talk, firstly, the definition of BMs has been given to be identical to the absorbable metallic biomaterials in ASTM--F3160, and its classification has been illustrated. Secondly, metallic elements in periodic table with accessible data have been screened for being the candidate elements as BMs from two criterions, biodegradability and biocompatibility. Regarding biodegradability, electrode potential, galvanic series and Pourbaix diagram have been adopted as parameters to classify degradable and non-degradable. Considering the biocompatibility, serum concentration of elements, dietary average daily intake and recommended daily intake, 50% Lethal dose and 50% inhibitory concentration, preclinical and clinical safety and efficacy, have been adopted as parameters to comprehensively reflect biosafety. Thirdly, for the material design of BMs, "mechanical property" "chemical property", "physical property" and "biocompatibility and biological function" , should be considered to guarantee the BMs be adaptive to the host. The suitable alloying elements and their optimal additive amount has been proposed for Mg-based, Fe-based and Zn-based BMs. Finally, additional three points, microstructural regulation, surface modification and device configuration are proposed for guiding the medical device design of BMs.

9:00-9:30 Keynote

Novel Hot-Warm Rolled Zn-0.8Li Alloy with Superior Mechanical Properties and Ideal Degradation Rate for Stents

Luning Wang, University of Science and Technology Beijing, China

Zinc and its alloys have been paid much attention as candidates for biodegradable metals in most recent decade. Alloying with nutrient elements seems a promising strategy to highly enhance the mechanical

properties of pure zinc. Fabricated through a newly developed hot-warm rolling process, yield strength (YS), the ultimate tensile strength (UTS) and elongation to failure (EL) of Zn-0.8Li (in wt.%) alloy respectively reach 261.5MPa, 401.4MPa and 80.8%, far beyond the clinical benchmark for biodegradable stents (i.e., YS＞200MPa, UTS＞300MPa, EL＞15%~18%). Li distribution is determined by three dimensional atom probe (3D-AP), which reveals the formation of metastable α-Li_2Zn_3 precipitates with an average size of 4.4nm and a number density of $7.16\times10^{22}m^{-3}$. Through transmission electron back-scatter diffraction (T-EBSD), it is revealed that the alloy contains sub-micron Zn grains with an average size of 640nm, which exhibit a strong basal structure. Precipitation of α-Li_2Zn_3 and sub-micron grains contribute to the superior mechanical properties. The degradation rate of the alloy is 9.8μm/y in simulated body fluid (SBF), fulfilling the clinical benchmark (i.e., <20μm/y). In vivo evaluation has been carried out to prove that the Zn-0.8Li alloy shows nearly ideal degradation behaviour during long term implantation.

9:30-9:50

Advanced Biodegradable Materials for Electrical Regeneration of Peripheral Nerve

Seung-Kyun Kang, Sung-Geun Choi, Ju-Yong Lee, Kyung-Sub Kim, Korea Advanced Institute of Science and Technology, Korea

Biodegradable materials are widely used as regenerative scaffold, surgical adhesive, drug delivery vehicle and others with unique feature of automagical elimination. Recent developments in soft electronic fabrication have introduced bioresorbable devices in which all materials are composed of biodegradable classes. This system dissolves in biofluid within programmed time, thus there is no need of removal surgery. This type of electronics minimizes the chance of inflammation of residual implant and secondary damage of additional surgery. Here we report the recent advances in the study of the dissolution kinetics of bioresorbable metal and dielectrics. Bioresorbable metal including Mg, Zn, and alloy of them can be integrated in electronic grade with comparable performance of conventional electronic metals like Au, Ag and Cu. The silicon oxides and nitrides have the dissolution chemistry and their kinetics have been investigated in various environmental condition. Increase of temperature and pH accelerate the dissolution of silicon oxides and silicon nitrides by increasing of reaction possibility with OH- ion. Also, the film formation method affects to the physical density of the silicon oxides and silicon nitrides film. Thus, the dissolution rate is tunable by change of fabrication method via control of physical structure of films. Unusual transfer printing technology allow transfer ultra-thin film layers to the soft and biodegradable polymer. Integrating the transferred circuit, the complex level of bioresorbable device is available. The wireless electrical stimulator that offers a therapeutic pulse on an injured peripheral nerve will be introduced as a demonstration of integrated medical device. Providing electrical stimulation, the transected nerve shows improved functional recovery in a point of EMG, residual muscle mass and muscle force. There was no inflammation via implanted materials. The introduced system is applicable to other temporary electrical stimulator in cardiac pacemake, muscle stimulation, and spinal cord stimulation with minimized advertise effect of implantation and removal surgery.

9:50-10:10

Biodegradable Zn-Mn Based Alloys: a Recent Development

Zhangzhi Shi, Xuefeng Liu, Luning Wang, University of Science and Technology Beijing, China

Zn-Mn based alloys with minor Mn additions have emerged as a new kind of biodegradable Zn alloys. The present authors have done a series of fundamental researches on biodegradable Zn-Mn based alloys, which paves the way for their further optimization and future application. Beside Zn matrix, the major second phase in these alloys is MnZn13 compound, which plays a vital role in microstructure evolution during thermomechanical processing. It is found that twinning can be activated in the compound with a base-centered monoclinic structure. All the twinning elements of the observed twins are deduced theoretically, agreeing well with EBSD measurements. During heat treatment, MnZn13 precipitates can form within Zn grains, which exhibit lath-like morphology, characterized by phase transformation with an invariant line strain. The orientation relationship (OR) between Zn matrix (m) and MnZn13 precipitates (p) is firstly reported to be [101]p ~// [2-1-10]m, (-131)p ~5.4 from (0002)m, which is an irrational OR.

Zn-Mn binary alloys are very brittle in as-cast status, but they become super ductile at room temperature after proper thermomechanical processing. Their elongation reaches near 100%, suggesting that Zn-Mn binary alloy is an excellent base alloy system for further compositional design. Effects of minor addition of Fe, Cu, Ag and Ca on microstructure and properties of Zn-Mn alloys have be investigated. Their minor additions are possible to make big difference of the microstructure and enhance mechanical properties significantly. Minor Fe addition leads to formation of (Fe, Mn)Zn13 phase, a large fraction of which have a core/shell structure with MnZn13 as the shell. The two phases exhibit a coherent OR owing to their similar crystal structures and the core/shell structure is likely to form during solidification due to epitaxial growth of MnZn13 on (Fe, Mn)Zn13. However, out of expectation, there exists an interlayer in nano-

scale between the core and the shell, which exhibits an irrational OR with respect to either of them. The reason of its formation is still unknown.

10:10-10:30

In Vitro and in Vivo Studies on Mg-30Sc Alloys with Different Phase Structure for Potential Usage within Bone

Jianing Liu, Dong Bian, Yufeng Zheng, Peking University, China; Yulin Lin, The Fifth Affiliated Hospital of Guangzhou Medical University, China; Ming Wang, Southern Medical University, China; Yinong Liu, The University of Western Australia, Australia

Most magnesium alloys are mainly composed of α phase with hexagonal close packed (hcp) structure, of which the fewer slip systems limit the plastic deformation capacity of alloys. Proper addition of scandium (Sc) into magnesium alloy could transform its matrix phase from α phase with hexagonal closed-packed (hcp) structure into β phase with body-cubic centered (bcc) structure. In the present work, the Mg-30wt.% Sc alloys with single α phase or β phase as well as dual phases (α+β) were developed and their potential usage within bone was comprehensively investigated. After three different heat treatments, the as-extruded alloys all recrystallized and both two single phase alloys displayed a pattern of equiaxed grains. By altering the heat-treatment routines, the microstructures and mechanical properties of Mg-30wt.%Sc alloys could be adjustable. The β phased Mg-30wt.% Sc alloy showed the best mechanical performance with an ultimate compressive strength of 603 ± 39MPa and a compressive strain of 30.7 ± 2.6%. In vitro degradation test showed that scandium could effectively incorporate into the corrosion film, form a double-layered structure, and further protect the matrix. No cytotoxic effect was observed for both single α phased and β phased Mg-30wt.% Sc alloys on MC3T3 cell line. Moreover, the β phased Mg-30wt.%Sc alloy displayed excellent corrosion resistance in vivo (0.09mm/y) and maintained mechanical integrity up to 12 weeks. The degradation process did not significantly influence the hematology indexes of inflammation, hepatic or renal functions. After 4 weeks' implantation, no abnormalities in main organs of Mg-30wt% Sc group were observed by histological observations. The bone-implant contact ratio of 38.1±3.5% after 12 weeks implied satisfactory integration between β phased Mg-30wt.%Sc alloy and the surrounding bone. These findings indicate a potential usage of the bcc-structured Mg-Sc alloy within bone and might provide a new strategy for future alloy designs.

10:30-10:45 Tea Break

10:45-11:05 (1361063)

Wound Dressings Based on Rubidium-Doped Bioactive Glass Nanospheres Promote Diabetic Wound Healing

He Xiang, Yong Liu, Yanni Tan, Songzhu Luo, Saili Duan, Central South University, China; Yufang Ding, Qinghai Zeng, Third Xiangya Hospital, China; Jian Song, Technical University of Munich, German; Chen Peng, Key Laboratory of Advanced Manufacturing Technology of Zhejiang Province, China

An improved Stöber method was successfully adopted to synthesize the rubidium-doped bioactive glass nanospheres (Rb-BGNs) with excellent homogeneity and integrity. The in vitro results show that the ionic dissolution product of Rb-BGNs stimulated human umbilical vein endothelial cells (HUVECs) to proliferate, migrate and promote tubule forming by inducing HIF-1α-driven angiogenesis-related molecules. And the ionic dissolution product of Rb-BGNs also promoted the proliferation and migration of both the fibroblasts (FBs) and human immortal keratinocytes (HaCaTs). Meanwhile, growth-promoting factors (such as TGF-β1, FGF2, PDGF, and EGF) and ERK/P38 signaling pathways of FBs and HaCaTs were activated by the ionic dissolution product of Rb-BGNs. And in vivo study demonstrated that Rb-BGNs could improve wound healing through the synergetic effect on promoting angiogenesis and re-epithelialization as well as collagen deposition on wound surface of diabetic foot ulcer. Furthermore, EGF loaded Rb-BGNs were freeze-dried for further study. And the results show that the EGF loaded Rb-BGNs improved wound healing better than Rb-BGNs, which indicates that Rb-BGNs not only have the ability to promote wound healing itself, but also can deliver other drugs to synergistically facilitate the process. Therefore, our work proves that Rb-BGNs is a promising nanoparticle filler for wound healing of diabetic foot ulcer.

11:05-11:25 (1234662)

Porous Structure and Mechanical Properties of 3D Printed PLA Gyroid Scaffolds for Biomedical Applications

Mona Alizadeh Osgouei, Yuncang Li, Cuie Wen, RMIT University, Australia

Bone-related disorders are becoming one of the main worldwide clinical health issues, in particular for the elderly. To repair and treat broken hard tissues, various types of biomaterials and devices have been widely applied in damaged parts of skeletal systems. Polymers as the third generation of biomaterials have been widely studied for biomedical applications. Synthetic polymers such as polylactic acid (PLA) can be considered as one of the best options for many biomedical applications, owing to their biocompatibility with host tissue without the need for a second surgery, along with its ease of manufacturing, hydrophobic nature, and biodegradability. Additive manufacturing (AM) is a new and modern

technique that shows great potential to offer complete control of architectural details such as pore size. In this study, fused deposition modelling (FDM) as one of the most common variations of the additive manufacturing method is used to produce PLA gyroid scaffolds with three different unit cell sizes. The mechanical properties of the scaffolds are evaluated through the compression and tensile tests in both of the building and transverse directions. Archimedes principles and micro-CT analysis are used to measure the porosity of scaffolds. The microstructure and morphology of the scaffolds are investigated by optical microscopy and scanning electron microscopy (SEM). The results indicate that gyroid scaffolds could be considered as promising structures for scaffolds for bone tissue engineering.

11:25-11:45

Study of Porous Ti-Ta-Nb-Zr for Biomedical Applications

Boqiong Li, Jinzhong University, China / Dalian Jiaotong University, China; Xing Lu, Dalian Jiaotong University, China

In order to prevent stress shielding in postoperative patients, young's modulus of implant should be as low as that of the human bone. Therefore, Ti-Nb-Ta-Zr alloy has been a new type of titanium alloy developed for biomaterials due to low modulus and improved strength. In general, the materials with higher young's modulus show lower resilience, which is more favorable for surgical operations. In this paper, low resilience porous Ti-Nb-Ta-Zr alloys with the porosity of <55% and macro-pore size of 100~400 micrometer for biomedical applications were successfully fabricated by diffusion bonding method. The microstructure, compressive and tensile properties, Vickers hardness, pseudoelastic and electrochemistry behavior were studied. It results that a few Ti-rich phase and Ta-rich phase co-exist in β matrix of the porous Ti-35Nb-5Ta-7Zr alloy, which failed mainly by mixture feature with the feather cleavage and a few voids in compression. With the increase of process control agent (PCA) during ball milling, the compressive modulus and strength of porous Ti-35Nb-5Ta-7Zr alloys with the porosity of 40% and the macro-pore size of 110 ± 35 micrometer rise from 0.8GPa to 1.3GPa and from 88MPa to 165MPa, respectively. The influence of pore structure on the mechanical properties has been analyzed by finite element calculation and Gibson-Ashby model. For comparison, bulk Ti-Nb-Ta-Zr alloys fabricated by arc melting and diffusion bonding have been investigated. The melted Ti-Nb-Ta-Zr alloys present higher strength (1224MPa) and corrosion potential in Simulated Body Fluid (-0.34V), while sintered Ti-Nb-Ta-Zr alloys show higher pseudoelastic strain ratio (12.3%, larger than 2.7% for porous Ti-Nb-Ta-Zr alloys). The stress-strain curves of bulk Ti-Nb-Ta-Zr alloys show the elastic-plasitc deformation feature under compression and linear-elastic with slight yield phenomenon in tension. The reasons have been discussed based on the microstructure of the Ti-Nb-Ta-Zr alloys.

G. Smart and Magnetic Materials: Magnetostrictive Materials and Soft Materials

Symposium Organizers:

Shaoxiong Zhou, Center Iron & Steel Research Institute, China; Chengbao Jiang, Beihang University, China; Satoshi Sugimoto, Tohoku University, Japan; Haein Yim, Sookmyung Women's University, Korea; Sean Li, New South Wales, Australia; Bob Shull, National Institute of Standards and Technology, USA

Thursday AM — Room: Yulan Hall-220 (2nd Floor)
August 22, 2019 — Symposium: G

Chairs:
Kiyonori Suzuki, Monash University, Australia
Sen Yang, Xi'an Jiaotong University, China

8:30-8:55 Invited

Recent Progress of Large Magnetostriction Induced by Magnetic MPB and Strain Glass

Sen Yang, Chao Zhou, Shuai Ren, Xiaobing Ren, Xi'an Jiaotong University, China

In this study, we report two novel ways to acquire a large magnetostriction with low triggered magnetic field: one way is magnetic morphotropic phase boundary (MPB) and the other way is the magnetic strain glass. For the MPB, we first report the existence of a MPB in a ferromagnetic system $TbCo_2$-$DyCo_2$ between a ferromagnetic rhombohedral phase and a ferromagnetic tetragonal phase. Such a magnetic MPB involves a first-order magnetoelastic transition, at which both magnetization direction and crystal structure change simultaneously. The MPB composition demonstrates a 3~6 time larger "figure of merit" of magnetostrictive response compared with that of the off-MPB compositions. For strain glass, we acquired a large magnetostriction (800ppm) triggered by a low saturation field (0.8kOe) in iron-palladium (Fe-Pd) alloys. Magnetostriction enhancement jumping from 340ppm to 800ppm was obtained with a slight increase in Pd concentration from 31.3at.% to 32.3at.%. Further analysis showed that such a slight increase led to suppression of long-range ordered martensitic phase and resulted in frozen short-range ordered strain glass state. Our study provides a way to design novel high-performance magnetostrictive and even magneto-electric materials.

8:55-9:20 Invited

Diffusional Phase Transition in Fe-Ga Alloys and the Resultant Novel Properties

Tianyu Ma, Junming Gou, Ruihua Qiao, Xiaobing Ren, Xi'an Jiaotong University, China

Magnetic materials with large magnetostriction (magnetic-

field-induced distortion) can convert a large portion of electromagnetic energy into mechanical energy or vice versa, hence have found wide applications in actuators, sensors and transducers. The binary Fe-Ga solid solution is a landmark material with large magnetostriction under low switching field and good mechanical properties. Tetragonal magnetostriction as high as 400ppm has been obtained in Fe-Ga alloys, which can fulfill the large gap between the traditional Fe or Ni metals and the brittle rare-earth based intermetallic compounds. Thus, Fe-Ga alloys have stimulated extensive investigations to put forward their applications since 2000. In addition to the large magnetostriction, here we shall show that unique functional properties can be achieved in Fe-Ga alloys through controlling the diffusional phase transition from D03 (ordered bcc) to L12 (ordered fcc). At proper compositions and heat-treatment conditions, the alloys form a natural ferromagnetic composite containing both D03 and L12 phases. These two phases with different intrinsic properties (such as saturation magnetization, magnetocrystalline anisotropy, magnetostriction sign, and elastic modulus) have differential responses to the external temperature, stress and magnetic fields, hence giving rise to novel properties. i) The Fe73Ga27 composite exhibits highly thermal-stable magnetization up to 617˚c due to the gradual transformation from the D03 phase with lower magnetization to the L12 phase with higher magnetization upon heating. ii) When the two phases have proper volume fractions, the Fe73Ga27 composite can possess stress-insensitive magnetic permeability due to the compensation of stress-induced anisotropies between the D03 phase with positive magnetostriction and the L12 phase with negative magnetostriction. iii) The magnetostriction sign of such composites can be tuned by increasing magnetic field strength due to the preferable domain switching of the bcc phase with weaker magnetocrystalline anisotropy and the subsequent domain switching of the fcc phase with stronger magnetocrystalline anisotropy. These unique properties in Fe-Ga composites may lead to important applications.

9:20-9:40

Direct Observation of Tri-Axial Lattice Strains under Magnetic Field for Fe-Ga Single Crystal Alloy by X-Ray Diffraction

Muneyuki Imafuku, Masaki Fujita, Takehito Ikeuchi, Akihiro Koyama, Tokyo City University, Japan; Shigeru Suzuki, Tohoku University, Japan

Since the discovery of giant non-volume-conserving or non-Joulian magnetostriction for Fe-Ga alloy in 2015, various studies have been reported concerning the volume change for Fe-Ga, Fe-Al and Fe-Ge magnetostrictive alloys. These studies are based on measuring the macroscopic shape change by using strain gauges or Joule's liquid displacement method. In this study, we focused on the microscopic approach that measures the lattice strains directly by using x-ray diffraction method under magnetic field. We used a cube-oriented Fe-18%Ga single crystal disk of 10mm in diameter and 0.5mm thickness produced by the Czochralski method. The magnetic field was applied in (001) plane on the disk with various directions. In-situ tri-axial magnetostriction analysis was done for the specimens before and after annealing. Although the periodic change in tri-axial magnetostriction with the direction of applied magnetic field was clearly observed for both specimens, those amplitudes are not the same between them. Moreover, the magentostriction in perpendicular direction, [001] changed with the direction of applied magnetic field, which cannot be derived from the classical theory. We analyzed these magnetostrictive behaviors by using magnetostriction theory considering the magnetic domain structures. As a result, we could evaluate the initial orientation ratio of magnetic domains and found that of biased distribution for the as-prepared specimen eliminated after annealing.

9:40-10:00

Studies of Fe(NiCoMn) Alloys with Moderate Magnetostriction and Good Mechanical Properties

Hao Jin, Yiling Lian, Zhihua Nie, Beijing Institute of Technology, China

The magnetostrictive effect, a change of shape or dimension in magnetic materials by applying magnetic fields, attracts much attention due to broad applications in actuators and sensors. Up to date, many magnetostrictive materials are developed including RT2 intermetallic compounds (R= rare earth, T= Co, Fe), Ni-Mn-based ferromagnetic shape memory alloys and Fe-Ga alloys. However, the magnetostrictive materials show a disappointing response in the tensile stress condition which may restrict their practical application.
In this work, a series of Fe1-x(NiCoMn)x (13≤x≤45, at.%) polycrystalline alloys was studied. The Fe1-x(NiCoMn) x alloys were prepared by arc-melting in an argon atmosphere. The effect of NiCoMn addition on the crystal structure, microstructure, magnetic and mechanical properties in Fe1-x(NiCoMn)x alloys was investigated using the synchrotron-based high-energy x-ray diffraction (HE-XRD), electron back-scatter diffraction (EBSD), vibrating sample magnetometer (VSM) and loading machine. With increasing x value, the phase of alloys changed from pure body-centered cubic (bcc) structure to the coexistence of bcc and face-centered cubic (fcc) structures, then to a pure fcc phase. The bcc and fcc phases were ferromagnetic and paramagnetic, respectively. In the bcc region, with increasing x value, the lattice parameter, magnetostriction, yield strength and tensile enlongation of the alloys increased

monotonically. The magnetostriction of the Fe1-x(NiCoMn)x alloys dropped dramatically when the fcc phase generated. The Fe75(NiCoMn)25 alloy contained ~4% fcc phase, which showed a proper magnetostriction of 50ppm. At meanwhile, the Fe75(NiCoMn)25 alloy had good mechanical properties with the tensile strength more than 1000MPa and elongation up to 10%. The crystallography relationship between the fcc phase and bcc phase was further studied by pole figure using EBSD technique. The two phases had Kurdjumov-Sachs (K-S) relationship with (111)fcc // (110)bcc, [110]fcc // [111] bcc. All these merits make this alloy system attractive for potential magnetostriction applications. This study is instructive for the development of high-performance magnetostrictive materials with good mechanical properties.

10:00-10:20

Microstructural Evolution and Magnetic Property of Rapidly Solidified Co-Mo Hypereutectic Alloy

Sha Sha, Weili Wang, Jian Chang, Yuhao Wu, Bingbo Wei, Northwestern Polytechnical University, China

In recent years, binary Co-Mo eutectic-type alloys had aroused much attention due to their potential applications in electronic industries. However, both the rapid solidification kinetics and magnetic property optimization of these alloys were still rarely explored by now. In this work, the non-equilibrium solidification mechanisms of hypereutectic Co62Mo38 alloy were investigated by electromagnetic levitation (EML) and drop tube (DT) techniques, while the magnetism properties of rapidly solidified samples were characterized using a vibrating sample magnetometer (VSM). During EML experiments, the obtained maximum undercooling of levitated alloys reached up to 203K (0.12 TL), and the final solidification microstructures consisted of primary e-Co7Mo6 dendrites and interdendritic (e-Co7Mo6+a-Co) eutectic. Clearly, the macroscopic magnetism of Co62Mo38 alloy was dominated by the solid solution a-Co phase. As the alloy undercooling increased, the volume fraction and cobalt content of e-Co7Mo6 compound monotonously enhanced, whereas the a-Co phase reduced gradually. Based on this variation, the saturated magnetization and remanence of bulk Co62Mo38 alloy linearly decreased with the rise of undercooling. Mean- while, the grain refinement took place in highly undercooled state, resulting in a conspicuous decrease of coercive force and hysteresis loss for hypereutectic Co62Mo38 alloy. As a comparison, the free fall experiment of liquid Co62Mo38 alloy droplets was also performed with a drop tube, and their phase compositions were consistent with those under EML condition. The theoretical calculations indicated that the smaller droplets possess the larger undercooling and cooling rate. With the decrease of droplet size, the isothermal magnetization curves were weakened remarkably. This represented that all mentioned magnetic parameters shows a decreasing trend. Nevertheless, if the droplet size continuously reduced below 392mm, the 'faceted dendrite-equiaxed dendrite' morphological transition of primary phase was induced, leading to an abrupt decrease of the volume fraction and cobalt content for e-Co7Mo6 compound. Such a variation contributed to the tiny increase of the coercive force at this threshold value.

10:20-10:35 Tea Break

10:35-11:05 Keynote

Formation of Nano-Meter Scale Microstructures from Binary Amorphous Precursors

Kiyonori Suzuki, Monash University, Australia

Nano-mater scale grains with a diameter of 10 to 20nm are known to be prepared by primary crystallization of rapidly-quenched amorphous precursors with carefully designed alloy compositions. A commercially successful example of this processing route is nanocrystalline Fe73.5Si13.5B9Nb3Cu1 where exceptionally high permeability is obtained due to the exchange averaging effect on the magnetocrystalline anisotropy energy. These nanocrystalline alloys contains alloying elements for retarded crystal growth and/or accelerated nucleation for the formation of nano-meter scale microstructures. However, we have recently demonstrated that magnetically soft nanocrystalline alloys can be prepared from simple Fe-B based precursors when the heating rate during annealing is increased to 103 ~ 104K/s. Owing to the high concentration of Fe in these Fe-B based alloys, the resultant microstructure exhibits exceptionally high magnetic polarization (up to 1.92T). The formation of nano-meter scale microstructures in a simple binary system unlocks previously unavailable alloy design strategies in nanostructured materials which is not only relevant to magnetic materials but, also to structural materials. In this talk, the effects of heating rate on the microstructural and magnetic properties in Fe-B alloys are discussed along with some latest results on the kinetics of nano-crystallization investigated under isothermal conditions.

11:05-11:35 Keynote

Novel Soft Magnetic Properties of Rare Earth-Transitional Metal Compounds at High Frequency

Jinbo Yang, Guanyi Qiao, Wenyun Yang, Changsheng Wang, Shunquan Liu, Peking University, China

It is well known that rare earth-transitional metal intermetallic compounds such as $Nd_2Fe_{14}B$ have become high performance permanent magnets primarily due to their high axial magnetocrystalline anisotropy. However, their magnetocrystalline anisotropy covers not only easy axial anisotropy, but also cone anisotropy and planar

anisotropy. In combination of the high Curie temperature and large saturation magnetization when compared to those of the ferrites, a material with such properties can have a higher Snoek limit, initial permeability, and working frequency, which shows promising potential to work as "soft" magnetic materials at high frequency such as microwave absorber. Here, we will report our results about the magnetic and microwave absorption properties in the high frequency region for a series of the rare earth-transitional metal compounds/paraffin composites. As an example, R2(Fe, M)17(Nx) was prepared and the R2(Fe, M)17(NX) paraffin composite improves the Snoek limit and exhibits high microwave reflection loss of up to -60dB at about 10GHz due to its high saturation magnetization and high ratio of the magnetocrystalline anisotropy field to the basal plane anisotropy field. The maximum RL value of the Sm1.5Y0.5Fe15.5Si1.5 paraffin composite reaches -52dB, and the RL value exceeding -20dB ranges from 4.5GHz to 18GHz due to a better electromagnetic match. Hence, it presents an advantage for use as a high-performance thin layer microwave absorber. This opens up broad prospects for technology applications.

11:35-11:55

Magnetic Softness and High Frequency Characterization of FeSiBNbCu(P, Mo Alloys

Aina He, Huiyun Xiao, Yaqiang Dong, Anding Wang, Ruiwei Li, Xincai Liu, Ningbo Institute of Materials Technology and Engineering, Chinese Academy of Sciences, China

Fe-based nanocrystalline alloys have excellent combination of soft magnetic properties such as higher permeability (μ), lower coercivity (Hc), lower core loss (P), and better high-frequency characteristics, compared to conventional soft magnetic materials. With the rapid development of technology and concerning on energy saving, modern electronic devices tend to be miniaturized, lightweight, and high energy efficient. Finemet alloys (representative Fe73.5Si13.5B9Nb3Cu1 alloy) have two shortcomings of low saturation magnetization (Bs) and high content of Nb element, which become increasingly obvious for inhibiting miniaturization and high performance-price ratio. By devoting subsequent great efforts, a variety of high Bs of Nanoperm (Fe88M6B6), Hitperm ((Fe0.5Co0.5)88M6B6) and Nanomet (Fe83Cu1(Si, B, P, C)16) were successfully developed. Yet, these nanocrystalline alloys exhibit high Hc above 3A/m, poor high-frequency characteristic and low amorphous forming ability (AFA) due to high content of Fe element and low content of amorphous forming elements. In this study, the thermal behavior, magnetic softness and dynamic magnetization process of FeSiBNbCu(P, Mo) nanocrystalline alloys were investigated systematically. On the other hand, we fabricated Fe76Si13B8Nb2Cu1 nanocrystalline alloy ribbons with industrial raw materials (IRMs) and industrial processes, investigated the influence of impurities and produce processes. Ribbons with high surface quality, ductility and commercially useable width were also successfully produced. Contrast experiments with pure raw materials and processes in lab were performed to comprehensively understand the effects of raw materials and surface crystallization on the amorphous formation ability (AFA), manufacturability, thermal performance and magnetic properties. The reasons of IRM ribbons exhibit excellent magnetic properties were discussed. These results would give a valuable reference for industrialization of the high Bs and low loss nanocrystalline alloys.
High Fe content Fe76Si13B8Nb2Cu1 alloy ribbons with excellent quality and width of 20~55mm were successfully produced with industrial processes and raw materials, showing the superb manufacturability and impurity tolerance. It is found that impurities and ribbon width have a negligible influence on crystallization behavior, by comparing with samples prepared with high purity materials. The wide annealing time window can be over 50min in the optimal temperature range of 500~600˚C . Besides, industrialized Fe76Si13B8Nb2Cu1 alloy ribbons exhibit outstanding magnetic properties, including high saturation magnetic flux density (Bs) of 1.39T, high effect permeability of 2.88×10^4 at 1kHz and low coercivity of 3.5A/m, which are equivalent to ribbon prepared with pure materials. Extreme low core losses of 0.91W/kg at 1T and 1kHz were also obtained in ring samples. It is found that fine nanostructure and wide stripe domains are the origins of excellent magnetic properties. This alloy with excellent performance has great potential in applications of high working B and of high working B and frequency devices and will also be a new reference for industrialization of nanocrystalline alloy.

11:55-12:15

High Filling Alumina/Epoxy Nanocomposite as Coating Layer for Fe-Based Amorphous Powder Cores with Enhanced Magnetic Performance

Yaqiang Dong, Yiqun Zhang, Lei Liu, Bang Zhou, Liang Chang, Qiang Chi, Xinmin Wang, Ningbo Institute of Materials Technology & Engineering, Chinese Academy of Sciences, China

Soft magnetic composites (SMCs) containing magnetic powders surrounded by insulation coatings are allowed for revolutionized designs of electromagnetic devices to improve efficiency and reduce weight and costs, without sacrificing magnetic performance. Ferromagnetic powders have shown the most potential as core materials, compared with the traditional magnetic materials, such as pure Fe, Fe-Si, Fe-Ni, Fe-Ni-Mo, and Fe-Si-Al, the Fe-based amorphous alloys exhibit high resistive and low coercivity, as a result, Fe-based amorphous powder cores (AMPCs) show the advantages of 3D

isotropic magnetic fields, high saturation induction, high permeability under a DC magnetic bias field, high resistivity, high thermal conductivity, relatively low core loss and flexibility of design. Nevertheless, the permeability of Fe-based AMPCs is relatively low, it is not advisable to sacrifice much permeability by introduce inordinate non-magnetic materials to reduce core loss. Therefore, an appropriate insulation coating is crucial for Fe-based AMPCs.

For high frequency applications, the insulation coating is critical to increase the electrical resistivity and achieve low core loss. Besides the high electrical resistivity, satisfactory cohesiveness and thermal stability are also highly desirable for the insulation layer to provide sufficient mechanical strength and to allow high-temperature annealing for stress relaxation. Organic polymers, usually epoxy, silicone, polyimide, phenolic and hybrids of these, can create an embedded matrix on the surface of the powders. However, the thermal stability of the polymers is usually bad, which limits the annealing temperature of the cores. Inorganic materials, such as phosphates, oxides, water glass and ferrite, can form an encapsulation around each particle. However, additional lubricant is needed to decrease the hysteresis loss (Ph), which will reduce the magnetic volume fraction and permeability. Recently, micro- or nanoparticle/polymer composites have been used as insulating layers for SMCs. For example, SiO_2, $ZnSO_4$ and Fe_3O_4 have been mixed with the phenol-formaldehyde resin and epoxy-modified silicone resin, respectively, as the insulating layers for pure Fe SMCs. The hybrid insulating layers result in a defect-free structure of prepared green compacts, which consequently exhibit lower eddy current losses.

Furthermore, Al_2O_3 nanoparticles have been coated around pure Fe powders directly before being treated with organic resin. But the insulating layer is not uniform at all, which introduce more pores and defects then drastically reduced the permeability. In order to get the uniform insulation, high filling alumina/epoxy nanocomposite has been designed as coating layer for Fe-based AMPCs in this work. Alumina nanoparticles were embedded into the epoxy resin matrix through convenience mixing process, for compare, alumina directly coated were also discussed. The content and effects of the alumina hybrid nanocomposite on the magnetic properties and microstructure were investigated. Compared with organic coating, the organic-inorganic hybrid coating cores exhibited superior magnetic properties without sacrificed saturation magnetization and much permeability. Meanwhile, the core loss declined for 40% and the quality factor was 13% higher as a half alumina was introduced into epoxy resin matrix. the Fe-based AMPCs with convenience insulation coating process have the advantage of low cost compared with the FeNi magnetic powder cores, which renders the Fe-based AMPCs become a potential candidate for a variety of industrial applications.

K. Nanocrystalline Materials, and Ultra-Fine Grained Materials: VI

Symposium Organizers:

Yue Zhang, University of Science and Technology Beijing, China; Zhiyong Tang, National Center for Nanoscience and Technology, China; Nobuhiro Tsuji, Kyoto University, Japan; Jae-il Jang, Hanyang University, Korea; Kenong Xia, University of Melbourne, Australia; Nathan Mara, University of Minnesota, USA

Thursday AM
August 22, 2019

Room: 309(3rd Floor)
Symposium: K

Chairs:
Kyung-Tae Park, Hanbat National University, Korea
Fei Chen, Wuhan University of Technology, China

8:30-9:00 Keynote

Fabrication and Mechanical Behavior of Porous Cu via Chemical De-Alloying Method

Fei Chen, Hao Wang, Qiang Shen, Lianmeng Zhang, Wuhan University of Technology, China; Lavernia, University of California Irvine, America

We report on a study of the synthesis and deformation of two different porosity structure: nano-sized and micron-sized porous Cu, processed via chemical de-alloying of Cu-Al intermetallic compounds and Cu-Fe solid solution in 20 wt% NaOH aqueous solution and 5 wt% H_2SO_4 respectively. We studied the relationship between phase composition/microstructure of the precursor alloys and structural properties (volume fraction of porosity, density, pore size distribution) of porous Cu. Moreover, the compressive strength of bulk nano/micron porous Cu were measured and the effect of volume fraction of porosity on mechanical properties was studied. The results show that the microstructure of both nanoporous Cu and micron porous Cu are characterized by bi-continuous interpenetrating ligament-pores. The ligament size of nanoporous Cu is 130±20nm -170±20nm, and its corresponding compressive strength increases with decreasing volume fraction of porosity; as porosity increased 56.372% to 73.972%, the compressive strength decreased from 17.1871MPa to 2.7170.5MPa. Moreover, the average pore size of micron porous Cu is in the range of 1.5~4.0μm. Our mechanical behavior results reveal that the yield stress of micron porous Cu increases from 3.9MPa to 58.6MPa as the volume fraction of porosity decreases from 78.9 % to 39.3%.

9:00-9:30 Keynote

Dynamic Tensile Extrusion Behavior of OFHC Cu Having Ultrafine Grains and Fine Grains

Kyung-Tae Park, Hanbat National University, Korea; Keunho Lee, Keunho Lee, LeeJu Park, Seong Lee, Agency for Defense Development, Korea

A series of dynamic tensile extrusion (DTE) tests was performed on ultrafine grained (UFG) OFHC Cu to examine the metal jet formability under dynamic loading conditions (i.e. deformation at extremely high strain rates).The UFG Cu bars were fabricated by equal channel angular pressing (ECAP) with the route Bc and then annealing was conducted at 150˚c and 200˚c for 1hr in order to control the grain size. The as-ECAPed grain size of ~0.9 micrometer increased to 2.8 micrometer and 4.7 micrometer after 150˚c and 200˚c annealing. The spherical balls of the diameter 7mm were carefully machined from the as-ECAPed bar and the subsequently annealed bar. The DTE tests were conducted by launching the balls to the conical DTE die at a speed of ~ 480m/s using a vacuumed gas gun system. The DTE fragments were softly recovered and their microstructure was characterized by using EBSD technique. The DTE ductility (the sum of elongation of each fragment) increased as increasing the grain size under the present grain size range. The computational analysis showed that the temperature of the specimen during DTE increased over ~ 600˚c locally due to adiabatic heating, and the maximum strain rate reached 10^6/s. The EBSD analysis revealed that, regardless of the initial grain size, <001> + <111> dual fiber texture was strongly developed along the DTE direction. Besides, it was evident that dynamic recrystallization in the as-ECAPed condition was more frequent compared to the annealed condition. Based on the present extremely high strain rate DTE tests, the metal jet formability of OFHC having the grain size ranging from ultrafine size (~ 1 micrometer) to fine size (2~5 micrometer) is discussed.

9:30-9:55 Invited

Grain Refinement in a Metastable Beta Ti Alloy Deformed to Large Strains at High Strain Rates

Ahmad Zafari, The University of Melbourne, Australia

It has long been known that severe plastic deformation (SPD) can effectively refine grains in metallic materials. However, the roles played by stress induced transformation, in particular martensitic transformation, as well as strain rate in the grain refinement have received little attention. Hence, we studied these two factors in a metastable β Ti-5Al-5V-5Mo-3Cr (Ti-5553) after conducting high pressure torsion (HPT) and shear punching (SP) at different strain rates of 0.02~200s^{-1}. It was revealed that the presence of the martensitic α" in Ti-5553 resulted in grains of 30~50nm, much smaller than those of 100nm formed in more stable β Ti alloys, such as Ti-20Mo, in which no stress induced martensitic transformation (SIMT) occurred. The formation of thin α" plates divided β grains into smaller domains and imbalanced dislocation generation and diffusion at grain boundaries. The rates of dislocation generation and absorption at the boundaries were further manipulated by varying strain rate during SP. SP to large plastic strains up to 40 was conducted at various speeds, creating severe plastic deformation at high shear rates up to 200s^{-1}. Grain refinement in the resulting shear bands (SBs), which experienced even faster deformation due to strain localisation, was studied using extensive TEM. Significant grain refinement occurred at < 40s^{-1}, producing β grains of ~5~10nm, considerably smaller than those obtained by HPT to a much higher strain of 240 at a slow shear rate of 0.5s^{-1}. The applied shear strain rate of 2s^{-1} was found to be an optimum for attaining a pure nano-β grain structure thanks to maximum dislocation activity and complete α" to β reverse transformation. However, some stress induced α" remained as strain rate deviated from this value and much coarser β grains formed at the strain rats of > 40s^{-1}. The effects of strain rates on grain refinement and the minimum achievable grain sizes at high strain rates are explained based on classical dislocation dynamics.

9:55-10:15

Microstructures and Tensile Properties of Ultrafine Grained Al-Mg Alloys Fabricated by High Pressure Torsion and Subsequent Annealing

Xiaodong Lan, Si Gao, Myeong-heom Park, Akinobu Shibata, Nobuhiro Tsuji, Kyoto University, Japan/ Element Strategy Initiative for Structural Materials, Japan

Al-Mg alloys have been widely used because of their good combination of low density, high strength and excellent formability. Previous studies have shown that increasing Mg content leads to simultaneous improvement of strength and ductility of Al-Mg alloys. On the other hand, it is well-known that grain-size refinement can effectively improve strength of metallic materials according to Hall-Petch effect, but ductility is deteriorated when the grain size is decreased down to sub-micrometer sizes (ultrafine range), which is known as a trade-off relation between strength and ductility. Although intensive studies have been carried out on Al-Mg alloys, the combined effect of Mg contents and grain size on mechanical properties of Al-Mg alloys remains unclear, especially when the grain size is refined down to the ultrafine grain size range. The present study aims to investigate microstructure and mechanical properties of UFG Al-Mg alloys having different Mg contents.

Al-xMg (x=2.5, 5 and 7.5wt.%) specimens having different grain sizes were fabricated by high pressure torsion (HPT) and subsequent annealing process. Microstructural characterizations were conducted on transverse sections of the HPT disks by using SEM-BSE and EBSD. Tensile test was conducted at a strain rate of $8.3\times10^{-4}s^{-1}$ at ambient temperature, using miniaturized tensile test specimens cut from the HPT discs. Digital image correlation (DIC) method was used to characterize local deformation behavior as well as to precisely measure tensile elongation in the tensile tests. It was found that yield strength and ultimate tensile strength significantly increased by refining the grain size down to sub-micrometer but tensile elongation substantially decreased by the grain refinement in all three kinds of Al-Mg alloys. However, at all the grain sizes, specimens with higher Mg content maintained larger tensile ductility than those with lower Mg content. It was found that strain hardening rate during the tensile test significantly increased with increasing Mg content at similar grain sizes, which should account for the larger tensile ductility in the specimens with higher Mg content. On the other hand, it was noteworthy that yielding behavior changed from continuous yielding to discontinuous yielding with decreasing the grain size in all alloys. The effects of grain size and Mg content on the yielding behavior, yield strength and strain hardening behavior of the specimens are discussed in details by comparing Al-xMg alloys with pure Al in the presentation.

10:15-10:35

Influence of Cryomilling and High Pressure on the Consolidation of Aluminum by Spark Plasma Sintering

Dongming Liu, Zhongyu Wang, Jiale Zheng, Shandong University, China

There has been a significant interest in the development of bulk nano-structured or ultra-fine grained materials because the grain refinement may lead to substantial changes in both mechanical and physical properties. We report on cryo-milling as well as spark plasma sintering (SPS) are employed to consolidate nano-structured pure aluminum.

Cryomilling is a special kind of a mechanical attrition technique, in which the powder and the milling balls are immersed in a cryogenic medium (e.g., liquid nitrogen or liquid argon) during the milling process. In the case that liquid nitrogen is used as the cryogenic medium, the extremely low temperature can suppress the recovery and recrystallization and lead to finer grain structures and more rapid grain refinement. Meanwhile, the incorporation of the nitrogen into the powder particles improves the mechanical properties and the thermal stability of the microstructure.

Spark plasma sintering (SPS) is a recently developed powder consolidation technology, in which a pulsed high-amperage, direct current (DC) is used concurrently with a superimposed uniaxial pressure to consolidate powders. In comparison with well-established consolidation methods such as hot pressing, where the samples are heated externally, the thermal energy during SPS is generated in-situ, i.e., by the powder being sintered in case of conductive powder as well as by the mold elements. This technique possesses the advantage of sintering powders under conditions of high heating rate (up to 1000˚C/min). Consequently, materials can be consolidated at relatively low temperatures and in a shorter time interval, and thereby minimize changes to the starting microstructures, relative to conditions generally present during conventional consolidation methods.

In this paper, nearly full dense bulk nanostructured aluminum is fabricated by cryomilling and high-pressure spark plasma sintering. The consolidated material demonstrates a compressive yield stress as high as 380MPa, which is significant higher than commercial strain hardened aluminum. Microstructural observation shows that it has a bimodal structure, i.e., ultra-fine grains are embedded a nano-sized grain of aluminum. In addition, the effect of cryomilling and high pressure (up to 500MPa) on the consolidation is thoroughly analyzed. It is also shown that the change in the carbon and oxygen level is insignificant during spark plasma sintering. There is a slight decrease in the nitrogen content. And the hydrogen level is significantly reduced. Quantitative calculation was performed to analyze the contributors to the high strength. It is shown that the strengthening mechanisms include grain boundary strengthening, second phase strengthening and dislocation strengthening.

10:30-10:45 Tea Break

11:45-11:10 Invited

Phase Transformation of Ti-Mg Alloys by Heavy Plastic Deformation

Yoshikazu Todaka, Nozomu Adachi, Toyohashi University of Technology, Japan; Armando Tejeda Ochoa, Toyohashi University of Technology, Japan / Research Center for Advanced Materials (CIMAV), Japan; Jose Martin Herrera Ramirez, Research Center for Advanced Materials (CIMAV), Japan; Masatoshi Mitsuhara, Toyohashi University of Technology, Japan / Kyushu University, Japan; Wansong Li, Kyushu University, Japan

The phase transformation of Ti100-xMgx(x = 0, 25, 50, 75 and 100at%) alloys by means of heavy plastic deformation processes,i.e.ball milling (BM) and high-pressure torsion (HPT) processes, was investigated. It was found by XRD analysis that the powders of Ti100-xMgx alloys with x = 0, 25, 50 and 75at% transform from hcp phase to a metastable fcc phase during BM. Mg element seems to

accelerate this phase transformation. In the Ti50Mg50 alloy powder after BM for 75h, the nanostructure with around 10nm in grain size and fcc phase was observed by TEM analysis. While, in the pure hcp-Mg powder, no other phases were observed after BM. Moreover, the Ti50Mg50 alloy powder with retained hcp phase after BM for 25h was further deformed by HPT-straining under 5GPa. The retained hcp phase transformed to fcc phase during HPT-straining. On the other hand, the as-blended powder of pure Ti (hcp) and pure Mg (hcp) without BM did not transform to fcc phase by HPT-straining under 5GPa, instead hcp-Ti phase transformed to simple hexagonal (ω) -Ti phase. In this presentation, I will discuss the effect of heavy plastic deformation on the phase transformation from hcp phase to fcc phase in Ti-Mg alloys.

11:10-11:35 Invited

The Effect of Solutes and Second-Phase Particles on Grain Refinement during ECAP in Al Alloys

Yan Huang, Brunel University London, England

The exploitation of the optimized effect of solute additions and second-phase particles has potential to develop commercially viable routes for producing true bulk nanograined aluminium alloys. In the present work, the effect of solute elements and second-phase particles in aluminium on inhibiting dynamic recovery and pinning boundary migration during SPD by equal channel angular pressing (ECAP) was investigated. ECAP was carried out, at room temperature and cryogenic temperatures down to 77K, using either a 90° or 120° die and following route A, to various true strains of up to 15. The deformed microstructures were characterized by FEGSEM, TEM and EBSD. Experimental results showed that increased Mg addition led to more instability in the early stages of deformation and consequently improved grain refinement as medium to high angle boundaries were generated by shear banding. At room temperature, the average grain width after a strain of 10 was stabilized at ~550nm in an Al-0.1Mg alloy and ~120nm in an Al-3Mg alloy. However, shear banding in the supersaturated Al-4Cu was found even more severe and the shear bands carried most of the strains in the first two ECAE passes. The grain width obtained after the same strain of 10 was down to ~65nm, which is a true nanoscale. The combined effect of Al_3Sc particles and Mg solute in Al-0.2Sc-0.1Mg and Al-0.2Sc-1Mg alloys resulted in finer structures than in the Al-0.1Mg and Al-1Mg solid solutions. In the Al-4Cu alloy, the nanoscale equilibrium q-phase (Al_2Cu) particles showed limited impact on the microstructure upon further deformation. The minimum grain width decreased with decreasing processing temperature, although the effect of temperature was not as strong as expected based on thermal activation analysis. Shear banding was found to be most effective in the grain refinement during early stages of deformation. Second-phase particles played an important role in stabilizing the obtained fine grain structure. The mechanisms of grain refinement during ECAP are discussed in the paper in association with the contribution of solute atoms and second-phase particles.

11:35-12:00 Invited

Effect of Severe Plastic Deformation and Subsequent Aging on Strength-Ductility Balance of Ultra-Fine Grained Al-Si-Mg Alloy

Daisuke Terada, Chiba Institute of Technology, Japan

Ultra-fine grained metallic materials fabricated by severe plastic deformation processes exhibit quite high strength, but these ductility is often small. Several researchers report combination of ultra-fine grained microstructure with precipitates can improve the ductility. However, the relationships between mechanical properties and process conditions, such as deformation strain and heat treatment temperature have not been clarify yet. Thus, in this study, age hardenable aluminum alloys was deformed with various strain and aged under various conditions, and the mechanical properties were investigated.
Al-Mg-Si alloy sheets were solution treated and then deformed by cold-rolling with various reductions or severely deformed by accumulative roll-bonding (ARB) process. The deformed sheets were subsequently aged at 100˚C or 170˚C with various aging time. Hardness test and tensile tests for these specimens were carried out.
In the specimens deformed by cold-rolling with reduction below 50%, the yield stress and tensile strength were increased and total elongation was decreased by aging at 170˚C. The result shows trade-off relationship between the strength and ductility. On the other hand, both strength and ductility increased during aging in the specimens deformed with reduction above 50% or by ARB process. The result indicates that the strength and ductility were related to positive correlation when the specimens were pre-deformed severely. When the deformed specimens aged at 100˚C, trade-off relationship was observed in the specimen deformed below 10% reduction. In the specimen deformed with reduction above 20%, positive relationship of the strength and ductility appeared. The results indicate that the mechanical properties depend on strain of deformation and aging temperature, and the relationships between strength and ductility can be controlled.

12:00:12:20

Effect of Grain Size on Mechanical Properties of Mg-0.3at.%Y Dilute Alloy

Ruixiao Zheng, Chaoli Ma, Beihang University, China; Nobuhiro Tsuji, Kyoto University, Japan

In this study, a Mg-0.3at.%Y alloy was provided for a severe plastic deformation by high pressure torsion (HPT) and subsequent annealing. After the HPT by 5 rotations, nanocrystalline structures with a mean grain size of about 240nm having deformed characteristics

were obtained. Fully recrystallized microstructures with mean grain sizes ranging from sub-micron to several tens of micrometers were obtained by subsequent annealing at various temperatures for different holding times. Room temperature tensile tests revealed that ultrafine grained (UFG; grain sizes smaller than 1μm) specimens exhibited very high yield strength over 250MPa but quite limited tensile ductility. In contrast, good balance of strength and ductility was realized in fine grained specimens with grain sizes around 2 to 5μm. Particularly, the yield strength and total tensile elongation of a specimen with a mean grain size of 2.13μm were 180MPa and 37%, respectively, which were much higher than those of pure Mg having a similar grain size. The deformation microstructures of typical fine grained and coarse grained Mg-Y specimens were systematically observed by electron backscattered diffraction (EBSD) and transmission electron microscopy (TEM). It was found that the dominant deformation mode has been changed in the fine grained specimen. The significant effects of grain size and Y addition on the change of deformation mechanisms were discussed.

L. Computational Design and Simulation of Materials: VI

Symposium organizers:

Tongyi Zhang, Shanghai University, China; Zhimei Sun, Beihang University, China; Shigenobu Ogata, Osaka University, Japan; Byeong-Joo Lee, Pohang University of Science and Technology (POSTCEH), Korea; Salvy Russo, RMIT, Australia; Saryu Fensin, Los Alamos National Lab, USA; Michele Manuel, University of Florida, USA

Thursday AM
August 22, 2019

Room: 204 (2nd Floor)
Symposium: L

Chairs:
Mike Ford, University of Technology Sydney, Australia
Qingmiao Hu, Institute of Metal Research, Chinese Academy of Sciences, China

08:30-08:55 Invited

DFT Calculations of Generalized Stacking Fault Energies and Critical Shear Stresses of Alpha-Titanium Alloys: On the Plastic Deformation Anisotropy and Dwell Fatigue Susceptibility

Hui Yu, Institute of Metal Research, Chinese Academy of Sciences, China / Shenyang University of Technology, China / Northeastern University, China; Shuo Cao, Rui Yang, Qingmiao Hu, Institute of Metal Research, Chinese Academy of Sciences, China; Yang Qi, Northeastern University, China

Dwell fatigue of titanium alloys reduces significantly the life-time of the blades and disks of gas turbine engine in a jet aircraft. The dwell fatigue susceptibility of titanium alloys depends highly on the alloy composition. Understanding the mechanism underlying such dependence is demanded for the rational design of titanium alloys so as to improve the service life-time of the blades and disks. The dwell fatigue of titanium alloys originates from the plastic deformation anisotropy of the alpha phase with hexagonal close packed crystal structure as the critical shear stress of the <c+a> slip system is 3 to 4 times higher than that of the <a> slip system. In the present work, the plastic deformation anisotropy and its composition dependence are investigated by calculating the generalized stacking fault energies of <a> and <c+a> slip systems of alpha titanium alloys using a first-principles method based on density functional theory. The critical shear stresses of the slip systems are then evaluated with the semi-discrete variational Peierls-Nabarro model. We try to establish a predictive model of the dwell fatigue susceptibility of titanium alloys against the alloy composition based on the critical shear stress anisotropy. The work provides fundamental understanding on the composition dependence of the dwell fatigue susceptibility of titanium alloys at electronic structure level, and will hopefully help the design of titanium alloys with low dwell fatigue susceptibility.

08:55-09:20 Invited

In-Silico Investigation of Electrode Materials for Rechargeable Magnesium Batteries

Nikhil Medhekar, Mingchao Wang, Jodie Yuwono, Vallabh Vasudevan, Nick Birbilis, Monash University, Australia

Rechargeable Mg-ion batteries (MIBs) are rapidly emerging as a plausible alternative to Li-ion batteries (LIBs) in terms of energy density, scalability and operation safety. However, key challenges in addressing the electrochemical stability and cyclability of potential electrodes, such as Mg metal as anode and layered transition-metal dichalcogenides (TMD) as cathode, pose questions regarding their feasibility as electrodes in MIBs. The inadequate understanding of reaction mechanisms during (de)magnesiation process hinders the practical application and optimal design of electrode materials. Here we carry out first-principles calculations to investigate the electrochemical behavior of Mg metal and Group 14 as anodes, as well as layered TMD as cathodes. We find that unexpected self-catalytic behavior of Mg induced by surface hydroxylation can be effectively controlled by impurity enrichment (alloying with Group 14 and 15 elements) and surface oxidation. To replace Mg by Group 14 elements as MIB anodes, comprehensive kinetic and thermodynamic investigations reveal that amorphous Ge and crystalline Sn can work as potentially effective anode for Mg-ion batteries. We also find out that a small overpotential

is necessary for avoiding aggregation of Mg at anode/electrolyte interfaces during Mg-X reactions. In addition to anodes, our studies demonstrate that the expansion of layer spacing in TMDs (i.e. TiS_2 and MoS_2) enables faster intercalation and diffusion of $MgCl^+$ species in TMD interlayers owing to the low energy barrier, and further enhancing the theoretical energy capacity of MgxTMD.

09:20-09:40

A Study of Migration of Grain Boundary and Mechanism of Dislocation Interaction under Applied Biaxial Strain: Atomistic and Continuum Modeling

Yingjun Gao, Physical School of Guangxi University, China

The Phase Field Crystal method is applied to study the cooperative dislocation motion of the grain boundary (GB) migration, the manner of the nucleation of the grain and of the grain growth in two dimensions (2D) under the deviatoric deformation at high temperature. Three types of the nucleation modes are observed by the PFC simulation: The first mode of the nucleation is that through splitting the GB into two sub-GBs (SGB); The second mode is that through the reaction of the SGB dislocations, such as, the generation and annihilation of a pair of partial Frank sessile dislocation in 2D. This process can be considered as the nucleation of dynamic recrystallization; The third mode is that two rows of the dislocations of these SGBs are oncoming by gliding, crossing and passing each other and forming new gap between the two rows of the passing dislocations, which is the nucleation place of the new deformed grain. The research shows that due to the nucleation of different modes, the mechanism of the grain growth by means of the SGB migration is different, and therefore, the grain growth rates are also different. Under the deviatoric deformation of the applied biaxial strain, the grain growth is faster than that of the grain growth without external applied stress. It is observed that the cooperative dislocation motion of the GB migration under the deviatoric deformation accompanies with local plastic flow and the state of the stress of the system changes sharply. When the system is in the process of recrystallized grain growth, the system energy is in an unstable state due to the release of the strain energy to cause that the reverse movement of the plastic flow occurs. The area growth of the deformed grain is approximately proportional to the strain square and also to the time square. The rule of the time square of the deformed grain growth (DGG) can also be deduced by establishing the continuum dynamic equation of the biaxial strain-driven migration of the GB and the grain growth. The copper metal is taken as an example of the calculation, and the obtained result is a good agreement with that of the experiment.

09:40-10:00

Energy Analysis on Dislocation-Particle Bypassing Process by Dislocation Dynamics Simulation

Jianbin Liu, Shinji Muraishi, Tokyo Institute of Technology, Japan

In order to achieve better understanding the process of dislocation bypassing the misfitting particle, discrete dislocation dynamics (DDD) based on the Green' s function method is utilized to the computation of the stress fields of dislocation and misfitting particle. The present research is aimed at quantitatively describing the effect of the key parameters (eigenstrain, distance between a particle and slip plane, particle size, etc.) on interaction energy required for edge dislocation to overcome the misfitting particle. Strengthening ability of the particle blocking the motion of dislocation is analyzed by DDD method in terms of interaction energy between particle and dislocation. According to the simulation results, dislocation bypassing process is varied depending on dislocation bypassing geometry of particle, where magnitude of interaction force is proportionally changed with eigenstrain independent to particle size, while contour area of internal stress field depends on particle size. Although strong interaction force operated on the dislocations lying on the slip plane across the particle, simultaneous dislocation cross slip and prismatic loop formation reduce interaction energy sum throughout dislocation bypassing process. Maximum interaction energy sum throughout bypassing process is achieved by dislocation slip in absence of cross-slip when the dislocation slip plane located on the periphery of the particle. Interaction energy analysis by present study proved that interaction force acted on dislocation greatly influence existence of dislocation cross slip in bypassing process, which reduce amount of work done by external stress.

10:00-10:20

Oscillation Behavior of Electrostatically Levitated Metallic Droplets at High Temperatures

Mingxing Li, Pengfei Zou, Xiao Cai, Haipeng Wang, Northwestern Polytechnical University, China

Droplet oscillation is of great importance in the interdisciplinary physics of nonlinear physics, oscillation dynamics, fluid dynamics, complex systems, space science, and computational physics. It is quite essential to study the oscillation behaviors and understand the underlying mechanism of the droplet oscillation. Especially, the metallic droplets at high temperatures own the characteristics of large surface tension and high activities, the oscillation research of which requires critical experimental condition and excitation method. Thus, it will be very meaningful to figure out the following problems: (i) what cause the formation of

different oscillation patterns? (ii) The change of fluid flow inside the droplet during the oscillation. (iii) The inherent relationships between the oscillation frequency and droplet size, density and surface tension. (iv) Is it possible to realize the stable levitation and conduct the oscillation research of metallic droplets with a diameter of 10mm in a liquid state?

To study the oscillation behavior of electrostatically levitated metallic droplets at high temperatures, the electrostatic levitation (ESL) method was employed and the metallic zirconium droplet was chosen as the experimental object. With increasing the size of levitated droplet, it was observed that the oscillation pattern changes from stable levitation without appreciable oscillation to the second-order zonal oscillation, and then to third-order zonal oscillation. By capturing the morphology evolution during the droplet oscillation, the oscillation pattern, oscillation frequency and oscillation amplitude of zirconium droplet with various sizes at different temperatures were analyzed. As a supplement, a mathematical model was proposed to simulate the droplet deformation and oscillation. By numerical simulation, the internal flow was obtained visually during the droplet oscillation, and the evolution characteristics of higher-order oscillations were predicted. Besides, the inherent relationships between the oscillation frequency and the droplet size, density and surface tension of metallic droplets were investigated systematically. Moreover, a stability factor model was defined as a function of the surface tension and density to quantitatively describe the suspension stability of different metallic droplets. With the guidance of stability factor, the levitation and oscillation of Al and Ti droplet in centimeter size have been simulatively realized.

10:20-10:40 Tea Break

10:40-11:05 Invited

High Throughput Materials Discovery Using a Combination of Density Functional Theory and Artificial Intelligence

Mike Ford, University of Technology Sydney, Australia / Shanghai University, China; Sherif Tawfik, University of Technology Sydney, Australia; Olexandr Isayev, University of North Carolina, USA; Catherine Stampfl, University of Sydney, Australia; Joe Shapter, University of Queensland, Australia / Flinders University of South Australia, Australia; David Winkler, CSIRO, Australia / La Trobe University, Australia / Monash University, Australia; Marco Fronzi, University of Technology Sydney, Australia / Xi'an Jiaotong University China

There are now many examples of naturally occurring materials that can exist in a two-dimensional form, that is, as atom-thick single layer materials. Graphene and MoS_2 are the classic examples, and more recently phosphorene , metal oxides, transition metal dichalcogenides and the more complex MXenes. Many of these 2D layers have useful properties in their own regard, such as the recently discovered quantum emission from hBN and are being combined to create hybrid materials and devices such as quantum light emitting diodes. In Nature in 2013, Geim and Grigorieva foreshadowed a rapid expansion in these van der Waals heterostructures. With such a large parameter space to explore it is important to develop techniques to screen these heterostructures rapidly for useful materials. Density functional theory (DFT) based calculations are important for understanding the properties of 2D materials, however they are too time intensive for undertaking rapid materials screening. Here we use a combination of DFT and machine learning to rapidly explore the very large number of possible combinations of 2D building blocks.

These results demonstrate how machine learning approaches can be effectively used to predict structural and electronic properties of van der Waals heterostructures. Based on a library of 53 2D monolayers, we have used DFT calculations on a small subset of 267 bilayers to train machine learning approaches to predict the properties of all possible 1431 bilayer combinations of these monolayers. Given that the computational time spent in the machine learning predictions is negligable relative to the 267 DFT calculations this represents a 5 fold speed up in screening time. In principle, using our trained machine learning approaches, we can now also predict properties for around 2 million bilayers built from the 1800 2D building blocks identified recently.

This work is supported by resources provided by the National Computational Infrastructure (NCI), and Pawsey Supercomputing Centre with funding from the Australian Government and the Government of Western Australia. Financial support is provided by the Australian Research Council through grants DP150103317 and DP160101301

11:05-11:25

First Principles Calculation of Specific Heat for Si-Ge Alloys within a Broad Temperature Range

Qing Wang, Haipeng Wang,Delu Geng, Mingxing Li, Northwestern Polytechnical University, China

The correlation among the specific heat and temperature is significantly helpful to explore the effect of electrons and lattice vibration within Si-Ge alloys, and thus guiding the potential applications. In this work, the first principles calculation combined with the quasiharmonic approximation are preformed to calculate the equilibrium volume Ve, the specific heat at constant volume CV, the bulk modulus B and the thermal expansion α, of Si and Ge. It is found that a violent increase of CV occurs before 400 K for both Si and Ge. When the temperature

reaches 400K, the CV changes slowly and converges to 24.76J·mol^{-1}·K^{-1} and 24.83J·mo^{l-1}·K^{-1}, respectively. The relationship between the equilibrium volume, the bulk modulus and temperature are discussed. The Si and Ge present the negative thermal expansion when temperature is lower than 118K and 31K, respectively. The lowest calculated thermal expansion for Si is -1.57×10^{-6}K^{-1} at 74K. As for Ge, the lowest thermal expansion appears at 22K, which is -1.2×10^{-7}K^{-1}. Furthermore, the specific heat at constant pressure Cp, of Si and Ge is derived by Ve, CV, α and B from 0K to their melting points. A comparison is performed between the calculated and experimental results. At 298K, the calculated specific heat value for Si is 20.07J·mol^{-1}·K^{-1}. There exist 1.66J·mol^{-1}·K^{-1} difference between the measured value. The calculated and the measured results for Ge at 298K are 23.40J·mol^{-1}·K^{-1} and 23.09J·mol^{-1}·K^{-1}, respectively, exhibiting 1.34% difference. The electronic and the lattice vibrational contribution to the specific heat is discussed through the comparison. The calculated and measured results are nearly identical. Thus, it can be concluded that the lattice vibrational contribution dominates the specific heat of Si and Ge lattices in the temperature range of 123 ~ 823K.

11:25-11:45

Photo-Induced Phase Transition in $MoTe_2$: A Nucleation-Growth Picture via Diffusion-Controlled Vacancy Clustering

Chen Si, Beihang University, China

Polymorphism is a fascinating feature of two-dimensional (2D) transition metal dichalocogenides (TMDs), which make them distinct from other 2D materials such as graphene and hexagonal boron nitride (h-BN). Tailoring the structural transitions between multiple polymorphs of TMDs with different physical properties has led to a host of intriguing applications ranging from electronic, optical and quantum devices to electrochemical catalysis. Recently, local transformations from the semiconducting hexagonal 2H phase to the metallic monoclinic 1T' phase in $MoTe_2$ have been induced by laser irradiation [Science 2015, 349, 625-628], however, a complete microscopic picture for this phase transition remains elusive, particularly, due to the lack of an understanding on the kinetic process of the transition.

Here, we show that nonequilibrium dynamics plays a central role in the photo-induced 2H-to-1T' phase transition of $MoTe_2$, where the transition takes place by a vacancy-mediated nucleation and growth of the 1T' phase in the original 2H lattice, rather than by a collective sliding of a whole atomic layer of Te as perceived before. First, a local 1T' region is formed near a vacancy cluster, even if it is as tiny as a Te di-vacancy. Second, the local 1T' region grows as more Te vacancies are accumulated to the region. Critically important is the fact that the processes are boosted by photo-generated carriers, which enhance the Te vacancy diffusion, increase the speed of the vacancy clustering, and accelerate the 1T' phase transition. By uncovering the interplay between vacancy clustering and photo-excited carriers in photo-induced phase transition of $MoTe_2$, our work sheds new lights on the phase engineering of transition-metal dichalcogenides.

N. Additive Manufacturing and Powder Metallgufy: Refractory Metal & Superalloy

Symposium Organizers:

Huiping Tang, Northwest Institute for Nonferrous Metal Research, China; Yong Liu, Central South University, China; Yuichiro Koizumi, Osaka University, Japan; Kee-Ahn Lee, Inha University, Korea; Qian Ma, RMIT, Australia; Ed Herderick, Ohio State University, USA

Thursday AM
August 22, 2019

Room: 402 (4th Floor)
Symposium: N

Chairs:
Koji Kakehi, Tokyo Metropolitan University, Japan
Xuezhe Zhang, Northwest Institute for Nonferrous Metal Research, China

8:30-9:00 Keynote

Selective Laser Melting of Titanium for Biomedical Applications

Tim Sercombe, The University of Western Australia, Australia

For patients with extensive bone loss or deformities, standard off-the-shelf orthopaedic implants often do not provide an acceptable clinical solution. In order to successfully treat such patients, customized devices with the external geometry derived from the patient's computed tomography or magnetic resonance imaging data must be manufactured. Such customized devices have the potential to reduce surgery, recovery and rehabilitation times, restore correct joint kinetics, improve implant fixation and reduce the likelihood of revision surgery. These combined factors reduce the patients' pain and suffering, and should result in a considerable reduction in hospitalization time and medical costs. Additive manufacturing technologies such as selective laser melting (SLM) are providing the ideal platform for the creation of these customized devices. SLM facilitates the manufacture of parts with almost no geometric constraints and is economically feasible down to a batch size of one. It is a powder-based, layer-

additive manufacturing technology, whereby parts are built by melting selected areas of a powder layer using a high-intensity laser beam. Three-dimensional parts are then manufactured by sequential production of these two dimensional layers.

Titanium and its alloys are currently the favoured material for load bearing applications due to its high strength and corrosion resistance, relatively low modulus and good biocompatibility. The majority of studies on SLM-produced titanium alloys have been focused on the either commercially pure titanium or the traditional Ti-6Al-4V. However, driven by the mismatch in Young's modulus between these materials and the surrounding bone which can lead to the well-known "stress-shielding" phenomenon, low modulus beta titanium alloys are also gaining attention. In this work we will look at the various classes of titanium alloys and explore their suitability for use in Selective Laser Melting. We will look at the effect of the processing variables on the properties, the production of lattice structures, as well as post process heat treatment and surface finishing techniques have on the properties of the printed parts.

9:00-9:25 Invited

Net-Shape Forming and Microstructure Controlling of Tungsten Products

Xuanhui Qu, Lin Zhang, Mingli Qin, University of Science and Technology Beijing, China

Tungsten exhibits attractive properties, such as high melting point, excellent thermal conductivity and superior mechanical properties at high temperature, which is irreplaceable material for some applications in national defense, atomic energy and electric industries, et al. Due to the high hardness and room temperature brittleness, tungsten products with complex geometries is very difficult to be fabricated. Near-shape forming technology of complex shaped tungsten components is realized by utilizing powder injection molding technology in this study. Two kinds of tungsten components with different microstructure were investigated: ultrafine grained tungsten with high densification and porous tungsten with uniform pore structure.

For the ultrafine grained tungsten, Nano-sized W-based composite powder W-La_2O_3 was fabricated by solution combustion synthesis (SCS) followed by hydrogen reduction. Solution combustion synthesis is an exothermal redox reaction between an oxidizer (e.g. metal nitrates) and a fuel (e.g. glycine, urea, citric acid.) in an aqueous solution within a short time (on the order of minutes). The advantage of the method is that all the elements are mixed at the molecular level, which guarantees the uniformity of the reactant, compared to solid-solid or solid-liquid methods. Needle-like $W_{18}O_{49}$/lanthanum tungstate composite powder was usually obtained with SCS, and after hydrogen reduction process, the W-based composite powder W-La_2O_3 with the grain size of 30nm could be produced. The synthesis process, densification behavior of the powder, grain growth kinetics and strengthen mechanisms, as well as the resulting mechanical properties of the alloy were discussed. The relative density the fabricated W-La_2O_3 is 95.0% at 1500˚C. The grain size of is only 0.57μm, and the micro hardness and compressive strength reach up to 680 HV0.2 and 2119MPa, respectively.

For the porous tungsten, the tungsten products with high open porosity and narrow pore size distribution were fabricated by using near spherical with high dispersity. With commercial tungsten powder, the products exhibit very non-uniform pore structure due to highly agglomeration phenomenon of the powder. Jet milling is found to be an effective approach to achieve deagglomeration of tungsten powder. During the air jet milling process, the powders were forced by high speed and high purity nitrogen into the milling chamber, where the powders were collided with each other, and deagglomeration and morphological modification were achieved. After jet milling, the agglomeration of the initial powders disappeared and the particle morphology tend to be nearly spherical. The dispersed tungsten powder exhibits good flowability, lending to enhanced packing density of tungsten powder and powder loading of the injection molded preform. This is beneficial for the formation of contiguous open pores and uniform pore size. The influence of particle size and sintering temperature on pore structure were investigated in detail.

Finally, the typical applications and the potential applications of ultrafine grained tungsten and porous tungsten were introduced.

9:25-9:50 Invited

Refractory Metals Fabricated by Selective Electron Beam Melting

Huiping Tang, Guangyu Yang, Kun Yang, Nan Liu, Liang Jia, Jian Wang, Northwest Institute for Nonferrous Metal Research, China; Pengwei Yang, Northeastern University, China

Refractory metals (tungsten, molybdenum, tantalum, niobium, etc.) with the high melting point, the high stability and the wear resistance are very important high temperature structural materials. In addition, for their special properties, such as the high density of tungsten, the high rigidity of molybdenum, the high specific volume and good biocompatibility of tantalum and niobium, they are also very important functional materials used in the fields of aerospace, new energy, military and other major engineering, etc. For the very high melting point, the main route in refractory metal manufacturing is powder metallurgy and plastic processing, but the high temperature producing and the further processing are all difficult and costly. Selective electron beam melting (SEBM) is a typical additive manufacturing technology,

which is characterized by higher energy input of electron beam. It has obvious advantages in the preparation of refractory metals.
Refractory metals, such as W, Mo, Ta, Nb, and their alloys were fabricated by SEBM, and the effect of the parameters on the density and microstructure of the metals were also studied. Metal bulks without obvious defects such as holes and cracks were formed. The relative density is 99%, and the mechanical properties meet or exceed that of the metals prepared by traditional powder metallurgy. During the SEBM process, the heat conduction among molten pool, formed area, powder bed and start plate is complex for the complex temperature field. Grains were formed by epitaxial growth, and it appears as columnar crystals. Furthermore, the morphology of columnar crystals was affected remarkably by the heat conduction. Lastly, the application of refractory metal manufactured by SEBM was also introduced.

9:50-10:10

Influence of the Powder Manufacturing Technique on the Structure and Properties of the Test Specimens from Inconel 718 Alloy

Oleksii Pedash, Valery Shylo, Nataliya Lysenko, Volodymir Klochykhin, MOTOR SICH JSC, Ukraine

The present presents result of the comparative examination of test specimens from the heat resistant superalloy Inconel 718 3D printed with the use of the powders produced by different techniques: Vacuum Induction-melting Inert Gas Atomization (VIGA) and Plasma Rotated Electrode Process (PREP). Tensile strength and impact strength tests as well as micro- and macro structural examination were made on the test specimens 3D printed in vertical (Z axis) and horisontal (X-Y) by the Laser Powder Bed Fusion (L-PBF) technology and subsequently subjected to a standard heat treatment.
The examination of the tensile and impact strength specimens after the testing revealed that the fractures the specimens produced by both techniques are fine-grained and characterized by a ductile fracture. The macro- and microstructure of the specimens homogeneous, fine-grained and oriented along the build-up direction, typical for Inconel 718 in as heat treated condition.
It is important to note a presence of micro porosity with the pores sized up to 15 micrometers in the test specimens produced from the powder manufactured by PREP whereas the specimens produced from the powder manufactured via VIGA had the pores with sizes up to 35 micrometers. Oxide inclusions sized respectively 10 and 25 micrometers have also been identified.
The authors believe that the identified microporosity in the fractures and the microstructure necessitates mandatory Hot Isostatic Pressing of the 3D printed parts in order to perform a substantial healing of the structure. The parts used in the aerospace industry are of a special concern.
For both the studied powder manufacturing processes the specimens 3D printed in the horizontal position demonstrate a slightly higher level of the strength characteristics, whereas for the ductility characteristics an opposite relationship was observed. It should be noted, that the test specimens processed from the powder produced by PREP demonstrate significantly higher(by a factor of 3 to 4) impact strength than those from the powder obtained using VIGA process. The use of the PREP powder manufacturing process has been found to be a positive factor that contributed to increased (1.5~2 times) stress-rupture strength as compared to the test specimens from the powder produced by VIGA.

10:10-10:30

Microstructures and Properties of Tungsten Alloys Prepared Using Laser Melting Deposition Process

Guomin Le, Yingpei Wang, Yuzhao Zhou, Institute of Materials, China Academy of Engineering Physics, China

Tungsten alloys have wide applications due to the properties of high melting point and high density. Traditional preparation of tungsten alloys using liquid phase sintering (LPS) usually has a large material waste, and is hard to avoid distortion. Due to a near net forming capacity, and a small heat influence volume during fabrication, a laser melting deposition (LMD) additive manufacturing technique has been applied in this study to fabricate thin wall tungsten alloy samples, by applying laser powers of 500 W, 600W, 700W, 800W, and 900W, a scanning speed of 400mm/min, and a dual directional scanning strategy. The used raw materials is a mixture of tungsten powders, iron powders, and nickel powders. Effects of process parameters on the microstructure evolutions and properties of the fabricated tungsten alloys have been studied. The tungsten alloys consist of two phases of FCC (Ni, Fe) bonding matrix and BCC tungsten particles, similar to those prepared using LPS, unless the tungsten particles are not of spherical shapes. The tungsten particles resume the sizes and shapes of raw tungsten powders for lower laser powers, due to partial dissolutions of tungsten. As the laser power increases, some tungsten particles show dendritic shapes, due to the dissolution and precipitation of tungsten during the melting and solidification process. As the laser power increases, the density of the tungsten alloy increases, and the distribution of tungsten particles becomes more homogenous. Near full dense tungsten alloys with a tungsten content up to 88% have been

successfully prepared using laser powers of 800W and 900W. The fabricated tungsten alloys show tensile strength up to 1000MPa, which is comparable or higher than those of tungsten alloys prepared using LPS. However, the elongations of the fabricated tungsten alloys are as low as 4%. Further studies are planned to improve the ductility of tungsten alloys prepared using LMD technique.

10:30-10:45 Tea Break

10:45-11:10 Invited

Microstructure and High-Temperature Properties of Ni-Base Superalloys Fabricated by Selective Laser Melting

Koji Kakehi, Tokyo Metropolitan University, Japan

To clarify the effects of the unexpected precipitation, interdendritic segregation and recrystallization, which are characteristic phenomenon in the selective laser melting process on the microstructure and high-temperature mechanical properties in Ni-base superalloys, the effects of degradation factors on the mechanical properties in IN718, CM247LC and IN939 alloys will be discussed. The microstructure, tensile and creep properties were examined. In IN718 alloy which is strengthened γ"-γ' precipitation, the creep rupture life and ductility of materials produced by additive manufacturing were lower than those of a conventional material at 650˚C. The horizontal-direction specimen exhibited inferior creep life and worse ductility than the vertical-direction specimen because of the direction of the interdendritic δ-phase precipitates, which were arrayed perpendicular to the stress axis in the former specimen. The morphology and a row of interdendritic δ-phase with incoherent interfaces were found to affect the materials' creep life and ductility in IN718. In SLM CM247LC, the segregation of alloy elements, Hf and Zr along the interdendritic region brought about solidification crack. Whereas, as for IN939 alloy which is strengthened by γ' precipitation, crystals oriented along [001] orientation and high density of dislocations were observed in the as-built specimen. However, the recrystallization during heat treatment and creep deformation were found to affect the materials' creep life and ductility both at 650˚C and 816˚C.

11:10-11:30

Microstructure and Mechanical Behavior of GH 4099 Superalloy Fabricated by Electron Beam Melting

Hui Peng, Hongbo Guo, Xiaodan Teng, Shengkai Gong, Beihang University, China

Ni-based superalloys are widely used in hot sections in aerospace industry. Recently, additive manufacturing (AM) of superalloys exhibits great potential in fabricating complex parts. The mechanical properties of superalloys can also be preserved or even improved due to the tailored microstucture processed by AM. In this work, a Chinese superalloy GH4099, was fabricated by electron beam melting (EBM). Argon gas atomization (AA) and plasma rotation electrode process (PREP) powders with the similar compositions and size distributions were used as raw materials for comparison. Microstructure and mechanical properties of both the as-EBMed and post-treated alloy samples were investigated. The results show that the different powder characteristics resulted in the different building temperatures for AA and PREP samples, which were 1253K and 1373K, respectively. With increasing the building temperature, the EBM processing window shifted towards the higher velocity direction. Furthermore, intergranular cracking was observed for the PREP sample as a result of the slightly concentrated Si at grain boundaries. The cracks were completely eliminated by post hot isostatic pressing (HIP). Fine spheroidal gamma prime phase precipitated after solution treatment and aging (STA). The tensile strength of the HIP+STA samples was ~920MPa in the building direction and ~850MPa in the horizontal direction, comparable with that of the wrought alloy.

11:30-11:50

Effect of Heat Treatment on the Microstructural Evolution of a Precipitation-Hardened Superalloy Produced by Selective Laser Melting

Mang Ni, Chao Chen, Kechao Zhou, Central South University, China

Additive manufacturing technologies are receiving widespread attention due to the potential to create customized components with unique microstructures and high performances in structural applications. Inconel 718 (IN718) is a widely known nickel-based precipitate-strengthened superalloy of good weldability, which is ideally suited for the selective laser melting (SLM) process. This study systematically evaluates the microstructural evolution and mechanical properties of a SLM-processed IN718 alloy under solution-aging treatment, which led to novel microstructures combining solidification cellular structures and full precipitation of a strengthening phase in the SLM-fabricated IN718 alloy. It was demonstrated that the fraction of low angle grain boundaries (LAGBs) and the aspect ratio of the grains decreased with the increase of the solution temperature, while the average grain size increased after solution treatment. Aging treatment promoted full precipitation of the strengthening phase. The fraction of the γ' and γ" phases exceeded 45.5% compared to 24% of the as-fabricated alloy. Heat treatment also

eliminated the anisotropic mechanical properties of the SLM-processed IN718, as the columnar grains transformed to equiaxed grains with the increase of the solution temperature. Consequently, the static tensile properties showed a combination of high strengths ($\sigma_{0.2}$=1276MPa and UTS=1505MPa) and excellent ductility (elongation exceeded 13%) of the SLM-processed IN718 after low temperature (980℃) solution and double aging treatments. The superior mechanical properties were attributed to the combination of hierarchically heterogeneous microstructures (solidification enabled sub-micron cellular structure and large fraction of LAGBs) formed in the SLM process and the full precipitation of the γ' and γ" phases in the aging treatment. Furthermore, this study demonstrated the method proposed herein was an economical and environment-friendly process for enhancing the strength of the SLM-processed IN718 by direct aging treatment without the energy-intensive solution treatments. The approach could also potentially provide guidance for improving the mechanical properties in other SLM-processed precipitate-strengthened alloys by excluding energy-intensive solution treatment methods.

11:50-12:10

Metastable Cellular Microstructure and Its Effects on Phase Transformations in Selective Laser Melted Maraging Steel

Yingjie Yao, Zhigang Yang, Chi Zhang, Hao Chen, Tsinghua University, China

Metastable cellular microstructures are frequently found in various additive manufactured alloys, especially those made by the selective laser melting (SLM) or electron beam melting (EBM). A high density of defects and alloying elements segregation were usually observed at the boundaries of the cells, which were deduced to be boundaries of columnar sub-grains formed during the rapid solidification. The cellular microstructure was found to play an important role in phase transformations and mechanical properties of the additive manufactured alloys. In this study, maraging steel samples are fabricated by the SLM method. TEM, AES-EBSD and other techniques were used to characterize the cellular microstructure in the samples. Dislocations and alloying element distribution are depicted, showing a dislocation network with almost no segregation along the cells' boundaries in the as-fabricated state of samples. The SLM fabricated steels were aged at ~500℃ for 1~10 hours, and the effects of cellular structures on precipitation and austenite reversion were analyzed. The boundaries of the cellular structures were found to act as the nucleation sites of austenite grains, and a three-dimensional network of retained austenite can be obtained along the cells' boundaries. Enrichment of alloying elements, especially Ni and Co, was observed in retained austenite. A high density of nanosized precipitates are observed in the aged samples, which leads to a significant improvement in the microhardness of the samples. To study the thermal stability of the cellular microstructure and its effects on martensitic transformation, the additive manufactured samples were heated to the fully-austenite region and kept for different times followed by quenching to room temperature. The cellular microstructure was found to be metastable at elevated temperatures due to dislocation recovery and alloying element diffusion, while it can be retained if the austenization duration is short. The metastable cellular microstructure plays a significant role in the phase transformations, and it opens a new route to create new microstructures and improve mechanical properties of the additive manufactured steels.

12:10-12:30

The Effect of Homogenization Temperature on the Microstructure and High Temperature Mechanical Performance of IN718 Fabricated by SLM

Yang Gao, Ming Cao, Runping Chen, Junyuan Deng, Beijing University of Technology, China

Microstructure and mechanical properties at elevated temperature (650℃) of Inconel 718 manufactured by Selective Laser Melting (SLM) were investigated in this paper. The spherical powder Inconel 718, which has been produced by gas atomization, was used as powder bed material. The diameters of the gas-atomized powers range from 5~45μm. Four kinds of heat treatments with different homogenization heat treatment processes under the condition of keeping the same solution treatment and aging process were carried out to regulate the microstructure of the SLM-ed IN718 alloy in order to obtain the optimum comprehensive mechanical performance at high temperature. The dimension and morphology of grains, subgrains, different precipitates including δ phase, strengthening phase, carbides and nitrides were investigated. In addition, their evolution mechanism was also analyzed deeply. Furthermore, aiming at figuring out the effects of microstructures on the mechanical performance, creep rupture test and tensile test at 650℃ were carried out to compare the performance differences of heat-treated samples. The results demonstrated that the heat-treated samples show the better creep rupture performance and higher tensile strength at elevated temperature than that of the wrought. In addition, the sample with homogenization heat treatment in 1080℃, solution treatment in 980℃ and conventional aging treatment shows the optimum mechanical properties in 650℃.

12:30-12:50

Research of Texture and Mechanical Performance of Molybdenum Sheets for Vacuum Electron Devices

Yan Li, Zenglin Zhou, Zhilin Hui, Xueliang He, Xiaoying Fu, Wenshuai Chen, GRIMAT Engineering Institute Co.,Ltd., China

Microstructure and texture of molybdenum sheets for vacuum electron devices were studied by electron back-scattered diffraction (EBSD) and metallography analysis. The correlation of microstructure and texture with mechanical performance was discussed. The results show that the molybdenum sheets with excellent processability have some characteristics: Observed microstructures are mostly flat cloud-flake grains arrayed orderly along rolling direction and paralleled to rolling surface. Grain orientation distribution which is relatively weaker and more dispersed, consists of {001}<110> and {112}<110> components of α-fiber, {111}<110> and {111}<112> of γ-fiber, the shear texture {112}<111> and the cube texture {001}<100>. The maximum component of the texture in the center is {001}<110>, with high texture intensities on {112}<110>. In the surface layer, the maximum shifts to {112}<110> with few γ-fiber and undetected copper component. Relatively less high-angle boundaries with $\theta > 50°$ are detected. Therefore, the Mo sheets show higher yield ratio and elongation, and weaker elongation anisotropy in RD, TD, and 45° -RD directions.

A. Advanced Steels and Processing: VIIII

Symposium Organizers:

Han Dong, Shanghai University, China; Zhigang Yang, Tsinghua University, China; Yoshitaka Adachi, Nagoya University, Japan; Dong-Woo Suh, Pohang University of Science and Technology (POSTCEH), Korea; Christopher Hutchinson, Monash University, Australia; Amy Clarke, Colorado School of Mines, USA

Thursday PM Room: 205+206+207(2nd Floor)
August 22, 2019 Symposium: A

Chairs:
Qingdong Liu, Shanghai Jiaotong University, China
Guangrui Jiang, Shougang Group, China

13:30-13:55 Invited

Effect of Prior Ni Plating on Selective Oxidation Behavior and Galvanisability of High Strength Steel

Guangrui Jiang, Haiquan Wang, Huaxiang Teng, Shougang Group, China

Much more kinds of hot-dip galvanized advanced high strength steel (AHSS) were widely applied on the car body due to requirement on safety and economy. However, the galvanisability of AHSS was dramatically deteriorated on account of the selective oxidation of alloying elements, such as Si, Mn, Cr, on the external surface after being annealed. To figure out this problem, some new technology were developed, including prior plating technology. In this study, a prior Ni plating with 50 to 300nm thickness was electrodeposited on a C-Mn-Si high strength steel followed. Then samples were annealed and galvanized through a Hot Dip Process Simulator. To studied the selective oxidation behavior of the high strength steel with the prior Ni plating, scanning electron microscopy, glow discharge optical emission spectroscopy, X-ray photoelectron spectroscopy and transmission electron microscopy were applied. Moreover, the morphology of the coating was analyzed by scanning electron microscopy and the composition was analyzed by energy disperse spectroscopy. It could be found that the prior Ni plating with no less than 100nm thickness could remarkably suppress enrichment of Si to the external surface. Compared with Si, Mn could easily be found on the external surface of the prior Ni plating no matter how thick the prior Ni plating is. With decreasing the thickness of the prior Ni plating, more alloying elements could diffuse to the external surface during annealing. Moreover, A large amount of Si and Mn appear at the boundary of the prior Ni plating. Under the Ni plating, some mixed oxides with Si and Mn could be found. After being galvanized, it could be found that hardly any defect could be found on the Ni plating zone and much naked matrix could be found on the no Ni plating zone. As analyzed by SEM and EDS, a continuous Al enrichment layer could be found between the Zn coating and the Ni plating while the Al enrichment layer for the sample without prior Ni plating is cracked, which indicated improvement coating adhesion and galvanisability by the prior Ni plating.

13:55-14:15

Development and Application of Square Turbulence Inhibitor in a Slab Caster Tundish

Yanzhao Luo, Research Institute of Technology, Shougang Group Co., China

Tundish is an important metallurgical reactor that links steelmaking and casting operations, allowing the continuous casting operations to be performed without any disruption. Exposed steel in the tundish can cause reoxidation, leading to the formation and growth of inclusions and affecting steel cleanliness. Gases such as oxygen and nitrogen present in air have high affinity to react with dissolved elements in steel like Al, Mn, Ti, etc. to form harmful inclusions. The primary inclusions

formed are Al_2O_3 during open eye formation in tundish. These inclusions generally have dendritic or cluster-like shapes, which allows them to easily get attached to the walls of the nozzles and cause clogging, which affect product quality and productivity. One reoxidation event at the caster is known as a Tundish Open Eye. The formation of open eyes in tundish can lead to the reoxidation of molten steel and the formation of harmful inclusions. In addition, it is also a place for gas absorption, heat loss and slag emulsification. All these factors make it necessary for us to understand the basic principles of open eye formation, which in turn enables us to prevent or control its harmful effects. The flow field and temperature field of 80 ton tundish continuous casting process were simulated by ANSYS Fluent software. The results show that the stagnation time of round and square turbulence inhibitors increases from 136s to 147s, the average residence time increases from 655s to 663s, the percentage of dead zone increases from 5.65% to 4.26%, and the flow area increases from 68.4% to 74.89%, which is beneficial for inclusion floating removal. The total oxygen content of round and square turbulence inhibitors was 20.8ppm and 18ppm, respectively. Compared with the hot rolling and cold rolling results with different turbulence inhibitor, the rates are 0.6%, 1.2% and 1.31%, 1.86%. The square turbulence inhibitor shows the good results.

14:15-14:35

Effect of Annular Argon Blowing at Upper Nozzle on Behavior of Steel and Slag Interface in Tundish

Xufeng Qin, Changgui Cheng, Yang Li, Shifa Wei, Yan Jin, Wuhan University of Science and Technology, China

The process of annular argon blowing at the upper nozzle of tundish can effectively purify the molten steel and prevent the tundish nozzle from clogging, an unreasonable process parameters may cause the risk of slag entrapment and molten steel exposure to atmosphere. In order to utilize the purification effect of argon bubbles in the annular argon blowing, according to the process parameter of a continuous slab casting, the water model and the numerical simulation of coupling the volume of fluid model with the discrete phase model were established to study the effects of the flow rate of argon blowing, the parameters of annular permeable brick and the casting speed on the behavior of the steel-slag interface in tundish. The results showed that the behavior of steel-slag interface in tundish obtained by numerical simulation was in good agreement with the experimental results of the water model. Under the action of blowing argon at upper nozzle, the flow of molten steel was active in the surrounding area of the stopper rod, and there existed significant recirculatory flows in the leftside and frontside of the stopper rod, in which the turbulent kinetic energy and flow velocity in steel-slag interface were large. With the increase of flow rate of argon blowing, the interface velocity and turbulent kinetic energy around the stopper increased, which reinforced the fluctuation of the steel-slag interface, and the molten steel exposure to atmosphere and slag entrapment may be possible. To avoid the tundish open eye, the flow rate of argon blowing should be less than 3L/min. With the increase of casting speed, the number of bubbles floating to liquid steel and slag interface decreased, and the fluctuation of steel-slag interface was weakened for the impact force of upwelling bubble plumes on the steel slag interface became lower. With increased the width of annular permeable brick, the bubble size decreased, which can effectively reduce the risk of slag entrapment and the molten steel exposure to atmosphere. These results can provide a theoretical basis to optimize the parameters of the argon blowing process and improve slab quality.

14:35-14:55

Theoretical Calculation and Evolution Mechanism of Inclusions Precipitation During Continuous Casting of High-Titanium Steel

Huazhi Yuan, Yuanbing Wu, Shengping He, Qian Wang, Qiangqiang Wang, Chongqing University, China; Jianhua Zeng, Min Zhang, The Iron & Steel Research Institute, Panzhihua Iron & Steel Co, China

The application of titanium in the steel industry is mainly based on titanium microalloyed steel, which is used to improve the strength and the serviceability of steel products. However, as the Ti content in the molten steel increases, more titanium-containing inclusions are precipitated. The precipitation of TiC can effectively improve the wear-resistance of the steel, but the excess precipitation of TiN will seriously affect the quality of the slab and the fatigue performance of the product. Therefore, for the wear-resistance steel with high titanium content (>0.2%), the way to precisely control the precipitation of inclusions, such as titanium carbide, titanium nitride and solid solution titanium carbonitride formed during the continuous casting process, is of great significance to the final product quality. However, the research on the precipitation of titanium-containing inclusions in high-titanium steel is scarce, especially about TiC. Against this background, the current study carried out systematic research of the precipitation behavior of inclusions during the cooling and solidification process in the continuous casting of high-titanium steel. In this study, the effect of segregation of solute elements on the precipitation of inclusions is considered in thermodynamics and kinetic calculations. Main results show that the precipitation of TiC in the liquid steel does not satisfy the corresponding thermodynamic conditions. And the enrichment of solute elements in mushuy zone will increase the concentration range of TiC precipitation. Furthermore, the growth theory of inclusion particles at the solidification front

was analyzed. The analysis results showed that TiC inclusions can only precipitate when the solidification is nearly completed under the controlled conditions used in this study for the manufacture of high-titanium steel; the radius of TiC particles decreases as the Ti and C contents decrease and as the cooling rate increases. Therefore, the ultimate size of TiC inclusions can be reduced by lowering the concentration of C and Ti as well as by increasing the cooling rate.

14:55-15:15

Morphology Characteristics of Carbon Segregation in High Carbon Steel Billet by CC Based on Fractal Dimension and Dimensionless Perimeter

Jianghai Cao, Zibing Hou, Dongwei Guo, Zhongao Guo, Ping Tang, Chongqing University, China

Segregation of solute elements is an inherent feature during alloy solidification. Macro/semi-macro segregation are considered more harmful to final steel properties, as they cannot be eliminated even with prolonged heat treatments. High carbon steel billet by continuous casting (CC) is an important base material for the production of high end rod and wire rod, whereas macro/semi-macro segregation is more severe in high carbon steel billet owing to its high carbon content and low equilibrium distribution coefficients. In order to control segregation defects of high carbon steel billet delicately and effectively, the morphology characteristics of carbon segregation in 82B cord steel (the carbon content is 0.82wt%) produced in a factory are investigated based on fractal dimension and dimensionless perimeter. It is shown that the segregation extent is relatively minimum in the columnar to equiaxed transition (CET) region of billet. And the whole segregation extent is mostly influenced by the large segregation point, the segregation ratio will be increased when increasing the area of the large segregation point. Meanwhile, it is found that fractal is a very important characteristic of the segregation point morphology in the billet. The both parameters of the fractal dimension and the dimensionless perimeter are effective to quantitatively evaluate the complexity of the segregation point morphology. Fractal dimension and dimensionless perimeter are reduced from the outer to the middle zones of the billet, this indicates that the complexity of segregation point morphology is reduced. Moreover, compared to dimensionless perimeter, fractal dimension can be used as a good criterion for measuring the segregation degree. The segregation degree will be increased when increasing the corresponding fractal dimension. In addition, the fractal dimension decreases with increasing second dendrite arm spacing (SDAS) and local solidification time. It can be considered that the fractal dimension of segregation point is determined mainly by local solidification time. This result demonstrates the potential of the fractal dimension as a parameter for estimating local solidification time of the billet in which the measurement of SDAS is difficult, thereby serving the further optimization of continuous casting process and the production of high-end steel.

15:30-16:10 Tea Break

16:10-16:30

Research and Modeling on the Correlation Among Microstructure, Yield Strength and Process of Bainite/Martensite Steel

Jiajia Qiu, Min Zhang, Guhui Gao, Zhunli Tan, Xiaolu Gui, Beijing Jiaotong University, China; Bingzhe Bai, Beijing Jiaotong University / Tsinghua University, China

Bainite/martensite multiphase rails have attracted great attention in the last decade due to excellent mechanical properties and service performances. Conventional production process of bainite/martensite multiphase rails is air cooling after rolling, which is susceptible to seasonal and regional influence. Controlled cooling process has been proved to improve the uniformity of microstructure, increase the strength and toughness of rail steel and reduce the influence of environment. For the purpose of reducing the cost of trial production, experiments and finite-element simulations were combined to explore the controlled cooling process of rails. In the present work, mechanical properties of rails produced by controlled cooling process have been measured and yield strength decreased continuously from 5mm to 45mm under the tread. Dislocation density and substructure size of rail steel were measured by scanning electron microscope (SEM), e-beam sustained discharge (EBSD) and X-ray diffraction (XRD). Microstructures of present steel contained bainite (B), martensite (M) and retained austenite (RA) at room temperature. In order to simplify the following analysis, microstructures were regarded as a mixture of α' phase (containing M and B) and γ phase (RA) based on crystal structure. Lath thickness and block size increased while the dislocation density decreased from 5mm to 45mm under the tread. Based on the correlation among lath thickness, dislocation density and yield strength, a physical model was proposed to predict the yield strength of rail steel. Controlled cooling production process was simulated and the temperature field of rails was obtained. It was shown that the temperature increased gradually from 5mm

to 45mm under the tread. Dislocation density and lath thickness revealed good correlations with temperature. The contribution of dislocation strengthening and grain boundary strengthening to yield strength was about 70%. Finally, a prediction model combining temperature field simulation with yield strength was established and could predict the yield strength at different positions under the rail tread. Fair agreement between predicted and experimental values was obtained and the simplification of the microstructure was feasible. This model could help to obtain the relationship between controlled cooling process and yield strength of rail steel and provide suitable parameters for production.

16:30-16:50

Effect of Intercritical Quenching Temperature on Microstructure and Yield Ratio of Constructional Steel

Can Zhang, Xuemin Wang, Jinghua Cong, Lujie Wei, University of Science and Technology Beijing, China

Effects of intercritical quenching temperatures on the microstructure and yield ratio of constructional steel were systematically investigated. In order to achieve this purpose, the RQ+IQ (reheated quenching and intercritical quenching) process with different intercritical quenching temperatures and massive technical methods such as tensile test, metallographic observation, SEM and TEM observation were used. The results show that a composite microstructure of ferrite and martensite is obtained by RQ+IQ process. Most of the ferrite and a small amount of martensite were observed in the experimental steel when quenching temperature was 740℃. With the increase of quenching temperature, the amount of martensite increased and the ferrite coarsened. When quenching temperature was 820℃, the microstructure consisted of a large amount of martensite and a small amount of ferrite. With the increase of intercritical quenching temperature, the yield strength and tensile strength of the experimental steel increase and the yield ratio drops firstly and then rises. The increase of tensile strength comes from the increasing martensite transformation percentage and the increase of yield strength comes from the increasing dislocation density of ferrite. The yield ratio (yield-to-tensile strength ratio) of the test steel declined from 0.658 to 0.649 in the range of quenching temperature from 740 to 760℃ and rose at quenching temperatures above 760℃. The reason for this phenomenon is that as the quenching temperature of the two-phase region increases, the austenite transformation increases, but the carbon and manganese content in the austenite gradually decreases, resulting in a decrease in martensite strength after quenching. So with the yield strength continuously increasing, the maximum difference between yield strength and tensile strength occurred at around 760℃, at which time the yield ratio was the lowest.

16:50-17:10

Heterogeneous Retained Austenite in Quenching and Partitioning Steels

Ran Ding, Yang Zhigang, Chi Zhang, Hao Chen, Tsinghua University, China

The heterogeneous retained austenite of a low alloyed Fe-C-Mn-Si steel (QP980) processed by intercritical annealing and quenching & partitioning is systematically characterized by a correlative application of auger electron spectrometer (AES) and electron back scattered diffraction (EBSD), which simultaneously provides nanoscale phase/elements distribution and crystallographic information. The mechanism of retained austenite formation during intercritical annealing and the following Q&P process is discussed based on thermodynamic simulations as well as experimental observations. Various kinds of retained austenite with different C/Mn content, crystallographic orientation and size are expected to lead to heterogeneity in their thermal and mechanical stability.

17:10-17:30

Effect of interfacial Mn partitioning on carbon partitioning and interface migration during the Quenching and Partitioning process

Zongbiao Dai, Zhigang Yang, Chi Zhang, Hao Chen, Tsinghua University, China

The present study elucidates the critical role of interfacial Mn partitioning on carbon partitioning and martensite/austenite interface migration during the quenching and partitioning process. Two Q&P models (QP-LE and QP-PE), in which effects of substitutional alloying elements have been considered by assuming Local Equilibrium or Paraequilibrium at the martensite/austenite interface, are proposed to simulate the kinetics of carbon partitioning and interface migration in the Fe-C-Mn-Si steels. The QP-LE and QP-PE models predict that whether the interface migrates or not and its moving direction are dependent on quenching/partitioning temperatures and alloy composition. A careful comparison between experiments and model predictions indicates that the dependence of interface migration behavior on quenching/partitioning temperatures measured by experiments during the Q&P process could be explained reasonably well by the QP-LE model, rather than the QP-PE model and the constrained carbon equilibrium model. The current study suggests that interfacial partitioning of Mn plays a significant role in carbon partitioning and interface migration during the Q&P process, which should be considered in the design of Q&P steels in the future.

C1. Light Metals and Alloys-Aluminum: VI

Symposium Organizers:

Baiqing Xiong, GRINM Group Co. Ltd., China; Yoshihito Kawamura, Kumamoto University, Japan; Young Min Kim, Korea Institute of Materials Science (KIMS), Korea; Jian-Feng Nie, Monash University, Australia; Diran Apelian, Worceste Polytechnic Institute, USA

Thursday PM Room: Presidium Conference Room
August 22, 2019 Symposium: C1

Chairs:
Timothy Langan, Clean TeQ, United States

13:30-13:55 Invited

Precipitation of Stable Sc-Containing Dispersoids in High Strength Aluminum Alloys

Timothy Langan, Clean TeQ, United States

Scandium, the most potent alloying element that can be added to aluminum, has been shown to improve performance of alloys in a number of ways including; i) refining grain size during solidification, ii) reducing or eliminating recrystallization in wrought product, iii) precipitation of very potent stable coherent disperdoids and iv) enhanced nucleation of strengthening phases (e.g., refined distribution of theta prime phase in Al-Cu alloys). Early work by Willey at Alcoa demonstrated that modified heat treatment schedules can be used to enhance strengthening in Sc-containing alloys. This talk will review the recent development of heat treatments designed to optimize precipitation of stable Sc-containing dispersoids in commercial aluminum alloys. Work will be highlighted that elucidates the effects of alloying and trace elements in commercial alloys on nucleation, growth and stability of these dispersoids. Specifically looking at interactions with Cu in Al-Cu 2xxx alloys; Mg in Al-Zn-Mg 7xxx and Al-Mg 5xxx; and Si in Al-Si-Mg 6xxx. Results of advanced characterization studies have been used to guide these efforts. Work shows that interactions between Sc, vacancies and other alloying elements impacts nucleation of both the Sc-containing dispersoids and strengthening phases. Approaches to incorporate heat treat schedules designed to precipitate Sc-dispersoids into conventional heat treat schedules used to homogenize commercial alloys will also be discussed.

13:55-14:15

Effects of Ultrasonic Treatment on Microstructure and Mechanical Properties of Mg-6Zn-0.5Y-2Sn Magnesium Alloys

Zhihui Xing, Gaozhan Zhao, Ming Li, Jianquan Tao, Zhiwei Huang, No.59 Institute of China Ordnance Industry, China; Hansong Xue, College of Materials Science and Engineering, Chongqing University, China

In this paper, the effects of melt ultrasonic treatment on the microstructure and mechanical properties of Mg-6Zn-0.5Y-2Sn magnesium alloy was studied by means of ultrasonic vibration treatment with different powers (0W, 300W, 500W and 700W) during solidification process of Mg-6Zn-0.5Y-2Sn magnesium alloy. The results show that the appropriate ultrasonic treatment can not only improve the microstructure of the as-cast and extruded experimental alloys, but also significantly improve their mechanical properties.

The microstructure of the as-cast Mg-6Zn-0.5Y-2Sn alloy is mainly consisted of α-Mg phase, $MgZn_2$ phase, MgSnY phase, Mg_2Sn phase and I-phase (Mg_3Zn_6Y, with small amount). With the application of ultrasonic treatment, the small amount I-phase and the existed coarse dendrites microstructure nearly disappear, and with the increase of the ultrasonic treatment power, the coarse dendrites microstructure is gradually changed into roundish equiaxed grains. And the morphologies of $MgZn_2$ phase, MgSnY phase and Mg_2Sn phase are transformed from coarse, semi-continuous and non-uniform to fine, discontinuous, uniform and dispersive. When the ultrasonic treatment power is 700W, the best ultimate tensile strength (245.6MPa) and elongation (20.2%) of Mg-6Zn-0.5Y-2Sn alloy are obtained, the best 0.2% tensile yield strength (83.0MPa) is achieved when the power is 500W. Compared with the untreated alloy, the best 0.2% tensile yield strength, ultimate tensile strength and elongation are improved by 43.1%, 30.2% and 66.9%, respectively.

The microstructure of the as-extruded Mg-6Zn-0.5Y-2Sn alloy is mainly consisted of α-Mg phase, MgSnY phase and Mg_2Sn phase. After 700W ultrasonic treatment, the microstructure of the as-extruded Mg-6Zn-0.5Y-2Sn alloy is mainly consisted of α-Mg phase and MgSnY phase. The MgSnY phase is fine, dispersive and uniform. The Mg_2Sn phase has been broken into fine and dispersive particles and dissolved into α-Mg matrix significantly. The average recrystal grain size reduces from about 21μm to 15μm. When the ultrasonic treatment power is 300W, the best 0.2% tensile yield strength (178.8MPa) is achieved. When the ultrasonic treatment power is 500W, the best elongation (19.6%) is achieved. When the ultrasonic treatment power is 700W, the best tensile strength (327.7MPa) is achieved. Compared with the untreated alloy, the best 0.2% tensile yield strength, ultimate tensile strength and elongation are improved by 7.2%, 12.3% and 74.3%, respectively.

14:15-14:35

Microstructural Investigation of High Strength Self-Piercing Riveted Joints of Different Car Body Aluminum Alloys

Ebad Bagherpour, Yan Huang, Zhongyun Fan, Brunel Centre for Advanced Solidification Technology (BCAST), Brunel University London, United Kingdom

Self-piercing riveting (SPR) as a solid-state joining technology has extended its application in the automobile industry in recent years, mostly in the joining of car body aluminum sheets. A number of investigations have been carried out to study the effect of the rivet, die and process parameters including material stacks on the joint quality either by physical experiment or computer simulation. However, most investigations have been able to focus only on the effect of a limited rivet and die conditions and process parameters. In particular, the characteristic features of microstructures around the joint and their dependence on the rivet and die conditions and process parameters, which are important to understand material behavior during the joining process, optimize process parameters and improve joint quality, are not considered in these investigations. In the present work, a comprehensive investigation is conducted to study the performance of the SPR process for car body aluminum alloys including AA6111, AA6082, AC170, and RC5754. A wide range of rivet and die conditions and process parameters are tested under various stacks between similar and dissimilar aluminum alloy sheets with different thickness. Shear and peel tests are performed to evaluate the joint mechanical properties. The microstructures of typical joints are examined by optical microscopy, scanning electron (SEM) microscopy and electron back-scatter diffraction (EBSD), and material flow pattern during joining is characterized accordingly with much higher accuracy than that from low magnification observations. Also, the effect of riveting on the texture of the sheets was investigated. It was confirmed that the area around the outer wall of the tail of the rivet in the lower sheet exhibited the highest deformation and possibly tolerated the highest tensile stress. Besides, the best conditions of joining for the various car body aluminum alloys were defined in order to achieve the best combination of peel and shear strengths.

14:35-14:55

Influence of Continuous Pulsed Current Treatment on the Dynamic Behavior of Mg/Al Composite Plate Fabricated by Explosive Welding

Xiaoqing Cao, Xuewen Zhang, Xinxiao Zhu, Xiaolei Cui, Peng Lin, Taiyuan University of Technology, China

In recent decades, the research and preparation of laminated metal composite plates have attracted wide attention of scholars and experts due to their excellent physical, chemical and mechanical properties by taking into account the characteristics of its member metal materials. The preparation of Mg/Al laminated composite plates with lightweight, high strength and corrosion resistance which has both advantages of components metals and achieves the complementary and optimum properties has attracted much attention. Explosive welding has high bonding strength, relatively thin diusion layer, no porosity and other defects. But there is a little work reported on the dynamic behavior of Mg/Al composite plates especially the one fabricated by explosive welding. In this study, Mg/Al composite plate was prepared by explosive welding with good bonding strength. After explosive welding, Mg/Al composite is usually heat treated (annealing) to eliminate high residual stress from explosive wave, but this process will cause brittle intermetallic compounds between magnesium alloy and aluminum alloy and damaged the property of the composite plate. Continuous pulse current treatment is an useful way to reduce the detriment according some researchers work. The magnesium plate and Mg/Al composite plastic fabricate by explosive welding were treated by continuous pulsed current with different current density respectively, and their dynamic behavior under different strain rates were tested by Hopkinson pressure bar test system to indicate the effect of pulsed current treat. To clarify the mechanism of pulsed current treat, the microstructure change before and after continuous pulsed current treatment of magnesium and Mg/Al composites were observed by OM, SEM, EBSD. The results showed that Mg/Al composite plate by explosive welding has better response under dynamic condition compared with magnesium plate under both conditions, i.e. with and without continuous pulsed treatment. The results will help to widen the use of magnesium alloy in collision condition such as automobile buffer beam and weapons.

14:55-15:15

The Microstructure, Tensile Properties and Wear Behavior of High-Speed DC Cast Al-16%Mg_2Si Composite

Dongtao Wang, Haitao Zhang, Soochow University, China / Northeastern University, China; Jianzhong Cui, Northeastern University, China; Hiromi Nagaumi, Soochow University, China

In this paper, the improved cooling system was used for the high-speed DC casting. The high-speed DC casting of Al-16%Mg_2Si billet (106mm diameter) was achieved to increase the casting speed to 300mm/min. The results showed that when the casting speed increased from 50mm/min to 300mm/min, primary Mg_2Si particles became finer and its average size was reduced from

22μm to 10μm, the average spacing of primary Mg_2Si phases decreased from 53μm to 15μm, the size difference of primary Mg_2Si phase decreased also and its distribution became more uniform at the different billet positions. With the increase in casting speed, the morphology of primary Mg_2Si transformed from irregular shape to regular and polyhedral shapes, the eutectic Mg_2Si transformed from lamellar shape to short rod-like shape and the spacing of the eutectic Mg_2Si decreases from 2.1μm to 0.5μm. The solid solubility of Mg and Si in α-Al increased according to the change of diffraction peak angle of α-Al in XRD. The hardness, tensile strength and elongation of the Al-16%Mg_2Si billet improved with the increase in casting speed. The wear tests showed that the mass loss, wear rate and friction coefficient of Al-16%Mg_2Si billet decrease with the increase of the casting speed. The refinement and morphology transformation of primary Mg_2Si particles at the high casting speed (300mm/min) is the major factor for the improvement of tensile and wear properties in the Al-16%Mg_2Si composite.

15:15-16:10 Tea Break

16:10-16:30

Superhydrophobic Film with Ordered Arrangement of Graphene for Protection of MAO Ceramic Layer Against Corrosion

Tianlu Li, Fei Chen, Li Li, Beijing Institute of Petrochemical Technology, China

Superhydrophobic materials have extensive research and many applications in the fields of self-cleaning, antifouling, microfluidics transportation, drag reduction and corrosion protection. In the field of corrosion resistance, the preparation of superhydrophobic film on the metal surface can separate metal surface from the external corrosion environment, and so it is a simple and effective corrosion prevention method. Research shows that the addition of graphene has a certain shielding effect on corrosion. But in the previous study, graphene is disordered in the coating, so gaps existing between graphene will still cause corrosion. In this study, a composite interfacial layer of graphene and hydrophobic polymer was prepared on the aluminum alloy substrate after microarc oxidation, and the corrosion resistance of the metal was studied. Through the interaction between cations of polyelectrolyte and graphene, and the hydrophobic interaction between graphene and hydrophobic polymer, strong binding strength between the microarc oxidation layer and the graphene/polymer layer is established, and thus the superhydrophobic properties are obtained. Moreover, microarc oxidation layer and superhydrophobic graphene/polymer layer provide double protection for aluminum alloy and the corrosion resistance is improved. Firstly, PDDA aqueous solution and PVDF dissolved in of DMF solution were prepared. And graphene immersed in 10mL of deionized water and vigorous stirred to form homogeneous dispersions. Then, the sample was immersed in PDDA solution, and washed by deionized water and dried. Then, the sample was immersed in graphene dispersion and PVDF solution respectively, and dried when taken out, and we get the first layer. Then repeating precious step for n times (n=1,2,3,4,5). And we get MAO/G/PVDFn specimens. The surface characterization of aluminum alloy and MAO ceramic layer and MAO/G/PVDF film were investigated by SEM (JEOL JSM-7500, Japan) with an accelerating voltage of 20kV. The chemical composition of allium alloy substrate, MAO ceramic layer, and MAO/G/PVDF film was detected by X-ray diffraction technic (Rigaku Ultima IV) and Raman spectra analysis. Contact angle measurements: CAs of the samples were measured on an SL200KS machine at ambient temperature. A water droplet (about 5μL) was dropped carefully onto the prepared surface. CA was adopted as the average value of three to five measurements at different positions of one sample. The electrochemical corrosion test was performed on electrochemical station (CS series) by three-electrodes system in 0.05mol/L NaCl solution. The prepared sample with size of 1cm^2 was used as work electrode, SCE was used as conference electrode, and platinum was used as assistance electrode.

16:30-16:50

The Preparation of Al-V Alloy and Its Characteristics

Yihan Liu, Northeastern University, China

With the development of aviation, national defense, high-speed train and other vehicles, the aluminum alloys have changed rapidly in high technology areas. Vanadium—the vital national strategic metal resources—has been widely used in the aluminum alloy, which become an important means to improve the microstructure and properties of alloy.

In this study, the liquid aluminum reduction smelting process is selected to produce Al alloy containing low content of V. The influence of V on the microstructure, mechanical properties and corrosion resistance of Al-V alloys was studied by optical microscopy (OM), Scanning electronic microscopy (SEM), mechanical

properties testing and electrochemical workstation. The results reveal as follow:

(1) It is possible for smelting process to produce Al-V alloy. When smelting temperature is 1150˚C and V_2O_5 addition amount is 5.5% and hold time is 6h the liquid aluminum reduction smelting process is able to produce Al-V alloy, and the V content is about 4.5%.

(2) As-cast alloy is composed of α-Al, Al21V2 and Al45V7. The high temperature nonstationary phase Al45V7 all become Al21V2 after homogenization treatment.

(3) The mechanical properties of Al-V alloy indict that: The addition of V can clearly improve the hardness, tensile strength and yield strength. But the elongation is decreased obviously.

16:50-17:10

Study on Ultrahigh-Frequency Fatigue Behaviors of As-Extruded AZ31 Magnesium Alloy and Its Friction Welded Joint

Yuwenxi Zhang, Gaofeng Quan, Mingyang Zhou, Southwest Jiaotong University, China

Magnesium alloys are expanding into more critical applications in aerospace, automotive and rail transportation industries with their excellent properties. And these structural components, including their welding parts, inevitably withstanding low and dynamic loading in service. So it is necessary to understand high even ultrahigh cycles fatigue properties of magnesium alloys and their welded joints. This work aim to investigate the ultrahigh frequency fatigue behaviors of as-extruded AZ31 magnesium alloy and its continuous drive friction welded joint via ultrasonic fatigue test at a resonance frequency of 20kHz and a stress ratio of $R = -1$. Microstructure analysis, mechanical performance testing and SEM fracture surface characterization were performed to explain the mechanism underlying crack initiation in AZ31 magnesium base alloy and welded joint.

The results showed that under ultrahigh frequency fatigue condition, AZ31 magnesium alloys have conventional fatigue characteristics, and all of these specimens only have conditioned fatigue limits. The conditioned fatigue limits of as-extruded AZ31 base alloy at 10^9 cycles is 90MPa, higher than that of its welded joints 61MPa, which is not corresponding to their ultimate tensile strength, 209MPa and 255MPa respectively, while the tensile strength of friction welded joint is close to that of base material. The ratio of endurance limit at one billion cycles to the tensile strength (σ_{-1}/σ_b) is 0.33, belonging to moderate fatigue strength. In both base alloy and welded joint, the fatigue failure mainly originated from the specimen surface or near surface at 10^6 ~ 10^8 cycles, while their fatigue cracks initiated in subsurface or internal area where inclusion defects were found exist in crack nucleation sites at high cycle numbers close to 10^9 cycles. And by observing microstructures of post-fatigued specimens, the slip and twining were activated during the fatigue testing process, and played important roles in fatigue life of both AZ31 magnesium alloy and its welded joint.

17:10-17:30

TEM Observation of Al-7Si-0.4Mg Casting Alloy Extracted by the Thermal Phenol Method

Makita Yuki, Tsuchiya Taiki, Seungwon Lee, Saikawa Seji, Ikeno Susumu, Matsuda Kenji, University of Toyama, Japan

Al-Si alloys have been used as casting materials for automobile parts. Al-Si-Mg alloys enhance its ductility and castability due to formation of metastable phase (Mg_2Si). Moreover, it is effective for increasing both strength and corrosion resistance with Mg addition. However, precipitation sequence is not clear in T5 (casting + aging treatment) process. The aim of this research is to estimate mechanical properties and to classify precipitates by micro Vickers hardness measurement and transmission electron microscopy (TEM) of Al-7%Si-0.4%Mg (mass%) alloy in T5 condition. Al-7%Si-0.4%Mg alloy was fabricated by casting using Fe Y-block mold, then, alloy was cooled in the mold as is to 773K, and quenched into cold water. Specimens were taken from mold bottom were used in this research. After casting, artificial aging was carried out. Micro Vickers hardness measurement was conducted using Mitutoyo HV-101 (load: 0.98N, duration time:15s). Microstructure observation were conducted the samples of aged using scanning ion microscopy (SIM, HITACHI FB-2100), SEM (HITACHI S-3500H) and TEM (TOPCON EM-002B operated at 120kV). Micro Vickers hardness values were decreased and time to reach to peak-aging was shortened. Eutectic Si and α-Al matrix were observed by SIM aged at 473K for 7.2ks. Particles size of ~50nm were observed only far from eutectic Si. Uneven precipitates occurred depending from eutectic Si. With close inspection of TEM images and SAED pattern, Si, β", preprogram precipitate and Type-A precipitates were observed in the peak-aged samples by analysis results of HR-TEM images and SAED patterns. We analyzed Type-A precipitates in detail by the thermal phenol method. We got SAED patterns and EDS analysis results from a number of rod-shaped precipitates and analyzed SAED patterns. We can make stereographic projection of diffraction pattern of Type-A precipitates. The chemical composition of Type-A precipitates were proven Mg: Al: Si= 1: 4: 5 from EDS analysis result in this alloys.

L. Computational Design and Simulation of Materials: VII

Symposium Organizers:

Tongyi Zhang, Shanghai University, China; Zhimei Sun, Beihang University, China; Shigenobu Ogata, Osaka University, Japan; Byeong-Joo Lee, Pohang University of Science and Technology (POSTCEH), Korea; Salvy Russo, RMIT, Australia; Saryu Fensin, Los Alamos National Lab, USA; Michele Manuel, University of Florida, USA

Thursday PM
August 22, 2019

Room: 204 (2nd Floor)
Symposium: L

Chairs:
Ming Xu, Huazhong University of Science and Technology, China
Marlies Hankel, The University of Queensland, Australia

13:30-13:55 Invited

First-Principles-Based Novel Materials Design for Pb-Free Hybrid Perovskite

Donghwa Lee, Pohang University of Science and Technology, Korea

Perovskite is the class of compounds that have the crystal structure of ABC3, where A and B are cation sites having different charge states while C is an anion site. Recently, organic-inorganic hybrid perovskite, which has organic molecule in A site, transition metal in B site and Iodine ion in C site, such as $MAPbI_3$ or $FAPbI_3$ has been received a great attention for a photoactive layer in solar cell or a resistance switching layer in memristor since a simple manufacturing process leads to outstanding performances. However, there are still several remaining issues that have to be resolved for their practical usage. For examples, environmental and thermal stability have to be ensured for them to be used for device applications. Another big challenge is toxicity of this material. The inclusion of toxic lead has increased the necessity of developing Pb-free materials that can replace the current Pb-based perovskite structure. However, the combinations of organic molecules and inorganic constituents are too numerous to investigate all possible candidate materials experimentally. In this study, therefore, a computational approach is used to find out alternative perovskite materials that can replace conventional pb-based hybrid perovskite materials. Especially, First-Principles-based novel materials design technique is employed to reduce time and cost required for synthesis and characterization of traditional experimental approaches. We have extensively studied numerous candidate materials by incorporating different transition metal elements or organic molecules into various backbone structures to find out Pb-free perovskite materials. Our study has identified a couple of candidates that can possibly switch current Pb-based perovskite photoactive layer or resistance switching layer. In addition, analysis on electronic structure has led the understanding of the relationship between constituent elements and properties. This work is supported by the National Research Foundation of Korea (NRF) funded by the Ministry of Science, ICT & Future Planning No. NRF-2015M1A2A2053003 and NRF-2015R1C1A1A01054315 and NRF-2016M3D1A1027665 and NRF-2017R1A4A1015811.

13:55-14:20 Invited

Layered Two-Dimensional Materials as Anode and Cathode in Metal Ion Batteries

Marlies Hankel, Debra Bernhardt, The University of Queensland, Australia

Carbon structures have been extensively studied over recent decades as energy storage materials. One of the industry applications is as the anode of lithium (Li) ion batteries (LIBs). Graphite, a layered material consisting of sp2 bonded carbon sheets is currently the predominant anode material offering a theoretical capacity of LiC6 with Li inserted between the layers. Aluminium ion batteries (AIBs) have been proposed as an alternative to LIBs for energy storage. Recent work employed graphite as a cathode material with the AlCl4 molecule intercalating between the carbon layers. This showed high stability but low capacity.
To achieve higher storage capacity for LIB anodes and AIB cathodes, we pursue novel materials such as carbon allotropes, carbon nitrides or graphene composites. We have investigated the energy storage capacity of porous graphitic carbon nitrides, g-C_3N_4, g-CN, hC_2N as well as other CxNy configurations and their composites with other two-dimensional materials. Our studies also include carbon only membranes such as biphenylene, graphdiyne and hydrogenated graphdiyne. Some materials, that surpass the capacity of graphite for Li storage and that show similar performance to graphite for $AlCl_4$ have been identified.
Density functional theory (DFT) calculations are employed to obtain the maximum Li/$AlCl_4$ storage capacity. We also calculate diffusion barriers for the Li/$AlCl_4$ movement from one site to another to determine their mobility. In addition to this we also show how the Li/$AlCl_4$ binds to the material by consideration of the charge density distribution and the charge transfer from the Li/$AlCl_4$ to and from the material. The volume change of the material on the insertion of Li/$AlCl_4$ is determined by employing a bilayer or bulk configuration of the material.

14:20-14:40

Hydrogen Embrittlement Mechanism: A Perspective from Atomistic Modeling Study

Liang Wan, Wuhan University, China / Osaka University, Japan; Wen Tong Geng, Osaka University, Japan / University of Science and Technology Beijing, China; Akio Ishii, Hajime Kimizuka, Osaka University, Japan; Jun-Ping Du, Shigenobu Ogata, Osaka University, Japan / Kyoto University, Japan; Qingsong Mei, Wuhan University, China; Nobuyuki Ishikawa, JFE Steel Corporation, Japan

Hydrogen atoms absorbed by metals in the hydrogen-containing environments can lead to the premature fracture of the metal components used in load-bearing conditions. This degradation of mechanical performance of the metals used in practice is considered as a key technological challenge in many industrial applications. Although a number of theories such as the hydrogen enhanced decohesion (HELP), hydrogen enhanced localized plasticity (HELP), and hydrogen enhanced strain induced vacancy (HESIV), etc. have been proposed, the underlying atomistic mechanism for hydrogen embrittlement of metals is still not well understood and wild controversy remains. Since metals used in practice are mostly polycrystalline, grain boundaries can play an important role in hydrogen embrittlement of metals. Taking H in alpha-Fe as an example, here we show that the reaction of grain boundaries with lattice dislocations is a key component in hydrogen embrittlement mechanism for polycrystalline metals. We use atomistic modeling methods to investigate the mechanical response of grain boundaries in alpha-iron with various hydrogen concentrations. It is found that fracture of the material occurs via void nucleation and growth at grain boundary, or by cleavage along the grain boundary, depending on the hydrogen concentration. Both void nucleation/growth and cleavage are preceded by dislocations emission and impingement on the grain boundary. Analysis indicates that dislocations impingement and emission on the grain boundary can provoke it to locally transform into an activated state with a more disordered atomistic structure, and introduce a local stress concentration. The activation of the grain boundary segregated with hydrogen atoms can greatly facilitate decohesion of the grain boundary. We propose a hydrogen embrittlement model that can give better explanation of many experimental observations. Based on the new hydrogen embrittlement model proposed, we briefly discuss the viable strategies that can be adopted for design of advanced metals and alloys with improved hydrogen embrittlement resistance.

14:40-15:00

A FEM Analysis of Mn-Si-Cr Bainite/Martensite Steel

Yu Tian, Zhunli Tan, Min Zhang, Bo Gao, Bingzhe Bai, BeiJing JiaoTong University, China

Mn-Si-Cr bainite/martensite steels have been used widely because of its superior properties such as better combination of strength and toughness. While for their large-scale parts such as train wheel, owing to the difference of thermal transport and phase transportation between surface position and center, there often exist inhomogeneity of properties and sometimes this diversity would affect the application. Therefore, it is important to make measures to decrease this difference degree. For a given composition of large-scale component, the study of heat treatment processing is the key factor for decrease this difference. while it is hard to adjust the process by experiments and simulation becomes an effective way for this. For Mn-Si-Cr bainite/martensite steels, especially the large-scale parts, there is seldom related simulation study about transient change of temperature and phase transformation kinetics during heat treatment currently. So, temperature changes dynamically and related microstructure during the water spray quenching process were researched by finite element simulation in this paper.

The results showed that when the cooling rate is between 0.5℃/s and 4℃/s, the microstructure of as-employed steels mainly contains bainite and martensite. 100% martensite(M) corresponds to cooling rate over 8℃/s. The activation energy of bainitic transformation and the Avrami exponent *n* are 52.17kJ / mol and 1.52187 by JMAK equation, respectively.

The finite element model of large ring forging determined by these parameters, to some degree, can predict the difference of temperature between surface and center as well as simulate microstructure distribution at different water spraying intensity and spraying angle. Related simulated results showed that the temperature of large ring forgings is distributed in gradient with the increase of surface water spraying intensity, keeping almost total martensite in surface layer. As the radial depth increases, the hardness decreases gradually, which is consistent with the measured locations of the temperature and hardness. The error is less than 5%.

15:00-15:20

CUDA-Accelerated Spinodal Decomposition Study of Fe-Cr Binary Alloy: Effect of the Negative Mobility of Interdiffusion Process

Kunok Chang, Jeonghwan Lee, Kyung Hee University, Korea

Fe-Cr-Al ferritic alloy system is one of the candidate

material systems for the accident tolerant fuel cladding. It has the advantage of high temperature oxidation resistance comparing to the Zr cladding materials. In the Fe-Cr based ferritic alloys such as Fe-Cr and Fe-Cr-Al, it is well known that spinodal decomposition occurs. Since spinodal decomposition of chrome-rich and chrome-depleted phases can damage the mechanical integrity of the materials, quantitative prediction of the spinodal decomposition kinetics are a quite significant task. A phase-field method has been actively applied to predict spinodal decomposition process of Fe-Cr alloys. Most of the former studies, they assumed that the mobility of the interdiffusion process is always positive. However, since the mobility of the diffusion is inversely proportional to the second derivative of the free energy with respect to the compoisition in the binary system. Within the spinodal region, the second derivative of the free energy with respect to the composition is negative, so the mobility of the interdiffusion process becomes negative. In this study, we examine a role of the negative mobility in microstructural evolution. Since the mobility diverge to the infinity when second derivatvie of the free energy converge to 0, so we made some numerical assumptions to avoid this situation. Incorporating quantitative value of the mobility in the phase-field modeling generally reduces the numerical stability of the calculation. To compensate for this performance reduction, we adopted CUDA parallelization technique to enhance the computational efficiency.

15:20-16:00 Tea Break

16:00-16:20

Atomistic Simulation Study of the Solid-Liquid Interfacial Premelting at the Solid-Liquid Interfaces of Pb Inclusions Embedded in Al Matrix

Umar D. Muhammad, Xiangming Ma, Hongtao Liang, Yang Yang, East China Normal University, China

With the increasing demand for higher quality aluminum cast products, especially in the automotive and aerospace industries, attentions have been paid to the nano-sized inclusions in the aluminum matrix. Lead inclusions (in aluminum) are of keen interest because they could cause hot shortness and segregation during casting; meanwhile they could improve machinability and assist in chip formation. The current study is motivated by a series of transmission electron microscopy (TEM) experimental observations, done by Uli Dahmen et al. at Lawrence Berkeley National Laboratory, on the equilibrium shape evolution and the novel Brownian motions for the nano-sized liquid Pb inclusions in Al matrix. Our study is also motivated by recent progress in the atomistic simulation studies on the Al-Pb solid-liquid interfaces by Yang et al., including the discovery of a new category of premelting phenomenon and its significant impact on the spreading kinetics mechanism and wetting thermodynamics.

In this talk, we first report the simulation technique in setting up the equilibrium solid matrix/liquid inclusion system, and a few affiliated analysis and calculation methods. Including the characterization, the structural and thermodynamic properties along the radial direction for the liquid Pb inclusion; the Irving-Kirkwood methods for the calculation of the pressure and stress components; the measurements of the surface tension, solubility, inner pressure of the liquid inclusion and the premelting width of the interfacial Al. Following methodology, a few interesting findings will be reported and discussed, including i) statistical averaging reveals a weak anisotropy in the premelted liquid skin surrounding Pb inclusion. ii) the presence of the solid-liquid interfacial premelting layer is significantly affecting the capillarity and the thermodynamic properties inside the liquid inclusion, while the extent of the premelted solid-liquid interface is also remarkably influenced by the inclusion. iii) the inclusion size, temperature and mass density dependence of the premelting is compared with the planar interface cases.

16:20-16:40

Exploring the Materials Genes of Phase-Change Memory

Ming Xu, Huazhong University of Science and Technology, China

The local structure (scale: < 6Å) of materials largely determines the properties. Phase change memory materials (PCMs) have so many unique physical properties that are linked with the local structure. For example, the local order determines the fragility of glass, resulting in the rapid crystallization of PCM; the resistance drift in PCM devices is due to evolution of local structure upon time (glass aging); the local defects and distortions could induce the amorphization of crystal to reduce the power consumption. The local structure of PCMs has been intensively studied by both experiments and ab initio calculations over past decades. Yet, a lot of issues are still to be resolved on the analysis of ab initio models. We employed the atomic cluster alignment (ACA) method to study the local structure of several prototypical PCMs. Some new structural features and physical properties have been revealed.

The glass forming of Sb_2Te_3 and $Ge_2Sb_2Te_5$ (GST) from melts has been investigated by ACA method. The ACA method may contain some neighboring atoms which contribute to both short- and medium-range order, and thus the method enables us to explore the changes of cluster structures in a larger scale. Obviously, the liquid contains large degree of disorder. The tetrahedrons show an aggregation in liquid and supercooled liquid,

in contrast to the octahedrons which present a notable aggregation in amorphous GST. With rapid cooling, the overall coordination number becomes higher until the local structure approaches the octahedral scenario. These octahedral clusters are connected via edge-sharing fourfold rings.
The ACA method can obtain a 3D description of the average structure ordering in the system. We provide useful insight into the local structural characteristics and phase change mechanisms of PCMs, having important implications on the design of memory devices.

16:40-17:00

Modelling Defect Structures and Processes in TCO

Qing Hou, Alexey A. Sokol, John Buckeridge, Richard Catlow, University College London, England

The combination of high optical transparency and high electrical conductivity in transparent conducting oxides (TCOs) results in the class of materials being widely used in many fields, including solar cells, liquid crystal displays, electrochromic plating and smart windows. The most commonly used n-type TCO materials are SnO_2, In_2O_3, which tend to be oxygen deficient due to the occurrence of oxygen vacancies, and tin-doped In_2O_3(indium tin oxide, ITO). The n-type conductivity has intuitively been attributed to the presence of these vacancies, but other sources have also been proposed and the matter remains a topic of debate. Accurate modelling of intrinsic and extrinsic defects is needed to understand the source of conductivity.
ITO is a disordered system, which necessitates large length scale simulations of multiple atomic environments in the presence of charge carriers to understand its structural and electronic properties. Fully ab initio approaches to such problems are limited by both computational resources and methodological problems in the study of charged defects. Computational techniques based on interatomic potentials, in contrast, are particularly well suited to explore such systems, but require sufficiently accurate and transferable parameterisa- tion. As shown below, previous work on the parameterisation of interatomic potentials suffered from a number of problems related to transferability and/or accuracy in the reproduction of essential physical properties of both parent SnO_2 and In_2O_3 compounds.
We present a consistent interatomic forcefield for indium sesquioxide and tin dioxide that has been derived to reproduce lattice energies and, consequently, the oxygen vacancy formation energies in the respective binary compounds. The new model predicts the dominance of Frenkel-type disorder in SnO_2 and In_2O_3, in good agreement with ab initiodefect calculations. The model is extended to include free electron and holepolarons, which compete with charged point defects to maintain charge neutrality in a defective crystal. The stability of electrons and instability of holes with respect to point defect formation rationalizes the efficacy of n-type doping in tin doped indium oxide (ITO), a widely employed transparent conducting oxide in optoelectronic applications. We investigate the clustering of Sn substitutional and oxygen interstitial sites in ITO, finding that the dopants substitute preferentially on the cation crystallographic dsite in the bixbyite unit cell, in agreement with experiment. The forcefield described here provides a useful avenue for investigation of the defect properties of extended transparent conducting oxide systems.

N. Additive Manufacturing and Powder Metallgufy: Steel & Other Alloys

Symposium Organizers:

Huiping Tang, Northwest Institute for Nonferrous Metal Research, China; Yong Liu, Central South University, China; Yuichiro Koizumi, Osaka University, Japan; Kee-Ahn Lee, Inha University, Korea; Qian Ma, RMIT, Australia; Ed Herderick, Ohio State University, USA

Thursday PM
August 22, 2019

Room: 402 (4th Floor)
Symposium: N

Chairs:
ShiHoon Choi, Sunchon National University, Korea
Takeshi Fujita, Kochi University of Technology, Japan

13:30-13:55 Invited

Deformation and Fracture Behaviors of 316L Stainless Steels Fabricated by SPS and SLM Techniques under Uniaxial Tension

ShiHoon Choi, Amol B. Kale, Jaiveer Singh, WiGeol Seo, Sunchon National University, Korea; Mike Reece, Queen Mary University of London, UK

316L austenitic stainless steels (SS) alloy is highly demanded in several industries due to their excellent corrosion resistance and high mechanical strength, as well as better formability, weldability. Therefore they have been used in the petrochemical industry, the medical sector, and the nuclear industry. The well-known manufacturing techniques of 316L SS are mainly casting, forging and extrusion. These techniques have limited degrees of freedom and manufacturing of metal parts with complex shape geometries need post-processing, in particular, machining, which is

accompanied with considerable wastage of material and time. The most effective additive manufacturing (AM) technique for fabricating 316L SS parts is a selective laser melting (SLM) due to its excellent advantages, such as high process flexibility, high material utilization, short production time, and excellent corrosion resistance.
In this study, 316L stainless steel (316L-SS) specimens fabricated by spark plasma sintering(SPS) and selective laser melting(SLM) techniques were investigated. The specimens fabricated by SPS with partially sintered regions have relatively low densities compared to the SLM specimens. Microstructural observation showed that the SPS specimens consisted of fully and partially sintered regions and contained initial pores which are located at the grain boundaries. SPS specimens have relatively low density and low kernel average misorientation(KAM) values near the interface of pores and matrix. The spatial distribution of KAM in the SLM specimens indicated that melt pool boundaries (MPBs) and grain boundaries (GBs) are not equivalent. In order to reveal the fracture mechanisms of the SPS and SLM specimens, the surfaces of the fractured specimens were analyzed via field emission scanning electron microscope(FE-SEM). The fracture surfaces of the SPS specimen revealed that fine cup-like dimples were observed in the fully sintered region, while in the partially sintered region was identified as a decohesion of the interface between the powder and the matrix. Fracture mechanism of SLM specimen at different strain levels indicated that the occurrence of crack initiation was due to the presence of second phase particles.

13:55-14:20 Invited

Hierarchical Nanoporous Copper by 3D Printing Technique for Highly Efficient Catalysts

Takeshi Fujita, Yongzheng Zhang, Kochi University of Technology, Japan; Xiaohao Sun, Naoyuki Nomura, Tohoku University, Japan

Recently, 3D printing, as the most common method in additive manufacturing, has shown great potential as an advanced manufacturing technique for a growing range of applications, including metal structures, soft robots, ceramics, nano-devices, and silica glass. In particular, the manufacture of metal structures by selective laser melting (SLM) 3D printing is becoming more and more popular, and plays an critical role in the aerospace, medical, and automotive industries.
Nanoporous metals represent a class of functional materials with unique bicontinuous open porous structural properties, making them ideal candidates for various catalyst applications. However, the pursuit of nanoporous properties, extremely small pores and high surface area, results in the restricted mass transport. Although several metallic powders such as Ti alloys are preset for SLM fabrication, optimal fabrication parameters, including powder size and laser power, are largely unknown for unexplored alloy powders.
In this work, we introduce an alternative approach for hierarchical nanoporous Cu prepared by 3D printing with Cu-Mn alloy powders as an electrocatalyst for methanol oxidation. An extensive variety of digitally controlled architectures with complex geometries were processed rapidly and consistently by a SLM 3D printing technique. After SLM and a subsequent one-step dealloying process, hierarchical nanoporous Cu architectures with fast mass transport and highly efficient catalytic activity were obtained. The digitally controlled hierarchical structure with macro- and nano-scaled pores is utilized for promoting and directing mass transport as well as for the enhancement of catalytic properties. This work highlights a facile and low-cost strategy for hierarchical nanoporous structure design that can be applied to multicomponet alloys for various functional applications.

14:20-14:40

Mechanism and Control of Grain Morphology and Texture in a Co-Cr-Mo Alloy Fabricated by Electron Beam Additive Manufacturing

Yufan Zhao, Yuichiro Koizumi, Kenta Aoyagi, Kenta Yamanaka, Akihiko Chiba, Yufan Zhao, Tohoku University, Japan

Co–Cr–Mo (CCM) alloys have been widely used for medical prosthetic implants because CCM is a non-magnetic alloy exhibiting high strength, corrosion resistance, and excellent wear resistance. Thus, CCM alloys are the materials of choice for applications such as knee implants, metal-to-metal hip joints, and dental prosthetics. Additive manufacturing plays a significant role in the development of medical implants via computer-aided design. It provides extensive customization based on the individual patient data that can be captured by computed tomography and magnetic resonance imaging technology.
Grain morphology, size, and growth direction are crucial in determining the performances of metallic implant components. Understanding the effects of the manufacturing characteristics of powder bed fusion with an electron beam (PBF-EB), an additive manufacturing process, on microstructure formation and anisotropy development during solidification is essential to achieve flexible microstructure control.
In this study, PBF-EB was employed to fabricate a Co-Cr-Mo alloy and the grain morphology and texture formation with different process parameters were analyzed by experimental characterization with the aid of computational thermal–fluid dynamics simulations. It was found that the epitaxial growth with resulting columnar grain and near-cubic texture tended to be

dominant in the solidification process, due to competitive grain growth and the heat flow characteristics in the snake-scanning strategy. However, the molten pool connection between adjacent melt tracks resulted in the random orientation of <001> in the horizontal plane, producing a fiber-like texture. In addition, nucleation and new grain growth rather than extensive epitaxial growth could be achieved by manipulating the molten pool geometry and overlap between adjacent melt tracks. Increasing the slope of the solid/liquid interface of the molten pool and decreasing the remelting fraction of adjacent melt tracks favored the formation of new grains with random orientations to restrict the extensive epitaxial growth of the columnar grains and attenuate the microstructural anisotropy.

14:40-15:00

The Effects of Selective Laser Melting on the Microstructure and Associated Properties in Co-Cr-Mo Alloys

Zhi Wang, South China University of Technology, China; Konda Gokuldoss Prashanth, Tallinn University of Technology, Australia; Jürgen Eckert, Austrian Academy of Sciences, Australia; Sergio Scudino, IFW Dresden, Australia

The selective laser melting (SLM) process was applied to Co-Cr-Mo alloy and its microstructure; mechanical properties were investigated and compared with as-cast alloy to determine whether this method of fabrication is appropriate for high temperature and biomedical applications.

The results show that the γ and ε phase was dominant for as-cast alloy while ε phase was prevalent for SLM build samples at room temperature. The unique microstructure of SLM build samples consisted of columnar and cellular cells with laser hatch boundaries whereas the as-cast samples exhibited a dual phase microstructure. Higher yield strengths, UTS, hardness and elongation could be obtained for the SLM builds compared to as-cast ones and thus established the suitability of the process for biomedical implants.

Isothermal annealing was conducted for the SLM build and as-cast samples at different temperatures and the mechanical properties were investigated by correlating with microstructural analysis. The optimum properties were obtained at 873K for SLM build samples. Yield strength exhibited by this sample was ~922MPa and fracture strain was ~10.3% due to the fact that SIMT ε-hcp phase along with thickening of isothermal martensites forms a network with elongated σ phase precipitates hindering the motion of dislocations. Heating compression tests were also conducted for both as-cast and SLM build samples which showed that the latter possessed much improved properties in service conditions compared to the former and thus justified that the SLM process for the Co-Cr-Mo alloy is a talented candidate for high temperature applications.

15:00-15:20

Laser Shock Peening: a Promising tool for Tailoring Metallic Microstructures in Selective Laser Melting

Ke Huang, Xi'an Jiaotong University, China /École polytechnique fédérale de Lausanne (EPFL), Switzerland; Nikola Kalentics,Roland Logé, École polytechnique fédérale de Lausanne (EPFL), Switzerland

Selective Laser Melting (SLM) is a very well-known metal Additive Manufacturing process, in which the part is built in a layer-wise manner. A powder bed is deposited and selectively fused by a focused laser beam, and this sequence is repeated until completion of the part. SLM gives the ability to produce parts with increasingly complex geometries which are difficult or impossible to produce by conventional methods. However, the undesirable microstructure still presents an important limitation of the process. During the fabrication, due to the low thermal conductivity of the surrounding powder, the heat deposited by the laser beam is mostly extracted through the previously solidified layers. This results in a thermal gradient along the building direction and directional solidification. Excellent studies demonstrate that, after solidification, the grain structure is most of the time columnar and grain size in the building direction can extend considerably, as a result of an "epitaxial" growth along a preferred crystallographic orientation, which is <100> in alloys with a cubic structure. The combination of a coarse grain structure in the build direction with a strong crystallographic texture leads to non-optimal anisotropic mechanical properties of the parts made by SLM, which represents a known limitation of the SLM process. In this paper, Laser Shock Peening (LSP) was performed on a 316 L stainless steel part fabricated by SLM. The following conclusions can be drawn: i) The LSP treatment increases the stored energy and the microhardness of SLM AB parts in the near surface region but does not change grain size; ii) In the LSP affected zone, recrystallization kinetics is strongly accelerated upon heat treatment, resulting in a refined, equiaxed grain structure, very different from the AB SLM microstructure; iii) The combination of SLM with Laser Shock Peening offers a promising new route for the 3D control of microstructures and mechanical properties of SLM parts.

A. Advanced Steels and Processing

Symposium Organizers:

Han Dong, Shanghai University, China; Zhigang Yang, Tsinghua University, China; Yoshitaka Adachi, Nagoya University, Japan; Dong-Woo Suh, Pohang University of Science and Technology (POSTCEH), Korea; Christopher Hutchinson, Monash University, Australia; Amy Clarke, Colorado School of Mines, USA

August 19-21, 2019
Place: Exhibition Area (3rd Floor)

A-1: Influence of Aging Time on Precipitation Behavior of Lean Duplex Stainless Steel 2101

Haijian Xu, Xiaochun Sha, Jingsong Meng, Wenzhong Wang, Fang Li, Angang Steel Company Limited, State Key Laboratory of Metal Material for Marine Equipment and Application, China; Zhaodong Wang, Northeastern University, China; Wanqing Hu, Weijuan Li, University of Science and Technology Liaoning, China

Duplex stainless steels are an important class of stainless steels, with a dual-phase microstructure consisting of approximately equal volume fractions of ferrite (α) and austenite (γ). The balance between the two phases is obtained by means of heat treatment, whose temperature depends on the chemical composition of the alloy. As a result of an interesting combination between the austenitic and ferritic stainless steels, these duplex stainless steels combine the best features of both alloys, e.g., stress corrosion cracking resistance and good weldability and reduced costs due to the minor presence of alloying elements in comparison with other stainless steels. In this topic, microstructure of a grade 2101 duplex stainless steel was studied. Samples were annealed at different temperatures, to change the α/γ proportion, to precipitate undesirable phases (for example, chromium nitrides), and to study the effect of the microstructure on the mechanical behaviors. Samples with a thickness of 1.8mm were prepared according to ASTM standards and tested at room temperature. Tensile tests were conducted using displacement control at a rate of 5 mm/min. Secondary phases precipitating after aging treatment at certain temperature in 2101 duplex stainless steel will influence the properties of the duplex stainless steel. Correlation between secondary phase precipitation and aging treatment of hot-rolled 2101 duplex stainless steel was studied by employing optical microscope (OM) and scanning electron microscopy (SEM) with energy-dispersive spectrum (EDS) system to observe microstructure changes of precipitates as well as to analyze chemical composition of precipitates and matrix. The results show that the total solid solution temperature of Cr_2N precipitation in 2101 is around 1050˚c. The calculation results and experimental results are in good agreement. The finishing hot rolling temperature must be above the total solid solution temperature in the practical production process to prevent Cr_2N precipitation. With prolonging aging time, the content of ferrite phase decreases, and both the precipitates and austenite increase. The mechanical properties of the steel were significantly changed due to the changed microstructure. The results demonstrate the sensitivity of the steel to the annealing temperature.

A-2: Effect of Si-Cr-Mo Element of Cold Rolled Duplex Steel on Oxidation Characteristics and Surface Quality

Chang Wang, Shou Gang Group, China

Based on the phase transformation strengthening mechanism, the dual-phase steel composed of ferrite and martensite has been developed into a kind of advanced high-strength stamping steel for automobile. In the widespread use of the C-Si-Mn system, the mass percent of Mn element exceeds 1.5%, which mainly provide the hardenability of dual phase steel during continuous annealing process. The mass percent of Si element is controlled between 0.2 and 1.5%, which can improve the austenitic hardenability and improve the purity of the ferrite. However, when the mass percent of Si is more than 0.2%, the red scale defect are easily generated during hot rolling process, which can finally form the surface color difference defect on the finished product. According to the requirements of the coating performance and high surface quality standards, sometimes the Si element is not used as the main addition element, and is replaced by Cr or Cr-Mo element to form the C-Mn-Cr/C-Mn-Cr-Mo composition system. In this paper, the interactive effects of Si-Cr-Mo alloy elements on interfacial oxidation characteristic in dual-phase steel are studied. Thermal simulation, scanning electron microscopy (SEM) and electron probe analysis are carried out, and the influence of different alloy elements on hot coil surface quality under industrial production conditions is also discussed. Results show that the oxidation resistance of Si-Cr steel is higher than Si-Cr-Mo steel, because the interface oxidation of Cr element under high temperature. Compared with steel only adding Si element, the primary scale of the Si-Cr and Si-Cr-Mo steel is easier to remove, owing to the reduction of anchor scale structure at the interface between scale and substrate. However, Si and Cr element will form dense oxide film under 1100˚C at the interface, which increases the difficulty of finishing descaling. Mo is mainly enriched at the surface, and it reduces the activity of Si and Cr, blocks the diffusion channel of Si and Cr elements, and weakens the formation Si-Cr oxide film at the interface. Therefore the surface quality of Si-Cr-Mo steel is significantly improved under industrial production. This work can provide useful guidance for production of this kind of dual-phase steel.

A-3: Study on Microstructure and Properties of High Strength Seismic, Fire and Weatherproof Hot Rolled H-Beam for 460MPa Grade Structures

Zhendong Song, Ya Tao, Xiangdong Bu, Xiaomin Zhao,Technical Center of Steel Union Co. Ltd. of Baotou Steel (Group) Corp, China; Chengjia Shang, Technical Center of Steel Union Co. Ltd. of Baotou Steel (Group) Corp / University of Science and Technology Beijing, China

With the rapid development of national economy, the strength level of steel grades used in steel structure engineering will be higher and higher. At present, with the development of high-rise and long-span building structures, high-strength steel must be used in building structures to reduce the weight of structures, reduce construction costs, reduce the thickness of steel materials and improve their safety and reliability. The Twelfth Five-Year Plan of the state also puts forward some suggestions for promoting the steel structure industry, It is necessary to strengthen the revision of relevant design standards and codes for steel structures, improve the steel standards for buildings, bridges and containers in China, promote the development and application of high-performance steel products, and focus on the development of steel plates and profiles with high strength, high toughness and good weldability, so as to provide replacement and upgrading materials for the manufacture of buildings, bridges, containers and marine equipment. Famous earthquake studies at home and abroad show that serious damage or collapse of buildings such as houses is the most important cause of casualties and property losses, which also prompts people to fully realize the seismic capacity of public buildings. The disadvantage of steel structure is that its fire resistance and weatherability are poor, which requires that steel materials have seismic, fire resistance and weatherability at the same time. In this paper, the hot rolled H-beam with high strength, seismic resistance, fire resistance, weatherability and other comprehensive properties was prepared by chemical composition design of low carbon and multi-alloy composite strengthening. By controlling steelmaking process and rolling process, nano-ferrite + bainite structure is obtained. Under air-cooled condition, the yield strength of H-section steel is not less than 460MPa, the yield strength ratio is not more than 0.85, the yield strength is not less than 310MPa at 600˚C, the low temperature toughness at -20˚C is greater than 31J, and the weathering index factor I is greater than 6.

A-4: Influence of Relaxation Process on Microstructure and Mechanical Properties of Weathing Bridge Steel

Leqing Huang, Yanfeng Wang, Yongda Yang, Changwen Ma, Guobiao Di, Shougang Research Institute of Technology, China

With the development of rail transportation, more and more bridge was built in China. Contrasted with ordinary bridge steel and antiseptic treatment, weathering bridge steel has advantages over cost in whole life cycle and harmonious with environment, so more and more bridges selected weathering bridge steel as their construction materials. In this paper, in order to study the influence of relaxation process on mechanical and corrosion properties of weathering bridge steel, 420MPa weathering bridge steel produced by relaxation time of 0s, 30s, 85s and 270s were topics of research and studied by means of microstructure observation, mechanical property test, EPMA test and accelerate corrosion test of dry-wet cyclic immersion. The results show that: with the extension of relaxation time, the microstructure of the steel changed from AF+GB to F+B, and further to F+P, the rate of yield strength declined so faster than tensile strength that Y/T (yield strength / tensile strength) ratio decreased from 0.88 to 0.62, the elongation fluctuated from 20 to 24 percent, impact absorbed energy decreased from 247 to 174J at -40˚C. Results of accelerate corrosion test of dry-wet cyclic immersion showed corrosion rate of the steel did not cause a large fluctuation. Results of microstructure observation of accelerate corrosion test show that surface of samples were covered with corrosion pit. Results of EPMA test of relaxation time of 30s, 85s show that C element had obvious diffusion during relaxation process but there was no significant diffusion of the weathering elements such as Cr during the relaxation process. In summary, relaxation process could reduce Y /T ratio and corrosion properties and mechanical properties such as strength, elongation and impact absorbed energy stayed at elevated levels. In this way, we adopt relaxation process in weathering bridge steel commercial production, product quality meet the requirements of the standard of GB/T 714-2015 and EN 10025, the products applied in Guanting Reservoir Bridge which is the first non-coating high way steel bridges.

A-5: Thermophysical Properties of Undercooled Liquid NiFeCo Ternary Alloys

Jiongfei Zhao, Haipeng Wang, Northwestern Polytechnical University, China

The thermophysical properties of liquid alloys, such as density, diffusion and thermal expansion, are considerable importance in understanding solidification processes. The Ni-based high temperature alloys has been extensively used in aerospace gas turbine shafting, nuclear reactors and industrial gas turbine producing. The present study aims at study the concentration dependence of structural and thermophysical properties of liquid NiFeCo ternary alloys. The Molecular dynamics (MD) simulation has been employed to study the structural evolution, thermodynamics and dynamics properties of liquid NixFe0.5(100-x)Co0.5(100-x) (x=0, 20, 40, 60, 80, 100) ternary alloys in a wide temperature range based upon 2NN modified embedded atom

method (2NN MEAM) models. The calculated density, radial distribution function and static structure factor are good agreement with experimental data. The densities of NiFeCo ternary alloys at 1800K increase from 7.425g/cm^3 to 7.738g/cm^3 and then reduce to 7.660g/cm^3 with the increase of the content of Ni, which reaches the maximum at 60at.% Ni content. In all cases, the densities of NiFeCo ternary alloys with different compositions are larger than those of the ideal solution and the maximum difference is 0.172g/cm^3 at 60at.% Ni content. The liquid NiFeCo alloys show a negative excess volume and a negative mixing enthalpy, which could be attributed to the strong attractive interactions between Ni, Fe and Co atoms. The partial radial distribution function $g_{\alpha\beta}(r)$ and total radial distribution function $g_{total}(r)$ are all similar to each other, which suggests that both Ni, Fe and Co atoms pack almost identically and through substitutional replacement upon changing the concentration. The partial static structure factor S(q) of Co-Co and Ni-Ni display a 'prepeak', which indicate that there is the medium-range chemical ordering in liquid NiFeCo alloys. Furthermore, the concentration dependence of diffusion has been discussed. The diffusion coefficients is reduced first and then increased with the increase of the content of Ni atoms.

A-6: Effects of Pre-Deformation Process on Nanobainite Transformation Kinetics

Shixin Xu, Zhijun Luo, Suhuai Deng, Qisong Sun, Research Institute of Technology, Shougang Group Co., Ltd. China; Wei Yu, University of Science and Technology Beijing, China

As a new steel, nanobainitie steel has favourable strength and good plasticity, but the bainitie transformation needs a longer time, so as to severely slow production efficiency down. So, the research of acceleration methods of bainitie transformation is of significance. In this work, in order to accelerate the bainitie transformation rate, the effects of pre-deformation temperature and amount on nanobainitie transformation kinetics and microstructure of the medium carbon nanobainitie steel were investigated. The results showed that pre-deformation process obviously shortened the incubation time of bainitie transformation. When the temperature range is from 300˚C to 850˚C and the pre-deformation amount is 20%, low pre-deformation temperature could accelerate bainitie transformation at whole isothermal region, while high pre-deformation temperature accelerated bainitie transformation at the initial stage, and hindered bainitie transformation at later stage. Volume fraction and increasing rate of bainite ferrite were decreased with increasing pre-deformation temperature. Bainite ferrite lath thickness was increased with decreasing pre-deformation temperature. The pre-deformation process increased the frequency of small angle grain boundary of bainite transformation microstructure, and the frequency of small angle grain boundary of low pre-deformation temperature was higher than that of high pre-deformation temperature. When the pre-deformation amount is from 0 to 30% and the pre-deformation temperature is 300˚C, volume fraction and increasing rate of bainite ferrite were increased and then decreased with increasing pre-deformation amount. The kinetic parameters *n* of bainitie transformation was calculated by the analytical model, the model of nucleation and growth were identified, the pre-deformation process changed the nucleation position of bainitie transformation. The crystal edge and the crystal face nucleation were mainly obtained through high pre-deformation temperature, and the crystal corner nucleation was mainly obtained through low pre-deformation temperature. Nucleation position was mainly changed from the crystal edge and the crystal face to the crystal corner with increasing pre-deformation amount in the low pre-deformation temperature process.

A-7: Synchrotron Radiation Analysis of Controlling Mechanism to Emerge Excellent Strength and Ductility Balance in Low Carbon-2%Si-5%Mn Fresh Martensitic Steels

Taiga Fuse, Shiro Torizuka, Atsushi Ito, Hiroki Adachi, University of Hyogo, Japan

In the automobile industry, higher strength and higher ductility materials require with satisfying both collision safety and fuel economy. However, there is a trade-off relationship between strength and ductility. When strength increases, ductility decreases. Therefore, it is very difficult to improve both simultaneously. We have reported that 0.1%C-2%Si-5%Mn fresh martensitic steel exhibits excellent strength of 1400MPa and total elongation of 15%. We also reported that the mechanism of simultaneous improvement of strength and ductility by the effect of the addition of Mn is due to improvement of work hardening ability in 0.1%C-2%Si-5% Mn fresh martensitic steel. The increase in Mn content from 1.5 to 5% enables martensitic structure to increase dislocation density from 2.5x10^{15} to 4.4x10^{15}mm/mm^3 , resulting in higher work hardening rate. Good agreement was obtained between the relationship the dislocation arrangement parameter obtained by the XRD result and TEM observation result.
However, the effect of C on 2% Si - 5% Mn fresh martensitic steel is not clear. In this study, to investigate the effect of C on strength and ductility is carried out with in-situ X-ray diffraction during tensile tests by the synchrotron radiation in SPring-8. The relationship between the work hardening behavior and the dislocation density is analyzed. The dislocation density was calculated with modified Williamson-Hall method and modified Warren Averbach method. XAFS measurement was also performed to investigate the interaction between Mn and C. The increase in C content from 0.075 to 0.2% C enables martensitic structure to increase dislocation density from 3.7x10^{15} to 5.8x10^{15}mm/mm^3, resulting in higher work hardening rate. We found that the tensile

strength is determined by the upper limit of dislocation density and the uniform ductility is determined by the increasing rate of the dislocation density.

A-8: Synchrotron Radiation Analysis of the Mechanism to emerge 1500MPa-30% Excellent Mechanical Properties of Ultrafine Ferrite+Austenite Structure in Low C-2%Si-5%Mn Steels

Kazuki Minoda, Shiro Torizuka, Hiroki Adachi, University of Hyogo, Japan

In recent years, improvement of fuel consumption and reduction of exhaust gas have become important issue in the automobile industry, and development of steel sheets for automobiles having both high strength and high ductility are strongly required. However, its realization is very difficult because high strength and high ductility are in trade off relationship. TRIP steel has large elongation and strength-ductility balance 30000MPa% level, but tensile strength is 1000MPa at most.

5%Mn steels have attracted a lot of attention and are researched all over the world. High tensile strength of 30000MPa% level has been reported.

However, in any of the high tensile strength steels, the tensile strength is about 1000MPa, and it does not exceed 30000MPa% at high strength 1500MPa grade. Although TRIP steel has high elongation by utilizing deformation induced martensitic transformation, its tensile strength is not sufficient due to its small austenite volume fraction. Therefore, high strength and high ductility can be achieved at the same time by increasing the γ volume fraction of TRIP steel.

We reported that 0.1%C-2%Si-5%Mn ultrafine a (ferrite) + g (austenite) steel has a high γ volume fraction (30%). In this study, the change in γ volume fraction during tensile deformation was investigated by in-situ XRD in 0.1~0.3%C-2%Si-5% Mn steels. Especially, the effect of C content is focused. Microstructures of the starting and deformed materials were analyzed by SEM-EBSD. The change in strength and ductility with changing in C addition and heat treatment temperature were focused. As a result, 0.15%C-2%Si-5%Mn ultrafine a + g steel annealed at 700˚C for 1 hour has the strength-ductility balance exceeding 30000MPa% at TS of 1500MPa level. Also, it is investigated that the mechanism to emerge its excellent strength-ductility balance.

A-9: The Study of Microstructure and Properties of High Nitrogen Stainless Steel in Watch Case Application

Wei Peng, Hongshan Zhao, Chundong Hu, Hengchang Lu, Xintong Lian, Tengshi Liu, Jing Xu, Han Dong, Shanghai University, China

High nitrogen stainless steel has been widely concentrated on the application of human body biomaterials, such as stent in blood vessels, artificial valves in the heart, and replacement of implants in shoulders, keens, hips, elbows, and dental structures. Also, it has been used in orthopedic implant devices to aid healing, correct deformities and restor the lost functions of the original part in order to improve the longevity of humans. It is notably that all these applications are inside the human body. But in this present, the microstructure and properties of high nitrogen stainless steel (HNSS) for the application in watch case has been investigated. HNSS microstructure mainly consists of austenite phase after solid solution treatment, and tensile tests show that a good ductility and high strength. It also presents favorable forming performance during product manufacturing. In addition, better corrosion resistance and quite low Ni dissolution rate are detected. Hence, the field of studied HNSS cannot only apply on the implant materials in human body, but also use in other aspect which the material can contact human's skin. In the past, the watch case materials are mainly stainless steel with a lot of Ni element, the anaphylactic reaction will be occurred on human skin after a long period of wearing. The low Ni dissolution rate of our studied HNSS cannot arouse anaphylactic reaction with human skins, which is suitable for manufacturing watch case. For the application of watch case, it needs high strength, good forming performance, wear resistance, good corrosion resistance and so on, all these properties can be met by high nitrogen stainless steel. As a perspective material for high nitrogen stainless steel, we can predict that it is not only using the human body implant materials and the contact materials with human skin, but also applying on other aspects too.

A-10: Control of Carbides in High-Carbon Martensitic Stainless Steels

Hongshan Zhao, Yudan Yang, Chundong Hu, Han Dong, Shanghai University, China

Martensitic stainless steels are high performance engineering steels. The high mechanical properties with moderate good corrosion resistance can meet those of engineering applications like cutting tools, bearings, shafts, bolts and so on. The type and size of carbides in martensitic stainless steel are key factors controlling the service performance such as mechanical properties and corrosion resistance, especially for high carbon types. Besides the solidification process, the carbides are controlled by the thermal-mechanical treatment. Three types of high carbon martensitic stainless steels, 5Cr15MoV, 6Cr16MoMA and 9Cr18MoV, are used to study the carbide evolution during deformation process and heat treatment. The phase diagrams of the three steel have been calculated by thermal calc, and the effect of deformation at different temperatures

on the carbides will be studied by thermo-mechanical simulation testing machine. Different annealing and quenching and tempering heat treatments will be applied to these steels. The type and size of carbides will be characterized by XRD, SEM, TEM; the mechanical properties will be tested by hardness, tensile and impact testing; the corrosion behavior will be studied by electrochemical method and salt spray test. The carbide evolution study and controlling will be helpful to further improve the properties of martensitic stainless steels and the product quality.

A-11: Effects of Solution Treatment on Microstructure and Impact Toughness of S31803 Duplex Stainless Steel

Xingrun Chen, Guoguang Cheng, University of Science and Technology Beijing, China / Hongxing Iron & Steel Co. Ltd., Jiuquan Iron and Steel Group Corporation, China; Jixiang Pan, Hongxing Iron & Steel Co. Ltd., Jiuquan Iron and Steel Group Corporation, China

S31803 duplex stainless steels (DSS), a fascinating combination of ferritic and austenitic steel features, have stirred a considerable research interest around the world since they are discovered in 1940s, and are replacing austenitic steels employed extensively in a variety of applications such as ocean and bridge structure engineering, petroleum and power generation industries because of their optimal compromise between the mechanical properties, the corrosion resistance and the economic advantages. The effects of solution treatment on microstructure and impact toughness of S31803 duplex stainless steel (DSS) were investigated in details. The results demonstrate that the holding time has little effect on expansion amount of S31803 DSS at the different solution temperatures. The solution temperature plays a key role on the phase transformation when the holding time is more than 5 minutes. This trend is in good agreement with the equilibrium phase diagrams during solidification calculated with Thermo-Calc thermodynamic computational software. The white austenitic phase islands embed in the black matrix ferrite phase and no significant secondary phase precipitates can be found in the specimen. The volume fraction of ferrite phase gradually increases with increase of solution temperature. The impact toughness of the S31803 increases with the solution temperature increasing, and, typically, it is larger than the 100J in the case of solution temperature at 1373K (1100℃). The SEM morphology of impact fracture shows a significant ductile fracture, illustrating that solution treatment can markedly improve the toughness of S31803 DSS due to the presence of large number of dimples in impact test.

A-12: Research on Hydrogen Induced Delayed Cracking of DP780

Chunqian Xie, Yun Han, Limei Pan, Shougang Group Co. Ltd., Research Institute of Technology, China / Beijing Key Laboratory of Green Recyclable Process for Iron & Steel Production Technology, China

With the development of light-weight and safe automotive, more and more high strength steel has been used in "body in white" of car. The application of 780MPa grade and above high strength steel has decreased the weight of car body, reduced emissions, and improved safety performance of the car. Among these high strength steels, DP steel is the most widely used one due to its low yield strength, high tensile strength and high work-hardening rate.

Hydrogen induced delayed cracking is a phenomenon in which a material undergoes sudden brittle after a certain period of time under static stress. This phenomenon is one kind of environmental embrittlements induced by the interaction of material, environment and stress. Besides, as the strength of steel increases, the problem of hydrogen embrittlement usually becomes more seriously. Recently, 780MPa grade dual-phase steel (DP780) is the most widely used high strength steel in automotive industry. And the hydrogen induced delayed cracking of DP780 should be researched in order to increase the safety of automotive and protect passengers.

In this work, the hydrogen induced delayed cracking behavior of two cold rolled DP780 steels for automotive with different chemical compositions was studied by electrochemical hydrogen charging, slow strain rate test(SSRT), thermal desorption spectroscopy (TDS) analysis, SEM and TEM. The results show that the microstructure of DP780-1 is composed of ferrite matrix and banding martensite, while DP780-2 is composed of ferrite matrix and martensite island. And there were more hydrogen condition in DP780-1 than DP780-2 after charging at the same condition. According to the results of SSRT, the tensile strength of DP780-1 after hydrogen charging was reduced by 13%, while it was just 5.3% for DP780-2. The reasons for better resistance of hydrogen induced cracking of DP780-2 are the dispersed martensite island and the TiNbC Precipitates as hydrogen trapping.

A-13: Austenite Grain Evolution Mechanism of High Carbon Rail Based on Thermal Technology

Jun Yuan, Pangang Group Research Institute Co., Ltd., China

Aiming at the special requirements of high-toughness and high-performance rails for high-speed railway, the safe and stable operation of high-speed railway in China is guaranteed. By combining basic research with industrial production, through industrial exploration, the characteristics of austenite grain formation are

revealed, industrial heating and rolling processes are simulated, and innovative experimental research methods such as different heating and heat treatment are carried out on real rails in laboratory. Austenite grain size of high carbon rails under different hot working processes is established for the first time. Transfer characteristics with microstructures and key properties. The test results show that the austenite grain size of U71Mn and U75V industrial production process for high-speed railway is 4.0~5.0 grade; the austenite grain size of high-carbon rail is remarkably refined after simulated rolling; when the holding temperature is increased from 800 to 1300℃, the austenite grain size of high-carbon rail steel decreases and austenite grain is gradually coarsened. The tensile strength increases slightly at first, then decreases slightly, and the overall tensile strength has little effect on heating temperature. With the increase of heating temperature, the elongation and impact toughness of high carbon rail decrease. When the holding temperature is 1000℃, the holding time increases from 10min to 50min, and the influence of rail strength and toughness is small. The heating temperature of high carbon rail combined with austenite grain size shows that the heating temperature has a great influence on austenite grain size, and has the most obvious influence on the toughness of high carbon rail. Combining with industrial production data and laboratory research results, the heating temperature of laboratory rail is the most suitable in the process of heat treatment. For industrial batch production, it is suggested that the temperature of soaking section of high carbon rail billet should be less than 1250℃, which is beneficial for matching strength and toughness of high carbon rail for high speed railway.

A-14: Effect of Hot Rolling on Properties of 15Cr-ODS Steels

Zhengyuan Li, Shenyang University of Technology, China

Nano-structured oxide dispersion strengthened (ODS) ferritic/martensitic steels are the leading candidate materials for the fast reactor fuel cladding application due to their excellent high-temperature strength and radiation tolerance due to their characteristic microstructure of ultra-high density of nano-scale clusters/precipitates, ultrafine grains and high-density of dislocations. At present, the research of nano-structured ODS steel focuses mainly on the optimization of alloy composition, mechanical alloying and heat curing parameters to improve the microstructure and mechanical properties of nano-structured ODS steel. However, the research on hot rolling is limited.

In this thesis, two different Cr content of nano-structured ODS steels containing Al and Zr elements (9Cr-ODS steel and 15Cr-ODS steel) were prepared by mechanical alloying (MA) and hot isostatic pressing (HIP), followed by different hot rolling deformation. The effects of hot rolling on the microstructures, including the types, size and density of nanoscale precipitated phases, before and after hot rolling were studied by electron back scattered diffraction (EBSD), scanning electron microscopy (SEM) and transmission electron (TEM). The mechanical properties were measured too. This research could provide theoretical foundation for the research and application of nano-structured ODS steel microstructures and performances optimization. The following results were obtained:

(1)The relative densities of 9Cr-ODS steel and 15Cr-ODS steel prepared by mechanical alloying and HIP are both more than 98%, and reach up to ~99% after hot rolling. The quantity of rolling deformation has little influence on the relative density.

(2)The average grain size before rolling is about 1.6μm, and the average grain size of 15Cr-ODS steel after hot rolling is 0.78μm (TD) and 1.05μm (ND). Hot rolling can significantly refine the grains of ODS steels.The grains are elongated along the rolling direction in TD surface, and significant cubic texture (Φ1= 0° , Φ= 0° , Φ2 =0°) {0 0 1} <1 0 0>and brass-R texture (Φ1= 0° , Φ= 55° , Φ2 =45°) {1 1 1} <1 1 0> are observed.

(3)Hot rolling can also significantly improve the tensile strength of ODS steels. The tensile strength of ODS steels after hot rolling at room temperature is 100MPa higher than the HIPed ODS steels before hot rolling. The tensile strength of ODS steel before and after rolling decrease with the rise of temperature. The total elongation of ODS steel rises first and decreases with the increasing temperature, and reaches the highest at 600℃. The fracture mechanism changes from quasi-cleavage fracture to dimple fracture with the increasing temperature. The effect of rolling reduction on the tensile strength and elongation is not obvious. Compared with other ODS steel, the toughness and total elongation of nano-structured ODS steel with Al and Zr addition is significantly improved without intensity reduced. showing excellent mechanical properties.

A-15: Nanoindentation Investigation in Strengthening Mechanism in a Medium Manganese Steel

Lijuan Zhang, Mingyang Liang, Zongqiang Feng, Ling Zhang, GuiLin Wu, Chongqing University, China; Wenquan Cao, Special Steel Department of Central Iron and Steel Research Institute (CISRI), China

Remarkable enhancement of impact toughness, good combination of strength and ductility in laminated structure has been reported in some multilayered composites and single phase materials.

Dual phase steel, due to its alternating two phase nature, has big potential to achieve this goal if the granular microstructure can be tuned into laminated structure. In a previous study, laminated 5Mn3Al dual phase steels have been designed by adding Mn and

Al elements to stabilize austenite and ferrite phases at high temperatures and suppress the growth of lamellae to granular shape. The interfaces between the ferrite and martensite phase were considered to be very important in affecting the strength, ductility and impact toughness of the material. Its effect on deflecting crack (delamination of lamellae and interfaces) has been reported in previous investigations. However, it's effect on strength is less studied since it is hard to evaluate by normal testing method, such as tensile test and Vickers hardness test. Nanoindentation technique has been widely used because of its ability to measure the mechanical properties of a precise site at the nanometer scale, and the technique is thought to be a good method to separate individual contributions from various factors. In this study, nanoindentation technique was carried out to evaluate the contribution of the interface on strength in a 0.1C5Mn3Al (wt%) laminated steel.

From the present investigation, it can be concluded that in the 0.1C5Mn3Al dual phase steel, decreasing in phase thickness can lead to hardening of the phase interior and thus harder interface or phase boundary. A lamella structure can give better strength and ductility combination than that of granular structure. Low load pop-in event in the phase interior and high load pop-in event near the phase boundary were observed due to dislocation formation and dislocation-interface interactions. The hardening of the interface itself may contribute to the strength of the material. While, a good combination of microstructure and strength of the interface is more essential to improve the elongation.

A-16: Online Softening and Spheroidization of Pearlite for Middle Carbon Steel

Hengchang Lu, Chundong Hu, Han Dong, Shanghai University, China; Jinzhong Zuo, Zhenwei Su, Miao Zhou, Yu Liu, Zenith Steel Group Co., Ltd, China

The middle carbon (0.35Cwt.%) steel is possible to be spheroidizing annealed for a better ductility to cold heading or extruding in the process of fastener making. However, it will consume a lot of energy and release pollutants in the annealing process. Thus a trial of online softening and spheroidizing of pearlite of 0.35Cwt.% carbon steel wire rod was taken by thermal mechanical transformation (TMT) technology. The dynamic CCT curve of 0.35Cwt.% carbon steel shows that the morphology of pearlite will be spheroidizing when the cooling rate is lower than 0.5℃/s after deformation at 800℃ with a deforming rate of $10s^{-1}$. The results of thermal machanical test by Gleeble 1500D show that the amount of deformation induce ferrite (DIF) will be increase by a decrease of deformation temperature and an increase of rate. The Zener-hollomon parameter of 0.35Cwt.% carbon steel can be expressed by, and the deformation stored energy can be expressed by. Combine with DIF, spheroidal & degenerate pearlite using extreme thermal mechanical controlling process (TMCP), the tensile strength of the 0.35C wt.% carbon steel wire rod can be reduced by about 80MPa, which make the spheroidizing annealing process be omitted for cold heading.

A-17: Effect of V on Continuous Cooling Transformation Characteristic of Bainitic Steels

Pengyu Fan, Guhui Gao, Yu Tian, Beijing Jiaotong University, China

By using thermal expansion method, combined with metallographic method, the determination of the hardness method, including V (0.2%) and does not contain V bainite test steel continuous cooling transformation curve (CCT curve), and using optical microscope (OM), scanning electron microscope (SEM), vickers hardness and X ray diffraction analyses the V elements of supercooling austenite bainitic steel continuous cooling transformation rules, microstructure, especially the bainite microstructure transformation rules, microhardness and the influence of residual austenite content. The results show that the critical points of Ac1, Ac3 and Ms are reduced by V. At the same time, V element has significant influence on the morphology and distribution of bainite. V element can significantly improve the hardness of the steel in the bainite transition zone. With the increase of cooling rate, the hardness of the steel with V increases gradually and finally stabilizes around 780HV, which is significantly improved compared with the steel without V element (720HV). The residual austenite content of the test steel was measured by X-ray diffractometer. The steel content in both tests increased with the increase of cooling rate. The steel with V element was finally stabilized at about 10%, while the steel without V was about 8.5%.

A-18: Performance Testing of Weathering Steel

Zheng Liu, Hongshan Zhao, Yudan Yang, Shanghai University, China

Low carbon steel is the most common type of steel. It is widely used in construction, transportation and bridge. So its corrosion problem is particularly important. Compared with carbon steel, weathering steel has better resistance to atmospheric corrosion because of the addition of alloying elements, such as Cu, P, Cr, and Ni. In addition, inclusions in steel often become the source of pitting corrosion, pitting corrosion gradually expanded and further developed into general corrosion. Rare earth elements have the effect of inclusion modification. Therefore, this study is mainly for a series of performance tests on these three materials of Q235, 09CuPCrNi, 09CuPCrNiRE by inclusion rating, aspex, SEM, EPMA, electrochemical experiment and indoor accelerating corrosion test (alternate immersion corrosion test and salt spray test). These tests were designed to research the mechanism of action of RE on steel and the reason why the addition of RE could

improve atmospheric corrosion resistance. It is found that the rare earth elements can be segregated at the grain boundaries because of large atomic radius and actively chemistry and form spherical rare earth compounds with sulfur and oxygen, which reduces the size and density of inclusions and improves the atmospheric corrosion resistance of the materials.

A-19: Dissolution and Precipitation of Carbides in a Medium Carbon Cr-Mo-V Steel Sheets

Chundong Hu, Xing He, Hongshan Zhao, Han Dong, Shanghai University, China

The evolution behavior of carbides under various austenitizing (900~1100˚c) and tempering (600~700˚c) temperatures in a Cr-Mo-V secondary hardening steel was investigated. Characterization methods of scanning electron microscopy (SEM), electron back-scattered diffraction (EBSD), transmission electron microscopy (TEM), carbon extraction replica, electrochemical extraction and X-ray diffraction (XRD) were applied. Carbides of MC, M2C, M3C, M6C, M7C3 and M23C6 were identified. During the austenitizing process, the M7C3, M23C6 and M6C are completely dissolved in 900~950˚c, 950~1000˚c and 1000~1025˚c, respectively, while there are still some MC remaining at 1100˚c. The whole solution temperature of MC is increased because of Nb. The growth of the grain size can be inhibited effectively when the amount of MC is more than 0.14wt.%. When tempered from 600 to 700˚c after being austenitized at 1050˚c, the amount of MC and M2C precipitation is increased from 1.26 to 1.81wt.%, while the M3C is reduced greatly from 1.91wt.% at 650˚c to 0.92wt.% at 675˚c. The M7C3 starts to precipitate at 675˚c, indicating that the M3C is converted to M7C3. It seems that the low impact toughness between 600~650˚c is due to the high amount of M3C

A-20: Formation and Growth of Intermetallic Phases on Steels Hot-Dipped in Al-Zn-Si-Mg Alloy Melts

Seung-Hui Ko, Joo-Youl Huh, Korea University, Korea; Il-Jeong Park, Seok-Gyu Lee, Technical Research Laboratories, POSCO, Korea

Hot-dip aluminized (HDA) steel sheets have superior corrosion resistance compared to the conventional hot-dip galvanized steel sheets due to the formation of a dense Al_2O3 layer which provides an excellent barrier protection. Al has a higher melting point than Zn and thus, the liquid metal embrittlement (LME) phenomenon can be avoided in the HDA steel sheets. However, the HDA coatings are lack of sacrificial corrosion resistance which is required to protect cut edges from corrosion. Therefore, Al-Zn-Si alloy coatings have drawn much attention in the steel industry since they can exhibit both protective and sacrificial corrosion resistances without LME phenomenon during spot welding. It is known that the adhesion of hot-dipped Al-Zn-Si coatings is deteriorated by increasing Zn content in the coating alloy. Moreover, Mg is often added to the Al-Zn-Si bath to enhance the corrosion resistance of the alloy coatings. Therefore, it is necessary to understand how the Zn and Mg contents in Al-Zn-Si-Mg baths influence the formation and growth of intermetallic phases and, thus, the interfacial adhesion of Al-Zn-Si-Mg alloy coatings. In this study, 1180TRIP (transformation-induced plasticity) and EDDQ (extra deep drawing quality) steel sheets were hot-dip coated using two molten Al-Zn-Si alloy baths with and without 3wt.% Mg in a HDA simulator. The effects of the Mg addition on the formation and growth of intermetallic phases were investigated by changing the dipping time from 5 to 80s for two different bath temperatures of 580˚c and 600˚c. A scanning electron microscope (SEM) equipped with an energy dispersive spectroscope (EDS) were used to characterize the thickness, composition, and morphology of the intermetallic phases formed at the steel/coating interface. Phase identification of the intermetallic phases was also performed using X-ray diffraction (XRD) and an electron probe micro-analyzer (EPMA).

A-21: Characterization of Nano-Sized Precipitation and Dislocations and the Correlation with Mechanical Properties of a Low Alloy TRIP-Aided Seel

Zhenjia Xie, C.J. Shang, University of Science and Technology Beijing, China; B. Langelier, S.V. Subramanian, X.P. Ma, McMaster University, Canada; Y.T. Tsai, J.R. Yang, National Taiwan University; China; W.H. Zhou, Hunan Valin Xiangtan Iron and Steel Co. Ltd., China

High strength low alloy (HSLA) steels are very important materials for structure and infrastructure applications, due to their excellent combination of strength, toughness, weldability and economy. Driven from energy consumption and safety concern, there is a continuous and increasing trend to higher strength with improved ductility and low temperature toughness for all applications. However, great challenges are generally entailed to enhance the comprehensive properties. Most importantly, increasing the strength invariably deteriorates toughness, especially at low temperature. To overcome such inversion problem, retained austenite is introduced to low carbon martensitic steels containing 8~15 weight percent (wt%) nickel, processed by quenching and tempering/annealing. Excellent combination of strength and toughness has been achieved due to the transformation-induced-plasticity (TRIP) effect of retained austenite, though the addition of Ni/Mn comes with increased cost. Recently, we have produced low carbon low alloy steels with stable retained austenite at room temperature. Due to

the low carbon and lean alloying elements content, two cycles of intercritical heat treatment, namely, intercritical annealing and intercritical tempering were designed to stabilize austenite. The first cycle of intercritical annealing was conducted by annealing at a high temperature in the ferrite (α) plus austenite (γ) two-phase region followed by air cooling, secondary ferritic laths containing intermediate Mn content were obtained. The second cycle was carried out by tempering at a lower temperature to promote further diffusion of Mn into Mn-enriched austenite, such that retained austenite was stabilized after cooling to room temperature. Unfortunately, these cyclic high temperature heat treatments usually induce significant softening of the steel due to dislocations recovery.

Precipitation strengthening is an effective approach to compensate for the loss in strength. For instance, microalloying elements, such as Nb and V, were added to conventional TRIP steels and quenching and partitioning (Q&P) steels for precipitation strengthening. In addition, copper is usually used to increase strength in steels processed by multi-step heat treatment, via forming nano-sized Cu-enriched particles. Based on the above concept, both Nb and Cu were added in multi-step heat treated steel in our previous studies. The combination of retained austenite and nano-scale precipitation provided superior mechanical properties. Intensive efforts have been made by using TEM to explore microstructure–mechanical property relationship, with particular emphasis on precipitation strengthening. However, little quantitative study was made. APT has been widely used to study nano-sized atomic clusters and precipitates in metallic materials. APT offers a possible route to measure the composition, size, number density and volume fraction of nano-sized clusters and precipitates, though this information is limited to coming from a very small volumes of analyzed material.

The present work focuses on structure-property correlation in a new low alloy multi-phase microstructure steel engineered with retained austenite via Cu alloying plus a three-step heat treatment, namely, intercritical annealing, intercritical tempering and sub-critical tempering of a as hot rolled structure. Particular attention was paid to characterizing nano-sized precipitates and dislocations after the three-step heat treatment by atom probe tomography (APT) and transmission electron microscopy (TEM), in order to establish their respective contribution to the yield strength. Cu-rich atomic clusters and ultra-fine precipitates were obtained in intercritical ferrite after the three-step heat treatment. The average radius of clusters and precipitates was 1.3 ± 0.4nm and 5.6 ± 0.7nm, respectively. The number density of clusters and precipitates was estimated as $2.55 \times 10^{23} m^{-3}$ and $1.68 \times 10^{21} m^{-3}$, respectively. The strength contribution from clusters and precipitates was ~72MPa and ~101MPa, respectively, assuming the number density of the APT dataset to represent the whole material. In addition, a large number of dislocations were observed in the intercritical ferrite by TEM study. The average density of dislocations was measured to be ~$1.66 \times 1014 \pm 7.12 \times 10^{13} m^{-3}$, which contributed ~272MPa to yield strength according to the Bailey–Hirsch relationship.

A-22: Optimization of Austempered Gray Cast Iron(AGI) Heat Treatment Conditions by Aluminum Content

Dong Hyuk Kim, Si Geun Choi, Jae Il Jeong, Jae Won Kim, Bok Seong Choe, Jong Hyoung Kim, Korea Institute of Industrial Technology(KITECH), Korea

Aluminum cast iron has excellent oxidation resistance, resistance to sulfide and corrosion. Compared with Ti and Ni alloys, it is expected to be a substitute material for structural materials and stainless steels because it is relatively inexpensive to use Fe, which is a non-strategic element. In case of iron, excellent non-strength has the same level of strength when manufacturing parts. This results in a weight reduction effect of about 30% as compared with the case of using stainless steel. However, their practical use has been limited because their room-temperature ductility is insufficient and strength is rapidly reduced at temperatures of 600℃ or higher. For heat-resistant cast iron, high-temperature materials containing Cr and Ni account for 30%~50% or more. However, such high-temperature materials are costly and aluminum heat-resistant cast iron is considered a heat-resistant cast iron material to replace such expensive heat-resistant materials.

To this end, in this study, aluminum cast iron specimens with 1~4wt.% aluminum added to flake graphite cast iron are fabricated using high-frequency induction melting furnace. The microstructure analysis in terms of aluminum content and austempering heat treatment conditions revealed two phases: austenite and ferrite. The cooling curve experiment and solidification simulation show that the austenitizing temperature is insufficient for forming austenite phase in the 4wt.% Al cast-iron to establish the optimum os tempering heat treatment condition. When the austenitizing temperature is 1000℃, the ausferrite fraction is higher than that obtained at 900℃. Based on the mechanical properties, phase map analysis, and distribution fraction of 2wt.% Al cast-iron, the most optimized heat treatment condition was identified as the os tempering temperature of 320℃. The microstructure and phase analyses, mechanical properties, and oxidation resistance according to the heat treatment conditions are investigated to establish the optimal austempering heat-treatment conditions

A-23: Analysis of Tensile Specimens Fracture Delamination of Low Alloy High Strength Steel Plate

Shuang Wang, Haiyang Hu, Diandong Sun, Bingyu Yan, Ansteel Group Iron and Steel Research Institute, China

Low alloy high strength steel plate is a very important kind of structural steel plates, its performance has great significance to the safety and long-term

reliability of the whole structure. With the development of science, technology and the improvement of people's requirements for structural properties, higher requirements have been put forward for low alloy high strength steel plates, which requires stringent chemical composition and mechanical performance, and should have good microstructure stability, weld ability, cold processing and fatigue strength under operating temperature. In recent stage, a batch of Q460C steel plates produced by our factory showed the phenomenon of fracture delamination of tensile specimens in the normal temperature mechanical property test. Therefore, this paper solved the problem of fracture delamination by analyzing and studying the layered samples. In view of the fracture delamination in the tensile test of Q460C steel, the fracture morphology, non-metallic inclusions and microstructure of the tensile test specimens were analyzed. The results showed that sulfide and titanium nitride inclusions existed in the thick center of the plate, and tissue segregation of martensite + bainite + ferrite were the main cause of fracture delamination. The improvement measures are mainly in smelting. First, the harmful element S is further reduced from 0.008% to below 0.003%. Secondly, to reduce the degree of superheat of molten steel, through the accurate control of refining of molten steel temperature, make molten steel pouring superheat from 25 ~ 35℃ to 15℃ below, at the same time, improve the electromagnetic stirring parameters, from 800A, 4Hz to 1000A, 3.5Hz are adjusted to further reduce the composition segregation of tissue segregation in the end. After adjustment, the dendrite test and non-metal inclusion test were conducted for the continuous casting billet and the steel plate. It can be seen that the central segregation of the continuous casting slab has been reduced from B1.5 to B0.5, and manganese sulfide and titanium nitride inclusions have been effectively controlled.

A-24: Development of W-1.1wt% TiC Using a MA-HIP Process

Hiroyuki Noto, Yoshimitsu Hishinuma, Takeo Muroga, National Institute for Fusion Science, Japan; Hideo Benoki, Nippon Tungsten Co., Ltd., Japan

Tungsten (W) is a candidate material for plasma facing components of fusion reactors in terms of high thermal conductivity, high melting point and low tritium retention etc. However, tungsten has critical issues for the application such as recrystallization-embrittlement at high temperature. As a possible solution of the issue, W-1.1wt%TiC has been investigated. The W-1.1wt%TiC is known as an advanced W alloy which applied the role of Titanium-carbide (TiC) to decrease the density of grain boundaries which are known to act as driving force of recrystallization. The W-1.1wt%TiC in previous study exhibited high resistance to heat loading and the Ductile-brittle transition temperature (DBTT) being below room temperature. Those materials were fabricated by 3MPDA (three mutually perpendicular directions agitation) ball mill - GSMM (Grain Boundary Sliding-based Microstructural Modification) treatment. However, this process has some critical issue such as the complexity of the process and the limited volume of the products. Therefore, we have adopted a new fabrication process based on Mechanical Alloying (MA) - Hot Isostatic Pressing (HIP) methods which are applied to ODS ferritc steels for W-1.1wt%TiC. In the present study, the effect of alloying process on mechanical properties was investigated.

In the production of W-1.1wt%TiC, the initial elements were mixed and mechanically alloyed in a planetary-type ball mill using tungsten carbide balls of 1.6mm and 3.0mm in a 250cc MA pot with ball-powder ratio of 2:1. The alloying was carried out with a rotating rate of 360rpm for 64h in a pure argon gas atmosphere. The mechanically alloyed powders were compressed by cold isostatic pressing (CIP), and were then pre-sintered in hydrogen gas atmosphere at high temperature. The pre-sintered W-1.1wt%TiC were then sintered by HIP at 1750℃ for 1.5h with a pressure of 186MPa. The microstructures were characterized by Transmission Electron Microscope and the Energy dispersive X-ray spectroscopy.

XRD showed that the peak broadening was more prominent in the case when larger MA balls (3.0mm) were used. In this case, the peak was broadened after 64h MA, indicating that elements of W and TiC reached a metastable state. The particle refining proceeded more rapidly in the case of 3.0mm balls MA than that of 1.6mm balls MA. The HIPed W-1.1wt%TiC after MA using 3.0mm balls, exhibited fine micro-structure, and high hardness relative to those using 1.6mm balls. The sintered microstructure was analyzed by Electron Back Scatter Diffraction (EBSD) Patterns, and exhibited recrystallized state caused by low rate of coincident site lattice (CSL) boundary (sigma3～sigma29b). The EBSD result indicated the possibility of strengthening of recrystallized grain boundaries by TiC.

A-25: Combustion Characteristics and Kinetics of Chlorine-Containing Bituminous Coal

Cui Wang, Jianliang Zhang, Kexin Jiao, Guangwei Wang, University of Science and Technology Beijing, China

With the rapid growth of the world population, serious pollution of our surroundings and the rising demand for water by industry, the world is facing the danger of running out of fresh water. In order to meet the requirements of the national water saving, the blast furnace (BF) dry-dedusting system has been widely introduced into iron-making plant in many countries. However, the released HCl and other acid gases in BF bring hazards to gas pipelines, BF top gas recovery turbine unit and so on,

which should have been absorbed by gas washing water in BF wet-dedusting system. Chlorine in BF usually comes from iron ores, coke and pulverized coal. Recently, as the injection rate of pulverized coal into BF is constantly increasing and the low-quality coals are extensively utilized for injection, the increase in chlorine affects the BF smelting process, metallurgical properties of raw materials and coke, characteristics of molten slag, as well as the combustion characteristics of pulverized coal simultaneously, and the certain extent of circulation and accumulation of chlorine in BF makes these effects more obvious.

Therefore, it is urgently required to clarify the behavior and influence of chlorine on the combustion characteristics of coals injected into BF under the new situation. In order to better understand the influence of chlorine on the combustion performance of coal in BF tuyere raceway at high temperature, the fundamental influence at low temperature is studied beforehand. Hu et al investigated the effect of chlorine on combustion process of pulverized coal in tuyere zone, it was found that the chlorine influence was depended on the existence form of chorine in coal. If the chlorine existed as chloride, such as NaCl, KCl, $CaCl_2$, etc., the combustion process of the pulverized coal was prevented. On the contrary, the combustion process was improved if chorine was present in the form of combination with HCl and nitrogen functional groups of coal macromolecules. However, the basic influence of chlorine on coal combustion characteristics is not referred to, especially the process parameters, such as the initial reaction temperature, final reaction temperature, maximum reaction rate, etc., which play great roles in measuring the coal combustion performance. In order to clarify the fundamental influence of chlorine on the coal combustion process, the combustion characteristics and kinetics of chlorine-containing bituminous coal, which usually accounts for a certain proportion in the pulverized coal injected into BF tuyere raceway, were performed systematically in this study.

The thermogravimetric method was applied to the investigation of the combustion process of Shenhua bituminous coal (SH) with 0.047%, 0.204%, 0.952% and 3.044% chlorine from ambient temperature to 1173K in air atmosphere. The results showed that the SH combustion characteristics were affected by increasing chlorine, the thermogravimetric analysis further revealed that the SH combustion was inhibited by chlorine addition, while the reactivity was improved by increasing heating rate. The average apparent activation energies derived from the iso-conversional method (iterative KAS method) were 105.160, 114.045, 113.155 and 124.869kJ/mol, respectively. As a slight variation was observed for the change of the apparent activation energies for each of different chlorine-containing SH combustion with the degree of conversion, the combustion process was treated as a single-step reaction mechanism. The most probable mechanism funtion was determined to be the random nucleation reaction, the integral form of which was $g(a)= - \ln(1 - a)$ and differential form was $f(a)= 1 - a$. The mechanism function of the nucleation kinetic model was then employed to estimate the pre-exponential factor, and the average values of pre-exponential factor were 1.14×10^6, 6.08×10^6, 1.22×10^7 and $2.96\times10^7 s^{-1}$, respectively.

A-26: Hot Deformation Behavior of Nb-Bearing High Carbon Steel by CSP Process

Xinli Song, Rongdong Chen, Yu Cao, Wuhan University of Science and Technology, China; Aimin Guo, Zhongzhu Liu, Wuhan University of Science and Technology, CITIC-CBMM Microalloying Center, China

High carbon steels are widely used for automobile and high quality saw blade and construction equipment and so on because of the their high strength and high hardness and wear resistant and fatigue resistant. Compact strip production(CSP) process for high carbon steel has significant advantages in its technical and economic benefit. Compared with the traditional production process, The short time and large pass reduction in CSP line is benefit to reduce the decarbonization behavior and element segregation and refine non-metallic inclusion. Niobium in high carbon steel can refine the microstructure and improve the ductility. In this paper the hot deformation behavior of Nb-bearing high carbon steel was investigated using single hit compression tests on Gleeble-3800 simulator at the temperature range of 900~1150℃ and strain rate range of $0.1\sim10s^{-1}$. The austenite grains and precipitation were analyzed by OM and TEM respectively. The results showed that the hot deformation behavior of Nb-bearing high carbon was susceptible to both deformation temperature and strain rate. The dynamic recrystallization behavior occurred and the equiaxed grains were obtained at the temperature of 1080 and 1150℃ and low strain rate of $0.1s^{-1}$. There was only work hardening behavior and the elongation grains obtained at the temperature of 900℃. The dynamic recovery phenomena occurred for the sample deformed at high strain rate of $5s^{-1}$ and $10s^{-1}$ at the temperature of 950 ~1150℃.The mixed grain microstructure occurred at the temperature of 1000℃ and strain rate range of $0.1\sim10s^{-1}$. The fine nano-size NbC precipitates were found in the hot deformation sample. The recrystallization active energy Q was 328.02×10^3J. The dynamic recrystallization constitutive equation of Nb-bearing high carbon steel is as following: $\varepsilon = 4.536\times10^{12}\sinh(0.0082\sigma)5.532\exp(-328020/RT)$. The results could provide the process parameters for the Nb-bearing high carbon steel produced by CSP.

A-27: Study on Reduction Behaviors of Low Ti-Bearing Sinter in the Lump Zone of Blast Furnace

Yapeng Zhang, Dongqing Wang, Wen Pan, Huaiying Ma, Zhixing Zhao, Shougang Group Co., Ltd Research Institute of Technology, China

Low Ti-bearing sinter (LTS) is an important burden material to prolong the service time of blast furnace (BF), especially at the later stage of campaign. The mineral composition and mineralogical morphology of LTS are very different from ordinary sinter, which lead to the particular reduction performance in the lump zone of BF. In this paper, the reduction degradation behavior, phase transformation, microstructure changes, and reduction kinetics of LTS with high basicity at low and medium temperature conditions were studied and analyzed with application of scanning electron microscope (SEM), X ray diffraction analyses (XRD). The reduction of LTS was conducted in a vertical resistance furnace with simulating the gas composition in lump zone of BF to study the kinetics of LTS reduction. The apparent activation energy was calculated with Arrhenius formula. The results showed that when the reduction temperature was 500˚C, LTS basically maintained the sample structure before reduction, combined with little weightlessness. When the reduction temperature was 600˚C, the original structure of LTS was destroyed with many cracks in LTS and led to its reduction degradation. Compared to 600˚C, as the reduction temperature reached 700˚C and 900˚C, less cracks and more weight loss were found. With increase of reduction temperature, the peak strength of hematite and silico-ferrite of calcium and aluminum (SFCA) in sinter gradually weakened, while the peak strength of magnetite and wustite gradually strengthened in XRD patterns. This phenomenon indicated that increasing reduction temperature could promote the reduction of LTS in lump zone. With the same reduction time, higher reduction temperature would lead to higher weight loss of LTS. At 1100˚C, weight loss would keep increase with the extension of reduction time, and the content of Fe and FeO in the sample would keep rising. It's well to be reminded that the slope of weight loss ratio curve within 30min of reduction was greater than that of 30min later, indicating that the reduction reaction started at a faster speed and slowed down after 30min. With kinetic analysis of reduction in the temperature range of 500˚C to 900˚C, it's found that the apparent activation energy of LTS reduction reaction had a tendency to reduce with the extension of reduction. The average apparent activation energy was 38599.98J/mol.

A-28: The Effect of MnS and AlN Compound Precipitation on Their Growth Behavior in 3% Silicon Steel

Ryutaro Yamagata, Nobusato Morishige, Takashi Kataoka, Nippon Steel & Sumitomo Metal Corporation, Japan

The growth behavior of MnS and AlN compound precipitates in 3% silicon steel was studied. To focus on the effect of the compound precipitation on their growth behavior, two thermo-mechanical treatments and additional isothermal treatment were designed. The thermo-mechanical treatments were composed of the same homogenizing treatment (600s at 1623K), compression (50% in $10s^{-1}$ at 1373K) and holding time (1230s at 1373K), while intermediate cooling and reheat timings were differently set. The intermediate cooling and reheat are designed to induce the nucleation of AlN on prior MnS in low temperature where the system is in the supersaturated state. The long holding time before intermediate cooling and reheat caused the system to experience the low magnitude of supersaturation of AlN, accordingly the nucleation rate of AlN expected to be reduced. In order to control compound precipitation, these timings are set in 30s or 1200s after the compression so as to divide holding duration. The additional isothermal treatments for 3.6ks and 230ks at 1373K are designed to evaluate the difference in the growth behavior of precipitates between the specimens which underwent different thermo-mechanical treatments. The thermo-mechanical treatments were carried out under He atmosphere using a hot-deformation simulator (Thermec Mater-Z, Fuji Electronic Industrial Co., Ltd.), and the additional isothermal treatments are carried out for the samples sealed in vacuum SiO_2 tube, using an electric furnace. Microscopic observation was carried out to measure the sizes of precipitates. A number of single precipitates (MnS) and compound precipitates (MnS and AlN) were found in both specimens, but the ratios of the compound precipitates to all precipitates were different. In the case of the steel with the earlier cooling and reheat timing, the compound precipitates were found more frequently and they remained relatively small in size after the additional annealing. Thus it is considered that the growth rate of precipitates is affected by the ratio of the compound precipitates to all precipitates.

A-29: Development Status and Prospect of Hot Metal Pretreatment Desulfurizer

Tengfei Ma, Wufeng Jiang, Suju Hao, Yuzhu Zhang, North China University of Science and Technology, China

The iron element contained in iron ore and coke during blast furnace ironmaking will increase the crack thermal sensitivity, anisotropy and reduce the impact toughness of steel, which is one of the harmful elements in steel. Therefore, there are strict requirements on the sulfur content of steel in the process of production, especially pipeline steel, ship plate, aviation steel and so on. The hot metal pretreatment desulfurization is the best choice in the steel production process, considering the thermodynamic and kinetic conditions of the desulfurization reaction, or the goal of improving the

production efficiency and steel performance of the steel mill. The way to reduce the sulfur content in molten iron is to develop an economical and efficient desulfurizing agent and a reasonable method for desulfurization and slag removal in the hot metal pretreatment stage. After several decades of development and improvement, the desulfurization and slag removal method has formed a complete and mature system, and the process has little change. The desulfurization agent has become the main research direction of low-cost desulfurization in recent years due to its low development cost.

This paper mainly introduces the desulfurization method commonly used in the hot metal pretreatment desulfurization process and the desulfurization mechanism and application status of several desulfurizers, and reviews the problems of improving the desulfurization ability of desulfurizer, improving the problem of desulfurization and reducing the desulfurization cost in recent years. Some improvement measures and innovations. Through summarization and analysis, it is concluded that under the precursors with little change in the current desulfurization slag method, a single desulfurizer with good desulfurization performance can not maximize the desulfurization effect, and the slag has good physical and chemical properties. Provide a guarantee for the smooth separation of slag iron. The future research and development of desulfurizers will focus on the development of multi-diversity and multi-functionality.

A-30: The Effects of Ni and Cr Addition on Cryogenic Impact Toughness in Bainite-Martensite Steels

Zishan Yao, Guang Xu, Man Liu, Zhoutou Wang, Wuhan university of science and technology, China

Three low-carbon bainite-martensite steels, i.e. basic steel, Ni-bearing steel and Ni + Cr bearing steel, were designed to investigate the effects of Ni and Cr addition on cryogenic impact toughness under two different heat treatment procedures. Dilatometry, scanning electron microscope, transmission electron microscopy were used to observe microstructure and measure the volume fraction of different phases. The amount of retained austenite was measured by X-ray diffraction. Cryogenic impact toughness and surface hardness tests were conducted. For the isothermal treatment process (ITP), specimens were heated to 950℃ for austenitizing for 10min, then quickly cooled to 380℃ at a cooling rate of 20℃/s for isothermal treatment for 30min and finally cooled to room temperature at a cooling rate of 5℃/s. For the continuous cooling process (CCP), specimens were heated to 950℃ for 10min, then quickly cooled to 380℃ at a cooling rate of 20℃/s, followed by cooling to room temperature at a cooling rate of 5℃/s. The results show that due to the occurrence of carbide during isothermal treatment, the addition of Ni and Cr has little improvement in cryogenic impact toughness compared with the basic specimen. In addition, for continuous cooling process, single Ni addition improves cryogenic impact toughness by refining microstructures, while the composite addition of Ni and Cr decreases the cryogenic impact toughness. This is because of the increased ductile-brittle transition temperature and the formation of granular bainite and twin marstenite by Cr addition. Furthermore, microstructures of specimens by ITP and CCP show obvious difference. Compared with the basic specimen, the Ni-bearing specimen has more lath-like bainite and less martenite, while the Ni + Cr bearing specimen has the largest volume fraction of bainite by ITP. The microstructures of specimens by CCP mainly consist of bainite-martensite structures, and no retained austenite and carbide precipitation are observed obviously. The work provides the reference for improving the cryogenic impact toughness of high-strength bainite-martensite steels.

A-31: Influence of Mo, Ti and Nb Contents on the Microstructures and the Low Cycle Fatigue Properties of Ferritic and Bainitic Steels for Seismic and Fire-Resistant Applications

Jung-Ho Sim, Hyun-Uk Hong, Changwon National University, Korea; Chang-Hoon Lee, Joon-Oh Moon, Ferrous Alloy Department, Korea Institute of Materials Science, Korea; Joon-Ho Jeong, Incheon R&D Team, Hyundai Steel Company, Korea

To satisfy the requirements for seismic-resistance, steels must have a low yield ratio(the ratio of yield strength to tensile strength), reflecting a capability to accommodate deformation prior to fracture. Furthermore, it is compulsory that the yield strength at 600℃ should exceed two-thirds of the yield strength at room temperature to satisfy a critical requirement for fire-resistant applications. In this study, low-carbon ferritic and bainitic steels containing different contents of Mo, Ti, and Nb were designed for seismic and fire-resistant applications. The microstructure of steel containing 0.3wt% Mo and 0.02wt% Nb(Steel A) was mainly composed of bainite. By contrast, the microstructure of steel with 0.2wt% Mo and 0.1wt% Ti(Steel B) almost consisted of ferrite with a high density of nano-sized MX precipitates. We conducted tensile tests at 25℃ and 600℃ as well as low cycle fatigue tests to investigate which microstructure combination is favorable to satisfy seismic and fire-resistant characteristics. As results of tensile test at 25℃, the Steel B containing MX precipitates in the ferrite matrix, presented higher yield stress and elongation than Steel A. However, after 600℃ tensile test, the reduction of yield stress for Steel B was so significant that the yield stress for Steel A is higher than Steel B. The Steel A satisfied the requirement for the fire-resistance applications(YS@600℃ ≥ 2/3 YS@ RT). After the thermal exposure at 600℃ for 200, 500, and 1000h, tensile tests were conducted. The yield stress of the Steel A at 25℃ after thermal exposure was

lower, whilst higher at 600˚c than the Steel B. These results indicate that the bainitic microstructures (Steel A) are quite favorable to higher temperature strength due to better thermal stability, while a high volume fraction of nano-sized MX particles(Steel B) contribute largely to lower yield ratio. From strain-controlled fatigue testing at room temperature, it was found that the Steel A showed better fatigue life. Microstructure evolutions and their influence were discussed in terms of performance for both seismic and fire-resistant applications.

A-32: Development Status and Existing Problems of Non-Blast Furnace Ironmaking

Tianhao Sun, Suju Hao, Wufeng Jiang, Yuzhu Zhang, North China University of Science and Technology, China

The present situation of modern ironmaking technology and the development history of non-blast furnace ironmaking are introduced in this paper. The research status of gas-based direct reduction process and coal-based direct reduction process are introduced, including mainstream rotary hearth furnace process, external thermal reaction tank process, shaft furnace process and fluidized bed process. At the same time, the problems that need to be solved urgently in the process development are also put forward. The analysis shows that the problem of bonding loss of flow of iron ore powder in non-blast furnace ironmaking process needs to be solved urgently. Three types of bonding loss of flow are briefly described: iron whisker bonding, new iron bonding and low melting point eutectic formation; and the factors affecting bonding loss of flow are reduction degree, metallization rate, reduction temperature and reaction gas velocity. Four measures to inhibit bond loss are summarized: reducing reduction temperature, carbon coating on the surface of ore powder, controlling morphology of fresh iron and controlling gas velocity of reduction reaction. Four kinds of restraining measures are compared and analyzed. Reducing reduction temperature can restrain the bonding loss in the reduction process of iron ore powder, but the reduction efficiency can not reach the original intention of saving energy in non-blast furnace ironmaking process. The major disadvantage of increasing reaction gas velocity is the low utilization rate of gas and the increase of kinetic energy consumption. It is difficult to control the morphology of new iron in the process, so this method is abandoned. Carbon coating on the surface of ore powder has many advantages, and has good potential for industrial application: i) It is easy to attach carbon to ore powder in the reduction process; ii)Carbon attachment can not only inhibit the loss of bond flow, but also reduce the reaction with ore to improve the reflection efficiency. Therefore, carbon coating on the surface of ore powder has important guiding significance for the development of non-blast furnace ironmaking.

A-33: Atomistic View on C Partitioning Effect into κ-Carbide and Dislocation Behavior by Si Addition after Aging Heat Treatment in Fe-Mn-Al-C Lightweight Cast Steel

ByeongHun Park, Chiwon Kim, Mathieu Terner, Jaehyun Lee, Hyunuk Hong, Changwon National University, Korea; Joonoh Moon, Seongjun Park, Jaehoon Jang, Ferrous Alloy Department, Korea Institute of Materials Science, Korea; Bongho Lee, Center for Core Research Facilities, Daegu Gyeongbuk Institute of Science & Technology, Korea; Youngju Lee, Research Institute of Industrial Science & Technology, Korea

Fe-Mn-Al-C steels which have excellent combination of strength and ductility have been studied for improvement of efficiency in transportation. In these steels, high content of Al (>6wt.%) contributes to about 15% weight reduction compared to conventional steels. In the present study, Si addition was investigated because Si effectively decreases the melting point of molten metals therefore improving castability. Fe-Mn-Al-C steels are age-hardenable by precipitation of κ-carbides with an ordered fcc crystal structure (L'12). The aim of this study is to study the effect of Si addition on mechanical properties, precipitation behavior and deformation mechanism in Fe-30Mn-9Al-0.9C-0.5Mo(-1Si) cast steels. After the solution treatment, mechanical properties were similar in spite of Si addition. However, after aging heat treatment at 550˚c for 100 hours, the Si-added steel was significantly stronger than the Si-free steel. Transmission-Electron-Microscopy (TEM) analyses showed that precipitation of nano-sized κ-carbides was accelerated in the Si-added steel (18 nm precipitates) compared to the Si-free steel (11nm). In addition, dislocations cut through κ-carbides in limited slip systems resulting in unidirectional shearband-Induced-Plasticity (SIP) in the Si-added steel whereas dislocations cut through κ-carbides in multiple slip systems resulting in multidirectional SIP in the Si-free steel. 3D Atom Probe Tomography (3D-APT) highlighted the effect of Si addition on the precipitation of κ-carbides. After aging heat treatment, Si was segregated at the interface between γ-matrix and κ-carbide while C atoms were excessively partitioned into κ-carbides in the Si-added steel. C partitioning by Si addition is thus believed to increase the number of Al-C bonding. The results from first-principles calculations indicate that the energy required for a/2<110> shearing of κ-carbide increases due to unfavorable Al-C bonding, from which the limited deformation was evidenced. In order to assess the dominant deformation mechanism, a theoretical investigation based on the precipitation hardening model was conducted. In the result of theoretical investigation, it was confirmed that shearing mechanism can be activated if there are κ-carbides with radius less than 13.4nm whereas Orowan looping can be activated

with the radius larger than 13.4nm.

A-34: Centerline Segregation and Its Influence on Variability in Mechanical Properties of Corresponding Plates of X70 Pipeline Steel

Fujian Guo, Wenle Liu, Xuelin Wang, Chengjia Shang, University of Science and Technology Beijing, China

The high performance of pipeline steel is determined by fiber structure. Microstructure uniformity is a necessary condition for achieving the above high performance. However, for multi-phase microstructure uniformity control, continuous casting slab uniformity (macro internal quality) is an important factor affecting the fiber uniformity of hot rolled steel plates. Although it is impossible to make the continuous casting slab absolutely uniform, it is necessary to recognize the quantitative relationship between degree of segregation of slabs and the performance stability of plates. Therefore, controlling the quality of continuous casting slab is the necessary method to improve the performance of pipeline steel. Through our research, it is found that control of centerline segregation in continuously cast slab can effectively improve low temperature toughness and elongation of pipeline steel. The objective of this study is to elucidate the influence of centerline segregation in continuously cast slab on variability in mechanical property of X70 pipeline steel. Manneasmann rating method was used to evaluate the degree of segregation of two groups slabs and its effect on variability in mechanical properties of corresponding plates. The results indicated that the degree of segregation significantly causes the tensile strength scatter and deteriorates ductile-brittle transition temperature (DBTT). Microstructural characterization indicated that Mn was enriched in the segregated area.

A-35: Tensile Properties and Microstructures of Pre-deformed and Tempered Advanced High Strength Steel CP800 for Torsion Beam

Suyun Li, Yiding Pei, Yongan Min, Shanghai University, China; Peiyao Xu, Xiumian Gong, Baoliang Sun, Shanghai Huizhong Automobile Manufacturing Co., Ltd., China

Nowadays advanced high strength steel (AHSS) CP800 is a competitive candidate for automobile torsion beams in consideration of weight reduction and energy saving. During the manufacture process of torsion beams with CP800 steel, after mechanical forming, a subsequent optimized tempering treatment is necessary and critical to such torsion beam, so as to release the residual mechanical stress and adjust the deformed microstructures. In this paper various degrees of tensile strain between 0% to 7% were carried out on CP800 tensile specimens. These different strain specimens were tempered at certain temperature of 673~973K for 600、1800 or 7200 second. Brinell hardness was tested on different strain specimens before and after the tempering treatment. Then tensile properties of above pre-deformed and tempered specimens were obtained by tensile test. Microstructures of CP800 in different states were studied with optical microscope (OP)、scanning electron microscope(SEM) 、X-ray Diffraction(XRD)、atom probe tomography(APT). The results show larger strain lead to lower product of strength and elongation (PSE) on insufficient tempered specimens. Proper sufficient tempering endows CP800 steel with high PSE of 16KMPa%. The values of full width at half maximum(FWHM) of crystal plane (211) α show quite in accord with the strain hardening and temper recovering. SEM and APT analyses reflect segregation of elements and precipitation of second phase particles during tempering treatment, which are helpful to understand the change of PSE.

A-36: A Study on Permanent Deformation during Grain Boundary Migration under Applied Stress using Molecular Dynamics Simulation

Simoon Sung, Heung Nam Han, Seoul National University, Korea; Jae hoon Jang, KIMS(Korea Institute of Material Science), Korea

It is known that permanent deformation occurs during the solid-solid phase transformation of the metal even under stress condition lower than the yield stress. This permanent deformation is called transformation plasticity because it is closely related to the phase transformation. To explain the transformation plasticity phenomenon, Greenwood and Johnson argued that the summation of the externally applied stress and the internal stress due to the volume change occurring during phase transformation cause plastic deformation. Han et al. suggested that the choice of energetically favorable variants generates the permanent deformation when a diffusionless transformation, such as martensitic transformation, occurs. However, since the permanent deformation is observed in the recrystallization and grain growth processes without the volume change, the above theories can not explain this permanent deformation phenomenon. Therefore, Han et al. proposed the concept of interface migration-induced plasticity and derived a constitutive equation. In this study, a molecular dynamics simulation for polycrystalline pure iron using Large-scale Atomic / Molecular Massively Parallel Simulator (LAMMPS) was conducted to verify the interface migration-induced plasticity model under various external stress and temperature conditions.

A-37: Cyclic Deformation Behavior and Microstructure Evolution of Hot Rolled DP600 Steel

Xinli Song, Wuhan University of Science and Technology, China

The low cyclic deformation behavior and microstructure development of the hot rolled DP600 steel was

investigated by MTS fatigue test machine and OM and SEM and TEM respectively. The results showed that the microstructure was composed of ferrite and martensite, the volume fraction of martensite was 10% or so. Some dislocation lines were found in the matrix of ferrite of the hot rolled DP600 steel. The cyclic hardening and softening behavior obtained for the sample under the strain amplitude of 0.6% and stress ratio of -1.0. Where the cyclic softening-hardening-softening phenomena was obtained for the samples under the strain amplitude of 0.3% and stress ratio of -0.1 and -1.0 respectively. The dislocation development at the strain amplitude of 0.3% and 0.6% contributed to the cyclic deformation behavior. The number of cycles of the sample with strain amplitude of 0.3% are 34489 which is about 10.4 times that of the sample with strain amplitude of 0.6%. The fatigue cracks were initiated at the interface of martensite and ferrite and the surface and crack propagation along the ferrite grain boundaries and the interface of martensite and ferrite. Some secondary fatigue cracks and fatigue striation were found in the matrix of fatigue fracture samples.

A-38: Effect of Quenching and Tempering on Microstructure and Properties of 15MnNi4Mo Carburized Steel

Renbo Song, Chi Chen, Shengrui Su, Yongjin Wang, Jiakang Li, University of Science and Technology Beijing, China

The effects of quenching temperature, tempering temperature, tempering time and quenching agent on the strength, toughness, hardness and microstructure of 15MnNi4Mo carburized steel were studied by orthogonal experiment. The quenching temperatures were 760℃, 800℃ and 840℃ respectively, and the quenching time was 1h. The quenching agents were air cooling, wind cooling and oil cooling. The tempering temperatures were 140℃, 170℃ and 200℃ respectively, and the tempering times were 1h, 2h and 3h. After heat treatments, the cross section of the sample was observed and the microhardness from the surface to the core was measured. Meanwhile, the standard tensile and impact specimens were cut for mechanical properties test. The results show that, lath martensite can be obtained by oil cooling, and bainite can be obtained by wind cooling and air cooling in the core. Plate martensite can be obtained in the surface by the three methods. Tempering process has a greater impact on the surface hardness and quenching process has a greater impact on strength and toughness. The surface hardness can be effectively improved by controlling the quenching temperature to control the amount of carbides in the surface. Holding at 760℃ for 1h, air cooling to room temperature and tempering at 140℃ for 1h, the highest surface hardness can be obtained, and the value is 702HV.

A-39: Investigations of the Fire Resistant Property of Low Carbon Structural Steels and the Effects of Mo and Nb Addition(1234301)

Hyo-Haeng Jo, Joonoh Moon, Chang-Hoon Lee, Sung-Dae Kim, Seong-Jun Park, Tae-Ho Lee, Korea Institute of Materials Science, Korea

In this study, the effects of Mo and Nb addition on the microstructure and high temperature strength of low carbon fire-resistant steels were investigated. For this purpose, five alloys with different Mo and Nb contents were prepared by vacuum induction melting and hot-rolling process. After hot-rolling, normalizing heat treatments with different cooling modes of air cooling and water quenching were carried out for all alloys.
The microstructures of the base steels were analyzed using scanning electron microscopy (SEM) and transmission electron microscopy (TEM). Air-cooled samples consisted of ferrite and pearlite microstructure, while water-quenched samples consisted of bainite and martensite microstructure with high dislocation density. Tensile tests were performed at room temperature and high temperature of 600℃, and then the fire-resistant property was evaluated quantitatively by the ratio of yield strengths at room temperature (σ room) and 600℃ (σ 600℃), i.e., higher ratio of yield strength (σ 600℃/ σ room) means higher fire-resistant characteristics. In addition, this study also carried out constant load tests. The constant load test is a test method to measure the temperature at which failure occurs during continuous heating with applying constant load. The results of tensile tests and constant load tests indicated that Mo and Nb added bainitic steel had the most excellent fire-resistant property.

A-40: Numerical Simulation Study on Structure of Two-Roll Thin Strip Cast Steel Delivery System

Yong Zhong, AiPing Zhang, Bing Huang, Chongqing University, China.

The twin-roll strip delivery system plays an important role in achieving a stable strip casting process and improving the quality of the strip. In this paper, a two-roll thin strip cast steel delivery system with a roll diameter of 900 mm and a roll width of 1800mm is taken as the research object. Based on ANSYS fluent software, the effects of different delivery system lengths and the arrangement of the edge holes of the delivery system (straight type, staggered type) on the uniformity of the liquid level in the molten pool were studied. The standard deviation of the liquid surface velocity of the molten pool between the two rolls is analyzed under different delivery system schemes; And the comprehensive liquid surface temperature field is compared, and the optimal delivery system length and edge hole arrangement scheme are

obtained .As a result, the length of the delivery system mainly affects the liquid surface temperature and the arrangement of the edge holes of the delivery system can effectively improve the uniformity of the liquid level of the molten pool, which provides a reference for the twin-roll thin strip cast steel.

A-41: The Effect of Retained Austenite on the Wear-Resistance Mechanism of Bainite Ductile Iron at a Varying Impact Load

Renbo Song, Liang Huang, Yu Pei, University of Science and Technology Beijing, China; Ke Guo, University of Science and Technology Liaoning, China / Angang Group Mining Design and Research Institute Co., Ltd, China

In this study, two test bainite ductile iron was produced to investigate the effect of different retained austenite on impact wear resistant. In order to acquire different content and morphologies of retained austenite, the test samples were separately austenitized at 920 and 960˚C for 2 hours, and then quenching in sodium chloride solution. Subsequently, they were all tempered at 200˚C for 2 hours, followed by air cooled, which were named as Material A and Material B, respectively. The volume fraction of phase was carried out using X-ray diffractometer (XRD). As the austenitizing temperature increased from 920 and 960˚C, the volume of retained austenite climbed from 9% to 17% and it grew from fine filmy to bulky. Using an impact abrasive wear testing equipment, the results were obtained and showed that a better wear performance of the sample of Material A rather than another one. The wear mass loss of Material A is less than that of Material B. The wear resistance of material A is about three times of latter under 4 J impact load. The worn surface was characterized and analyzed by XRD and scanning electron microscope (SEM). The experiment results demonstrate that strain induced martensite phase transformation occurred in all samples after impact wear. Meanwhile, the morphology of retained austenite of the bainite ductile iron, has a significant effect on the wear resistance. In high energy impact wear, only the thin filmy retained austenite with highly dispersed is favourable for impact wear, while the bulky and low stability retained austenite will be transformed into brittle martensite, will dramatically reduce the wear resistance of the material. In addition, the wear mechanism of Material A is mainly plough wear and fatigue wear, while that of Material B is plough wear, fatigue wear and deformation fatigue flake.

A-42: Behavior of Hydrogen in High Strength Steel Weldments

Takanori Hino, Toshiaki Manaka, Mitsuharu Todai, National Institute of technology, Niihama College, Japan.

The high strength steels which can reduce the weight of welded components have been desired in the field of construction and industrial machinery. However, the application of high strength steel thick plates for the welding has been limited since they are susceptible to cold-cracking and delayed fracture arisen from hydrogen embrittlement. In order to prevent hydrogen-induced cracking in the high strength steel weldments, preheating and post-weld heat treatment are performed. These processes increase work load of an operator, results in high cost. To achieve high strength steel weldments without heat treatment before and after the welding, we need to reveal the behavior of hydrogen in steels.

In the present study, the behavior of hydrogen in a low carbon martensitic steel with tensile strength of 950MPa class was investigated by means of tensile testing, thermal desorption spectroscopy (TDS) and silver decoration technique. Gas metal arc welding was conducted using the plates in 12mm thick by multi-pass. Microstructural characterization was performed on the welds with optical microscopy and scanning electron microscopy (SEM). The tensile pieces were cut from the weldments at different thickness position to evaluate effect of microstructure on hydrogen embrittlement sensitivity. The specimens were pre-charged with hydrogen by cathodic electrolytic method for 48h. The amount of diffusive hydrogen was measured with TDS from room temperature to 300˚C. Slow strain rate tensile testing at room temperature was performed and the fracture surfaces were examined with SEM. Hydrogen embrittlement sensitivity defined as reduction ratio of elongation to failure with and without hydrogen was compared among the specimens. Silver decoration technique, which can visualize hydrogen as metallic silver on the specimen surface was applied to reveal the distribution of hydrogen with metallographic microstructure. Relationship between hydrogen embrittlement sensitivity and microstructure was discussed based on the hydrogen distribution.

A-43: The Effects of Pre-Deformation on the Tensile Properties of Hot Rolled High Strength Steel

Jia Guo, Shougang Research Institute of Technology, China

The effects of pre-deformation with no less than 3% and the tensile rate within 2mm/min on the tensile properties of hot rolled high strength bainite steels were investigated in this paper. The results indicated that whatever the rate of pre-deformation varying under 2mm/min, yield strength increased apparently with increasing the amount of pre-deformation to 2%, whereas it reduced once the amount of pre-deformation

exceeded 2%. Besides, the tensile strength declined with the amount of pre-deformation rising to 0.5% and ascended with the amount of pre-deformation up to 1%, later, it declined again with the amount of pre-deformation rising from 1% to 3%. Meanwhile, elongation was first increased and then decreased along with enhancing the amount of pre-deformation, and peak elongation came out when the value of pre-deformation equal to 0.5%. The amount of pre-deformation under 2% affected the tensile properties faintly. The yield strength and tensile strength dropped apparently whereas elongation went up when the amount of pre-deformation exceeded 2%. The effects of both the amount and the rate of pre-deformation on tensile properties were due to the changing of tensile curves associated with the retained austenite and dislocation density. The microstructure of the steel was dominated by bainite, besides, about 8% retained austenite was contained. Some amounts of retained austenite were transformed to martensite during the processed of pre-deformation. The results of X-ray declared that the amounts of retained austenite declined about 5% comparing to that was contained in steel without per-deformation. The plasticization of retained austenite has been weakened after pre-deformation, which corresponding to the changes of tensile curves with values of yield strength was improved apparently and the elongation was somewhat restrained. Furthermore, dislocation density appeared the trend of first rising and then decreasing with increasing both the amount and the rate of pre-deformation. The resistance of deformation during tensile test will enhance when the dislocation density was improved, which is in coincidence with the promoting of both yield strength and tensile strength and the declining of elongation. Conversely, the yield strength and tensile strength will be restrained and elongation will be improved when reducing the dislocation density.

A-44: Effect of Deformation in Unrecrystallized Austenite Zone on Microstructure and Properties of 70mm Low Carbon Microalloyed Heavy Plate

Qun Li, Zhanbin Dong, Kaizhao Shen, Shougang Jingtang United Iron and Steel Co., China; Guobiao Di, Shaopo Li, Shougang Research Institute of Technology, China

The effect of three kinds of Austenite Deformation (40%, 50%, 60%) in the unrecrystallized zone on the microstructure and properties of 70mm low carbon microalloyed plate was studied in this paper. By selecting 400mm continuous casting slab and Industrialized experimental rolling was carried out on a wide and heavy plate mill. The results show that with the increase of deformation in the unrecrystallization zone, the microstructure type does not change, quasi-polygonal ferrite and low carbon bainite are dominant in the quarter and the center, but the grains are more uniform and fine, the acicular ferrite content of steel increases and the granular bainite matrix structure becomes finer. The strength of steel reaches 420MPa, but the change is not obvious. The impact toughness at - 20˚c and - 40˚c did not change significantly, but at - 60˚c the impact toughness was greatly improved, and the impact energy reached 200J level. By reasonably designing the deformation in the unrecrystallized zone, the rolling effect can be significantly strengthened and controlled. Combining with a certain continuous cooling process, The ductile-brittle transition temperature of steel can be significantly reduced, the high strength and toughness low carbon microalloyed thick plate can be developed.

A-45: Design of ESR Slags for Remelting Rotor Materials of COST-FB2 by Utilizing Factsage

Leizhen Peng, Zhouhua Jiang, Xin Geng, Xing Li, Boyang Li, Xiaokai Li, Yu Hou, Northestern University, China

COST-FB2 is the promising rotor material for A-USC thermal power plant and the B is the main and key strengthened element to largely inprove the creep property at high temperature. But the B content range is narrow and B is an active element to burn loss during the remelting process, so the proper slag is necessary to melt the qualified ingot during ESR process. This word is mainly focused on the slag design using Factsage 7.2. The basic slag component and proportion is attained but using the phase diagram mould. T hen the optimized slag for remelting COST-FB2 is got via using the equilibrium mould to simulate reaction between slag and molten steel. The physical properties of the optimized slag are also calculated using Factsage. All the results show that: when the MgO addition is 3%, the liquid area is maximum. The wt (CaO)/wt (Al_2O_3) should be less than 1 to get a better stability of melting temperature with slag content varying and relatively low melting temperature. When the additional amounts of B_2O_3 is 0.5%, B can be controlled within the target scope. The calculated melting temperature and the viscosity of the three slags with 0.5%, 1.0%, 1.5% B_2O_3 added into the 55%CaF_2-20%CaO-22%Al_2O_3-3%MgO are all satisfied with the required physical properties of slag for ESR remelting process.

A-46 Effects of Surface Roughness on the Grain Size and Crystallographic Texture of Hot-Dip Galvanized Coatings on Steel Sheets

Gi-Jin Chung, Joo-Youl Huh, Korea University, Korea; Seong-Gyoon Kim, Kunsan National University, Korea; Hyun-Seok Hwang, Sang-Heon Kim, POSCO, Korea

Hot-dip galvanizing (HDG) is widely used as a surface treatment for anti-corrosion of steel sheets. For automotive applications, it is necessary to control the grain or spangle size of the galvanized coating layer below ~100μm for the anti-galling property in the stamping process and the gloss property after painting. Moreover, to avoid the coating layer delamination by low-temperature brittleness, it is essential to reduce the preferred (0001) texture of the galvanized coating layer. In general, the cooling rate and the surface condition of steel sheets are known to be important factors affecting the grain size and texture of the hot-dipped coating layer. Although the surface roughness of steel sheets has long been known to simultaneously reduce both the grain size and the basal plane texture, there seems to be no established explanation for what kinds of surface roughness are effective in reducing the grain size and (0001) texture. In this study, the effects of surface roughness and cooling rate on the grain size and crystallographic texture were systematically studies by coating on drawing quality (DQ) steel sheets with Zn-0.2wt.% Al using a HDG simulator. Prior to galvanizing, the surface roughness of the DQ steel sheets was modified by various methods, such as polishing, indentation, and brushing, and then evaluated using a confocal laser scanning microscope. The grain size and texture of galvanized coating layers were evaluated using optical microscopy and electron back-scattered diffraction.

A-47: Design of Advanced High Strength Steels Using Machine Learning

Yi Zong, Zhigang Yang, Chi Zhang , Hao Chen, Tsinghua University, China

Quenching & Partitioning (Q&P) and Medium Manganese steels (MMS) , which are regarded as the 3rd generation advanced high strength steels (AHSSs) for future automotive applications, have been receiving intensive attention due to their excellent mechanical properties. An efficient design of these AHSSs is therefore of great practical importance. However, up to now, it is still challenging to establish a precise relationship between composition-process-properties by the conventional computational calculations or experiments. Here we employed machine learning (ML) method based on Random forest (RF) algorithms to efficiently establish the composition-processing-properties linkages for Q&P and MMS using more than three hundred experimental datasets. The link between the input features of composition/processing and the mechanical property was analyzed in details. The prediction models were also used to design the new composition and process of Q&P and MMS for target mechanical properties.

A-48: Microstructure Evolution and Rolling Contact Fatigue Characteristics of a Carbide-Free Bainite Wheel-Rail Steel

Baifeng An, Tsinghua University/Central Iron & Steel Research Institute, China; Chi Zhang, Hao Chen, Zhigang Yang, Tsinghua University, China; Zhunli Tan, Beijing Jiaotong University, China; Mingru Zhang, Maanshan Iron & Steel Co., Ltd., China; Yuqing Weng, Tsinghua University/Central Iron & Steel Research Institute/Beijing Jiaotong University, China

The carbide-free bainitic (CFB) microstructure, a mixture of bainitic ferrite（BF） and retained austenite (RA), has been thoroughly investigated by numerous researchers. In this research, the microstructure evolution and Rolling Contact Fatigue Characteristics on the rolling surface of a bainitic wheel-rail steel subjected to rolling-sliding and pure rolling contact loading was systematically investigated. Experimental results showed that the bainite structure of the surface layer in the rolling-sliding sample transformed into nano-structured. The decrease in the stability of film retained austenite reduced the volume fraction of retained austenite. Using the technique that layer-by-layer X-ray diffraction methodology to observe microstructural evolution, accurate quantification of the volume fraction of RA at different depths from the surface. In addition to the highly refined microstructure, the RA transformation under strain to martensite (TRIP effect), contributes to the surface hardness during testing, thus reducing the wear rate. Maintaining good toughness, which prevent brittle cracking. It exhibits excellent rolling contact fatigue resistance. Microhardness depth profiles of the rolling-sliding and pure rolling samples also showed different trends.

B. High Temperature Structural Materials

Symposium Organizers:

Qiang Feng, University of Science and Technology Beijing, China; Shengkai Gong, Beihang University, China; Hyun Uk Hong, Changwon National University, Korea; Damon Kent, University of Sunshine Coast, Australia; Sammy Tin, Illinois Institute of Technology, USA; Hiroyuki Yasuda, Osaka University, Japan; Jun Zhang, Northwestern Polytechnical University, China

August 19-21, 2019
Place: Exhibition Area (3rd Floor)

B-1: Effect of Unique Layered Microstructure on High-Temperature Fatigue Property of TiAl Alloys Fabricated by Electron Beam Melting

Fukuoka Takuma[1], Ryota Kobayashi[1], Jong Yeong Oh[1], Ken Cho[1], Hiroyuki Y. Yasuda[1], Takayoshi Nakano[1], Mitsuharu Todai[2], Ayako Ikeda[3], Minoru Ueda[4], Masao Takeyama[5]
1. Osaka University, Japan
2. Institute of Niihama National College of Technology, Japan
3. National Institute for Material Science, Japan
4. Metal Technology Co., Ltd., Japan
5. Tokyo Institute of Technology, Japan

Recently, TiAl alloys have been used as a heat-resistant material for low-pressure turbine blades of aircraft jet engine due to their excellent high-temperature strength, corrosion resistance and lower density compared to Ni-based superalloys. Electron beam melting (EBM) is one of the suitable manufacturing processes for TiAl alloys because it can fabricate near net shape products based on 3D computer-aided design (CAD) data. In previous study, we found that the cylindrical rods of Ti-48Al-2Cr-2Nb (at.%) alloy fabricated by EBM with appropriate process parameters exhibit unique layered microstructure consisting of equiaxed gamma grains regions (gamma bands) and duplex-like regions perpendicular to building direction. Moreover, the rods fabricated at an angle between building and cylinder direction of 45 deg. (45 deg. rods), exhibit high RT elongation (more than 2%). This high ductility of the rods is attributed to the shear deformation along the deformable gamma bands. In addition, the unique layered microstructure also has beneficial effect on other mechanical properties such as fatigue property.
In the present study, fatigue properties at room and high temperature (1023K) of 45 deg. rods were investigated. As a result, we found that 45 deg. rods without hot isostatic pressing (HIP) treatment exhibit better fatigue strength at both room and high temperature than cast alloys with HIP treatment. This is because the large ductility of the rods suppresses crack initiation. However, some pores can be found on the fracture surface of the specimens fatigued at high temperatures. These results indicate that the small cracks were initiated at the pores, which influences the crack propagation and fatigue failure at high temperature. Therefore, in order to improve fatigue strength at high temperature, 45 deg. rods were subjected to HIP treatment under optimum conditions for maintaining the unique layered microstructure. HIP treatment decreased volume fraction of pores and consequently improved fatigue strength in high-cycle fatigue life region due to inhibition of crack initiations at pores

B-2: Improvement of High-Temperature Strength of Fe-Al-Ni-Ti Alloys by Controlling Lattice Misfit and Thermal Stability of $L2_1$-Ni_2Al(Ti, V) Precipitates Through V Addition

Shinya Maegawa[1], Ken Cho[1], Hiroyuki Y. Yasuda[1]
1. Osaka University, Japan

Recently, extensive efforts have been made to develop ferritic heat-resistant steels for advanced ultra-supercritical steam turbine application. In many cases, these ferritic alloys are strengthened by precipitates. Among them, Fe-Al-Ni-Ti alloys have attracted much attention as candidates for high-temperature application and consist of the bcc-Fe matrix and the $L2_1$-Ni_2AlTi precipitates which show high thermal stability. Based on our recent research, if the dislocations in the bcc matrix shear the $L2_1$ precipitates, these alloys exhibit excellent high-temperature strength because of difference in primary slip systems between the bcc matrix and the $L2_1$ precipitates (<111> slip and <110> slip, respectively). However, Fe-Al-Ni-Ti alloys demonstrate low high-temperature strength because lattice misfit between matrix and precipitates is so large and $L2_1$ precipitates are so coarse that the dislocations in the bcc matrix cannot shear but bypass the precipitates. In the present study, we investigate the effect of V addition to Fe-Al-Ni-Ti alloy on lattice misfit and thermal stability of $L2_1$ precipitates, and the mechanical properties of Fe-Al-Ni-Ti-V alloys through changing the ratio of Ti and V. As a result, V addition to Fe-Al-Ni-Ti alloy changes the $L2_1$ precipitates from Ni_2AlTi to Ni_2Al(Ti, V), resulting in a decrease in misfit strain whereas the thermal stability of the $L2_1$ precipitates is lowered generally. But, by optimizing the ratio of Ti and V, low misfit and high thermal stability can be realized concurrently. In terms of mechanical property, the Fe-Al-Ni-Ti-V alloy furnace-cooled to room temperature exhibit lower high-temperature strength than Fe-Al-Ni-Ti alloy, owing to the existence of coarse $L2_1$-Ni_2Al(Ti, V) precipitates which cannot be cut by the dislocations in the bcc matrix. However, after solutionization followed by aging treatment at 973K, the Fe-Al-Ni-Ti-V alloy exhibit much higher high-temperature strength than that of furnace-cooled alloy. This is because the $L2_1$ precipitates are

dispersed finely through the aging treatment so that the dislocations can shear the precipitates.

B-3: Effect of Al and Cr on Oxidation Behavior of MoSiBTi$_2$C Alloy

Xi Nan[1], Tomotaka Hatakeyama[1], Kyosuke Yoshimi[1]
1. Tohoku University, Japan

Mo–Si–B alloys exhibit great potentials for advanced structural materials because of their high melting point and impressive creep strength at high temperature. Recently, a series of TiC added-Mo-Si-B alloys (MoSiBTiC alloys) have been developed to improve the room-temperature fracture toughness and decrease the density. Nevertheless, the insufficient oxidation resistance of the MoSiBTiC alloys have prevented their practical use. A recent work by Hatakeyama et al. showed that the introduction of Ti_5Si_3 into MoSiBTiC alloy improved the oxidation resistance, but it is still insufficient at 800˚C. As Al and Cr are generally considered as the useful elements for oxidation resistance, a comparative study is carried out to investigate the effects of Al and/or Cr additions on the microstructure of a Ti_5Si_3-containing MoSiBTiC alloy (MoSiBTi$_2$C alloy) and the oxidation behavior at 800 and 1100˚C in this study.
The multiphase alloys with the composition of 36Mo–28Ti-14Si-6C-6B-(10-x)Cr-xAl (x = 0, 4, 6, 10) (at.%) were prepared by arc melting and then annealed at 1600˚C for 10h under Ar atmosphere. Microstructure was characterized by XRD, SEM, EDX and EPMA. Oxidation tests were performed isothermally at 800 and 1100˚C for 12 hours using TGA. Oxidized specimens were also examined using XRD, SEM and EDX.
10at.% Cr added alloy is composed of Moss, Mo_5SiB_2, Ti_5Si_3 and TiC, which is the same as those in the MoSiBTi$_2$C alloy. By the Al additions, Mo_3Si appeared and increased with increasing Al content in the alloys. At 800˚C, more than 6at.% Cr added alloys exhibit enhanced oxidation resistance, but the oxidation resistance of the alloys with higher Al contents were still insufficient. Both Cr and Al added MoSiBTi$_2$C alloys show improved oxidation resistance at 1100˚C. It was found from the obtained results that Al and Cr are effective to improve the high-temperature oxidation resistance of the MoSiBTi$_2$C alloy.

B-4: Microstructure and Oxidation Resistance of Ti, Cr, and Al co-added MoSiBTiC Alloy

Motoyuki Tsukamura[1]
1. Tohoku University, Japan

Recently, a series of TiC added-Mo-Si-B alloys (MoSiBTiC alloys) have been developed to improve the room-temperature fracture toughness and decrease the density. Although MoSiBTiC alloys show superior mechanical properties, the oxidation resistance of MoSiBTiC alloys is poor due to the low Si content. To improve the oxidation resistance, the addition of Al and Cr has been considered. However, Al macroalloying leads to Mo_3Al(A15) formation and macro Cr alloying may make Mo solid solution phase brittle due to solid solution strengthening. To avoid these problem, Ti, Cr, Al co-addition to MoSiBTiC alloys is attempted. In this study, Microstructure and oxidation resistance of Ti, Cr, Al co-added MoSiBTiC alloy is studied.
A series of Ti, Cr, Al co-added MoSiBTiC alloy with the composition of (75-x-y-z)Mo-xCr-yTi-5Si-zAl10C-10B (at.%)($6 \leqslant x \leqslant 10$, $15 \leqslant y \leqslant 25$, z=3, 5) were prepared by arc melting and then annealed at 1600˚C for 24h under Ar atmosphere. Microstructure characterization was performed using XRD, SEM and EDX. Oxidation tests were performed isothermally at 800˚C for 8 to 24 hours using TGA. Oxidized specimens were also examined using XRD, SEM and EDX.
In low Ti, Cr region, both of the 3Al and 5Al alloys are composed of Moss, Mo_5SiB_2, A15 and TiC. However, by choosing a composition in the region of $-1.1 \times Al + 0.16 \times Cr + 0.92Ti > 18.8$(at.%), the constituent phases of the Ti, Cr, and Al co-added MoSiBTiC alloys are Moss, Mo_5SiB_2, and TiC, which are the same as those in MoSiBTiC alloy. Ti, Cr, and Al co-added MoSiBTiC alloys showed negative parabolic oxidation behavior at 800˚C and its oxidation resistance were better than those of Cr added MoSiBTiC alloys and Ti and Cr co-added MoSiBTiC alloys. From the obtained results, it was found that the Ti, Cr, Al co-addition to MoSiBTiC alloys improves. the oxidation resistance at 800˚C without A15 formation.

B-5: Characterization of the Microstructures and the Creep Properties of Inconel 718 Fabricated by Selective Electron Beam Melting with Different Focus Offset

Sunyoung Jun[1], Hyun Uk Hong[1], Soyoung Im[1], Byeongsoo Lee[2], Haejin Lee[2]
1. Changwon National University, Korea
2. Korea Institute of Industrial Technology, Korea

In this study, the selective electron beam melting (SEBM) process was used to fabricate Inconel 718 superalloy as an alternative processing method. The proper SEBM condition ensuring a relative density higher than 99.9% was found in electron beam current range of 24 to 28mA at a scanning speed of 4500mm/s and focus offset of 1mA, from which the sound cylindrical bars with 15mm diameter and 100mm length were obtained. The SEBMed Inconel 718 exhibited a columnar grain microstructure with a strong <100> textures along building direction. In order to investigate the influence of the focus offset, we varied its value from 1 to 50mA. A high focus offset (higher than 30mA) induced a large spot area with insufficient fusion heat energy, leading to low density. The microhardness increased until the focus offset reached 12mA (452HV) and then decreased with the focus offset. It is interesting to observe that γ''

precipitates formed in as-built condition regardless of focus offset, and their size increased with increasing focus offset from 1 to 12mA. The samples built with focus offset of 12mA showed the highest tensile strengths of 1.3GPa and 1.0GPa at room temperature and 650˚C, respectively. The creep rupture time of samples built with focus offsets of 12mA showed 2 time longer than that of conventional forged Inconel 718 under creep condition of 650˚C/700MPa. EBSD analysis on the crept samples indicated that strain accumulation was so significant at the porosities and the high angle grain boundaries. Additionally, the grain boundaries inclined to loading axis were more damaged during creep. From the TEM analysis on the crept samples, lots of matrix dislocations were tangled and stored at the γ'' particles. The γ'' particles were occasionally sheared by matrix dislocations with Burger vector of a/2<110>, without leaving stacking faults behind. The enhanced creep property of SEBMed Inconel 718 superalloy, which was fabricated with focus offset of 12mA, can be attributed to the columnar microstructure with a strong <100> texture and the high density of dislocations resulted from strong interaction with the γ'' particles.

B-6: Refining Effect of Inconel 718 by Hydrogen Plasma Arc Melting

Dosung Lee[1]
1. Chonbuk National University, Korea

Ni based superalloys have characteristics such as high strength and excellent resistance to creep, low-cycle fatigue failure, and oxidation even at elevated temperatures (~650˚C). As these characteristics are heavily influenced by the presence of impurities, sound melting techniques in vacuum are generally used in their production. Typical gaseous impurities are oxygen and nitrogen. As the oxygen concentration increases, the stress-rupture life decreases sharply. The higher the nitrogen concentration in Ni-based superalloys, the more the microporosity in them. Nitrogen also reacts with titanium to form brittle TiN particles in the molten Inconel 718 and replaces carbon in MC and M_6C. Due to this adverse effect, the recommended maximum oxygen and nitrogen concentrations in Ni-based superalloys are 50 and 10ppm respectively.

In the present study, refining effects and behaviors of gas and metallic impurities on Inconel 718 by hydrogen plasma arc melting method were investigated. The solid-type Inconel 718 scraps were used as a raw material. The concentrations of oxygen, nitrogen and metallic impurities in the scraps were analyzed as 173, 53 and 2934ppm, respectively. In the ingot refined by HPAM for 30min the concentration of oxygen and nitrogen was reduced to 40ppm and 3ppm. The metallic impurities were removed to 1215ppm. The refined ingot satisfied the criteria of the recommended Inconel 718 ingot. The hydrogen added to the argon plasma generation gas in HPAM made the plasma arc to be contracted by thermal pinch effect and increase the temperature of the plasma arc. The surface temperature of the molten Inconel 718 is raised, thereby accelerating the generation of metal vapor. In addition, the chemical reactions caused by the activated hydrogen atom acts as the main mechanism of oxygen and nitrogen reduction and enhance the evaporation rate of the impurities.

B-7: Manufacturing High Purity Tantalum Wire from Tantalum Scrap by EBM and Drawing

Jiwon Yu[1,2], Sanghoon Choi[1,2], Jaejin Sim[1], Kyongdeok Seo[1,2], Soongkeon Hyun[2], Kyongtae Park[1]
1. Korea Institute of Industrial Technology, Korea
2. In-Ha University, Korea

A study has been carried out on recycling of tantalum scrap by electron beam melting(EBM) and drawing techniques. The purity of recycled tantalum metal was compared to that of scrap. The purity of scrap, which was 3N, was increased to more than 5N by recycling process including the EBM. These high-purity tantalum metal can be used in other applications such as sputtering targets and spring-type electrode material of lithography lamp for semiconductor processing. In addition, hardness and oxygen concentration of recycled tantalum metal were 149HV and less than 300ppm, respectively. The above properties show similar or better grades than commercial products or virgin metal. The EBM process can remove volatile elements using the difference in vapor pressure of various impurities at high temperature. Actually, these facts are supported by easy removal of impurities such as Fe, Ni, Si, Al on the scrap during EBM process. Subsequently, drawing of the recycled tantalum metal was conducted by drawing dies. Owing to continuous drawing, the diameter of the tantalum wire decreased to 0.5mm from 10mm and the hardness of it was 232.12HV. The tantalum wire having these properties is sufficient for use as an electrode material of lithography lamp. Not only this, the processes used in this study is properly techniques as recycling method of refractory metal and it can also be utilized for recycling of various industrial wastes related on refractory metal. In conclusion, our study contains total processing from refining of raw material to recycling of scrap and it is possible that the properties of recycled metal are higher than that of original metal or commercial products. In other words, it can be described as upcycling process that was performed by EBM and drawing.

B-8: Effect of Water Vapor and Temperature on the Oxidation of High-Temperature Structural Materials Sanicro 25, HR6W, 617B and 282

Zhiyuan Liang[1], Miao Yu[1], Yong Gui[1], Qinxin Zhao[1]
1. Xi'an Jiaotong University, China

It's well known that increasing the steam parameter of boilers is the most effective method to improve the efficiency of supercritical power plants and decrease industrial pollutants. Reliable structural steels and alloys are needed against the higher steam temperature and pressure. Conventional austenitic heat-resistant steels are not suitable due to the lower high-temperature strength and corrosion resistance. Several commercial high-strength steels and alloys were developed to meet this rigorous demand. However, systematic study of the oxidation behaviors of these materials is lacked. The aim of this paper is to investigate the oxidation behaviors of Sanicro 25, 617B, 282 and HR6W at 750˚C and 810˚C and to reveal the effect of water vapor and temperature on their oxidation behaviors. Oxidation experiments were conducted at 750˚C and 810˚C for 250h, 500h, 750h and 1000h under laboratory air and air/steam conditions. X-ray diffraction and scanning electric microcopy were employed to characterize the oxidation products. Results show that the oxidation kinetics of investigated materials followed a parabolic oxidation law. Oxidation products of investigated materials in air were mainly Cr_2O_3, which provides the oxidation resistance and hinders the quick oxidation at higher temperatures. Internal oxidation and prior oxidation at the grain boundaries were observed at Ni-base alloys 617B and 282, as shown in Figure 1 and Figure 2. In the air/steam environment, investigated materials suffered more server oxidation than that in air at 810˚C, as shown in Figure 3. Fe oxides were found on Sanicro 25 and HR6W, which was attributed to the breakaway of Cr-rich oxide scale. The depths of internal oxidation and prior oxidation of 617B and 282 were much higher in the air/steam environment. This result could be explained by the evaporation of Cr_2O_3 under air/steam condition. In last, the most excellent oxidation resistance of investigated materials was 617B.

B-9: Influence of Heat Treatment on Microstructure and Stress Rupture Property of a Weldable Superalloy K439B

Jingyang Chen[1], Leilei Zhang[1,2], Mingjun Zhang[1], Qing Yang[2], Xin Tang[1], Chengbo Xiao[1]
1. Beijing Institute of Aeronautical Materials, China
2. Xi'an University of Technology, China

The main superalloy used to prepare the large-scale casting component in both aero and industrial gas turbines is K4169 in China at present, which temperature capability is only about 650˚C. With the development of advanced turbine, K4169 could not meet the need of the increasing turbine inlet temperature. Recently, K439B alloy was developed by Beijing Institute of Aeronautical Materials (BIAM) in order to meet this demand. K439B is a hot corrosion resistant superalloy with temperature capability up to about 850˚C. In addition, K439B has good weldability, castability and ductility, which is suitable for the application in both aero and industrial gas turbines. These applications include large IGT vane segments, low pressure (LP) and pressure turbine (PT) integral nozzles (vane rings), high temperature capable combustor and turbine casings, transition ducts, heat shields and burner nozzles, as well as turbine containment ring components.
In this study, the microstructure and stress rupture property of K439B with different heat treatments were investigated by using stereo microscope, optical microscopy (OM), scanning electron microscopy (SEM), transmission electron microscopy (TEM) and stress rupture testing. The results indicated that the average grain size of K439B was 0.5mm. The as-cast microstructure consisted of γ matrix and γ' precipitate in the dendrite core and interdendritic region. Meanwhile, γ/γ' eutectic and MC carbides was also observed in the interdendritic region and at the grain boundary. The average stress rupture life of K439B after conventional and modified heat treatments was 35.4h and 109.1h, respectively. The current results suggested that the stress rupture life increased significantly after modified heat treatment. And the average stress rupture life after modified heat treatment was about 3.1 times that after conventional heat treatment. The relationship among heat treatment parameters, microstructure and stress rupture property of K439B will also be discussed in this study.

B-10: Formation and Widening Mechanisms of Envelope Structure and Its Effect on Creep Behavior of a Multiphase Ni3Al-Based Intermetallic Alloy

Jing Wu[1], Yongchang Liu[1], Chong Li[1], Yuting Wu[1], Zongqing Ma[1], Haipeng Wang[2]
1. Tianjin University, China
2. Northwestern Polytechnical University, China

In present work, the envelope structure (about 1.1μm in width, and 3vol.% of volume fraction) in a multiphase Ni_3Al-based intermetallic alloy is characterized in detail, and the formation and widening mechanisms of the envelope structure during solidification and aging treatment and its effect on creep behaviors of alloy are also investigated by 800˚C/1000h long-term aging treatment. Results show that the envelope structure located between the $\gamma'+\gamma$ dendrite and the interdendritic β phase is a γ'-Ni_3Al phase with ordered fcc ($L1_2$) structure. The γ'-envelope phase exhibits the orientation relationship of [101] γ'-envelope//[01-1] γ-matrix with the γ-matrix phase in the $\gamma'+\gamma$ dendrite, and the orientation relationship between the γ'-envelope

and the interdendritic β phase can be described as non-coherent, which is one of the weakest interfaces, except for the grain boundaries in alloy. The γ'-envelope structure is mainly formed during solidification near 1190˚C , before the precipitation of primary γ' phase and after the formation of the interdendritic β phase and in alloy. The enrichment of Ni in the residual liquidoid after the precipitation of interdendritic β phase is the primary formation mechanism of the γ'-envelope during solidification. The widening mechanism of γ'-envelope during long-term aging treatment is mainly due to the diffusion of Ni, Al, Hf and Mo atoms at the phase interfaces of γ'-envelope and the γ'+γ dendrite and interdendritic β phase under thermal activations. Besides, instead of one side, the γ'-envelope can extend to both sides of γ'+γ dendrite and interdendritic β phase at the same rate of widening, and the corresponding phase tranformation can be simply described as: β (NiAl) + γ (Ni) → γ' (Ni_3Al). The widening of γ'-envelope has double-edged effects on creep properties of alloy. On the one hand, it can result in the decrease of the volume fraction of β phase and the increase of the volume fraction of γ' phase, which is beneficial to improve the high temperature properties of alloy. On the other hand, it may lead to the deterioration of the weldability and thermoplasticity of alloy by decreasing of the volume fraction of β phase, and the deterioration of the creep properties of alloy by gradually surrounding the carbides, located at the interfaces, and subsequently cause the initiation of microcracks or holes at the sourrounded carbides in the widened γ'-envelope during deformation, thus leading to creep fracture.

B-11: Microstructural Evolution of a Co-Al-W-Base Single Crystal Superalloy During Creep at 900℃ - 420MPa

Haijing Zhou[1,2], Longfei Li[2], Stoichko Antonov[2], Qiang Feng[2,3]
1. Central Iron & Steel Research Institute, China
2. University of Science and Technology Beijing, China
3. Beijing Advanced Innovation Center for Materials Genome Engineering, China

The discovery of the γ'-$Co_3(Al,W)$ phase with $L1_2$ structure in the Co-Al-W ternary system by Sato et al. enabled the design of high temperature capability Co-base superalloys. Subsequently, creep experiments performed at 900~1000˚C on simple-composition single-crystal Co-base superalloys have demonstrated a creep resistance comparable to 1st generation Ni-base superalloys. As the solidus and liquidus of Co-base alloys are about ~100~150˚C higher than those of advanced Ni-base single-crystal superalloys, Co-based superalloys have the potential to surpass Ni-based superalloys in terms of high temperature capability. Moreover, the limited segregation of alloying elements in the dendritic structure in Co-base single-crystal alloys, as compared to Ni-base single-crystal alloys, results in a higher resistance to the formation of convective instabilities and freckles, which is beneficial for the production of large scale blades and turbine components.

In order to increase the γ' solvus temperature of Co-Al-W-base alloys, which is highly responsible for the creep resistance at high temperature in γ-γ' two-phase alloys, various alloying additions have been investigated. Both the γ' solvus temperature and creep properties can be raised by additions of Ta and Ti. Moreover, the synergistic effect of Ta and Ti additions further improved the γ-γ' two-phase microstructural stability of Co-Al-W-base alloys, and the creep resistance of Co-Al-W-Ta-Ti alloys exceeds that of previously reported Co-Al-W-base alloys.

Recently, the deformation mechanisms in crept Co- and CoNi-base alloys have been investigated, and the analyses reveal a high density of stacking faults (SFs) extending across γ' precipitates. This is considerably different to Ni-base superalloys, where a second coupled partial dislocation follows the leading partial and reestablishes the order. Unfortunately, investigations on the substructural evolution of Co-base superalloys during creep at high temperature are still rare.

In the current research, the creep behavior of a Co-Al-W-Ta-Ti alloy was systematically investigated at 900˚C - 420MPa. Several creep tests were interrupted after appropriate creep strains, which were selected according to the divisions of creep regions. The observation of microstructural and substructural evolution were performed at each creep region to understand the creep deformation mechanism.

Four distinct creep regions were exhibited in the creep strain rate versus time curve. The activation of run and stop mechanism appeared to contribute to the sharp decrease of strain rate in the initial region. The formation of enclosed γ channels, the γ/γ' interfacial dislocation networks and the formation of Lomer-Cottrell locks in γ' precipitates were responsible for the steady-state region. The formation of directionally coarsening γ' precipitates and the extension of stacking faults across multiple γ' precipitates resulted in the increase of strain rate before the steady-state region, while the initiation and propagation of microcracks appeared to contribute to the increase of strain rate after the steady-state region.

B-12: Effect of Initial Microstructure on the Hot Deformation Behavior of a Ni_3Al-Based Alloy

Yuting Wu[1], Yongchang Liu[1], Chong Li[1], Jing Wu[1]
1.Tianjin University, China

With the development of aerospace technology, conventional high-temperature alloys such as Fe-based, Ni-based and Co-based alloys cannot meet

the stringent performance requirements of the high-temperature components. Ni_3Al-based alloys have gotten considerable attention in recent years for its excellent properties at elevated temperature. In order to investigate the effect of initial microstructure on the hot deformation behavior of a Ni_3Al-based alloy, the flow behavior, microstructure evolution and critical conditions of dynamic recrystallization during hot deformation of the studied alloy with two different microstructures were discussed. The isothermal compression tests were performed at 1100℃ and 1200℃ with strain rate of $0.01s^{-1}$, $0.1s^{-1}$ and $1s^{-1}$. The results show that the hot deformation behavior of the Ni_3Al-based alloy is sensitive to the initial microstructure, particularly under low deformation temperature and high strain rate. During the hot compression, the dynamic recrystallization occurs in specimens with different initial microstructure at all the tested conditions. The stress-strain curves signified that the peak stress for the alloy with coarse γ' precipitates was higher than that for the alloy with fine γ' precipitates at a given deformation temperature and strain rate. In addition, based on the experimental data, the critical conditions for the occurrence of dynamic recrystallization were determined. It is found that the critical strain is affected by deformation temperature, strain rate and initial microstructure. The critical strain of dynamic recrystallization significantly decreases with the increase of strain rate or decrease of deformation temperature. Moreover, for different initial microstructure, the critical stress and strain for the alloy with coarse γ' precipitates were higher than that for the alloy with fine γ' precipitates. When the deformation temperature is high enough, the dissolution of coarse γ' precipitates easily occurs, which leads to that the effect of initial microstructure on hot deformation behavior of the Ni_3Al-based alloy is weakened.

B-13: Effect of Dual Aging Treatments on Phase Transformation and Microstructure in a Pre-Deformed Ti_2AlNb-Based Alloy Containing O + β/B2 Structures

Hongyu Zhang[1], Yongchang Liu[1]
1.Tianjin University, China

Compared with the conventional Ti_3Al (α_2)-based and TiAl (γ)-based alloys, the Ti_2AlNb-based alloys exhibit higher specific strength, excellent oxidation resistance, creep resistance and fracture toughness, hence it can be considered as a potential high-temperature structural application for advanced aerospace. According to the lattice structure, the Ti_2AlNb-based alloy typically are comprised of O (cm symmetry Ti_2AlNb) phase, body-centered cubic (bcc) structured B2 (ordered) or β (disordered) phase, and hexagonal close-packed (hcp) α_2 (Ti_3Al) phase. The O phase possesses excellent creep resistance in the temperature range between 650℃ to 750℃ when compared to the traditional α_2 phase and matrix β/B2 phase. The effect of dual aging treatment on phase morphology, composition, and microstructure evolution of a pre-deformed Ti_2AlNb-based alloy were investigated in this study. The 1040℃-pre-deformed alloys were dual aged at different temperature in O + β/B2 region followed by 750℃-aged treatment. The experimental results show that coarse O lath and lamellar O + β/B2 were formed when the aging temperature is lower than 950℃ while globular O appeared when aging temperature is higher than 950℃. Widmanstätten O + β/B2 laths were obtained after secondary aging treatment at 750℃ when the first aging temperature is higher than 910℃. Complete lamellar O + β/B2 precipitation and coarse O lath, in particular, were obtained in the 910℃ and 750℃ dual aged alloy with no Widmanstätten O + β/B2 laths appeared. The phase content is closely related to the aging temperature. When the 970℃-aged alloy put into the secondary aging at 750℃, coarse O laths which were fragmented or partially spheroidized and globular O during 970℃-aged process were dissolved and the Widmanstätten O began to precipitate inside. The results will be guidance for a better understanding for the microstructure control of Ti_2AlNb alloys and optimizing their heat treatment routes.

B-14: Microstructural Feature and Evolution of Rapidly Solidified Ni_3Al-Based Superalloys

Yefan Li[1], Chong Li[1], Jing Wu[1], Huijun Li[1], Yongchang Liu[1], Haipeng Wang[2]
1. Tianjin University, China
2. Northwestern Polytechnical University, China

The effect of solidification cooling rate on the morphological evolution, elements segregation and interface characteristic in a Ni_3Al-based superalloy was discussed. The original as cast Ni_3Al-based superalloy used in this work was produced by vacuum induction melting (VIM) and electro slag remelting (ESR) techniques. The microstructure consists of primary dendrites and interdendritic regions. As to the as cast superalloy, cuboidal γ' precipitates are distributed with the mean size of 0.5μm and separated by γ phase channels filled with nanometer γ' particles. The γ and γ' phase present a typical complete coherent orientation relationship. Cr and Fe elements are segregated into γ phases while Ni and Al are segregated into γ' phase in the areas of dendritic cores. The Ni_3Al based superalloy was rapidly solidified in the form of droplets with varying diameters. The cooling rate (Rc) is a function of diameter (D) of droplet. With the decrease of droplet sizes (increase of the cooling rates), the volume fraction of interdendritic structure increases from 21.31% (D=1400μm, $Rc=3.6\times10^2Ks^{-1}$) to 36.31% (D=270μm, $Rc=2.3\times10^3Ks^{-1}$). Moreover, in dendritic cores, the feature of γ' precipitate is also obviously changed with increasing cooling rate. The bimodal size distributions of γ' precipitates disappear, which is normal in as cast

alloys. Instead, it can be seen that the γ' phase with size about 30~50nm presents unimodal distribution in the γ phase in the droplets due to high nucleation burst. For original as cast alloy, there are some lattice distortions without dislocation in the area of γ/γ' interface, however, in the case of rapid solidification condition, edge dislocations with Burgers vector of a/3<111>, which can relax the high interface energy formed during rapid solidification process, were observed on (111) planes, and the result shows that the increase of solidification rate leads to the expansion of lattice misfit between γ and γ' phases.

B-15: Hot Corrosion Behaviours of a γ'-Strengthened Co-Al-W-Mo-Ta-B Alloy with Additions of Ce at 800℃

Jiangbo Sha[1], Fei Zhong[1,2], Yan Li[1]
1. Beihang University, China
2. Hubei Engineering University, China

Hot corrosion resistance, corrosion scale evolution and failure mechanism of Ce doped Co-9Al-4.5W-4.5Mo-2Ta-0.02B alloy (doped 0.01, 0.05, 0.1 and 0.2at.% Ce, referred to as 0.01Ce, 0.05Ce, 0.1Ce and 0.2Ce alloys hereafter, respectively) exposed at 800℃ in corrosion solution of 75%Na_2SO_4+25%NaCl were investigated. The weight measurements of each specimen were conducted at each oxidation time to obtain the corrosion kinetics curve and the corrosion scale at different corrosion time was observed using SEM. Aged at 850℃ for 50h, the 0.01Ce and 0.05Ce alloys consisted of a Co solid-solution matrix (γ-CoSS) and nano-scale cuboidal γ'-$Co_3(Al, W)$ precipitates, while for the 0.1Ce and 0.2Ce alloys, k-$Co_3(W, Mo)$ precipitates and γ'-depleted zone were present at the grain boundaries in addition to the γ/γ' microstructure in the grain interior. It was found the oxidation kinetics curves of the four Ce doped alloys exhibited a parabolic time dependency, and with an increasing nominal Ce content from 0.01 to 0.2at.%, the weight gain of the Co-9Al-4.5W-4.5Mo-2Ta-0.02B alloy significantly decreased, approximately from 45mg•cm^{-2} to 9.8mg•cm^{-2}, when exposed at 800℃ for 50h. During whole corrosion process, a three-layer corrosion scale composed of an outer Co_3O_4 + CoO layer, an intermediate layer containing oxides of $CoAlO_4$, $CoWO_4$, $CoSO_4$ and Al_2O_3, and an inner layer of sulfide plus γ/Co_3W zone adhering to the γ/γ' substrate gradually formed. Heavy spallation of the corrosion scale occurred in the 0.01Ce, 0.05Ce and 0.1Ce alloys, whereas no spallation was present in the 0.2Ce alloy. The excellent corrosion resistance of the 0.2Ce alloy was mainly attributed to the thickest Al_2O_3 plus spinel oxide ($CoAlO_4$, $CoWO_4$ and $CoSO_4$) layer during entire corrosion process. Due to un-formation of the continuous Al_2O_3 layer, four alloys have insufficient corrosion resistance, which is needed to be improved further.

B-16: Effect of Boron Addition on Solidification Behavior and Segregation of a Directionally Solidified Nickel-Base Superalloy

Baoping Wu[1], Jiantao Wu[1], Juntao Li[1], Jianxin Dong[2]
1. Central Iron and Steel Research Institute, China
2. University of Science and Technology Beijing, China

Historically boron is an element employed to enhance the grain boundary strength of the Ni-based superalloys. In the past decades, the effects of the boron addition on the microstructure and properties of Ni-base alloys, such as conventional casting and DS superalloys, have been discussed in many papers. The general results indicate that boron segregation at grain boundaries increases cohesion or decreases grain boundary diffusivity, thereby increasing the stress rupture property of Ni-base alloy. In addition, Boron addition also influences the solidification behavior of alloy. Despite many investigations indicated that liquidus and solidus temperature would decreased with the addition of boron to the directionally solidified superalloys, previous work often concentrated on the synergistic effect of boron and other minor elements such as zirconium and carbon. Moreover, Boron addition would lead to complex solidification path, partition of elements and precipitated phases in the solidified alloys, which would influence the mechanical properties of directionally solidified nickel-base superalloy. Studies about effect of boron on solidification behavior and segregation of directionally solidified nickel-base superalloys are lacking up to now. The aim of the present work is therefore to examine the effect of boron additions alone on solidification behavior and segregation of a directionally solidified nickel-base superalloy.

The results indicate that boron addition decreases the liquidus and solidus temperature, and increases the freezing range of alloy. Furthermore, the solidification rate of alloy changes with the different content of boron, which will also alter the segregation of the solute elements. The segregation of the solute elements results in the thermal solutal convection which may contribute to the homogenization of solution elements. At the beginning of the solidification, the solidification rate of alloy decreases with the addition of boron ranging from 0.0007% to 0.024%, which will results in the temperature of dendrite contact decreasing. Then the segregation of the solute elements will have enough time to be homogenized. Consequently, the segregation degrees of W, Ti and Nb decrease with the addition of boron ranging from 0.0007% to 0.024%. However, when the content of boron reaches to 0.033%, the solidification rate of alloy increases, and then the temperature of dendrite contact increases too, which will suppress the thermal solutal convection. Therefore, the segregation degrees of W, Ti and Nb increase.

This paper reports the fundamental underlying relationships between solidification behavior and

segregation. Such knowledge will be significant helpful to understand the effect of boron addition on solidification behavior, segregation and mechanical properties of directionally solidified nickel-base superalloy.

B-17: Influence of Cr on the High-Temperature Oxidation Behavior of New γ-γ' Co-Ni-Base Superalloys

Yingxin Zhu[1], Hongyao Yu[2,3], Yongchang Liu[1], Zhongnan Bi[2,3]
1. Tianjin University, China
2. Central Iron and Steel Research Institute, China
3. Beijing Key Laboratory of Advanced High Temperature Materials, China

Since the discovery of the γ' phase in the Co-Al-W system in 2006, the γ'-strengthened Co-Ni-base superalloys have been intensively studied. A dispersion of γ'-phase precipitated in the matrix provides them with a yield strength exceeding in some cases that of their nickel counterparts above 900℃. The higher melting temperature of pure cobalt also opens up the possibility of pushing their upper operating temperature above the temperature of the nickel-base superalloys. Co-Ni-base superalloys have the potential for high temperature application, i.e. gas turbines and aircraft engines. Since alloying elements have different effects on the properties, the current research focuses on the influence of the Cr element on oxidation resistance performance of the new type γ-γ' Co-Al-W-Ni-Cr-Ti superalloys. Specimens were tested in high temperature exposition (12, 48 and 100h) in air environment at 900℃. The oxidized surfaces have been analyzed by scanning electron microscope (SEM), energy dispersive x-ray spectroscopy (EDX) and x-ray diffraction (XRD). The results indicated that the microstructure of oxidized surfaces of the Co-Ni based superalloys at 900℃ can be divided into three layers. The outer layer consists mainly of CoO, and the inner layer was identified as Al_2O_3. The middle layer is Cr oxides. Moreover, the oxidation performances of the Co-Ni base superalloys can be roughly divided into three stages at 900℃, i.e. a transient stage, a steady stage, and an unsteady stage. Thus, Cr has a great influence on the oxidation performance of Co-Ni base superalloys.

B-18: Microstructure Evolutions of NiCrAlY Coatings on DZ125 Superalloy Sheet under Effect of Thermal and Thermal-Stress Coupling at 950℃

Dongxu Nie[1], Weiwei Zheng[1], Qiang Feng[1], Wei Wang[2], Longfei Li[1]
1. University of Science and Technology Beijing, China
2. AECC Shenyang Engine Design Institute, China

NiCrAlY coating has good high temperature oxidation resistance and high temperature corrosion resistance, and has little influence on the mechanical properties of the base alloy. It is not only a common bonding layer of thermal barrier coating, but also often used as a high temperature protective coating. At present, the research on NiCrAlY coating mainly focuses on the oxidation property and the element diffusion behavior, and there are few reports on the microstructure degradation during the service of NiCrAlY coating.
In this paper, microstructure evolutions of NiCrAlY coatings on DZ125 superalloy sheets were investigated systematically. The relationship between service condition and microstructure degradations was established by the experimental simulation including thermal simulation and thermal-stress coupling simulation. The results showed that microstructures in NiCrAlY coating and the inter diffusion layer had almost the same degradation process during the thermal simulation at 950℃ and thermal-stress coupling simulation at 950℃/101MPa、950℃/135MPa. With the increase of thermal exposure and thermal-stress coupling time, the thickness of inter diffusion layer increased, the volume fraction of α-Cr phase decreased and disappeared quickly, the volume fraction of γ' phase decreased gradually till the formation of γ single phase zone at the upper half of the coating and the inter-diffusion layer. This research laid the foundation for the assessment of microstructure degradation during the service of NiCrAlY coating

B-19: Alloying Effects on the Microstructure and Oxidation Resistance of Multicomponent γ'-Strengthened Wrought Cobalt-Based Superalloys

Xiaoli Zhuang[1], Longfei Li[1], Qiang Feng[1]
1.University of Science and Technology Beijing, China

Since some unique properties, γ'-strengthened Cobalt-based superalloys have attracted much attention since their discovery in 2006. However, most researches are primarily focused on Cobalt-based single crystal superalloys with low components, i.e. ternary to quinary alloys. In this study, a set of multiple-component γ'-strengthened Co-Al-W-Ti-Ta-Ni-Cr (at%) wrought superalloys with different contents of W, Ti, Ta as well as with or without the addition of Mo, were designed in order to investigate the effects of these alloying elements on the microstructure after aging at 850℃ for 50h to 300h and the oxidation resistance at 800℃ to 1000℃. All investigated alloys showed typical γ/γ' two-phase microstructure at 850℃. However, a higher content of W or a higher Ti/W ratio would decrease the microstructural stability and promoted the precipitation of μ and β phases, respectively. The increase of Ti content or Ti/W ratio could improve the cubic degree of γ' phase, but resulted in a faster coarsening rate of γ' phase. While, The increase of W content or the addition of Mo could decrease the cubic degree of γ' phase and had limited effect on the coarsening rate of γ' phase. In comparison with that after aging at 850℃ for 50h, the Vickers hardness of each alloy was higher after aging at 850℃ for 300h, due to higher fraction of γ'

phase. The increase of W content or the addition of Mo could improve the Vickers hardness and the increase of Ti content or Ti/W ratio would decrease the Vickers hardness. The oxidation resistances of all studied alloys are comparable to that of U720Li at 800℃, and well than it at 900℃ and 1000℃. The current study is helpful to futher design and optimize multicomponent γ'-strengthened wrought Cobalt-based superalloys.

B-20: The Characteristics and High Temperature Annealing Behavior of As-Cast GH5605 Cobalt-Base Superalloy

Jiang He[1], Jianxin Dong[1], Chao Liu[1], Yongji Niu[2]
1. University of Science and Technology Beijing, China
2. Beijing Beiye Functional Materials Corporation, China

The cobalt-base superalloy is widely used in high temperature environment in consideration of the good high temperature stability and mechanical property. GH5605 is a solution strengthened Co-Cr-Ni base wrought superalloy. Though there have been a number of investigations on similar superalloys, however, there is little report on the characteristics of as-cast GH5605 ingot, including the element segregation behavior, microstructure characteristics, precipitation distribution, high temperature annealing behavior and so on. In present work, GH5605 ingot with a diameter of 243mm was prepared by vacuum induction melting (VIM) and electroslag remelting (ESR) was used for investigation. Multiple methods, such as thermo-dynamic calculation, microstructure observation and differential scanning calorimeter (DSC) test, were carried out to study the microstructure characteristics of as-cast GH5605 ingot. The element segregation degree of as-cast GH5605 is not that apparent, and the element segregation index is in the range of 0.9~1.4. The major segregation elements are W and Cr. $M_{23}C_6$ carbide and eutectic phase are the primary precipitates in the as-cast GH5605 ingot. Microstructure and phase evolution during high temperature annealing was also investigated. Dendrites and element segregation can be eliminated after 1120℃ high temperature annealing for 8h. The optimized high temperature annealing treatment is determined by microstructure observation and isothermal hot compression test.

B-21: Influence of Composition Homogeneity on Residual Stress of Cast & Wrought Superalloy GH4169 Parts

Yong Zhang[1], Kang Wei[1], Wei Cao[1], Guoqing Zhang[1]
1. Beijing Institute of Aeronautical Materials, AECC, China

A study has been performed to investigate the effect of composition homogeneity on residual stress of large scale Cast & Wrought Superalloy GH4169 billet was researched in the paper. Two type methods machining chemical composition specimens were designed. In virtue of sample variance analysis to detected data, the partial segregation of large scale GH4169 billets was analyzed comparatively with different melting method, VIM (Vacuum Induction Melting) +VAR (Vacuum Arc Remelting) and VIM+ ESR(Electro Slag Remelting)+ VAR. The result indicated that tri-melting process is better than duplex melting process for reducing composition segregation. Also, comparative research work was conducted about chemical composition, macrostructure, microstructure, δ phase and main mechanical properties of cast & wrought superalloy GH4169 (Inconel718) manufactured by tri-melting(VIM+ ESR+VAR) at home and abroad. Based on the design method, composition homogeneousness of GH4169 and American Inconel 718 billet was measured. X-ray residual stress instrument was introduced to investigate the residual stress in billet and subsequently forged disk of domestic and international GH4169. The results show that chemical composition, purity, grain size, δ phase control and mechanical property of domestic large diameter GH4169 billet has approached Inconel718 standards. However, there is still margin in partial segregation of composition, occurrence probability of metallurgical defects, control of residual stress, stability of batches between home and abroad. Smelting process and material standard need further improvement. Compared with foreign materials, the residual stress of disk forged by domestic GH4169 billet is higher, directly leading to the deformation of GH4169 disk used in aero engines, the basic cause of which is the partial segregation of composition within the material resulted from smelting process.

B-22: Microstructural Evolution of a Nickel-Base Single Crystal Superalloy during Long-Term Aging at 980℃ for 10000h

Fan Lu[1], Yunsong Zhao[2], Siliang He[1], Jian Zhang[2], Longfei Li[1], Qiang Feng[1]
1. University of Science and Technology Beijing, China
2. Beijing Institute of Aeronautical Materials, China

Long-term microstructural stability, including the degeneration of γ' phase and the formation of TCP precipitates, of nickel-base single crystal superalloys is very important to the long-term service safety of aeroengine turbine blades. However, limited investigations about the microstructural stability of nickel-base single crystal superalloys over thousands of hours have been reported. In this study, the microstructural evolution of a second generation nickel-base single crystal superalloy during long-term aging at 980℃ for 500 to 10000h was investigated, using multi-scale characterization, including microstructure, sub-microstructure, lattice misfit and Vickers hardness. Quantitative microstrucutural characterization was

conducted in terms of volume fraction of γ' and TCP phase, γ' size and interface dislocation network spacing. With the increase of aging time, the initial cuboidal γ' phase began to grow in size primarily and lost the cuboidal morphology after 1000h. After then, the γ' phase rafted gradually in longitudinal sections, which may be attributed to the initial high lattice misfit of γ/γ' phases. A small number of TCP phases participated in dendrite core after aging for 5000h due to the enrichment of refractory elements, i.e. Re and W. While, the interfacial dislocation network which was formed to release the misfit stress between γ/γ' phases became intensive gradually with the increase of aging time and the lattice misfit tended to be zero simultaneously. Vickers hardness tests indicated that the mechanical properties decreased gradually and tend to be stable with the increase of aging time. The relationship between aging time, micro/sub-microstructure, γ/γ' lattice misfit and Vickers hardness of this nickel-base single crystal superalloy during long-term aging was established, which provides a reference for the design and application of second generation nickel-based single crystal superalloys in aeroengine turbine blades for long-term service.

B-23: Effect of Heat Treatment on the Microstructure and Mechanical Properties of a Co-Based Superalloy Strip

Yongji Niu[1]
1. Beijing Beiye Functional Materials Corporation, China

In this paper, the effect of heat treatment on the microstructure and mechanical properties of a deformed Co-Cr-Ni-W superalloy strip was investigated. The cold-rolled superalloy was annealed at different temperatures 500～1240℃ for 10min. It was found that hardness increased in the range temperature 500～800℃, the annealing had ageing strengthening effect, this was due to the fcc~hcp transformation. As the annealing temperature is higher than 800℃, the hardness decreased with the increase of the annealing temperature. There were four inflection points in the influence of annealing temperature on the hardness of the alloy, which were about 800℃, 900℃, 1050℃and 1150℃. From 800℃ to 900℃, the hardness of the alloy decreased rapidly, recovery and recrystallization was initial. From 900℃ to 1050℃, the hardness of the alloy decreased slower, recrystallization was finished and grain growth slowly. The temperature reaches 1050℃ to 1150℃, the hardness curve decreased rapidly, carbides dissolution and grain growth was considerable. Above 1150℃, the hardness tended to be stable, the grain growth of the alloy was obvious, and more annealing twins were also formed. As the annealing temperature increased, the tensile strength decreased and the elongation increased.

The research results can provide the basis for the performance control of GH605 alloy.

B-24: Synergistic Strengthening Symphony of Nanograins, Nanophases and Nanotwins

Gan Bin[1], Jun Zhang[1], Lin Liu[1], Hengzhi Fu[1]
1. Northwestern Polytechnical University, China

Recently, equiatomic CrCoNi medium entropy alloys have been found to possess both excellent cryogenic strength and ductility without suffering from the detrimental ductile-to-brittle transition. This catalyzed a global interest in delineating the underlying deformation mechanisms operated in cryogenic temperatures, and invigorated teams of people around the world to exploit the full potential of strengthening residing in this new alloy system. CrCoNi alloys have a very low stacking fault energy (SFE) and a high propensity for forming nanotwins. Considering that nanotwins can not only impede dislocation motion but are also able to accommodate plastic deformation, the population of nanotwins in the microstructure may be a superior strategy for achieving high strength and ductility in these alloys. The distribution of obstacles can also have a significant influence on the mechanical properties of materials. Recently, gradients or heterogeneous distributions of strengthening defects (nanotwins, dislocation substructures, high-angle boundaries, low-angle boundaries, etc.) have been reported to possess an excellent combination of high strength and good ductility. Several novel gradient deformation approaches (high energy shot peening, surface mechanical grinding treatment (SMGT), surface mechanical attrition treatment (SMAT) and simple torsion have been developed to produce a spatial variation of grain sizes or twin sizes in the surface layers of bulk metals. In this work, the role of nanotwin gradients induced by cryogenic pre-torsion and annealing on the strengthening of CrCoNi alloys is investigated. The influence of the applied torsional strains in cryogenic environments on the microstructure and hardness of CrCoNi is probed using electron microscopy and nanoindentation, and their subsequent impacts on the corresponding tensile behavior and deformation mechanisms are investigated. Systematic microstructural characterization reveals that the sequential torsion and tension tests lead to the observed hierarchical microstructure through activation of different twinning systems and stacking faults, leading to the significant increase strength while retaining a good ductility. Following this study, the synergistic strengthening symphony of nanograins, nanophases and nanotwins is investigated by the tuning the alloying addition of Al and Ti into the CrCoNi alloy system, combined with the variation of thermal-mechanical history, so as to optimize the mechanical properties and illustrate the underlying deformation mechanisms.

B-25: Site Specific Study of Precipitate Coarsening in an Alumina-Forming Austenitic Stainless Steel During Creep

Hongyuan Wen[1], Ze Chen[1], Bingbing Zhao[1], Xianping Dong[1], Jing Wang[2], Jiashi Zhou[2], Langting Zhang[1]
1. Shanghai Jiao Tong University, China
2. Semiconductor Manufacturing International Corporation (SMIC) Shanghai, China

Due to the combination of excellent oxidation resistance and high creep resistance at elevated temperature, alumina-forming austenitic (AFA) stainless steels are considered as a promising candidate structural material for advanced ultra-supercritical power plant. AFA steel can sustain creep/rupture at 700℃ under 150MPa for 3000h. However, the fracture mode is mainly intergranular, and secondary cracks in front of fracture surface always extend along normal grain boundary (NGB) other than twin boundary (TB). To distinguish the precipitation behaviors on NGBs and TBs, a comprehensive site specific study has been performed using specimens crept for 0, 50, 500 and 3000h under 700℃/150MPa. Both NGBs, TBs and matrix are free of precipitates before creep/rupture. After creep for 50h, nanosized MC and $L1_2$ dispersions began to appear inside the grain. Only a small amount of Mo segregation was noticed at TB. However, a large number of B_2 and $M_{23}C_6$ phases ~200nm started to appear at NGB, which also cause a $L1_2$ phase precipitate free zone (PFZ) nearby. With the extension of creep time, Laves phase began to nucleate and grow at both boundaries, and the precipitation behaviors at both boundaries tended to be similar. Up to 3000h, micrometer size B2, $M_{23}C_6$ and Laves phase appeared at both boundaries and the width of $L1_2$ precipitate free zone increased to ~4mm. Even though the precipitates at both the boundaries are similar after 3000h, fracture occurred almost along the NGBs. This suggests that the strength of NGB is inferior to that of TB during long term creep/rupture. It may be attributed to the relatively slow precipitation kinetics at TB compared with NGB and the difference in crystallographic orientation of the precipitates at these two boundaries. The present study offers an in-depth insight of the creep/rupture mechanism in AFA stainless steel.

B-26: Multiphase-Field Study of γ' Precipitates during Two-Step Aging in Single Crystal Superalloy DD6

Yaqian Zhang[1], Cong Yang[1], Qingyan Xu[1], Baicheng Liu[1]
1. Tsinghua University, China

Phase field method has been an effective tool for predicting microstructure evolution such as solidification, solid-state phase transformation and so on. In this paper, a multiphase-field model incorporating elastic driving forces in the presence of lattice misfit is developed to simulate the microstructure evolution and elements distribution of γ' precipitates during two-step aging treatment in multicomponent DD6 superalloy. In the model, artificial order parameter fields (ϕ1mm, ϕ2mm, ϕ3mm, ϕ4mm) are used to distinguish the four types of γ' precipitates described by long-range order (LRO) parameters (1,1,1)η_0, (-1,-1,1)η_0, (-1,1,-1) η_0, (1,-1,-1)η_0. The antiphase domains (APDs) formed as a result of $L1_2$ ordering are considered. To solve the elastic and lattice misfit between γ and γ' phase, stresses are kept same in the diffuse interface between the two elastically inhomogeneous phases and the lattice misfit is coupled through eigenstrain strain. The commercial software Pandat was used to provide realistic superalloy thermodynamic and kinetic data for the multiphase-field simulation. It is found that γ' precipitates grow quickly in the first 1120℃/4h aging with γ' forming elements such as Al, Ta diffusing into precipitates while γ forming elements such as Co, Cr diffuse away from the growth path, and the diffusion of elements slows down due to the decrease of temperature in the second 870℃/4h aging process. The effect of elastic energy and the APDs on the morphology evolution of γ' precipitates are analyzed. The simulation results indicate that the γ' phase grows into cubical shape under the influence of inhomogeneous elastic energy. In addition, the γ' precipitates with same LRO parameters can merge together and grow into rectangular or L-shaped while γ' precipitates with different LRO parameters will not due to the anti-phase effect of γ' phases. The simulated elements distribution and γ' morphology are in good agreement with the experimental results by three dimensional atom probe (3DAP) and scanning electron microscope (SEM) analysis.

B-27: Effect of Reactive Element Ti Addition on the Oxidation Resistance of CoNiCrAlY Alloys

Liang Yang[1], Yu Zheng[1], Chi Zhang[1], Hao Chen[1], Zhigang Yang[1]
1.Tsinghua University, China

With different contents of reactive element Ti (0, 0.1, 0.3, and 0.5wt.%) added in CoNiCrAlY alloy (Co: Bal., Ni: 32wt.%, Cr: 20wt.%, Al: 8wt.%, Y: 0.4wt.%), the multi-scale distribution of Ti in microstructure and the effect of Ti addition on the features of oxide pegs (density, length, width, Al_2O_3 sheath thickness, and growth direction and so on), cohesiveness of the thermally grown oxide (TGO) to the alloy, and phase constituents of CoNiCrAlY alloy will be investigated. Combining computational calculations (thermodynamics and first principle calculations) and experimental characterization (scanning electron microscopy combined with energy dispersive spectrometer, X-ray diffraction, atomic force microscope, and electron probe micro-analyzer), multi-scale Ti distribution in microstructure will be

investigated. A cyclic oxidation experiment (holding samples in the furnace at 1150˚C for 4.5h followed by air cooling for 0.5h; these samples were subjected to 20 circulations for a total of 100h) and an isothermal oxidation experiment (holding samples in the furnace at 1150˚C for, respectively, 0.5, 1, 2, 5, 10, 20, and 50h) have been carried out, so that diffusion and segregation of oxygen, nucleation and growth of oxide pegs, evolution of phases in alloy, the mass variation of different samples, and stress distribution during the experiment process will be get, and their interactions will also be systematically analyzed. The effect of Ti addition on the features of oxide pegs and cohesiveness of thermally grown oxide to the alloy will be revealed, and a theoretical guide for rational Ti addition will thus be provided to improve oxidation resistance of CoNiCrAlY alloy. This project will provide theoretical foundation for future modification by reactive elements addition in MCrAlY alloy and make contribution to improve intrinsic properties of high-temperature bond coat materials for airspace engine.

B-28: Oxidation Behavior on Re-Rich Ni-Based Superalloy Nano Lamella by In-Situ TEM

Yanhui Chen[1], Yunsong Zhao[2], Chunhui Wang[1], Haibo Long[1], Ang Li[1]
1. Beijing University of Technology, China
2. AIC Beijing Institute of Aeronautical Materials, China

Rhenium are an important element for improved high-temperature properties of Ni-based single-crystal superalloys. Higher performance on longer-lasting components and higher fuel efficiencies of superalloys can be realized by moderate addition of Re. Re-rich containing about 7wt% third generation Ni-based superalloys prepared by our group had been improved an enhanced lasting time about 41% under 1050˚C/83MPa. Its oxidation behavior, however, is another important behavior than its mechanical ones in service under a severe environments with high temperature and stress applied. Recent research on the oxidation of Ni-based superalloys focused on the role of micro alloying in the oxidation kinetics and oxide layer formation. Our work focused on oxidation behavior of Re and other elements during hot oxidation behavior by advanced in-situ high resolution technique. Direct in situ TEM observation of micro-structural evolution of single crystal Re-rich Ni-based superalloys alloy during oxidation were carried out to investigate its oxidation mechanism. The in-situ oxidation experiments utilized a dedicated Cs corrected transmission electron microscope equipped with energy dispersive X-ray spectrum and Electron energy loss spectroscopy (EELS). The specimen temperature was maintained at 350~1100˚C using a DENS nano-chip based heating holder. There was not an obvious oxidation change when oxidation temperature lower than 450˚C. Real-time in-situ structural variation indicates that γ phase has priority of oxidation than γ' phase and it follows a sequence of surface oxidation of γ phase and then tend to γ/γ' boundary and continue to thicker γ phase. In-situ selective phase and elemental oxidation experiments provide direct clues on alloy design.

B-29: Critical Assessment of Dynamic Recrystallization during Hot Deformation of Metallic Materials

Hongkai Zhang[1], Hao Xiao[1], Ke Huang[1]
1. Xi'an Jiaotong University, China

Most of the metallic parts have been subjected to hot deformation, during which dynamic recrystallization (DRX) often takes place. Dynamic recrystallization has been well documented in steels and aluminium alloys, which are two types of the most used structural metallic materials. However, the dynamic recrystallization behaviour in more recent metallic materials such as titanium alloys, nicke-based superalloys, magnesium alloys, which are currently being extensively investigated, seem to be quite different as those found in steels and aluminium alloys. In this study, the critical problems related to dynamic recrystallization during hot deformation of metallic materials are analyzed. The most serious problem in dynamic recrystallization studies is related to the possible temperature gradient within the deformed samples, which can easily lead to strain localization. A routine way to preserve the hot deformation microstructure for most alloys is to immediately quench the deformed samples. The quench delay, which is often raised by the equipment, after the termination of hot deformation results in static or post dynamic recrystallization. For some materials, the hot deformation structures are obliged to be destroyed by the phase transformation during cooling after hot deformation. All the above-mentioned issues give misleading results when examining the post-mortem microstructures. Moreover, most industrial alloys contain a matrix phase and dispersed second-phase particles. Second-phase particles may retard or accelerate recrystallization, depending on their size and spatial distribution, among others. But the effect of second-phase particles on dynamic recrystallization is often oversimplified or totally neglected. Nucleation of recrystallization is never a homogeneous process in any sense. It takes place in regions that contain microstructural heterogeneities such as grain boundaries, micro or shear bands, or around large second-phase particles. Single EBSD/optical micrograph with small analyzed area is often not enough to get statistically reliable data to give solid conclusions. Procedures to avoid and/or verified solutions to these encountered problems related to

dynamic recrystallization are proposed.

B-30: Effects of Long-Term Aging on Microstructure and Properties of a Tungsten Bearing Heat Resistant Alloy

Zhihua Gong[1,2], Gang Yang[2], Hansheng Bao[2]
1. Inner Mongolia University of Science & Technology, China
2 Central Iron and Steel Research Institute, China

In this study, the effects of long-term aging at 700℃ and 750℃ on microstructure and mechanical properties of a new developed tungsten bearing heat resistant alloy used for advanced ultra-supercritical (A-USC) power plant was investigated both experimentally and thermodynamically. Experimental results showed that the mechanical properties remained excellent stability after long-term aging at 700℃ for 10000h, while the impact absorbing energy decreased sharply after 1000h aging and then kept constant till 10000h. The thermodynamic calculations showed that the equilibrium precipitation phase of the alloy consisted of $M_{23}C_6$ and MC, no M_6C appeared. The main precipitations after long-term aging at 700℃ and 750℃ were $M_{23}C_6$, MC and homogeneous γ'. The mass fraction of $M_{23}C_6$ carbides increased with the increase of aging time, and the $M_{23}C_6$ carbides precipitated in shape of chains and lamellas in the vicinity of grain boundaries. The slight decrease of MC carbides during aging may be due to degradation reaction. The weight fraction of γ' increased with the aging time, then changed little after 5000h; the γ' phase exhibited excellent microstructure stability and low coarsening rate during long-term aging at 700℃, however the coarsening rate of γ' phase was much higher at 750℃.

B-31: Influence of Small Angle Deviation from [111] Orientation on Creep Properties of a Ni-Base Single Crystal Superalloy

Bin Hu[1], Yanling Pei[1], Shusuo Li[1], Shengkai Gong[1], Huibin Xu[1]
1. Beihang University, China

The creep behavior of a Ni-Base single crystal superalloy near [111] orientation has been investigated under different stress at 760℃. It is found that precisely [111] orientation showed the best creep strength in spite of poor strain hardening. With the increase of orientation deviation from [111] to [011], the creep properties decrease more significantly compared with the deviation from [111] to [001]. While specimens deviate toward [001] have a distinct incubation creep stage with relatively low initial creep rate. TEM and EBSD have been used for further analysis of dislocations and lattice rotation. The results showed that the dominant slip systems are {111} <112> during creep test. However, almost no γ' cutting was observed during the incubation stage. It can be inferred that the deformation mechanism in the incubation period is mainly the {111} <110> slip systems in γ channel. For {111} <110> slip systems, deviation from [111] to [011] correspond to coplanar double slip, which is conducive to the occurrence of a<112> ribbon forming by two a/2 <110> matrix dislocations with different Burgers vectors on the same {111} plane, resulting in a relatively high initial creep stage. While [111]-[001] boundary is non-coplanar double slip orientation and the formation of a<112> ribbon is impeded.

B-32: Effects of Mo and Re Content on Stress Rupture Properties of γ'- Rich Ni_3Al-Based Single Crystal Superalloy at 1200℃

Jiapeng Huang[1], Yanling Pei[1], Shusuo Li[1], Shengkai Gong[1]
1. Beihang University, China

The effect of Mo and Re concentration on creep properties of Ni-Al-Ta-xMo-yRe single crystal superalloy with (x-0.3, x and x+0.3) Mo and (y-0.3, y and y+0.3) Re (wt.%) at 1200℃/ 80MPa was investigated. The initial microstructure of alloys and microstructural evolution during the creep deformation were characterized by scanning electron microscopy (SEM) and transmission electron microscopy (TEM). The results showed that after heat treatment, all the five alloys were composed of γ and γ' phase (it's volume fraction about 80%) without TCP phase precipitation. Both Mo and Re could increase the γ/γ' lattice misfit and density of interfacial dislocations which profited to the creep resistance at high temperature and low stress condition. The inferior thermal stability of γ' phase in alloys resulted from excessive Mo instead of its enhanced by Re addition. The stress–rupture life of the original alloys was 152h, which is better than the lives of alloys with lower or higher Mo concentration. In contrast, the longer creep lives and the lower minimum creep rate of alloys as the Re concentration is increased. The smallest amount of strain of alloys with (y+0.3) Re element in the primary stage of creep although its total strain is the largest attributed to the earlier and more complete rafted γ' phase. Moreover, the higher content of strengthening elements such as Ta and Mo in the γ' phase make it strengthened due to the addition of Re element.

B-33: Effect of Pt-Aluminide Bond Coating on Creep Behavior of a Single Crystal Superalloy with Different Thickness

Yuan Liu[1], Heng Zhang[1], Yi Ru[1], Zehao Chen[1], Weiwei Qu[1], Yanling Pei[1], Shusuo Li[1], Shengkai Gong[1]
1. Beihang University, China

The effect of Pt-aluminide bond coating on creep properties of a nickel-base single crystal superalloy has been investigated. The specimens were given a diffusion treatment at 1040℃ for 2h after electroplated

with an approximately 2μm thick Pt layer. Subsequently, they were aluminized by chemical vapor deposition at 870℃ for 6h. Creep experiments were carried out on the single crystal Ni-base superalloy IC21 at 850℃/450MPa, 980℃/250MPa, 1100℃/137MPa. Coated and uncoated specimens with different substrate thickness (0.3mm, 0.5mm and 1.0mm) were applied to these creep tests. The creep life of coated specimens was inferior to those of the uncoated alloy at all test temperatures. A decrease in creep life with decreasing thickness was also observed. This can be ascribed to the reduction of substrate loaded area. In contrast to 980℃ and 1100℃, a sharp decline of creep life (more than 50% for 1.0mm specimens) arises at 850℃. Both coated and uncoated specimens show outstanding ductility at 980℃ and 1100℃ compared to specimens at 850℃. Ductility decline also occurs at thinner specimens. The ductility of substrate and coating various at each temperature leads to the results. In all tests, Creep behavior of 1.0mm specimens exhibits excellent consistency in duplicated tests, thinner specimens show more discrete meanwhile.

B-34: The Study of the Hot Corrosion Behavior of Single Crystal Superalloys with Different Cr Content under Cold and Hot Fatigue

Zehao Chen[1], Shusuo Li[1], Weiwei Qu[1], Yuan Liu[1], Jiapeng Hang[1], Tao Dong[1], Yi Ru[1], Heng Zhang[1], Shengkai Gong[1]
1. Beihang University, China

The industry gas turbines' (IGT) service life and use intensity are troubled by hot corrosion environment generally in spite of it has the highest efficiency of thermal -power conversion and considerable service time. There is no doubt that improving the inlet temperature can effectively improve the operating efficiency of gas turbines, so the adoption of air-cooling technology has become an important choice to improve the efficiency of gas turbines. The effect of internal stress and microcrack caused by drill on the hot corrosion of the alloy is worthy of attention seriously. In this paper, three alloys of different composition were used and two different sizes of holes were drilled, and then the cold and hot fatigue between heat at 900℃ in air and immersed in a saturated salt solution(75%Na_2SO_4+25%NaCl) at room temperature was carried. The samples were heat in 900℃ for 10 minutes, immersed in salt solution for 15 seconds, evaporated residual water for 30 seconds with heat preservation as one circulation, 80~100 cycles were used totally. The corrosion results were analyzed and found that compared with the general cold and hot cycle, the salt solution cold and hot cycle has more severe reaction degree and more obvious cracks. Among them, the reaction of low chromium alloy is more intense and the crack is more obvious. At the same time, obvious difference of element distribution was found at the cracks, especially the distribution of molybdenum and sulfur on one side and aluminum on the other side was consistent with the distribution law of hot corrosion reaction. All of the above can prove that after the perforation process, the hot corrosion of the alloy does affect the properties around the holes and the growth of cracks.

B-35: High Temperature Cyclic Deformation Microstructural Characteristic in GH4720Li Ni-Based Superalloy

Xingfei Xie[1], Jinglong Qu[1], Jinhui Du[1]
1. Central Iron and Steel Research Institute, China

GH4720Li Ni-based superalloy with high volume fraction of γ' phases has been widely used for turbine disks in aeroengines because of its combination of superior mechanical properties and excellent oxidation resistance at high temperature. The fatigue failure of Ni-based superalloy has become the major damage mechanism and design consideration for aeroengines. The microstructural characteristic during high temperature fatigue behavior for GH4720Li superalloy remains unclear. In this work, the strain-controlled axial fatigue test was conducted at 550℃ on MTS fatigue testing machine for GH4720Li superalloy which was prepared through smelting, hot forging and conventional heat treatment. The metallurgical observation of GH4720Li superalloy was performed by scanning electron microscope (SEM). The microstructural characteristic of dislocation substructure and mechanical twin formed in GH4720Li superalloy subjected to high temperature fatigue was investigated by transmission electron microscope (TEM) and high-resolution transmission electron microscope (HRTEM) operating at 300 kV. The sample for TEM analysis was cut along the transverse sections of fatigue-tested specimen and prepared by double-jet electrochemical polishing. The interaction mechanism between dislocation substructure and mechanical twin was further discussed. The results show that the dislocation substructure reveals both planar slip and cross slip characteristic in the interior of γ' phases or around γ' phases in GH4720Li superalloy during high temperature cyclic deformation. The mechanical twin and deformation band segment the deformed austenitic grains. The deformation band consisting of high density dislocation was produced on the closely parallel primary glide plane. The dislocation movement can be hindered on the slip planes oblique to twin boundary and also be promoted on the slip planes parallel to twin boundary. In addition, certain chemical elements tend to be concentrated near the coherent twin boundary during high temperature cyclic deformation. The twin boundary could effectively facilitate dislocation multiplications

contributing to ductility of GH4720Li superalloy during high temperature cyclic deformation.

B-36: Development of GH4169 L-Shaped Extrusion Profile in Aero-Engine

Qiliang Nai[1], Baoshun Wang[1], Cheng Su[1], Zhengzhou Li[1]
1. Zhejiang JIULI Hi-Tech Metals Co. Ltd., China

At present, GH4169 L-shaped Profile in Aero-engine are mostly manufactured by hot rolling process. However, the mechanical properties and the finished product rate of the hot rolled profiles are worse than that manufactrued by extrusion forming. Due to the GH4169 alloy has high deformation resistance and poor hot plasticity, the L-shaped Profile is very difficult to manufacture by hot extrusion. In this paper, the influence of billet temperature, extrusion rate, extrusion ratio and other process parameters on the extrusion behavior of GH4169 alloy L-shaped profile by finite element method were studied. The evolution law of metal flow behavior, temperature distribution and extrusion load change during the extrusion process were researched thoroughly. Based on the finite element calculation results, the reasonable extrusion process for GH4169 L-shaped Profile was explored. Then pilot production of GH4169 L-shaped profile were carried out on 42MN extruder. The tensile and stress rupture tests of the extrusion profile were carried out at room temperature and 650˚C. The results show that the export velocity of metal flow and the temperature of the billet increases with the increase of the extrusion ratio during the extrusion process. When the temperature of the billet higher than 1230 ˚C, the excessive temperature can make the surface of the L-shaped extrusion profile cracking. The L-shaped Profile of GH4169 alloy has a good extrudability at 1120 ~ 1220 ˚C, and the extrusion speed should be controlled in 40 ~ 150 mm/s during the whole extrusion process . The GH4169 L-shaped extrusion profile has a nice surface quality, and the crystal degree of the extrusion profile is above 4 grade. At 650˚C, the tensile strength of the L-shaped extrusion profile is above 1100 MPa, the yield strength is more than 860 MPa, and the elongation . And other mechanical properties of the GH4169 L-shaped extrusion profile can comply with relevant technical requirements.

B-37: On the Influence of Multiaxial Stress States on the Kinetics of Rafting During Creep of Ni-Base Single Crystal Superalloys

Lijie Cao[1], David Buerger[1], Gunther Eggeler[1]
1. Ruhr-University Bochum, Germany

Ni-base superalloy single crystals are used for turbine blades which operate in the creep regime. To study their creep behaviors, researches have been carried out extensively with a focus on the evolution of microstructure during uniaxial creep, while less effort was devoted to the effect of multiaxial stress states. The present work introduces a new circular notched miniature tensile creep specimen which can be used to study the influence of multiaxial stress state on the rafting during creep of Ni-base single crystal (SX) superalloys. We first explain briefly how circular notches affect the stress state in the notch root during elastic loading, and why the stresses redistribute under creep conditions. Then finite element method (FEM) was used to study the stress and strain distributions in the notch region. Based on the FE analysis, a new miniature circular notched specimen was designed, and a series of interrupted creep experiments on Ni-base single crystal superalloy ERBO1 (CMSX-4 type) were performed at 950˚C with miniature uniaxial and circular notched <100> tensile specimens. The evolution of microstructure is investigated carefully after 81, 169 and 306 hours in both types of specimens. In the uniaxial experiments, rafting occurs homogeneously in the specimen and starts from the beginning on. In the circular notched specimens rafting is delayed and different coarsening rates are observed at different positions in the notch region. The results are discussed in the light of previous work on the influence of circular notches on creep and on the influence of multiaxial stress states on rafting.

B-38: Creep and Rejuventation by Hot Isostatic Pressing of a Single Crystal Ni-Base Superalloy

Oliver Horst [1], Benjamin Ruttert[1], David Bürger[1], Larissa Heep[1], Hongcai Wang[1], Antonin Dlouhy[2], Werner Theissen[1], Gunther Eggeler[1]
1. Ruhr-University Bochum, Czech
2. Academy of Science of the Czech Republic, Czech

The present work deals with the effect of hot isostatic pressing (HIP) rejuvenation treatments on the creep behavior of a pre-crept single crystal Ni-base superalloy of type CMSX-4. Precisely oriented [001] miniature tensile creep specimens are tested up to different strains resulting in different microstructures. HIP rejuvenation treatments of the pre-crept specimens should restore the microstructure and creep behavior. Quantitative analysis of scanning and transmission electron micrographs and further creep experiments prove the effect of the rejuvenation treatments. A HIP-rejuvenation treatment significantly improves creep strength of specimens with pre-strain of 5.0%. However, the microstructural damage induced by the creep pre-deformation could not be fully removed. A series of sequential creep/HIP/creep-experiments has shown that, increasing levels of pre-deformation result in increasing levels of creep rates even after identical HIP-rejuvenation treatments. This phenomenon is related to

an accumulation of permanent microstructural damage, which is not associated with rafting or cavitation. The mechanical results obtained in the present work are interpreted based on microstructural results on the γ/γ'-microstructure (γ-channel widths and γ'-size), on the pore population (number density of pores, pore size distributions and pore area fractions) and dislocation substructures which have formed during creep. The results are discussed in the light of previous results reported in the literature.

B-39: Thermodynamic Constitution of the Al–Cu–Ni System Modeled by CALPHAD and Ab Initio Methodology for Designing High Entropy Alloys

Wei Wang [1,2], Hai-Lin Chen[3], Henrik Larsson[2,3], Mao Huahai[2,3]
1. Northeast Electric Power University, China
2. KTH Royal Institute of Technology, Sweden
3. Thermo-Calc Software, China

The Al–Cu–Ni system has been thermodynamically assessed over the whole composition and temperature range based on a critical literature review. The $L1_2$ and B2 phases, in conjunction with their disordered counterparts, are described using partitioning models. Ab initio calculations were performed to support the assessment of these phases. A set of self-consistent thermodynamic parameters for describing the Gibbs energy of individual phases was obtained. The assessment was validated by comparing various calculations such as invariant reaction equilibria, thermochemical properties, isothermal and isoplethal sections with all available experimental data. The Al–Cu–Ni ternary is a vital subsystem of many high entropy alloys (HEAs), which can probably be attributed to the existence of stable ordered and disordered FCC and BCC structures. In near-equiatomic compositions of this ternary system, the phase formation and equilibrium and non-equilibrium solidification curves were calculated using the present thermodynamic description. The phase competitions and their impacts on the design of HEAs are discussed, e.g. the relative stability of the disordered FCC and BCC for dual-phase HEAs, and the equilibria between disordered FCC_A1 and ordered B2 phases for ductile high strength HEAs. This thermodynamic database can also be used to design Ni-based high-temperature alloys.

C1. Light Metals and Alloys-Aluminum

Symposium Organizers:

Baiqing Xiong, GRINM Group Co. Ltd., China; Yoshihito Kawamura, Kumamoto University, Japan; Young Min Kim, Korea Institute of Materials Science (KIMS), Korea; Jian-Feng Nie, Monash University, Australia; Diran Apelian, Worceste Polytechnic Institute, USA

August 19-21, 2019
Place: Exhibition Area (3rd Floor)

C1-1: Finite Element Analysis of Residual Stress with Quenching Rate of 6061 Aluminum Alloy

GyuSeok Lim, SukCheol Kwon, HwaYoung Woo, Chungnam National University, Korea; JongHyeon Lee, Chungnam National University, Korea / Rapidly Solidified Materials Research Center, Korea / Graduate school of Energy Science and Technology, Korea

Aluminum (Al) alloy is an important material for the environmentally friendly industry including the automobile industry and the aerospace industry because of its light weight, good processability and high noble strength. The 6061 aluminum alloy, in which magnesium (Mg) and silicon (Si) are added to aluminum as an alloy element, is a precipitation hardening type alloy and has a relatively high strength and excellent corrosion resistance. In order to achieve precipitation hardening, solution treatment is essential, and if thermal deformation occurs at a stage of holding and quenching at a high temperature, a large residual stress is generated inside the specimen. This causes distortion during subsequent machining and reduces the precision of the part. Therefore, in order to increase the precision of the component, it is important to minimize the residual stress generated during quenching and to analyze the residual stress distribution in the aluminum alloy. This study simulated the quenching of Al 6061 alloy billets using finite element method. The thermal flow and residual stress distribution were calculated by varying the cooling rate through water temperature change during quenching. From these results, it is expected that it will provide guidelines for the change of residual stress due to quenching of aluminum alloy and improve the reliability and mechanical properties of the material.

C1-2: Effect of Heating Rate on Microstructure and Mechanical Properties of Al 7055 Alloy

Seunggyu Choi, Seok-Jae Lee, Chonbuk National University, Korea

Nowadays, 7xxx aluminum alloys has been widely used as structural materials that requires high strength in automotive, aircraft, and defense industries.

A precipitation hardening is a key strengthening mechanism to improve the strength in 7xxx Al alloys. The characteristics of precipitates such as mean particle size, volume fraction, average distance among particles, total number of particles, and so on could be controlled during an artificial T6 aging treatment after a solid solution treatment. Even though the same T6 aging condition was adopted, the mechanical properties of the aged 7xxx Al alloys might be different depending on the solid solution treatment. Previous studies reported that the chemical composition of matrix and the condition of precipitates are influenced by solid solution temperature, cooling rate, etc. which resulted in the variation of mechanical properties. In the present study, we investigated the influence of heating rate on mechanical properties of Al 7055 alloy. The dissolution and formation kinetics of precipitates existed in the sample before the solid solution treatment were affected depending on the heating rate because the dissolution and formation of precipitate particles are diffusional controlled. A dilatometric test was carried out to control the heating rates in the solid solution treatment. The mechanical properties were evaluated using hardness test and compressive test while the microstructural features were observed by XRD, OM, and TEM.

C1-3: Effect of AlP in Aluminum System Alloys AA365

Yiyang Zhao, Satoru Ishihara, Seiji Saikawa, University of Toyama, Japan; Hisao Kazuta, University of Toyama (Present: NIDEC CORPORATION), Japan; Susumu Ikeno, University of Toyama, Japan

From the perspective of protecting the atmosphere, in the automotive industry, attempts have been made to convert iron-based materials for automotive parts into aluminum, aluminum, magnesium, and resins with low specific gravity to reduce the weight of the body to reduce carbon dioxide emissions and improve fuel economy. AA365 alloy is applied to automobile parts because it is easier to recycle, cheap and environmentally friendly than resin. As a result of, it has been widely used for automobile road wheels, suspension arms.
We investigated the effect of AlP on the microstructure of Al-10mass%Si-Mg system alloy by using different purity aluminum (to reduce the nucleation frequency of AlP caused by P content). In DTA cooling curve of using low purity Al-10mass%Si-0.8mass%Mg alloy, we observed unknown peak. The peak was researched with quench at any temperature during solidification. In the result, it was found that the peak occured by growth of plate-like eutectic Si phase formed with AlP as the heterogenius nucleation site. In this study, has investigated influence of P content on AA365 alloy by using different purity aluminum. In order to do this, we used 2N alloy and 5N alloy that different of P content due to investigate effect of AlP was prepared. Aluminum of commercial purity (2N 99.7mass%) or high purity (5N 99.999mass%) was melted with crucible made by alumina in electric resistant furnace. For investigation of the solidification sequence, measured crystallization temperature and quenched microstructure. The result of this study, supercooling at about 2˚c was observed only in 5N alloy. And a plate-like Si phase have formed AlP as a core was only observed at 2N material at any temperature. Further, before the Al-Si binary eutectic reaction, the number of the plate-like Si phases in the 2N material increases, and the number of the plate-like Si phases increases and the behavior increases.

C1-4: Microstructure Observation of Al-1.6mass%Mg_2Si Alloy with and without Homogenization

Takara Umezawa, Taiki Tsuchiya, Seungwon Lee, Kenji Matsuda, Susumu Ikeno, University of Toyama, Japan; Ken-ichi Ikeda, Hokkaido University, Japan; Tomoyuki Homma, Nagaoka University of Technology, Japan

Al-Mg-Si alloys (6xxx Al alloy series) are one of age-hardenable aluminum alloys. The precipitation sequence can be described as follows: Super Saturated Solid Solution (ssss) → clusters / GP zones → needle shaped β''/ Parallelogram type precipitates → rod shaped β'/ Type A / Type B / Type C precipitates → plate shaped β (Mg_2Si) precipitates. Al- Mg- Si alloys are extensively used in chassis part of window frames, automotive and high-speed train, due to their high strength-to-weight ratio, high ductility, good extrudability and excellent corrosion resistance by anodizing. These chassis are usually produced by extrusion process. But the speed of extrusion is restricted by occurring cracks that is called "pick-up fault" with increasing extrusion speed. It is reported that pick-up fault could be reduced by homogenization treatment. However, the reports are few about effect of homogenization treatment against Al- Mg- Si alloys without impurities. It is known that initial microstructure can influence to extruded microstructure by casting microstructure, for example segregation of alloying elements, dendrites and dispersoids. Aim of this research is to investigate the influence of homogenization treatment on microstructure of Al- Mg- Si alloys. Two kinds of samples were prepared; (1) non-homogenization and (2) homogenizing treatment at 848K for 7.2ks. Microstructure evolution was investigated each alloy using optical microscope (OM), electron probe micro analyzer (EPMA) and transmission electron microscope (TEM) at 120kV. In non-homogenization sample, the contrast thought of as dispersoids and precipitates around dispersoids mainly are observed. In homogenized sample, the contrast thought of as

dispersoids, equilibrium phase and precipitates are observed. Precipitates are not seen very often around big dispersoids and equilibrium. TEM observation from the [100]Al direction, it was possible to observe rod-like precipitation and their cross sectional plane. Rod-like precipitation have orientation relationship with matrix; parallel to the <100>Al direction.

C1-5: Effect of Cold-Rolling on Aging Behavior of Al-Cu-Mg Alloy with Different Cu/Mg Ratio

Masaki Matsumoto, Taiki Tsuchiya, Seungwon Lee, Kenji Matsuda, Susumu Ikeno, University of Toyama, Japan; Ken-ichi Ikeda, Hokkaido University, Japan; Tomoyuki Homma, Nagaoka University of Technology, Japan

Al-Cu-Mg alloys are known as 2xxx series aluminium alloys which is represented by the duralumin and super duralumin, and it is widely used in aerospace and transportation industries due to its excellent mechanical properties. It has been reported that mechanical properties of 2xxx series aluminium alloys can be enhanced by cold-rolling before aging. The precipitation sequence for Al-Cu-Mg alloys is generally described as followed as: S.S.S.S.→ G.P. Zone→ metastable θ' phase→ stable θ phase or S.S.S.S.→ G.P.B. Zone→ metastable S' phase → stable S phase. The precipitation sequence of this alloy series is related with the Cu/Mg ratio. In addition, many studies on the high concentration side as represented by the A2024 alloy have been made, but few studies are dealt with aging precipitation behaviour in the cold rolling before aging on the low concentration side. Therefore, the purpose of this research is to investigate the effect of cold-rolling on age hardening behaviour of low concentration Al-Cu-Mg alloys with different Cu/Mg ratio (Cu/Mg=1, 3) aged at 473K. In this study, four types of cold-rolling before artificial aging were used: these are 0%, 10%, 30%, 60%. To estimate mechanical properties, Micro Vickers hardness measurement was conducted. Microstructure observation was carried out using TEM. Samples for microstructure observation was prepared by twin-jet electropolishing method. As the result of Micro Vickers hardness measurement, the Micro Vickers hardness of cold-rolled samples was increased and the aging time to peak-hardness was shortened with the increase of thickness after cold-rolling. The aging time to peak-hardness was shortened with the increase of Cu/Mg ratio. As the result of t Microstructure observation, the number density of S' phases and θ' phase in cold-rolling samples was increased. The reason why the precipitation process was promoted is that the dislocations what is introduced by cold-rolling would be the nucleation site of the precipitation.

C1-6: Influence of Ag Addition on Microstructure of Al-Mg-Ge Alloy

Shu Umemura, Graduate School of Science and Engineering for Education, Japan; Taiki Tsuchiya, Seungwon Lee, Kenji Matsuda, Susumu Ikeno, University of Toyama, Japan; Ken-ichi Ikeda, Hokkaido University, Japan; Tomoyuki Homma, Nagaoka University of Technology, Japan

Several reports are available about a substitution for Si to Ge in Al-Mg-Si alloy can improve its mechanical property by aging treatment at relatively high temperatures. Precipitation sequence of Al-0.43%Mg-0.20%Ge (mol.%) alloy is suggested to S.S.S.S → Cluster → G.P. zone → Random type → Parallelogram type, β'' → β', A type → β.
It is known that Ag addition on Al-Mg-Si alloys can enhance their mechanical properties and age-hardenability due to increase of precipitates. Also, it is reported that Ag addition can precipitate β' Ag which has smaller a-axis than β' phase. Ag enters the composition of β' phase, shrinking its hexagonal network from a=0.715nm in the Ag-free phase to a=0.69nm, while the c direction remains the same 0.405nm. β' Ag phase has Al, Mg, Si and Ag in its composition. Further, β' Ag phase has a space group different from β' phase. The aim of this research is to understand the effect of Ag on aging behavior and mechanical property on Al-Mg-Ge-Ag alloy. Chemical compositions of alloys are Al-0.43%Mg-0.20%Ge (Base alloy) and Al-0.47%Mg-0.23%Ge-0.23%Ag (Ag added alloy) (mol.%). Aging treatment was carried out at 423K, 473K, 523K. Vickers microhardness measurement was conducted to estimate the mechanical properties of alloys. TEM observation was conducted by using Topcon, EM-002B with accelerated voltage of 120kV. Ag added alloy showed a significant increment of hardness at the initial stage of aging. The number density of precipitates in the Ag added alloy at the initial stage and peak hardness condition was remarkably increased compared to Base alloy. In the case of over-aged condition, β' phase, A type and β phase were observed in Ag added alloy. β' phases with different a-axis were found. A type existed on grain boundary. Interplanar spacing of A type in the Ag added alloy was no change compared to A type in the Base alloy.

C1-7: Effect of Homogenization on the Microstructure in an Excess Silicon Al-Mg-Si Alloy

Shuaishuai Qin, Graduate School of Science and Engineering for Education, Japan; Taiki Tsuchiya, Seungwon Lee, Kenji Matsuda, Susumu Ikeno, University of Toyama

Widely used Al-Mg-Si(6XXX) alloys usually need an extrusion process. Before extrusion, the as-casted billets often require a homogenization treatment,

because homogenized billets not only extrude easier and faster and give better surface finish than cast billets, but also can make the as-cast billet capable of undergoing extensive plastic deformation without cracking and local melting. Despite there are detailed studies of how homogenization affect extrudability in the Al–Mg–Si alloys, less attention was focused on the effect of homogenization on the final microstructure after artificial aging.

In the present work, we used Al-0.33at%Mg-0.67at%Si alloy to investigate how homogenization affects the final microstructure. The as-cast microstructure is typical dendritic structure. The temperature of homogenization is 575℃ and the samples were held for 2h, then the samples were cooled in air and furnace, respectively. After homogenization, optical microscope(OM) showed that the predominant phase formed in the matrix is rod-like, the length of the rod-like precipitates in furnace-cooling samples is longer than in air-cooling, however, there are many boundaries can be found in the grains of air-cooling samples after homogenization, at the same time, the rod-like precipitates trend to distribute along these boundaries. In order to identify these precipitates and boundaries, TEM observation was conducted by using Topcon, EM-002B with accelerated voltage of 120kV, according to the diffraction patterns, these precipitates were β', and also, many low angle grain boundaries were observed in air-cooling samples after homogenization. After one hour of solution heat treatment, few particles can be observed in air-cooling samples, however, there are many particles remained in the matrix of no-homogenization samples. Moreover, the average grain size is also calculated and the no-homogenization samples exhibit the finest grains. Finally, artificial aging treatment was carried out at 473K, the hardness was measured and no-homogenization group exhibits the lowest peak-hardness. Under peak aging condition, TEM observation revealed that the precipitates in no-homogenization samples are coarser than the homogenized samples.

C1-8: Influence of P Content in Crystallization Behavior of Pseudo-Binary Al-Mg_2Si

Arisa Osugi, Hisao Kazuta, Satoru Ishihara, Susumu Ikeno, Seiji Saikawa, University of Toyama, Japan

In recent years, weight reduction of vehicle body has been required in the automobile industry because of protection of the environment. The application of aluminium alloy have been expanded in the auto parts. Al-Mg-Si alloy has both of good strength and high ductility without heat treatment, which is attracting attention as new die-cast alloy. However, the castability in this alloy is inferior to other aluminum alloy.

In our previous study, the castability of Al-2~6%Mg-1~3%Si system alloy. As a result, the composition that hot-tear decresed was Al-6%Mg-3%Si alloy, because the composition of this alloy was close to pseudo-binary eutectic of Al-Mg_2Si. In addition, it is found that hot-tearing was not occurred in the case of 0.04%Sr addition to Al-6%Mg-3%Si alloy. Eutectic Mg_2Si phase of Sr-free alloy was observed plate-like Mg_2Si having AlP nuclei. On the other hands, Eutectic Mg_2Si phase of 0.04%Sr addition alloy was the remarkable refinement and not present plate-like Mg_2Si.

In this study, for the purpose of clarifying the crystallization behavior of plate-like Mg_2Si phase with AlP as the nucleus, Al-6%Mg-3%Si alloy the crystallization behavior was investigated in detail.

2N alloys and 5N alloys that different of P content due to investigate effect of AlP was prepared. The target compositions were Al-6%massMg-3mass%Si. The melt was held at any temperature and time, and the tissue was frozen by quenching in water. The quenching specimens were polished with sandpaper, buffed with 1μm diamond paste and etched in a 0.5%HF solution. The microstructures were observed by optical microscope and the average diameter and number of plate-like Mg_2Si phases were investigated. The plate-like Mg_2Si phase formed with AlP as the heterogeneous nucleation site was observed only in 2N alloy. In the case of 5N, no such nuclei existed, there were very fine lamellar eutectic phase. In the case of the molten metal was held for a long time, the number of plate-like Mg_2Si phases decreased.

C1-9: Characterizations of the Microstructural and Tensile Properties of Al-9Si-0.3Fe-0.15Mn Alloy with Ti and V Additions

Zeze Xiao, Kazuhiro Matsugi, Zhefeng Xu, Taishi Matsuoka, Tomoshi Uomi, Hirohshima University, Japan; Nobuyuki Oda, Hironobu Kominato, Hirohshima University, Japan / Mazda Motor Corporation, Japan; Yasuo Uosaki, Mazda Motor Corporation, Japan

The effects of 0.2wt% Ti and 0.2wt% V additions on the Al-9Si-0.3Fe-0.15Mn base alloy were investigated for development of low-cost alloys which could be used for the as-cast applications. It was found that the grain size of α−Al phase in the base, 0.2wt% Ti and 0.2wt% V addition alloys measured by image analysis were 43.7μm, 53.7μm and 30.1μm, respectively. Dendritic structures were observed in the base and 0.2wt% V addition alloy. The secondary dendrite arm spacing in 0.2wt% V addition alloy was 31.1μm, which was smaller than that of the base alloy. The microstructure of the base alloy exhibited the α−Al, flake-like Si eutectic and a small amount of the intermetallic compounds, such as the polyhedral-shaped Al15$(Mn, Fe)_3Si_2$ compound and rod-shaped β-Al5(Fe, Mn)Si compound. The introduction of 0.2wt% Ti to base alloy resulted in the formation of Al_3Ti compound, which distributed in the eutectic region. The polyhedral-shaped $Al_{15}(Mn, Fe, V)_3Si_2$ compound

and rod-shaped β-Al_5(Fe, Mn, V)Si compound appeared in the 0.2wt% V addition alloy. The liquidus temperature was increased by the addition of 0.2wt% Ti and 0.2wt% V, which led to the promotion of the segregation degree in the α–Al phase and Si eutectic region. Three alloys showed the same levels in tensile properties ($\sigma_{0.2}$: 79 ~ 83MPa, σ_{UTS} : 148.7 ~ 152.8MPa and ε_f : 5.6%~ 6.3%), which correlated to segregation degree at the as-cast condition. The effect of 0.2wt% Ti and 0.2wt% V additions on tensile properties were discussed in the view of the characteristic microstructural. The findings of this study can benefit and contribute to developing a new Al-9Si series alloys for as-cast applications intended for lightweight materials for the automobiles.

C1-10: Investigation of H Effect into Solid Solution Decomposition in an Al-Zn-Mg Alloy System

Artenis Bendo, Taiki Tsuchiya, Seungwon Lee, Kenji Matsuda, Katsuhiko Nishimura, Norio Nunomura, University of Toyama, Japan; Hiroyuki Toda, Kazuyuki Shimizu, Kyushu University, Japan; Tomohito Tsuru, Masatake Yamaguchi, Japan Atomic Energy Agency, Japan

Hydrogen (H), the basic element on the periodic table, is researched in material science and material physic for its applications and deteriorating effects. H interaction with microstructural defects such as vacancies, defects, dislocations, grain boundaries and interphase boundaries in crystalline materials is an area of research for its implications in mechanical and physical properties. Reports of ten-fold enhanced diffusion in Ni-Cu diffusion couples and lattice contraction in numerous metals when subjected to H atmosphere in high pressures and temperatures, suggests of strong atomic H interaction with point defects. In this regard, possible H effect into precipitation phenomena in Al-Zn-Mg alloy system is investigated. Samples were H charged immediately after quenching from solid solution treatment. Hardness tests showed an inconsiderably slight shift of age-hardening curve to shorter ageing time in H-charged and aged samples. Transmission Electron Microscopy (TEM) was employed for microstructure investigation during ageing treatment to provide insight into microstructure decomposition. Investigation directions were [110]Al, [100]Al and [112] Al. Precipitation density and morphology did not show any consistent difference between H-charged and H-free samples, due to hindering of accurate measurement because of thicknesses variations of investigated regions. However, high resolution transmission electron (HRTEM) images along [110]Al revealed that regions rich in high aspect ratio GP-II zones were observed in H-charged and aged samples, and were absent in the number of HRTEM images analyzed for H-free ones. They had a heterogenous ditribution in Al matrix, with regions rich and absent in these zones. High aspect ratio GP-II zones are reported to be occasionally observed in samples which were solid solution treated at temperature higher than 450˚C indicating a strong depence on vancancy concetration. Higher probability of observing these zones in hydrogen charged and aged samples is probably related to H-point defect interaction and H previously reported effect on vacancy formation and stabilization. Higher presence of high aspect ratio GP-II zones neccesitates a higher presence of vacancies which are required for clustering on {111}Al planes and creating vacancy rich clusters as seeds of nucleation.

C1-11: Effects of Homogenizing Treatment on Dispersive Precipitates and Recrystallized Grains of Si-Bearing Al-Mg Alloys

Cheng Guo, Haitao Zhang, Zibin Wu, Ping Wang, Baomian Li, Jianzhong Cui, Northeastern University, China; Hiromi Nagaumi, Soochow University, China

In this research, microstructural evolutions of Si-bearing Al-Mg alloys were investigated in detail by optical microscope (OM), scanning electronic microscope (SEM), energy dispersive spectrum (EDS) and transmission electronic microscope (TEM). For the as-cast alloy, the microstructures consist of Mg_2Si, Al_6(Mn, Fe) and Al_{12}(Mn, Fe)$_3$Si phases. The amount of the primary phase increased with the content of Si. In the homogenization process, the dimension, distribution and quantity of the dispersoids were influenced significantly by the temperature and time of heat treatment. The precipitates of the two-step homogenized samples were higher density and better dispersed distribution than the single homogenized samples. For the two-step homogenization heat treatment, the purpose of the first step homogenization was to precipitate β' (Mg_2Si) from the supersaturated solid solution. The fine-scale β' phases decomposed into Si-rich "u-phase" at the subsequent high-temperature homogenization stage, which provided nucleation sites for dispersed α-Al (Mn, Fe) Si. The volume fraction of the dispersed zone of the two-step homogenized samples increased as well as the dispersoid free zone (DFZ) decreased comparing with that of single homogenizing. By comparing the volume fraction of the precipitates under different homogenization conditions, the optical phase distribution was obtained when the alloy homogenized at 235˚C/6h+580˚C/8h.

The dispersive precipitates can restraint the recrystallization of the alloy effectively in the hot working and annealing process. After rolling, the dispersed α-Al (Mn, Fe) Si played the role of pinning dislocations and hindering the migration of grain boundary and sub-boundary. The alloy which processed by two-step homogenizing had finer grain size than the single homogenized sample. Besides, the amount of the precipitates increased with the content of Si in the process of homogenization. So the grain size of

the alloys decreased with the increasing of Si after annealing. The strengths of the two-step homogenized alloys were higher than those of the single homogenized alloys, as the dispersed precipitates plays an important role in the plastic deformation process.

C1-12: Additional Interface Strengthening in Aluminum Alloy Laminated Plate with Bimodal Distribution of Grain Size

Taiqian Mo, Zejun Chen, Chongqing University, China

The objective of the present study is to obtain aluminum alloy laminated plate with high yield strength and good ductility through a multiscale coarse/ultrafine-grained design, fabricated by the difference in recrystallization of constituent metals using different strain path and annealing processes. Experimental results showed that, with increasing annealing temperature, where pronounced grain coarsening of the 1100Al layers occurs, but for the 7075Al layers the change in grain structures is not obvious. The difference in recrystallization degree of two alloys results in the producing of the bimodal distribution of grain size in whole laminated plate. Moreover, in order to analyze the effect of strain incompatibility on the mechanical properties, laminated plates with different properties of constituent layers were comparatively studied. Results showed that the cross rolling, compared with direct rolling, give rises to somewhat more effective mechanical properties improvement after annealing treatment due to higher strain incompatibility across the interface. For the different processes, the difference in flow properties between the constituent layers plays an important role in interface strengthening mechanism. During tensile test, high density of geometrically necessary dislocations (GNDs) were observed to distribute in the interface due to the mechanical incompatibility across the interface. The high yield strength of the plate with multi-scale grain structure is attributed to back stress strengthening associated with the formation of geometrically necessary dislocations and the good ductility results from the high strain hardening rate during plastic deformation.

C1-13: Aging Behavior of Al-7%Si-0.3%Mg Casting Alloy Demolded at 473K in T5 Process at 473K

Keigo Muro, Taiki Tsuchiya, Seungwon Lee, Seji Saikawa, Susumu Ikeno, Kenji Matsuda, University of Toyama, Japan

Al-Si-Mg cast alloys are widely used in automotive industry to produce components and parts (i.e. engine cylinders) at lower cost. These alloys have excellent castability and good strength to weight ratio. Where dimensional accuracy is concerned, industrial Al-Si-Mg cast alloys (i.e. A357, A356) are in many cases performed T5 heat treatment (Artificial aging after casting). Artificial aging treatment is carried out at temperatures above ambient, typically in the range of 423~473K. The precipitates in Al-Si-Mg alloys is presumed to correspond with excess Si-type Al-Mg-Si alloys. The precipitation sequence of excess Si-type Al-Mg-Si alloys is known to be as follows:

S.S.S.S.→GP zones→β", Parallelogram-type→Type-A, Type-B, Type-C→β, Si

However, the correlation between the microstructures and hardness in Al-Si-Mg alloys have not been clarified. The casting was done using metal permanent Y-mold. The alloy was cooled in the mold as is. The demolding carried out at the temperature of 473K, then, Y-block was quenched into ice water. Specimens were taken from the mold bottom were used in this research. After casting, artificial aging was carried out at the 3 selected temperatures (423K, 473K and 523K). Micro Vickers hardness measurement was conducted using Mitutoyo HV-101 (load: 0.98N, duration time:15s). The microstructures were observed by OM (Olympus BX51M), SEM (HITACHI S-3500H) and TEM (TOPCON EM-002B operated at 120kV). SEM specimens were conducted deep etching. TEM specimens aged in a silicone oil bath at 473K were cut from the ingot by the precision cutter and thinned by the single jet electro-polishing technique. Electrolytes were 10% perchloric acid-ethanol solution and 25% nitric acid-methanol.

Micro Vickers hardness measurement of Al-7%Si-0.3%Mg alloy demolded and aged at 473K shows that reaches peak hardness at 6ks. TEM observation showed that the precipitate density around eutectic Si was lower Si in the case of aged at 473K for 6ks. The selected area electron diffraction (SAED) patterns were in agreement with Type-A precipitate and Si.

C1-14: Effect of Microstructure on Discharge Performance of Al-0.8Sn-0.05Ga-0.9Mg-1.0Zn (wt%) Alloy as Anode for Seawater Activated Battery

Zibin Wu, Haitao Zhang, Cheng Guo, Jing Zou, Ke Qin, Ban Chunyan, Jianzhong Cui, Northeastern University, China

The discharge behavior of Al-0.8Sn-0.05Ga-0.9Mg-1.0Zn (wt%) alloys in as-cast, homogenized and annealed states was investigated through potentiodynamic polarization, electrochemical impedance spectroscopy, galvanostatic discharge, and battery test in 3.5wt% NaCl solution. An influence mechanism of rolling process on anode discharge performance is proposed. Results suggest that the mechanism can explain properly that rolling and subsequent annealing improves the discharge properties of the Al-0.8Sn-0.05Ga-0.9Mg-1.0Zn (wt%) alloy. The results indicate that rolling and subsequent annealing can greatly improve the microstructure of the Al-0.8Sn-0.05Ga-0.9Mg-1.0Zn (wt%) alloy, thereby improving its electrochemical performance. The 400˚C annealed Al-0.8Sn-0.05Ga-0.9Mg-1.0Zn (wt%) alloy exhibits stronger discharge activity than the as-cast, homogenized and 150˚C annealed ones, attributed to more grain boundaries being activated as a reaction channel. The 400˚C annealed Al-0.8Sn-0.05Ga-0.9Mg-1.0Zn (wt%) alloy show higher anodic efficiency than the as-cast and homogeneous ones because of the more uniform distribution of Sn in the aluminum matrix.

Moreover, the discharge capacitance (2514.23 $mAh \cdot g^{-1}$) and anodic efficiency ((84.37 ± 0.72)%) of the seawater activated battery using the 400°C annealed Al-0.8Sn-0.05Ga-0.9Mg-1.0Zn (wt%) alloy is higher than those with magnesium alloys, and the peak power density (61.3$mW \cdot cm^{-2}$) of the battery is close to the seawater activated battery with pure Mg, Mg-Li-Al-Ce-Y and Mg-Al-Pb anodes.

C1-15: Residual Stress Analysis of 7075 Aluminum Billet with Cooling Rate

HwaYoung Woo, Sukcheol Kwon, Gyu-Seok Lim, Jong-Hyeon Lee, Chungnam National University, Korea

Aluminum alloys are widely used in many structural materials and industrial fields due to their high strength and corrosion resistance. The properties vary depending on the content and type of the alloy element, and aluminum alloys having suitable physical properties are used depending on the use. Among aluminum alloys, 7075 aluminum is a precipitation-hardening aluminum alloy containing zinc and magnesium as alloying elements, and has the highest strength. Especially, 7075 aluminum is used in aircraft structure, mold tools, gears and shafts, mechanical equipment and fixture where high strength and corrosion resistance are required. However, for precipitation hardening, internal residual stress due to cooling rate difference occurs in the process of quenching after solution treatment. This residual stress impairs the accuracy of the product during the subsequent processing and poses a risk of stability. In this study, Ansys simulation program was used to calculate the cooling rate of aluminum billet depending on the temperature of cooling media and the geometry. The residual stress was measured and compared with calculation data. The correlation between processing parameters and residual stress was mathematically derived. From the results obtained, we expect to reduce the cost of the process for removing residual stress by optimizing the machining parameters.

C1-16: Effect of Hydrogen on Age Hardening in Al-Zn-Mg Alloy Containing Low Zn/Mg Ratio

Kengo Takamoto, Artenis Bendo, Kazuyuki Shimizu, Taiki Tsuchiya, Seungwon Lee, Kenji Matsuda, Katsuhiko Nishimura, Norio Nunomura, Susumu Ikeno, University of Toyama, Japan; Hiroyuki Toda, Kyosuke Hirayama, Hongye Gao, Kyusyu University, Japan; Masatake Yamaguchi, Ken-ichi Ebihara, Mitsuhiro Itakura, Tomohito Tsuru, Japan Atomic Energy Agency, Japan; Susumu Ikeno, University of Toyama, Japan

7xxx series alloy (Al-Zn-Mg alloy) has a high strength compared to other Al alloys due to its good age hardenability. The precipitation sequence of this series alloy is known to be as follows:

S.S.S.S. → G.P.zone → η', T' → η, T

This series alloy also has problems about high stress corrosion crack susceptibility, it is considered that the cause is due to the propagation of hydrogen embrittlement. Behavior of the hydrogen embrittlement mechanism is revealing, but that in Al alloy isn't still completely understood. We propose that elucidating behavior of hydrogen in the alloy plays a major role for solving this problem. In this work, we use 2 types alloy which hydrogen charged Al-Zn-Mg alloy and not charged same alloy. We investigated the aging behavior and the type of precipitate of hydrogen charged sample and not charged by means of hardness tests and transmission electron microscopy (TEM) microstructure observations. We prepared Al-Zn-Mg alloy by casting. The chemical composition is Al-1.8mol.%Zn-3.5mol.%Mg. Solution heat treatment was conducted at 748K for 3.6ks, and then quenched in cold water. Hydrogen charging to the alloy was conducted by electron discharge machining. We call the hydrogen charged sample "EDM" and not charged sample "NoEDM". Micro-Vickers hardness was measured using Mitutoyo HM-101 (load: 0.98N, holding time 15s). TEM (Topcon EM-002B) observation was conducted under the accelerated voltage of 120kV.

The result that Micro-Vickers hardness test of aged at 393K, EDM had higher maximum hardness and shorter time to reach it compared with NoEDM. The results from selected area electron diffraction (SAED), both of EDM and NoEDM had the same diffraction spots reported as η', η_1, η_4, T' phases in Al-Zn-Mg alloys. And the TEM bright field image of EDM showed that it had more precipitation ratio of η' phase and less that of T' phase than NoEDM sample.

C1-17: Effect of Different Aging Treatments on Microstructure and Mechanical Properties of Extruded 7136 Aluminum Alloy

Huiyan Li, Yue Ma, Beijing University of Aeronautics and Astronautics, China

The retrogression and reaging (RRA) is an emerging hot treatment technology that addresses many classic shortcomings of more traditional aging treatment processes. In this work, the microstructure evolution of the extruded 7136 aluminum alloy under different aging treatments were investigated via optical microscopy (OM), scanning electron microscope (SEM) and transmission electron microscope (TEM). Meanwhile, the mechanical properties and conductivity of the alloy during the different aging were studied by tensile testing, hardness testing and electrical conductivity testing. When the number of RRA treatment was less than 3, matrix precipitates (Mpt) grew up moderately, while grain boundaries precipitates (GBP) gradually became coarser, and the width of the precipitate free zone (PFZ) increased. As a result, the electrical conductivity

increased gradually over the cycle times due to the decreased of the electron scattering centres which were closely related to the localized strain fields and the solute concentration in the matrix. 16.29% enhancement in conductivity was achieved after 3 RRA treatment. Furthermore, the fine GP zone and the η' phase in the crystal kept the ultimate tensile strength and hardness of the material at a high level (705MPa, 217HV). However, when the number of RRA treatment reached 4, the significantly coarsened matrix precipitates result in a dramatic decline in the tensile strength and hardness. The intrinsic mechanism of the influence of the multiple RRA treatment on the microstructure, mechanical property, and the electrical conductivity was discussed. RRA treatment on aluminum alloy was confirmed to be a simple and effective way to significantly improve the electrical conductivity while maintaining its tensile strength.

C1-18: Effect of Silicon Content on Age Hardening Behavior in Hypoeutectic Al-Si-Mg System Alloy

Satoru Ishihara, Hisao Kazuta, Seiji Saikawa, University of TOYAMA, Japan; Susumu Ikeno, Professor emeritus at University of Toyama, Japan

In the automobile industry, lightweight materials are needed to improve fuel economy. Especially Al-7mass%Si-0.3mass%Mg system alloy is widely used for aluminum die-casting alloys having excellent mechanical properties and castability. For these alloys, T6 heat treatment is applied for the purpose of improving the mechanical properties. However, there are few reports on age hardening behavior of Al-Si-Mg cast alloys, and the effect of Si content on age hardening behavior has not been known. In this study, the influence of Si content on the age hardening behavior of Al-Si-Mg based alloy was investigated by varying Si content from 4 to 10 mass%.

Alloys with target compositions of Al-4mass%Si-0.3mass%Mg, Al-7mass%Si-0.3mass%Mg and Al-10mass%Si-0.3mass%Mg were cast. Based on the target compositions, pure Al, Al-20 mass% Si and Al-10mass%Mg ingots were weighed and melted at a temperature of 993K with an electric furnace. After the melting, Al-10mass%Sr alloy was added to the melt in an amount of 0.012 to 0.015% in order to improve eutectic silicon structure and the Ar gas was supplied to the melt for the degasification. The melt was cast into a copper mold having a Y block shaped cavity, when the melt and the mold temperatures were 973K and 453K, respectively. After the pouring, when the temperature of the cast alloys decreased to 773K, the cast alloys were released from the casting mold and were immediately water-quenched. After the water-quenching, test specimens with dimensions of 10mm×12mm×2.5mm were cut out within 1.8ks from the obtained casting at room temperature. Solution treatment was carried out for 36.0ks at 813K. Vickers hardness was measured using a micro hardness testing machine under a load of 2.94N at a load time of 10s.

The microstructure of the as-cast alloys was consisted of primary crystallized α-Al and secondary crystallized eutectic phases. Amount of the eutectic phase increased with increasing Si content. In addition, the value of the age hardening ΔHV also increased with increasing Si content. It is considered that the amount of the area of the interface between the eutectic Si and the α-Al matrix phase influences the age hardening behavior.

C1-19: Effect of SiC Particles Addition on Morphology of Primary Si Crystal in Hypereutectic Al-Si Alloy

Masayuki Mizumoto, Takuto Hayashi, Satoru Nishikawa, Iwate University, Japan

Hypereutectic Al-Si alloys are applied to piston and cylinder block in engine due to their excellent abrasion resistance, high temperature strength and low thermal expansion. In the present work, the effect of SiC particles addition on the morphology of primary Si crystal in hypereutectic Al-Si alloy was investigated. SiC particles (mean particle size: 17μm) were added in the form of MMC (40vol% SiC particles/Al alloy composite). Hypereutectic Al-40wt%Si ally was melted and held at 1273K. MMC (1~10wt%) was added into the alloy melt and held for predetermined time. When MMC was added more than 5wt%, the morphology of primary Si crystal was changed from coarse needle-like to fine polygonal shape and the primary Si crystal size was decreased to less than half of that observed in the specimen without MMC addition. Most of SiC particles were attached on the primary Si crystals. These results suggest that SiC particles in MMC would act as nuclei for the crystallization of primary Si crystal. However, the Si crystal size was almost constant, even when MMC was added more than 10wt%. The many segregated SiC particles were observed in the microstructures of the specimens with more than 10wt% MMC addition. Thus it is suggested that the SiC particle segregation would result in the decrease of the number of effective nuclei. The Si crystal size was gradually increased with increasing the holding time and was increased to almost half of that observed in the specimen without MMC addition. It is considered that, although the SiC particle segregation would be promoted with increasing the holding time, the SiC particles were thermodynamically stable in the alloy melt and could act as nuclei.

C2. Light Metals and Alloys-Magnesium

Symposium Organizers:

Xianhua Chen, Chongqing University, China; Yoshihito Kawamura, Kumamoto University, Japan; Young Min Kim, Korea Institute of Materials Science (KIMS), Korea; Jian-Feng Nie, Monash University, Australia; Diran Apelian, Worceste Polytechnic Institute, USA

August 19-21, 2019

Place: Exhibition Area (3rd Floor)

C2-1: Effect of LPSO Template and Precipitation Behavior on Mechanical Properties in Mg-Y-Al Alloys

Qingchun Zhu, Yangxin Li, Yuxuan Liu, Huan Zhang, Xiaoqin Zeng, Shanghai Jiao Tong University, China

To date, the applications of Magnesium alloys are still limited due to their low strength, low ductility as well as low creep resistance. Magnesium alloys containing rare earth (RE) in conjunction with other alloying elements, such as Zn, have drawn increasing interest due to their high strength, high ductility and high creep-resistance with the existence of long period stacking ordered (LPSO) phases.

It is widely accepted that intragranular precipitates strengthen the matrix via impeding the movement of dislocations, and the magnitude of strengthening effect on the matrix strongly depends on the size, morphology and crystallography of precipitates. Since the LPSO phase is essentially periodic stacking faults that usually form on the basal plane, it is very difficult to achieve a significant improvement in strength by merely introducing dispersive LPSO precipitates at ambient temperature. In addition, it is well-know that LPSO phase exhibit high stability at elevated temperature, showing excellent pinning effect for grain boundaries. Meanwhile, the LPSO phase can obstruct the movement of <a+c> dislocation which can enhance the mechanical properties of magnesium alloys performing at high temperatures. Therefore, the combination of LPSO and other strengthening precipitates, such as the plate-shaped β' phase (c-axis base-centered orthogonal, a = 0.642nm, b = 2.224nm, c = 0.521nm) that forms on prismatic plane of α-Mg matrix, is believed to be a promising approach to achieve excellent mechanical properties both at the ambient and elevated temperatures.

In our work, superior thermal stability of refined grains was found in the Mg-11.7Y-1Al (wt.%) alloys at elevated temperatures. The observed 18R-LPSO phase, of which distribution can be controlled by solution treatment parameters, can pin the grain boundary and impede grain growth during solution treatment. After solution treatment at 550˚C for 16 hours, the LPSO phase was mainly formed at grain boundary. After solution treatment at 520˚C for 8h, the refined LPSO phase was uniformly distributed within the grains and formed a template with an average distance of 100 nm. The peak hardness was attributed to the precipitation of β' phase obtained during ageing at 225˚C for 10 days. The size of β' particles can be limited when they are formed between LPSO laths, which leads to an abnormal yield strength increase at elevated temperatures.

C2-2: Effects of High Strain Rate on the Microstructure Evolution of GW103K Magnesium Alloy

Huan Zhang, Yangxin Li , Qingchun Zhu, Yuxuan Liu, Xiaoqin Zeng, Shanghai Jiao Tong University, China

As the lightest metallic structure material, magnesium alloys have a large range of applications in automotive industry due to their low density and high specific strength. However, it is crucial for automotive components to withstand high strain rate impact without failure. As we all know, strain rate is an important factor for the deformation of magnesium alloys, which influences both dislocations and twinning modes. However, the deformation mechanism of magnesium alloys with high strain rates has not been thoroughly investigated yet, especially for magnesium alloys containing rare-earth (RE) elements.

In this work, the microstructure evolution of GW103K alloy with different conditions (T4 and T6) is investigated after high strain rate deformation by split Hopkinson bar (SHPB) at room temperature. A considerable amount of mechanical twins were observed both in the T4 and T6 GW103K alloys after SHPB treatment, where the {10-12}<10-11> extension twin and {10-11}-{10-12} double twin are commonly found in TEM and EBSD. In addition, a high density of stacking faults was found to be uniformly distributed both in the matrix and mechanical twins.

Magnesium alloys usually exhibit poor ductility with quasi-loading at room temperature. The activation of multiple twinning modes can effectively improve the plasticity because twins can accommodate the deformation along c axis. After SHPB deformation, the Vickers hardness was increased a lot due to the work hardening in both the T4 and T6 alloys. However, for the T6 alloy, the existence of β' phase limits the formability of high strain rate deformation and suppresses the occurrence of other twinning modes, compared with the T4 alloy under the same strain, where the unusual {11-21}<11-26> extension twin was also observed. In addition, a high density of <c+a> dislocations were activated. Therefore, multiple mechanical twinning modes and dislocation slip systems during the SHPB deformation lead to a better formability of the T4 alloy.

C2-3: Multi-Scale Study on Tensile Plastic Deformation Mechanism of Biaxially Separated Non-Basal Textured AZ31 Magnesium Alloy Sheet at Room Temperature

Yu Chen, Tu Jian, Hu Li, Tao Zhou, Chongqing University Of Technology, China

As to AZ31 magnesium alloy sheet fabricated by the conventional plastic processing technology, the poor deformability at room temperature results from its forming stable basal texture, and therefore its maximum deformation degree per pass in the process of rolling at room temperature has never exceeded 22%. However, in the present study, based on the technique of equal channel angular rolling continuous bending (ECAR-CB), AZ31 magnesium alloy sheet with the bimodal non-basal texture is fabricated, in which the basal poles are completely separated. As a result, its maximum deformation degree per pass in the process of rolling at room temperature has reached 32%, which illustrates that the unfavorable effect of basal texture on the deformability in the process of rolling at room temperature can be basically eliminated, and moreover the breakthrough with regard to bottleneck in the application of traditional wrought magnesium alloy is overwhelmed with expectation. However, deformation mechanisms of AZ31 magnesium alloy sheet with this kind of special non-basal texture are still not clear. Therefore, it is meaningful to investigate the relative deformation mechanism, from the macroscale, mesoscale, microscale and nanoscale perspective, by combining microstructure characterization experiment of materials and crystal plasticity finite element simulation, it shall be able to lay the theoretical and technical foundations for the industrial production of magnesium alloy sheet with perfect properties by means of exploring the basic laws of microstructure evolution of sheet inthe case of rolling at room temperature, analyzing the interaction mechanisms between dislocation and dislocation, between dislocation and twin, between twin and twin, between dislocation and grain boundary during rolling process of sheet at room temperature, establishing the crystal plasticity constitutive model in consideration of the synergetic interaction between dislocation and twin, revealing the deformation mechanisms of AZ31 magnesium alloy sheet with the bimodal non-basal texture in the process of rolling at room temperature.

C2-4: Effects of the Heat Treatment Conditions on the Creep Properties and Microstructure Evolution of Mg-10Gd-0.4Zr Alloy

He Qin, Guangyu Yang, Wanqi Jie, Northwestern Polytechnical University, China

Effects of the heat treatment conditions on the creep properties and microstructure evolution of Mg-10Gd-0.4Zr magnesium alloy under the applied stress of 80MPa and the temperature of 523K have been investigated by high resolution transmission electron microscopy (HRTEM) and high-angle annular detector dark-field scanning transmission electron microscopy (HAADF-STEM) in this work. It is found that the creep resistance of T4 and T6 state experimental alloys are much higher than that of the as-cast alloy respectively, which mainly owing to the coarse and unevenly distributed intergranular second phase in the as-cast alloy. It is also showed that the strain of T4 state alloy within the primary creep stage is larger than that of T6 state alloy due to the less precipitated phase. However, the steady creep rate of T4 sate alloy is lower than that of T6 state alloy. The main reason for this lies in the fact that the ellipsoidal β' precipitates gradually form and then grow into prismatic plates to enhance the creep resistance of T4 state alloy, and the formation and coarsening of β_1 and β phases at the expense of β' precipitates in T6 state alloy lead to the deterioration in creep resistance during the steady state creep stage.

C2-5: The Formation and Orientation of Static Recrystallization Grains in Mg-Zn-Gd Alloys

Lingyu Zhao, Institute of Metal Research, Chinese Academy of Sciences, China / University of Science and Technology of China, China; Hong Yan, Rongshi Chen, Enhou Han, Institute of Metal Research, Chinese Academy of Sciences, China

The formation of non-basal texture is reported to be associated with the recrystallization process in magnesium-rare earth alloys. The orientation and misorientation of static recrystallization (SRX) grain relative to the matrix in cold-rolled Mg-Zn-Gd alloys during annealing at 300~400˚C for 1h were investigated using electron backscattered diffraction method. Our results show that the orientation of SRX grains varies with SRX mechanism. SRX grains formed at grain boundary (GB) show random orientations. In addition, the misorientation between these SRX grains and matrix is mostly more than 50° . However, the orientation of SRX grain formed by sub-grain is near the matrix and the misorientation is less than 30° . Interestingly, a new way to form SRX grains is observed in this study. That is, many small sub-grains surrounded by short low angle GBs are in the original matrix grain. Then short low angle GBs transform into long low angle GBs which divide the matrix into several parts. With the transformation from long low angle GBs to long high angle GBs, these parts become new SRX grains at last. SRX grains formed by this new way show larger size than traditional SRX grains and similar orientation to the matrix (the misorientation is less than 35° .

C2-6: Bending Deformation Behavior of Mg-Y Alloy Single Crystals

Kenta Oka, Ryota Fukumori, Masayuki Tsushida, Hiromoto Kitahara, *Shinji Ando*, Kumamoto University, Japan

Magnesium has a hexagonal close-packed (hcp) structure with low symmetry, and the main slip and

twin systems of magnesium is basal slip and {10-12} twin, respectively. However, when the loading axis is perpendicular or parallel to basal planes, basal slips never occur geometrically. Also, when the loading direction is perpendicular to basal planes in compression tests, or parallel to basal planes in tension tests, {10-12} twinning does not occur. It is, therefore, known that the deformation behavior of magnesium shows strong orientation dependence. Here, bending deformation is a key process for producing various products from magnesium sheets. In bending tests, both tensile and compressive stresses simultaneously loaded in a specimen. Thus, bending deformation behavior is more complex, compared to that in tensile and compression tests. Therefore, bending deformation behavior of magnesium remains unclarified. In recent years, it has been reported that bending deformation behavior of pure magnesium single crystals shows strong orientation dependence. In this study, Mg-Y alloy single crystals with different crystal orientations and yttrium contents were prepared, and then they were subjected to three-point bending tests to investigate the influence of yttrium on the bending deformation behavior, ductility and strength. The composition of each specimen was Mg-0.07at%Y and Mg-0.15at%Y. Three-point bending tests were carried out at room temperature and the loading rate was 1.67×10^{-2}mm / s. Specimens whose neutral planes are parallel to (0001) and neutral axes are [11-20] deformed due to basal slips and showed gull-shape. Yield stresses were found to increase with increasing yttrium contents and to be determined by the shear stress loading on the basal plane. On the other hand, when the neutral planes are parallel to (1-100) and neutral axes are [11-20], the specimens deformed due to {10-12} twinning occurred in the compressive side and showed V-shape. It was also found that twinning also occurs in the tensile side of magnesium in three-point bending tests when yttrium was added.

C2-7: Microscopic Phase Structure of the As-Cast and the Peak-Aged Mg-Yb-Zn-Zr Alloy

Deping Zhang, Tohoku University, Japan / Changchun Institute of Applied Chemistry Chinese Academy of Sciences, China; Soo-Hyun Joo, Jing Jiang, *Hidemi Kato*, Tohoku University, Japan; Qiang Yang, Jian Meng, Changchun Institute of Applied Chemistry Chinese Academy of Sciences, China; Yaqin Zhang, Taiyuan Institute of Technology, China

Detailed microstructures of the as-cast and the peak-aged metal mould casting Mg-xYb-0.5Zn-0.4Zr (x = 0.5, 1, 2, and 3wt.%) alloys were thoroughly investigated. The results indicate that Yb has better grain refinement effect, solid solution strengthening effect and dispersion enhancement effect of precipitated phase under peak-aged on the Mg-Zn-Zr based alloys compared with the conventional rare earth elements such as Nd, Sm, and Gd, and the dominant intermetallic phase in the as-cast samples is Mg_2Yb, although with a few $Mg41Sm_5$ particles. In addition, the studied alloys also exhibit good aging hardening response when aged at 200˚C. During aging treatment, obvious precipitation of T phase formed on grain boundaries can be observed in the alloys with Yb is less than 2wt.%, while Mg_2Yb precipitate chains in the grain center and discrete Mg_2Yb particles homogeneously distributed near grain boundaries in the samples with Yb addition over 2wt.%. Under the same aging conditions, with the increase of Yb content, the type, size, shape, quantity and distribution of the second phase changed obviously. At the same time, the precipitate chains precipitated in the grain center can effectively prevent the grain dislocation slip, and the dispersed phase particles uniformly distributed near the grain boundary can pin the grain boundary and avoid the occurrence of grain boundary slip. The coexistence of the two phases results in the alloy having the most superior comprehensive properties at this time. Finally, ultra-fine needle-like precipitates were detected in all peak-aged samples, although with distinct difference on sizes and distribution densities. Based on energy dispersive spectrometer mappings of Mg, Yb, Zn and Zr and the SAED patterns, the needle-like precipitates were identified as g' phase (MgZnRE containing, hexagonal structure, a = 0.55nm and c = 0.52nm) and followed an orientation relationship as (1.0)g'||(11.0)Mg and [00.1]g'||[00.1]Mg.

C2-8: Effect of Y on Microstructure Evolution and Mechanical Properties of Mg-13Li-3Al Alloys

Lili Chang, Jing Guo, Shandong University, China

Mg-13Li-3Al (wt%) alloys with different amounts of addition Y were prepared by vacuum melting followed by hot-extrusion and annealing process. Microstructure evolution was characterized by using optical microscopy, scanning electrical microscopy, transmission electrical microscopy, X-ray diffraction and mechanical properties were examined by tensile test. The results indicated that the main phase constitutes of Mg-13Li-3Al ingots included β-Li、AlLi and $MgLiAl_2$. When Y was added in to Mg-13Li-3Al, Al_2Y was detected. Fine AlLi partiles located inside grain interior, blocky MgLiAl2 phases distributed along grain boundaries, while corase Al2Y clusters aggregated inside β-Li matrix. After hot-extrusion, an typical equiaxed grain structure was obserced, indicating dynamic recrystallization occuured during extrusion and the average grain size was in the range of 117~144μm. Except phases in the ingots, Mg17Al12 was characterized by XRD. The macrotexture results by XRD indicated a weak basal texture was formed in Mg-13Li-3Al due to hot-extrusion and the maximum intensity of basal texture was about 2. After annealing at 300 degree for 2h, compared to the parameters of mechanical properties, the ultimate tensile strength

was decreased due to softening while elongation at room temperature was enhanced. Mg-13Li-3Al withou Y addition exhibits a better comprehensensive mechanical properties with an ultimate tensile strength of 209MPa and a elongation of 31%.

C2-9: Microstructure and Corrosion Evolution of As-Rolled Mg-4Li-6AlSi Alloy(1221504)

Cheng Zhang, Liang Wu, Guangsheng Huang, Fusheng Pan, Chongqing University, China

The microstructure and corrosion evolution of the two hot-rolled alloys, Mg-4Li and Mg-4Li-6AlSi alloys (weight percent) were investigated. The microstructure and composition were carried out by using a X-ray fluorescence (XRF), an optical microscope (OM) and a scanning electron microscope (SEM) equipped with an Oxford electron backscattered diffraction (EBSD) system and also equipped with an energy-dispersive X-ray spectroscopy (EDS). The corrosion behavior was investigated by hydrogen evolution tests, weight loss tests and potentiodynamic polarization curves.
The grain size of the Mg-4Li alloy is relatively coarse, and there are a lot of low-angle grain boundaries which can provide the ability and nucleation points for further dynamic recrystallization. The grain orientation of the Mg-4Li alloy mostly tends to (0001) orientation while the grain orientation of the Mg-4Li-6AlSi alloy mostly tends to cone and cylinder direction, and the texture are mostly formed with the conical and cylindrical texture. Moreover, the addition of 6wt.% AlSi can achieve the effect of weakening and dispersing the texture of the base surface. For the Mg-4Li-6AlSi alloy, the dynamic recrystallization grain is the least, and the dynamic recrystallization tends to nucleate at the crystal. It is also easy to produce dislocation entanglement at the grain boundaries, and can also provide a nucleation point for dynamic recrystallization. In addition, the results of corrosion tests show that the Mg-4Li alloy has much better corrosion resistance compared with the Mg-4Li-6AlSi alloy. The hydrogen evolution rate of the Mg-4Li-6AlSi alloy was measured to be as high as 0.145 $mL \cdot cm^{-2}$, while the hydrogen evolution rate of the Mg-4Li alloy was 0.048$mL \cdot cm^{-2}$. The addition of 6wt.% AlSi results in the precipitation of Al3Li and Mg_2Si within the hot-rolled alloys by OM and EBSD, which precipitates as some small spherical particles. The increase of the corrosion rate might be attributed to the precipitation strengthening imparted by the Al3Li and Mg_2Si phases.

C2-10: Effect of Temperature on Deformation Behaviors of Mg-0.1at.%Y Alloy Having Various Grain Sizes

Kazuhiro Oki, Akinobu Shibata, Nobuhiro Tsuji, Kyoto University, Japan; Ruixiao Zheng, Kyoto University, Japan / Beihang University, China

Magnesium (Mg) alloys are drawing great interest as structural material because of its light weight and good strength-to-weight ratio. It is well known that addition of rare-earth, such as Yttrium (Y), improves strength and ductility even if the alloying amount is very small. Recently it was found that there is a strong grain size dependence of deformation mechanism in Mg-Y dilute alloy. On the other hand, testing temperature has been revealed to be very important parameter which affect the mechanical property of Mg alloys. However, these works were mostly carried out at elevated temperature with conventional coarse grain specimens. Therefore, the present study aimed to systematically investigate the effect of testing temperature on deformation behaviors of a Mg-0.1at.%Y having various grain sizes. Mg-0.1at.%Y alloy specimens with various grain sizes ranging from 0.4μm to several tens of micrometers were prepared by high pressure torsion (HPT) and subsequent annealing. Mechanical property of the specimens was examined by a tensile test at room temperature and -196˚C with an initial strain rate of $8.3 \times 10^{-4} s^{-1}$. Microstructures of the specimens before and after the tensile deformation were characterized by scanning electron microscopy (SEM), electron backscatter diffraction (EBSD) and transmission electron microscopy (TEM). At room temperature, the yield strengths obeyed a typical linear relationship (Hall-Petch relationship) when the grain size was larger than 1μm, and a clear softening from the Hall-Petch relationship was observed in the ultrafine grained (d < 1μm) specimens. However, the softening phenomenon was less pronounced at -196˚C, which was believed to be due to the inhibition of grain boundary sliding at low temperature. In addition, for a given grain size, the work-hardening rate (ds/de) at -196˚C was much higher than that at room temperature. EBSD observations of the tensile deformed specimens suggested enhanced activity of {10-12} deformation twinning at -196˚C, which seemed one of the reasons for the enhanced work-hardening rate. Furthermore, all the specimens tested at -196˚C showed premature fracture before achieving Considère plastic instability condition. Fracture surfaces of the specimens tested at -196˚C were almost covered by intergranular fracture patterns, especially in the coarse grained specimens. The fracture behavior will be furthermore discussed based on micro-crack observations using EBSD.

C2-11: Microstructure Observation of Mg-Zn-Ag Alloy Aged at 473K

Rie Kudo, Tomoyoshi Maeda, Taiki Tsuchiya, Lee Seungwon, Susumu Ikeno, Kenji Matsuda, University of Toyama, Japan

Several reports are available about precipitation hardening of Mg-Zn alloys. Nie et al. suggested the precipitation sequence of Mg-Zn alloy like: S. S. S. S. → G.P. zone → β_1'→ β_2'. The recent study showed Mg-Zn alloy combined trace addition of Ag has more aging effectiveness. C.L. Mendis et al and T. Bhattacharjee et al. However, nucleation sequence, crystal structure

and orientation relationship with a matrix of Mg-Zn-Ag alloy are not clearly revealed yet. In this study, Mg-Zn alloy and Mg-Zn-Ag alloy by detailed microstructure observant using high-resolution transmission electron microscopy (HRTEM) and the effect of added elemental has been investigated. Mg-2.2mol%Zn (2Zn) and Mg-2.2mol%Zn-0.2mol%Ag (2ZQ) were prepared by gravity casting. 2Zn alloy and 2ZQ were homogenized at 603K for 12h and at 653K for 48h , and alloys were undergone the hot rolling from 3mm to 1mm thickness, respectively. Then, samples were subjected to solution treated at 603K and 653K respectively for 1h using a quartz tube of argon atmosphere and quenched into water. Aging process was conducted using an oil bath at 473K. The mechanical property was investigated using Vickers microhardness measurement. Microstructure observation was conducted using TEM (transmission electron microscopy, TOPCON EM-002B) under accelerated voltage of 120kV. Thin foils were prepared by twin-jet electron polishing using a solution of nitro acid: phosphoric acid: methanol = 1.5 : 1.5 : 7. Microstructure observation was carried using HRTEM simulation used Mac Tempas X the multi-slice method. 2ZQ alloy showed higher the number of precipitation density than 2Zn. It is responsible for the higher hardness level of 2ZQ. TEM observation of peak hardness of 2ZQ indicated that dark contrast in mother phase is β_1' and β_2' of the precipitation in Mg-Zn alloy. The structure analysis was clear that the structure of β_1' is MgZn2 (C14 structure and C15 structure) and the structure of Mg_4Zn_7.

C2-12: Microstructure Observation of Mg-2.2at.%Zn Alloy Aged at 473K

Tomoyoshi Maeda, Graduate School of Science and Engineering for Education, Japan; Taiki Tsuchiya, Seungwon Lee, Susumu Ikeno, Kenji Matsuda, University of Toyama, Japan

General interest in Mg alloy is increasing due to its good mechanical properties as structural application. Zn addition can enhance room temperature strength by solid solution effect. Also Mg-Zn alloy can be strengthened by precipitation hardening by aging treatment using super saturated solid solution (S.S.S.S). Recent studies have revealed the structure and morphology of precipitates of Mg-Zn alloys, and the precipitation sequence of Mg-Zn alloy is suggested that like : S.S.S.S→G.P.zones→β_1'→ β_2'→ β. β_1' phase is considered as a reinforcing phase has a rod shape and parallel to the [0001] Mg direction of matrix. β_2' phase forms from β_1' and has plate shape on (0001) Mg plane of matrix.Recent work has reported that the Mg_4Zn_7 and $MgZn_2$ phases can coexist in β_1'. However, precipitation process, nucleation and growth process of precipitates are not completely known. In this study, Mg-2.2 at.%Zn alloy was prepared to observe the precipitation sequence.
In this study, Mg-2.2at.%Zn alloy was prepared to observe the precipitation sequence. This alloy was prepared by gravity casting. Homogenization was carried out at 603 K for 43.2ks, and the sample cut to a thickness of 3mm was hot rolled to 1mm. The solution treatment was performed at 603K, 3.6ks in an argon atmosphere and then quenched into water at 293K. Aging treatment was conducted at 473K. TEM specimens were prepared by twin jet electrolytic polishing method and then using a solution of nitric acid: methanol = 1: 3 cooled to 253 K. Microstructure observation was carried out using transmission electron microscope (TEM) Topcon EM-002B under accelerated voltage of 120kV. At the initial stage of aging of the Mg - 2 at.% Zn alloy, the structure observation and the HRTEM simulation were carried out, and the aging precipitation behavior of this alloy and the structure of the precipitate were investigated.

C2-13: Room-Temperature Tensile Behavior and Plasticity Improvement of Columnar Crystal Mg-Gd-Y Alloy

Shengshi Zhao, Northeastern University at Qinhuangdao, China; Xiaoping Lin, Northeastern University at Qinhuangdao, China / Northeastern University, China,

Columnar crystal Mg-xGd-0.5Y (x=3,6) with vertical grain boundaries and less lateral grain boundaries were prepared by directional solidification technique at a pulling speed of 50 μ m/s. Back scattered electron diffraction (EBSD) technology was employed to investigate the effects of columnar crystal growth orientation and grain boundaries on the room-temperature tensile behavior of the alloy. The results showed that in the Mg-3Gd-0.5Y alloy, the angle between the c-axis of the columnar crystal and the tensile direction (ie, the direction of temperature field) were 30° ~60° (A orientation, taking up about 60%) and 80° ~90° . (B orientation, taking up about 40%), and consequently the majority of grain boundaries were determined as A-A and the less ones were A-B. During deformation, the {101(—)2} tensile twins were preferentially activated at the A-oriented grain near the A-B grain boundary and expanded into the interior of the A grain. As the deformation continued, the {101(—)1} compression twins were activated in the B-oriented grains (near the A-B grain boundary) with a misorientation of 56° with the matrix. The {10-12} twins tended to be activated in the {101(—)1} compression twins, forming {101(—)1}-{101(—)2} double twins. The compression twins and double twins formed on both sides of the B-oriented crystal grains simultaneously expanded into the crystal, and stopped growing after colliding with each other. As the deformation continued, small angle grain boundaries stacked up near the twin boundary and A-B grain boundary, causing severe stress concentration, resulting in alloy fracture at ε = 13%.
In the Mg-6Gd-0.5Y alloy, the angles of the c-axis between the stretching axis were 30° ~60° , and the grain boundary type were identified as A-A. At

the early stage of deformation, the {101(—)2} tensile twins were activated on both sides of the A-A grain boundary and expanded into the crystal, turning the c axis to be perpendicular to the stretching direction (ie, B orientation). With the continuation of the deformation, the new orientation crystal with the same orientation with B undergone compression twinning and double twinning again (such as Mg-3Gd ~0.5Y) and eventually caused the material to break at ε = 36%.

C2-14: Dynamic Tension-Compression Asymmetry and Microstructure Evolution of Extruded EW75 Magnesium Alloy at High Strain Rates

Jincheng Yu, Wuxi Institute of Technology, China; Yuanding Huang, Helmholtz-Zentrum Geesthacht, Germany

The tension-compression asymmetry of extruded EW75 magnesium alloy deformed at high strain rates (from 1000s^{-1} to 3000s^{-1}) along extrusion direction (ED) were investigated by Split Hopkinson Tension Bar (SHTB) and Split Hopkinson Pressure Bar (SHPB). The specimens after dynamic tension and dynamic compression were examined with optical microscope (OM), scanning electron microscope (SEM), electron back-scatter diffraction (EBSD) and transmission electron microscope (TEM). The results show that extruded EW75 magnesium alloy along ED exhibits positive strain-rate sensitivity both in dynamic tension and dynamic compression. Due to the strong basal texture, extruded EW75 magnesium alloy exhibits a significant dynamic tension-compression asymmetry that dynamic compressive flow stresses are higher than dynamic tensile flow stresses. The dynamic tensile $\sigma_{0.005}$ at the strain rate of 3010s^{-1} is only 63MPa while the dynamic compressive $\sigma_{0.005}$ at the strain rate of 2826s^{-1} is 160 MPa (dynamic tensile $\sigma_{0.005}$ / dynamic compressive $\sigma_{0.005}$ = 0.39). The dynamic tensile σmax at the strain rate of 3010s^{-1} is only 271MPa while the dynamic compressive σ_{max} at the strain rate of 2826s^{-1} is 534MPa (dynamic tensile σmax / dynamic compressive σ_{max} = 0.51). Microstructure analysis demonstrates that {10-12 }<11-20 > tensile twinning causes the dynamic tension-compression asymmetry of extruded EW75 magnesium alloy along ED. High density dislocations, deformation twins and strong twin-dislocation interactions were observed in the TEM micrographs of extruded EW75 magnesium alloy under dynamic deformation at high strain rates. Dislocation pile-ups and twin intersections could increase the flow stress and strain hardening during dynamic plastic deformation. A kind of Nanocrystalline were observed after dynamic deformation. Fracture surfaces are relatively flat and significant amounts of deformed micro-dimples are produced during dynamic compression. It can be observed that this area consists of continuous tiny steps which suggests the dynamic compressive behavior of extruded EW75 magnesium alloy becomes more ductile at higher strain rate.

C2-15: Annealing Effect on Recrystallization and Grain Growth of Caliber-Rolled AZ31 Mg Alloys

Taein Kong, Byung Je Kwak,Taekyung Lee, Pusan National University, Korea

Mg alloys have recently attracted a great deal of interest for lightweight structural applications in the automotive industry due to their low density and superior specific strength. Researchers and engineers have made an effort to improve the strength and toughness to substitute other competitive metals. Although severe plastic deformation (SPD) processes, such as equal-channel angular pressing and high-pressure torsion, have been developed for this purpose, the applications are limited to the laboratory scale owing to a small product, low productivity, and necessity of additional heat treatment to recover ductility. Multi-pass caliber-rolling can be an alternative approach in the current situation. We fabricated a caliber-rolled AZ31 Mg alloy with a bulk dimension and satisfying mechanical strength. Tensile strength monotonically increased as the number of caliber-rolling passes was increased due to the grain-boundary strengthening. The 7-pass caliber-rolled alloy exhibited yield strength of 280MPa and with bulk dimension (~1m in length) for the industrial applications. Effect of annealing for this alloy at 473~673K and 10~360min were investigated in terms of recrystallization, grain growth, and mechanical characteristics. Increasing annealing temperature led to the reduction of strength in general as a result of grain growth. Though, the annealing at 473K resulted in a fine-grained structure (d ~ 2μm) and enhanced ductility with rarely decreased tensile strength. Such a mechanical enhancement was attributed to the inhibited activation of mechanical twins. In a coarse-grained AZ31 alloy, the tension loading perpendicular to the c-axis facilitates {10-11} contraction twinning and subsequent {10-12} extension twinning. These double twins degrade a ductility by dislocation pile-ups at twin boundaries. They were inhibited for the caliber-rolled AZ31 alloy annealed at the low temperature, since the caliber-rolling process increased the stress required for the onset of twinning. In conclusion, the inhibited mechanical twinning contributed to the enhanced ductility.

C2-16: Enhanced Yield Isotropy and Mechanical Strength of Caliber-Rolled ZK60 Mg Alloy

Byung Je Kwak, Taein Kong, *Taekyung Lee*, Pusan National University, Korea; Jeong Hun Lee, Korea Institute of Industrial Technology, Korea

Multi-pass caliber rolling, often called groove rolling, has attracted particular attentions for a recent decade since the report of 1600% increase in Charpy V-notch impact energy of a low-alloy steel caused by a ultrafine-grained

structure and nano-sized precipitates (Y. Kimura, T. Inoue, F. Yin, K. Tsuzaki, Science 320 (2008) 1057–1060). A recent study attributed the mechanical improvement via this process to its capability of imposing higher strain with more uniform distribution due to complex three-dimensional stress states. It is also worthwhile noting the industrial applicability of the caliber-rolling as the process is able to manufacture ultrafine-grained bulk products (T. Lee, M. Koyama, K. Tsuzaki, Y.-H.H. Lee, C.S. Lee, Mater. Lett. 75 (2012) 169–171; T. Lee, D.S. Shih, Y. Lee, C.S. Lee, Metals 5 (2015) 777–789), which had been difficult with conventional severe plastic deformation (SPD) processes including equal-channel angular pressing and high-pressure torsion. In spite of the importance of this process, studies on caliber-rolled Mg alloys have been focused only on Mg-Al-Zn alloys owing to the short history of research (T. Inoue, H. Somekawa, T. Mukai, Adv. Eng. Mater. 11 (2009) 654–658; A. Tripathi, S.V.S.N. Murty, P.R. Narayanan, J. Magnes. Alloy. 5 (2017) 340–347). This is the first report applying the caliber-rolling to a Mg-Zn-Zr alloy. The homogenized cast alloy was heated at 673K for 1 h and then subjected to the caliber-rolling process with a reduction of area of 84%. The material exhibited tensile yield strength (TYS) of 340MPa, ultimate tensile strength of 390MPa, and the total elongation was 18%. This is a marked increase in mechanical strength with preserved ductility compared to conventionally extruded ZK60 alloys. Interestingly, its compressive yield strength was nearly comparable to TYS, resulting in the yield point symmetry ratio of 0.99. We have analyzed such mechanical characteristics in terms of microstructural evolution.

C2-17: Effect of Extrusion Ratio on the Microstructure and Mechanical Properties of Mg-8Gd-4Y-1Zn-0.5Al Alloy Sheet

Han Ma, Yi Yao, Hao Zhang, Guangdong Institute of Materials and Processing, China / Xi'an University of Technology, China; Zhenghua Huang, Guangdong Institute of Materials and Processing, China; Zhongming Zhang, Chunjie Xu, Xi'an University of Technology, China

The microstructure, texture and mechanical properties of extruded Mg-8Gd-4Y-1Zn-0.5Al alloy sheet with different extrusion ratios (ER=9 and 22) were systematically investigated in the present paper. The two as-extruded alloy sheets are both composed of the fine dynamic recrystallized (DRXed) grains with random orientation, coarse hot-worked grains with strong basal texture, and the broken long-period stacking ordered (LPSO) structure and Mg4Y2ZnAl3 phase aligned along the extrusion direction. The broken LPSO structure and Mg4Y2ZnAl3 phase can promote dynamic recyrstallization (DRX) via particle stimulated nucleation mechanism during the hot-extrusion process. When the DRXed grains contact with the particles, the grain boundaries will be pinned by these particles and then prevent the growth of grains further. The distribution of LPSO structure and Mg4Y2ZnAl3 phase are more small and dispersive with ER of 22, which result in the fine average size of DRXed grains. Smaller grain size could reduce the slip distance of the dislocations, then release the stress concentration at the grain boundaries and improve the ductility of the alloy. Furthermore, the volume fraction of DRXed grains increases significantly with increasing the ER. Consequently, the maximum pole intensity of the extruded alloy sheet with higher ER is significantly weakened. As the ER increases, the ultimate tensile strength increases from 345MPa to 364MPa, and the elongation to failure obviously increases from 6.5% to 11.0%, which can be seen as a result of the weaker texture and fine grains. In addition, many deep dimples were clearly observed in fracture surface of higher ER alloy, showing significant ductile characteristics. The peak-aged alloy with ER of 22 during isothermal aging at 473K obtains the highest mechanical properties, with the ultimate tensile strength and yield strength of 438MPa and 348MPa, respectively. The improvement in strengthen is mainly ascribed to fine DRXed grains, coarse hot-worked grains with strong basal texture, and dense distribution of the fine β' precipitates in Mg matrix.

C2-18: Refining the Microstructure, Modifying the Texture and Enhancing the Toughness of AZ31B Alloy Rod by the Extrusion and Upsetting

Zhenghua Huang, Guangdong Institute of Materials and Processing, China; Yi Yao, Han Ma, Hao Zhang, Guangdong Institute of Materials and Processing, China / Xi'an University of Technology, China; Zhongming Zhang, Chunjie Xu, Xi'an University of Technology, China

Ultrafine grained (UFG) materials exhibit attractive mechanical properties including the high strength and good ductility. Severe plastic deformation (SPD) is an effective technique in fabricating bulk UFG materials. Some SPD methods, like equal channel angular extrusion (ECAE), multidirectional forging (MDF), and cyclic extrusion and compression (CEC), have been employed to prepare UFG magnesium alloy materials successfully, and change the texture. Based on the grain refinement and texture change, the mechanical properties including the strength and ductility of the processed materials can be enhanced significantly. Moreover, in recently several new SPD methods have also been proposed and employed successfully to prepare bulk UFG magnesium alloy materials, such as integrated forward extrusion and torsion deformation, repetitive upsetting (RU), accumulative back extrusion (ABE), and repetitive extrusion and upsetting (REU). However, the above-mentioned methods are complex,

expensive and hard to be industrialized. Therefore, the present paper will propose a simple, inexpensive and novel SPD method for grain refinement and texture modification, named extrusion and upsetting (EU), consisting of conventional direct extrusion (CDE) and upsetting.

AZ31B alloy rods with a diameter of 35mm were prepared by a novel severe plastic deformation method combined EU and CDE, respectively. The microstructure and texture of the rods were investigated by optical microscopy (OM) and electron back-scatter diffraction (EBSD). Meanwhile, the hardness, tensile and compressive mechanical properties, and impact toughness were tested. The results show that the totally fine dynamically recrystallized (DRXed) grains are obtained for the EUed specimen. However the CDEed specimen exhibits a bimodal microstructure comprising coarse elongated hot-worked grains and fine DRXed grains. Both of the specimen exhibit strong texture, however the types of texture are completely different. The (0001) basal plane is parallel to the extrusion direction (ED) for the CDEed specimen, while it is perpendicular to the ED for the EUed specimen. And the change in texture strongly influences the yield strength of the alloys. Due to the grain refinement and texture modification, the EUed specimen exhibits much better ductility, where the elongation increases from 13.5% and 41.0% for the CDEed specimen to 26.0% and 106.0% at room and elevated temperatures. Meanwhile, the corresponding mechanical anisotropy decreases from 0.47 to 1.21. EU is an effective and simple method to refine the grain size, modify the texture and enhance the elongation to failure of wrought magnesium alloys.

C2-19: In Situ Synchrotron X-Ray Total Scattering Studies of the Atomic Structures of Mg Alloys During Solidification

Shifeng Luo, Northwestern Polytechnical University, China / University of Hull,UK; Jiawei Mi, University of Hull, UK; Guangyu Yang, Wanqi Jie, Northwestern Polytechnical University, China

The atomic structures of Gd containing Mg based alloys during solidification were investigated in situ by synchrotron X-ray total scattering at the I15 beamline of Diamond Light Source, UK. The alloys were melted, contained and processed in a special designed quartz tube crucible which can effectively prevent samples from oxidation during experiments. The total scattering data were analysed using pair distribution functions. The research is focused on studying the atomic structures of Gd added Mg alloys and the different roles played by Gd, Nd and Zr elements in nucleating nanoscale crystals. In addition, anomalous X-ray scattering at the absorption edge of elements was also used to obtain the information of element partial atomic pairs with the aim of clarifying the contribution of each individual element on the formation of the short-range-ordered and medium-range-ordered atomic structures in the liquid state and immediately before nucleation occurs. Using the combined total scattering and anomalous scattering techniques, we are able to elucidate, for the first time, the atomic structures of multiple-component Mg alloys in liquid state and the effectiveness of Gd, Nd and Zr on nucleation. The research provides much more quantitative understanding on how to design novel and high performance Mg based alloys for critical engineering applications.

C2-20: Effect of the LPSO Content on the Mechanical Properties of As-Cast Mg-Ni-Y Alloys

Cheng Liu, Qun Luo, Qian Li, Shanghai University, China

In recent years, the ternary Mg–RE–X (RE: Y, Gd, Dy, Ho, Er, Tm or Tb; X: Zn, Cu, Ni or Co) alloys have attracted considerable attention due to the formation of long-period stacking ordered (LPSO) phase and excellent mechanical properties. In this work, the effect of LPSO phase content on mechanical properties of as-cast Mg-Ni-Y alloys were investigated. Four key alloys Mg96.0Ni1.2Y2.8, Mg92.3Ni2.0Y5.7, Mg91.2Ni2.4Y6.4 and Mg89.3Ni3.2Y7.5 (designated as1#, 2#, 3# and 4#) were selected based on the thermodynamic calculation. The microstructure and mechanical properties of the alloys were investigated by optical microscopy (OM), scanning electron microscopy equipped (SEM) with energy dispersive spectrum(EDS), X-ray diffraction(XRD) and tensile tests at room temperature (RT). The experiment results indicate that the four alloys are composed of α-Mg and LPSO phase. They exhibit typical cast microstructure of primary α-Mg dendrites and network LPSO phases. The LPSO phase contents of the four alloys are 15wt.%, 25wt.%, 35wt.% and 45wt.%, respectively. The EDS results indicate that the average chemical compositions of LPSO phase in 1~4# alloys are Mg90.41Ni4.33Y5.26, Mg91.57Ni3.44Y4.99, Mg91.85Ni3.43Y4.72 and Mg91.43Ni4.21Y4.36, respectively. Therefore, all of the network LPSO phases in 1~4# alloys might belong to 14H-type. The tensile tests at room temperature exhibit that the 1# alloy shows the optimal mechanical properties with the ultimate tensile strength of 222MPa and elongation of 10.5%. In order to investigate the influence of LPSO phase content on the mechanical properties, the fracture microstructure of the alloys was analyzed. There exist the small-size dimples which are distributed on the fracture surface of 1# and 2# alloys. However, the dimples disappear and large-sized cleavage facets and deep cracks dominate the whole fracture surface of 3# and 4# alloys. The results show that with the increasement of LPSO phases, the fracture mechanism of as-cast alloys transforms quasi-

cleavage fracture to cleavage fracture.

C2-21: Influence of Yttrium and Lithium on Activities of Non-Basal Slips of Magnesium

Keisuke Takemoto, Haruka Miyano, Hiroaki Rikihisa, Hiromoto Kitahara, Shinji Ando, Kumamoto University, Japan

Light weight and high specific strength, magnesium alloys has gained attention for use in transport industries. However, magnesium shows low ductility at room temperature. Not only {0001}<11-20> basal slips (BS) but also non-basal slips, such as {10-11}<11-23> first order pyramidal <c+a> slip (FPCS) or {11-22}<11-23> second order pyramidal <c+a> slip (SPCS) must be activated required to deform a crystal to any arbitrary shape. Therefore, controlling slip systems is a key to improving ductility of magnesium. However, details of slip systems and their influence by alloy element addition have yet to be elucidated. Rikihisa et. al. has reported that tensile tests of single crystalline and polycrystalline Mg-Y alloys were carried out at room temperature. Mg-(0.6~1.1)at%Y alloy single crystals yielded due to the FPCS. Yield stress and ductility of Mg-Y alloy single crystals and polycrystals were higher than those of pure magnesium. The number of grains where SPCS were activated was the largest in those where non-basal slips were activated in pure magnesium, while those where FPCS were activated was the largest in Mg-0.9at%Y alloy. High ductility of Mg-0.9at%Y alloy would be caused by activation of FPCS due to yttrium addition. And it was reported that critical resolved shear stress of SPCS was decreased when lithium added. However, details of activation of non-basal slip have yet to be elucidated in Mg-Li polycrystals. In this study, tensile tests of Mg-(0.5, 1.2at)Y alloy and Mg-6.2at%Li alloy polycrystals were carried out to investigate that influence of yttrium and lithium on non-basal slip systems and considered the relationship between ductility and yield stress of magnesium and activation of slip systems. Rolled Mg-Y alloy and Mg-Li alloy sheets were annealed to obtain grains with the sizes of approximately 60μm and cut into tensile specimens parallel to its rolling direction. Tensile tests were carried out at room temperature. In Mg-Y alloy polycrystals, the yield stress was increased with increasing yttrium addition. The ductility was 20% when yttrium content was 0.5at% and 0.9at%, however it decreased to 15% at 1.2at%. Slip lines of BS, FPCS, SPCS and PS were observed. The frequency of FPCS didn't change when yttrium content was 0.5at% and 0.9at%, however it decreased at 1.2at%. The frequency of SPCS decreased and PS increased with increasing yttrium content, respectively. In Mg-6.2at%Li alloy polycrystals, the ductility was slightly increased in comparison with pure Mg. The frequency of FPCS was increased, while those of SPCS and PS were not affected by lithium addition. These results indicate that to improve ductility of magnesium alloy require increasing totally frequency of non-basal slips.

C2-22: Effect of Ca, Y Addition on Recrystallization and Texture Evolution of Mg-Al Based Alloy Sheets

Young Min Kim, Su Mi Jo, Bong Sun You, Korea Institute of Materials Science, Korea

With respect to the improvement in the room-temperature formability of magnesium sheets, many researchers have carried out to investigate the modification of texture through the addition of alloying elements such as rare-earth (RE) elements (e.g. Ce, Nd, Y) and non-RE elements (e.g. Zn, Zr, Ca). Recently it was reported that the addition of Ca or Y into Mg-Zn based wrought magnesium alloys led to texture weakening by activating non-basal slip systems and twinning, which can resultantly improve the room-temperature formability. However, there were few reports that investigated the effect of Ca and Y addition on recrystallization behavior and texture modification of Mg-Al based alloys.
The present study aims at investigating the effect of alloying elements and process parameters on recrystallization and texture evolution of modified AZ31 magnesium alloys with Ca and Y addition subjected to a cold rolling and subsequent recrystallization annealing process. In this study, it was found that severely deformed structures such as shear bands formed during cold rolling could provide nucleation sites of new grains during annealing. Cold-rolled and annealed sheets showed much finer grain size and lower maximum intensity of basal pole, indicating better mechanical properties and formability. In addition, the studied alloys shows dramatically increased ignition temperature and corrosion resistance. Detailed analyses with EBSD and TEM on microstructural evolution and texture changes during annealing will be shown in this presentation.

C2-23: Pair Interaction Energy in Stacking-Faulted Mg Matrices and Formation Mechanism of Stacking Order in LPSO Mg Alloys

Taku Murakami, Nobuhisa Fujima, Toshiharu Hoshino, Shizuoka University, Japan; Mitsuhiro Takeda, Kazuya Konno, Sendai National College of Technology, Japan

Magnesium-Metal-Rare-Earth (Mg-M-RE) ternary alloys with the long-period stacking ordered (LPSO) phase have attracted much attention as new light-weight structural materials because of their high tensile strength, elongation, high heat resistance, and so on. In recent years based on these knowledges about LPSO materials, it is widely attempted to extend research targets to various Mille-feuille materials, which are consisted of hard layers and soft layers. In

order to develop more functional Mille-feuille candidate materials, it must be very important to understand the formation mechanism of LPSO structure, especially, why and how the in-plane and stacking orders of the impurity clusters are formed.
In this research, we calculate the pair-interaction energy (PIE) between two impurity elements, M-M, M-RE and RE-RE with M=Al, Zn and RE=Y, in Mg matrices with periodic stacking faults, namely, PIE through both hcp and fcc environments, by using first-principles calculation based on density functional theory (DFT). For the calculations, we use a unitcell, Mg1054i2 (i=M and/or RE), consisting of 22 layers of 4✓3 aMg × 4✓3 aMg rhombus to generate the stacking sequences of 10H, 14H, 18H and 22H in Ramsdell notation. Also, we investigate effects of the lattice distortion around the impurity elements in these stacking faulted structures. Through this work, we clarify the differences between impurity-impurity interactions in the Mg matrices with the periodic stacking fault and those in the pure hcp and/or fcc Mg. Finally, by comparing of the results in the cases of M=Zn and M=Al, we reveal how this difference contributes to the formation of long-range stacking order of LPSO structure and discuss the origin of the difference between the cluster ordering in Mg-Al-Y alloy and that in Mg-Zn-Y alloy.

C2-24: Corrosion Resistance and Super-Hydrophobicity of Poly(3-Aminopropyltrimethoxysilane)/Polypropylene Composite Coatings on AZ31 Magnesium Alloys

Zhaoqi Zhang, Shandong University of Science and Technology, China / Luoyang Ship Material Research Institute, China; Rongchang Zeng, Shandong University of Science and Technology, China; Cunguo Lin, Luoyang Ship Material Research Institute, China

Recently, there has been increasing attention given to magnesium (Mg) and its alloys for a number of applications in the automotive, aerospace and electronics industries by virtue of their low density, high strength-to-weight ratio, good castability and recycling potential. However, the high susceptibility to corrosion of Mg alloys has so far limited their widespread applications.
A super-hydrophobic Mg alloy surface was successfully fabricated via amino-silane (PAPTMS) pretreatment, and subsequently covered with a polypropylene (PP) film. The surface morphologies, microstructures and chemical compositions were investigated using FE-SEM, XRD and FT-IR. The corrosion resistance of the composite coatings was evaluated using the electrochemical and hydrogen evolution tests. The results indicate that the PAPTMS/PP composite coatings exhibited a good super-hydrophobicity with a water contact angle (CA) of 162 ± 3.4° . The current density (Icorr) from 4.9 ± 0.06 × 10^{-5}A·cm^{-2} to 9.08 ± 0.09 × 10^{-8}A·cm^{-2}, obviously, the Icorr of the PAPTMS/PP composite coatings decreased approximately three orders of magnitude compared to the substrate, suggesting that the PAPTMS/PP composite coatings can effectively protect the Mg alloy from corrosion. Additionally, a corrosion mechanism of the composite coatings were proposed and discussed.

C2-25: Microstructure and Deformation Behavior of Mg-9%Al Alloy Reinforced with in Situ Formed AlN Particles

Alireza Maldar, Jie Wang, Leyun Wang, Xiaoqin Zeng, Shanghai Jiao Tong University, China

Between the various in-situ composites fabrications, the gas bubbling is considered a promising method that reactive gases are bubbled into the melt and the reinforced particulates are formed during the reaction between the gas or its decomposition product and the melt or its alloying elements. In the present study, Mg-AlN composite has been fabricated by bubbling nitrogen gas into a molten Mg-9%Al alloy. The in-situ synthesis was done in a furnace with SF6/CO_2 protection and nitrogen gas with high purity (99.999%) bubbled into the melt through a rotating steel lancer for 1.5h. The molten alloy was then poured into a permanent mould. Mechanical properties were investigated by tensile and compression tests in as-cast, solutionized, and hot extrude conditions. The results confirm the formation and the uniform distribution of AlN phases in the alloy. Thus, the shape of β-Mg17Al12 phases were changed, and grain size of Mg-α has been changed due to presence of AlN particles. As results, higher ultimate tensile strength and higher fracture elongation were simultaneously improved for MgAl/AlN composites in solution and extruded conditions. However, the as-cast composite has a weaker mechanical properties in tensile conditions, which is due to the existence of the brittle β-phase that overcomes AlN particles effect.

C2-26: The Effect of Double Extrusion on the Microstructure and Mechanical Properties of AZ80RE Alloy

Qiyu Liao, Qichi Le, Northeastern University, China

The Mg-8.10Al- 0.42Zn- 0.51Mn- 1.52La- 1.10Gd (wt. %, AZ80RE alloy, RE=rare earth) alloy was subjected to double extrusion, and the influence of the double extrusion on the microstructure and mechanical properties of the extruded alloy was investigated. The secondary extrusion process could strongly refine the recrystallized grains and disperse the fine RE-containing phases. The second phase mainly composed of Mg17Al12, Al11La3 and Al3Gd. The fine dispersed particle could supply more available dynamic recrystallization nucleation sites with deformation zone. The ductility of the AZ80RE alloy was also promoted, due to the grain refinement and the basal texture

weakening. The texture weakening of the alloy after secondary extrusion was attributed to the lower yield stress at a higher pass number. The elongation was significantly prolonged from the initial 13.3% to 28.5% after secondary extrusion. The basal texture weakening slightly deteriorated the yield stress of the AZ80RE alloy. The yield stress was declined from 218MPa to about 172MPa after secondary extrusion. Furthermore, The secondary extrusion temperature has obvious effects on the microstructures and mechanical properties. The extrusion temperature is inversely proportional to the grain size and also inversely proportional to the elongation. The lower extruding temperature was beneficial for finer grains and better ductility.

C2-27: A Melt Processing for Fabrication of Carbon Nanotube Reinforced Magnesium Matrix Composite

Hailong Shi, Xiaojun Wang, Harbin Institute of Technology, Chian

Magnesium (Mg) is one of the lightest structural materials which possesses high specific strength, high stiffness as well as low density. The density of Mg is only 2/3 of aluminium, 2/5 of titanium, 1/5 of steel and only slightly higher than many polymers. It is therefore regarded as potential structural materials for structure lightening. However, the poor mechanical behavior of Mg limited its application. Fabrication of Mg matrix composites provides us with a solution to strengthen Mg while maintaining its low density. Carbon nanotubes (CNTs) are regarded as the ideal reinforcement for metal matrix composites because of their extremely high elastic modulus and strength as well as good thermal and electrical properties. Because CNTs have good compatibility with magnesium even at high temperature. It is necessary to study the melt processing for CNTs reinforced magnesium matrix composites. In our work, a melt processing which consists of mechanical stirring and ultrasonic vibration process was developed to prepare CNTs reinforced magnesium matrix composites, which realized uniform distribution of CNTs in the composites and simultaneous strength and ductile improvement compared with the matrix. Grain refinement and load transfer of the CNTs were attributed to the improvement of the mechanical properties of the Mg/CNT composite.

C2-28: Strain Hardening Behavior of Mg-Y Alloys after Extrusion Process

Chaoyue Zhao, Teng Tu, Chongqing University, China; Xianhua Chen, Fusheng Pan, Chongqing University, China / Chongqing Academy of Science and Technology, China; Zhu Luo, Chongqing University, China; Andrej Atrens, The University of Queensland, Australia

The strain hardening is an effective mode of enhancing mechanical properties in alloys. In this work, the strain hardening behaviors of Mg-xY (x = 1, 2, and 3wt.%) magnesium alloys after extrusion process was investigated and the strain hardening rate was obtained from true stress-true plastic strain curves testing by uniaxial tensile tests at $10^{-3}s^{-1}$. Results suggest that the as-extruded Mg-Y alloys are mainly composed of α-Mg matrix and a little second phase Mg24Y5. The average grain size reduces from 19.8μm to 12.2μm with the Y content adds from 1wt.% to 2wt.%. Nevertheless, when Y content reaches 3 wt.%, the grain size of Mg-3Y is 12.9μm, which is close to that of Mg-2Y. The strain hardening rate decreases from 883MPa to 798MPa at $(\sigma-\sigma_{0.2})$ = 40MPa, and Mg-2Y and Mg-3Y have the similar strain hardening response. Moreover, Mg-1Y shows an obvious ascending stage after the steep decreasing stage, which is mainly caused by the activation of twinning. The strain hardening behavior of as-extruded Mg-Y alloys is explained based on understanding the roles of the deformation mechanisms via deformation microstructure analysis and Visco-Plastic Self Consistent (VPSC) model. The variation of strain hardening characteristics with increasing Y content is related to the effects of grain size and texture.

C2-29: A High-Ductility Mg–Zn–Ca Magnesium Alloy

Teng Tu, Chongqing University, China

A new kind of Mg-2Zn-0.6Ca (wt%) alloy was fabricated by casting and hot extrusion as a high-ductility structural material. The as-extruded Mg-2Zn-0.6Ca alloy exhibits a superior elongation of ~30%, yield strength of 130MPa and ultimate tensile strength of 280MPa along the extrusion direction at room temperature. Microstructure, texture and tensile properties of the as-extruded Mg-2Zn-0.6Ca alloy were investigated in details. Hereinto, the fine and equiaxed grains was obtained in as-extruded Mg-2Zn-0.6Ca alloy and the average grain size was ~10μm in diameter. In addition, a small number of $Ca_2Mg_6Zn_3$ precipitates were formed in as-extruded Mg-2Zn-0.6Ca alloy with the average grain size of less than 1μm. Moreover, the as-extruded Mg-2Zn-0.6Ca alloy showed a texture intensity of 9.06, weaker than the texture intensity of 22.19 in as-extruded Mg-Zn alloy, because the addition of Ca to Mg-2Zn alloy can suppress the formation of basal texture by providing a random texture in the extrusion. The high ductility of as-extruded Mg-2Zn-0.6Ca alloy was attributed to three main reasons：the refined grains, a small number of $Ca_2Mg_6Zn_3$ precipitates and the weakened texture. Firstly, the refined grains of as-extruded Mg-2Zn-0.6Ca alloy lead to the increase in grain boundary and reduces the whole stress concentration, it is favorable for the

activation of non-basal slip near the grain boundaries at room temperature and improve ductility. Secondly, the number of $Ca_2Mg_6Zn_3$ precipitates is limited and the inhibition of dislocation movement by the second phase is weakened hardly, which is beneficial to the process of plastic deformation and improves ductility. Finally, the weakened texture can be beneficial to the enhancement of ductility, because the majority of grains in the tilted texture have an orientation favorable for both basal slip and tensile twins. Our study shed lights on the design of new Mg alloys with high ductility.

C2-30: Effect of Ultrasonic Melt Treatment on Corrosion of ZW61 Magnesium Alloy

Xingrui Chen, Qichi Le, Shaochen Ning, Ruizhen Guo, Northeastern University, China

Considering the excellent grain and phase refinement ability of dual-frequency ultrasonic field (DUF), this technology is employed to refine the quasicrystal-reinforced Mg-Zn-Y alloy (i.e. Mg-6%Zn-1%Y (ZW61)). Microstructural evolution, corrosion behavior and electrochemical behavior of cast ZW61 alloy with and without DUF treatment are investigated systematically. Results revealed that the DUF treatment can refine the α-Mg grain and the I-Mg3Zn6Y quasicrystals dramatically. The average grain size reduces from $568 \pm 51\mu m$ to $89 \pm 9\mu m$ after dual-frequency ultrasonic treatment. The I phase also become tiny and has a homogeneous distribution. Consequently, the corrosion resistance is improved as well, showing the decrease of corrosion rate from 5.29mg/cm^2/day to 2.22mg/cm^2/day after dual-frequency ultrasonic treatment. The corrosion potentials and corrosion current density are reduced after dual-frequency ultrasonic treatment. Based on the microstructure observation, the corrosion process of untreated ZW61 alloy can be divided into three stages, namely, the galvanic couple corrosion, the filiform corrosion and the pitting corrosion. However, the dual-frequency ultrasonic treatment can prohibit the filiform corrosion. It is also found that the dual-frequency ultrasonic treatment can increase the solid solubility in grain boundary of Mg matrix. Thus, the increase of segregation of solute Zn element at grain boundaries, the morphology change of I-phase and the prohibition of filiform corrosion should respond the promoting of corrosion resistance.

C3. Light Metals and Alloys: Ti and Others

Symposium Organizers:

Yongqing Zhao, Northwest Institute for Nonferrous Metal Research, China; Yoshihito Kawamura, Kumamoto University, Japan; Young Min Kim, Korea Institute of Materials Science (KIMS), Korea; Jian-Feng Nie, Monash University, Australia; Diran Apelian, Worceste Polytechnic Institute, USA

August 19-21, 2019
Place: Exhibition Area (3rd Floor)

C3-1: Effect of β Annealing on the Microstructures and Mechanical Properties of TC18 Alloy *Chaohua Li*, Weiwei Zheng, Feng Zhang, University of Science and Technology Beijing, China

TC18(Ti-5Al-5Mo-5V-1Cr-1Fe) titanium alloy is a new type of α+β high strength titanium alloy. The strength of the alloy after annealing is 1100MPa, which is one of the highest strength titanium alloys in the annealed state. The microstructure characterizations such as the size, content and distribution of the constituent phases are very sensitive to the heat treatment and processing parameters, which directly affect the final mechanical properties of the alloy. In this paper, microstructure characterizations after a series of different annealing heat treatment processes were quantitatively investigated by using SEM, and TEM, and the mechanical properties at room temperature corresponding to different microstructures were tested. The results showed that during the primary annealing process, the volume fraction of α plates increased with the decrease of the intermediate temperature and the increase of the holding time. The length of the α plates, the thickness of α plates in β grains and the width of the grain boundary α plates all increased with the holding time. Furthermore, the width of the grain boundary α plates was always greater than the thickness of α plates in β grains. Increasing the intermediate holding time of the primary annealing could only improve the strength slightly and had almost no effect on the plasticity. During the secondary annealing, the secondary acicular α phase precipitated from the metastable β phase retained during the primary annealing process, the annealing twins appeared in the α plates formed during the primary annealing process, the thickness of the α plates decreased and spheroidization of α phase occurred simultaneously. The volume fraction of α plates had the greatest influence on tensile property and fracture toughness. The larger the volume fraction, the higher the strength and the lower the crack growth rate. Fine secondary acicular α phase could significantly improve the strength, and had little influence on the fracture toughness, but led to obvious decrease of the plasticity. Therefore, the mechanical properties of the TC18 titanium alloy could be improved by controlling

the intermediate holding temperature in the primary annealing process.

C3-2: Effect of Strain Rate and Temperature on Compressive Behaviour of TiAlMn Alloy

Lihong Su, University of Wollongong, Australia; Dong Ruan, Guoxing Lu, Swinburne University of Technology, Australia; Huon Bornstein, Defence Science and Technology Group, Australia

TiAl based alloys have been considered novel light-weight structural materials due to their advantages of low density, high specific strength, good oxidation resistance and creep resistance at elevated temperature. This research investigates the compressive behaviour of Ti-45Al-8Mn alloy subjected to compressive loading at various strain rates and temperatures.

Room temperature compressive stress strain curves showed characteristics of a typical compression curve of brittle materials showing marked failure. At a strain rate of 0.001/s and room temperature, the specimen fractured at a strain of approximately 30% and shattered into pieces. Cross-sectional microstructure and fracture surface characterisation indicated that there was no plastic deformation for the tests at room temperature. At 600˚C and the strain rate of 0.001/s, the stress of the specimen was higher than that at the room temperature. Obvious plastic deformation could be observed in the specimen as well as large amount of micro cracks. At 800˚C and above, the shape of the stress strain curve showed characteristics of compression curve of ductile materials. Microstructure observation indicated occurrence of plastic deformation and phase transformation. Fracture was not observed for the tests at 600˚C and above.

At high strain rates above 1000/s, the flow stress increased compared to the low strain rate for the tests at room temperature, and it increased with increasing strain rate, which indicates that there was a slight strain rate hardening effect. At elevated temperature and high strain rate, the flow stress decreased compared to that at room temperature with similar strain rate levels and the stress reduced with increasing testing temperature.

It can be concluded from the results that the Ti-45Al-8Mn material is intrinsically brittle. At 600˚C , the material showed higher stress and better ductility than room temperature, indicating that the material may be more suitable to be used at elevated temperature.

C3-3: Lattice Deformation and High Temperature Oxidation Behavior of Ti-6Al-4V Alloy Powders Prepared by Heat Treatment under Ar+H_2 Atmosphere

Gye-Hoon Cho, Jung-Min Oh, Jae-Won Lim, Chonbuk National University, South Korea

Developments in the 4th industry and 3D printing technology have raised interest in powder metallurgy products. The advantage of powder metallurgy is that can easily produce high melting point metallic products. In addition, it is possible to decrease waste of raw materials by reducing scraps occurrence. Accordingly, the use of titanium and titanium alloy powders is also gaining attention. Ti and Ti alloys are one of materials used throughout the industry because of its high strength and excellent corrosion resistance. In particular, they are a major material for artificial bones and implants due to their biocompatible properties. Recently, because of the development of 3D printing technology, complex shapes of artificial bones can be processed. As a result, the demand for Ti and Ti alloy powders is increasing significantly.

The problem of powder metallurgy is that the mechanical properties of final products are lower because the density is not perfect. In addition, the oxygen contents of powders has a large effect on the final density. Therefore, recent trends are toward lowering oxygen contents and increasing the density of final products.

In the present work, new heat treatment that dissolve hydrogen was developed without forming hydride. Dissolved hydrogen will have a good effect on sintering properties such as oxidation resistance and green density. In the experiment, commercially available Ti-6Al-4V alloy powders were used. The powders were annealed using tube furnace in argon atmosphere at 700˚C and 900˚C during 120min. Hydrogen was injected temporarily during argon annealing to dissolve hydrogen, and continuously a dehydrogenation process was performed in argon atmosphere. The prepared powders were analyzed by X-ray diffraction and gas analysis, and confirmed that hydrogen was dissolved. Hydrogen was first solubilized on the beta phase and expanded the beta phase’s cell volume. The dissolved hydrogen contents were determined by the temperature. TGA analysis was carried out to evaluate the oxidation resistance, and it was confirmed that hydrogen dissolved Ti-6Al-4V alloy powders improved oxidation resistance than the raw material.

C3-4: Influence of Cutting Oil on the Scraps During Ti-30Fe Ingot Preparation

Suhwan Yoo, Chonbuk National University, South Korea

Mechanical and chemical properties of titanium alloys with high strength, stiffness, toughness, low-density and good corrosion resistance at various temperatures enable weight reductions in aerospace structures and other high performance applications. Ti is used in not only aerospace but also daily products like glasses frames, golf club, tennis racket, bicycle and wrist watch. Furthermore Ti is used in implant. Despite having great properties, it has difficult processability. Because Ti

is hardly formable, it generates a lot of scraps during processing. Various researches are under way to recycle this scraps. As a part of this, the use of Ti deoxidation additive in steel making process can be mentioned. The Ti deoxidizer is used as a substitute which can avoid the effect of nitrogen aging of Al deoxidizer in the steel making process. The Ti deoxidizer used at this time is required to be grade B or higher according to the ASTM standard. In this paper degreasing process of Ti scraps and making CP Ti-30Fe ingots are discussed. For degreasing process, the variables of solution concentration and temperature were set for optimization of cleaning conditions. And then, in order to analyze the influence of cutting oil adhered to Ti scraps, Ti scraps were degreased with NaOH with Tetrasodium Pyrophosphate(TSPP). To further see the influence of stirring, Ti scraps were agitated in NaOH aqueous solution and TSPP as additive to variable to remove cutting oil by washer. Two types of washers are used: Ultra-sonic washer, simple stirring washer. CP Ti scraps and CP Ti scraps degreased in NaOH with TSPP with washer were investigated. Thereafter, a Ti-30Fe ingot was prepared by washed Ti scraps and pure electrolytic iron. The washed Ti scraps and pure iron are melted in vacuum arc melting furnace. The influence of cutting oil on the Ti scraps during Ti-30Fe ingot preparation was investigated.

C3-5: Influence of Mo to Fe Ratio on Heat-Treatment Effects in Ti-Mo-Fe Alloys

Masahiko Ikeda, Masato Ueda, Yuka Sakai, Kansai University, Japan

Iron (Fe) is a typical impurity in titanium (Ti) and its alloys, and its maximum acceptable concentration is limited because of its detrimental effect on the mechanical properties of the alloy. However, Fe has recently been adopted as an alloying element for Ti due to its lower cost than other beta stabilizing elements and its high abundance. In beta Ti, Fe undergoes abnormally fast diffusion, in contrast to the typical beta stabilizing element molybdenum (Mo), whose diffusion coefficient is lower than other beta stabilizers at the same temperature. Since the diffusion coefficient for Fe is almost two orders of magnitude greater than that for Mo, it is of interest to study the effects of co-addition of both Fe and Mo during heat treatment. Therefore, the Fe and Mo content was varied while keeping the ratio of the number of valence electrons to the number of atoms fixed, and the effects of heat treatment on these alloys was investigated based on electrical resistivity, Vickers hardness, and X-ray diffraction (XRD) measurements. The XRD results indicated that in all heat-treated specimens, only the beta phase was present. The resistivity at both room temperature and liquid nitrogen temperature decreased with increasing Mo content, as Fe was substituted by Mo. The temperature dependence of the resistivity was negative. During aging tests, the time until the initiation of precipitation increased with increasing Mo content. Details of the heat treatment results will be presented at the conference.

C3-6: Optimization of both Composition and Manufacturing Process for α-Type Titanium Alloys and Their Characterizations

Xilong Ma, Kazuhiro Matsugi, Zhefeng Xu, Yongbum Choi, Hiroshima University, Japan; Jie Hu, Xingang Liu, Hao Huang, Yanshan University, China

α-type titanium alloys which contain α stabilizers such as aluminum, zirconium and tin were widely used for chemical and cryogenic applications, as well as building materials of offshore drilling. New designed α-type titanium alloys were proposed with both electron parameters (bond order (Bo) and d-orbital energy level (Md)). The contour lines estimating the ultimate tensile strength (σ_{UTS}) values could be indicated by connecting the reported α-type titanium alloys in the Bo-Md diagram. The practically alloy Ti-5Al-2.5Sn showed 750MPa and 15% in the σ_{UTS} and fracture strain (ε_f), respectively. These values and its hot corrosion resistance were used as objectives. New designed alloy Ti-5Al-4Zr-3.6Sn (Md: 2.422, Bo: 3.430) and Ti-6Al-1.7Sn-1.3Zr (Md:2.422, Bo:3.487) were proposed on the basis of the contour lines. The Ti-6Al-1.7Sn-1.3Zr alloy had both same Bo and Md values as those of reference alloy Ti-5Al-2.5Sn. Three α-type alloys were produced by the cold crucible levitation melting (CCLM) technique as the single manufacturing process, which cooling solidification rate were controlled by adjusting its magnitude of current. The single α phase with size of 800μm was identified in three α-type alloys. The homogeneous microstructures were observed in three α-type alloys, which was attribute to the effect of CCLM. The σ_{UTS} and εf values were shown on Ti-5Al-4Zr-3.6Sn alloy: 801MPa, 16% and Ti-6Al-1.7Sn-1.3Zr alloy: 695MPa, 15%, respectively. Their values were improved compared with those of reference alloy: 598MPa, 15%. In contrast, the hot corrosion results at as-cast condition showed the ratio of weight loss of Ti-5Al-4Zr-3.6Sn, Ti-6Al-1.7Sn-1.3Zr and Ti-5Al-2.5Sn were 3.86%, 4.15% and 4.85%, respectively. The results of σ_{UTS}, ε_f and hot corrosion resistance were achieved by new designed alloy Ti-5Al-4Zr-3.6Sn, which meant the new designed alloy Ti-5Al-4Zr-3.6Sn was a possible potential material even at as-cast condition for practical applications.

D.Advanced Processing of Materials

Symposium Organizers:

Wanqi Jie, Northwestern Polytechnical University, China; Jianguo Li, Shanghai Jiaotong University, China; Hideyuki Yasuda, Kyoto University, Japan; Myoung-Gyu Lee, Seoul National University, Korea; Huijun Li, University of Wollongong, Australia; Dan Thoma, University of Wisconsin- Madison, USA

August 19-21, 2019
Place: Exhibition Area (3rd Floor)

D-1: An Experimental Study of Surface Properties in Ultrasonic Vibration Assisted Grinding

Zhihua Li, Kan Zheng, Wenhe Liao, Nanjing University of Science and Technology, China

Ultrasonic vibration assisted grinding (UVAG) technology has been applied to fabricate hard-to-machine materials due to its excellent advantages compared with ordinary grinding (OG), such as low cutting force, fabulous material removal rate and so on. However, the surface properties in UVAG in different cutting parameters and vibration parameters are still not clear. Thus, in order to investigate the effect of ultrasonic vibration on surface properties, a series of experiments in UVAG and OG are conducted in this paper. A three-dimensional (3D) surface roughness parameter Sa is introduced to evaluate the surface quality machined by UVAG and OG in different cutting conditions. Surface topography and profile are observed to verify surface properties of UVAG, compared with OG. The results show that Sa in UVAG is lower than that in OG in the same cutting condition because ultrasonic vibration is introduced. Sa has the opposite trend between UVAG and OG as spindle speed increases. With feed rate rising from 40mm/min to 50mm/min, Sa has little changed. Sa in OG presents an upward trend when cutting depth is from 5μm to 15μm, while there is no significant different in UVAG. When ultrasonic power ratio increases from 0% to 100%, it can be seen Sa is smaller if ultrasonic vibration is introduced. Besides, from the results of surface topography and profile, it shows that regular structure can be found on the surface machined by UVAG, while a great deal of large defect formed by pre-processing is remained on the surface machined by OG. Therefore, ultrasonic vibration assisted grinding can reduce the impact of pre-processing on surface quality. In summary, surface roughness Sa can be improved by introducing ultrasonic vibration. At the same time, the impact of pre-processing on surface quality can be reduced. Thus, this study can act as a reference for further understanding ultrasonic vibration assisted grinding technology.

D-2: Optimization of Multifunction Cavitation Technology for Development of High-Temperature and High-Pressure Bubble Generation

Ijiri Masataka, Tokyo Denki University, Japan; Shimonishi Daichi, Nakagawa Daisuke, Yoshimura Toshihiko, Sanyo-Onoda City University, Japan

Multifunction cavitation (MFC) combines ultrasonic cavitation technology and water jet peening (WJP) technology. In this processing technique, it has been reported that the residual stress necessary for improving the fatigue strength on the pure Al surface is large, whereas the amount of surface scraping by this processing is small. Moreover, improvement of the corrosion resistance of the surface of Al-Cu alloys has been reported. In the development this technology, it has been clarified that varying the cycle of ultrasonic waves influences the improvement of the corrosion resistance and residual stress of the surface of MFC-processed Cr-Mo steel specimens. This suggests that the state of the cavitation bubbles generated by the water jet (WJ) nozzle has changed. However, the cause of the cycle of ultrasonic waves in cavitation bubbles cannot be clarified. Furthermore, when the ultrasonic output is increased, the temperature in the cavitation bubbles increases, and as the machining progresses, diffusion decarburization accelerates on the Cr-Mo steel surface. It is reported that this diffusion decarburization does not occur uniformly on the surface but only sparsely. Other cases, it has been suggested that in addition to the frequency of the ultrasonic wave, the inner wall of the reactor, which reflects the ultrasonic wave, also influences the physical parameters inside of the cavitation bubbles. In fact, it has been reported that the change in the resonance state in the reactor varies with the water surface height and water temperature even if the frequency is held constant. Thus, a wide range of influencing factors must be considered when assessing the governing mechanisms of this technology. In this study, to improve the efficiency and accuracy of MFC technology, the dependence of the surface condition, residual stress, and surface roughness on the distance from the water jet nozzle (standoff distance) to the specimen surface were evaluated.

D-3: Formability of Corrugated Cup by Deep Drawing (1222601)

Harada Yasunori, Nishikubo Yuki, University of Hyogo, Japan

In the present study, corrugated cup having concavo-convex shapes were formed to enhance the functionality of drawn cup. Deep drawing, which is one of press processing, is known as the most severe three-dimensional forming process. It is a technology to make a seamless hollow three dimensional casing from one

sheet. There are various types and shapes of products made by this processing technology. For example, there are living goods such as aluminum cans and dishes, and industrial goods such as automobile parts and motor cases. As described above, deep-drawing containers are used in various fields, so improvement in functionality of containers themselves is required. There are technologies such as embossing and thickening of thickness as functional improvement. However, there are few processing methods that improve the functionality of cup only by deep drawing. In this study, the drawability of the corrugated cup was investigated by the deep drawing process. In the experiment, the materials were commercially extra-low carbon steel SPCC and austenite stainless steel SUS304. The initial thickness of the sheet was 0.2 to 0.5mm in thickness. The blank diameter is 70mm or more. The special die was used to enhance the functionality of the drawn cup. To form the corrugated surface at the side wall of the cup, the die has a groove in the shoulder part, and a steel ball is arranged in the groove. In addition, the balls rotate freely during forming. The steel ball is a bearing steel SUJ2 having a diameter of 10mm. The blank is formed into a cylindrical cup by means of a punch that presses the blank into the die cavity. The lubricant used was the solid powders of molybdenum disulfide. The deep drawing process was performed using an oil hydraulic press at a forming speed of about 10mm/min. In the drawn cup, to evaluate the formability of the cup, its height and diameter were measured. Hardness distribution and plate thickness strain distribution were also measured. The formability of the corrugated cup was good. There was no fracture of wall cracks and bottom cracks. In the side wall portion of the drawn cup, the interval between the convex portions was about 8.5 mm. The height of the container of the corrugate was lower than that of the drawn cup formed by conventional processing. The decrease rate was about 15%. The drawn cup was work hardened by plastic deformation. In the side wall of the drawn cup, the hardness distribution was wavy. Hardness showed high values at convex portions. By using a die with steel balls, it was found that the corrugated cup could be formed.

D-4: Interaction between Bubbles and Intermetallic Compounds in Heating Al-Mn Alloy

Wenquan Lu, Shanghai Jiao Tong University, China

In contrast to solidification process, the microstructure evolution of Al-Mn alloy has its peculiarity during heating process and can take complex pathways in response to compositions and processing conditions. Due to opacity and high temperature of alloy melts, the behaviors of bubbles and intermetallic compounds (IMCs) as well as their interaction in Al-Mn alloy during heating still remain lack of information and are poorly understood. Here, using synchrotron X-ray radiography, we provide direct visualization of the microstructural evolution in heating Al-5wt.% Mn and Al-10wt.% Mn alloy. IMCs can act as bubble nucleation sites and deform bubble shape. The bubbles mainly present three kinds of shapes with increasing temperature and finally changed to ball shape. Not all of bubbles grow, some ones gradually became smaller or even disappeared. There are two different reasons for bubble growth, bubbles aggregation and the hydrogen distribution around bubbles, while bubble annexation and hydrogen bubble dissolution result in bubble shrinkage. As the continuous heating process is not in an asymptotically stationary state, the behavior of group bubbles in heating Al-Mn alloy cannot be described by Ostwald ripening model. And this reason for inconformity with the Ostwald ripening model is different with that in solidifying Al-Bi alloy, where Bi atoms segregated at bubble/liquid interface and then change the bubbles size distribution. The bubbles have great effect on IMCs dissolution, i.e. the dissolution rate of IMCs changes with changing bubbles volume, and the IMCs around bubbles completely dissolve in matrix melt prior to those which are far away from the bubbles. Bubble collapse can promote the growth of the surrounding bubble, and it has a greater influence than the IMCs dissolution on the bubble growth. We also found that the variation of the IMCs area with time can be described by a logistic population model.

D-5: Hydrogen Storage from Crystal Water via Regeneration of Sodium Borohydride

Liuzhang Ouyang, Min Zhu, South China University of Technology, China

In the early 2000s, sodium borohydride ($NaBH_4$) emerged as a promising hydrogen storage material for proton exchange membrane fuel cell (PEMFC) and direct borohydride fuel cell (DBFC) systems with a theoretical gravimetric hydrogen storage capacity of 10.8wt.%, excellent hydrolysis controllability and high hydrogen purity. But, after a 10-year effort, the United States DOE recommended a no-go decision on $NaBH_4$ based on its low effective gravimetric hydrogen storage capacity, high cost and the inefficiency for recycling its hydrolysis by-product ($NaBO_2$). Overall, reducing the regeneration costs and increasing the hydrolysis yields are two critical targets for the commercial utilization of $NaBH_4$. Recently, the regeneration of $NaBH_4$ was actualized via a reaction between $NaBO_2$ and MgH_2 by ball milling with the maximum yield being 76%, but the real hydrolysis by-product of $NaBH_4$ is $NaBO_2 \cdot xH_2O$ and expensive MgH_2. In this study, based on the substitution of expensive MgH_2 with cheap Mg base alloy or compound and $NaBO_2$ with $NaBO_2 \cdot xH_2O$ to reduce costs, hydrogen storage via $NaBH_4$ regeneration from crystal water from the real hydrolysis by-products ($NaBO_2 \cdot 2H_2O$ and $NaBO_2 \cdot 4H_2O$) via ball milling with Mg base alloy or

compound was reported. The transition process from H^+ in the coordinate water to H^- in $NaBH_4$ was fulfilled and the intermediate $[BH_3(OH)]^-$ and $[BH(OH)_3]^-$ were also observed. In this case, a convenient and economical method for $NaBH_4$ regeneration was also developed without hydrogen or hydrides introduced during ball milling process. Simple to say, the real hydrolysis by-products served as hydrogen suppliers, instead of dehydrated sodium metaborate ($NaBO_2$) were applied for the regeneration of $NaBH_4$ with Mg at room temperature and atmospheric pressure. The regeneration yields of $NaBH_4$ were 64.06% and 68.55% from Mg reacted with $NaBO_2$•$4H_2O$ and $NaBO_2$•$2H_2O$, respectively. The cost of $NaBH_4$ regeneration showed about 30-fold reduction compared with that of using MgH_2 as the reduction agent.

D-6: Production of an Anisotropic Nd2Fe14B Magnet Via Electromagnetic Vibration Processing

Mingjun Li, Tamura Takuya, National Institute of Advanced Industrial Science and Technology (AIST), Japan

An anisotropic Nd2Fe14B magnet is conventionally produced by hot pressing melt-sun ribbons and thus the Nd2Fe14B platelets can be well aligned. Alternatively, Nd2Fe14B powder can be first highly oriented in in a static magnetic field and then sintered to fabricate an anisotropic magnet. In this study, we used a kit of suitable electromagnetic vibration (EMV) processing parameters to solidify the Nd70Cu30-30wt% Nd2Fe14B alloy, by which the magnetic Nd2Fe14B compound could be segmented into short laths and their easy magnetization axes of these platelets could be highly aligned, as revealed by electron backscatter diffraction (EBSD) patterns.Magnetic properties showed that the alloy exhibited strong anisotropy in magnetism. Our present results opened a new avenue for the simple production of anisotropic Nd2Fe14B magnets via solidification without the powder metallurgy routine.

D-7: Effects of Brazing Temperature on Microstructure and Mechanical Properties of ZTA/Ni-Ti/ZTA Joints

Qi Zhang, Juan Wang, Guangdong Institute of Materials and Processing, China

ZTA ceramics had been joined to themselves using active braze alloy Ni-50Ti at.%, the brazing temperature was changed between 1320℃ and 1450℃, the holding time was set as 30min. In this study, the interfacial microstructure of the joints was characterized by scanning electron microscope(SEM) equipped with energy dispersive spectrometer(EDS), transmission electron microscopy(TEM) and electron backscattered diffraction(EBSD). Efforts were made to identify the reaction products and investigate the effects of brazing temperature on the interfacial microstructure and mechanical properties of the joints and analyze the interfacial reaction mechanism and the fracture mechanism of the joints. The hardness and Young's modulus of the reaction products were characterized by nano-indentation. The results revealed that sound brazed joints could be obtained in the study, when the brazing temperature was 1320℃, a Ni_2Ti_4O layer were formed at the interface, and the Ni_2Ti_4O layer became thicker when the temperature rise to 1350℃. However, when the brazing temperature reached 1400℃, a disordered layer were observed at the interface, Ni_2Ti_4O, TiO and $AlNi_2Ti$ were identified in the layer, in addition, large amount of black TiO particles exist in the seam. The microstructure didn't show remarkable change when the brazing temperature was 1450℃. The diffusion and reaction of active Ti element were the main factors to obtain excellent bonding of the ceramics. The shear strength of the joints increased with the increase of brazing temperature, and the maximum strength of 145.6MPa was achieved when brazed at 1450℃ for 30min. The hardness and Young's modulus of Ni_2Ti_4O phase that observed at 1350℃ were 14.8GPa and 264.8GPa, respectively. The average hardness and Young's modulus of the disordered layer that formed at 1400℃ were 17GPa and 277.4GPa, respectively, and the TiO particles in the seam had the hardness of 21.3GPa and Young's modulus of 314.7GPa.

D-8: Influence of HIP Temperature on Yttria Dispersed Copper Alloys during In-Situ Fabrication Process

Bing Ma, The Graduate University for Advanced Studies, Japan; Bo Huang, Kyoto University, Japan; Hishinuma Yoshimitsu, Noto Hiroyuki, Muroga Takeo, The Graduate University for Advanced Studies, Japan / National Institute for Fusion Science, Japan

Copper (Cu) alloys are the most promising candidates for the heat sink materials of divertors for fusion reactors mainly because of their good thermal conductivity. Considering the instability of microstructure at high temperature, and loss of strength and ductility because of irradiation-induced softening and hardening, respectively, some new Cu-based materials have been developed using Oxide Dispersion Strengthening (ODS) method. In order to prevent the aggregation of the dispersive oxide particles during the fabrication, which is known to occur in the internal oxidation method for fabricating Cu-Al_2O_3, the in-situ fabrication method applied for Cu-Y_2O_3 particles was developed by our research group. In this study, pure Y was used to reduce CuO forming uniform the dispwersiveY_2O_3 by Mechanical Alloying (MA) and Hot Isostatic Pressing (HIP) methods. We investigated to explore the influence of HIP temperature on the properties of ODS-Cu during the in-situ fabrication process.Cu-3.0wt.% Y_2O_3 alloys

were produced by MA and HIP methods. The MA process passed through the two steps. Firstly, the Cu and Y powders were mixed and mechanically alloyed in a planetary-type ball mill using 5mm stainless steel (SUS) balls in the steel MA pot with ball/powder ratio of 7/3 for 16 hours in a pure argon gas atmosphere. Secondly, CuO powders were added into the milled powders and the MA process continued to the additional 16 hours. In this study, the total MA process time was 32 hours. The mechanical alloyed powders were packed into the steel capsules and degassed at 500˚C for 1 hour in 0.1Pa vacuum.During the HIP treatment, the steel capsules was kept in the pressure of 150MPa and temperature of 850˚C, 900˚C and 950˚C for 1 hour. The samples after HIP were characterized in terms of morphology, X-ray diffraction (XRD) spectrum, Vickers hardness, and thermal conductivity.We found that CuO remained in the HIP sample treated at 850˚C and 900˚C, but not at 950˚C from the XRD patterns. This means that most of in-situ reactions occurred during the HIP process instead of MA process, and the in-situ reaction rate increased with the HIP temperature. The lattice constant parameter decreased with the increase of the HIP temperature approaching of pure Cu. This is because Y alloyed with Cu during MA process precipitated out to form yttria during the HIP process at high temperature.The relative density and hardness increased with the HIP temperature. The relative density increased from 97.56% at 850˚C to 100% at 950˚C, and the Vickers hardness increased from HV172 at 850˚C to HV234 at 950˚C. These suggested that higher HIP temperature enhanced and promoted the thermal activation processes with increasing of the relative density and hardness.

D-9: A Numerical Model for Evaluating the Formability of Multi-Layered Metal-Polymer Sheet

Jaeseung Kim, Myoung-Gyu Lee, Seoul National University, Korea; Kim Daeyong, Korea Institute of Materials Science, Korea

Multi-layered sheets have received increasing attentions from various industries for their functional advantages such as higher specific strength, better damping characteristic etc. For example, the combination of metals and polymers has been applied to the structure parts of automotive and the components of Li-ion battery cell or pouch. Although the mechanical properties of the integrated sheets can be readily measured by standard test methods, the effect of each component in the multi-layered metal-polymer sheet on the overall mechanical properties has not been fully understood. In particular, the formability of the multi-layered sheet needs to be carefully investigated in consideration of the role of each component layer and the interaction between the neighboring layers. The numerical analysis might be an efficient approach for this purpose. In this study, formability of metal-polymer multi-layered sheet is evaluated by the numerical method based on the Marciniak–Kuczynski (M–K) forming limit scheme. The plastic strain rate potential for the metal sheet under rigid-viscoplasticity increases the numerical efficiency owing to the reduced unknowns for the calculation of equilibrium and kinematic compatibility conditions. The overall numerical algorithm is formulated by the incremental deformation theory on the basis of the minimum plastic work path. Also, the rotation of anisotropic axes of metal sheet in the localized zone (or groove zone in the M-K model) is accounted for in the present formulation. The material properties of the polymers are represented by the hyperelastic constitutive law and the interfacial condition between the metal and polymer layers is also considered to investigate the effect of interface property on the delamination and overall formability of the multi-layered sheet. Various validation and sensitivity studies are provided to discuss the effect of material properties of individual component and geometry of the integrated system on the overall formability.

D-10: Development of the Sphericalization Technology for a Glass Frit

Yunseok Choi, Korea Institute of Science and Technology, Korea / Korea University, Korea; Cho Sohye, Korea University, Korea; Chung Jaewon, Korea Institute of Science and Technology, Korea / University of Science and Technology, Korea

Aluminosilicate glass frits are used for the ceramic dental filler and typically produced by melting of oxide components, and subsequent cooling and pulverizing. The particle size of the pulverized glass frits is tens of micronmeter but for the better performance as a dental filler, submicron-size particles are demanded in the dental market. However, when the size of the glass frits is submicron, it becomes difficult to well disperse the frits in the dental resin. One way to imporve the dispersity of the frits to the resin is to shape the glass frits to spheres with smooth surface. When the frits are sphericalized, the cement strength increases because of reduced void space and lower the surface and secondary damages by round surface edge. Also, packing density and flowability can be enhanced. In this study, we used spray flame method for sphericalization. The frit powders is sprayed into the flame by the rotational powder feeder and the burner is designed for adjusting the flame temperature and residence time and the thermophoretic collector is applied in the end stage. Also, the melting temperature of the glass frit is measured for the flame condition by ash fusion determinator (SE-AF 4000) and shape of spherical powder is analyzed by FE-SEM (inspect F50). The component differences are confirmed with XRD (D8 ADVANCE) analysis. We found that the

powders is sphericalized evenly, and the component phase is maintained as the amorphous condition.

D-11: High Mechanical Property and Excellent Electrical Conductivity of Cu–25Cr Alloys Prepared by the Combination of High Ratio Differential Speed Rolling and Heat Treatment

Hye Sung Kim, Chan Soo Lee, Hee Chang Lee, Pusan National University, Korea

Since the solid solubility of Cr element in Cu matrix for Cu-Cr alloy is quites small, the conductivity of the copper is not substantially reduced by the addition of Cr element. It has been investigated that the conductivities and mechanical properties were observed in various processed Cu-Cr alloys. Especially, strong deformation processed Cu-Cr alloy has attracted the interest of many researches due to possibility of ultra high strength. Relatively low cost high temperature stability renders chromium an attractive reinforcing phase for Cu based alloys. Nonetheless, most studies on Cu-Cr alloys have been conducted from binary Cu-Cr alloy containing below 5wt%Cr because high Cr addition in Cu matrix make ductility of Cu-Cr alloy deteriorate.In this study, ultra fine-grained (UFG) microstructures of Cu-25wt%Cr alloy were prepared by high ratio differential speed rolling (HRDSR) processing. The effect of heat treatment after HRDSR-processing on the mechanical property and the electrical conductivity was investigated from Cu alloy with high chromium content of 25wt%. The mechanical property was slightly reduced even in high temperatures, while the electrical conductivity increased to a similar level with non-HRDSR. Our study shows that a combination of high strength and excellent electrical conductivity can be achieved by the proper combination of HRDSR-processing and heat-treatment.

E. Thin Films and Surface Engineering

Symposium Organizers :

Chuang Dong, Dalian University of Technology, China; Hongbo Guo, Beihang University, China; Hiroshi Masumoto, Tohoku University, Japan; Ho Won Jang, Seoul National University, Korea; Mingxing Zhang, University of Queensland, Australia

August 19-21, 2019

Place: Exhibition Area (3rd Floor)

E-1: Preferred Orientation and Electrical and Optical Properties of NiO Films Deposited by Reactive Pulsed DC Magnetron Sputtering with Different Sputtering Powers

Nan Wang, Dalian Jiaotong University, China

Up to now, NiO films with preferred orientation have been prepared by spray pyrolysis, pulsed laser deposition, sol-gel spin coating, chemical vapor deposition, RF magnetron sputtering, DC reactive magnetron sputtering, and so on. Among these methods, magnetron sputtering is more widely used because it is more suitable for industrial large-scale production. Generally, NiO films are deposited by RF magnetron sputtering from NiO ceramic target, but by DC reactive magnetron sputtering from Ni metal target. Evidently, high quality metal target can be more easily fabricated than high quality ceramic target, and the film preparation process based on DC magnetron sputtering can be more easily controlled than that based on RF magnetron sputtering. Therefore, DC reactive magnetron sputtering is promising in the preparation process of NiO films. In previous studies, the NiO films deposited by RF magnetron sputtering usually presented (1 1 1) or (2 0 0) preferred orientation, but those deposited by DC reactive magnetron sputtering generally showed (2 0 0) or (2 2 0) preferred orientation. Such difference of the NiO films in preferred orientation should be determined by the different magnetron sputtering modes and the different sputtering parameters. However, the study on the NiO films deposited by pulsed DC reactive magnetron sputtering is still lacking, and then the preferred orientation of the NiO film deposited by the sputtering method also is not known. In this paper, the NiO films were deposited at room temperature by reactive pulsed DC magnetron sputtering from a Ni target, and the effects of the sputtering power on the preferred orientation and the electrical and optical properties of the deposited films were discussed systematically. The films deposited at the lower sputtering powers presented (2 0 0) orientation, but those deposited at the higher sputtering powers showed (1 1 1) orientation. With increasing the sputtering power, the carrier concentration of the films increased, but the carrier mobility decreased, and then the resistivity decreased.

E-2: Properties of Cu_2ZnSnS_4 Films Prepared by Single-Target Magnetron Sputtering at Different Sputtering Pressures

Chaoqian Liu, Dalian Jiaotong University, China

Single-target magnetron sputtering method is boomingly developed in preparing CZTS films and numerous correlative studies were reported. For magnetron sputtering method, it is well accepted that the deposition parameters (such as substrate temperature, sputtering power, sputtering pressure, etc.) can seriously affect the growth behavior of the films. There are a lot of literatures reporting the effects of substrate temperature and sputtering power on the properties of CZTS films deposited by the single-target magnetron sputtering. There are only several groups studying the effects of sputtering pressure. Our group recently studied the effects of sputtering pressure on the preferred orientation of the CZTS films deposited at room temperature, and indicated the preferred orientation was gradually

converted from (2 2 0) to (1 1 2) with increasing sputtering pressure. However, it is still very limited in the study of sputtering pressure affecting the physical properties of the CZTS film deposited by a single quaternary ceramic target at higher substrate temperature without sulfurization process. In the present work, the effects of the sputtering pressure were investigated on the phase, preferred orientation, composition, morphology, and electrical and optical properties of the CZTS films deposited by single-target magnetron sputtering method at 400˚c. The effects of the sputtering pressure on the composition, phase, preferred orientation, surface morphology, and electrical and optical properties of the CZTS films were studied. The results indicated that the content of Zn was remarkably affected by the sputtering pressure. All the deposited films exhibited the single kesterite phase and the well-preferred orientation of (112), and the spatial distribution of the preferred orientation was not almost affected by sputtering pressure. With increasing the sputtering pressure, the granule boundaries became more and more clear, but compactness of the films became poor. Moreover, the electrical properties of the films were seriously affected by the elemental content and the morphology. All the optical bandgaps were almost constant.

E-3 Surface Roughness and Work Function of ITO Films by Ion Bombardment Treatment

Hualin Wang, Dalian Jiaotong University, China

Transparent conducting oxides is still a hot topic in material science field, such as tin-doped indium oxide (ITO), aluminum doped zinc oxide and antimony doped tin oxide. ITO is a highly degenerate n-type semiconductor, which has excellent electrical conductivity and highly transparence to the visible light. Due to these unique properties, ITO films have been utilized in devices such as flat panel displays, solar cells, lamps, and so on, especially as the anodes in organic light emitting diodes (OLEDs). As the anode in OLEDs, there is a large demand for ITO films with excellent optical and electrical properties, smooth surface and high work function. Due to the as-deposited ITO films can not meet the requirements. Therefore, the relationship between the properties of ITO and various surface treatments has been widely studied. The most commonly used ITO treatments are polishing, oxygen plasma treatment, ultraviolet (UV) ozone treatment and so on.

In this paper, ITO films were prepared by direct current pulse magnetron sputtering from a ceramic In_2O_3:SnO_2 (90wt.%:10wt.%) target. Due to the high demand for ITO films as the anode in OLEDs, the deposition parameters were optimized. And post-processings by ion bombardment were performed with a linear ion source (AE, PinnacleTM Plus+ 5kW). The thickness, optical and electrical properties, surface morphology and surface work function of ITO films were investigated systematically by the step profiler, spectrophotometer, Hall effect measurement system, atomic force microscopy and kelvin probe force microscopy.

The as-deposited ITO films were bombarded with Ar ion or O ion at different times and ion energies. It was found that O ion bombardment had a significant effect on the work function of ITO, while Ar ion bombardment had a significant effect on the roughness of ITO surface. Bombarding with higher energy of Ar ion at a short time (<2min), could promote the flowing of atoms on the surface of ITO films, and the roughness of ITO films reduced. Due to the selectivity of the sputtering of Ar ion, the roughness of ITO films increased with a longer bombardment time. The work function of ITO films increased from 4.50eV to 4.96eV with the increasing of bombardment time from 0 min to 2min. When the bombardment time was more than 2min, the work function of ITO films didn't increase again. But the sheet resistance of ITO films kept on increasing with the increasing of bombardment time.

In summary, Ion bombardment is a considerable post-processing method to improve the surface flatness and work function of ITO films using for OLED.

E-4: Calcium-Magnesium-Alumina-Silicate (CMAS) Resistance Property of $LaTi_2Al_9O_{19}$ for Thermal Barrier Coating Applications

Weiwei Qu, Shusuo Li, Yanling Pei, Yi Ru, Zehao Chen, Yuan Liu, Jiapeng Huang, Shengkai Gong, Beihang University, China

The higher operating temperatures in gas turbine engines made possible by thermal barrier coatings (TBCs) are engendering a new problem: environmentally ingested airborne silicate particles (sand, ash) melt on the hot TBC surfaces and form calcium-magnesium-alumina-silicate (CMAS) glass deposits. The molten CMAS glass degrades the TBCs, leading to their premature failure. In our study, a kind of newly developed TBC ceramic, $LaTi_2Al_9O_{19}$ (LTA), is found to have high resistance to the penetration of molten CMAS at 1250˚c. The formation of a continuous, dense crystalline layer, mainly composed of anorthite ($CaAl_2Si_2O_8$), between the sample surfaces and LTA contributed to this desirable attribute. The accumulation of Al and Ti in the molten CMAS triggered the crystallization of the melt, leading to the formation of many $CaAl_2Si_2O_8$ anorthite crystals above the LTA layer, which could reduce the mobility of the molten CMAS by reducing the amount of Si entering the LTA or YSZ matrix. In this context, we study the resistance of LTA bulk and APS-LTA/YSZ coating to CMAS, and the mechanisms by which the CMAS attacks LTA samples are discussed. The results indicate that Ti is an effective element for altering CMAS composition, and LTA can be an attractive way of mitigating CMAS attack.

E-5: Surface Modification of Mg Alloy by Mechanochemical Cavitation

Daichi Shimonishi, Toshihiko Yoshimura, Sanyo-Onoda City University, Japan; Masataka Ijiri, Tokyo Denki University, Japan; Yasunori Sakai, Shibaura Institute of Technology, Japan

Among metals with practical uses, Mg is the lightest, with a specific gravity one-quarter that of Fe and two-thirds that of Al. Moreover, it has a high specific strength and specific rigidity, and excellent properties in terms of electromagnetic wave shielding ability and recyclability. However, Mg has the lowest standard electrode potential among practical metals and is chemically very active, so it is easily corroded. Therefore, to increase the corrosion resistance, it is necessary to improve the surface of Mg, and typical Mg surface treatments include anodizing and chemical conversion. Anodic oxidation treatment is used industrially because corrosion resistance is improved by using sealing treatment and painting in combination. However, for Mg anodizing treatment, unlike the alumite treatment for Al alloys, an electrolytic solution for maintaining current-carrying holes, such as a sulfuric acid bath, has not been developed. As a result, to form a thick film on the magnesium surface, it is necessary to grow an oxide film with dielectric breakdown due to spark discharge during its formation. Therefore, it is necessary to increase the current density, and accordingly the cost of the power supply and cooling equipment increases. Chemical conversion treatment is a method for chemically treating a metal surface and forming a coating of an insoluble compound. This method combines high versatility and low cost, and it is applied industrially. In typical chemical conversion treatment of Mg alloys, a liquid containing a large amount of hexavalent chromic ions, such as anhydrous chromic acid and dichromic acid salt, is used. However, due to growing "green" social demands, such as the EC Restriction of Hazardous Substances Directive, to limit the use of hazardous substances for electronic devices, chromic-free chemical conversion is required. At present, there are two types of practical chromic-free chemical conversion treatments: phosphate and permanganate. Between them, the phosphate type is more commonly applied to Mg alloys. The most proven coating system is the calcium phosphate-X system (where X denotes a metal such as Mn and V). The film formed by this system is excellent for resisting corrosion. However, the corrosion resistance of the produced calcium phosphate-manganese type film is not sufficient and needs improvement. To improve the corrosion resistance of the Mg alloy, a new processing technique is required. In this study, basic research on the formation of a film for improving the corrosion resistance of a Mg alloy (AZ31) surface was carried out by the addition of dilute phosphoric acid during water jet peening (WJP) and multifunction cavitation (MFC).

E-6: Effect of TiO_2 Doping on the Mechanical and Thermo-Physical Properties of Y_2O_3 Stabilized HfO_2

Fangde MA, Yue MA, Beihang University, China

The fracture toughness of ceramics has an important influence on the service life of thermal barrier coatings. 8 mol% Y_2O_3 stabilized HfO_2 (YSH) ceramics doped with different TiO_2 contents ((Hf1-xTix)0.92Y0.08O1.96 , x=0 , 0.05, 0.1, 0.15, 0.2 and 0.25) were synthesized by solid-state reaction at 1550˚C for 5h. The phase composition, mechanical properties and thermal conductivity of TiO_2-doped YSH were investigated. The ceramics were composed of monoclinic phase and cubic phase when the TiO_2 concentration varied from 0 to 0.1. As TiO_2 concentration was between 0.15 and 0.2, more oxygen deficient $YTiO_{2.085}$ phase was observed. As TiO_2 content reached 0.25, hafnium titanate was detected. The fracture toughness of (Hf1-xTix)0.92Y0.08O1.96 ceramic increased as Ti^{4+} ion concentration increased, and reached 3.2MPa·$m^{1/2}$ when x=0.25, nearly 52% higher than that of Hf0.92Y0.08O1.96. This enhancement of fracture toughness of the (Hf1-xTix)0.92Y0.08O1.96 ceramic by emerging the residual stress as a result of the increased amount of the second phase when TiO_2 doping content increased. The thermal conductivity of (Hf1-xTix)0.92Y0.08O1.96 ceramics decreased as Ti^{4+} ion concentration increased. Specifically, 25mol% TiO_2-doped YSH had the lowest thermal conductivity (1.8W/m*K at 1200˚C), which was about 24% lower than that of Hf0.92Y0.08O1.96. This reduction was due to the lattice distortion of the unit cell, upon substituting Ti^{4+} for the Hf^{4+} cation with a mismatch in atomic mass and ionic radius. Lattice defects scattered the phonon transmission effectively, resulting in the phonon mean free path as well as the thermal conductivity reduced. Meanwhile, 25mol% TiO_2-doped YSH kept good phase stability between room temperature and 1400˚C. Considering the comprehensive properties, 25mol% TiO_2 doped YSH was considered as a promising thermal barrier coating ceramic.

E-7: Synthesis and Characterization of Gadolinium Zirconate Feedstocks for PS-PVD

Shan Li, Liangliang Wei, Jia Shi, Hongbo Guo, School of Materials Science and Engineering, Beihang University, China

Plasma spray-physical vapor deposition (PS-PVD) is an advanced coating fabrication technology which can produce multiple microstructures, such as "columnar structure", "dense lamellar structure", and "quasi-columnar structure". Recently, columnar structured thermal barrier coatings made of yttria stabilized zirconia (YSZ) manufactured by PS-PVD has been reported presenting excellent thermal cycling lifetime. Gadolinium zirconate (GZO) is very promising ceramic

material suggested as a substitute of YSZ. In this study, pyrochlore structured GZO feedstocks for PS-PVD were successfully synthesized. Two kinds of starting powders were prepared by reverse titration coprecipitation and solid-state reactions, which were in nanoscale (NP) and microscale (MP), respectively. Afterwards, GZO feedstocks for PS-PVD were obtained through spray drying. The characteristics of the two feedstocks were studied by Laser particle size analyzer (LPSA), Scanning electron microscope (SEM), X-ray diffraction (XRD), and Hall funnel. Results revealed that the phase composition, the size distribution and their flowability of the NP and MP feedstocks were similar while the porosity of the NP feedstocks was lower than that of MP feedstocks. GZO coatings were fabricated by PS-PVD with same spraying parameters. It showed that the coating deposited from MP feedstock was typical columnar structure and was thicker, which indicates that the MP feedstock was more suitable for PS-PVD.

E-8: Study on the Preparation Process and Microstructure of Yb_2SiO_5 Environment-Barrier Coating Prepared by Plasma Spray Physical Vapor-Deposited

Jie Xiao, Dongrui Liu, Qian Guo, Hongbo Guo, Beihang University, China

In this paper, the spraying parameters of Yb_2SiO_5 environmental barrier coating prepared by PS-PVD were optimized and determined by orthogonal experiments. The typical morphologies of the coating under different spraying parameters were analyzed. The variation of the morphology and thickness of the coating along the radial direction of the jet was studied, and the deposition mechanism of the coating prepared under the optimal spraying parameters was analyzed. The results show that the coatings prepared by spraying parameters of 1200A gun current, 10mbar vacuum and 900mm spraying distance have high density, high hardness and fast deposition rate. With the increase of beam heating, small solid particles, large solid particles, liquid phase layered structure, silicon-poor particles and silicon-rich gas cylinders can be formed separately. The farther away from the center of the beam flow, the heating ability of the beam on the powder is weakened, and the solid and liquid particles will migrate downward under the influence of gravity. Under the optimum parameters, the coating is mainly liquid phase deposition. With the increase of deposition thickness, the liquid layer becomes uniform gradually, and the proportion of gas and solid phase deposition is small.

E-9: Structure, Magnetic and Dielectric Properties of Co-$SrTiO_3$ Nano-Composite Films

Moe Kimura, Yang Cao, Hanae Aoki, Hiroshi Masumoto, Shigehiro Ohnuma, Tohoku University, Japan; Nobukiyo Kobayashi, Shigehiro Ohnuma, Research Institute for Electromagnetic Materials, Japan

The magnetoelectric effect in materials that consist of magnetic and dielectric components has been demanded for the magnetoelectric applications such as sensors, and tunable devices. Although many candidate materials were previously studied, the magnetoelectric effects are too weak at room temperature because of their low magnetic transition temperature. In our group, the tunneling magneto-dielectric (TMD) effect was observed in FeCo-MgF nano-composite films for the first time. These films comprise two-phase components with the room temperature TMD effect, which holds high potential for device application. In this study, we prepared Co-$SrTiO_3$ nano-composite films using differential pressure sputtering (DPS), that can control Co (ϕ3") and $SrTiO_3$ (ϕ3") sputtering condition, respectively. Metal-oxide nano-composite systems, which are expected to expand the application range of TMD effect, has been used instead of metal-fluoride composite. The Si(100), Si/Ti/Pt, Si/Ti/Au and quartz were used. Magnetic property was observed by Vibrating Sample Magnetometer. Electric resistivity was tested by resistivity meter. Dielectric constant was analyzed by LCR meter. The Co-$SrTiO_3$ films exhibit nano-composite structure, with Co granules embedded in $SrTiO_3$ matrix. At Co=29 at.%, film shows super-paramagnetic properties and the electric resistivity is more than $1.0 \times 10^4 \Omega \cdot m$. TMD effect at room temperature has been found in Co-$SrTiO_3$ nano-composite films.

E-10: Highly Conductive and Stable Silver Nanowire Transparent Electrodes Fabricated by Electrodeposition

Sangyeob Lee, Hanbat National University, Korea

Transparent conducting electrodes (TCEs) have been one of key components in various electronic and energy applications such as photovoltaic devices, flat panel display devices, and light emitting diodes. So far, Indium tin oxide (ITO) has been the most commonly used material for TCEs owing to its high transmittance (T >90%) and low sheet resistance (Rs <10Ω/m^2). Despite the high transmittance, however, the inherent brittleness of ITO proves to be insufficient for flexible device application. Furthermore, the relatively high cost of ITO in materials and processing has still been problematic to wider the application of TCE. Thus, various materials such as carbon nanotubes, graphene and metal nanowires, have been studied as alternatives to ITO thin films. Among them, metal nanowire networks including silver nanowire has attracted tremendous interests, due to the capability of solution process that enable to reduce processing time and cost as well as its flexibility resulting from the networks structure and ductility of metal. On the other hands, the critical properties of AgNWs network as a TCE such as the sheet resistance,

transparency, surface roughness and thermal stability need to be improved with reliable processes in order to be commercially utilized in the market. Here we demonstrate a method to improve aforementioned properties in silver nanowire network by using electrodeposition. The electrodeposition enhanced the conductance of silver nanowire by increasing diameter of nanowire and lowering the contact resistance between each silver nanowire. Our experimental data demonstrate that the silver nanowire network with larger diameter showed lower sheet resistance than with smaller diameter at the same transparency, implying that electrodeposition is the effective method to improve optical and electrical properties of nanowire transparent electrode. In addition to the enhancement of optical and electrical properties, electrodeposition method also improved surface roughness and thermal stability of silver nanowire network. Additional silver is uniformly deposited on the surface of the nanowires to smooth the surface morphology of the silver nanowire network. By increasing the diameter of silver nanowire up to 300nm, the silver nanowire network preserves its conductance up to 550℃, proving that the thermal instability of silver nanowires due to surface diffusion was greatly improved by electrodeposition. A CIGS thin-film solar cell with an electrodeposited sliver nanowire TCE shows nearly equal device performance to that of a cell with a sputtered AZO TCE. We expect that electrodeposited sliver nanowire networks can be used as high-performance and robust TCEs for various optoelectronic applications.

F:Biomaterials

Symposium Organizers:

Yufeng Zheng, Peking University, China; Luning Wang, University of Science and Technology Beijing, China; Takayoshi Nakano, Osaka University, Japan; Seung-Kyun Kang, Korea Advanced Institute of Science and Technology (KAIST), Korea; Cuie Wen, RMIT University, Australia; Marc Meyers, University of California, San Diego, USA

August 19-21, 2019

Place: Exhibition Area (3rd Floor)

F-1: Microstructure and Shape Memory Properties of Bionaocomposites Based on Cellulose Nanocrystals and PLLA/PLCL Polymer Blends

Fang Zou, Rui Zuo, Bingwei Yu, Xili Lu, Harbin Engineering University, China

Celluloses nanocrystalline (CNC) were prepared by acid hydrolysis from microcrystalline celluloses and were surface-grafted by direct polymerization of L-lactic acid. The efficiency of grafting was determined by FTIR. The resulting PLLA-g-CNCs were incorporated in PLLA/PLCL polymer blends by solution casting methods at different compositions. The microstructure and shape memory properties of the PLLA-g-CNC/PLLA/PLCL bionanocomposites were characterized. DSC result revealed that the PLLA-g-CNCs exhibit a significant influence on the crystallinity and spherulite morphology of the nanocomposites. The mechanical properties and shape memory properties of the nanocomposites were enhanced by incorporating the PLLA-g-CNCs. It was found that the elastic modulus of the nanocomposite reached the maximum when the content of PLLA-g-CNCs was 2.5wt%. When the content of PLLA-g-CNCs was 1.0wt%, the nanocomposite had the best shape memory effect. Furthermore, the addition of PLLA-g-CNCs allowed the nanocomposites to recover their original shape at 40℃, effectively reduced the recovery temperature of the nanocomposites and imparted water-induced shape memory properties to the nanocomposite. These shape memory nanocomposites had great application prospects in the biomedical field, such as surgical sutures, tissue scaffolds and drug delivery systems.

F-2: Mussel-Inspired Poly(Aspartic Acid) Injectable Nanocomposite Hydrogel with Adhesive Properties and Anti-Bacterial Performance

Guodong Xu, Harbin Engineering University, China

Injectable hydrogels systems based on polymeric materials and the catecholic amino acid 3, 4-Dihydroxyphenyl-L-alanine (DOPA) have attractive considerable attention in tissue engineering because of their water-resistant adhesive characteristics. In this work, a synthetic dopamine-modified poly (aspartic acid) polymer was combined with MgO nanoparticles to form a novel injectable naoncomposite hydrogel (PASP-DP). The resulting hydrogels were charcterized by FTIR, 1H-NMR and UV-Vis-UV spectra. The physical properties, mechanical properties, degradation properties and antibacterial properties of the hydrogels were also investigated. The study demonstrated that incorporation of up to 5wt% MgO significantly reduced the geling time while enhancing the mechanical and adhesive properties. The measured gel times reduced from 230s to 10s for the hydrogels at 25℃ when the content of MgO is 5wt%. PASP-DP nanocomposite hydrogels showed at least twice times stronger tissue adhesion strength over the clinically used fibrin glue. The adhesion strength of the hydrogels varied from 60kPa to 150kPa with different MgO content. The gel contents of the PASP-DP hydrogels increased with the addition of MgO and the degradation rate of the hydrogels also increased with the increasing of MgO content. Furthermore, the addition of MgO nanoparticles not only improved the crosslinking effect but also made hydrogel system possess the antibacterial properties. The results of antimicrobial experiments showed that MgO nanoparticles as well as PASP-DP hydrogel had good antibacterial activity against Escherichia coli.

All these results indicated that this novel PASP-DP nanocomposites hydrolgel was a promising biomimetic material for wound repair, tissue engineering, and other biomedical applications.

F-3: Effect of EDTA on Corrosion Resistance of In-Situ Growth of Nano-Sized $Mg(OH)_2$ on Micro-Arc Oxidized Magnesium Alloy AZ31

Changyang Li, Rongchang Zeng, Shandong University of Science and Technology, China

One of the major obstacles for the clinical use of biodegradable magnesium (Mg)-based materials is their high corrosion rate. Micro-arc oxidation (MAO) coatings on Mg alloys provide mild corrosion protection owing to their porous structure. Hence, in this study a dense $Mg(OH)_2$ film was fabricated on MAO-coated Mg alloy AZ31 in an alkaline electrolyte containing ethylenediamine tetraacetic acid disodium (EDTA-2Na) to reinforce the protection degree. Surface morphology, chemical composition and growth process of the MAO/$Mg(OH)_2$ hybrid coating were examined using FE-SEM, EDS, XRD, XPS and FT-IR. Corrosion resistance of the coatings was evaluated via potentiodynamic polarization curves and hydrogen evolution tests. The results manifested that the $Mg(OH)_2$ coating possessed a porous nano-sized structure and completely sealed the micro-pores and micro-cracks of the MAO coating. The intermetallic compound of AlMn phase in the substrate played a key role in growth of the $Mg(OH)_2$ film. The current density of $Mg(OH)_2$-MAO composite coating decreased three orders of magnitude in comparison with its substrate, indicating its excellent corrosion resistance. The composite coating was beneficial to the formation of calcium and phosphorus corrosion products on the surface of Mg alloy AZ31, demonstrating a great promise for orthopaedic applications.

F-4: Biological Research on n-HA/CMCS/PDA Bone Repairing Materials Fabricated by Additive Manufacturing

Tao Chen, Beihang University/ National Institutes for Food and Drug Control, China; Yan Li, Beihang University, China; Bufang Fu, National Institutes for Food and Drug Control, China

The repairing of bone defects caused by bone tumors and trauma has always been a difficult problem in clinical treatment of bone repairing. Synthetic bone repairing materials have an irreplaceable effect in bone transplant, and it is urgent to find superior biological repairing materials. Here, we explored the biocompatibility of nano-hydroxyapatite/carboxymethyl chitosan/polydopamine (n-HA/CMCS/PDA) composite bone repairing materials fabricated by additive manufacturing technology. Firstly, some basic characterization of n-HA/CMCS/PDA have been carried out. From the results of infrared spectroscopic (IR), there was no change happens for raw materials' chemical structure before and after preparation, and it was observed that new chemical bond firmed interface and made composite performance better. -NH_2 of CMCS bonded with -OH of n-HA. The inside of the material was a porous structure from the scanning electronic microscope (SEM) results. The composite had pore diameters of 50~500μm. The pH value in phosphate buffer saline (PBS) solution changed among 7.0~7.4 for 8 weeks, which was in line with human microenvironment. In addition, we evaluated the biological properties of n-HA/CMCS/PDA. The cytotoxic properties were determined by a 3-day continuous exposure MTT assay with mouse fibroblast cell line L929. And the results showed that the material was not cytotoxic. Hemolysis test of rabbit results showed that the material did not undergo hemolysis in vitro. Animal intradermal reaction test and guinea pig maximum dose test were carried out in sequence. The results showed that n-HA/CMCS/PDA did not cause skin irritation of rabbit and skin sensitization of guinea pig. Finally, we assessed the systemic toxicity of the material by acute systemic toxicity of kunming mouse. And we concluded that n-HA/CMCS/PDA did not result in death and acute systemic toxicity of mice.
In this study, we have prepared porous and biocompatible bone repairing materials. The n-HA/CMCS/PDA bone repairing materials meet the biological requirements, and has a good potential application in the field of bone repairing. Further studies are therefore necessary to determine the osteoconductive and osteointegrative effects of the materials.

F-5:Mechanism of Deposition of Biophosphonates on Hydroxyapatite

Chen Zhuang, South China University of Technology / Peking University Shenzhen Institute, China

The high concentration of mineral present in bone and pathological calcifications is unique compared with all other tissues and thus provides opportunity for targeted delivery of pharmaceutical drugs, including radiosensitizers and imaging probes. Targeted delivery enables accumulation of a high local dose of a therapeutic or imaging contrast agent to diseased bone or pathological calcifications. Bisphosphonates (BPs) are the most widely utilized bone-targeting ligand due to exhibiting high binding affinity to hydroxyapatite mineral. BPs can be conjugated to an agent that would otherwise have little or no affinity for the sites of interest. This article summarizes the current state of knowledge

and practice for the use of BPs as ligands for targeted delivery to bone and mineral deposits. The clinical history of BPs is briefly summarized to emphasize the success of these molecules as therapeutics for metabolic bone diseases. Mechanisms of binding and the relative binding affinity of various BPs to bone mineral are introduced, including common methods for measuring binding affinity in vitro and in vivo. Current research is highlighted for the use of BP ligands for targeted delivery of BP conjugates in various applications, including (i) therapeutic drug delivery for metabolic bone diseases, bone cancer, other bone diseases, and engineered drug delivery platforms; (ii) imaging probes for scintigraphy, fluorescence, positron emission tomography, magnetic resonance imaging, and computed tomography; and (iii) radiotherapy. Last, and perhaps most importantly, key structure–function relationships are considered for the design of drugs with BP ligands, including the tether length between the BP and drug, the size of the drug, the number of BP ligands per drug, cleavable tethers between the BP and drug, and conjugation schemes.

F-6: Design of Biomedical TiNbTaZrMo High Entropy Alloy with bcc Structure

Tatsuru Awabori, Mitsuharu Todai, National Institute of Technology, Niihama College, Japan; Takeshi Nagase, Aira Matsugaki, Takayoshi Nakano, Osaka University, Japan

A new generation of metallic biomaterials with superior biocompatibility and mechanical properties is strongly desired to meet the future demands of the medical field. Recently, a new class of structural materials, termed as high entropy alloys (HEAs), has been developed. In this study, we developed a novel equi-atomic TiNbTaZrMo high-entropy alloy (HEA) as a new metallic biomaterial. Novel HEA with bcc structure was designed by the parameters such as the mixing enthalpy (Hmix), omega parameter, delta parameter, and the valence electron concentration theory (VEC). In the present study, heat of mixing (Hmix), delta parameter, which determines the atomic-size difference in multi-component alloys. Omega parameter, which is defined by the combination of Smix, Hmix, and melting temperatures of the constituent elements were used in this study. As a results, the bcc solid solution phases were obtained in as-cast states of TiNbTaZrMo alloy. An equi-axis fine dendrite structure was observed in the as-cast TiNbTaZrNb HEA, and this was independent of the position in ingots. The formation of this fine dendrite is closely related to the distribution coefficients during solidification. This HEA showed considerable strengthening with superior biocompatibility comparable to pure Ti. This study implies the possibility of using HEAs as a new class of metallic biomaterials.

G. Smart and Magnetic Materials

Symposium Organizers:

Shaoxiong Zhou, Center Iron & Steel Research Institute, China; Chengbao Jiang, Beihang University, China; Satoshi Sugimoto, Tohoku University, Japan; Haein Yim, Sookmyung Women's University, Korea; Sean Li, New South Wales, Australia; Bob Shull, National Institute of Standards and Technology, USA

August 19-21, 2019
Place: Exhibition Area (3rd Floor)

G-1: Magnetic and Mechanical Properties of High Purity Fe-3 mass%Si-1 mass%Mn Alloy

Iwao Sasaki, Takashi Kakimoto, Ryo Isa, Masaaki Takezawa, Hidenori Era, Kyushu Institute of Technology, Japan; Zhe Lei, Nippon Koshuha Steel, Japan; Satoshi Hata, Kyushu University, Japan; Toshifumi Ogawa, Fukuoka Industrial Technology Center, Japan

Electromagnetic steel has excellent soft magnetic properties and is a material used as the iron core of electrical products. This material is required not only magnetic properties but also good mechanical properties such as the strength to withstand external forces applied, and good workability for thinning at the rolling step. It is reported that adding Mn to an Fe-Si based magnetic steel sheet is effective for improving the mechanical properties of the electromagnetic steel. However, the additive effect of influence and mechanism on the Mn in the electromagnetic steel sheet have not been clarified. In this study, a high purity alloy was prepared using a cold crucible levitation melting apparatus same as our high purity Fe-Si alloys research previously. And raw materials of the alloy were electrolytic iron having a purity of 99.99mass%, silicon having a purity of 99.999 mass%, and manganese having a purity of 99.999mass%. Magnetic and mechanical properties were evaluated to investigate the effect of Mn addition to Fe-3mass% Si alloy. The sample of high purity Fe-3mass%Si-1mass% Mn alloy was cut out from the ingot and magnetically measured using a DC magnetization characteristic test apparatus. The mechanical properties were determined by tensile test. The results showed improvement for the maximum permeability which increased from 8600 to 9200 by adding of Mn, but no effect for the iron loss which changed from 0.75W/kg to 0.89W/kg. The result of the tensile test was an improvement by adding Mn which showed a yield stress of 1.13 times which was found to be superior to the previous reported result of 1.06 times increase. In addition, the elongation was 1.14 times by adding of Mn, suggesting improved workability.

G-2: Electric Behaviors in Multiferroic 0.7BaTiO3-0.3Pr0.65Ca0.35MnO3 Core Shell under Laser Light

Osami Yanagisawa,Takashi Fujimoto, National Institute of Technology, Yuge College, Japan; Kazuhiro Kitamura, Aichi University of Education, Japan

The multi-functional application devices with new physical property control by external fields are developed intensively. The multiferroic caused by the coupling between ferroelectric, ferromagnetic, ferroelastic and etc is one of candidate. 0.7BaTiO3-0.3Pr0.65Ca0.35MnO3 core shells were prepared by the chemical method to approach to the multiferroic between ferroelectric, $BaTiO_3$ and the photo-induced effect, Pr0.65Ca0.35MnO3 mediated with strain. Electric behaviors in multiferroic 0.7BaTiO3-0.3Pr0.65Ca0.35MnO3 under external magnetic field are studied comparatively with 0.7BaTiO3-0.3NiFe2O4. The powder XRD profiles conform the 0.7BaTiO3-0.3Pr0.65Ca0.35MnO3 core shell samples are composites of $BaTiO_3$ and Pr0.65Ca0.35MnO3 single phase without a chemical reaction between two phases. The sectional SEM images show the samples have inhomogeneous particle size, distribution of the Pr0.65Ca0.35MnO3 core observed as black color in the image in the $BaTiO_3$ shell observed as gray color and inhomogeneous micro structure. The EDXS shows the samples have a good chemical composition as $BaTiO_3$ as the gray color part and Pr0.65Ca0.35MnO3 as the black color part in the SEM image. Temperature dependence of the normalized voltage in 0.7BaTiO3-0.3NiFe2O4 with the magnetic field 280mT show a dramatic increase below temperature 210K and decrease above 210K compared with no magnetic field. Temperature dependence of the dielectric constant with measurement frequency 100, 1k, 10k and 100k Hz with the magnetic field show a dramatic increase at low temperature. Temperature dependence of the normalized voltage in 0.7BaTiO3-0.3Pr0.65Ca0.35MnO3 with the magnetic field show a decrease below temperature 170K and increase above 170K. Temperature dependence of the dielectric constant with the magnetic field show a dramatic increase at low temperature. These behaviors are reversible without and with the magnetic field. These behaviors in $BaTiO_3$, $NiFe_2O_4$ and Pr0.65Ca0.35MnO3 single phase show different behaviors with the magnetic field respectively. These behaviors in BaTiO3-0.3Pr0.65Ca0.35MnO3 may be attributed to the multiferroic between piezoelectricity and the photo-induced effect through strain which is similar kind of mechanism in 0.7BaTiO3-0.3NiFe2O4.. In this case the photo-induced effect which is transition from the CO insulator state associated with AF spin order to the CD state associated F spin order by laser light, is caused by the magnetic field. This effect may give us great future possibility to reach multiferroic device which can control the dielectric constant with the laser light. Electric behaviors in 0.7BaTiO3-0.3Pr0.65Ca0.35MnO3 under external laser light with various wavelength will be purported comparatively with 0.7BaTiO3-0.3NiFe2O4.

G-3: Effects of Powder Particle Size and Component Ratio on the Magnetic Properties of Anisotropic Bonded NdFeB/SmCo Permanent Magnets

Shizhong An, Wuhui Li, Ting Yin, Yanfeng Zhu, Henan University of Science and Technology, China

Anisotropic bonded NdFeB/SmCo permanent magnets have wide potential applications in the areas such as small and special electric machines due to their excellent processing property and high magnetic properties. The effects of powder particle size distribution and combination of anisotropic NdFeB powder and SmCo powder on the magnetic properties of the bonded magnets are investigated. When the particle size of the anisotropic NdFeB powder produced by HDDR method decreases from 420~178μm to 38~45μm, the energy product of the bonded NdFeB magnets first increases, peaks at 150~75μm of 19.1 MGOe, and then decreases. It is found that with the decreasing of the particle size from 420~150μm to 38~45μm the energy product of the bonded SmCo magnets decreases from 14.0 MGOe to 11.0 MGOe. However, when the SmCo powder is mixed with NdFeB powder to form bonded NdFeB/SmCo magnets, a lowest energy product of 18.3 MGOe is obtained when SmCo particles are in the size of 150~75μm, and a highest energy product of 19.4 MGOe is obtained when SmCo particles are in the size of less than 38μm. Analysis shows that the filling effect of the powder plays a key role in the effect of particle size on magnetic properties. A model is proposed to clarify the filling effect of the powder with different particle size. In addition, the effects of component ratio on the magnetic properties of anisotropic NdFeB/SmCo magnets are also revealed. With the increase of SmCo mass percent in the NdFeB/SmCo bonded magnets, a reduced degradation of the magnetic properties when the temperature increases is observed, showing that the addition of SmCo in the bonded magnets improves the temperature stability. And through adjusting the mass ratio between NdFeB and SmCo, from 23~125˚C the remanence temperature coefficient and coercivity temperature coefficient can be tuned in the range of -0.13%~-0.04% and -0.57%~-0.13%, respectively. When the mass percent of the SmCo exceeds 80%, the bonded SmCo/NdFeB magnets have a remanence of >7.4kGs, a coercivity of >11.7 kOe, and a maximum energy product of >11.2 MGOe, the operation temperature of the bonded magnets can reach 150˚C.

G-4: In Situ Observation of Internal Micro Structure and Chemical Composition of Casted Ti-50.5at%Ni before and after the Transformation Temperature

Kazuhiro Kitamura, Aichi University of Education, Japan; Osami Yanagisawa, Takashi Fujimoto, National Institute of Technology, Yuge College, Japan

Recently the shape memory alloy are studied intensively

to wider industrial application area especially micro machine and medical application which can expect high added value. The casting is very good cost performance method to avoid difficult and expensive cutting and processing of shape memory alloy ingot.

Our research group evaluates the shape memory alloy physical properties of specimens cast from self-propagating high temperature synthesis (SHS) ingots. The transformation temperature width of these specimens are wider than that of general SHS ingots. This is assumed to be caused by the fluctuation of chemical composition of the specimens and the grain size differs greatly between the surface and inside of the specimens. The aim of this study is to clarify the relationship between internal micro structure and transformation temperature by casting specimen by lost wax method from SHS ingot.

Ti-50.5at%Ni ingots were prepared by SHS process from elementary Ti and Ni powder. This powder were filled into graphite die and combustion synthesized in vacuum chambers using SHS machine. The cast Ti-Ni superelastic plates were made by the casting machine from SHS ingot. The transformation temperature of the specimen is measured by differential scanning calorimetry (DSC). The scanning electron microscope (SEM) was employed to analysis characteristics of internal micro structure of the specimen surface. The energy dispersive X-ray spectroscopy (EDXS) was employed to analysis chemical composition of the specimen surface. In situ observation of SEM and EDAX of the specimen surface in the warming run and cooling run before and after the martensitic transformation temperature with precise temperature control with ceramic heater and platinum resistance thermometer located under sample stage in vacuum chamber were carried out. The X-ray diffraction (XRD) was carried out of identifying the phase of the specimens.

These results revealed that there is area with different chemical compositions in the specimens. In addition, the crystal grain size is much larger at inside of the specimens than at surface. The results of in situ observation of internal micro structure and chemical composition of the specimens before and after the transformation temperature will be reported.

G-5: Study on Magnetic Nondestructive Testing Technology of Oxide Skin

Jingyi Du, Jiacheng Wang, Kang Chen, Xi'an University of Science and Technology, China; Aijun Yan, Xi'an Thermal Power Research Institute Co., Ltd, China

As the demand for power is growing faster, the importance about energy security and environmental situation is increasing. The development of China's thermal power units is toward the larger capacity and higher parameter of supercritical and (ultra-)supercritical coal-fired units .With the improvement of equipment structure and thermal system technology, the equipment safety need to be improved too, and the operation and control have become more complicated .

Since 2018, preliminary investigations have been conducted on the superheating and reheating of superheaters and reheaters in 32 units of 12 power plants. The existing problems were preliminary analyzed from a relatively finite sample of studies. After a long time running, adverse environmental conditions would cause the oxidation of superheater and reheater pipe walls, forming oxide-scale in the internal surface of the wall. When environmental conditions change dramatically, the oxide-scale is easy spalling. and the spalling oxide-scale would accumulate in the elbow of the superheater and reheater pipe, and block the pipe seriously, resulting in the heating pipes burst. The metal oxidation of boiler tubes becomes one of the main factors which affect the safe operation of the utility boiler.

This paper introduced a magnetic nondestructive testing method is presented used to austenitic stainless steel tubes of super-heater pipelines in nondestructive testing method under high temperature and high pressure conditions. After excitation of external magnetic field, the density of oxide skin magnetic induction will change with growing accumulation of oxide skin. At the same time it causes a change of the voltage signal generated by the magneto sensor. And the curves are obtained between the voltage of detection apparatus and the thickness of oxide. Research show that in the position of the interface between oxide skin and the non-oxidized skin in the tube, the magnetic induction intensity changes significantly. Finally, simulation of ANSYS and detection device comparison experiments were carried out, and the experimental results show that the method can effectively detect the oxides and its height of stainless steel tube by the change of voltage value.

G-6: Advancement of Next Alternative with Rare-Earth-Free Permanent Magnet

Haein Yim, Sookmyung Women's University, Korea

The purpose of this research is to realize L10 FeNi phase with hard magnetic characteristics by annealing the amorphous alloy ribbon for a long time. Rare earth materials, which are currently used in the permanent magnet industry, have mutually common problems such as unbalance of supply and demand and decrease of coercive force at high temperature. Advancement of non-rare-earth permanent magnet materials can be a solution to this. Most of all, L10 FeNi with hard magnetic properties found in meteorites has high theoretical performance to replace rare earth permanent magnets, but it takes several hundreds of millions of years to form by nature. In this research, the new composition progress method is combined with the process technology constructed in this laboratory to shorten the time required for the artificial L10 FeNi phase to several tens of days to realize a high-order non-rare-earth permanent magnet. We substitute Ni with atomic percent (at.%)

corresponding to half of Fe in multiple compositions of soft iron-based amorphous alloys and find optimal heat treatment conditions to develop a hard magnetic L10 FeNi phase at the minimum annealing time. Ultimately, we plan to obtain a customized amorphous composition for the L10 FeNi phase by adding other elements to the 1: 1 atomic percent composition of Fe and Ni.

G-7: Theoretical Prediction of Physical and Electronic Structure for Mn Based Mn_2NiX (X=Ga, In) Alloys

Jing Bai, Northeastern University at Qinhuangdao, China / Northeastern University, China; Jinlong Wang, Northeastern University at Qinhuangdao, China; Haile Yan, Xiang Zhao, Liang Zuo, Northeastern University, China

Significant attention has been attracted on the Mn based Mn-Ni-Ga ferromagnetic shape memory alloy due to its unique physical properties, e.g. 4% magnetic field controllable shape memory effect, high Curie temperature up to 588K and high martensitic transformation temperature close to room temperature. The Hg_2CuTi structure is widely accepted for the parent phase of the Mn_2NiGa alloy. However, such a structure does not satisfy with the mechanical stability criteria.
In this work, we systematically investigated the possible austenitic structures by the first-principles calculations. Moreover, the magnetic properties and electronic structure were discussed in detail. For the stoichiometric Mn_2NiX (X=Ga, In) alloy, a more reasonable configuration of L21 structure has been determined. Its total energy is lower than that of the Hg_2CuTi structure. Moreover, the elastic constants of this new structure can satisfy the criteria of mechanical stability. This suggests that the new proposed L21 structure is more likely than Hg_2CuTi-type for the parent phase of the Mn_2NiX (X=Ga and In) alloys. The magnetic moments of Mn1 and Mn2 atoms are anti-parallel arrangement, thus the magnetism of the parent phase in the Mn_2NiX is antiferromagnetic. Since the physical properties of Heusler alloys are very sensitive to their crystal structure, the present results are particularly useful in promoting composition optimization and performance design.

G-8: Phase Identification of Fe1-xGax and (Fe1-xGax)99.8Tb0.2 (19⩽x⩽29) As-Cast Alloys

Tingyan Jin, Hui Wan, Chengbao Jiang, Huibin Xu, Beihang University, China

Owing to the combination of large magnetostriction and good mechanical properties, Fe-Ga alloys have been attracting extensive attention for their application in actuators, sensors and transducers. Recently, in the Fe-17at.% Ga alloys, modified-D03 (m-D03) nanoheterogeneities was found dispersing in the A2 matrix, which are regarded to induce tetragonal distortion of the A2 matrix, leading to the enhanced magnetostriction. Meanwhile, minor doping with rare earth atoms in binary FeGa (~ 17at.% Ga) alloys was found to significantly enhance the tetragonal distortion of the m-D03 and the matrix, resulting in the remarkable improvement in magnetostriction. However, it is unclear that whether the m-D03 nanoheterogeneities still exist and contribute to the magnetostriction in FeGa or trace rare earth doped FeGa alloys when Ga content is larger than 19.0at.%, therefore, we carried out the detailed study of magnetostriciton and phase structure in FeGa and FeGaTb alloys with Ga content ranging from 19at.% to 29at.%.
The magnetostriction was measured by strain gauge method with the magnetic field along the length of the samples. The magnetostriction exhibits two peaks with the variation of Ga content in both Fe1-xGax and (Fe1-xGax)99.8Tb0.2 alloys, consistent with the literatures [5]. The magnetostriction of (Fe1-xGax)99.8Tb0.2 alloys increases by 15% on average compared with that of the un-doped alloys.
Furthermore, the structure of as-cast Fe1-xGax and (Fe1-xGax)99.8Tb0.2 (19≤ x ≤29) alloys was investigated by X-ray diffraction and transmission electron microscope. XRD results indicate that the major structure in the alloys is A2 phase. Moreover, an obvious splitting was observed in the samples with x=27 and x=29, indicating the existence of A2+D03 mixture in these samples. Further TEM analysis revealed the microstructure and the phase structural evolution in the Fe1-xGax and (Fe1-xGax)99.8Tb0.2 (x =19, 23 and 27) alloys. Especially, the evolution of m-D03 nanoheterogeneities in Fe-Ga and Fe-Ga-Tb alloys with the increase of Ga content was studied in detail. The effect on the number density and the size of m-D03 nanoheterogeneities by trace Tb doping was also investigated. Our TEM results can well explain the magnetostriction variation with the evolution of m-D03 nanoheterogeneities in Fe-Ga and Fe-Ga-Tb alloys.

G-9: D-hcp Phase in the Incompletely Decomposed Sm-Co-Fe-Cu-Zr Magnets

Xin Song, Fan Ye, Tianyu Ma, Xi'an Jiaotong University, China

2:17 type Sm-Co-Fe-Cu-Zr permanent magnet is highly desirable for high temperature applications. Its hard magnetism originates from the unique nano-cell structure, which is formed by the spinodal decomposition from the hexagonal 1:7H solid solution into rhombohedral 2:17R cell phase, hexagonal 1:5H cell boundary phase and lamellar Zr-rich 1:3R phase. Incomplete decomposition cannot produce continuous 1:5H boundaries to provide sufficient pinning sites for the domain walls of each 2:17R nano-cells, hence leading to low coercivity. The untransformed region lies mainly at some crossover regions of 1:5H cell boundaries but its structure is still in

controversy. This region has been considered as either 1:3R, hexagonal 2:17H or the mixture of 2:17H and 2:17R (partially ordered 2:17R). The main difficulty to differentiate them is that all these phases are coherent with the surrounding 2:17R phase and 1:5H phase, and themselves are also coherent with each other. Here, we performed a HRTEM study and proposed a crystallographic model to identify that this region has double hexagonal close packed (d-hcp) structure. We selected a commercial Sm-Co-Fe-Cu-Zr magnet with maximum magnetic energy product of 30.11 MGOe and coercivity of 26.5 kOe for study. The 1:5H cell boundary phase was found to be discontinuous, demonstrating its incomplete decomposition nature. Plane defects (stacking faults) are displayed at the crossover regions with the size of 20~40nm when tilting the specimen to [100]-2:17R zone axis. The corresponding FFT patterns show additional superlattice reflections at (001)*, (002)*, (010)* and (020)* positions, which cannot be indexed as either 1:3R or 2:17H phase. It is an intermediate state for the transformation from a hexagonal structure with a stacking of two types of mixed planes ABABAB··· to a rhombohedral structure with a staking of three types of mixed planes ABCABC···. We proposed a model to understand how this intermediate state can produce a d-hcp structure with local fault of ABCABA···. Our work may add important insights into understanding the coercivity-microstructure relation of the pinning-type Sm-Co permanent magnets.

G-10: A Piezoelectric, Strain-Controlled Antiferromagnetic Memory Insensitive to Magnetic Fields

Zexin Feng, Beihang University, China

Spintronic devices based on antiferromagnetic (AFM) materials hold the promise of fast switching speeds and robustness against magnetic fields. Different device concepts have been predicted and experimentally demonstrated, such as low-temperature AFM tunnel junctions that operate as spinvalves, or room-temperature AFM memory, for which either thermal heating in combination with magnetic fields or Néel spin–orbit torque is used for the information writing process. On the other hand, piezoelectric materials were employed to control magnetism by electric fields in multiferroic heterostructures, which suppresses Joule heating caused by switching currents and may be useful for tuning exotic physical phenomena unveiled recently in AFM materials. Here, we combine the two material classes to explore changes in the resistance of the high-Néel-temperature antiferromagnet MnPt induced by piezoelectric strain. We find two non-volatile resistance states at room temperature and zero electric field that are stable in magnetic fields up to 60T. Furthermore, the strain-induced resistance switching process is insensitive to magnetic fields. Integration in a tunnel junction can further amplify the electroresistance. The tunnelling anisotropic magnetoresistance reaches ~11.2% at room temperature. Overall, we demonstrate a piezoelectric, strain-controlled AFM memory that is fully operational in strong magnetic fields and has the potential for low-energy and high-density memory applications.

G-11: A New Strategy to Synthesize Dispersible $SmCo_5$ Particles

Ying Dong, Tianli Zhang, Hui Wang, Chengbao Jiang, Huibin Xu, Beihang University, China

$SmCo_5$ was the first-generation rare-earth permanent magnetic material and it is still irreplaceable for some application due to its extraordinary magneto-crystalline anisotropy of $17MJ{\cdot}m^{-3}$ and high Curie temperature of 747˚C. Dispersible $SmCo_5$ particles are important for making magnetic materials with large coercivity, investigating hard/soft exchange coupled magnetic materials and could also have important applications such as in high-density data storage and as medical drug carriers. It is therefore important to develop methods to produce $SmCo_5$ particles in a dispersible form. A combined method of chemical synthesis and calciothermic reduction is very useful to prepare $SmCo_5$ particles. However, it is difficult to obtain particles that can be dispersed as sintering easily occurs during the high-temperature calciothermic reaction, which is an irreplaceable process as Sm is too electronegative to be reduced. This study presents a new strategy to synthesize dispersible $SmCo_5$ particles by co-precipating a precursor of amorphous $Sm(OH)_3$ and coherent nanoscale $Ca(OH)_2$ and $Co(OH)_2$. After reaction at 860˚C with calcium metal, fine CaO particles dehydrolized from $Ca(OH)_2$ form a core-shell structure with $SmCo_5$ as the core and CaO as the shell, which prevents the $SmCo_5$ particles from sintering. The particles show high coercivity and can be aligned magnetically in a magnetic field.

G-12: The Irreversible Loss of Sm-Co Permanent Magnet

Wei Xia, Hui Wang, Tianli Zhang, Jinghua Liu, Chengbao Jiang, Huibin Xu, Beihang University, China

Permanent magnet material has gradually become leading influence on human life and social development, which is mainly embodies in energy generation and energy efficient utilization. Today, the elevated temperatures permanence magnets have received widely attention, and some special devices need high performance magnets capable of operating at 400˚C and higher, especially in the field of aerospace such as gyroscope, accelerometer, reaction and momentum wheel of satellite. An optimized permanent magnet has a square hysteresis loop where the coercivity Hc

comfortably exceeds half the remanence Mr. Alnico magnets are useable at 500˚C or more, but it has to be awkwardly shaped to reduce the demagnetizing field to less than the achievable coercivity, limiting the energy product (BH)max to about 40kJ/m^3. Energy products of Nd-Fe-B magnets are ten times greater, but its Curie temperature is very low which limits their applications to temperature below about 180˚C, even with the help of Dy or Tb substitution for Nd to enhance the anisotropy and coercivity, and Co substitution for Fe to raise the Curie temperature. Good remanence and better high-temperature performance is achieved in 2:17Sm-Co magnets, which have a much higher Curie temperature of 917˚C, and can exhibit a coercivity that is comparable to the remanence at 500˚C. The Sm-Co magnets are fabricated by a complex process of milling, alignment, sintering, solution treatment and ageing. Nevertheless, they are subject to irreversible losses, especially at the upper end of their operating temperature range.

These losses depend somehow on magnet shape, hysteresis loop shape and temperature. The uncertainty regarding irreversible losses in permanent magnets used in electronic devices causes difficulties for efficient magnetic circuit design, where a precise knowledge of the magnetic stray fields is required. Pre-treatment at a temperature about 50˚C above the maximum operating temperature is normally recommended to saturate the irreversible losses, which prevents the magnets from deteriorating further under working conditions. However, the pre-treatment cannot eliminate uncertainty about the irreversible losses in differently-shaped magnets, and it definitely degrades magnetic performance. Therefore, it is very important to quantify the factors that limit our ability to precisely set the magnetic field. Although, it is well established that the losses are thermally activated, resulting in a long-time decay of remanence that varies as the logarithm of time, the spatial distribution of the demagnetization and the initial trigger for magnetization reversal have received much less attention.

The irreversible remanence loss in high-temperature 2:17Sm-Co magnets was investigated, which become increasingly serious as temperature exceeds 300˚C. By examining the magnetization and domain structure in successive magnet slices, both experimentally and via computer simulation, the variation of the irreversible loss with number of thermal cycles, operating temperature, magnet shape, and hysteresis loop shape is established. We find that the irreversible loss of remanence does not occur uniformly throughout the magnet and that a partly-demagnetized outer 'skin' forms, which protects the bulk from further demagnetization after heating. The skin is a consequence of the non-uniformity of the demagnetizing field. A simple and effective magnetic image approach is proposed to reduce the irreversible losses, thereby substantially improving high-temperature magnet performance.

G-13: Anisotropic Exchang-Coupled L10-FePt/Co Core/Shell Nanoparticles

Xin Liu, Hui Wang, Tianli Zhang, Chengbao Jiang, Huibin Xu, Beihang University, China

Anisotropic exchange-coupled nanocomposites provide us a salient candidate for the new generation of permeant magnet due to their boosted maximum energy product (BH)max. However, previous researches basically focused on bulk materials or thin films, therefore limiting the applications and further understanding of anisotropic exchange-coupling. Here, L10-FePt/Co core/shell nanoparticles with different Co shell thickness were successfully synthesized by chemistry method in liquid phase. The core/shell nanoparticles were further dispersed in liquid epoxy resin under an aligning external magnetic field. After the solidification of epoxy resin, nanoparticle-based anisotropic exchange-coupling nanocomposites were obtained. The nanoparticles/epoxy composites have been investigated by vibrating sample magnetometery (VSM). It was found that the coercivity(Hc) of L10-FePt/Co core/shell nanoparticles got smaller with the thickness of Co coated layers decreased. On the contrary, the remanence(Mr) were just the opposite. The hysteresis loops of all samples showed single phase magnetic properties, indicating the magnetically hard core and the magnetically soft shell were strongly coupled, which was further proved by Henkel plot. After aligning in an external magnetic field, the hysteresis loops showed obvious anisotropy, which means the easy-axis of L10-FePt/Co core/shell nanoparticles were aligned. The enhanced Hc and Mr of the easy-axis give the nanocomposites a higher maximum magnetic energy product((BH)max) than the isotropic samples (83% improved). The anisotropic exchange-coupling nanocomposites extends our knowledge of the preparation methods and the magnetic properties of anisotropic exchange-coupling nanocomposites, therefore showing great potential in multifarious permanent magnet applications and fundamental researches.

G-14: Effect of Al Substitution on the Magnetocaloric Properties of Ni-Co-Mn-Sn Multifunctional Alloy

Lian Huang, Hunan Institute of Engineering, China

Multiferroic magnetic shape memory alloys with first-order magneto structural transformation exhibit much enhanced magnetocaloric effect which incorporates the latent heat associated with the phase transformation itself. The effect of Al on the structural, magnetic and magnetocaloric effect (MSE) of Ni-Co-Mn-Sn Heusler alloys was studied. With minor Al substitution we greatly reduced the thermal hysteresis and transformation temperature interval while conserving the large

magnetization difference between the two phases. It was disclosed that the thermal hysteresis (ΔThys) of martensitic transformation is totally dominated by the geometric compatibility condition between austenite and martensite. Therefore, in-situ high energy X-ray diffraction technique was using to elucidate the origin of the effect of Al substitution on the magnetocaloric properties of Ni-Co-Mn-Sn multifunctional alloy, it is shown the good geometric compatibility between martensite and austenite. Remarkable enhancement of MCE is observed near room temperature upon Al substitution. The maximum magnetic entropy change of 32J/Kg.K was achieved in a field of 50 koe. The significant increase in the magnetization with large magneto-structural coupling associated with the reverse martensitic transition is responsible for the giant MCE in these compounds, which are quite beneficial for practical applications. Incorporating the advantages of low cost, environment friendliness and easy fabrication, this alloy shows great potential for magnetocaloric applications.

G-15: Strain Induced Martensite Stabilization and Shape Memory Effect of Ti–20Zr–10Nb–4Ta Alloy

Qiquan Li, Yan Li, Chengyang Xiong, Beihang University, China

The phase transformation, the microstructure and the shape memory effect of the Ti–20Zr–10Nb–4Ta alloy are investigated. Alloy ingots was prepared using high-purity raw materials via the non-consumable arc-melting method, then cutted into pieces for cold rolling and heat treatment. The X-ray diffraction measurements indicated that the alloy is composed of single orthorhombic α'' -martensite. The alloy showed a two stage yielding behavior upon tension at 0.5% and 6% strain with a yield stress of 215MPa and 565MPa, respectively. The strain induced martensite stabilization was identified because the reverse martensite transformation start temperature of the alloy increases from 348K to 405K, with the pre-strain increasing from 0% to 8%. This can be ascribed to the martensite reorientation that occurred at a low strain level and the dislocations formed at a large strain level. TEM images and SAED patterns of the Ti-20Zr-10Nb-4Ta alloy with different pre-strains reveal the transformation of martensite variants in the process of tensile. The strain induced martensite stabilization can be attributed to the martensite reorientation that occurred at the low strain level and the dislocations formed at the high strain level. The experimental data of recovery strain upon heating after loading-unloading tensile indicated the maximum shape memory strain is 3.3% in the Ti-20Zr-10Nb-4Ta alloy, which means this alloy has superior property in shape memory effect than many Ti-Zr based alloys.

G-16: Promising Applications of Advanced Functional Materials in the Oil Field

Gufan Zhao, Weina Di, SINOPEC Research Institute of Petroleum Engineering, China

The new round of technological revolution driven by information technology, biotechnology, and new materials is surging. Technological innovations in the oil and gas sector will also usher in major opportunities and further demonstrate the trend of rapid development. The exploration and development of complex oil and gas reservoirs like deep seas, exploration of remaining oil and gas, and exploitation of unconventional oil and gas resources have become the main fields for oil and gas exploration and development. High temperature, high pressure, and high acidity make more and more requirements for petroleum engineering technology. Supporting equipment, downhole tools, and the oil field fluids place higher demands. Major oil companies and technical service companies have increased investment in the research and development of new technologies, introduced new materials and technologies, and upgraded their own technology. Domestic companies should continue to pay attention to the latest progress in advanced functional materials and provide new ideas for the research and development of new technologies. In the oil field, the technological advancement of related disciplines has played an increasingly significant role in promoting drilling technology. Many advanced functional materials have been used in oil and gas exploration and production and achieved good economic and social benefits. Advanced functional materials show broad application prospects in the oil field. Based on the technical requirements of drilling engineering for functional materials, the properties and application environment of new materials such as polyurea self-healing materials, the nanomaterials dispersion and the cellulose nanofibers were analyzed. The potential applications in drilling engineering need to be further combined with the technical environment of oil and gas drilling for application and development. Future development of drilling engineering would rely on the comprehensive integration of new technologies and application of advanced functional materials. The application of CNF and other advanced functional materials could provide innovative ideas, research and foundation for the future development of the oil and gas drilling technology, and contribute to achieving a major technological breakthrough and improve the overall level of the oil and gas drilling technology.

G-17: Recycling of Nd-Fe-B Sludge by Reduction-Diffusion Process to Regenerate Sintered Magnets

Xiantao Li, Shaoxiong Zhou, Guangqiang Zhang, Baoshao Dong, Zongzhen Li, Wei Zheng, Qian Zhang, Jiangsu JITRI Advanced Energy & Materials Research Institute Co., Ltd., China; Ming Yue, Beijing University of Technology, China

Nowadays, recycling of Nd-Fe-B sludge has drawn

tremendous attention due to the rapid growth of demand for Nd-Fe-B magnets and volatility in the price of rare earth elements such as Nd and Dy. However, the reports are rare on recycling of Nd-Fe-B sludge to prepare sintered magnets. In present study, the Nd-Fe-B sludge is recycled by co-precipitation, calcium reduction-diffusion and doping NdHx nanoparticles to regenerate sintered magnets.

The Nd-Fe-B sludge was dried, and then put into sufficient hydrochloric acid. Oxalic acid was added to the solution to generate oxalate precipitation to obtain mixed oxide by filtering and roasting. The mixed oxide, Fe, FeB, Ca and CaO were mixed and reduction-diffusion process was carried out in an argon atmosphere. The resulting powders were washed with de-ionized water and aqueous solution of glycerol to remove CaO. The rengenerated Nd-Fe-B powders mixed with NdHx nanoparticles were ball milled then pressed and sintered to obtain regenerated sintered magnets.

New recycling route from Nd-Fe-B sludge to regenerated sintered magnets is set up. First, co-precipitation technique is applied to obtain mixed oxide powders containing rare earth and main transition metal from the sludge. Second, calcium reduction-diffusion technique is used to prepare Nd-Fe-B powders. Finally, NdHx nanoparticles are doped into the powders to regenerate sintered magnets via conventional sintering technique. Based on analysis to specific mechanism of above method process, key preparation conditions are optimized. The mixed oxide, obtained from the sludge powder, contains mainly Fe_2O_3, Nd_2O_3, and $FeNdO_3$. The optimum reaction temperature for the Ca reduction-diffusion process is 1323~1373K. The particle size of the regenerated Nd-Fe-B powder decreases with the increase of the ball milling time, and the optimum time is 4 hours. The regenerated sintered magnets with doping 10wt.% NdHx nanoparticles bear magnetic properties of Br of 1.2T, Hci of 517.6kA/m, and (BH)max of 258kJ/m^3.

G-18: Synthesis and Characterization of Copper Oxalate and Mesoporous Copper Oxide (CuO) Using Inverse Micelle Method

Sung Gue Heo, Korea Institute of Industrial Technology, Korea / Kora University, Korea; Won-Sik Yang, Taek-Soo Kim, Seok-Jun Seo, Korea Institute of Industrial Technology, Korea; Soong Ju Oh, Kora University, Korea

Synthesis of mesoporous transition metal oxides by typical micelle base hydrolysis and condensation process, called soft template method, is difficult due to weak interaction between surfactant and transition metal ion. Therefore, the mesoporous transition metal oxides are generally synthesized using hard template such as mesoporous silica or mesoporous carbon, however, this method requires the complicated process. On the other hand, sol-gel based inverse micelle method solves the problem of multi-step process for synthesis of mesoporous transition metal oxides such as manganese oxide, iron oxide, cobalt oxide, and nickel oxide. However, it is difficult to synthesize mesoporous copper oxide with high specific surface area via this process due to relatively high stability constant of hydroxo complex. In this study, we successfully synthesized mesoporous copper oxide with a specific surface area of more than 100m^2/g by inducing a mesophase, copper oxalate, and converting it to CuO by heat treatment. In order to form an ordered mesoporous copper oxide structure, optimal synthesis conditions were obtained by adjusting the concentration of the precursor, pH and heat treatment temperature of the reactants. Analysis was performed by means of specific surface area analyzer (BET), pore size distribution (BJH), FT-IR, FE-SEM, HR-TEM and X-ray diffraction (XRD).

G-19: Evidence of Non-Joulian Magnetostriction for Fe-Ga and Fe-Al Single Crystal Alloys

Masaki Fujita, Akihiro Koyama, Takehito Ikeuchi, Muneyuki Imafuku, Tokyo City University, Japan; Sigeru Suzuki, Tohoku University, Japan

In recent years, securing of power source for convenient IoT equipment has been great issue in our society. One of the promising candidates of its solutions is vibration power generation devices using Fe-based magnetostrictive alloys, such as Fe-Ga and Fe-Al. The hot topic of physical properties in these materials is non-Joulian magnetostriction behavior and its origin. In this study, we investigated angular dependence of magnetostriction for cube-oriented specimen Fe-18%Ga alloy single crystal having diameter of 10mm and thickness of 4mm and Fe-15%Al single crystal alloy having length of one side 7mm. The magnetostriction in [100], [010] and [001] directions were measured by using strain gauges under magnetic field applied in (001) plane. We observed periodic magnetostriction in each direction and the maximum magnetostriction when the magnetic field was applied in easy magnetostrictive axis of [100], [010] and [001]. The volume strain can be calculated by summation of magnetostrictions in [100], [010] and [001]. In the results, we found large volume strain of c.a.120ppm and 60ppm for Fe-Ga and Fe-Al alloy single crystals, respectively. That is to say, these alloys are both auxetic non-Joulian magnetostrictive materials. In this presentation, we will discuss the origin of these behavior by the change of magnetic domain structure.

G-20: Study on The Process and Magnetic Properties of Fe-6.5wt% Si Thin Sheet Prepared by Three Stage Warm Rolling

Gongtao Liu, Chao Wang, Lin Cheng, Yunxia Liu, Zhiyuan Hu, Dongyang An, Shougang Zhixin Qian'an Electromagnetic Material Co., Ltd, China

Cold rolled sheets of Fe-6.5wt% Si high silicon electrical

steel with thicknesses of 0.2mm were fabricated by three stage warm rolling, and the microstructure, texture and magnetic properties of the intermediate processing samples were investigated. The roles of warm rolling temperature, the third warm rolling reduction and final annealing temperature in influencing the magnetic induction and core loss were clarified. The results demonstrate that more shear bands increasingly formed in the deformed structure of high silicon steel with the decrease of warm rolling temperature, which is conducive to the improvement of magnetic induction and the reduction of high frequency iron loss. The volume fraction of < 001>/ RD texture in finished products increased from 21% to 40%, when the reduction rate of the third warm rolling increased from 33.3% to 53.5%. For the samples with a thickness of 0.2mm with higher third warm rolling reduction, the typical magnetic induction B800 and the core loss P1.0/400 reached 1.435T and 6.55W/kg, respectively. The effect of increasing the reduction rate of the third warm rolling on magnetic properties was more significant than that of the warm rolling temperature. Furthermore, the optimization of process for preparing high silicon steel strip by three-step warm rolling was established as follows: the reduction rate of the third warm rolling is 50%~60% and the final annealing temperature is 1000˚C.

G-21: Effect of Heat Treatment on Thermal Radiation Properties of TC4 Alloy Coating

Yang Liu, Xiaoxi Zhu, Weiyu Li, Beijing Spacecrafts, China

TC4 alloy coating has been used for structure design of aircraft in space and may have thermal and magnetic functional performance due to its excellent characteristic, as the development of manned spaceflight and deep space exploration. Thermal radiation properties (solar absorptance and hemispheric emittance) of TC4 alloy coating are becoming important design indexes. In this paper, TC4 alloy coatings with different heat treated conditions were prepared. We investigated TC4 alloy coatings with different surface conditions, and the effect of heat treated conditions on solar absorptance and hemispheric emittance. The wavelength coverage of solar absorptance is between 200nm to 2600nm, and hemispheric emittance of TC4 alloy coatings is tested in room temperature. The results show that heat treated conditions of TC4 alloy coatings have slight effect on solar absorptance of the coatings. The change of heat treated conditions (heated temperature and heated time) , which is related to the microstructure of coatings, transforms the surface condition of TC4 alloy coatings. As the surface roughness of coating increases, solar absorptance of the coating increases. Hemispheric emittance is sensitive to heat treated conditions of TC4 alloy coatings. Hemispheric emittance of TC4 alloy coatings increases as heated temperature and heated time of the coatings add.

G-22: Understanding the Magneto-Structural Coupling of Ni50Mn35.4In14.6 Alloy from First-Principles Calculations

Die Liu, Jinlong Wang, Northeastern University, China / Northeastern University at Qinhuangdao, China; Jing Bai, Northeastern University, China / Northeastern University at Qinhuangdao, China / Hebei Provincial Laboratory for Dielectric and Electrolyte Functional Materials, China; Xinzeng Liang, Haile Yan, Xiang Zhao, Liang Zuo, Northeastern University, China; Yudong Zhang, Claude Esling, University of Lorraine, France

The discovery and study of thermal-magnetic coupling phase transition in magnetic shape memory alloy results in a series of rich physical effects, such as magnetic field-induced shape memory effect, magnetostrictive strain, magnetocaloric effect and magnetoresistance. The magneto-structural coupling of Mn-rich non-stoichiometric Ni50Mn35.4In14.6 alloy is investigated by the first-principles calculations DFT method in view of phase stability and magnetic properties of the austenite, the six-layered modulated (6M) martensite, and the non-modulated (NM) martensite. Extra-Mn atoms at the sublattice of deficient In atoms tend to be uniformly distributed. The 6M and NM martensites are energetically more stable than the L21 parent phase. From an energy dynamics perspective, the calculated martensitic phase transformation sequence of the Ni50Mn35.4In14.6 alloy is Paramagnetic Austenite (PA)→ Ferromagnetic Austenite (FA)→ Ferrimagnetic 6M (FIM 6M)→Ferrimagnetic NM (FIM NM) as a function of temperature. When the Mn-Mn interatomic distance is less than a certain value, MnMn-MnIn coupling may be antiferromagnetic. Shorter Mn-Mn distance breaks the ferromagnetic Mn environment, causing total magnetic moment decrease during martensitic transition. This is a typical magneto-structural coupling phenomenon. The martensitic transformation is attributed to the Jahn-Teller splitting of the spin-down total DOS peak near the Fermi level. The Ni 3d state electrons play an important role in driving martensitic transformation for the Ni50Mn35.4In14.6 alloy.

G-23: Formation of TiO_2/ZrO_2 Nanotube/ Nanoporous Heterostructure on Silicon Substrates Using an Anodization Process

Yang Yu, Yujie Zhao, Yan Li, Beihang University, China

Metal oxide nanostructures display unique electrical, optical and chemical properties. Among various methods of processing nanostructured metal oxides, anodization is generally known as a useful method for modifying the surface structures to obtain the nanoporous or

nanotubular structures. However, most of the work focuses on the anodization of metal or alloy foils, which structure are inflexible and difficult to apply the micro and nano device. In this work, Ti/Zr/Ti multilayer film as an anodized substrate was prepared by magnetron sputtering. Subsequently, the TiO_2/ZrO_2 nanotube/nanoporous heterostructure was obtained by anodizing. In this work, Ti/Zr/Ti multilayer films were deposited on single-crystal Si wafers using DC magnetron sputtering then anodized. The TiO_2/ZrO_2 nanotube/nanoporous heterostructure were characterized by X-ray diffraction (XRD), scanning electron microscope (SEM) and energy dispersive X-ray spectroscopy (EDS).
For the results of scanning electron microscope (SEM), the cross-section morphology of the Ti/Zr/Ti multilayer films prepared by magnetron sputtering show a columnar structure and Ti layers are more denser than the Zr layer. And a flake-like surface morphology of the top Ti layer can be observed. After the anodizing treatment, the upper and lower Ti layer are transformed into a nanotube structure. The nanotubes are open on the top while on the bottom they are closed, and the tubes diameter are about 90nm. Different from the Ti layer, the Zr layer in the middle is transformed into a nanoporous structure. Because of Zr layer with more inter-columnar voids, the electrolyte has access not only to the top surface, but also to the side walls of the columns. Each column would individually experience the typical anodization process, involving pit nucleation and growth resulting in a sponge-like structure. The EDS and XRD results indicate the formation of a TiO_2/ZrO_2 nanotube/nanoporous heterostructure.

G-24: Formation of TiO_2/ZrO_2 Nanotube/Nanoporous Heterostructure on Silicon Substrates Using an Anodization Process

Yang Yu, Yujie Zhao,Yan Li, Beihang University, China

Metal oxide nanostructures display unique electrical, optical and chemical properties. Among various methods of processing nanostructured metal oxides, anodization is generally known as a useful method for modifying the surface structures to obtain the nanoporous or nanotubular structures. However, most of the work focuses on the anodization of metal or alloy foils, which structure are inflexible and difficult to apply the micro and nano device. In this work, Ti/Zr/Ti multilayer film as an anodized substrate was prepared by magnetron sputtering. Subsequently, the TiO_2/ZrO_2 nanotube/nanoporous heterostructure was obtained by anodizing. In this work, Ti/Zr/Ti multilayer films were deposited on single-crystal Si wafers using DC magnetron sputtering then anodized. The TiO_2/ZrO_2 nanotube/nanoporous heterostructure were characterized by X-ray diffraction (XRD), scanning electron microscope (SEM) and energy dispersive X-ray spectroscopy (EDS).
For the results of scanning electron microscope (SEM), the cross-section morphology of the Ti/Zr/Ti multilayer films prepared by magnetron sputtering show a columnar structure and Ti layers are more dense than the Zr layer. And a flake-like surface morphology of the top Ti layer can be observed. After the anodizing treatment, the upper and lower Ti layer are transformed into a nanotube structure. The nanotubes are open on the top while on the bottom they are closed, and the tubes diameter are about 90nm. Different from the Ti layer, the Zr layer in the middle is transformed into a nanoporous structure. Because of Zr layer with more inter-columnar voids, the electrolyte has access not only to the top surface, but also to the side walls of the columns. Each column would individually experience the typical anodization process, involving pit nucleation and growth resulting in a sponge-like structure. The EDS and XRD results indicate the formation of a TiO_2/ZrO_2 nanotube/nanoporous heterostructure.

H. Materials Characterisation and Evaluation

Symposium Organizers:

Zhiwei Shan, Xi'an Jiaotong University, China; Xiaodong Han, Beijing University of Technology, China; Satoshi Hata, Kyushu University, Japan; Ju-Young Kim, Ulsan Institute of Science and Technology (UNIST), Korea; Jin Zou, University of Queensland, Australia; Jennifer Carter, Case Western Reserve University, USA

August 19-21, 2019
Place: Exhibition Area (3rd Floor)

H-1: Effects of Orientation Relationship on Stress Concentration at Grain Boundaries in Cu Bicrystals

Tomotaka Miyazawa, Ryosuke Suganuma, Toshiyuki Fujii, Tokyo Institute of Technology, Japan

Local stress distributions were studied by using some techniques to investigate stress localization phenomena in metallic materials. However, the mechanism of stress concentration at grain boundaries has not been revealed completely yet, because it is difficult to measure the local stress distributions near the grain boundaries. On the other hand, recently, several methods of stress/strain measurement using the synchrotron X-ray have been developed to analyze the deformation mechanism of polycrystalline metals. The energy dispersive X-ray diffraction microscopy (EXDM) with the synchrotron white X-ray micro beam is one of these methods measuring the local stress distribution under the external stress and that was successfully applied to the measurement of the stress concentration at grain boundaries in polycrystalline Cu

and Al. Thus, in this study, to discuss the mechanism of the stress concentration at grain boundaries, the local stress distributions in Cu bicrystals were measured by the EXDM technique. Three different Cu bicrystals grown by the Bridgman method were cut into tensile specimens with a single grain boundary perpendicular to the stress axis. The orientation relationships between grains in the bicrystals were [-10 0 1](2 -3 20)/[-89 -37 -14](20 -41 -19), [35 -36 1](14 11 -99)/[77 57 23](-25 -5 96), and [48 -45 -74](40 -64 65)/[85 -46 -19](1 -6 19), respectively. The local stress distribution around the grain boundary in each specimen under the external tensile stress of 0 and 10 MPa was measured by the EXDM method at BL28B2 in SPring-8. The stress concentration behavior at the grain boundaries were different from each other. The magnitude of the stress concentration had no dependence on misorientation angles between two adjacent grains. There was also no relationship between the stress concentration and Taylor factor ratios. In contrast, a linear relationship was found between the elastic strain energy due to the strain compatibility of the two grains and the values of the stress concentration.

H-2: Fabrication and Microstructural Evolution of Copper/Aluminium Dissimilar Friction Stir Butt Welds

Waraporn Piyawit, Panya Buahombura, Suranaree University of Technology, Thailand

Friction stir welding is a solid state joining process that has been developed since early 1990's. The advantages of this welding method compared to the conventional joining techniques are absence of porosity, hot cracking and availability of dissimilar materials joining. However, dissimilar joining of Al to Cu has not been widely employed due to low mechanical properties and formation of welding defects in large extent. In our recent work, we successfully prepared the Al/Cu dissimilar butt joining by friction stir welding with aluminium on the tool advancing side. Dissimilar system welds were produced on 6mm thick workpiece of AA6063 and pure copper. Cylindrical H13 hot work tool steel with 24mm shoulder diameter, 6mm pin diameter and 5.2mm pin depth was used for the stirring tool. The welding process was conducted at ambient atmosphere with the tool rotational speed and traveling speed of 900 rounds/min and 28mm/min, respectively. The microstructural and microchemical characteristics were investigated using optical and electron microscopy equipped with energy dispersive X-ray spectroscopy. The determination of material mixing in the weld nugget zone and the dominant alloying elements across the zone were revealed through the micrograph examinations. The vortex-like pattern and lamella structure were found in the weld nugget stir zone. The hardness distributions across the welds showed that the hardness of the copper adjacent nugget was considerably higher than at the aluminium side. Hardness across thermomechanically affected zone and heat affected zone were simultaneously decreased. The intermetallic phases in the weld nugget zone promoted the hardness of joint area. The different forms of intermetallic compounds were found across the welds. The irregular particles found in Al stir zone were consisted of different intermetallic compound layers due to extremely deformation. The formation of intermetallic phases between Al and Cu could be driven by the interdiffusion instead of phase transformation because the operating temperature of friction stir welding process is well below the melting points of materials. Intermetallic phases Al_2Cu and Al_4Cu_9 were identified by energy dispersive X-ray spectroscopy and X-ray diffraction pattern. CuSi particles were thoroughly dispersed in Cu stir zone. The stir zone hardness was increased because of the hard and brittleness of intermetallic compound particles.

H-3: Effect of Morphology-Directing Agents on Structure, Morphology and Optical Properties of CuI

Weiwei Jiang, Dalian Jiaotong University, China

Copper(I) iodide (CuI) has characteristics which are stable physical-chemical properties and low cost of preparation. It is a p-type semiconductor with 3.2eV wide bandgap and transparent during the visible light wavelength range. It has three kinds of crystal structures which are α, β and γ. α-CuI is of cubic blende structure and it exists stably at temperature higher than 392℃. β-CuI is of cubic crystal structure too and ionic conductor. γ-CuI exists when the temperature is lower than 350℃. Moreover, organic catalysis process includes adsorption and activation of reagents on the specific surface of solid catalyzer, chemical reaction of adsorbate and desorption of products.

CuI acts as organic synthesis catalyst due to non-toxicity, environment friendly and accelerating rate of organic reaction. Their catalyze properties are not very well and the reacting conditions are not soft enough.

The photoelectrical property and chemical catalyze property of CuI are relevant to the structure and morphology of material closely. In this paper, CuI is prepared by precipitation method with morphology-directing agents (MDAs) which are C6H8O6 and C11H12N2O2 assisted. The effects of MDAs on the structures, morphologies and optical properties of CuI were studied. The XRD results showed all of the samples had cubic marshite structure. The relations between morphologies and optical properties of CuI were also discussed. The results show that MDAs can affect CuI morphologies because they increase space steric hindrance. CuI prepared with MDA- C11H12N2O2

has smaller particles sizes and very different particles shapes from CuI prepared with MDA-none and MDA-$C_6H_8O_6$ because $C_{11}H_{12}N_2O_2$ intertwines on particles surfaces. Furthermore, it is results from the morphologies difference of samples that all of CuI samples have strong absorption in the UV wavelength range but different absorption in the visible wavelength range.
This work report is good foundation for CuI application in optoelectronic and catalytic fields.

H-4: Dislocation Substructure-Controlled Softening of Cu-20Ni-20Mn Alloy

Fuxin Luo, Huaichao Peng, Huiming Chen, Xiangpeng Xiao, Weibin Xie, Hang Wang, Bin Yang, Jiangxi University of Science and Technology, China

The Cu-Ni-Mn alloys have drawn considerable interest as potential candidates for aerospace and mining applications owing to their high strength, excellent flexibility, and corrosion resistance. The high strength of Cu-Ni-Mn alloy is related to NiMn precipitation, which acts as strengthening phase with an ordered face-centered tetragonal structure, and dislocation strengthening. Most investigations into Cu-Ni-Mn alloys have examined its precipitation characteristics and strengthening mechanism associated with microstructure evolution. However, little attention has been devoted to the softening behaviors of Cu-Ni-Mn alloys or their corresponding substructure characteristics, particularly the relationship of softening with the dislocation substructure. The dislocation strengthening effect is generally considered to be controlled by dislocation density, and a linear relationship between the strain strengthening and the square root of dislocation density (Taylor equation) and the effects of the dislocation substructure have been ignored. However, in the present study the dislocation substructure is shown to play an even more important role for Cu-20Ni-20Mn alloy. In this paper, the hardness and microstructural evolution during annealing in a hot-forged Cu-20Ni-20Mn alloy are investigated. The microstructures of the forged and annealed samples are characterized by electron back-scatter diffraction and transmission electron microscopy. Microstructure analysis of annealed samples indicated variation in the number of dislocations and dislocation substructure related to softening of the Cu-20Ni-20Mn alloy during static recovery. The tangled dislocations formed a regular array during annealing at 600℃, leading to a high softening fraction of 95%. In addition, rapid dislocation annihilation and sub-boundary disintegration occurred during annealing owing to the dislocation climb at 650℃. dislocation substructure evolution in the temperature can be characterized by the following shifts: numerous tangled dislocations → subgrain and parallel dislocations → a few isolated dislocations. The number of mobile dislocations within the grains decreased considerably, leading to softening in the Cu-20Ni-20Mn alloy annealed at 650℃.

H-5: Analysis of Grain Refinement and Stability Effect on Deformation Induced Martensitic Transformation in Austenitic Stainless Steels by Synchrotron Radiation

Yusuke Izuta, Shun Furukane, Shiro Torizuka, University of Hyogo, Japan

Austenitic stainless steel is a very widely used material. But austenitic stainless steels are metastable and deformation induced martensitic transformation often occur, which is sometimes harmful for austenitic stainless steels. In order to suppress the deformation induced martensitic transformation, additional elements such as Cu and Mo are usually added, but they are expensive. On the other hand, grain refinement is also known to be effective on suppressing deformation induced martensitic transformation without the addition of expensive elements. Nohara reported the Equation Md30,
Md30 = 541 - 462(C + N) - 9.2Si - 8.1Mn - 13.7Cr-29.0(Ni + Cu) - 18.5Mo - 68Nb - 1.42(ν−8.0). v denotes ASTM grain size number. This equation clearly shows that smaller grain suppress deformation induced martensitic transformation. However, Matsuoka et.al. reported that grain refinement is not effective on the suppression of deformation induced martensitic transformation. Therefore, it is still not clear whether grain refinement is effective or not on the suppression. Therefore, in this study, we focused and investigated the effect of grain refinement on suppression of deformation induced martensitic transformation. The materials used are SUS304, SUS301 and SUSXM7. Warm multi pass grooved rolling were carried out at 500℃ to obtain 1mm grained structure. And for comparison, coarse grained structures were also produced by heat treatment at 1100℃ for 10 minutes. Then, to occur deformation induced martensitic transformation, the specimens were rolled at 50℃ and 0℃ by 10 to 60% reduction with a flat rolling machine. The volume fraction of deformation induced martensite was measured by a transmission X-ray diffraction of synchrotron radiation in SPring-8. In SUS 301, the volume fraction of deformation induced martensite was smaller with smaller grain size than with coarse grain. However, in SUS304 and SUSXM7, the volume fraction was smaller with coarser grain size than with smaller grain. Grain size dependence on the suppression of deformation induced martensite is varied with the stability of austenite."

H-6: Analysis on the Effects of Grain Refinement and Stability on Deformation Induced Martensitic Transformation in Austenitic Stainless Steels by Synchrotron Radiation

Yusuke Izuta, Shun Furukane, Shiro Torizuka, University of Hyogo, Japan

Austenitic stainless steel is a very widely used material.

But austenitic stainless steels are metastable and deformation induced martensitic transformation often occur, which is sometimes harmful for austenitic stainless steels. In order to suppress the deformation induced martensitic transformation, additional elements such as Cu and Mo are usually added, but they are expensive. On the other hand, grain refinement is also known to be effective on suppressing deformation induced martensitic transformation without the addition of expensive elements. Nohara reported the Equation Md30,

Md30 = 541 - 462(C + N) - 9.2Si - 8.1Mn - 13.7Cr- 29.0(Ni + Cu) - 18.5Mo - 68Nb - 1.42(ν −8.0). ν denotes ASTM grain size number. This equation clearly shows that smaller grain suppress deformation induced martensitic transformation. However, Matsuoka et.al. reported that grain refinement is not effective on the suppression of deformation induced martensitic transformation. Therefore, it is still not clear whether grain refinement is effective or not on the suppression. Therefore, in this study, we focused and investigated the effect of grain refinement on suppression of deformation induced martensitic transformation.

The materials used are SUS304, SUS301 and SUSXM7. Warm multi pass grooved rolling were carried out at 500℃ to obtain 1mm grained structure. And for comparison, coarse grained structures were also produced by heat treatment at 1100℃ for 10 minutes. Then, to occur deformation induced martensitic transformation, the specimens were rolled at 50℃ and 0℃ by 10 to 60% reduction with a flat rolling machine. The volume fraction of deformation induced martensite was measured by a transmission X-ray diffraction of synchrotron radiation in SPring-8.

In SUS 301, the volume fraction of deformation induced martensite was smaller with smaller grain size than with coarse grain. However, in SUS304 and SUSXM7, the volume fraction was smaller with coarser grain size than with smaller grain. Grain size dependence on the suppression of deformation induced martensite is varied with the stability of austenite."

H-7: Performance Testing of High Carbon Martensitic Stainless Steel

Yudan Yang, Hongshan Zhao, Zheng Liu, Shanghai University, China

Due to high strength and hardness, excellent wear resistance and good corrosion resistance, high carbon martensitic stainless steels are widely used in the manufacture of wear parts, high quality knife and scissors, medical equipment, precision molds and so on. This study is mainly for a series of performance tests on high carbon martensitic stainless steels with different carbon and chromium contents. The stainless steels were austenized at 1025~1100℃ with oil and tempered at 160℃. After that, the mechanical properties (hardness, impact toughness, tensile strength), corrosion resistance (electrochemical pitting performance, salt spray corrosion performance) and abrasion resistance of the materials were tested. It is found that after quenching and tempering, the hardness of the material increases first and then decreases with the increasing of austenitizing temperature, reaching a maximum value (>58HRC) at around 1050~1075℃. The toughness of the materials is low (A_{KU2}<10J), and increases with austenitizing temperature. Under the same heat treatment, the corrosion resistance of high carbon martensitic stainless steel mainly depends on the composition ratio of chromium/carbon, and is also closely related to its microstructure. Abrasion resistance is greatly affected by the hardness of materials, but it is not entirely dependent on hardness.

H-8: Maximum Prediction of Carbon Element Content in Continuous Casting Billet of 82B Cord Steel

Dongwei Guo, Zibing Hou, Jianghai Cao, Zhongao Guo, Yi Chang, Chongqing University, China

82B cord steel is an important raw material for the production of wire rod products. However, macrosegregation defects are prone to occur during the continuous casting process owing to the high carbon content and low equilibrium distribution coefficients. The statistics of extreme values (SEV) is introduced for the first time In this study to predict the maximum value of carbon element along the casting direction, which can quantitatively characterize the segregation degree and explore the influence of different technological conditions on the maximum value of carbon element. The experiment is conducted by considering the effect of superheat, casting speed and cooling intensity on the maximum value of carbon element. It's shown that the SEV method can predict the maximum value of carbon element effectively by analyzing the distribution and fluctuation of carbon element in continuous casting billet. To some extent, the SEV method can get rid of the limitation of sampling length and sampling quantity by predicting the maximum value of carbon element on a larger range of continuous casting billet with few samples. During the continuous casting process, the equiaxed grain region in the billet can be enlarged with lower superheat, which can prevent the solute-enriched liquid from accumulating to the center of the billet and decrease the maximum value of carbon element. The action area of the end electromagnetic stirring increase with the augment of the casting speed, which can reduce the concentration of carbon element in the center of the billet. The increase of cooling intensity makes the surface shrinking rate increase ans slows down the flow of solute-enriched liquid to the center and the maximum value of carbon element can also be decreased

finally. This research can provide a new theoretical reference for the quantitative calculation of segregation carbon elements in continuous casting billet and the quality evaluation of continuous casting billet.

H-9: Combinatorial Evaluation for Biocompatibility of High Formable Shape Memory Alloys

Kaname Chizuwa, Chiemi Oka, Seiichi Hata, Junpei Sakurai, Nagoya University, Japan

Recently, Ti-Ni based high formable shape memory alloys (HFSMAs) are expected the structural and functional materials, because HFSMAs are excellent in workability due to viscous flow in the supercooled liquid region, and these alloys are fromed into complex 3D-structure. Thus, after annealing, SMA devices with 3D-structure can be fabricated. Although these HFSMAs are expected to apply for medical devices as well as Ti-Ni binary SMAs, biocmpatibility of HFSMAs has not been evaluated.
In this study, we proposed combinatorial evaluation methods for corrosion resistance which is one of the biocompatibility evaluation indicators. Proposed combinatorial evaluation substrates were fabricated by micro electro mechanical systems process. 9 HFSMAs samples with different compotision were prepared on the glass substrate by a carousel sputtering system. We performed anodic polarization test to evaluate corrosion resistance of HFSMAs. In the anodic polarization tests, the fabricated substrate were immersed in phisioligical saline (NaCl solution of 9g/L, 37±0.5℃), and the polarization curves were obtained by sweeping the potential at a scan rate of 40 mV/min, a scan range of -0.2V to 2.0V. Their corrosion resistance were collectively evaluated.
The current density in passive state (ips) of each composition were read from the polarization curves and these values were compared. The ips of Ti-Ni-Zr varied depending on the composition, and their values were equal or higher than that of Ti48Ni52 which is used medical devices. Moreover, ips of Ti-Ni-Zr tended to be lower as the content of Ti increased and that of Ni decreased. We found HFSMAs with corrosion resistance equivalent of Ti48Ni52.

H-10: Characterization of Road Surface Defects Using Nondestructive Evaluation Techniques

Jeongguk Kim, Korea Railroad Research Institute, Korea

Various types of nondestructive evaluation (NDE) techniques were used to characterize the defects on the road surface. The NDE techniques in this investigation include infrared (IR) thermography, line laser, and vision image technology. On the road surface, various defects could exist such as pothole and line defects on the pavement. In order to characterize and/or detect such defects on the road, NDE techniques were employed. IR thermography was used to detect road defects in terms of thermal images with 2-dimensional presentation of temperature contour. The abnormalities on the road were well detected with temperature difference on the road surface. Moreover, the thermal images were compared with the vision image results, and more obvious characterization was provided. The line laser technology was applied on the road surface to examine the surface profile difference. Using the profile difference information, the existence of defects on the road surface was characterized. After the preliminary experiments with those NDE techniques, the road surface monitoring system was developed to scan defects during driving. In this research, the road surface monitoring system was developed using various types of NDE techniques, and the performance testing was conducted. The development process and performance testing results would be introduced and presented.

H-11: Effect of Thermal Cycling on the Martensitic Transformation Behavior in Equiatomic CuZr Alloy

Shota Hisada, Mitsuhiro Matsuda, Kumamoto University, Japan; Minoru Nishida, Kyushu University, Japan; Carlo Alberto Biffi, Ausonio Tuissi, National Research Council of Italy, CNR-ICMATE, Italy

The equiatomic CuZr alloy has a martensitic transformation from the B2 parent phase to two martensitic phases (space group: P21/m and Cm) below 423K. It has been reported that the reverse transformation starts temperature (As) increased and the martensitic transformation start temperature (Ms) decreased by thermal cycling. Furthermore, based on the DSC measurements, peaks A* and M* indicating a new transformation appeared at the 4th cycle. The peak areas of A and M gradually decreased with increase of thermal cycle, while those of A* and M* increased. On the 7th cycle, the A and M peaks disappeared, and only A* and M* peaks remained around 253K until further 50 cycles. However, the change in the microstructural morphology and crystal structure accompanying the peak shift due to these thermal cycles has not been clarified yet. We investigated the effect of thermal cycle on the microstructure and martensitic transformation of equiatomic CuZr alloy on the basis of TEM observations. The solution-treated CuZr alloy consists of the plate-like variants of a few hundred nm with monoclinic P21 / m and Cm. The 10th cycled specimens are composed of the fine plate-like variants of about 10nm, and a lamellar eutectoid structure having $CuZr_2$ and $Cu_{10}Zr_7$ on the variant. Therefore, the decrease of A and M peaks is originated from the promotion of eutectoid reaction, leading to the suppression of the martensitic transformation of the CuZr phase. From the above results, the formation of the lamellar eutectoid structure

due to thermal cycle has a great influence on martensitic transformation behavior.

H-12: Combination Effects of Deformation and Precipitation Hardening on Morphology of CuAgZr Alloy

Pimsiri Rattanasopa, Panya Buahombura, Waraporn Piyawit, Suranaree University of Technology, Thailand

CuAgZr alloys have been remarkably known for their good combination of strength and electrical conductivity. The specific characteristic of nanosized Ag continuous precipitates that orderly aligned on {111} Cu matrix was the key factor for combining these two desirable properties. However, there are cellular precipitates or discontinuous precipitates also presenting along the grain boundaries in nondeformed alloys. Nonhomogeneity of these precipitates would be adverse effect to strength and conductivity. Therefore, this study investigated the morphological evolution of Ag precipitates in Cu- 7wt.%Ag-0.05wt.%Zr alloy after cold deformation. CuAgZr solid solution samples were initially cold drawn with 90%CW at room temperature. Precipitation temperature of cold drawn samples was identified using differential scanning calorimetry (DSC). The drawn samples were subsequently aged at 260˚C for 1, 2, and 4 hours. Structural and morphological characterizations were carried out by using X-ray diffraction (XRD) and scanning electron microscopy (SEM), respectively. Peak broadening in as-drawn samples showed the existence of the small crystallize sizes. Cu peak shifting was corresponding to Ag substitutional solute atoms in Cu matrix. After precipitation hardening of the drawn samples, nanosized Ag precipitates were randomly distributed in Cu matrix without preferred crystallographic planes. Their sizes were increased with increasing aging times. This was in good agreement with small angle X-ray scattering (SAXS) measurements. There was no evidence of cellular precipitates found in the deformed samples. Therefore, strength and electrical conductivity would be enhancing through the microstructural tailoring with homogenously dispersed nanosized Ag precipitates.

H-13: Corrosion Resistance of Nanostructured $Mg(OH)_2$ Coating on Magnesium Alloy AZ31 in Presence of EDTA

Xiaoli Fan, Rongchang Zeng, Shandong Univerdity of Science and Technology, China

Magnesium (Mg) alloys have attracted widespread attention in automotive, aerospace and 3C (computer, communication and customer electronic) electronics industries. However, a bottleneck, blocking the broad engineering applications of Mg alloys, is their poor corrosion resistance in aqueous environments due to their low standard corrosion potential (-2.37V vs. SHE). $Mg(OH)_2$ coating possesses good corrosion resistance and flame retardancy. Herein, a hexagonal $Mg(OH)_2$ nanosheet coating was prepared through a one-step hydrothermal method using LiOH solution as mineralizer and then modified by ethylenediaminetetraacetic acid (EDTA). The morphology and structure of the coating was evaluated using filed emission-scanning electron microscopy (FESEM), Fourier transform infrared spectra (FTIR), and X-ray diffraction (XRD) patterns. The corrosion resistance was characterized by electrochemical polarization and impedance spectroscopy, hydrogen evolution measurements. The bonding strength was conducted on nanoscratch tests. The results demonstrated that $Mg(OH)_2$ coating in presence of EDTA had better corrosion resistance, thicker thickness and higher bonding strength than the $Mg(OH)_2$ coating without EDTA. The formation mechanism of $Mg(OH)_2$ coating was attributed to EDTA's superior complexation with Mg^{2+}. First, EDTA combines with Mg^{2+} to form a complex; and the complex further forms $Mg(OH)_2$ in an alkaline solution. $Mg(OH)_2$ was first formed in the vicinity of the intermetallic compound AlMn particles and gradually covered the entire surface, showing the important role of the second phase of Mg alloy.

H-14: Relation between Grain Boundary Effect and Etch Resistance of PVT and CVD SiC

Je Jun Jeong, Jong Beom Kim, Je Hoon Oh, Myoung-woon Moon, Joon Hyeong Kim, Kyu Hwan Oh, Seoul National University, Korea

Silicon carbide (SiC) is an excellent material for various applications such as high power, high temperature and high frequency electronic devices. Recently, in the semiconductor process, the ring-shape SiC component, which is fabricated via physical vapor transport (PVT) method, is widely used to protect the electrostatic chuck, to guide the Si wafer and to achieve the uniform plasma distribution. Therefore, the SiC ring is required to possess a low etch rate to plasma as well as the electrical resistance. It was reported that the etch resistance had strong relation with the growth direction of SiC crystal and also 4H-SiC has better structural stability than 6H-SiC because of its highest attractive interaction between the stacking layers.
In this study, we have investigated the effect of grain boundary of SiC crystal on the etch resistance in comparing the etch depths, produced by the O_2 or CF_4 plasma, of SiC crystals, grown by PVT and CVD methods. As a result, we can determine both the plane direction and grain size of SiC crystals, which can maximize the etch resistance to plasma. The preferential growth direction of SiC crystals, grown by PVT and CVD method, was determined by the electron back scattered diffraction (EBSD), and the accurate etch rate of SiC crystals was measured by the ion beam irradiation in

the focused ion beam (FIB) system and the 3D laser scanning confocal microscope.

H-15: Electron-Beam Irradiation Induced Reversible Phase Transition of $Ge_1Sb_2Te_4$

Tingting Jiang, Jiangjing Wang, Lu Lu, Chuansheng Ma, Danli Zhang, Chunlin Jia, Wei Zhang , Xi'an Jiaotong University, China; Rao Feng, Shenzhen University, China

Fast and reversible phase transitions in chalcogenide phase-change materials (PCMs), in particular, Ge-Sb-Te compounds, are not only of fundamental interests, but also make PCMs based random access memory (PRAM) a leading candidate for non-volatile memory and neuromorphic computing devices. To RESET the memory cell, crystalline Ge-Sb-Te has to undergo phase transitions firstly to a liquid state and then to an amorphous state, corresponding to an abrupt change in electrical resistance. In this work, we demonstrate a progressive amorphization process in GeSb2Te4 thin films under electron beam irradiation on transmission electron microscope (TEM). Melting is shown to be completely absent by the in situ TEM experiments. The progressive amorphization process resembles closely the cumulative crystallization process that accompanies a continuous change in electrical resistance. Our work suggests that if displacement forces can be implemented properly, it should be possible to emulate symmetric neuronal dynamics by using PCMs. The chief TEM parameters for these transitions are found to be accelerating voltage, beam intensity, and irradiation time. The in-situ irradiation experiments provide a real-time and real-space view of progressive structural evolution between the two solid state phases, where melting is completely absent. The knock-on collision effect of E-beams drives this non-thermal amorphization process.

H-16: In-Situ Transmission Electron Microscopy Observation of Mass Transport in Graphene Encapsulated Copper Nanowire

Cheol-Woong Yang, Byeong-Seon An, Sungkyunkwan University, Korea

Cu interconnect distributes the clock and other signals and provides power/ground to the various microelectronic devices. The Cu interconnect requires a diffusion barrier layer to avoid Cu diffusion into the surrounding dielectric and to obtain low electrical resistance. In general, Ta/TaN, Co and Ru deposited by physical vapor deposition (PVD) or chemical vapor deposition (CVD) methods are used as barrier material in Cu interconnects. However, the size of advanced Cu interconnect has been significantly reduced, reaching the current 10 nm node technology and below, and thus advanced Cu interconnect requires ultrathin and reliable diffusion barrier. Recently, graphene has been suggested as a new candidate for ultrathin Cu diffusion barrier material. With scaling, in addition, the physical properties such as electrical resistivity and electromigration (EM) in Cu interconnect are increasingly influenced by Cu microstructure and adhesion between metallic interconnect and barrier materials. Therefore, it is necessary to investigate the EM mechanism of advanced narrow Cu interconnects wit ultrathin diffusion barrier.

Instead of patterned Cu interconnect, in this study, graphene encapsulated Cu nanowires were synthesized and a mechanism of EM occurred during the current sweep was investigated by in-situ transmission electron microscopy (TEM). Pristine Cu nanowires with a diameter of about 25nm were synthesized by a rapid and facile hydrothermal method. Then, Cu nanowires were directly encapsulated with transfer-free graphene by using a thermal CVD process. TEM specimens for in-situ experiment were prepared by transferring Cu nanowires onto the electrical MEMS chips using lift-out system. The resistance-time (R-T) characteristics were investigated by TEM operated at 200kV. The relationship between EM phenomena and microstructure of Cu nanowire was observed simultaneously by using in-situ experiment. Direct observation of the microstructural evolution and failure phenomena with electrical measurement allowed us to understand the EM mechanism clearly.

H-17: High-Resolution Three-Dimensional Visualization of Dislocations in Mo Using Weak-Beam Dark-Field Electron Tomography

Yifang Zhao, Hirotaka Sakai, Hikaru Saitou, Satoshi Hata, Kyushu University, Japan

Since a pioneering work by Barnard et al., electron tomography (ET) has become one of the conventional techniques for three-dimensional (3D) observation of dislocation networks in materials. In their original work, a series of weak-beam dark-field (WBDF) images were recorded every few degrees over a large tilt range, while ensuring that the used reciprocal lattice vector was parallel to the tilt axis so that the diffraction condition was constant through the data acquisition.

Last decade, the diffraction contrast ET technique has been customized in our group by development of a high-angle triple-axis (HATA) specimen holder capable of high-angle tilting for the primary horizontal axis with tilting capability in the other horizontal and vertical axes. The use of scanning transmission electron microscopy (STEM) mode has also improved experimental data quality in terms of obvious contrast, where strong beam conditions (or two beam excitations) have been chosen. Indeed, the STEM mode has an advantage in avoiding from the chromatic aberration, resulting in a successful reconstruction of dislocation arrangement

from an α-Fe specimen with a 400nm thick by a 300kV electron microscope. However, as suggested in Ref. , the strong beam (SB) conditions are not always the best choice especially regarding spatial resolution. WBDF-STEM has the potential to give further improvement to dislocation tomography.

In this study, we have examined how WBDF-STEM improves data quality for 3D reconstruction comparing the conventional SB condition. SB- and WBDF-STEM were compared by obtaining the two sets of tilt series on the exactly same dislocation network in a Mo film specimen. In the experiment, a transmission electron microscope Titan Cubed G2 (Thermo Fisher Scientific) was operated at an acceleration voltage of 300kV, under the "microprobe STEM mode" enabling a parallel beam illumination so that each diffraction disk can be detected by "bright-field detector" separately. The diffraction conditions were managed using the HATA holder (Mel-Build Corporation) through a large tilt range of ±70° . As a result, the 3D reconstruction obtained by WBDF has higher spatial resolution and more detail information than the conventional SB condition.

H-18: Revealing the Growth and Dopants Distribution of III-V Nanowires with Atom Probe Tomography

Jiangtao Qu, Rongkun Zheng, Julie Cairney, The University of Sydney, Australia

The bottom-up nanowire growth has been raising increasing attention since 1964 when Wagner and Ellis initially grew Si whiskers with the assistance of Au particles, which they termed as the vapour-liquid-solid mechanism. It has been argued that the metallic seeds (such as Au, Ni,) is capable of absorbing the adatoms from ambient precursors, and precipitating them in the form of crystals at the metal/semiconductor interface. As a result, the nanowire can grow along either in-plane or out of plane direction with respect to their substrate orientation. However, the growth mechanism of nanowires with a complex structure is still not clear on the aspects of structural evolution and dopants distribution, which handicap their future applications.

In this work, we use atom probe tomography (APT) to volumetrically map one single nanowire from free-standing core-shell InGaAs nanowires and GaAs heterojunction planar nanowire. Accordingly, the chemical distribution of the nanowire has been visualized by taking advantage of spatial resolved APT technique with high detection capacity.

Our tomography demonstrates: (i) the InGaAs nanowires are prone to form a core-shell structure with a Ga rich core and an In rich shell; (ii) there is an elemental inter-diffusion between the core and shell, Ga and In migrate inward and outward respectively; and (iii) the nanowires experience an anisotropic growth of {112}A and {112}B facets, i.e. faster growth rate on {112}A facets with lower In concentration. The findings on planar nanowire are direct evidence of Zn redistribution during nanowire synthesis and accumulation at the interfaces. Meanwhile, Si was not inclined to incorporate into GaAs nanowire catalytically at growth temperature 460℃. The ratios between doping and Ga were 4.15×10^{-5} and 1.59×10^{-3} for Si and Zn respectively, which are beyond the detectable ability of traditional microscopes. These findings provide fresh insights into the compound III-V nanowire growth and doping.

I. Composite Materials

Symposium Organizers:

Lin Geng, Harbin Institute of Technology, China; Boming Zhang, Beihang University, China; Junya Inoue, Tokyo University, Japan; Sang Bok Lee, Korea Institute of Materials Science (KIMS), Korea; Hao Wang, University of Southern Queensland, Australia; Rusty Gray III, Los Alamos National Lab, USA

August 19-21, 2019

Place: Exhibition Area (3rd Floor)

I-1：Dielectric Properties of PTFE Composites

Hoy Yul Park, Keri, Korea

Dielectric properties of PTFE (polytetrafluoroethylene) composites for circuit breaker nozzle was investigated. PTFE has been used widely as a nozzle material for circuit breakers. Radiation is considered to be the major energy transport mechanism in a circuit breaker. The fraction of the radiation power is emitted out of the arc and reaches the nozzle wall, causing ablation at the surface and in the depth of the wall. The energy concentration in the material cause depolymerization and eventually lead to the generation of decomposed gas as well as some isolated carbon particles. The generation of the decomposed gas in the depth of the material causes inner explosion. The surface of nozzle becomes uneven. The flow of gas is not uniform due to the unevenness of the surface. Small pieces of nozzle material after explosion have a negative effect on the performance of circuit breakers because it may clog the gap between piston and cylinder.

The light reflectance of nozzle materials is very important for high power circuit breakers, since the arc energy is transferred to the materials by the mechanism of radiation. The reflectance of PTFE in the visible and ultraviolet region at room temperature is very high, so that PTFE can well reflect the arc radiation. However, in the high temperature over its melting point, the light reflectance of PTFE significantly decreases, since it becomes transparent by melting. In these cases, PTFE is degraded severely because the arc energy penetrates into the material. Adding some filler into PTFE is

expected to be efficient for improving the endurability against radiation.

In this experiment, three kinds of fillers that have endurance in the high temperature environment were added into PTFE. Dielectric constant, dissipation factor, electrical resistivity and dielectric strength of PTFE composites were investigated. Dielectric constant and dissipation factor of the PTFE composites increased with increasing contents of the fillers. Electrical resistivity and dielectric strength of the PTFE composites decreased with increasing contents of the fillers.

I-2: Effect of Thermal Exposure on the Interfacial Strength of a Continuous SiC Fiber Reinforecd Aluminum Matrix Composite

Desheng Chu, Yue Ma, Beihang University, China; Peiyong Li, Beijing Institute of Aeronautical Materials, China

The continuous SiC fiber reinforced aluminum matrix (SiCf/Al) composite is an important potential structural material in aerospace, due to its outstanding properties including high specific strength, high specific stiffness, and high temperature performance. The interfacial strength between SiC fiber and aluminum matrix is related to the mechanical properties of the composite. In this work, the effect of thermal exposure on the interfacial strength of a SiCf/Al composite was investigated. The SiC fibers coated with aluminum alloy were firstly hot isostatic pressed to obtain the sample of SiCf/Al composites. Secondly, the 0.5mm-thick slices of the composite sample were thermally exposed at temperatures of 300~450˚c for 20h to 100h. The interfacial strengths of the SiCf/Al composites before and after thermal exposure were measured by the push-out method. The microstructure of the composite samples was investigated by scanning electron microscopy (SEM) and transmission electron microscopy (TEM). The results showed that the interfacial strength of the SiCf/Al composite after thermal exposure decreased compared to that before exposure. When exposed at temperatures below 400˚c for 20h, the exposure temperature had almost no influence on the interfacial strength. When exposed at temperature above 400˚c for more than 50h, the interfacial strength decreased dramatically. According to the SEM and TEM results, which showed that the elements of C, Al, Fe, Si diffused across the interface between the fiber and matrix, and discontinuous zone appeared near the carbon layer on the SiC fiber, it may be postulated, when the SiCf/Al composite was exposed at 400˚c for 50h, the oxidation reaction of the carbon layer between the interface between SiC fiber and aluminum matrix leads to the decrease of the interfacial strength. In addition, the cooling process of thermal exposure treatment was simulated by finite element method. It was found that the residual stress would increase when the SiCf/Al composite material cooled down from higher temperature to room temperature. Under this residual stress, the interface with low interfacial strength would be easy to damage.

I-3:Products and Application Development of Stainless Steel Clad Plate

Liyan Wei, Yunhong Dai, Xiaoyong Wang, Research Institute of Technology of Shougang Group Limited Company, China

In today's society, the requirement of material application is increasing with the change of environment. Especially steel materials, it requires not only higher strength, but also better corrosion resistance. In addition, from the economic point of view, reducing maintenance and shortening the duration of the project are also important conditions for selecting materials. Moreover, the recyclability of iron and steel materials is one of its important advantages. Stainless steel clad steel sheet is a very practical steel material, the base material of stainless steel clad steel sheet is carbon steel or low alloy steel, which has good mechanical properties. The clad steel is stainless steel, which has good corrosion resistance. The metallurgical combination of the two makes it tightly bonded and has good machinability and weldability. With the development of production and processing technology of stainless steel clad steel sheet, the product has won more and more recognition for its unique performance. In this paper, the research and development progress and product characteristics of stainless steel clad steel sheet are studied, the explosive cladding process and rolling cladding process were compared and analyzed, the production and application standards of products are enumerated. It is pointed out in the report that the welding process is one of the most important processes and a bottleneck in improving the application scope of rolling clad plate. The corresponding analysis is given in the report.. This paper investigates the production and equipment of stainless steel clad steel products in key iron and steel enterprises in China and Japan. At the same time, the application field of the product was explored, for example, in the field of petrochemical industry, seawater desalination, paper industry, pressure vessels, etc. the existing and potential markets were analyzed, and the demand characteristics of stainless steel clad steel plate in the future market were described in detail.

I-4: Friction Stir Lap Welding of WC-12Co Cermet and Medium Carbon Steel by Using a Ni Interlayer

Toru Nagaoka, Osaka Research Institute of Industrial Science and Technology, Japan; Marie-Noëlle Avettand-Fènoël, Roland Taillard, UMET, University of Lille, France; Hidetoshi Fujii, Joining and Welding Research Institute, Osaka University, Japan

WC-Co cermet which consists of WC particles and Co

metallic binder has a superior balance of high hardness and high toughness. Therefore, it has been widely used for cutting tools, dies, molds, and so on. Conventionally, brazing is often applied to joining of WC-Co cermet and steel. But the bonding strength is relatively low because the filler is made of softer materials. In this study, friction stir lap welding of WC-12 mass%Co and 0.45 mass%C steel with or without Ni interlayer was carried out in order to obtain high strength joins. The steel plate was overlapped on the cermet plate. The thickness of the steel plate and the cermet plate was 2.4mm and 2.0mm, respectively. The rotating tool made of silicon nitride was plunged into the steel. The length of the probe was 2.4mm. FSW was carried out by load control. The tool tilt angle was 3° and the load was 12.5kN. The rotation speed was 800 rpm. The traveling speed was 50mm/min. The thickness of Ni interlayer was changed from 0.05mm to 2mm. At the Ni-steel interface, some tongues were turned towards either the advancing side (AS) or the retreating side (RS) according to their AS or RS location. Conversely, the Ni-cermet interface is rather flat on a mesoscopic scale. It proves that the probe did not touch the cermet during the welding process. The addition of a Ni interlayer improved the feasibility of welding of the cermet and the steel. During shear tests, fracture initiated at the steel-cermet interface and propagated in the cermet in the case of Ni free joints. On the other hand, it occurred in the base material for the joints with Ni interlayer. Some interdiffusion zones were observed at the steel-cermet, steel-Ni and Ni-cermet interfaces. Supersaturated Co based solid solutions in Fe or in Ni was formed. The formation of Fe-Ni and Ni-Co solid solutions which avoids the formation of brittle phase at the steel-cermet interface should improve the mechanical properties of the bonding interface.

I-5: Microstructure, Phase Transformation and Mechanical Property of NiMnGa/Sn Composites

Zhaoxin Liu, Bin Tian, Yunxiang Tong, Feng Chen, Li Li, Harbin Engineering University, China

NiMnGa magnetic shape memory alloys have been extensively studied because of their large magnetic field induced strain and high response frequency, which present large potential applications in the field of high-power underwater sonar, micro-displacement sensors, vibration and noise control, linear motors, microwave devices and robotics. However, since such alloys belong to intermetallic compound, the polycrystalline material is relatively brittle. To overcome this problem, making composites consisting of NiMnGa particles and ductile matrix has been developed, in which the matrix ensures integrity of the composites and NiMnGa particles provides functional property. In the previous studies, polymer is mostly used as the matrix and damping property of the composites has been enhanced based on the twin boundary motion of NiMnGa particles. Metal Sn has large plasticity and good damping properties, and the damping factor tanδ can reach ~0.13 after a shear deformation of 30%. Therefore, Sn might be a promising candidate as matrix to composite with NiMnGa particles. In this paper, NiMnGa/Sn composites were prepared by pressureless sintering of NiMnGa alloy particles and Sn powder. The microstructure, martensitic transformation and mechanical property of the composites with different content of NiMnGa particles are systematically investigated.

The SEM results show that the NiMnGa particles are widely distributed in the Sn matrix for the composite with 40wt% NiMnGa particles, and the local aggregation of NiMnGa particles occurred when the content of NiMnGa particles is increased to 50wt% and 60wt%. XRD results show that the composites mainly consist of the diffraction peaks of Sn and NiMnGa particles and the diffraction peak belonging to interfacial reaction phase is not observed, indicating that the interfacial reaction between NiMnGa particles and Sn matrix is very weak. Susceptibility measurement results show that the martensitic transformation and reverse transformation of the composites occur at 300~340K, and the Curie transition is at ~368K, which is consistent with the phase transformation temperatures of NiMnGa particles. Mechanical testing results demonstrate that the compressive strength of the composites are significantly improved as compared to that of the pure Sn. As the content of NiMnGa particles increases, the maximum compressive strength of the composites increases gradually, but the elongation of the composites decreases. When the NiMnGa content is 40wt%, the composite exhibit both high compressive strength and plasticity.

I-6: Structure and Hydrogen-Permeation Properties of Mo-Doped V-Based Solid Solutions

Xiaofeng Yan, Zhongmin Wang, Taijun Chen, Huaiying Zhou, Guilin University of Electronic Technology, China

Vanadium and other group V Metals and alloys exhibit much higher hydrogen permeabilities than palladium alloys, but the heavy hydrogen embrittlement limits its application in practical production. Hydrogen permeation experiments have been confirmed that alloying was an effective way to solove the problem menmtioned above. Therefore, the X-ray diffraction (XRD) analysis, Pressure-Composition-Temperature (PCT) measurement, electrochemical tests and three-point bending test were used to investigate the structural and hydrogen permeation properties of V100-xMox (x = 2.5, 5, 10) solid solutions in our study. All samples in this study were prepared by arc melting in purified

argon atmosphere using V, Mo (99.99 mass% purity for all) as raw meterials. The results of our works indicated that obvious lattice deformation have been observed in V-Mo samples. With the increase of Mo-doped content, the hydride-formation enthalpy, diffusion coefficient for H atom, and mechanical property of anti-hydrogen embrittlement for the alloys increase at the same time. The diffusion coefficient for H atom in V90Mo10 solid solution is almost 1.273×10^{-9}cm/s, which is about twice times of that in V97.5Mo2.5 sample. The work suggests that Mo doping can reduce the stability of V-Mo hydride, contribute to hydride dehydrogenation, H-diffusion ability and mechanical property of anti-hydrogen embrittlement can be improved significantly

I-7: Study on the Deformation Behaviors of Isothermally Compressed TA1/AZ31B Laminated Composites

Bing Zhang, Su Yao, Qiuyu Wang, Tianli Zhao, Wen Wang, Jun Cai, Kuaishe Wang, Xi'an University of Architecture & Technology, China; Juan Li, Dong Zhang, State Key Laboratory of Nickel and Cobalt Resource integrated utilization, China

In this study, the deformation behaviors of isothermally compressed TA1/AZ31B laminated composites in the deformation temperature range from 573K to 723K, the strain rate range from $0.01s^{-1}$ to $10.0s^{-1}$ and the height reduction range from 30% to 50% has been investigated in depth. Effect of the strain on the flow stress and the microstructure evolution for deformation of isothermally compressed TA1/AZ31B laminated composites is analyzed. The results show that the difference in plastic deformation between TA1 and AZ31B during at the same time isothermally compressed. Below 623K temperature, both metals of TA1/AZ31B laminated composites are involved in deformation; the flow stress presents work hardening with the strain increasing. Form 623K to 723K, the AZ31B layer deformation was dominated, the flow stress presents work hardening first, and then softening with the strain increasing, and the work hardening appeared predominantly in TA1 layers during the isothermally compressed deformation processing. The Arrhenius-type constitutive equation could precisely predict the flow stress behavior of TA1/AZ31B composites, and the value of R was 0.991 when that of AARE is 3.976%. Combined with macrostructure observations and experimental results were established based on the dynamic material model (DMM), The optimum parameters were determined at the temperature of 723K and the strain rate of $0.01s^{-1}$ with power dissipation's maximum efficiency of 28%. With the strain increasing, the middle TA1 layer is subjected to larger shearing stress due to two AZ31 layers plastic elongation deformation and pressuring, the middle TA1 layer occurs necking and fracture.

I-8: Effect of Initial Particles Size on the Microstructure and Ion Conductivity of $BaZr0.1Ce0.7Y0.1Yb0.1O3-\delta$ Mixed Ion Conductor Applied for Micro-Tubular Intermediate Temperature Solid Oxide Fuel Cell

Changcheng Chen, Long Li, Zhanmin Wang, Xi'an University of Architecture and Technology, China; Yuan Dong, Xi'an University of Posts & Telecommunications, China; Mingfei Liu, Georgia Institute of Technology, United States

The influence of starting powder's initial particle size (micron and nano-sized) on the structural characterization, morphology, and ionic conductivity of the mixed ion conductor $BaZr0.1Ce0.7Y0.1Yb0.1O3-\delta$ (BZCYYb) are investigated. The BZCYYb materials are employed as electrolyte to achieve anode-supported proton conducting micro-tubular solid oxide fuel cells (MT-SOFCs) with configuration of Ni-$BaZr0.1Ce0.7Y0.1Yb0.1O3-\delta$ | $BaZr0.1Ce0.7Y0.1Yb0.1O3-\delta$ | $La0.6Sr0.4Co0.2Fe0.8O3-\delta$-$Sm0.2Ce0.8O2-\delta$. The influence of initial particle size on the electrochemical performance as well as impedance spectra of single cell are thoroughly studied. Achieved results include: i) X-Ray Diffractometer results showed that the pure perovskite phase could be obtained in BZCYYb-ZnmCμm material which fabricated with mixed initial nano-sized ZrO_2 and micron-sized CeO_2 powders; ii) Raman vibrations appear near 350, 430 and 650cm^{-1} in BZCYYb-ZnmCμm material, while the perovskite structure of BZCYYb has rhombohedral distortion; iii) BZCYYb-ZnmCμm sample exhibits outstanding conductivities of 1.011, 0.750, 0.564, 0.473, 0.339, 0.259, 0.186, 0.123 and 0.072 $\times 10^{-2}\Omega^{-1}\cdot cm^{-1}$ at 800, 750, 700, 650, 600, 550, 500, 450 and 400°C under the air condition, respectively. iv) the single cell exhibits uniform distribution of micro sponge-like pores electrode is well-adhered to the dense, crack-free 12μm thick BZCYYb-ZnmCμm electrolyte layer observed by Scanning Electron Microscope; v) the cells show excellent electrochemical performance with the maximum power densities of 1.07, 0.98, 0.81 and $0.70W\cdot cm^{-2}$ at 750, 700, 650 and 600°C, respectively, characterized by Electrochemical Impedance Spectroscopy; vi) the cell design especially gives a very low concentration polarization value (0.01 and $0.02\Omega\cdot cm^2$ at 750 and 700°C). Noticeably, it is the first time that a model of particle size effect on both phase structure and conductivity of mixed ion conductor BZCYYb is developed. Moreover, it is the first time that an investigation of particle size effect on both electrochemical performance and impedance spectra of MT-SOFCs ever reported.

I-9: Study on Dispersion of Nano ZrO_2 Particles Applied to Pure Iron Based on High Temperature Laser Confocal

Yiming Du, Shengli Li, Xingang Ai, Shaoguang Yang, University of Science and Technology Liaoning, China

The dispersion of nanoscale particles in molten steel due to their easy agglomeration, were studied. Because of the unique agglomeration characteristics of nano particles, The non-uniform distribution of second phase nanoparticles in molten steel is one of the main difficulties in strengthening the mechanical properties of steel. In order to solve this problem, it is particularly important to study the distribution and dispersion of nano particles. Nano ZrO_2 particles were modified and their structures were analyzed and characterized. The distribution and dispersion of ordinary nano ZrO_2 particles and pre-dispersed nano ZrO_2 particles were compared. Instead of traditional induction heating furnace, physical melting model was constructed by high temperature laser confocal microscope. Pre-dispersed modified nano ZrO_2 particles and untreated nano ZrO_2 particles were added to the iron powder respectively. The movement and morphology of nanoparticles during solidification of molten steel were observed. Scanning electron microscopy was used to observe the distribution of nanoparticles. Morisita’s index was used to calculate the dispersion uniformity quantitatively. The results show that the common nano ZrO_2 particles agglomerate at the edge, and it is difficult to exist stably in the metal. The pre-dispersed nano ZrO_2 particles are evenly dispersed in molten steel without obvious agglomeration and have better dispersion.

I-10: Research on 2Cr13 Cutting Edge Strengthened by Plasma Surfacing

Taixu Xu, Zhijun He, Xiao Han, University of Science and Technology Liaoning, China

In order to enhance the performance of cutting edge, make efficient use of high-quality cutting materials and reduce waste of high-quality materials. The experiment uses the plasma surfacing method to form the 8Cr13MoV powder surfacing layer as the cutting edge on the surface of the 2Cr13 common cutter material.The specimens were corroded by mixed corrosion solution of picric acid, hydrochloric acid and ethanol, and the bonding between surfacing layer and matrix was observed by optical microscope. Detection of comprehensive hardness of surfacing layer by Rockwell hardness tester and Vickers hardness tester The wear resistance of surfacing layer was tested by spherical friction and wear tester. The impact toughness was tested by composite specimens, and the potential polarization curve and planned resistance of surfacing layer were tested by electrochemical workstation.The experimental results show that the bonding mode of 8Cr13MoV surfacing layer and 2Cr13 matrix is metallurgical bonding, and the crystallization mode of fusion zone is epitaxial crystallization. The hardness of 8Cr13MoV surfacing layer is good, the macrohardness is 56.7HRC and the microhardness is 604HV5. Due to the higher hardness, the wear resistance of the surfacing layer is about 4 times higher than that of the matrix. The impact toughness and corrosion resistance of 8Cr13MoV surfacing layer are equal to that of 2Cr13 matrix

J. Amorphous and High Entropy Alloys

Symposium Organizers:

Weihua Wang, The Institute of Physics, Chinese Academy of Sciences, China; Zhaoping Lv, University of Science and Technology Beijing, China; Hidemi Kato, Tohoku University, Japan; Hojin Ryu, Korea Advanced Institute of Science and Technology (KAIST), Korea; Michael Ferry, New South Wales, Australia; Evan Ma, Johns Hopkins University, USA

August 19-21, 2019
Place: Exhibition Area (3rd Floor)

J-1: Heating Rate Effect on Soft Magnetic Properties and Crystallization of Fe-Si-B-P-Cu(-C) Amorphous Alloy System

Yan Zhang, Tohoku University, Japan

Soft magnetic materials have been widely used for power transformers, motors, communications devices, and microelectronics, etc. Si-steel is widely used for soft magnetic material due to its low cost and high saturation magnetic flux density. However, an inescapable disadvantage of Si-steel shows much higher core loss than Fe-based amorphous/nano-crystalline materials because of the high coercivity. Among the various Fe-based amorphous/nano-crystalline alloys based on FINEMET (Fe-Si-B-Nb-Cu), NANOPERM (Fe-M-B, M=Zr, Hf, Nb) and NANOMET (Fe83.3-85-Si-B-P-Cu) with excellent soft magnetic properties, the Fe-rich Fe-Si-B-P-Cu nano-crystalline materials have been developed, which reduce production costs by eliminating expensive materials such as Nb, Zr and Hf. A high heating rate (> 300K/min) is necessary to achieve a nano-crystalline alloy in NANOMET. However, the annealing process for more than 30 sheets at the same time tends to be uncontrollable at high heating rate, during which ribbon stacking density is limited in industrial application. To realize the mass industrial production of magnetic cores, two-step annealing process seems to be unavoidable. Obviously, the heat treatment process conditions need to be ameliorated and explored further. In the present work, the excellent magnetic softness is realized in

Fe81.5Si0.5B4.5P11Cu0.5C2 (at.%) nano-crystalline alloy through an optimum annealing with low heating rate (10K/min). For the Fe-rich soft magnetic materials, the crystallization mechanism during annealing process with high and low heating rate in this alloy is analyzed which is different from Fe83.3-85-Si-B-P-Cu nano-crystalline alloy.

In this research, the ribbon samples (about 5~10mm in width and 20μm in thickness) of Fe-Si-B-P-Cu-(-C) were fabricated by single-roller melt spinning in air. Nano-crystallization behavior was performed by annealing in an infrared furnace at the heating rate of 5~1000K/min. Thermal and structural analyses were performed by using differential scanning calorimetry (DSC), X-ray diffractometry (XRD) and transmission electron microscopy (TEM). Magnetic properties were measured and analyzed by using B-H curve tracer and vibrating sample magnetometer (VSM). The result details will be presented in the conference session.

J-2: A thermodynamic-Elastic Energy Criterion for Composition Design of HEAs

Lei Zhang, Guangxi College of Education, China; Hongmei Chen, Xiaoma Tao, Yifang Ouyang, Guangxi University, China

High entropy alloys (HEAs) have useful properties, such as excellent specific strength, superior mechanical performance at high temperatures, exceptional ductility and toughness at cryogenic temperatures, superparamagnetism, and superconductivity. HEAs usually intend to form BCC and/or FCC solid solution rather than intermetallic compounds.

The thermodynamic properties are used to predict which phase will be formed for the HEAs. The mixing enthalpies for binary alloys can be calculated successfully by Miedema's theory, and the thermodynamic properties of multicomponent alloy systems can be evaluated by the extrapolation from constituent binary systems. Zhang et al used a criterion with the parameter δ and parameter Ω to determine the forming ability of HEAs. Senkov et al proposed combined parameters associated with mixing enthalpy, entropy and annealing temperature. This criterion should determine the annealing temperature before prediction of composition. The mixing enthalpy of HEAs in above methods was evaluated by way proposed Takeuchi et al.

The thermodynamic properties of multicomponent alloy systems can be evaluated by the geometrical model from those of constituent binary systems by including the interaction among constituent elements. The thermodynamic-elastic energy criterion was proposed and verified by using 107 HEAs, the enthalpies of mixing have been calculated by Miedema's theory and geometrical model. The mixing enthalpies and elastic energies of multicomponent alloys exhibit a clear relationship, that is the enthalpies of mixing should be in the range of -22 to 5kJ/mol and the elastic energy should be less than 6.06kJ/mol. The lager the atomic size difference, the lager the elastic energy is. The more negative enthalpy will be benefit to forming of the intermetallic compound. The present criterion is compared with that with the parameter δ and parameter Ω, and the agreement is reasonable. It also shows good coincidence with experiment. The present criterion should be help to design the composition and new system of HEAs.

Acknowledgements:This work was financially supported by the National Natural Science Foundation of China (51531009, 11464001), the Natural Science Foundation of Guangxi Province (2016GXNSFBA380166), and the Science Foundation of Guangxi Education Department (2017KY1472).

J-3: High-Temperature Properties of TRIP Refractory High-Entropy Alloy

Jie Wang, Yu Tang, Shuxin Bai, National University of Defense Technology, China

The concept of high-entropy alloys(HEAs) has been proposed since 2004. HEAs is a kind of alloys containing more than 4 principle elements, for which their configurational entropy is high. Deviating from the Gibbs' rule, though HEAs has complex elements, they get simple phase, usually single phase, because of the phase-stabilizing contribution of high configurational entropy. HEAs usually show a good strength and ductility due to the special strengthening mechanism caused by the random atom occupation and single solid solution structure. As more special properties of HEAs, such as sluggish diffusion, anti-radiation and corrosion resistance, are discovered successively, the great applications in different condition are exploited.

Refractory high-entropy alloys (RHEAs) is a family of HEAs contains at least 4 refractory elements. Except the characteristic the same as other HEAs, RHEAs have an intrinsic high melting point, probably higher than 2000˚C, which endues RHEAs a great potential to substitute Ni-based superalloys. However, most of the reported RHEAs have poor plasticity at room temperature, which is the primary reason restricting the real application of RHEAs.

Fortunately, the transformation-induced plasticity (TRIP) effect, which was widely used in high-Mn steels and titanium alloys, provides a way to overcome the poor plasticity of RHEAs. The basis of TRIP effect is mechanically induced martensitic transformation, which leads to a remarkable plastic-deformation ability. And the increased phase boundary density due to transformation creates additional obstacles of dislocation slip, thereby contributing to the strain hardening. Because of this special transformation mechanism, TRIP effect can increase plasticity without decreasing the strength. Since the TRIP effect was firstly introduced in HEA at 2016, its

effect on improving the plasticity of RHEAs has been demonstrated by HfZrTiTa0.5 and NbZrTiTa systems. But there is still a lot of work to do before RHEAs' real application, because only a few reports about the high-temperature properties of RHEAs, including high-temperature creep strength, thermal structural stability and anti-oxidation capability, all of which are critical to high-temperature structural material, have been presented. Therefore, it is significant to study the service characteristics of RHEAs.

In this work, the properties including the mechanical behavior, structural stability and anti-oxidation capability at high temperature of TRIP RHEAs were measured. The mechanism behind these service characteristics of TRIP RHEAs were investigated. Above all, the potential of TRIP RHEAs as high-temperature structural material was revealed, and some improvement ways were provided. This work is helpful for the development of both HEAs and high-temperature alloys.

J-4: The Characterisation of the Microstructure and Mechanical Properties of Mg35Al25Gd20Y10Zn10 High-Entropy Alloy

Dan Xu, Ning Liang, Northeastern University at Qinhuangdao, China; Xiaoping Lin, Liwei Quan, Yun Dong, Runguo Zhen, Northeastern University at Qinhuangdao,China / Northeastern University, China

In recent years, the strengthening of magnesium alloys and high-entropy alloys (HEAs) have attracted more and more attentions and become hot research. Based on the idea of high-entropy alloy design, Al, Gd, Y, Zn were selected as the principal elements with obvious "solid solubility effect" with Mg according to the Hume-Rothery solid solubility theory and the existing high-entropy alloy criterion. Then Mg35Al25Gd20Y10Zn10 high-entropy alloy was designed according to non-equal molar ratio and prepared by vacuum melting. The microstructure and phase composition of the experimental alloy were determined by X-ray diffraction (XRD), scanning electron microscopy (SEM) and Energy Dispersive Spectroscopy (EDS). Meanwhile, the mechanical properties of the alloy were examined by microhardness tester and universal testing machine. The results showed that the alloys are composed of two kinds of magnesium-based solid solutions with blocky or granular second phases dispersed on it. The solid solubility (wt.%) of Gd, Zn, Y and Al in the two magnesium-based solid solutions were about 4.90, 1.60, 0.83, 0.03 and 21.10, 9.20, 4.48 and 0.93, respectively; and the microhardness was 101HV and 128HV, respectively. The atomic ratio of the main elements in the blocky or granular second phase was nearly Al:Gd:Y=6:2:1, with a small amount of solid-solved Zn. The dimension of the second phase was about 2~20μm, and the microhardness was 427HV. The engineering stress-strain curves of the alloy at room temperature compression engineering shows obvious work hardening tendency. Besides, the yield strength was 419MPa, compressive strength was 451MPa, compression rate after fracture was 17.23%, and strength-plastic product was 6850MPa·%, which is much higher than that of cast magnesium alloy and deformed magnesium alloy reported at present. Magnesium-based solid solution with high solid solubility and the second phase with high hardness dispersed on it are the main reasons for the ultra-high-strength plastic product of the alloy.

J-5: Microstructural Evolution and Compressive properties of AlCuSiFe-X (X = Cr, Zn, Mn) High Entropy Alloys

Ashutosh Sharma, Ajou University, Minseok Oh, Kwanil Kim, Byungmin Ahn, Ajou University, Korea

High entropy alloys (HEAs) are currently of great research potential in materials research community. Compared to traditional binary or ternary element alloys. Multicomponent HEAs exhibit simple solid solutions in contrast to conventional alloys where a number of complex compounds form. There are various routes of metals and alloy fabrication like casting, spraying, vapor deposition techniques and chemical methods. Most of the HEAs are often produced by casting and solidification approach which are highly sensitive to casting defects, metals segregations and inclusions. Therefore, compared to popular casting methods, powder metallurgy route which consists of high energy ball milling (HEBM) and compaction steps can successfully eliminate the drawbacks of traditional metal fabrication processes. In addition, PM process is simple, safe and can be scaled to the industrial level.

In the present work, the alloying behavior of equiatomic AlCuSiFe-X (X = Cr, Zn, Mn) was investigated using X-ray diffraction, scanning electron microscopy, and transmission electron microscopy. The HEAs were prepared by HEBM and subsequent consolidation by spark plasma sintering (SPS). The results indicate that single phase FCC and BCC phases evolve after HEBM; whereas BCC/FCC phase separation, evolution of sigma (σ) phases, and fluctuations of the Al and Cu-X compositions in Al-Cu-X rich regions occur after SPS. It appears that entropy of mixing plays a key role in determining the phase formation in HEAs after SPS. Further, compressive properties of AlCuSiFeZn, AlCuSiFeCr, and AlCuSiFeMn alloys together with their hardness values were evaluated. The as-sintered bulk hardness and compressive stress values were maximum for AlCuSiFeCr followed by AlCuSiFeZn and AlCuSiFeMn. The results are discussed in terms of compositional fluctuations governed by the mixing entropy of the binary systems. It is also reported that a combination of cheaper metals like Al, Cu, Si, Fe,

Zn in this alloy can reduce down the overall cost with a comparable or better structural properties in some cases compared to the popular Mn, Cr based HEAs.

J-6: In Situ XRD Studies of Atomic Structure of Two Fe-Based Metallic Glasses

Shi Huang, Jiawei Mi, University of Hull, UK

In-situ synchrotron high energy X-ray diffraction were used to study the atomic structure evolution of Fe48Cr15Mo14C15B6Gd2 and Fe48Cr15Mo14C15B6Y2 metallic glass on the process of solidification at the I15 beamline of Diamond Light Source UK. Atomic structural changes occurring in these two amorphous alloys during the process of solidification were investigated. The metallic glasses were melted with a constant heating rate, after that the temperature were held isothermally, and then the sample was cooled. The research is mainly focused on studying the atomic structure of Gd alloys in Fe-based amorphous alloys and the role played by Gd and Y element in the nanocrystallization. By combining total scattering and anomalous scattering techniques, we are able to recognize the atomic structures of multicomponent Fe-based amorphous alloys in liquid state. Real space analysis by means of the atomic pair distribution function (PDF) demonstrated that the rate and extent of the thermal expansion strongly depend on the interatomic separation. The PDF proved to be a reliable method for the description of crystallization kinetics. To clarify the role played by Gd and Y element, the difference of atomic structure and crystallization kinetics of these two Fe-based amorphous alloys were compared. This research indicated that how the local short-range ordered structure of an amorphous phase evolves into the long-range periodic structure of a crystalline phase in some Fe-based metallic glasses. It is very important in designing and developing new metallic alloys.

J-7: Porous Ceramic Composite Networks Prepared by Sintering of Metallic Glass Nanospheres

Zhifeng Wang, Mo Zhu, Yonghui Yan, Chunling Qin, Hebei University of Technology, China

Porous ceramics with high specific surface area contains special physical and chemical properties, and presents potential applications in bone tissue engineering, water treatment, drug delivery systems, optical sensors, nuclear fuel materials, heat transfer and thermal energy storage. However, the fabrication of porous ceramic is still challenging.

Yttrium titanate $Y_2Ti_2O_7$ is an important member of the pyrochlore family because it exhibits various properties which make it suitable for potential applications in different fields, such as optical and fuel cells applications. So far, the fabrication of porous $Y_2Ti_2O_7$ pyrochlores has been rarely reported. Here we report a new route to obtain porous $Y_2Ti_2O_7$ pyrochlore composite networks by sintering of metallic glass nanospheres at high temperature. The metallic glass nanospheres were synthesized by selective phase etching of a two-phase amorphous alloy precursor ribbon. Then the as-obtained metallic glass nanospheres were sintered at different temperatures open to air. The changes in composition and morphology with different temperatures were detailedly analysed.

The lattice parameter, electrical conductivity, X-ray analysis, Fourier Transform-Infrared Spectroscopy (FTIR) and thermal expansion coefficient (TEC) were obtained in order to study its suitability in the field of solid oxide fuel cells. The results show that the crystalline structure and phase composition of the products are highly influenced by sintering temperature. When the sintering temperature is lower than 1000˚C, porous TiO_2 and Y_2O_3 composites can be obtained. When the sintering temperature is higher than 1100˚C, porous $Y_2Ti_2O_7$ pyrochlore composites can be synthesized. The further study shows that the original sizes of metallic glass nanospheres and sintering time play important roles in porosity of the porous $Y_2Ti_2O_7$ pyrochlore composites, and finally influence the electrical and thermal properties of the materials when used in solid oxide fuel cells.

This work also opens a door for the synthesis of various porous ceramic networks by sintering of nanostructured amorphous alloy precursors, and may promote the development of both dealloying and amorphous alloy fields.

J-8: Study on Soft Magnetic Properties and Microstructure for FeCoNixCuAl (x = 0.75~1.75) High-Entropy Alloys

Zhongyuan Wu, Zhong Li, Chenxu Wang, Xiaohua Tan, Hui Xu, Shanghai University, China

In the past few decades, the emergence of high-entropy alloys (HEAs) has broken the design philosophy of traditional alloys. Its severe lattice distortion and slow diffusion leads the alloys to have high strength, hardness and high temperature resistance. In the previous research of our group, it is found that FeCoNiCuAl alloy has good mechanical properties and good soft magnetic properties. In this paper, we changed the content of Ni to investigate the changes of soft magnetic properties and microstructure in the FeCoNixCuAl (x = 0.75~1.75) HEAs. The ingots of this alloys were produced by

vacuum arc melting for four times. And it was sucked into a 100mm × 10mm × 2mm water-cooled Cu mold. The coercivity (Hc), hysteresis losses (Pu), remanence (Br), initial magnetic permeability (μi), and maximum magnetic permeability (μm) were obtained from hysteresis curves (DC) test system. With increasing Ni content, the values of μi and μm increase while the values of Br, Hc and Pu decrease, when the magnetic field is added to 25000A/m. The results of X-ray diffraction (XRD) reveal that all samples contain BCC plus FCC duplex phases and the formation of FCC phase was promoted with the increase of Ni element. It suggests that the magnetic properties are closely related to the phase composition of FeCoNixCuAl (x = 0.75~1.75) HEAs. In the process of adding Ni, the electrical resistivity of the alloy also increases with the increase of Ni content.

J-9: High Temperature Deformation in Non-Equiatomic FeMnNiCoCr High Entropy Alloy

Hee-Tae Jeong, Soo-Young Chae, Woo-Jin Kim, Hongik University, Korea

High temperature tensile deformation behavior and microstructural evolution in a non-equiatomic Fe40Mn27Ni26Co5Cr2 high entropy alloy (HEA) which has face-centered cubic (fcc) single phase was studied. The HEA was processed by severe plastic deformation, High ratio differential speed rolling (HRDSR) and post annealing. In order to investigate the high temperature tensile deformation behavior, uni-axial tensile tests were conducted at high temperatures in range of 973~1173K and at strain rate from 10^{-4} to $10^{-1}s^{-1}$ on ultrafine grained (~ 1.3μm), fine grained (~ 10.4μm) and coarse grained (~ 314.0μm) HEAs. To investigate the microstructural evolution, the microstructure of HEAs was observed by using optical microscopy (OM), scanning electron microscopy (SEM) and electron backscatter diffraction (EBSD) techniques. In order to examine the existed phases in HEA deformed at high temperatures, X-ray diffraction (XRD) was performed. Compared with the excellent ductility and fracture toughness at room temperature, ductility and fracture toughness dramatically decreased by increasing deformation temperature albeit the HEA had recrystallized fine grains and coarse grains. In addition, dislocation climb creep (DCC) exhibited at low strain rates and at high temperatures (973~1173K) as the rate-controlling deformation mechanism in coarse grained HEA. However, grain boundary sliding (GBS) appeared at low strain rate and at high temperatures and DCC exhibited at high strain rates and at high temperatures as the rate-controlling deformation mechanism in fine grained and ultrafine grained HEA. This GBS became obvious as the temperature increased and grain size decreased. The activation energies for plastic flow at high temperature were estimated and strain rate sensitivity (m) was examined in order to understand tensile deformation behavior at high temperatures and wide strain rate. For a better understanding of tensile deformation behavior at high temperatures, the correlation between high temperature tensile deformation behavior and microstructure of HEA was also discussed.

J-10: Preparation of Metallic Glass/Crystalline Composites Using Electroless Plating Copper on Glassy Powders

Zhiwei Huang, Guoqiang Xie, Zhenwei Wu, Xi Cheng, Harbin Institute of Technology (Shenzhen), China

Spherical Cu50Zr43Al7 metallic glassy powder was produced by the gas-atomized process, and a layer of crystalline copper was coated on the Cu-based glassy powder by electroless plating to form metallic glass / crystalline Cu composite powder to improve the electrical conductivity and the ductility of the consolidated composite. The metallic glass / crystalline composite powder was densified by spark plasma sintering to obtain bulk metallic glass composite. The powder and Cu50Zr43Al7/Cu composite were characterized by X-ray diffraction and field emission scanning electron microscope. The relative density, thermal stability, mechanical and electrical properties of the specimens were tested. The effects of sintering temperature, loading pressure, holding time and particle size on the properties of samples were studied. The results show that the composite has a hardness of 320HV and a compressive strength of over 1000MPa. The strength and hardness decrease obviously with the addition of ductile crystalline copper. On the contrary, the conductivity increases continuously. Compared with amorphous materials, sintering can be carried out under lower loading pressure, and the plasticity of composites has been improved obviously. In addition, the conductivity is over $5.0 \times 10^{4}(\Omega \cdot cm)^{-1}$, which is of great significance for the research of composite materials with high strength and high conductivity.

J-11: Investigation of Mechanical Properties of CoCrFeMnNi High Entropy Alloys Fabricated by Rapid Solidification Process

Hyeon Jeong You, Kwang Yong Jeong, Nagarjuna Cheenepalli, Soon JIk Hong, Kongju National University, Korea

High entropy alloys (HEAs) are very attractive materials due to their outstanding properties such as high strength, good thermal stability and high temperature strength, and exceptional corrosion resistance. High

entropy alloys (HEAs) usually containing at least five principal elements by adding 5~35 at% each element unlike the conventional multi-element alloys. As a result, high mixed entropy occurs, so that an intermetallic compound is not formed and a single solid solution is formed, so that the mechanical properties are relatively higher than those of the conventional alloy. In this study, we have fabricated FCC structured single phase of CoCrFeMnNi high entropy alloys (HEAs) by the combination of two approaches, and systematically investigated and comparted their mechanical properties. Initially High entropy alloys (HEAs) was fabricated by the casting plus rolling method, and characterized their properties. Secondly, High entropy alloys (HEAs) was fabricated by the new powder metallurgy process such as gas atomization, followed by spark plasma sintering. (SPS) The crystal structure of the specimens from both processes was analyzed by X-ray diffraction. The fracture surfaces, and cross-sectional micrographs of the High entropy alloys (HEAs) specimens were characterized by scanning electron microscopy (SEM), and transmission electron micrograph (TEM) respectively. The mechanical properties including the compressive strength, micro vickers hardness were analyzed.

J-12: Microstructure and Properties of Corrosion-Resistant Al-Cr-Fe-Co-Ni High Entropy Alloys

Xiaolei Yan, Hui Guo, Shujie Pang, Tao Zhang, Beihang University, China; Qing Wang, Dalian University of Technology, China; Peter K. Liaw, The University of Tennessee, USA

The AlxCrFeCoNi high entropy alloys (HEAs) with both ductile face-centered cubic (FCC) phase and tough body-centered cubic (BCC) phase have attracted extensive attentions due to their high strength and good ductility. However, pitting corrosion tends to occur at the surface of the BCC phase in Cl−-contained solutions, which may limit the applications of the AlxCrFeCoNi HEAs. In this presentation, we will report an Al-Cr-Fe-Co-Ni alloy with integration of excellent corrosion resistance, high strength and good ductility synthesized by increasing Cr content, and the influences of Cr on microstructure, corrosion behaviors and mechanical properties of the Al-Cr-Fe-Co-Ni HEAs. It was found that increasing Cr content could lead to the change in the phase structure of the alloys from single FCC to duplex FCC+BCC. For the Al-Cr-Fe-Co-Ni HEAs with duplex FCC+BCC structure, the BCC phase exhibited higher content of Cr than the FCC matrix and hence did not cause deterioration of the corrosion resistance of the alloys. The pitting corrosion resistance of the Al-Cr-Fe-Co-Ni HEAs was enhanced with increasing Cr content, and the alloys with relatively high contents of Cr exhibited no pitting corrosion in 3.5wt.% NaCl solution. Moreover, the formation of BCC phase in the Al-Cr-Fe-Co-Ni HEAs with relatively high Cr contents effectively enhanced the tensile strength, though decrease the ductility. It is notable that the Al-Cr-Fe-Co-Ni HEA with high Cr-content exhibited tensile yield strength over 600MPa and elongation of 12% besides excellent corrosion resistance.

J-13: High-Temperature Deformation Mechanisms and Processing Maps of Equiatomic CoCrFeMnNi High-Entropy Alloy

Hee-Tae Jeong, Woo-Jin Kim, Hongik University, Korea; Hyung-Ki Park, Kwangsuk Park, Tae-Wook Na, Korea Institute of Industrial Technology, Korea

The hot compressive deformation mechanism and processing maps of the equiatomic FCC CoCrFeMnNi high-entropy alloy (HEA) were studied in the temperature range between 1023 and 1323K and in the strain rate range between 10^{-3} and $10s^{-1}$. At high strain rates above $1s^{-1}$, strain hardening was dominant even at the very high temperature of 0.84Tm, which may be attributed to the sluggish diffusion coefficient and low stacking fault energy of the CoCrFeMnNi HEA, leading to suppression of dynamic recovery. According to the processing maps, the best condition for hot working was near $10^{-3}s^{-1}$ at 1323K. Power-law breakdown and unstable flow occurred at low temperatures and high strain rates where the strain hardening was pronounced. The activation energy for plastic flow measured in the power-law creep regime when considering the dependence of elastic modulus on temperature was 312.2kJ/mol; this value is close to the activation energy for the weighted diffusion coefficient calculated by weighting the contribution of each element in the CoCrFeMnNi HEA (284kJ/mol). The size and fraction of the dynamically recrystallized grains increased as the strain rate decreased and the temperature increased, as in conventional metals. Both discontinuous dynamic recrystallization and continuous dynamic recrystallization (CDRX) occurred. CDRX became more distinct as the temperature increased. The deformation mechanism and behavior of the CoCrFeMnNi HEA were very similar to those of FCC pure metals in terms of the stress exponent and the effect of the stacking fault energy and diffusivity on the creep rates.

K. Nanocrystalline Materials, and Ultra-Fine Grained Materials

Symposium Organizers:

Yue Zhang, University of Science and Technology Beijing, China; Zhiyong Tang, National Center for Nanoscience and Technology, China; Nobuhiro Tsuji, Kyoto University, Japan; Jae-il Jang, Hanyang University, Korea; Kenong Xia, University of Melbourne, Australia; Nathan Mara, University of Minnesota, USA

August 19-21, 2019
Place: Exhibition Area (3rd Floor)

K-1: Engineering on Ni-Co-S Bifunctional Electrocatalyst for Water-Splitting

Jing Wu, Huijing Guo, Zhuo Kang, Yue Zhang, University of Science and Technology Beijing, China; Yue Zhang, University of Science and Technology Beijing, China

Efficient evolution of hydrogen and oxygen simultaneously with earth-abundant, highly active, and robust bifunctional electrocatalysts has been a significant concern for water splitting. Herein, non-noble metal based Ni-Co-S bifunctional catalysts with tunable stoichiometry and morphology were realized. The electronic structure engineering and subsequent morphological design synergistically contributed to significantly elevated electrocatalytical performance. Overpotentials $\eta 10$ of 243mV (vs.RHE) for OER and 80mV for HER in 1M KOH solution, as well as Tafel slopes of 54.9mV/dec for OER and 58.5mV/dec for HER were demonstrated together with prominent stability. In addition, DFT calculation was conducted to indicate the optimal electronic structure via visually mapped electron density difference of catalysts, and representatively verify that the enhanced OER activity of $NiCo_2S_4$ nanosheets is concerned with the Co top site on (110) surface. Moreover, the tandem bifunctional $NiCo_2S_4$ anode and cathode exhibited a required voltage down to 1.58V ($J=10mA/cm^2$) for simultaneous OER and HER, and no obvious performance decayed after 72h. When integrated with a GaAs solar cell, such photo-assisted water splitting electrolyzer acquired a certificated solar-to-hydrogen efficiency up to 18.01%, further demonstrating the feasible engineering protocols as well as the promising potential of bifunctional $NiCo_2S_4$ for large-scale overall water splitting.

K-2: Magnetic Metal Cobalt/Reduced Graphene Oxide (M-Co/RGO) Nanocomposites with Tunable and High Performance Electromagnetic Wave Absorption Capabilities

Qi Li, Qingliang Liao, Yue Zhang, University of Science and Technology Beijing, China

From the half-century, with the broad application of electronic devices and wireless communication equipment in civil and military fields. Electromagnetic interference (EMI) or electromagnetic pollution have been paid more and more widespread attention all over the world. To address the problem effectively are not only beneficial for national defense security, but also for the improvement of the harmonious human living environment. The magnetic metal nanoparticles have attracted considerable attention due to the excellent EM wave absorption properties as well as the controllable synthesis of dimensions and shapes. Consequently, RGO has been functionalized by various magnetic metal nanoparticles. Herein, the prepared M-Co nanoparticles have relative high saturation magnetization (Ms) and hysteresis, which have potentials to be employed as excellent magnetic loss EM wave absorption materials. Magnetic metal cobalt (M-Co) nanoparticles are evenly dispersed on reduced graphene oxide (RGO) without pronounced aggregation. The M-Co/RGO nanocomposites exhibit tunable and high-performance electromagnetic (EM) wave absorbing properties. The excellent EM wave absorbing properties are due to the dielectric-magnetic loss synergistic effect as well as the well-matched impedance matching. When the mass ratio of M-Co and RGO is 5:1 and the filler loading of the nanocomposite is 20%, the maximum RL reach as strong as –32.8dB at 11.7GHz with a thickness of 2.2mm, and the effective absorption bandwidth up to 5.7GHz at a thickness of 1.8mm. The highly excellent EM wave absorbing performance mainly originates from synergistic effect of dielectric loss and magnetic loss as well as well-matched impedance matching. The EM wave absorbing mechanisms of M-Co/RGO nanocomposites including dipole polarization relaxation, interfacial polarization relaxation, eddy current loss, natural resonance and conductive loss. The novel M-Co/RGO nanocomposites have superior potentials to be designed as tunable and high-performance absorbents.

K-3: Crystal Orientation Engineering of NiOx Hole Transport Layer in Perovskite Solar Cells

Mingyue Shi, Haonan Si, Zhuo Kang, Yue Zhang, University of Science and Technology Beijing, China

Hybrid organic-inorganic perovskite solar cells (PSCs) have attracted great attention over the past years due to their high solar to electric power conversion efficiency (PCE). The hole transporting material (HTM) is an essential component in perovskite solar cells (PSCs) for efficient charge extraction and transport. NiOx is a potential candidate owing to its wide bandgap and good stability. Materials with low crystal symmetry often exhibit anisotropic properties, allowing the tuning of their physical and chemical properties via crystallographic orientation and exposed facet control.

Herein, for the first time we have demonstrated that NiOx with a [111] growth orientation and exposed (111) facets exhibits excellent charge transport properties. The NiOx film is fabricated using RF sputtering technique. We use [111]-oriented NiOx as hole transport layer in perovskite solar cells with a configuration of ITO/NiOx/CH3NH3PbI3/ZnO/Ag. The orientation of the NiOx film influences the arrangement, coordination, surface energy and structural defect of surface atoms and their band structure. As a result, the NiOx film with a [111] crystal orientation not only increase electrical conductivity, carrier mobility and charge extraction ability in the hole transport layer, but also improve morphology of the perovskite film, which contribute to an improvement of PCE and negligible hysteresis. Therefore, the crystal orientation engineering effectively modulates the carrier transporting behavior, which eventually gives rise to the enhanced performance of PSCs.

K-4: Pulsed Laser Ablation Assisted Synthesis of Graphene Quantum Dots

Ho Jun Lee, Jung-Il Lee, Jeong Ho Ryu, Korea National University of Transportation, Korea

Graphene quantum dots (GQDs) have attractive properties and potential applications. However, their various applications are limited by a current synthetic method which requires long processing time. Here, we report a facile and remarkably rapid method for production of GQDs exhibiting excellent optoelectronic properties. We employed the pulsed laser ablation (PLA) technique to exfoliate GQDs from multi-wall carbon nanotube (MWCNTs), which can be referred to as a pulsed laser exfoliation (PLE) process. Strikingly, it takes only 6min to transform all MWCNTs precursors to GQDs by using PLE process. Furthermore, we could selectively produce either GQDs or graphene oxide quantum dots (GOQDs) by simply changing the organic solvents utilized in the PLE processing. The synthesized GQDs show distinct blue photoluminescence (PL) with excellent quantum yield (QY) up to 12% as well as sufficient brightness and resolution to be suitable for optoelectronic applications. We believe that the PLE process proposed in this work will further open up new routes for the preparation of different optoelectronic nanomaterials.

Moreover, we present the GQDs and GOQDs can be selectively prepared by easy and simple pulsed laser ablation in liquid (PLAL) method by controlling the laser wavelength. The obtained GQDs and GOQDs showed a significantly different optoelectronic nature mainly due to the existence of surface oxygen-rich functional groups (e.g. carboxyl or hydroxy groups). Also, we described a possible mechanism for the formation of oxygen functional groups during the PLAL process based on the Coulomb explosion model, which can give further insight for designing functional carbon materials.

K-5: Temperature Dependence of Harmonic Structure Designed SUS316L Austenitic Stainless Steel Deformation

Koki Yagi, Morihiro Hariki, Masashi Nakatani, Bhupendra Sharma, Mie Kawabata, Kei Ameyama, Ritsumeikan University, Japan; Cinzia Manapace, University of Trento, Japan

SUS316L austenitic stainless steel has variety of industrial applications because of its favorable ductility and corrosion resistance properties. However, relatively low yield strength may make it unsuitable for many structural applications. In stainless steel, the high strength can easily be achieved by many grain refinement methods, but usually with a pronounced sacrifice of ductility. In recent years, to solve this strength-ductility trade-off problem, a new concept of heterogeneous microstructural design called "Harmonic Structure" has been proposed. Harmonic Structure (HS) consists of coarse-grains areas like island surrounded by a continuous fine-grains counterpart three-dimensional network structure. At room temperature, the Harmonic structured SUS316L specimen presented a good combination of high strength and improved uniform elongation. However, under different temperature conditions, the mechancial properties of Harmonic structured SUS316L is not reported yet. Therefore, the present study focuses on the analysis of mechanical properties of Harmonic structured SUS316L at various temperatures.

The SUS316L steel powder, prepared by plasma rotating electrode process (PREP), was used as a starting material. Average particle size in the initial powder was approximately 140μm. Mechanical milling was carried out in a planetary ball mill using SUS304 steel pots and balls (5mm diameter). The milling was carried out under argon gas atmosphere, at room temperature, wherein the ball-to-powder weight ratio was maintained at 2:1. Mechanical milling was carried out for 180ks, 360ks, and 540ks at a constant milling speed of 150 rpm. Subsequently, the milled powders were sintered by Spark Plasma Sintering (SPS) at 1223K temperature for 5.4ks under 50MPa load. In addition, the reference compacts of homogeneous structured SUS316L were prepared from initial powder (IP). The microstructure observations were carried out by scanning electron microscopy (SEM) and electron backscatter diffraction (EBSD). The mechanical properties were examined by tensile and compression tests at various temperatures between 223K and 1073K. The specimens for tensile and compression tests were machined by wire-spark cutting (3mm gauge length, 1mm gauge width and 1mm gauge thickness for tensile tests and 5mm diameter and 10mm height for compression tests). Tensile and compression tests were carried out at a nominal strain rate of $5.6 \times 10^{-4} s^{-1}$ and $1.0 \times 10^{-3} s^{-1}$, respectively, at all temperatures.

The HS designed SUS316L exhibited superior mechanical properties at temperatures below 873K, whereas at higher temperature (1073K) it showed almost similar mechanical property than that of the conventional IP counterparts. Those uniqueness in mechanical properties are attributed to the heterogeneity of the HS materials.

K-6: Improvement of Mechanicalproperties of Harmonic Structured Pure-Ti via Multi-Thermo-Mechanical Process

Akito Shimamura, Motoki Miyakoshi, Hupendra Sharma, Mie Kawabata, Kei Ameyama, Ritsumeikan University, Japan

The Harmonic Structured (HS) materials consist of heterogeneous bimodal microstructure with coarse grained area "Core" surrounded by fine grained area "Shell" exhibited the excellent combination of mechanical properties. However, the Harmonic Structured materials have a limited improvement in mechanical properties as compared to its conventional homogeneous counterparts. Therefore, the present study focuses on the further improvement of mechanical properties of Harmonic Structured titanium (HS-Ti) by multi thermomechanical (Multi-TMP) process.
In the present study, the Harmonic Structured pure-Ti was prepared by mechanical milling (540ks) followed by spark plasma sintering (1073K, 1.8ks) of PREP Ti powder. Then Multi-TMP process was carried out on as-fabricated HS-Ti specimens. The TMP conditions were as follows: accumulative cold rolling (CR) for 3 passes of 10%, 19%, and 27%, and subsequent annealing at 873K for 1.8ks after each pass. The microstructural analysis was performed by SEM and EBSD techniques. Preliminary microstructure analysis revealed that the microstructure of Multi-TMP processed specimens (CR + annealed) was apparently similar to the as-fabricated HS-Ti specimen. Moreover, the Shell and Core grain size including with overall grain size was approximately similar in all the cases. However, interestingly, the mechanical properties were significantly different. In particular, with increasing CR passes, the strength remarkably increases without significant reduction in ductility. The Kernel Average Misorientation (KAM) image presented that the misorientation increases, at Shell areas, with increasing cold rolling passes. In many HS materials, stress concentration has been reported to take place especially into the Shell region in the early stage of deformation and, as a result, dislocation emission and accumulation occurs in the vicinity of the Shell. Therefore, it was expected that due to those dislocations remained in the Shell region even after "CR + annealing" step, the dislocation density gradient successively generated by each Multi-TMP process. That is, it can be expected that the increasing strength after each CR pass is due to the dislocation strengthening, which play an important role as same as "ultra-fine grain Shell strengthening" in HS materials. In other words, as same as "grain size gradient", "dislocation density gradient" is quite effective mechanism for improving the mechanical properties in HS materials.

K-7: Selective Recrystallization in Harmonic Structure Designed Pure Titanium via Thermo-Mechanical Processing

Mie Ota Kawabata, Motoki Miyakoshi, Akito Shimamura, Kei Ameyama, Ritsumeikan University, Japan; Guy Dirras, David Tingaud, Université Paris 13, Japan

Harmonic Structure (HS) is one of heterogeneous microstructures, and it is characterized as 3D ultra-fine grains (UFGs) network structure, named "Shell", with uniformly dispersed coarse grains, "Core". The HS designed materials are able to achieve high strength and high ductility at the same time, compared with the homogeneous coarse grains structure materials. Distribution of strain at the Shell grains during plastic deformation exhibits such superior mechanical properties. In this study, thermo-mechanical processing (TMP), i.e. cold rolling and annealing, was applied to the HS designed pure Titanium, and its microstructure evolution and the mechanical properties are discussed. Fabrication of the HS is based on powder metallurgy route. That is, pure titanium powder was processed by Mechanical Milling (MM) for 360ks at room temperature under Argon gas atmosphere. During MM, nano grains formed in the surface layer of the powder by severe plastic deformation, whereas coarse grains were remained in the middle of powder particles. The Milled powder was subsequently consolidated at 873K for 3.6ks under vacuum by a Spark Plasma Sintering process. The sintered compacts have a topological three-dimensional connected UFG network structure, which is so called "Harmonic Structure". Average grain size and volume fraction of the shell were 19.7mm and 15.7%, respectively. Those compacts were provided to the TMP, that is, 10% cold rolling at room temperature followed by annealing at 873K for 1.8ks. There was few change in the Shell grain size after the TMP, while volume fraction of the shell increased from 15.7% to 23.1%. It is noteworthy that TEM observation revealed existence of dislocation free grains in the Shell region, though a typical deformed structure was observed in the Core region. These results imply that a selective recrystallization took place in the Shell region, but not in the Core grains. Mechanical properties were evaluated by tensile tests. Outstanding mechanical properties such as high proof strength, high UTS, a large elongation and a large tensile toughness were obtained in the TMP-HS Titanium. Increase of UFGs by the selective recrystallization in the Shell resulted not only in higher proof strength, but also the higher UTS

with superior ductility. In other words, the remarkable improvement of mechanical properties was attributed to the development of the Shell structure by a selective recrystallization in the Shell. This work was supported by JSPS KAKENHI Grant Number JP18H05256. These supports are gratefully acknowledged.

K-8: Preparation and Application of High-Performance Graphene-Reinforced Copper Tungsten Alloys

Yi Ding, Zhixiang Zhu, Baoan Chen, Qiang Zhang, Xin Chen, Yu Han, Global Energy Interconnection Research Institute Co., Ltd., China

In this work, the failed samples were analyzed. The method of damage for CuW80 products used for ultra-high voltage SF6 circuit breaker are mainly cracking, ablation and exfoliation. Therefore, the graphene was selected to add into the electrical contact material of CuW, and the threshold of graphene oxide content was achieved through the calculation based on the percolation model. Furthermore, the process of surface modification and dispersibility improvement of graphene oxides was systematically studied. The optimal process parameters were gotten by a series of work on the fabrication and characterization of RGO/Cu composites. The relationship between density of skeletons and compacting pressure was established and green compacts of skeleton with different components for CuW electrical contact materials were prepared based on the relation curve. Then, CuW electrical contact materials with target composition were obtained by sintering at 930˚C for 2h and infiltrating at 1050˚C. Simultaneously, two processes of preparation were explored, including infiltration with pure tungsten and activated sintering infiltration.

CuW80 electrical contact materials modified with graphene (0.002~0.2wt.%) were fabricated by activated sintering infiltration method. The properties of the as-prepared materials, including density, hardness, electrical conductivity and bending strength, could reach the national standard of GB/T8320-2003, which completely meet the technical requirement of the research contents.

The results revealed that the hardness, electrical conductivity and bending strength of the materials firstly increased and then decreased with an increase of the graphene content. The CuW80 possessed the best performance at the content of 0.002wt.% graphene in the matrix, specially, the wear extent, wear rate and the friction coefficient were 53%, 55% and 76% of the CuW80 products in use, respectively. The performance could satisfy the technical requirement of the project, where the wear performance should improve 20%. In addition, the arc erosion resistance of the as-prepared electrical contact materials under the condition of AC4 (AC, 380V and 120A) was evaluated through mass loss after experienced over 20 and 35 operations. It demonstrated that the mass loss was 44% and 63% of the ultra-high voltage electrical contact materials. The arc erosion resistance also reached the technical requirement of the project that a decrease of 20% in mass loss during arc erosion should achieved.

L. Computational Design and Simulation of Materials

Symposium Organizers:

Tongyi Zhang, Shanghai University, China; Zhimei Sun, Beihang University, China; Shigenobu Ogata, Osaka University, Japan; Byeong-Joo Lee, Pohang University of Science and Technology (POSTCEH), Korea; Salvy Russo, RMIT, Australia; Saryu Fensin, Los Alamos National Lab, USA; Michele Manuel, University of Florida, USA

August 19-21, 2019

Place: Exhibition Area (3rd Floor)

L-1: First-Principles Calculation of Hydrogen Dissolution and Diffusion Properties in V-Mo-W Alloy Membranes

Jiayao Qin, Guilin University of Electronic Technology, China; Zhongmin Wang, Dianhui Wang, Chaohao Hu, Huaiying Zhou, Guilin University of Electronic Technology, China / Guangxi Key Laboratory of Information Materials, China

Vanadium-based alloys have been identified as one of the most promising hydrogen separation membrane materials due to their high hydrogen permeability and cost less. In this paper, we systematically studied the effect of W doping on the structure, mechanics, H-dissolution and H-diffusion properties of V-Mo alloy by using the first-principles method. Calculations reveal that the absorption of a single H atom at the tetrahedral interstitial site (TIS) is the most thermodynamically stable one among all the tetrahedral interstitial site (TIS), the diagonal interstitial site (DIS), and octahedral interstitial site (OIS); and H solution enthalpy at TIS are 32.23kJ/mol, -20.55kJ/mol and -0.97kJ/mol for V16H, V12Mo4H and V8Mo4W4H, respectively. The optimal way of H-diffusion is TIS-to-TIS; and H-diffusion energy in V16H, V12Mo4H and V8Mo4W4H are 0.138 eV, 0.132eV and 0.188eV, respectively. The values of H-difusion coefcient (D) are $1.68\times10^{-8}m^2/s$, $8.31\times10^{-9}m^2/s$, and $1.87\times10^{-8}m^2/s$ for V, V-Mo, and V-Mo-W, respectively, at 673K. The calculation results also show that V-Mo-W alloy also has good elastic properties. These results indicate that the addition of W element not only further reduces the solubility of hydrogen and inhibits hydrogen embrittlement, but also enhances hydrogen diffusivity and improves the mechanical properties of V-Mo alloy. This provides a theoretical

reference for the design of the ternary alloy and further obtains a better hydrogen permeable membrane.

L-2: Molecular Dynamic Simulation of the Structure and Viscosity Properties of CaO-SiO_2-Al_2O_3 Slags with Low Basicity

Boran Jia, Min Li, Sai Wang, Qiangqiang Wang, Qian Wang, Shengping He, Chongqing University, China

CaO-SiO_2-Al_2O_3 melt is the main components of slag in ironmaking and steelmaking processes. As a typical amphoteric oxide, it is important to study the effect of Al_2O_3 concentration on the microstructures of CaO-SiO_2-Al_2O_3 melt for predicting the macroscopic physical and chemical properties of metallurgical slag. The effect of Al_2O_3 concentration on the microstructures of CaO-SiO_2-Al_2O_3 melt with low basicity was studied by means of molecular dynamics simulation in this study. The Born-Mayer-Huggins pair potential function was adopted to describe the interaction among atoms in melt. The NVT ensemble was selected to prevent the shape of the simulation cell changed. The position coordinates at the end of the calculation are analyzed to obtain the structure information and transport characteristics of the melt. The results showed that $[SiO_4]^{4-}$ tetrahedron is more stable than $[AlO_4]^{5-}$ tetrahedron at 1873K. With the increase of Al_2O_3 concentration, Non-bridging Oxygen decreased and oxygen tricluster increased in the melt, indicating that a more complex network structure was formed. The Average Coordination Number of Al (CNAl-O) increased from 4.25 to 4.43, suggesting that $[SiO_4]^{4-}$ tetrahedron was replaced by $[AlO_4]^{5-}$ tetrahedron. The increasing of high-coordination Al leaded to the instability of melt structure. In the acidic region with low Al_2O_3 concentration, with the increase of Al_2O_3 content, the amount of degree of polymerization (DOP) in the melt increases, which leaded to the complexity of the melt structure and the increase of its viscosity. In the acidic regions with high Al_2O_3 concentration, with the increase of Al_2O_3 content, the structure of melt tends to be unstable, resulting in the decrease of its viscosity, indicating that the part of Al_2O_3 is alkaline. The study indicated the expression of amphoteric properties of Al_2O_3 in aluminosilicate melt, which can provide a guidance to how to select or control slags used in ironmaking and steelmaking.

L-3: Ab Initio Materials Design to Enable Sub-Nanosecond Memory Writing

Yuxing Zhou, Getasew M Zewdie, Wei Zhang, Xi'an Jiaotong University, China; Evan Ma, Xi'an Jiaotong University, China / Johns Hopkins University, United States

Operation speed is a key challenge for phase change random access memory (PCRAM) technology. The further increase to the writing speed for the commercialized phase change storage meets its bottleneck due to the stochastic nature of phase change materials (PCMs) during the crystallization process. In this work, a new phase change material, Sc0.2Sb2Te3 (SST), is designed to enable the sub-nanosecond writing operation through systematic screening across the Periodic Table of Element. This scandium antimony telluride compound allows a writing speed of only 700 picoseconds, compared with the speed of tens of nanoseconds in the conventional phase change devices, such as $Ge_2Sb_2Te_5$. By thorough ab initio based simulations, the abundance of ABAB rings are observed in amorphous SST and those squares are revealed to be steadily existing during the thermal fluctuation at elevated temperatures, which leads to the reduction of the stochasticity and the enhanced incubation without any preprogramming. In addition, to further understand the mechanism of ultrafast nucleation in SST, we explore the intrinsic properties of its parent compounds, namely Sc_2Te_3 and Sb_2Te_3, in their amorphous forms. Though there are huge similarities between two compounds in terms of bonds and angles, amorphous Sc_2Te_3 exhibits a much more ordered amorphous network with the absence of homopolar bonds and odd rings, leading to the abundance of ABAB squares. The bonding strength of Sc-Te is proved to be larger than that of Sb-Te via chemical bonding analysis, but higher-membered primitive rings in a-Sc_2Te_3 deviate from the targeted crystalline counterpart. All the evidences mentioned above give rise to the enhanced incubation upon our materials design by alloying a small amount of the Sc into amorphous Sb_2Te_3, breaking the barrier for cache-type phase change memory.

L-4: Alloy Design of Fe-Based Bulk Metallic Glasses Using Neural Network and Optimization Algorithm

Junhyub Jeon, Seok-Jea Lee, Chonbuk National University, Korea; Hyunjoo Choi, Kookmin University, Korea; Hwi-Jun Kim, Liquid Processing & Casting R&D Group, Korea Institute of Industrial Technology, Korea; Min-Ha Lee, Advanced Process and Materials R&D Group, Korea Institute of Industrial Technology, Korea

The classical methods to design alloys are generally based on a 'trial-and-error' process that spends lots of time, effort, and cost. A more effective approach to design alloys using computational model has received much attention as computational technologies develop. In the present work, we chose computational approaches to effectively model the design of Fe-based bulk metallic glasses (BMG) for achieving better physical properties rather than previous Fe-based BMG alloys. An artificial neural network (ANN) was applied to design novel Fe-based BMG alloys based on literature data. ANN has been vastly applied to present a non-linear relationship between input variables and output results in diverse areas including science, engineering, economy, and so on. Simultaneously, optimization algorithms (OA) were employed to research an optimized alloy composition which shows target properties. The principal thermal properties that like glass transition temperature,

crystallization temperature, and melting temperature of Fe-based BMG alloys are predicted by ANN and OA. The relation of alloying elements with the thermal properties is quantitatively analyzed. The optimal alloy composition is proposed based on the predicted results and validated the prediction accuracy with experimental work. We suggest a computational alloy modeling process for novel Fe-based BMG alloys and expected that this approach could be applied to predict other properties of Fe-based BMG alloys and research novel composition of diverse series of Fe-based BMG alloys.

L-5: First-Principles Simulation of Grain Boundary Segregation in Steels

Jingliang Wang, Chengjia Shang, University of Science and Technology Beijing, China

Segregation of alloying elements to the grain boundaries can modify a wide range of properties, among which the influence on cohesive properties of grain boundaries is of greatest concern when the embrittlement of steels is considered. The experiments have long revealed that certain alloying elements such as C and B have beneficial effect on the grain boundary strength while other elements, such as P and S are known as harmful impurities. To understand the mechanism behind this, however, one has to turn to atomic scale computer modeling, which can provide insight into the electronic structures so that the chemical bonding between atoms can be characterized. First-principles density functional theory, as a fully quantum-mechanical method, thus has been widely used in the investigation of segregation behavior of alloying elements at grain boundaries in steels. In practice, one must identify the segregation sites first and then can further determine the effect of segregation on the grain boundary energy and cohesive properties. Recently, we proposed a geometric criterion to predict the segregation site for interstitial C. Rice-Wang thermodynamic model and ab-initio tensile tests were then applied to characterize the grain boundary cohesive properties. This method was then extended to other alloying elements.

L-6: L-6: Li^{2+} as a Paradigm for Understanding the Competition between Attosecond Charge Migration and Charge Transfer Induced by Nuclear Motion

Likun Yang, Jeffrey R. Reimers, Rika Kobayashi, Noel S. Hush, Shanghai University, China; University of Technology Sydney, The Australian National University, Australia, The University of Sydney, Australia, Australia

Attosecond spectroscopy presents opportunities for the control of chemical reaction dynamics and products, as well as for quantum information processing. Results are often interpreted using very extensive quantum dynamics simulations, however, rather than through simple chemical models. We show how Hush's 1975 theory depicting core-ionized mixed-valence X-ray photoelectron spectroscopy (XPS) can be applied to interpret properties of core-ionized Li2+, which, along with H^{2+} and N^{2+}, provides a relatively simple paradigm scenario for understanding the principles controlling attosecond dynamics. Indeed, Li^{2+} is the simplest molecule with both core and valence electrons, also providing the simplest system in which charge migration strongly interacts with nuclear dynamics following attosecond-timescale excitation. Dynamics is considered following simultaneous excitation of 8 different pairs of core-ionized states, as well as for six model sets of potential-energy surfaces, showing how subtle changes in surface properties can have profound effects on dynamics.

L-7: Theoretical Prediction of Boron-Based MAX Phases M2AB and M2AB2

Nanxi Miao, Junjie Wang, Artem R Oganov, Northwestern Polytechnical University, China

Two types of new boron-based MAX phases, include Hf2BiB, Hf2PbB, Hf2InB2, Hf2SnB2, Zr2TlB2, Zr2PbB2 and Zr2InB2, were predicted through combining first-principles calculations and a systematic variable-composition evolutionary structure exploration. Therefore, the X elements, which were limited to carbon and nitrogen in the conventional MAX phases, can be extended to boron. Besides the traditional form of Mn+1AXn, a new prototype of MAX phase M2AX2 can be formed in the boron-based system. The coexistence of covalent, ionic, and metal bonds in the newly predicted MAX results in high cohesive energy, which is favorable for experimental synthesis. The effect of various functional groups on the stabilization, mechanical properties and electronic of derivative two-dimensional (2-D) MXenes from predicted M2AB and M2AB2 was also investigated. It shows that the functionalized 2-D MXenes possess improved mechanical flexibly than bare 2-D MXenes. Moreover, the predicted 2-D Zr2B2 exhibits an extremely high theoretical capacity due to its large adsorption area and strong adsorption ability for Li^+ and shows low Li^+ migration energy barriers. Therefore, the predicted 2-D Zr_2B_2 can be an excellent candidate anode material for lithium ion batteries.

L-8: Crystal and Electronic Structure Engineering of Tin Monoxide by External Pressure

Kun Li, Junjie Wang, Northwestern Polytechnical University, China; Artem R Oganov, Skolkovo Innovation Center, Russia

The layered tin monoxide (-SnO) with the space group P4/nmm, having the excellent electronic property, is a p-type semiconductor and shows promise as anode

material in lithium rechargeable battery and thin film transistors. However, compared to the SnO_2, the narrow band gap of SnO limits it from a more general application, e.g. solar cell and transparent conductor. The development of material synthesis and material prediction motivates us to modify band gap of tin monoxide and synthesize a new tin monoxide with wider band gap. In this work, a theoretical investigation within the framework of density functional theory was carried out on the structural and electronic properties of several SnO material with various vdW correction under different pressures. Our calculations revealed that a metastable SnO (β -SnO), owing the space group of P21/c, could be more stable than the -SnO under the high pressure and possesses a band gap of 1.5eV suitable for photofunctional applications. Combining the topological analysis, we concluded that -SnO could be converted from -SnO via a high-pressure intermediate phase. A semiconductor-to-metal transition was observed and suggests possible enrichment of application of -SnO.

M. Renewable Energy Materials and Nuclear Materials

Symposium Organizers :

Min Zhu, South China University of Technology, China; Yuan Deng, Beihang University, China; Guanghong Lu, Beihang University, China; Tetsuya Uda, Kyoto University, Japan; Taek-Soo Kim, Korea Institute of Industrial Technology (KITECH), Korea; Dmitri Golberg, Queensland University of Technology, Australia; Assel Aitkaliyeva, University of Florida, USA

August 19-21, 2019

Place: Exhibition Area (3rd Floor)

M-1: Phase-Field Simulation of Void Formation During Radiation

Wenbo Liu, Di Yun, Libin Sun, Xi'an Jiaotong University, China

Phase-field simulation is a powerful method in capturing the morphological evolution of interfaces in various materials science processes. A phase-field method (PFM) had been developed to simulate the void formation during radiation. The void formation and growth behavior during irradiation, especially the effects of GBs on the voids morphology evolution, were studied using the phase-field method. By constructing the total free energy as a function of vacancy concentration, interstitial concentration and the phase-field variable, the void morphology during irradiation was simulated using PFM. Both the radiation-produced point defects (GBs) and gas atoms were considered. By incorporating a simple orientation dependent surface energy with sharp cusps on given crystallographic orientations, experimentally observed void shape with facets and rounded corners is captured. When applied to polycrystalline materials, grain dependent void morphologies are predicted, and the simulation results are qualitatively similar to reported void morphologies in irradiated copper. In addition, the formation of void denuded zones and vacancy depleted zones adjacent to the GBs in bicrystalline and polycrystalline structures are studied. The effect of grain boundaries on the formation of voids was also studied, and the anisotropic of surface energy on the void evolution was also systematically analyzed. In addition, all the effect of other parameters on the void formation during radiation were also discussed. The annihilation of vacancies in GBs and the appearance of void denuded zone near GBs were also simulated by considering the interaction between GBs and point defects produced during irradiation. In addition, voids are preferred to form and grow near GBs during post-irradiation process if the vacancy formation energy is lower and the diffusion coefficients of point defects, including vacancy and interstitial atom, are higher than that inside grains, which has been experimentally observed during post-irradiation annealing, and both two-dimensional (2D) and 3D simulation results agreed well with the experimental observations.

M-2: Research Progress on Recovery Annealing of Reactor Pressure Vessels Steel

Haidong Wang, Xiaoyong Wu, Lu Wu, Jianjun Mao, Rongjian Pan, The First Sub-Institute, Nuclear Power Institute of China

The reactor pressure vessel (RPV) of nuclear power plants (NPPs) is rated as the highest priority component considered practically and economically impossible to be replaced, its service security determines the operation safety and life time of NPPs. During high energy neutron irradiation, the phenomenon of hardening and embrittlement of RPV steels occurs, which causes the yield strength increase and the ductile brittle transition temperature move to high temperature region. Therefore, irradiation embrittlement is pronounced in two consequences: firstly, it narrows the "pressure - temperature" operation window for normal operating conditions, and second, it limits RPV lifetime as the transition temperature of RPV materials cannot be higher than that determined from the pressurized thermal shock calculations. Recovery annealing is the most effective method that it could practically restore initial mechanical properties of RPV materials. In this paper, the restoration of mechanical properties and mechanism of post-irradiation annealing RPV steels are presented. Based on previous studies, this work was performed in the framework of a larger project where irradiated (I), irradiated and annealed (IA) and re-irradiated (IAI) materials were characterized. It is noted that irradiation induced formation of clusters (mainly Cu) and segregation of impurities (mainly P) are the main factors that lead to RPV steels hardening and embrittlement. In addition, Annealing temperature at least 150˚C more than the irradiation temperature is required

for at least 100 to 168 hours to obtain a significant recovery toughness. Furthermore, the re-embrittlement rates upon subsequent re‐irradiation were similar to the embrittlement rates observed prior to the thermal anneal. The following problems are discussed in the review: evolution of RPV materials properties and nano-structure under irradiation and post irradiation annealing; models for embrittlement recovery and re-embrittlement due to post-annealing irradiation RPV steels; chemical composition and neutron fluence effect on transition temperature of irradiated RPV materials recovery.

M-3: Compositional and Structural Optimization of $ZrFe_2$ Based Alloys for High Pressure Hydrogen Storage Application

Min Zhu, Hui Wang, Chao Zhou, School of Materials Science and Engineering, South China University of Technology, Guangdong Provincial Key Laboratory of Advance Energy Storage Materials, China

Hydrogen is an ideal energy carrier without causing any pollution. However, the lack of effective and safe hydrogen storage technology limits the large-scale application of hydrogen energy. In addition to the widely known gaseous-, solid-, and liquid-state hydrogen storage systems, the gas-solid hybrid hydrogen storage mode combines the high pressure gaseous hydrogen storage with materials-based solid-state hydrogen storage. Therefore, the hybrid hydrogen tank has higher gravimetric or volumetric hydrogen density compared with conventional hydrogen storage techniques. Thus it is feasible to reduce the volume and operating pressure (to 35 ~ 45MPa) of high-pressure hydrogen tank without the loss of hydrogen capacity, and the safety of hydrogen storage system could be also improved.

To match the fast hydrogen charging and discharging performances of hybrid hydrogen tank within the working pressure range, it demands hydrogen storage alloys with high equilibrium pressure, fast kinetics, low hydride formation enthalpy (less than 20kJ·mol^{-1} H_2) and high cycle ability. Meanwhile, the small hysteresis coefficient (Hf) between absorption and desorption is also one of the criteria to weigh the performance of high-pressure hydrogen storage alloys.

$ZrFe_2$ alloy has great potential as high-pressure hydrogen storage medium because of its high equilibrium pressure and fast kinetics at ambient temperature. Nevertheless, its ultrahigh equilibrium pressure and low hydrogen capacity hinder its further application. To improve the thermodynamic properties and hydrogen storage performances of $ZrFe_2$, we study the alloying with Cr, Mn, V, Ti elements and its effect on the structure and hydrogen storage behaviors of $ZrFe_2$. The dependence of lattice constant, electron concentration, and the volume modulus on the composition (stoichiometry, atomic size ratio of A-/B- site elements) of alloys, and the corresponding effects on the de-/hydriding plateau characteristics were systematically investigated. A series of ternary and quaternary alloys have been prepared by arc-melting, their hydrogen storage properties including the capacity, equilibrium pressure, hydrogen sorption rate have been evaluated.

M-4: Effect of Heat Treatment on $M_{23}C_6$ Carbide Precipitation and Its Effect on Tensile Properties of Alloy 690 Tubes

Taehyuk Lee, Korea Institute of Geoscience and Mineral Resources, Korea; Jonghyeon Lee, Chungnam National University, Korea

Alloy 690, a nickel-based alloy having high chromium content (27~31wt.%), was developed as a replacement for alloy 690 in the steam generators of PWRs in NPPs, and is now widely used owing to its excellent resistance to SCC, pitting corrosion, and corrosion fatigue in aggressive primary water environments. These special properties are dependent on the size and distribution of precipitates in the matrix. Generally, under the conditions of heat treatment or during high-temperature service, $M_{23}C_6$, as a typical carbide commonly precipitates at the grain boundary in alloy 690. The precipitation behavior then could be affected by the alloy composition (such as carbon content) and heat treatment conditions. Hence, it is very important to study carbide precipitation behavior according to the heat treatment conditions, such as solution annealing and thermal aging and its effect on mechanical properties of alloy 690. In this study, we investigated the effect of solution annealing and aging treatment on the intergranular carbide precipitation behavior of alloy 690 tubes for steam generators. The carbides precipitated on the grain boundaries were identified as chromium-rich $M_{23}C_6$ carbide, which has a cube-cube orientation relationship with the matrix on one side of neighboring grains. The carbide precipitation behavior is closely related with the interaction between the solubility of carbon in Ni-based matrix and diffusion of alloying elements. The ultimate tensile strength and elongation of the solution annealed alloy 690 tubes at 300°C are 638.8 ± 12.4MPa and 43.2 ± 4.2%, respectively. In the early stage of precipitation, the ultimate tensile strength increased to 720.4 ± 13.5MPa. The carbides function as reinforcement in alloy 690 and provide strength enhancement with aging time reached 15 hours. However, when the aging time passed 15 hours, this property gradually decreased to 710.6 ± 12.6MPa due to the low bonding strength between the carbide and matrix.

M-5: Comparison of Different Interatomic Potentials for Tensile Simulation of α-Fe at 723K

Heng Rui, Huiping Zhu, Baochen Chang, Ting Zhou, Fenglei Niu, Yan Ma, North China Electric Power University, China

The mechanical properties of structural materials which are mainly iron-based materials in nuclear power

plants affecting the safe operation severely. Hence, it is necessary to study the mechanical properties and microstructure evolution of materials under different working conditions. The molecular dynamics (MD) simulation technology can reveal the microscopic dynamic process of materials and calculate the relevant mechanical parameters. However, the accuracy of the simulation bases on the reliability of the used interatomic potentials. Thus, the interatomic potentials used for the MD simulation need to be verified by testing their capability in relevant material properties. This paper using MD method to compare different interatomic potentials for tensile simulation of body-centered cubic (bcc) iron in high temperature, and determine a suitable interatomic potential for subsequent in-depth research. Considering the high temperature of the material under actual working conditions, the stretching temperature was set to 723K and compared with the room temperature. Through the simulated stress-strain curves, the tensile strength and yield strain of different potential models at different temperatures were calculated. Open Visualization Tool (OVITO) software was used for visualizing the microstructure evolution, and the local structure around each atom was resolved by using the common neighbor analysis (CNA) technique. Meanwhile, Dislocation analysis (DXA) was applied to analyze the dislocations during tensile loading. The results showed that the tensile strength and yield strain were both reduced with the increasing temperature, the phase transformation is advanced and the phase transformation process is increased during the stretching at 723K, but no significant influence on the formation of dislocations was found. At the start of stretching, the body-centered cubic (bcc) structure remained intact. After reaching the yield strength, the phase transition occurred and the new phase of face-centered cubic (fcc) structure increased. The 1/2<111> dislocations were generated and migrated subsequently. Besides, different interatomic potentials had different performances in predicting the stress-strain curves and microstructure variation. The details were discussed in the full paper.

M-6: Study on Corrosion Resistance of Ti_3SiC_2 in LBE at 500℃

Baochen Chang, Huiping Zhu, Heng Rui, Baikun Huang, Sihao Huang, Ting Zhou, Fenglei Niu, North China Electric Power University, China

Liquid lead and lead bismuth have been considered as coolants for future Accelerator Driven Systems (ADS) and Lead cooled Fast Reactors (LFR). Hence, one of the main key issues to be addressed in the development of ADS and LFR is the compatibility of the structural materials in contact with the high temperature liquid lead-based coolant. As a ceramal material, MAX-phase material possesses some of the most attractive proprieties of both ceramics and metals, such as high temperature resistance, corrosion resistance, good heat conduction and plasticity, which makes it an important candidate structural material for LFR and ADS. To understand the LBE corrosion resistance of this material, a typical MAX-phase material Ti_3SiC_2 was immersed in static LBE with saturated oxygen concentration at 500˚C for 300~1000h. After the corrosion experiment, multiple analysis methods have been used to analyze the corrosion layer evolution of Ti_3SiC_2. By combining the analysis results of scanning electron microscopy (SEM), energy dispersion X-ray spectroscopy (EDS) and X-ray diffraction (XRD), information of the morphology of both the sample surface and sample cross section, the thickness of corrosion layer, the element distribution and configuration has been clearly obtained. The results showed that the surface smoothness of Ti_3SiC_2 samples degenerated after LBE corrosion. No stratification was observed in all corroded samples but the transition layer was found in the surface region of corroded samples and its thickness increased with the increase of corrosion time. More experimental content and test results will be discussed in the manuscript in detail.

M-7: Current Status and Development Trend of Impact Limiter Filling Materials for Nuclear Spent Fuel Transport Cask

Youdong Xing, Siyi Yang, Yukun An, Ertuan Zhao, Zhongfang Li, Pengfei Zhang, Shandong University of Technology, China

With the widespread use of nuclear fuel, the transportation of nuclear spent fuel is also particularly important. In China or other countries, nuclear spent fuel is carried out by transport casks. In order to ensure the safety of the transport cask during lifting and transportation, impact limiters must be installed at top and end of the cask to avoid unpredictable consequences caused by fallen leakage spent fuel. The impact limiter acts to absorb energy, control overload and ensure structural integrity, consisting of the outer cladding material and the inner filler material. The filling material is an important part of the impact limiter energy absorption.

The traditional filler material of the impact limiter is mainly wood. In addition, polyurethane foam and honeycomb aluminum material also have the case of being an impact limiter filling material; all of the above three materials have good energy absorption and light weight characteristics, which are suitable for impact limiters , however, the above materials also have defects. The wood has texture, which leads to the directionality of mechanical properties, also it has perishable defect. Polyurethane foam has flammability and low strength, and energy absorption needs large size. Honeycomb aluminum materials have unidirectional mechanical

properties, and the manufacturing process of honeycomb aluminum materials is complicated.

As an important part of the impact limiter, how to make it have excellent energy absorption performance, light weight and fire resistance is the focus of research on filling materials. Our team aims to apply two kinds of metal materials (bi-directional corrugated honeycomb aluminum, aluminum foam) as the filling material for the impact limiter. Between them, the bi-directional corrugated honeycomb aluminum material is made as the nuclear fuel storage cask impact limiter filling material has been used in other country like USA without China. The bi-directional corrugated honeycomb aluminum has mechanical properties in two directions, and its weight is lighter than that of the same volume of aluminum. It implies superb energy absorption characteristics after researched. We aims to design and optimize the bi-directional corrugated honeycomb aluminum material to make it have better use characteristics. Additionally, our team creatively proposed to use aluminum foam as an impact limiter filling material, and launched a new application for aluminum foam. In the new direction, the next step is to study and manufacture large foam aluminum blocks with more uniform structure and better energy absorption characteristic. Through the above work, we will do our utmost to research and manufacture the impact limiter filling materials and denote our passion.

M-8: High Performance of Si-Organic Hybrid Solar Cells by Optimizing Interfacial Junction Quality and Light Trapping Ability

Zudong He, Kunming University of Science and Technology / Faculty of Metallurgical and Energy Engineering, China

Recently, the organic-inorganic hybrid heterojunction solar cells (HHSCs) with simple preparation process and low cost are gaining increasing attention. Among various types, the Silicon-poly (3,4 ethylenedioxythiophene): polystyrene sulfonate (PEDOT:PSS) was considered promising one. Here, nanotexture of inverted pyramid (SiIPa) and nanowires (SiNWs) were fabricated by copper (Cu) and siliver (Ag) nanoparticle assisted chemical etching for improving the light trapping ability and interfacial junction area to ensure the improvement of energy efficiency. Compared with planar silicon wafers, nano-structured silicon wafers exhibit better light absorption performance in the wavelength range of 200~1200nm, and the light reflectivity is less than 7%. However, nanotextured silicon surface leads to a large number of surface defect states and causes charge recombination, and the minority carrier lifetime of silicon wafers with inverted pyramid and nanowires are lower than that of planar silicon. Therefore, the surface was smoothed by tetramethylammonium hydroxide (TMAH) solution to enhance the minority carrier lifetime. What is more, a novelty technological process of pressurized spin coating was proposed to increase heterojunction contact area. The results show that interfacial junction area between PEDOT:PSS and nanotextured silicon prepared by pressurized spin coated is larger than that of natural gravity infiltration. In addition, compared with the reference devices, the energy conversion efficiency of the hybrid solar cells prepared by the pressurized spin coating process is improved by 10%~15%. Metal-assisted chemical etching is a sustainable and simple technique for introducing microstructures into the surface of silicon wafers, and the resulting PEDOT:PSS/Si hybrid solar cells (HSCs) with SiIPa and SiNWs show a promising PCE. The novel external assisted spin coating provides a new method to optimize interfacial junction quality between PEDOT:PSS and the textured silicon substrate.

M-9: Indium Recovery from Indium-Tin Scrap by Electrorefining in Molten Fluoride Salt

Hyun-gyu Lee, Sang-Hoon Choi, Jae-Jin Sim, Kyoung-Tae Park, Korea Institute for Rare Metals, Korea Institute of Industrial Technology, Korea; Hyun-gyu Lee, Sang-Hoon Choi, Soong-Keun Hyun, Department of Advanced Materials Engineering, In-Ha University, Korea

The essentiality of indium in electronic devices has increased many fold during recent past. At the same time indium is rare in natural abundance indium is obtained as a byproduct of zinc metal refining so that the need for recycling of indium has increased dramatically in the near past. Out of other recycling methods, molten salts based electrorefining holds promising future because it provides high conductivity, purity and eco-friendly process. General methods of molten salt electrorefining presents that solid anode and cathode is adapted and handled to get refined metal, but in this study indium and tin is used. Impure scrap containing indium-tin alloy shows lower melting temperature than electrolyte, LiF-KF system, so electrorefining specially carried out using molten anode(In-Sn impure) and cathode(purifiyed indium) materials. Herein, we report electrorefining of indium at the tungsten and molybdenum electrode as anode and cathode, respectively. Process temperature was holded at 700˚C and electrolyte is molten LiF–KF eutectic (49~51mol.%). Contents of InF_3, initiative compounds was controlled for reducing polarization of potential in electrolytic cell. Chemical stability between fluoride electrolyte and materials used in this expermnets such as In-Sn alloy, alumina crucible was pre-analyzed before electrolysis. Concentration of InF_3 was changed from 3wt% to 7wt% and it was found that the electrochemical reduction of indium at the cathode

site and then it was directly move into the bottom crucible as a liquid phase. Cyclic voltammetry(CV) was performed to evaluate the electrochemical behavior of the In electrorefining. Mo was used as a working electrode in conjunction with a tungsten rod as counter electrode Ni wire Electrode was used as a pseudo-reference electrode, serving only to monitor and control the potential of working electrode during the experiments. The cathode was molybdenum metal. Electrochemical measurements were performed using a potentiostat/galvanostat. To get the In deposition, chronopotentiometry (CP) analysis was performed to compare the variation of potential for various applied current densities at the cathode during electrolysis of the In-Sn impure. It was observed that recovery rate of indium increases by increasing time. As a result, In-Sn alloy was recycled into pure In with low levels of impurities.

M-10: Co-Substitution Enhances the Rate Capability and Cyclic Stability of O_3-Type Cathode NaNi0.45-xMn0.25Ti0.3CoxO2 for Sodium-Ion Storage at High Voltage

Lichun Yang, Chaojin Zhou, South China University of Technology, China

To promote the practical application of O_3-type $NaNiO_2$-based cathode materials, increasing their energy density to the commercial level of lithium-ion batteries is necessary. It is effective to enhance the energy density of SIBs by expanding their operating voltage. However, O_3-type $NaNiO_2$-based cathode materials suffer irreversible phase transition when they are charged to above 4.0V in sodium-ion batteries. To solve this problem, we partially substitute Ni^{2+} in O_3-type NaNi0.45Mn0.25Ti0.3O2 by Co^{3+}. NaNi0.45Mn0.25Ti0.3O2 with Co-substitution possesses an expanded interlayer and exhibits higher rate capability, as well as cyclic stability, compared with the pristine cathode in 2.0~4.4V. The optimal NaNi0.4Mn0.25Ti0.3Co0.05O2 delivers discharge capacities of 180 and 80mAh·g^{-1} at 10 and 1000mA·g^{-1}. At 100mA·g^{-1}, NaNi0.4Mn0.25Ti0.3Co0.05O2 exhibits 152mAh·g^{-1} in the initial cycle and maintains 91.4mAh·g^{-1} after 180 cycles. Through ex situ X-ray diffraction, Co-substitution is demonstrated to be effective in enhancing the reversibility of P3-P3" phase transition from 4.0 to 4.4V. Electrochemical impedance spectroscopy indicates that higher electronic conductivity is achieved by Co-substitution. Moreover, cyclic voltammetry and the galvanostatic intermittent titration technique demonstrate faster kinetics for Na^+ diffusion due to the Co-substitution. This study provides a reference for further improvement of electrochemical performance of cathode materials for high-voltage sodium-ion batteries.

M-11: 2-Step Degradation of Hydrogen Permeability Through Pd-53mol%Cu Alloy Membrane with B2 Crystal Structure at Low Temperature

Hiroshi Yukawa, Suzuki Asuka, Nagoya University, Japan; Hideki Araki, Mizuno Masataka, Sugita Kazuki, Osaka University, Japan; Higemoto Wataru, Japan Atomic Energy Agency, Japan

Pd-53mol%Cu (Pd-40wt%Cu) alloy membrane with B2 crystal structure is widely used as hydrogen separation membrane. The activation energy for hydrogen permeation is much smaller for Pd-53mol%Cu alloy than ordinary Pd-Ag alloys (e.g., Pd-25wt%Ag) with fcc crystal structure, indicating that Pd-Cu alloy membrane has a potential to show higher hydrogen permeability than Pd-Ag alloy membrane at low temperature, e.g., room temperature. However, the temperature dependence of hydrogen permeability for Pd-Cu alloy membrane have not been investigated in detain especially below about 250˚C. In this study, the hydrogen permeability of Pd-53mol%Cu alloy membrane at low temperature region has been investigated in a fundamental manner.
A thin foil of Pd-53mol%Cu alloy with a thickness of 20μm is prepared. XRD analysis is performed in order to conform the sample is composed of a single phase with B2 crystal structure. The hydrogen permeation tests are performed from 350˚C down to room temperature. During the test, the hydrogen pressures at feed and permeation sides of the membrane are kept constant of 0.10MPa and 0.01MPa, respectively.
The the hydrogen permeability at 350˚C is in good agreement with previous study. The hydrogen permeability decreases with decreasing temperature and obeys Arrhenius-type relation above 200˚C. However, the hydrogen permeability declines more and deviates from the linear relationship below about 150˚C. It is found that the hydrogen permeability at room temperature decreases about one order of magnitude in two steps during 4 days after cooling down to room temperature. Such a slow and large decrement in hydrogen permeability at low temperature for Pd-Cu alloy membrane has not been reported. It is noted that the hydrogen permeability recovers to the original value when the the sample cell is heated up to 350˚C again.

M-12: Effects of Glass Chemistry and Additives in Ag Paste on Fire-Through Contact Formation onto Boron Emitters of N-Type Si Solar Cells

Sung-Hu Kim, Hee-Soo Kim, Ji-Gun Park, ,Joo-Youl Huh, Korea University, Korea

N-type Si wafers have higher efficiency potentials compared to p-type Si wafers owing to higher carrier lifetime and the absence of light induced degradation. The solar cells based on n-type Si wafers are commonly realized by forming boron emitters. However, it has

long been known that the conventional Ag pastes used for contacting phosphorous emitter are not capable to reliably contact boron emitters, leading to contact resistances above 5×10^{-2} ohm·cm^2. This problem has been partially resolved by adding a small amount of Al to the Ag paste. Although the addition of Al to Ag paste was reported to produce boron emitter contacts with specific contact resistances below 1×10^{-2} ohm·cm^2, it can cause other detrimental effects, such as shunting behavior and higher line resistivity. Recently, a significant progress in Ag paste has been made by replacing the conventional PbO-based glass frit with TeO_2-based glass frit, which enables to fabricate high-quality ohmic contacts to the phosphorous emitter with a sheet resistance of ~100ohm/sq. In this study, we used Ag paste containing tellurite glass frit to search a possibility to contact boron emitters without adding Al. By varying the tellurite glass chemistry and adding inorganic additives to Ag paste, we examined the contact microstructure and contact properties. In the presentation, we will discuss the roles of the glass chemistry and additives in the contact firing reactions for boron emitter contacts based on the contact microstructure observations and contact resistance measurements.

M-13: Effect of Ball Milling Time on the Thermoelectric Properties of Bi-Sb-Te Alloys with Dispersion of Cu

Seok min Yoon, Chul Hee Lee, May Likha Lwin, Sharief Pathan, Soon JIk Hong, Kongju National University, Korea

Thermoelectric materials are capable of converting waste heat into electricity and vice versa. They are used in power generation and cooling devices; which are adverse advantageous such as low maintenance and environment friendly. Bi-Sb-Te thermoelectric materials have been used for room temperature applications. However, the energy conversion efficiency of the commercialized products is still below about 10%, most of the studies focused on increasing thermoelectric performance of the existing materials.

It has been reported that the addition of a small amount of Cu to the Bi-Sb-Te thermoelectric material reduces the lattice thermal conductivity and significantly improves the electrical conductivity, thereby improving the thermoelectric performance.

In order to effectively disperse the Cu into Bi0.5Sb1.5Te3 powder, we have utilized low energy ball milling with various milling time. Then as-prepared powder was consolidated using Spark Plasma Sintering process. (SPS)

The crystal structure of BST-Cu powder and bulks were analyzed by X-ray diffraction (XRD). The microstructure and chemical composition of BST-Cu samples were characterized using Scanning Electron Microscope (SEM) and Electron probe micro-analyzer (EPMA) techniques respectively. The result indicate that electrical conductivity increased with milling time while Seebeck coefficient decreased. The thermal conductivity decreased with increasing milling time, as a result, ZT was improved.

M-14: Monolayer MoS_2 on Nanoporous Graphene as a Electrocatalyst for Hydrogen Evolution Reaction

Yongzheng Zhang, Fujita Takeshi, Kochi University of Technology, Japan

2D layered materials have attracted much attention in recent years due to their remarkable properties and potential for highly active catalysts. MoS_2, two-dimensional layered materials, is highly stable, active, nano-structured and shows promising activity for hydrogen evolution reaction (HER). However, the 2D electrocatalysts usually suffer from lower photoelectrochemical efficiency because of the challenges in effectively utilizing the 2D electrocatalysts in three-dimensional electrodes with a reserved surface area and 2D electronic properties. The efficient electrons, as well as proton transport processes in the electrocatalysts, are the key factors for HER activity. Graphene is regarded as superior electron mobility and excellent electronic behavior material for modification of conduction. In addition, graphene could be used as an efficient and low-cost cocatalyst for electrocatalytic reactions because of its high specific surface area and good electron transfer abilities. Herein, we report that MoS_2 /nanoporous graphene hybrid catalysts of monolayer MoS_2 sheets coating on nanoporous graphene with the high surface area are fabricated and applied for HER. The fabrication process of 3D nanoporous graphene is shown in the Scheme. And the BET surface area of synthesized nanoporous graphene was above 600m^2·g^{-1}. MoS_2 was deposited on nanoporous graphene by chemical vapor deposition (CVD) method. Different deposited time and temperature were studied. By controlling time and temperature, monolayer MoS_2 with different loading amount were obtained. The HER test results showed that the onset potential is -80mV with the Tafel slope of 60mv/dec for best MoS_2/graphene sample.

M-15: Corrosion Model Study of Cu Cr Zr Alloy for Fusion Reactor

Pengwei Yang, Baikun Huang, Yan Ma, North China Electric Power University, China

As a fusion of divertor heat sink and the first wall material of copper, Cu Cr Zr alloy under the condition of the running of the fusion, will contact with the pile of high temperature and high pressure in the cooling water, which corrosion occurs , the Cu Cr Zr alloy corrosion products will be on the surface of the cooling water,

washed down with cooling water migration, and will eventually deposition on the surface of the other parts of the cooling circuit. These corrosion products are irradiated and thus become part of activated corrosion products, which may be irradiated by factory workers inspecting or maintaining cooling loop equipment. After experiments, all the test specimens were analyzed and examined by weight change method to determine the corrosion mechanism and factors affecting the corrosion rate. The model was established by referring to the inherent model and verified by comparing the experimental data. The result of the experiment shows: In the flowing water, the corrosion weight of Cu Cr Zr changes linearly with time, and in the continuous water, the corrosion weight changes exponentially with time. Then referenc grey model, and build corrosion model in the flowing water and in the continuous water, which means that the corrosion behavior of Cu Cr Zr alloys in different water environments was studied by grey model. And the model was verified by comparing with the experimental data .

N. Additive Manufacturing and Powder Metallgufy

Symposium Organizers :

Huiping Tang, Northwest Institute for Nonferrous Metal Research, China; Yong Liu, Central South University, China; Yuichiro Koizumi, Osaka University, Japan; Kee-Ahn Lee, Inha University, Korea; Qian Ma, RMIT, Australia; Ed Herderick, Ohio State University, USA

August 19-21, 2019

Place: Exhibition Area (3rd Floor)

N-1: Effect of Solid Solution Treatment on the Microstructure and Properties of Rapidly Solidified Powder Metallurgy Al-20Si-7.5Ni-3Cu-1Mg-0.25Fe Alloy

Pengjun Tang, Peiyong Li, Xingyuan Wang, AECC Beijing Institute of Aeronautical Materials / Beijing Engineering Research Center of Advanced Aluminum Alloys and Applications, China; Desheng Chu, AECC Beijing Institute of Aeronautical Materials / Beihang University, China

In this paper, the Al-20Si-7.5Ni-3Cu-1Mg-0.25Fe alloy was prepared by gas atomization, sieving, canning, degassing and hot extrusion. The as-extruded alloys were solid solution treated at temperatures from 470˚C to 490˚C for 1hour. The microstructure and mechanical properties of as-extruded and as-heat treated alloys were studied by optical microscopy, scanning electronic microscopy, transmission electronic microscopy, X-ray diffraction, and tensile test. The results show that this alloy mainly consisted of Al, Si, Al_3Ni, Al_3Ni_2, Al_7Cu_4Ni, and $Al_4Cu_2Mg_8Si_7$ phases. After solid solution treatments, the contents of metallic compounds and Si phase increased, while the amount of Al matrix decreased, comparing with as-extruded alloy. Meanwhile, the spheroidization and Ostwald coarsening of large primary β(Si) blocks happened, following the dissolution of very fine Si particles. Additionally, the coarsening of metallic compounds also was observed during solid solution treatments. And with the increase of the solid solution temperature, the primary β(Si) blocks and metallic compounds became larger. Furthermore, $Al_4Cu_2Mg_8Si_7$ phase particles partially transformed into the metallic compounds containing Fe or Ni elements during the solid solution treatment. The tensile properties were improved by solid solution treatment and artificial ageing at 180˚C for 6h, following nature ageing for 24h. The ultimate tensile strengths of the alloys, solid solution treated at 470˚C, 480˚C, and 490˚C, increased by 4.4%, 7.7%, and 3.3%, respectively, comparing to as-extruded alloy. While the yield strengths increased up 28.1%, 31.3%, and 34.4%. When solid solution treated at 480˚C for 1h, combining with appropriate artificial ageing, the ultimate tensile strength, yield strength and Young's modulus at room temperature of the sample are 490MPa, 420MPa and 95GPa, respectively. The improvement of mechanical properties after heat treatments are mainly due to the precipitation of G.P. zones, spheroidization of large primary Si blocks, and numerous of fine metallic compounds dispersed in Al matrix.

N-2: Effect of Mo Addition on Phase Transformation and Microstructure of Powder Metallurgic Ti-22Al-25Nb Alloy during Quenching and Furnace Cooling

Yaran Zhang, Yongchang Liu, Tianjin University, China; Qi Cai, Shanghai University, China

Ti_2AlNb-based alloy comprises B_2/β phase, O phase, and α_2 phase. B_2 phase is the matrix, and O phase is the mainly strengthening phase, which brings the balance of strength and room-temperature ductility to the Ti2AlNb-based alloy. The B_2 and O phase commonly form Widmannstatten B_2+O bimodal microstructure, and this microstructure would improve the hardness and room-temperature ductility. Powder metallurgic Ti_2AlNb alloys with Mo addition were sintered at 900˚C, 1000˚C, 1070˚C, and 1150˚C for 12h, followed by water quenching and furnace cooling. These sintering temperatures, which were determined from the recorded DSC curves, correspond to the B_2+O, α_2+B_2+O, α_2+B_2, and B_2 phase region, respectively. The phase composition and the microstructure of the sintered Ti-22Al-23.4Nb-1.1Mo compacts were then characterized by X-ray diffraction and scanning electron microscopy, respectively. Before the microstructure observation, the alloys were chemically etched with Kroll's reagent. The room temperature hardness was measured by the Vickers hardness test. Comparisons

of phase and microstructure between the quenched and furnace cooled Mo-modified alloys and between the Mo-modified and Mo-free alloys were carried out to illustrate the phase transformation and microstructure evolution during the cooling process and to reveal the function of Mo element, respectively. Mo addition accelerated the solution of α_2 and O phase during the high-temperature preservation, and Widmannstatten B_2+O structure, which contributes to the properties, was induced by furnace cooling from all the phase regions. The Widmanstatten structure included B_2 matrix, primary O, and secondary O precipitates. However, Mo alloying refined the Widmanstatten structure only when the alloys were solution treated and then cooled from the single B_2 phase. Although the hardness of Mo-modified alloys were lower than that of Mo-free alloys sintered in the same phase region, an enhancement of hardness, 488.4±28.5HV, was obtained in the alloy solution treated in the single B_2 region for a short time.

N-3: Dimension Prediction Model of Single-pass Multi-layer Thin Wall Based on CMT (Cold Metal Transfer) Wire-Arc Additive Manufacturing

Xuewei Fang, Changxing Wang, Bingheng Lu, Xi'an Jiaotong University, China; Hao Bai, Chuanqi Ren, Lijuan Zhang, National Innovation Institute of Additive Manufacturing, China

Based on the CMT (cold metal transfer) wire-arc Additive Manufacturing process, 2319 aluminum wire as the filling material, the C+PA welding source mode has a lower heat input. which is not suitable forming on substrate. So using C+P welding source mode to forming two different layer number primer, it was found that the three layers primer was suitable for forming subsequent thin wall using C+PA welding source mode. Based on this, the design of the regression experiment was carried out by Box Behnken Design (BBD) to form single-pass 16 layers thin wall, consist of three layers primer and subsequent 13 layers part by C+PA welding source mode. The process parameters (wire feeding speed, welding speed, interlayer temperature) and the cross-section size of single-pass multi-layer thin wall were established. According to the obtained regression equations of W (width) and ΔH (the average height), the error between the predicted value of the regression equation and the experimental measured value is calculated. The W error distribution of the measured value and the predicted value is Within 2%, The ΔH error between the measured value and the predicted value is within 5%.Through five groups of verification experiment, the prediction error of the model is less than 7%. it indicates that the predicted value and the measured value are in good agreement with each other. Through further analysis the results show that the effect of wire feeding speed on the forming width is greater than the interlayer temperature; the effect of welding speed on the average height ΔH is greater than the wire feeding speed than the interlayer temperature. When the wire feeding speed increases, the W and ΔH of C+PA forming parts increase linearly. When the welding speed increases, the W and ΔH of C+PA forming parts decrease. When the interlayer temperature increases, the W of C+PA forming increases but the ΔH decreases.

N-4: The Monitoring System for Measurement of the Layer Height and Track Width Based on Multiple Sensors in CMT-WAAM

Xuewe Fang, National Institute Corporation of Additive Manufacturing, China / Xi'an Jiaotong University, China; Chuanqi Ren, Xi'an Jiaotong University, China

To substantially shorten the period for developing products, forming-patterns and moulds, maximize profits through changing the modern advanced processes, several enterprises and research institutes have focused on additive manufacturing(AM). The process of cold metal transfer additive manufacturing (CMT-AM) was noted for high efficiency, outstanding metallurgical bonding and much lower capitalized cost. To obtain a better surface and high dimension accuracy and a comprehensive understanding of specific forming process, the monitoring system for acquisition of forming information has been established and which was based on multiple sensors. The sensors involved are mainly divided into follow categories by different function in forming, in which vision sensor(CCD), laser profile scanner, hall current and voltage sensors and temperature sensor are included. Various data from actual manufacturing, either digital/analog quantity or image information, are embedded in this intricate monitoring system.

As we all know that temperature is one major factors in welding additive manufacturing and improper setting may have great harmful influences on metal flow, metallurgical combination of interlayer, and even lead to coarse grains. Making comprehensive consideration of various situations, thermocouples are buried in the special substrate which could ensure the initial heat input during forming. The infrared thermometer is expanded to get the on-line temperature of welding pool in a non-contact and nondestructive form, whereas the precondition is that both relative locations keep keeps invariant. Image data are captured by the CCD, which mainly contains the geometric characteristics of the welding pool on time.

Layer height is transmitted to industrial computer by laser profiler, meanwhile, the electrical signals parameters are collected by Hall sensors. The layer height data and the welding current and voltage are simultaneously fed back to the operator in the form of waveforms. The system can fully monitor the forming process of CMT and improve the automation of equipment to a certain extent, and which also provides a basis for the realization

of precision forming.

N-5: A New Finite Element Method for the Residual Stress Prediction of Large-Sized Component Additively Manufactured by Wire and Arc

Xuewei Fang, Lijuan Zhang, Bingheng Lu, Jiyuan Zhao, Xi'an Jiaotong University / National Innovation Institute of Additive Manufacturing, China; Jiannan Yang, National Innovation Institute of Additive Manufacturing, China; Ke Huang, Xi'an Jiaotong University, China

With the increasing development of wire and arc additive manufacturing (WAAM) technology, especially for the large-scaled metallic components, WAAM was supposed to be one of the promising building methods due to its high deposition rate and material utilization rate, together with comparatively low production and equipment cost. Owing to the flexibility of the large-sized components' structure, it's hard to predict the stress distribution and distortion with great precision, while finite element analysis was considered to be one of the best approaches to figure out the stress and distortion evolution. And the simulation was usually contained of a transient thermal analysis and a following structural analysis with the temperature load obtained from the thermal analysis. The most problem was the simulation efficiency, particularly for the large-sized component fabricated by WAAM. In this research, a new finite element method was come up with to optimize the simulation procedure and finally reduce the whole cost of time. Specifically, the WAAM deposited component was divided into several parts according to the depositing plan and the structural characteristics. The transient thermal analysis of each model was then conducted one by one. The point was that the initial condition of each simulation was the same as the last results in the previous model. And then these thermal analysis results of the divided models were employed to finish the structural analysis like the traditional procedure. The time costs of each layer for the new and general finite element method were compared quantitatively. On the one hand, dividing the whole solid model of the large-sized component could clearly help to reduce the count of elements that contributed to the calculation of current layer, which would be much too lower than that of the whole model. On the other hand, due to the procedure limitation of the finite element analysis, the structural analysis must be done until the thermal analysis had already be completed. But when the whole model was divided, the time line of the structural analysis could intersect that of the thermal analysis. It's believed that this new finite element model would attracted more researchers' attention on the residual stress prediction of large-sized component additively manufactured by wire and arc.

N-6: A Fractographic Study Exploring the Relationship between Bending Vibration Fatigue and Metallurgical Properties of 3D Laser-Deposited Ti–6Al–4V Alloy

Yan He, Weiguo Guo, Northwestern Polytechnical University, China

Titanium alloy Ti-6Al-4V, widely used in turbine and compressor blades, was subjected to high cycle fatigue loading. As of now, little work has been done on the fatigue performance of these materials. In the present paper, the vibration-based fatigue behavior of Ti-6Al-4V alloy prepared by the 3D laser deposition technology, is studied in an effort to address the relationship between bending vibration fatigue and metallurgical properties. Based on economic considerations, and adapt to the micro-vibration equipments, the micro-sample is designed. The vibration fatigue specimens were cut out from blocks in two orientations with respect to the deposition direction, and then cycled in the first bending mode to reach a certain max stress amplitude, which is indirectly controlled by the displacement of the fixed point at the end of the sample. The microstructure of the undeformed and deformed samples was examined through optical microscopy(OM) and scanning electron microscope (SEM). An extensive fractographic evaluation was carried out to explore the relationship between bending vibration fatigue and the metallurgical properties. The experimental results show the followings: (i) in order to save the 3D laser-deposited Ti–6Al–4V alloy,a noval method with micro-sample for vibration fatigue process is achievable; (ii) fractography revealed the presence of a range of manufacturing defects located at or near the surface of the specimens. Accordingly Lack-of-Fusion (LOF) defects were primarily responsible for fatigue crack initiation. The reduction in fatigue life appeared to be affected by the location, size and shape of the LOF defect; (iii)significant anisotropic behavior are found in the microstructure and in the fracture surface, and the crack propagation path has also been studied combined with electron backscattered diffraction (EBSD) and energy dispersive spectrometer(EDS); (iv) the crack initiation extends from bicontinental surface to the center position and finally fracture in an instant because of the fatigue of symmetrical bending vibration, while there are few surface defects.

N-7: High Strain Rate Compressive Property of Sintered Metal Fiber Felts

Jun Ma, Xi'an Jiaotong University / North West Institute for Nonferrous Metal Research, China; Jianzhong Wang, Huiping Tang, North West Institute for Nonferrous Metal Research, China; Weidong Song, Beijing Institute of Technology, China; Feng Jin, Xi'an Jiaotong University, China

Sintered metal fiber felts are transversely isotropic porous

materials fabricated by high temperature sintering. The deformation is the stretching-dominated mode loaded along in-plane direction, leading to high specific strength, so they have potential for dynamic energy absorption application. The energy absorption property of metal foam and metal honeycomb had been discussed by many researchers, and it shown that the pore structure has a large effect on the energy absorption property. For example, closed-cell foam has stronger rate effect than open-cell one. Compared with metal foam, the sintered metal fiber felts have far smaller pores and thinner pore walls, also different pore morphology. Due to the good plasticity of metal fibers and the metallurgical bonding between fibers, the sintered metal fiber felts wouldn't crack during dynamic loading process, while the metal foam is opposite. In this study, the energy absorption property of sintered metal fiber felts was investigated by the splited Hopkinson's bar experiments loaded along in-plane direction. The strain rate effect and the deformation mode under high speed compression were analyzed. The dynamic compressive property was simulated based on the 3D pore structure obtained from μ-CT images of the materials. The experimental results disclosed the strong strain rate effect at densification stage of stress-strain curves but relative weak strain rate effect at plateau stage of stress-strain curves.

N-8: Effects of Nickel Powder Addition on the Mechanical Properties, and Phase Composition of Sintered 3YSZ Composites

Yongzhi Chen, Rutie Liu, Central South University, China; Jia Lou, Xiangtan University, China; Hao He, Guangxi University of Science and Technology , China; Yimin Li, Central South University/ Guangxi University of Science and Technology , China

In recent years, the use of ceramic materials has greatly increased in various applications due to its low density and high comprehensive mechanical properties. However, the brittleness of ceramic material limits its development. Increase the toughness of ceramic material has been a main content of ceramic science research. 3Y-ZrO_2 ceramics have obvious advantages in bending strength and fracture toughness which is based on the martensite phase transformation (tetragonal to monoclinic phase transformation) when 3Y-ZrO_2 ceramics crack. However, the increase of toughness by phase transition is limited. The most promising method to improve the toughness of ceramics is to introduce a ductile phase. The deformation, withdrawal, and fracture of the ductile phase can absorb a majority of the fracture energy of the propagating cracks. In previous studies, the ductility phases, such as Ta, Nb, Ag, Mo, and stainless steel, were added to zirconia, and a favorable toughening effect occurred. As a common ductile metal, Ni is also used in improving ceramic toughness. Some scientists think that Ni/ZrO_2 is a perfect system. This is mainly because Ni and ZrO_2 have similar elastic modulus and crystal parameters .In this study, we have investigated the effects of nickel powder on the sintering of yttria-stabilized zirconia in vacuum environments, and a Ni/ZrO_2 composite material with high comprehensive mechanical properties was prepared. It was found that nickel inclusions had obvious pull-out phenomenon which improve mechanical properties of composite. But with the increase of Ni concentration, the constitution of monoclinic Phase(M), cubic phase(C), and Tetragonal phase(T) changed. The transformation of T Phase to M Phase and C Phase depends on the element segregation, and this can be confirmed by EDS in the system ZrO –Ni. We also found the segregation is related to the cooling speed, and has nothing to do with the holding time. Therefore, we believe that the elastic strain energy which was caused by heat mismatch between Ni and ZrO_2 matrix during the cooling process, promote the element segregation.

N-9: Effect of Energy Parameters on Microstructure and Mechanical Properties of Ti-48Al-2Cr-2Nb Alloy Fabricated by Selective Electron Beam Melting

Yulin Sun, Nanjing University of Science and Technology / Northwest Institute for Nonferrous Metal Research, China; Nan Liu, Liang Jia, Huiping Tang, Northwest Institute for Nonferrous Metal Research, China; Guang Chen, Nanjing University of Science and Technology, China

Selective electron beam melting (SEBM) is a promising manufacturing technology, which offers the possibility to change several parameters to tailor the microstructure of TiAl alloy. The amount of energy supplied by the electron beam has considerable influence on the final build quality in the SEBM process. Energy input is comprised of the beam voltage, beam current, scan speed, and line offset. However, if the energy input is constant, different energy input parameters will also affect the microstructure and mechanical properties of TiAl alloy. In this research, the beam current and the scan speed were varied to reflect the influence of different energy parameters on microstructure and mechanical properties of Ti-48Al-2Cr-2Nb alloy fabricated by SEBM. With the increased of scan speed and beam current in a certain range, the microstructure becomes more uniform, and its compression performance is also improved. Scanning electron microscopy and X-ray diffraction investigations were carried out to understand this phenomenon. The results showed that the reason for this phenomenon lies in the number of B_2 phase and the distribution of Al element. Meanwhile, the correlation of scan speed and beam current with B_2 phase and Al element distribution was investigated.

N-10: Effect of Temperature on the Hollow Ratio of Aerosolized Milling Particles

Shaokun Yu, Linchen Deng, Tietao Zhou, Beihang University, China; Peng Gao, AECC Beijing Hangke Engine Control System Science and Technology Co. Ltd., China

Tin bronze alloys are often used in the electrical, mechanical and metallurgical fields due to their excellent wear resistance and corrosion resistance. Although the traditional tin bronze processing methods having been widely used, they have disadvantages such as thin plating, poor bonding performance with the substrate, or poor surface quality. Compared with conventional processing methods, the cladding process can solve these problems well, so the use of cladding to repair tin bronze parts is becoming more and more popular.
As a raw material for the cladding process, the quality of the tin bronze powder has a great influence on the quality of the cladding layer. At present, the commonly used powder preparation method is gas atomization milling, but the powder obtained by this method often forms some solidification shrinkage holes, and these holes have a great influence on the wear resistance of the tin bronze cladding layer, for example, it will cause a decline in corrosion resistance and reduce the service life.
Therefore, this paper mainly studies the relationship between the temperature of aerosolized tin bronze powder and the hollow rate of metal powder, and then according to the conclusions obtained, the guidance of the gas atomization milling process is made to optimize the process.

N-11: Relationship between Solidification Microstructure and Particle Size Distribution of Microcladding Tin Bronze

Linchen Deng, BeiHang University, China

Aiming at the difficult problem of establishing the relationship between the solidification structure of cladding and the related main process parameters, a finite element numerical model was established to simulate the relationship and mutual transformation between the related process parameters, such as input power, scanning rate and particle size distribution of powder material used in cladding. In this experiment, argon arc was used as a heat source to fuse in the microregion of copper substrate to prepare tin bronze cladding layer. The microstructure of cladding prepared with different particle size distributions was observed and analyzed by means of metalloscope and electron probe, so as to determine the relationship between microstructure and particle size distribution of powder used in cladding. Then through ANSYS software for energy transport mechanism of micro zone in the molten pool numerical simulation, determine the cladding powder particle size distribution of molten pool used internal crystal form, size and distribution and supercooling degree and the relationship between the cooling rate model, and then determine the cladding material with the best organization performance when used in powder material particle size distribution and the input power, scan rate, the number of relations between, in turn, get the best process parameters, improve production efficiency and product performance.

N-12: Isotropic Microstructure and Mechanical Properties of Additively Manufactured Ti-based Alloy

Gwanghyo Choi, Won Seok Choi, Pyuck-Pa Choi, Korea Advanced Institute of Science and Technology (KAIST), Korea

Direct laser deposition (DLD) is a metal-based additive manufacturing (AM) technique, also referred to as laser-based direct energy deposition (DED). This manufacturing technique enables to make the physical realization of 3D model data via involving incremental layer-by-layer deposition, as opposed to subtractive manufacturing methodologies. The deposition is conducted by fusing metallic powders with a high-energy laser. However, additively manufactured Ti-based alloy has suffered from anisotropic microstructure and mechanical properties due to rapid cooling rate and significant heat gradient. We obtained non-columnar microstructure and random texture via modifying powder mixtures and processing parameters. The microstructure and the texture were investigated using X-ray diffraction (XRD), electron back scattered diffraction (EBSD), and scanning / transmission electron microscopy (SEM / TEM).
The ratio of powder mixtures and processing parameters were optimized by means of high-throughput laser-aided fabrication. This resulted in isotropic mechanical properties irrespective of deposition direction. The thermodynamic stability of intermetallic phases was controlled by alloying composition in order to improve the material toughness. We also investigated the influence of solid solution strengthening and grain size on the mechanical properties of deposited materials. This study suggests an alloy design concept for additive manufacturing and provides a viable route for tailoring microstructure and mechanical properties.

N-13: Microstructure and Mechanical Properties of Ti-Cu-Ni-Sn-Nb Nanostructure-Dendrite Composite

Quan Zhou, Northeastern University / Northwest Institute for Non-ferrous Metal Research, China; Huiping Tang, Jianzhong Wang, Liqing Wang, Ping Tan, Northwest Institute for Non-ferrous Metal Research, China

Ti-Cu-Ni-Sn-Nb alloys possess high strength, low elastic

modulus and large plasticity, which would be a promising candidate as structural and biomedical material. High performance of Ti-Cu-Ni-Sn-Nb multicomponent alloys can be easily available by directly casting method, while traditional amorphous and nanocrystalline alloys for high strength purpose require a multi-step process.
In this study, large size Ti62.5Cu14Ni12Sn4Nb7.5 (atom percent) alloy specimen with the diameter of 260 mm and the height of 400mm was prepared by vacuum arc melting. Characterization of the Ti62.5Cu14Ni12Sn4Nb7.5 parts by SEBM were observed by Optical Microscope (OM), Scanning Electron Microscopy (SEM), X-ray Diffraction (XRD) and Differential Scanning Calorimeter (DSC). The sample microstructure is composed of nanostructured matrix and β-Ti solid solution dendrite phase. This composite with dendrite and ultrafine structures exhibit low elastic modulus (49.8GPa) and high fracture strength (2149.6MPa). For this alloy, the compressive deformation mechanism occurs through a shear-banding in the matrix, and the dislocation movement in dendrite. Accordingly, nanostructured matrix as tough part is responsible for the alloy's high strength, meanwhile β-Ti dendrite in situ formed as ductile phase restricts high excessive shear banding, which attributes to a large plastic strain.

N-14: Effect of Aging Behavior during Selective Laser Melting Process at Various Temperatures on Mechanical Properties in Al-Si-Mg Alloy

Kazuto Sugai, Daisuke Terada, Shigeto Yamasaki, Masatoshi Mitsuhara, Hideharu Nakashima, Jun Kusui, Mituru Adachi, Chiba Institute of Technology, Japan

The purpose of this study was to investigate mechanical properties and relationship between the mechanical properties and position in additive manufactured Al specimens. The Al-10Si-0.4Mg alloy specimens were fabricated by selective laser melting (SLM) process at various temperatures of 72˚C, 140˚C, 162˚C and 200˚C. Hardness of these specimens was measured at various position from a base plate for the SLM process along building direction. It was found that hardness of the specimens fabricated at 72˚C was constant and independent of the position. On the other hand, the hardness of the specimens fabricated above 140˚C depended on distance from the base plate. In the specimens fabricated at 140˚C and 162˚C, the hardness increased with increasing the distance from the base plate and showed maximum values near the top surface, and then decreased. In case of the fabricated at 200˚C, the hardness increased monotonically with increasing the distance from the base plate. From the result of the DSC measurement, it was expected that these specimens were thermodynamic non-equilibrium state because exothermic peaks were observed during temperature rising. In Al-Si-Mg alloys, it is known that age precipitation from supersaturated solid solution, Thus, it is considered that supersaturated solid solution was created during the SLM process and the exothermic peak means precipitation. Additionally, the exothermic heat value decreased with decreasing the distance from the base plate in the specimens fabricated above 170˚C. The decrease of exothermic heat value indicated that precipitation also occurred during the SLM process above 170˚C. In other words, the specimens were aged during the SLM process. The change in hardness can be explained by the aging behavior during the SLM process at various temperatures.

N-15: Effect of Addition on the Properties of Ta-Cu Composite

Kyoung Deok Seo, Hyun Gyu Lee, Ji Won Yu, Korea Institute of Industrial Technology / In-Ha University, Korea; Jae Jin Sim, Kyoung Tae Park, Korea Institute of Industrial Technology, Korea; Soong Keun Hyun, In-Ha University, Korea; Yong Jin Park, Shin Saeng Metal, Korea

The Electrical contact materials are used for electric switching. Its main characteristics are electrical conductivity, arc resistance, melting point, oxidation resistance. From endurance properties in high temperature, contact materials is classified and selected. Among the contact materials, Ag or Cu matrix composite typically regards most popular materials because they have excellent electrical conductivity, heat resistance as well as it could change to various shaper of materials like a foil, wire, clad. However, when using Ag or Cu contact materials for long time, The problem of arc heat generated by high voltage and current cause welding problems at Ag and Cu interface. Ag-CdO-based composites lies in medium/ high current contact materials category, and account for more than 70% of the contact market. However Ag-CdO-based composites are causing soil pollution and making it difficult to use due to heavy metals and regulations on the use of certain hazardous substances. In case of Cu-W contact material difficulty lies in machining. In order to solve these problems, Ta and Cu with environmental friendliness and plastic processing properties was selected.
The Cu powder was ball-milled with additive (CeO_2, WC) having thermally stability for 8 hour at 200rpm. Then, the Ta powder was simple mechanical mixed at 150rpm for 2 hours. Liquid Sintering (LS) method was used to sinter them into bulk. In order to analyze the physical properties of the sintered sample according to each additive various characterizations were performed. Electrical conductivity decreased to 0.2 from 11 (%IACS) and Hardness increased to 0.5 from 20HV with additive content. Microstructure analysis of sintered bulk was showed that additive was showed for uniform dispersion in Cu matrix.

N-16: Study on High Temperature Mechanical Properties of Extruded TZM Alloy

Xingang Wang, Xin Chen, Chon Zhao, Zhanwei Yuan, Chang'an University, China

In this study, the molybdenum alloy TZM (0.5wt.% Ti, 0.08wt.% Zr) bar was prepared by the powder metallurgy and high-temperature extrusion processing with 65% extrusion deformation ratio. The TZM alloy bar was annealed at 1300˚C for 1hr. The microstructure was examined by scanning electron microscopy (SEM), electron backscattering diffraction (EBSD) and transmission electron microscopy (TEM). The results show that the microstructure of extruded TZM alloy has <110> deformation texture, and the grain is significantly elongated along extruding direction. Meanwhile, the grain with the fibrous and equiaxed shape is distorted and refined at the cross section of specimen. The nanoscale second phase particles distributed in the grain uniformly. The high temperature uniaxial tensile tests were performed at different temperatures using plate-shaped specimen. The peak stress is 806.6MPa, 430.4MPa, 368.7MPa, 279.3MPa and 83.6MPa for room temperature, 1000˚C, 1200˚C, 1400˚C and 1600˚C respectively, and the elongation at break is 27.1%, 16.15%, 17.6%, 24.4%, 59.6% correspondingly. When the temperature is lower than 1400˚C, the stress decreases quickly with the increase of strain after elastic deformation stage in the tensile stress-strain curve. However, when the temperature is more than 1400˚C, the stress increases firstly during about 15% elongation and then decrease rapidly till rupture with the increase of strain. TZM alloy presents a characteristic of strain-hardening after elastic deformation stage. TZM alloy present a mixture mode of dimple and transgranular fracture for tensile specimen at room temperature. But the tensile fracture for all high temperatures exhibit the typical dimple morphology after ductile fracture.

N-17: Effect of Carbon Addition on Austenite Stability and Strain-Induced Martensite Transformation of Nanocrystalline Fe-Ni Alloy

Namhyuk Seo, Junhyub Jeon, Seok-Jae Lee, Chonbuk National University, Korea

In this study, we investigated the effect of carbon addition on the austenite stability and strain-induced martensite transformation of nanocrystalline Fe-11wt.%Ni alloys by means of X-ray diffraction (XRD), field emission scanning electron microscopy (FE-SEM), and a mechanical test. The FeNiC alloy samples with nanosized crystallite were fabricated by spark plasma sintering (SPS) which required extremely short densification time, resulting in not only achieving a theoretical density value, but also preventing grain growth. A room temperature compressive tests were carried out to observe the strain-induced martensite transformation. The quantitative phase change during the deformation was analyzed using XRD whereas the microstructural characteristics was observed with FE-SEM. The nanosized crystallites in the sintered alloys contributed to increase the austenite stability. The addition of carbon, which is a strong austenite stabilizer, influenced the initial volume fraction of retained austenite and the variation of volume fraction of retained austenite during the deformation by changing the austenite stability. Thus, the volume fraction of retained austenite was varied with both the carbon addition and the crystallite size of FeNiC alloys. The transformation kinetics of the strain-induced martensite from the decomposition of retained austenite was evaluated and discussed using the empirical equation considering the austenite stability factor.

N-18: Incorporation of Luminescent Compounds into Binders for Use in Metal Binder-Jet 3D Printing

Adrian Trinchi, Shirley Shen, Linda Varadi, Adam Best, CSIRO Australia, Australia

The advent of additive manufacturing, particularly metal-based 3D printing, has stimulated enormous research interest, and as the field progresses, so does interest in introducing embedded function into components. It is envisaged that such printing will be extended to incorporate functional composites, which can offer a variety of functions, one of which is embedded sensing. A challenge faced in this endeavour is the ability to incorporate materials into the binder systems to allow the composite material to be deposited at an intended location, as well as compatibility with the bulk matrix, and the ability to visualise or interrogate such embedded functional materials.

Herein we present our research findings on embedding luminescent functionality into binders which could be used in the manufacture of future metal binder-jet based 3D printed products. Methods for embedding luminescent and optical/coloured non-metallic functional powders (FPs) into binder-jet based 3D printed products have been explored, as well as the material properties and performance of the produced samples. The approach consists of incorporating the nano and micro-sized FPs into the polymeric binder (via appropriate mixing and dispersing), which can then be deposited (jetted/sprayed) directly onto the metal powder during the 3D printing/layering process. A range of FPs (particularly luminescent ceramics) with different optical properties,

capable of withstanding the processing conditions and being compatible with the material-binder systems have been investigation.

The embedded FPs may provide a number of unique primary enhancements and capabilities, ranging from as the ability to print in colour for branding/visual identity, all the way through to sensors. They may also exhibit secondary functions, such as assist in grain refining or serve as phase stabilizers. A miniature deposition process has been developed for small scale sample production so as to emulate a 3D binder-jetting process, on which samples were produced.

P. Dynamic Behaviour of Materials

Symposium Organizers :

Marc Andre Meyers, University of California, USA; Na Yan, Northwestern Polytechnical University, China

August 19-21, 2019

Place: Exhibition Area (3rd Floor)

P-1: Experimental and Numerical Study on Impact Resistance of Composite Ice-Resistant Plate

Yu Wang, Tao Suo, Northwestern Polytechnical University, China

The ice-resistant plate of a turbo-prop airplane is a layer of attached skin, which usually is symmetrically outside the fuselage and corresponding area of the propeller plane. In order to prevent the fuselage from being damaged by the ice block throwed from the propeller. Therefore, the Impact resistance design of the ice-resistant plate is particularly important.In the present work, by using the gas gun, The experiment of the ice block impacting the different ice-resistant plates was made. In the meantime, a three-dimensional digital image correlation (3D-DIC) method was employed to measure the deformation field of the ice-resistant plate under ice block impact. By comparing the Strain-time curve and displacement-time curve between the glass fiber reinforced composite ice-resistant plates and aluminum alloy ice-resistant plates, The results indicated that glass fiber reinforced composites ice-resistant plate can reduce the weight on the premise of ensuring its impact resistance. In the numerical model, the VUMAT subroutine of ABAQUS was used to define the mechanical properties and damage parameters of the composite ice-resistant plate and the Smooth Particle Hydrodynamic (SPH) method was used to build the ice block model to simulate the complex impact process of ice block on the ice-resistant plate. The finite element model was found to be in excellent agreement with experimental data. The simulation results indicated that the closer the ice block was to the vertical impact, the higher deformation of the fuselage would be; If the initial angle of impact changed within 10 degrees, the influence on the experiment result can be ignored; Under the condition of a fixed layer thickness, changing the composite layup can influence the impact resistance of the ice-resistant plate, the glass-fiber reinforced composite with layup shows excellent impact resistance.

P-2: Effect of Cr and W Contents on Charpy Impact Properties of Fe-Cr-W Oxide Dispersion Strengthened Steels

Daehyun Kwon, Gunhee Lee, Jonghee Baik, Jung Gu Lee, Univeristy of Ulsan, Korea; Sanghoon Noh, Korea Atomic Energy Research Institute (KAERI), Korea

Oxide dispersion strengthened (ODS) ferritic/martensitic (F/M) steels are considered to be the most promising structural materials for several types of advanced nuclear systems, in which they would most likely compose the materials in the cladding tube for fast reactors and the blanket for fusion reactors. The homogeneous distribution of nanosize yttrium oxide particles in the ODS steels improves high-temperature strength and creep properties, and it also benefits irradiation resistance because of the effective sink of interface between oxide particles and matrix for irradiation-induced point defects and helium atoms. By means of powder metallurgical routes, mechanical alloying offers an economical and appropriate method of synthesizing complex ODS alloys by high energy ball milling at room temperature. However, it is well known that ODS F/M steels produced by mechanical alloying exhibit relatively weak Charpy impact properties and low fracture toughness with respect to conventional F/M steels. Such brittle features generally depends on multiple factors, which not only include the oxide morphology and distribution, but also microstructural factors, such as effective grain size, plastic anisotropy, and microtexture. In this study, the effects of Cr and W contents on the microstructure and Charpy impact properties of Fe-Cr-W ODS steels were investigated. ODS steels was fabricated by mechanical alloying and hot isostactic pressing, followed by hot rolling. The Charpy impact was tested at -40˚C in longitudinal-transverse (LT) and longitudinal-short transverse (LS) orientations. The high contents of Cr and W induced strong <110> texture in the elongated F/M matrix, which is associated with the deformation mechanism during hot rolling. This microstructural anisotropy resulted in splitting of crack-divider type in LT specimens during impact testing, while crack-arrester type was observed in LS specimens. On the other hand, when the contents of Cr and W were relatively low, the equiaxed grains were produced with the segregation of coarse oxide particles along the grain boundaries. With this microstructure, the similar impact fracture behaviors were observed irrespective of the specimen orientation. In addition, the total absorbed energy during impact testing was separated into the energies for crack initiation and propagation, and the relative portion of each energy was interpreted by correlating it with the corresponding microstructure.

PRICM 10

Author Index

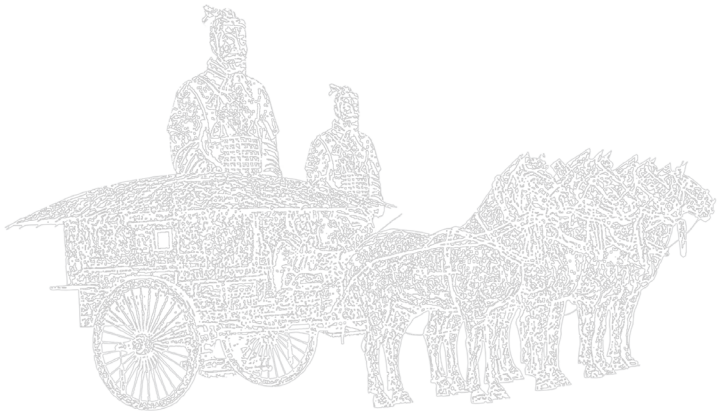

Author Index

Author Index

Author Index

Author Index

Author Index

Author Index

Author Index

Author Index

Author Index

Author Index

Author Index

Author Index

Author Index

Author Index

Important Notice to Participants

Welcome to Xi'an to attend The 10th Pacific Rim International Conference on Advanced Materials and Processing (PRICM10). For the convenience of your stay in Xi'an, the following information has been provided for your reference.

Official Language

The official language of the conference is English

Registration

1. Registration:

Time: 18 August, 13:00-21:00 | 19 August, 07:30-16:00 | 20-22 August, 08:00-16:00
Location: First Floor of Xi'an Qujiang International Conference Center (QICEG)
Address: No.15 Huixin Road, Qujiang New District, Xi'an, Shaanxi Province, China
Tel.:+86-29-87655888

2. Fee (On-site Registration):

Registration Fee	CNY 5900	Regular Participant
	CNY 3400	Student Participant (Not included Welcome Reception on 18 August and Conference Dinner on 20 August)
	CNY 1400	Accompanying Person
Additional Conference Proceedings USB	CNY 400/Copy	Payment on-site
Additional Conference Technical Program Book	CNY 200/Copy	Payment on-site

* Note: 1. The receipt will be given at the registration desk.
2. Students are requested to submit the copy of their student ID.

3. The following materials will be provided at registration desk:

- Name Badge
- Conference Proceedings USB
- Technical Program Book
- Ticket for Welcome Reception on 18 August (Only for Regular Authors & Participants)
- Ticket for Conference Dinner on 20 August (Only for Regular Authors & Participants)
- 4 Lunch Tickets for 19-22 August

*Notes: 1. Please wear your name badge to attend meetings and take your tickets for lunch, welcome reception and conference dinner.
2. Please sign your name to finish your registration procedure.
3. Please hand over your poster when you register.

Conference Venue and Time

No.	Activity	Time	Venue
1	Plenary Session	Morning, 19 August	Golden Hall (1st Floor) of QICEC
2	Parallel Sessions	Afternoon, 19 August 20-22 August	1st , 2nd, 3rd and 4th Floor of QICEC
3	Exhibition and Poster Sessions	19-21 August	3rd Floor of QICEC

Paper Presentations

Please read the Technical Program of PRICM10 and pay attention to your presentation time. Time for plenary papers is 40 minutes including 5 minutes' discussion, for keynote papers at parallel sessions is 30 minutes including

5 minutes' discussion, for invited papers at parallel sessions is 25 minutes including 5 minutes' discussion and for contributed papers at parallel sessions is 20 minutes including 5 minutes' discussion.

*Notes: Please leave the business card or the short resume of presenter's at the registration desk for the introduction by the session chairmen.

Exhibition and Poster Presentations

The Exhibition and Poster Sessions will be opened on 19-21 August at the 3rd Floor of QICEC. If you have been noticed to give a poster presentation at PRICM10, please stay at the 3rd floor to answer the participants' questions during tea break in the afternoon of 19-21 August.
The excellent poster winners will be given during tea break in the afternoon of 20 August.

Meals

- Breakfast | Location: At your staying hotel
- Welcome Reception (18:00-19:30, 18 August) | Location: At Golden Hall (1st Floor) of QICEC
- Conference Dinner (19:00-21:00, 20 August) | Location: At Golden Hall (1st Floor) of QICEC
- Conference Lunch: (12:00-13:30, 19-22 August) | Location: At the 1st Floor of QICEC

Events

1. Workshop

Company: Carl Zeiss (Shanghai) Co., Ltd. | Time: 14:30-18:00, 18 August
Location: Room 305 (3rd Floor) of QICEC
Topics: Studying Structure-Property Relations in Materials Using Analytical and In Situ Microscopy Characterization Technique

2. Big Data Intelligence and Knowledge Services Forum 2019

Time: 08:30-17:30, 20 August | Location: International Reporting Hall (3rd Floor) of QICEC

3. 2nd China-Korea Symposium on Light Metals

Time: 09:00-17:00, 21 August | Location: Room 304 (3rd Floor) of QICEC

Conference Policies

Badges

All attendees must wear registration badges at all times during the conference to ensure admission to events included in the paid fee such as technical sessions, exhibition, receptions, conference dinner, etc.

Photography Notice

By registering for this conference, all attendees acknowledge that they may be photographed by conference personnel while at events and that those photos may be used for promotional purposes.

Audio/Video Recording Policy

Recording of sessions (audio, video, still photography, etc.) intended for personal use, distribution, publication, or copyright without the express written consent of CSM and the individual authors is strictly prohibited.

Cell Phone Use

In consideration of attendees and presenters, we kindly request that you minimize disturbances by setting all cell phones and other devices on “silent” while in meeting rooms.

Conference Secretariat

Prof. Qing Song Cell phone: 13651002794
Mr. Xin Zhao Cell phone: 13439682609
Ms. Fang Liu Cell phone: 13810162102